Electrokinetic Remediation for Environmental Security and Sustainability

UNCORRECTED PROOFS

UNCORRECTED PROOFS

Electrokinetic Remediation for Environmental Security and Sustainability

Alexandra B. Ribeiro
Center for Environmental and Sustainability Research
Department of Environmental Sciences and Engineering
NOVA School of Science and Technology
NOVA University Lisbon
Caparica
Portugal

M. N. V. Prasad
Department of Chemistry
School of Life Sciences
University of Hyderabad
Hyderabad
Telangana
India

UNCORRECTED PROOFS

WILEY

This edition first published 2021
© 2021 by John Wiley & Sons, Inc. All rights reserved.

All rights reserved. No part of this publication may be reproduced, stored in a retrieval system, or transmitted, in any form or by any means, electronic, mechanical, photocopying, recording or otherwise, except as permitted by law. Advice on how to obtain permission to reuse material from this title is available at http://www.wiley.com/go/permissions.

The right of Alexandra B. Ribeiro and M. N. V. Prasad to be identified as the author of this work has been asserted in accordance with law.

Registered Offices
John Wiley & Sons, Inc., 111 River Street, Hoboken, NJ 07030, USA
John Wiley & Sons Ltd, The Atrium, Southern Gate, Chichester, West Sussex, PO19 8SQ, UK

Editorial Office
The Atrium, Southern Gate, Chichester, West Sussex, PO19 8SQ, UK

For details of our global editorial offices, customer services, and more information about Wiley products visit us at www.wiley.com.

Wiley also publishes its books in a variety of electronic formats and by print-on-demand. Some content that appears in standard print versions of this book may not be available in other formats.

Limit of Liability/Disclaimer of Warranty
In view of ongoing research, equipment modifications, changes in governmental regulations, and the constant flow of information relating to the use of experimental reagents, equipment, and devices, the reader is urged to review and evaluate the information provided in the package insert or instructions for each chemical, piece of equipment, reagent, or device for, among other things, any changes in the instructions or indication of usage and for added warnings and precautions. While the publisher and authors have used their best efforts in preparing this book, they make no representations or warranties with respect to the accuracy or completeness of the contents of this work and specifically disclaim all warranties, including without limitation any implied warranties of merchantability or fitness for a particular purpose. No warranty may be created or extended by sales representatives, written sales materials or promotional statements for this work. This work is sold with the understanding that the publisher is not engaged in rendering professional services. The advice and strategies contained herein may not be suitable for your situation. You should consult with a professional where appropriate. Neither the publisher nor author shall be liable for any loss of profit or any other commercial damages, including but not limited to special, incidental, consequential, or other damages. The fact that an organization, website, or product is referred to in this work as a citation and/or potential source of further information does not mean that the publisher and authors endorse the information or services the organization, website, or product may provide or recommendations it may make. Further, readers should be aware that websites listed in this work may have changed or disappeared between when this work was written and when it is read. Neither the publisher nor authors shall be liable for any loss of profit or any other commercial damages, including but not limited to special, incidental, consequential, or other damages.

For general information on our other products and services or for technical support, please contact our Customer Care Department within the United States at (800) 762-2974, outside the United States at (317) 572-3993 or fax (317) 572-4002.
Wiley also publishes its books in a variety of electronic formats. Some content that appears in print may not be available in electronic formats. For more information about Wiley products, visit our web site at ww.wiley.com.

Library of Congress Cataloging-in-Publication Data

Ribeiro, Alexandra B.; Prasad, M. N. V.
Electrokinetic Remediation for Environmental Security and Sustainability
ISBN: 978-1-119-67011-7

Cover image: [Production Editor to insert]
Cover design by [Production Editor to insert]

Set in 9.5/12.5pt STIXTwoText by SPi Global, Chennai, India

10 9 8 7 6 5 4 3 2 1

UNCORRECTED PROOFS

Trim Size: 170mm x 244mm Single Column Loose Ribeiro670117 ftoc.tex V1 - 12/15/2020 7:03pm Page v

Contents

Contributors *xix*

1 An Overview of the Modeling of Electrokinetic Remediation *1*
Maria Villen-Guzman, Maria del Mar Cerrillo-Gonzalez, Juan Manuel Paz-Garcia, and Jose Miguel Rodriguez-Maroto
1.1 Introduction *1*
1.2 Reactive Transport *3*
1.2.1 One-Dimensional Electromigration Model *3*
1.2.2 One-Dimensional Electromigration and Electroosmosis Model *7*
1.2.3 One-Dimensional Electrodialytic Model *9*
1.2.4 One-Dimensional Electroremediation Model Using Nernst-Planck-Poisson *16*
1.3 Chemical Equilibrium *18*
1.4 Models for the Future *24*
1.4.1 Combining Chemical Equilibrium and Chemical Reaction Kinetics *24*
1.4.2 Multiscale Models *26*
1.4.3 Two- and Three-Dimensional Models *29*
1.4.4 Multiphysics Modeling *29*
Acknowledgments *30*
References *30*

2 Basic Electrochemistry Tools in Environmental Applications *35*
Chanchal Kumar Mitra and Majeti Narasimha Vara Prasad
2.1 Introduction *35*
2.1.1 Electrochemical Half-Cells *37*
2.1.2 Electrode Potential *38*
2.1.3 Electrical Double Layer *40*
2.1.4 Electrochemical Processes *41*
2.1.4.1 Polarization (Overvoltage) *41*
2.1.4.2 Slow Chemical Reactions *42*
2.2 Basic Bioelectrochemistry and Applications *44*

UNCORRECTED PROOFS

Trim Size: 170mm x 244mm Single Column Loose Ribeiro670117 ftoc.tex V1 - 12/15/2020 7:03pm Page vi

2.3 Industrial Electrochemistry and the Environment *44*
2.3.1 Isolation and Purification of Important Metals *44*
2.3.2 Production of Important Chemical Intermediates by Electrochemistry *45*
2.4 Electrokinetic Phenomena *45*
2.4.1 Electroosmosis in Bioremediation *46*
2.5 Electrophoresis and Its Application in Bioremediation *47*
2.6 Biosensors in Environmental Monitoring *48*
2.6.1 What Are Biosensors? *48*
2.6.2 Biosensors as Environmental Monitors *49*
2.7 Electrochemical Systems as Energy Sources *52*
2.8 Conclusions *55*
References *55*

3 Combined Use of Remediation Technologies with Electrokinetics *61*
Helena I. Gomes and Erika B. Bustos
3.1 Introduction *61*
3.2 Biological Processes *62*
3.2.1 Electrobioremediation *62*
3.2.2 Electro-Phytoremediation *64*
3.3 Permeable Reactive Barriers *67*
3.4 Advanced Oxidation Processes *67*
3.4.1 Electrokinetics-Enhanced In Situ Chemical Oxidation (EK-ISCO) *67*
3.4.2 Electro-Fenton *70*
3.5 *In Situ* Chemical Reduction (ISCR) *71*
3.6 Challenges for Upscaling *71*
3.7 Concluding Remarks *73*
References *73*

4 The Electrokinetic Recovery of Tungsten and Removal of Arsenic from Mining Secondary Resources: The Case of the Panasqueira Mine *85*
Joana Almeida, Paulina Faria, António Santos Silva, Eduardo P. Mateus, and Alexandra B. Ribeiro
4.1 Introduction *85*
4.2 Tungsten Mining Resources: The Panasqueira Mine *86*
4.2.1 The Development of the Industry *86*
4.2.2 Ore Extraction Processes *88*
4.2.3 Potential Risks *88*
4.3 The Circular Economy of Tungsten Mining Waste *89*
4.3.1 Panasqueira Old Slimes vs. Current Slimes *89*
4.3.2 Tungsten Recovery *90*
4.3.3 Building Material–Related Applications *92*

UNCORRECTED PROOFS

Trim Size: 170mm x 244mm Single Column Loose Ribeiro670117 ftoc.tex V1 - 12/15/2020 7:03pm Page vii

4.4 Social, Economic, and Environmental Impacts *93*
4.5 Final Remarks *94*
Acknowledgments *94*
References *95*

5 Electrokinetic Remediation of Dredged Contaminated Sediments *99*
Kristine B. Pedersen, Ahmed Benamar, Mohamed T. Ammami, Florence Portet-Koltalo, and Gunvor M. Kirkelund
5.1 Introduction *99*
5.2 EKR Removal of Pollutants from Harbor Sediments *101*
5.2.1 Pollutants and Removal Efficiencies *101*
5.2.1.1 Metals *102*
5.2.1.2 Organic Pollutants and Organometallic Pollutants *104*
5.2.2 Influence of Experimental Settings and Sediment Properties on the Efficiency of EKR *105*
5.2.2.1 Enhancement of EKR – Changes in Design *106*
5.2.2.2 Enhancement of EKR – Chemical Agents and Surfactants *106*
5.2.2.3 Sediment Characteristics *108*
5.3 Case Studies of Enhancement Techniques *111*
5.4 Evaluation of the Best Available EKR Practice *120*
5.4.1 Energy Consumption *120*
5.4.2 Environmental Impacts *122*
5.5 Scaling Up EKR for Remediation of Polluted Harbor Sediments *123*
5.5.1 Results and Comments *125*
5.6 Future Perspectives *129*
References *131*

6 Pharmaceutically Active Compounds in Wastewater Treatment Plants: Electrochemical Advanced Oxidation as Onsite Treatment *141*
Ana Rita Ferreira, Paula Guedes, Eduardo P. Mateus, Alexandra B. Ribeiro, and Nazaré Couto
6.1 Introduction *141*
6.1.1 Emerging Organic Contaminants *141*
6.1.2 Occurrence and Fate of EOCs *141*
6.1.2.1 EOCs in WWTPs *143*
6.1.3 Water Challenges *144*
6.1.4 Technologies for Wastewater Treatment – Electrochemical Process *146*
6.2 Electrochemical Reactor for EOC Removal in WWTPs *148*
6.2.1 Experimental Design *148*
6.2.1.1 Analytical Methodology *148*

UNCORRECTED PROOFS

Trim Size: 170mm x 244mm Single Column Loose Ribeiro670117 ftoc.tex V1 - 12/15/2020 7:03pm Page viii

6.2.2 Electrokinetic Reactor Operating in a Continuous Vertical Flow Mode *150*
6.3 Conclusions *153*
Acknowledgments *153*
References *153*

7 Rare Earth Elements: Overview, General Concepts, and Recovery Techniques, Including Electrodialytic Extraction *159*
Nazaré Couto, Ana Rita Ferreira, Vanda Lopes, Stephen Peters, Sibel Pamukcu, and Alexandra B. Ribeiro
7.1 Introduction *159*
7.1.1 Rare Earth Elements: Characterization, Applications, and Geo-Dependence *159*
7.1.2 REE Mining and Secondary Sources *162*
7.1.3 REE Extraction and Recovery from Secondary Resources *163*
7.2 Case Study *164*
7.3 Conclusions *166*
Acknowledgments *167*
References *167*

8 Hydrocarbon-Contaminated Soil in Cold Climate Conditions: Electrokinetic-Bioremediation Technology as a Remediation Strategy *173*
Ana Rita Ferreira, Paula Guedes, Eduardo P. Mateus, Pernille Erland Jensen, Alexandra B. Ribeiro, Nazaré Couto
8.1 Introduction *173*
8.1.1 Hydrocarbon Contamination *173*
8.1.2 Oil Spills in Arctic Environments *174*
8.1.3 Remediation of Petroleum-Contaminated Soil *175*
8.1.3.1 Electrokinetic Remediation (EKR) *176*
8.2 Case Study *177*
8.2.1 Description of the Site *177*
8.2.2 Soil Sampling *178*
8.2.3 Electrokinetic Remediation (EKR) Experiments *178*
8.2.4 Analytical Procedures *179*
8.2.4.1 Soil Characterization *179*
8.3 Determination of Metals and Phosphorus *180*
8.3.1 Results and Discussion *180*
8.3.1.1 Soil Characteristics *180*
8.3.1.2 EKR Experiments *182*
8.4 Conclusions *186*
Acknowledgments *186*
References *186*

UNCORRECTED PROOFS

Trim Size: 170mm x 244mm Single Column Loose Ribeiro670117 ftoc.tex V1 - 12/15/2020 7:03pm Page ix

9 Electrochemical Migration of Oil and Oil Products in Soil *191*
V.A. Korolev and D.S. Nesterov
9.1 Introduction *191*
9.2 Specific Nature of Soils Polluted by Oil and Its Products *192*
9.3 Influence of Mineral Composition *193*
9.4 Influence of Soil Dispersiveness *195*
9.5 Influence of Physical Soil Properties *198*
9.6 Influence of Physico-Chemical Soil Properties *201*
9.7 Influence of the Initial Water/Oil Ratio in a Soil *203*
9.8 Influence of the Oil Aging Process *207*
9.9 Influence of Oil Composition *212*
9.10 Conclusions *221*
Acknowledgments *221*
List of Abbreviations *221*
References *222*

10 Nanostructured TiO_2-Based Hydrogen Evolution Reaction (HER) Electrocatalysts: A Preliminary Feasibility Study in Electrodialytic Remediation with Hydrogen Recovery *227*
Antonio Rubino, Joana Almeida, Catia Magro, Pier G. Schiavi, Paula Guedes, Nazare Couto, Eduardo P. Mateus, Pietro Altimari, Maria L. Astolfi, Robertino Zanoni, Alexandra B. Ribeiro, and Francesca Pagnanelli
10.1 Introduction *227*
10.1.1 Electrokinetic Technologies: Electrodialytic Ex Situ Remediation *228*
10.1.2 Nanostructured TiO_2 Electrocatalysts Synthesized Through Electrochemical Methods *230*
10.2 Case Study *231*
10.2.1 Aim and Scope *231*
10.2.2 Experimental *232*
10.2.2.1 TiO_2 Based Electrocatalyst Synthesis and Characterization *232*
10.2.2.2 ED Experiments *233*
10.2.3 Discussion *235*
10.2.3.1 Blank Tests: Electrocatalyst Effectiveness toward HER *235*
10.2.3.2 ED Remediation for Sustainable CRMs Recovery *236*
10.3 Final Considerations *242*
Acknowledgments *244*
References *244*

11 Hydrogen Recovery in Electrodialytic-Based Technologies Applied to Environmental Contaminated Matrices *251*
Cátia Magro, Joana Almeida, Juan Manuel Paz-Garcia, Eduardo P. Mateus, and Alexandra B. Ribeiro
11.1 Scope *251*
11.2 Technology Concept *253*

UNCORRECTED PROOFS

Trim Size: 170mm x 244mm Single Column Loose Ribeiro670117 ftoc.tex V1 - 12/15/2020 7:03pm Page x

11.2.1 Potential Secondary Resources *253*
11.2.2 Electrodialytic Reactor *254*
11.2.2.1 Electrodes *254*
11.2.2.2 Ion-Exchange Membranes *256*
11.2.2.3 PEMFC System *258*
11.3 Economic Assessment of PEMFC Coupled with Electroremediation *260*
11.3.1 Scenario Analysis *260*
11.3.2 Hydrogen Business Model Canvas *262*
11.3.3 SWOT Analysis *264*
11.4 Final Remarks *264*
Acknowledgments *266*
References *266*

12 Electrokinetic-Phytoremediation of Mixed Contaminated Soil for Environmental Remediation *271*
Joana Dionísio, Nazaré Couto, Paula Guedes, Cristiana Gonçalves, and Alexandra B. Ribeiro
12.1 Soil Contamination *271*
12.2 Phytoremediation *272*
12.3 Electroremediation *274*
12.3.1 EK Process Coupled with Phytoremediation *275*
12.3.2 EK-Assisted Bioremediation in the Treatment of Inorganic Contaminants *277*
12.3.3 EK-Assisted Bioremediation in the Treatment of Organic Contaminants *278*
12.4 Case Study of EK and Electrokinetic-Assisted Phytoremediation *279*
12.5 Conclusions *281*
Acknowledgments *282*
References *282*

13 Enhanced Electrokinetic Techniques in Soil Remediation for Removal of Heavy Metals *287*
Sadia Ilyas, Rajiv Ranjan Srivastava, Hyunjung Kim, and HummaAkram Cheema
13.1 Introduction *287*
13.2 Electrokinetic Mechanism and Phenomenon *288*
13.3 Limitations of the Electrokinetic Remediation Process *289*
13.4 Need for Enhancement in the Electrokinetic Remediation Process *290*
13.5 Enhancement Techniques *292*
13.5.1 Surface Modification *292*
13.6 Cation-Selective Membranes *293*
13.7 Electro-Bioremediation *294*
13.8 Electro-Geochemical Oxidation *295*
13.9 Lasagna™ Process *296*

UNCORRECTED PROOFS

Trim Size: 170mm x 244mm Single Column Loose Ribeiro670117 ftoc.tex V1 - 12/15/2020 7:03pm Page xi

13.10 Other Potential Processes *296*
13.11 Summary *298*
Acknowledgments *299*
References *299*

14 Assessment of Soil Fertility and Microbial Activity by Direct Impact of an Electrokinetic Process on Chromium-Contaminated Soil *303*
Prem Prakash, Prasun Kumar Chakraborty, and Brijesh Kumar Mishra
14.1 Introduction *303*
14.2 Experimental Section *304*
14.2.1 Soil Characteristics and Preparation of Contaminated Soil *304*
14.2.2 Electrokinetic Tests, Experimental Setup, and Procedure *305*
14.2.3 Testing Procedure *306*
14.2.4 Extraction and Analytical Methods *306*
14.2.5 Soil Nutrients *306*
14.2.6 Soil Microbial Biomass Carbon Analysis *307*
14.2.7 Quality Control and Quality Assurance *307*
14.3 Results and Discussion *308*
14.3.1 Electrokinetic Remediation of Chromium-Contaminated Soil *308*
14.3.1.1 Electrical Current Changes During the Electrokinetic Experiment *308*
14.3.2 pH Distribution in Soil During and After the Electrokinetic Experiment *309*
14.4 Removal of Cr *310*
14.4.1 The Distribution of Total Cr and Its Electroosmotic Flow During the Electrokinetic Experiment *310*
14.5 Effects of the Electrokinetic Process on Some Soil Properties *312*
14.5.1 Soil Organic Carbon *312*
14.5.2 Soil-Available Nitrogen, Phosphorus, Potassium, and Calcium *314*
14.5.3 Soil Microbial Biomass Carbon *318*
14.6 Conclusion *318*
References *319*

15 Management of Clay Properties Based on Electrokinetic Nanotechnology *323*
D.S. Nesterov and V.A. Korolev
15.1 Introduction *323*
15.2 Objects of the Study *326*
15.3 Methods of the Study *328*
15.4 Results and Discussion *330*
15.4.1 Regulation of Soil pH *330*
15.4.2 Regulation of Oxidation-Reduction Potential *332*
15.4.3 Regulation of Soil Particle Surface-Charge Density *332*
15.4.4 EDL Parameter Regulation *339*
15.4.5 Regulation of Clay CEC *343*

UNCORRECTED PROOFS

Trim Size: 170mm x 244mm Single Column Loose Ribeiro670117 ftoc.tex V1 - 12/15/2020 7:03pm Page xii

15.4.6 Regulation of Physico-Chemical Parameters of Soils *345*
15.4.7 Regulation of Soil Texture and Structure *346*
15.4.8 Regulation of Physical Clay Properties *352*
15.4.9 Regulation of Soil Strength and Deformability *353*
15.5 Conclusions *354*
Acknowledgments *355*
Abbreviations *355*
References *357*

16 Technologies to Create Electrokinetic Protective Barriers *363*
D.S. Nesterov and V.A. Korolev
16.1 Introduction *363*
16.2 Conventional Electrokinetic Barriers *366*
16.2.1 Cationic Contaminants *366*
16.2.2 Anionic Pollutants *367*
16.2.3 Advanced EKB Implementations *367*
16.2.4 Using EKBs for Soil Remediation *368*
16.3 Electrokinetic Barrier with Ion-Selective Membranes (IS-EKB) *369*
16.4 Electrokinetic Barrier Based on Geosynthetics (EKG-B) *370*
16.5 Bio-Electrokinetic Protective Barrier (Bio-EKB) *371*
16.6 Electrokinetic Permeable Reactive Barriers (EK-PRB) *376*
16.6.1 EK-PRBs Based on Activated Carbon *377*
16.6.2 EK-PRBs Based on Iron Compounds *379*
16.6.2.1 ZVI-Based EK-PRBs *379*
16.6.2.2 EK-PRBs Based on Ferric/Ferrous Compounds *381*
16.6.3 EK-PRBs Based on Red Mud *382*
16.6.4 EK-PRBs Based on Zeolites *383*
16.6.5 EK-PRBs Based on Clays or Modified Soils *383*
16.6.6 Other Materials for the Creation of EK-PRBs *384*
16.7 Electrokinetic Permeable Reactive Barriers to Prevent Radionuclide Contamination *397*
16.8 Conclusion *401*
Acknowledgments *401*
Abbreviations *401*
References *403*

17 Emerging Contaminants in Wastewater: Sensor Potential for Monitoring Electroremediation Systems *413*
Cátia Magro, Eduardo P. Mateus, Maria de Fátima Raposo, and Alexandra B. Ribeiro
17.1 Scope *413*
17.2 Removal Technologies: Electroremediation Treatment *416*
17.3 Monitoring Tool: Electronic Tongues Devices *417*
17.3.1 Sensor Design *418*
17.3.1.1 Thin-Film Nanomaterials *419*

UNCORRECTED PROOFS

Trim Size: 170mm x 244mm Single Column Loose Ribeiro670117 ftoc.tex V1 - 12/15/2020 7:03pm Page xiii

17.3.1.2 Promising Thin-Film Deposition Techniques *420*
17.3.1.3 Electrical Measurements: Impedance Spectroscopy *422*
17.3.2 Data Treatment *424*
17.4 Critical View on Coupling EK and Electronic Tongues *424*
17.5 Final Remarks *427*
Acknowledgments *428*
References *428*

18 Perspectives on Electrokinetic Remediation of Contaminants of Emerging Concern in Soil *433*
Paula Guedes, Nazaré Couto, Eduardo Mateus, Cristina Silva Pereira, and Alexandra B. Ribeiro
18.1 Introduction *433*
18.1.1 Soil Pollution *433*
18.1.2 Contaminants of Emerging Concern *434*
18.2 Electrokinetic Process *436*
18.2.1 Removal Mechanisms *437*
18.2.2 Electro-Degradation Mechanisms *439*
18.2.3 Enhanced Bio-Degradation *442*
18.3 Conclusion *445*
Acknowledgments *446*
References *446*

19 Electrokinetic Remediation for the Removal of Organic Waste in Soil and Sediments *453*
S.M.P.A Koliyabandara, Chamika Siriwardhana, Sakuni M. De Silva, Janitha Walpita, and Asitha T. Cooray
19.1 Introduction *453*
19.2 Organic Soil Pollution *453*
19.2.1 The Fate of Organic Soil Pollutants *455*
19.2.2 Biomagnification and Bioaccumulation of Soil Pollutants *455*
19.3 Soil Remediation Methods *456*
19.3.1 Physical Methods *456*
19.3.1.1 Capping *456*
19.3.1.2 Thermal Desorption *457*
19.3.1.3 Soil Vapor Extraction (SVE) *458*
19.3.1.4 Incineration *458*
19.3.1.5 Air Sparging *458*
19.3.2 Chemical Methods *458*
19.3.2.1 Soil Washing/Flushing *459*
19.3.2.2 Chemical Oxidation Remediation *459*
19.3.3 Bioremediation *460*
19.3.3.1 Microbial Remediation *460*
19.3.3.2 Phytoremediation *460*
19.4 Electrokinetic Remediation (EKR) *461*

UNCORRECTED PROOFS

Trim Size: 170mm x 244mm Single Column Loose Ribeiro670117 ftoc.tex V1 - 12/15/2020 7:03pm Page xiv

19.4.1 Basic Principles of EKR *461*
19.4.1.1 Electrolysis of Pore Water *462*
19.4.1.2 Electromigration *462*
19.4.1.3 Electroosmosis *464*
19.4.1.4 Electrophoresis *464*
19.5 EKR for the Treatment of Soils and Sediments *464*
19.5.1 Enhancement Techniques Coupled with EKR *466*
19.5.1.1 Techniques Used to Enhance the Solubility of Contaminants *466*
19.5.1.2 Techniques to Control Soil pH *466*
19.5.1.3 Coupling with Other Remediation Techniques *467*
19.5.2 Facilitating Agents for PAH Removal *468*
19.5.2.1 Cyclodextrin-Enhanced EK *468*
19.5.2.2 Surfactant-Enhanced EK *468*
19.5.3 Cosolvent-Enhanced EKR *469*
19.5.4 Biosurfactant–Enhanced EKR *469*
19.6 Factors Affecting the Efficiency of Electrokinetic Remediation *470*
19.6.1 Effect of pH *470*
19.6.2 Effect of Electrolytes *470*
19.6.3 Effect of Soil Characteristics *470*
19.6.4 Effect of the Voltage Gradient *471*
19.7 Conclusions and Future Perspective *471*
Acknowledgments *471*
References *472*

20 The Integration of Electrokinetics and In Situ Chemical Oxidation Processes for the Remediation of Organically Polluted Soils *479*
Long Cang, Qiao Huang, Hongting Xu, and Mingzhu Zhou
20.1 Introduction *479*
20.2 Principles Underlying EK-ISCO Remediation Technology *480*
20.2.1 Desorption and Migration of Organic Pollutants *480*
20.2.2 Oxidant Migration *482*
20.3 Factors that Influence EK-ISCO Technology *484*
20.3.1 Soil Properties *484*
20.3.2 Dosage and Methods Used to Add Oxidants to Soil *485*
20.3.3 Concentration and Aging of Organic Pollutants *486*
20.4 Enhanced EK-ISCO Remediation Methods *486*
20.4.1 Electro-Fenton Process *486*
20.4.2 pH Control *487*
20.4.3 Ion-Exchange Membranes *488*
20.4.4 Adding Solubilizers *488*
20.4.5 Electrode Activation/Electrode Thermal Activation *489*
20.4.6 Nanomaterial-Enhanced Methods *490*
20.5 Pilot/Field-Scale Studies of EK-ISCO Remediation Technologies *490*
20.5.1 Experimental Design *490*

UNCORRECTED PROOFS

Trim Size: 170mm x 244mm Single Column Loose Ribeiro670117 ftoc.tex V1 - 12/15/2020 7:03pm Page xv

20.5.1.1 Electrode Materials *490*
20.5.1.2 Configuring Electrode Settings *491*
20.5.1.3 Power Supply Modes *492*
20.5.2 Pilot Cases *493*
20.6 Conclusions *494*
Acknowledgments *494*
References *495*

21 Electrokinetic and Electrochemical Removal of Chlorinated Ethenes: Application in Low- and High-Permeability Saturated Soils *503*
Bente H. Hyldegaard and Lisbeth M. Ottosen
21.1 Introduction *503*
21.1.1 Chlorinated Ethenes *503*
21.1.2 Low-Permeability Saturated Soils *506*
21.1.3 High-Permeability Saturated Soils *507*
21.2 Electrokinetically Enhanced Remediation in Low-Permeability Saturated Soils *508*
21.2.1 Electrokinetically Enhanced Bioremediation (EK-BIO) *508*
21.2.1.1 EK-Induced Delivery of Microbial Cultures and Electron Donors *509*
21.2.1.2 Current State of Development from an Applied Perspective *510*
21.2.2 Electrokinetically Enhanced In Situ Chemical Oxidation (EK-ISCO) *511*
21.2.2.1 EK-Induced Delivery of Oxidants *512*
21.2.2.2 Current State of Development from an Applied Perspective *513*
21.2.3 Electrokinetically Enhanced Permeable Reactive Barriers (EK-PRB) *514*
21.2.3.1 EK-Induced Mobilization of Chlorinated Ethenes *514*
21.2.3.2 EK-Controlled Reactivity of the Filling Material *515*
21.2.3.3 Current State of Development from an Applied Perspective *515*
21.3 Electrochemical Remediation in High-Permeability Saturated Soils *516*
21.3.1 Electrochemistry in Complex Environmental Settings *517*
21.3.2 Electrochemical Remediation in Complex Environmental Settings *519*
21.3.2.1 Electrochemically Induced Changes in Hydrogeochemistry *522*
21.3.2.2 Current State of Development from an Applied Perspective *525*
21.4 Summary *527*
References *528*

22 Chlorophenolic Compounds and Their Transformation Products by the Heterogeneous Fenton Process: A Review *541*
Cetin Kantar and Ozlem Oral
22.1 Introduction *541*
22.2 Heterogeneous Fenton Processes *545*
22.2.1 Effect of Catalyst Type and Possible Reaction Mechanisms *546*

UNCORRECTED PROOFS

Trim Size: 170mm x 244mm Single Column Loose Ribeiro670117 ftoc.tex V1 - 12/15/2020 7:03pm Page xvi

22.2.1.1 Iron Oxides *547*
22.2.1.2 Pyrite *552*
22.2.1.3 Zero-Valent Iron (ZVI) *553*
22.2.1.4 Multimetallic Iron-Based Catalysts *555*
22.2.1.5 Supported Iron-Based Catalyst Materials *560*
22.3 Factors Affecting CP Removal Efficiency in Heterogeneous Fenton Processes *565*
22.3.1 Effect of Catalyst Size *565*
22.3.2 Effect of Catalyst Dosage *565*
22.3.3 Effect of pH *566*
22.3.4 Effect of Hydrogen Peroxide Dose *567*
22.3.5 Effect of Organic Ligands *568*
22.4 Reaction By-Products *569*
22.5 Mode of Implementation, Reactor Configuration, and Biodegradability *571*
22.6 Conclusions *572*
References *574*

23 Clays and Clay Polymer Composites for Electrokinetic Remediation of Soil *587*
Jayasankar Janeni and Nadeesh M. Adassooriya
23.1 Introduction *587*
23.2 Electrokinetic Remediation Technique: An Overview *588*
23.3 Clay Soil and Minerals *588*
23.4 Clay Mineral Classifications and Structure *589*
23.5 Layer Charge *590*
23.6 Active Bond Sites in Clay Minerals *590*
23.7 Properties of Clay Minerals *591*
23.8 Clay Minerals and Their Modifications *591*
23.9 Organoclays and Their Properties *591*
23.10 Factors Affecting the Mechanism of Transporting Contaminants in Clay Soils *593*
23.10.1 Structural Parameters *593*
23.10.2 Mass Transport *593*
23.10.3 Electrokinetic Potential (Zeta Potential) *595*
23.10.4 Polymeric Agent Enhanced Electrokinetic Decontamination of Clay Soils *596*
23.10.5 Future Perspectives *597*
23.11 Summary *598*
References *598*

24 Enhanced Remediation and Recovery of Metal-Contaminated Soil Using Electrokinetic Soil Flushing *603*
Yudha Gusti Wibowo and Bimastyaji Surya Ramadan
24.1 Introduction *603*

UNCORRECTED PROOFS

Trim Size: 170mm x 244mm Single Column Loose Ribeiro670117 ftoc.tex V1 - 12/15/2020 7:03pm Page xvii

24.2 Metal Contamination in Mining Areas *604*
24.3 Treatment of Metal-Contaminated Soil Using EKSF *605*
24.3.1 Soil Flushing *605*
24.3.2 Fundamental Equation for EK Remediation *606*
24.3.3 Electrokinetic Soil Flushing (EKSF) *609*
24.3.4 Flushing Fluid Enhanced EKSF Performance *610*
24.3.5 Preventing pH from Acidification *617*
24.3.6 Other Factors that Enhance EKSF Performance *618*
24.3.7 Energy Requirements and Future Perspectives *618*
24.4 Conclusion *620*
References *620*

25 Recent Progress on Pressure-Driven Electro-Dewatering (PED) of Contaminated Sludge *629*
Bimastyaji Surya Ramadan, Amelinda Dhiya Farhah, Mochtar Hadiwidodo, and Mochamad Arief Budihardjo
25.1 Introduction *629*
25.2 Electro-Dewatering for Sludge Treatment *630*
25.2.1 Conventional Sludge Treatment Systems *630*
25.2.2 Overview of Electro-Dewatering Systems *630*
25.2.3 Fundamental Equations of EDW Systems *632*
25.3 Design Considerations for PED Systems *636*
25.3.1 Reducing Electrical Resistance in PED Systems *638*
25.3.2 Maintaining Optimum pH and Salinity *639*
25.3.3 Determining Sludge Characteristics and Properties *641*
25.3.4 Operating PED Under Constant Voltage or Current *641*
25.3.5 Determining Appropriate Electrodes (Anodes and Cathodes) *642*
25.3.6 Reducing Energy Consumption *643*
25.4 Future Perspectives *644*
25.5 Conclusion *647*
References *647*

26 Removing Ionic and Nonionic Pollutants from Soil, Sludge, and Sediment Using Ultrasound-Assisted Electrokinetic Treatment *653*
Bimastyaji Surya Ramadan, Marita Wulandari, Yudha Gusti Wibowo, Nurani Ikhlas, and Dimastyaji Yusron Nurseta
26.1 Introduction *653*
26.2 Overview of Technologies *654*
26.2.1 Ultrasonication *654*
26.2.2 Electrokinetic Remediation *656*
26.3 Desorption and Degradation Mechanism *659*
26.3.1 Removing Contaminants by Ultrasonication *659*
26.3.2 Ultrasonic Wave Effect *660*
26.3.2.1 Cavitation *660*

UNCORRECTED PROOFS

Trim Size: 170mm x 244mm Single Column Loose Ribeiro670117 ftoc.tex V1 - 12/15/2020 7:03pm Page xviii

26.3.2.2 Thermal Effect *661*
26.3.2.3 Chemical Effect *661*
26.3.2.4 Biological Effect *662*
26.3.3 Electrokinetic Remediation Process *662*
26.3.3.1 Electrolysis *662*
26.3.3.2 Electromigration and Electrophoresis *664*
26.3.3.3 Electroosmosis *664*
26.3.3.4 Electrooxidation/Reduction *665*
26.4 Ultrasonication-Assisted Electrokinetic Remediation *666*
26.4.1 Recent Progress in Ultrasonication-Assisted Electrokinetic Remediation (US-EK) *666*
26.4.2 Factors Affecting Performance *666*
26.4.2.1 System Parameters *666*
26.4.2.2 Contaminant and Environmental Parameters *669*
26.4.3 Future Directions *671*
26.5 Conclusions *671*
References *672*

Index *679*

UNCORRECTED PROOFS

Contributors

Nadeesh M. Adassooriya,
Department of Food Science & Technology
Wayamba University of Sri Lanka
Makandura
Sri Lanka

Joana Almeida
CENSE – Center for Environmental and Sustainability Research, Department of Environmental Sciences and Engineering, NOVA School of Science and Technology
NOVA University Lisbon
Caparica Campus, Caparica
Portugal

and

Department of Civil Engineering
NOVA School of Science and Technology,
NOVA University Lisbon
Caparica Campus, Caparica
Portugal

Pietro Altimari
Department of Chemistry
Sapienza University of Rome
Rome
Italy

and

Eco Recycling Srl
Rome
Italy

Mohamed T. Ammami
Department of Civil Engineering
Le Havre Normandie University
Le Havre
France

Maria L. Astolfi
Department of Chemistry
Sapienza University of Rome
Rome
Italy

Ahmed Benamar
Department of Civil Engineering
Le Havre Normandie University
Le Havre
France

UNCORRECTED PROOFS

Trim Size: 170mm x 244mm Single Column Loose Ribeiro670117 flast.tex V1 - 12/15/2020 7:01pm Page xx

Mochamad Arief Budihardjo
Department of Environmental Engineering, Faculty of Engineering
Universitas Diponegoro
Semarang
Indonesia

Erika B. Bustos
Centro de Investigación y Desarrollo Tecnológico en Electroquímica
S.C. Parque Tecnológico Querétaro
Sanfandila, Querétaro
Mexico

Long Cang
Key Laboratory of Soil Environment and Pollution Remediation
Institute of Soil Science
Chinese Academy of Sciences, Nanjing
China

Maria del Mar Cerrillo-Gonzalez
Department of Chemical Engineering
Faculty of Science
University of Malaga
Malaga
Spain

Humma Akram Cheema
Mineral and Material Chemistry Lab
Department of Chemistry
University of Agriculture
Faisalabad
Pakistan

Asitha T. Cooray
Department of Chemistry, Faculty of Applied Sciences
University of Sri Jayewardenepura
Nugegoda
Sri Lanka

and

Instrument Centre, Office of the Dean
Faculty of Applied Sciences
University of Sri Jayewardenepura
Nugegoda
Sri Lanka

Nazaré Couto
CENSE – Center for Environmental and Sustainability Research
Department of Environmental Sciences and Engineering
NOVA School of Science and Technology
NOVA University Lisbon
Caparica
Portugal

and

Department of Civil and Environmental Engineering
Lehigh University
Bethlehem, Pennsylvania
USA

Sakuni M. De Silva, Instrument Centre
Office of the Dean, Faculty of Applied Sciences
University of Sri Jayewardenepura
Nugegoda
Sri Lanka

UNCORRECTED PROOFS

Trim Size: 170mm x 244mm Single Column Loose Ribeiro670117 flast.tex V1 - 12/15/2020 7:01pm Page xxi

Joana Dionísio
CENSE – Center for Environmental and Sustainability Research, Department of Environmental Sciences and Engineering
NOVA School of Science and Technology, NOVA University Lisbon
Caparica
Portugal

Amelinda Dhiya Farhah
Department of Environmental Engineering, Faculty of Engineering
Universitas Diponegoro
Semarang
Indonesia

Paulina Faria
Department of Civil Engineering
NOVA School of Science and Technology
NOVA University Lisbon
Caparica Campus, Caparica
Portugal

and

CERIS – Civil Engineering Research and Innovation for Sustainability
Instituto Superior Técnico, University of Lisbon
Lisbon
Portugal

Ana Rita Ferreira
CENSE – Center for Environmental and Sustainability Research, Department of Environmental Sciences and Engineering, NOVA School of Science and Technology
NOVA University Lisbon
Caparica
Portugal

and

Department of Civil and Environmental Engineering
Lehigh University
Bethlehem, Pennsylvania
USA

Helena I. Gomes
Food, Water, Waste Research Group
Faculty of Engineering
University of Nottingham
University Park, Nottingham
UK

Cristiana Gonçalves
CENSE – Center for Environmental and Sustainability Research, Department of Environmental Sciences and Engineering, NOVA School of Science and Technology
NOVA University Lisbon
Caparica
Portugal

UNCORRECTED PROOFS

Trim Size: 170mm x 244mm Single Column Loose Ribeiro670117 flast.tex V1 - 12/15/2020 7:01pm Page xxii

Paula Guedes
CENSE - Center for Environmental and Sustainability Research, Department of Environmental Sciences and Engineering, NOVA School of Science and Technology
NOVA University Lisbon
Caparica
Portugal

and

Instituto de Tecnologia Química e Biológica António Xavier
NOVA University Lisbon
Oeiras
Portugal

Mochtar Hadiwidodo
Department of Environmental Engineering, Faculty of Engineering
Universitas Diponegoro
Semarang
Indonesia

Qiao Huang
Key Laboratory of Soil Environment and Pollution Remediation
Institute of Soil Science, Chinese Academy of Sciences
Nanjing
China

and

College of Resources and Environment
University of the Chinese Academy of Sciences
Beijing
China

Bente H. Hyldegaard
Department of Civil Engineering
Technical University of Denmark
Lyngby
Denmark

Nurani Ikhlas
Department of Environmental Engineering, Faculty of Engineering
Institut Teknologi Pembangunan
Surabaya
Indonesia

Sadia Ilyas
Department of Mineral Resources and Energy Engineering
Jeonbuk National University
Jeonju, Jeonbuk
Republic of Korea

Jayasankar Janeni
Postgraduate Institute of Science
University of Peradeniya
Peradeniya
Sri Lanka

Pernille Erland Jensen
Department of Civil Engineering
Technical University of Denmark
Kongens Lyngby
Denmark

Cetin Kantar
Department of Environmental Engineering
Canakkale Onsekiz Mart University
Canakkale
Turkey

UNCORRECTED PROOFS

Trim Size: 170mm x 244mm Single Column Loose
Ribeiro670117 flast.tex V1 - 12/15/2020 7:01pm Page xxiii

Hyunjung Kim
Department of Mineral Resources and Energy Engineering
Jeonbuk National University
Jeonju, Jeonbuk
Republic of Korea

and

Department of Environment and Energy
Jeonbuk National University
Jeonju, Jeonbuk
Republic of Korea

Gunvor M. Kirkelund
Department of Civil Engineering
Technical University of Denmark
Lyngby
Denmark

S.M.P.A Koliyabandara
Department of Chemistry, Faculty of Applied Sciences
University of Sri Jayewardenepura
Nugegoda
Sri Lanka

V.A. Korolev
Department of Engineering and Ecological Geology, Faculty of Geology
M.V. Lomonosov Moscow State University
Moscow
Russia

Vanda Lopes
CENSE – Center for Environmental and Sustainability Research, Department of Environmental Sciences and Engineering, NOVA School of Science and Technology
NOVA University Lisbon
Caparica
Portugal

and

Department of Civil and Environmental Engineering
Lehigh University
Bethlehem, Pennsylvania
USA

Catia Magro
CENSE – Center for Environmental and Sustainability Research, Department of Environmental Sciences and Engineering, NOVA School of Science and Technology
NOVA University Lisbon
Caparica
Portugal

Eduardo P. Mateus
CENSE – Center for Environmental and Sustainability Research, Department of Environmental Sciences and Engineering
NOVA School of Science and Technology
NOVA University Lisbon
Caparica Campus, Caparica
Portugal

Chanchal Kumar Mitra
Department of Biochemistry
University of Hyderabad
Hyderabad, Telangana
India

UNCORRECTED PROOFS

Trim Size: 170mm x 244mm Single Column Loose Ribeiro670117 flast.tex V1 - 12/15/2020 7:01pm Page xxiv

D.S. Nesterov
Department of Engineering and Ecological Geology, Faculty of Geology
M.V. Lomonosov Moscow State University
Moscow
Russia

Dimastyaji Yusron Nurseta
Bioprocess Engineering, Department of Agricultural Engineering, Faculty of Agricultural Technology
Universitas Brawijaya
Indonesia

Ozlem Oral
Department of Environmental Engineering
Canakkale Onsekiz Mart University
Canakkale
Turkey

Lisbeth M. Ottosen
Department of Civil Engineering
Technical University of Denmark
Lyngby
Denmark

Francesca Pagnanelli
Department of Chemistry
Sapienza University of Rome
Rome
Italy

and

Eco Recycling Srl
Rome
Italy

Sibel Pamukcu
Department of Civil and Environmental Engineering
Lehigh University
Bethlehem, Pennsylvania
USA

Juan Manuel Paz-Garcia
Department of Chemical Engineering
Faculty of Science
University of Malaga
Malaga
Spain

Kristine B. Pedersen
Department of Environment
Akvaplan-niva AS
Fram Centre – High North Research Centre for Climate and the Environment
Tromsø
Norway

and

Department of Chemistry,
UiT – The Arctic University of Norway
Tromsø
Norway

Cristina Silva Pereira
Instituto de Tecnologia Química e Biológica António Xavier
NOVA University Lisbon
Oeiras
Portugal

Stephen Peters
Department of Earth and Environmental Sciences
Lehigh University
Bethlehem, Pennsylvania
USA

UNCORRECTED PROOFS

Trim Size: 170mm x 244mm Single Column Loose Ribeiro670117 flast.tex V1 - 12/15/2020 7:01pm Page xxv

Florence Portet-Koltalo
University Institute of Technology
Rouen Normandie University
Evreux
France

Majeti Narasimha Vara Prasad
School of Life Sciences
University of Hyderabad
Hyderabad, Telangana
India

Bimastyaji Surya Ramadan
Department of Environmental Engineering, Faculty of Engineering
Universitas Diponegoro
Semarang
Indonesia

Maria de Fátima Raposo
CEFITEC, Department of Physics
NOVA School of Science and Technology
NOVA University Lisbon
Caparica
Portugal

Alexandra B. Ribeiro
1CENS – Center for Environmental and Sustainability Research
Department of Environmental Sciences and Engineering, NOVA School of Science and Technology
NOVA University Lisbon
Caparica Campus, Caparica
Portugal

Jose Miguel Rodriguez-Maroto
Department of Chemical Engineering
Faculty of Science
University of Malaga
Malaga
Spain

Antonio Rubino
Department of Chemistry
Sapienza University of Rome
Rome
Italy

Pier G. Schiavi
Department of Chemistry
Sapienza University of Rome
Rome
Italy

António Santos Silva
Department of Materials, National Laboratory for Civil Engineering
Lisbon
Portugal

Chamika Siriwardhana
Department of Chemistry, Faculty of Applied Sciences
University of Sri Jayewardenepura
Nugegoda
Sri Lanka

Rajiv Ranjan Srivastava
Center for Advanced Chemistry
Institute of Research and Development
Duy Tan University
Da Nang
Vietnam

and

Faculty of Natural Sciences
Duy Tan University
Da Nang
Vietnam

Maria Villen-Guzman
Department of Chemical Engineering
Faculty of Science
University of Malaga
Malaga
Spain

UNCORRECTED PROOFS

Trim Size: 170mm x 244mm Single Column Loose Ribeiro670117 flast.tex V1 - 12/15/2020 7:01pm Page xxvi

Janitha Walpita
Instrument Centre, Office of the Dean
Faculty of Applied Sciences
University of Sri Jayewardenepura
Nugegoda
Sri Lanka

Yudha Gusti Wibowo
Department of Environmental Science
School of Postgraduate Studies
Universitas Jambi
Jambi
Indonesia

Marita Wulandari
Environmental Engineering
Department
Institut Teknologi Kalimantan
Balikpapan
Indonesia

Hongting Xu
Key Laboratory of Soil Environment
and Pollution Remediation
Institute of Soil Science
Chinese Academy of Sciences
Nanjing
China

Robertino Zanoni
Department of Chemistry
Sapienza University of Rome
Rome
Italy

Mingzhu Zhou
Key Laboratory of Soil Environment
and Pollution Remediation
Institute of Soil Science, Chinese
Academy of Sciences
Nanjing
China

UNCORRECTED PROOFS

Trim Size: 170mm x 244mm Single Column Loose Ribeiro670117 c01.tex V1 - 12/02/2020 10:43pm Page 1

1

An Overview of the Modeling of Electrokinetic Remediation

Maria Villen-Guzman, Maria del Mar Cerrillo-Gonzalez, Juan Manuel Paz-Garcia and Jose Miguel Rodriguez-Maroto

Department of Chemical Engineering, Faculty of Science, University of Malaga, Malaga 29071, Spain

1.1 Introduction

Electrokinetic remediation (EKR) is based on the application of an electric field to porous solid matrices [1] or suspensions (i.e. solid particles suspended in a well-stirred aqueous solution) [2]. Due to transport phenomena associated with the applied electric field, ionic and non-ionic species are mobilized toward the electrodes. Electrokinetic technology has also been widely applied to mobilize reactive particles, such as zero-valent iron (n-ZVI), through the soil and groundwater [3].

The basic principle of EKR is the application of an electric potential between two or more electrodes inserted into a solid matrix, resulting in a direct electric current through the medium [4]. At the electrode-electrolyte interface, the electric current transported by electron flow is transformed into ionic current that flows through the system. The electric current, transported mainly by ionic species, generates hydraulic, chemical, and electric potential gradients through the solid-fluid system. In EKR, five transport mechanisms coexist: (i) *electromigration* – movement of ion species (cations and anions) induced by an applied electric current toward the electrode of the opposite charge; (ii) *electroosmosis* – transport of ionic and non-ionic species through the porous media as a result of the movement of pore water; (iii) *electrophoresis* – movement of positive and negative-charged colloids; (iv) *diffusion* – movement of species as a result of the concentration gradient; and (v) *advection* – movement of water as a result of pressure gradients [5]. During in situ and *ex situ* application of EKR to a porous matrix, the contribution of the latter three mechanisms is not significant to the global transport process and therefore can usually be neglected in mathematical models.

In addition to transport processes, upon electric field application, electrochemical reactions including reduction (species gain electron from the external circuit) and oxidation (species donate electrons to the external circuit) occur at the cathode and

Electrokinetic Remediation for Environmental Security and Sustainability, First Edition.
Edited by Alexandra B. Ribeiro and M.N.V. Prasad.
© 2021 John Wiley & Sons Ltd. Published 2021 by John Wiley & Sons Ltd.

UNCORRECTED PROOFS

Trim Size: 170mm x 244mm Single Column Loose Ribeiro670117 c01.tex V1 - 12/02/2020 10:43pm Page 2

anode, respectively. For example:

$$\text{Cathode.Reduction} : Me^{2+} + 2\,e^{-} \longrightarrow Me^{0} \tag{1.1}$$

$$\text{Anode.Oxidation} : 2\,Cl^{-} - 2\,e^{-} \longrightarrow Cl_2 \tag{1.2}$$

Under normal operation conditions, decomposition of water occurs at the electrodes, generating oxygen gas and hydrogen ions at the anode and hydrogen gas and hydroxyl at the cathode. These reactions generate an acidic front at the anode migrating toward the cathode, which can aid the mobilization of some contaminants, such as heavy metals, since most heavy metal cations are dissolved in acidic conditions. Simultaneously, the basic front generated at the cathode, which migrates through the soil toward the anode, can cause the precipitation of heavy metals in the soil. In addition, the generation of water from encountering both fronts can involve the creation of a low-electrical-conductivity zone, which can make the technique ineffective. These problems can be avoided by neutralizing the basic front via acid addition at the cathode, neutralizing the acid front via basic addition at the anode, or using complexation agents at one or both electrodes [6]. Using exchange membranes at the electrode compartments has also been proposed to avoid problems associated with pH changes through the solid matrix [7]. This technique is referred to as electrodialytic remediation (EDR). These enhancement methods cause important changes in the initial chemical system, such as incorporating new ionic species or transport phenomena across the exchange membranes, which must be considered in mathematical models.

Transport phenomena are also influenced by chemical reactions in the aqueous phase and by solid-fluid interactions. Acid-base reactions, reduction-oxidation (redox) reactions, complexation, adsorption-desorption processes, and ion exchange and surface complexation reactions are some of these interactions. Some examples are:

$$H^{+} + OH^{-} \rightleftarrows H_2O \tag{1.3}$$

$$Pb^{+2} + 2\,OH^{-} \rightleftarrows Pb(OH)_2 \tag{1.4}$$

$$[SiO]^{-} + 2H^{+} \rightleftarrows [SiO - H_2]^{-} \tag{1.5}$$

$$[SiO]^{-} + H^{+} \rightleftarrows [SiO - H]^{0} \tag{1.6}$$

The complexity of the processes occurring under an electric field requires the development of mathematical models not only to increase the overall understanding of the technology but also to allow predictions of field applications.

These mathematical models should describe the most relevant physical-chemical processes with a minimal number of equations and parameters. In other words, models should be as simple as possible while describing the behavior of the system's primary species. However, based on studies reported in the literature, EKR models have become more complex since the 1990s, to properly describe advances in the technique.

Mathematical models describing EKR are based on the equation of mass conservation:

$$\frac{\partial C_i}{\partial t} = -\vec{\nabla} \cdot \vec{J}_i + G_i \tag{1.7}$$

UNCORRECTED PROOFS

Trim Size: 170mm x 244mm Single Column Loose Ribeiro670117 c01.tex V1 - 12/02/2020 10:43pm Page 3

where C_i (kmol m^{-3}) and G_i (kmol m^{-3} s^{-1}) are the concentration and rate of production of the ith ion per unit of volume of pore water, respectively, and J_i (kmol m^{-2} s^{-1}) is the flux of the ith ion. This flux includes all the previously described transport mechanisms. However, mathematical models usually assume some simplifications, such as neglecting one or more transport phenomena to simplify the numerical model.

The first reported works dealing with the implementation of a mathematical model for EKR considered only one transport mechanism, such as the electroosmotic transport of water [8–10] or electromigration [11, 12]. In most cases, electrophoresis, i.e. the movement of charged particles toward the electrode of the opposite polarity, is of limited importance in compacted solid systems. Therefore, electrophoresis transports can often be neglected in EKR models. However, mass transport by electrophoresis can become significant in some specific cases, such as when contaminants are adsorbed onto charged particles, when a technique application is based on the transport of reactive particles, when using a surfactant as facilitating agent, or when using electroremediation of sludge treatment.

This chapter covers aspects of relevance for applying EKR modeling to solid matrices. First, reactive transport models are described, from simple unidimensional models proposed in the 1990s to the most complex models assisted by computer software. Then, chemical equilibrium models are discussed. The last section provides new insights on future EKR models, including the combination of chemical equilibrium and chemical reaction kinetics, multiscale models, two- and three-dimensional models, and Multiphysics modeling.

1.2 Reactive Transport

1.2.1 One-Dimensional Electromigration Model

The implementation of a one-dimensional electromigration model is based on the mass conservation equation applied to a soil completely saturated with water:

$$\frac{\partial C_i}{\partial t} = -\vec{\nabla}\cdot\vec{J_i} + G_i = -\vec{\nabla}(-u_i C_i \vec{\nabla}\varphi - K_{eo} C_i \vec{\nabla}\varphi - D_i \vec{\nabla} C_i + C_i \vec{v}) + G_i \qquad (1.8)$$

where the terms in parentheses in the right-hand expression represent, respectively, the electromigration, electroosmotic, diffusive, and advective flux, $u_i = z_i D_i F/RT$; (m^2 V^{-1} s^{-1}) is the ionic mobility; z_i is the ion charge (equiv. mol^{-1}); F is the Faraday constant ≈96 485 C mol^{-1}; R is the gas constant (8.314 J mol^{-1} K^{-1}); D_i (m^2 s^{-1}) is the effective diffusion coefficient of the ith ion; k_{eo} (m^2 V^{-1} s^{-1}) is the electroosmotic permeability of the soil; v is the advective velocity of the pore water (m s^{-1}); and $\nabla\varphi$ is the electrical voltage gradient (V m^{-1}).

The mathematical model described in this section is based on an electrical circuit analogy [11], schematically depicted in Figure 1.1. Thus, the electrical potential distribution is a function of the electrical resistance of the soil, which depends on the instantaneous local concentration and mobility of ionic species in pore water. The model neglects the electrical conduction through the solid of the soil.

UNCORRECTED PROOFS

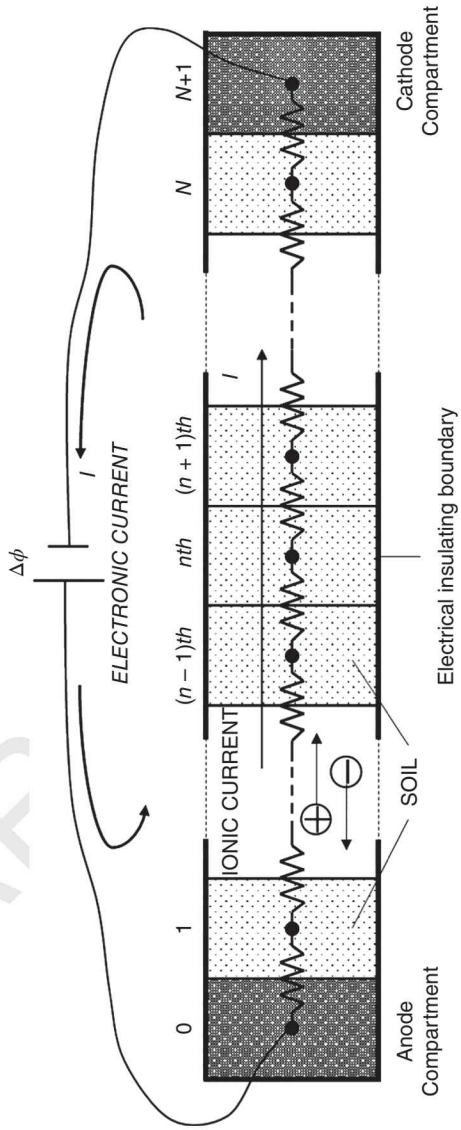

Figure 1.1 One-dimensional electromigration model scheme.

UNCORRECTED PROOFS

Trim Size: 170mm x 244mm Single Column Loose Ribeiro670117 c01.tex V1 - 12/02/2020 10:43pm Page 5

The potential drop in the electrode compartments can be assumed very low compared with the potential drop in the soil, because the electrode compartments are well stirred, and the concentration of electrolyte solutions is usually very high. Since the system is assumed to be electrically insulated, the current only flows in the soil regions between the electrodes. Therefore, the electrical potential gradient can be expressed as

$$\Delta\phi = \mid E \mid + IR \tag{1.9}$$

where $|E|$ is the voltage drop in the electrode processes (V), I is the electrical current (A), and R is the total resistance of the soil (Ω) obtained as the sum of the resistance of each volume element R_n and N is the number of elements into which the solid column of length L (m) was divided.

The electrode reactions considered in this model are water oxidation at the anode and water reduction at the cathode. Therefore, the voltage drop resulting from the electrode processes can be obtained from both the standard reduction potentials of the half-reactions at the electrodes and the Nernst equation. Considering values of 1 atm for the partial pressures of the gases and 25 °C for the temperature:

$$\text{Cathode}: 4\,H_2O + 4e^- \rightleftarrows 4\,OH^-\,(aq) + 2\,H_2\,(gas)\; E^0 = -0.828\,V \tag{1.10}$$

$$\text{Anode}: 2\,H_2O \rightleftarrows 4\,H^+\,(aq) + O_2\,(gas) + 4\,e^-\; E^0 = -1.229\,V \tag{1.11}$$

Therefore, the electrical potential difference between the electrodes can be obtained as the sum of these two voltage drops:

$$\Delta\varphi = |-1.228 - 0.059(pH_{cat} - pH_{an})| + I\sum_{n=1}^{N}\frac{\Delta x\cdot\tau}{S\cdot\theta}\left(\frac{1}{\sum_i^{N_i}\lambda_i C_{in}}\right) \tag{1.12}$$

where pH_{cat} and pH_{an} are the pH values at the anode and cathode, respectively; $\Delta x = L/N$ is the thickness of the volume element (m); τ is the tortuosity of the soil (−); S is the cross-sectional area (m^2); θ is the porosity of the water-saturated soil (−); N_i is the number of ions existing in the soil pore water (−); λ_i is the molar conductivity of the ith ion, obtained as $\lambda_i = z_i\,u_i\,F$ ($\Omega^{-1}\,m^2\,kmol^{-1}$); and C_{in} is the concentration of the ith ion in the porous water of the nth volume element ($kmol\,m^{-3}$).

Regarding transport phenomena, electromigration is the only significant mechanism considered in some cases, such as soils contaminated with heavy metals and higher values of ionic conductivity for the pore fluid. Therefore, the mass conservation equation can be simplified as

$$\frac{\partial C_i}{\partial t} = -\vec{\nabla}\cdot\vec{J_i} + G_i = -\vec{\nabla}(-u_i C_i \vec{\nabla}\varphi) + G_i \tag{1.13}$$

Applying this equation for each ion in the pore water results in a set of differential equations strongly coupled through the electrical potential distribution, which should be simultaneously integrated. With this aim, the one-dimensional system is divided into $N + 2$ volume elements. The electrode compartments are located at both ends of the system (0 and $N + 1$), and the inner volume elements contain the soil or solid waste to be treated.

UNCORRECTED PROOFS

Trim Size: 170mm x 244mm Single Column Loose Ribeiro670117 c01.tex V1 - 12/02/2020 10:43pm Page 6

The numerical integration of the equation system is based on a time-iterative scheme composed of two sequential steps for each time increment. The assumption of reactive-transport under local chemical equilibrium conditions, described in more detail in Section 1.3, allows the application of this procedure. First, transient concentrations are calculated, considering ionic transport between each cell. These concentrations are used in the second step to solve chemical equilibria and charge and mass balances within each volume element. The concentration values obtained through the chemical equilibrium calculations are then used to obtain the next time-step concentration values.

The transport step, i.e. the first step of the iterative numerical integration described above, is presented in the following. The mass conservation equation for a volume element of the soil ($1 \le n \le N$), considering electromigration as the only transport phenomenon, is given by

$$(\Delta x A \theta)\frac{dC_{in}}{dt} = \frac{-I\lambda_i}{z_i F 10^3}\left(\frac{C_{in}S(z_i) + C_{in+1}S(-z_i)}{\sum_{i=1}^{N_i}\lambda_i(C_{in}S(z_i) + C_{in+1}S(-z_i))} - \frac{C_{in-1}S(z_i) + C_{in}S(-z_i)}{\sum_{i=1}^{N_i}\lambda_i(C_{in-1}S(z_i) + C_{in}S(-z_i))}\right) \tag{1.14}$$

$$(\Delta x A \theta)\frac{dC_{in}}{dt} = \frac{-I}{z_i F 10^3}(t_{in} - t_{in-1}) \tag{1.15}$$

where $S(x)$ is a "key function" introduced to take into consideration the different movement of cations and anion, whose value is one if x is higher than zero ($S(x) = 1$ if $x > 0$) and zero if x is less than or equal to zero ($S(x) = 0$ if $x \le 0$); and t_{in} is the fraction of the total current carried by the ith ions between each two cells divided into the total conductivity at the boundary face, known as the *transport number*. The total conductivity (denominators of the terms inside the parentheses of Eq. (1.14)) is given by the sum of the contribution of the cations migrating toward the cathode and the anions migrating toward the anode between the nth and $(n+1)$th and $(n-1)$th and nth, respectively.

Since the anode ($n = 0$) and cathode ($n = N + 1$) compartments are electrically isolated, there is no molar flow through the right and left sides of the cathode and anode, respectively. Consequently, the first term of Eq. (1.14) in the parentheses should be zero for the cathode, and the second term should be zero for the anode. Furthermore, the electrolysis of water and the addition of protons or hydroxyls via acid or base addition, respectively, as enhancing agents must be considered in the mathematical model. Therefore, the generation of hydroxyl ions because of water reduction and the neutralization of a percentage of hydroxyl ions generated at the cathode by acid addition are considered as follows:

$$V_{N+1}\frac{dC_{iN+1}}{dt} = \frac{-I\lambda_i}{z_i F 10^3}\left(-\frac{C_{iN}S(z_i) + C_{iN+1}S(-z_i)}{\sum_{i=1}^{N}\lambda_i(C_{iN}S(z_i) + C_{iN+1}S(-z_i))}\right) + a\frac{I}{|z_i|F10^3} \tag{1.16}$$

UNCORRECTED PROOFS

Trim Size: 170mm x 244mm Single Column Loose Ribeiro670117 c01.tex V1 - 12/02/2020 10:43pm Page 7

where V_{N+1} is the volume of the cathode compartment (m^3); and a is zero for all ions except hydroxyl ions, for which $a = (1-f)$, and for anions of the acid used in the enhanced EKR $a = f$, where f is the fraction of hydroxyl ions neutralized.

Analogously, for the anode compartment,

$$V_0 \frac{dC_{i0}}{dt} = -\frac{I\lambda_i}{z_i F 10^3}\left(\frac{C_{i0}S(z_i) + C_{i1}S(-z_i)}{\sum_{i=1}^{N}\lambda_i(C_{i0}S(z_i) + C_{i1}S(-z_i))}\right) + a\frac{I}{|z_i|F10^3} \tag{1.17}$$

where V_0 is the volume of the anode compartment (m^3); a is zero for all ions except for protons, for which $a = (1-f)$; and $a = f$ for cations corresponding to the base used in the enhancement (if this is the case), where f is the fraction of protons neutralized.

From the numerical solution of Eqs. (1.15)–(1.17), new values of concentrations at the time $t + \Delta t$ can be obtained:

$$C^*_{in}(t + \Delta t) = C^*_{in}(t) + \left(\frac{dC_{in}}{dt}\right)\Delta t \tag{1.18}$$

The concentration values obtained from Eq. (1.18) for each volume element are not at chemical equilibrium since only transport phenomena have been considered above. According to the model hypotheses, reaction rates are high enough to consider the local equilibrium reached. Therefore, concentration values obtained from this first step will be used as a starting point in the second step to achieve chemical equilibria between all species. Given that the chemical equilibrium model is also applied for most models reported in this chapter, it will be described in Section 1.3.

1.2.2 One-Dimensional Electromigration and Electroosmosis Model

The mathematical model presented in this section was published by Baraud et al. to provide a useful prediction tool for EKR applications [13]. This model considers electromigration and electroosmosis as dominant transport phenomena. A theoretical expression for the linear velocity of charged species in the pore solution allows predictions. In addition, sorption phenomena of contaminants onto a solid surface are integrated, defining a retardation factor. Interactions of chemical species with the solid matrix, including surface complexation, surface precipitation, and ion exchange, depend on the chemical species, the nature of the solid, and the pore fluid's properties. This model assumes that the sorption is fast and reversible; hence, the concentration of the chemical species adsorbed onto the solid surface can be supposed to be at equilibrium with the adjacent liquid phase. In most studies, adsorption models such as Langmuir and Freundlich isotherms are applied to assess sorption phenomena. For low concentrations, the linear relationship between solid (C_{iS}) and liquid phase (C_i) concentrations represents the sorption process as

$$C_{iS} = K_{di} \cdot C_i \tag{1.19}$$

where K_{di} is the partition coefficient for the ith component.

Thus, the influence of sorption on contaminant transport can be considered by a retardation factor R_i defined from the mass balance for each component i:

$$C_{itotal} = \theta C_i + \rho C_{iS} = \theta C_i + \rho K_{di} C_i \tag{1.20}$$

UNCORRECTED PROOFS

Trim Size: 170mm x 244mm Single Column Loose Ribeiro670117 c01.tex V1 - 12/02/2020 10:43pm Page 8

where C_{itotal} is the concentration of contaminant per unit volume of soil,

$$R_i = 1 + \frac{\rho}{\theta} K_{di} \tag{1.21}$$

where dry soil density (ρ), porosity (θ), and the partition coefficient (K_{di}) may be obtained from EKR experiments. Simple empirical expressions obtained from batch experiments, such as $logK_{di} = a_i pH + b_i$, let us easily obtain the value of R_i (1.21) with a simple pH measurement.

Concerning the transport of charged contaminant species, anions, and cations, the global velocity can be obtained as the sum of electromigration and electroosmosis velocities:

$$V_i = V_{EM} + V_{EO} = \left(\frac{u_i}{\tau} + \frac{K_{eo}}{\theta} \right) \cdot \vec{\nabla} \varphi \tag{1.22}$$

where V_i is the net linear velocity corresponding to cation and anion movement (a positive value when the movement is toward the cathode) (m s^{-1}), V_{EM} is the linear velocity of ions by electromigration (m s^{-1}), V_{EO} is the average linear velocity by electroosmosis (m s^{-1}), u_i is the ionic mobility (m^2 V^{-1} s^{-1}), τ is the tortuosity of the solid matrix ($\tau > 1$), K_{eo} is the electroosmotic permeability of the solid (m^2 V^{-1} s^{-1}), and $\nabla\varphi$ is the electrical potential gradient (V m^{-1}).

On the other hand, the outlet molar flow rate of the contaminant species ($Q_i(t)$) (kmol s^{-1}) is given by

$$Q_i(t) = \theta C_i(t) V_i S \tag{1.23}$$

Therefore, the mass balance for the ith contaminant after a period of time (t) is

$$R_i L \frac{Q_i(t)}{V_i} = R_i \theta C_i(t) SL = N_{Si}^0 - \int_0^t Q_i(t) dt \tag{1.24}$$

where S is the cross-sectional area (m^2), L is the length of the solid column (m), and N_{Si}^0 is the initial quantity of contaminant ith (kmol).

This model also defines the ratio of removed to initial contaminant concentration ($\eta_i(t)$) as

$$\eta_i(t) = \frac{\int_0^t Q_i(t) dt}{N_{Si}^0} \tag{1.25}$$

Combining Eqs. (1.24) and (1.25):

$$\frac{d\eta_i(t)}{1 - \eta_i(t)} = \frac{V_i}{LR_i} dt \tag{1.26}$$

Integrating Eq. (1.26) and expressing η_i as a percentage of decontamination:

$$\eta_i(\%) = 100 \left[1 - exp \left(-\frac{V_i t}{R_i L} \right) \right] \tag{1.27}$$

The described procedure can be used as a simple tool to predict EKR performance, assuming electromigration and electroosmosis as dominant mechanisms. As previously described, the percentage of decontamination can be estimated from a few preliminary studies aimed at determining specific soil characteristics (porosity, tortuosity) and pH, K_{di}, and R_i. Thus, we can predict the treatment time required to

UNCORRECTED PROOFS

Trim Size: 170mm x 244mm Single Column Loose Ribeiro670117 c01.tex V1 - 12/02/2020 10:43pm Page 9

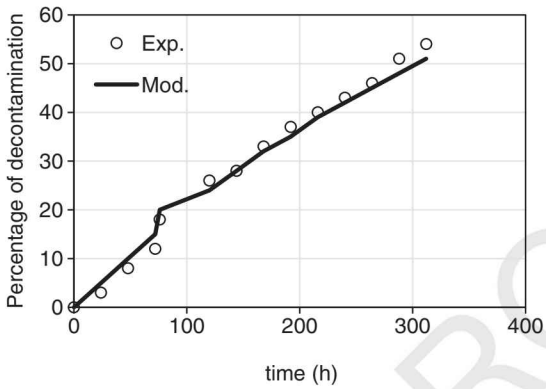

Figure 1.2 Experimental and model results of decontamination percentage of strontium during treatment time. Source: Adapted from Baraud et al. [13].

obtain an acceptable percentage of decontamination and also the economic and energy costs of remediation.

This model was applied to predict the EKR performance for spiked kaolinite containing 62 mg kg^{-1} of Sr^{2+}. Experiments were carried out at a constant voltage of 1 V cm^{-1}, with acetic acid and sodic acetate added as enhancing agents to the cathode and anode, respectively.

Comparing the experimental and simulation results (Figure 1.2) indicates that the model predicts the experimental results fairly well. Thus, this approach played an important role in obtaining a better understanding of transport phenomena involved in EKR applications. However, some important phenomena during EKR treatment, such as precipitation, complexation, and diffusion, are not included in this model. These results encourage further studies to improve modeling of EKR treatment by including the processes mentioned.

1.2.3 One-Dimensional Electrodialytic Model

EDR is an emerging technology widely applied to solid matrices, such as soils contaminated with heavy metals [14–17]. The technique consists of applying an electric current together with semipermeable membranes [18], in a similar way to conventional electrodialysis processes. The solid matrix to be treated is placed in a central compartment, which is separated from the electrode compartments by ion-exchange membranes. The electric current mobilizes charged species contained in the central compartments toward an electrolyte solution. The ion-exchange membranes reduce the amount of energy "wasted" on the transport of highly mobile ions that differ from the target contaminants and prevent contaminants from the electrolyte solutions from re-entering the solid matrix [7, 19, 20]. To avoid ionic species in the soil interfering in the electrode processes, additional exchange membranes can be used to isolate the electrode compartments. To date, EDR has been used to remove metals such as Cu, Cd, Cr, Pb, Hg, and Zn from polluted soils [21–24].

This section will describe the most relevant aspects of modeling EDR technology. From reported studies, it can be concluded that the implementation of specific characteristics of the processes through membranes entails the development of more

UNCORRECTED PROOFS

Trim Size: 170mm x 244mm Single Column Loose Ribeiro670117 c01.tex V1 - 12/02/2020 10:43pm Page 10

complex models. Specifically, such a model should describe the transport of anions and protons through an anion-exchange membrane (AEM) and of cations across a cation-exchange membrane (CEM) during the application of an electrical potential gradient.

Among other key parameters, the characterization of membranes must be considered to develop mathematical models. De Lara et al. proposed a method to characterize CEMs and AEMs based on measuring the membrane potential and electrical resistance under operating conditions [25]. Electrical potential differences between the two sides of the membrane were performed for $CdCl_2$ and NaCl solutions at different concentrations. These experimental results were compared with values of the electrical potential for an ideal CEM ($t^+ = 1$) and AEM ($t^- = 1$). The cation and anion transport numbers in the membranes are determined using

$$\Delta\varphi = -\frac{\nu}{\nu_i}\frac{RT}{F}t_+ ln\frac{a_+}{a_-} \tag{1.28}$$

where T is the thermodynamic temperature of the system (K), ν_i is the stoichiometric coefficient of the anion and cation ($\nu = \nu_+ + \nu$) (−), a_+ and a are the activity coefficients of the cathode and anode compartments (−), respectively, and t_+ is the cation transport number (fraction of the total current carried by the cations, ($t^+ + t^- = 1$)) (−).

The electrical resistance of the membrane system and the influence of the solution pH on the membrane potentials and, subsequently, on the transport number were also considered. As described in previous sections, water decomposition in the electrode compartments involves generating protons and hydroxyls whose movement is a critical factor in EDR processes. Thus, it is essential to evaluate the permeability of membranes to protons and hydroxyls when no current is applied. For this case, the concentration gradient is the only driving force for the transport of protons:

$$V\frac{d[H^+]_{Na}}{dt} = KS([H^+]_{No} - [H^+]_{Na}) \tag{1.29}$$

where K is the mass transport coefficient through the membrane (m s^{-1}), V is the solution volume of the half-compartment (m^3), S is the membrane surface area in contact with the solutions (m^2), and $[H^+]_{No}$ and $[H^+]_{Na}$ are the concentrations of protons (kmol m^{-3}) measured in the solutions of HNO_3 and $NaNO_3$, respectively.

In the absence of an electric field, the transport of H^+ through the AEM is significant even though this movement is slower than movement through the CEM. On the other hand, hydroxyls are not allowed to pass through the AEM.

The aspects previously described allow us to model ionic transport through the exchange of ionic membranes under dynamic conditions. De Lara et al. proposed a unidimensional model to simulate the electrodialytic decontamination of kaolin spiked with Cd [25]. The transport of Cd^{2+}, Cl^-, H^+, and OH^- through the CEM and AEM was simulated.

Applying mass balance for the ith ion:

$$V\frac{dC_i}{dt} = \frac{t_i I}{z_i F} + G_i \tag{1.30}$$

UNCORRECTED PROOFS

Trim Size: 170mm x 244mm Single Column Loose Ribeiro670117 c01.tex V1 - 12/02/2020 10:43pm Page 11

where V is the volume of solution in anode or cathode electrode (m^3), C_i is the concentration of the ion ith (kmol m^{-3}), t_i is the transport number of the ith chemical specie.

From equations (1.31) and (1.32), transport number for cations and anions in the membranes could be obtained:

$$[t_{i+}]_m = \frac{f_{i+} z_{i+} u_{i+} [C_i^{z+}]_{an}}{\sum_{i=1}^{2} f_{i+} z_{i+} u_{i+} [C_i^{z+}]_{an} + \sum_{i=1}^{2} f_{i-} z_{i-} u_{i-} [C_i^{z-}]_{cat}} \tag{1.31}$$

$$[t_{i-}]_m = \frac{f_{i-} z_{i-} u_{i-} [C_i^{z-}]_{cat}}{\sum_{i=1}^{2} f_{i+} z_{i+} u_{i+} [C_i^{z+}]_{an} + \sum_{i=1}^{2} f_{i-} z_{i-} u_{i-} [C_i^{z-}]_{cat}} \tag{1.32}$$

where u_{i+} and u_{i-} are the electrochemical mobilities for cations and anions (–), respectively, $[C_i^{z+}]_{an}$ and $[C_i^{z-}]_{cat}$ are the concentrations of the cations inside the anode and cathode cell (mol m^{-3}), respectively, f_i is the quotient of the product $u_i C_i$ inside the membrane and in the solution, the denominator is the sum of the electrical transport of all ions through the membrane.

Ribeiro et al. (2007) applied the previously described model to simulate the removal of Cr, Cu and As from a saturated bed of chromated copper arsenate (CCA)-treated wood chips via dialytic and electrodialytic treatment [26]. The movement of the target species was mathematically described considering diffusive transport through the solid matrix. Furthermore, the transport of ionic species through exchange membranes was simulated as previously discussed. Hence, the CEM and AEM were described as filters that avoid the transport of anions and cations, respectively, not including protons, which were slowed but allowed to pass through the AEM. The primary ionic species included in the model were H^+ and OH^- (generated at the electrodes by water electrolysis), Na^+ and NO_3^- (used as electrolyte solutions), and oxalate ions and H^+ (incorporated with the oxalic acid solution contained in the pretreated wood chips). The addition of HNO_3 as an enhancing agent in the cathode compartment was implemented to consider the neutralization of OH^- generated during water decomposition. The numerical model, like those previously described, consists of the combination of two coupled sections: one for simulating the kinetic process through the integration of the reactive-mass transport equations and another for chemical equilibrium. In this study, the proposed complex chemical system consists of 17 species (N). The simulation of the electromigration transport of each ion through both sides of each volume element (V_n), not including electrode compartments and their limiting cells ($n = 2$ to $N-1$), is performed using the transport number concept [11, 27], previously described in Section 1.2.1:

$$t_{in} = \frac{\lambda_i [C_{in-1} S(z_i) S(C_{in-1}) + C_{in} S(-z_i) S(C_{in})]}{\sum_{i=1}^{N_i} \lambda_i [C_{in-1} S(z_i) S(C_{in-1}) + C_{in} S(-z_i) S(C_{in})]} \tag{1.33}$$

Equation (1.33) must be adapted to describe the specific characteristics of the anode and cathode compartments and their limiting cells, such as the presence of the ion-exchange membrane. Thus, the effective transport number of a proton (t_{1am}) and of the rest of the ions through the AEM (t_{iam}) and the transport number of cations

UNCORRECTED PROOFS

Trim Size: 170mm x 244mm Single Column Loose Ribeiro670117 c01.tex V1 - 12/02/2020 10:43pm Page 12

through the CEM (t_{icm}) are

$$t_{1am} = \frac{f_1\lambda_1 C_{10} S(C_{1,0})}{f_1\lambda_1 C_{10} S(C_{10}) + \sum_{i=1}^{N_i} \lambda_i [C_{i1} S(-z_i) S(C_{i1})]} \tag{1.34}$$

$$t_{iam} = \frac{\lambda_i C_{i1} S(-z_i) S(C_{i,1})}{f_1\lambda_1 C_{10} S(C_{10}) + \sum_{i=1}^{N_i} \lambda_i [C_{i1} S(-z_i) S(C_{i1})]} \tag{1.35}$$

$$t_{icm} = t_{iN} = \frac{\lambda_i [C_{iN} S(z_i) S(C_{i,N})]}{\sum_{i=1}^{N_i} \lambda_i [C_{iN} S(z_i) S(C_{i,N})]} \tag{1.36}$$

where $(f_1\lambda_1)$ is the effective molar conductivity of protons through the AEM [25].

Diffusive transport in the ED process is calculated only for non-ionic species of the chemical system since this transport mechanism is considered insignificant compared to electromigration [1]. Thus, the mass balance equation for diffusive transport from $n = 2$ to $N - 1$ volume elements is given by

$$V_n \left(\frac{dC_{ij}}{dt}\right)_D = \frac{D_i^* (C_{in-1} - 2C_{in} + C_{in+1}) \Longleftrightarrow S}{\Delta x} \tag{1.37}$$

where D_i^* is the effective diffusion coefficient ($m^2\ s^{-1}$). For cells next to electrode compartments ($n = 1$ and $n = N$) and for anode and cathode compartments ($n = 0$ and $n = N + 1$):

$$V_1 \left(\frac{dC_{i1}}{dt}\right)_D == \frac{D_i^* (2C_{i0} - 3C_{i1} + C_{i2}) S}{\Delta x} \tag{1.38}$$

$$V_N \left(\frac{dC_{iN}}{dt}\right)_D = \frac{D_i^* (C_{iN-1} - 3C_{iN} + 2C_{iN+1}) S}{\Delta x} \tag{1.39}$$

$$V_0 \left(\frac{dC_{i0}}{dt}\right)_D = \frac{2D_i^* (C_{i1} - C_{i0}) S}{\Delta x} \tag{1.40}$$

$$V_{N+1} \left(\frac{dC_{iN+1}}{dt}\right)_D = \frac{2D_i^* (C_{iN} - C_{iN+1}) S}{\Delta x} \tag{1.41}$$

To simulate the dialytic process, the diffusive transport of ions must be considered since the concentration gradient is the primary impulsive force for the ion mass flux in the absence of an applied electrical potential.

For electrode compartments, the advective flow represents a fresh supply of electrolyte solution ($NaNO_3 \approx 10^{-2}$ M), which aims at obtaining good conductivity, pH control, and sample collection from the electrode compartments:

$$V_0 \left(\frac{dC_{i0}}{dt}\right)_A = Q(C_i - C_{i0}) \tag{1.42}$$

$$V_{N+1} \left(\frac{dC_{iN+1}}{dt}\right)_A = Q(C_i - C_{iN+1}) \tag{1.43}$$

where Q is the mean inward and outward flow from the electrode compartments ($m^3\ s^{-1}$), and C_i is the concentration of the ith species in the fresh electrolyte (kmol m^{-3}).

UNCORRECTED PROOFS

Trim Size: 170mm x 244mm Single Column Loose Ribeiro670117 c01.tex V1 - 12/02/2020 10:43pm Page 13

As usual for models consisting of two steps, the concentration values obtained from the reactive-mass transport module must be modified to satisfy chemical equilibrium. Specifically, this model implements four equilibria groups: water ionization, acid ionization, precipitation-dissolution, and complex formation. A detailed description of the chemical equilibrium can be found in Section 1.3.

In summary, this model consists of differential equations to describe the transport of ionic and non-ionic species through the solid matrix or exchange membranes and the chemical equilibria equations to obtain the concentration of these species. The cumulative quantities of target contaminants obtained from samples collected from electrode compartments are given by

$$\frac{dM_A}{dt} = (QC_{i0}) \tag{1.44}$$

$$\frac{dM_C}{dt} = (QC_{iN+1}) \tag{1.45}$$

The electrical neutrality conditions were guaranteed in the electrodialytic and dialytic processes due to the numerical procedure proposed [12, 28]; in addition, this condition was continuously checked during the simulation for each element of volume:

$$\sum_{i=1}^{N_i} z_i C_{in} = 0 \tag{1.46}$$

A comparison of experimental and simulation results along slices of the central cell compartments for electrodialytic removal of Cr, As, and pH profile from pretreated wood chips is shown in Figure 1.3.

From these results, it was concluded that the model accurately predicts the partial and total removal of Cr and As from the solid matrix located at the central cell compartments. As can be observed, a high proportion of both contaminants was removed at the end of the experiments.

Lima et al. proposed a one-dimensional model with similar characteristics to simulate the electrodialytic and dialytic treatment of fly ash [2] containing Cd (82 ± 12 ppm), Cu (543 ± 50 ppm), and Pb (2644 ± 218 ppm) collected at Valorsul, a Portuguese municipal solid waste (MSW) incinerator [29]. In this case, the model was applied to two experimental EDR setups: a three-compartment cell for treating stationary solid ash and a stirred ash suspension (Figure 1.4). The transport of Cd, Cu, and Pb has been described, considering diffusion through the exchange membranes and the electromigration of ionic, simple (Cd^{2+}, Cu^{2+}, and Pb^{2+}), and complex species during treatment. Other non-contaminant species in the system (H^+, OH^-, Ca^{2+}, CO_3^{2-}, SO_4^{2-}, Na^+, NO^{3-}, citrate, and ammonium) were also considered in the model to describe water decomposition, ash, and the addition of electrolyte solution and enhancing agents.

As mentioned earlier, the simulation of the EDR experiments applied to a stirred suspension of ash is the most relevant innovation of this model. As shown in Figure 1.4b, the experimental setup developed and patented at Technical University of Denmark (PCT/DK95/00209) basically consisted of three compartments: the

UNCORRECTED PROOFS

UNCORRECTED PROOFS

Trim Size: 170mm x 244mm Single Column Loose

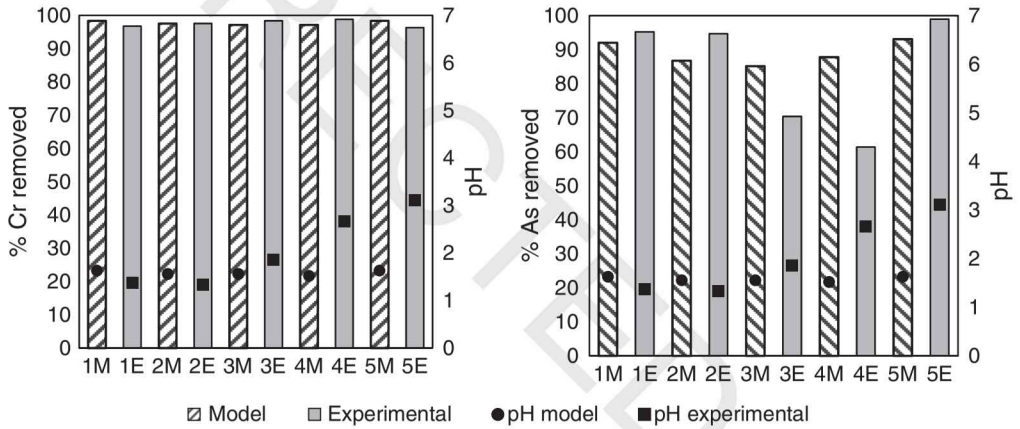

Figure 1.3 Experimental and simulation results along the solid slices of central cell compartment for EDR applied to CCA-wood chips. Source: Adapted from Ribeiro et al. [26].

Ribeiro670117 c01.tex V1 - 12/02/2020 10:43pm Page 14

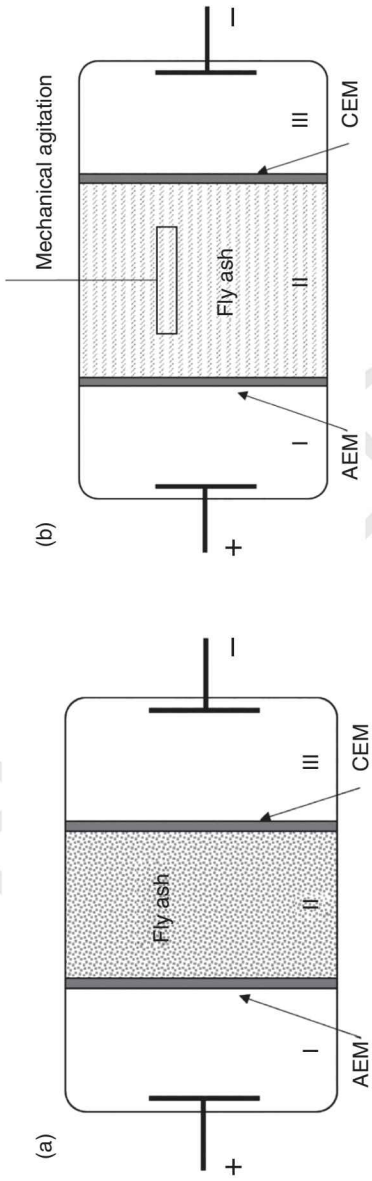

Figure 1.4 Electrodialytic cells for (a) unstirred ash; (b) stirred ash suspension.

UNCORRECTED PROOFS

Trim Size: 170mm x 244mm Single Column Loose Ribeiro670117 c01.tex V1 - 12/02/2020 10:43pm Page 16

solid matrix is placed in the central compartment, which is separated from the cathode and anode compartments by a CEM and an AEM, respectively [27, 30]. To simulate ash treatment, perfect mixing was assumed in the three cell compartments due to peristaltic pump circulation of the electrolytes in the electrode compartments and mechanical agitation of the ash suspension in the central cell.

Mass transport through the membranes due to concentration gradients is calculated as

$$V_0\left(\frac{dc_{i0}}{dt}\right)_D = (N_{i,1})_D A = k(c_{i1} - c_{i0})A \tag{1.47}$$

$$V_{N+1}\left(\frac{dc_{iN+1}}{dt}\right)_D = (N_{i,N})_D A = k(c_{iN} - c_{iN+1})A \tag{1.48}$$

where k is the global mass transfer coefficient (h^{-1}).

The model properly reproduces not only the evolution of contaminant (Cd, Cu, Pb) and non-contaminant (Na, Ca, Al, Zn, etc.) species but also the pH values in the three-compartment cell.

1.2.4 One-Dimensional Electroremediation Model Using Nernst-Planck-Poisson

The primary difference between models based on a Nernst-Planck-Poisson (NPP) system and those described in previous sections is the procedure applied to calculate the electric potential gradient. Models based on NPP apply the Poisson equation to obtain the induced electrical potential due to the local charge imbalance produced when several ions migrate at a different rate, whereas previous models applied electroneutrality conditions. The electrical potential distribution is generated even without applying an external electric field because of different diffusion ionic rates. Simultaneously, this diffusion potential involves electromigration transport leading to the electroneutrality of the global system.

Paz-Garcia et al. proposed a model for EKR transport phenomena based on an NPP system integrated by a finite element method. The concentrations of the individual ionic species are obtained by the Nernst-Planck equations, whereas, as mentioned earlier, the electrical potential is calculated by the Poisson equation. The authors performed several simulations with non-reactive systems to assess the model [31]. To include electrode processes in the model, a constant voltage difference or current density is applied as a boundary condition.

In this model, application of the mass balance equation for each chemical species in a fluid medium considers diffusion and electromigration as the most relevant transport phenomena. Electromigration and diffusion terms must be considered for charged particles even when there are free diffusion problems because of electrical interaction between ions. Thus, the flow of any ith chemical species can be defined as

$$\vec{J}_i = (-u_i^{eff} C_i \vec{\nabla}\varphi - K_{eo} C_i \vec{\nabla}\varphi - D_i^{eff} \vec{\nabla} C_i) \tag{1.49}$$

$$D_i^{eff} = \frac{D_i \theta}{\tau} \tag{1.50}$$

UNCORRECTED PROOFS

Trim Size: 170mm x 244mm Single Column Loose Ribeiro670117 c01.tex V1 - 12/02/2020 10:43pm Page 17

where D_i^{eff}, K_{eo}, and u_i^{eff} are the effective diffusion, electroosmotic coefficient, and effective ionic mobility obtained from the Einstein-Nernst relation. The value of the electroosmotic permeability coefficient is usually in the narrow range of 10^{-5} to 10^{-4} $cm^2\ s^{-1}\ V^{-1}$. Since the electromigration and electroosmosis terms are similar, they can be written as

$$A_i = (u_i^{eff} + K_{eo}) \tag{1.51}$$

where A_i is a coefficient representing the electromigration and electroosmosis transport.

Concerning chemical reaction phenomena, water–chemical equilibrium and the electrochemical reaction at the electrodes are taken into account. Subsequently, the generation term is not included in the continuity equation. The chemical equilibrium is modeled, as usual, as a coupled step with an iterative solution of a nonlinear system of equations.

Integrating the unidimensional Nernst-Planck equation for each ionic species over the region limited by the electrodes obtains the concentration profile for a given set of boundary conditions:

$$\frac{\partial C_i}{\partial t} = -\frac{\partial}{\partial x}\left(-D_i\frac{\partial C_i}{\partial x} - A_i C_i \vec{\nabla}\varphi\right) \tag{1.52}$$

For a system with M species, the state variable number will be $M+1$ depending on the time and the position, M profiles of molar concentration, and the electrical potential distribution. Therefore, the system will consist of M Nernst-Planck equations for each species and the Poisson equation defined as

$$\varepsilon\frac{\partial^2\varphi}{\partial x^2} = F\sum_{i=1}^{M} z_i \rightleftarrows C_i \tag{1.53}$$

where $\varepsilon = \varepsilon_r\varepsilon_o$ is the water permittivity, ε_o is the vacuum permittivity, and ε_r is the relative electric permittivity of water.

To solve the coupled NPP equation system described in the one-dimensional region, a finite element procedure is applied. By discretization, nodal values are obtained using matrix algebra.

The strong nonlinearity of the coupled NPP system causes the solution of the system to be indirect. In other words, since the electromigration and electroosmosis terms in the NPP system depend on the product of the molar concentration and the electric potential distribution, an iterative method is required to solve the system.

High consistency was demonstrated in the simulation results since, by establishing a constant density at the electrodes, it is maintained constant along distance and time. The computational time, a key parameter in the development of models, showed the high efficiency of the implemented EKR simulation.

The consistency and versatility of the model led to its application in several multispecies chemical systems to evaluate the EKR application. Paz-Garcia et al. proposed to simulate the desalination of brick pieces contaminated with sodium or potassium chloride [32]. In this case, the dissolution/precipitation of calcite in the presence of 25 chemical species was described, taking into account not only porosity changes but also the formation and release of CO_2 bubbles during the process.

UNCORRECTED PROOFS

Trim Size: 170mm x 244mm Single Column Loose Ribeiro670117 c01.tex V1 - 12/02/2020 10:43pm Page 18

In this case, the mass balance equation for water is also included as

$$\frac{\partial W}{\partial t} = -\frac{\partial}{\partial x}\left(-D_W \frac{\partial W}{\partial x} - A_i W \vec{\nabla}\varphi\right) + G_W \tag{1.54}$$

where W is the water content (kg of water m^{-3} of the pore), and G_W is the water generation (kg m^{-3} s^{-1}).

The model allows us to obtain the total water quantity decreasing with time, as the electrode processes release gases. From the results, it was concluded that the consumption of water near the cathode was double that in the anode under constant current conditions. However, a net flow of water was driven toward the cathode by electroosmotic transport despite the counteracting effect of moisture transport. Results for water profiles predicted almost constant water profile inside the bricks, with slightly higher water content at the cathode compartment.

Paz-Garcia et al. proposed to evaluate electro-desalination techniques enhanced with carbonated clay to prevent salt-induced deterioration problems of masonry and other construction materials by an NPP model [33]. The removal efficiency for chlorides, nitrates, and sulphate ions was evaluated by a chemical system consisting of 28 species in solution and 18 solid species. From the results, it was concluded that protons produced at the anode are neutralized by the dissolution of calcite with a simultaneous release of CO_2 from mineral dissolution and gases produced in the electrochemical reactions (O_2, H_2, and Cl_2). Simulation results showed that the EKR treatment was highly efficient for removing chloride and nitrates, whereas sulphates were retained because of gypsum precipitation.

1.3 Chemical Equilibrium

This section provides conceptual and practical aspects of chemical equilibrium models by revising implemented models reported in the literature. These models can be used for chemical reactions that are fast enough to reach equilibrium. Under equilibrium conditions, the reactant and product concentrations can be assumed constant [34]. In other words, the species concentration at equilibrium can be obtained from the law of mass actions for the involved chemical reaction coupled with the electroneutrality of the aqueous phase.

Early models for EKR proposed the construction of a stoichiometry tree to solve the equilibrium equations numerically. This procedure considers chemical reactions assumed to be at equilibrium during EKR [11, 12]. The stoichiometry tree applied to simulate the removal of cadmium from polluted soil is shown in Figure 1.5. The equilibrium constant used for this example is presented in Table 1.1.

The synergetic effects of multiple chemicals, such as the ionic strength of water and activity coefficients, were not considered in this model. The influence of temperature on chemical equilibrium constants and adsorption equilibrium was not implemented in the first published models. All of that leads to important capacity limitations.

UNCORRECTED PROOFS

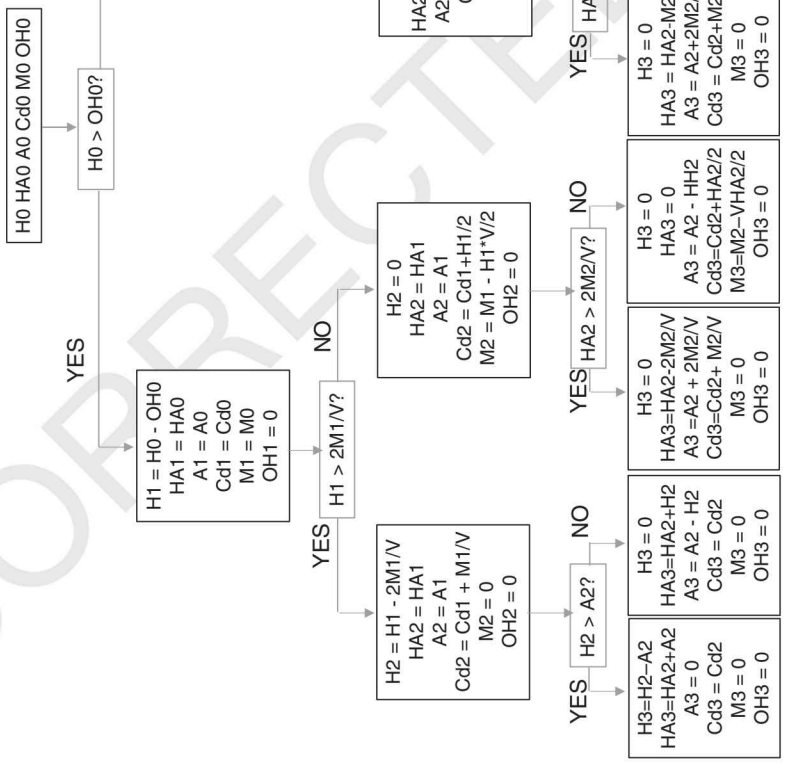

Figure 1.5 Stoichiometry tree to model the removal of cadmium from soil by EKR. Source: Adapted from Wilson et al. [12].

UNCORRECTED PROOFS

Trim Size: 170mm x 244mm Single Column Loose Ribeiro670117 c01.tex V1 - 12/02/2020 10:43pm Page 20

Table 1.1 Equilibrium constants for the example of electroremediation enhanced with acetic acid from soil contaminated with cadmium hydroxide.

Reaction	Log (K_{eq})
$HAc \rightleftarrows H^+ + Ac^-$	−4.744
$H_2O \rightleftarrows H^+ + OH^-$	−14.000
$Cd(OH)_2 \rightleftarrows Cd^{2+} + 2OH^-$	−13.699

Subsequent EKR models defined the concept of *master species* that represent each of the elements in the chemical system. These models applied further complex numerical methods to implement the chemical equilibrium model. The most widely applied procedure for computing multispecies chemical equilibrium (MSCE) is based on Morel's Tableau [35, 36], which basically consists of classifying chemical species as master and secondary species. The secondary species can be described as a function of the master species (M). That is, the total chemical species (N) should be described by ($R = N - M$) chemical equilibrium reactions. The stoichiometric equations for each of the R reactions is given by

$$\sum_{i=1}^{N} \nu_{ir} C_i = 0 r = 1, 2, \ldots . R \tag{1.55}$$

where C_i is the concentration of each ith species (kmol m^{-3}), and ν_{ir} is the stoichiometric coefficient for the ith species in the rth reaction. The example discussed in this section consisted of $N = 6$ chemical species: 3 secondary species are described as a function of $M = 3$ master species by $R = N–M = 3$ chemical equilibria.

The description of stoichiometric equations takes into consideration negative coefficients for reagents. It should also be highlighted that each secondary species is present only in one rth equation. The mathematical solution of strongly nonlinear equations systems describing MSCE usually requires iterative methods.

The fundamental procedure is to write every equation as a function of a minimum set of chemical species, i.e. one species (master species) for each element or valence state of an element. These master species should be used to describe dissolution, complex formation, and surface complex reactions. The primary master species is also needed to describe reactions for all aqueous species. That way, the equation describing the primary master species is basically an identity reaction. For the case of redox species, the primary master species is also a secondary master species. For example, let us consider the calculation of the mass balance of total iron (Fe), total ferric iron (Fe^{2+}), and total ferrous iron (Fe^{3+}). In this case, Fe^{2+} is the primary master species for Fe, and Fe^{2+} and Fe^{3+} are the secondary master species for Fe^{2+} and Fe^{3+}, respectively.

As previously described, a system with N species and M master species is described by $R = N - M$ formation reactions. Using the master species concentration as an

UNCORRECTED PROOFS

Trim Size: 170mm x 244mm Single Column Loose Ribeiro670117 c01.tex V1 - 12/02/2020 10:43pm Page 21

independent variable:

$$K_r = \frac{C_r}{\prod_{i=1}^{M} C_i^{\nu_{ir}}} \text{ for aqueous reactions and } K_p = \prod_{i=1}^{M} C_i^{\nu_{ip}} \text{ for precipitation} \quad (1.56)$$

where K_r is the equilibrium constant for the aqueous phase reactions or the solubility product for the solid-fluid equilibrium.

The logarithmic form of these equations allows us to obtain the non-master species concentration in the aqueous phase as a function of the master species concentrations:

$$LogC_r = LogK_r + \sum_{i=1}^{M} \nu_{ir} LogC_i \quad (1.57)$$

For the example of the removal of Cd from soil using HAc as an enhancing agent, since H^+ and Ac^- are selected as master species,

$$Log[HAc] = 4.744 + Log[Ac^-] + Log[H^+] \quad (1.58)$$

For water (solvent):

$$Log[OH^-] = -14.000 - Log[H^+] \therefore pOH = 14 - pH \quad (1.59)$$

And the saturation index of the rth species (SI_r) for precipitation reactions is

$$SI_p = Log\frac{\prod_{i=1}^{M} C_i^{\nu_{ip}}}{K_p} = -LogK_p + \sum_{i=1}^{M} \nu_{ip} LogC_i \quad (1.60)$$

$$SI(Cd(OH)_2) = Log\frac{\prod_{i=1}^{M} [Cd^{2+}][OH^-]^2}{K_r} = Log[Cd^{2+}] - 14.301 + 2pH \quad (1.61)$$

where $SI_r = 0$ when the precipitate is at equilibrium with the aqueous phase; if it is negative, $SI_r < 0$, the system is undersaturated (the solid tends to be solubilized) with respect to that species; and if it is positive, $SI_r > 0$, the solution is supersaturated (the solid tends to increase). If a species is precipitated or dissolved, a new master species must be included or removed from the system.

In addition, the system must satisfy the mass balance conditions for the reference compounds, given by

$$T_m = \sum_{i=1}^{N} \nu_{ir} C_i + \sum_{i=1}^{N} \nu_{is} C_{is} \quad (1.62)$$

where the first term represents the contribution of compound concentrations in the aqueous phase and the second term represents the contribution of the compound concentrations in the solid phase per unit of volume, to represent precipitation, sorption, exchange, and surface complexation; and T_m is the total concentration of the mth master species, whose value is usually known before equilibrium (T_m^*) because it has been calculated from the values of concentrations obtained after the transport step $C_{in}^*(t + \Delta t)$.

The mass balance for protons is replaced by the charge balance with the aim of avoiding the role of water as a chemical species in the system and ensuring electroneutrality.

UNCORRECTED PROOFS

Trim Size: 170mm x 244mm Single Column Loose Ribeiro670117 c01.tex V1 - 12/02/2020 10:43pm Page 22

The mathematical solution of this nonlinear system of equations is usually obtained by applying an iterative numerical procedure, such as Newton-Raphson (NR) and Marquardt. The iterative procedure is as follows: the concentration of the non-master species (C_r) is obtained as a function of an initial set of values of master species (C_i) using the logarithmic Eq. (1.57). Afterward, the total concentration of each master species (T_m) is calculated by mass balance. The divergences between the total concentration of master species obtained by mass balance and those obtained from the transport step ($T_m - T_m^*$) are known as *residues*. By comparing residues with a tolerance value, the iterative method can indicate the new set of values for the concentration of master species to be used in the next iteration if the residues were higher than the tolerance value. This iterative method will continue until all the mass balance residues are below the tolerance value.

Moreover, the electron concentration can be considered the master species (*pE* value) required to calculate the concentration of the aqueous species involved in a redox pair. The mass balance equation for each redox pair is coupled to eliminate the electron concentration of the equations, i.e. as if a set of redox pairs were at redox equilibrium. The concentration values obtained after this step are used as a starting point to repeat the two sequential steps for the next time increment – i.e. it is a forward time integration method.

Before applying the integration method, it is necessary to define the initial chemical conditions. To do so, the most probable distribution of metals among different chemical species (speciation) according to the initial conditions of the soil (pH, initial metal concentration, redox potential, etc.) can be provided by software packages (PHREEQC [37], Visual MINTEQ [38], and WATEQ4F [39], among others). This way, it is also possible to select the primary species and equilibrium to be included in the chemical equilibrium model.

In addition to stoichiometric algorithms, numerical strategies for computing chemical equilibrium problems can be addressed by non-stoichiometric methods [40–43]. These algorithms consist of a direct minimization of the Gibbs energy coupled with mass balances for each chemical species. Paz-Garcia et al. proposed a mathematical model based on this approach to describe a set of chemical equilibrium equations in a multispecies and multiphase chemical system [44]. This model includes the effect of the ionic strength of the electrolyte media to calculate the equilibrium in an unsaturated system:

$$f_r(x_r) = \sum_{i=1}^{N} \nu_{ir} Loga_i - LogK_r \tag{1.63}$$

where a_i is the activity defined from the molar concentration (mol kg^{-1}), $f_r(x_r)$ is the residual function representing the distance to the equilibrium state for the *r*th reaction, and x_r is an independent state variable used to describe the reaction progress, whose value can be positive or negative if the reversible reaction proceeds toward the products or the reactants, respectively.

UNCORRECTED PROOFS

Trim Size: 170mm x 244mm Single Column Loose Ribeiro670117 c01.tex V1 - 12/02/2020 10:43pm Page 23

Table 1.2 Stoichiometric coefficients to be expressed as matrix *M*.

	H^+	OH^-	Cd^{2+}	Ac^-	H_2O	$Cd(OH)_2(s)$	HAc
H_2O	1	1	0	0	−1	0	0
$Cd(OH)_2(s)$	0	2	1	0	0	−1	0
HAc	1	0	0	1	0	0	−1

The total concentration of each species at equilibrium can be obtained by the mass balance as

$$\sum_{i=1}^{N} \nu_{ir} n_i = 0 r = 1, 2, \ldots . R \tag{1.64}$$

$$n_i = n_i^* + \sum_{r=1}^{R} \nu_{ir} x_r i = 1, 2, \ldots \ldots N \tag{1.65}$$

where n_i(mol) is the total amount of the ith chemical species after calculation and n_i^* before each iteration (mol).

The system can be expressed in matrix notation as

$$\begin{bmatrix} n_1 \\ n_2 \\ \ldots \\ n_N^* \end{bmatrix} = \begin{bmatrix} n_1^* \\ n_2^* \\ \ldots \\ n_N^* \end{bmatrix} + M^T \begin{bmatrix} x_1 \\ x_2 \\ \ldots \\ x_R \end{bmatrix} \tag{1.66}$$

where M^T is the transpose stoichiometric matrix, where the stoichiometric matrix M is formed from the set of stoichiometric equations describing the system.

For the example we are following in this section, the stoichiometric matrix M for the system must be written as (Table 1.2):

$$\begin{bmatrix} f_1(x_1 \ldots x_r) \\ f_2(x_1 \ldots x_r) \\ \ldots \\ f_R(x_1 \ldots x_r) \end{bmatrix} = M \begin{bmatrix} lna_1(x_1 \ldots x_r) \\ lna_2(x_1 \ldots x_r) \\ \ldots \\ lna_N(x_1 \ldots x_r) \end{bmatrix} - \begin{bmatrix} lnK_1 \\ lnK_2 \\ \ldots \\ lnK_R \end{bmatrix} \tag{1.67}$$

The purpose of this numerical model is to obtain a value of x_r for each rth chemical reaction, which entails activity values (a_i) minimizing the value of f_r (x_r). The value of the reaction extents (x_r) is obtained by an iterative procedure, which ensures global equilibrium as

$$x_r(new) = x_{ro} + \lambda \delta x_r \tag{1.68}$$

where

$$\begin{bmatrix} \delta x_1 \\ \delta x_2 \\ \ldots \\ \delta x_R \end{bmatrix} = -\begin{bmatrix} \frac{\partial f_1(x_1 \ldots x_r)}{\partial x_1} & \frac{\partial f_1(x_1 \ldots x_r)}{\partial x_2} & \ldots & \frac{\partial f_1(x_1 \ldots x_r)}{\partial x_R} \\ \frac{\partial f_2(x_1 \ldots x_r)}{\partial x_1} & \frac{\partial f_2(x_1 \ldots x_r)}{\partial x_2} & \ldots & \frac{\partial f_2(x_1 \ldots x_r)}{\partial x_R} \\ \ldots & \ldots & \ldots & \ldots \\ \frac{\partial f_R(x_1 \ldots x_r)}{\partial x_1} & \frac{\partial f_R(x_1 \ldots x_r)}{\partial x_2} & \ldots & \frac{\partial f_R(x_1 \ldots x_r)}{\partial x_R} \end{bmatrix}^{-1} \begin{bmatrix} f_1(x_1 \ldots x_r) \\ f_2(x_1 \ldots x_r) \\ \ldots . \\ f_R(x_1 \ldots x_r) \end{bmatrix} \tag{1.69}$$

UNCORRECTED PROOFS

Trim Size: 170mm x 244mm Single Column Loose Ribeiro670117 c01.tex V1 - 12/02/2020 10:43pm Page 24

and λ is a scalar factor used to control the magnitude of the increment calculated by the NR method. Its optimal value is obtained by a try-and-error algorithm, following a decreasing sequence given by a geometric progression, with an initial value of $\lambda = 1$.

For precipitation-dissolution reactions, the value of the residual function ($f_r(x_r)$) is used as an indicator of the saturation index (SI_r) ($SI_r \geq 0$: saturated [i.e. solid precipitate], $SI_r < 0$: undersaturated [complete dissolution]).

The primary advantage of using this method is that it is compatible with a kinetically controlled model, which simultaneously describes chemical equilibrium and chemical kinetics. For a given value of the reaction progress, mass and charge balances are always achieved.

On the other hand, the model's main drawback is that it has a significant tendency to fall into a local minimum.

In addition, as is widely known, the reversible reaction in the aqueous phase is usually characterized by taking place at equal rates in the direct and reverse directions; that is, the chemical equilibrium assumption may be used in most cases. For example, acid-base ionization and water auto-ionization can reach the equilibrium state in microseconds or less. In the case of aqueous complexation reactions, the equilibrium state is achieved on the order of micro- to milliseconds. However, the kinetic rates of heterogeneous reactions, such as adsorption-desorption, ion-exchange, and precipitation-dissolution, can be similar to transport rates. For these cases, the chemical equilibrium assumption involves relevant limitations to describe the system properly.

1.4 Models for the Future

The progress of EKR models over the last 25 years has been presented throughout this chapter: from simple models describing only one transport mechanism to more complex and efficient mathematical models describing relevant physical-chemical phenomena in detail. Most recent multispecies EKR models are based on the NPP coupled system of equations and describe multiple transport phenomena. Furthermore, these models allow the prediction of porosity evolution, the water content in solid matrices, and gas released during treatment. The theoretical advance in models has been supported by an increase in the availability of software and hardware. Although guessing the future is not possible, this section will cover new trends in EKR models, which will be decisive in their development.

1.4.1 Combining Chemical Equilibrium and Chemical Reaction Kinetics

As described in Section 1.3, most EKR models assume chemical equilibrium conditions. In other words, models for reactive transport in porous media suppose that the rates of chemical reactions are higher than the rates of transport phenomena. Although this assumption has been demonstrated suitable for many real cases, some disagreement can be found in concentration profiles between experimental and simulation results. In these cases, the simulation results usually show sharper profiles,

UNCORRECTED PROOFS

Trim Size: 170mm x 244mm Single Column Loose Ribeiro670117 c01.tex V1 - 12/02/2020 10:43pm Page 25

Table 1.3 Time scales for the primary chemical and transport processes involved in EKR.

Transport processes		**Chemical processes**	
Electromigration	**10^{-2} s**	**Proton transfer to H_2O**	**10^{-12} s**
Electro-osmosis	10^{-4} s	Dissociation of strong acid	10^{-8} s
Diffusion	10^{-5} s	Dissociation of weak acid	10^{-6} s
		Inorganic complexation	10^{-6} s
		Adsorption/Ion exchange	$10^{-2} - 10^{4}$ s
		Dissolution/Precipitation	10^{2}–10^{7} s

Source: Jacobs and Probstein [46].

indicating the importance of kinetic processes [45]. Therefore, the prediction capability of EKR models can be improved by considering the kinetics of chemical reactions. However, kinetics laws are very case-specific for multispecies and multiphase systems, so it is not easy to collect the data necessary for describing a kinetic system. Software dealing with numerical integration presents difficulties when solving stiff partial and differential systems of equations since, in general, chemical reaction are several orders of magnitude higher than transport processes [46].

To improve the prediction ability for local chemical equilibrium transport models, it is a good approach to consider only the kinetics of slower reactions: i.e. heterogeneous reactions (liquid-solid). Table 1.3 shows the characteristic time scales for several processes involved in EKR. As can be observed, surface complexation and precipitation-dissolution reactions are characterized by kinetic rates on the same order as those for transport phenomena in porous media.

For most polluted solid matrices, the contaminant is retained on the solid matrix either as a mineralized compound or as adsorbed species. Thus, the release rate of target contaminants from their non-mobilizable form to the aqueous phase is essential to processes involved in EKR. For example, for EKR enhanced with acid addition, the acid front generated at the anode tends to dissolve the contaminant within a solid mineral into a mobile species. However, the acid front's progress is hindered by the presence of buffering compounds, such as calcite. According to M. Villen-Guzman et al., the dissolution of carbonates does not occur under equilibrium conditions [47].

Masi et al. developed a model to further predict the role of dissolution kinetics based on the combination of local chemical equilibrium and the kinetics model [48]. The modeled system was based on the EKR of Pb-contaminated soil contained a high concentration of carbonates [49]. In this case, although a previous model had predicted the experimental results fairly well, sharp concentration profiles for Ca and Pb were obtained, indicating the critical role of the dissolution-precipitation processes [45]. Therefore, the kinetics of calcite dissolution was included by the following simplified empirical kinetic law:

$$\frac{\partial m}{\partial t} = kA_0\left(\frac{m}{m_0}\right)^{\alpha} \frac{\partial m}{\partial t} = kA_0\left(\frac{m}{m_0}\right)^{\alpha} \tag{1.70}$$

UNCORRECTED PROOFS

Trim Size: 170mm x 244mm Single Column Loose Ribeiro670117 c01.tex V1 - 12/02/2020 10:43pm Page 26

where A_0 is the initial specific surface area ($m^2\ kg^{-1}$), m is the amount of solid (g), α is an indicator for changes in the specific surface area of the particles during dissolution (−), and k (mol $m^{-2}\ s^{-1}$) is the specific rate constant given by

$$k = k_f\left[1 - \left(\frac{IAP}{K_{sp}}\right)^{\beta}\right] \tag{1.71}$$

where k_f is a constant (mol $m^{-2}\ s^{-1}$), IAP is the ion activity product (−), K_{sp} is the solubility product constant (−), and β is a coefficient associated with the stoichiometry of the reaction (−) ($\beta = 2/3$ for calcite, assuming spherical particles). It should be noted that $(IAP/K_{sp}) > 1$ for supersaturation, $(IAP/K_{sp}) < 1$ for undersaturation, and $(IAP/K_{sp}) = 1$ in precipitation-dissolution equilibrium. Thus, as can be concluded, the kinetics law applied is a function of the distance to equilibrium and describes precipitation and dissolution processes.

Simulation results reproduced experimental data with higher accuracy compared with those obtained using the local equilibrium assumption for all reversible reactions, especially in the soil close to the anode compartment (Figure 1.6). In other words, the model's prediction ability was clearly improved by considering the kinetics of calcite dissolution. The authors concluded that the observed divergences between experimental and simulated results should be associated with precipitation processes occurring in soil close to the cathode compartment. It should be noted that the developed model represents a useful tool for other porous matrices such as sludge and sediments.

1.4.2 Multiscale Models

Physical systems for electrokinetic treatment can be described at three scales: nano, micro, and macro. However, mathematical models usually treat the three scales as a group, which means some details are neglected.

Igreja et al. proposed a model considering the three scales to describe EKR in kaolinite clays [50]. They assumed a stratified microstructure of kaolinite composed of parallel particles to describe the physical system. To describe the electroosmosis phenomena and the ionic transport in the proximity of the electrode compartment, Danckwerts' conditions were imposed. The developed model is a coupled system of nonlinear partial differential equations.

The primary advantage of multiscale models with respect to macroscopic models is the possibility of obtaining a more meticulous derivation of the constitutive laws for the effective coefficient applied in the macroscopy model. Thus, the correlation of electrochemical phenomena on the local level and the macroscopic response of the medium are better described [51–53].

The definition of *nanoscale* is based on the electrical double layer (EDL) concept in the proximity of charged solid particles. The Helmholtz-Smoluchowski slip condition is included, to take into account EDL effects on the microscopy scale.

The homogenization technique of periodic structures is applied for scale change from nanoscale and microscale to macroscale [54]. Thus, based on microscale

UNCORRECTED PROOFS

UNCORRECTED PROOFS

Trim Size: 170mm x 244mm Single Column Loose

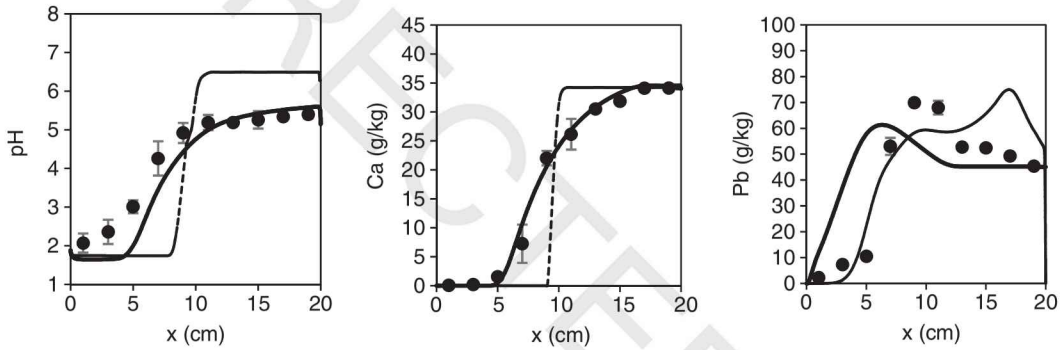

Figure 1.6 Experimental data and simulation results obtained using local chemical equilibrium and chemical kinetic models. Source: Adapted from Masi et al. [48].

Ribeiro670117 c01.tex V1 - 12/02/2020 10:43pm Page 27

Trim Size: 170mm x 244mm Single Column Loose Ribeiro670117 c01.tex V1 - 12/02/2020 10:43pm Page 28

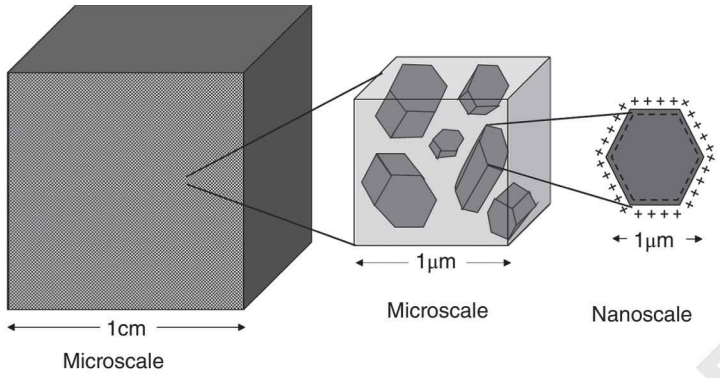

Figure 1.7 Natural-length scales in kaolinite. Source: Adapted from Lima et al. [55].

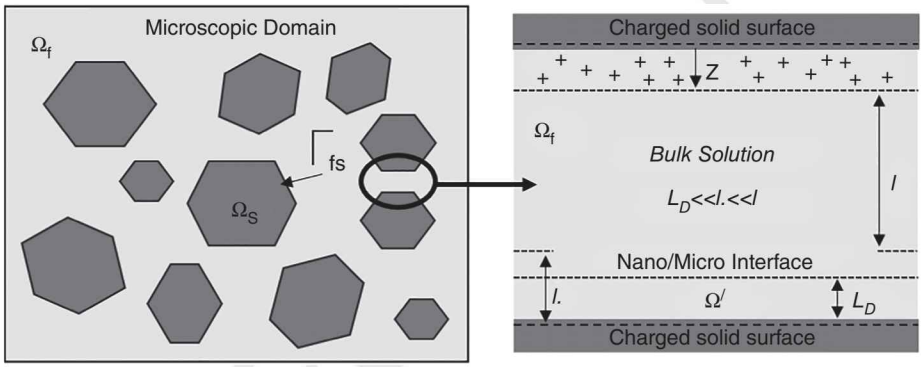

Figure 1.8 Microscale and nanoscale of kaolinite. Source: Adapted from Lima et al. [55].

through the application of electrodynamics continuum laws coupled with NPP, it is possible to link microscale with the Darcy scale.

The three scales mentioned earlier are schematically represented in Figure 1.7 for the case modeled by Igreja et al. [50].

The interfacial phenomena are conducted by electrochemistry of the EDL and the protonation-deprotonation reactions at nanoscale (10^{-9} m). The aqueous phase is described as a bulk fluid containing ionic solutes at microscale (10^{-6} m). Finally, the medium at macroscale is defined as solid-fluid with averaged properties defined at each macroscopy position.

Using kaolinite as an example, Figure 1.8 shows microscale and macroscale schematically. As can be observed, the microscopy domain is occupied by a biphasic medium composed of solid particles and micropores containing bulk fluid. At nanoscopic scale, the solid phase consists of solid particles of kaolinite with a charged surface and pores containing electrolyte solution composed of water and ionic solutes.

UNCORRECTED PROOFS

Trim Size: 170mm x 244mm Single Column Loose Ribeiro670117 c01.tex V1 - 12/02/2020 10:43pm Page 29

First nanoscale was described, then microscale, and finally, the macroscale model, defining effective parameters such as electroosmotic permeability, hydraulic permeability, and diffusivity, among others, to connect the nanoscale and microscale models with the macroscale model.

1.4.3 Two- and Three-Dimensional Models

A wide variety of one-dimensional models for EKR were presented in Section 1.2. However, a limited number of theoretical models exist under two-dimensional geometries [6, 28, 46].

As previously described, the analytical solution of one-dimensional models is not viable, and therefore, numerical methods must be applied. It is even more difficult to find an analytical solution for two-dimensional models, which entails using a more complex numerical model. In addition, the boundary conditions for electric current and mass flow should be carefully defined because they are not as direct as for one-dimensional models.

Although one-dimensional approaches provide the required information in most cases, predictions obtained from two- and three-dimensional models are more important for field applications, specifically to assess the influence of soil heterogeneities and anisotropies on electric field lines and, subsequently, on treatment evolution.

1.4.4 Multiphysics Modeling

Coupled transport phenomena combined with chemical and electrochemical reactions involved in EKR treatments and solid-liquid interactions imply that the design, analysis, and implementation of mathematical models is a complex task. Hence, assumptions and simplifications have traditionally been required in the development of such models. But the availability of the Multiphysics software package for this purpose, such as COMSOL Multiphysics [56], allows us to solve differential equations representing coupled transport phenomena, including kinetics and/or chemical equilibriums. Furthermore, improving the mathematical model's convergence behavior allows us to increase the complexity of the problem while maintaining solution efficiency.

Lopez-Vizcaino et al. proposed a Multiphysics model implemented in COMSOL aiming at a better understanding of processes occurring in natural soils and pore waters under natural conditions [57]. They developed an extended geochemical model defining 9 partial differential equations for describing mass balance in the soil, 16 ordinary differential equations for mass balance in the electrolyte wells, and 11 algebraic equations for chemical speciation.

Sprocati et al. proposed a mathematical model for EKR consisting of a coupling between COMSOL Multiphysics, applied to simulate fluid flow, solute mass transfer, and electrostatic processes based on the NPP system; and PhreeqcRM, used as a geochemical engine [58]. They evaluated the ability of the proposed model to operate at

UNCORRECTED PROOFS

Trim Size: 170mm x 244mm Single Column Loose Ribeiro670117 c01.tex V1 - 12/02/2020 10:43pm Page 30

different dimensions (1D, 2D, and 3D). Comparing the simulation results with previously obtained analytical and numerical solutions suggested the potential application of the model to describe electrokinetic processes for environmental remediation purposes and also in other fields dealing with electrokinetic processes.

As reflected by the content of this section, future EKR models will be based on multiphysics and multidimensional geometry, definitions of chemical equilibrium as well as kinetically controlled reactions, and NPP formulations including coupling transport mechanisms and multiscale environments.

Acknowledgments

This work has received funding from the European Union's Horizon 2020 research and innovation program under Marie Skłodowska-Curie grant agreement No. 778045. Financial support from the E3TECH Excellence Network under project CTQ2017-90659-REDT (MCIUN, Spain) is acknowledged. Paz-Garcia acknowledges financial support from the program "Proyectos I+D+i en el marco del Programa Operativo FEDER Andalucía 2014-2020," No. UMA18-FEDERJA-279. Villen-Guzman acknowledges the postdoctoral fellowship obtained from the University of Malaga. Cerrillo-Gonzalez acknowledges the FPU grant obtained from the Spanish Ministry of Education.

References

1 Acar, Y.B. (1993). Principles of electrokinetic remediation. *Environmental Science & Technology* 27 (13): 2638–2647.
2 Lima, A.T., Ribeiro, A.B., Rodríguez-Maroto, J.M. et al. (2010). Experimental and modeling of the electrodialytic and dialytic treatment of a fly ash containing Cd, Cu and Pb. *Journal of Applied Electrochemistry* 40 (9): 1689–1697.
3 Gomes, H.I., Rodríguez-Maroto, J.M., Ribeiro, A.B. et al. (2015). Numerical prediction of diffusion and electric field-induced iron nanoparticle transport. *Electrochimica Acta* 181: 5–12.
4 EPA Office of Solid Waste and Emergency Response. (1995). In situ remediation technology status report: Electrokinetics.
5 Ribeiro, A. and Rodríguez Maroto, J. (2006). Electroremediation of heavy metal-contaminated soils -processes and applications. In: *Trace Elements in the Environment*, 325–340. CRC Press. Taylor & Francis.
6 Vereda-Alonso, C., Heras-Lois, C., Gomez-Lahoz, C. et al. (2007). Ammonia enhanced two-dimensional electrokinetic remediation of copper spiked kaolin. *Electrochimica Acta* 52 (10): 3366–3371.
7 Ottosen, L.M., Hansen, H.K., Laursen, S., and Villumsen, A. (1997). Electrodialytic remediation of soil polluted with copper from wood preservation industry. *Environmental Science & Technology* 31 (6): 1711–1715.

UNCORRECTED PROOFS

Trim Size: 170mm x 244mm Single Column Loose Ribeiro670117 c01.tex V1 - 12/02/2020 10:43pm Page 31

8 Shapiro, A.P., Renaud, P.C., and Probstein, R.F. (1989). Preliminary studies on the removal of chemical species from saturated porous media by electroosmosis. *PCH Physicochemical Hydrodynamics* 11 (5–6): 785–802.

9 Bruell, C.J., Segall, B.A., and Walsh, M.T. (1992). Electroosomotic removal of gasoline hydrocarbons and TCE from clay. *Journal of Environmental Engineering* 118 (1): 68–83.

10 Eykholt, G.R. and Daniel, D.E. (1994). Impact of system chemistry on electroosmosis in contaminated soil. *Journal of Geotechnical Engineering* 120 (5): 797–815.

11 Wilson, D.J., Rodríguez-Maroto, J.M., and Gómez-Lahoz, C. (1995). Electrokinetic remediation. I. Modeling of simple systems. *Separation Science and Technology* 30 (15): 2937–2961.

12 Wilson, D.J., Rodriguez-Maroto, J.M., and Gomez-Lahoz, C. (1995). Electrokinetic remediation. II. Amphoteric metals and enhancement with a weak acid. *Separation Science and Technology* 30 (16): 3111–3128.

13 Baraud, F., Fourcade, M.C., Tellier, S., and Astruc, M. (1997). Modelling of decontamination rate in an electrokinetic soil processing. *International Journal of Environmental Analytical Chemistry* 68 (2): 105–121.

14 Ottosen, L.M., Hansen, H.K., Bech-Nielsen, G., and Villumsen, A. (2000). Electrodialytic remediation of an arsenic and copper polluted soil - continuous addition of ammonia during the process. *Environmental Technology* 21 (12): 1421–1428.

15 Ottosen, L.M., Kristensen, I.V., Pedersen, A.J. et al. (2003). Electrodialytic removal of heavy metals from different solid waste products. *Separation Science and Technology* 38 (6): 1269–1289.

16 Pedersen, A.J., Ottosen, L.M., and Villumsen, A. (2003). Electrodialytic removal of heavy metals from different fly ashes: influence of heavy metal speciation in the ashes. *Journal of Hazardous Materials* 100 (1–3): 65–78.

17 Villen-Guzman, M., Guedes, P., Couto, N. et al. (2018). Electrodialytic phosphorus recovery from sewage sludge ash under kinetic control. *Electrochimica Acta* 287: 49–59.

18 Villen-Guzman, M., Arhoun, B., Vereda-Alonso, C. et al. (2019). Electrodialytic processes in solid matrices. New insights into battery recycling. A review. *Journal of Chemical Technology and Biotechnology* 94 (6): 1727–1738.

19 Hansen, H.K., Ottosen, L.M., Kliem, B.K., and Villumsen, A. (1997). Electrodialytic remediation of soils polluted with Cu, Cr, Hg, Pb and Zn. *Journal of Chemical Technology and Biotechnology* 70 (1): 67–73.

20 Hansen, H.K., Ottosen, L.M., Laursen, S., and Villumsen, A. (1997). Electrochemical analysis of ion-exchange membranes with respect to a possible use in electrodialytic decontamination of soil polluted with heavy metals. *Separation Science and Technology* 32 (15): 2425–2444.

21 Jakobsen, M.R., Fritt-Rasmussen, J., Nielsen, S., and Ottosen, L.M. (2004). Electrodialytic removal of cadmium from wastewater sludge. *Journal of Hazardous Materials* 106 (2–3): 127–132.

UNCORRECTED PROOFS

Trim Size: 170mm x 244mm Single Column Loose Ribeiro670117 c01.tex V1 - 12/02/2020 10:43pm Page 32

22 Ottosen, L.M., Hansen, H.K., Ribeiro, A.B., and Villumsen, A. (2001). Removal of Cu, Pb and Zn in an applied electric field in calcareous and non-calcareous soils. *Journal of Hazardous Materials* 85 (3): 291–299.

23 Pedersen, A.J. (2003). Characterization and electrodialytic treatment of wood combustion fly ash for the removal of cadmium. *Biomass and Bioenergy* 25 (4): 447–458.

24 Velizarova, E., Ribeiro, A.B., and Ottosen, L.M. (2002). A comparative study on Cu, Cr and As removal from CCA-treated wood waste by dialytic and electrodialytic processes. *Journal of Hazardous Materials* 94 (2): 147–160.

25 De Lara, R., Rodriguez-Postigo, J., Garcia-Herruzo, F. et al. (2005). Decontamination of soils by membrane processes: characterization of membranes under working conditions. *Industrial and Engineering Chemistry Research* 44 (2): 400–407.

26 Ribeiro, A.B., Rodríguez-Maroto, J.M., Mateus, E.P. et al. (2007). Modeling of electrodialytic and dialytic removal of Cr, Cu and As from CCA-treated wood chips. *Chemosphere* 66 (9): 1716–1726.

27 Ribeiro, A.B., Rodriguez-Maroto, J.M., Mateus, E.P., and Gomes, H. (2005). Removal of organic contaminants from soils by an electrokinetic process: The case of atrazine. Experimental and modeling. *Chemosphere* 59 (9): 1229–1239.

28 Vereda-Alonso, C., Rodríguez-Maroto, J.M., García-Delgado, R.A. et al. (2004). Two-dimensional model for soil electrokinetic remediation of heavy metals: application to a copper spiked kaolin. *Chemosphere* 54 (7): 895–903.

29 Ferreira, C., Ribeiro, A., and Ottosen, L. (2003). Heavy metals in MSW incineration fly ashes. *Journal De Physique IV* 107: 463–466.

30 Ottosen, L.M. and Hansen, H.K. (1992). *Electrokinetic Cleaning of Heavy Metal Polluted Soil*. Denmark: Technical University of Denmark.

31 Paz-García, J.M., Johannesson, B., Ottosen, L.M. et al. (2011). Modeling of electrokinetic processes by finite element integration of the Nernst-Planck-Poisson system of equations. *Separation and Purification Technology* 79 (2): 183–192.

32 Paz-García, J.M., Johannesson, B., Ottosen, L.M. et al. (2012). Modeling of electrokinetic desalination of bricks. *Electrochimica Acta* 86: 213–222.

33 Paz-García, J.M., Johannesson, B., Ottosen, L.M. et al. (2013). Simulation-based analysis of the differences in the removal rate of chlorides, nitrates and sulfates by electrokinetic desalination treatments. *Electrochimica Acta* 89: 436–444.

34 De Bortoli, Á.L., Andreis, G.S.L., and Pereira, F.N. (2015). Chapter 1 - Chemical Equilibrium. In: *Modeling and Simulation of Reactive Flows*, 1–10. Elsevier.

35 Morel, F. and Morgan, J. (1972). Numerical method for computing equilibriums in aqueous chemical systems. *Environmental Science & Technology* 6 (1): 58–67.

36 Morel, F.M.M. and Hering, J.G. (1993). *Principles and Applications of Aquatic Chemistry*. Wiley. (A Wiley-Interscience publication).

37 Parkhurst, D.L. and Appelo, C.A.J. (1999). User's guide to PHREEQC (Version 2): A computer program for speciation, batch-reaction, one-dimensional transport, and inverse geochemical calculations. US Geological Survey Water-Resources Investigations Report 99-4259: 312.

38 Peterson, S.R., Hostetler, C.J., Deutsch, W.J., and Cowan C.E. (1987). MINTEQ user's manual. https://www.osti.gov/servlets/purl/6364793.

UNCORRECTED PROOFS

Trim Size: 170mm x 244mm Single Column Loose Ribeiro670117 c01.tex V1 - 12/02/2020 10:43pm Page 33

39 Ball, J.W. and Nordstrom, D. (1991). WATEQ4F - User's manual with revised thermodynamic data base and test cases for calculating speciation of major, trace and redox elements in natural waters. US Geological Surv Open-File Rep.; 91–183: 1–189.

40 Brassard, P. and Bodurtha, P. (2000). A feasible set for chemical speciation problems. *Computational Geosciences* 26 (3): 277–291.

41 Blomberg, P.B.A. and Koukkari, P.S. (2011). A systematic method to create reaction constraints for stoichiometric matrices. *Computers and Chemical Engineering* 35 (7): 1238–1250.

42 Carrayrou, J., Mosé, R., and Behra, P. (2002). New efficient algorithm for solving thermodynamic chemistry. *AICHE Journal* 48 (4): 894–904.

43 van Baten, J. and Szczepanski, R. (2011). A thermodynamic equilibrium reactor model as a CAPE-OPEN unit operation. *Computers and Chemical Engineering* 35 (7): 1251–1256.

44 Paz-García, J.M., Johannesson, B., Ottosen, L.M. et al. (2013). Computing multi-species chemical equilibrium with an algorithm based on the reaction extents. *Computers and Chemical Engineering* 58: 135–143.

45 Paz-Garcia, J.M., Villen-Guzman, M., Garcia-Rubio, A. et al. (2015). A coupled reactive-transport model for electrokinetic remediation. In: *Electrokinetics Across Disciplines and Continents: New Strategies for Sustainable Development*, 251–278. Springer International Publishing.

46 Jacobs, R.A. and Probstein, R.F. (1996). Two-dimensional modeling of electroremediation. *AICHE Journal* 42 (6): 1685–1696.

47 Villen-Guzman, M., Paz-Garcia, J.M., Amaya-Santos, G. et al. (2015). Effects of the buffering capacity of the soil on the mobilization of heavy metals. Equilibrium and kinetics. *Chemosphere* 131: 78–84.

48 Masi, M., Paz-Garcia, J.M., Gomez-Lahoz, C. et al. (2019). Modeling of electrokinetic remediation combining local chemical equilibrium and chemical reaction kinetics. *Journal of Hazardous Materials* 371: 728–733.

49 Villen-Guzman, M., Paz-Garcia, J.M., Rodriguez-Maroto, J.M. et al. (2015). Scaling-up the acid-enhanced electrokinetic remediation of a real contaminated soil. *Electrochimica Acta* 181: 139–145.

50 Igreja, I., Lima, S.A., and Klein, V. (2017). Asymptotic analysis of three-scale model of pH-dependent flows in 1:1 clays with Danckwerts' boundary conditions. *Transport in Porous Media* 119 (2): 425–450.

51 Mainka, J., Murad, M.A., Moyne, C., and Lima, S.A. (2014). A modified effective stress principle for unsaturated swelling clays derived from microstructure. *Vadose Zone Journal* 13 (5): 1–17.

52 F. RV, P., Murad, M.A., and Lima, S.A. (2013). A two-scale computational model of pH-sensitive expansive porous media. *Journal of Applied Mechanics* 80 (020903) https://doi.org/10.1115/1.4023011.

53 Gupta, A., Coelho, D., and Adler, P.M. (2008). Universal electroosmosis formulae for porous media. *Journal of Colloid and Interface Science* 319 (2): 549–554.

54 Sánchez-Palencia, E. (1980). *Non-homogeneous Media and Vibration Theory*, Lecture Notes in Physics, vol. 127. Springer.

UNCORRECTED PROOFS

Trim Size: 170mm x 244mm Single Column Loose Ribeiro670117 c01.tex V1 - 12/02/2020 10:43pm Page 34

55 de Lima, S.A., Murad, M.A., Moyne, C., and Stemmelen, D. (2008). A three-scale model for pH-dependent steady flows in 1:1 clays. *Acta Geotechnica* 3 (2): 153.

56 Comsol. (2019). *COMSOL Multiphysics Reference Manual*. https://doc.comsol.com/5.5/doc/com.comsol.help.comsol/COMSOL_ReferenceManual.pdf.

57 López-Vizcaíno, R., Yustres, A., León, M.J. et al. (2017). Multiphysics implementation of electrokinetic remediation models for natural soils and porewaters. *Electrochimica Acta* 225: 93–104.

58 Sprocati, R., Masi, M., Muniruzzaman, M., and Rolle, M. (2019). Modeling electrokinetic transport and biogeochemical reactions in porous media: A multidimensional Nernst–Planck–Poisson approach with PHREEQC coupling. *Advances in Water Resources* 127: 134–147.

UNCORRECTED PROOFS

Trim Size: 170mm x 244mm Single Column Loose Ribeiro670117 c02.tex V1 - 12/02/2020 11:05pm Page 35

2

Basic Electrochemistry Tools in Environmental Applications

Chanchal Kumar Mitra[1] *and Majeti Narasimha Vara Prasad*[2]

[1] *Department of Biochemistry, University of Hyderabad, Hyderabad, Telangana 500046, India*
[2] *School of Life Sciences, University of Hyderabad, Hyderabad, Telangana 500046, India*

2.1 Introduction

In simple terms, electrochemistry deals with chemical changes brought about by the passage of electricity, more specifically electric current through a liquid or a solution. In metals, electricity is carried by electrons, and the electrons are free to move around (electrons in the conduction band). Whereas all matter has electrons, in insulators, the electrons are not free to move. The motion of electrons in solids per se does not cause any chemical changes. In solutions, some solutes (salts, for example) can dissociate to form ions (both positive and negatively charged), and they too can conduct current when subjected to an external electric field. Conventionally, the external electric field is usually applied with a pair of metal rods or plates (electrodes) in physical contact with the solution. Chemical changes take place when electrons from the metal surface interact with ions in the solution. This interaction can lead to oxidation-reduction reactions and also other secondary chemical processes. Essentially, all electrochemical processes take place at or close to the electrode surface, with the electrode acting as a source or sink for electrons.

In some cases, the reverse process, i.e. production of electric potential and generation of an external current, can also take place due to chemical reactions. Usually, two electrodes of different metals (sometimes a graphite or carbon rod) are used in a solution, and the electrodes themselves (or materials in intimate contact with the electrodes) take part in the chemical reaction. As a result, the electrodes develop electric potential and can supply currents to an external circuit. Such an electrochemical setup is often called an *electrochemical cell* (one or more combinations of electrochemical cells is a *battery* used as a source of electric power). An oxidation-reduction reaction (that has a net negative free energy change) takes place in the electrochemical cell while an electric current to an external circuit is delivered.

Whether chemical changes are produced by electric current or electric potential is produced by a chemical reaction does not make any fundamental difference

Electrokinetic Remediation for Environmental Security and Sustainability, First Edition.
Edited by Alexandra B. Ribeiro and M.N.V. Prasad.
© 2021 John Wiley & Sons Ltd. Published 2021 by John Wiley & Sons Ltd.

UNCORRECTED PROOFS

Trim Size: 170mm x 244mm Single Column Loose Ribeiro670117 c02.tex V1 - 12/02/2020 11:05pm Page 36

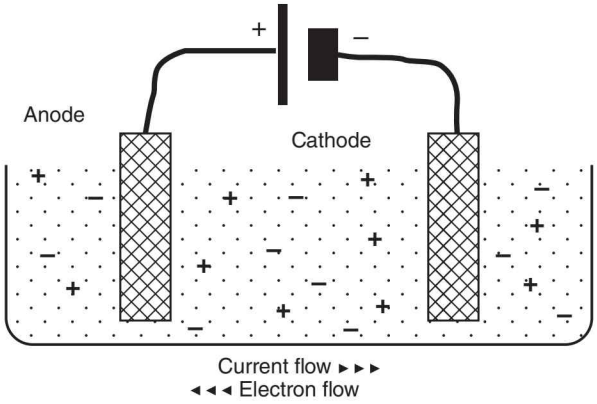

Figure 2.1 Two electrodes (possibly indifferent; they are not involved in the electrochemical reactions) are placed in one beaker. The beaker is filled with a salt solution that provides both positive and negative ions that are essential for the current flow. Electric current is supplied by an external battery. At the positive electrode, negative ions give up their charge to the electrode, and thus oxidation (at the anode) takes place. Similarly, positive ions take up electrons from the negative electrodes, and thus reduction takes place (at the cathode). Conventional current flows from the positive side of the negative end, but the electron flow is in the opposite direction. All primary electrochemical processes take place close to the surface of the electrodes.

(except in terms of free energy of the chemical reaction), and we will not make any distinction unless specifically noted. However, electric energy (in the form of potential and current) from electrochemical processes is an important source of convenient energy that has wide commercial and environmental significance.

In simple pictorial terms, a basic electrochemical setup (often called an *electrochemical cell*, or simply a *cell*) has three major components: two electrodes (essential to make electrical connections) and a solution (or a liquid, e.g. a molten salt, serving as an electrolyte) containing ions (responsible for the conduction of electricity in the solution) (Figure 2.1). A solution must have equal numbers (equivalents) of positive and negative ions (so that the solution is essentially neutral electrically). The electrons leave the negative electrode (called the *cathode*), pass through the external electrical circuit, and reach the positive electrode (anode), and are taken up by the positively charged ions (*cations*) in solution. Therefore, at the electrode surface, new ions may be created or consumed during the electron flow. Note that neither protons nor electrons can exist freely in a solution (due to their small size, they have very high surface potential) but can exist as solvated charges. Protons, for example, are easily solvated in acidic, basic, or amphoteric solvents but not in aprotic solvents. Similarly, electrons are released by the discharge of negatively charged ions (*anions*) at the positive electrode (called the *anode*). The transfer of electrons at the electrodes (to ions at the electrode solution interface) is responsible for the oxidation-reduction process. Therefore, the gain of electrons at the cathode by the cations at the electrode surface is a reduction process, and the loss of electrons at the anode by the anions is an oxidation process. Solvated electrons can have only a transient existence in water and rapidly decay by redox processes. Current flow in

UNCORRECTED PROOFS

Trim Size: 170mm x 244mm Single Column Loose Ribeiro670117 c02.tex V1 - 12/02/2020 11:05pm Page 37

a solution is always associated with oxidation-reduction processes at the respective electrodes (often called the *charge transfer process*).

2.1.1 Electrochemical Half-Cells

Because electrochemical reactions take place close to the surface of the electrodes and the rest of the solution plays only a relatively minor role, it is often convenient to discuss the two electrodes and the associated processes independently. This is similar to acid-base reactions in which acid and base properties can be considered independently (or to redox reactions). Because electrochemical reactions are closely related to oxidation-reduction processes (redox reactions), (relative) strengths of oxidants and reductants are often reported by their electrochemical potential. However, half-cells cannot be used alone: they must be paired for any practical applications. For example, we illustrate with a common galvanic cell (an electrochemical cell that can supply electric power) using Cu and Zn electrodes – two half cells connected with a salt bridge internally and with a lamp externally (as the effective load) (Figure 2.2).

For an acid-base reaction, we usually write

$$HA + B \rightleftarrows A^- + BH^+$$

which is considered the result of two half-reactions (one acid and one base): essentially, one proton is transferred from the acid to the base.

$$\text{HA} \rightleftarrows H^+ + A^- \ldots \text{(a Bronsted acid)}$$

$$B + H^+ \rightleftarrows BH^+ \ldots \text{(a Bronsted base)}$$

Similarly, for an oxidation-reduction (redox) reaction, we usually write

$$Ox_1 + Red_2 \rightleftarrows Red_1 + Ox_2$$

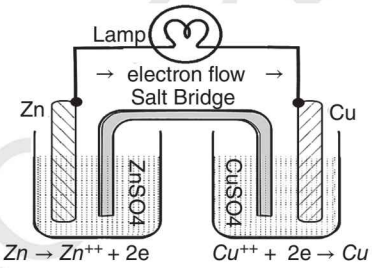

Figure 2.2 Daniell cell: An example of an electrochemical cell that provides electrical current at some given potential. The cell consists of Zn /Zn(II) SO_4; a salt bridge; Cu(II)SO_4/ Cu; and an external circuit completed via a lamp. The salt bridge helps connect the two halves of the electrochemical cell. Oxidation of Zn takes place at the Zn electrode ($Zn \rightarrow Zn^{+2} + 2e$), and reduction of Cu(II) ions takes place at the Cu electrode ($Cu^{+2} + 2e \rightarrow Cu$). The two electrons responsible for the redox process moves via the external circuit (through the lamp as shown), and the internal circuit is completed via the movement of Zn^{+2} and Cu^{+2} ions. In this example, the chemical energy associated with the reaction $Zn + Cu^{+2} \rightarrow Zn^{+2} + Cu$ is transformed into electrical energy.

UNCORRECTED PROOFS

Trim Size: 170mm x 244mm Single Column Loose Ribeiro670117 c02.tex V1 - 12/02/2020 11:05pm Page 38

which are similarly considered the result of two half-reactions (one oxidation and one reduction): one or more electrons are transferred from the reductant to the oxidant.

$$Ox_1 + e \rightleftarrows Red_1 \ldots \text{(the oxidant gains electron(s))}$$

$$Red_2 \rightleftarrows Ox_2 + e \ldots \text{(the reductant loses electron(s))}$$

Oxidation-reduction processes are best studied as electrochemical processes, even if no electrochemistry is directly involved. The free-electron shown above does not exist in solution (except perhaps a brief solvated existence), and we therefore need an arbitrary reference to compare the strengths of oxidants and reductants. In comparison, the strengths of acids and bases are often compared with respect to the acidic nature of the solvent (water, most commonly, can be considered as an acid by virtue of its autoionization: $H_2O + H_2O \rightleftarrows H_3O^+ + OH^-$).

2.1.2 Electrode Potential

An electrochemical cell (or a galvanic cell) has the three essential components: two electrodes separated by a conducting solution or a liquid (the electrolyte). Electrons enter the electrolyte via one electrode (the cathode) and leave via the other electrode (the anode). Free electrons do not exist in solution, and the electrons that enter the solution are taken up by one of the chemical species resulting in reduction. Similarly, the electrons that leave the solution via the cathode result in oxidation. It is convenient to study these two processes independently. Since only the potential of a full cell is directly measurable (half-cell potentials cannot be measured because the electrical circuit is incomplete), we always consider a hydrogen electrode as a standard reference (https://chem.libretexts.org/Bookshelves/Analytical_Chemistry/Supplemental_Modules_(Analytical_Chemistry)/Electrochemistry/Redox_Chemistry/Standard_Reduction_Potential). A standard hydrogen electrode, by definition, has a zero potential under standard conditions.

Consider a copper (Cu) metal rod (the electrode) placed in a solution of copper sulfate ($CuSO_4$). The following equilibrium process takes place close to the surface of the electrode:

$$Cu \rightleftarrows Cu^{+2} + 2e$$

where in the forward reaction, the metal atom tends to go into the solution but leave two electrons on the surface; whereas in the reverse process

$$Cu^{+2} + 2e \rightarrow Cu$$

the copper ion in solution tends to take up two electrons from the electrode surface and gets deposited on the electrode. As a result of this equilibrium, the electrode acquires a potential with respect to the bulk of the solution. But this potential cannot be measured directly because only potential differences between two electrodes can be physically measured. Hence we must couple a standard hydrogen electrode (another half-cell) with this system that makes a complete electrochemical cell with two electrodes. The potential measured this way is called the *redox potential*

UNCORRECTED PROOFS

Trim Size: 170mm x 244mm Single Column Loose Ribeiro670117 c02.tex V1 - 12/02/2020 11:05pm Page 39

Table 2.1 Standard reduction potential (in volts) for several redox species. All components are in their standard state.

$F_2(g) + 2e \rightarrow 2F^-(aq)$	+2.87
$S_2O_8^{-2}(aq) + 2e \rightarrow 2SO_4^{-2}(aq)$	+2.01
$O_2(g) + 4H^+(aq) + 4e \rightarrow 2H_2O(l)$	+1.23
$Br_2(l) + 2e \rightarrow 2Br^-(aq)$	+1.09
$Ag^+ + e \rightarrow Ag(s)$	+0.80
$Fe^{+3}(aq) + e \rightarrow Fe^{+2}(aq)$	+0.77
$I_2(l) + 2e \rightarrow 2I^-(aq)$	+0.54
$Cu^{+2}(aq) + 2e \rightarrow Cu(s)$	+0.34
$Sn^{+4}(aq) + 2e \rightarrow Sn^{+2}(aq)$	+0.15
$S(s) + 2H^+(aq) + 2e \rightarrow H_2S(g)$	+0.14
$2H^+(aq) + 2e \rightarrow H_2(g)$	**0.00**
$Sn^{+2}(aq) + 2e \rightarrow Sn(s)$	−0.14
$V^{+3}(aq) + e \rightarrow V^{+2}(aq)$	−0.26
$Fe^{+2}(aq) + 2e \rightarrow Fe(s)$	−0.44
$Cr^{+3}(aq) + 3e \rightarrow Cr(s)$	−0.74
$Zn^{+2}(aq) + 2e \rightarrow Zn(s)$	−0.76
$Mn^{+2}(aq) + 2e \rightarrow Mn(s)$	−1.18
$Na^+(aq) + e \rightarrow Na(s)$	−2.71
$Li^+(aq) + e \rightarrow Li(s)$	−3.04

Source: Chemistry LibreTexts, https://chem.libretexts.org/Bookshelves/Analytical_Chemistry/Supplemental_Modules_(Analytical_Chemistry)/Electrochemistry/Redox_Chemistry/Standard_Reduction_Potential. Licensed under CC-BY-3.0.

(more specifically, the *oxidation potential*) of the Cu/Cu^{+2} system. Redox potentials of systems not involving a metal can also be measured by using an indifferent electrode (e.g. a Pt electrode inserted in a solution of Fe^{+2}/Fe^{+3} ions measures the redox potential of the Fe^{+2}/Fe^{+3} couple). The Pt electrode is the source of electrons in the following redox equilibrium process: $Fe^{+3} + e \rightleftarrows Fe^{+2}$.

A list of standard reduction potentials is shown in Table 2.1. More detailed and exhaustive tables are available online at http://www2.ucdsb.on.ca/tiss/stretton/Database/Standard_Reduction_Potentials.htm. For biochemical and environmental applications, these values (biochemical redox potentials are often called *formal potentials*) may be considered approximate because of several other factors that deviate considerably from ideal behavior.

Looking at the table, we see that for the cell described, the Zn electrode will have a potential of −0.76 v (from the table; with reference to the standard hydrogen electrode), and the Cu electrode will have a potential of 0.34 v; the total voltage across the cell will be 1.1 v (with the Zn electrode being more negative). This voltage will depend on the concentrations of the solutions (of $ZnSO_4$ and $CuSO_4$; more

UNCORRECTED PROOFS

Trim Size: 170mm x 244mm Single Column Loose Ribeiro670117 c02.tex V1 - 12/02/2020 11:05pm Page 40

accurately, the concentrations of Zn^{+2} and Cu^{+2} ions close to the respective electrodes) and also on the temperature. The overall chemical reaction that takes place is $Zn + Cu^{+2} \rightarrow Zn^{+2} + Cu$. This reaction is spontaneous (net free energy change for the reaction is negative; free energy is liberated as the products have lower free energies compared to the reactants), and the excess free energy is recovered as the electrical energy (otherwise, it would have dissipated as heat).

2.1.3 Electrical Double Layer

It is seen that a Zn electrode dipped in a solution of $ZnSO_4$ (effectively, a solution containing Zn(II) ions; the anion plays no role in the present discussion) acquires a definite potential. This potential is present at (close to) the metal-solution interface, because the equilibrium $Zn \rightleftarrows Zn^{+2} + 2e$ can be possible only at or near the interface; but the actual distribution of potential close to the interface is interesting for various reasons. Theoretically, we expect the potential to drop to zero far from the electrode (the bulk solution). If the electrode is negatively charged, positive ions (cations) will be attracted close to the electrode surface (vs. anions), and this asymmetric distribution of ions will result in a potential close to the electrode surface. In the Stern model of the electrochemical double layer, some of the ions are strongly adsorbed at the electrode surface (Stern layer), some of the ions are weakly adsorbed, and the rest of the ions are relatively free (Figure 2.3). Although the thickness of the electrochemical double layer is a few nanometers at best (with ionic strengths of 0.1), this plays an important role in several electrokinetic processes in which there is relative movement of the solution with respect to the electrode.

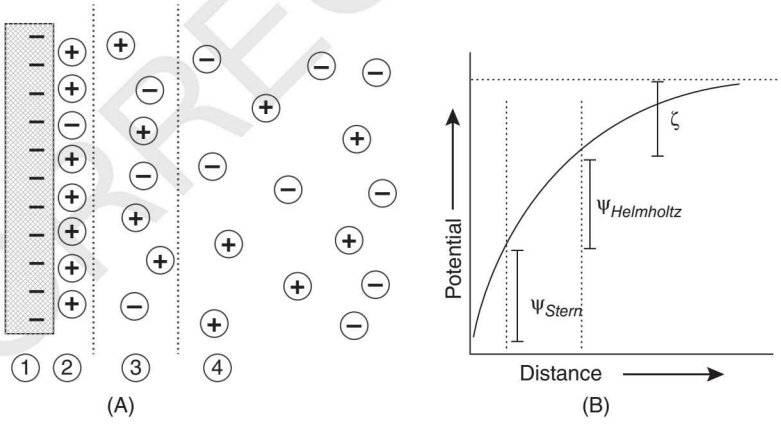

Figure 2.3 (a) A metal electrode in a solution of (e.g. a Zn electrode in a $ZnSO_4$ solution) acquires a potential with respect to the bulk of the solution. The total potential on the solution side is due to (i) the metal electrode (ii), the adsorbed ionic layer, (iii) the diffuse ionic layer, and (iv) the bulk of the solution. (b) The potential distribution as a function of the distance from the surface is seen qualitatively in this graph. The potential in the bulk phase, ζ, usually called the *zeta-potential*, is responsible for various electrokinetic phenomena (flow of a conducting liquid over an electrically charged surface).

UNCORRECTED PROOFS

Trim Size: 170mm x 244mm Single Column Loose Ribeiro670117 c02.tex V1 - 12/02/2020 11:05pm Page 41

Figure 2.3 shows that the total potential developed across the electrode is the sum of the three potentials: the voltage across the adsorbed layer, the voltage across the diffuse layer, and the voltage across the mobile layer. In the figure, a positive ion in the bulk faces little resistance to reach the electrode surface, but a negative ion cannot reach the electrode surface easily (due to electrostatic repulsion). This double layer is also associated with a capacitance that is used in the construction of electrolytic capacitors.

The actual potential of the ideal system (H_2(Pt)/H^+,Zn^{+2}/Zn(s)) will be determined by the Nernst equation [1]:

$$E = E_0 + 2.303\frac{RT}{nF}log[Zn^{+2}]$$

where E is the actual electrode potential, E_0 is the standard electrode potential, R is the ideal gas constant, T is the absolute temperature, n is the number of electrons involved in the redox equation (two in this particular case), and $[Zn^{+2}]$ is the concentration (activity) of Zn^{+2} ions in solution. The activity of a pure solid (Zn electrode) is always 1 (unity) by definition. If we apply an external potential to the Zn electrode that is greater than E, Zn will dissolve (until the Zn^{+2} concentration and the potential satisfy the above equation) and vice versa.

2.1.4 Electrochemical Processes

Electrochemical processes (chemical reactions taking place close to the electrode) in real life are far from ideal, and the two most important aspects that contribute to inefficiency (theoretical vs. actual potential) are (i) slow electron transfer and (ii) chemical reactions (we include diffusion and other rate processes) prior to or post electron transfer.

2.1.4.1 Polarization (Overvoltage)

When an appreciable current flows through the electrode, the actual electrode potential deviates significantly from the ideal value (E, as seen from the Nernst equation). In simple terms, the process is now disturbed from equilibrium and is governed by the laws of rate processes. In any given sequence of processes, the overall rate is governed by the slowest step. In the present case, the deviation from the ideal potential is due to slow processes, and the effect is known as *polarization* (electrochemical polarization at the electrode solution interface), which is a qualitative measure of the deviation from the ideal behavior. The most common cause of the polarization is slowness of the charge-transfer process across the electrode solution interface. The polarization can be different for anodic and cathodic processes (forward and reverse reactions). The excess potential (over the ideal value as predicted by the Nernst equation) needed for an electrochemical process to occur at an appreciable rate is also known as *electrode overvoltage*. The slow process can be considered as a chemical reaction (rate) with high activation energy. An ideally polarizable electrode has very high activation energy (no charge transfer process is possible), although this does not exist in reality. For example, a Zn(s)/Zn^{+2} half cell shows very little polarization except for some concentration effects at high

UNCORRECTED PROOFS

Trim Size: 170mm x 244mm Single Column Loose Ribeiro670117 c02.tex V1 - 12/02/2020 11:05pm Page 42

current densities, whereas O_2(Pt)/OH^- shows considerable overpotential. The effect depends on the nature of the electrode and also the exact composition of the electrolyte [2].

2.1.4.2 Slow Chemical Reactions

Electron-transfer processes may be coupled with chemical reactions in various ways. The overall kinetics can be complicated, but we simply list several possibilities as per the classical treatment by Bard and Faulkner [3]:

(a) CE reaction: A chemical process takes place prior to electron transfer:

$$Y \rightleftarrows O; O + ne \rightleftarrows R$$

(b) EC reaction: A chemical reaction takes place after the electron transfer:

$$O + ne \rightleftarrows R; R \rightleftarrows X$$

(c) EC′ reaction: A catalytic reaction in which one of the electroactive species is regenerated:

$$O + ne \rightleftarrows R; Z + R \rightleftarrows O + Y$$

(d) EE reaction: Two consecutive electron-transfer processes:

$$A + e \rightleftarrows B; B + e \rightleftarrows C$$

(e) ECE reaction: Two electron-transfer processes separated by a chemical reaction:

$$O_1 + n_1 e \rightleftarrows R_1; R_1 + Z \rightleftarrows O_2; O_2 + n_2 e \rightleftarrows R_2$$

(f) $\overleftarrow{E}C\vec{E}$ reaction: Oxidation process followed by a chemical reaction followed by a reduction:

$$A + e \rightleftarrows A^-; A^- \rightleftarrows B^-; B^- - e \rightleftarrows B$$

Several variants of coupled electron transfer and chemical reactions are possible.

Case Study

Global production of metallic aluminum in 2018 was 60 million metric tons [3]. The metal is obtained by the electrolysis of aluminum oxide (Al_2O_3) dissolved in molten cryolite (Na_3AlF_6) at an approximate temperature of 1000 °C (Heroult Hall process) (Figure 2.4). Aluminum is widely distributed on the earth's crust, but bauxite is the only mineral currently used for the production of aluminum. The world reserve of bauxite is estimated to be 55–75 billion metric tons. China accounts for more than 50% of the world's production of the metal. Aluminum oxide is obtained from bauxite by a simple chemical purification step. The electrolytic production process is highly energy-intensive. Crude aluminum is further refined for most applications by another electrolytic process (Hoopes

UNCORRECTED PROOFS

Trim Size: 170mm x 244mm Single Column Loose Ribeiro670117 c02.tex V1 - 12/02/2020 11:05pm Page 43

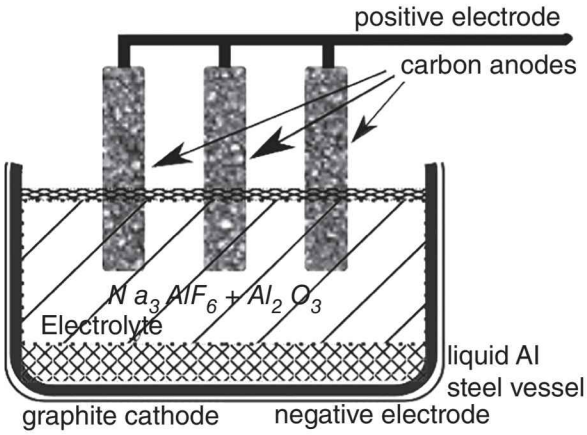

Figure 2.4 Aluminum electrolytic cell. The cathode is a graphite lined steel vessel, and the electrolyte is cryolite (Na_3AlF_6) containing dissolved aluminum oxide. The temperature is around 1000 °C, and the product (metallic aluminum) and the electrolyte are in liquid state. The reaction at the cathode, $AlF_6^{-3} + 3e \rightarrow Al + 6F^-$, takes place with a low overpotential. The reaction at the anode is $2O^{-2} + 4e \rightarrow O_2$; $C + O_2 \rightarrow CO_2$ has a high overpotential. The cell uses about 5 V in operation but with currents of 100 kA (depending on the size of the cell). The liquid aluminum collects at the bottom and is withdrawn periodically. The reaction at the anode is of type EC; the top of the cell is sprinkled with carbon powder that reacts with oxygen produced at the anode to produce mostly carbon dioxide. The energy efficiency of the cell is around 50%, and the waste energy is used to keep the cell at the operating temperature. HF and F_2 are the two major pollutants produced in the process.

process). The primary production of the metal needs 14 221 kWh per metric ton (theoretical value: 6164 kWh; https://prd-wret.s3-us-west-2.amazonaws.com/assets/palladium/production/s3fs-public/atoms/files/mcs-2019-alumi.pdf), and refining the metal costs about the same. Most of the electrochemical energy input is dissipated as heat (>50%). Aluminum is the second most widely used metal, and parts made from the metal have a design lifetime of approximately 10 years – in other words, the parts being recycled are about 10 years old on an average and need electrochemical refining. In 2018, the world consumed 868 TWh of energy in the production of aluminum (primary aluminum smelting power consumption), and more than 60% of this electrical energy was derived from coal-powered plants (http://www.world-aluminium.org/statistics/primary-aluminium-smelting-energy-intensity/#data). This does not include the energy used in the processing of bauxite (the raw material) to the finished product, alumina (Al_2O_3), ready to be added to the electrolytic cell. Another important chemical, caustic soda (NaOH) is also produced industrially by an electrolytic process.

Several other metals, notably magnesium and sodium, are also obtained by electrolysis, but the amounts are far smaller. World magnesium production in 2018 was 970 thousand metric tons, with China being a major (~80%) producer

Trim Size: 170mm x 244mm Single Column Loose Ribeiro670117 c02.tex V1 - 12/02/2020 11:05pm Page 44

(http://www.world-aluminium.org/statistics/metallurgical-alumina-refining-energy-intensity/#data). Magnesium is mainly used as an alloy with aluminum. A significant amount of magnesium is also used in other industries (desulfurization of iron and steel, reduction agent for metals production, etc.). Similarly, sodium is mostly obtained by the electrolysis of molten sodium chloride (NaCl), and the world production of the metal was >100 000 metric tons in 2005 (https://prd-wret.s3-us-west-2.amazonaws.com/assets/palladium/production/atoms/files/mcs-2019-mgmet.pdf). The metal is widely used as a reducing agent in the chemical industry and a coolant in nuclear reactors.

2.2 Basic Bioelectrochemistry and Applications

Wikipedia says, "Bioelectrochemistry is a branch of electrochemistry and biophysical chemistry concerned with electrophysiological topics like cellular electron-proton transport, cell membrane potentials and electrode reactions of redox enzymes" – a definition that is very broad to be really useful. We use a somewhat restrictive definition of *bioelectrochemistry* as electrochemical principles in biology and biological aspects of electrochemistry [4].

2.3 Industrial Electrochemistry and the Environment

Electrochemical methods are useful in the isolation of several metals, purification of many important metals (refining), and also in the production of important industrial chemicals; e.g. production of sodium hydroxide by chlor-alkali method is a very large industry. Electrochemistry is also involved in electroplating, electroforming, and other similar processes (organic or inorganic compounds). Production of sodium hydroxide using a mercury cell (Castner Kellner process) is now obsolete because of extensive pollution caused by mercury. In general, electrochemical processes tend to be relatively less polluting compared to other chemical industries.

2.3.1 Isolation and Purification of Important Metals

As mentioned earlier, aluminum is an important metal, both isolated and refined from the ore (bauxite) by electrolysis. Other metals, e.g. magnesium, sodium, lithium, are also obtained by electrolysis of their respective salts (metal chlorides), but the actual production volumes are much smaller. However, a significant quantity of copper and zinc are also isolated by electrolysis (depending on the local cost of electricity). Several other metals, e.g. cadmium, silver, gold, nickel, gallium, thallium, etc., are also produced by electrolysis, but the respective amounts are rather small. If high-purity metals are needed, all the above metals are purified by electrolysis [5].

UNCORRECTED PROOFS

Trim Size: 170mm x 244mm Single Column Loose Ribeiro670117 c02.tex V1 - 12/02/2020 11:05pm Page 45

2.3.2 Production of Important Chemical Intermediates by Electrochemistry

The most common and important electrolysis process for the production of inorganic chemical industrial raw materials is the chlor-alkali process. Basically, a solution of sodium chloride (NaCl) is electrolyzed to produce sodium hydroxide (NaOH; caustic soda or lye), chlorine (Cl_2 gas; used in several plastics and in a large number of solvents), and hydrogen (H_2 gas). Both sodium hydroxide and chlorine are very important intermediates in various chemical processes. In 2018, European countries produced 9479 kilotons of chlorine and 9383 kilotons of sodium hydroxide (https://www.chlorineindustryreview.com/manufacturing-applications). In 1990, the US produced 10.9 million tons of chlorine; the amount of caustic soda was not mentioned but should be similar; see https://www3.epa.gov/ttnchie1/ap42/ch08/final/c08s11.pdf. The production of chlorine and caustic soda should be similar for the rest of the world. Roughly, the annual world chlorine production was noted at 3.5×10^7 tons and uses about 100 TWh of electricity.

Other chemicals are also produced by electrochemical means: fluorine, sodium chlorate, sodium bromate, peroxosulfates, etc. They have modest demands, and we will not go into the details.

2.4 Electrokinetic Phenomena

In general, in an electrochemical setup, the electrodes and solution are stationary with respect to each other. Thus the electrical double layer (Figure 2.3) is essentially a static description. However, if the solution moves with respect to the electrode surface, the electrical double layer experiences a shearing force, and part of the double layer – outside the Helmholtz double layer, corresponding to the ζ potential – moves. The electrode in Figure 2.3 need not be a metal surface; it can be a simple charged particle. Clay particles (containing silicates) can lose a few sodium or calcium ions to the solution and become charged. Similarly, a gel made of polyacrylamide can acquire a negative charge; in prolonged contact with water, some of the amide groups hydrolyze to give carboxylic acids that can ionize to give a negative charge. A solution flowing through a porous clay plug or a gel of polyacrylamide can show electrokinetic behavior.

Wikipedia says, "Electrokinetic phenomena are a family of several different effects that occur in heterogeneous fluids, or in porous bodies filled with fluid, or in a fast flow over a flat surface. The term heterogeneous here means a fluid containing particles. Particles can be solid, liquid, or gas bubbles with sizes on the scale of a micrometer or nanometer" (https://en.wikipedia.org/wiki/Electrokinetic_phenomena). We will focus on electroosmosis as applied in bioelectroremediation of toxic compounds from soil.

UNCORRECTED PROOFS

Trim Size: 170mm x 244mm Single Column Loose Ribeiro670117 c02.tex V1 - 12/02/2020 11:05pm Page 46

2.4.1 Electroosmosis in Bioremediation

If we consider a capillary tube that has electric charges fixed on the inner surface – a glass capillary has negatively charged silicate functional groups on its surface and the cations are relatively mobile – it also has a characteristic electric double layer (when filled with a dilute salt solution). If an electric field is now applied along the length of the tube, the fixed charges cannot move, but the diffuse layer (with the associated potential ζ) does move along with the solvent and other electrically neutral molecules. This process is called *electroosmosis* or *electro-endosmosis* (flow of solvent under an electric field). A porous clay plug can also be considered an array of microcapillary tubes and also shows the same effect. This is also seen in gels (colloid with a continuous liquid dispersion medium) and is important in electrophoresis [6]. The pore size (or the inner diameter of the capillary tube) should not be much larger than the Debye length (effective thickness of the double layer) because only liquid close to the double layer (diffuse layer) can move in this process. The direction of flow depends on the charges on the surface and the counter-charges.

In the classical osmosis experiment, two compartments are separated by a membrane that is impermeable to the solute. The two compartments contain solutions with different concentrations of the same solute (hence different chemical potentials). Because the solute is impermeable (it cannot cross the membrane), the solvent flows across the membrane from the lower concentration (of the solute) to the higher concentration. This is a spontaneous process because the (solutes in) solution on both sides tends to reach the same concentration. In electroosmosis, however, work is done by the electric field in transporting ions (and associated solvents) across the membrane and is not a spontaneous process. The direction of flow can be reversed by changing the direction of the electric field. As in the case of osmosis, the flow of solution can be stopped by applying an external force (osmotic pressure). In the case of electroosmosis, the pressure is dependent on the electric field applied and the ζ potential for the given membrane and the solution but otherwise independent of the physical dimensions of the membrane. Electroosmosis can be effective in dilute solutions and can transport highly solvated uncharged molecules (like sugars, urea etc.), but macromolecules or nonpolar molecules (that are less solvated) are transported poorly.

In classical osmosis, if an external pressure is applied to the side containing solute with higher concentration, the solvent can be made to flow from the higher concentration (of the solute) to the lower concentration; in normal osmosis, the solvent flows spontaneously from higher solvent concentration to lower solvent concentration. The process is known as *reverse osmosis* and has been widely used in desalination plants. Similarly, if water is forced through a glass capillary tube, a potential is produced across the two ends of the tube (streaming potential) [7–10]. Both these effects show that the processes (osmosis and electroosmosis) are reversible in principle and the basic principles of thermodynamics hold good.

Electroosmosis has been used in an experimental setup for soil remediation and waste treatment. Shapiro and Probstein used treated clay as the electroosmotic medium in an experimental study [11]. The pollutant studied were phenol and

UNCORRECTED PROOFS

Trim Size: 170mm x 244mm Single Column Loose Ribeiro670117 c02.tex V1 - 12/02/2020 11:05pm Page 47

acetic acid, respectively. The experiment can be considered only a partial success because the clay got saturated with the pollutants and could not prevent pollutants from being removed efficiently. For removing acetic acid, the pH was an important factor because at high pH, considerable amounts of acetate were carried over as the negatively charged ions. The authors conclude that electroosmosis can be cost-effective when hazardous wastes are involved, for which cleanup costs can be considerable.

2.5 Electrophoresis and Its Application in Bioremediation

Electrophoresis is concerned with the movement of electrically charged particles under an external electric field (https://www.merriam-webster.com/dictionary/electrophoresis). Although the movement of charged ions in gases can be considered under this definition, usually movement of a charged particle in a liquid (e.g. water) or in a gel (e.g. agar, polyacrylamide, or damp cellulose or paper) is considered under this definition. The motion was first observed with colloidal particles, but in the laboratory, it has become a powerful tool in the analysis of proteins and nucleic acids. We present a very simplified description of the process below.

A particle with a net charge ne in an external electric field E experiences a net force equal to neE. As a result, the particle begins to move, and this force is counterbalanced with the frictional force due to viscosity as given by the Stokes' law: $6\pi\eta r_0 v$, where η is the viscosity of the medium, r_0 is the radius of the particle, and v is the velocity of the particle. A steady terminal velocity is obtained when these two forces balance each other: $6\pi\eta r_0 v = neE$. This gives the terminal velocity as $v = (neE)/(6\pi\eta r_0)$. Thus the terminal velocity depends on the charge/size (e/r_0) of the particle and is directly proportional to the applied electric field.

For an initially homogeneous solution, the effect will be most pronounced close to the electrode surface. This is illustrated in Figure 2.5.

Electrokinetic remediation (EKR) has been extensively studied in the literature on an experimental basis [12]. It is important to use low-strength electric fields and a longer period of application for meaningful results. Results suggest that toxic metal ions (Cu, Cd, Pb, and Zn) can be effectively remediation from soil using both electric field and phytoremediation. Although the exact mechanism is not clear, it appears that (i) application of low electric potential reduces electrolysis at the electrodes and use of AC potential reduces any large change of pH at (or near) the electrodes; and (ii) the metal ions are perhaps present within structures (or complexes) where EDTA or other chelating agents do not have access; the electric field liberates the metal ions, and then they are free to complex with various chelating agent (and can be phytoremediation), and other factors (iii) like electroendoosmosis cannot be ruled out to play a role.

Gomes et al. have reported some success in degrading organochlorine compounds (some common pesticides and insecticides) using EKR techniques [13]. These compounds are endocrine disruptors, show carcinogenic effects, and are slowly degraded

UNCORRECTED PROOFS

Trim Size: 170mm x 244mm Single Column Loose Ribeiro670117 c02.tex V1 - 12/02/2020 11:05pm Page 48

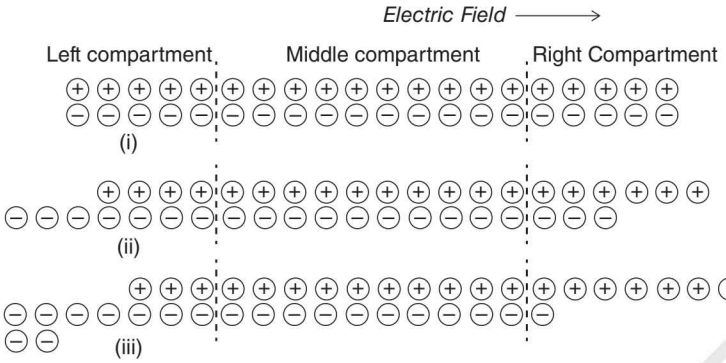

Figure 2.5 Movement of charged particles in an external electric field. The left and right compartments are close to the electrodes, but the central or middle compartment represents the bulk of the solution. To fix our ideas, let us assume that the positive charges have a mobility of one unit, whereas the negative charges have mobility of two units. The top diagram (i) shows the state before the electric field is applied. The middle diagram (ii) shows the state after some time when one positively charged particle moves one place to the right and two negatively charged particles move two places to the left. The bottom diagram shows the state when two positively charged particles move to the right by two places and four negatively charged particles move four places to the left. Both left and right compartments show equal changes in the concentrations, but the middle compartment is unaffected. For current to flow continually, ions must be discharged at the electrodes at the same rate; often, H^+ and OH^- are discharged instead of the migrating ions, and that can cause a change in pH close to the electrodes.

in nature. As they are mostly uncharged molecules, they are not subject to the electric field and do not electrophorese. However, close to the electrode, they are subject to secondary chemical reactions and can undergo an oxidation reduction process. Although the exact reaction mechanism is not certain, it has been reported that the molecules can be transported by electroosmosis, and some degree of remediation can be observed [14, 15].

2.6 Biosensors in Environmental Monitoring

Although biosensors are mostly useful in detecting and monitoring organic and biological pollutants in air, water, or soil samples, they are not directly useful in soil or water remediation. They are useful in the rapid measurements of various organic and biological toxic compounds, and most are simple enough to be used in a field. They are essential tools in estimating the progress of any major remediation program and are very cost-effective.

2.6.1 What Are Biosensors?

Biosensors are devices to detect and quantify some analyte of interest using a bioselective component as the first recognition step. When the analyte binds to the biorecognition element, a signal is produced that is transduced into another form

UNCORRECTED PROOFS

Trim Size: 170mm x 244mm Single Column Loose Ribeiro670117 c02.tex V1 - 12/02/2020 11:05pm Page 49

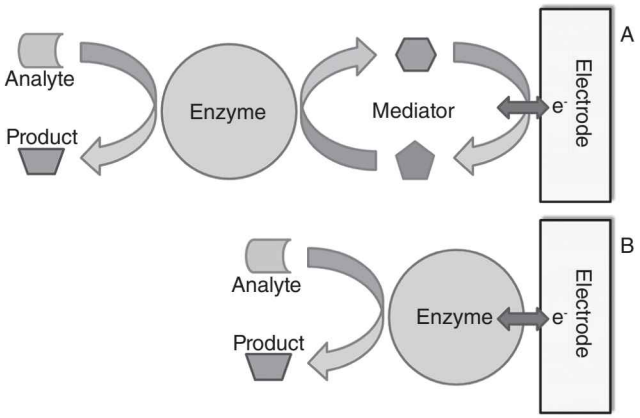

Figure 2.6 A schematic diagram of a modern biosensor. (a) A conventional glucose biosensor that uses a mediator molecule to ferry electrons between the enzyme and the electrode. The analyte can be glucose, the product can be gluconolactone, the enzyme can be glucose oxidase, the mediator can be ferrocene-carboxylic acid, and the electrode can be simple glassy carbon or gold. (b) The same system, but without using the mediator; the enzyme is modified so that fast electron transfer with the electrode is possible.

that can be more conveniently processed. The bioselective element is chosen based on the analyte to be detected; both quantitative and semi-quantitative detections are useful. The bioselective element can be DNA, protein (enzyme, antibody, carrier, receptor, special amino acid sequence, etc.), or even whole cells or tissue slices. The bioselective (also called *biorecognition*) component is intimately coupled to a signal transducer that can be electrochemical, optical, mass (piezoelectric, gravimetric, surface acoustic wave-based etc.), thermometric (heat change), etc. Biosensors based on electrochemical transduction are the most common (including amperometric, potentiometric, and impediometric methods), with optical transduction being a close second [16]. Enzymes are the most common bioselective elements, with antibodies being the next most common. The basic principle of operation is explained in Figure 2.6.

2.6.2 Biosensors as Environmental Monitors

During the last 40 years, research and development in the broad area of biosensors has grown exponentially. A simple literature search on Scopus (www.scopus.com) reveals the number of publications in a given year (Figure 2.7).

Most biosensors have applications in medical diagnostics, but the number of biosensors used today in environment applications is also very large [17]. The most common pollutants analyzed with the help of biosensors are pesticides (in both soil and water). Biosensors are popular for this purpose because they are usually small, simple, fast, and accurate for field analysis. Although one specific biosensor cannot measure different types of pesticides, they are generally useful if the nature of the pesticide is known in advance. For example, many pesticides work as nerve agents, and they function as inhibitors of acetylcholine esterase enzyme. A large number

UNCORRECTED PROOFS

Trim Size: 170mm x 244mm Single Column Loose Ribeiro670117 c02.tex V1 - 12/02/2020 11:05pm Page 50

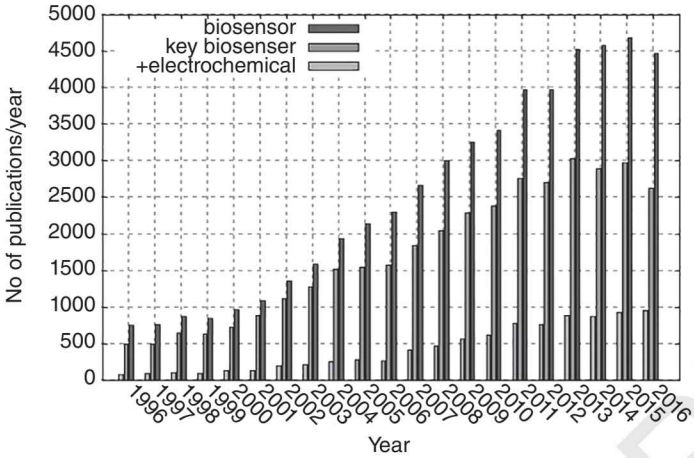

Figure 2.7 Number of publications with *biosensors* in the title, abstract, or keyword (purple bars); *biosensors* in the keyword (green bars); and also having *electrochemical* in the keyword (blue bars). The initial exponential growth has tapered off in recent years (as it must), suggesting that the technology has matured. Most publications came from the US and China.

of organophosphate and carbamate pesticides can be detected by using a biosensor that measures the degree of inhibition of the acetylcholine esterase enzyme. The most popular detection method has been the following:

$$\text{acetyl choline} + H_2O \overset{\text{AchE}}{\rightarrow} \text{acetate}^- + \text{choline}^+$$

AchE is the acetylcholine esterase enzyme; this is being targeted by the pesticide. With a higher concentration of the pesticide, the enzyme will be inhibited, and this reaction will proceed slowly.

In electrochemical detection, we use acetylthiocholine as the substrate; the product is thiocholine. Thiocholine is easier to detect electrochemically, with fewer side effects because the oxidation of thiocholine takes place at a lower potential. The product (thiocholine) can be now detected electrochemically:

$$2\,\text{thiocholine} \overset{\text{oxidation}}{\rightarrow} \text{bis} - \text{thiocholine} + 2\,H^+ + 2\,e$$

With higher pesticide concentration, there will be greater inhibition of the enzyme, which will result in a slower rate of production of thiocholine, giving rise to a lower current at the sensor. This scheme works with most organophosphates, carbamates, and nerve gases (chemical warfare agents). Although this is the simplest scheme, there are proposals that involve two or more enzymes on the same electrode. For the two-enzyme-based sensors, choline oxidase is most common as the second enzyme [18].

For increased convenience and faster response, an enzyme-linked immunosorbent assay (ELISA) – a test that depends on very high specificity of antigen-antibody binding – has been adapted as an electrochemical biosensor [19]. Like ELISA, it uses two

UNCORRECTED PROOFS

Trim Size: 170mm x 244mm Single Column Loose Ribeiro670117 c02.tex V1 - 12/02/2020 11:05pm Page 51

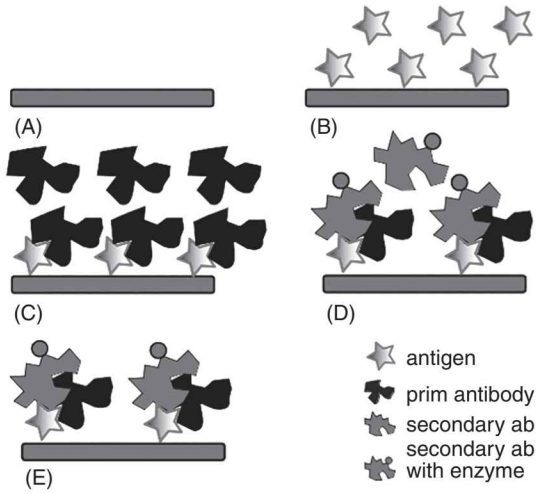

Figure 2.8 A brief outline of the steps involved in the electrochemical detection of pesticides using antibodies following a protocol similar to ELISA. The pesticide acts like an antigen, and the steps involved are very similar to the colorimetric test commonly referred to as ELISA (enzyme-linked immunosorbent assay). (a) The bare electrode, ready to attach to the antigen (pesticide). Often the attachment is non-covalent, but for optimum performance, we prefer a spacer arm attached covalently to the electrode surface and the antigen. (b) The antigen is anchored to the electrode surface. The unbound antigen is removed by a simple wash with a plain buffer (the wash cycle is not shown in the diagram). (c) The primary antibody is introduced and is allowed to bind with the antigen. Sufficient time is allowed so that a near-complete binding takes place. After the binding is complete, the excess antibody is washed off using a conventional buffer. (d) We add another antibody (secondary antibody) that binds selectively to the antigen-antibody complex formed in the previous step. This secondary antibody is chemically modified by attachment with a redox enzyme: horseradish peroxidase (HRP) is the most popular because it is stable and widely available. As before, the excess secondary antibody is washed off. (e) Finally, we add a redox substrate and hydrogen peroxide, which is catalyzed by the enzyme. The current produced is now proportional to the amount of enzyme present on the electrode surface. TMB (tetramethylbenzidine, a popular redox substrate) is oxidized by H_2O_2, and this follows the electrochemical reaction TMB(reduced) $+ H_2O_2 \rightarrow$ TMB(oxidized).

specific antibodies, and the first antibody is attached covalently close to the electrode surface. This is dipped in the solution containing the specific antigen, and part of the antigen in solution will bind to the primary antibody. Once this is washed, the electrode is next dipped into the secondary antibody, which is often tagged with a redox enzyme (most commonly horseradish peroxidase). The secondary antibody binds with a high affinity to the antigen-primary antibody complex already present on the electrode surface. The amount of enzyme bound to the electrode is assayed using a redox mediator molecule (Figure 2.8).

Production of antibodies is often messy and time-consuming and involves animal experiments. A simple, efficient, completely chemical method that does not involve animal experiments is now available. A DNA sequence is generated (called *aptamers*) using selection evolution of ligands by exponential enrichment (SELEX), which can recognize and bind with high efficiency with a given molecule.

UNCORRECTED PROOFS

Trim Size: 170mm x 244mm Single Column Loose Ribeiro670117 c02.tex V1 - 12/02/2020 11:05pm Page 52

These aptamers can be used as biosensors for pesticides with high selectivity using techniques like surface plasmon resonance (SPR), impedance spectroscopy, mass changes, etc.).

AQ1

2.7 Electrochemical Systems as Energy Sources

Electrochemical cells, or batteries, are among the most widely used energy sources for portable devices. They come in different shapes, sizes, and capacities to fit different purposes. The intrinsic chemistries also vary widely. The most commonly used batteries are shown in Figure 2.9. Their small size, low cost, easy availability, and reasonable capacity has made them very popular. The cheapest ones, the $ZnCl_2$-based AA or AAA size, are the most widely used.



Figure 2.9 Electrochemical devices as power sources. They are widely used in many portable devices, and there are many more different types not shown here (coin cells or watch batteries). Left: ZnCl2-based, 1.5 V output, AAA size disposable cell. Several years ago, these batteries contained small amounts of mercury, but most modern cells are free from mercury. The active electrolyte is in the form of a paste, and a carbon rod serves as a positive electrode. These cells can provide around 500–1000 mAh capacity. The next cell is a larger size (AA) and can be recharged multiple times but provides a lower voltage (1.2 V) and is based on Ni-MH (nickel-metal hydride) chemistry. The positive electrode is made of nickel (undergoes oxidation to nickel oxide), and the negative electrode is an intermetallic compound (contains rare earth metals) that adsorbs the H produced after the reduction of H^+. The active electrolyte is KOH, and the cells are similar to NiCd cells (but Cd is highly toxic) in performance. The next cell shown is again Zn-based and disposable, with an alkaline electrolyte; it is more expensive but has better performance. The next one is a larger size (usually described as 18 650 cell) and higher voltage (3.7 V) and is based on the Li-ion chemistry (non-aqueous electrolyte). Some portable instruments, including many electronic instruments, need higher voltage and low current, and the 9 V disposable (also available in rechargeable version) battery is less common. Not shown are the coin cells used in watches and some remotes.

UNCORRECTED PROOFS

Trim Size: 170mm x 244mm Single Column Loose Ribeiro670117 c02.tex V1 - 12/02/2020 11:05pm Page 53

Table 2.2 Recent developments in electrochemical remediation.

Research contribution	References
Dewatering for the removal of oxyfluorfen from a coagulation/flocculation sludge	Acosta-Santoyo et al. 2020 [20]
Treatment and management of contaminated soil	Annamalai and Sundaram 2020 [21]
Fenton process for the remediation of soil	Anshy Oonnittan 2020 [22]
Wastewater treatment and carbon sequestration	Anwer et al. 2020 [23]
Wastewater management	Arellano, Sanromán, and Pazos 2020 [24]
Removal of harmful emerging salt pollutants from saline-sodic soil	Bessaim et al. 2020 [25]
Sodic-saline soil remediation	Bessaim et al. 2020; Ghernaout and Elboughdiri 2020 [26, 27]
Wastewater remediation	Brillas 2020 [28]
Contaminated soils, sediments, and groundwater	Cameselle, Gouveia, and Urréjola 2019 [29]
phytoremediation amended with electric current	Cameselle and Reddy 2019 [30]
Remediation of organic contaminants	Cheng, Karthikeyan, and Wong 2019 [31]
Soil washing effluents polluted with atrazine	Contreras et al. 2020 [32]
Desalination	Dai et al. 2020 [33]
Recovery of heavy metals from canola (*Brassica napus*) and soybean (*Glycine max*) biomasses	Delil et al. [34]
Metal recovery	Dominguez-Benetton, Varia, and Pozo 2019 [35]
Renewable energy–driven electrochemical wastewater/soil decontamination	Ganiyu, Martínez-Huitle, and Rodrigo 2020 [36]
Ciprofloxacin degradation	He et al. 2020 [37]
Cleaning chromium pollution	He et al. 2020 [38]
Tetrachloroethylene contamination in realistic aquifer settings	Hyldegaard, Jakobsen, and Ottosen 2020 [39]
Transformation of tetrachloroethylene	Hyldegaard, Ottosen, and Alshawabkeh 2020 [40]
Remediation of sites' total petroleum hydrocarbons	Kuppusamy et al. 2020 [41]

UNCORRECTED PROOFS

Trim Size: 170mm x 244mm Single Column Loose Ribeiro670117 c02.tex V1 - 12/02/2020 11:05pm Page 54

Table 2.2 (Continued)

Research contribution	References
Electrochemical technology	Lacasa et al. 2019 [42]
Remediation of Pb-contaminated saturated sand	Li et al. 2020 [43]
Removal of *Microcystis aeruginosa*	Lian et al. 2020 [44]
CNT-based membranes for environmental applications	Liu et al. 2020 [45]
E-waste remediation	Liyanage and Walpita 2020 [46]
Coupled electrochemical and ion-exchange technologies to remove recalcitrant micropollutants	Martins et al. 2020 [47]
CO_2 and its derived products valorization	Mateos et al. 2019 [48]
Removal of naphthalene	McQuillan, Stevens, and Mumford 2020 [49]
Treatment of wastewater effluents	Millán et al. 2020 [50]
Electrochemical oxidation in combination with adsorption processes	Muñoz-Morales et al. 2020 [51]
Remediation of soil contaminated with HCB	Oonnittan and Sillanpää 2020 [52]
Remediation of low-permeability soil contaminated with persistent organic pollutants	Pham and Sillanpää 2020 [53]
Electrokinetically enhanced bioremediation technologies for pH	Saini et al. 2020 [54]
Photolytic treatments with electrochemical technology	Souza et al. 2020 [55]
Charge interactions, reaction kinetics, and dimensionality effects on electrokinetic remediation	Sprocati and Rolle 2020 [56]
Water desalination, ion separation, and the recovery of elements	Srimuk et al. 2020 [57]
Municipal wastewater treatment	Tang et al. 2019 [58]
Remediation of soils polluted with lindane	Vidal et al. 2020 [59]
Petroleum hydrocarbons using microbial electrochemical technology	Wang, Lu, and Ren 2019 [60]
Microbial electrochemistry for bioremediation	Wang et al. 2020 [61]
Microbial fuel cell system for pollutant removal and environmental remediation	Wu et al. 2020 [62]

UNCORRECTED PROOFS

Trim Size: 170mm x 244mm Single Column Loose Ribeiro670117 c02.tex V1 - 12/02/2020 11:05pm Page 55

Table 2.2 (Continued)

Research contribution	References
Electrochemical treatment of organic pollutants in landfill leachate using a three-dimensional electrode system	Yu et al. 2020 [63]
Electrochemical oxidative degradation of indigo wastewater based on a chlorine-containing system	Zhang et al. 2020 [64]
Remediation of persistent organic pollutants	Zhi et al. 2020 [65]

Although consumer batteries are widely used and available, they represent only a small amount of portable power. The bulk of portable power is used in cars (12 V lead-acid cells), buses and trucks (often 24 V lead acid cells), trains, and aircraft. Most modern aircraft have switched over to lithium cells, and some electric cars also use Li-ion cells. In 1992, about 3 million tons of lead were used in the manufacture of batteries (https://en.wikipedia.org/wiki/Lead%E2%80%93acid_battery). Total world production (primary production plus recycling) of lead in the same year was 5.48 million tons (https://www.ila-lead.org/lead-facts/lead-production--statistics). China is the largest producer of lead in the world. Because the metal is cheap, it has not been possible to find a safer replacement for the metal in the battery industry. However, lead is widely and efficiently recycled.

2.8 Conclusions

Because electrochemical processes are relatively free from side effects (undesired product formation), they are an attractive candidate for remediation technology. However, this is a nascent technology, and wide application has been slow. Although electric energy is relatively expensive, its inherent cleanliness has been the primary driving force. Table 2.2 lists some of the recent studies toward electrochemical remediation of soil and/or water from heavy metals, toxic compounds, or undesirable products (including process treatments).

References

1 Nernst, W. (1889). Die elektromotorische wirksamkeit der jonen. *Zeitschrift für Physikalische Chemie* 4 (1): 129–181.
2 Glasstone, S. (1942). *An Introduction to Electrochemistry*, 435–480. Litton Educational Publishing, Inc.

UNCORRECTED PROOFS

Trim Size: 170mm x 244mm Single Column Loose Ribeiro670117 c02.tex V1 - 12/02/2020 11:05pm Page 56

3 Bard, A.J. and Faulkner, L.R. (2001). *Electrochemical Methods, Fundamentals and Applications*, 2e. Wiley.

4 Klemm, A., Hartmann, G., and Lange, L. (2005). Sodium and sodium alloys. In: *Ullmann's Encyclopedia of Industrial Chemistry*. Weinheim: Wiley-VCH https://doi.org/10.1002/14356007.a24_277.

5 Pletcher, D. and Wash, F.C. (1990). *Industrial Electrochemistry*, 2e. Springer Science & Business Media.

6 Glasstone, S. (1942). *An Introduction to Electrochemistry*, 521–544. Litton Educational Publishing, Inc.

7 Kruyt and Willigen (1928). *Kolloid-Zeitschrift und Zeitschrift für Polymere* 45: 307.

8 Briggs, D.R. (1928). *The Journal of Physical Chemistry* 32: 641.

9 Fairbrother, F. and Balkinm, M. (1931). *Journal of the Chemical Society* 3S9.

10 Bull, H.B. and Moyer, L.S. (1936). *The Journal of Physical Chemistry* 40: 9.

11 Shapiro, A.P. and Probstein, R.F. (1993). Removal of contaminants from saturated clay by electroosmosis. *Environmental Science & Technology* 27 (2).

12 Chirakkara, R.A. and Reddy, K.R. (2013). Electrokinetic-enhanced phytoremediation of soils: Status and opportunities Claudio Cameselle. *Chemosphere* 93: 626–636.

13 Gomes, H.I., Dias-Ferreira, C., and Ribeiro, A.B. (2012). Electrokinetic remediation of organochlorines in soil: enhancement techniques and integration with other remediation technologies. *Chemosphere* 87: 1077–1090.

14 Lu, X. and Yuan, S. (2009). Electrokinetic removal of chlorinated organic compounds. In: *Electrochemical Remediation Technologies for Polluted Soils, Sediments and Groundwater* (eds. K.R. Reddy and C. Cameselle), 219–234. Hoboken, NJ: Wiley.

15 Karagunduz, A. (2009). Electrokinetic transport of chlorinated organic pesticides. In: *Electrochemical Remediation Technologies for Polluted Soils, Sediments and Groundwater* (eds. K.R. Reddy and C. Cameselle), 235–248. Hoboken, NJ: Wiley.

16 Mitra, C.K., Shantilatha, R., and Varma, S. (2003). Designing a simple biosensor. In: *Advances in Biosensors: perspectives in Biosensors*, 1e (eds. A.P.F. Turner and B.D. Malhotra).

17 Sassolas, A., Prieto-Simón, B., and Marty, J.-L. (2012). Biosensors for pesticide detection: new trends. *American Journal of Analytical Chemistry* 03 (03): 210–232. https://doi.org/10.4236/ajac.2012.33030.

18 Upadhyay, S., Rao, G.R., Sharma, M.K. et al. (2009). Immobilization of acetylcholineesterase-choline oxidase on a gold-platinum bimetallic nanoparticles modified glassy carbon electrode for the sensitive detection of organo-phosphate pesticides, carbamates and nerves agents. *Biosensors and Bioelectronics* 25 (4): 832–838. https://doi.org/10.1016/j.bios.2009.08.036.

19 Ahirwal, G.K. and Mitra, C.K. (2010). Gold nanoparticles based sandwich electrochemical immunosensor. *Biosensors and Bioelectronics* 25 (9): 2016–2020.

20 Rodrigo, M.A. (2020). Electrochemically assisted dewatering for the removal of oxyfluorfen from a coagulation/ flocculation sludge. *Journal of Environmental Management* 258: 110015.

UNCORRECTED PROOFS

Trim Size: 170mm x 244mm Single Column Loose Ribeiro670117 c02.tex V1 - 12/02/2020 11:05pm Page 57

21 Annamalai, S. and Sundaram, M. (2020). Electro-bioremediation: an advanced remediation technology for the treatment and management of contaminated soil. In: *Bioremediation of Industrial Waste for Environmental Safety*, 183–214. Singapore: Springer.

22 Oonnittan, A. and Sillanpää, M. (2020). Application of electrokinetic Fenton process for the remediation of Soil. In: *Advanced Water Treatment: Advanced Oxidation Processes*, vol. 43, 57. Elsevier Inc.

23 Anwer, A.H., Khan, M.D., Khan, M.Z., and Joshi, R. (2020). Microbial electrochemical cell: an emerging technology for waste water treatment and carbon sequestration. In: *Modern Age Waste Water Problems*, 339–360. Cham: Springer.

24 Arellano, M., Sanromán, M.Á., and Pazos, M. (2020). Sulfate radicals-based technology as a promising strategy for wastewater management. In: *Frontiers in Water-Energy-Nexus—Nature-Based Solutions, Advanced Technologies and Best Practices for Environmental Sustainability*, 113–115. Cham: Springer.

25 Bessaim, M.M., Missoum, H., Bendani, K. et al. (2020). Effect of processing time on removal of harmful emerging salt pollutants from saline-sodic soil during electrochemical remediation. *Chemosphere* 253: 126688.

26 Bessaim, M.M., Missoum, H., Bendani, K. et al. (2020). Sodic-saline soil remediation by electrochemical treatment under uncontrolled pH conditions. *Arabian Journal of Geosciences* 13 (5): 1–3.

27 Ghernaout, D. and Elboughdiri, N. (2020). Electrochemical technology for wastewater treatment: dares and trends. *Open Access Library Journal* 7 (1): 1–7.

28 Brillas, E. (2020). A review on the photoelectro-Fenton process as efficient electrochemical advanced oxidation for wastewater remediation. Treatment with UV light, sunlight, and coupling with conventional and other photo-assisted advanced technologies. *Chemosphere* 250: 126198.

29 Cameselle, C., Gouveia, S., and Urréjola, S. (2019). Sustainable soil remediation. Phytoremediation amended with electric current. In: *Environmental Geotechnology*, 51–61. Singapore: Springer.

30 Cameselle, C. and Reddy, K.R. (2019). Electrochemical remediation for contaminated soils, sediments and groundwater. In: *Engineering Tools for Environmental Risk Management: 4. Risk Reduction Technologies and Case Studies*, 447. CRC Press.

31 Cheng, K.Y., Karthikeyan, R., and Wong, J.W. (2019). Microbial electrochemical remediation of organic contaminants: possibilities and perspective. In: *Microbial Electrochemical Technology*, 613–640. Elsevier.

32 Contreras, M.B., Camacho, J.V., Fernández-Morales, F.J. et al. (2020). Biodegradability improvement and toxicity reduction of soil washing effluents polluted with atrazine by means of electrochemical pre-treatment: influence of the anode material. *Journal of Environmental Management* 255: 109895.

33 Dai, J., Wang, J., Hou, X. et al. (2020). Dual-zinc electrode electrochemical desalination. *ChemSusChem* 13 (10): 2792–2798.

34 Delil, A.D., Köleli, N., Dağhan, H., and Bahçeci, G. (2020). Recovery of heavy metals from canola (*Brassica napus*) and soybean (Glycine max) biomasses using electrochemical process. *Environmental Technology & Innovation* 17: 100559.

UNCORRECTED PROOFS

Trim Size: 170mm x 244mm Single Column Loose Ribeiro670117 c02.tex V1 - 12/02/2020 11:05pm Page 58

35 Dominguez-Benetton, X., Varia, J.C., and Pozo, G. (2019). *Microbial Electrochemical Technology Drives Metal Recovery*. Microbial Electrochemical Technologies.

36 Ganiyu, S.O., Martínez-Huitle, C.A., and Rodrigo, M.A. (2020). Renewable energies driven electrochemical wastewater/soil decontamination technologies: a critical review of fundamental concepts and applications. *Applied Catalysis B: Environmental* 270: 118857.

37 He, C., Gu, L., Xu, Z. et al. (2020). Cleaning chromium pollution in aquatic environments by bioremediation, photocatalytic remediation, electrochemical remediation and coupled remediation systems. *Environmental Chemistry Letters*: 1–6.

38 He, J., Li, N., Zhang, D. et al. (2020). Real-time monitoring of ciprofloxacin degradation in an electro-Fenton-like system using electrochemical-mass spectrometry. *Environmental Science: Water Research & Technology* 6 (1): 181–188.

39 Hyldegaard, B.H., Jakobsen, R., and Ottosen, L.M. (2020). Electrochemical transformation of an aged tetrachloroethylene contamination in realistic aquifer settings. *Chemosphere* 243: 125340.

40 Hyldegaard, B.H., Ottosen, L.M., and Alshawabkeh, A.N. (2020). Transformation of tetrachloroethylene in a flow-through electrochemical reactor. *Science of the Total Environment* 707: 135566.

41 Kuppusamy, S., Maddela, N.R., Megharaj, M., and Venkateswarlu, K. (2020). Approaches for remediation of sites contaminated with total petroleum hydrocarbons. In: *Total Petroleum Hydrocarbons*, 167–205. Cham: Springer.

42 Lacasa, E., Cotillas, S., Saez, C. et al. (2019). Environmental applications of electrochemical technology. What is needed to enable full-scale applications? *Current Opinion in Electrochemistry* 16: 149–156.

43 Li, G., Li, Y., Zhang, J., and Liu, J. (2020). Study on electrokinetic remediation of Pb-contaminated saturated sand. *International Journal of Electrochemical Science* 15: 1486–1497.

44 Lian, H., Xiang, P., Xue, Y. et al. (2020). Efficiency and mechanisms of simultaneous removal of Microcystis aeruginosa and microcystins by electrochemical technology using activated carbon fiber/nickel foam as cathode material. *Chemosphere* 252: 126431.

45 Liu, Y., Liu, F., Ding, N. et al. (2020). Recent advances on electroactive CNT-based membranes for environmental applications: the perfect match of electrochemistry and membrane separation. *Chinese Chemical Letters*.

46 Liyanage, D. and Walpita, J. (2020). Organic pollutants from E-waste and their electrokinetic remediation. In: *Handbook of Electronic Waste Management*, 171–189. Butterworth-Heinemann.

47 Martins, V.L., Ogden, M.D., Jones, M.R. et al. (2020). Opportunities for Coupled Electrochemical and Ion-Exchange Technologies to Remove Recalcitrant Micropollutants in Water. *Separation and Purification Technology* 239: 116522.

48 Mateos, R., Escapa, A., Vanbroekhoven, K. et al. (2019). Microbial electrochemical technologies for CO2 and its derived products valorization. In: *Microbial Electrochemical Technology*, 777–796. Elsevier.

49 McQuillan, R.V., Stevens, G.W., and Mumford, K.A. (2020). Electrochemical removal of naphthalene from contaminated waters using carbon electrodes, and

UNCORRECTED PROOFS

Trim Size: 170mm x 244mm Single Column Loose Ribeiro670117 c02.tex V1 - 12/02/2020 11:05pm Page 59

viability for environmental deployment. *Journal of Hazardous Materials* 383: 121244.

50 Millán, M., Lobato, J., Cañizares, P., and Rodrigo, M.A. (2020). Prediction and management of solar energy to power electrochemical processes for the treatment of wastewater effluents. *Electrochimica Acta* 335: 135594.

51 Muñoz-Morales, M., Sáez, C., Cañizares, P., and Rodrigo, M.A. (2020). Improvement of electrochemical oxidation efficiency through combination with adsorption processes. *Journal of Environmental Management* 262: 110364.

52 Oonnittan, A. and Sillanpää, M. (2020). Application of electrokinetic Fenton process for the remediation of soil contaminated with HCB. In: *Advanced Water Treatment*, 57–93. Elsevier.

53 Pham, T.D. and Sillanpää, M. (2020). Ultrasonic and electrokinetic remediation of low permeability soil contaminated with persistent organic pollutants. In: *Advanced Water Treatment*, 227–310. Elsevier.

54 Saini, A., Bekele, D.N., Chadalavada, S. et al. (2020). A review of electrokinetically enhanced bioremediation technologies for PHs. *Journal of Environmental Sciences* 88: 31–45.

55 Souza, F.L., Sáez, C., Cañizares, P., and Rodrigo, M.A. (2020). Improving photolytic treatments with electrochemical technology. *Separation and Purification Technology* 235: 116229.

56 Sprocati, R. and Rolle, M. (2020). Charge interactions, reaction kinetics and dimensionality effects on electrokinetic remediation: a model-based analysis. *Journal of Contaminant Hydrology* 229: 103567.

57 Srimuk, P., Su, X., Yoon, J. et al. (2020). Charge-transfer materials for electrochemical water desalination, ion separation and the recovery of elements. *Nature Reviews Materials*: 1–22.

58 Tang, J., Zhang, C., Shi, X. et al. (2019). Municipal wastewater treatment plants coupled with electrochemical, biological and bio-electrochemical technologies: opportunities and challenge toward energy self-sufficiency. *Journal of Environmental Management* 234: 396–403.

59 Vidal, J., Carvela, M., Saez, C. et al. (2020). Testing different strategies for the remediation of soils polluted with lindane. *Chemical Engineering Journal* 381: 122674.

60 Wang, H., Lu, L., and Ren, Z.J. (2019). *Enhanced Bioremediation of Petroleum Hydrocarbons Using Microbial Electrochemical Technology*. Microbial Electrochemical Technologies.

61 Wang, X., Aulenta, F., Puig, S. et al. (2020). Microbial electrochemistry for bioremediation. *Environmental Science and Ecotechnology* 1: 100013.

62 Wu, Q., Jiao, S., Ma, M., and Peng, S. (2020). Microbial fuel cell system: a promising technology for pollutant removal and environmental remediation. *Environmental Science and Pollution Research* 27: 1–6.

63 Yu, D., Cui, J., Li, X. et al. (2020). Electrochemical treatment of organic pollutants in landfill leachate using a three-dimensional electrode system. *Chemosphere* 243: 125438.

UNCORRECTED PROOFS

Trim Size: 170mm x 244mm Single Column Loose Ribeiro670117 c02.tex V1 - 12/02/2020 11:05pm Page 60

64 Zhang, W., Lv, W., Li, X., and Yao, J. (2020). *Electrochemical oxidative degradation of indigo wastewater based on chlorine-containing system*. Pigment & Resin Technology.

65 Zhi, D., Lin, Y., Jiang, L. et al. (2020). Remediation of persistent organic pollutants in aqueous systems by electrochemical activation of persulfates: a review. *Journal of Environmental Management* 260: 110125.

UNCORRECTED PROOFS

Trim Size: 170mm x 244mm Single Column Loose Ribeiro670117 c03.tex V1 - 12/02/2020 11:04pm Page 61

3

Combined Use of Remediation Technologies with Electrokinetics

Helena I. Gomes[1] *and Erika B. Bustos*[2]

[1] *Food, Water, Waste Research Group, Faculty of Engineering, University of Nottingham, University Park, Nottingham NG7 2RD, UK*
[2] *Centro de Investigación y Desarrollo Tecnológico en Electroquímica, S.C. Parque Tecnológico Querétaro, Sanfandila, 76703 Querétaro, Mexico*

3.1 Introduction

Soil is a non-renewable natural resource at the human scale and is essential for our survival as a species, as soils provide food for a growing future population [1]. Contamination is one of the threats to soil quality and can be caused by improper solid waste management, leachates from mismanaged landfills, unsafe storage of hazardous chemicals and nuclear waste, and uncontrolled dumping of municipal waste, industrial plants, and mining. A systematic assessment of the status of soil pollution at a global level has never been undertaken, despite agricultural intensification, industrial output, and urbanization continuing at a rapid pace [2]. Soil contamination by potentially toxic elements (e.g. arsenic, lead, and cadmium), persistent organic chemicals like polychlorinated biphenyls (PCBs) and polycyclic aromatic hydrocarbons (PAHs), and pharmaceuticals (such as antibiotics or endocrine disruptors) poses severe direct risks to human health [3].

Electrokinetic and electrodialytic remediation are technologies based on the application of low-level direct current to induce mechanisms that allow the transport or degradation of contaminants. Electroremediation is superior to other technologies for being applicable to fine-grain soils where other techniques are unsuccessful [4]. However, the complexity of soil contamination, due to the presence of both organic and inorganic contaminants, age of contamination, soil heterogeneity, site-specific factors, and the need to develop and implement cost-effective solutions that incorporate the strengths of remediation technologies, has led to the use of different techniques in sequence (treatment trains) or simultaneously (combination). Electrokinetics (EK) can help overcome some limitations of current remediation technologies [5–7], and in the last five years, several novel approaches have been developed.

This chapter will focus on recent case studies where electrokinetic remediation was combined with other remediation technology to achieve remediation criteria

Electrokinetic Remediation for Environmental Security and Sustainability, First Edition.
Edited by Alexandra B. Ribeiro and M.N.V. Prasad.
© 2021 John Wiley & Sons Ltd. Published 2021 by John Wiley & Sons Ltd.

UNCORRECTED PROOFS

Trim Size: 170mm x 244mm Single Column Loose Ribeiro670117 c03.tex V1 - 12/02/2020 11:04pm Page 62

and fitness for reuse. Case studies are described, illustrating routes to maximize contaminant removal or degradation, focusing on *in situ* application. Both bench-scale and pilot studies were considered, examining the efficiency of remediation carried out by combining techniques and the factors that can affect it. Advantages and disadvantages, as well as current knowledge gaps, of these combined technologies are described.

3.2 Biological Processes

3.2.1 Electrobioremediation

Bioremediation can be combined with electroremediation to enhance the bioavailability of nutrients, electron acceptors, and electron donors for catabolically active microorganisms [8]. Biological remediation techniques are considered cost-effective, efficient, and environmentally friendly. The combination of both technologies has been used to target different contaminants, mainly organics, such as PAHs [9–11], petroleum hydrocarbons [12–15], diesel [16, 17], cycloparaffinic hydrocarbons [18], herbicides [19], phthalate esters [20], metals such as Cr [21], As [22], and mixed contaminations [23, 24]. The synergistic effect between EK and bioremediation results from the fact that direct current allows electrochemical oxidation to occur, breaking down contaminants [14]. The combination of both remediation techniques can coincide or alternate. Alternating bioremediation and EK on the remediation of n-hexadecane spiked sandy loam soil enhanced the percentage of degradation to 79% after 45 days of treatment [25]. A recent review of electrokinetically enhanced bioremediation technologies for petroleum hydrocarbons details advances in electrokinetic bioattenuation, biostimulation, and bioaugmentation [26].

As soil is heterogeneous, biological processes occurring there are not as simple as those occurring in the liquid phase, and finding the conditions in which pollutants, microorganisms, and nutrients meet in the same treatment region becomes a key concern [16, 17]. Bioremediation can also be enhanced with electrokinetic soil flushing (EKSF), which is based on the use of a flushing solution to enhance removal of pollutants from soil by direct current [16, 17, 27]. The flushing fluid may contain surfactants, chelating agents, nutrients and salts, pH regulators, or other microorganisms that can aid in the efficient removal of pollution [16, 17, 28]. The addition of surfactant in electrobioremediation almost doubled the removal of a non-polar herbicide (oxyfluorfen) from a spiked clayey real soil [19, 29]. Electrokinetic injections of nutrients (e.g. nitrate, ammonia, phosphate) can also allow potentiating bioremediation [30] including removal of radioactive pollutants [31], e.g. Co^{2+} [32].

Several case studies using surfactant–enhanced electrokinetic treatment [33–38] are presented in Table 3.1, with specific cases of hybrid systems flushing chemical compounds to enhance electrokinetic treatment.

Another approach is the combined use of bioleaching (extraction of metals using living organisms) with EK. It was tested to remove metals from contaminated soil at

UNCORRECTED PROOFS

Trim Size: 170mm x 244mm Single Column Loose Ribeiro670117 c03.tex V1 - 12/02/2020 11:04pm Page 63

Table 3.1 Summary of recent research using surfactant-enhanced electrokinetic treatment.

Target contaminant	Surfactant	Experimental conditions	Removal efficiency (%)	Ref
Acenaphthene, phenanthrene, fluoranthene, pyrene, benzo(a)pyrene, and benzo(g,h,i)perylene	Tween 80	196.50 g l^{-1} Tween 80 in presence of Pt as anode, carbon – felt as cathode, 0.15 M Na_2SO_4, 2000 mA current, pH 3, 0.060 ± 0.013 mM Fe^{2+}, 0–40 mg l^{-1} O_3, pH 5.3–5.4 for 8 h	99	[114]
^{99m}Tc and ^{24}Na	Tween 80	4 h applying a current density of 0.06 mA cm^{-2} with a cell potential of 5 V in the presence of 50% Ultima Gold XR™ and 50% water (1 : 1) as scintillation liquid	61 and 72, respectively	[115]
Anthracene	Tween 80	3% Tween 80 with a constant voltage gradient of 1.5 V cm^{-1} for 10 days	38	[116]
Pb, Zn, Ni, and phenanthrene	Tween 80 and Brij 35	Tween 80 and Brij 35 with Na_2-EDTA applying 1.5 V cm^{-1} for 15 days	61, 48, and 65, respectively	[117]

an industrial site, achieving metal solubilization rates >70% for Cu, Zn, and Cr and >40% for Pb [39]. With current density higher than 1 mA cm^{-2}, the metal solubilization rates did not increase with increasing current density. These results at bench scale are a proof of concept that the combined use of both technologies can effectively lower the metal contents in the soil to environmentally safe levels, improve remediation efficiency, and shorten the operation time of bioleaching [39].

The use of electrobioremediation for contaminated groundwaters has also raised interest [40]. Benefits of the combined approach include the following: (i) electrodes can directly serve as electron donors or acceptors to support microbial metabolism; (ii) increased mass transport and mixing, driven by the formed electric field near the electrodes; and (iii) stimulation of microbial activity [40]. However, field application is limited by knowledge gaps in understanding the microbiology in groundwaters and tailoring the approach for site-specific process engineering [40].

There is also the potential to use EK to enhance the transport of microorganisms into low-permeability soils, namely organic contaminant degrading bacteria *Sphingomonas paucimobilis* EPA505 and *Mycobacterium vanbaalenii* PYR-1, for *in situ* bioaugmentation and remediation of PAH-contaminated soils [41].

The alteration of soil pH due to the acid and alkaline fronts from the anode and cathode, respectively, can be unfavorable for bacteria [30]. Polarity reversal of the electric field was shown to be an efficient option for pH, moisture, and temperature control for soil contaminated with diesel and petroleum hydrocarbons [16, 17, 42],

UNCORRECTED PROOFS

Trim Size: 170mm x 244mm Single Column Loose Ribeiro670117 c03.tex V1 - 12/02/2020 11:04pm Page 64

also enhancing nutrients distribution, microbial growth, and biodegradation of pyrene [10]. Polarity reversal was effective in minimizing extreme pH fronts in the soil and avoiding the need for a buffer for pH control [43, 44]. Other studies showed increased efficiency in contaminant removal but also a greater decrease in the microorganism population [45]. One of the drawbacks of polarity reversal is the fact that it requires continuous pH monitoring, which, in some cases, can be challenging and costly [30]. Other approaches for overcoming the issue of pH control in electrobioremediation include a novel anode-cathode compartment (ACC) [46] and the use of ion-exchange membranes [24]. However, up to now, both have only been tested at bench scale, and further research is needed for upscaling.

Potential shortcomings of electrobioremediation are as follows: (i) the need to maintain optimal conditions for microbial growth and proliferation; (ii) the process of mass transfer limits contaminant degradation [14]; (iii) limited studies on mixed contamination and the efficacy of both techniques combined; and (iv) upscaling of the combined technologies is conditioned by the lack of pilot and field studies to optimize variables such as positioning, type (material), and number of electrodes required. High energy consumption increases the overall cost of the remediation process and may become a major factor restricting the field application of two technologies combined without [47] or with circulation (circulation-enhanced electrokinetics [CEEK], [48, 49]). The use of solar panels can help overcome this challenge [9].

Advanced technologies – in particular, biotechnology and synthetic biology – provide excellent opportunities for enhancing electrokinetic bioremediation with reduced cost. This may involve several research components including prolonging the survival and function of the microbes in contaminated sites, identifying new bacterial strains with better performance in bioremediation, enhancing the metabolic ability of indigenous bacteria through microbial genetic engineering, exploring the rich microbial sources for potent contaminant degrading enzymes using metagenomics, and designing smart engineering tools for efficient bioremediation [30, 47].

3.2.2 Electro-Phytoremediation

This combined technology is based on the enhanced transport of contaminants by EK and the use of hyperaccumulator plants. These plants can accumulate high amounts of metals in a small volume of biomass, which makes them easier and cheaper to operate for either metals recovery or safe disposal [50–52]. Electro-phytoremediation has also been tested for mixed organic and metal contaminants [53]. The combination of EK with phytoremediation can enhance plant survival and growth rates and may be used to boost the remediation process for recalcitrant contaminants in complex subsurface conditions [53]. Table 3.2 presents a summary of recent studies using electro-phytoremediation.

Variables that can affect the efficacy of electro-phytoremediation include electric field intensity, use of alternate (AC) or direct (DC) current, mode of voltage application, electrodes configuration, and use of amendments to increase the bioavailability

UNCORRECTED PROOFS

UNCORRECTED PROOFS

Trim Size: 170mm x 244mm Single Column Loose

Ribeiro670117 c03.tex V1 - 12/02/2020 11:04pm Page 65

Table 3.2 Summary of recent research using electro-phytoremediation.

Target contaminant	Plant species	Electric field(V cm^{-1})	Voltage(V)	Duration(days)	Ref
Pb, Cs, and As	*Brassica juncea, Spinacia oleracea, Brassica rapa*	1	—	15	[118]
Pb	*Helianthus annuus*	—	10 and 30	14	[58]
Metals	*Eucalyptus globulese*	—	2, 4, and 10	30	[119]
Metals and PAH	*Lolium perenne*	0.2	—	30	[54]
Cd, Pb, and Cu	*Eucalyptus globulus*	—	4	14	[57]
Atrazine	*Zea mays*	2 and 4	—	14	[120]
Cd, Cu, Pb, and Zn	*Noccaea caerulescens*	—	2, 4, and 10	7	[59]
Pb	*Zea mays*	0.8	—	7	[48]
Metals and PAH	*Brassica rapa*	1 (DCV and ACV)	—	10	[55]
Petroleum hydrocarbons	*Helianthus annuus*	1	—	20	[121]
Petroleum hydrocarbons	*Lolium perenne L*	1	—	60	[122]

(Continued)

UNCORRECTED PROOFS

Trim Size: 170mm x 244mm Single Column Loose

Table 3.2 (Continued)

Target contaminant	Plant species	Electric field(V cm^{-1})	Voltage(V)	Duration(days)	Ref
Atrazine	*Lolium perenne*	1	—	20	[123]
Atrazine	*Zea mays*	2 and 4	—	14	[124]
Uranium	*Helianthus annuusBrassica juncea*	1	—	9	[125]
Cd, Zn, and Pb	*Brassica napus* and *Glycine max*	—	−0.6	2	[80]
Metals	*Vetiver grass*	1 (DCV) and 2 (ACV)	—	21	[126]
Atrazine	*Lolium perenne*	0.6	—	24	[127]
Atrazine	*Lolium perenne L.*	0.6	—	19	[128]

Note: DCV = direct current voltage; ACV = alternate current voltage.

Ribeiro670117 c03.tex V1 - 12/02/2020 11:04pm Page 66

Trim Size: 170mm x 244mm Single Column Loose Ribeiro670117 c03.tex V1 - 12/02/2020 11:04pm Page 67

of the contaminants or the growth of the plants [52]. Alternate current has displayed better results in case of mixed contaminations [54, 55]. Chelating agents, such as poultry manure extract, cow manure extract, and ethylenediaminetetraacetic acid (EDTA) were tested as enhancements for electro-phytoremediation, with EDTA being the most effective [49, 56–58]. The spatial distribution of the electrodes in soil has a decisive influence on the distribution of the electric field in soil. For lab applications, side-by-side electrodes are recommended because of the uniform electric field distribution. In field applications, parallel anode and cathode on the soil surface are recommended for straightforward implementation [55].

The use of electro-phytoremediation has an associated risk of some metals being mobilized and enriched in leachate instead of hyperaccumulated in plants. In mixed contaminated sites, combining EK and phytoremediation should be conducted with caution due to potential secondary environmental risks caused by mobile, non-hyperaccumulated metals [59].

3.3 Permeable Reactive Barriers

Permeable reactive barriers (PRBs) are a well-established, passive in situ technology for groundwater remediation. Although PRBs were initially applied to treat chlorinated hydrocarbon plumes, other applications include inorganic contaminants such as trace metals (e.g. chromium, manganese, uranium, zinc, lead) and anionic contaminants (sulfate, nitrate, phosphate, arsenate) [60]. Several bench-, large-, and pilot-scale studies of PRBs have been reported in the last 25 years [61]. The combination of electrokinetic remediation with PRBs has raised increased interest in the last five years, with several studies published (Table 3.3), most of them at bench scale. The use of both technologies together benefits from the fact that EK mobilizes the contaminants in low-permeability soils (mainly through electromigration and electroosmosis) and allows more uniform transport of contaminants. The acid generated at the anode also helps prevent the passive layer of iron corrosion products when zero-valent iron is used in the PRBs [62]. Complementary PRBs have the advantage of removing, degrading, or immobilizing contaminants through reduction, oxidation, adsorption, and/or precipitation [63].

Different materials and types of barriers have been developed and tested to tackle different contaminants, to optimize the efficacy of both techniques used (Table 3.3), but further effort in scaling up and test with real contaminated soils, preferably on-site, must be made to advance the implementation of EK and PRBs.

3.4 Advanced Oxidation Processes

3.4.1 Electrokinetics-Enhanced In Situ Chemical Oxidation (EK-ISCO)

In situ chemical oxidation (ISCO) is a mature technology used on contaminated soils and groundwaters, involving the injection or direct mixing of chemical oxidants

UNCORRECTED PROOFS

UNCORRECTED PROOFS

Trim Size: 170mm x 244mm Single Column Loose

Ribeiro670117 c03.tex V1 - 12/02/2020 11:04pm Page 68

Table 3.3 Summary of recent research using electroremediation combined with permeable reactive barriers.

Target contaminant	Soil	Type of barrier	Maximal removal (%)	Electric field ($V\,cm^{-1}$)	Voltage (V)	Duration (days, d; hours, h)	Ref
Nitrate	Model soil – kaolin	Anion exchange resin (Purolite A-520E)	90	1.0–2.0		7 d	[129]
Metals	Municipal solid waste incineration fly ash	Activated charcoal	80	1.5	—	10 d	[130]
Diesel	Model soil – kaolin	Biological (from active sludge)	30	1	—	14 d	[131]
Metals	Industrial contaminated soil	Electrospun polyacrylonitrile nanofiber membrane	99.7	—	10, 25, 50	13 d	[132]
Mercury	Soil from mining site	Zero-valent iron (Fe^0)	84	—	20	3 d	[133]
Perchloroethylene (PCE)	Spiked farmland soil	Zero-valent iron (Fe^0)	80	1	—	10 d	[134]
Diesel	Model soil – kaolin	Biological (from active sludge)	29	0.5 and 1	—	14 d	[135]
Diesel	Model soil – kaolin	Biological (from active sludge) with polarity reversal	36	1.5	—	15 d	[136]
Copper	Model soil – kaolin	Activated carbon	97	1	—	4 d	[137]
Fluorine	Real contaminated soil	Modified activated alumina	76	2	—	10 d	[138]
Fluorine	Model soil – kaolin	Bamboo charcoal	76	1 and 1.5	—	7 d	[139]
Cadmium	Spiked soil	Humin	44	—	20	10 d	[140]
Chlorsulfuron and 2,4-D	Model soil – kaolin	Reversible adsorption barrier (microscale Pd/Fe PRB)	72	1	—	15 d	[141]
Phenanthrene (PHE) and 2,4,6-trichlorophenol (TCP)	Spiked clay soil	Zero-valent iron/activated carbon	64	1	—	15 d	[142]

(Continued)

UNCORRECTED PROOFS

Trim Size: 170mm x 244mm Single Column Loose

Ribeiro670117 c03.tex V1 - 12/02/2020 11:04pm Page 69

Table 3.3 (Continued)

Target contaminant	Soil	Type of barrier	Maximal removal (%)	Electric field ($V\,cm^{-1}$)	Voltage (V)	Duration (days, d; hours, h)	Ref
Atrazine and oxyfluorfen	Model soil – kaolin	Reversible adsorption barrier (microscale Pd/Fe PRB)	90	1	—	15 d	[143]
Chromium	Spiked clay soil	CaAl-LDH permeable reaction barrier	96	1, 1.5, 2	—	5 d	[144]
Nitrate	Synthetically contaminated water	Activated carbon (with in situ regeneration)	76	1.25	—	3 d	[145]
Clopyralid	Spiked silty loam soil	Permeable reactive barrier; reversible electrokinetic adsorption barrier (activated carbon)	57	1	—	30 d	[146]
Chlorinated hydrocarbons	Natural soil from a quarry located in Mora (Toledo, Spain)	Permeable reactive barrier (zero-valent iron)	60	1	—	850 h	[147]
2,4-dichlorophenoxyacetic acid (2,4-D)	Spiked clay soil	Biological permeable reactive barrier (biofilm)	85	1	—	10 d	[148]
Selenite	Model soil – kaolin	Reactive barrier (activated carbon loaded with nanoscale zero-valent iron)	85	0.5, 1, 2	—	1–12 d	[149]
Cr (VI)	Model soil – quartz sand	Permeable reactive barrier hybrid system (polypyrrole – linen fabric, PPy – LF)	80.8	1	—	72 h	[150]
Arsenic	Historically contaminated soil	Permeable reactive barrier (zero-valent iron)	45	1	—	4 d	[151]
Lindane	Natural soil from a quarry located in Mora (Toledo, Spain)	Permeable reactive barrier (zero-valent iron)	67	1	—	720 h	[152]
Cadmium	Model soil – kaolin	Permeable reactive barrier (zeolite and zero-valent iron)	93	1.5–3.0	—	5 d	[63]

Trim Size: 170mm x 244mm Single Column Loose Ribeiro670117 c03.tex V1 - 12/02/2020 11:04pm Page 70

for rapid and complete degradation of contaminants (mainly organic; in particular, chlorinated solvents and petroleum hydrocarbons). It is often used in zone sources and contaminant plumes with moderate to high contamination, significant sorbed contamination, and, in some cases, the presence of residual, separate-phase contamination.

Commonly used chemical oxidants (permanganate and persulfate) are negatively charged and highly mobile through electromigration in low-permeability soils, so the combination of EK and ISCO allows a better distribution of the oxidants in the contaminated area [7, 64]. Both used together overcome the limited ability to penetrate low-permeability soils presented by ISCO.

The use of EK enhances the transport of an oxidant – permanganate – to degrade persistent organic contaminants such as PCBs [65, 66], organochlorine compounds [67], trichloroethene (TCE) [68], δ-triazine herbicides [69], phthalate esters [20], and ibuprofen [70]. The combined use of both technologies can enhance the remediation of low-permeability soils/matrices and simultaneously limit the extent of contaminant back-diffusion [68]. Electrokinetic oxidant soil flushing was tested with sodium hypochlorite (NaOCl), potassium permanganate ($KMnO_4$), and sodium persulfate ($Na_2S_2O_8$) for petroleum hydrocarbons in real historically contaminated soil, showing 40–60% removal [71].

Cheng et al. ([35], [36]) reported a combination of hydroxypropyl-β-cyclodextrin, citric acid, and sodium persulfate with Fe^{2+} to remove metals and persistent organic pollutants such as Cu, Pb, Ni, PCBs, PAHs, and polybrominated diphenyl ethers between 180 and 240 minutes with removal efficiencies of 69%, 74%, 97%, 93%, and 96%, respectively.

3.4.2 Electro-Fenton

Electro-Fenton is an integrated technology incorporating chemical oxidation by Fenton's process with the electrokinetic treatment. In this combined technology, there is *in situ* generation of hydroxyl radicals due to the decomposition of H_2O_2 by the catalytic action of iron present in the matrix, mobilized through the soil by the action of direct current [38, 72–74]. A detailed review of the application of electro-Fenton can be found in Oonnittan and Sillanpää [75].

The electrokinetic-Fenton technology, coupled with surfactants for *ex situ* treatment of real soils historically polluted with petroleum hydrocarbons, showed promising results (>72% removal) [38]. Batch tests with electrokinetic-Fenton technology enhanced by citric acid showed 58% removal of total petroleum hydrocarbons from an industrially contaminated soil [76].

Organochlorine pesticides, such as hexachlorocyclohexane soprocide (HCH) and dichloro-diphenyl-trichloroethane (DDT), were also treated with electro-Fenton technology in historically contaminated soils, showing removals higher than 72% in the enhanced treatment with pH control and addition of a solubilizer and electrolyte [77].

Soil acidification, polarity reversal, positioning, configuration, and type of electrodes are variables to consider in optimizing an electro-Fenton application [75, 78].

UNCORRECTED PROOFS

Trim Size: 170mm x 244mm Single Column Loose Ribeiro670117 c03.tex V1 - 12/02/2020 11:04pm Page 71

Regarding the type of electrodes, carbon materials [38, 79], Pt/Pb [80], or Fe/Al [81] were used for both organic and inorganic contaminants. However, electro-Fenton is essential to generate the oxidant species close to the anode, e.g. hydroxyl radical ($^{\bullet}$OH). For this reason, dimensionally stable anodes are preferable, such as Ru/Ir oxides [12, 82–84], Ir/Ta oxides [85, 86], and boron-doped diamond (BDD, [87, 88]).

3.5 *In Situ* Chemical Reduction (ISCR)

The use of zero-valent iron nanoparticles (nZVI) combined with EK for in situ chemical reduction (ISCR) of persistent organic pollutants has been extensively studied for heavy metals and chlorinated organic compounds [89], PCBs ([90–95]), and chlorinated ethenes [96]. Other contaminants, such as chromium [97], arsenic [98], and the herbicide molinate [99] were also targeted. A review of the dynamic processes occurring in EK coupled with nanoparticles can be found in Herrada et al. [100].

The numerical modeling of zero-valent iron nanoparticle transport under direct current was described in Gomes et al. [101]. A recent long-term study of the combined use of nZVI at pilot scale for the remediation of a site contaminated with chlorinated ethenes showed that there were economic benefits to using both techniques simultaneously, with excellent activity and low toxicity for the remotion of heavy metals and organic pollutants [102, 103]. The economic effectiveness was approximately six times higher than the deployment of nZVI alone, making the application of nZVI with EK competitive with chemical oxidation [104].

3.6 Challenges for Upscaling

Much of the knowledge of EK and the use of combined technologies is limited to results obtained in studies conducted at bench scale in a controlled environment, where soil is in airtight cells. Also, in most cases, model soils such as kaolin are used in the tests, which do not adequately represent the complex matrices in real historically contaminated soils. Therefore, extrapolating these results to real applications is questionable, leading to the need to scale the process [105]. Site-specific conditions must also be considered when conceptualizing a soil-remediation treatment and contemplating the use of combined technologies.

Pilot studies on the use of combined technologies targeting different contaminants in the last five years include:

- Electrochemically assisted fences for the electroremediation of soils polluted with 2,4-dichlorophenoxy acetic acid (2,4-D) [106]
- Mock-up electrokinetic reactor at pilot scale (volume of 0.175 m^3) and a prototype with a capacity of 16 m^3 to treat 2,4-D contaminated soil [105]
- Pilot of 3.3 m^3 of real pelic-type Vertisol contaminated with petroleum hydrocarbons, using a 2D circular arrangement of electrodes combined with a process of advanced oxidation for leachate treatment [84]

UNCORRECTED PROOFS

Trim Size: 170mm x 244mm Single Column Loose Ribeiro670117 c03.tex V1 - 12/02/2020 11:04pm Page 72

- EKSF with facing rows of electrodes for 2,4-D at pilot scale (0.175 m^3) [107]
- EKSF with a surrounding electrode arrangements for 2,4-D at pilot scale (0.175 m^3) [108]
- EKSF with linear rows of electrodes for oxyfluorfen at pilot scale (0.175 m^3) [109]
- EKSF with surrounding electrodes for oxyfluorfen at pilot scale (0.175 m^3) [110]
- Electrobioremediation at prototype scale (32 m^3) of oxyfluorfen and 2,4-D acid contaminated soil [111]
- Electro-phytoremediation at field scale (0.6 m^3) in a metal (Pb)-contaminated site using *Zea mays* [48]
- Pilot study of electrobioremediation of PAH-contaminated soil (157.5 m^3) with alternating polarity [11]
- Long-term (three-year) pilot test using EK and nZVI for chlorinated ethenes [104]

These pilot studies have shown that volatilization of pollutants due to soil heating is a critical issue that should be accounted for in the design of full-scale processes ([106, 107]). Volatilization is caused by an increase in temperature, which in turn is due to ohmic loses [111]. Also, evaporation and possible leaks are important. These processes should be identified and quantified because they influence the development of the EK process itself, altering the soil's water content and possibly promoting the formation of soil cracks [105]. Perimeter control of the pilot-scale reactor is a crucial aspect, and drainage wells should be included that allow for identifying possible leaks [105].

Several difficulties were found regarding optimizing simultaneously electrokinetic and biological processes, as most of the processes caused by the electric field negatively affect the viability of the microorganisms [111]. Further research on electrobioremediation at pilot scale should address these issues.

Another critical factor is the sampling procedure for monitoring the remediation process. Although liquid samples taken at boreholes can be used to monitor changes in the soil during remediation, the results obtained are not as accurate as those obtained by a postmortem analysis [111].

The different physicochemical properties of soil are important to increase the removal efficiency of remediation technologies combined with EK at the lab, pilot, and field scales to remove organic, inorganic, or mixed pollutants from soil [35, 36, 112]. The change of scale considerably influences the amount of electric energy consumed in the process and, consequently, the intensity with which the different electrokinetic processes are developed [105]. Also, the running time of the pilot studies is critical. The only long-term study published showed that EK used in conjunction with zero-valent nanoparticles required annual reinstallation of anodes due to their oxidative disintegration [104]. Despite this, the method provides significantly improved chlorinated ethane reduction, remediation of low-permeable zones, and extended efficiency, and it is five times cheaper when compared to the nZVI used alone. Rede et al. [74] indicated that chemical soil remediation could be more prejudicial for terrestrial organisms than contaminated soil. In this sense, Gong et al. [113] indicated that combined technologies are better than single technologies alone, although requiring complex operating conditions to take into account technical, economic, and sustainability issues.

UNCORRECTED PROOFS

Trim Size: 170mm x 244mm Single Column Loose Ribeiro670117 c03.tex V1 - 12/02/2020 11:04pm Page 73

3.7 Concluding Remarks

The soil contamination problem worldwide demands cost-effective, sustainable alternatives for *in situ* application with minimal disturbance of the site. The combined use of electrokinetic remediation with other technologies can result in synergistic effects, where some of the drawbacks of each technology can be overcome. Electrokinetics is particularly suited for low-permeability soils where most of the traditional remediation technologies show limited efficacy.

Currently, there is no one-solution-fits-all for remediation of contaminated soils, and solutions should be tailored to each site. In the case of coupled technologies, optimizing operation conditions to deal with soil properties, contamination, and site-specific problems (e.g. drainage, connection to electric power) and monitoring and control of the process are essential for success.

There is potential for the remediation of emerging contaminants, mixed contaminations, and further development of combinations of electrokinetics with novel remediation technologies.

References

1 Oberle, B., Bringezu, S., Hatfield-Dodds, S. et al. (2019). *Global Resources Outlook 2019: Natural Resources for the Future we Want. A Report of the International Resource Panel*. Nairobi, Kenya: United Nations Environment Programme.

2 Rodríguez-Eugenio, N., McLaughlin, M., and Pennock, D. (2018). *Soil Pollution: A Hidden Reality*. FAO.

3 Carré, F., Caudeville, J., Bonnard, R. et al. (2017). Soil contamination and human health: a major challenge for global soil security. In: *Global Soil Security* (eds. D.J. Field, C.L.S. Morgan and A.B. McBratney), 275–295. Cham: Springer International Publishing.

4 Ottosen, L.M., Larsen, T.H., Jensen, P.E. et al. (2019). Electrokinetics applied in remediation of subsurface soil contaminated with chlorinated ethenes – a review. *Chemosphere* 235: 113–125.

5 Cameselle, C. and Gouveia, S. (2018). Electrokinetic remediation for the removal of organic contaminants in soils. *Current Opinion in Electrochemistry* 11: 41–47.

6 Kuppusamy, S., Thavamani, P., Venkateswarlu, K. et al. (2017). Remediation approaches for polycyclic aromatic hydrocarbons (PAHs) contaminated soils: technological constraints, emerging trends and future directions. *Chemosphere* 168: 944–968.

7 Lima, A.T., Hofmann, A., Reynolds, D. et al. (2017). Environmental electrokinetics for a sustainable subsurface. *Chemosphere* 181: 122–133.

8 Gomes, H.I., Dias-Ferreira, C., and Ribeiro, A.B. (2012a). Electrokinetic remediation of organochlorines in soil: enhancement techniques and integration with other remediation technologies. *Chemosphere* 87: 1077–1090.

UNCORRECTED PROOFS

Trim Size: 170mm x 244mm Single Column Loose Ribeiro670117 c03.tex V1 - 12/02/2020 11:04pm Page 74

9 Hassan, I., Mohamedelhassan, E., Yanful, E.K., and Yuan, Z.-C. (2017). Solar power enhancement of electrokinetic bioremediation of phenanthrene by *Mycobacterium pallens*. *Bioremediation Journal* 21: 53–70.

10 Li, T., Wang, Y., Guo, S. et al. (2016). Effect of polarity-reversal on electrokinetic enhanced bioremediation of pyrene contaminated soil. *Electrochimica Acta* 187: 567–575.

11 Li, F., Guo, S., Wu, B., and Wang, S. (2019a). Pilot-scale electro-bioremediation of heavily PAH-contaminated soil from an abandoned coking plant site. *Chemosphere* 244: 125467.

12 Cappello, S., Cruz Viggi, C., Yakimov, M. et al. (2019). Combining electrokinetic transport and bioremediation of enhanced removal of crude oil from contaminated marine sediments: results of a long-term, mesocosm-scale experiment. *Water Research* 157: 381–395.

13 Daghio, M., Aulenta, F., Vaiopoulou, E. et al. (2017). Electrobioremediation of oil spills. *Water Research* 114: 351–370.

14 Fan, R., Guo, S., Li, T. et al. (2015). Contributions of electrokinetics and bioremediation in the treatment of different petroleum components. *CLEAN – Soil, Air, Water* 43: 251–259.

15 Ossai, I.C., Ahmed, A., Hassan, A., and Hamid, F.S. (2020). Remediation of soil and water contaminated with petroleum hydrocarbon: a review. *Environmental Technology & Innovation* 17: 100526–100568.

16 Ramírez, E.M., Camacho, J.V., Rodrigo, M.A., and Cañizares, P. (2015a). Combination of bioremediation and electrokinetics for the in-situ treatment of diesel polluted soil: a comparison of strategies. *Science of the Total Environment* 533: 307–316.

17 Ramírez, E.M., Jimenez, C.S., Camacho, J.V. et al. (2015b). Feasibility of coupling permeable bio-barriers and electrokinetics for the treatment of diesel hydrocabons polluted soils. *Electrochimica Acta* 181: 192–199.

18 Yuan, Y., Guo, S., Li, F. et al. (2016). Coupling electrokinetics with microbial biodegradation enhances the removal of cycloparaffinic hydrocarbons in soils. *Journal of Hazardous Materials* 320: 591–601.

19 Barba, S., Villaseñor, J., Rodrigo, M.A., and Cañizares, P. (2017). Effect of the polarity reversal frequency in the electrokinetic-biological remediation of oxyfluorfen polluted soil. *Chemosphere* 177: 120–127.

20 Yang, G.C.C. (2019). Integrated electrokinetic processes for the remediation of phthalate esters in river sediments: a mini-review. *Science of the Total Environment* 659: 963–972.

21 He, J., He, C., Chen, X. et al. (2018). Comparative study of remediation of Cr(VI)-contaminated soil using electrokinetics combined with bioremediation. *Environmental Science and Pollution Research* 25: 17682–17689.

22 Roy, M., Giri, A.K., Dutta, S., and Mukherjee, P. (2015). Integrated microbial remediation for sustainable management of arsenic in soil and water. *Environment International* 75: 180–198.

23 Feng, Y., Yang, S., Xia, L. et al. (2019). In-situ ion exchange electrocatalysis biological coupling (i-IEEBC) for simultaneously enhanced degradation of

UNCORRECTED PROOFS

Trim Size: 170mm x 244mm Single Column Loose Ribeiro670117 c03.tex V1 - 12/02/2020 11:04pm Page 75

organic pollutants and heavy metals in electroplating wastewater. *Journal of Hazardous Materials* 364: 562–570.

24 Ma, Y., Li, X., Mao, H. et al. (2018). Remediation of hydrocarbon–heavy metal co-contaminated soil by electrokinetics combined with biostimulation. *Chemical Engineering Journal* 353: 410–418.

25 Wang, S., Guo, S., Li, F. et al. (2016). Effect of alternating bioremediation and electrokinetics on the remediation of n-hexadecane-contaminated soil. *Scientific Reports* 6: 23833.

26 Saini, A., Bekele, D.N., Chadalavada, S. et al. (2020). A review of electrokinetically enhanced bioremediation technologies for PHs. *Journal of Environmental Sciences* 88: 31–45.

27 Morillo, E. and Villaverde, J. (2017). Advanced technologies for the remediation of pesticide-contaminated soils. *Science of the Total Environment* 586: 576–597.

28 Ramadan, B.S., Sari, G.L., Rosmalina, R.T. et al. (2018). An overview of electrokinetic soil flushing and its effect on bioremediation of hydrocarbon contaminated soil. *Journal of Environmental Management* 218: 309–321.

29 Barba, S., Carvela, M., Villaseñor, J. et al. (2019b). Improvement of the electro-bioremediation process of a non-polar herbicide-polluted soil by means of surfactant addition. *Science of the Total Environment* 650: 1961–1968.

30 Hassan, I., Mohamedelhassan, E., Yanful, E.K., and Yuan, Z.-C. (2018b). Enhancement of bioremediation and phytoremediation using electrokinetics. *Advances in Bioremediation and Phytoremediation* 169: 169–189.

31 Zhang, X., Gu, P., and Liu, Y. (2019). Decontamination of radioactive wastewater: state of the art and challenges forward. *Chemosphere* 215: 543–553.

32 Thanh, I.H.V. and Liu, J.C. (2017). Flotation separation of strontium via phosphate precipitation. *Water Science Technology* 75: 2520–2526.

33 Ammami, M.T., Portet-Koltalo, F., Benamar, A. et al. (2015). Application of biosurfactants and periodic voltage gradient for enhanced electrokinetic remediation of metals and PAHs in dredged marine sediments. *Chemosphere* 125: 1–8.

34 Burger, A. and Lichtscheidl, I. (2018). Stable and radioactive caesium: a review about distribution in the environment, uptake and translocation in plants, plant reactions and plants' potential for bioremediation. *Science of the Total Environment* 618: 1459–1485.

35 Cheng, M., Zeng, G., Huang, D. et al. (2017a). Advantages and challenges of Tween80 surfactant-enhanced technologies for the remediation of soils contaminated with hydrophobic organic compounds. *Chemical Engineering Journal* 314: 98–113.

36 Cheng, F., Luo, Z., Liu, G. et al. (2017b). Remediation of electronic waste polluted soil using a combination of persulfate oxidation and chemical washing. *Journal of Environmental Management* 204: 170–178.

37 Karthick, A., Roy, B., and Chattopadhyay, P. (2019). A review on the application of chemical surfactant and surfactant foam for remediation of petroleum oil contaminated soil. *Journal of Environmental Management* 243: 187–205.

UNCORRECTED PROOFS

Trim Size: 170mm x 244mm Single Column Loose Ribeiro670117 c03.tex V1 - 12/02/2020 11:04pm Page 76

38 Sandu, C., Popescu, M., Rosales, E. et al. (2016). Electrokinetic-Fenton technology for the remediation of hydrocarbons historically polluted sites. *Chemosphere* 156: 347–356.

39 Huang, Q., Yu, Z., Pang, Y. et al. (2015a). Coupling bioleaching and electrokinetics to remediate heavy metal contaminated soils. *Bulletin of Environmental Contamination and Toxicology* 94: 519–524.

40 Li, W.-W. and Yu, H.-Q. (2015). Electro-assisted groundwater bioremediation: fundamentals, challenges and future perspectives. *Bioresource Technology* 196: 677–684.

41 Secord, E.L., Kottara, A., Van Cappellen, P., and Lima, A.T. (2016). Inoculating bacteria into polycyclic aromatic hydrocarbon-contaminated oil sands soil by means of electrokinetics. *Water, Air, & Soil Pollution* 227: 288.

42 Zhang, M., Guo, P., Wu, B., and Guo, S. (2020). Change in soil ion content and soil water-holding capacity during electro-bioremediation of petroleum contaminated saline soil. *Journal of Hazardous Materials* 387: 122003.

43 Mena, E., Villaseñor, J., Rodrigo, M.A., and Cañizares, P. (2015b). Combination of bioremediation and electrokinetics for the in-situ treatment of diesel polluted soil: a comparison of strategies. *Science of the Total Environment* 533: 307–316.

44 Mena, E., Villaseñor, J., Cañizares, P., and Rodrigo, M.A. (2016a). Effect of electric field on the performance of soil electro-bioremediation with a periodic polarity reversal strategy. *Chemosphere* 146: 300–307.

45 Barba, S., Villaseñor, J., Rodrigo, M.A., and Cañizares, P. (2018b). Can electro-bioremediation of polluted soils perform as a self-sustainable process? *Journal of Applied Electrochemistry* 48: 579–588.

46 Hassan, I., Mohamedelhassan, E., Yanful, E., and Bo, M.W. (2018a). Enhanced electrokinetic bioremediation by pH stabilisation. *Environmental Geotechnics* 5: 222–233.

47 Hassan, I., Mohamedelhassan, E., Yanful, E.K., and Yuan, Z.-C. (2016). A review article: Electrokinetic bioremediation current knowledge and new prospects. *Advances in Microbiology* 6: 57.

48 Chang, J.-H., Dong, C.-D., and Shen, S.-Y. (2019). The lead contaminated land treated by the circulation-enhanced electrokinetics and phytoremediation in field scale. *Journal of Hazardous Materials* 368: 894–898.

49 Chang, J.-H., Dong, C.-D., Huang, S.-H., and Shen, S.-Y. (2020). The study on lead desorption from the real-field contaminated soil by circulation-enhanced electrokinetics (CEEK) with EDTA. *Journal of Hazardous Materials* 383: 121194–121200.

50 Couto, N., Guedes, P., Ribeiro, A.B., and Zhou, D.-M. (2015). Phytoremediation and the electrokinetic process: potential use for the phytoremediation of antimony and arsenic. In: *Phytoremediation: Management of Environmental Contaminants*, vol. 2 (eds. A.A. Ansari, S.S. Gill, R. Gill, et al.), 199–209. Springer International Publishing, Springer.

51 Guedes, P., Couto, N., Ribeiro, A.B., and Zhou, D.-M. (2016). Chapter 16. Phytoremediation coupled to electrochemical process for arsenic removal from

UNCORRECTED PROOFS

Trim Size: 170mm x 244mm Single Column Loose Ribeiro670117 c03.tex V1 - 12/02/2020 11:04pm Page 77

soil. In: *Electrokinetics across Disciplines and Continents. New Strategies for Sustainable Development* (eds. A.B. Ribeiro, E.P. Mateus and N. Couto), 313–329. Springer International Publishing.

52 Mao, X., Han, F.X., Shao, X., and Su, Y. (2015). Coupled electrokinetic remediation and phytoremediation of metal (loid) contaminated soils. *Journal of Bioremediation & Biodegradation* 6: e163.

53 Chirakkara, R.A., Cameselle, C., and Reddy, K.R. (2016). Assessing the applicability of phytoremediation of soils with mixed organic and heavy metal contaminants. *Reviews in Environmental Science and Bio/Technology* 15: 299–326.

54 Acosta-Santoyo, G., Cameselle, C., and Bustos, E. (2017). Electrokinetic – enhanced ryegrass cultures in soils polluted with organic and inorganic compounds. *Environmental Research* 158: 118–125.

55 Cameselle, C. and Gouveia, S. (2019). Phytoremediation of mixed contaminated soil enhanced with electric current. *Journal of Hazardous Materials* 361: 95–102.

56 Khalid, S., Shahid, M., Niazi, N.K. et al. (2017). A comparison of technologies for remediation of heavy metal contaminated soil. *Journal of Geochemical Exploration* 182: 247–268.

57 Luo, J., Cai, L., Qi Sh, W.J., and Gu, X.W.S. (2018). The interactive effects between chelator and electric fields on the leaching risk of metals and the phytoremediation efficiency of *Eucalyptus globulus*. *Journal of Cleaner Production* 202: 830–837.

58 Tahmasbian, I. and Safari Sinegani, A.A. (2016). Improving the efficiency of phytoremediation using electrically charged plant and chelating agents. *Environmental Science and Pollution Research* 23: 2479–2486.

59 Luo, J., Xing, X., Qi, S. et al. (2019). Comparing the risk of metal leaching in phytoremediation using *Noccaea caerulescens* with or without electric field. *Chemosphere* 216: 661–668.

60 Bekele, D.N., Naidu, R., Birke, V., and Chadalavada, S. (2018). Choosing the best design and construction technologies for permeable reactive barriers. In: *Permeable Reactive Barrier. Sustainable Groundwater Remediation* (ed. V.B. Ravi Naidu), 56–77. CRC Press.

61 Floris, B., Galloni, P., Sabuzi, F., and Conte, V. (2017). Metal systems as tools for soil remediation. *Inorganica Chimica Acta* 455: 429–445.

62 Suzuki, T., Oyama, Y., Moribe, M., and Niinae, M. (2012). An electrokinetic/Fe0 permeable reactive barrier system for the treatment of nitrate-contaminated subsurface soils. *Water Research* 46: 772–778.

63 Zhou, H., Xu, J., Lv, S. et al. (2020). Removal of cadmium in contaminated kaolin by new-style electrokinetic remediation using array electrodes coupled with permeable reactive barrier. *Separation and Purification Technology* 239: 116544.

64 Huang, D., Hu, C., Zeng, G. et al. (2017). Combination of Fenton processes and biotreatment for wastewater treatment and soil remediation. *Science of the Total Environment* 574: 1599–1610.

UNCORRECTED PROOFS

Trim Size: 170mm x 244mm Single Column Loose Ribeiro670117 c03.tex V1 - 12/02/2020 11:04pm Page 78

65 Fan, G., Cang, L., Gomes, H.I., and Zhou, D. (2016). Electrokinetic delivery of persulfate to remediate PCBs polluted soils: effect of different activation methods. *Chemosphere* 144: 138–147.

66 Zhou, Z., Liu, X., Sun, K. et al. (2019). Persulfate-based advanced oxidation processes (AOPs) for organic-contaminated soil remediation: a review. *Chemical Engineering Journal* 372: 836–851.

67 Suanon, F., Tang, L., Sheng, H. et al. (2020). TW80 and GLDA-enhanced oxidation under electrokinetic remediation for aged contaminated-soil: does it worth? *Chemical Engineering Journal* 385: 123934–123944.

68 Chowdhury, A.I.A., Gerhard, J.I., Reynolds, D. et al. (2017). Electrokinetic-enhanced permanganate delivery and remediation of contaminated low permeability porous media. *Water Research* 113: 215–222.

69 Chen, L., Hu, X., Yang, Y. et al. (2018). Degradation of atrazine and structurally related δ-triazine herbicides in soils by ferrous-activated persulfate: kinetics, mechanism and soil-types effects. *Chemical Engineering Journal* 351: 523–531.

70 Liu, Y., Wang Sh, W.Y., Chen, H. et al. (2019). Degradation of ibuprofen by thermally activated persulfate in soil systems. *Chemical Engineering* 356: 799–810.

71 Sandu, C., Popescu, M., Rosales, E. et al. (2017). Electrokinetic oxidant soil flushing: a solution for in situ remediation of hydrocarbons polluted soils. *Journal of Electroanalytical Chemistry* 799: 1–8.

72 Maletic, S.P., Beljin, J.M., Roncevic, S.D. et al. (2019). State of the art and future challenges for polycyclic aromatic hydrocarbons in sediments: sources, fate, bioavailability and remdiation techniques. *Journal of Hazardous Materials* 365: 467–482.

73 Poza-Nogueiras, V., Rosales, E., Pazos, M., and Sanromán, M.A. (2018). Current advances and trends in electro-Fenton process using heterogeneous catalysts - a review. *Chemosphere* 201: 399–416.

74 Rede, D., Santos, L.H.M.I.M., Ramos, S. et al. (2016). Ecotoxicological impact of two soil remediation treatments in *Lactuca sativa* seeds. *Chemosphere* 159: 193–198.

75 Oonnittan, A. and Sillanpää, M. (2020). Chapter 2 - application of electrokinetic Fenton process for the remediation of soil contaminated with HCB. In: *Advanced Water Treatment* (ed. M. Sillanpää), 57–93. Elsevier.

76 Popescu, M., Rosales, E., Sandu, C. et al. (2017). Soil flushing and simultaneous degradation of organic pollutants in soils by electrokinetic-Fenton treatment. *Process Safety and Environmental Protection* 108: 99–107.

77 Ni, M., Tian, S., Huang, Q., and Yang, Y. (2018). Electrokinetic-Fenton remediation of organochlorine pesticides from historically polluted soil. *Environmental Science and Pollution Research* 25: 12159–12168.

78 Usman, M., Hanna, K., and Haderlein, S. (2016). Fenton oxidation to remediate PAHs in contaminated soils: a critical review of major limitations and counter-strategies. *Science of the Total Environment* 569–570: 179–190.

UNCORRECTED PROOFS

Trim Size: 170mm x 244mm Single Column Loose Ribeiro670117 c03.tex V1 - 12/02/2020 11:04pm Page 79

79 Bocos, E., Fernández-Costas, C., Pazos, M., and Sanromán, M.A. (2015). Removal of PAHs and pesticides from polluted soils by enhanced electrokinetic-Fenton treatment. *Chemosphere* 125: 168–174.

80 Delil, A.D., Köleli, N., Daghan, H., and Bahceci, G. (2020). Recovery of heavy metals from canola (*Brassica napus*) and soybean (*Glycine max*) biomasses using electrochemical process. *Environmental Technology and Innovation* 17: 100559–100570.

81 Hung, C.-H., Yuan Ch, W.M.-H., and Chang, Y.-C. (2018). Electrochemical degradation of ibuprofen-contaminated soils over Fe/Al oxidation electrodes. *Science of the Total Environment* 640–641: 1205–1213.

82 Cuevas, O., Herrada, R.A., Corona, J.L. et al. (2016). Assessment of IrO_2-Ta_2O_5|Ti electrodes for the electrokinetic treatment of hydrocarbon-contaminated soil using different electrode arrays. *Electrochimica Acta* 208: 282–287.

83 Herrada, R.A., Medel, A., Manríquez, F. et al. (2016). Preparation of IrO_2-Ta_2O_5|Ti electrodes by immersion, painting and electrophoretic deposition for the electrochemical removal of hydrocarbons from water. *Journal of Hazardous Materials*: 102–110.

84 Ochoa, B., Ramos, L., Garibay, A. et al. (2016). Electrokinetic treatment of polluted soil at pilot level coupled to an advanced oxidation process of its wastewater. *Physics and Chemistry of the Earth, Parts A/B/C* 91: 68–76.

85 Pérez-Corona, M., Plank, Z., and Bustos, E. (2016). The electrokinetic treatment of polluted soil by hydrocarbon: from laboratory to field. In: *Soil Contamination - Current Consequences and Further Solutions* (eds. I. Larramendy and S. Soloneski), 289–305. InTech.

86 Pérez-Corona, M., Rodríguez-Maroto, J.M., Gómez-Lahoz, C., and Bustos, E. (2018). Electroremediation of sodium bentonite contaminated with phenanthrene and its modeling with a Nernst-Planck equation. *Journal of Applied Electrochemistry* 48: 1373–1380.

87 Dos Santos, E.V., Sáez, C., Martínez-Huitle, C.A. et al. (2015). Combined soil washing and CDEO for the removal of atrazine from soils. *Journal of Hazardous Materials* 300: 129–134.

88 Medel, A., Patiño, D., Méndez, E. et al. (2015). Novel electrokinetic remediation system - boron doped diamond (EKR - BDD) process for the destruction of polyaromatic hydrocarbons (PAHs) in liquid phase. *Environmental Engineering and Management Journal* 14: 879–886.

89 Xue, W., Huang, D., Zeng, G. et al. (2018). Performance and toxicity assessment of nanoscale zero valent iron particles in the remediation of contaminated soil: a review. *Chemosphere* 210: 1145–1156.

90 Fan, G., Cang, L., Qin, W. et al. (2013). Surfactants-enhanced electrokinetic transport of xanthan gum stabilized nanoPd/Fe for the remediation of PCBs contaminated soils. *Separation and Purification Technology* 114: 64–72.

91 Gomes, H.I., Dias-Ferreira, C., Ottosen, L.M., and Ribeiro, A.B. (2014a). Electrodialytic remediation of polychlorinated biphenyls contaminated soil with iron nanoparticles and two different surfactants. *Journal of Colloid and Interface Science* 433: 189–195.

UNCORRECTED PROOFS

Trim Size: 170mm x 244mm Single Column Loose Ribeiro670117 c03.tex V1 - 12/02/2020 11:04pm Page 80

92 Gomes, H.I., Dias-Ferreira, C., Ottosen, L.M., and Ribeiro, A.B. (2015a). Electroremediation of PCB contaminated soil combined with iron nanoparticles: effect of the soil type. *Chemosphere* 131: 157–163.

93 Gomes, H.I., Ottosen, L.M., Ribeiro, A.B., and Dias-Ferreira, C. (2015b). Treatment of a suspension of PCB contaminated soil using iron nanoparticles and electric current. *Journal of Environmental Management* 151: 550–555.

94 Gomes, H.I., Fan, G., Ottosen, L.M. et al. (2016a). Chapter 17. Nanoremediation coupled to electrokinetics for PCB removal from soils. In: *Electrokinetics across Disciplines and Continents. New Strategies for Sustainable Development* (eds. A.B. Ribeiro, E.P. Mateus and N. Couto), 331–350. Springer International Publishing.

95 Gomes, H.I., Rodríguez-Maroto, J.M., Ribeiro, A.B. et al. (2016b). Chapter 14. Electrokinetics and zero valent iron nanoparticles: experimental and modeling of the transport in different porous media. In: *Electrokinetics across Disciplines and Continents. New Strategies for Sustainable Development* (eds. A.B. Ribeiro, E.P. Mateus and N. Couto), 279–294. Springer International Publishing.

96 Cernik, M., Nosek, J., Filip, J. et al. (2019). Electric-field enhanced reactivity and migration of iron nanoparticles with implications for groundwater treatment technologies: proof of concept. *Water Research* 154: 361–369.

97 Gomes, H.I., Dias-Ferreira, C., Ribeiro, A.B., and Pamukcu, S. (2012b). Electrokinetic enhanced transport of zero valent iron nanoparticles for chromium(VI) reduction in soils. *Chemical Engineering Transactions* 28: 139–144.

98 Baragaño, D., Alons, J., Gallego, J.R. et al. (2020). Zero valent iron and goethite nanoparticles as new promising remediation technique for as-polluted soils. *Chemosphere* 238: 124624–124634.

99 Gomes, H.I., Fan, G., Mateus, E.P. et al. (2014b). Assessment of combined electro-nanoremediation of molinate contaminated soil. *Science of the Total Environment* 493: 178–184.

100 Herrada, R.A., Pérez–Corona, M., Shrestha, R.A. et al. (2014). 3. Electrokinetic remediation of polluted soil using nano-materials: Nano-iron case. In: *Evaluation of Electrochemical Reactors as a New Way to Environmental Protection* (eds. J.M. Peralta-Hernández, M.A. Rodrigo-Rodrigo and C.A. Martínez-Huitle), 41–46. Kerala, India: Research Signpost.

101 Gomes, H.I., Rodríguez-Maroto, J.M., Ribeiro, A.B. et al. (2015c). Numerical prediction of diffusion and electric field-induced iron nanoparticle transport. *Electrochimica Acta* 181: 5–12.

102 Boente, C., Sierra, C., Martínez-Blanco, D. et al. (2018). Nanoscale zero-valent iron-assisted soil washing for the removal of potentially toxic elements. *Journal of Hazardous Materials* 350: 55–65.

103 Jiang, D., Zeng, G., Huang, D. et al. (2018). Remediation of contaminated soils by enhanced nanoscale zero valent iron. *Environmental Research* 163: 217–227.

104 Černíková, M., Nosek, J., and Černík, M. (2020). Combination of nZVI and DC for the in-situ remediation of chlorinated ethenes: an environmental and economic case study. *Chemosphere* 245: 125576.

UNCORRECTED PROOFS

Trim Size: 170mm x 244mm Single Column Loose Ribeiro670117 c03.tex V1 - 12/02/2020 11:04pm Page 81

105 López-Vizcaíno, R., Navarro, V., León, M.J. et al. (2016). Scale-up on electrokinetic remediation: engineering and technological parameters. *Journal of Hazardous Materials* 315: 135–143.

106 Risco, C., Rodrigo, S., López-Vizcaíno, R. et al. (2015). Electrochemically assisted fences for the electroremediation of soils polluted with 2,4-D: a case study in a pilot plant. *Separation and Purification Technology* 156: 234–241.

107 Risco, C., López-Vizcaíno, R., Sáez, C. et al. (2016a). Remediation of soils polluted with 2,4-D by electrokinetic soil flushing with facing rows of electrodes: a case study in a pilot plant. *Chemical Engineering Journal* 285: 128–136.

108 Risco, C., Rodrigo, S., López-Vizcaíno, R. et al. (2016b). Electrokinetic flushing with surrounding electrode arrangements for the remediation of soils that are polluted with 2,4-D: a case study in a pilot plant. *Science of the Total Environment* 545–546: 256–265.

109 Risco, C., Rodrigo, S., López Vizcaíno, R. et al. (2016c). Removal of oxyfluorfen from spiked soils using electrokinetic soil flushing with linear rows of electrodes. *Chemical Engineering Journal* 294: 65–72.

110 Risco, C., Rubí-Juárez, H., Rodrigo, S. et al. (2016d). Removal of oxyfluorfen from spiked soils using electrokinetic soil flushing with the surrounding arrangements of electrodes. *Science of the Total Environment* 559: 94–102.

111 Barba, S., López-Vizcaíno, R., Saez, C. et al. (2018a). Electro-bioremediation at the prototype scale: what it should be learned for the scale-up. *Chemical Engineering Journal* 334: 2030–2038.

112 Lim, M.W., Lau, E.V., and Poh, P.E. (2016). A comprehensive guide of remediation technologies for oil contaminated soil - present works and future directions. *Marine Pollution Bulletin* 109: 14–45.

113 Gong, Y., Zhao, D., and Wang, Q. (2018). An overview of field-scale studies on remediation of soil contaminated with heavy metals and metalloids: technical progress over the last decade. *Water Research* 147: 440–460.

114 Mousset, E., Huguenot, D., Van Hullebusch, E.D. et al. (2016). Impact of electrochemical treatment of soil washing solution on PAH degradation efficiency and soil respirometry. *Environmental Pollution* 211: 354–362.

115 Valdovinos, V., Monroy-Guzmán, F., and Bustos, E. (2016). Electrokinetic removal of radionuclides contained in scintillation liquids absorbed in soil type Phaeozem. *Journal of Environmental Radioactivity* 162–163: 80–86.

116 Estabragh, A.R., Lahoori, M., Javadi, A.A., and Abdollahi, J. (2019). Effect of a surfactant on enhancing efficiency of the electrokinetic method in removing anthracene from a clay soil. *Journal of Environmental Chemical Engineering* 7: 103298–103303.

117 Mohamadi, S., Saeedi, M., and Mollahosseini, A. (2019). Enhanced electrokinetic remediation of mixed contaminants from a high buffering soil by focusing on mobility risk. *Journal of Environmental Chemical Engineering* 7: 103470–103479.

118 Mao, X., Han, F.X., Shao, X. et al. (2016). Electrkinetic remediation coupled with phytoremediation to remove lead, arsenic and cesium from contaminated paddy soil. *Ecotoxicology and Environmental Safety* 125: 16–24.

UNCORRECTED PROOFS

Trim Size: 170mm x 244mm Single Column Loose Ribeiro670117 c03.tex V1 - 12/02/2020 11:04pm Page 82

119 Luo, J., Cai, L., Qi, S. et al. (2017). A multi-technique phytoremediation approach to purify metals contaminated soil from e-waste recycling site. *Journal of Environmental Management* 204: 17–22.

120 Sánchez, V., López-Bellido, F.J., Cañizares, P., and Rodríguez, L. (2018). Can electrochemistry enhance the removal of organic pollutants by phytoremediation? *Journal of Environmental Management* 225: 280–287.

121 Rocha, I.M.V., Silva, K.N.O., Silva, D.R. et al. (2019). Coupling electrokinetic remediation with phytoremediation for depolluting soil with petroleum and the use of electrochemical technologies for treating the effluent generated. *Separation and Purification Technology* 208: 194–200.

122 Huang, H., Tang, J., Niu, Z., and Giesy, J.P. (2019b). Interactions between electrokinetics and rhizoremediation on the remediation of crude oil-contaminated soil. *Chemosphere* 229: 418–425.

123 Sánchez, V., Francisco, López-Bellido, J. et al. (2019a). Enhancing the removal of atrazine from soils by electrokinetic-assisted phytoremediation using ryegrass (*Lolium perenne* L.). *Chemosphere* 232: 204–212.

124 Sánchez, V., López-Bellido, F.J., Rodrigo, M.A., and Rodríguez, L. (2019b). Electrokinetic-assisted phytoremediation of atrazine: differences between electrode and interelectrode soil sections. *Separation and Purification Technology* 211: 19–27.

125 Li, J., Zhang, J., Larson, S.L. et al. (2019b). Electrokinetic-enhanced phytoremediation of uranium-contaminated soil using sunflower and Indian mustard. *International Journal of Phytoremediation*: 1–8.

126 Siyar, R., Ardejani, F.D., Farahbakhsh, M. et al. (2020). Potential of Vetiver grasss for the phytoremediation of a real multi-contaminated soil, assisted by electrokinetic. *Chemosphere* 246: 125802–125812.

127 Sánchez, V., López-Bellido, F.J., Cañizares, P. et al. (2020a). Scaling up the electrokinetic-assisted phytoremediation of atrazine-polluted soils using reversal of electrode polarity: a mesocosm study. *Journal of Environmental Management* 255: 109806–109815.

128 Sánchez, V., López-Bellido, F.J., Rodrigo, M.A. et al. (2020b). A mesocosm study of electrokinetic-assisted phytoremediation of atrazine-polluted soils. *Separation and Purification Technology* 233: 116044–116054.

129 García, Y., Ruiz, C., Mena, E. et al. (2015). Removal of nitrates from spiked clay soils by coupling electrokinetic and permeable reactive barrier technologies. *Journal of Chemical Technology & Biotechnology* 90: 1719–1726.

130 Huang, T., Li, D., Kexiang, L., and Zhang, Y. (2015b). Heavy metal removal from MSWI fly ash by electrokinetic remediation coupled with a permeable activated charcoal reactive barrier. *Scientific Reports* 5: 15412.

131 Mena, E., Ruiz, C., Villaseñor, J. et al. (2015a). Biological permeable reactive barriers coupled with electrokinetic soil flushing for the treatment of diesel-polluted clay soil. *Journal of Hazardous Materials* 283: 131–139.

132 Peng, L., Chen, X., Zhang, Y. et al. (2015). Remediation of metal contamination by electrokinetics coupled with electrospun polyacrylonitrile nanofiber membrane. *Process Safety and Environmental Protection* 98: 1–10.

UNCORRECTED PROOFS

Trim Size: 170mm x 244mm Single Column Loose Ribeiro670117 c03.tex V1 - 12/02/2020 11:04pm Page 83

133 Robles, I., Lozano, M.J., Solís, S. et al. (2015). Electrokinetic treatment of mercury-polluted soil facilitated by ethylenediaminetetraacetic acid coupled with a reactor with a permeable reactive barrier of iron to recover mercury (II) from water. *Electrochimica Acta* 181: 68–72.

134 Kebria, D.Y., Taghizadeh, M., Camacho, J.V., and Latifi, N. (2016). Remediation of PCE contaminated clay soil by coupling electrokinetics with zero-valent iron permeable reactive barrier. *Environmental Earth Sciences* 75: 699.

135 Mena, E., Villaseñor, J., Cañizares, P., and Rodrigo, M.A. (2016b). Influence of electric field on the remediation of polluted soil using a biobarrier assisted electro-bioremediation process. *Electrochimica Acta* 190: 294–304.

136 Mena, E., Villaseñor, J., Rodrigo, M.A., and Cañizares, P. (2016c). Electrokinetic remediation of soil polluted with insoluble organics using biological permeable reactive barriers: effect of periodic polarity reversal and voltage gradient. *Chemical Engineering Journal* 299: 30–36.

137 Zhao, S., Fan, L., Zhou, M. et al. (2016). Remediation of copper contaminated kaolin by electrokinetics coupled with permeable reactive barrier. *Procedia Environmental Sciences* 31: 274–279.

138 Zhou, M., Zhu, S., Yi, Y., and Zhang, T. (2016). An electrokinetic/activated alumina permeable reactive barrier-system for the treatment of fluorine-contaminated soil. *Clean Technologies and Environmental Policy* 18: 2691–2699.

139 Zhu, S., Han, D., Zhou, M., and Liu, Y. (2016). Ammonia enhanced electrokinetics coupled with bamboo charcoal adsorption for remediation of fluorine-contaminated kaolin clay. *Electrochimica Acta* 198: 241–248.

140 Ding, L., Lv, W., Yao, K. et al. (2017). Remediation of Cd(II)-contaminated soil via humin-enhanced electrokinetic technology. *Environmental Science and Pollution Research* 24: 3430–3436.

141 Souza, F.L., Sáez, C., Lanza, M.R.V. et al. (2017). Removal of chlorsulfuron and 2,4-D from spiked soil using reversible electrokinetic adsorption barriers. *Separation and Purification Technology* 178: 147–153.

142 Sun, Y., Gao, K., Zhang, Y., and Zou, H. (2017). Remediation of persistent organic pollutant-contaminated soil using biosurfactant-enhanced electrokinetics coupled with a zero-valent iron/activated carbon permeable reactive barrier. *Environmental Science and Pollution Research* 24: 28142–28151.

143 Vieira dos Santos, E., Sáez, C., Cañizares, P. et al. (2017). Reversible electrokinetic adsorption barriers for the removal of atrazine and oxyfluorfen from spiked soils. *Journal of Hazardous Materials* 322: 413–420.

144 Xu, Y., Xia, W., Hou, H. et al. (2017). Remediation of chromium-contaminated soil by electrokinetics and electrokinetics coupled with CaAl-LDH permeable reaction barrier. *Environmental Science and Pollution Research* 24: 20479–20486.

145 Ghaeminia, M. and Mokhtarani, N. (2018). Remediation of nitrate-contaminated groundwater by PRB-Electrokinetic integrated process. *Journal of Environmental Management* 222: 234–241.

UNCORRECTED PROOFS

Trim Size: 170mm x 244mm Single Column Loose Ribeiro670117 c03.tex V1 - 12/02/2020 11:04pm Page 84

146 Rodrigo, S., Saez, C., Cañizares, P., and Rodrigo, M.A. (2018). Reversible electrokinetic adsorption barriers for the removal of organochlorine herbicide from spiked soils. *Science of the Total Environment* 640–641: 629–636.

147 Vidal, J., Saez, C., Cañizares, P. et al. (2018). ZVI-reactive barriers for the remediation of soils polluted with clopyralid: are they really worth? *Chemical Engineering Journal* 350: 100–107.

148 Barba, S., Carvela, M., Villaseñor, J. et al. (2019a). Fixed-bed biological barrier coupled with electrokinetics for the in situ electrobioremediation of 2,4-dichlorophenoxyacetic acid polluted soil. *Journal of Chemical Technology & Biotechnology* 94: 2684–2692.

149 Huang, T., Liu, L., Zhang, S., and Xu, J. (2019a). Evaluation of electrokinetics coupled with a reactive barrier of activated carbon loaded with a nanoscale zero-valent iron for selenite removal from contaminated soils. *Journal of Hazardous Materials* 368: 104–114.

150 Wang, Y., Huang, L., Wang, Z. et al. (2019). Application of polypyrrole flexible electrode for electrokinetic remediation of Cr(VI)-contaminated soil in a main-auxiliary electrode system. *Chemical Engineering Journal* 373: 131–139.

151 Yao, W., Cai, Z., Sun, S. et al. (2019). Electrokinetic-enhanced remediation of actual arsenic-contaminated soils with approaching cathode and Fe^0 permeable reactive barrier. *Journal of Soils and Sediments*.

152 Vidal, J., Carvela, M., Saez, C. et al. (2020). Testing different strategies for the remediation of soils polluted with lindane. *Chemical Engineering Journal* 381: 122674–122683.

UNCORRECTED PROOFS

Trim Size: 170mm x 244mm Single Column Loose Ribeiro670117 c04.tex V1 - 12/11/2020 11:51pm Page 85

4

The Electrokinetic Recovery of Tungsten and Removal of Arsenic from Mining Secondary Resources: The Case of the Panasqueira Mine

Joana Almeida[1,2], Paulina Faria[2,3], António Santos Silva[4], Eduardo P. Mateus[1], and Alexandra B. Ribeiro[1]

[1] *CENSE – Center for Environmental and Sustainability Research, Department of Environmental Sciences and Engineering, NOVA School of Science and Technology, NOVA University Lisbon, Caparica Campus, 2829-516 Caparica, Portugal*
[2] *Department of Civil Engineering, NOVA School of Science and Technology, NOVA University Lisbon, Caparica Campus, 2829-516 Caparica, Portugal*
[3] *CERIS – Civil Engineering Research and Innovation for Sustainability, Instituto Superior Técnico, University of Lisbon, 1049-001 Lisbon, Portugal*
[4] *Department of Materials, National Laboratory for Civil Engineering, 1700-066 Lisbon, Portugal*

4.1 Introduction

Mining industries today are producing a larger volume of residues than ever. To access ore, waste rock needs to be removed, and other residues are generated in the process [1]. The accumulation of these residues in open pits leads to landscape problems and environmental deterioration. For example, the Panasqueira mine in Portugal has been active for more than a century and is one of the largest tin (Sn) – tungsten (W) deposits in Europe. The mining residues are low-grade secondary resources that contain not only W, from wolframite, but also elements of environmental concern, including arsenic (As) from arsenopyrite [2].

The electrodialytic (ED) process has been studied to remove metals and metal oxides from a wide range of porous solid matrices in the environment [3–7]. This process consists of applying a low-level direct current between pairs of electrodes. The electric field generated inside a reactor promotes the removal or separation of substances from contaminated matrices [8]. In addition, natural deep eutectic solvents are another strategy for extracting metals from environmental matrices and have economic and environmental advantages compared to conventional ionic liquids [9].

Natural deep eutectic solvents and/or ED processes were applied to secondary mining resources from the Panasqueira mine to remove or separate elements [10, 11]. Considering European Commission targets, the recovery of critical raw materials [12] and removal of harmful compounds from secondary resources contributes to close loops of by-products and move toward a circular economy [13].

Electrokinetic Remediation for Environmental Security and Sustainability, First Edition.
Edited by Alexandra B. Ribeiro and M.N.V. Prasad.
© 2021 John Wiley & Sons Ltd. Published 2021 by John Wiley & Sons Ltd.

UNCORRECTED PROOFS

Trim Size: 170mm x 244mm Single Column Loose Ribeiro670117 c04.tex V1 - 12/11/2020 11:51pm Page 86

AQ1

Additionally, worldwide, construction products have extremely high embodied energy and consume large amounts of raw materials. EU targets from 2021 to 2030 [14] call for reducing greenhouse gas emissions by 40% (comparing with 1990 levels) and improving energy efficiency by more than 32.5%. The valorization of residues as binder replacers or additions in cementitious construction products may be a sustainable alternative for the construction and mining sectors, alleviating primary resources needs and residue disposal.

Mining wastes from the Panasqueira mine have been successfully reused in the construction sector using different approaches [15, 16]. The introduction of Panasqueira W mining waste resources in construction products was assessed, emphasizing the advantages and drawbacks of the material's properties [17]. The feasibility of innovative technologies, namely the ED process, to remove and recover elements from secondary resources for subsequent use in construction product formulations was also studied.

4.2 Tungsten Mining Resources: The Panasqueira Mine

4.2.1 The Development of the Industry

The Panasqueira mine is located in the Centro region of Portugal and is described as the largest Sn–W deposit in Western Europe [18]. Tungsten market downturns have influenced the plant's dynamics over the years, regarding the optimization of mechanical processes and exploring alternative ores (Figure 4.1).

Panasqueira began W exploration in 1896, when the mining company Tungsten Mines Society of Portugal was founded. Wolframite ore was firstly extracted from Cabeço do Pião (now known as Rio). In 1904, the plant was improved, and 41 t of ore were produced by integrating a new mechanized treatment using the Zêzere river for a water supply. Although the first underground drifts were opened in Rio, mining activities decreased at this site due to richer veins in the Panasqueira area [19].

In 1911, Wolfram Mining and Smelting Company was formed and acquired all the rights and concessions of the previous company. Investments in machinery and equipment were made to increase ore production. From a social perspective, the need for more workers to manage the plant processes increased employment in the region. The production of wolframite concentrates was estimated to be 267 t of 65% WO_3 mined from 11 000 t of vein and 86 000 t of host rock [19].

During the World War I, the mining operation grew; production increased, and the plant facilities were enlarged. Also, the mine began to recover Sn from cassiterite. In 1928, the price of W fluctuated, which affected its exploration. To overcome the W "crisis," the recovery of Sn was intensified. The company reorganized itself and changed its name to Beralt Tin and Wolfram Company [19].

During the World War II, peak production of W was reported, and the price of W increased again in 1934. Manpower was also boosted from 750 workers in 1933 to 5800 in 1943. However, from the end of the war to 1950, the W market declined. The production of Sn was maintained, and Cu (copper) recovery was introduced to the

UNCORRECTED PROOFS

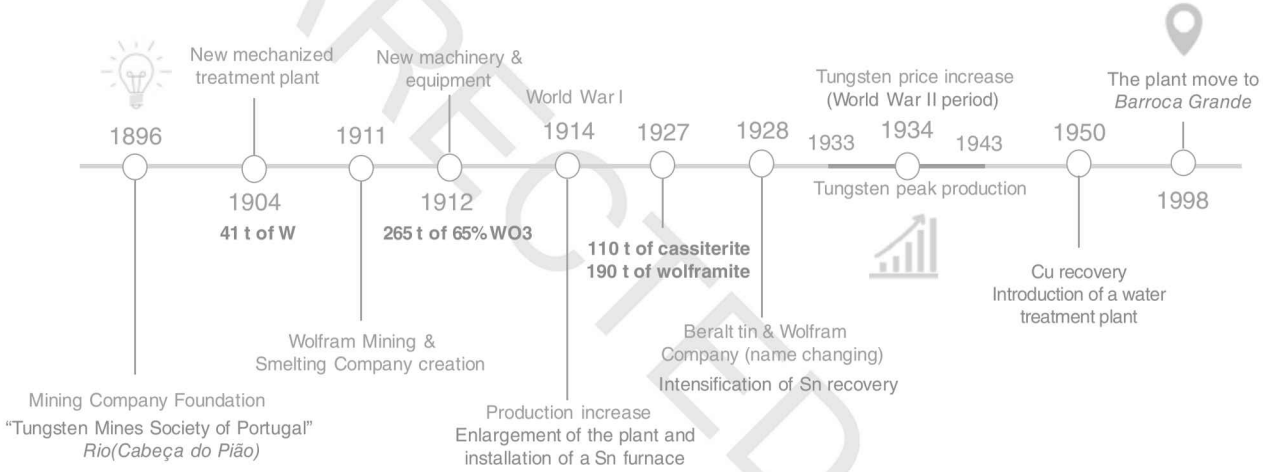

Figure 4.1 Highlights of the Panasqueira mine timeline.

UNCORRECTED PROOFS

Trim Size: 170mm x 244mm Single Column Loose

Ribeiro670117 c04.tex V1 - 12/11/2020 11:51pm Page 87

Trim Size: 170mm x 244mm Single Column Loose Ribeiro670117 c04.tex V1 - 12/11/2020 11:51pm Page 88

plant to compensate for W depreciation. In addition, water treatment was integrated into the system to address water quality issues. The Zêzere river is one of Lisbon's water supplies, so constant water monitoring was necessary [18, 19].

Later, the company mechanized underground operations, reducing labor expenses. In 1998, the remaining plant at Rio was moved to Barroca Grande, where it is located today. The mine has a production plan for more than 30 years in the future [19].

4.2.2 Ore Extraction Processes

Tungsten is a high valuable transition metal that can be extracted from the two W minerals that are commercially mined: scheelite ($CaWO_4$) and wolframite ((Fe, Mn)WO_4) [20]. Panasqueira mine ore deposits are characterized by a series of sub-horizontal, stacked, and hydrothermal quartz veins that promote the mineralization of wolfram-bearing schists and shales. The mineralized area is 2500 m long, 400–2200 m wide, and 500 m deep. Wolframite, chalcopyrite, and cassiterite are extracted and recovered to produce concentrates of W, Sn, and Cu, respectively [21].

The current extraction technology is based on a room-and-pillar method, taking into account an analysis of the geomechanical and geological properties of the rock mass. The ore extraction process starts with a heavy media separation between fine and coarse fractions. This step removes 80% of the ore that does not contain W. Then, this pre-concentrated fraction is subjected to a conventional gravity concentration technique, followed by flotation (with sulfide) and dry magnetic separation [21].

4.2.3 Potential Risks

The final concentrate production procedures are carried out in the Barroca Grande plant. A huge tailings pile and two mud dams are currently in the area. One dam is still being filled with material (mud and coarse material) without W ore as a result of extraction operations [22].

More than 27 million t of rock were extracted in the first 50 years of mining. During this period, around 92 800 t of W concentrate, 4800 t of Sn concentrate, and 28 600 t of Cu concentrate were produced [22] (Figure 4.2).

Now production has been optimized and is estimated to yield 85 000–95 000 t of W concentrate per year, which is almost equal to the total W production during the first 50 years of Panasqueira mining. Currently, the W concentrate grade is approximately 75% WO_3, representing one of the best W products available on the global market [21].

Panasqueira extraction and processing generate two types of mine tailings: (i) coarse waste-rock tailings from rock blasting and (ii) waste-mud tailings transferred into mud dams. Panasqueira has accumulated these rejected fractions for a long time, and they now have enormous proportions. The total amount of accumulated residues is a problem: it is estimated that to date, 8 200 000 m^3 of mining waste have been disposed of. Even more concerning is the quantity of residue disposed of in

UNCORRECTED PROOFS

Trim Size: 170mm x 244mm Single Column Loose Ribeiro670117 c04.tex V1 - 12/11/2020 11:51pm Page 89

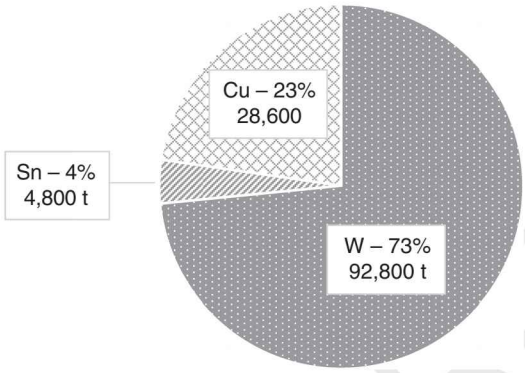

Figure 4.2 Tungsten, copper, and tin concentrate production in the first 50 years of Panasqueira mining.

open air impoundments, since only around 23% of the total mining waste estimated is effectively at dam facilities (1 924 919 m^3) [22].

Besides harming the landscape, the piles of accumulated mining waste are exposed to environmental conditions. Thus, these residue impoundments are unstable and prone to landslides, erosion, and leaching of harmful compounds. Waste mud contains high proportions of arsenic and other sulfide-related heavy metals, e.g. lead (Pb), copper (Cu), cadmium (Cd) and zinc (Zn). The oxidation of sulfides and their release from open impoundments are reported as the main threat to the Panasqueira area since they are associated with the migration and mobilization of metals/metalloids into the environment [23].

Although secondary resources from the Panasqueira mine have been successfully valorized in several applications, there are other potential risks. The presence of metals and metalloids, including arsenic (As), Cd, chromium (Cr), Cu, Pb, and Zn, has been reported in different streams (rhizosphere soils, irrigation water, road dust, and vegetables in local gardens). The mean concentrations exceed standards values and cause potential risks for habitants [24].

4.3 The Circular Economy of Tungsten Mining Waste

Europe's flagship initiative supports the shift to a resource-efficient, low-carbon economy to achieve sustainable growth. Reusing mining waste contributes to moving away from a linear economy model (take-make-use-dispose) and toward circular economic principles as set by the European Commission [13].

4.3.1 Panasqueira Old Slimes vs. Current Slimes

Reprocessing old tailings from Cabeço do Pião can be a solution to extract more ore concentrate and minimize the residues disposed of in the area [25]. However, research on old and current Panasqueira W slimes have shown varying efficiencies for the processes at the plant.

UNCORRECTED PROOFS

Trim Size: 170mm x 244mm Single Column Loose Ribeiro670117 c04.tex V1 - 12/11/2020 11:51pm Page 90

Panasqueira wolframite froth flotation (selective separation of hydrophobic from hydrophilic materials) has shown inconsistent results when comparing current tailings with old dam tailings. The old dam tailings have difficulty during flotation, which may be related to surface weathering. The finest wolframite is not effectively recovered by high-intensity magnetic separation (low to moderate fields) since the differential needed between wolframite, siderite, and other magnetic minerals is not achieved. With the application of higher fields, a substantial recovery of magnetic silicates and low-weight rejection is reported [26].

A three-stage gravity-separation process with a middle step of sulfide flotation can produce a wolframite concentrate of 55% WO_3. Tungsten minerals have extremely fine particles, and wolframite particles in Panasqueira mine tailings are less than 25 μm. Thus, the complex mineralogy and low-grade ore have led to the pursuit of a combination of enrichment techniques (e.g. flotation, magnetic, and gravity separation). The process for recovering ultrafine wolframite was optimized to enable efficient reprocessing of old mine tailings and current plant slime tailings from the Panasqueira mine [26].

4.3.2 Tungsten Recovery

Tungsten is both scarce and extremely important economically: it was reported as a critical raw material in the EU 2017 Critical Raw Material list [12]. Thus, alternative ways to recover W from secondary resources are now gaining attention. The Panasqueira mine has tons of accumulated secondary mining resources as a result of the extraction process, as reported in Section 4.2.3.

The electrodialytic process (ED) has been studied for removing organic and inorganic contaminants from liquid and solid environmental matrices by applying a low-level direct current to the system [27]. In the construction sector, ED has been demonstrated to be an effective pretreatment for immobilizing metals in solid matrices and improving the physical, chemical, and microstructural properties [28–31] for matrix reuse in mortars production.

Toward this end, research has been conducted to assess the feasibility of recovering W from secondary Panasqueira mining resources [10, 11]. Following the work of Almeida et al. [10], ED treatment was applied to W mining residues to (i) recover W contents, (ii) remove harmful compounds (As), and (iii) provide a suitable matrix for further reuse in the construction sector.

Tests also demonstrated the feasibility of adding biodegradable acid adjuvants – natural deep eutectic solvents – to the ED process [10]. The main goals of this combination were to improve the As and W extraction ratios and separate the extracted elements from the matrix.

Recovering W and removing As were assessed in a two-compartment ED cell (Figure 4.3). Tests were performed for four days at 100 and 50 mA. The electrolyte ($NaNO_3$ 0.01 M) was placed in the anode compartment, and the matrix was introduced in the cathode compartment in a water suspension (liquid-solid ratio of 9).

The tested conditions allowed the extraction of As (35%) and W (22%). Additionally, the conditions generated in the cell promoted the extraction and migration of

UNCORRECTED PROOFS

Trim Size: 170mm x 244mm Single Column Loose Ribeiro670117 c04.tex V1 - 12/11/2020 11:51pm Page 91

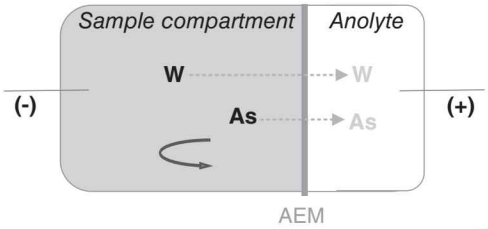

Figure 4.3 Two-compartment electrodialytic cell with an anion exchange membrane (AEM) interposed.

the studied elements. The elements extracted from the original matrix electromigrated into the anode compartment: 82% of the As and 77% of the W. Also, As and W can be further separated from the anolyte [10].

Simultaneously, research has been conducted for W recovery using other strategies. The hydrometallurgical recovery of W from minerals, tailings, and scrap involves several stages. Digesting and purifying these secondary raw materials allows the leaching of the concentrate and, consequently, extraction by the solvent. Tungsten from secondary scheelite can be processed through alkali leaching, where wolframite is dissolved in NaOH or Na_2CO_3 at temperatures between 125 and 200 °C or by high-pressure digestion. Then, silicates, phosphates, fluorides, As, antimony (Sb), bismuth (Bi), Pb, and cobalt (Co) can be selectively precipitated by other reagents. This purification step is accompanied by a W concentration step by either solvent extraction or ion-exchange resins [32].

However, the precipitation of contaminants leads to a loss of W. Therefore, direct solvent extraction of W from the alkaline medium was proposed with quaternary ammonium carbonate salts applied as extractants [32]. Trioctyl methyl ammonium chloride was transformed in quaternary ammonium carbonate and used as an extractant, removing almost all the impurities (e.g. phosphorus [P], As, silicon [Si], and Sn) [32].

Tungsten can also be selectively recovered from W-bearing scrap by biosorption. *Escherichia coli* and beer yeast have high uptake capacities for W biosorption (0.16 g W/g biosorbent and 0.29 g W/g biosorbent, respectively), comparable to ion-exchange resins [33].

Emulsion liquid membranes are another strategy for W recovery and consist of two consecutive steps: extraction and stripping. The emulsion membrane phase is based on (i) a homogeneous mixture of extractant, (ii) an organic diluent, (iii) an internal aqueous stripping phase, and (iv) a surfactant to stabilize the emulsion. Transporting the solute with the species through the liquid membrane is coupled with counter-transport of ions (H^+/OH^-) from the internal stripping phase to the external feed phase, which allows high enrichment concentrations. The enriched solute can be recovered by breaking the emulsion [34].

Recent developments in microprocess engineering have helped to intensify existing solvent extraction processes for various metals [35, 36]. Microextraction processes are designed for slug flow in a microchannel with alternating drops of the aqueous and organic phases, non-dispersively in surface-modified microchannels or with an extra membrane between the two phases [37].

UNCORRECTED PROOFS

Trim Size: 170mm x 244mm Single Column Loose Ribeiro670117 c04.tex V1 - 12/11/2020 11:51pm Page 92

4.3.3 Building Material–Related Applications

From the perspective of a circular economy, and in line with the EU desire to close secondary resources loops [13], mining residues from Panasqueira and other mines were broadly tested in construction material products [17].

Together with sources of alumino-silicates, alkali-activated binders can be obtained. Some examples are calcinated clays (e.g. kaolin) and other industrial byproducts. Alkali-activated binders, also known as *geopolymers*, are gaining increasing attention because their properties are in some instances superior to other cementitious products [38].

Tungsten mine waste mud was used to produce geopolymeric binders. Formulations were performed with dehydroxylated mine waste, CaOH, NaOH (as an activator), and water-glass solutions. Regarding fresh and hardened characterizations, the tests standards may not be appropriate to measure the benefits of introducing residues in the formulation. For instance, since the formulation includes a viscous residue (water glass), it may bond to metallic surfaces of the material used to measure consistency and, indirectly, workability, affecting the results [39].

In-depth research of geopolymer optimization coupled with the incorporation of other reagents and wastes has been conducted. Tungsten mining waste was combined with red clay brick waste. When higher amounts of red clay brick waste were added to the mixture, there was an increase in compressive strength from 25 to 59 MPa with 10 and 50% of red clay brick waste, respectively [40].

Together with W mining waste, waste glass, and metakaolin, several precursors were tested to produce alkali-activated foams. A foaming agent (aluminum powder) was added to the mixture. The compressive strength of the final foamed material can be enhanced by reducing the precursors' particle size [41].

Tungsten mining waste mud was also combined with other mixtures, concentrations, and liquid-solid ratios of alkaline activator solutions. Some examples are Na_2SiO, NaOH, KOH, and waste glass powder dissolved in NaOH, aiming to enhance the compressive strength and microstructure of hybrid alkaline binders. By adding ground granulated blast furnace slag to secondary resources from W mining, a compressive strength of 32.8 MPa was obtained in 28 days of cure. This strategy's major drawbacks are the alkaline activator solutions, which are the most expensive component to prepare a hybrid alkaline binder [15].

The feasibility of reusing waste-rock piles from the Panasqueira W mine was assessed, aiming to develop a polymer-based composite material. These materials have the potential for technical-artistic applications in rehabilitation as building coatings and for conserving sculptures, although polymer-based composite products are probably incompatible with the conservation of historical monuments [42].

Panasqueira secondary resources as aggregates were successfully applied as a refractory lining in a foundry of non-ferrous metals [43]. Also, cementitious grouts were formulated with milled glass and Panasqueira waste mud for the road industry [44].

UNCORRECTED PROOFS

Trim Size: 170mm x 244mm Single Column Loose Ribeiro670117 c04.tex V1 - 12/11/2020 11:51pm Page 93

The influence of sodium carbonate on the thermal reactivity performance of materials produced with Panasqueira mine waste mud was also assessed. Although compressive strength achieved 40 MPa in 28 days of cure, Na_2CO_3 did not lead to a stable structure or, consequently, enhanced thermal reactivity [45].

The potential of tungsten mine waste mud to repair ordinary Portland cement (OPC) concrete was studied. A geopolymeric binder formulated with W mining waste was used as a repair material. This geopolymeric binder showed excellent bond strength and was not affected by its low roughness. On the other hand, commercial repair products are characterized by low bond strength and are highly dependent on surface treatment roughness [46].

Additionally, W mine tailings were studied to determine their potential for use in commercial glass production. $CaCO_3$ and $NaCO_3$ were added since they are essential for glass manufacture. Tungsten mine tailings showed suitable properties for commercial glass manufacture and also retained toxic elements, preventing environmental deterioration [47].

4.4 Social, Economic, and Environmental Impacts

The impacts of mining activities involve social, economic, and environmental pillars. Mining residues can affect the environment as a result of their chemical and mineralogical composition, physical properties, volume and surface occupied, and need for waste disposal. As a consequence, water quality and availability may also be affected. The potential for acid mine drainage is high, since mine tailings, rock residues, and heap and dump leach materials are quarried and exposed to oxygen and water, increasing the probability of acids being formed due to the presence of sulfide minerals (pyrite) [48]. Toxic constituents can leach even if acidic conditions are not present. Elevated levels of cyanide and nitrogen compounds have been found in waters at mine sites, from heap leaching and blasting. Also, landslides can occur on high deposits [49].

Particulate matter is transported by the wind as a consequence of mining activities (e.g. excavations, blasting, transportation of materials, wind erosion). In addition, exhaust emissions from the vehicles involved in mining areas increase these particulate levels [49].

Current demand and metal prices have potentiated the interest in old mining waste. As mentioned before, this waste can be considered a secondary mining resource for critical/raw materials. The recycling of W has lower-energy negative impacts (below $6000\,kWh\,t^{-1}$) compared to virgin production ($10\,000\,kWh\,t^{-1}$), depending on the grade and cut-off. However, depending on the market conditions, energy savings associated with W recycling do not make recycling cheaper than conventional W production [50].

To overcome the drawback of recycling costs, innovative methods require lower processing energies, lower carbon emissions, and waste rock generation from excavation activities, wastewater, and leachates from mining operations. Also, new technologies should have an eco-friendly perspective for the W processing

UNCORRECTED PROOFS

Trim Size: 170mm x 244mm Single Column Loose Ribeiro670117 c04.tex V1 - 12/11/2020 11:51pm Page 94

industry by reducing the reagents needed and/or the production of harmful/useless byproducts [50].

Future developments may consider redesigning models to optimize the environmental, social, and economic consequences of managing mining waste throughout the value chain. Orebody characterization, mine planning, processing, disposal, reprocessing, recycling, and reuse should be integrated. Economically, avoiding mining waste is at the top of the list, followed by reuse > recycling > recovery treatment > disposal. However, circular business models supported by public policies may have strategic importance [51]. To achieve social acceptance, special incentives may be provided to reward W producers or processors. These benefits should optimize the recycling management system to increase recycling rates [50].

4.5 Final Remarks

Reusing secondary mining resources may be a key factor in facing dependence on primary raw materials and improving sustainability in the industries that produce and reuse mine residues.

Although W mining wastes were reported as a feasible source to be reused, the presence of harmful elements may lead to potential risks. Applying a pretreatment before reusing secondary mining resources can recover critical raw materials, remove harmful compounds, and make it possible to safely reuse this matrix in other applications.

In the construction sector, geopolymerization proved to be able to stabilize hazardous compounds in formulations with W mining wastes for cementitious or clayish construction products. In addition to geopolymerization, other applications also seem feasible. Thus, W mining wastes are a valid secondary resource to empower a circular economy while mitigating primary resource needs in the construction sector without the loss of building materials' properties.

The imminent threat of climate change is a powerful motor for innovation in the field of raw material replacement for eco-efficient production of construction materials.

Acknowledgments

This work has received funding from the European Union's Horizon 2020 research and innovation program under the Marie Skłodowska-Curie grant agreement No. 778045. The authors acknowledge the Portuguese Foundation for Science and Technology (FCT) for the support given to CENSE and CERIS through the strategic projects UIDB/04085/2020 and UIDB/04625/2020, respectively, and for the J. Almeida PhD fellowship PD/BD/135170/2017 from the EcoCoRe Doctoral program. This work is anchored by the RESOLUTION LAB, a laboratory at the NOVA School of Science and Technology.

UNCORRECTED PROOFS

Trim Size: 170mm x 244mm Single Column Loose Ribeiro670117 c04.tex V1 - 12/11/2020 11:51pm Page 95

References

1 Schmidt, S., Berghau, W., and Hutten, A. (2012). From deposit to concentrate: the basics of tungsten mining part 1: project generation and project development. *International Tungsten Industry Association* 4 (June): 1–20.

2 Candeias, C., Melo, R., Ávila, P.F. et al. (2014). Heavy metal pollution in mine-soil-plant system in S. Francisco de Assis - Panasqueira mine (Portugal). *Applied Geochemistry* 44: 12–26.

3 Guedes, P., Mateus, E., Almeida, J. et al. (2016). Electrodialytic treatment of sewage sludge: current intensity influence on phosphorus recovery and organic contaminants removal. *Chemical Engineering Journal* 306: 1058–1066.

4 Guedes, P., Mateus, E.P., Fernandes, J.P., and Ribeiro, A.B. (2019). Electro-technologies for the removal of 2,4,6-trichloroanisole from naturally contaminated cork discs: reactor design and proof of concept. *Chemical Engineering Journal* 361: 80–88.

5 Ribeiro, A.B., Mateus, E.P., Ottosen, L.M., and Bech-Nielsen, G. (2000). Electrodialytic removal of cu, Cr, and as from chromated copper arsenate-treated timber waste. *Environmental Science & Technology* 34 (5): 784–788.

6 Ribeiro, A.B. and Mexia, J.T. (1997). A dynamic model for the electrokinetic removal of copper from a polluted soil. *Journal of Hazardous Materials* 56 (3): 257–271.

7 Ferreira, C., Jensen, P., Ottosen, L., and Ribeiro, A. (2005). Removal of selected heavy metals from MSW fly ash by the electrodialytic process. *Engineering Geology* 77 (3–4): 339–347.

8 Ribeiro, A.B., Mateus, E.P., and Couto, N. (eds.) (2016). *Electrokinetics across Disciplines and Continents: New Strategies for Sustainable Development*, 427 p. Springer International Publishing.

9 Paiva, A., Craveiro, R., Aroso, I. et al. (2014). Natural deep eutectic solvents - solvents for the 21st century. *ACS Sustainable Chemistry & Engineering* 2 (5): 1063–1071.

10 Almeida, J., Craveiro, R., Faria, P. et al. (2020). Electrodialytic removal of tungsten and arsenic from secondary mine resources — deep eutectic solvents enhancement. *Science of the Total Environment* 710: 136364.

11 Almeida, J., Magro, C., Mateus, E.P., and Ribeiro, A.B. (2020). Electrodialytic hydrogen production and critical raw materials recovery from secondary resources. *Water* 12 (5).

12 European Comission. (2017). Communication from the Comission to the European Parliament, the Council, the European Economic and Social Committee and the Committee of the Regions on the 2017 list of critical raw materials for the EU.

13 European Commission. (2015). Communication from the Comission to the European Parliament, the Council, the European Economic and Social Committee and the Committee of the Regions - Closing the loop - An EU action plan for the circular economy.

UNCORRECTED PROOFS

Trim Size: 170mm x 244mm Single Column Loose Ribeiro670117 c04.tex V1 - 12/11/2020 11:51pm Page 96

14 European Commission. (2014). 2030 climate and energy policy framework.

15 Sedira, N. and Castro-Gomes, J. (2020). Effect of activators on hybrid alkaline binder based on tungsten mining waste and ground granulated blast furnace slag. *Construction and Building Materials* 232: 117176.

16 Almeida, J., Santos Silva, A., Faria, P., and Ribeiro, A. (2020). Assessment on tungsten mining residues potential as partial cement replacement. *KnE Engineering* 5 (4): 228–237.

17 Almeida, J., Ribeiro, A.B., Silva, A.S., and Faria, P. (2020). Overview of mining residues incorporation in construction materials and barriers for full-scale application. *Journal of Building Engineering* 29: 101215.

18 Candeias, C., Ávila, P.F., Da Silva, E.F. et al. (2014). Acid mine drainage from the Panasqueira mine and its influence on Zêzere river (Central Portugal). *Journal of the African Earth Sciences* 99: 705–712.

19 Almonty. (2019). Panasqueira Mine. https://almonty.com/project/panasqueira/ (accessed 6 January 2020).

20 Yang, X. (2018). Beneficiation studies of tungsten ores – a review. *Minerals Engineering* 125: 111–119.

21 Franco, A., Vieira, R., and Bunting, R. (2014). The Panasqueira mine at a glance. *Tungsten* 3: 1–12.

22 Ávila, P.F., da Silva, E.F., Salgueiro, A.R., and Farinha, J.A. (2008). Geochemistry and mineralogy of mill tailings impoundments from the Panasqueira mine (Portugal): implications for the surrounding environment. *Mine Water and the Environment* 27 (4): 210–224.

23 Godinho, B., Abreu, M., and Magalhães, M. (2010). Avaliação biogeoquímica dos solos e do medronheiro na área mineira da Panasqueira. *Revista de Ciencias Agrarias* 33 (1): 226–235.

24 Ávila, P.F., Ferreira da Silva, E., and Candeias, C. (2017). Health risk assessment through consumption of vegetables rich in heavy metals: the case study of the surrounding villages from Panasqueira mine, Central Portugal. *Environmental Geochemistry and Health* 39 (3): 565–589.

25 Figueiredo, J., Vila, M.C., Matos, K. et al. (2018). Tailings reprocessing from Cabeço do Pião dam in Central Portugal: a kinetic approach of experimental data. *Journal of Sustainable Mining* 17 (3): 139–144.

26 Clemente, D., Newling, P., Botelho de Sousa, A. et al. (1993). Reprocessing slimes tailings from a tungsten mine. *Minerals Engineering* 6 (8–10): 831–839.

27 Lepp, N.W. (2006). Trace elements in the environment. *Journal of Environmental Quality* 35 (3): 956–956.

28 Magro, C., Guedes, P., Kirkelund, G.M. et al. (2016). Incorporation of different fly ashes from mswi as substitute for cement in mortar: an overview of the suitability of electrodialytic pre-treatment. In: *Electrokinetics across Disciplines and Continents* (eds. A.B. Ribeiro, E.P. Mateus and N. Couto), 225–247. Cham: Springer International Publishing.

29 Kappel, A., Ottosen, L.M., and Kirkelund, G.M. (2017). Colour, compressive strength and workability of mortars with an iron rich sewage sludge ash. *Construction and Building Materials* 157: 1199–1205.

UNCORRECTED PROOFS

Trim Size: 170mm x 244mm Single Column Loose Ribeiro670117 c04.tex V1 - 12/11/2020 11:51pm Page 97

30 Kirkelund, G.M., Jensen, P.E., Ottosen, L.M., and Pedersen, K.B. (2019). Comparison of two- and three-compartment cells for electrodialytic removal of heavy metals from contaminated material suspensions. *Journal of Hazardous Materials* 367: 68–76.

31 Magro, C., Paz-Garcia, J.M., Ottosen, L.M. et al. (2019). Sustainability of construction materials: Electrodialytic technology as a tool for mortars production. *Journal of Hazardous Materials* 363: 421–427.

32 Zhang, W., Yang, J., Zhao, Z. et al. (2016). Coordination leaching of tungsten from scheelite concentrate with phosphorus in nitric acid. *Journal of Central South University* 23 (6): 1312–1317.

33 Makino, T., Nagai, S., Iskandar, F. et al. (2018). Recovery and recycling of tungsten by alkaline leaching of scrap and charged amino group assisted precipitation. *ACS Sustainable Chemistry & Engineering* 6 (3): 4246–4252.

34 Noble, R.D. and Stern, S.A. (1995). *Membrane Separations Technology: Principles and Applications*. Elsevier.

35 Willersinn, S. and Bart, H.J. (2015). Reactive mass transfer in a membrane-based microcontactor. *Chemical Engineering and Processing Process Intensification* 95: 186–194.

36 Willersinn, S. and Bart, H.J. (2016). Kinetics of Ge(IV) extraction using a microstructured membrane contactor. *International Journal of Chemical Kinetics* 48 (10): 609–621.

37 Kenig, E.Y., Su, Y., Lautenschleger, A. et al. (2013). Micro-separation of fluid systems: a state-of-the-art review. *Separation and Purification Technology* 120: 245–264.

38 Silva, I., Castro-Gomes, J.P., and Albuquerque, A. (2012). Effect of immersion in water partially alkali-activated materials obtained of tungsten mine waste mud. *Construction and Building Materials* 35: 117–124.

39 Pacheco-Torgal, F., Castro-Gomes, J., and Jalali, S. (2008). Properties of tungsten mine waste geopolymeric binder. *Construction and Building Materials* 22 (6): 1201–1211.

40 Sedira, N., Castro-Gomes, J., and Magrinho, M. (2018). Red clay brick and tungsten mining waste-based alkali-activated binder: microstructural and mechanical properties. *Construction and Building Materials* 190: 1034–1048.

41 Beghoura, I., Castro-Gomes, J., Ihsan, H., and Estrada, N. (2017). Feasibility of alkali-activated mining waste foamed materials incorporating expanded cork. *Mining Science* 24: 7–28.

42 Castro-Gomes, J.P., Silva, A.P., Cano, R.P. et al. (2012). Potential for reuse of tungsten mining waste-rock in technical-artistic value added products. *Journal of Cleaner Production* 25: 34–41.

43 Montoya Herrera, J., Durán Suarez, J.A., Silva, A.P. et al. (2013). Reciclagem de agregados das minas da Panasqueira como revestimento refratário da fundição de metais. *Ciencia e Tecnologia dos Materiais* 25 (2): 129–137.

44 Afonso, M.L., Dinis-Almeida, M., Pereira-De-Oliveira, L.A. et al. (2016). Development of a semi-flexible heavy duty pavement surfacing incorporating recycled

UNCORRECTED PROOFS

Trim Size: 170mm x 244mm Single Column Loose Ribeiro670117 c04.tex V1 - 12/11/2020 11:51pm Page 98

and waste aggregates - preliminary study. *Construction and Building Materials* 102: 155–161.

45 Pacheco-Torgal, F. and Jalali, S. (2010). Influence of sodium carbonate addition on the thermal reactivity of tungsten mine waste mud based binders. *Construction and Building Materials* 24 (1): 56–60.

46 Pacheco-Torgal, F., Castro-Gomes, J.P., and Jalali, S. (2008). Adhesion characterization of tungsten mine waste geopolymeric binder. Influence of OPC concrete substrate surface treatment. *Construction and Building Materials* 22 (3): 154–161.

47 Alfonso, P., Tomasa, O., Garcia-Valles, M. et al. (2018). Potential of tungsten tailings as glass raw materials. *Materials Letters* 228: 456–458.

48 Oluwasola, E.A., Hainin, M.R., Aziz, M.M.A. et al. (2014). Potentials of steel slag and copper mine tailings as construction materials. *Materials Research Innovations* 18: 250–254.

49 Elaw (2010). *Guidebook for Evaluating Mining Project EIAs*, 1e. Environmental Law Alliance Worldwide.

50 Okvist, L., Ye, G., and Hu, X. (2016). Innovation potential in the recovery of refractory metals from secondary resources. MSP-REFRAM H2020 project (D3.3).

51 Velenturf, A.P.M., Archer, S.A., Gomes, H.I. et al. (2019). Circular economy and the matter of integrated resources. *Science of the Total Environment* 689: 963–969.

UNCORRECTED PROOFS

Trim Size: 170mm x 244mm Single Column Loose Ribeiro670117 c05.tex V1 - 12/09/2020 3:19pm Page 99

5

Electrokinetic Remediation of Dredged Contaminated Sediments

Kristine B. Pedersen[1,2], Ahmed Benamar[3], Mohamed T. Ammami[3], Florence Portet-Koltalo[4], and Gunvor M. Kirkelund[5]

[1] *Department of Environment, Akvaplan-niva AS, Fram Centre – High North Research Centre for Climate and the Environment, 9007, Tromsø, Norway*
[2] *Department of Chemistry, UiT – The Arctic University of Norway, 9037 Tromsø, Norway*
[3] *Department of Civil Engineering, LOMC UMR CNRS 6294, Le Havre Normandie University, 76600 Le Havre, France*
[4] *University Institute of Technology, COBRA UMR CNRS 6014, Rouen Normandie University, 27000 Evreux, France*
[5] *Department of Civil Engineering, Technical University of Denmark, 2800 Lyngby, Denmark*

5.1 Introduction

Harbor sediments are the final recipient for pollutants caused by past and present anthropogenic activities in the harbor and onshore. The pollution in harbors often has a complex composition of a wide variety of organic and inorganic pollutants. In sediments, heavy metals, persistent organic pollutants (POPs) such as polycyclic aromatic hydrocarbons (PAHs) and polychlorinated biphenyls (PCBs), and tribytultin (TBT) are of concern due to potential toxicity. Pollution is considered hazardous when it exceeds sediment quality criteria for adverse effects, as defined by national environmental authorities. The need for action to remediate harbor sediments arises during the development of harbors, when increasing navigational depths, or through governmental intervention with environmental requirements to mitigate adverse effects on the marine environment and human health. The choice of remediation technology depends on sediment properties, pollutant composition, and availability, as well as site-specific conditions and cost-effectiveness. In situ remediation of sediments is often based on decreasing the bioavailability of pollutants – for instance, by capping polluted sediments [1] – and is relevant in areas with limited risk of disturbance to the sediments. However, various activities may disturb sediments, e.g. upwhirling by ship propellers, and in situ remediation is relevant only in parts of the harbor with deep-sea basins and areas where increasing navigational depth is not anticipated. Accordingly, there is a need for ex situ management of large volumes of dredged sediments.

It was estimated in 2004 that in Europe alone, around 200 million m^3 of sediments were dredged annually [2]. Since then, the amount of dredged sediments in Europe

Electrokinetic Remediation for Environmental Security and Sustainability, First Edition.
Edited by Alexandra B. Ribeiro and M.N.V. Prasad.
© 2021 John Wiley & Sons Ltd. Published 2021 by John Wiley & Sons Ltd.

UNCORRECTED PROOFS

Trim Size: 170mm x 244mm Single Column Loose Ribeiro670117 c05.tex V1 - 12/09/2020 3:19pm Page 100

has increased, although it has not been quantified. In France, 55 million m^3 of sediments are dredged annually, of which 24 million m^3 are contaminated; this total is expected to increase to 70 million m^3 within the next 10 years. Managing polluted dredged sediments is restricted by legislation and environmental impacts. The prevailing method for managing dredged sediments is marine disposal: e.g. 440 000 m^3 of dredged contaminated sediments from Oslo harbor were transported 3 km to a marine disposal site in the period 2004–2008 [3]. The disposal of marine sediments cannot be sustainable, and alternative solutions are necessary. Disposal on land also has environmental implications, e.g. leaching of pollutants, dispersion into the environment, and greenhouse gas emissions. In addition, many disposal sites in Europe have reached their maximal storage capacities. Although investigation into the treatment of sediment has been extensive, the implementation of these technologies has been limited compared to disposal, due to both practical and financial considerations. A greater emphasis on identifying and developing methods for separating pollutants from sediments will lead to an increase in the possibilities for recycling sediments as non-polluted material and, in addition, provide the option of recycling pollutants (where desirable) or at least reducing the amount of hazardous waste. A first step is often the physical separation of dredged sediment to retrieve the finer fractions in which most pollution is bound [4, 5]. Subsequent treatment can be divided into physical, biological, and chemical technologies, including thermal degradation/extraction, biological decontamination, chemical oxidation/reduction/separation, electrokinetics, stabilization/solidification, and washing [1, 4–6]. Of these, electrokinetic remediation (EKR) is a reliable method for separating pollutants from different polluted materials.

EKR was initially developed as a mitigation method for polluted soil [7], and during the last 30 years it has been recognized as a practical in situ and ex situ remediation technique for clay-rich soils and fine-grained, low-permeability harbor sediments. In short, supplying an electric potential through the sediment via embedded electrodes results in electromigration, electroosmosis, and electrophoresis, which simultaneously affect the migration process of pollutants (inorganic and organic) that move toward the electrodes. The method has been extensively researched and developed in both laboratory and field studies for various pollutants in soil (e.g. [8–16]). One of the first EKR studies of polluted marine sediments was conducted in 1999 [17] the development of EKR for sediments is not as extensive as for soil and was initially based on knowledge transfer from EKR studies of soil. The remediation goals and challenges for harbor sediments differ from those in soils, due to the often more complex pollutant composition and risk of exposure to the marine environment. Salt concentration and organic matter composition affecting the availability of pollutants are the main difference between soil and sediment [18, 19]. In addition, sediments are often dredged, making EKR relevant as an ex situ treatment, as opposed to many cases with soil, in which excavation would be an unnecessary disturbance. Dredged sediments are a slurry of solid particles and water, making it possible to treat sediments in both stationary and stirred setups. The differences in challenges between soil and sediment treatment are reflected in the development of EKR for polluted sediments.

UNCORRECTED PROOFS

Trim Size: 170mm x 244mm Single Column Loose Ribeiro670117 c05.tex V1 - 12/09/2020 3:19pm Page 101

The first studies focused on one or a few metals; recent studies have investigated the potential for simultaneous remediation of metals and POPs. To optimize the removal of pollutants, most EKR studies have included enhancement techniques or combinations with other remediation technologies. This chapter presents the development of EKR for harbor sediments in relation to removal efficiency, types of pollutants, and influences of variables and sediment characteristics (Section 5.2). Subsequently, case studies illustrate recent developments for simultaneous removal of metals and POPs, employing physically and chemically enhanced EKR (Section 5.3). To evaluate the environmental impacts of EKR of harbor sediments, studies of energy consumption, leaching of pollutants from sediments after EKR, and effects on copepods to estimate toxicity are reviewed (Section 5.4). A case study highlights challenges related to scaling up EKR (Section 5.5). In the final part of the chapter (Section 5.6), future perspectives and challenges for developing EKR of harbor sediments are discussed.

5.2 EKR Removal of Pollutants from Harbor Sediments

Studies have been conducted on spiked sediment and have revealed the potential for EKR of harbor sediments [20–22]. However, the results are not realistic representations for aged pollutions [23–26] and may overestimate the removal of pollutants [27]. Many studies have focused on aged pollutions and will remain the focus of this chapter.

5.2.1 Pollutants and Removal Efficiencies

In the 20 years since the first study of EKR of marine sediments was published in 1999, approximately 71 studies on the topic have been published in scientific journals. Most of the studies have been published in the past 10 years (Figure 5.1),

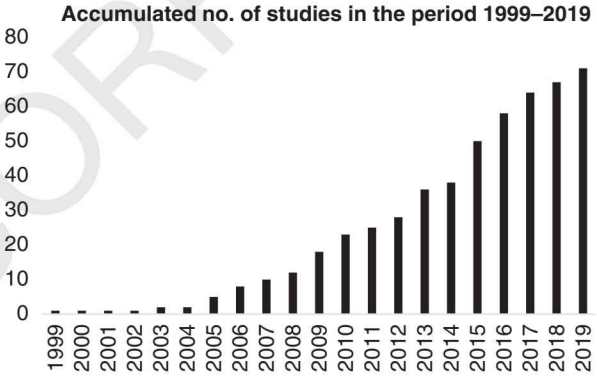

Figure 5.1 Accumulated number of published articles in scientific journals on the topic of EKR of marine sediments in the period 1999–2019. Source: Based on records of published articles in the Web of Science and Google Scholar search engines (accessed 20 January 2020).

UNCORRECTED PROOFS

Trim Size: 170mm x 244mm Single Column Loose Ribeiro670117 c05.tex V1 - 12/09/2020 3:19pm Page 102

peaking in 2015 with 12 publications. The published studies cover a range of pollutants and various enhancement techniques to optimize the removal efficiencies of pollutants and provide a good foundation for assessing and further developing the method.

Table 5.1 summarizes removal efficiency ranges of studied pollutants and the enhancement techniques applied for the highest removal in previous studies. It is worth noting that obtaining the highest possible removal of targeted pollutants is not necessarily a remediation goal; instead, the goal is to achieve concentrations that no longer pose a risk for human health and the environment according to the use of sediment, based on criteria set by national environmental authorities. However, high removal efficiencies indicate whether the remediation technology is relevant; and in the following, EKR is assessed in relation to the maximum reported removal efficiencies (Table 5.1).

5.2.1.1 Metals

Seven EKR studies of harbor sediments covering sites in Asia, Europe, and North America have focused on removing one target heavy metal, whereas 41 studies have investigated the simultaneous removal of multiple metals. It is seldom that all metals exceed concentrations that could cause potential adverse effects for the marine environment in harbors, and no study has included all priority metals as defined by European and North American legislation (most commonly As, Cd, Cr, Cu, Hg, Ni, Pb, and Zn). For this reason, target metals differ depending on the local environmental conditions in the reported studies.

The reported maximum removal efficiencies are above 80% for As, Cd, Cu, Ni, Pb, and Zn (Table 5.1). Cu, Pb, and Zn are included in most of the studies (36–39 studies), with the highest reported removal efficiencies above 90%. Ni and Cd are included in 24 studies, with the highest removal efficiencies being, respectively, 84% and 98%. For these five metals, the highest removal efficiencies are achieved in stirred setups with the application of ion-exchange membranes [28, 29]. Stirring has a higher impact on the mobilization of metals than applying ion-exchange membranes [29, 30]. As is included in 10 studies, with the highest removal efficiency of 88% obtained by using surfactants and chelating agents during EKR treatment [31].

Cr and Hg have the lowest reported removal efficiencies (69–71%), achieved by using surfactants and chelating agents [32, 33]. The electrokinetic mobilization and removal of Cr has been investigated in 20 studies, and the mobility of Cr is generally lower than the other studied metals. However, Cr is seldom highly prioritized in the remediation of marine sediments, so optimization efforts may not have been pursued in the same way as for other metals. Although Hg is highly prioritized by environmental authorities and international conventions (e.g. OSPAR), it has not been elaborately investigated and is included in only three studies. The reason Hg has not been included in more EKR studies could be due to analytical challenges (different analysis than other metals) or workplace health and safety. More studies of Hg are necessary to assess whether electrokinetic removal of Hg from harbor sediments can be optimized.

Although high removal efficiencies of individual metals have been reported (Table 5.1), studies of the simultaneous removal of metals have revealed differences in the removal efficiencies of each metal. For instance, Kirkelund et al. found a difference in removal efficiencies in the order Cd (98%) > Zn (78%) > Pb (65%) > Cu (44%) using a stirred setup and ion-exchange membranes [34]. Two studies

UNCORRECTED PROOFS

Trim Size: 170mm x 244mm Single Column Loose Ribeiro670117 c05.tex V1 - 12/09/2020 3:19pm Page 103

Table 5.1 Pollutants, reported removal efficiencies, and enhancement techniques used for the highest removal efficiencies.

Pollutant	No. of studies	Range of removal efficiencies reported	Enhancement
Metals			
Arsenic	10	3–88%	Surfactants and chelating agents
Chromium	20	0–69%	
Mercury	3	55–71%	
Cadmium	24	14–98%	Stirred setups and ion-exchange membranes
Copper	38	6–94%	
Nickel	24	9–92%	
Lead	39	5–96%	
Zinc	36	5–97%	
TBT	1	0–80%	Stirred setups and ion-exchange membranes
PCB7	2	15–62%	
TPH	2	90%	Combination with Fenton
Polyaromatic hydrocarbons (EPA16)			
2-ringed PAHs			
Acenaphtylene	4	0–50%	Surfactants and chelating agents
Acenaphtene	4	0–44%	
Fluorene	4	0–92%	
Naphtalene	4	39–70%	
3-ringed PAHs			
Anthracene	4	0–60%	Surfactants and chelating agents
Fluoranthene	5	0–70%	
Phenanthrene	6	0–75%	
4-ringed PAHs			
Benzo(a)anthracene	4	0–58%	Surfactants and chelating agents
Benzo(b)fluoranthene	5	0–74%	
Benzo(k)fluoranthene	4	0–78%	Stirred setup and ion-exchange membranes
Chrysene	5	0–86%	Surfactants and chelating agents

UNCORRECTED PROOFS

Trim Size: 170mm x 244mm Single Column Loose Ribeiro670117 c05.tex V1 - 12/09/2020 3:19pm Page 104

Table 5.1 (Continued)

Pollutant	No. of studies	Range of removal efficiencies reported	Enhancement
Pyrene	5	0–90%	
5-ringed PAHs			
Benzo(a)pyrene	4	0–60%	Surfactants and chelating agents
Dibenzo(a,h)anthracene	4	0–70%	
Indeno(1,2,3 cd)pyrene	4	0–65%	Stirred setup and ion-exchange membranes
6-ringed PAHs			
Benzo(ghi)perylene	4	0–47%	Stirred setup and ion-exchange membranes
Sum PAH16	10	5–70%	Combined with bioremediation

a) Source: The table was created based on 54 studies of EKR of aged polluted harbor sediments: Pedersen et al. [28]; Nystroem, Ottosen, and Villumsen [29]; Hahladakis et al. [31]; Andreottola et al. [32]; Falciglia, Malarbì, and Vagliasindi [33]; Kirkelund, Ottosen, and Villumsen [34]; Song et al. [35]; Pazos et al. [36]; Pedersen et al. [37]; Yan and Reible [38]; Ammama et al. [39]; Hahladakis, Latsos, and Gidarakos [40]; Hahladakis, Calmano, and Gidarakos [41]; Benamar et al. [42]; Falciglia et al. [43]; Tian et al. [44]; Yoo et al. [45]; Iannelli et al. [46]; Ottosen et al. [47]; Kirkelund, Ottosen, and Villumsen [49]; Nystroem, Ottosen, and Villumsen [50]; Nystroem et al. [51]; Kim et al. [57]; Ammami et al. [65]; Jiang et al. [70]; Yan and Reible [71]; Cappello et al. [72]; Reddy and Ala [73]; De Gioannis et al. [74]; Merkx et al. [75]; Masi et al. [76]; Song et al. [77]; Mao, Shao, and Zhang [85]; Pedersen and Gerdner [98]; Nystrøm, Ottosen, and Villumsen [99]; De Gioannis et al. [100]; Yuan et al. [101]; Shin [102]; Guoliang, Dehan, and Diqin [103]; Colacicco et al. [104]; Haroun, Chilingar, and Pamukcu [105]; Rozas and Castellote [106]; Kim et al. [107]; Pedersen et al. [108]; Pedersen et al. [109]; Pedersen et al. [110]; Pedersen et al. [111]; Masi and Losito [112]; Yoo et al. [113]; Missaoui et al. [114]; Luo, Connor, and Ngothai [115]; Masi, Ceccarini, and Iannelli [116]; Krcmar et al. [117]; Kirkelund et al. [118].

applying ethylenediaminetetraacetic acid (EDTA) conditioning in the electrolytes found a difference in the order of metal removal. Andreottola et al. found removal in the order As (81%) > Cr (69%) > Cu (40%) > Pb (33%) > Zn (22%) [32], while Song et al. found removal efficiency in the order Pb (60%) > Ni (54%) > Cr (43%) > Zn (34%) > As (30%) > Cu (27%) > Cd (15%) [35]. It is obvious that the experimental setup and settings along with sediment characteristics influence the efficiency of EKR for removing metals.

5.2.1.2 Organic Pollutants and Organometallic Pollutants

Few studies of EKR for PCBs, TBT, and total petroleum hydrocarbons (TPHs) in harbor sediments have been reported, but high removal efficiencies have been achieved. Removal efficiency of 90% of TPH was achieved by combining EKR with Fenton's

UNCORRECTED PROOFS

Trim Size: 170mm x 244mm Single Column Loose Ribeiro670117 c05.tex V1 - 12/09/2020 3:19pm Page 105

reagent and EDTA [36]. Removal efficiencies of 62% for PCBs and 80% for TBT were achieved in a stirred setup with ion-exchange membranes [37].

Ten studies on the electrokinetic removal of a total of 16 EPA-prioritized PAHs have been published; six of these included individual removal efficiencies for some of the compounds (Table 5.1). The highest removal efficiency for the sum of the 16 PAHs was 70% [38], achieved by enhancing natural degradation by EKR. The highest removal efficiencies for each of the 16 PAH compounds varied from 44% to 92%. For pyrene and fluoranthene, up to 90–92% was removed/degraded during EKR [31, 39], while only 44–47% of acenaphtene and benzo(ghi)perylene was removed/degraded [37]. The highest removal efficiencies for the 16 PAH compounds were generally achieved using surfactants [31, 39–41], although for a few of the four- to six-ringed PAHs, using a stirred setup achieved the highest removal efficiencies [37].

A limited number of studies have investigated the simultaneous EKR of organic pollutants and metals. In the study that remediated 90% of TPH, 55–60% of Cu, Hg, Pb, and Zn [36] were simultaneously removed. Removal efficiencies of 54% for PAH and 8–52% for metals [42] or 30% for PAH and 41–83% for metals [40] have been reported, and one study has reported similar removal efficiencies for PAH (59%) and mercury (66%) by using surfactants [43].

Two studies have looked at the simultaneous removal of metals, PAHs, and PCBs. In the first study, removal efficiencies of 38% for PCBs, 29% for PAHs, and 5–28% of metals were achieved [44]. In the second study, TBT was included, and the highest removal efficiencies were 64–85% for metals (Cu, Pb, and Zn), 34% for PAHs, 62% for PCBs, and 80% for TBT. However, the highest removal efficiencies were not achieved for the same experimental settings. For the greatest removal of TBT, the removal efficiencies of the metals were 43–80%, 34% for PAHs, and 20% for PCBs. For the greatest removal of PCBs, the removal efficiencies of the other pollutants were 4% for PAHs, 3–78% for metals, and 0% for TBT [37].

5.2.2 Influence of Experimental Settings and Sediment Properties on the Efficiency of EKR

It has been well established that experimental variables, experimental settings, types of pollutants, pollutant availability, and sediment characteristics influence pollutant removal efficiencies during EKR. Current density and remediation time are among the most important experimental variables influencing EKR [45]. EKR experiments performed at higher current densities and remediation times generally obtain higher removal efficiencies for both inorganic and organic pollutants [46]. Higher current densities decrease acidification times, increase the availability/desorption of metals and POPs, and increase the availability of microorganisms and nutrients, enhancing natural degradation in the sediment. There is, however, a limit to increasing the settings, since high current densities may impede the removal of metals and increase resistance in the EKR cell. The current efficiency regarding the transport of metals through the EKR cell decreases strongly with time, partly due to declining rates of metal desorption after acidification, and partly due to increasing protons carried by the current with decreasing pH [7]. Optimization of EKR of polluted harbor sediments is related to enhancement techniques increasing the availability of pollutants and reducing the transport time of pollutants through the sediment.

UNCORRECTED PROOFS

Trim Size: 170mm x 244mm Single Column Loose Ribeiro670117 c05.tex V1 - 12/09/2020 3:19pm Page 106

5.2.2.1 Enhancement of EKR – Changes in Design

An EKR system can involve two compartments (anode embedded in the sediment) or three compartments (two electrolyte compartments). In the first case, pollutants are recovered only in the catholyte, limiting EKR to cations, while in the second configuration, anions and cations can be recovered in the electrode compartment of the opposite charge. Chemically inert and electrically conductive materials such as graphite, coated titanium, and platinum are widely used for electrodes. Obviously, selecting electrode materials focuses primarily on electrical conductivity and electrochemical activity. A vertical parallel electrode configuration (flat or cylindrical) has been widely applied in EKR because it provides a direct, efficient electric field for horizontal ionic migration. The most common system for removing organic and inorganic pollutants involves three compartments: two electrode reservoirs containing additive solutions (electrolytes) and a central compartment filled with sediment to be treated (Figure 5.3). This design leads to the easy recovery and simultaneous removal of several pollutants within electrolytes but is limited for the electrode approaching technique.

By applying ion-exchange membranes between the electrolyte compartments and the compartment containing sediment, it is possible to control the transport of ions between the compartments, referred to as *electrodialytic remediation* (EDR). An anion exchange membrane between the anode and sediment prevents the transport of cations into the sediment, making the applied current more efficient for removing sediment compared to unenhanced EKR [47]. Acidification of the sediment is not achieved by the transport of protons from electrolysis reactions at the anode, as is the case with unenhanced EKR, but rather by water splitting at the anion-exchange membrane [48]. The formation of an alkaline front from the cathode is prevented by a cationic exchange membrane between the cathode and sediment compartments, thus preventing hydroxyl ions formed by electrolysis reactions on the cathode from entering the sediment. Stirring ensures faster acidification due to faster dissolution of carbonates caused by increased availability and mobility of protons [30]. In addition, stirring increases oxidation of the sediment, making pollutants bound in organic fractions more available [34, 49]. Stirred setups ensure faster removal of metals than increasing the current density in a stationary setup. The stirring rate, liquid/solid ratio of the sediment slurry, and EDR cell design (two to five compartments) also influence removal, depending on the availability of the pollutant in the sediment [50]. In a two-compartment cell, the anode is placed directly in the sediment slurry, decreasing the acidification time and enhancing oxidation of the sediment by the electrolysis reaction on the anode. By increasing the stirring rate or applying a two-compartment cell, higher desorption of metals bound in the organic fraction has been observed [28, 34]. In addition to increasing heavy metal removal, oxidation of the sediment increases the availability of hydrophobic pollutants. This is, for instance, relevant for the chemical decomposition of PCBs, which increases at $pH < 5$ [13] and could explain the relatively high 62% removal efficiency in [37].

5.2.2.2 Enhancement of EKR – Chemical Agents and Surfactants

Enhanced EKR technology is highly dependent on the type of processing solutions added to the electrode compartments (electrolyte conditioning). Enhancing additives increase contaminant desorption from the solid substrate, solubilization in the

UNCORRECTED PROOFS

Trim Size: 170mm x 244mm Single Column Loose Ribeiro670117 c05.tex V1 - 12/09/2020 3:19pm Page 107

pore water, and migration to the electrode compartments. But targeted contaminants differ in their physicochemical properties, and the chemical compounds added to the electrode compartments can be very different. In the case of metals, an acidic pH enhances their solubilization and transport to the cathode. The main reaction inherent to the EKR process is water electrolysis: it generates H+ at the anode side and OH- at the cathode side and thus causes metals to precipitate (hydroxides) near the cathode. Therefore, acids are suitable candidates as enhancing agents near the cathode. Strong inorganic acids such as nitric acid and hydrochloric acid are obviously efficient for controlling the pH and acidifying the solid substrate [51, 52]. But these strong acids considerably degrade the treated sediment quality. Less drastic weak acids can also be added to the cathode compartment, such as acetic acid or citric acid (CA) [53].

Adding complexing agents or chelators can also convert soil-bound metals into soluble coordination or metal-chelate complexes and enhance their removal [54]. EDTA, ethylenediaminedisuccinic acid (EDDS), nitrilotriacetic acid (NTA), diethylenetriamine pentaacetic acid (DTPA), and ethyleneglycoltetraacetic acid (EGTA) were used to remove metals from soils [35, 36, 55, 56]. But these additives can potentially increase the toxicity of the sediment, so more environmentally friendly alternatives have been tested. CA is the most commonly used chelating agent; it is relatively inexpensive and environmentally benign [42, 44]. It has been extensively used because it contributes not only to control the pH and form negative metal complexes that better migrate to the anode side but also to significantly increase the electroosmotic flow (EOF), which is favorable for the multi-decontamination of neutral organic compounds [57]. Electrolyte conditioning has also been used to treat organic pollutants [58]. Controlling pH at the cathode by acidification of the solid substrate appeared to be favorable for removing PCBs and tributyl tin (TBT) [37]. In the case of organic pollutants such as the 2,4D organochlorine pesticide, which is dissociated in anionic species, pH conditioning at the anode using NaOH to keep an alkaline pH was more favorable for electromigration [59].

Introducing surfactants can also help better solubilize and mobilize heavy metals during EKR. Surface active agents are amphiphilic molecules, with a hydrophobic part and a hydrophilic part, which can be neutral (but polar), anionic, or cationic. Due to this asymmetric structure, surfactant monomers can aggregate into micellar structures and reduce interfacial and surface tension. Cationic surfactants are not used in EKR because they adsorb to the negatively charged soil or sediment surface and inhibit the formation of micelles. Anionic surfactants such as sodium dodecyl sulfate (SDS) are used more often because they have an affinity for cationic metals and can better transport them [60], but nonionic surfactants such as Tween 80 also enhance metal removal [31]. Recently, biodegradable biological surfactants (biosurfactants) produced by various bacteria, which have higher ecological safety, were also tested for metal removal: rhamnolipids, saponins, and sophorolipids proved to enhance metal removal [42, 61]. Among the surfactants used to increase PAH solubilization, nonionic and biological surfactants are chosen more often because cationic surfactants have high toxicity and anionic surfactants tend to migrate toward the anode opposite to the direction of EOF. One of the most-used synthetic

UNCORRECTED PROOFS

Trim Size: 170mm x 244mm Single Column Loose Ribeiro670117 c05.tex V1 - 12/09/2020 3:19pm Page 108

surfactants is Tween 80, but Igepal, Brij, Merpol, Tergitol, Tyloxapol, Nonidet, APG, and Calfax have also been examined [40, 62, 63]. For PAHs, the highest removal has been reported using Nonidet P40 (48% removal) and Poloxamer 407 (43% removal). Among the biological surfactants, rhamnolipid glycolipids, which are commercially available, are the most applied for EKR of PAHs [64], but other classes of biosurfactants such as cyclolipopetides, produced by bacteria, have also been tested [65]. However, biosurfactants appear less efficient than synthetic surfactants, probably because of their higher degradability, particularly at the anode side where oxidation occurs. Adding the anionic SDS surfactant was favorable for eliminating nonpolar organochlorine pesticides that give anionic species [66]. In contrast, adding nonionic surfactants (Igepal) or the saponin biosurfactant was favorable for PCB elimination, which migrates to the cathode side by electroosmosis [67, 68]. Cyclodextrins were also tested for removing hexachlorobenzene pesticide [69].

Combining surfactants with chemical/complexing agents has shown promise in simultaneous removal from PAH and metal-spiked sediments, removing 54–56% of PAH and 10–91% of metals by using either Tween 20 and CA, or Tween 80 combined with MGDA [39, 43]. The promising results of applying Tween 20 in combination with CA have been confirmed in experiments with aged sediments, albeit with lower removal efficiencies [65]. Hahldakis et al. found the best combination to be Nonidet P40 combined with acetic acid at the cathode, enabling simultaneous removal of 41–83% of metals and 30% total of 16PAH, with some PAH compounds up to 70% [40]. By applying CA and saponin, it was possible to mobilize and remove 4–16% of metals, 29% of PAHs, and 38% of PCBs [44].

EKR technology has also been used in combination with other remediation technologies for contaminated sediment, primarily chemical oxidation, and bioremediation. By combining EKR with electrolyte conditioning and chemical oxidation, Jiang et al. showed that it was possible to remove up to 61% of Cr [70], while Pazos et al. were able to simultaneously remove 90% of petroleum hydrocarbons and 55–60% of metals from contaminated marine sediments [36]. Electrokinetics has been combined with bioremediation by controlling the redox potential, thereby providing electron acceptors to enhance the natural degradation of PAHs [38]. Based on these results, the authors developed a reactive cap for covering polluted sediments, enhancing degradation, and decreasing exposure of PAHs to the marine environment [71]. Cappello et al. also used electrokinetics to obtain aerobic conditions in oil-polluted sediments, whereby aromatic hydrocarbons were made more available for removal via electroosmosis and simultaneously enhanced the biodegradation of low-weight molecular alkanes [72].

5.2.2.3 Sediment Characteristics

The efficiency of EKR, whether unenhanced, enhanced, or combined with other remediation technologies, has repeatedly been shown to be highly affected by the characteristics of the sediment. Buffer capacity, organic matter, pollutant availability, mineral composition, grain size, and salt influence EKR [42, 73, 74]. A high buffer capacity can retard the acidification and subsequent desorption/extraction of pollutants in the sediment [43]. Organic matter can contribute to the buffer capacity and

UNCORRECTED PROOFS

Trim Size: 170mm x 244mm Single Column Loose Ribeiro670117 c05.tex V1 - 12/09/2020 3:19pm Page 109

further retard acidification and removal of pollutants. The adsorption and binding of pollutants in the sediments also affect the efficiency of EKR. Organic pollutants and metals can be strongly adsorbed to organic matter, metals can also be bound in minerals, and the mineral composition will also influence how available the metal is for desorption/dissolution during EKR [75]. Salt in the sediment may form complexes and decrease the current efficiency [51]. Several studies have investigated how to overcome challenges met in contaminated sediments with characteristics that retard or prevent adequate removal, e.g. by using electrolyte conditioning in high-buffer-capacity sediments [76] and sediment with high organic matter content [77], or by using stirred setups in sediments with high organic matter content [37].

Case Study 5.1

Assessing the Relative Importance of Experimental Variables and Sediment Characteristics

EDR studies from 2014 to 2017 investigated the influence of experimental variables on 6 different sediments in 47 experiments. Projection onto latent structure (PLS) models have been calculated to evaluate variable importance in the 47 experiments. PLS is a chemometric tool in which correlations between variance in the variables (here, experimental settings and sediment characteristics) and the variance in responses (here, final concentrations of Cu, Pb, and Zn) are calculated. Variable importance is assessed in loading plots. Results presented here are supplement results in [78], in which individual models of Cu, Pb, and Zn were presented. Here they are merged in the same models. The experimental space and sediment characteristics are summarized in Table 5.2; for more detailed information, the reader is referred to [78].

Table 5.2 Sediment characteristics and pollutant concentrations in 47 EDR experiments.

Parameter	Unit	Range	Parameter	Unit	Range
Metals			Carbonate	%	0.7–45
	mg/kg		Organic matter	%	4.8–14.7
Al		4250–8650	Total carbon	%	3.1–10.1
Ba		121–1350	Sulfur	%	0.2–1.2
Ca		4500–145 600	Nitrogen	%	0.01–0.5
Fe		6400–18 700	pH		7.0–8.2
K		1450–4440	*Grain size*		

(Continued)

UNCORRECTED PROOFS

Trim Size: 170mm x 244mm Single Column Loose Ribeiro670117 c05.tex V1 - 12/09/2020 3:19pm Page 110

Case Study 5.1 (Continued)

Table 5.2 (Continued)

Parameter	Unit	Range	Parameter	Unit	Range
Mg		3450–7560	Clay (<2 μm)	%	1.6–8.9
Mn		70–132	Silt (2–63 μm)		18–52
V		25–77	Sand (63–2000 μm)		54–77
Cd		0.1–1.1	Gravel (>2 mm)		0.7–5.1
Cr		15–47	*Experimental variables and settings*		
Cu		54–216	Remediation time		25–672 h
Hg		0.01–1.2	Time after pH 4		0–572 h
Ni		10–23	Current density		0.04–1.0 mA cm^{-2}
Pb		42–152	Liquid–solid ratio		2–12 l kg^{-1}
Zn		83–960	Stirring rate		1–1300 rpm
Chloride	mg/kg	6240–14 100	Suspension liquid		Distilled/tap water
Conductivity	mS/cm	7.0–20	Light[a)]		Light/no light
Cation exchange capacity	meq/100 g	1.8–12.8			

a) The influence of daylight was investigated due to the Arctic locations of the sampled sediments.

To investigate the relative influence of experimental variables and sediment characteristics on the different phases of EDR, three PLS models were calculated based on pH-dependent desorption tests of the metals [78]:

1) Acidification phase, in which limited desorption/removal of metals was observed at pH>3.6
2) Fast removal phase, in which most of the metals were removed for pH range 2–4
3) Slow removal phase after the fast removal phase when pH < 2

The results of the three PLS models are presented in loading plots (Figure 5.2). Variables/sediment characteristics located farthest from (0,0) have the greatest influence on the models, parameters located close to each other are correlated, and parameters located opposite each other are inversely correlated.

UNCORRECTED PROOFS

Trim Size: 170mm x 244mm Single Column Loose Ribeiro670117 c05.tex V1 - 12/09/2020 3:19pm Page 111

The sediment characteristics generally have a greater influence on the different phases of EDR than experimental variables. In the acidification phase, the remediation time and liquid/solid ratio are most influential on the final concentrations of Cu, Pb, and Zn, with high settings increasing the removal (opposite position in Figure 5.2a). In the fast metal removal phase, the stirring rate and remediation time are important for removing metals, with high settings increasing removal. A high stirring rate ensures better mixing of the sediment and increased oxidation of the sediment, thereby releasing metals bound in organic matter. In the final phase of EDR, in which pH has reached levels below 2, the experimental variables do not significantly influence removal. In this phase of EDR, removing metals appears to be more dependent on sediment properties, which indicates lower availability of metals in the sediment.

The influence of carbonate is strongest in the initial phase of EDR (Figure 5.2b) and decreases in the following phases in which carbonate is depleted. The influence of organic matter is greatest after the acidification phase, with high organic matter content resulting in higher final concentrations of metals. This indicates that the release of metals from the organic fraction in the sediment is slower than for metals bound in other fractions of the sediment. The correlation between Cu and sulfur in the fast removal phase suggests that Cu remains bound to sulfur at pH 2–4. The increasing influence of chloride in the final phase of EDR is correlated to Pb and Zn (Figure 5.2c), suggesting that the differences in the final concentrations are related to complexing with chlorides. The reason for chloride not having much influence in the preceding models (i.e. initial EDR phases), for which complexing may be expected, is that processes other than complexing with chloride are predominant. The strong influence of grain size during EDR indicates that the relative binding of heavy metals in gravel, sand, silt, and clay is essential for removal and may be due to the relatively higher amounts of metals bound in clay and silt.

The results show that sediment characteristics are important, the relative importance changes in the different phases of EDR, and multivariate analysis can be used to identify important variables and interactions between experimental variables and sediment characteristics. This can in turn be used to design the remediation according to the assigned goals by adjusting experimental settings or expanding the experimental space to optimize removal.

5.3 Case Studies of Enhancement Techniques

Successful laboratory-scale EKR tests have been reported for several years for contaminated sediments. EKR technology is highly dependent on the system components, such as power for the electric field, electrode material and placement, and electrolyte solutions. The enhancement of EKR is ongoing by the selection of these parameters and by adopting appropriate electrochemical conditions for each kind of pollutant, as illustrated here with three case studies.

UNCORRECTED PROOFS

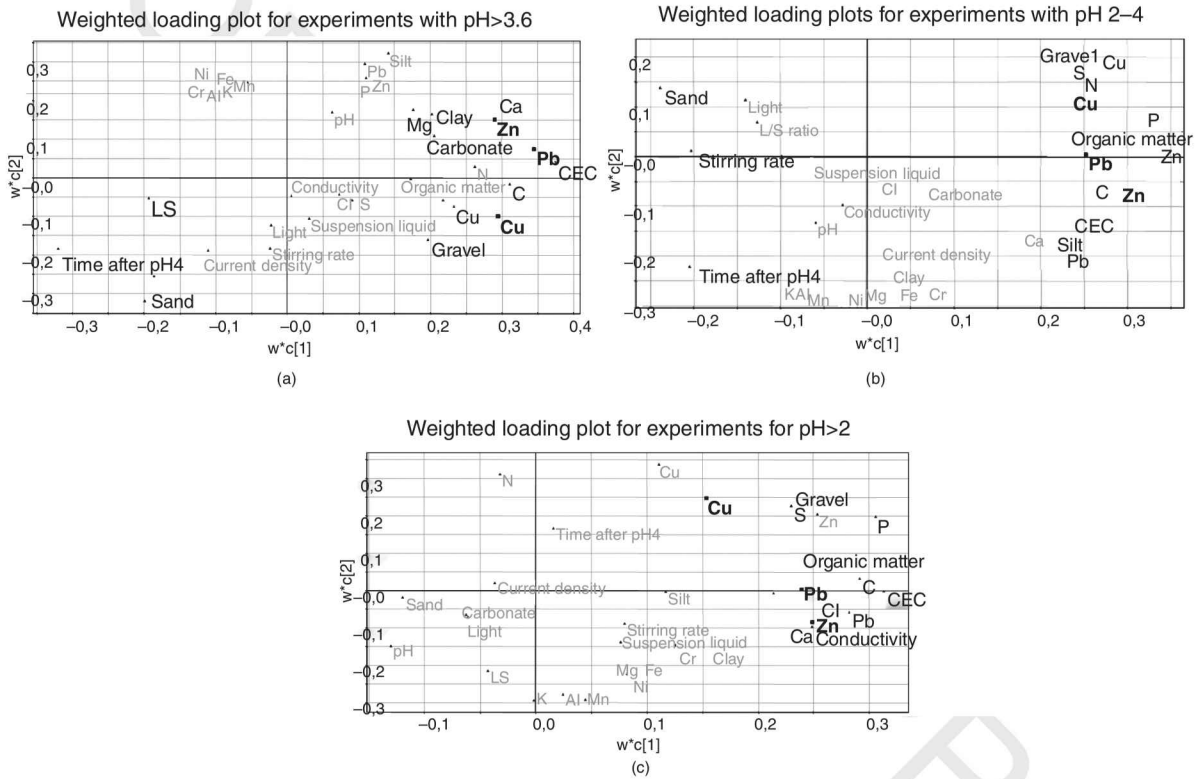

Figure 5.2 Weight plots of variables (w*) and responses (c) for the first and second component of the three PLS models: (a) pH > 3.6, explaining 55% of the variance in the dataset; (b) pH 2–4, explaining 64% of the variance in the dataset; and (c) pH < 2, explaining 68% of the variance in the dataset. Correlated parameters are located adjacent to one another. Responses of Cu, Pb, and Zn are highlighted in bold. Parameters with major influence on the models (variable importance in the projection values > 1) are highlighted in black font; parameters with low-moderate influence on the models (variable importance in the projection values < 1) are in smaller gray font.

UNCORRECTED PROOFS

Trim Size: 170mm x 244mm Single Column Loose
Ribeiro670117 c05.tex V1 - 12/09/2020 3:19pm Page 112

Trim Size: 170mm x 244mm Single Column Loose Ribeiro670117 c05.tex V1 - 12/09/2020 3:19pm Page 113

case study 5.2

Voltage Gradient

Natural dredged sediments were used for the EKR experiments, which aimed to optimize the electrochemical parameters to enhance the removal of pollutants (organics and inorganics). The materials were collected from a French harbor disposal site in Normandy (France), localized near important urban centers and industrialized areas. The pooled sediment samples were homogenized and stored at 4 °C. The physicochemical properties of the sediment are presented in Table 5.3. The sediment had high moisture content and low hydraulic conductivity owing to its fine-grained composition. The high carbonate and fairly high organic matter make this sediment interesting regarding the high buffer capacity.

Table 5.3 Characteristics of the sediment sample.

	Parameter	Values	Method
Sediment sample	Clay	6.3%	Particle size analyzer Multisizer 2000-Malvaern
	Silt	86.2%	
	Sand	7.5%	
	Water content	93%	NF P 94–050
	Organic matter	11.6%	At 450 °C for 6 h
	Carbonate	30.5%	Bernard Calcimeter
	Hydraulic conductivity	$1.0\ 10^{-7}$ m s^{-1}	Falling-head method
	pH (1 : 10 water)	8.4 ± 0.2	(1 : 10) Sediment-water
	EC (1 : 10 water)	1.57 ms cm^{-1}	
Initial metal contaminant concentration (mg kg^{-1} dry matter)	As	14.9	Microwave acid mineralization and ICP-AES
	Cd	4.6	
	Cr	136.3	
	Cu	64.0	
	Ni	39.0	
	Pb	63.9	
	Zn	222.8	
Initial POPs concentration (µg kg^{-1} dry matter)	∑16PAH priority	2114 ± 63	Microwave solvent extraction + GC-MS
	∑ PCB7 (indicators)	192 ± 1	Microwave solvent extraction + GC-MS

(Continued)

UNCORRECTED PROOFS

Trim Size: 170mm x 244mm Single Column Loose Ribeiro670117 c05.tex V1 - 12/09/2020 3:19pm Page 114

case study 5.2 (Continued)

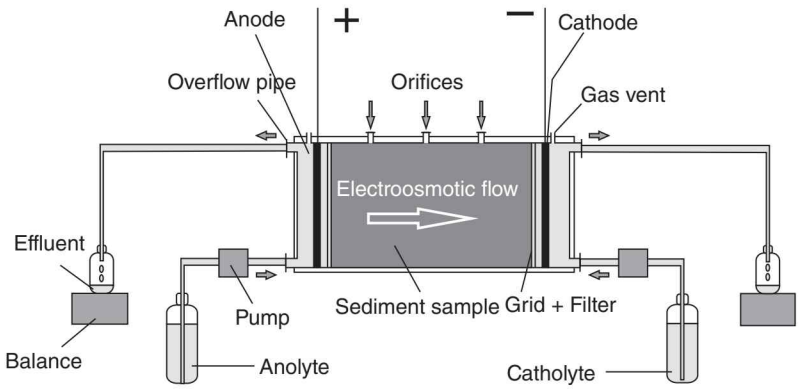

Figure 5.3 A schematic diagram of the experimental setup.

The natural wet sediment was fully packed into a cylindrical chamber made of Teflon PTFE (4.9 cm inner diameter × 14.2 cm length). Two graphite electrode plates were placed in each electrode compartment (4.9 cm diameter × 5 cm length), which were separated from the sediment by perforated grids and porous fiberglass papers (0.45 μm). Two pumps fed the electrode reservoirs with aqueous solution (anolyte or catholyte) at a low flow rate (Figure 5.3). EOF was calculated from the difference between the volume generated by the imposed flow and the periodic measurement of the effluent volume flowing from the electrode compartments. A voltage gradient (1 V cm^{-1}) was applied continuously or pulsed (alternating five days on and two days off), and the electrical current was measured periodically.

The experimental conditions are summarized in Table 5.4. Chelating agents and surfactants were combined as electrolyte solutions to increase metal and PAH mobility. The results are shown in Table 5.5.

Table 5.4 Conditions of EKR tests.

Test	Anolytes and catholytes	days	Voltage gradient/mode
1	Tween 20 (4.94 g·l^{-1}) + citric acid (0.1 mol·l^{-1})	21	1 V·cm^{-1}/continuous
2	Tween 20 (4.94 g·l^{-1}) + citric acid (0.1 mol·l^{-1})		1 V·cm^{-1}/alternate

UNCORRECTED PROOFS

Trim Size: 170mm x 244mm Single Column Loose Ribeiro670117 c05.tex V1 - 12/09/2020 3:19pm Page 115

Table 5.5 Metal and PAH removal (%).

	Test 1	Test 2
Metals		
Cd	12.8	34.9
Cr	1.3	8.5
Cu	1.6	5.6
Pb	12.9	28.8
Zn	43.0	50.2
PAHs		
Naph	38.4	44.5
Ace	30.4	42.2
Acy	67.5	73.1
Fluo	35.7	32.9
Phen	20.4	32.9
Ant	31.9	40.8
Flt	32.5	45.8
Pyr	30.8	44.6
B[*a*]ant	31.7	48.5
Chry	54.6	63.0
B[*b*]flt	9.1	24.3
B[*k*]flt	48.0	62.8
B[*a*]pyr	22.6	44.0
I[1.2.3-*cd*]pyr	43.0	57.4
Db[*ah*]ant	26.0	50.1
B[*ghi*]per	42.8	63.3
Total PAH removal	**35.3**	**48.1**

CA was added to the purging fluid for two primary reasons: (i) to generate H^+, particularly near the cathode, in order to hinder the transport of OH^- generated by the electrolysis of water and to avoid the formation of an alkaline front, causing metal precipitation (formation of hydroxides); and (ii) to generate citrate ions, which can form anionic metal complexes and favors their solubilization into the interstitial fluid and migration to the anode side. But the high buffering capacity of the natural sediment counteracted the acidification of the sediment column and consequently prevented metal solubilization and electromigration. Indeed, Zn tends to precipitate as hydroxide at pH above 7, whereas Cr, Cu, and Pb precipitate at pH above 4–5. So, Zn was easier to remove in its cationic form in the natural sediment ($pH > 6$ at the end of the EKR process), and it was preferentially found in the cathode compartment. Cr and Cu remained immobilized in the sediment in experiment 1 and did not

UNCORRECTED PROOFS

Trim Size: 170mm x 244mm Single Column Loose Ribeiro670117 c05.tex V1 - 12/09/2020 3:19pm Page 116

form soluble complexes with CA. Concerning Pb, which precipitated as hydroxide at pH conditions of the tested sediment, its removal could be attributed to the formation of chelates with CA, which migrated preferentially to the anode compartment. Cd was atypical since it formed hydroxides only at pH > 8 but its migration as a free cation was low, preferentially to the cathode. In fact, Cd is more likely to bind to organic matter than other metals and is difficult to mobilize. Moreover, the stability of Cd complexes with citrate is low [54], which prevents its migration to the anode. Applying an alternative voltage gradient (experiment 2) enhanced the decontamination of the overall sediment column, but only slightly better near the cathode: the greater pulsed current intensity was favorable for metal removal (Table 5.5). Switching off the EKR system leads the matrix to re-equilibrate: adsorbed charged elements move to the depleted fluid phase to reach equilibrium again. Switching on reactivates the ionic mobility of the enriched fluid toward the electrode with opposite charge.

Removal of lipophilic compounds such as PAHs can be attributed to the combined effect of (i) the ability of the purging fluid to desorb and solubilize the contaminants and (ii) the possible migration of the dissolved contaminants to the electrodes. PAH desorption and solubilization were possible because of the presence of the nonionic surfactant (Tween20) in the purging solution, which can form micellar aggregates at concentrations higher than the critical micelle concentration (CMC) and solubilize PAHs in their hydrophobic interior. EOF is a major factor when we consider removing neutral compounds such as PAHs or PAHs incorporated in nonionic surfactants. Table 5.5 shows that PAH removal was also increased, from 35.3% for the sum of the 16 priority PAHs (test 1) to 48.1% (test 2). Applying a periodic voltage gradient was beneficial for PAH removal: desorption and solubilization of PAHs are rate-limited processes, and during the "down-time" voltage interval, re-equilibration at the solid-liquid interface occurs, and more PAHs can be solubilized into micellar aggregates.

The experiment performed with an alternative voltage gradient was the most powerful for removing metals, in particular Zn, Cd, and Pb. The treated dredged sediment contained large amounts of carbonates and so had a high buffering capacity, which appeared detrimental for metal removal. But using large amounts of CA, a periodic voltage gradient, and a sufficiently long treatment (to stabilize the sediment at a more acidic pH) seems necessary. With regard to PAHs, adding not only a surfactant but also CA had a positive effect on their removal; considering energy and additive consumption, test 2 was more favorable.

case study 5.3

Removal of Metals by Chelating Agents

To investigate improvement of metal removal with chelating agents, a series of EKR tests were made. This section evaluates and compares the enhancement effect of CA, EDTA, EDDS, and NTA for removing trace elements (As, Cd, Cr, Cu, Ni, Pb, and Zn) from dredged contaminated sediment. Arsenic is not a metal but

UNCORRECTED PROOFS

Trim Size: 170mm x 244mm Single Column Loose Ribeiro670117 c05.tex V1 - 12/09/2020 3:19pm Page 117

a metalloid and has a particular behavior compared to cationic metallic ions because it is mainly available in neutral or anionic forms (arsenites or arsenates). Moreover, in alkaline and reductive media, the reduced form (AsIII) is more mobile than the oxidized form (AsV). The chelating agents EDTA, EDDS, and NTA help to desorb metals from the sediment and form anionic complexes, which migrate from the cathode to the anode [45, 79]. Solutions of chelates were prepared (0.1 mol l^{-1}) and used to feed both electrode compartments. The tests were performed under an electrical field of 1 V cm^{-1} for 21 days. As a control test, distilled water (DW) was previously used as an electrolyte. The initial pH of the sediment was measured at 8.2. At the end of the tests, sediment pH was in the range (from anode to cathode) 6.8 to 9.5 for DW, 7.9 to 8.8 for EDTA, 8.2 to 10.1 for EDDS, 3.4 to 7.3 for NTA, and 6 to 7.2 for CA tests.

Figure 5.4 shows that removal efficiency with EDTA for five trace elements: Zn, Pb, Ni, Cr, and As, reached the highest overall values. EDTA could be considered the most effective processing additive for removing trace elements in this research. In the EDTA test, much of the Pb and Ni was extracted from sediment, Pb being the most mobile metal (about 60% removed) and Cd the least mobile (about 15% removed). The best recoveries were obtained in the order Pb > Ni > Cr > Zn > As > Cu > Cd. It is known that Pb-$EDTA^{2-}$ is the dominant form under neutral and alkaline sediment pH. Therefore, negatively charged Pb-EDTA complexes were transported toward the anode by electromigration [45]. The stability constants of M-EDTA complexes are much higher than those of other complexes. EDTA can be attached to a metal ion at up to six sites, makes metals desorb from the particulate surface, and increases the migration rate of metal ions through the material [79]. The pH of the system and the environment can affect the stability and effectiveness of the chelating system. EDTA dissolves better in more alkaline solutions [80]. In the EDDS-test, the results (Figure 5.4) indicate that the best-removed metal is Cu (about 51%), and Zn is the least-recovered metal (about 26%). By the end of the experiment, the best recoveries were obtained in the order Cu > Ni > Cr > Cd ≈ Pb > As > Zn. The competition with major ions in the system, such as Ca, Mg, or Fe, can affect the chelation of minor contaminants. But the constant stability values for Ca, Mg, and Fe complexed with EDTA or EDDS are lower than for Cr, Cu, Ni, Cd, and Pb at neutral or alkaline pH. At the end of the EKR tests using EDTA and EDDS, sediment pH was neutral near the anode and alkaline near the cathode. This leads to a reduction of the competition between major cations and metals for complex formation in the case of EDDS and EDTA and shows significant extraction efficiencies for Cr, Cu, Ni, Cd, and Pb.

When using NTA, M-NTA-complexes were formed with Cd, Cr, Cu, Ni, and Zn, and they migrated toward the anode. At the end of the experiment, 43% of Cr, 38% of Cd, and 34% of Cu and Ni were removed from the sediment (Figure 5.4). As and Pb remained immobilized in the sediment and apparently did not form large amounts of soluble complexes with NTA. The order of extraction efficiency is Cr > Cd > Cu ≈ Ni > Zn > Pb ≈ As. Using CA as an additive, trace element removal

UNCORRECTED PROOFS

Trim Size: 170mm x 244mm Single Column Loose Ribeiro670117 c05.tex V1 - 12/09/2020 3:19pm Page 118

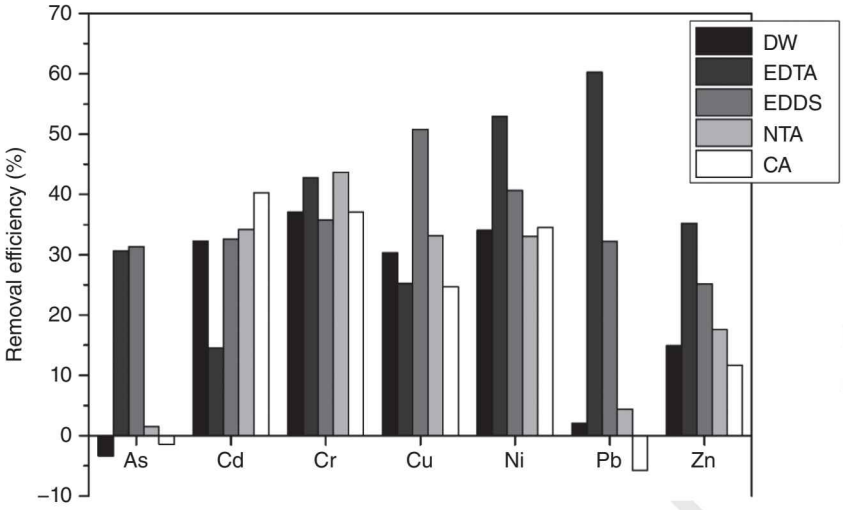

Figure 5.4 Metal removal efficiency after each EKR test.

efficiencies were better, in the order Cd > Cr > Ni > Cu > Zn > As > Pb. As and Pb did not form large amounts of soluble complexes with CA (Figure 5.4).

As a result of the high pH value in the sediment after EDTA and EDDS tests, As in its reduced and more mobile form (AsIII) was more effectively removed from the sediment matrix. In the presence of CA, the sediment pH was acidified, and the less mobile form of As(V) could not be removed.

The results of the EDTA and EDDS tests do not illustrate their chelate enhancement on Cd compared to the DW test, due to the low pH value involved in this test. In these cases, the sediment pH remains neutral or alkaline, which was not favorable for Cd complexation. Using NTA or CA could slightly increase Cd removal efficiency. Indeed, in these two cases, the sediment pH was acidified, particularly at the anode side, which was more favorable for Cd release from organic matter and further complexation.

Ni exists as Ni (II) cations when the pH is less than about 6.0 and precipitates as $Ni(OH)_2$ when the pH becomes greater than around 8.0 [81]. So, Ni removal presents similar removal efficiency (~33–35%) for NTA and CA tests, where acidic conditions allow Ni to be removed (Figure 5.4). However, the removal efficiency of Ni was increased (reaching 40.5% and 52.7%) after the EK treatment enhanced by EDDS and EDTA, in quite alkaline conditions. The enhancement involving EDTA compared with DW and CA has also been reported by Iannelli et al. and is due to higher chelating constants with Ni in neutral or alkaline conditions [46].

NTA and CA were not effective for releasing Pb compared to EDTA or EDDS in a lower-pH environment (pH < 8). However, the Pb removal efficiency for the EDTA test was two times higher than the Pb removal efficiency with EDDS because EDTA has an excellent affinity for Fe (III), and most of the Pb was adsorbed to Fe-Mn oxides [82, 83]. So the release of Fe(III) was also favorable to the release of Pb and further complexation. Some authors reported that M-EDTA complexation depends on the

UNCORRECTED PROOFS

Trim Size: 170mm x 244mm Single Column Loose Ribeiro670117 c05.tex V1 - 12/09/2020 3:19pm Page 119

fractionation of metals in sediments and might be limited to metals bound to easily extractable fractions [83].

No enhancement of Cu removal by EDTA and CA could be observed compared to the DW test. Similar results have been obtained by Iannelli et al. and Ammami et al. [46, 65]. The enhancement of EDDS was better reflected in Cu removal (52% removed), this value being two times higher than that obtained in the EDTA test. Chen et al. observed the high capacity of EDDS to form complexes with Cu [84].

Figure 5.4 shows that Zn was more significantly removed using EDTA, EDDS, and NTA compared to pure water. The removal efficiencies in DW and CA tests were low (respectively, 14.6% and 11.5%). Zn tends to precipitate as a hydroxide at pH > 7, so free Zn was not mobile in neutral-alkaline conditions [65]. But using chelating agents increased the removal efficiency of this metal in the order EDTA > NTA > EDDS, thus even in quite alkaline conditions. In the case of CA, the complex with Zn formed in acidic conditions (around pH = 4), which were not encountered in the sediment specimen. This study confirms that the metal removal efficiency through EKR is related to the stability constants of metal-chelate complexes and so depends on the type of chelating agent, the sediment's pH, the aqueous solution, and also the metal mineral speciation.

case study 5.4

Simultaneous Removal of PAHs and PCBs by Chelating Agents

This case study was devoted to the investigations of EKR efficiency for mobilizing and removing PAHs and PCBs from dredged sediments by using combinations of chelating agents and surfactants (Table 5.6).

Table 5.6 Summary of EKR tests and removal results for PAHs and PCBs.

Test	Voltage (V cm^{-1})	Anolyte/Catholyte	Duration (days)
EK1	1 (5 d on/2 d off)	Saponin (0.85 g l^{-1}) + citric acid (0.2 M)	28
EK2	1 (5 d on/2 d off)	Saponin (0.85 g l^{-1}) + citric acid (0.1 M)	
EK3	1 (5 d on/2 d off)	Saponin (5 g l^{-1}) + EDDS (0.1 M)	

The greatest removals of PAHs and PCBs were obtained in the EK 1 and EK 2 tests, respectively, using enhancing additives (Table 5.7). PCB removal was tightly related to the cumulative EOF at the cathode side of each EKR test, the EOF being enhanced when adding CA compared to EDDS. The higher the cumulative EOF was, the greater the removal of PCBs. It was reported that in the presence of a nonionic surfactant, PCBs were transported via EOF [68]. With PCBs, adding a biosurfactant helped in PAH removal. But EK 3 was less efficient for PAH remediation, owing to the alkaline environment due to EDDS, which

(Continued)

UNCORRECTED PROOFS

Trim Size: 170mm x 244mm Single Column Loose Ribeiro670117 c05.tex V1 - 12/09/2020 3:19pm Page 120

case study 5.4 (Continued)

could not hinder the formation of the alkaline front at the cathode side: saponin was partially charged negatively and so was unable to desorb the PAHs quantitatively from the negatively charged sediment surface. So, in this test, even if the concentration of saponin was six times higher than in the EK 1 and EK 2 tests, the removal results were worse, removing only 5.2% of PAHs. The desorption of PCBs in the EK 3 test was also less significant than in the EK 2 test, but the removal was better than for PAHs (38.7%). It is suggested that after being desorbed by the biosurfactant, PCBs, as polarized molecules, were then surrounded by water molecules and could be transported by the pore fluid with EOF. Compared to PAHs, PCB migration depends more on the pore fluid migration, while PAH mobilization depends on the surfactant micelles' migration.

Table 5.7 Metal, PAH, and PCB removal (%).

	Removal (%)	
Test	**Σ16PAH**	**Σ7PCB**
EK1	29.2	38.2
EK2	13.1	50.2
EK3	5.2	38.7

5.4 Evaluation of the Best Available EKR Practice

The design of EKR for remediation of harbor sediments depends on remediation goals, pollutant(s), pollutant availability, and sediment characteristics. Accordingly, EKR should be efficient in removing pollutants, have efficient energy consumption, and have limited environmental impacts during and after treatment. These will be among important considerations for evaluating EKR as a relevant method for reusing sediments, scaling up, and potential commercial use of EKR.

5.4.1 Energy Consumption

On land, dredged polluted sediments are managed as polluted material, or sometimes as hazardous waste. Disposal as polluted waste in the EU typically costs 50–150 € t^{-1}, depending on the pollutant concentration and composition. In addition, there are costs for dewatering sediments and transport; the distance to the closest landfill licensed for polluted waste can, in some cases, be more than 1000 km. It is difficult to determine a specific threshold for using energy for driving current through sediment during EKR: it depends on the cost of the EKR design (e.g. pumps, mechanical stirring, installation, etc.) and the added value of treated

UNCORRECTED PROOFS

Trim Size: 170mm x 244mm Single Column Loose Ribeiro670117 c05.tex V1 - 12/09/2020 3:19pm Page 121

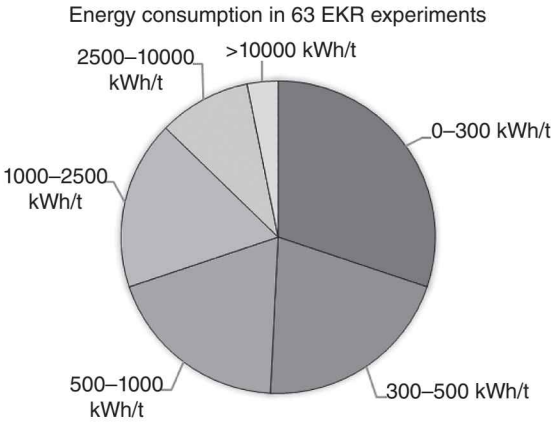

Figure 5.5 EKR experiments and energy consumption (kWh/t). Source: Based on 63 published EKR experiments in 12 articles: Pedersen et al. [28]; Hahladakis et al. [31]; Song et al. [35]; Pedersen et al. [37]; Hahladakis, Latsos, and Gidarakos [40]; Hahladakis, Calmano, and Gidarakos [41]; Benamar et al. [42]; Iannelli et al. [46]; Ottosen et al. [47]; Colacicco et al. [104]; Pedersen et al. [111]; Krcmar et al. [117]. Reported energy consumption of kWh/m^3 has been converted to kWh/t by average sediment density of 1.6 t m^{-3}.

sediments for reuse compared to the total cost of disposal on land. However, if the energy consumption for EKR treatment remains within the cost of polluted waste disposal at landfills, there is the potential for cost-efficient remediation technology. In Europe, the cost of non-household electricity was 0.06–0.17 € kWh^{-1} in 2019 (Eurostat). Converting the disposal cost of 50–150 € t^{-1} gives an energy consumption range of 300–2500 kWht^{-1} of sediment. If an electric field in EKR exceeds 2500 kWht^{-1}, it is highly likely that further optimization to ensure increased energy efficiency is necessary.

In the literature, some EKR studies of marine sediments have calculated energy consumption based on the applied current and voltage during the experiments. Approximately one-third of the experiments had an energy consumption of 300 kWht^{-1}, and almost 90% were below 2500 kWht^{-1} (Figure 5.5). This is a good indication of the potential for using EKR for remediation of marine sediments. A few experiments had an energy consumption above 10 000 kWht^{-1} and were related to sediment characteristics [28, 74]. The lowest energy consumption levels have been observed in stirred setups, with several below 50 kWht^{-1}; stirring ensures better mixing and less resistance in the sediment. The lowest energy consumption levels, down to 3 kWht^{-1}, were achieved in two-compartment cells in which placing the anode directly in the sediment reduces the energy needed for acidification and transport across an anion-exchange membrane [28]. Other experiments that reported energy consumption levels below 300 kWht^{-1} included washing the sediment prior to EK treatment to reduce salt levels [74] and using biosurfactants or the surfactant Tween 20 [42].

It is important to note that energy consumption is seldom related to cleanup levels after EKR. Low energy consumption levels, however, indicate the potential for

UNCORRECTED PROOFS

Trim Size: 170mm x 244mm Single Column Loose Ribeiro670117 c05.tex V1 - 12/09/2020 3:19pm Page 122

ensuring efficient use of the current during EKR. For future experiments and to scale up, there is a need to relate removal efficiencies and energy consumption to remediation goals and remediation alternatives. In addition, there are no studies relating energy consumptions in lab-scale experiments to scaling up, and a linear correlation between the two may not exist. For instance, a pilot-scale experiment has shown that it is possible to remove 90% of Pb in marine sediments with an energy consumption below 1 $kWht^{-1}$ [85], indicating the potential for reducing the energy consumption per quantity of sediments when scaling up.

5.4.2 Environmental Impacts

An essential aspect of evaluating and choosing the best available EKR methodology for remediating marine sediments is assessing environmental aspects during and after EKR. The environmental benefits of remediation should preferably outweigh the environmental impacts. These include the use of chemicals, energy consumption, effect on organisms in the sediment during EKR treatment, availability of residual pollution, leaching of pollutants, potential remaining toxic chemicals in the sediment, and impacts of the final use of the sediment. There have been limited studies on the environmental effects of EKR of marine sediments. The few that have been published have focused on one environmental impact per study, and no studies have been undertaken to assess the total impact of EKR on the environment.

To our knowledge, no studies have been made of the effect of the use and replacement of potentially toxic chemicals during EKR. For instance, it has been well established that EDTA, one of the more efficient chemicals in EKR, has adverse effects on organisms and plants [86, 87]. A study has revealed a lethal effect on copepods after EKR using chemical agents; this could, however, be a combined effect of chemical agents, low pH, and residual pollutants [42]. Another study revealed that using CA and biosurfactants did not negatively impact copepods [44]. Studies that isolate the effect on the residual concentration of toxic chemicals or on the effects of the waste management of electrolyte liquids after EKR are needed. Replacing potentially toxic chemicals with green chemicals will be related to removal efficiencies, energy consumption, and the final use of the sediment.

During EKR, the availability of pollutants in the sediment increases; EKR could potentially make residual pollution more available for desorption/solubilization, thereby increasing the risk of leaching with an adverse effect on the environment. For instance, it was revealed that the leaching of metals at neutral pH was similar before and after EDR, which removed 35–95% of targeted metals in the sediment [88]. The potential adverse effects of leaching residual pollutants in sediments have not been fully investigated. A study of the adverse effects on copepods has indicated that residual pollution can affect marine organisms [44].

The final use of treated sediments affects cleanup levels and potential environmental impacts. If sediments are reused in the environment, there will be a higher focus on toxicity, whereas if they are used in construction materials, stabilization and strength may be more significant criteria. Marine sediments have been used in harbor foundations.

UNCORRECTED PROOFS

Trim Size: 170mm x 244mm Single Column Loose Ribeiro670117 c05.tex V1 - 12/09/2020 3:19pm Page 123

5.5 Scaling Up EKR for Remediation of Polluted Harbor Sediments

EKR studies aim to address the effectiveness of remediating polluted sediments, and the operating conditions selected at bench scale are generally the starting point for large-scale treatments. Most of the EKR in the literature deals with small-scale experimental devices, and few land features have been developed to treat large amounts of sediment. To scale up small laboratory-scale tests to treat land features, an intermediate-scale investigation is of great interest [89, 90]. In EKR, various rate constants (linked to kinetics parameters), transfer coefficients (linked to equilibrium constants), and transport properties (linked to fluid dynamics), as well as the reactor dimensions, must be taken into account to understand the complex processes. The complex nature of the field conditions (soil heterogeneity, unsaturated medium, large volume) and the inability to predict field EKR performance using selected laboratory operating parameters led to unexpected efficiency in the field [46]. Among the key parameters to be investigated is the predicted time required for efficient remediation. Control of electrolyte additives and pH were the key features of the electrokinetic technology to enhance the removal of pollutants from soils and sediments. Limited field experiments for harbor sediments have been conducted; field experiments in soil mainly employed simple electrode configurations involving vertical or horizontal electrodes in the polluted site, and drilling wells or trenches around the area of concern. Scaling up electrochemical process units requires similar values for corresponding dimensionless groups. From the literature [91], several primary similarity criteria have been suggested: geometric similarity (but high voltage drops and increased energy costs arise), kinematic similarity (concerns the flow velocities within a system), thermal similarity (maintaining the same temperature in corresponding reactors), and current/potential similarity (maintaining a constant inter-electrode gap).

case study 5.5

Example of Scaling Up EKR

A preliminary scale-up investigation is reported in this section and involves two reactors (small and intermediate scale) devoted to evaluating the potential for the EKR process and effect of scaling up. Mixtures of eco-friendly enhancing additives for the treatment of multi-contaminated harbor sediment were used, and efficiency was measured through the pollutants' removal. Additives providing better metal removal at the small scale (involving less than 0.4 kg of sediment) during EKR were used to perform tests at a medium scale with more than 40 kg of sediment. The electrochemical process's primary controlled parameters are the voltage gradient, electrode installation, reactor dimensions, the sediment porosity, and enhancing additives.

(Continued)

UNCORRECTED PROOFS

Trim Size: 170mm x 244mm Single Column Loose Ribeiro670117 c05.tex V1 - 12/09/2020 3:19pm Page 124

case study 5.5 (Continued)

The sediment was dredged from a waterway in a harbor in Normandy (France), and its physicochemical properties are presented in Table 5.8. The fine-grained sediment involves large fines content (silt) and high organic matter and carbonate contents.

Table 5.8 Summary of physical and chemical characteristics of tested sediment.

Particle size distribution (%)	Particles <2 μm (clays)	5.9 ± 1.7
	Particles from 2 to 63 μm (silts)	75.1 ± 1.6
	Particles from 63 to 2000 μm (sand)	18.9 ± 3.3
Physical and chemical properties	Organic matter content (%)	11
	Carbonate content (%)	30
	Hydraulic conductivity ($m\,s^{-1}$)	10^{-7}
	pH (n = 3)	8.3 ± 0.1
	Electrical conductivity ($\mu S\,cm^{-1}$) (n = 3)	2200 ± 80
	Redox potential (mV) (n = 3)	-76 ± 8
	PAHs ($mg\,kg^{-1}$ DW) (n = 5)	$\sum = 2.114 \pm 0.063$
	PCBs ($mg\,kg^{-1}$ DW) (n = 5)	$\sum = 0.192 \pm 0.014$
	Metals ($mg\,kg^{-1}$ DW) (n = 5)	$\sum = 410.51 \pm 21.29$
	Cd	4.02 ± 0.05
	Cr	136.68 ± 18.58
	Cu	39.21 ± 0.06
	Pb	59.88 ± 0.58
	Zn	170.72 ± 2.02

Two devices were designed as reactors (Figure 5.6) for EKR of dredged sediment: a small cylindrical cell 14 cm long and 5 cm in diameter, with three compartments (two electrode boxes and a specimen container) and a rectangular tank 60 cm long with a cross-section of $20 \times 20\,cm^2$. Before designing the large-scale reactor, considerations of which electrochemical parameters to keep constant were made. The voltage gradient was set with a ratio of 2 in the corresponding reactors (Table 5.9), plate electrodes were used, and the system was closed. The pulse voltage gradient was applied in both reactors by alternating five days on and two days off. The additives were $5\,g\,l^{-1}$ Tween 20 as anolyte and $5\,g\,l^{-1}$ Tween 20 + 0, $1\,mol\,l^{-1}$ CA as catholyte.

UNCORRECTED PROOFS

Trim Size: 170mm x 244mm Single Column Loose Ribeiro670117 c05.tex V1 - 12/09/2020 3:19pm Page 125

Table 5.9 Operating parameters of the EKR process at two scales.

Parameters	Small scale	Large scale	ratio
Electrodes gap (m)	0.14	0.60	4.3
Sediment volume (l)	0.28	24	85
Voltage gradient ($V\,cm^{-1}$)	1	0.5	0.5
Additives flow rate ($ml\,h^{-1}$)	5	50	10
Average value of EOF ($ml\,h^{-1}$)	0.2	6	30
Average current density ($mA\,cm^{-2}$)	0.5	0.75	1.5
Treatment duration (d)	21	56	2.7

5.5.1 Results and Comments

In this first approach of scaling up, the sediment temperature in the two reactors was maintained as similar as possible, around 20 °C. Most of the parameters are adjusted to achieve similar current density, which is the most important similarity. Figure 5.7 shows the evolution of current intensity during EKR. The results indicated that a high current value rises at the start of the EKR process, more than 10 times for the large reactor, and decreases more quickly for the small reactor. So, the average value of the current density (Table 5.9) remains similar in the two reactors. The alternate nature of the applied voltage leads to the reactivation of the current at each cycle.

Regarding EOF, the results from Figure 5.8 indicate that in the small-scale reactor, the main EOF was directed from the anode to the cathode, while in the large-scale reactor, the EOF occurs toward the two electrodes and was more activated by the current density. The amount of transported fluid was greater toward the cathode, but the volume recovered in the anode was not as significant, indicating that the EOF reverse direction increases due to the modification of chemical conditions. The pH values recorded within the sediment from the large specimen indicated low values in the upper sections. The electrical conductivity measured at the end of tests shows high recorded data near the anode where ions primarily concentrate.

The objective of scaling up is to adapt laboratory operating parameters (following similarity factors) to reach similar removal results at field or bench scale. This objective is not easily reached if any compartment of the large reactor has local conditions that hinder that EKR process's efficiency. The results of pollutant removal (Table 5.10) indicate that the large reactor can provide better removal of many metals and PAHs. The additives used in these tests help to remove PAHs and PCBs efficiently, and the chemical parameters measured after treatment provided a distribution showing the accumulation of pollutants in the local zones of the large

UNCORRECTED PROOFS

UNCORRECTED PROOFS

Trim Size: 170mm x 244mm Single Column Loose



Figure 5.6 View of the two scale devices used for sediment EKR.

Ribeiro670117 c05.tex V1 - 12/09/2020 3:19pm Page 126

Trim Size: 170mm x 244mm Single Column Loose Ribeiro670117 c05.tex V1 - 12/09/2020 3:19pm Page 127

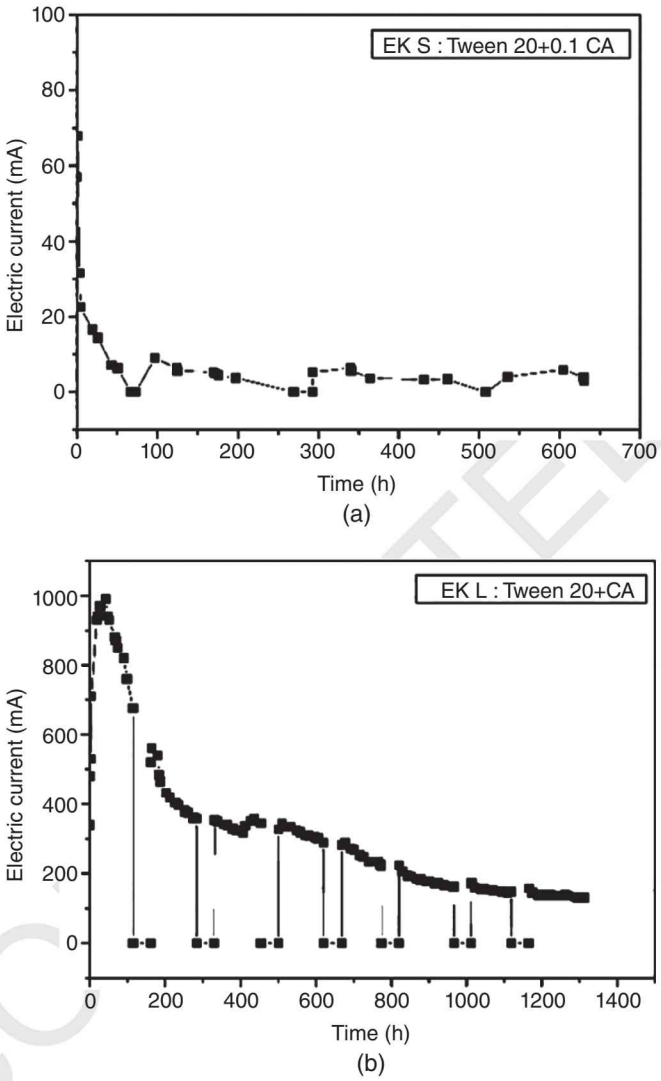

Figure 5.7 Evolution of electric current during EKR in (a) the small reactor; (b) the large reactor.

UNCORRECTED PROOFS

Trim Size: 170mm x 244mm Single Column Loose Ribeiro670117 c05.tex V1 - 12/09/2020 3:19pm Page 128

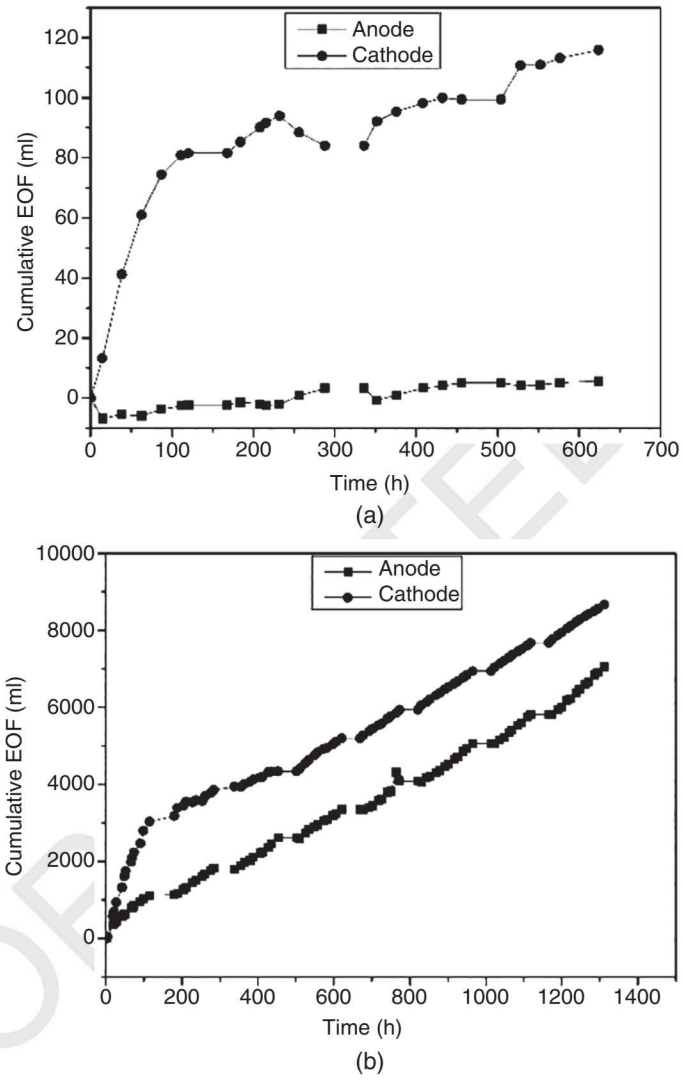

Figure 5.8 Variation of electroosmotic flow during EK treatment in (a) the small reactor; (b) the large reactor.

UNCORRECTED PROOFS

Trim Size: 170mm x 244mm Single Column Loose Ribeiro670117 c05.tex V1 - 12/09/2020 3:19pm Page 129

Table 5.10 Pollutant removal from two different-scale reactors.

Removal (%)	Small-scale reactor	Large-scale reactor
Cd	4.5 ± 0.8	No significant value
Cr	3.1 ± 1.8	22.7 ± 1.2
Cu	No significant value	5.3 ± 2.4
Pb	3.5 ± 0.7	9.5 ± 1.4
Zn	2.3 ± 0.9	No significant value
∑16PAH	**No significant value**	**20.5 ± 7.6**
∑7PCB	**22.8 ± 3.7**	**21.5 ± 8.1**

reactor and the transport of species toward the deeper layers, hindering the transport of pollutants toward the cathodes. The great inter-electrode gap at the large scale may lead to potential drop, affecting the electric field within the specimen, reducing the horizontal transferability of the species. When using large-scale EKR devices including a large volume of sediment, the contaminants could also migrate downward along with the liquid through dispersion and diffusion, although they mainly migrated according to the horizontal electric field [35]. To eliminate the effects of downward transport, electrode placement can be changed by introducing an upward EKR technology using vertical non-uniform electric fields between the top cathode and bottom anode to remove heavy metals from the contaminated soil. Moreover, this electrode's disposition provides upward migration of pollutant ions to the surface of the sediment, which facilitates the excavation and disposal of a soil layer. This method concentrates the pollutants within a sediment upper layer but cannot remove contaminants within a catholyte solution, from which pollutant extraction is easier. Except for Cr, metal removal remains low with these additives, while extraction of PAHs and PCBs is more interesting at large scale EKR. Overall, greater removal is obtained in the large-scale reactor compared to the lab scale, indicating that all the promising results obtained in other laboratory-scale experiments using different additives have the potential to be scaled up and even optimized.

5.6 Future Perspectives

The full potential of the EKR technique as a sediment treatment alternative is yet to be fully realized. It is still an optimized process that requires a more fundamental understanding of improved engineering design. EKR includes complex chemical and physical processes and phenomena. There is, however, a need for scientific research to investigate and understand these phenomena, which limits the engineering design of the EKR reactor for optimum performance and field-developed technology.

The focus of research in recent years has been on optimizing engineering design, such as optimization of an electrode configuration for EKR. Extracting

UNCORRECTED PROOFS

Trim Size: 170mm x 244mm Single Column Loose Ribeiro670117 c05.tex V1 - 12/09/2020 3:19pm Page 130

contaminants using EKR technology requires applying appropriate electric fields through the sediment. In some cases, the further addition of appropriate chemicals helps the dissolution, and thus removing the pollutants to demonstrate a suitable system configuration can make this technology an excellent choice in terms of environmental sustainability [92]. The enhancement concerned the electrodes' material and shape, their position, and the nature of the additives; and the use of a permeable reactive barrier at the electrodes must be improved. Many combined EKR technologies have been reported with constant improvement, but scaling up remains a limitation for the industrial development of such technologies. The scale-up experience revealed that it affects the treatment rate and also shows poor reproducibility of results obtained on the laboratory scale. Multidisciplinary aspects (from sediment compaction to electrode position) are of concern. Further research is needed before full-scale applications can be carried out [93].

Enhanced technologies must also be sustainably powered with regard to environmental impact. The high energy cost of EKR becomes a major barrier to its widespread application. Alternate voltage has a significant advantage in the EKR of pollutants versus continuous voltage. To reduce the energy consumption of EKR, a pulsed sinusoidal electric field has also been applied to EKR systems with more success. Compared with traditional DC power supplies, solar energy may be an alternative to lower technology costs and environmental impact since alternate gradient voltage demonstrated its efficiency for reactivating the electric current during EKR [94]. Using stirred setups with mechanical stirring has also been shown to improve removal significantly and is relevant for developing ex situ remediation and appears to be a feasible solution when dealing with dredged sediments.

The focus of research in recent years has been using this technology to remove particularly hazardous organics from soil [95] or marine and river sediments [96]. The enhancement of EKR using friendly environment additives (biosurfactant, biochelatant) opens the possibility of developing the technology in the field without disseminating pollutants around the treated area. Presently, the two challenges for EKR success as a widely used technology for sediments are assessing the similarity parameters that ensure the reproduction of laboratory performance and finding combinations of green additives that will achieve significant pollutant removal without impacting the environment.

Attempts to model electrokinetic processes reported in the literature for porous media contaminated by toxic metals need more understanding. A two-dimensional reactive-transport model was implemented to simulate the transport of chemical species by diffusion, electromigration, and electroosmosis, coupled with a geochemical model that calculates precipitation and dissolution of species, adsorption and desorption reactions, and aqueous speciation [97]. Modeling can help provide a fundamental understanding of interaction processes at laboratory scale and be used as a foundation to apply appropriate modeling for full-scale treatment.

UNCORRECTED PROOFS

Trim Size: 170mm x 244mm Single Column Loose Ribeiro670117 c05.tex V1 - 12/09/2020 3:19pm Page 131

References

1 Perelo, L.W. (2010). Review: in situ and bioremediation of organic pollutants in aquatic sediments. *Journal of Hazardous Materials* 177: 81–89.

2 Salomons W. and Brils, J. (2004). Contaminated sediments in European river basins. European Sediment Research Network SedNet. EC Contract No, in EVKI-CT-2001-20002, Key Action 1.4.

3 Vidgren, H., Helland, A., and Lepland, A. (2015). Stability of capped dredged sediments in a confined disposal facility at Malmøykalven, Oslofjord, SE Norway. *Soil and Sediment Contamination: An International Journal* 24: 675–693.

4 Mulligan, C.N., Yong, R.N., and Gibbs, B.F. (2001). An evaluation of technologies for the heavy metal remediation of dredged sediments. *Journal of Hazardous Materials* 85: 145–163.

5 Chapman, P.M., Wang, F., Janssen, C. et al. (1998). Ecotoxicology of metals in aquatic sediments: binding and release, bioavailability, risk assessment, and remediation. *Canadian Journal of Fisheries and Aquatic Sciences* 55: 2221–2243.

6 Peng, J.-f., Song, Y.-h., Yuan, P. et al. (2009). The remediation of heavy metals contaminated sediment. *Journal of Hazardous Materials* 161: 633–640.

7 Acar, Y.B. and Alshawabkeh, A.N. (1993). Principles of electrokinetic remediation. *Environmental Science & Technology* 27: 2638–2647.

8 Cabrera-Guzmán, D., Swartzbaugh, J.T., and Weisman, A.W. (1990). The use of electrokinetics for hazardous waste site remediation. *Journal of the Air & Waste Management Association* 40: 1670–1676.

9 Hansen, H.K., Ottosen, L.M., Kliem, B.K., and Villumsen, A. (1997). Electrodialytic remediation of soils polluted with Cu, Cr, Hg, Pb and Zn. *Journal of Chemical Technology & Biotechnology: International Research in Process, Environmental AND Clean Technology* 70: 67–73.

10 Maini, G., Sharman, A.K., Knowles, C.J. et al. (2000). Electrokinetic remediation of metals and organics from historically contaminated soil. *Journal of Chemical Technology & Biotechnology: International Research in Process, Environmental & Clean Technology* 75: 657–664.

11 Park, S.-W., Lee, J.-Y., Yang, J.-S. et al. (2009). Electrokinetic remediation of contaminated soil with waste-lubricant oils and zinc. *Journal of Hazardous Materials* 169: 1168–1172.

12 Dong, Z.-Y., Huang, W.-H., Xing, D.-F., and Zhang, H.-F. (2013). Remediation of soil co-contaminated with petroleum and heavy metals by the integration of electrokinetics and biostimulation. *Journal of Hazardous Materials* 260: 399–408.

13 Gomes, H.I., Dias-Ferreira, C., Ottosen, L.M., and Ribeiro, A.B. (2014). Electrodialytic remediation of polychlorinated biphenyls contaminated soil with iron nanoparticles and two different surfactants. *Journal of Colloid and Interface Science* 433: 189–195.

UNCORRECTED PROOFS

Trim Size: 170mm x 244mm Single Column Loose Ribeiro670117 c05.tex V1 - 12/09/2020 3:19pm Page 132

14 Sörengård, M., Niarchos, G., Jensen, P.E., and Ahrens, L. (2019). Electrodialytic per-and polyfluoroalkyl substances (PFASs) removal mechanism for contaminated soil. *Chemosphere* 232: 224–231.

15 Chen, F., Li, X., Ma, J. et al. (2019). Remediation of soil co-contaminated with decabromodiphenyl ether (BDE-209) and copper by enhanced electrokinetics-persulfate process. *Journal of Hazardous Materials* 369: 448–455.

16 Acar, Y.B., Li, H., and Gale, R.J. (1992). Phenol removal from kaolinite by electrokinetics. *Journal of Geotechnical Engineering* 118: 1837–1852.

17 Chung, H.I. and Kang, B.H. (1999). Lead removal from contaminated marine clay by electrokinetic soil decontamination. *Engineering Geology* 53: 139–150.

18 Hedges, J.I. and Oades, J.M. (1997). Comparative organic geochemistries of soils and marine sediments. *Organic Geochemistry* 27: 319–361.

19 Hur, J., Lee, D.-H., and Shin, H.-S. (2009). Comparison of the structural, spectroscopic and phenanthrene binding characteristics of humic acids from soils and lake sediments. *Organic Geochemistry* 40: 1091–1099.

20 Chung, H.I. (2006). Dewatering and decontamination of artificially contaminated sediments during electrokinetic sedimentation and remediation processes. *KSCE Journal of Civil Engineering* 10: 181–187.

21 Virkutyte, J. and Sillanpää, M. (2007). The hindering effect of experimental strategies on advancement of alkaline front and electroosmotic flow during electrokinetic lake sediment treatment. *Journal of Hazardous Materials* 143: 673–681.

22 Altaee, A., Smith, R., and Mikhalovsky, S. (2008). The feasibility of decontamination of reduced saline sediments from copper using the electrokinetic process. *Journal of Environmental Management* 88: 1611–1618.

23 Hatzinger, P.B. and Alexander, M. (1995). Effect of aging of chemicals in soil on their biodegradability and extractability. *Environmental Science & Technology* 29: 537–545.

24 Alexander, M. (2000). Aging, bioavailability, and overestimation of risk from environmental pollutants. *Environmental Science & Technology* 34: 4259–4265.

25 Wang, J., Schlenk, D., and Gan, J. (2019). A direct method for quantifying the effects of aging on the bioavailability of legacy contaminants in soil and sediment. *Environmental Science & Technology Letters* 6: 148–152.

26 Smolders, E., Oorts, K., Van Sprang, P. et al. (2009). Toxicity of trace metals in soil as affected by soil type and aging after contamination: using calibrated bioavailability models to set ecological soil standards. *Environmental Toxicology and Chemistry: An International Journal* 28: 1633–1642.

27 Ottosen, L.M., Lepkova, K., and Kubal, M. (2006). Comparison of electrodialytic removal of cu from spiked kaolinite, spiked soil and industrially polluted soil. *Journal of Hazardous Materials* 137: 113–120.

28 Pedersen, K.B., Jensen, P.E., Ottosen, L.M., and Lejon, T. (2015). An optimised method for electrodialytic removal of heavy metals from harbour sediments. *Electrochimica Acta* 173: 432–439.

UNCORRECTED PROOFS

Trim Size: 170mm x 244mm Single Column Loose Ribeiro670117 c05.tex V1 - 12/09/2020 3:19pm Page 133

29 Nystroem, G.M., Ottosen, L.M., and Villumsen, A. (2005). Electrodialytic removal of Cu, Zn, Pb, and Cd from harbor sediment: influence of changing experimental conditions. *Environmental Science & Technology* 39: 2906–2911.

30 Ottosen, L.M., Jensen, P.E., Kirkelund, G.M. et al. (2012). Electrodialytic remediation of heavy metal polluted soil–treatment of water saturated or suspended soil. *Chemical Engineering* 28: 103–108.

31 Hahladakis, J.N., Lekkas, N., Smponias, A., and Gidarakos, E. (2014). Sequential application of chelating agents and innovative surfactants for the enhanced electroremediation of real sediments from toxic metals and PAHs. *Chemosphere* 105: 44–52.

32 Andreottola, G., Bonomo, L., De Gioannis, G. et al. (2010). Lab-scale feasibility tests for sediment treatment using different physico-chemical techniques. *Journal of Soils and Sediments* 10: 142–150.

33 Falciglia, P.P., Malarbì, D., and Vagliasindi, F.G. (2016). Removal of mercury from marine sediments by the combined application of a biodegradable non-ionic surfactant and complexing agent in enhanced-electrokinetic treatment. *Electrochimica Acta* 222: 1569–1577.

34 Kirkelund, G.M., Ottosen, L.M., and Villumsen, A. (2009). Electrodialytic remediation of harbour sediment in suspension—evaluation of effects induced by changes in stirring velocity and current density on heavy metal removal and pH. *Journal of Hazardous Materials* 169: 685–690.

35 Song, Y., Ammami, M.-T., Benamar, A. et al. (2016). Effect of EDTA, EDDS, NTA and citric acid on electrokinetic remediation of As, Cd, Cr, Cu, Ni, Pb and Zn contaminated dredged marine sediment. *Environmental Science and Pollution Research* 23: 10577–10586.

36 Pazos, M., Iglesias, O., Gómez, J. et al. (2013). Remediation of contaminated marine sediment using electrokinetic–Fenton technology. *Journal of Industrial and Engineering Chemistry* 19: 932–937.

37 Pedersen, K.B., Lejon, T., Jensen, P.E., and Ottosen, L.M. (2017). Simultaneous electrodialytic removal of PAH, PCB, TBT and heavy metals from sediments. *Journal of Environmental Management* 198: 192–202.

38 Yan, F. and Reible, D.D. (2012). PAH degradation and redox control in an electrode enhanced sediment cap. *Journal of Chemical Technology & Biotechnology* 87: 1222–1228.

39 Ammami, M.T., Benamar, A., Wang, H. et al. (2014). Simultaneous electrokinetic removal of polycyclic aromatic hydrocarbons and metals from a sediment using mixed enhancing agents. *International Journal of Environmental Science and Technology* 11: 1801–1816.

40 Hahladakis, J.N., Latsos, A., and Gidarakos, E. (2016). Performance of electroremediation in real contaminated sediments using a big cell, periodic voltage and innovative surfactants. *Journal of Hazardous Materials* 320: 376–385.

41 Hahladakis, J.N., Calmano, W., and Gidarakos, E. (2013). Use and comparison of the nonionic surfactants Poloxamer 407 and Nonidet P40 with HP-β-CD cyclodextrin, for the enhanced electroremediation of real contaminated sediments from PAHs. *Separation and Purification Technology* 113: 104–113.

UNCORRECTED PROOFS

Trim Size: 170mm x 244mm Single Column Loose Ribeiro670117 c05.tex V1 - 12/09/2020 3:19pm Page 134

42 Benamar, A., Tian, Y., Portet-Koltalo, F. et al. (2019). Enhanced electrokinetic remediation of multi-contaminated dredged sediments and induced effect on their toxicity. *Chemosphere* 228: 744–755.

43 Falciglia, P.P., Malarbì, D., Greco, V., and Vagliasindi, F.G. (2017). Surfactant and MGDA enhanced–Electrokinetic treatment for the simultaneous removal of mercury and PAHs from marine sediments. *Separation and Purification Technology* 175: 330–339.

44 Tian, Y., Boulangé-Lecomte, C., Benamar, A. et al. (2017). Application of a crustacean bioassay to evaluate a multi-contaminated (metal, PAH, PCB) harbor sediment before and after electrokinetic remediation using eco-friendly enhancing agents. *Science of the Total Environment* 607: 944–953.

45 Yoo, J.-C., Yang, J.-S., Jeon, E.-K., and Baek, K. (2015). Enhanced-electrokinetic extraction of heavy metals from dredged harbor sediment. *Environmental Science and Pollution Research* 22: 9912–9921.

46 Iannelli, R., Masi, M., Ceccarini, A. et al. (2015). Electrokinetic remediation of metal-polluted marine sediments: experimental investigation for plant design. *Electrochimica Acta* 181: 146–159.

47 Ottosen, L.M., Nystrøm, G.M., Jensen, P.E., and Villumsen, A. (2007). Electrodialytic extraction of Cd and Cu from sediment from Sisimiut harbour, Greenland. *Journal of Hazardous Materials* 140: 271–279.

48 Ottosen, L., Hansen, H., and Hansen, C. (2000). Water splitting at ion-exchange membranes and potential differences in soil during electrodialytic soil remediation. *Journal of Applied Electrochemistry* 30: 1199–1207.

49 Kirkelund, G.M., Ottosen, L.M., and Villumsen, A. (2010). Investigations of cu, Pb and Zn partitioning by sequential extraction in harbour sediments after electrodialytic remediation. *Chemosphere* 79: 997–1002.

50 Nystroem, G.M., Ottosen, L.M., and Villumsen, A. (2005). Acidification of harbor sediment and removal of heavy metals induced by water splitting in electrodialytic remediation. *Separation Science and Technology* 40: 2245–2264.

51 Nystroem, G.M., Pedersen, A.J., Ottosen, L.M., and Villumsen, A. (2006). The use of desorbing agents in electrodialytic remediation of harbour sediment. *Science of the Total Environment* 357: 25–37.

52 Ammami, M.T. (2013). Contribution à l'étude des processus électrocinétiques appliqués aux sédiments de dragage. Doctoral dissertation, Le Havre.

53 Cameselle, C. and Pena, A. (2016). Enhanced electromigration and electroosmosis for the remediation of an agricultural soil contaminated with multiple heavy metals. *Process Safety and Environmental Protection* 104: 209–217.

54 Gidarakos, E. and Giannis, A. (2006). Chelate agents enhanced electrokinetic remediation for removal cadmium and zinc by conditioning catholyte pH. *Water, Air, and Soil Pollution* 172: 295–312.

55 Giannis, A., Nikolaou, A., Pentari, D., and Gidarakos, E. (2009). Chelating agent-assisted electrokinetic removal of cadmium, lead and copper from contaminated soils. *Environmental Pollution* 157: 3379–3386.

UNCORRECTED PROOFS

Trim Size: 170mm x 244mm Single Column Loose Ribeiro670117 c05.tex V1 - 12/09/2020 3:19pm Page 135

56 Suzuki, T., Moribe, M., Okabe, Y., and Niinae, M. (2013). A mechanistic study of arsenate removal from artificially contaminated clay soils by electrokinetic remediation. *Journal of Hazardous Materials* 254: 310–317.

57 Kim, K.-J., Kim, D.-H., Yoo, J.-C., and Baek, K. (2011). Electrokinetic extraction of heavy metals from dredged marine sediment. *Separation and Purification Technology* 79: 164–169.

58 Huang, D., Xu, Q., Cheng, J. et al. (2012). Electrokinetic remediation and its combined technologies for removal of organic pollutants from contaminated soils. *International Journal of Electrochemical Science* 7: 4528–4544.

59 Vizcaíno, R.L., Yustres, A., Asensio, L. et al. (2018). Enhanced electrokinetic remediation of polluted soils by anolyte pH conditioning. *Chemosphere* 199: 477–485.

60 Giannis, A., Gidarakos, E., and Skouta, A. (2007). Application of sodium dodecyl sulfate and humic acid as surfactants on electrokinetic remediation of cadmium-contaminated soil. *Desalination* 211: 249–260.

61 Tang, J., He, J., Xin, X. et al. (2018). Biosurfactants enhanced heavy metals removal from sludge in the electrokinetic treatment. *Chemical Engineering Journal* 334: 2579–2592.

62 Yang, J.-W., Lee, Y.-J., Park, J.-Y. et al. (2005). Application of APG and Calfax 16L-35 on surfactant-enhanced electrokinetic removal of phenanthrene from kaolinite. *Engineering Geology* 77: 243–251.

63 Von Lau, E., Gan, S., Ng, H.K., and Poh, P.E. (2014). Extraction agents for the removal of polycyclic aromatic hydrocarbons (PAHs) from soil in soil washing technologies. *Environmental Pollution* 184: 640–649.

64 Gonzini, O., Plaza, A., Di Palma, L., and Lobo, M. (2010). Electrokinetic remediation of gasoil contaminated soil enhanced by rhamnolipid. *Journal of Applied Electrochemistry* 40: 1239–1248.

65 Ammami, M.T., Portet-Koltalo, F., Benamar, A. et al. (2015). Application of biosurfactants and periodic voltage gradient for enhanced electrokinetic remediation of metals and PAHs in dredged marine sediments. *Chemosphere* 125: 1–8.

66 dos Santos, E.V., Souza, F., Saez, C. et al. (2016). Application of electrokinetic soil flushing to four herbicides: a comparison. *Chemosphere* 153: 205–211.

67 Cao, M., Hu, Y., Sun, Q. et al. (2013). Enhanced desorption of PCB and trace metal elements (Pb and Cu) from contaminated soils by saponin and EDDS mixed solution. *Environmental Pollution* 174: 93–99.

68 Fan, G., Cang, L., Fang, G., and Zhou, D. (2014). Surfactant and oxidant enhanced electrokinetic remediation of a PCBs polluted soil. *Separation and Purification Technology* 123: 106–113.

69 Li, T., Yuan, S., Wan, J., and Lu, X. (2010). Hydroxypropyl-β-cyclodextrin enhanced electrokinetic remediation of sediment contaminated with HCB and heavy metals. *Journal of Hazardous Materials* 176: 306–312.

70 Jiang, H., Liu, G., He, S., and Guo, J. (2018). Effects of complexes and ph buffer solution in electrokinetic oxidation treatment on sediments chromium removal. *Wuhan University Journal of Natural Sciences* 23: 265–269.

UNCORRECTED PROOFS

Trim Size: 170mm x 244mm Single Column Loose Ribeiro670117 c05.tex V1 - 12/09/2020 3:19pm Page 136

71 Yan, F. and Reible, D. (2015). Electro-bioremediation of contaminated sediment by electrode enhanced capping. *Journal of Environmental Management* 155: 154–161.

72 Cappello, S., Viggi, C.C., Yakimov, M. et al. (2019). Combining electrokinetic transport and bioremediation for enhanced removal of crude oil from contaminated marine sediments: results of a long-term, mesocosm-scale experiment. *Water Research* 157: 381–395.

73 Reddy, K.R. and Ala, P.R. (2006). Electrokinetic remediation of contaminated dredged sediment. *Journal of ASTM International* 3: 1–14.

74 De Gioannis, G., Muntoni, A., Polettini, A., and Pomi, R. (2009). Electrokinetic treatment of contaminated marine sediments. In: *Electrochemical Remediation Technologies for Polluted Soils, Sediments and Groundwater* (eds. K.R. Reddy and C. Cameselle), 149–177.

75 Merkx, O., Loch, J., Lima, A. et al. (2013, 1667). The effectiveness of electro-remediation of aged, metal-contaminated sediment in relation to sequential extraction of metals. *Water, Air, & Soil Pollution* 224.

76 Masi, M., Iannelli, R., and Losito, G. (2016). Ligand-enhanced electrokinetic remediation of metal-contaminated marine sediments with high acid buffering capacity. *Environmental Science and Pollution Research* 23: 10566–10576.

77 Song, Y., Benamar, A., Mezazigh, S., and Huaqing, W. (2018). Citric acid-enhanced electroremediation of toxic metal-contaminated dredged sediments: effect of open/closed orifice condition, electric potential and surfactant. *Pedosphere* 28: 35–43.

78 Pedersen, K.B., Lejon, T., Jensen, P.E., and Ottosen, L.M. (2017). The influence of sediment properties and experimental variables on the efficiency of electrodialytic removal of metals from sediment. *Journal of Environmental Chemical Engineering* 5: 5312–5321.

79 Zhang, T., Zou, H., Ji, M. et al. (2014). Enhanced electrokinetic remediation of lead-contaminated soil by complexing agents and approaching anodes. *Environmental Science and Pollution Research* 21: 3126–3133.

80 Chang, F.-C., Lo, S.-L., and Ko, C.-H. (2007). Recovery of copper and chelating agents from sludge extracting solutions. *Separation and Purification Technology* 53: 49–56.

81 Reddy, K.R., Danda, S., and Saichek, R.E. (2004). Complicating factors of using ethylenediamine tetraacetic acid to enhance electrokinetic remediation of multiple heavy metals in clayey soils. *Journal of Environmental Engineering* 130: 1357–1366.

82 Kim, C., Lee, Y., and Ong, S.K. (2003). Factors affecting EDTA extraction of lead from lead-contaminated soils. *Chemosphere* 51: 845–853.

83 Yoo, J.-C., Lee, C.-D., Yang, J.-S., and Baek, K. (2013). Extraction characteristics of heavy metals from marine sediments. *Chemical Engineering Journal* 228: 688–699.

84 Chen, L., Liu, T., and Ma, C.a. (2010). Metal complexation and biodegradation of EDTA and S, S-EDDS: a density functional theory study. *The Journal of Physical Chemistry A* 114: 443–454.

UNCORRECTED PROOFS

Trim Size: 170mm x 244mm Single Column Loose Ribeiro670117 c05.tex V1 - 12/09/2020 3:19pm Page 137

85 Mao, X., Shao, X., and Zhang, Z. (2019). Pilot-scale electrokinetic remediation of lead polluted field sediments: model designation, numerical simulation, and feasibility evaluation. *Environmental Sciences Europe* 31: 25.

86 Duo, L., Yin, L., Zhang, C., and Zhao, S. (2019). Ecotoxicological responses of the earthworm Eisenia fetida to EDTA addition under turfgrass growing conditions. *Chemosphere* 220: 56–60.

87 Grčman, H., Velikonja-Bolta, Š., Vodnik, D. et al. (2001). EDTA enhanced heavy metal phytoextraction: metal accumulation, leaching and toxicity. *Plant and Soil* 235: 105–114.

88 Gardner, K.H., Nystroem, G.M., and Aulisio, D.A. (2007). Leaching properties of estuarine harbor sediment before and after electrodialytic remediation. *Environmental Engineering Science* 24: 424–433.

89 Kim, B.-K., Baek, K., Ko, S.-H., and Yang, J.-W. (2011). Research and field experiences on electrokinetic remediation in South Korea. *Separation and Purification Technology* 79: 116–123.

90 López-Vizcaíno, R., Yustres, A., Sáez, C. et al. (2019). Techno-economic analysis of the scale-up process of electrochemically-assisted soil remediation. *Journal of Environmental Management* 231: 570–575.

91 Sulaymon, A. and Abbar, A. (2012). *Scale-up of Electrochemical Reactors*, chapter 9 in Electrolysis (ed. J. Kleperis), 189–202. IntechOpen https://doi.org/10.5772/48728.

92 Vocciante, M., Caretta, A., Bua, L. et al. (2016). Enhancements in ElectroKinetic remediation technology: environmental assessment in comparison with other configurations and consolidated solutions. *Chemical Engineering Journal* 289: 123–134.

93 Lacasa, E., Cotillas, S., Saez, C. et al. (2019). Environmental applications of electrochemical technology. What is needed to enable full-scale applications? *Current Opinion in Electrochemistry* 16: 149–156.

94 Yuan, S., Zheng, Z., Chen, J., and Lu, X. (2009). Use of solar cell in electrokinetic remediation of cadmium-contaminated soil. *Journal of Hazardous Materials* 162: 1583–1587.

95 Moussa, D.T., El-Naas, M.H., Nasser, M., and Al-Marri, M.J. (2017). A comprehensive review of electrocoagulation for water treatment: potentials and challenges. *Journal of Environmental Management* 186: 24–41.

96 Mukimin, A., Zen, N., Purwanto, A. et al. (2017). Application of a full-scale electrocatalytic reactor as real batik printing wastewater treatment by indirect oxidation process. *Journal of Environmental Chemical Engineering* 5: 5222–5232.

97 Masi, M., Ceccarini, A., and Iannelli, R. (2017). Model-based optimization of field-scale electrokinetic treatment of dredged sediments. *Chemical Engineering Journal* 328: 87–97.

98 Pedersen, A.J. and Gardner, K.H. (2003). Electrochemical remediation of dredged material for beneficial use. In: *Beneficial Use of Recycled Materials in Transport Applications* (ed. T.T. Eighmy), 389–399. Air and Waste Management Association Press.

UNCORRECTED PROOFS

Trim Size: 170mm x 244mm Single Column Loose Ribeiro670117 c05.tex V1 - 12/09/2020 3:19pm Page 138

99 Nystrøm, G.M., Ottosen, L.M., and Villumsen, A. (2005). Test of experimental setups for electrodialytic removal of Cu, Zn, Pb and Cd from different contaminated harbour sediments. *Engineering Geology* 77: 349–357.

100 De Gioannis, G., Muntoni, A., Polettini, A., and Pomi, R. (2008). Enhanced electrokinetic treatment of different marine sediments contaminated by heavy metals. *Journal of Environmental Science and Health Part A* 43: 852–865.

101 Yuan, S., Wu, C., Wan, J., and Lu, X. (2009). In situ removal of copper from sediments by a galvanic cell. *Journal of Environmental Management* 90: 421–427.

102 Shin, H.-M. (2009). Removal of Cr, Pb and Cd from reservoir sediment by Electrokinetic technique. *Journal of Soil and Groundwater Environment* 14: 68–77.

103 Guoliang, X., Dehan, W., and Diqin, C. (2009). Remediation of heavy metals polluted sediment by electrokinetics and bamboo charcoal. *Journal of Huazhong Agricultural University* 28: 174–178.

104 Colacicco, A., De Gioannis, G., Muntoni, A. et al. (2010). Enhanced electrokinetic treatment of marine sediments contaminated by heavy metals and PAHs. *Chemosphere* 81: 46–56.

105 Haroun, M., Chilingar, G.V., and Pamukcu, S. (2010). The efficacy of using electrokinetic transport in highly-contaminated offshore sediments. *Journal of Applied Electrochemistry* 40: 1131–1138.

106 Rozas, F. and Castellote, M. (2012). Electrokinetic remediation of dredged sediments polluted with heavy metals with different enhancing electrolytes. *Electrochimica Acta* 86: 102–109.

107 Kim, K.-J., Yoo, J.-C., Yang, J.-S., and Baek, K. (2013). Electrokinetic extraction of metals from marine sediment. *Korean Chemical Engineering Research* 51: 733–738.

108 Pedersen, K.B., Kirkelund, G.M., Ottosen, L.M. et al. (2015). Multivariate methods for evaluating the efficiency of electrodialytic removal of heavy metals from polluted harbour sediments. *Journal of Hazardous Materials* 283: 712–720.

109 Pedersen, K.B., Lejon, T., Jensen, P.E., and Ottosen, L.M. (2016). Applying multivariate analysis as decision tool for evaluating sediment-specific remediation strategies. *Chemosphere* 151: 59–67.

110 Pedersen, K.B., Lejon, T., Ottosen, L.M., and Jensen, P.E. (2015). Screening of variable importance for optimizing electrodialytic remediation of heavy metals from polluted harbour sediments. *Environmental Technology* 36: 2364–2373.

111 Pedersen, K.B., Ottosen, L.M., Jensen, P.E., and Lejon, T. (2015). Comparison of 2-compartment, 3-compartment and stack designs for electrodialytic removal of heavy metals from harbour sediments. *Electrochimica Acta* 181: 48–57.

112 Masi, M. and Losito, G. (2015). Spectral induced polarization for monitoring electrokinetic remediation processes. *Journal of Applied Geophysics* 123: 284–294.

113 Yoo, J.-C., Kim, E.-J., Yang, J.-S., and Baek, K. (2015). Step-wise extraction of metals from dredged marine sediments. *Separation Science and Technology* 50: 536–544.

UNCORRECTED PROOFS

Trim Size: 170mm x 244mm Single Column Loose Ribeiro670117 c05.tex V1 - 12/09/2020 3:19pm Page 139

114 Missaoui, A., Said, I., Lafhaj, Z., and Hamdi, E. (2016). Influence of enhancing electrolytes on the removal efficiency of heavy metals from Gabes marine sediments (Tunisia). *Marine Pollution Bulletin* 113: 44–54.

115 Luo, E., Connor, J.N., and Ngothai, Y. (2016). Alternative processes for separating mineralised Port Pirie dredge material. Chemeca 2016: Chemical Engineering-Regeneration, Recovery and Reinvention.

116 Masi, M., Ceccarini, A., and Iannelli, R. (2017). Multispecies reactive transport modelling of electrokinetic remediation of harbour sediments. *Journal of Hazardous Materials* 326: 187–196.

117 Krcmar, D., Varga, N., Prica, M. et al. (2018). Application of hexagonal two dimensional electrokinetic system on the nickel contaminated sediment and modelling the transport behavior of nickel during electrokinetic treatment. *Separation and Purification Technology* 192: 253–261.

118 Kirkelund, G.M., Jensen, P.E., Ottosen, L.M., and Pedersen, K.B. (2019). Comparison of two-and three-compartment cells for electrodialytic removal of heavy metals from contaminated material suspensions. *Journal of Hazardous Materials* 367: 68–76.

UNCORRECTED PROOFS

UNCORRECTED PROOFS

Trim Size: 170mm x 244mm Single Column Loose Ribeiro670117 c06.tex V1 - 12/11/2020 11:51pm Page 141

6

Pharmaceutically Active Compounds in Wastewater Treatment Plants: Electrochemical Advanced Oxidation as Onsite Treatment

Ana Rita Ferreira[1], Paula Guedes[1,2], Eduardo P. Mateus[1], Alexandra B. Ribeiro[1], and Nazaré Couto[1]

[1]CENSE – Center for Environmental and Sustainability Research, Department of Environmental Sciences and Engineering, NOVA School of Science and Technology, NOVA University Lisbon, Caparica 2829-516, Portugal
[2]Instituto de Tecnologia Química e Biológica António Xavier, Universidade Nova de Lisboa, Oeiras 2780-157, Portugal

6.1 Introduction

6.1.1 Emerging Organic Contaminants

Emerging organic contaminants (EOCs) or contaminants of emerging concern can be defined as naturally occurring, manufactured, or manmade chemicals or materials whose associated risks cannot be properly evaluated due to the lack of data about their environmental fate and ecotoxicological or toxicological effects [1, 2]. A contaminant remains "emerging" as long as there is a scarcity of information in the scientific literature about the associated potential risks it could cause [1, 2].

EOCs broadly include "lifestyle compounds," personal care compounds, pharmaceuticals including hormones, and plasticizers [3]. Pharmaceutical products account for 70% of the approximately 4500 chemical compounds available in the world, and the production of pharmaceutical compounds and other medicines is still increasing [4]. Over the years, population growth and the development of new medicines to prevent or cure diseases with unknown fates and effects on the environment has made these compounds deserve special attention [5].

Over the last few decades, the subject of EOCs has become a worldwide issue of increasing environmental concern, and intensive research has been carried out on a range of different topics such as their occurrence and fate in the environment as well as treatment methods. A total of 117 papers were published in 2013 (Figure 6.1), and the number of studies has continued to increase since then to 330 in 2019 (almost two times more than five years before).

6.1.2 Occurrence and Fate of EOCs

One of the primary current worldwide concerns is the growth of pollution due to EOCs arising from many urban, industrial, and agricultural activities. Technological

Electrokinetic Remediation for Environmental Security and Sustainability, First Edition.
Edited by Alexandra B. Ribeiro and M.N.V. Prasad.
© 2021 John Wiley & Sons Ltd. Published 2021 by John Wiley & Sons Ltd.

UNCORRECTED PROOFS

Trim Size: 170mm x 244mm Single Column Loose Ribeiro670117 c06.tex V1 - 12/11/2020 11:51pm Page 142

AQ1

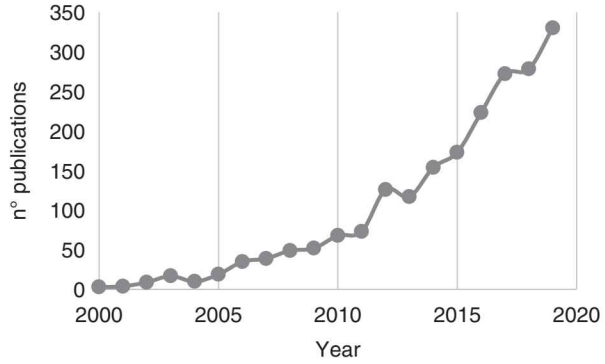

Figure 6.1 Number of publications on emerging organic contaminants from 2000 to 2019.

advances in analytical instrumentation and techniques have enabled researchers to detect and quantify EOCs in different environmental compartments (soil, air, and water) [6–8].

EOCs are now commonly detected in the environment due to their constant introduction through the disposal of wastewater, biosolids, and manure (Figure 6.2). Waste streams from hospitals, wastewater treatment plants (WWTPs), and sewage treatment plants have been identified as significant contributors to environmental contamination with EOCs [3, 9–11]. Besides the ubiquitous occurrences of EOCs in the environment, significant and measurable concentrations of ibuprofen, diclofenac, and carbamazepine were also found in drinking waters, e.g. [12, 13]. Surface water, groundwater, and soils are interrelated, and upon arrival in the environment, EOCs can undergo significant transformation including (bio)degradation, sorption at the sediment, and transport in the aqueous phase. This transformation depends on EOC physicochemical properties such as volatility, polarity, adsorption properties, persistence, and the properties of the interacting compartments: for example, the presence of a community of organisms that can transform the contaminants through metabolic networks and the bioavailability of contaminants, especially in sediments and soil [14, 15]. Generally, compounds with octanol/water partition coefficient (Log K_{ow}) lower than 3.0 are not expected to be adsorbed significantly to the particles, but compounds with relatively high Log K_{ow} values and pKa values below the pH of the wastewater are expected to be dissociated in the aqueous phase and not bound to the particles. Despite known chemical properties, it is difficult to predict their behavior in the environment as it depends on several variables [16].

In addition to direct sources of EOCs in the environment, other potential routes for these compounds may be considered. For example, reusing treated wastewater for irrigation in agriculture can also represent a risk to human health as EOCs might transfer to soil, potentially increasing the risk of consumption as they are not regulated and can be accumulated within crop plants. This fact has been already reported by several studies [15–20]. Malchi et al. [21] found 14 different EOCs, such as carbamazepine, caffeine, clofibric acid, diclofenac, ibuprofen, ketoprofen,

UNCORRECTED PROOFS

Trim Size: 170mm x 244mm Single Column Loose Ribeiro670117 c06.tex V1 - 12/11/2020 11:51pm Page 143

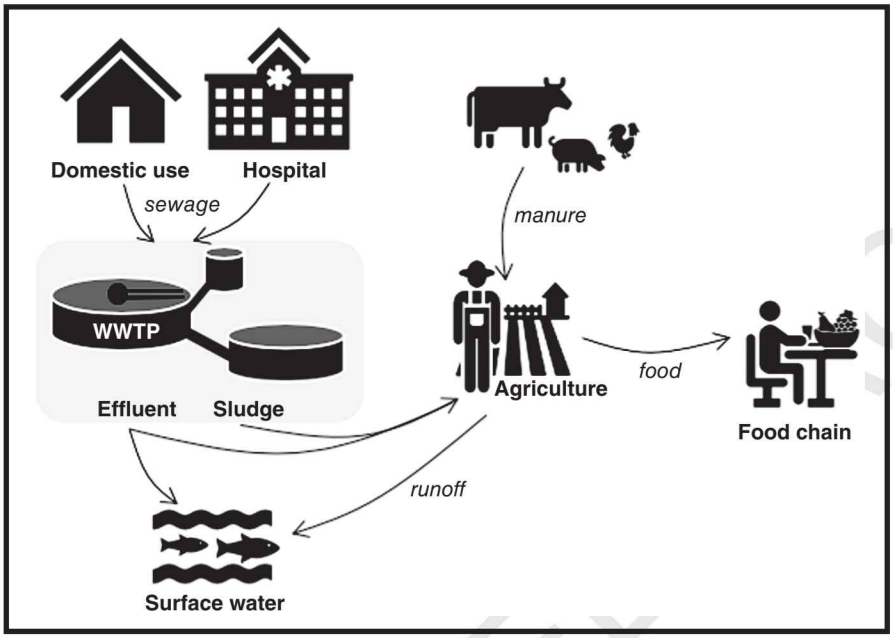

Figure 6.2 Origins of EOCs such as pharmaceuticals and routes into the environment.

and naproxen in carrots and sweet potatoes irrigated with treated wastewater. It is difficult to predict what environmental and public health implications may arise from the occurrence of these chemicals in the environment since EOCs are usually found in the environment at trace concentrations (i.e., between $ng\,l^{-1}$ and $\mu g\,l^{-1}$ or even lower). However, concerns are increasing about antimicrobial resistance [22] and chronic impacts on biodiversity, including endocrine-disrupting effects on fish [23–25]. Other effects/consequences of EOCs can be found summarized in the literature [10].

6.1.2.1 EOCs in WWTPs

Over the last two decades, the occurrence of several EOCs in the influents and treated effluents of WWTPs has been documented worldwide [3, 5, 11, 26]. In general, conventional WWTPs use a combination of primary (physical) and secondary (biological) methods. They were primarily designed to remove pathogens, suspended solids, and gross organic and inorganic matter, rather than remove the increasing numbers of new chemicals. Worldwide water scarcity is increasing the demand for non-conventional water resources. Nowadays, WWTPs have shown fairly limited effectiveness in EOC removal; there may still be significant concentrations of EOCs in effluents discharged into surface water bodies [27–29].

A combination of regulations and management measures with respect to discharging EOCs into the environment, as well as their occurrence in the environment, is fundamental to achieving efficient water resource management. Although there are no legal discharge limits for EOCs, some regulations have been published in the last

UNCORRECTED PROOFS

Trim Size: 170mm x 244mm Single Column Loose Ribeiro670117 c06.tex V1 - 12/11/2020 11:51pm Page 144

few years. Actions have been initiated across Europe, but Switzerland is currently the only country regulating pharmaceuticals and micropollutants in wastewater. Switzerland also aims to remove a total of 50% of micropollutants by upgrading one-seventh of all wastewater plants to use activated carbon and ozonation by 2040, as part of the Swiss micropollutants action plan ([30] and references therein).

Environmental quality standards for a minority of chemicals such as nonylphenol and bisphenol A have been stipulated in Directive 2008/105/EC. Nonylphenol and nonylphenol ethoxylates have also been recognized as toxic substances by the Canadian government [31]. Other EOCs, such as pharmaceutical and personal care products and steroid hormones, are not included in the list of regulated substances yet. To set regulatory limits, further research on biological responses to these compounds is needed [31].

Recent investigations have examined the fate of EOCs during wastewater treatment, focusing on their removal during conventional (e.g. activated sludge) and advanced (e.g. ozonation and membrane filtration) treatment processes. The results suggest that more studies in EOC remediation should fill the knowledge gaps [10]. The water industry will most likely undergo several changes in the coming years due to rapid urbanization, severe climate change, rising customer demand, and the implementation of emerging digital technologies.

6.1.3 Water Challenges

Water is an essential resource for sustaining humanity and life in general. Access to water, sanitation, and hygiene is a human right; however, half the world's population experiences severe water scarcity at least one month a year [32]. Although approximately 70% of the Earth's surface is covered with water, only a small fraction (2.5%) is freshwater compatible with terrestrial life. Nowadays, intensive pollution issues and, consequently, lack of water quality in many areas in the world have raised awareness about the importance of water. According to the European Environmental Agency Report, only around 40% of surface waters (rivers, lakes, and transitional and coastal waters) have a good ecological status or potential, and 38% have a good chemical status [33]. Nevertheless, effective strategies for addressing water contamination are latent in the modification and research of technologies aiming at wastewater treatment and integrating them into a holistic, circular water management system.

In this sense, various directives and protocols related to better water quality and management have been adopted in the last two decades. In 2000, the European Union (EU) introduced a list of 33 priority substances to control the chemical quality of water (Water Framework Directive, 2000/60/EC) [34], which was later updated to 45 substances in 2013 (Directive 2013/39/EU) [35].

According to the UN, the world population is expected to reach more than 9 billion people in 2050, and a continuous increase in water demand is observed as a consequence. The volume of wastewater generated by domestic, industrial, and commercial sources has been increasing along with population, urbanization, improved living conditions, and economic development [36]. At present, about 1 billion cubic meters of treated urban wastewater are reused annually, accounting

UNCORRECTED PROOFS

Trim Size: 170mm x 244mm Single Column Loose Ribeiro670117 c06.tex V1 - 12/11/2020 11:51pm Page 145

for approximately 2.4% of treated urban wastewater effluents and less than 0.5% of annual EU freshwater withdrawals. To make sure there is enough food for the growing population, it is estimated that global food production needs to increase by 70%; agriculture plays a key role and is a huge responsibility of water management, as it uses 70% of the available freshwater [37]. Thus, agricultural water consumption is also expected to grow by about 20% globally by 2050 [38]. In May 2018, the European Commission proposed new rules to stimulate and facilitate water reuse in the EU for agricultural irrigation [32]. The Regulation proposed by the Commission aims to alleviate water scarcity across the EU, and it will ensure that treated wastewater intended for agricultural irrigation is safe, protecting citizens and the environment. The proposal is part of the Commission's 2018 Work Programme, following up on the Circular Economy Action Plan, and completes the existing EU legal framework on water and foodstuffs.

Wastewater contains a great number of valuable resources such as nitrogen, phosphorus, energy, and other nutrients that can be recovered and reused in a circular economy to protect scarce and threatened resources in addition to reducing water consumption. However, changing from a linear model to a more circular economy requires rethinking traditional wastewater treatment models and understanding the interlinkages between the different Sustainable and Development Goals (SDGs). Some possible interlinkages that can be drawn from the SDG6 are shown in Figure 6.3. The SDG6 consists of the development of cost-efficient technologies to remove contaminants from wastewater, ensuring availability and sustainable management of water and sanitation for all. The SDG6 is an important element of the SDG2, promoting sustainable agricultural practices, as it will contribute to safe water reuse. At the same time, the SDG6 is also linked to other parts of Agenda 2030, such as those related to poverty, nutrition, health, education, gender,

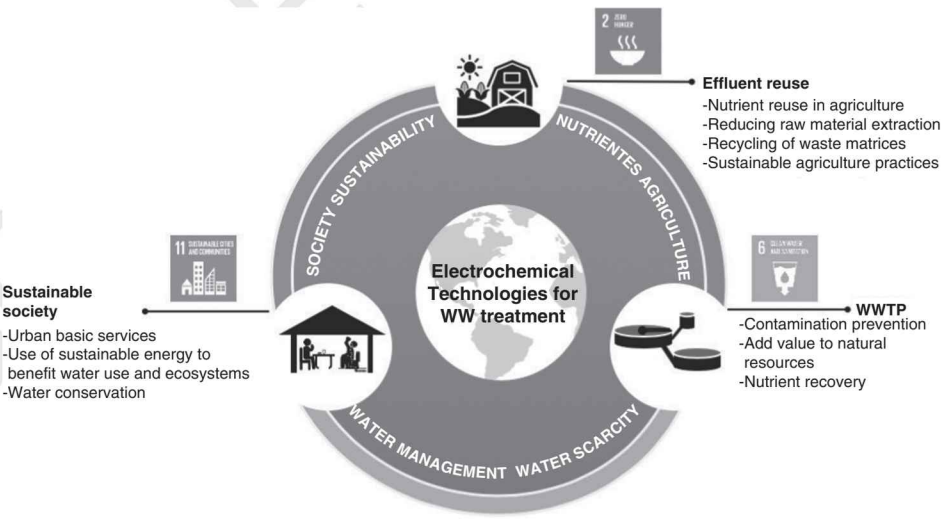

Figure 6.3 Interlink of Sustainable Development Goals addressing wastewater treatment challenges with electro-based technologies.

UNCORRECTED PROOFS

Trim Size: 170mm x 244mm Single Column Loose Ribeiro670117 c06.tex V1 - 12/11/2020 11:51pm Page 146

economic growth, and climate change. Explicit links can be made between SDG6.2 and those relating to basic urban services, with the proportion of urban solid waste regularly collected and with adequate final discharge out of total urban solid waste generated by cities (SDG11). The relative importance of these interlinkages can vary based on regional or socio-economic context [39].

6.1.4 Technologies for Wastewater Treatment – Electrochemical Process

The treatment of urban wastewater is one of the biggest challenges of the twenty-first century, and the development of cheaper, effective, and novel methods of decontamination is currently an active field of research, as shown by the numerous publications appearing each year (Figure 6.4).

In recent decades, research efforts have been made to develop more effective technologies for the remediation of waters containing organic pollutants. Several physicochemical techniques have been exploited, such as activated carbon adsorption, advanced oxidation processes (AOPs), nanofiltration, reverse osmosis, and membrane bioreactors, to achieve high levels of contaminant removal [40]. However, the application of such technologies implies a high cost for water treatment. In addition, these technologies in some cases do not achieve complete mineralization of the contaminant, sometimes leading to secondary pollution [41]. Successful mitigation strategies have not yet been established, and the search for alternative techniques is necessary to improve the degradation of organic contaminants (parent and secondary metabolites) and reduce the costs associated with effluent treatment in WWTPs, allowing its safe reuse [40, 42].

All the technologies have constraints not only in terms of cost but also in terms of feasibility, practicability, reliability, environmental impact, sludge production, operation difficulty, pretreatment requirements, and the formation of potentially toxic

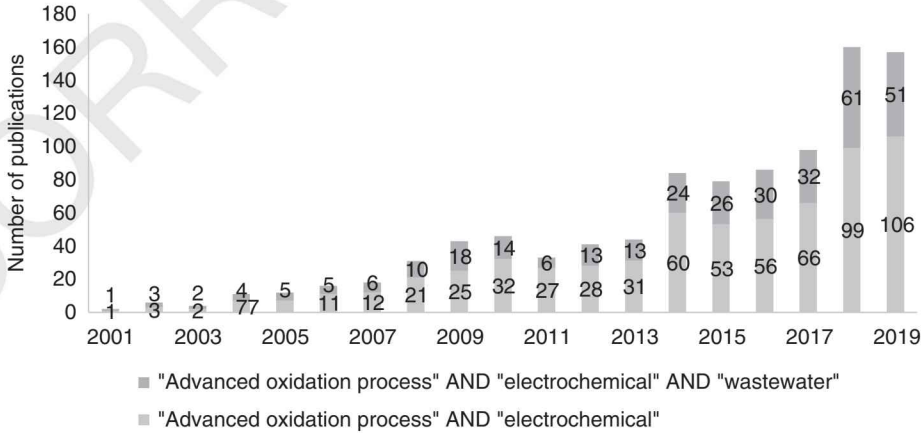

Figure 6.4 Number of publications from 2001 to 2019 on advanced oxidation processes with electrochemical technology and wastewater. .

UNCORRECTED PROOFS

Trim Size: 170mm x 244mm Single Column Loose Ribeiro670117 c06.tex V1 - 12/11/2020 11:51pm Page 147

byproducts. Among the various treatment processes currently cited for wastewater treatment, only a few are commonly employed by the industrial sector for technological and economic reasons [43].

The use of chemically strong oxidation agents such as hydroxyl radicals, chlorine, hydrogen peroxide, ozone, and combinations of these oxidants has been investigated for chemical oxidation of EOCs from wastewater. AOPs constitute important, promising, efficient, and environmentally friendly methods developed to principally remove organic pollutants from waters and wastewaters. Based on the ways oxidation agents are produced, AOPs can be classified in different ways such as Fenton oxidation catalytic ozonation, photocatalytic oxidation, and electrochemical oxidation [44].

Among the various technologies, the so-called electrochemical AOPs have generated increasing interest; over the last two decades, electrochemical technology or electrochemical-AOPs have gained increasing attention as a promising class of AOPs, representing half the publications in this field (Figure 6.4).

Electrochemical (EK) technology is a high-efficiency technology for oxidizing and removing a broad range of recalcitrant organic pollutants such as dyes, pesticides, herbicides, pharmaceuticals, antibiotics, hormones, chelating agents, and microcystin toxins [44–47]. EK processes have been investigated for wastewater treatment and offer a great advantage over conventional treatments since no additional chemicals are required as e.g. in electro-Fenton oxidation, and the electron may be considered as a "green" controllable reagent that does not generate sludge [48]. The great effectiveness of electrochemical methods is due to the production of the hydroxyl radical ($^{\bullet}OH$), which is a non-selective, very powerful oxidizing agent (2.8 V) that reacts with organics, giving dehydrogenated or hydroxylated derivatives until complete mineralization is reached [49]. Compared to other AOPs, electrochemicals are more efficient; for example, in [50], the study showed chemical oxygen demand (COD) degradation efficiency of 38.1%, which is higher than that obtained using ozonation (17.0%). Additionally, the specific energy demand is lower for electrochemical AOPs (93.6 kWh/kg m COD) than for ozonation (125.4 kWh/kg m COD) or the peroxone process (134.5 kWh/kg m COD).

The electrochemical oxidation of organic pollutants can take place in two ways: (i) direct electron exchange between the contaminant and the electrode surface, which can occur at relatively low potentials (i.e. prior to O_2 evolution); or (ii) by indirect in situ electro generation of catalytic species, which relies on the production of oxidizing species at the electrode that mediate the transformation of contaminants. The rates of direct electrolysis are affected by diffusion limitations, slow reaction kinetics, and a decrease in the catalytic activity of the electrode in the presence of dissolved solutes (i.e. poisoning) [51].

The effectiveness of electrochemical oxidation of organic pollutants depends largely on the properties of the anode material, such as the O_2 overpotential and adsorptive properties of the electrode surface [52–54]. Moreover, the reaction time, electrode separation distance, and electrode area might control the efficiency of EOC removal from wastewater [55].

UNCORRECTED PROOFS

Trim Size: 170mm x 244mm Single Column Loose Ribeiro670117 c06.tex V1 - 12/11/2020 11:51pm Page 148

Compared with conventional methods, the EK process has several advantages, such as ease of operation, short retention time, environmental compatibility, high-efficiency degradation, the potential for a high degree of automatization, robust performance, and the ability to adjust to variations in the influent composition and flow rate. However, the application of electrochemical treatment has been slowed by the relatively high costs of electrodes and concerns about toxic byproducts in the treated water [43].

6.2 Electrochemical Reactor for EOC Removal in WWTPs

A research study was carried out, aiming to investigate the electrooxidation performance of four different EOCs (Table 6.1) as a model for these experiments. The suitability of the electrode material and current density were studied, including sulfamethoxazole, carbamazepine, 17α-ethinylestradiol, and diclofenac from a real effluent sample. This investigation was undertaken to extend the knowledge of electro-degradation of EOCs in real effluents using different anode materials (graphite and Pt/Ti electrodes) and is part of the work carried out by the team and presented in [56]. The EOCs selected for the study include antibiotics, psychiatric drugs, hormones, and non-steroidal anti-inflammatory drugs that have been reported in rivers, lakes, and reservoirs around the world [10, 57–59]. In addition, all the EOCs present different physicochemical characteristics (e.g. solubility, octanol-water partition coefficient; Table 6.1) to give a representative study of EOC removal.

6.2.1 Experimental Design

Electrochemical experiments were carried out in a cylindrical reactor made of Plexiglas, 10 cm long and with an internal diameter of 8 cm (Figure 6.5). Electrodes were installed 2.5 cm from the middle of the reactor (5 cm apart from each other). The power supply (Hewlett-Packard E3612A) was used to maintain constant DC.

The vertical reactor was tested in a continuous flow mode with effluent at $2\,ml\,min^{-1}$. Two different anode materials – Pt/Ti (platinized coated titanium; length 5.5 cm, diameter 3 mm; Permascand®) and graphite (99.9995% metals basis; length 5.5 cm, diameter 3 mm; AlfaAesar) – were tested with a fixed Pt/Ti cathode. In addition to the effect of the anode material, two different current intensities were tested: 25 mA and 100 mA. Before EK treatment, the effluent was spiked with $3\,mg\,l^{-1}$ of each contaminant.

6.2.1.1 Analytical Methodology

Sulfamethoxazole, carbamazepine, diclofenac, and ethinylestradiol standards with high purity grade (>97%) were purchased from Sigma-Aldrich (Steinheim, Germany). The effluent samples were pre-cleaned/concentrated by soli-phase extraction (SPE) using Oasis HLB 500 mg (Waters; Saint-Quentin En Yvelines Cedex, France). The cartridges were placed in an SPE manifold connected to a

UNCORRECTED PROOFS

Trim Size: 170mm x 244mm Single Column Loose Ribeiro670117 c06.tex V1 - 12/11/2020 11:51pm Page 149

Table 6.1 Chemical structure and properties of emerging organic contaminants.

EOCs	Formula	Log K_{ow}	pKa	Solubility in water (mg l^{-1})	Category
Sulfamethoxazole (SFM)	$C_{10}H_{11}N_3O_3S$	0.89	5.7	610	Antibiotic
Carbamazepine (CBMP)	$C_{15}H_{12}N_2O$	2.45	13.9	18	Anticonvulsive
17α-ethinylestradiol (EE2)	$C_{20}H_{24}O_2$	3.67	10.3	11.3	Estrogen
Diclofenac (DCF)	$C_{14}H_{11}Cl_2NO_2$	4.51	4.15	2.37	Anti-inflammatory

Sources: PubChem, http://pubchem.ncbi.nlm.nih.gov; Sigma-Aldrich, Inc., www.SigmaAldrich.com.

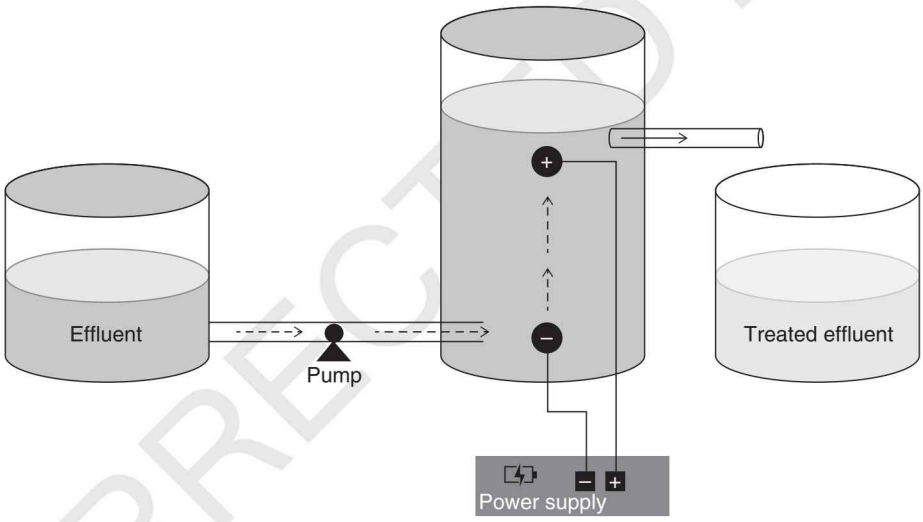

Figure 6.5 Electrochemical reactor design.

vacuum pump and operated as follows: conditioned by washing with 3 × 6 ml of MeOH, followed by re-equilibrium with 3 × 6 ml of Milli-Q water; for EOC enrichment, samples were acidified to pH 2 before extraction (nitric acid; deionized water, 1:1) and filtered through a 0.45 μm MF filter; 200 ml of the sample was passed through the cartridge at a flow rate of approximately 10 ml min^{-1}; then, the cartridges were dried for about 2 minutes by vacuum; finally, the extracts were eluted with two × 6 ml of MeOH. The samples were filtered before analysis through FILTER-LAB® polytetrafluoroethylene (PTFE) syringe filters (pore size 0.45 μm), previously passed through methanol. The EOC analysis was carried out by high-performance liquid chromatography (HPLC) with a diode array and fluorescence detectors (HPLC–DAD-FLD), 1260 Infinity II LC Systems (Agilent 1100

UNCORRECTED PROOFS

Trim Size: 170mm x 244mm Single Column Loose Ribeiro670117 c06.tex V1 - 12/11/2020 11:51pm Page 150

Series Technologies, USA) equipped with a quaternary pump and auto-sampler (1260). The RP-18e column (Chromolith High Resolution, 100 × 4.6 mm; VWR, Darmstadt, Germany) was used for analyte separation. LC OpenLab software was used for data processing.

6.2.2 Electrokinetic Reactor Operating in a Continuous Vertical Flow Mode

The initial effluent sample presented an alkaline pH (~8.6) and conductivity of ~1.8 mS cm^{-1}, and all the parameters were within the Portuguese legal limits for discharge into water bodies (DL 236/98). The pH, conductivity, and voltage values after EK treatment are listed in Table 6.2. The pH of the effluent had the tendency to decreases lightly, primarily when the higher current intensity was tested and when a graphite anode was used. The conductivity slightly decreased for the lowest current intensity and remained constant when applying a higher current intensity due to the greater production of ions in the electrode. The presence of Cl^- and other inorganic ions in the effluent yielded sufficient conductivity for direct EK treatment without adding any salt as supporting electrolyte. In both cases, using graphite or Pt/Ti as an anode, the voltage increased when higher current intensity was applied due to greater hydroxide ion generation.

Figure 6.6 shows the removal of the selected EOCs after EK treatment with low current intensity (25 mA) and with the current intensity increased four times (100 mA) for the two anode materials tested. An initial effluent screening was carried out, and the concentration of the target EOCs was below the analytical detection limits.

Compared with a control (without applied current), the effect of the lowest current applied (25 mA) promoted the removal of between 5 and 41% of EOCs; when the current intensity was increased to 100 mA, removal increased 10–36%. Regarding the differences among the contaminants for the two tested current intensities, CBMP and DCF showed the lowest level of removal. The compound's molecular structure has a strong influence on the success of electrochemical removal. Compounds characterized by the presence of electrophilic halogen groups with a negative inductive effect at the aromatic ring or by the absence of nucleophilic substituents with an activating effect on the aromatic ring like DCF are more recalcitrant because they

Table 6.2 pH, conductivity, and voltage drop after EK treatment.

Current intensity (mA)	Anode	pH	Conductivity (mS cm^{-1})	Voltage (V)
25	Graphite	8.11	1.72	7.2–7.0
	Pt/Ti	8.51	1.63	6.9–7.0
100	Graphite	7.25	1.85	14.8–16.7
	Pt/Ti	7.46	1.85	14.8–16.4

UNCORRECTED PROOFS

Trim Size: 170mm x 244mm Single Column Loose Ribeiro670117 c06.tex V1 - 12/11/2020 11:51pm Page 151

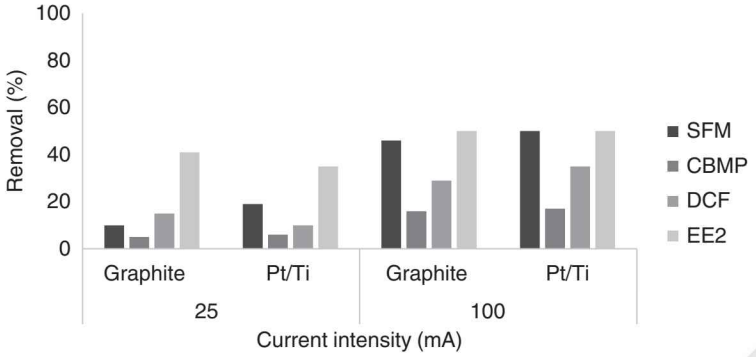

Figure 6.6 Removal (%) of EOCs after electrochemical treatment in a vertical continuous-flow reactor, applying different current intensities and anode materials.

decrease the reactivity toward oxidant agents and active chlorine species present in effluents [60].

- ***Current intensity***
  In several studies, current intensity is reported to affect electrochemical oxidation efficiency as it is the driving force of the reaction. The results from this study showed that EOC removal was enhanced by increasing current intensity. SFM removal increased by 36% when 100 mA were applied. Increasing current intensity promotes the generation of more OH, which is responsible for organic oxidation; hence, greater EOC removal can be expected in the tested conditions. Other research also found that an increase in current intensity enhances contaminant removal. For example, in [61], the effect of current density on the removal rate of COD of wastewater with sulfamethoxazole and trimethoprim (two well-known antibiotics) was investigated, and the results showed that COD removal efficiency increased when the current density increased from 10 to 100 mA cm^{-2}. However, when increased indefinitely, the current during EK treatment is not always proportional to the removal rate. The rate of parasitic reactions is also promoted, which leads to decreasing current efficiency and, consequently, less contaminant removal [47]. It is important to regular the amount of oxidizing species produced, taking into account the feasibility of the process in terms of electrical charge consumed and/or energy consumption [47]. In addition to energy dissipation, high current intensities can shorten the lifetime of the electrodes [62].
- ***Anode material***
  To improve process efficiency, several anode materials have been tested and show varied performance. In the tested conditions, no differences were found in terms of EOC degradation for the two tested anode materials, graphite and Pt/Ti. EK uses the electron as the primary reagent for contaminant removal: the generation of •OH from water oxidation at anode is crucial for EOC removal. Graphite and Pt/Ti are both considered active electrodes [63], and the electrogenerated •OH is expected to be converted in "adsorbed oxygen," which is consumed in the oxidation of organic compounds with the formation of selective oxidation products and

UNCORRECTED PROOFS

Trim Size: 170mm x 244mm Single Column Loose Ribeiro670117 c06.tex V1 - 12/11/2020 11:51pm Page 152

in an easy oxygen evolution [64]. Even though no differences were found between the two anodes in the tested conditions, the Pt electrode showed better performance than graphite. Some differences were also found for SFM and DCF removal in previous research such as [65]. The authors attributed the differences to the different adsorptions of •OH on these electrodes: due to Pt, the •OH are weakly adsorbed and have lower adsorption on the Pt surface. Consequently, they are very reactive and effective toward oxidation due to the faster reactions with all organics arriving at the surface and in the anode's vicinity. On the other hand, graphite has more •OH strongly adsorbed on its surface; thus it is less reactive toward EOC degradation [65].

After EK treatment, the graphite electrode showed signs of corrosion due to the effect of the applied current. Higher current could lead to electric energy transfer to thermal energy and result in a larger invalid consumption of the given charge. Even though high current intensity caused the electrode material to corrode, side reactions including oxygen evolution could also happen simultaneously, and no differences between the two electrodes in terms of EOC removal were registered for the tested conditions [66].

- ***Flow mode***

  The effect of current intensity can also be related to the continuous flow mode present in this work, which according to [64] is strongly interrelated, so they must be considered together. A continuous flow mode influences the direct oxidation of EOCs by the contact between electrode and effluent solution. In the vertical EK flow reactor, the effluent was in a continuous flow mode, passing first through the Pt/Ti cathode electrode, where reduction reactions take place, and going toward the anode, where •OH is generated. The oxidation of the organics by •OH generated from the water oxidation is so fast that the rate-determining step is the mass transport from the bulk solution to the anodic surface. When the rate of the mass transfer of the organic to the anodic surface is dramatically lower than the rate of oxidation, the concentration of the pollutant at the anodic surface/reaction layer is close to zero, and the oxidation process is under mass-transfer control [64]. Considering that the electrochemical oxidation of organics is limited by mass transport, high flow rates in the reactor might increase the mass transfer, thus allowing enhanced performance. If oxidation takes place by indirect electrolysis, high flow rates are reported to favor removal, meaning the oxidation is a diffusion-controlled process [67].

  The present results showed that electrochemical degradation is a promising method for EOC removal, but operational parameters need to be optimized: for example, by changing the flow mode and current intensity and testing different electrode materials. Experiments in batch mode were carried out by the team, and greater removal (> 90%) was achieved [56]. The results presented in [56] also show that in addition to the influence of the batch and flow mode, the electrode shape and material are key to a cost-efficient process. Greater EOC removal was achieved in a batch-mode system, with both the electrode's shape and material proving to be important parameters to improve the EK process, not only for

UNCORRECTED PROOFS

Trim Size: 170mm x 244mm Single Column Loose Ribeiro670117 c06.tex V1 - 12/11/2020 11:51pm Page 153

removing EOCs but also to make the process more efficient in terms of energy consumption.

6.3 Conclusions

To limit the presence of EOCs in the environment, efficient technologies should be implemented in WWTPs and stricter environmental quality standards should be established. The removal of EOCs with different physicochemical characteristics represents a real challenge in wastewater treatment. Research of electrochemical technologies to remove EOCs has been increasing, and the results show that treatment efficiency depends on reactor design and operational parameters such as flow mode and electrode material. The use of electrochemical technologies to remove EOCs from wastewater is a promising technology with the potential to reduce the environmental and human risks associated with the spread of contamination.

Acknowledgments

Financial support was provided by 4KET4Reuse (SOE1/P1/E0253) and CEMOWAS^2 (SOE2/P5/F0505), co-financed by the European Regional Development Fund (FEDER), the European Union's Horizon 2020 research and innovation program under the Marie Skłodowska-Curie grant agreement No. 778045; FCT/MCTES, Portugal, through UIDB/04085/2020 (research unit CENSE, Center for Environmental and Sustainability Research). Fundação para a Ciência e a Tecnologia is also acknowledged for P. Guedes' fellowship (SFRH/BPD/114660/2016) and N. Couto's contract established under the Individual Call to Scientific Employment Stimulus (CEECIND/04210/2017). The authors acknowledge and appreciate the support given to CENSE by the Portuguese Foundation for Science and Technology (FCT) through the strategic project UIDB/04085/2020. The authors would like to thank SIMARSUL, Dr. Cristina Santos, and Eng. Olga Paredes for providing the effluent samples, and the Laboratory of Control and Processes for assistance. This research is anchored by the RESOLUTION LAB, an infrastructure at NOVA School of Science and Technology.

References

1 Naidu, R., Jit, J., Kennedy, B., and Arias, V. (2016). Emerging contaminant uncertainties and policy: the chicken or the egg conundrum. *Chemosphere* 154: 385–390.

2 Sauvé, S. and Desrosiers, M. (2014). A review of what is an emerging contaminant. *Chemistry Central Journal* 8: 15.

UNCORRECTED PROOFS

Trim Size: 170mm x 244mm Single Column Loose Ribeiro670117 c06.tex V1 - 12/11/2020 11:51pm Page 154

3 Ebele, A.J., Abou-Elwafa Abdallah, M., and Harrad, S. (2017). Pharmaceuticals and personal care products (PPCPs) in the freshwater aquatic environment. *Emerging Contaminants* 3 (1): 1–16.

4 Khetan, S.K. and Collins, T.J. (2007). Human Pharmaceuticals in the Aquatic Environment: a challenge to green chemistry. *Chemical Reviews* 107 (6): 2319–2364.

5 Richardson, B.J., Lam, P.K.S., and Martin, M. (2005). Emerging chemicals of concern: pharmaceuticals and personal care products (PPCPs) in Asia, with particular reference to southern China. *Marine Pollution Bulletin* 50 (9): 913–920.

6 Li, M., Sun, Q., Li, Y. et al. (2016). Simultaneous analysis of 45 pharmaceuticals and personal care products in sludge by matrix solid-phase dispersion and liquid chromatography tandem mass spectrometry. *Analytical and Bioanalytical Chemistry* 408 (18): 4953–4964.

7 Barceló, D. and Petrovic, M. (2007). Pharmaceuticals and personal care products (PPCPs) in the environment. *Analytical and Bioanalytical Chemistry* 387 (4): 1141–1142.

8 Buchberger, W. (2011). Current approaches to trace analysis of pharmaceuticals and personal care products in the environment. *Journal of Chromatography A* 1218 (4): 603–618.

9 Archer, E., Petrie, B., Kasprzyk-Hordern, B., and Wolfaardt, G.M. (2017). The fate of pharmaceuticals and personal care products (PPCPs), endocrine disrupting contaminants (EDCs), metabolites and illicit drugs in a WWTW and environmental waters. *Chemosphere* 174: 437–446.

10 Gogoi, A., Mazumder, P., Tyagi, V.K. et al. (2018). Occurrence and fate of emerging contaminants in water environment: a review. *Groundwater for Sustainable Development* 6: 169–180.

11 Heberer, T. (2002). Occurrence, fate, and removal of pharmaceutical residues in the aquatic environment: a review of recent research data. *Toxicology Letters* 131 (1–2): 5–17.

12 Mompelat, S., Le Bot, B., and Thomas, O. (2009). Occurrence and fate of pharmaceutical products and byproducts, from resource to drinking water. *Environment International* 35 (5): 803–814.

13 A, L.G. and Pettigrove, M.E. (2006). Seasonal variations in concentrations of pharmaceuticals and personal care products in drinking water and reclaimed wastewater in southern California. *Environmental Science and Technology* 40 (3): 687–695.

14 Couto, N., Ferreira, A.R., Guedes, P. et al. (2018). Partition and remediation potential of caffeine, oxybenzone and triclosan in estuarine environment. *Environmental Science and Pollution Research* 25 (36): 35928–35935.

15 Grassi, M., Rizzo, L., and Farina, A. (2013). Endocrine disruptors compounds, pharmaceuticals and personal care products in urban wastewater: implications for agricultural reuse and their removal by adsorption process. *Environmental Science and Pollution Research* 20 (6): 3616–3628.

UNCORRECTED PROOFS

Trim Size: 170mm x 244mm Single Column Loose Ribeiro670117 c06.tex V1 - 12/11/2020 11:51pm Page 155

16 Zhang, D., Gersberg, R.M., Ng, W.J., and Tan, S.K. (2013). Removal of pharmaceuticals and personal care products in aquatic plant-based systems: a review. *Environmental Pollution* 184: 620–639.

17 Biel-Maeso, M., Corada-Fernández, C., and Lara-Martín, P.A. (2018). Monitoring the occurrence of pharmaceuticals in soils irrigated with reclaimed wastewater. *Environmental Pollution* 235: 312–321.

18 Calderón-Preciado, D., Jiménez-Cartagena, C., Matamoros, V., and Bayona, J.M. (2011). Screening of 47 organic microcontaminants in agricultural irrigation waters and their soil loading. *Water Research* 45 (1): 221–231.

19 Paltiel, O., Fedorova, G., Tadmor, G. et al. (2016). Human exposure to wastewater-derived pharmaceuticals in fresh produce: a randomized controlled trial focusing on carbamazepine. *Environmental Science and Technology* 50 (8): 4476–4482.

20 Hurtado, C., Domínguez, C., Pérez-Babace, L. et al. (2016). Estimate of uptake and translocation of emerging organic contaminants from irrigation water concentration in lettuce grown under controlled conditions. *Journal of Hazardous Materials* 305: 139–148.

21 Malchi, T., Maor, Y., Tadmor, G. et al. (2014). Irrigation of root vegetables with treated wastewater: evaluating uptake of pharmaceuticals and the associated human health risks. *Environmental Science and Technology* 48 (16): 9325–9333.

22 Piña, B., Bayona, J.M., Christou, A. et al. (2018). On the contribution of reclaimed wastewater irrigation to the potential exposure of humans to antibiotics, antibiotic resistant bacteria and antibiotic resistance genes – NEREUS COST action ES1403 position paper. *Journal of Environmental Chemical Engineering* 8 (1): 102131.

23 Meador, J.P., Yeh, A., Young, G., and Gallagher, E.P. (2016). Contaminants of emerging concern in a large temperate estuary. *Environmental Pollution* 213: 254–267.

24 Rosal, R., Rodea-Palomares, I., Boltes, K. et al. (2010). Ecotoxicity assessment of lipid regulators in water and biologically treated wastewater using three aquatic organisms. *Environmental Science and Pollution Research* 17 (1): 135–144.

25 Cunha, V., Burkhardt-Medicke, K., Wellner, P. et al. (2017). Effects of pharmaceuticals and personal care products (PPCPs) on multixenobiotic resistance (MXR) related efflux transporter activity in zebrafish (Danio rerio) embryos. *Ecotoxicology and Environmental Safety* 136: 14–23.

26 Boyd, G.R., Reemtsma, H., DA, G., and Mitra, S. (2003). Pharmaceuticals and personal care products (PPCPs) in surface and treated waters of Louisiana, USA and Ontario, Canada. *The Science of the Total Environment* 311 (03): 135–149.

27 Verlicchi, P., Al Aukidy, M., and Zambello, E. (2012). Occurrence of pharmaceutical compounds in urban wastewater: removal, mass load and environmental risk after a secondary treatment–a review. *The Science of the Total Environment* 429: 123–155.

UNCORRECTED PROOFS

Trim Size: 170mm x 244mm Single Column Loose Ribeiro670117 c06.tex V1 - 12/11/2020 11:51pm Page 156

28 Petrie, B., Barden, R., and Kasprzyk-Hordern, B. (2014). A review on emerging contaminants in wastewaters and the environment: current knowledge, understudied areas and recommendations for future monitoring. *Water Research* 72: 3–27.

29 De Jesus, G.V., Cardoso, V.V., Cardoso, E. et al. (2017). Occurrence and behaviour of pharmaceutical compounds in a Portuguese wastewater treatment plant: removal efficiency through conventional treatment processes. *Environmental Science and Pollution Research* 24 (17): 14717–14734.

30 European Federation of National Associations of Water Services, EurEau. (2019). Briefing note – Treating micropollutants at waste water treatment plants. 2019. http://www.eureau.org/resources/briefing-notes/3826-briefing-note-on-treating-micropollutants-at-the-wwtp/file.

31 Canadian Environmental Protection Act. (1999). Priority substances list assessment report, "nonylphenol and its ethoxylates".

32 European Comission. (2018). Environment. Water reuse. http://ec.europa.eu/environment/water/reuse.htm.

33 Kristensen, P., Whalley, C., and Klančnik, K. (2018). European waters assessment of status and pressures 2018. European Environment Agency. https://www.eea.europa.eu/publications/state-of-water.

34 EU (2000). Directive 2000/60/EC of the European Parliament and of the council establishing a framework for community action in the field of water policy off. *Journal of the European Communities* 327: 1–72.

35 EU (2013). Directive 2013/39/EU of the European Parliament and of the council amending directives 2000/60/EC and 2008/105/EC as regards priority substances in the field of water policy off. *Journal of the European Communities* 226: 1–17.

36 Qadir, M., Wichelns, D., Raschid-Sally, L. et al. (2010). The challenges of wastewater irrigation in developing countries. *Agricultural Water Management* 97 (4): 561–568.

37 Food and Agriculture Organization of the United Nations (FAO). (2018). Proportion of total water withdrawal withdrawn for agriculture (%). http://www.fao.org/nr/water/aquastat/maps/World-Map.WithA.Twith_eng.htm.

38 United Nations Department of Economic and Social Affairs. (2015). World population prospects: The 2015 revision. http://www.un.org/en/development/desa/news/population/2015-report.html.

39 Fritsche, U.R., Eppler, U., Fehrenbach, H., and Giegrich, J. (2018). Linkages between the Sustainable Development Goals (SDGs) and the GBEP Sustainability Indicators for Bioenergy (GSI). Global Bioenergy Partnership. http://www.globalbioenergy.org/fileadmin/user_upload/gbep/docs/Indicators/IINAS_IFEU__2018__Linkages_SDGs_and_GSIs_-_final.pdf.

40 Luo, Y., Guo, W., Ngo, H.H. et al. (2014). A review on the occurrence of micropollutants in the aquatic environment and their fate and removal during wastewater treatment. *The Science of the Total Environment* 473–474: 619–641.

41 Martínez-Huitle, C.A. and Ferro, S. (2016). Electrochemical oxidation of organic pollutants for the wastewater treatment: direct and indirect processes. *Chemical Society Reviews* 35: 1324–1340.

UNCORRECTED PROOFS

Trim Size: 170mm x 244mm Single Column Loose Ribeiro670117 c06.tex V1 - 12/11/2020 11:51pm Page 157

42 Schröder, P., Helmreich, B., Škrbić, B. et al. (2016). Status of hormones and painkillers in wastewater effluents across several European states—considerations for the EU watch list concerning estradiols and diclofenac. *Environmental Science and Pollution Research* 23 (13): 12835–12866.

43 Crini, G. and Lichtfouse, E. (2019). Advantages and disadvantages of techniques used for wastewater treatment. *Environmental Chemistry Letters* 17 (1): 145–155.

44 Ghime, D. and Ghosh, P. (2019). Removal of organic compounds found in the wastewater through electrochemical advanced oxidation processes: a review. *Russian Journal of Electrochemistry* 55 (7): 591–620.

45 Couto, N., Guedes, P., Ferreira, A.R. et al. (2015). Electrodialytic process of nanofiltration concentrates - phosphorus recovery and microcystins removal. *Electrochimica Acta* 181: 200–207.

46 Ai, Z., Li, J., Zhang, L., and Lee, S. (2010). Rapid decolorization of azo dyes in aqueous solution by an ultrasound-assisted electrocatalytic oxidation process. *Ultrasonics Sonochemistry* 17 (2): 370–375.

47 Moreira, F.C., Boaventura, R.A.R., Brillas, E., and Vilar, V.J.P. (2017). Electrochemical advanced oxidation processes: a review on their application to synthetic and real wastewaters. *Applied Catalysis B: Environmental* 202: 217–261.

48 Chu, Y.Y., Qian, Y., Wang, W.J., and Deng, X.L. (2012). A dual-cathode electro-Fenton oxidation coupled with anodic oxidation system used for 4-nitrophenol degradation. *Journal of Hazardous Materials* 199–200: 179–185.

49 Tung, C., Shen, S., Chang, J. et al. (2013). Treatment of real printing wastewater with an electrocatalytic process. *Separation and Purification Technology* 117: 131–136.

50 Haupt, D., Muddemann, T., Kunz, U., and Sievers, M. (2019). Evaluation of a new electrochemical concept for vacuum toilet wastewater treatment – comparison with ozonation and peroxone processes. *Electrochemistry Communications* 101: 115–119.

51 Wu, W., Huang, Z.-H., and Lim, T.-T. (2014). Recent development of mixed metal oxide anodes for electrochemical oxidation of organic pollutants in water. *Applied Catalysis A: General* 480: 58–78.

52 Cui, Y., Li, X., and Chen, G. (2009). Electrochemical degradation of bisphenol a on different anodes. *Water Research* 43 (7): 1968–1976.

53 Feng, L., Oturan, N., van Hullebusch, E.D. et al. (2014). Degradation of anti-inflammatory drug ketoprofen by electro-oxidation: comparison of electro-Fenton and anodic oxidation processes. *Environmental Science and Pollution Research* 21 (14): 8406–8416.

54 Li, X., Cui, Y., Feng, Y. et al. (2005). Reaction pathways and mechanisms of the electrochemical degradation of phenol on different electrodes. *Water Research* 39 (10): 1972–1981.

55 González, T., Domínguez, J.R., Palo, P. et al. (2011). Development and optimization of the BDD-electrochemical oxidation of the antibiotic trimethoprim in aqueous solution. *Desalination* 280 (1–3): 197–202.

UNCORRECTED PROOFS

Trim Size: 170mm x 244mm Single Column Loose Ribeiro670117 c06.tex V1 - 12/11/2020 11:51pm Page 158

56 Ferreira, A.R. (2018). Electro-based technologies for contaminants removal from soil and effluent targeting further reuses. PhD thesis, NOVA School of Science and Technology, NOVA University Lisbon.

57 Kolpin, D.W., Furlong, E.T., Meyer, M.T. et al. (2002). Pharmaceuticals, hormones, and other organic wastewater contaminants in U.S. streams, 1999-2000: a national reconnaissance. *Environmental Science & Technology* 36 (6): 1202–1211.

58 Paíga, P., Correia, M., Fernandes, M.J. et al. (2019). Assessment of 83 pharmaceuticals in WWTP influent and effluent samples by UHPLC-MS/MS: hourly variation. *Science of the Total Environment* 648: 582–600.

59 Oulton, R.L., Kohn, T., and Cwiertny, D.M. (2010). Pharmaceuticals and personal care products in effluent matrices: a survey of transformation and removal during wastewater treatment and implications for wastewater management. *Journal of Environmental Monitoring* 12 (11): 1956.

60 Garcia-Segura, S., Keller, J., Brillas, E., and Radjenovic, J. (2015). Removal of organic contaminants from secondary effluent by anodic oxidation with a boron-doped diamond anode as tertiary treatment. *Journal of Hazardous Materials* 283: 551–557.

61 Eleotério, I.C., Forti, J.C., and de Andrade, A.R. (2013). Electrochemical treatment of wastewater of veterinary industry containing antibiotics. *Electrocatalysis* 4 (4): 283–289.

62 Niu, J., Li, Y., Shang, E. et al. (2016). Electrochemical oxidation of perfluorinated compounds in water. *Chemosphere* 146: 526–538.

63 Rivera-Utrilla, J., Sánchez-Polo, M., Ferro-García, M.Á. et al. (2013). Pharmaceuticals as emerging contaminants and their removal from water. A review. *Chemosphere* 93 (7): 1268–1287.

64 Scialdone, O., Galia, A., and Randazzo, S. (2011). Oxidation of carboxylic acids in water at IrO_2–Ta_2O_5 and boron doped diamond anodes. *Chemical Engineering Journal* 174 (1): 266–274.

65 Sifuna, F.W., Orata, F., Okello, V., and Jemutai-Kimosop, S. (2016; 18;). Comparative studies in electrochemical degradation of sulfamethoxazole and diclofenac in water by using various electrodes and phosphate and sulfate supporting electrolytes. *Journal of Environmental Science and Health, Part A* 51 (11): 954–961.

66 Marselli, B., Garcia-Gomez, J., Michaud, P.-A. et al. (2003). Electrogeneration of hydroxyl radicals on boron-doped diamond electrodes. *Journal of the Electrochemical Society* 150 (3): D79.

67 Panizza, M., Barbucci, A., Ricotti, R., and Cerisola, G. (2007). Electrochemical degradation of methylene blue. *Separation and Purification Technology* 54 (3): 382–387.

UNCORRECTED PROOFS

Trim Size: 170mm x 244mm Single Column Loose Ribeiro670117 c07.tex V1 - 12/09/2020 3:20pm Page 159

7

Rare Earth Elements: Overview, General Concepts, and Recovery Techniques, Including Electrodialytic Extraction

Nazaré Couto[1,2], Ana Rita Ferreira[1,2], Vanda Lopes[1,2], Stephen Peters[3], Sibel Pamukcu[2], and Alexandra B. Ribeiro[1]

[1] *CENSE – Center for Environmental and Sustainability Research, Department of Environmental Sciences and Engineering, NOVA School of Science and Technology, NOVA University Lisbon, 2829-516 Caparica, Portugal*
[2] *Department of Civil and Environmental Engineering, Lehigh University, Bethlehem, PA 18015, USA*
[3] *Department of Earth and Environmental Sciences, Lehigh University, Bethlehem, PA 18015, USA*

7.1 Introduction

7.1.1 Rare Earth Elements: Characterization, Applications, and Geo-Dependence

Rare earth elements (REEs) are a group of 17 chemically similar elements composed of 15 lanthanides plus scandium and yttrium [1] (Table 7.1). The concentration of lanthanides varies in nature, except for promethium, which is not normally found due to the very short half-life of its isotopes [3, 4]. REEs can be divided into light rare earth elements (LREEs) and heavy rare earth elements (HREEs) according to their atomic number. In Europe, LREEs include elements between La and Sm, whereas in China, Sm is a HREE [3]. Although their electronic configurations are similar, with most of these elements partially occupying 4f electron orbitals, their distinct physical and chemical properties enable their use in a broad range of technologies [4]. Most REE become trivalent in a metallic state [5]. REEs have a small radius and high ionic charge due to their 3+ valence. The ionic radii decrease from LREEs to HREEs, and LREEs are more abundant than HREEs [3]. Lanthanides have specific characteristics: (i) the size of ions decrease from Ln^{3+} to Lu^{3+} (103–86 pm), known as the *lanthanide contraction* [6]; and (ii) the coordination number varies between 9 in light lanthanides and 8 in heavy lanthanides [7, 8].

REEs are crucial for modern technologies and used in a variety of industries. They can be used as catalysts, in ceramic and glass, metallurgical applications and alloys, polishing, and so on [9]. The importance and trade balance of REE is well known. It is considered that REEs, along with drinking water, oil, and phosphorous (for fertilizers) may be crucial and decisive for the redefinition of the international global balance [10].

The European Commission's Sustainable Development Goals (SDGs) and the decision of the G7 nations to promote actions to improve resource efficiency as

Electrokinetic Remediation for Environmental Security and Sustainability, First Edition.
Edited by Alexandra B. Ribeiro and M.N.V. Prasad.
© 2021 John Wiley & Sons Ltd. Published 2021 by John Wiley & Sons Ltd.

UNCORRECTED PROOFS

Trim Size: 170mm x 244mm Single Column Loose Ribeiro670117 c07.tex V1 - 12/09/2020 3:20pm Page 160

Table 7.1 Rare earth element characteristics.

	Atomic number	Atomic mass	Ionic radius (pm)	Oxidation state	Configuration
Lanthanum (La)	57	138.9	117	3	$[Xe]6s^2 5d^1$
Cerium (Ce)	58	140.2	115	3, 4	$[Xe]\ 4f^1 6s^2 5d^1$
Praseodymium (Pr)	59	140.9	113	3, 4	$[Xe]4f^3 6s^2$
Neodymium (Nd)	60	144.2	143	3	$[Xe]4f^4 6s^2$
Promethium (Pm) (radioactive)	61			3	$[Xe]4f^5 6s^2$
Samarium (Sm)	62	150.4	135	3, 2	$[Xe]4s^6 6s^2$
Europium (Eu)	63	151.9	131	3, 2	$[Xe]4f^7 6s^2$
Gadolinium (Gd)	64	157.3	108	3	$[Xe]\ 4f^7 6s^2 5d^1$
Terbium (Tb)	65	158.9	106	3, 4	$[Xe]4f^9 6s^2$
Dysprosium (Dy)	66	162.5	121	3	$[Xe]4f^{10} 6s^2$
Holmium (Ho)	67	164.9	104	3	$[Xe]4f^{11} 6s^2$
Erbium (Er)	68	167.3	103	3	$[Xe]4f^{12} 6s^2$
Thulium (Tm)	69	168.9	117	3, 2	$[Xe]4f^{13} 6s^2$
Ytterbium (Yb)	70	173.0	116	3, 2	$[Xe]4f^{14} 6s^2$
Lutetium (Lu)	71	174.9	100	3	$[Xe]\ 4f^{14} 6s^2 5d^1$
Yttrium (Y)	39	88.91	104–121.5	3	$[Kr]5s^2 4d^1$
Scandium (Sc)	21	44.96	88.5–102	3	$[Ar]4s^2 3d^1$

Source: Gollakota, Volli, and Sun [2] and references therein.

a core element of sustainable development [11] enforce the concept of maintaining the sustainability of natural resources. At a policy level, the Europe 2020 Strategy recognizes the need for broad-scale economic changes and includes a resource-efficient flagship initiative that aims to build a smart, inclusive, and sustainable economy – a circular economy [12]. Sustainable supply and increasing demand will have considerable influence on the stability of the market. Scientific advances in substitution, nontraditional sources, expansion of recycling and discovery, and extraction and processing of new large deposits will act as balancing influences [13].

REE mines are mostly located in China. For this reason, the country is the dominant global supplier, providing over 90% of the world supply. According to the 2019 US Geological Survey [9], in 2018, the *estimated mine production* in metric tons of rare-earth oxide (REO) equivalent was 120 000 for China; 20 000 for Australia; 15 000 for the US; 5000 for Myanmar; 2600 for Russia; 1800 for India; 1000 for Brazil, Burundi, and Thailand; 400 for Vietnam; and 200 for Malaysia. The largest reserves are estimated as being 44 000 000 in China, 22 000 000 in Brazil and Vietnam, 12 000 in Russia, and 6900 in India.

REEs are a fundamental part of the geopolitical strategy for the US and are included in the list of 35 minerals deemed critical to US national security and

UNCORRECTED PROOFS

Trim Size: 170mm x 244mm Single Column Loose Ribeiro670117 c07.tex V1 - 12/09/2020 3:20pm Page 161

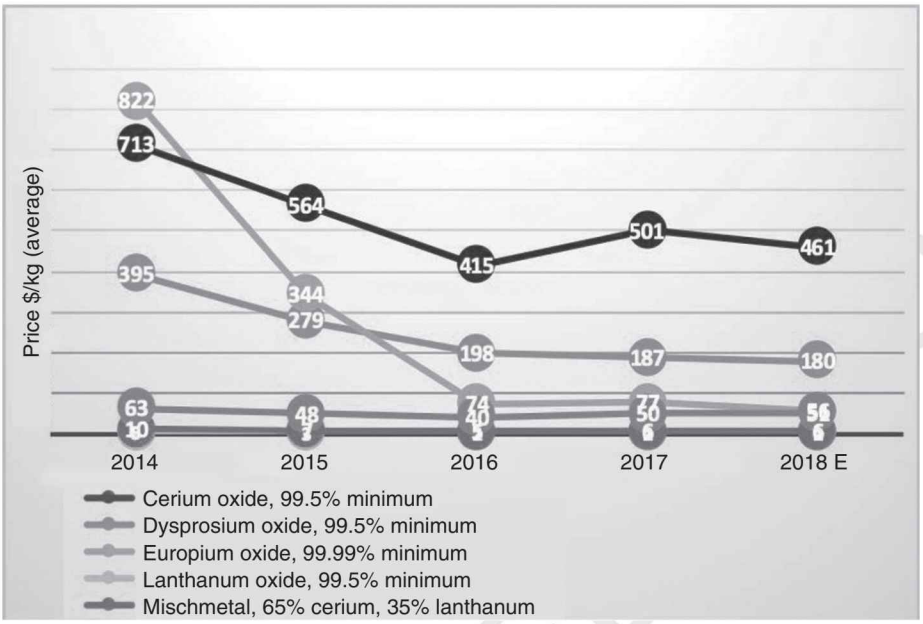

Figure 7.1 Price average (dollar per kilogram) in the US between 2014 and 2018. Source: Adapted from US Geological Survey [9].

the economy, published by the Department of the Interior on 18 May 2018 [14]. In 2017, the US imported 78% of REEs used domestically [15]. The estimated value of rare-earth compounds and metals imported by the country in 2018 was $160 million, an increase from $137 million in 2017 [9]. Figure 7.1 shows the average price in the US in the period between 2014 and 2018 [9]. In the summer of 2017, the government pledged $40 million to ramp up domestic exploration, a consequence of the Chinese partnered acquisition of the sole American REE mine, named Mountain Pass [15].

REEs are considered critical raw materials due to their importance in three main areas: (i) economic well-being, (ii) modern technology, and (iii) the environment [16]. The Critical Raw Materials List was created by the European Commission in 2011 and updated in 2014 and 2017 [17]. According to the review in [3], in 2011, REEs were grouped as critical raw materials (CRMs); in 2014, HREEs were more critical than LREEs, inverting the pattern in 2017. The list of CRMs reflects the situation at a specific moment, and the criticality normally reflects the average observed in the latest five years [3]. Unlike the US, the European Union is entirely dependent on imports of these CRMs. Furthermore, LREE and HREE substitution indexes are low (between 0.89 and 0.93 on a scale from 0 to 1, where 1 means non-substitutable), and the recycling rate is between 3% and 8% for LREEs and HREEs, respectively (Figure 7.2). In Europe and the US (in fact, worldwide), there is common ground: (i) economic importance (related to technical and cost performance of substitutes for individual applications) and (ii) supply risk with serious consequences for the industry and the value chain [7, 8].

UNCORRECTED PROOFS

Trim Size: 170mm x 244mm Single Column Loose Ribeiro670117 c07.tex V1 - 12/09/2020 3:20pm Page 162

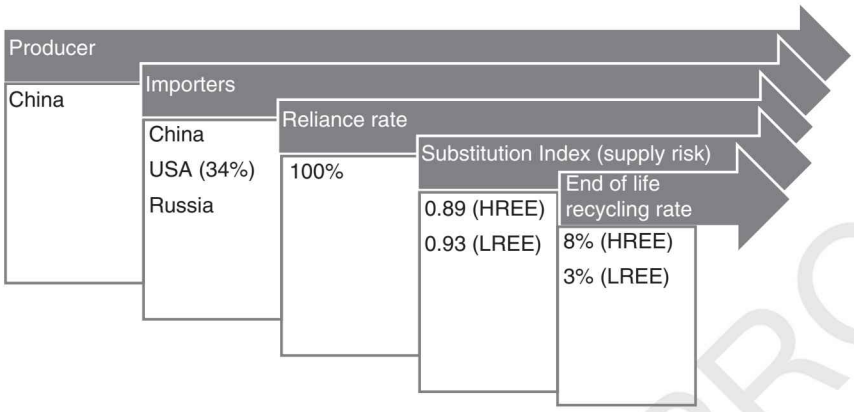

Figure 7.2 European overview of REEs. Source: Adapted from European Commission [16].

REE criticality is a dynamic and adaptable concept that depends on various parameters. Nd, Eu, Tb, Dy, and Y are/were considered critical in the US, Europe, and Japan [3]. Eu, Tb, and Y are used for phosphors in fluorescent lamps, and Nd and Dy are used in permanent magnets [3]. However, and due to market changes, REE criticality is changing [3]. Still, Nd and Dy are considered the elements with the highest criticality.

7.1.2 REE Mining and Secondary Sources

Sources of REEs are mainly divided into (i) primary mining from minerals such as bastnäsite, monazite, loparite, and the lateritic ion-adsorption clays [18] and (ii) secondary ores such as urban mines and industrial process residues.

In mining activities, it is not possible to extract a specific or wanted REE. The amount of REEs is not equally distributed in the respective ores, due to differences in their natural abundance [3]. REEs have specificities: (i) HREEs are less abundant than LREEs and (ii) elements with an even atomic number (Z) are more abundant than those with an odd atomic number, due to the Oddo-Harkins rule ([3] and references therein). Furthermore, bastnäsite and monazite are LREE-rich ores (Ce being dominant), whereas xenotime and ion-adsorption ores are HREE-rich ores (Y being dominant) [3].

The substitutes for REEs available for some applications may cause technical problems or loss of performance and/or have a high cost [19]. Thus, recovering REEs from secondary sources is necessary to avoid primary mining and promote a circular economy in the light of further reuse. Acid mine drainage, mine tailings, metallurgical slags, wastewater streams, and coal and by-coal products are examples of secondary sources for REE recovery [4, 20–37].

Power plant coal ash may be 8–10 times richer in REEs than feed coal [27, 36, 38, 39] and have a REE concentration analogous to or even greater than that in conventional ores [27, 40, 41]. High-demand REEs (Nd, Y, Dy, Er, Tb, and Eu) may make up 34–38% of total REEs compared to 15% in traditional ores [42]. If ashes are used

UNCORRECTED PROOFS

Trim Size: 170mm x 244mm Single Column Loose Ribeiro670117 c07.tex V1 - 12/09/2020 3:20pm Page 163

for secondary mining, in addition to the economic potential related to REE recovery and reuse, landfill deposition is also avoided. However, as coal ash may also be used for other purposes – e.g. in the cement industry, preparation of mesoporous materials or zeolites, asphalt filler, pavement base courses, soil stabilizers to prevent swelling by helping retain less water, geopolymers, silica aerogels, and carbon nanotubes [2] – they may be applicable for other purposes after REE extraction.

The possibility of using coal ash for REE recovery is also justified as coal still supplies 41% of global electricity needs, and China, US, Russia, and India are expected to be the major coal users in the future [41]. Today, India, China, and the US are the biggest coal fly ash producers (producing 112, 100, and 75 million tons per year), with a varying percentage of coal fly ash use: from 38% in India to 65% in the US [2]. Specifically, in the US, as 90% of coal is burned for power generation [43], and due to the existence of three geostrategic coal basins (Appalachian, Illinois, and Powder River), the country may find in coal ash an effective secondary source of REEs. In numbers, ~61 500 to 88 000 tons of REEs could be recovered from the 158 million tons of fly ash collected from four energy companies operating in the US [36].

The typical concentration range of REEs in coal ash is between ~200 and 1500 ppm [23, 32, 34, 44–47]. However, the concentration may vary between coal origin and power plant location [42, 48]. It is worth mentioning that, in general, the composition of fly ash, bottom ash, and slag is similar, indicating non-partitioning during coal combustion [41, 49]. However, it was also reported that fly ash might be enriched with HREEs [50]. In terms of mineralogical analysis, bottom ash shows a composition of ~60% of amorphous glass, whereas fly ash contains more than 70% of amorphous glass and less than 30% of mineral phases (mullite, quartz, and iron oxides) [50].

7.1.3 REE Extraction and Recovery from Secondary Resources

In brief, and as reviewed by [2], there is a broad range of available techniques and procedures to separate valuable elements from or by using coal fly ash: leaching (bioleaching, acid leaching, alkaline leaching, water leaching); digestion (acid digestion and alkaline digestion); electrolysis; ion exchange; sintering; calcination; chlorination; precipitation; sublimation; magnetic separation; flotation; and solvent extraction.

As typically happens with inorganic elements, REE recovery and selectivity may be limited by other metallic species when techniques such as sorption processes or solvent extraction are applied [51–53]. To solve this, selective extraction, separation, and purification processes are extremely beneficial. For example, knowledge of the behavior of REE precipitation and complex formation may avoid co-precipitation phenomena ([52] and references therein). Enrichment or increased efficiency of REE extraction can be achieved by physical separation processes such as particle size, magnetic, and density separations [34, 54, 55]; reprocessing methods; or sequential steps [45, 47, 48, 56, 57]. Membrane technologies such as electrodialysis, nanofiltration, and reverse osmosis may also be used ([53] and references therein). For example, nanofiltration may be applied to recover REEs from coal

UNCORRECTED PROOFS

Trim Size: 170mm x 244mm Single Column Loose Ribeiro670117 c07.tex V1 - 12/09/2020 3:20pm Page 164

fly ash leachate or acid mine drainage, separating REEs through the rejection of multi-charged ions such as transition metals and REEs, with mono-charged ions passing [58].

Focusing on one of the most common methodologies to extract metals, acid leaching, extraction efficiencies are dependent on the source and characteristics of the ashes [48]. Aluminosilicate glass, the predominant phase in fly ash, may hinder solubilization during acid leaching [48, 59]. As so, more complex leaching methods that first decompose the aluminosilicate glassy matrix of the ash, e.g. alkaline digestion, should be performed before acid leaching [48].

The electrodialytic (ED) process, detailed in other chapters of this book, is a technique with the capacity to remove metals from e.g. sewage sludge ashes in a two- or three-compartment cell [60–63]. This technique allows the separation of a broad range of contaminants by applying an electric field generated between electrodes and using ion-exchange membranes to separate the compartments.

7.2 Case Study

Coal ash from anthracite and bituminous origin were collected in the US. In both ashes, quartz, mullite, and hematite were present as well as an amorphous phase (Figure 7.3). A scanning electron microscopy (SEM) analysis (Figure 7.4) shows the morphology of anthracite coal and a particle, with the spectrum indicating three agglomerated REEs: Nd, Ce, and La.

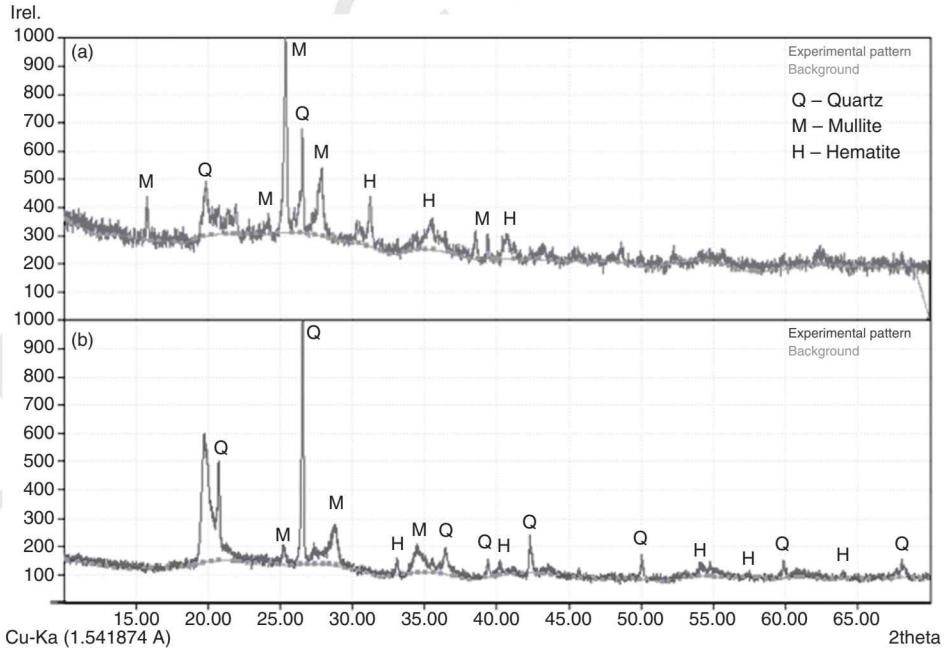

Figure 7.3 XRD analysis of bituminous ash (a) and anthracite ash (b).

UNCORRECTED PROOFS

Trim Size: 170mm x 244mm Single Column Loose Ribeiro670117 c07.tex V1 - 12/09/2020 3:20pm Page 165

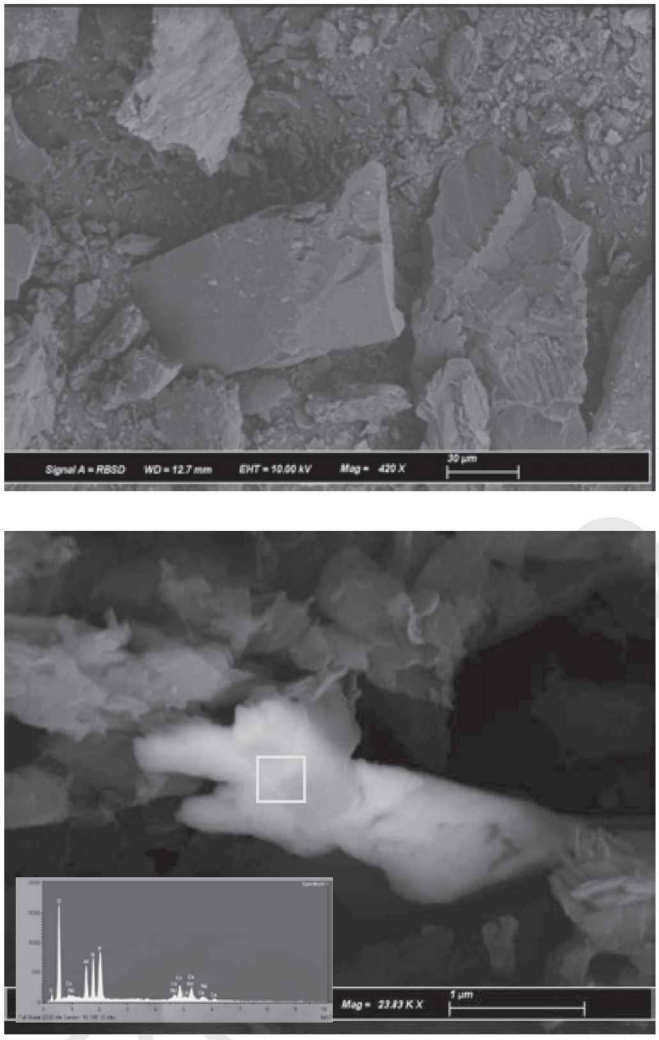

Figure 7.4 SEM micrographs of (a) anthracite coal; (b) particle detail.

A recent study [64] was performed aiming to understand the potential applicability of ED process to recover REE from these coal ashes. Bituminous and anthracite ash were compared in terms of total REE concentration, LREE and HREE fractions, and critical elements (focus on Dy, Tb, and Nd). Anthracite ash is about three times more enriched in total and critical elements than bituminous ash. To test the ED process, a two-compartment electrodialytic cell was used. The matrix was in the anode compartment to promote desorption from ash to the liquid phase due to acidic conditions, and the compartments were separated by a cation-exchange membrane. One of the study's primary conclusions is that the removal process is regulated by three main steps (Figure 7.5), which are related to the REE's position in the periodic table. HREE removal is primarily controlled by solubilization from the solid phase to the

UNCORRECTED PROOFS

Trim Size: 170mm x 244mm Single Column Loose Ribeiro670117 c07.tex V1 - 12/09/2020 3:20pm Page 166

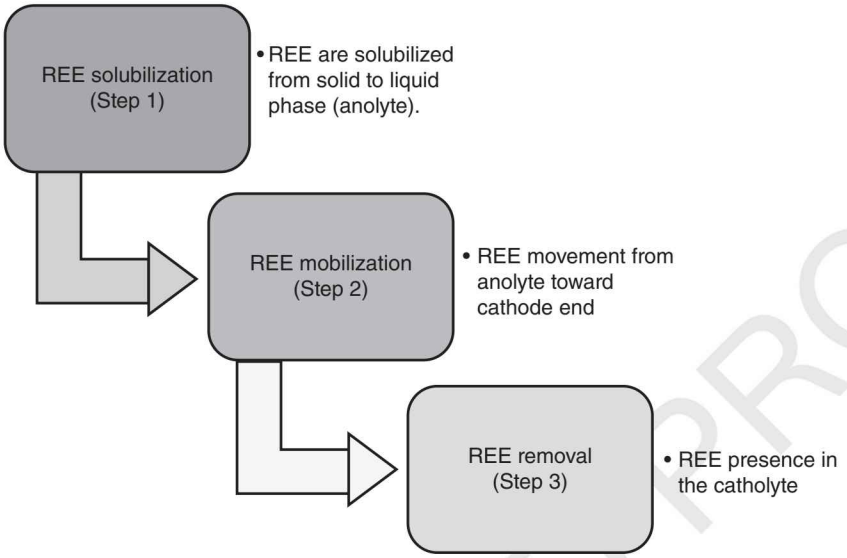

Figure 7.5 Schematic representation of the REE removal process in a two-compartment electrodialytic cell, separated by a cation-exchange membrane, with the matrix placed in the anode compartment. Source: Adapted from Couto et al. [64].

liquid phase (Step 1) and LREE by the movement from the anolyte toward the cathode end (Step 2) [64]. In the best tested conditions (three days of treatment; II 50 mA II pH adjustment in the catholyte [≈ 2]), more than 70% of REEs were extracted from anthracite ash, with a recovery of 62% and 74% (cathode end) for the critical elements Dy and Nd.

7.3 Conclusions

The importance of REEs in the world is undeniable: they are considered by some to be the *most critical* of the critical raw materials. The increasing variety of applications makes countries worldwide extremely dependent on REEs. In addition to the obvious REE criticality, geostrategic dependence is pushing many countries to develop efficient techniques to recover REEs from secondary sources. Efforts are being made to promote selective recovery with cost-effective, green, sustainable techniques.

The electrodialytic treatment of coal ashes, applied to anthracite ash due to its REE enrichment, is a potentially widely applicable technology that can effectively mobilize and recover critical REEs. It was proven that LREEs and HREEs do not behave the same way, opening perspectives for further optimization and selective recovery directed to specific socioeconomic parts of the world, depending on the most critical REEs.

UNCORRECTED PROOFS

Trim Size: 170mm x 244mm Single Column Loose Ribeiro670117 c07.tex V1 - 12/09/2020 3:20pm Page 167

Acknowledgments

Financial support was provided by the European Union's Horizon 2020 research and innovation program under the Marie Skłodowska-Curie grant agreement No. 778045. The authors acknowledge and appreciate the support given to CENSE by the Portuguese Foundation for Science and Technology (FCT) through the strategic project UIDB/04085/2020. FCT is also acknowledged for N. Couto's contract, established under the Individual Call to Scientific Employment Stimulus (CEECIND/04210/2017).

References

1 British Geological Survey. (2011). Rare earth elements profile.
2 Gollakota, A.R.K., Volli, V., and Sun, C.M. (2019). Progressive utilisation prospects of coal fly ash: A review. *Science of the Total Environment* 672: 951–989.
3 Binnemans, K., Jones, P.T., Müller, T., and Yurramendi, L. (2018). Rare earths and the balance problem: how to deal with changing markets? *Journal of Sustainable Metallurgy* 4 (1): 126–146.
4 Jowitt, S.M., Werner, T.T., Weng, Z., and Mudd, G.M. (2018). Recycling of the rare earth elements. *Current Opinion in Green and Sustainable Chemistry* 13: 1–7.
5 Strange, P., Svane, A., Temmerman, W.M. et al. (1999). Understanding the valency of rare earths from first-principles theory. *Nature* 399 (6738): 756–758.
6 Sonke, J.E. and Salters, V.J.M. (2006). Lanthanide–humic substances complexation. I. Experimental evidence for a lanthanide contraction effect. *Geochimica et Cosmochimica Acta* 70 (6): 1495–1506.
7 Cotton, S.A. (2005). Establishing coordination numbers for the lanthanides in simple complexes. *Comptes Rendus Chimie* 8 (2): 129–145.
8 Fernández, R.G. and Alonso, J.I.G. (2008). Separation of rare earth elements by anion-exchange chromatography using ethylenediaminetetraacetic acid as mobile phase. *Journal of Chromatography. A* 1180: 59–65.
9 US Geological Survey. (2019). Mineral commodity summaries. https://prd-wret.s3-us-west-2.amazonaws.com/assets/palladium/production/atoms/files/mcs-2019-raree.pdf.
10 Massari, S. and Ruberti, M. (2013). Rare earth elements as critical raw materials: focus on international markets and future strategies. *Resources Policy* 38 (1): 36–43.
11 UNEP. Resource efficiency: potential and economic implications. 2017.
12 EEA (2016). Circular economy in Europe. Developing the knowledge base. *European Environment Agency* (2): 37, 8–14. ISSN 1977-8449.
13 Ganguli, R. and Cook, D.R. (2018). Rare earths: a review of the landscape. *MRS Energy & Sustainability* 5 (i): 1–16.

UNCORRECTED PROOFS

Trim Size: 170mm x 244mm Single Column Loose Ribeiro670117 c07.tex V1 - 12/09/2020 3:20pm Page 168

14 US Geological Survey. (2018). Interior releases 2018's final list of 35 minerals deemed critical to U.S. national security and the economy. https://www.usgs.gov/news/interior-releases-2018-s-final-list-35-minerals-deemed-critical-us-national-security-and.

15 Williams, G. (2018). Trump admin targets Chinese rare earth imports. Investing News Network. https://investingnews.com/daily/resource-investing/critical-metals-investing/rare-earth-investing/trump-admin-targets-chinese-rare-earth-imports.

16 European Commission. (2017). Communication from the Commission to the European Parliament, the Council, the European Economic and Social Committee and the Committee of the Regions "on the 2017 list of Critical Raw Materials for the EU". COM(2017) 490.

17 European Commission. (2017). Study on the review of the list of critical raw materials: executive summary.

18 US Geological Survey. (2020). Rare earths statistics and information. National Minerals Information Center. https://www.usgs.gov/centers/nmic/rare-earths-statistics-and-information.

19 Garcia, M.V.R., Krzemien, A., Manzanedo del Campo, M.Á. et al. (2017). Rare earth elements mining investment: it is not all about China. *Resources Policy* 53: 66–76.

20 Seredin, V.V. (1996). Rare earth element-bearing coals from the Russian Far East deposits. *International Journal of Coal Geology* 30: 101–129.

21 Warwick, P.D., Crowley, S.S., and Ruppert, L.F. (1997). Petrography and geochemistry of selected lignite beds in the Gibbons Creek mine (manning formation, Jackson Group, Paleocene) of east-central. *Texas* 34: 307–326.

22 Hower, J.C., Ruppert, L.F., and Eble, C.F. (1999). Lanthanide, yttrium, and zirconium anomalies in the fire clay coal bed, Eastern Kentucky. *International Journal of Coal Geology* 39: 141–153.

23 Hower, J.C., Dai, S., Seredin, V.V. et al. (2013). A note on the occurrence of yttrium and rare earth elements in coal combustion products. *Coal Combustion and Gasification Products* 5: 39.

24 Honaker, R.Q., Hower, J.C., Eble, C.F., et al. (2014). Laboratory and bench-scale testing for rare earth elements. Final report, US Department of Energy, National Energy Technology Laboratory (NETL). Report ID 9bab59f6–4047-42cf-a851-cfee1791306e.

25 Schatzel, S.J. and Stewart, B.W. (2003). Rare earth element sources and modification in the lower Kittanning coal bed, Pennsylvania: implications for the origin of coal mineral matter and rare earth element exposure in underground mines. *International Journal of Coal Geology* 54 (3–4): 223–251.

26 Ketris, M.P. and Yudovich, Y.E. (2009). Estimations of Clarkes for carbonaceous biolithes: world averages for trace element contents in black shales and coals. *International Journal of Coal Geology* 78 (2): 135–148.

27 Seredin, V.V. and Dai, S. (2012). Coal deposits as potential alternative sources for lanthanides and yttrium. *International Journal of Coal Geology* 94 (0): 67.

UNCORRECTED PROOFS

Trim Size: 170mm x 244mm Single Column Loose Ribeiro670117 c07.tex V1 - 12/09/2020 3:20pm Page 169

28 Binnemans, K., Jones, P.T., Blanpain, B. et al. (2013). Recycling of rare earths: a critical review. *Journal of Cleaner Production* 51: 1–22.

29 Seredin, V.V., Dai, S., Sun, Y., and Yu, I. (2013). Coal deposits as promising sources of rare metals for alternative power and energy-efficient technologies. *Applied Geochemistry* 31: 1–11.

30 Dai, S., Yu, I., Seredin, V.V. et al. (2016). Metalliferous coal deposits in East Asia (Primorye of Russia and South China): A review of geodynamic controls and styles of mineralization. *Gondwana Research* 29 (1): 60–82.

31 Dai, S., Xie, P., Jia, S. et al. (2016). Enrichment of U-re-V-Cr-se and rare earth elements in the late Permian coals of the Moxinpo coal field, Chongqing, China: genetic implications from geochemical and mineralogical data. *Ore Geology Reviews* 80: 1–17.

32 Franus, W., Wiatros-motyka, M.M., and Wdowin, M. (2015). Coal fly ash as a resource for rare earth elements. *Environmental Science and Pollution Research* 22 (12): 9464–9474.

33 Rozelle, P.L., Khadilkar, A.B., Pulati, N. et al. (2016). A study on removal of rare earth elements from U.S. coal byproducts by ion exchange. *Metallurgical and Materials Transactions E* 3 (1): 6–17.

34 Lin, R., Howard, B.H., Roth, E.A. et al. (2017). Enrichment of rare earth elements from coal and coal by-products by physical separations. *Fuel* 200: 506–520.

35 Montross, S.N., Verba, C. A., and Collins, K.. (2017). Characterization of rare earth element minerals in coal utilization by products. US Department of Energy, National Energy Technology Laboratory. NETL-TRS-10-2017; NETL technical report series. DOI: 10.18141/1432615.

36 Huang, Z., Fan, M., and Tiand, H. (2018). Coal and coal byproducts: A large and developable unconventional resource for critical materials - rare earth elements. *Journal of Rare Earths* 36 (4): 337–338.

37 López, J., Reig, M., Torres, E. et al. (2018). Application of nanofiltration for acidic waters containing rare earth elements: influence of transition elements, acidity and membrane stability. *Desalination* 430: 33–44.

38 Smolka-danielowska, D. (2010). Rare earth elements in fly ashes created during the coal burning process in certain coal-fired power plants operating in Poland and upper Silesian industrial region. *Journal of Environmental Radioactivity* 101 (11): 965–968.

39 Stuckman, M.Y., Lopano, C.L., and Granite, E.J. (2018). Distribution and speciation of rare earth elements in coal combustion by-products via synchrotron microscopy and spectroscopy. *International Journal of Coal Geology* 195: 125–138.

40 Seredin, V. and Finkelman, R.B. (2008). Metalliferous coals: a review of the main genetic and geochemical types. *International Journal of Coal Geology* 76: 253–289.

41 Dai, S. and Finkelman, R.B. (2018). Coal as a promising source of critical elements: Progress and future prospects. *International Journal of Coal Geology* 186: 155–164.

UNCORRECTED PROOFS

Trim Size: 170mm x 244mm Single Column Loose Ribeiro670117 c07.tex V1 - 12/09/2020 3:20pm Page 170

42 Taggart, R.K., Hower, J.C., Dwyer, G.S., and Hsu-Kim, H. (2016). Trends in the rare earth element content of u.s.-based coal combustion fly ashes. *Environmental Science & Technology* 50 (11): 5919–5926.

43 U.S. Energy Information Administration. Quarterly Coal Report. 2019; (March).

44 Blissett, R.S., Smalley, N., and Rowson, N.A. (2014). An investigation into six coal fly ashes from the United Kingdom and Poland to evaluate rare earth element content. *Fuel* 119: 236–239.

45 Lanzerstorfer, C. (2018). Pre-processing of coal combustion fly ash by classification for enrichment of rare earth elements. *Energy Reports* 4: 660–663.

46 Das, S., Gaustad, G., Sekar, A., and Williams, E. (2018). Techno-economic analysis of supercritical extraction of rare earth elements from coal ash. *Journal of Cleaner Production* 189: 539–551.

47 Kumary, A., Parween, R., Chakravarty, S. et al. (2019). Novel approach to recover rare earth metals (REMs) from Indian coal bottom ash. *Hydrometallurgy* 187: 1–7.

48 King, J.F., Taggart, R.K., Smith, R.C. et al. (2018). Aqueous acid and alkaline extraction of rare earth elements from coal combustion ash. *International Journal of Coal Geology* 195: 75–83.

49 Dai, S., Seredin, V.V., Ward, C.R. et al. (2014). Composition and modes of occurrence of minerals and elements in coal combustion products derived from high-Ge coals. *International Journal of Coal Geology* 121: 79–97.

50 Wang, Z., Dai, S., Zou, J. et al. (2019). Rare earth elements and yttrium in coal ash from the Luzhou power plant in Sichuan, Southwest China: concentration, characterization and optimized extraction. *International Journal of Coal Geology* 203: 1–14.

51 de Vasconcellos, M.E., da Rocha, S.M.R., Pedreira, W.R., and Queiroz CA da S, Abrao A. (2008). Solubility behavior of rare earths with ammonium carbonate and ammonium carbonate plus ammonium hydroxide: precipitation of their peroxicarbonates. *Journal of Alloys and Compounds* 451: 426–428.

52 Kumari, A., Jha, S., Patel, J.N. et al. (2018). Processing of monazite leach liquor for the recovery of light rare earth metals (LREMs). *Minerals Engineering* 129: 9–14.

53 López, J., Reig, M., Gilbert, O., and Cortina, J.L. (2019). Integration of nanofiltration membranes in recovery options of rare earth elements from acidic mine waters. *Journal of Cleaner Production* 210: 1249–1260.

54 Yang, X., Werner, J., and Honaker, R.Q. (2019). Leaching of rare earth elements from an Illinois basin coal source. *Journal of Rare Earths* 37 (3): 312–321.

55 Rosita, W., Bendiyasa, I.M., Perdana, I., and Anggara, F. (2020). Sequential particle-size and magnetic separation for enrichment of rare-earth elements and yttrium in Indonesia coal fly ash. *Journal of Environmental Chemical Engineering* 8 (1): 103575.

56 Tang, M., Zhou, C., Pan, J. et al. (2019). Study on extraction of rare earth elements from coal fly ash through alkali fusion – acid leaching. *Minerals Engineering* 136: 36–42.

UNCORRECTED PROOFS

Trim Size: 170mm x 244mm Single Column Loose Ribeiro670117 c07.tex V1 - 12/09/2020 3:20pm Page 171

57 Zhang, W. and Honaker, R. (2019). Enhanced leachability of rare earth elements from calcined products of bituminous coals. *Minerals Engineering* 142: 105935.

58 Mutlu, B.K., Cantoni, B., Turolla, A. et al. (2018). Application of nanofiltration for rare earth elements recovery from coal fly ash leachate: performance and cost evaluation. *Chemical Engineering Journal* 349: 309–317.

59 Taggart, R.K., Hower, J.C., and Hsu-Kim, H. (2018). Effects of roasting additives and leaching parameters on the extraction of rare earth elements from coal fly ash. *International Journal of Coal Geology* 196: 106–114.

60 Kirkelund, G.M., Jensen, P.E., Ottosen, L.M., and Pedersen, K.B. (2019). Comparison of two- and three-compartment cells for electrodialytic removal of heavy metals from contaminated material suspensions. *Journal of Hazardous Materials* 367: 68–76.

61 Ottosen, L.M., Jensen, P.E., and Kirkelund, G.M. (2016). Phosphorous recovery from sewage sludge ash suspended in water in a two-compartment electrodialytic cell. *Waste Management* 51: 142–148.

62 Ebbers, B., Ottosen, L.M., and Jensen, P.E. (2015). Comparison of two different electrodialytic cells for separation of phosphorus and heavy metals from sewage sludge ash. *Chemosphere* 125: 122–129.

63 Guedes, P., Couto, N., Ottosen, L.M., and Ribeiro, A.B. (2014). Phosphorus recovery from sewage sludge ash through an electrodialytic process. *Waste Management* 34 (5): 886–892.

64 Couto, N., Ferreira, A.R., Lopes, V. et al. (2020). Electrodialytic recovery of rare earth elements from coal ashes. *Electrochimica Acta*; 359; DOI: https://doi.org/10.1016/j.electacta.2020.136934.

UNCORRECTED PROOFS

UNCORRECTED PROOFS

Trim Size: 170mm x 244mm Single Column Loose Ribeiro670117 c08.tex V1 - 12/11/2020 11:52pm Page 173

8

Hydrocarbon-Contaminated Soil in Cold Climate Conditions: Electrokinetic-Bioremediation Technology as a Remediation Strategy

Ana Rita Ferreira[1], Paula Guedes[1,2], Eduardo P. Mateus[1], Pernille Erland Jensen[3], Alexandra B. Ribeiro[1], and Nazaré Couto[1]

[1] *CENSE – Center for Environmental and Sustainability Research, Department of Environmental Sciences and Engineering, NOVA School of Science and Technology, NOVA University of Lisbon, 2829-516 Caparica, Portugal*
[2] *Instituto de Tecnologia Química e Biológica António Xavier, NOVA University of Lisbon, 2780-157 Oeiras, Portugal*
[3] *Department of Civil Engineering, Technical University of Denmark, 2800 Kongens Lyngby, Denmark*

8.1 Introduction

8.1.1 Hydrocarbon Contamination

Soil contamination refers to reduced soil quality and is considered a global issue. Health risks and environmental impacts associated with exposure to petroleum hydrocarbons have led to soil contamination being considered a major concern. There are more than 3 000 000 potentially contaminated sites worldwide, and they may represent a loss of economic opportunities and a threat to human health and the ecosystem [1]. If the current trend continues, the number of potentially contaminated sites is expected to increase by 50% by 2025 [2]. The leading causes of contamination vary widely across Europe but include past and present industrial and commercial activities and the disposal and treatment of waste.

In Europe, heavy metals and mineral oil are the most frequent soil contaminants (37.3 and 33.7%, respectively, at the investigated sites) [2]. Each year, thousands of oil spills occur on land and in water as the result of various types of incidents, including transportation and facility releases. The sources of petroleum hydrocarbons entering the environment are numerous as the number of individual hydrocarbon components is quite large [3]. Petroleum hydrocarbon contaminants can be characterized as the vast majority of organic compounds and byproducts classified as priority environmental pollutants, such as persistent organic pollutants (POPs) and polycyclic aromatic hydrocarbons (PAHs) due to their persistence and recalcitrant nature [3]. Long exposure to oil-containing waste may lead to the migration of hydrocarbons in the environment, resulting in secondary contamination sites [4, 5]. Moreover, petroleum hydrocarbons impose a significant ecological risk: they can inhibit plant

Electrokinetic Remediation for Environmental Security and Sustainability, First Edition.
Edited by Alexandra B. Ribeiro and M.N.V. Prasad.
© 2021 John Wiley & Sons Ltd. Published 2021 by John Wiley & Sons Ltd.

UNCORRECTED PROOFS

Trim Size: 170mm x 244mm Single Column Loose Ribeiro670117 c08.tex V1 - 12/11/2020 11:52pm Page 174

growth, damage soil structure and groundwater quality, and pose serious threats to human health [5].

Soil is a non-renewable resource and the basis for life and supporting livelihoods. The need to restore the natural quality of affected soil by the restitution of its functions and elimination or reduction of actual or potential risks to human health and the environment calls for the development of efficient remediation technologies. The physico-chemical properties of oil, such as its hydrophobic nature with low water solubility and a high octanol-water partition coefficient, make the development of a remediation strategy a challenge because oil adsorbs tightly to soil organic matter and thus is less susceptible to degradation [6]. Moreover, certain environments make the remediation challenge even more difficult.

8.1.2 Oil Spills in Arctic Environments

A broad range of new chemicals of emerging Arctic concern have been identified, and PAHs are included in the list [7]. Some researchers pointed out that residents in Arctic regions are exposed to high concentrations of POPs and heavy metals [8, 9]. Epidemiological studies established in the circumpolar area to investigate the link between exposure to contaminants and health outcomes showed links between exposure to contaminants and neurobehavioral, reproductive, cardiovascular, endocrine, and carcinogenic effects [10]. In addition, the bioaccumulation of hydrocarbons in the food chain of Arctic mammals was also reported [11], which represents a real threat as such hydrocarbons are mutagenic and carcinogenic [5].

Human activities in polar regions are oil-dependent, and in the future, the industry probably will expand, which increases the risk of adding more oil-contaminated sites. Hydrocarbon fuels are used extensively as the primary energy source for heating, transportation, power generation, and operating vehicles, aircraft, and ships. Generally, oil spills are related to accidental leaks during transport, management, or storage; and as a result of accidental spills and past disposal practices, petroleum contamination can be found in soils, especially around settlements [12]. Spills and releases include crude oil, oil byproducts (e.g. heating oil, refined fuels, and lubricants), and oil–chemical mixtures of various kinds [13].

The Arctic environment is very fragile to anthropogenic disturbances due to slow recovery times [14], and treating contamination is difficult due to suboptimal environmental conditions with a very short treatment season, remote sites, and limited local infrastructure [15].

Polar environments present significant challenges to oil spill mitigation. Extreme cold, snow and ice cover, frozen ground, variably wet and organic-rich soils, undulating surface cover (e.g. tundra, muskeg, and tussocks), and short summers hamper recovery and remediation of oil spilled in the Arctic.

Soil in the Arctic has specific characteristics that are different from other soil environments. Polar soils have unique periglacial features, including permafrost and numerous types of patterns, primarily due to freeze-thaw effects [16]. Permafrost environments are sensitive to heat and slow to recover from impacts. Thus, oil spills in permafrost environments are difficult to mitigate and clean up [13]. These soil

UNCORRECTED PROOFS

Trim Size: 170mm x 244mm Single Column Loose Ribeiro670117 c08.tex V1 - 12/11/2020 11:52pm Page 175

features might affect hydrocarbon remediation, as the activity of indigenous hydrocarbon-degrading microbes is limited, likely due to a combination of unfavorable conditions, cold and fluctuating temperatures, low nutrient levels, and low moisture [12, 15]. In addition to the growing interest and advances in environmental science in cold regions, much remains to be learned about spill response and remediation and how to manage spills in these cold, harsh environments [13].

8.1.3 Remediation of Petroleum-Contaminated Soil

Considerable efforts have been made to remediate petroleum-contaminated sites [17]. Remediation technologies for contaminated environments are site specific, and the variables are associated with the nature and composition of the contaminants together with the physical, chemical, and biological conditions of the environment [13].

Hydrocarbon soil remediation technologies can be mainly classified into two types: physical–chemical and biological [3, 18, 19]. The US EPA has documented inadequate performance of various remediation technologies, which may be attributed to (i) matrix characteristics (e.g. clayey soils are difficult to remediate because of their low permeability and organic content); (ii) heterogeneous conditions of the site (e.g. clayey within sand formation); (iii) physical and chemical characteristics of the contaminants; and (iv) co-existing inorganic and organic contamination. Very few technologies (e.g. washing/flushing soil and solidification/stabilization) have been successful in removing mixed contamination; most failed due to long treatment times and high cost [20, 21].

Some remediation actions involve the excavation and removal of the polluted soil, which causes site disturbance and adds to the cost of remediation treatment [17]. Research efforts have been focused on finding economic and suitable non-invasive methods for the remediation of oil-contaminated soil. Several in situ technologies have been investigated, such as bioremediation and phytoremediation, in which living bacteria, fungi, or green plants are used to clean up contaminated lands. Bioremediation, as a primary remediation technology to treat a wide range of hydrocarbons, has been a topic of considerable research interest over the last couple of decades, since it is effective and economical in removing oil with less undue environmental damage. Some studies have already proved that enrichment of oil-degrading microbial communities occurs soon after oil contamination, showing that cold-adapted indigenous microorganisms play an essential role in decontaminating cold climates [22, 23]. Nevertheless, successful bioremediation of petroleum hydrocarbons in soil has remained a challenge. It is a relatively slow process, and the degree of success depends on a number of factors such as soil type and structure, pH, association with co-pollutants, and temperature [24]. The temperature has been studied to accelerate the natural biodegradation rate during soil remediation [25]. Laboratory studies have demonstrated that mineralization can occur at low temperatures, but the rate of degradation is higher at elevated temperatures as they increase the degradation and volatilization rates of hydrocarbons. Given the low temperatures in subsurface soils and the short season during which soils are thawed

UNCORRECTED PROOFS

Trim Size: 170mm x 244mm Single Column Loose Ribeiro670117 c08.tex V1 - 12/11/2020 11:52pm Page 176

(one to two months) there is a need to control temperature, pH, nutrient levels, and moisture to optimize degradation rates [26, 27]. For example, the results from the study carried out by Fritt-Rasmussen [28] with soil from Greenland showed that oil degradation is greater at elevated temperatures and even more so when heat and nutrients are combined. Other studies have also shown the importance of coupling technologies to enhance hydrocarbon removal, such as biostimulation with active heating [25].

8.1.3.1 Electrokinetic Remediation (EKR)

Electrochemical remediation or electrokinetic remediation (EKR) is an emerging technology that consists of the controlled application of a low-intensity direct current through the soil between electrodes. A direct current is imposed on the contaminated soil to extract contaminants by the combined mechanisms of electroosmosis, electromigration, and/or electrophoresis. During electroremediation, electrolysis reactions at the inert electrodes produce protons at the anode and hydroxyl ions at the cathode. As a consequence, large pH gradients are caused by the transport of the generated protons and hydroxyl ions [29].

EKR is an effective and flexible technology that is versatile enough to be applied to different soil textures with moisture ranging from unsaturated to saturated [20, 30, 31]. However, the technology's effectiveness may be diminished by the sorption of contaminants on soil particle surfaces and various effects induced by the hydrogen ions and hydroxide ions generated at the electrodes.

Like all the remediation techniques, EKR also has drawbacks, including the limited desorption of some contaminants from the matrices, making it necessary to apply e.g. an enhancing solution. To improve EKR removal efficiency, many studies have been conducted using, for example, surfactants, enhancement solutions, pH control, desorbing agents, and pulse and alternating currents to facilitate the mobility of contaminants and test different variables [32].

EKR has been applied to a wide variety of pollutants including organic, inorganic, and mixed contaminants. EKR showed high efficiency in removing heavy metals (e.g. chromium, cadmium, copper, uranium, mercury, and zinc) [33], PAHs [34], polychlorinated biphenyls [35], atrazine [36], molinate, and bentazone from soil [37]. Regarding metals, the acid environment promotes metal extraction/dissolution, keeping metals in solution as cations that migrate toward the cathode end under the effect of the electric field. On the other hand, organic pollutants are transported by electromigration, electroosmosis, and electrophoresis if the organic molecules are ionizable during EKR [29]. The different nature of both types of contaminants (inorganic and organic) and their possible interactions make it challenging to optimize the operating conditions for their simultaneous extraction and transport out of the matrix [20, 31, 38].

EKR technology can be flexibly applied to soil remediation using in situ or ex situ treatment schemes. To overcome the isolated technology drawbacks and enhance removal, the application of EKR alone or combined with other techniques such as Fenton, surfactants, or biotechnologies has been demonstrated to be effective in reducing hydrocarbons in soil [39–42]. The combination of EKR with

UNCORRECTED PROOFS

Trim Size: 170mm x 244mm Single Column Loose Ribeiro670117 c08.tex V1 - 12/11/2020 11:52pm Page 177

bioremediation has been increasing over the years and demonstrates multiple advantages [42]. For example, using an alternating technology instead of simultaneous application has been shown to prevent competition between the isolated processes that would lower their efficiency in removing *n*-hexadecane from soil [43]. However, to the best of our knowledge, the effect of EKR coupled with bioremediation simulating in situ treatment aiming at removing hydrocarbons from polar soils was never studied. Hydrocarbon/oil remediation by EKR has been demonstrated, but studies have been focused primarily on ex situ bioremediation [25, 44–46]. Thus, treatment effectiveness in cold climate conditions and the development of strategies for in situ remediation in cold climates with limited environment disturbance is of great importance for the decontamination of oil spills.

8.2 Case Study

The present case study [47] examined the potential of EKR to stimulate biological degradation of oil pollution in soil in a simple setup with electrodes placed directly in the soil, applicable for in situ remediation strategies. Tests were done at two different temperatures resembling temperate and Arctic climates, and with three different current strategies: polarity-reversal at two different intervals and continuous application.

8.2.1 Description of the Site

The soil samples were collected in Sisimiut (66°56′ N, 53°40′ W), a town on the west coast of Greenland, approximately 75 km north of the Arctic Circle (Figure 8.1).



Figure 8.1 Map of Greenland, indicating the site where the soil was sampled.

UNCORRECTED PROOFS

Trim Size: 170mm x 244mm Single Column Loose Ribeiro670117 c08.tex V1 - 12/11/2020 11:52pm Page 178

This is the second-largest town in Greenland, with about 5230 inhabitants who use oil products for transport and heating buildings (www.qeqqata.gl).

The climate of polar regions is characterized by short, cold summers and extremely cold winters. Temperatures in Sisimiut range between −16 °C and 16 °C. The coldest months are January–March, with average maximum and minimum daily temperatures for the coldest day of −16 °C and −10 °C, respectively. The warmest months are July and August, with average daily low and high temperatures of 6 °C and 16 °C for the warmest day, respectively. The relative humidity ranges from 49% to 97% in a year, with the driest times in March and the most humidity around August (https://pt.weatherspark.com).

AQ2
AQ3
AQ4

8.2.2 Soil Sampling

The soil samples were taken at a Sisimiut dump site where barrels of waste oil are stored prior to incineration at the local waste incineration plant. Oil spills were visible (Figure 8.2). The soil was impacted as a result of leakage from an above-ground storage tank.

The soil under study was sampled from one of the identified spills in August 2017. During sampling, there was a strong odor of oil products, and free-phase oil was observed on the surface. The soil was dug up from a depth of 0 to 30 cm using a shovel and transported to Denmark in a polyethylene bucket. The EKR experiments took place at the Technical University of Denmark. In the laboratory, the soil was carefully homogenized by turning it continuously and removing larger particles such as stones, bricks, clinkers, and fibrous roots.

8.2.3 Electrokinetic Remediation (EKR) Experiments

Four strategies were tested at the laboratory scale: single bioremediation (Bio-control) performed as a control test; application of direct electric current to assess the influence of EKR as a combination of electrokinetic and biological (EKR-continuous); EKR with daily polarity reversal of the electric field (EKR-REP); and EKR with the current switched on/off every six hours (EKR-ON/OFF).

The influence of temperature was tested by comparing remediation at 6 °C and 22 °C (6 °C represented the summer temperature in the Arctic). The 6 °C



Figure 8.2 Soil sampling site.

UNCORRECTED PROOFS

Trim Size: 170mm x 244mm Single Column Loose Ribeiro670117 c08.tex V1 - 12/11/2020 11:52pm Page 179

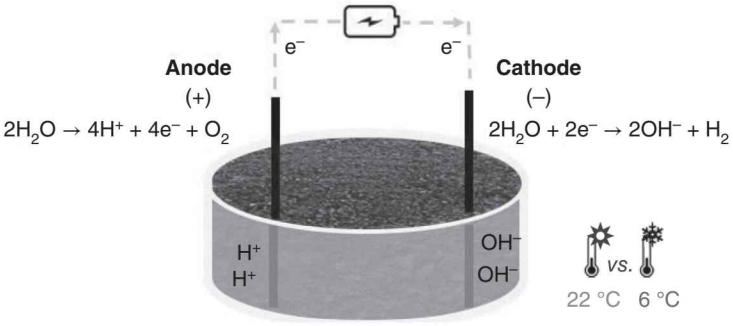

Figure 8.3 Experimental setup for EKR.

experiments were placed inside a refrigerator; 22 °C was the room temperature in the laboratory. The impact of the technology on soil properties was also assessed.

The experiments were carried out in a Plexiglas box (inner Ø = 8 cm; height = 4 cm) filled with 250 g of soil (Figure 8.3). The experiments lasted 14 days with an applied current intensity of 5 mA. The soil was initially weighed, and its moisture content was determined; to maintain an identical amount of water in the soil during EKR, the soil was weighed once a day in a digital balance, and deionized water was added if needed.

Mixed metal oxide (MMO) coated titanium electrodes 3 mm in diameter and 5 cm long (provided by FORCE® Technology, Denmark; Cathodic Protection) were used, and the power supply (Hewlett Packard E3612A) maintained constant direct current. The distance between the two electrodes in the EKR experiments was 4.5 cm.

8.2.4 Analytical Procedures

8.2.4.1 Soil Characterization

The studied soil was characterized in terms of oil content, phosphorus and metals, pH, conductivity, organic content, water content, and soil morphology. After EKR, the soil was divided in half – anode side and cathode side – and the same parameters were assessed.

- *General parameters*
  Dried soil (5.0 g) was agitated with KCl (1 M, 12.5 ml) for an hour, and pH was measured using a radiometric analytical electrode. For conductivity measurements, dried soil (10.0 g) was agitated with distilled water (25 ml) for an hour, and a radiometric analytical electrode was used. Organic matter was based on loss of ignition of dried soil (2.5 g) heated at 550 °C for an hour. Carbonate content was measured by treating dried soil (5.0 g) with HCl (3 M; 20 ml), and the developed CO_2 was measured volumetrically in a Scheibler apparatus calibrated with $CaCO_3$. Water content was calculated as weight loss at 105 °C for 24 hours.
  Laser and scanning electron microscopy with energy-dispersive X-ray spectroscopy (SEM-EDX) analysis was also carried out.

UNCORRECTED PROOFS

Trim Size: 170mm x 244mm Single Column Loose Ribeiro670117 c08.tex V1 - 12/11/2020 11:52pm Page 180

8.3 Determination of Metals and Phosphorus

The metals and major elements were measured after digestion: 20.0 ml (1:1) HNO_3 added in 1.0 g of dry soil were autoclaved (200 kPa, 120 °C for 30 minutes). Solid particles were subsequently removed by vacuum filtration through a 0.45 μm filter, and the liquid was diluted to 100 ml. The concentrations in the filtrate samples were analyzed with a Varian 720-ES inductively coupled plasma-optical emission spectrometer (ICP-OES). The digestion method is described in Danish Standard (DS) 259 [48].

- *TPH analysis*
  The soil samples were prepared with an internal standard consisting of three stock solutions with monobrobenzene, o-terphenyl, and squalan in pentane. The concentration was 10 000 mg l^{-1}. 1000 μl of each stock solution were added to a 100 ml volumetric flask filled with pentane. The concentrations of the internal standards were 100 mg l^{-1}.
  For oil extraction, 60 g of soil was shaken with 20 ml pentane in a 100 ml redcap glass; shaking stopped after a liquid suspension was reached (after about 30 s of handshaking). 20 ml of pentane with internal standard was added to the sample, and it was placed on a shaking table at 150 rpm for 24 hours. The organic phase was transferred into a vial from which further analyses were carried out. The oil content of the polluted soil was determined by gas chromatography using a flame ionization detector (GC-FID). Pentane controls and blinds were run randomly in the line sequence.
  The quantification of initial total petroleum hydrocarbons (TPH) in the range of C10–C40 was measured externally at a licensed laboratory following ISO/DIS 16703.

8.3.1 Results and Discussion

8.3.1.1 Soil Characteristics

The soil characteristics are summarized in Table 8.1. The soil has a sandy loam texture, which allows good drainage; a neutral pH (pH = 7.43); and both low buffer capacity (low content of carbonate, 1.9%) and organic matter (4.4%).

The phosphorus analysis did not show that the soil had a lack of nutrients. The concentration of metals found in the studied soil was below the limit values in soils in Denmark. Environmental quality criteria for oil compounds in soil specific to Greenland do not exist; instead, Danish environmental quality criteria values for health-related use of the soil were used as guidelines in this study. The soil sampled showed contamination of 69 500 ± 500 mg kg^{-1}, with 100 mg kg^{-1} being the quality criteria for soil in areas with very sensitive land use in Denmark [49].

In terms of the type of contamination, Figure 8.4 shows the chromatograms obtained for the soil extraction, from which it is possible to see that the soil contains low- to medium-molecular weight compound mixtures such as diesel fuel.

UNCORRECTED PROOFS

Trim Size: 170mm x 244mm Single Column Loose Ribeiro670117 c08.tex V1 - 12/11/2020 11:52pm Page 181

Table 8.1 Soil characteristics.

Characteristic	Value
pH	7.43 ± 0.02
Conductivity ($\mu S\ cm^{-1}$)	574 ± 75
Carbonate (%)	1.9
Organic matter (%)	4.4 ± 0
Water content (%)	10
Grain size	(%)
Clay	4.40
Silt	47.4
Sand	48.2
Metals and elements	($mg\ kg^{-1}$)
P	760 ± 24
Pb	37 ± 5
Al	5410 ± 502
Cr	22 ± 1
Cu	43 ± 11
Zn	85 ± 19
Fe	$12\,702 \pm 898$
Oil	($mg\ kg^{-1}$)
THC	$69\,500 \pm 500$

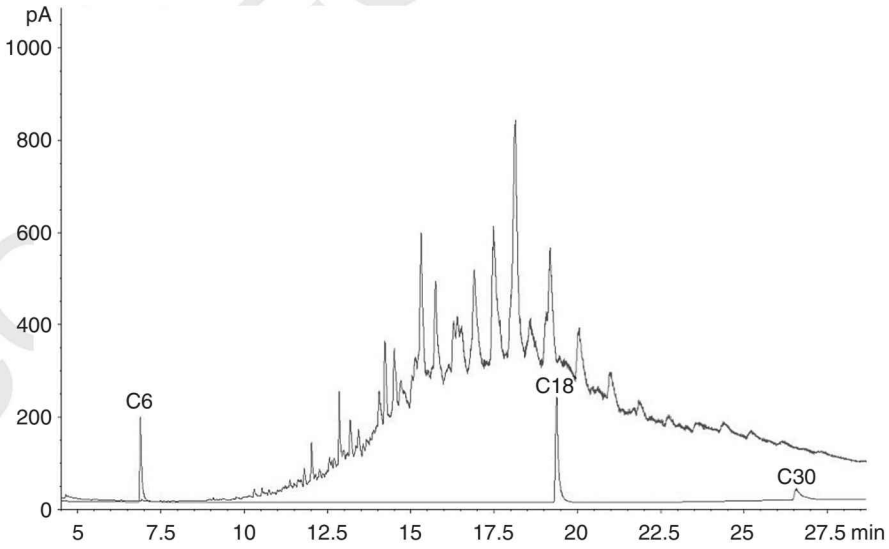

Figure 8.4 Chromatogram obtained from the initial soil extraction and internal standard (monobrobenzene, C6; o-terphenyl, C18, and squalan, C30).

UNCORRECTED PROOFS

Trim Size: 170mm x 244mm Single Column Loose Ribeiro670117 c08.tex V1 - 12/11/2020 11:52pm Page 182

8.3.1.2 EKR Experiments

- *General results*

To minimize environmental disturbances, it is important to monitor soil characteristics after EKR. The parameters analyzed after the experiments are shown in Table 8.2. After applying a continuous electric field (EKR-continuous), due to the electrolysis of water, the pH became more acidic and alkaline at the anode and cathode side, with values of 6.9 and 10.9 pH, respectively. When the electrode polarization was changed (EKR-REP), it prevented soil acidification and alkalization due to the shifting fronts counteracting each other. For the EKR experiments where the current was switched on/off every six hours, the soil pH changed only on the anode side, possibly due to an oxidation reaction that generated H^+ faster than OH^- and/or precipitation of hydroxides.

The initial voltage values were similar among the experiments and ranged from 17.2 to 23.2 V. Over time, voltage values fluctuated, and some high voltage levels were registered (up to 66.7 V), which can be explained by an increase in resistance in the soil matrix related to water evaporation. Even though the moisture content in the soil was controlled by adding deionized water, some water losses occurred during the day, which can explain the decrease in soil conductivity and consequent high voltages.

Soil conductivity increased when a continuous current was applied (except on the cathode side under the cold temperature). This might be associated with a significant increase in proton and hydroxyl ions concentrations as a consequence of the electrolysis of water. When reversed electrode polarization was applied, conductivity did not increase because the acid and basic fronts were partially balanced. Similar results were shown by other authors, e.g. Barba et al. [50].

Regarding organic content, no differences were found between controls (no applied electric current) and EKR experiments, suggesting that the current did not have any effect on organic matter degradation. The SEM analysis did not

Table 8.2 pH, conductivity, and organic content after EKR (bold values when pH > 8).

Temperature	Remediation strategy	Electrode charge	pH	Conductivity ($\mu S\ cm^{-1}$)	Organic content (%)
Room temperature	EKR-continuous	Anode	6.9	489	2.8
		Cathode	**10.9**	446	2.7
	EKR-REP	Anode	7.7	296	3.0
		Cathode	8.0	200	2.8
	EKR-ON/OFF	Anode	7.8	376	2.6
		Cathode	**10.8**	335	2.8
	Bio-control	*NA*	8.0	311	2.7
Cold	EKR-continuous	Anode	7.2	455	3.0
		Cathode	**10.8**	267	2.7
	Bio-control	*NA*	7.9	256	3.2

NA: not applicable

UNCORRECTED PROOFS

Trim Size: 170mm x 244mm Single Column Loose Ribeiro670117 c08.tex V1 - 12/11/2020 11:52pm Page 183

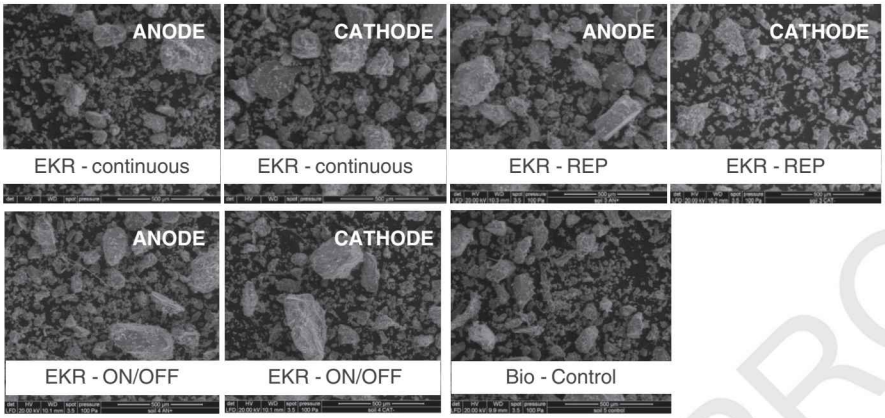

Figure 8.5 SEM analysis for the experimental soil after EKR on both the anode and cathode sides.

show any negative effect regarding physical characteristics when applying electric current (Figure 8.5).

- *Oil remediation*
  Overall reductions up to 78% were observed for TPH. Figure 8.6 shows the percentage of TPH left in the soil after experiments compared with the initial soil sample.

- *Bio-control* – without *electric current applied*
  Similar TPH removal (71 and 78%) was achieved at both temperatures, suggesting that the tested temperatures (6 °C and 22 °C) did not influence the remediation of oil degradation when current was not applied.
  Compared to the single bioremediation experiment (Bio-control) performed as a control with the initial TPH concentration, it is possible to attribute the loss of TPH to either bio or abiotic factors. Although the presence of indigenous cold-adapted microorganisms that persist in contaminated soils may have influenced oil degradation, hydrocarbon odors were noticed during the soil handling and experiments, suggesting that volatilization might also have played a significant role in TPH removal. Several studies reported that temperature directly affects the chemistry of oil as well as the physiology and diversity of microbial flora in the contaminated matrix [51]. However, the theory about the effect of temperature on microorganisms naturally present in soil is not linear. Some studies have demonstrated that hydrocarbon mineralization occurs in soils at low temperatures, but the rate and perhaps the extent of degradation are higher at elevated temperatures; thus, bioremediation levels are lower at cold temperatures [52, 53]. On the other hand, some studies showed that low temperatures did not influence the removal of hydrocarbons [54]. In the present study, even though no significant differences were found between controls at different temperatures, differences were found when electric current was applied.
- *EKR experiments*

UNCORRECTED PROOFS

Trim Size: 170mm x 244mm Single Column Loose Ribeiro670117 c08.tex V1 - 12/11/2020 11:52pm Page 184

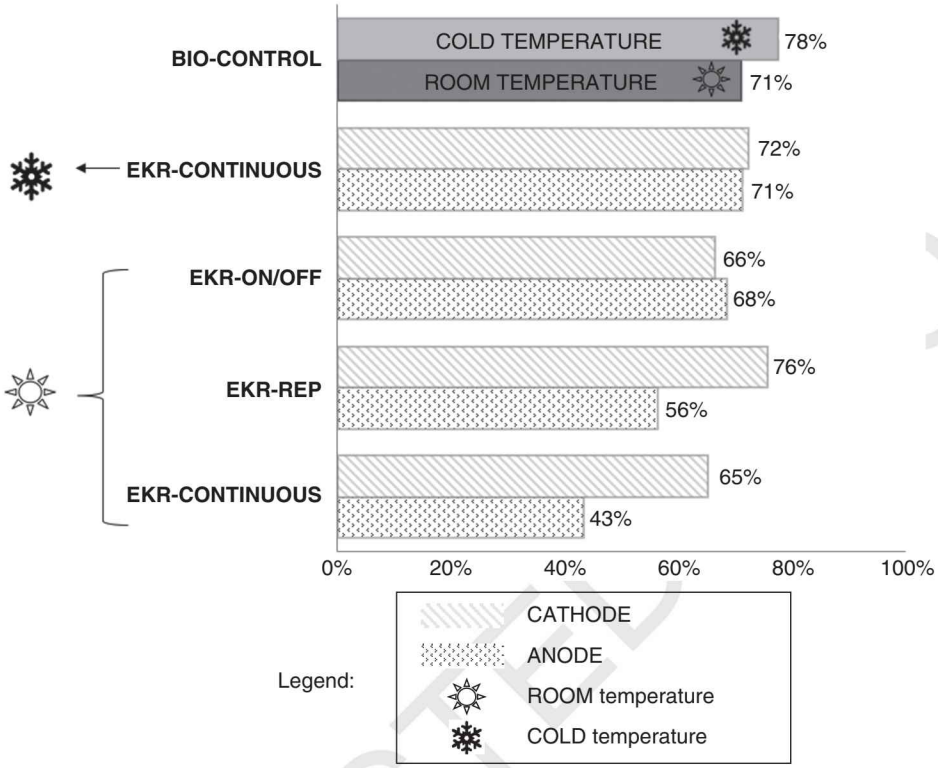

Figure 8.6 Removal of TPH from soil after 14 days of remediation.

Compared to the experiments where no electric current was applied, EKR did not improve oil remediation under the tested conditions (Figure 8.5). However, differences between EKR-continuous carried out at room and cold temperatures were detected, as well as when different electric current strategies were applied.

Among the EKR experiments, homogeneous TPH remediation was achieved when the EKR-ON/OFF current strategy was applied (68 and 66% at the anode and cathode, respectively). For EKR-continuous and EKR-REP, 20% of the difference was found between the anode and cathode sides in terms of TPH removal. The soil temperature was not measured during the experiments because low-intensity current (5 mA) was applied and no large changes in soil temperature were expected [55]. However, it is important to mention that the anode side in these experiments was clearly drier, and differences in the anode and cathode are probably attributed to electrical heating due to ohmic drops. The present results showed approximately 30% of the difference when comparing TPH removal at room and cold temperatures while applying a continuous current (43 vs. 71% at the anode at room and cold temperatures, respectively). Applying electrical current may produce excessive soil heating, which would lead to microbial inactivation [50, 56]. Temperature influences oxygen solubility, which decreases with increasing temperature and reduces the metabolic activity of aerobic microorganisms.

UNCORRECTED PROOFS

Trim Size: 170mm x 244mm Single Column Loose Ribeiro670117 c08.tex V1 - 12/11/2020 11:52pm Page 185

In EKR-REP, differences between the anode and cathode were also found, but heating phenomena are not expected to be the reason. The differences can be attributed to the electroosmotic flow, which decreased with the REP frequency, making the microbial distribution in soil not uniform [50]. Further studies should optimize the EKR-REP strategy, testing different periods of time. In the EKR-ON/OFF experiment, the effect of heating on the anode side was probably avoided by the current breaks. In addition, the off period has the advantage of less energy expenditure because the current is applied only half the time.

Keeping in mind the characteristics of the Arctic environment, the remediation technology developed must operate under challenging environmental conditions, be easy to operate, have low energy requirements, and have minimal impact on the environment. In addition, it is very important to keep the soil and experimental conditions such as pH and electrical conductivity within proper values for microbial life. When applying electric current, the conditions become more extreme around the electrodes as the experiment progresses, especially with respect to pH values. Negative impacts on microorganisms during EKR cannot be discarded and are most likely attributable to changes in pH rather than the influence of direct current. For example, the results in [57] showed the effect of soil pH on the degradation of PAHs, with a view to manipulating soil pH to enhance the bioremediation of PAHs. The author observed that soil at pH 7.5 was the most suitable for degrading PAHs, suggesting that changing pH using a liming process may be the most effective method to remediate soil contaminated with PAHs [57]. In this sense, the intensity and current strategy applied during soil remediation can be crucial for indigenous microorganisms. Thus, it is critical to control soil changes that may arise due to the application of electric current. One option to control soil pH is to use current strategies like EKR-REP and EKR-ON/OFF [58]. A study conducted by Ramírez et al. [56] showed that biological treatment was improved by the use of electrokinetic soil flushing, but only using the REP strategy. It is important to point out that the influence of applying an electric field on microbial communities is not completely explored yet, and the effect of the electric current is reported to have a limited effect [59] or even stimulate microbial activity [42, 50, 56, 60].

AQ5

REP contributed to decreasing the changes that the soil underwent as a consequence of the electrolysis of water because ~~they~~ ions are partially balanced in each polarity reversal. It is assumed that the EKR-REP strategy resulted in suitable conditions for biological processes, as it eliminates soil heating and extreme pH variation due to the acid and basic fronts. In addition, in theory, REP favors the homogenization of the system at a microscopic scale as it acts like a mixer that puts in contact pollutants, microorganisms, and nutrients [55, 56, 61]. Further optimization of EKR applied to oil-contaminated sites in cold regions is needed. Combined remediation between EKR-REP and EKR-ON/OFF could be a strategy to test together to optimize EKR: using less energy without changing soil characteristics or disturbing sites. Moreover, each remediation technology has advantages and limitations, and it is a challenge to find a universal method for oil-contaminated soil that can fulfill all the requirements [17]. Thus, further

UNCORRECTED PROOFS

Trim Size: 170mm x 244mm Single Column Loose Ribeiro670117 c08.tex V1 - 12/11/2020 11:52pm Page 186

research on combined technologies (EKR + bioremediation) should also be pursued to optimize the effect of the current application on soil microorganisms in cold climate conditions.

8.4 Conclusions

- The effect of electric current was not observed in the tested conditions, with the experiments showing similar removal for EKR and controls. Removal under cold temperatures was achieved with differences between the anode and cathode sides, probably due to heating phenomena in the anode.
- When applying REP, no changes in soil pH were verified. Switching the current on/off seems to be a feasible practice, as both sides (anode and cathode) showed similar oil remediation.
- Further studies are needed to find a strategy to make te EKR more efficient, and the combination of EKR-ON/OFF and EKR-REP can be a promising remediation strategy.

Acknowledgments

This work was financed by the Portuguese Polar Programme-PROPOLAR and supported by ARTEK, Department of Civil Engineering at the Technical University of Denmark. The authors would like to thank the Sisimiut municipality for help with sample collection and Kangerlussuaq for the accommodation at KISS. FCT is also acknowledged for P. Guedes' (SFRH/BPD/114660/2016) fellowship, and N. Couto's contract is established under the Individual Call to Scientific Employment Stimulus (CEECIND/04210/2017). The authors acknowledge and appreciate the support given to CENSE by the Portuguese Foundation for Science and Technology (FCT) through the strategic project UIDB/04085/2020.

References

1 Singh, B.K. and Naidu, R. (2012). Cleaning contaminated environment: a growing challenge. *Biodegradation* 23 (6): 785–786.
2 EEA, European Environment Agency. 2007. http://www.eea.europa.eu
3 Ossai, I.C., Ahmed, A., Hassan, A., and Hamid, F.S. (2020). Remediation of soil and water contaminated with petroleum hydrocarbon: a review. *Environmental Technology and Innovation* 17: 100526.
4 Truskewycz, A., Gundry, T.D., Khudur, L.S. et al. (201[illegible];). Petroleum hydrocarbon contamination in terrestrial ecosystems - fate and microbial responses. *Molecules* 24 (18): 3400.
5 Logeshwaran, P., Megharaj, M., Chadalavada, S. et al. (2018). Petroleum hydrocarbons (PH) in groundwater aquifers: an overview of environmental

UNCORRECTED PROOFS

Trim Size: 170mm x 244mm Single Column Loose Ribeiro670117 c08.tex V1 - 12/11/2020 11:52pm Page 187

fate, toxicity, microbial degradation and risk-based remediation approaches. *Environmental Technology and Innovation* 10: 175–193.

6 Trellu, C., Mousset, E., Pechaud, Y. et al. (2016). Removal of hydrophobic organic pollutants from soil washing/flushing solutions: a critical review. *Journal of Hazardous Materials* 306: 149–174.

7 Arctic Monitoring and Assessment Program (AMAP). (2017). AMAP assessment report: Arctic pollution issues.

8 Weihe, P., Bjerregaard, P., Bonefeld-Jørgensen, E. et al. (2016). Overview of ongoing cohort and dietary studies in the Arctic. *International Journal of Circumpolar Health* 75: 1–12.

9 Dallaire, F., Dewailly, É., Muckle, G., and Ayotte, P. (2003). Time trends of persistent organic pollutants and heavy metals in umbilical cord blood of inuit infants born in Nunavik (Québec, Canada) between 1994 and 2001. *Environmental Health Perspectives* 111 (13): 1660–1664.

10 Abass, K., Emelyanova, A., and Rautio, A. (2018). Temporal trends of contaminants in Arctic human populations. *Environmental Science and Pollution Research* 25 (29): 28834–28850.

11 Andersen, M.S., Fuglei, E., König, M. et al. (2015). Levels and temporal trends of persistent organic pollutants (POPs) in arctic foxes (Vulpes lagopus) from Svalbard in relation to dietary habits and food availability. *The Science of the Total Environment* 511: 112–122.

12 Mohn, W.W. and Stewart, G.R. (2000). Limiting factors for hydrocarbon biodegradation at low temperature in Arctic soils. *Soil Biology and Biochemistry* 32 (8–9): 1161–1172.

13 Filler, D.M., Kennicutt, M.C., Snape, I. et al. (2015). Arctic and Antarctic spills. Cold regions spills. Part XI. In: *Handbook of Oil Spill Science and Technology*, 1e (ed. M. Fingas), 495–512. Wiley.

14 Jorgenson, J.C., Hoef, J.M.V., and Jorgenson, M.T. (2010). Long-term recovery patterns of arctic tundra after winter seismic exploration. *Ecological Applications* 20 (1): 205–221.

15 Schiewer, S. and Niemeyer, T. (2006). Soil heating and optimized nutrient addition for accelerating bioremediation in cold climates. *Polar Record* 42 (1): 23–31.

16 Fitzpatrick, E.A. (1998). Arctic soils and permafrost. In: *Ecology of Arctic Environments* (eds. S.J. Woodin and M. Marquiss). Oxford: Blackwell Science.

17 Lim, M.W., Lau, E.V., and Poh, P.E. (2016). A comprehensive guide of remediation technologies for oil contaminated soil — present works and future directions. *Marine Pollution Bulletin* 109 (1): 14–45.

18 Alegbeleye, O.O., Opeolu, B.O., and Jackson, V.A. (2017). Polycyclic aromatic hydrocarbons: a critical review of environmental occurrence and bioremediation. *Environmental Management* 60 (4): 758–783.

19 Ranc, B., Faure, P., Croze, V., and Simonnot, M.O. (2016). Selection of oxidant doses for in situ chemical oxidation of soils contaminated by polycyclic aromatic hydrocarbons (PAHs): a review. *Journal of Hazardous Materials* 312: 280–297.

AQ6

UNCORRECTED PROOFS

Trim Size: 170mm x 244mm Single Column Loose Ribeiro670117 c08.tex V1 - 12/11/2020 11:52pm Page 188

20 Ricart, M.T., Pazos, M., Gouveia, S. et al. (2008). a. Removal of organic pollutants and heavy metals in soils by electrokinetic remediation. *Journal of Environmental Science and Health. Part A, Toxic/Hazardous Substances & Environmental Engineering* 43 (8): 871–875.

21 Reddy, K.R. (2013). Electrokinetic remediation of soils at complex contaminated sites: technology status, challenges, and opportunities. *Coupled Phenomena in Environmental Geotechnics*: 131–147.

22 Delille, D., Coulon, F., and Pelletier, E. (2004). Biostimulation of natural microbial assemblages in oil-amended vegetated and desert sub- Antarctic soils. *Microbial Ecology* 47 (4): 407–415.

23 Liu, H., Yao, J., Yuan, Z. et al. (2014). Isolation and characterization of crude-oil-degrading bacteria from oil-water mixture in Dagang oilfield, China. *International Biodeterioration and Biodegradation* 87: 52–59.

24 Bamforth, S.M. and Singleton, I. (2005). Bioremediation of polycyclic aromatic hydrocarbons: current knowledge and future directions. *Journal of Chemical Technology and Biotechnology* 80 (7): 723–736.

25 Couto, N., Fritt-Rasmussen, J., Jensen, P.E. et al. (2014). Suitability of oil bioremediation in an artic soil using surplus heating from an incineration facility. *Environmental Science and Pollution Research* 21 (9): 6221–6227.

26 Chang, W., Akbari, A., Snelgrove, J. et al. (2013). Biodegradation of petroleum hydrocarbons in contaminated clayey soils from a sub-arctic site: the role of aggregate size and microstructure. *Chemosphere* 91 (11): 1620–1626.

27 Naseri, M., Barabadi, A., and Barabady, J. (2014). Bioremediation treatment of hydrocarbon-contaminated Arctic soils: influencing parameters. *Environmental Science and Pollution Research* 21 (19): 11250–11265.

28 Fritt-Rasmussen, J. and Jensen, P.E. (2013). Remediation of oil-contaminated soil in Greenland. In: *ISCORD 2013*, 105–115. Anchorage, Alaska, United States: ASCE.

29 Acar, Y.B. and Alshawabkeh, A.N. (1993). Principles of electrokinetic remediation. *Environmental Science and Technology* 27: 2638–2647.

30 Cameselle, C. and Gouveia, S. (2013). *Advances in Electrokinetic Remediation for the Removal of Organic Contaminants in Soils*. IntechOpen.

31 Maturi, K., Reddy, K.R., and Cameselle, C. (2009). Surfactant-enhanced electrokinetic remediation of mixed contamination in low permeability soil. *Separation Science and Technology* 44: 2385–2409.

32 Moghadam, M.J., Moayedi, H., Sadeghi, M.M., and Hajiannia, A. (2016). A review of combinations of electrokinetic applications. *Environmental Geochemistry and Health* 38: 1217–1227.

33 Ottosen, L.M., Hansen, H.K., Laursen, S., and Villumsen, A. (1997). Electrodialytic remediation of soil polluted with copper from wood preservation industry. *Environmental Science and Technology* 31 (6): 1711–1715.

34 Lima, A.T., Ottosen, L.M., Heister, K., and Loch, J.P.G. (2012). Assessing PAH removal from clayey soil by means of electroosmosis and electrodialysis. *Science of the Total Environment* 435–436: 1–6.

UNCORRECTED PROOFS

Trim Size: 170mm x 244mm Single Column Loose Ribeiro670117 c08.tex V1 - 12/11/2020 11:52pm Page 189

35 Gomes, H.I., Dias-Ferreira, C., Ottosen, L.M., and Ribeiro, A.B. (2014). Electrodialytic remediation of polychlorinated biphenyls contaminated soil with iron nanoparticles and two different surfactants. *Journal of Colloid and Interface Science* 433: 189–195.

36 Ribeiro, A.B., Rodríguez-Maroto, J.M., Mateus, E.P., and Gomes, H. (2005). Removal of organic contaminants from soils by an electrokinetic process: the case of atrazine. Experimental and modeling. *Chemosphere* 59 (9): 1229–1239.

37 Ribeiro, A.B., Mateus, E.P., and Rodríguez-Maroto, J.M. (2011). Removal of organic contaminants from soils by an electrokinetic process: the case of molinate and bentazone. Experimental and modeling. *Separation and Purification Technology* 79 (2): 193–203.

38 Pedersen, K.B., Lejon, T., Jensen, P.E., and Ottosen, L.M. (2017). Simultaneous electrodialytic removal of PAH, PCB, TBT and heavy metals from sediments. *Journal of Environmental Management* 198: 192–202.

39 Pazos, M., Rosales, E., Alcántara, T. et al. (2010). Decontamination of soils containing PAHs by electroremediation: a review. *Journal of Hazardous Materials* 177 (1–3): 1–11.

40 Sandu, C., Popescu, M., Rosales, E. et al. (2016). Electrokinetic-Fenton technology for the remediation of hydrocarbons historically polluted sites. *Chemosphere* 156: 347–356.

41 Saichek, R.E. and Reddy, K.R. (2003). Effects of system variables on surfactant enhanced electrokinetic removal of polycyclic aromatic hydrocarbons from clayey soils. *Environmental Technology* 24 (4): 503–515.

42 Gill, R.T., Harbottle, M.J., Smith, J.W.N., and Thornton, S.F. (2014). Electrokinetic-enhanced bioremediation of organic contaminants: a review of processes and environmental applications. *Chemosphere* 107: 31–42.

43 Wang, S., Guo, S., Li, F. et al. (2016). Effect of alternating bioremediation and electrokinetics on the remediation of n-hexadecane-contaminated soil. *Scientific Reports* 6 (1): 1–13. p. 23833 https://www.nature.com/articles/srep23833.

44 Karppinen, E.M., Mamet, S.D., Stewart, K.J., and Siciliano, S.D. (2019). The charosphere promotes mineralization of 13 C-Phenanthrene by *Psychrotrophic* microorganisms in Greenland soils. *Journal of Environmental Quality* 48 (3): 559–567.

45 Cai, Z., Zhou, Q., Peng, S., and Li, K. (2010). Promoted biodegradation and microbiological effects of petroleum hydrocarbons by *Impatiens balsamina L.* with strong endurance. *Journal of Hazardous Materials* 183 (1–3): 731–737.

46 Pedersen, K.B., Lejon, T., Jensen, P.E., and Ottosen, L.M. (2016). Degradation of oil products in a soil from a Russian Barents hot-spot during electrodialytic remediation. *Springerplus* 5 (1): 168.

47 Ferreira, A.R. (2018). Electro-based technologies for contaminants removal from soil and effluent targeting further reuses. PhD thesis, NOVA School of Science and Technology, NOVA University Lisbon, Portugal.

48 Danish Standards Foundation. (2003). Determination of metals in water, sludge and sediments - General guidelines for determination by atomic absorption spectrophotometry in flame. DS259.

UNCORRECTED PROOFS

Trim Size: 170mm x 244mm Single Column Loose Ribeiro670117 c08.tex V1 - 12/11/2020 11:52pm Page 190

49 Miljøstyrelsen (Danish EPA). (2015). Liste over kvalitetskriterier i relation til forurenet jord og kvalitetskriterier for drikkevand.

50 Barba, S., Villaseñor, J., Rodrigo, M.A., and Cañizares, P. (2017). Effect of the polarity reversal frequency in the electrokinetic-biological remediation of oxyfluorfen polluted soil. *Chemosphere* 177: 120–127.

51 Skupińska, K., Misiewicz, I., and Kasprzycka-Guttman, T. (2004). Polycyclic aromatic hydrocarbons: physicochemical properties, environmental appearance and impact on living organisms. Vol. 61. *Acta Poloniae Pharmaceutica. Drug Research* 61: 233–240.

52 Paudyna, K., Rutter, A., Kerry Rowe, R., and Poland, J.S. (2008). Remediation of hydrocarbon contaminated soils in the Canadian Arctic by landfarming. *Cold Regions Science and Technology* 53: 102–114.

53 Aislabie, J., Saul, D.J., and Foght, J.M. (2006). Bioremediation of hydrocarbon-contaminated polar soils. *Extremophiles* 10 (3): 171–179.

54 Sanscartier, D., Laing, T., Reimer, K., and Zeeb, B. (2009). Bioremediation of weathered petroleum hydrocarbon soil contamination in the Canadian high Arctic: laboratory and field studies. *Chemosphere* 77 (8): 1121–1126.

55 Mena, E., Villaseñor, J., Rodrigo, M.A., and Cañizares, P. (2016). Electrokinetic remediation of soil polluted with insoluble organics using biological permeable reactive barriers: effect of periodic polarity reversal and voltage gradient. *Chemical Engineering Journal* 299: 30–36.

56 Ramírez, E.M., Camacho, J.V., Rodrigo, M.A., and Cañizares, P. (2015). Combination of bioremediation and electrokinetics for the in-situ treatment of diesel polluted soil: a comparison of strategies. *The Science of the Total Environment* 533: 307–316.

57 Pawar, R.M. (2015). The effect of soil ph on bioremediation of polycyclic aromatic hydrocarbons (PAHS). *Journal of Bioremediation and Biodegradation* 6: 291.

58 Harbottle, M.J., Lear, G., Sills, G.C., and Thompson, I.P. (2009). Enhanced biodegradation of pentachlorophenol in unsaturated soil using reversed field electrokinetics. *Journal of Environmental Management* 90 (5): 1893–1900.

59 Mena, E., Villaseñor, J., Cañizares, P., and Rodrigo, M.A. (2016). Influence of electric field on the remediation of polluted soil using a biobarrier assisted electro-bioremediation process. *Electrochimica Acta* 190: 294–304.

60 Shi, L., Müller, S., Loffhagen, N. et al. (2008). Activity and viability of polycyclic aromatic hydrocarbon-degrading Sphingomonas sp. LB126 in a DC-electrical field typical for electrobioremediation measures. *Microbial Biotechnology* 1 (1): 53–61.

61 Huang, D., Xu, Q., Cheng, J. et al. (2012). Electrokinetic remediation and its combined technologies for removal of organic pollutants from contaminated soils. *International Journal of Electrochemical Science* 7 (5): 4528–4544.

UNCORRECTED PROOFS

Trim Size: 170mm x 244mm Single Column Loose Ribeiro670117 c09.tex V1 - 12/11/2020 11:53pm Page 191

9

Electrochemical Migration of Oil and Oil Products in Soil

V.A. Korolev and D.S. Nesterov

Department of Engineering and Ecological Geology, Faculty of Geology, M.V. Lomonosov Moscow State University, Moscow, Russia, 119991

9.1 Introduction

The recultivation of oil-polluted areas is a well-known critical problem occurring all over the world [1]. Soil pollution by oil and its products takes place in different ways. According to statistical data, about 800 petroleum pipeline disruptions occur in Russia annually. Each such accident can be considered an ecologic catastrophe and results in the total demise of nearby ecosystems.

A considerable number of accidents having taken place during oil production and transportation in recent years. Some accidents, like the one at the oil-production platform in the Gulf of Mexico in 2010, had remarkable ecological and economic effects [2]. However, local oil-polluted areas pose an equal threat to ecosystems and human health [1].

Accordingly, various soil remediation methods have been proposed [3]. In particular, electrokinetic methods are considered one of the most promising ways to treat soil and remove oil within the soil mass (in situ). These methods are cheaper than microbiological approaches and can remediate the area more quickly. In many cases, soil pretreatment and nutrients for microorganisms are vital for successful bioremediation of oil-polluted soil [4]. That places some economic limitations on the ubiquitous use of microbiological treatment to remediate oil-contaminated areas. Also, electrokinetic methods are applicable during the winter when the majority of microbial technologies are unsuitable or require additional heat sources [5, 6].

The authors have performed extensive research on factors influencing the effectiveness of electrokinetic migration of oil and its products in various soils during the last two decades [7–12]. Clayey soils of varying dispersiveness and chemical and mineral composition were studied. In addition, a comprehensive study of the electrochemical migration behavior of oil in fertile soils was executed since typically these soils are the first to be subjected to oil pollution (for instance, during oil spills,

Electrokinetic Remediation for Environmental Security and Sustainability, First Edition.
Edited by Alexandra B. Ribeiro and M.N.V. Prasad.
© 2021 John Wiley & Sons Ltd. Published 2021 by John Wiley & Sons Ltd.

UNCORRECTED PROOFS

Trim Size: 170mm x 244mm Single Column Loose Ribeiro670117 c09.tex V1 - 12/11/2020 11:53pm Page 192

accidents during transportation, etc.). Herein, soil samples with undisturbed natural structures taken from various genetic horizons were studied so that the lab research results would be the most applicable for real field implementations.

9.2 Specific Nature of Soils Polluted by Oil and Its Products

Soil pollution by oil takes place not only due to pipe disruptions and oil spills but also in areas where oil is stored and refined. Different zones of oil pollution, represented by various oil fractions, form in a soil mass during the pollution process. The parameters of these zones need to be taken into account during electrokinetic treatment. The mobility of different oil fractions in such a soil mass varies considerably.

Oil and its products penetrate pores within oil-polluted soil. They fill the pores entirely or partially, adsorb onto soil particle surfaces, and cover the particles, forming continuous oil films that alter the soil structure.

The authors also conducted a study of the microstructure of sediments formed in emulsions prepared using water and oil or its products such as engine oil and kerosene. The soil or sediment microstructure transformed drastically due to the adsorption of oil and its products onto soil particle surfaces. As a result, soils became hydrophobous, and removing such oil films from the soil pore space is difficult.

In addition, it is essential to consider the sequence (or order) of oil intrusion into the soil. Oil penetrates dry soil rather quickly, making it hydrophobous. In contrast, oil effluence into moist soil is complicated since water films covering the soil particles prevent direct oil adsorption onto them.

The authors studied a wide range of factors influencing electrochemical oil migration in soils, including chemical and mineral composition of soils; their genesis, dispersiveness, and physical and physico-chemical properties; initial water/oil ratio in the soil; oil aging; and the composition and initial properties of oils from different oil fields.

Oil migration under DC electric field was proved to occur in all studied oil-water-saturated soils ranging from heavy clays to silty sands, including fertile soil horizons [12]. In addition, the oil redistribution effectiveness varied from 25 to 75% or more, depending on various internal and external factors.

Oil moves in the form of small droplets under the DC field alongside electroosmotic filtrate from the anode to the cathode being carried by electroosmosis flux due to viscous friction forces [12–14]. Also, some dissolved oil moves in the same direction as the electroosmotic flow due to its partial dissolution at the increased pH formed near the cathode [15]. In general, two mechanisms control the effectiveness of removing uncharged organics (including oil) from soils by electrokinetics: their desorption rate from the soil particles and the intensity of electroosmotic flow [16, 17]. Accordingly, many papers in the field of electrokinetic oil recovery from soils consider the use of oil-desorbing agents alongside the application of a DC field. Such chemicals are usually represented by various surfactants like sodium dodecyl sulfate [18] or Igepal CA-720 [16]. However, several studies found that a sufficient

UNCORRECTED PROOFS

Trim Size: 170mm x 244mm Single Column Loose Ribeiro670117 c09.tex V1 - 12/11/2020 11:53pm Page 193

amount of light oil fractions can be removed from soil solely by electrokinetics [18]. So, the authors of this work focused only on the study of soil and oil parameters that influence electrokinetic oil migration in soils. In other words, no desorbing additives were used in the present study.

The careful consideration of the influence of the factors mentioned on electrokinetic oil migration is given next.

9.3 Influence of Mineral Composition

The influence of mineral composition on electrokinetic oil migration was studied using a series of various clay soils. The samples included mono- and polymineralic soils. Kaolinite, illite, and montmorillonite clays were the first. The polymineralic soils under study were fertile soil horizons composed of various minerals.

The test carried out on *clay soils* of various mineral compositions demonstrated the extensive influence of that factor on oil migration rate under the voltage gradient. It affects oil migration efficiency by influencing the parameters of the soil's electrical double layer (EDL). The greater physico-chemical activity of clay soil leads to more extensive EDL development in the given conditions (moisture content, ionic strength, pH, and E_h). Accordingly, it results in more intensive electroosmotic transport and, consequently, more effective oil migration in clay soil.

The influence of *fertile soil horizon* mineral composition on the effectiveness of electrochemical oil migration in soil pores is shown in Figure 9.1. The percent of clay minerals in the studied samples increases as follows: Luvisol (gray forest soil in the Russian soil taxonomy) < Phaeozem (dark-gray forest soil) < meadowy

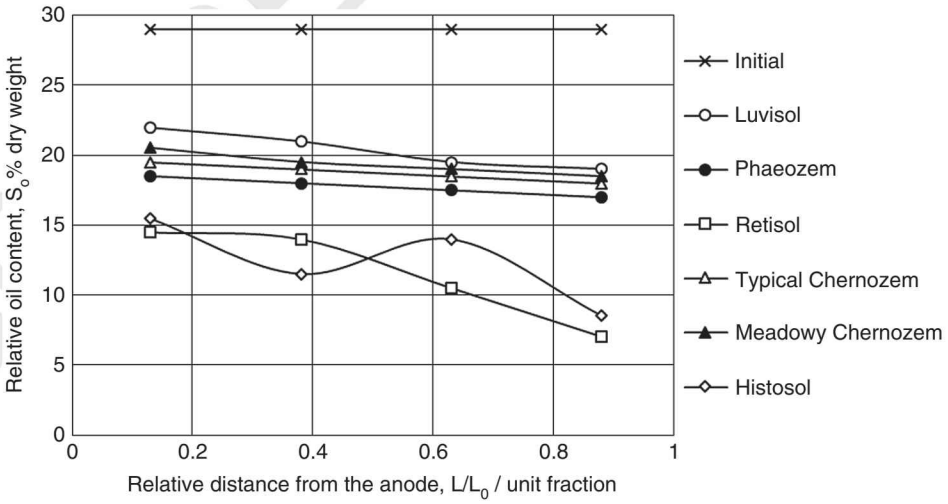

Figure 9.1 Oil redistribution along the length of the studied oil/water-saturated soils under electrokinetic treatment.

UNCORRECTED PROOFS

Trim Size: 170mm x 244mm Single Column Loose Ribeiro670117 c09.tex V1 - 12/11/2020 11:53pm Page 194

Chernozem < typical Chernozem < Retisol (soddy podzolic soil) < Histosol (peat soil) [19–21]. During the experiments, the relation of electrochemical oil distribution and clay mineral percent was obtained.

Electrokinetic removal of hydrocarbons increased with an increase in clay mineral percent in the studied soil horizons. It should be noted that the clay mineral fraction of Retisol was 11.5% of the bulk composition, and that of Luvisol was 3.4%.

The electroosmosis coefficient is generally defined by the thickness of the diffuse part of the EDL and, consequently, soil particle electrokinetic (ζ) potential [22]. Thus, the intensity of electrokinetic oil migration in soils should increase with an increase in their clay mineral content. A greater clay fraction percent results in the widening of the soil's EDL diffuse part (ζ-potential absolute value increases), other things being equal, and, consequently, an increased electroosmotic transport velocity P_{EO}.

It should be noted that comparable results were obtained by Shrestha et al. [23]. The authors of this study found that the most efficient oil recovery occurred in surrogate samples with a clay content of 10–20%. A decrease or increase in relative clay content percent resulted in a decreased oil recovery rate. This decline in oil removal efficiency occurred due to the EDL contraction and decrease in relative flow generated by increased current-carrier content in the soil pores, respectively.

In our study, soil characterization demonstrated that all the studied soil horizon samples were salinized to some extent. This being said, the amount of water-soluble salts increases as follows: Retisol < Histosol < typical Chernozem < meadowy Chernozem < Phaeozem < Luvisol.

The amount of hydrocarbons electrokinetically removed from soil increased with a decline in water-soluble salts content. Accordingly, the high effectiveness of oil removal from Retisol and Histosol was facilitated by the fact that these soils possess relatively low salt content compared to the other studied soil horizons. The electroosmosis intensity is known to decline as soil salinity increases, which can be explained by the decrease in the ζ-potential magnitude and thickness of the EDL diffuse part.

The study conducted allowed us to find a relation of oil removal rate based on the high-dispersed X-ray amorphous phase in soils. Soil samples with various X-ray amorphous phase content were used for experiments with oil/water-saturated soils. An increase in oil removal rate was detected as the X-ray amorphous phase percent grew.

Thus, the mineral composition of soils and their X-ray amorphous phase content and salinity determine the EDL composition and, consequently, electrochemical oil migration intensity. In turn, oil migration intensified as the clay mineral content increased and total soil salinity decreased: Histosol > Retisol > typical Chernozem > meadowy Chernozem > Phaeozem > Luvisol. The study of electrochemical oil migration was conducted on soil samples with various total organic carbon (TOC) content. However, the experiments did not show any clear relation between the final distribution of liquid hydrocarbons and TOC.

In general, the influence of chemical and mineral composition of clay soils, including fertile soil types, on their electrokinetic oil recovery rate operates through their

UNCORRECTED PROOFS

Trim Size: 170mm x 244mm Single Column Loose Ribeiro670117 c09.tex V1 - 12/11/2020 11:53pm Page 195

EDL parameters. The higher the physico-chemical activity of a clay mineral, the more effective the oil recovery rate of that soil should be.

9.4 Influence of Soil Dispersiveness

The influence of clay soil dispersiveness on its oil recovery efficiency was studied using a series of clay soils of various granulometric composition. The soils used varied from heavy clays to sandy loams (in the Russian classification), which corresponds to the range from clays to sandy silts in the International Organization for Standardization (ISO) regulation [24, 25]. Also, a selection of artificial sand-clay mixtures of different granulometric composition was prepared for this study.

The Russian soil particle-size classification system is similar to that created by Katschinski, except for the silt-clay boundary: it is shifted from 1 to 2 μm [26, 27]. Hereinafter, particles larger than 10 μm are referred to as *physical sand*, and particles smaller than 10 μm are referred to as *physical clay* [26].

The experiments demonstrated that an increase in soil dispersiveness intensified electrokinetic oil migration, while its decrease caused the opposite. Oil migration did not occur in pure sands, which can be explained by the insignificant EDL development and lack of clay fraction in such soils. Thus, granulometric composition influences the intensity of electrochemical migration in oil/water-saturated and water-saturated (without oil) soil the same way.

The influence of soil dispersiveness on the electrochemical treatment effectiveness of oil-contaminated soil was studied using model samples prepared by mixing pure quartz sand and mantle till loam. The study of this factor influence was carried out using 11 soil samples: 9 samples were sand-loam mixtures of various mass ratios, and the other 2 were pure sand and pure loam, respectively. The initial sample moisture content was adjusted to its liquid limit (LL); the sand's was 12.5%, which is slightly more than its maximum molecular moisture capacity (W_{mmc}). Generally, the soil liquid limit increased nonlinearly as the clay fraction content of the sample grew; and, accordingly, its physical sand rate decreased.

The voltage gradient increased from 3.4 to 20 Vcm^{-1} during the electrokinetic treatment to maintain the electric current at a constant level of 8 mA. The corresponding behavior of the voltage gradient alteration was diverse for the samples used (Figure 9.2). The initial voltage gradient (at the beginning of the experiment) increased from 3.4 to 11.4 Vcm^{-1} as the sand content of the model samples increased (from 0 to 90% sand) and was 20 Vcm^{-1} for pure quartz sand. This fact can be explained by the samples' variation in electrical resistivity, which increased with the sand content.

The voltage gradient of the oil/water-saturated sand was kept constant at a rate of 20 V cm^{-1} during its electrokinetic treatment. As the experiment proceeded, sand's electrical current decreased from 4.8 mA (at the start of the test) to 1.2 mA (when the setup was turned off). The model mixture samples' electrical current changed from 8 mA (at the beginning of the treatment) to 1–2 mA for all artificial sand-loam soils.

UNCORRECTED PROOFS

Trim Size: 170mm x 244mm Single Column Loose Ribeiro670117 c09.tex V1 - 12/11/2020 11:53pm Page 196

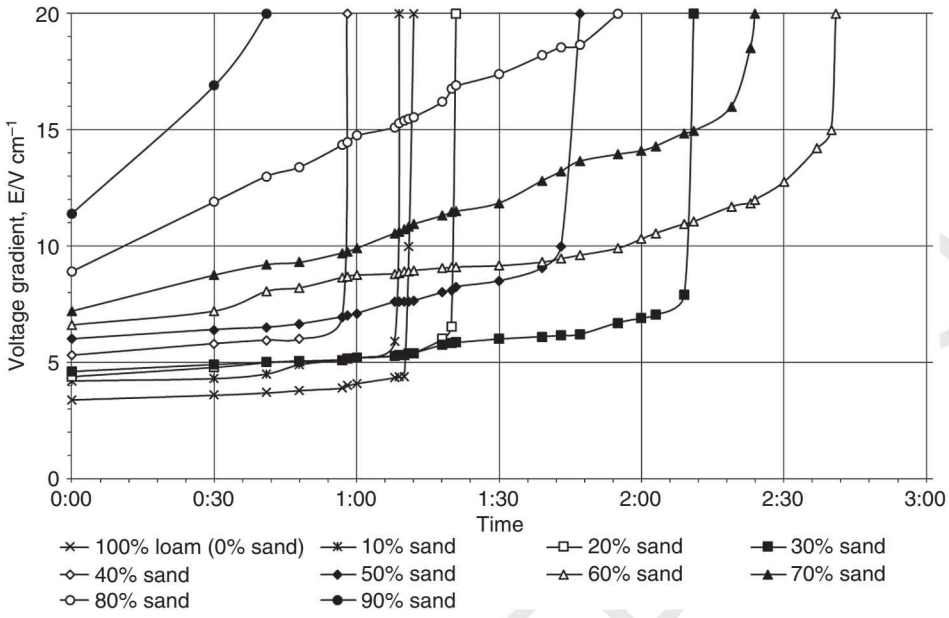

Figure 9.2 Electric field intensity (E, V cm^{-1}) variation with time (hours) during electrokinetic remediation of oil from model soil mixture samples.

Electroosmosis during the electrochemical treatment caused the dewatering of the soil samples (Figure 9.3). The total moisture loss differed among the samples studied, from 10.3% (for 100% loam) to 60% (soil samples with 80–90% sand content). So, generally, the soil drainage rate increased as the sand percent grew and initial moisture content decreased. The pure sand sample lost 37% of its total moisture content. The remaining soil moisture redistributed along the sample axis with its increase toward the cathode. However, the behavior of this redistribution was specific to each soil specimen and altered drastically with an increase in the sample's sand fraction. The least intense moisture redistribution occurred in the pure loam sample.

The more drained anodic zone of a sample stood out as its sand content increased. This zone gradually became more and more drained and protruded toward the cathode over time. Concurrently, continuous drainage of the near-cathode sector (L/L_0 = 0.5–0.75) of a soil sample occurred. The moisture content increased almost linearly from the anode to the cathode at sand content of 80–90%. In the case of the pure sand sample, significant drainage took place up to and including its near-cathode zone. The final moisture content exceeded the initial amount in the cathodic zone (L/L_0 = 0.75–1) for that sample due to water saturation caused by electroosmotic flow.

As a result of the electrokinetic treatment, the oil content decreased in all the studied samples (Figure 9.4). The efficiency of this process varied from 10 to 25% (at the initial oil saturation level of 90 to 170 g of oil per 1 kg of soil). The maximum treatment efficiency was achieved for the soil samples with 30–40% sand content (with a

UNCORRECTED PROOFS

Trim Size: 170mm x 244mm Single Column Loose Ribeiro670117 c09.tex V1 - 12/11/2020 11:53pm Page 197

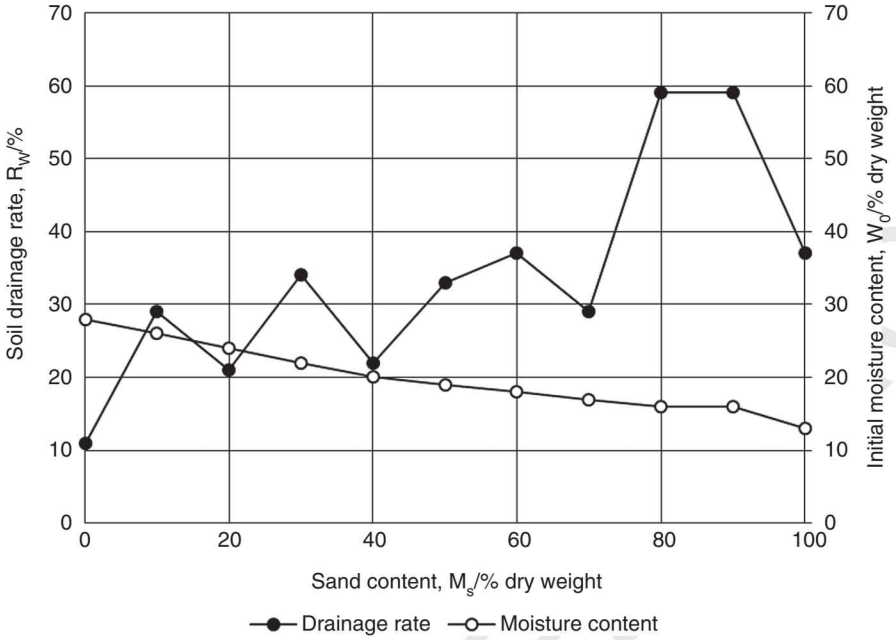

Figure 9.3 Drainage rate (moisture content loss in %) of the model mixture samples with different sand content, as a result of electrokinetic treatment.

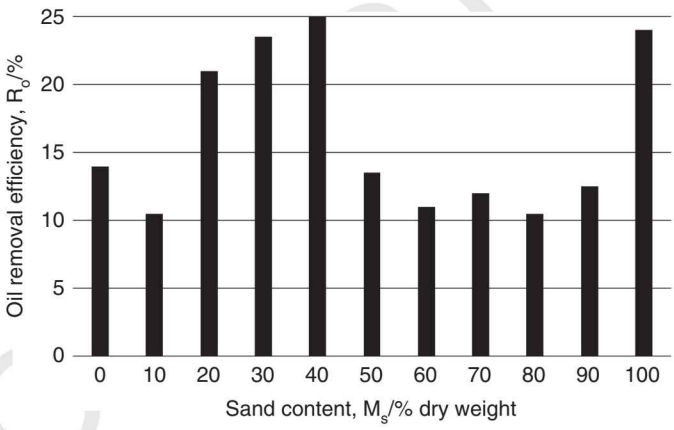

Figure 9.4 Influence of soil dispersiveness on the effectiveness of electrokinetic treatment to remove oil.

corresponding physical sand content of 68–75%). At the same time, soil samples with 0–10% and 50–90% sand fraction (58–63% and 72–88% of physical sand, respectively) demonstrated a treatment efficacy of only 10–13%. Special attention was paid to the electrochemical treatment of oil-contaminated sand, where the total treatment effectiveness was 24%.

UNCORRECTED PROOFS

Trim Size: 170mm x 244mm Single Column Loose Ribeiro670117 c09.tex V1 - 12/11/2020 11:53pm Page 198

According to electrosurface phenomena theory, sandy soils express negligible development of EDL at the mineral-water boundary in their porous space. Consequently, their EDL is considered to be neglected, and electrokinetic phenomena are not expected to occur in sands. So, oil removal was not expected to take place in the treated sand sample. However, these experiments have shown the possibility of electroosmosis in sands, the same as the Bolshakov study [28]. At least, electroosmosis can occur in the pure medium and fine sands used in the present study. This effect may relate to the increase in soil dispersiveness caused by oil since the oil droplets can be considered specific non-conductive particles. Thus, oil increases the total EDL percent in the contaminated soil due to the formation of the EDL at the oil/water boundary. This effect was given careful consideration in [14], and the authors of this work stated the increase in the electroosmotic flow intensity in the presence of the water/oil EDL.

Notably, oil removal occurred non-uniformly along the sample's length (Figure 9.5), which affected the redistribution of the remaining oil in the soil sample. In some cases, oil was recovered from only part of the soil. For instance, treating the 100% loam sample caused oil recovery (55%) only in the cathodic section ($L/L_0 = 0.75–1$) of the soil. On the other hand, the sample containing 20% loam and 80% sand was cleaned sufficiently only in its anodic part ($L/L_0 = 0–0.25$) at a rate of 40% (see Figure 9.5).

Generally, oil was recovered from soil samples either uniformly along their length or with a maximum in one zone (see Figure 9.5). Considering the electrokinetic oil removal efficiency in the various sample zones, one can conclude that the minimum treatment efficacy occurred in the central part of the soil: near-anode ($L/L_0 = 0.25–0.5$) and near-cathode ($L/L_0 = 0.5–0.75$) for all the soil samples (see Figure 9.5b,c). In the case of 100% loam and samples containing 80–90% sand, almost no oil was recovered from those zones.

The maximum oil removal took place in the anode and cathode sections of the soil samples (see Figure 9.5a,d). In the case of soil mixtures containing 40–80% sand, maximum oil recovery occurred in the anodic zone (40–42%). At the same time, the oil-contaminated sand sample achieved maximum treatment efficiency in its cathodic part (55%).

Thus, we can conclude that the optimum granulometric soil composition for the electrokinetic oil migration is a soil with 65–75% physical sand content. In that case, the free porous space is the most suitable for the electro-mass transfer of the two immiscible liquids – water and oil.

9.5 Influence of Physical Soil Properties

Of the physical soil properties, density and porosity affect electrokinetic oil migration the most. Figures 9.6 and 9.7 demonstrate the variation in oil removal efficiency for the studied *fertile soil horizons*, with their density and porosity. The graphs of the relation between oil removal efficiency and these physical soil properties appear as smooth curves, with the maximum for Retisol and the minimum for Luvisol.

UNCORRECTED PROOFS

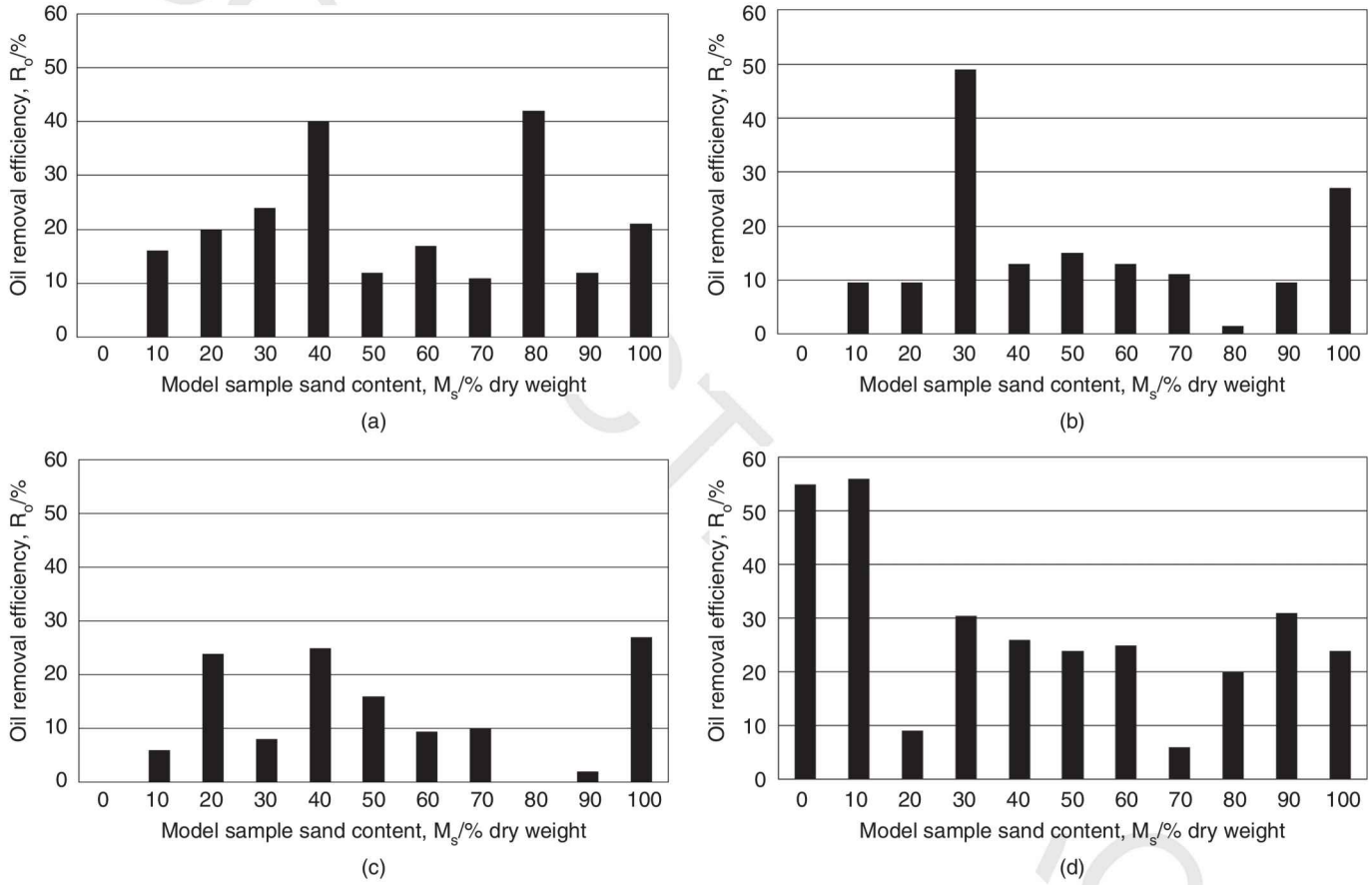

Figure 9.5 Effectiveness of sample remediation to remove oil in different zones: (a) anode zone ($L/L_0 = 0–0.25$); (b) near-anode zone ($L/L_0 = 0.25–0.5$); (c) near-cathode zone ($L/L_0 = 0.5–0.75$); (d) cathode zone ($L/L_0 = 0.75–1$). L/L_0, relative distance from the anode.

UNCORRECTED PROOFS

Trim Size: 170mm x 244mm Single Column Loose
Ribeiro670117 c09.tex V1 - 12/11/2020 11:53pm Page 199

Trim Size: 170mm x 244mm Single Column Loose Ribeiro670117 c09.tex V1 - 12/11/2020 11:53pm Page 200

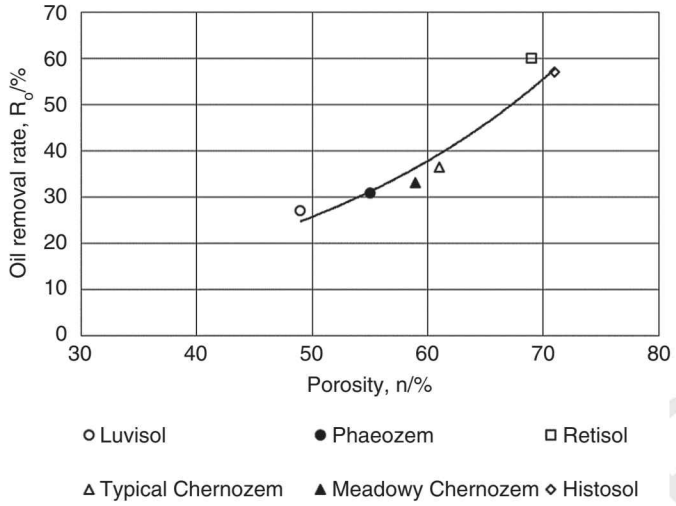

Figure 9.6 Relation of porosity (*n*) and electrokinetic soil remediation rate to remove oil (R_o).

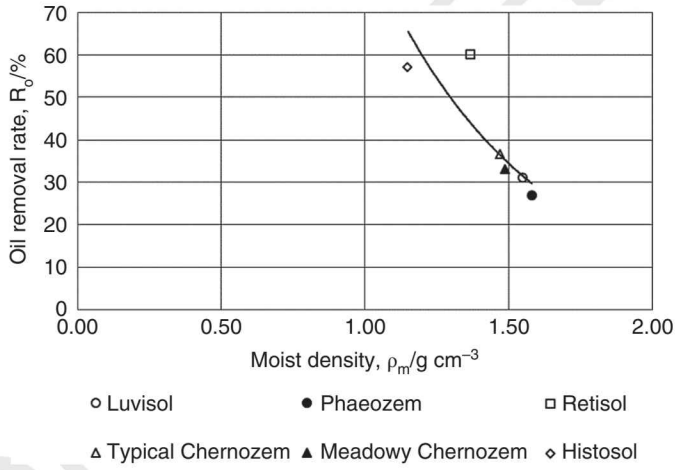

Figure 9.7 Relation of moist density (ρ_m) and electrokinetic soil remediation rate to remove oil (R_o).

Porosity of the soils studied increased in this order: Histosol > Retisol > typical Chernozem > meadowy Chernozem > Phaeozem > >Luvisol. Accordingly, the moist density of the soils grew: Luvisol > Phaeozem > meadowy Chernozem > typical Chernozem > Retisol > Histosol. The experimental data suggest that the greatest oil removal (around 60%) occurred in the Retisol and Histosol, which had the maximum porosity (69 and 71%, respectively). The minimum oil recovery efficiency (27%) was detected for Luvisol, with a porosity of 49% (see Figure 9.6). This regularity can be explained by the hypothesis that increased

UNCORRECTED PROOFS

Trim Size: 170mm x 244mm Single Column Loose Ribeiro670117 c09.tex V1 - 12/11/2020 11:53pm Page 201

porosity resulted in improved electrokinetic oil migration. Thus, more intensive oil extrusion by the electroosmotic flow occurred in the soils with the largest porosity.

Accordingly, the increase in moist soil density resulted in a decrease in the electrokinetic oil recovery rate. Consequently, the low oil migration by electroosmosis in Luvisol resulted from its denser constitution compared to the other soil samples (see Figure 9.7).

Thus, the tests conducted allowed us to find the relation between electrokinetic oil migration and physical soil properties: moist density and porosity. Also, the data obtained conformed with the relations found between oil recovery rate and other soil parameters (chemical and mineral composition, physico-chemical soil properties).

9.6 Influence of Physico-Chemical Soil Properties

The EDL parameters of clay soils depend significantly on their physico-chemical properties [17, 29] and, at the same time, determine some of them to a certain extent. Consequently, the electrokinetic oil removal efficiency of clay soils will depend on their physico-chemical parameters. Such variables include soil plasticity limits, soil activity, characteristic moisture parameters, etc.

For instance, the analysis of oil redistribution along the soil sample length after treatment demonstrated the relation between the oil remains and physico-chemical soil parameters. The oil recovery rate increased as the soil parameters grew, namely the plasticity index (PI), hydrophilicity index (K_h), and soil activity (K_a). PI was calculated as the difference between the soil liquid limit (LL) and plastic limit (PL) [30, 31]:

$$PI = LL - PL \tag{9.1}$$

Soil activity was determined as the ratio of PI to clay fraction content (M_c) [32]:

$$K_a = PI/M_c \tag{9.2}$$

The hydrophilicity index was calculated as the ratio of LL to soil clay content:

$$K_h = LL/M_c \tag{9.3}$$

The physico-chemical soil parameters increased in this order: Luvisol < Phaeozem < meadowy Chernozem < typical Chernozem < Retisol < Histosol. Luvisol and Phaeozem are slightly plastic, both Chernozems and Retisol are medium plastic, and Histosol is a highly plastic soil [30]. Considering soil activity, Luvisol, Phaeozem, and both Chernozems are inactive, Retisol is moderately active, and Histosol is active [32].

Figures 9.8 and 9.9 demonstrate the extensive influence of the physico-chemical soil parameters on electrokinetic oil migration. The maximum oil removal efficacy (around 60%) occurred in Retisol and Histosol. These soils possessed the highest PI (15–25%) and physico-chemical activity. The minimum treatment efficiency was observed for the soils with the lowest PI (see Figure 9.8).

UNCORRECTED PROOFS

Trim Size: 170mm x 244mm Single Column Loose Ribeiro670117 c09.tex V1 - 12/11/2020 11:53pm Page 202

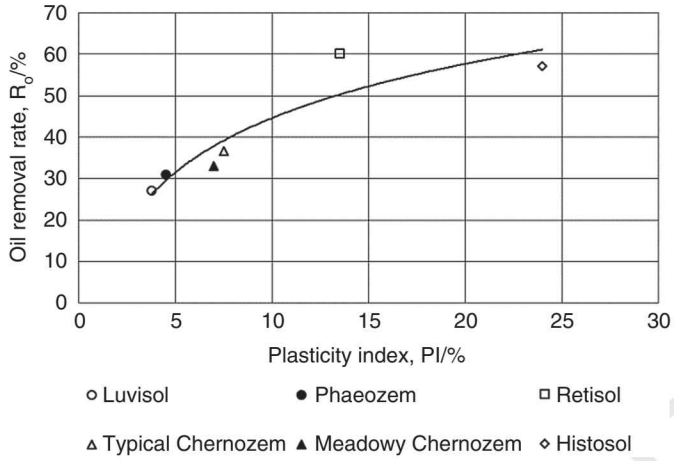

Figure 9.8 Relation of plasticity index (PI) and electrokinetic soil remediation rate to remove oil (R_o).

A similar relation occurred between the removal effectiveness and other soil parameters: hydrophilicity index (K_h) and soil activity (K_a). Sufficient oil removal took place in the soils with the most significant values for these parameters (see Figure 9.9). In the case of the other fertile horizons, the mass transfer intensity decreased, and the treatment efficacy was only 27–37%. That seems to be caused by the relatively small electrokinetic potential values and incomplete EDL development in inactive and moderate active soils.

Thus, the decrease in soil PI, K_h, and K_a caused a decline in electrokinetic oil migration and, consequently, the hydrocarbon removal rate of soils. These parameters determine the development of the EDL diffuse part, electroosmosis velocity, and its contribution to the total electrokinetic mass transfer.

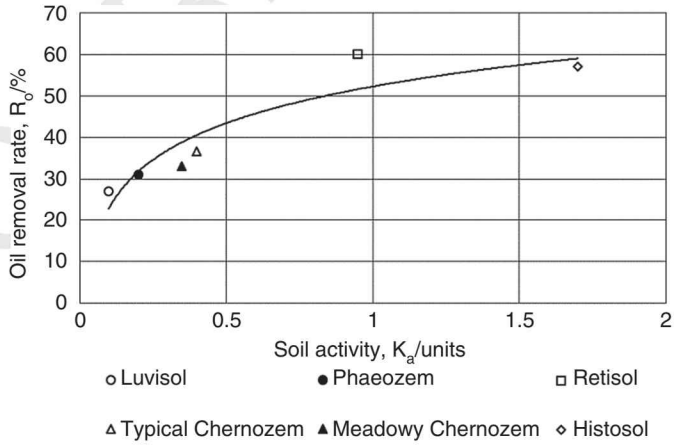

Figure 9.9 Relation of soil activity (K_a) and electrokinetic soil remediation rate to remove oil (R_o).

UNCORRECTED PROOFS

Trim Size: 170mm x 244mm Single Column Loose Ribeiro670117 c09.tex V1 - 12/11/2020 11:53pm Page 203

The results given were obtained during the experiments with no additional water source. However, the most effective electrokinetic soil treatment for oil contamination occurs with the use of a flow-through mode. This mode usually includes electrochemical washing of hydrocarbons with a leaching anolyte solution provided through the anode. The other study conducted by the authors demonstrated that the most efficient extraction agent among the chemicals studied was 0.1–0.2 M NaOH. On the one hand, sodium hydroxide as the anolyte caused the oil to solubilize not only in the cathode (alkaline) zone but along the entire sample length. The effect of high pH on the desorption of oil from mineral particles and emulsification of oil and water was studied deeply in [33]. On the other hand, adding NaOH caused an increase in the electrokinetic potential of the soil particles since its negative value generally increases with a rise in pH [29, 34]. Consequently, the use of NaOH solution caused increased electroosmotic flow in the soils [17]. Thus, in these tests, oil was removed by electroosmotic flow extrusion and partially in the dissolved form. That resulted in significant overall oil recovery from the soil samples.

9.7 Influence of the Initial Water/Oil Ratio in a Soil

The initial water/oil ratio in a soil's porous medium influences electrokinetic oil migration significantly. The study of the regularities of electrokinetic oil removal from clay soils was conducted using oil/water-saturated kaolinite clays and Quarternary mantle till loams at various water/oil ratios. First, clay samples were prepared by mixing dry matter with a water-electrolyte solution (0.01 M NaCl), and then the oil mass was added to the clayey paste. Oil from the Tarasovskoe field (western Siberia) was used for the study. The samples had a degree of oil/water saturation equal to 1 (in other words, there was no air in the soil pores). Kaolinite clay was chosen to determine the influence of oil content on the EDL parameters since this clay was monomineralic and washed to remove salts. That allowed interpreting the data obtained with adequate accuracy.

The research demonstrated that the volume ratio of the three soil phases (solid, water, and oil) influenced electrokinetic potential (ζ) and electroosmotic transport rate (P_{EO}) of clay significantly.

The isolines on the triangle diagram of the soil's phase composition show the values of ζ and P_{EO} (Figure 9.10). The degree of fluid saturation (K_f) for all the samples studied was 1. This diagram shows the volume percent of kaolinite, NaCl solution, and oil. It also depicts the areas of various EDL parameter values at different component ratios.

The results showed that ζ and P_{EO} decreased as soil moisture content dropped and oil content rose (see Figure 9.10).The triangle diagram demonstrates that the maximum values of ζ-potential (mV) and, consequently, P_{EO} are observed for clay with a water/oil ratio of 2:1 and a moisture content of 50.5%. This moisture percent corresponds to the free-swelling water content (W_{sw}) of the studied kaolinite clay.

The EDL transformation under various soil-phase compositions altered the electrokinetic potential. The soil-phase composition affected the degree of development

UNCORRECTED PROOFS

Trim Size: 170mm x 244mm Single Column Loose Ribeiro670117 c09.tex V1 - 12/11/2020 11:53pm Page 204

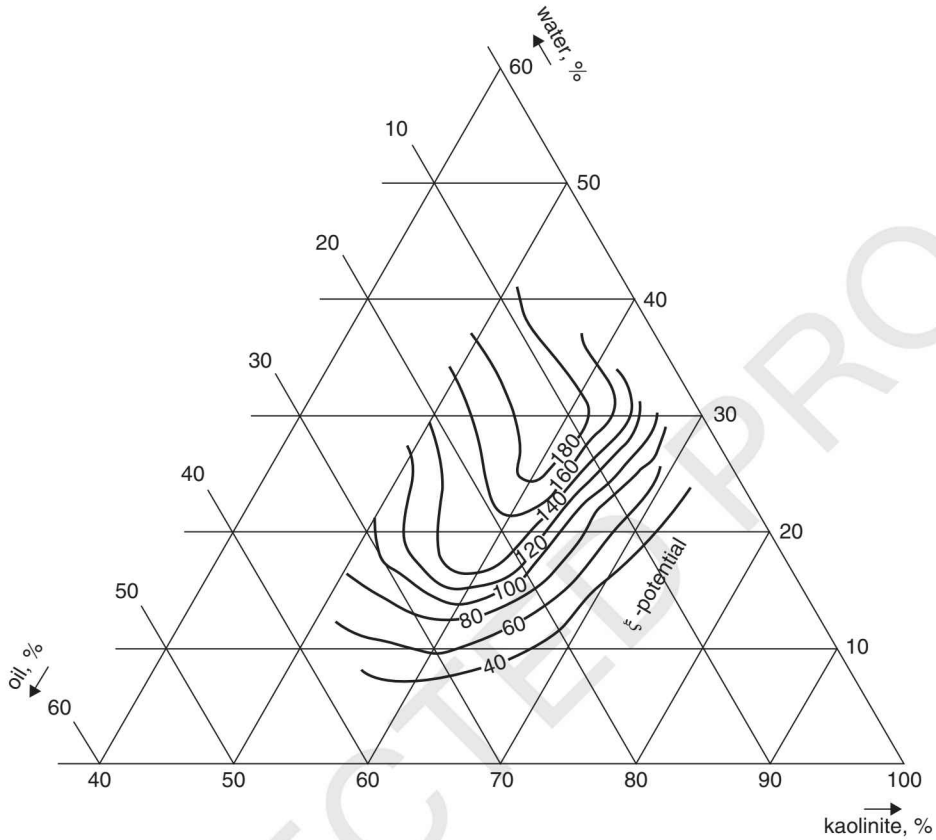

Figure 9.10 Triangular diagram of the ζ-potential values (mV) of oil/water-saturated kaolinite clay at various phase ratios.

and mutual overlap for the EDLs of the adjacent kaolinite particles. The overall soil electrosurface properties were complicated by the formation of the EDL at the water/oil boundary. The parameters of the water/oil EDL significantly depend on the volume ratio of water and oil in the soil pores.

Figure 9.10 depicts the trend of the most significant ζ alteration. It declined drastically as the kaolinite volume percent increased, and the moisture content decreased while the oil percent remained constant. This ζ-potential value drop occurred within the region of the kaolinite phase increase from 60 to 65% and evened out after that. The opposite effect was observed within the area of 50–60% kaolinite share, at a corresponding increase in oil percent from 15 to 30% and a simultaneous decline in NaCl solution content from 30–15%. The drop in ζ values (and P_{EO}, accordingly) was smooth within this diagram area and became sharper only with the increase in oil share over 25–30%. Considering these results, one can conclude that the volume content of clay minerals affected electrokinetic migration of the pore solution the same as in water-saturated soils without hydrocarbon pollutants. Also, one can deduce that electrokinetic oil migration occurred

UNCORRECTED PROOFS

Trim Size: 170mm x 244mm Single Column Loose Ribeiro670117 c09.tex V1 - 12/11/2020 11:53pm Page 205

alongside the electroosmotic flow of the pore solution in oil/water-saturated soils due to the viscous friction of the moving water. This effect was observed in [35] alongside the formation of an oil/water emulsion at high pH and its migration to the cathode.

In contrast, Pamukcu et al. reported that with high water content in saline oil-contaminated sediments, oil migration occurred in the anode direction [15]. Oil was found to migrate on the surface of solid particles carried by electrophoresis to the anode. This regularity is widely applied for the demulsification of oily sludges [36].

The EDL parameter values (such as ζ-potential, normalized diffuse layer thickness, and surface-charge density) determine the intensity of electroosmotic oil migration in oil/water-saturated soils. The larger these parameters are, the more intense the electrokinetic oil migration that occurs. It also demonstrates that the oil migration occurs alongside the electroosmotic flow and results from viscous water friction.

Thus, the tests conducted discovered the optimal phase ratio of clay soils for electrokinetic oil removal. The optimal moisture content for this purpose was close to the free-swelling water content of the clay, while the best water/oil ratio was 2:1 or more (Figure 9.11). Decreased moisture content and increased oil share caused a decline in the oil removal rate and, accordingly, electrokinetic oil migration intensity.

The influence of the water/oil ratio on electrokinetic treatment effectiveness was also studied for the fertile soil horizons. The study of the impact of the water/oil ratio on the Luvisol treatment efficiency showed that the oil removal rate increased with the growth of this ratio from 1:0.4 to 1:0.6. Further increase in oil content in the soil caused treatment efficacy to decline (Figure 9.12).

The oil removal rate for the Luvisol was 27% at a water/oil ratio of 1:0.4. Hydrocarbons migrated from the anodic zone to the cathodic zone with the electroosmotic flow. The pattern of electrokinetic oil migration did not change with an increase in the water/oil ratio to 1:0.5. In these conditions, the oil recovery rate achieved 57%. The direction of electroosmotic mass transfer remained the same at a water/oil ratio of 1:0.6. At the same time, its intensity increased drastically. At this ratio, the maximum hydrocarbon removal was achieved (60%). It is probably caused by specific aspects of EDL formation at that phase volume ratio. When oil covers a considerable share of the soil particle's surface, the water/mineral EDL impact on the electrokinetic mass transfer decreases. In this case, the direction and intensity of electroosmosis are defined by the composition of the water/oil boundary EDL.

Further increase in the water/oil ratio from 1:0.8 to 1:1.1 caused the electrokinetic mass transport to fade. The tests showed that the maximum oil removal efficacy (around 60%) was gained at a water/oil ratio of 1:0.6 (see Figure 9.12).

Thus, increasing the initial water/oil volume ratio from 1:0.4 to 1:0.6 intensified electrokinetic hydrocarbon migration. Further increase in that ratio resulted in a decrease in the oil removal rate. These facts are thought to be caused by specific features of the EDL formation at the water/mineral and water/oil boundaries and alterations in their contribution to the total electrokinetic oil migration at various water/oil volume ratios.

UNCORRECTED PROOFS

Trim Size: 170mm x 244mm Single Column Loose Ribeiro670117 c09.tex V1 - 12/11/2020 11:53pm Page 206

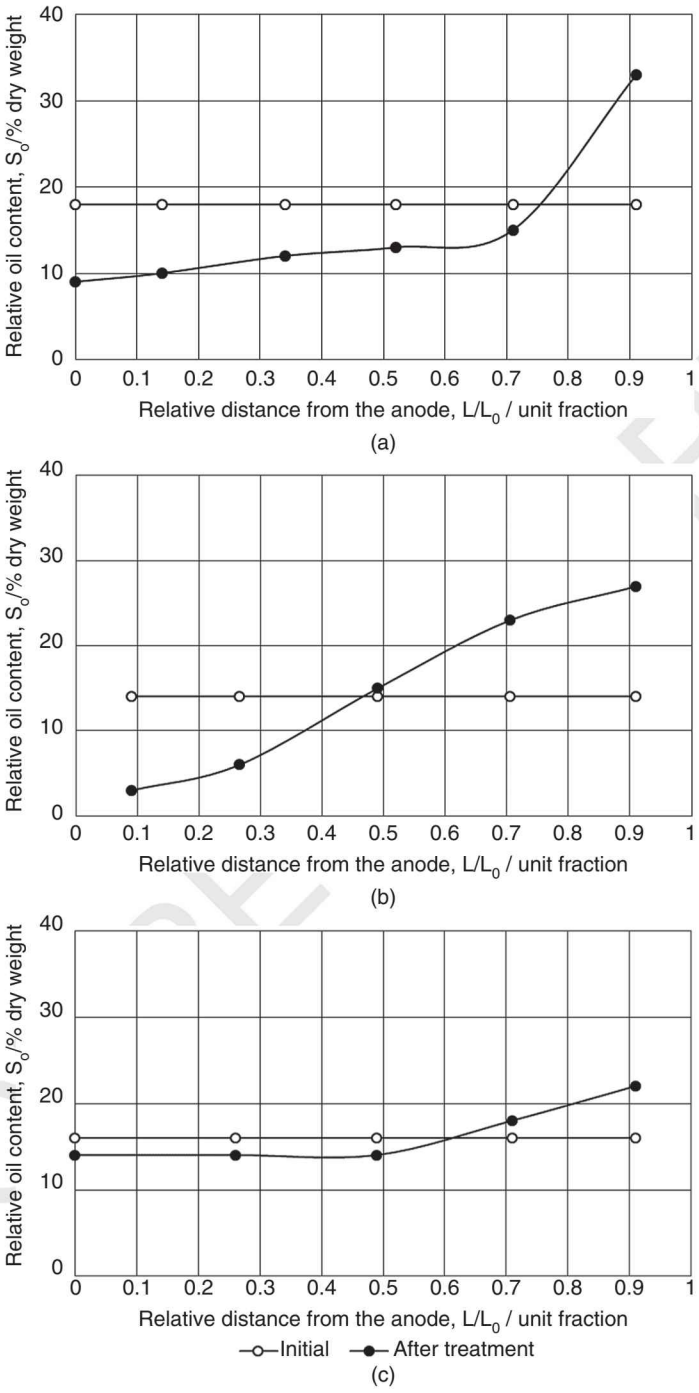

Figure 9.11 Oil redistribution alongside kaolinite clay samples during electrokinetic treatment at the relative initial water/oil volume rate: (a) 3 : 1; (b) 2 : 1; (c) 1 : 1.

UNCORRECTED PROOFS

Trim Size: 170mm x 244mm Single Column Loose Ribeiro670117 c09.tex V1 - 12/11/2020 11:53pm Page 207

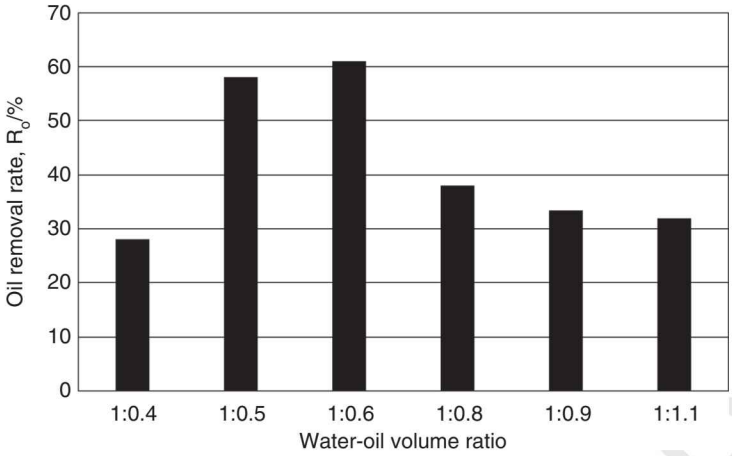

Figure 9.12 Relation of water/oil volume ratio and electrokinetic remediation rate to remove oil from Luvisol.

9.8 Influence of the Oil Aging Process

When oil accumulates in surface or near-surface soil horizons, it undergoes various transformations of its composition and properties due to the influence of different external thermodynamic factors [37]. Most of the oil light end vaporizes, and the oil composition changes due to its partial decomposition by microorganisms and atmospheric agencies, etc. The longer that process takes, the more profound the alterations in the oil composition that occur. These oil transformations are often referred to as oil *aging*.

Oil aging is thought to affect its electrokinetic mobility significantly. The influence of oil aging on the effectiveness of electrokinetic oil removal from oil-polluted soil was studied on model samples prepared using mantle till loam. Oil from the Usinskoe field was used in these tests. Electrokinetic soil treatment was carried out under lab conditions (at 20 °C) during various oil aging stages. The oil aging periods for the samples studied were 1 week, 2 weeks, 40 days, 1.5 months, 2 months, and 6 months (or 7, 14, 40, 46, 61, and 183 days).

Two types of behavior were observed in the current parameters during the electrokinetic treatment for the six samples under study. The first type occurred while treating the 1-week, 2-week, and 6-month aged samples. In this case, the initial voltage gradient was around 3 Vcm^{-1} (Figure 9.13). During the first 45 minutes, it increased to 4 Vcm^{-1}, and then it skyrocketed to 20 Vcm^{-1} within 3–5 minutes. The second type took place while treating the samples with oil aging periods of 40 days, 1.5 months, and 2 months. The initial voltage in that group was 40 V (with a corresponding gradient of 4 Vcm^{-1}). The increase in the voltage gradient to 20 Vcm^{-1} for this group of soil samples was more prolonged and steep. The maximum treatment duration occurred for the sample with 40-day oil aging. As the aging duration increased (over 40 days), the treatment time to achieve a voltage gradient of 20 Vcm^{-1} gradually decreased (see Figure 9.13).

UNCORRECTED PROOFS

Trim Size: 170mm x 244mm Single Column Loose Ribeiro670117 c09.tex V1 - 12/11/2020 11:53pm Page 208

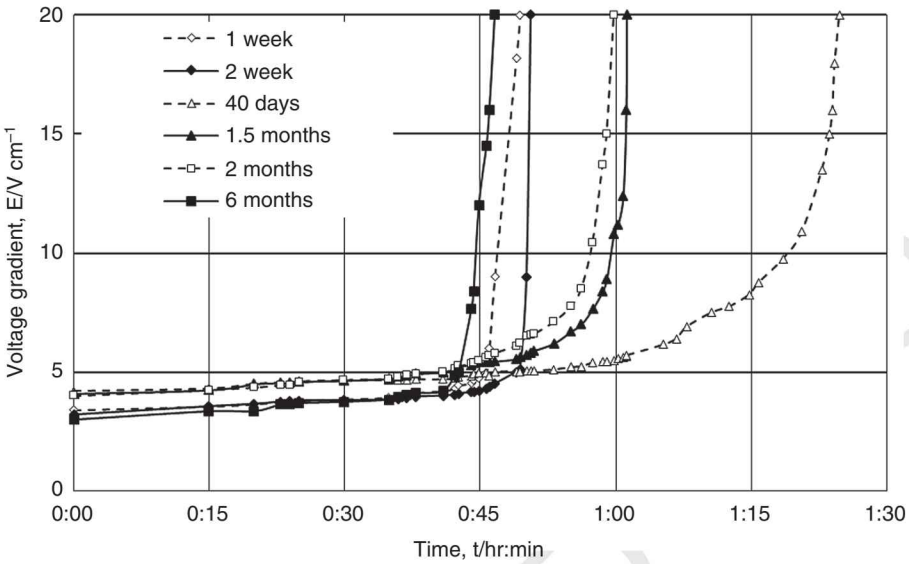

Figure 9.13 Voltage gradient alterations during electroosmotic treatment of soil samples with various oil ages.

Figure 9.14 demonstrates the moisture content redistribution in the samples studied after electrokinetic treatment. The water content redistribution profile showed the same behavior for the samples aged from one week to two months. However, the more extensive the aging period was, the less drainage that occurred in any section of the soil sample (see Figure 9.14). In the case of 1-week contamination, the moisture content of the anodic zone after treatment was 21.3% (initial value 27%), and water percent in the cathodic section was 25%. These values were 23.6 and 26.2%, respectively, for the 2-month sample. In contrast, treating the 6-month sample caused almost no water redistribution.

The total drainage rate for the 6-month sample was slightly higher than 1% (Figure 9.15). Considering the accuracy of moisture content detection (0.4%), one can assume that the water content of this sample almost did not change. These results can be explained considering the significant oil degradation over six months. During this period, some part of the oil components transformed into unsoluble and immobile forms. Consequently, the pore water was blocked between soil particles and heavy oil ends with high viscosity and low mobility. As a result, electroosmosis was almost entirely suppressed. Generally, the electroosmotic drainage rate decreased as the oil aging time increased (see Figure 9.15).

The remaining oil redistributed in this sample series due to electrokinetic treatment. As a consequence, the oil concentration decreased from the anode to the cathode (Figure 9.16). At the same time, oil accumulation occurred in the near-cathode zone (L/L_0 = 0.5–0.75) for all the soil samples except that aged for one week. The remaining oil content increased in the other soil zones (anodic, near-anode, and cathodic) for all the samples as aging time increased. Thus, the

UNCORRECTED PROOFS

Trim Size: 170mm x 244mm Single Column Loose Ribeiro670117 c09.tex V1 - 12/11/2020 11:53pm Page 209

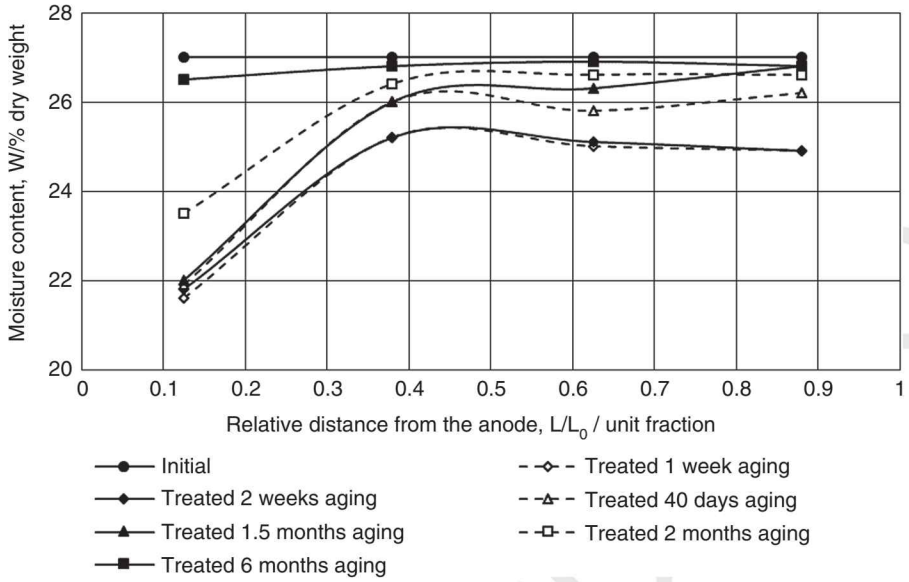

Figure 9.14 Redistribution of moisture content alongside the inter-electrode space for the model samples with various oil ages after electrokinetic treatment.

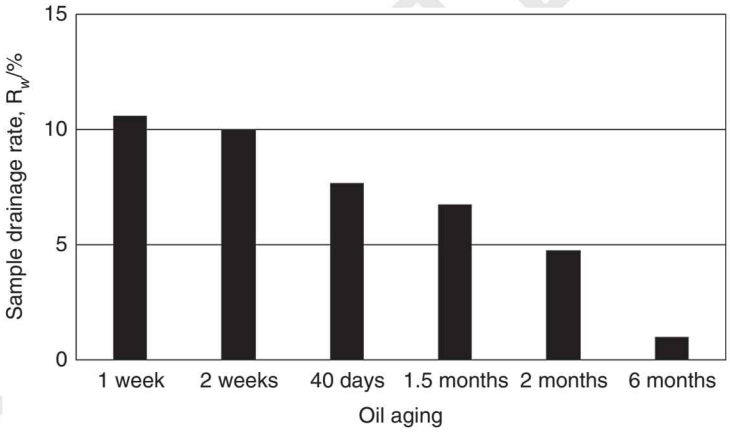

Figure 9.15 Drainage effect on model soil samples polluted with oil of various ages, achieved by electrokinetic treatment.

decrease in oil content in the near-cathode and cathodic soil sections contributed the most to total treatment efficiency for the sample aged for one week. Oil removal from the samples with more prolonged contamination periods occurred due to the oil content decrease in the soil's anodic and cathodic zones.

According to the results of the study, total treatment efficacy decreased as the contamination period increased. Generally, it dropped from 10.4% (1-week oil aging) to 2.9 and 0.6% in the case of the 2- and 6-month samples, respectively (Figure 9.17).

Trim Size: 170mm x 244mm Single Column Loose Ribeiro670117 c09.tex V1 - 12/11/2020 11:53pm Page 210

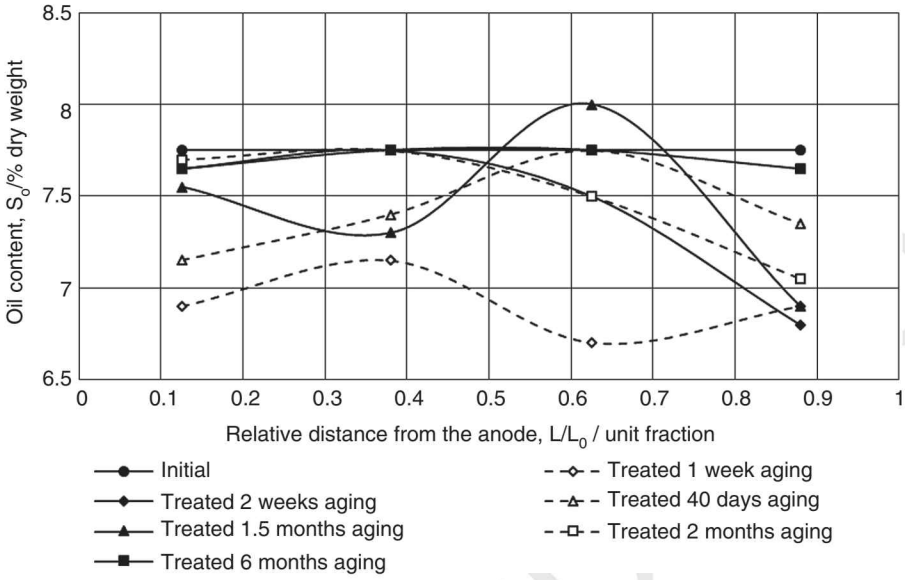

Figure 9.16 Redistribution of oil content resulting from electrokinetic treatment, alongside the length of samples contaminated with oil of various ages.

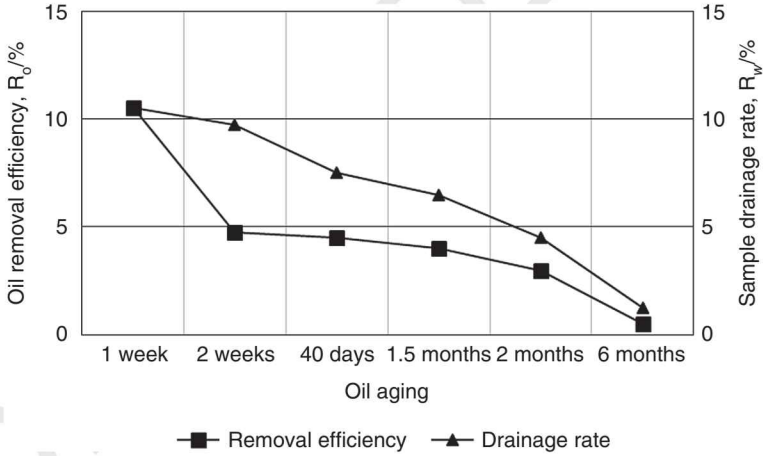

Figure 9.17 Relation between electrokinetic treatment effectiveness and drainage rate for soil samples contaminated with oil of various ages.

Also, a direct relation was found between the total drainage rate of the soil and oil removal effectiveness (see Figure 9.17). This fact proves the domination of electroosmosis in overall oil migration under the voltage gradient as well.

Considering the contribution of each soil sample zone in the total soil decontamination, one can conclude that the oil removal rate was equal in all the zones only in the case of the one-week sample (Figure 9.18). As the duration of oil aging increased further, the cathodic section contributed most to total treatment efficiency. This zone expressed the most substantial oil removal in almost all cases (see Figure 9.18).

UNCORRECTED PROOFS

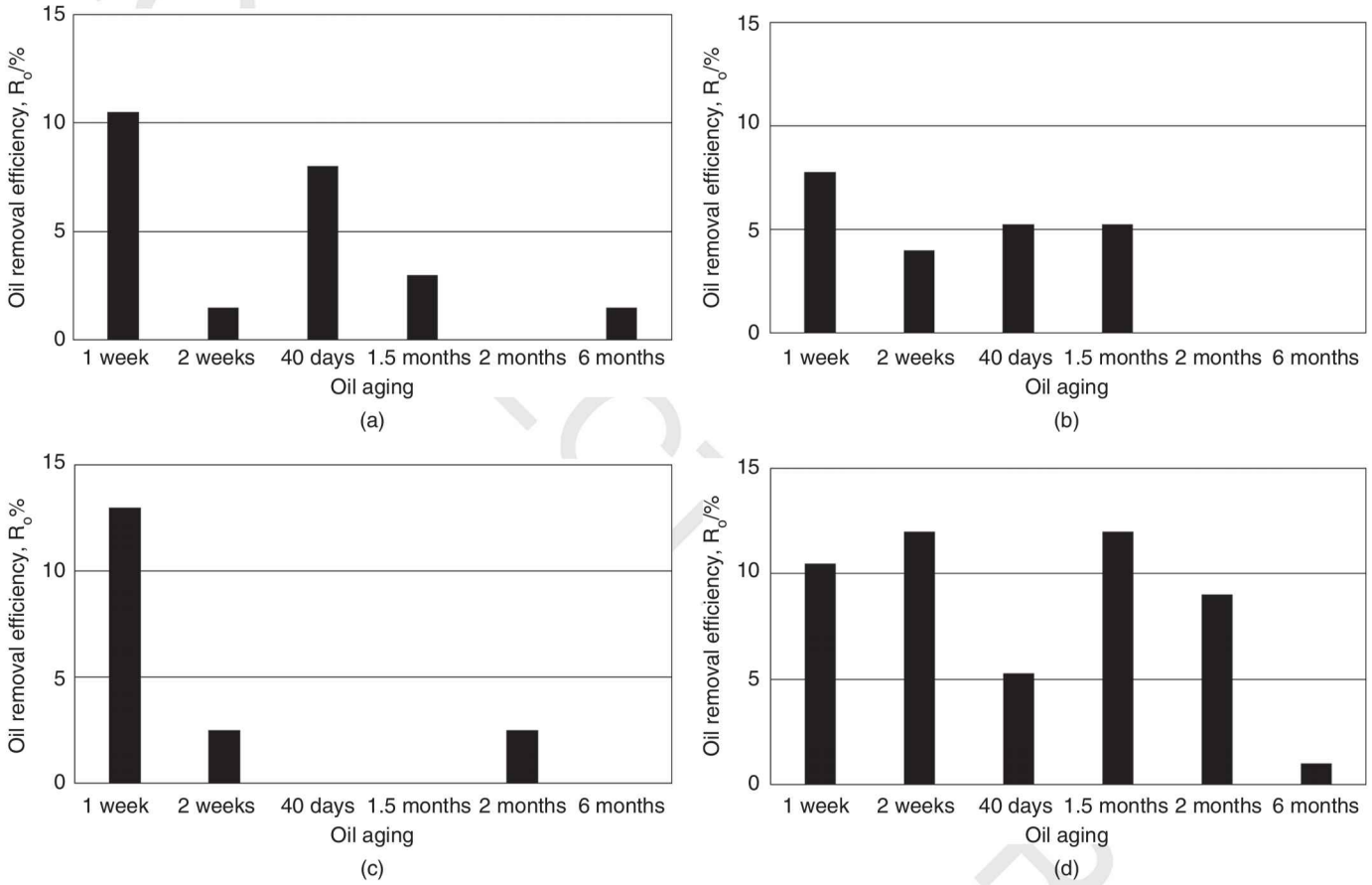

Figure 9.18 Effectiveness of electrokinetic treatment in soil samples contaminated by oil of various ages in four sample zones: (a) anode ($L/L_0 = 0–0.25$); (b) near-anode ($L/L_0 = 0.25–0.5$); (c) near-cathode ($L/L_0 = 0.5–0.75$); (d) cathode ($L/L_0 = 0.75–1$).

UNCORRECTED PROOFS

Trim Size: 170mm x 244mm Single Column Loose
Ribeiro670117 c09.tex V1 - 12/11/2020 11:53pm Page 211

Trim Size: 170mm x 244mm Single Column Loose Ribeiro670117 c09.tex V1 - 12/11/2020 11:53pm Page 212

On the other hand, the soils' near-cathode zone showed almost no oil removal (except for the 1-week sample), while the near-anode zone was cleaned only in the case of 1.5-month contamination.

Thus, a conclusion can be drawn that the use of electrokinetics to treat soils with an oil contamination period greater than six months will be ineffective. So, oil contamination age should be taken into account during the design of remediation projects for an oil-polluted soil mass. Degraded oil should be turned into mobile forms by the addition of surfactants or co-solvents. The other option is to apply an electrochemical leaching method, which allows the removal of viscous ends of the aged oil by the soil washing with a desorbing agent under the voltage gradient. A promising leaching solution for oil removal is an alkaline anolyte.

9.9 Influence of Oil Composition

Oil from different oil fields is known to vary significantly in its composition and properties. These differences are evident in the variation in oil density, viscosity, molecular weight, element content, and oil fractions: saturates, aromatics, resins, and asphaltenes. These differences in oil properties are thought to affect their electrokinetic migration in soils significantly.

The influence of oil composition on electrokinetic soil treatment efficiency was studied using model samples. These samples were prepared by mixing mantle till loam with an exact amount of oil. Three oil types varying in composition and density were used in the study (Tables 9.1 and 9.2). The American Petroleum Institute (API) degree values were calculated to classify each oil type:

$$API^{\circ} = [141.5/(D^4{}_s/\rho_{ws})] - 131.5 \tag{9.4}$$

where $D^4{}_s$ and ρ_{ws} are the densities of oil and water at ~15.6 °C (60 °F), respectively.

Oils are divided according to API values [38]: light (API > 31.1°), medium (22.3 < API < 31.1°), heavy (10 < API < 22.3°), and extra-heavy (API < 10°). The data on the electrokinetic oil migration in the loam is given in Table 9.3.

The initial voltage gradient while treating the sample contaminated by light oil from the Tarasovskoe field ($D^4{}_{20} = 0.816\ g cm^{-3}$) was 6 Vcm^{-1}. It increased gradually

Table 9.1 Composition and properties of the oils studied.

Oil type	$D^4{}_{20}$, g cm^{-3}	API°	API oil grade	ν, 10^{-6} m^2 s^{-1}	m_M, g mol^{-1}	M_e, % weight		M, % weight		
						^{14}N	^{32}S	Asphaltenes	Resins	Saturates (paraffins)
Tarasovskoe	0.816	42	Light	4.1	192	0.13	0.21	0.1	3.6	3.3
Usinskoe	0.854	34	Light	7.5	205	0.20	0.56	2.5	6.7	5.6
Yaregskoe	0.944	18	Heavy	86.3	452	0.37	1.11	3.7	20.1	1.7

$D^4{}_{20}$, oil density at 20 °C; ν, kinematic viscosity; $m_{M,}$ oil molecular mass; $M_{e,}$ percent of a chemical element (elementary composition); M, hydrocarbon group composition (oil component share).

UNCORRECTED PROOFS

Trim Size: 170mm x 244mm Single Column Loose Ribeiro670117 c09.tex V1 - 12/11/2020 11:53pm Page 213

Table 9.2 Fraction composition of the oils studied.

Oil type	Normal boiling point, t_b/° C	Up to 150 ° C	Up to 200 ° C	Up to 250 ° C	Up to 300 ° C
Tarasovskoe	58	22	32	48	69
Usinskoe	64	19	27	40	54
Yaregskoe	140	0.3	4	11	29

Table 9.3 Influence of oil composition on electrokinetic migration.

Oil type	Initial sample parameters: Moisture content, W/% dry weight	Initial sample parameters: Oil content, S_o/% dry weight	Final soil sample parameters	Parameter value at the relative distance from the anode, L/L_0: 0.13	0.38	0.63	0.88
Tarasovskoe	18.5	10.6	Moisture content, W/% dry weight	7.1	12.8	16.4	18.4
			Oil content, S_o /% dry weight	9.8	8.9	6.9	6.2
			Oil removal efficiency, R_o/%	7.2	16.3	34.9	42
Usinskoe			Moisture content, W/% dry weight	4.7	8.5	11.4	15
			Oil content, S_o /% dry weight	8.1	9.8	10	10.6
			Oil removal efficiency, R_o/%	23.6	10.3	4.9	16.8
Yaregskoe			Moisture content, W/% dry weight	10.2	14.4	15.5	15.6
			Oil content, S_o /% dry weight	9.8	10.2	9.8	10
			Oil removal efficiency, R_o/%	7.5	3.8	7.5	5.7

during the first 3 hours (up to 8 Vcm^{-1}) and then reached 20 Vcm^{-1} within 30 minutes. So, the treatment time until the voltage gradient increase to 20 $Vcm^{-1}$was 3.5 hours. A gradual increase in soil resistivity accompanied it. After that, a sharp decrease in current intensity occurred from 10 to 5 mA within 15 minutes, and then a more steep decrease took place to 2 mA (over 1.5 hours).

Electrokinetic treatment of the sample containing Tarasovskoe oil resulted in its drainage. Its final moisture content increased from 7.1 to 18.4% in the direction from the anode to the cathode (initial water percent W = 18.5%). The water redistribution

UNCORRECTED PROOFS

Trim Size: 170mm x 244mm Single Column Loose Ribeiro670117 c09.tex V1 - 12/11/2020 11:53pm Page 214

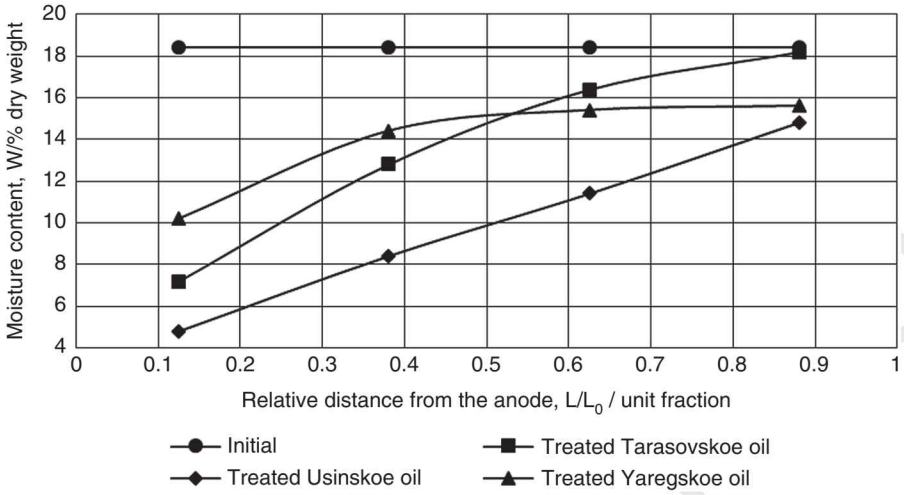

Figure 9.19 Moisture content redistribution along the soil sample's length after electrokinetic treatment of different oil types.

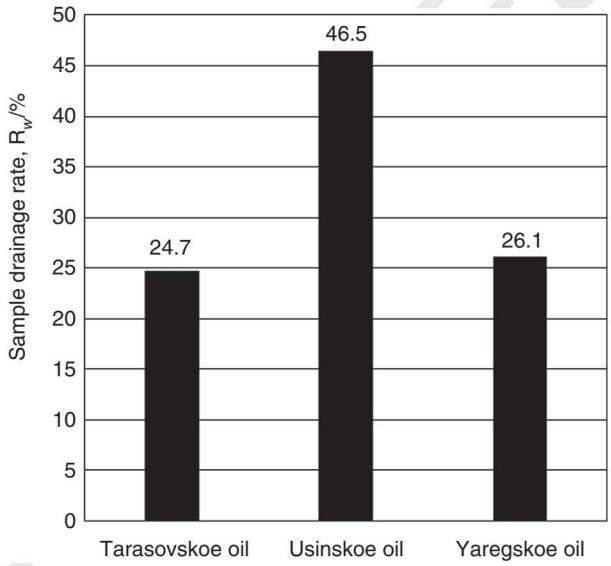

Figure 9.20 Total moisture loss in oil-containing soil samples after electrokinetic treatment of different oil types.

profile in this sample had the form of a smoothly curved bowing segment that rose in the cathode direction (Figures 9.19 and 9.20).

The oil redistribution profile in this sample is opposite that of water content. The oil content declined from 9.8 to 6.2% in the cathode direction (initial oil content 10.6%) (Figure 9.21). The redistribution of the remaining oil demonstrated

Trim Size: 170mm x 244mm Single Column Loose Ribeiro670117 c09.tex V1 - 12/11/2020 11:53pm Page 215

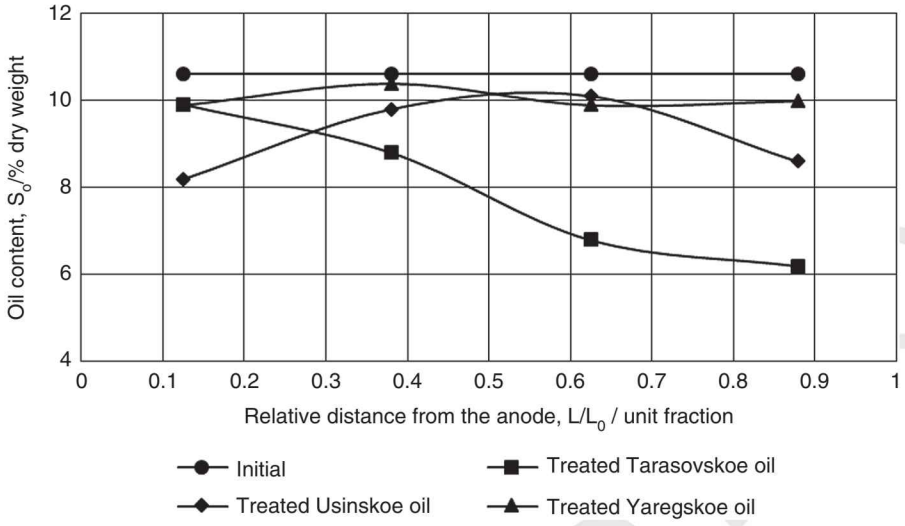

Figure 9.21 Redistribution of the remaining oil alongside soil specimens after electrokinetic treatment of various oil types.

once more that light, mobile Tarasovskoe oil moved predominantly with the electroosmotic flow and was carried out alongside the electroosmotic effluent in the cathodic zone. In this case, the oil outflow in the cathodic part of the sample dominated the influx from the anodic zone. That was why the oil concentration decreased gradually in the direction from the anode to the cathode.

The electrokinetic treatment efficiency for the loam with Tarasovskoe oil increased from the anodic zone (7.2%) to the cathodic zone, reaching a maximum of 42% (Figure 9.22). The oil removal rate increased by a factor of two in both the "anode – near-anode" and "near-anode – near-cathode" segments. The total oil recovery effectiveness of the sample was 25%, with 10% in the cathodic part (see Figure 9.22).

For the soil sample contaminated with Usinskoe oil ($D^4_{20} = 0.854\ gcm^{-3}$), the initial voltage gradient was $6\ Vcm^{-1}$, the same as for Tarasovskoe oil. It gradually increased to $20\ Vcm^{-1}$ over 5.5 hours. There was no intensive growth in soil resistivity as was observed for Tarasovskoe oil. After the voltage gradient achieved $20\ Vcm^{-1}$, the electric current decreased over 1 hour at a constantly declining rate.

The moisture content of this sample decreased sufficiently due to the treatment. It was 4.7% and 15% in the anodic and cathodic zones, respectively (initial W = 18.5%) (see Figure 9.22). The profile of the water content redistribution within the sample is shown by the right line ascending in the cathode direction.

The profile of the Usinskoe oil redistribution almost fit that of the Tarasovskoe type. It ascended in the cathode direction from 8.1% in the anodic zone to 10% in the near-cathode zone (initial oil content 10.6%) (see Figures 9.21 and 9.22). The oil percent in the cathodic zone descended to 8.8%. In this case, more dense Usinskoe oil cannot move with the electroosmotic flow as quickly as Tarasovskoe oil. For this reason, oil accumulated in the soil pores, with an increase in oil concentration in the

UNCORRECTED PROOFS

Trim Size: 170mm x 244mm Single Column Loose Ribeiro670117 c09.tex V1 - 12/11/2020 11:53pm Page 216

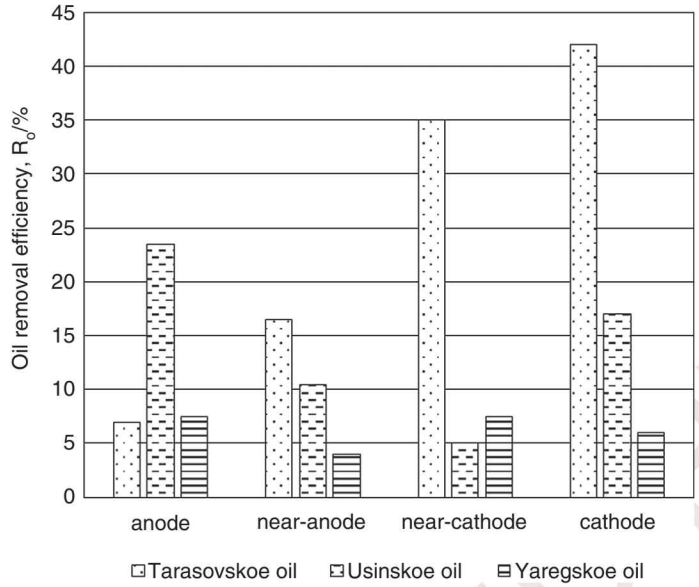

Figure 9.22 Electrokinetic oil removal effectiveness in various soil sample sections.

cathode direction. The process of alkaline leaching was not intense enough in that case to fully counteract oil accumulation. As a result, the oil influx from the anodic zone dominated its efflux into the cathodic zone within the near-cathode section.

Accordingly, the oil removal effectiveness decreased from the anodic part of the sample (23.6%) to the near-cathode part (4.9%).Then it increased in the cathodic zone up to 16.8% (Figures 9.21 and 9.22). Generally, treatment efficiency decreased by a factor of around 2.5 in both the "anodic – near-anode" and "near-anode – near-cathode" soil segments. The total treatment efficacy for the Usinskoe oil sample was 13.9%, with 6% in the anodic zone (see Figure 9.22).

The third oil type used was Yaregskoe oil. This oil was the most viscous (D^4_{20} = 0.944 g cm^{-3}). The initial voltage gradient was 4 Vcm^{-1} in the case of the Yaregskoe oil sample. It increased slowly to 5.7 Vcm^{-1} over 1 hour and 10 minutes and then ascended sharply to the maximum applied voltage gradient of 20 Vcm^{-1} within 7 minutes. After that, the electric current decreased to 3 mA within 2 minutes, and it declined further to 1 mA within 4 hours.

The water content of the Yaregskoe oil sample after treatment declined by a fifth. Moisture content in the anodic zone was 10.2%, and it reached 15.6% in the cathodic zone (initial water share 18.5%). The most distinctive drainage effect took place in the anodic zone. The rest of the soil zones drained relatively equally. As a result, the water percent redistribution profile represented a curve ascending almost linearly in the anodic and near-anode zones and continuing at one level up to the cathodic zone.

The Yaregskoe oil redistribution profile represents a curve at an average level of 10%, which is almost parallel to the initial oil content of 10.6% (see Figure 9.21). This fact demonstrates that there was almost no movement of viscous and low-mobile oil with the electroosmotic flow. In addition, since this oil contains a large number of

UNCORRECTED PROOFS

Trim Size: 170mm x 244mm Single Column Loose Ribeiro670117 c09.tex V1 - 12/11/2020 11:53pm Page 217

heavy fractions (resins and asphaltenes), these compounds could clog the light oil ends in soil mesopores and prevent their migration with electroosmotic flow [39]. The insignificant decline in oil content in this sample seems to be due to the vaporization of the light methane oil end.

The electrokinetic treatment efficacy varied from 3.8% in the near-anode zone to 7.5% in the anodic and near-cathode zones for the sample contaminated with Yaregskoe oil (see Figure 9.23). The total oil recovery rate was 6.1% (Figure 9.24), with a share in the anodic and near-cathode zones of 1.9%. However, this

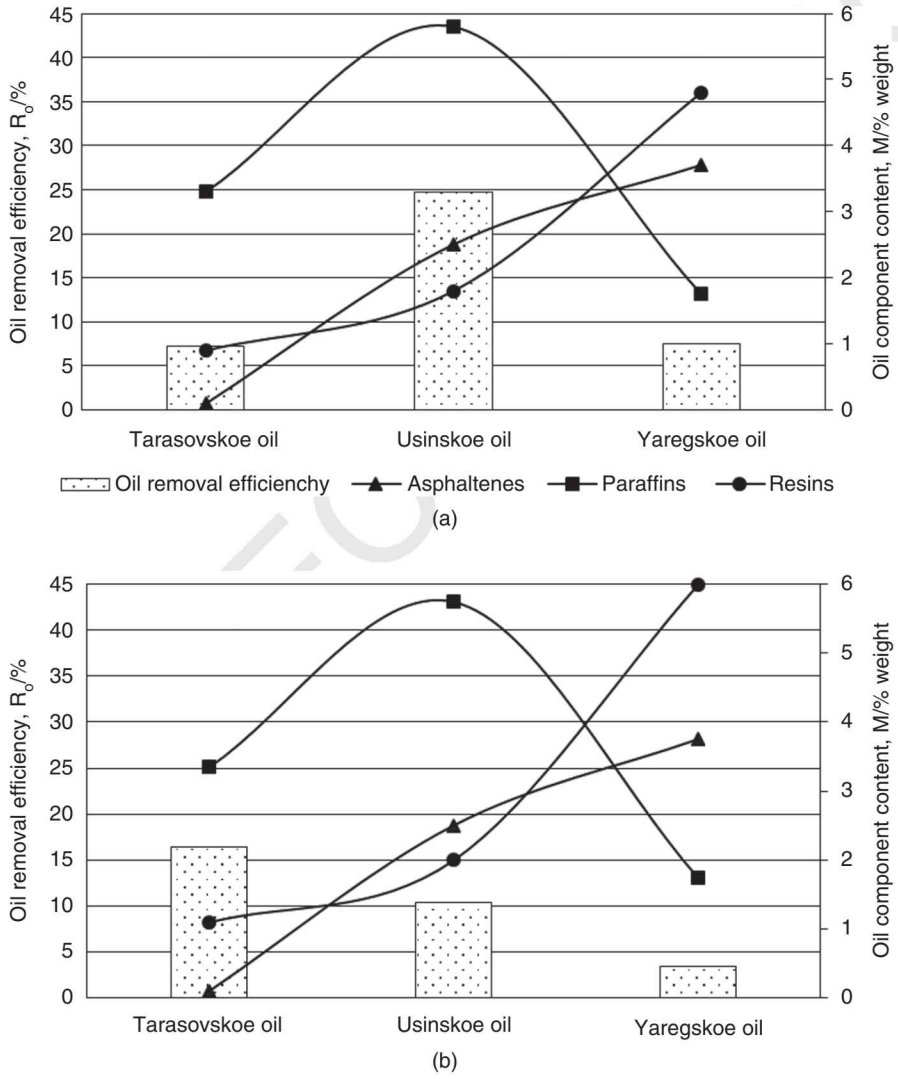

Figure 9.23 Oil removal efficiency in the anode (a), near-anode (b), near-cathode (c), and cathode (d) zones of the soil sample and the corresponding contents of asphaltenes, paraffins, and resins in the different oils.

Trim Size: 170mm x 244mm Single Column Loose Ribeiro670117 c09.tex V1 - 12/11/2020 11:53pm Page 218

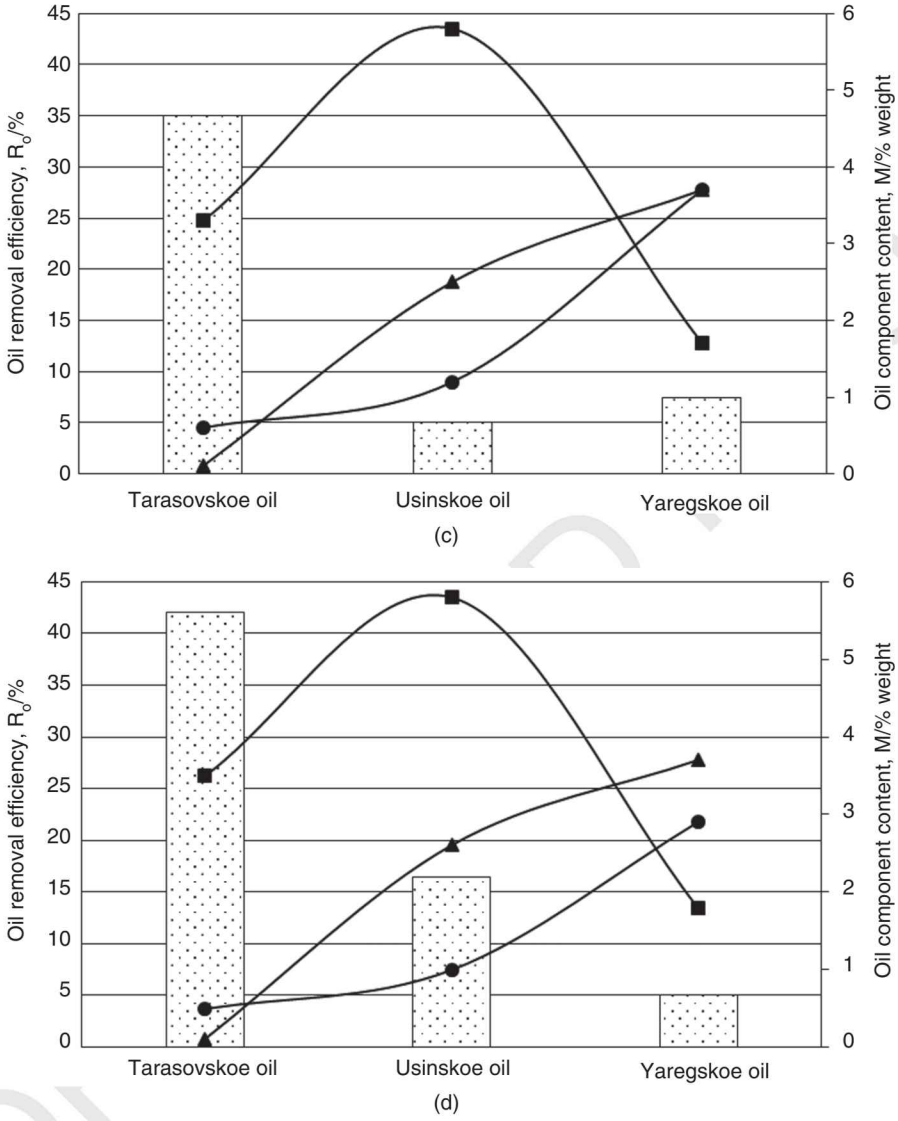

Figure 9.23 (*Continued*)

insufficient oil removal rate led to the conclusion that this sample experienced almost no purification.

Comparing the results of the study of electrokinetic treatment of soil contaminated by three oil types, one can draw several conclusions. The maximum drainage rate (46.5%) occurred during treatment of light, sour, low-in-tar paraffin oil from the Usinskoe field. A relatively smooth increase in the redistributed water content occurred from the anode to the cathode. In contrast, treating heavy, sulfurous, highly resinous paraffin oil from the Yaregskoe field resulted in insignificant

Trim Size: 170mm x 244mm Single Column Loose Ribeiro670117 c09.tex V1 - 12/11/2020 11:53pm Page 219

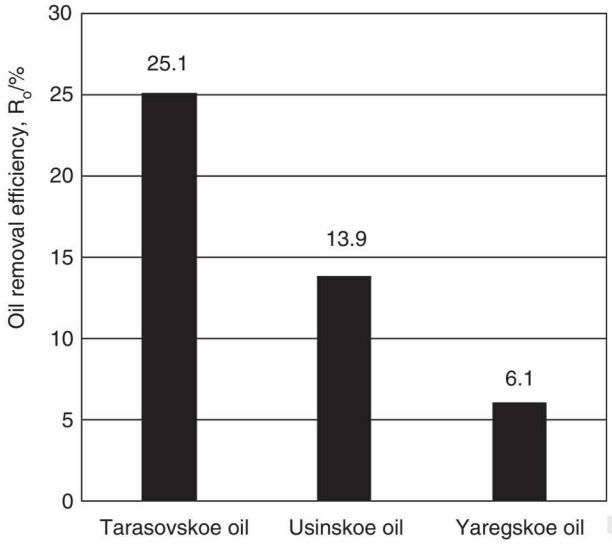

Figure 9.24 Overall electrokinetic treatment efficiency for mantle till loam contaminated with oil from the Tarasovskoe, Usinskoe, and Yaregskoe oil fields.

alteration of the moisture content along the sample axis except for the relatively drained anodic zone.

The most significant remaining oil redistribution occurred in the sample polluted by Tarasovskoe oil, with a decrease in its concentration in the cathode direction. Oil redistribution is insignificant in the case of soil treatment from Yaregskoe oil (see Figure 9.24).

Comparing the treatment effectiveness of various sample zones from different oil types (see Figure 9.23), one can conclude that the anodic zone was purified the best in the case of Usinskoe oil. The other three parts demonstrated a maximum removal rate during the treatment of Tarasovskoe oil. Considering the influence of oil type and hydrocarbon group composition on the oil recovery efficiency in each zone, one can find a positive relation of treatment efficacy in the anodic zone and paraffin percent of the oil (see Figure 9.23a). Also, a decrease in oil removal efficiency was observed in the near-anode and cathodic zones as the oil's resin and asphaltene content grew (Figure 9.23b,d).

The total electrokinetic treatment efficacy was 6.1% in the case of Yaregskoe oil, 13.9% for Usinskoe oil, and 25.1% for Tarasovskoe oil (see Figure 9.24).

Comparing the data on oil recovery rate and hydrocarbon group composition of various oil types (Figure 9.25) demonstrated that the treatment efficiency decreased as oil density grew. Oil removal efficacy declined as well with an increase in resin and asphaltene content in the oil. In contrast, the relation of oil removal rate and paraffin content was not pronounced. Thus, the most efficient electrokinetic treatment occurred in the case of light oils.

Generally, the study shows that the majority of organics, including toxic ones, in soils migrate to some extent in the DC electric field. Most organic compounds in

UNCORRECTED PROOFS

Trim Size: 170mm x 244mm Single Column Loose Ribeiro670117 c09.tex V1 - 12/11/2020 11:53pm Page 220

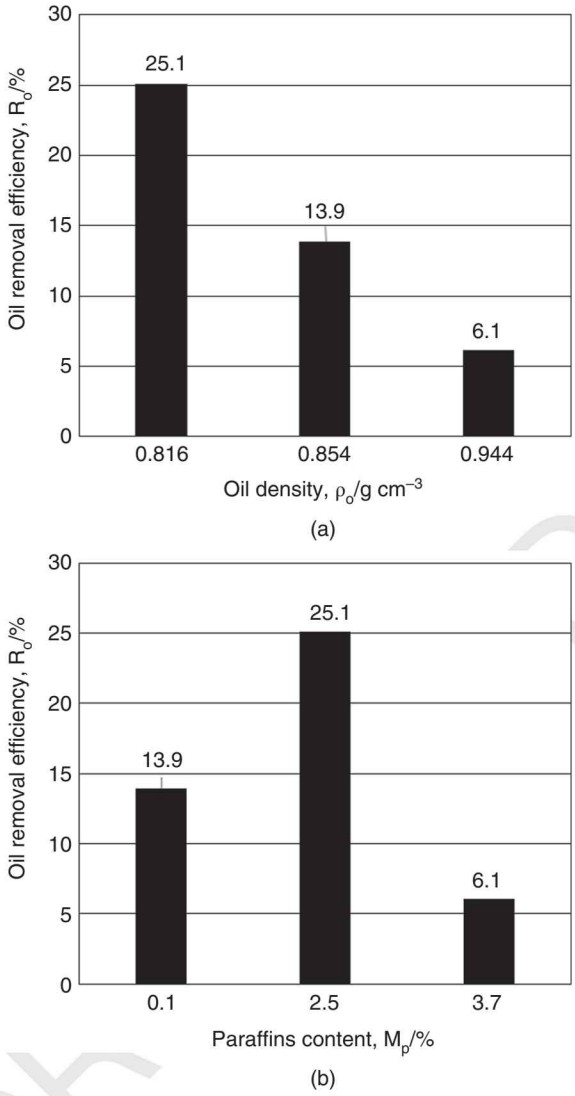

Figure 9.25 Relation of the soil electrokinetic treatment efficiency and the composition and properties of oil: (a) influence of oil density; (b) impact of paraffin percent.

soils are uncharged, so the predominant mechanism of their migration under the voltage gradient is electroosmosis. Some organics can form charged micelles, especially in the presence of surfactants. In that case, the charged micelles migrate by electrophoresis in the cathode (positively charged micelles) or anode (negatively charged micelles) direction. Moreover, the charged organic-metal complexes can move to the corresponding electrode by electromigration. Since no surfactants were used in this study, the predominant mechanism of oil migration in the DC electric field was electroosmosis.

Also, non-polar organics such as crude or industrial oil can migrate in water-saturated soils under a DC electric field by mechanisms other than viscous friction or electroosmotic flow. Those mechanisms include partial oil dissolution, micellization, oxidation-reduction reactions, and thermal influence.

UNCORRECTED PROOFS

Trim Size: 170mm x 244mm Single Column Loose Ribeiro670117 c09.tex V1 - 12/11/2020 11:53pm Page 221

9.10 Conclusions

The research conducted substantiates the development of technological schemes and industrial methods for the electrokinetic treatment of soils polluted by oil and its products. In turn, it will allow purposeful management of the ecological state of soils.

1. The predominant mechanism of oil migration in polluted soils is the electroosmotic movement of small oil droplets alongside the water flow due to viscous friction. An additional oil removal mechanism is oil's partial dissolution in an alkaline medium formed in the cathodic soil zone.
2. The physico-chemical activity of clay minerals determines the development of the soil EDL. The larger the soil EDL parameters, the more efficient the oil removal from this soil.
3. The type, composition, and aging of oil and its products influence the efficiency of electrokinetic treatment of the oil-polluted soil. Removing the aged oil, in which light ends have vaporized, is the most difficult.

Acknowledgments

The authors would like to thank A.M. Abyzova, M.A. Nekrasova, S.L. Polischuk, O.V. Romanyukha, and K.A. Sitar for their valuable contribution to the research presented in this chapter.

List of Abbreviations

API	Unit of relative oil density used by the American Petroleum Institute, API
D^4_{20}	Oil density at 20 °C, g cm^{-3}
D^4_s	Oil density at 15.6 °C (60 °F), g cm^{-3}
E	Voltage gradient, V cm^{-1}
EDL	Electrical double layer
K_a	Soil activity, units
K_f	Degree of fluid saturation, unit fraction
K_h	Hydrophilicity index, units
L_0	Sample length, cm
L/L_0	Relative distance from the anode, unit fraction
LL	Liquid limit, %
m_M	Oil molecular mass, g mol^{-1}
M	Oil component content, % weight
M_c	Clay content, % dry weight
M_e	Percent of a chemical element, % weight
M_p	Paraffin content, % weight
M_s	Sand content, % dry weight
n	Soil porosity, %

UNCORRECTED PROOFS

Trim Size: 170mm x 244mm Single Column Loose Ribeiro670117 c09.tex V1 - 12/11/2020 11:53pm Page 222

P_{EO}	Electroosmotic transport rate, $m^3\ A^{-1}s^{-1}$
PI	Plasticity index, %
R_o	Oil removal efficiency, %
R_w	Soil drainage rate, %
S_o	Relative oil content, % dry weight
t	Time, minutes
t_b	Normal boiling point, °C
W	Moisture content, % dry weight
W_{mmc}	Maximum molecular moisture capacity, % dry weight
W_0	Initial moisture content of soil, % dry weight
W_{sw}	Free-swelling water content, % dry weight
ζ	Electrokinetic potential of soil particles, mV
v	Kinematic viscosity, m^2s^{-1}
ρ_m	Moist soil density, g cm^{-3}
ρ_{ws}	Water density at 15.6 °C (60 °F), g cm^{-3}.

References

1 Trofimov, V.T. and Korolev, V.A. (2012). Engineering protection of territories and building in the system of engineering and environmental protection. *Moscow University Geology Bulletin* 67 (1): 50–55. https://doi.org/10.3103/S0145875212010103.

2 Michel, J., Owens, E.H., Zengel, S. et al. (2013). Extent and degree of shoreline oiling: Deepwater horizon oil spill, Gulf of Mexico, USA. *PLoS One* 8 (6): e65087. https://doi.org/10.1371/journal.pone.0065087.

3 Korolev, V.A. (2001). *The Cleaning of Soils from Pollution*. Moscow, Russia: MAIK/Interperiodica Publishing House [in Russian].

4 Elektorowicz, M. (1994). Bioremediation of petroleum-contaminated clayey soil with pretreatment. *Environmental Technology* 15: 373–380. https://doi.org/10.1080/09593339409385440.

5 Yang, S.-Z., Jin, H.-J., Wei, Z. et al. (2009). Bioremediation of oil spills in cold environments: a review. *Pedosphere* 19 (3): 371–381. https://doi.org/10.1016/S1002-0160(09)60128-4.

6 Couto, M.N.P.F.S., Fritt-Rasmussen, J., Jensen, P.E. et al. (2014). Suitability of oil bioremediation in an artic soil using surplus heating from an incineration facility. *Environmental Science and Pollution Research* 21 (9): 6221–6227. https://doi.org/10.1007/s11356-013-2466-3.

7 Korolev, V.A., Nekrasova, M.A., and Polischuk, S.L. (1997). The role of electrokinetic phenomena in the mechanisms of secondary oil migration. *Oil and Gas Geology* 6: 28–32. [in Russian].

8 Korolev, V.A. (2001). Laws of the electrochemical soils remediation from petroleum pollution. 3rd International Symposium and Status Report on Electrokinetic Remediation (EREM 2001), Karlsruhe, Germany (18–20 April).

UNCORRECTED PROOFS

Trim Size: 170mm x 244mm Single Column Loose Ribeiro670117 c09.tex V1 - 12/11/2020 11:53pm Page 223

9 Korolev, V.A. and Sitar, K.A. (2004). Remediationofoil-pollutedlands. *Ecological Bulletin of the Black-Sea Economical Partnership Research Centres (BEP)* 2: 69–76. [in Russian].

10 Korolev, V.A. and Romanyukha, O.V. (2007). Remediation of oil-polluted soils by the electrochemical lixiviation. 6th Symposium on Electrokinetic Remediation (EREM 2007), Vigo, Spain (12–15 June).

11 Korolev, V.A. (2008). Electrochemical soil remediation from environmental toxicants: results and prospects. *Moscow University Geology Bulletin* 63 (1): 11–18. https://doi.org/10.1007/s11969-008-1002-1.

12 Korolev, V.A., Romanyukha, O.V., and Abyzova, A.M. (2008). Electrokinetic remediation of oil-contaminated soils. *Journal of Environmental Science and Health-Part A: Toxic/Hazardous Substances and Environmental Engineering* 43: 876–880. https://doi.org/10.1080/10934520801974384.

13 Ghazanfari, E., Pervizpour, M., and Pamukcu S. (2012). Mathematical modeling of electrically assisted hydrocarbon transport in porous media. GeoCongress 2012, Oakland, California (25–29 March).

14 Ghazanfari, E., Pamukcu, S., Pervizpour, M. et al. (2014). Investigation of generalized relative permeability coefficients for electrically assisted oil recovery in oil formations. *Transport in Porous Media* 105 (1): 235–253. https://doi.org/10.1007/s11242-014-0368-6.

15 Pamukcu, S., Shrestha, S.R., Ribeiro, A.B. et al. (2016). Electrically induced displacement transport of immiscible oil in saline sediments. *Journal of Hazardous Materials* 313: 185–192. https://doi.org/10.1016/j.jhazmat.2016.04.005.

16 Saichek, R.E. and Reddy, K.R. (2005). Surfactant-enhanced electrokinetic remediation of polycyclic aromatic hydrocarbons in heterogeneous subsurface environments. *Journal of Environmental Engineering and Science* 4 (5): 327–339. https://doi.org/10.1139/s04-064.

17 Cameselle, C. and Reddy, K.R. (2012). Development and enhancement of electro-osmotic flow for the removal of contaminants from soils. *Electrochimica Acta* 86: 10–22. https://doi.org/10.1016/j.electacta.2012.06.121.

18 Pamukcu, S., Filipova, I., and Wittle, J.K. (1995). The role of electroosmosis in transporting PAH compounds in contaminated soils. In: *Proceedings of the Symposium on Electrochemical Technology Applied to Environmental Problems* (eds. E.W. Brooman and J.M. Fenton), 95–12. Reno, Nevada, the USA: The Electrochemical Society, PV.

19 Food and Agriculture Organization of the United Nations. (2014). World reference base for soil resources.

20 Egorov, V.V., Fridland, V.M., Ivanova, E.N. et al. (1977). *Classification and Detection of the USSR Soils*. Moscow, USSR: Kolos [in Russian].

21 Dokuchaev Soil Science Institute (2012). Russian soil classification, 2004. http://infosoil.ru/index.php?pageID=clas04mode (accessed 15 March 2020) [in Russian].

22 Pamukcu, S. (2009). Electrochemical transport and transformations. In: *Electrochemical Remediation Technologies for Polluted Soils, Sediments and Groundwater* (eds. K.R. Reddy and C. Cameselle), 29–64. Hoboken, NJ: Wiley.

UNCORRECTED PROOFS

Trim Size: 170mm x 244mm Single Column Loose Ribeiro670117 c09.tex V1 - 12/11/2020 11:53pm Page 224

23 Shrestha, R.A., Ghazanfari, E., and Pamukcu, S. (2012). Electrically assisted liquid hydrocarbon transport in porous media. *Electrochimica Acta* 86: 185–191. https://doi.org/10.1016/j.electacta.2012.04.077.

24 GOST 25100-2011 (2011). *Soils. Classification*. Moscow: Federal Agency on Technical Regulation and Metrology [in Russian].

25 ISO. (2018). Geotechnical investigation and testing identification and classification of soil - Part 1: Identification and description. EN ISO 14688-1:2018 E.

26 Katschinski, N.A. (1958). *Mechanical and Microaggregate Soil Composition, Methods of Its Study*. Moscow, USSR: USSR AS Publishing House [in Russian].

27 Deng, J., Ma, C., and Yu, H. (2018). Different soil particle-size classification systems for calculating volume fractal dimension – acase study of Pinus sylvestris var. Mongolica in Mu Us sandy land, China. *Applied Sciences* 8 (10): 1872–1885. https://doi.org/10.3390/app8101872.

28 Bolshakov, Y. (1995). *The Capillary Attraction Theory of Oil-and-Gas Accumulation*. Novosibirsk, Russia: RAS Siberian Branch Publishing House [in Russian].

29 Korolev, V.A. and Nesterov, D.S. (2018). Regulation of clay particles charge for design of protective electrokinetic barriers. *Journal of Hazardous Materials* 358: 165–170. https://doi.org/10.1016/j.jhazmat.2018.06.023.

30 Atterberg, A. (1911). Uber die physikalischeBodenuntersuschung and Uber die Plastizität der Tone. *Internationale Mitteilungenfür Bodenkunde* 1: 10–43. [in German].

31 Casagrande, A. (1932). Research on the Atterberg limits of soils. *Public Roads* 13 (8): 121–136.

32 Skempton, A.W. (1953). The colloidal "activity" of clays. 3rd International Conference on Soil Mechanics and Foundation Engineering, Zurich, Switzerland (16–27 August).

33 Elektorowicz, M., Habibi, S., and Chifrina, R. (2006). Effect of electrical potential on the electro-demulsification of oily sludge. *Journal of Colloid and Interface Science* 295: 535–541. https://doi.org/10.1016/j.jcis.2005.08.042.

34 Yukselen-Aksoy, Y. and Kaya, A. (2011). A study of factors affecting on the zeta potential of kaolinite and quartz powder. *Environmental Earth Sciences* 62 (4): 697–705. https://doi.org/10.1007/s12665-010-0556-9.

35 Miroshnik, A., Ghazanfari, E., Shrestha, R.A. et al. (2012). Electrically induced transport of immiscible hydrocarbons in clay soil. Proceedings of GeoCongress 2012, Oakland, California (25–29 March).

36 Taslimi Taleghani, S., Fellah Jahromi, A., and Elektorowicz, M. (2019). Electro-demulsification of oil-in-water suspensions enhanced with implementing various additives. *Chemosphere* 233: 157–163. https://doi.org/10.1016/j.chemosphere.2019.05.161.

37 Tang, J., Lu, X., Sun, Q. et al. (2012). Aging effect of petroleum hydrocarbons in soil under different attenuation conditions. *Agriculture, Ecosystems & Environment* 149: 109–117. https://doi.org/10.1016/j.agee.2011.12.020.

UNCORRECTED PROOFS

Trim Size: 170mm x 244mm Single Column Loose Ribeiro670117 c09.tex V1 - 12/11/2020 11:53pm Page 225

38 API. (2017). Standard test method for density, relative density, or API gravity of crude petroleum and liquid petroleum products by hydrometer method. ASTM D1298 − 12b.

39 Zhao, M., Wang, X., Liu, D. et al. (2020). Insight into essential channel effect of pore structures and hydrogen bonds on the solvent extraction of oily sludge. *Journal of Hazardous Materials* 389: 121826. https://doi.org/10.1016/j.jhazmat.2019.121826.

UNCORRECTED PROOFS

UNCORRECTED PROOFS

Trim Size: 170mm x 244mm Single Column Loose Ribeiro670117 c10.tex V1 - 12/11/2020 11:54pm Page 227

10

Nanostructured TiO_2-Based Hydrogen Evolution Reaction (HER) Electrocatalysts: A Preliminary Feasibility Study in Electrodialytic Remediation with Hydrogen Recovery

Antonio Rubino[1], Joana Almeida[2], Catia Magro[2], Pier G. Schiavi[1], Paula Guedes[2], Nazare Couto[2], Eduardo P. Mateus[2], Pietro Altimari[1,3], Maria L. Astolfi[1] Robertino Zanoni[1], Alexandra B. Ribeiro[2], and Francesca Pagnanelli[1,3]

[1] *Department of Chemistry, Sapienza University of Rome, Rome 00185, Italy*
[2] *CENSE – Center for Environmental and Sustainability Research, Department of Environmental Sciences and Engineering, NOVA School of Science and Technology, NOVA University Lisbon, Caparica 2829-516, Portugal*
[3] *Eco Recycling Srl, Rome 00156, Italy*
[4] *Instituto de Tecnologia Química e Biológica António Xavier, NOVA University Lisbon, Oeiras 2780-157, Portugal*

10.1 Introduction

The global growth in demand for energy in recent decades and environmental issues related to climate change led have to increasing attention on sustainable energy production [1]. In this scenario, hydrogen as an energy vector represents an attractive carbonless fuel. The only reaction product resulting from its oxidation is pure water, with little or null environmental impact [2]. Furthermore, thanks to its high versatility, it can be used directly in internal combustion engines [3] or converted into electricity using fuel cells [4].

On the other hand, even though it is one of the most abundant elements in the universe, the available hydrogen is almost always combined with other elements, such as carbon in hydrocarbons, oxygen in water, and both in biomass [5]. This aspect highlights that hydrogen is not a primary energy source; on the contrary, it needs to be produced, which requires energy consumption. Accordingly, producing hydrogen in a clean, sustainable, and economical way is a significant challenge [6].

Hydrogen can be produced from sources including both renewables (hydro, wind, solar, biomass, geothermal) and non-renewables (coal, natural gas, nuclear). To date, it is almost exclusively produced by reforming hydrocarbons (~96%) [5], using a well-mastered industrial process that remains less costly than water electrolysis [7]. Here, cost-effectiveness can be implemented, guaranteeing minimized overpotentials to sustain the electrolysis (i.e. it is preferable to operate under strongly acidic or alkaline conditions to minimize them) and contextually improving the efficiency of the energy conversion (i.e. increased catalytic activity of the electrodic materials)

Electrokinetic Remediation for Environmental Security and Sustainability, First Edition.
Edited by Alexandra B. Ribeiro and M.N.V. Prasad.
© 2021 John Wiley & Sons Ltd. Published 2021 by John Wiley & Sons Ltd.

UNCORRECTED PROOFS

Trim Size: 170mm x 244mm Single Column Loose Ribeiro670117 c10.tex V1 - 12/11/2020 11:54pm Page 228

AQ1

[8]. Thus it appears clear that a primary effort should focus on developing effective electrocatalysts.

The reactions involved in water electrolysis are the hydrogen evolution reaction (HER) and the oxygen evolution reaction (OER) for the cathode and anode, respectively. To date, the benchmark catalysts for OER are Ir/Ru-based compounds, while Pt-group metals are the most effective catalysts for HER [9]. The principal limit to the widespread use of these electrodic materials is related to their high cost and low abundance. This is why considerable research effort has been dedicated to developing highly efficient, non-precious-metal–based electrocatalysts [10, 11]. Most of these low-cost electrocatalysts show high activity in acidic media but are inactive or unstable in alkaline electrolytes and vice versa [12, 13]. As previously highlighted, to guarantee low overpotentials, it would be preferable to operate in strongly acidic or alkaline conditions. Consequently, when the two electrodes operate in the same pH range, as in conventional electrolytic cells, minimized overpotential for one of them would correspond to the ineffectiveness, or inactivation, of the other.

Minimized overpotentials can also be achieved by using nanostructured electrocatalysts instead of bulk materials [14, 15]. Transition to nanoscale, thanks to the strong reduction of dimensions, results in materials that exhibit novel and unique catalytic, electronic, magnetic, optoelectronic, and mechanical properties [16]. Based on that, the development of low-cost nanostructured electrocatalysts would contribute to further minimizing overpotential losses and, at the same time, increasing catalytic activity thanks to their characteristic high specific surfaces.

This strategy would be particularly appealing in conventional processes where hydrogen is produced as a byproduct. Here it can be recovered and used in tandem power production units to minimize the original cost and improve the overall process's sustainability. An example is offered by electrodialytic (ED) remediation. As reported by Magro et al. [17], the hydrogen byproduct in electrodialytic remediation can be directly used to produce power with a tandem proton exchange membrane fuel cell (PEMFC).

10.1.1 Electrokinetic Technologies: Electrodialytic Ex Situ Remediation

Electrokinetic technologies are generally used to carry out in situ remediation, removing organic and/or inorganic contaminants from soils or other porous matrices (sewage sludge, fly ash, etc.) that exhibit low permeability [18]. Such technologies consist of a direct current flow between two electrodes placed in the soil matrix, with the resulting electric field promoting contaminant mobilization [19]. During the current flow, transport phenomena such as electromigration, electroosmosis, and electrophoresis are involved (e.g. inorganic contaminants are transported as ions through electromigration, while organic contaminants and uncharged inorganic species are primarily transported by electroosmosis toward the electrodes).

Electrodialytic soil remediation is a specific ex situ electrokinetic technology developed for removing heavy metals from polluted soils. It combines the transport mechanisms involved during EK processes with the principles of electrodialysis [20]. As shown in Figure 10.1, electrodialytic cells are characterized by three

UNCORRECTED PROOFS

Trim Size: 170mm x 244mm Single Column Loose Ribeiro670117 c10.tex V1 - 12/11/2020 11:54pm Page 229

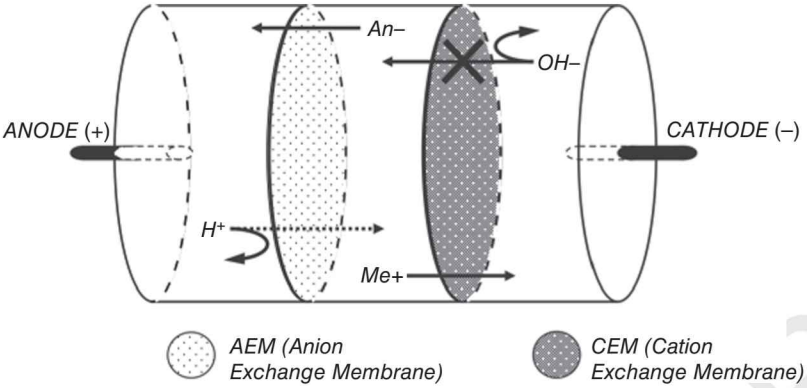

Figure 10.1 Schematic representation of a 3C ED cell during electric current flow.

compartments (3C), resulting from the use of ion-exchange membranes to separate the electrode compartments from the soil placed in the central compartment. According to the cell scheme, under the current flow, cations located in the central compartment move through the cationic exchange membrane (CEM) toward the cathode, while in the opposite direction, anions pass through the anionic exchange membrane (AEM) toward the anode, so they are separated in concentrated solutions [21, 22]. In addition to the transport mechanisms, considering the non-ideal selectivity of AEM to H^+ ions (i.e. H^+ pass through the AEM toward the central compartment), during the current flow, an acidic front forms toward the cathode, contributing to dissolving contaminants from the soil [20]. A further crucial factor in contaminant mobilization is stirring [23]. Together with the costs related to the power supply, stirring is one of the primary factors limiting the real use of such technology in remediation treatments.

To address this issue, as previously mentioned, a promising strategy to minimize overall cost can be directly derived from the primary cathodic reactions involved during the process:

$$2H^+ + 2e^- \rightarrow H_{2(g)} \tag{10.1}$$

$$2H_2O_{(l)} + 2e^- \rightarrow H_{2(g)} + 2OH^- \tag{10.2}$$

Here, the recovery of hydrogen, which can be kept as a valuable byproduct or directly used in tandem to produce power, would improve the sustainability of the original remediation process.

From this perspective, it is worth noting that during the current flow, according to the 3C ED cell scheme shown in Figure 10.3, fast acidification and alkalinization of the anodic and cathodic compartments, respectively, occurs [21]. Thus, the 3C ED cell scheme offers a significant advantage with respect to conventional electrolyzers, allowing the use of different electrocatalysts that are most effective when operated in different pH ranges. In addition, the fast pH variations in the electrodic compartments would contribute to minimizing the overpotential required to sustain electrolysis.

UNCORRECTED PROOFS

Trim Size: 170mm x 244mm Single Column Loose Ribeiro670117 c10.tex V1 - 12/11/2020 11:54pm Page 230

In spite of this, as reported by several authors in the available literature [20, 24–26], ED remediation treatments are generally carried out using the same commercial electrocatalyst (metal- and/or metal oxides-based) for both anode and cathode, in a symmetric electrode cell scheme, thus not fully exploiting the 3C ED cell advantages. At the same time, it is worth noting that this seems to be determined primarily by the tendency to prefer materials that can guarantee high stability with respect to the reaction environment and thus, from a scalability perspective, high electrocatalyst durability.

10.1.2 Nanostructured TiO_2 Electrocatalysts Synthesized Through Electrochemical Methods

In recent decades, scientific interest has grown regarding the study of nanomaterials and their applications. This is largely due to the novel and unique properties that nanostructures exhibit, compared to bulk materials [16], such as the high surface-to-volume ratio.

Nanostructured materials are synthesized through a large variety of methods including lithography [27], wet chemical techniques in microemulsion systems [28], electrochemical processes [29], photochemical processes [30], and soft chemical routes that include sol–gel techniques [31] and wet impregnation [32].

Of these, electrochemical synthesis routes guarantee precise control over the sizes and morphologies of the nanostructures [33–35], characteristics that primarily determine the catalytic activity [36]. These include *anodization*, where the electrochemical oxidation of metal substrates leads to the growth of nanostructured oxides and the electrodeposition of nanoparticles, namely the electrochemical reduction of ions over the working electrode. Both strategies are particularly effective when supported nanostructures over conductive substrates are needed, as in the case of TiO_2 nanotube (NT)-based electrode synthesis.

In reason of the nanotubular architecture, TiO_2 NTs are characterized by outstanding charge transport and carrier lifetime properties [37], which makes this material particularly appealing in advanced applications including sensors [38], dye-sensitized solar cells [39], photoelectrochemical systems for H_2 production [40], photocatalytic systems for CO_2 reduction [41], energy storage devices [42], supercapacitors [43], and alkaline electrolyzers [44]. It is worth noting at this stage that although the interest in TiO_2 is primarily due to its semiconductive features, which make it one of the most investigated photocatalysts, characteristics such as its chemical stability, non-toxicity, and raw material abundance, have led to growing interest in TiO_2 as a sustainable material in various applications [44].

TiO_2 NTs are generally synthesized in two-electrode cells, where the anodization of titanium sheets is carried out using a noble metal catalyst as a counter-electrode (e.g. Pt mesh as a cathode). The most diffused anodization method is based on double-step potentiostatic anodization where the sequence of two anodization steps, separated by the removal of the first formed disordered NT layer, guarantees the grown of highly ordered NTs during the second anodization step [45, 46].

UNCORRECTED PROOFS

Trim Size: 170mm x 244mm Single Column Loose Ribeiro670117 c10.tex V1 - 12/11/2020 11:54pm Page 231

On the contrary, there are very few works where the ordered NTs growth has been reached through single-step anodization [47, 48]. Among them, needs to be highlighted works where the authors proposed single-step methods characterized by the linear growth of the cell voltage in the early stage of the process followed by the conventional potentiostatic period [49], in agreement with our previous reports [50, 51]. It is worth noting that single-step methods improve the sustainability of the catalyst production process, guaranteeing two fewer operations and, consequently, less consumption of reagents in addition to energy savings.

By modulating parameters like cell voltage, pH, electrolyte composition, and time of electrolysis, anodization methods guarantee to control characteristics such as NT diameter and length [52–57]. In this regard, it is worth underlining that in many electrochemical reactions, electrolyte diffusion can be tuned by tailoring the pore sizes of the nanoporous electrocatalyst [58].

Titanium dioxide exists in three different crystalline phases – anatase, rutile, and brookite [59] – while the oxide resulting from anodization is generally characterized by an amorphous nature [60]. According to the specific application, crystallization of the amorphous oxide may be required (e.g. anatase is the most photoactive phase, while rutile is the thermodynamically stable phase). Some works report on partial crystallization achieved already during anodization for certain electrolyte compositions and anodization potentials [61, 62], anyway crystallization is generally promoted by thermal oxidation treatments at the end of the anodization [63–65]. Concerning this latter aspect, annealing temperature and duration are the parameters that allow control over the crystal phases ratio so that an increase in temperature and duration results in the transition from the anatase phase to the rutile phase [66]. Furthermore, annealing treatments can be carried out in controlled atmospheres, like argon, air, or nitrogen flow [53, 67], guaranteeing the contextual *doping* (i.e. introduction of foreign atoms to induce defects in TiO_2 lattice structure) of the NTs [68] and so contributing to improving the TiO_2 characteristics in relation to the specific application. Most recently, other approaches based on Ti^{3+} self-doping have been proposed [44, 69], including a strategy based on the electrochemical route [70]. Specifically, this consists of a facile electrochemical reduction to induce Ti^{3+} formation into TiO_2 lattice structure, which, from a scalability perspective, would allow closing in situ the synthesis loop of the nanostructured electrocatalyst at the end of the anodization.

Feng et al. demonstrated that the presence of low-coordinated Ti^{3+} ions would enhance the catalyst's electrical conductivity and favor the desorption of generated hydrogen [44], resulting in a low-cost and highly active HER catalyst to be used in alkaline media.

10.2 Case Study

10.2.1 Aim and Scope

The real use of technology such as electrodialytic remediation is primarily limited by the energy cost of sustaining the overall process. One of the strategies proposed

UNCORRECTED PROOFS

Trim Size: 170mm x 244mm Single Column Loose Ribeiro670117 c10.tex V1 - 12/11/2020 11:54pm Page 232

to overcome this limit is based on energy savings through the recovery of the hydrogen byproduct. To this purpose, it has been previously highlighted that 3C ED cells would offer the great advantage of having the electrodic compartments at different pH values, allowing the use of electrocatalysts that are effective when operating in tandem in different pH ranges. According to that, it is well recognized that benchmark catalysts for OER are Ir-/Ru-based compounds, while Pt-group metals are the most effective catalysts for HER.

As reported by several authors in the available literature, ED remediation treatments are instead carried out using commercial electrodes, like Ti/MMO (mixed metal oxides, Ti-/Ir-/Ru-based), for both anode and cathode. As highlighted earlier, these are benchmark catalysts for only one of the two primary reactions involved (i.e. OER) in ED remediation.

With the aim to improve the sustainability of the overall ED remediation process, the scope of the present work has been the development of non-precious-metal–based, highly efficient HER electrocatalysts that can be used to improve hydrogen production during ED remediation. To this purpose, the electrochemical synthesis of nanostructured titania-based electrodes offers the advantage of a versatile synthesis method, allowing control over the characteristics that primarily determine the electrocatalyst activity and facile scalability of the production process.

10.2.2 Experimental

10.2.2.1 TiO_2 Based Electrocatalyst Synthesis and Characterization

10.2.2.1.1 TiO_2 NTs through Single-Step Anodization

Electrocatalyst production is based on a single-step anodization method developed [50] and optimized in our previous works [51], briefly summarized here.

The anodizations are carried out in a two-electrode jacketed cell, kept at room temperature (24.5 ± 0.5) °C and magnetically stirred. The two electrodes are both titanium planar electrodes (Alfa Aesar 99.5%, annealed, thickness 0.25 mm) and are connected to a power supply (Aim-TTi CPX200DP DC power supply, dual outputs, 2×60 V/10A 180 W). The electrolyte employed is ethylene glycol (Alfa Aesar, 99 + %) based, containing $0.3\%_{wt}$ NH_4F (Alfa Aesar, 98% minimum) and $6\%_{v/v}$ H_2O. The cell voltage (V) is imposed in two stages: first, linear growth ($0.05\ V\ s^{-1}$) up to 60 V, reached which, it goes on in potentiostatic regime for 420 seconds.

10.2.2.1.2 Anatase TiO_2

To promote the formation of crystal phases, amorphous titania resulting from anodization is thermally treated in a muffle furnace (Nabertherm B410, Tmax 1100 °C, 1.2 KW). The annealing treatment adopted here was optimized for exclusive anatase formation in our previous report [50]. Briefly, the treatment starts with a heating rate of $8\ °C\ min^{-1}$ up to 580 °C, reached which the annealing proceeds at constant temperature for 60 minutes. At the end of the treatment, the samples are immediately ejected and cooled at ambient temperature.

UNCORRECTED PROOFS

Trim Size: 170mm x 244mm Single Column Loose Ribeiro670117 c10.tex V1 - 12/11/2020 11:54pm Page 233

10.2.2.1.3 Black TiO_2

Black TiO_2 is synthesized through an electrochemical post-treatment carried out at the end of the anodization in a two-electrodes cell. The TiO_2-based electrode resulting from the anodization is used as a cathode, with a titanium planar electrode (Alfa Aesar 99.5%, annealed, thickness 0.25 mm) as an anode. Electrodes are connected to a power supply (Aim-TTi CPX200DP DC power supply, dual outputs, 2×60 V/10 A 180 W) in $NaNO_3$ 0.01 M (Carlo Erba Reagent, $\geq 99.5\%$) at a constant current density of 20 mA cm^{-2} for 30 minutes.

10.2.2.1.4 Electrode Characterization

Morphological characterization of the synthesized electrodes is performed through field emission scanning electron microscopy (FE-SEM Zeiss Auriga), equipped with an energy-dispersive X-ray analyzer (EDX Bruker QUANTAX 123 eV) used for the elemental analysis of the nanostructures.

Diffuse reflectance spectroscopy (SHIMADZU UV-2600, 360–740 nm) is used to preliminary characterize the black TiO_2 light absorption.

The surface atomic composition of the synthesized electrodes was analyzed by X-ray photoelectron spectroscopy (XPS) using a modified Omicron NanoTechnology MXPS system. Experimental spectra were theoretically reconstructed by fitting the peaks to symmetric Voigt functions and the background to a Shirley or a linear function. XPS atomic ratios (~10% associated error) between relevant core lines were estimated from experimentally determined area ratios corrected for the corresponding theoretical cross-sections and for a square root dependence of the photoelectrons kinetic energies. All the samples were mounted on a magnetic stainless steel tip with conductive adhesive tape. The fit procedure was optimized, and peak assignments were given by reference to previous literature.

10.2.2.2 ED Experiments

10.2.2.2.1 ED Cell Configuration

The electrolytic cell used to carry out the tests is a three-compartment electrodialytic cell (Figure 10.1). In this configuration, anion (Ionics, AEM-AR204 SZRA B02249C) and cation exchange membranes (Ionics, CEM-CR67 HUY N12116B) are placed to separate the central compartment from the anodic and cathodic sides, respectively. The cell is made of Plexiglas with an 8 cm internal diameter. Each compartment is 5 cm long.

The anolyte and catholyte used in all the ED tests described were $NaNO_3$ 0.01 M (Carlo Erba Reagent, $\geq 99.5\%$), 250.0 ml for each compartment. The electrodes were placed 12.5 cm apart and connected to a power supply (Hewlett Packard E3612A, Palo Alto, USA).

All the electrodic configurations tested, listed in Table 10.1, foresee using commercial 5 cm Ti/MMO rods (Grønvold & Karnov A/S, Denmark - Ø 3 mm) as anodic material.

Blank Tests Preliminary blank tests were carried out to evaluate the hydrogen production rate of the cathodes listed in Table 10.1. Here, the central compartment

UNCORRECTED PROOFS

Trim Size: 170mm x 244mm Single Column Loose Ribeiro670117 c10.tex V1 - 12/11/2020 11:54pm Page 234

Table 10.1 Electrodic configurations tested in the ED cell.

	Electrodes	
Electrodic configuration	**Anode**	**Cathode**
S	Ti/MMO	Ti/MMO
A	Ti/MMO	Anatase TiO_2
B	Ti/MMO	Black TiO_2

was filled with tap water and 0.3 g of NaCl (Merck, Reag. Ph Eur). The experiment duration was fixed at 20 minutes, and a constant current flow was fixed in all the experiments at a current density of 21.2 mA cm^{-2}. The experiments were carried out in two replicates for each electrodic configuration.

The H_2 production rate was evaluated by connecting a volumetric variation indicator to the cathodic compartment outlet and registering the volume variation during the current flow.

ED Remediation Tests ED remediation experiments were carried out, investigating the electrodic configurations S and B listed in Table 10.1, in two replicates for each condition.

With respect to the blank tests, the cell configuration differs only for the central compartment, where the soil matrix (remediation target) is dissolved. Specifically, mine tailings residue from the Panasqueira mine in Covilhã, Portugal, referred to as MTAW (Mine Tailings As W), was dissolved in tap water with a solid/liquid ratio 1:9, and then 11.0 g of NaCl (Merck, Reag. Ph Eur) were added. The experiments' duration was set to 120 hours (5 days), while the current density was 21.2 mA cm^{-2}.

At the end of each experiment, liquid samples of the three compartments, referred to as ANOLYTE, CATHOLYTE, and CC ELECTROLYTE, were collected from the anodic, cathodic, and central compartment, respectively. The AEM and CEM membranes, as well as the Ti/MMO anodes, were leached in HNO_3 1.0 M (Panreac, Reag. Ph Eur) for 24 hours, after which a liquid sample of the relative leach liquor was collected (referred to as AEM, CEM, and ANODE respectively). At the end of the experiment, the solid fraction of the central compartment was first filtered and then dried for 24 hours, after which it was dissolved in 12 ml aqua regia with a solid-to-liquid ratio of 1:24 and stirred for 48 hours on a shaking table. The resulting liquid sample was collected (referred to as START MTAW).

Total concentrations of As, Cu, Sn, and W were determined through inductively coupled plasma with optical emission spectrometry (ICP–OES, Vista MPX CCD Simultaneous; Varian, Victoria, Mulgrave, Australia) in axial view mode and equipped with a cyclonic spray chamber. Here, radiofrequency power of 1.0 kW, plasma gas flow rate of 15.0 l min^{-1}, auxiliary gas flow rate of 1.5 l min^{-1}, and nebulizer gas flow rate of 0.75 l min^{-1} were used as operational conditions, as previously reported [71]. Y was chosen as an internal standard for all the measurements to

UNCORRECTED PROOFS

Trim Size: 170mm x 244mm Single Column Loose Ribeiro670117 c10.tex V1 - 12/11/2020 11:54pm Page 235

control the nebulizer efficiency. The following wavelengths (nm) were used: As 188.980, Cu 324.754, Sn 189.927, W 239.708, and Y 371.029.

All calibration standard solutions for ICP-OES were prepared from a multi-element standard solution ($1.000 \pm 0.005\,\mathrm{mg\,l^{-1}}$ As, Cu, Sn, and W; Ultra Scientific/Agilent Technologies, North Kingstown, RI, USA) by dilution with 2%v/v HNO_3 (according to the acid percentage in the samples) in deionized water. The limits of detection (LODs) were calculated based on $3.3\,\mathrm{SD} \cdot m^{-1}$ of 10 blanks, where m is the slope of the calibration curves and SD is the standard deviation, multiplied by the dilution factor used for sample preparation. LODs for As, Cu, Sn, and W were, respectively, 0.04, 0.02, 0.05, and $0.04\,\mathrm{mg\,l^{-1}}$.

10.2.3 Discussion

10.2.3.1 Blank Tests: Electrocatalyst Effectiveness toward HER

The first set of blank tests was carried out to evaluate the possibility of using non-commercial TiO_2-based electrodes as effective HER catalysts. To this purpose, anatase TiO_2 and black TiO_2 planar electrodes were synthesized and then used in comparison to commercial Ti/MMO rods.

The synthesized electrodes are characterized by an ordered nanotubes layer ~2 μm thick with inner tube diameters ≥50 nm, as FE-SEM images collected at the end of the anodization show (Figure 10.2). Figure 10.3 shows the equivalent absorption spectra collected for amorphous TiO_2 (a) achieved at the end of the anodization, and black TiO_2 (b) synthesized through a further electrochemical reduction step after the anodization. With respect to the amorphous TiO_2, black TiO_2 is characterized by a higher light absorption across the visible region ($\lambda > 400$ nm), characteristic of the

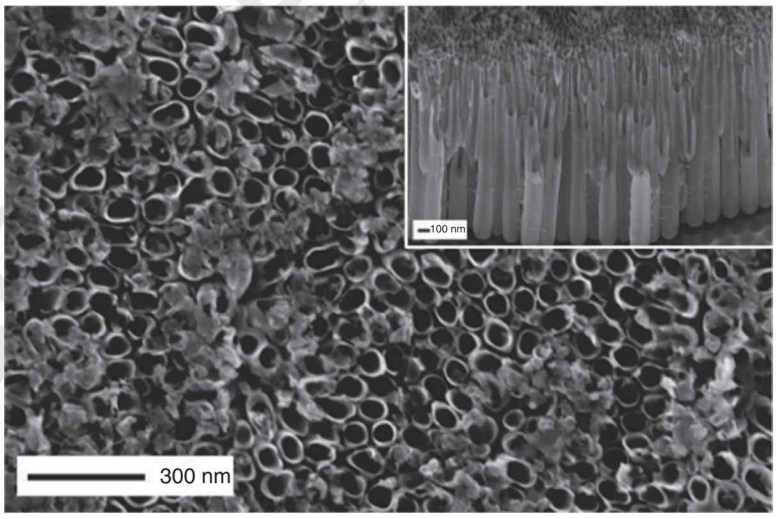

Figure 10.2 FE-SEM images. Top view of the TiO_2 NTs-based electrodes collected at the end of the anodization. The insert represents the corresponding cross-sectional view.

UNCORRECTED PROOFS

Trim Size: 170mm x 244mm Single Column Loose Ribeiro670117 c10.tex V1 - 12/11/2020 11:54pm Page 236

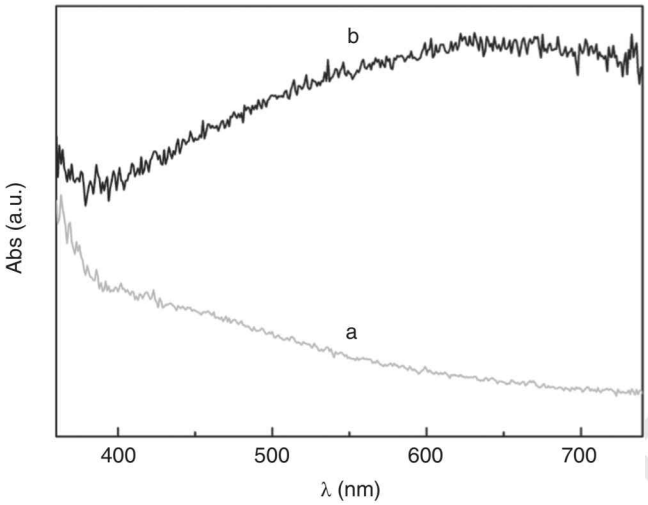

Figure 10.3 Equivalent absorption spectra from DRS analysis. (a) Amorphous TiO_2; (b) black TiO_2.

Ti^{3+} state's formation [72, 73]. Black TiO_2 was further characterized by XPS analysis. The analysis was performed in comparison to anatase TiO_2, achieved after the thermal treatment following the anodization, to emphasize differences in the Ti^{3+} states among the two synthesized electrocatalysts. As shown in Figure 10.4, in black TiO_2 at ~457 eV, a further peak is observable. This is attributable to the presence of Ti^{3+} states characteristic of black TiO_2 [69, 74]. This evidence confirms the effectiveness of the strategy based on the electrochemical closed-loop synthesis for Ti^{3+}-based catalyst production.

The results of the blank tests reported in Figure 10.5 show that black TiO_2 is the electrocatalyst characterized by the highest H_2 production rate, followed by anatase TiO_2 and then by the commercial Ti/MMO. Comparing the synthesized electrocatalysts, the improved performance registered by black TiO_2 can be attributed to the previously mentioned Ti^{3+} state and the formation of contextual oxygen vacancies, which significantly improve the catalytic activity [44, 75, 76].

10.2.3.2 ED Remediation for Sustainable CRMs Recovery

Based on the results of the blank experiments, the ED remediation experiments shown in this section were carried out, comparing the synthesized black TiO_2 and commercial Ti/MMO electrodes. The electrodic configurations tested were S and A (Table 10.1).

The ED remediation experiments performed fall in the researchers' exchange program within the activities of the e.THROUGH project (H2020-MSCA-RISE-2017, GA778045). Briefly, the aim of the project is to tackle EU dependency on Critical Raw Materials (CRMs) through strategies based on sustainable primary mining, recovery from secondary resources, and recycling. CRMs recovery in ED remediation of mine tailings residue is an example. This strategy prevents environmental issues caused by

UNCORRECTED PROOFS

Trim Size: 170mm x 244mm Single Column Loose Ribeiro670117 c10.tex V1 - 12/11/2020 11:54pm Page 237

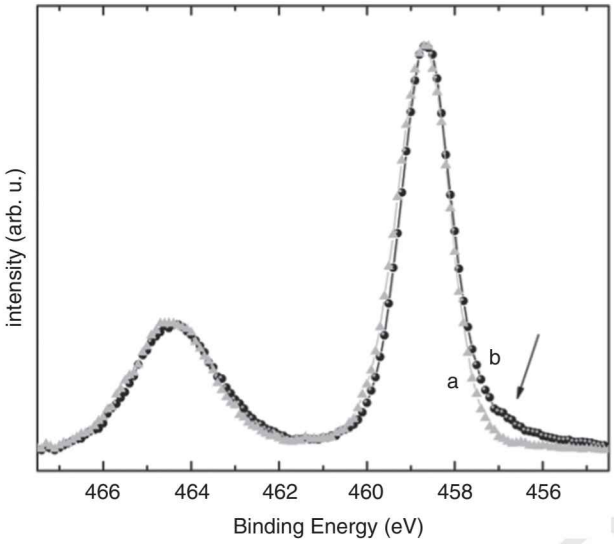

Figure 10.4 XPS spectra in the Ti 2p region: (a) anatase TiO_2 (light gray triangle); (b) black TiO_2 (black dot). The arrow highlights the peak in black TiO_2 attributable to Ti^{3+} states.

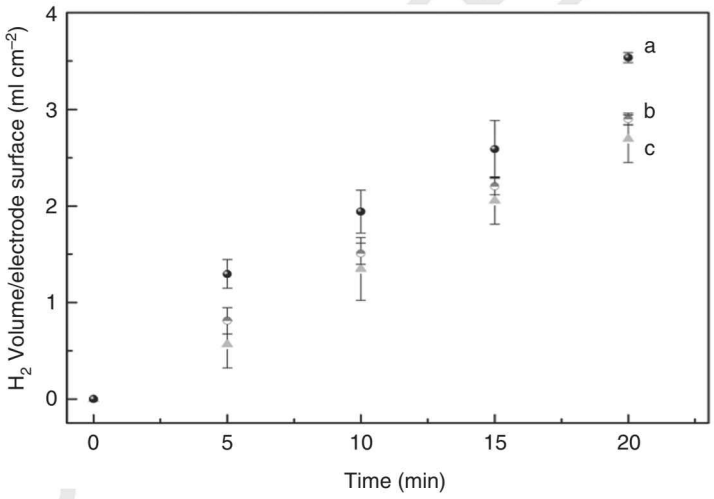

Figure 10.5 Blank experiments: evaluation of the H_2 production rate. (a) Black TiO_2; (b) anatase TiO_2; (c) commercial Ti/MMO.

open dump storage through the remediation and contextually exploitation of mine tailings residue as a secondary source of CRMs.

The mine tailings residue used was collected at the Panasqueira mine, one of the primary deposits of Sn and W in Europe in addition to secondary Cu production. The mine tailings residue, which is confined in open landfills, contains around 30% As due to the presence of arsenopyrite.

UNCORRECTED PROOFS

Trim Size: 170mm x 244mm Single Column Loose Ribeiro670117 c10.tex V1 - 12/11/2020 11:54pm Page 238

The ED remediation aimed at extracting W (as valuable CRM) and As (as remediation target). It is worth noting that the reduction of the heavy metals content in the treated matrix would allow its further reuse as inert material for building construction, further improving the overall sustainability of the remediation process. From this perspective, the extraction of Sn and Cu as value-added products was also evaluated. Based on previous experiences in ED remediation of mine tailings residue with Ti/MMO electrodes, the duration of the experiments at 100 mA employing Ti/MMO rods 5 cm long (i.e. 21.2 mA cm^{-2}) was fixed to a minimum of five days. This was primarily due to the high variability in the composition of the treated matrix: shorter durations that would not have guaranteed appreciable extractions, especially for the CRM target (i.e. W).

At the same time, according to the exchange program schedule, it is worth noting at this stage that the black TiO_2 electrocatalysts available to use in ED remediation were not specifically synthesized, taking into account the minimum time and current required to guarantee appreciable extraction. As a consequence, the maximum electrodic surface of the available black TiO_2 electrocatalysts was ~4 cm^2. Accordingly, at 21.2 mA · cm^{-2} current density, the resulting current flow was approximately equal to 85 mA. In these conditions, measuring the ED remediation time of the experiments performed in terms of the amount of transferred charge, it would be equal to 36 720 C for black TiO_2 experiments versus 43 200 C for Ti/MMO : ~15% less for black TiO_2. Consequently, in evaluating the data, it must be taken into account that the 15% difference in the amount of transferred charge (Q) inevitably affects extraction efficiency.

Table 10.2 shows the pH behavior during the ED remediation experiments, measured for each compartment before starting the current flow and at the end of the experiments. As expected, despite the electrocatalyst used and according to the 3C ED cell scheme (Figure 10.1), acidification and alkalization of the anodic and cathodic compartments took place, respectively, as well as the acidification of the central compartment [77].

The target metals distribution at the end of the ED remediation experiments (Tables 10.3 and 10.4) evidenced the high variability of the treated mine tailings residue, as confirmed by comparing the start metal contents. Figure 10.6 shows the extraction efficiencies for the target metals using the two kinds of electrocatalysts tested. The first evidence is for Sn and W, which were extracted only in the black TiO_2 experiments: 5.8 and 37.3%, respectively. With Ti/MMO, they were both less

Table 10.2 pH behavior in the 3C ED cell during the performed ED remediation experiments.

pH	Anolyte	Catholyte	CC electrolyte
Start	5.70 ± 0.30	5.70 ± 0.30	6.80 ± 0.50
End black TiO_2	1.45 ± 0.05	13.60 ± 0.10	1.90 ± 0.50
End Ti/MMO	1.03 ± 0.03	13.23 ± 0.13	1.83 ± 0.07

UNCORRECTED PROOFS

Trim Size: 170mm x 244mm Single Column Loose Ribeiro670117 c10.tex V1 - 12/11/2020 11:54pm Page 239

Table 10.3 ICP-OES analysis results.

	As (mg/kg)		Cu (mg/kg)		Sn (mg/kg)		W (mg/kg)	
	Mean	SD[a)]	Mean	SD[a)]	Mean	SD[a)]	Mean	SD[a)]
Final MTAW	1711	450	518	62	47.1	0.3	55.2	0.5
CC electrolyte	14.8	0.4	50	37	0.26	0.29	2.1	1.9
CEM	531	210	396	130	2.04	0.37	27.6	4.1
Catholyte	55	74	1.5	1.5	0.29	0.34	1.34	0.73
AEM	18	15	2.17	0.78	0.32	0.22	0.68	0.17
Anolyte	193	81	6.94	0.18	< LOD[b)]	< LOD[b)]	0.92	0.29
Anode	1.2	1.1	0.41	0.58	0.01	0.01	0.03	0.04
Start MTAW	2520	240	975	160	50.0	0.1	87.8	2.9

Target metal concentrations at the end of the electrodialytic remediation experiments using black TiO_2 (Q = 36 720 C).
a) Standard deviation.
b) Limit of detection.

Table 10.4 ICP-OES analysis results.

	As (mg/kg)		Cu (mg/kg)		Sn (mg/kg)		W (mg/kg)	
	mean	SD[a)]	mean	SD[a)]	mean	SD[a)]	mean	SD[a)]
Final MTAW	2180	290	298	76	48.4	6.0	127	61
CC electrolyte	428	58	210	3	< LOD[b)]	< LOD[b)]	< LOD[b)]	< LOD[b)]
CEM	1230	550	174	76	< LOD[b)]	< LOD[b)]	< LOD[b)]	< LOD[b)]
Catholyte	87	33	3.4	1.6	< LOD[b)]	< LOD[b)]	< LOD[b)]	< LOD[b)]
AEM	15.3	4.7	4.7	1.0	0.48	0.27	< LOD[b)]	< LOD[b)]
Anolyte	107	1	24.3	0.2	< LOD[b)]	< LOD[b)]	< LOD[b)]	< LOD[b)]
Anode	0.31	0.01	0.05	0.00	< LOD[b)]	< LOD[b)]	< LOD[b)]	< LOD[b)]
Start MTAW	4050	240	715	6	48.9	6.2	127	60

Target metal concentrations at the end of the electrodialytic remediation experiments using Ti/MMO (Q = 43 200 C).
a) Standard deviation.
b) Limit of detection.

than 1.0%, confirming the assumption on the minimum time required to achieve appreciable extraction. Regarding As and Cu, the diagrams show greater extraction using Ti/MMO electrodes: 14.4 and 11.3% more, respectively. These differences could be addressed in the first approximation to the higher amount of transferred charge for Ti/MMO-based experiments.

Figure 10.7 shows the percentage distribution related to the data shown in Tables 10.3 and 10.4, where the highest concentrations registered were, for almost

UNCORRECTED PROOFS

Trim Size: 170mm x 244mm Single Column Loose Ribeiro670117 c10.tex V1 - 12/11/2020 11:54pm Page 240

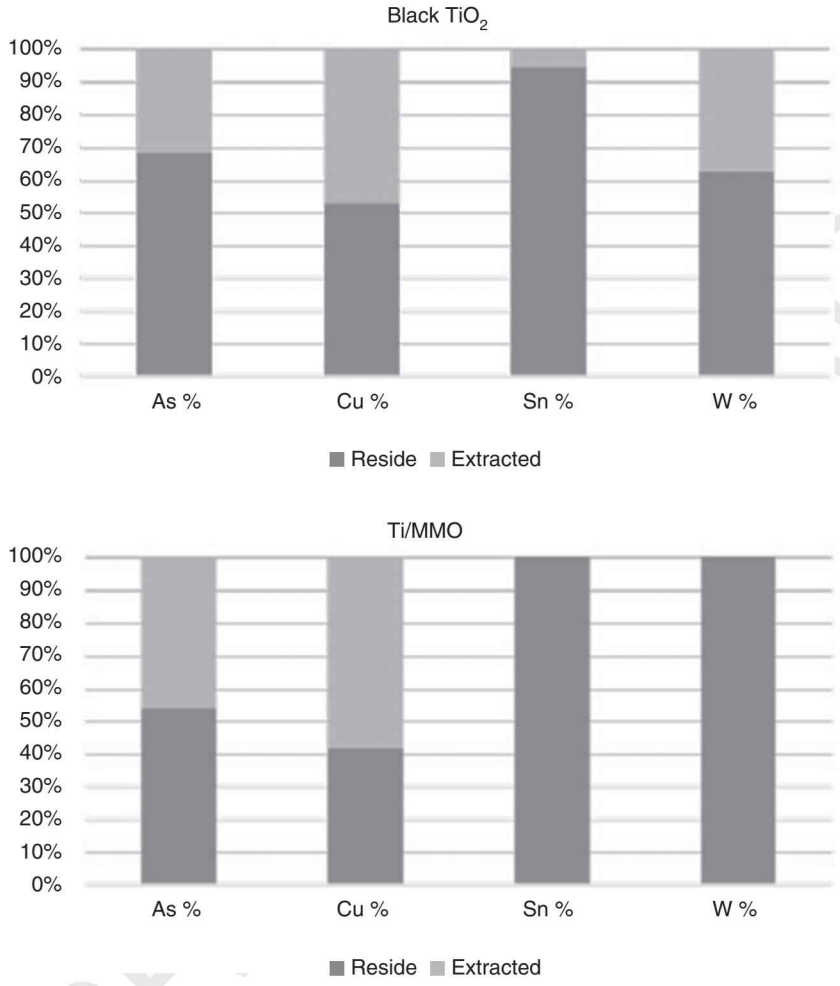

Figure 10.6 ED remediation experiments: evaluation of extraction efficiency (%) using black TiO_2 (left bar diagram) and commercial Ti/MMO (right bar diagram).

all the samples, in the CEM fraction. This is attributable to the strong alkaline environment that cations encounter as soon as they pass through the CEM, precipitating on it. Thus, proceeding with the remediation time, the formation of a solid layer (i.e. membrane fouling) on the cathodic side of the CEM cannot be prevented. This would lead to a progressive increase in the system resistance, negatively affecting both metal extraction and HER activity. The membrane fouling, according to the characteristics of the used electrocatalyst, could be prevented by guaranteeing the constant acidification of the catholyte. However, further studies should be performed first to verify the effect of catholyte acidification on the electrocatalyst's stability and HER effectiveness prior to evaluating the effectiveness of metal extraction during ED remediation. This is beyond the scope of the present study, where

UNCORRECTED PROOFS

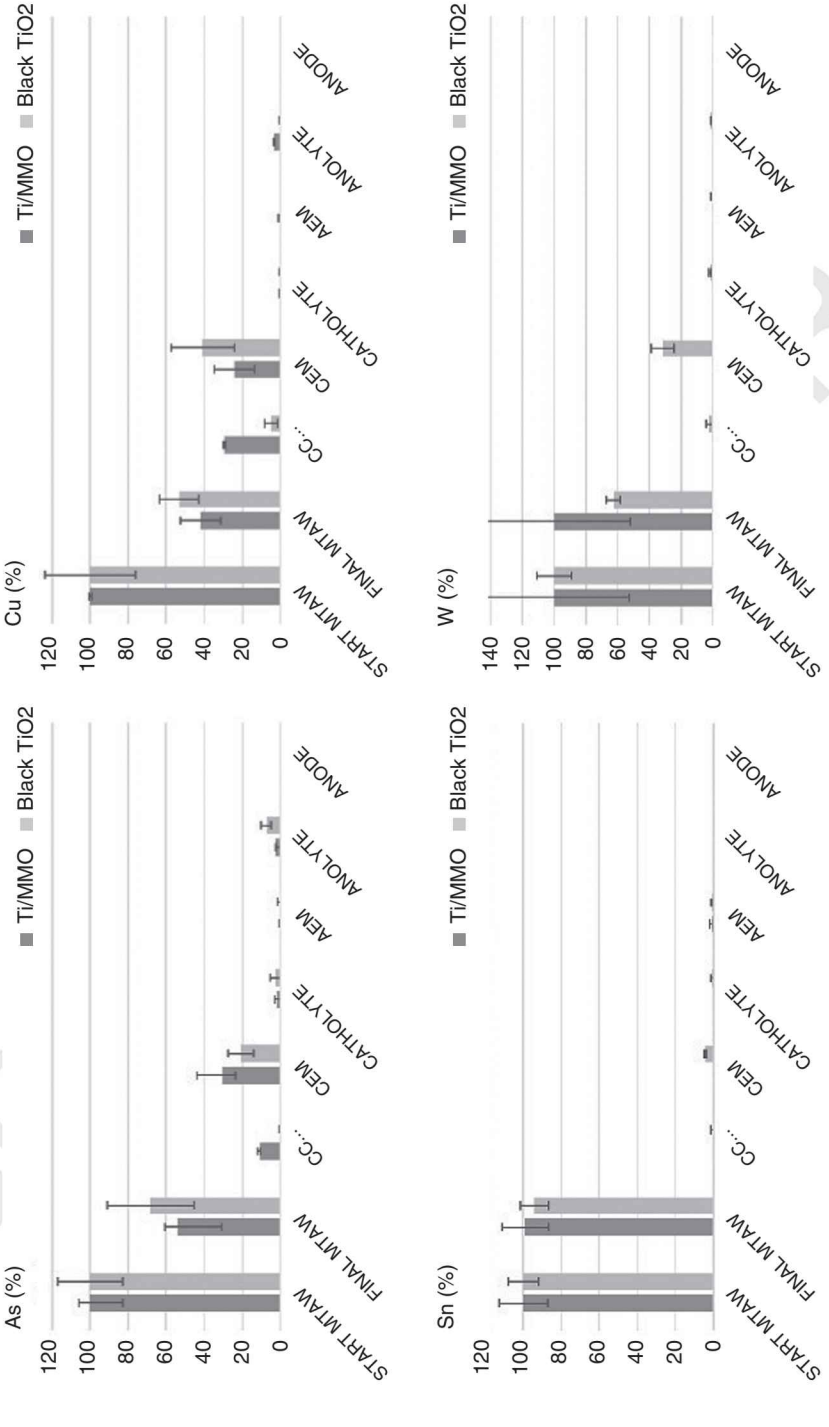

Figure 10.7 ED remediation experiments: estimated concentrations (%) in the different analyzed fractions. For each element, light gray bars indicate black TiO_2 and dark gray the commercial Ti/MMO electrodes.

UNCORRECTED PROOFS

Trim Size: 170mm x 244mm Single Column Loose Ribeiro670117 c10.tex V1 - 12/11/2020 11:54pm Page 242

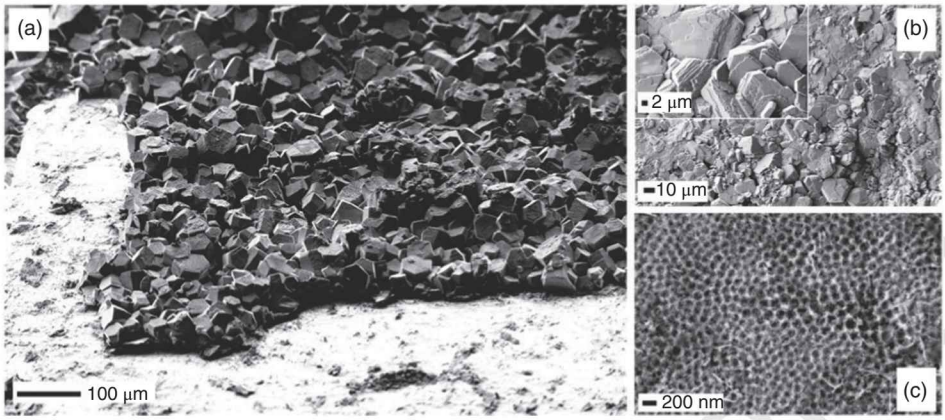

Figure 10.8 FE-SEM analysis. (a) Cross-sectional view of the deposits (dark part) overlying the NT layer (light part) in the black TiO_2 electrode at the end of the ED remediation treatment; (b) magnification of the deposited layer (top view); (c) magnification of the NTs underlying the deposits (top view).

the primary purpose was to preliminarily compare the different electrocatalysts' activity toward HER in alkaline environment to boost the production of hydrogen as a byproduct during ED remediation and minimize the overall process cost.

Tables 10.3 and 10.4 do not show concentration data for the cathodes. This is because leaching is a destructive analysis, not allowing further characterization. At the same time, the sample preparation for cross-sectional view FE-SEM analysis compromises the samples for further characterization. Figure 10.8 shows the FE-SEM images collected for black TiO_2-based electrodes at the end of the remediation treatment. Because of competing cathodic reactions, electrodeposition phenomena occur, as clearly observable in the images where the TiO_2 NTs are covered by a thick overlying layer. The elemental analysis carried out (Figure 10.9) further confirms the high heterogeneity of the treated matrix.

10.3 Final Considerations

The preliminary feasibility study carried out showed that the synthesized black TiO_2-based electrodes were the most effective electrocatalysts for HER during blank tests in the 3C ED cell. These tests highlighted the possibility of increasing the H_2 byproduct to further minimize the overall process cost.

The performance of commercial Ti/MMO and synthesized black TiO_2 electrocatalysts was further investigated through ED remediation tests. These experiments were carried out to evaluate the performance of the synthesized HER electrocatalyst for extracting target metals, the primary goal of the remediation process. Here, the extraction efficiency for As, Cu, Sn, and W was evaluated, focusing on As as remediation target and W as CRM recovery target. Experiments carried out with black TiO_2 electrodes highlighted the greatest extraction efficiency for W.

UNCORRECTED PROOFS

Trim Size: 170mm x 244mm Single Column Loose Ribeiro670117 c10.tex V1 - 12/11/2020 11:54pm Page 243

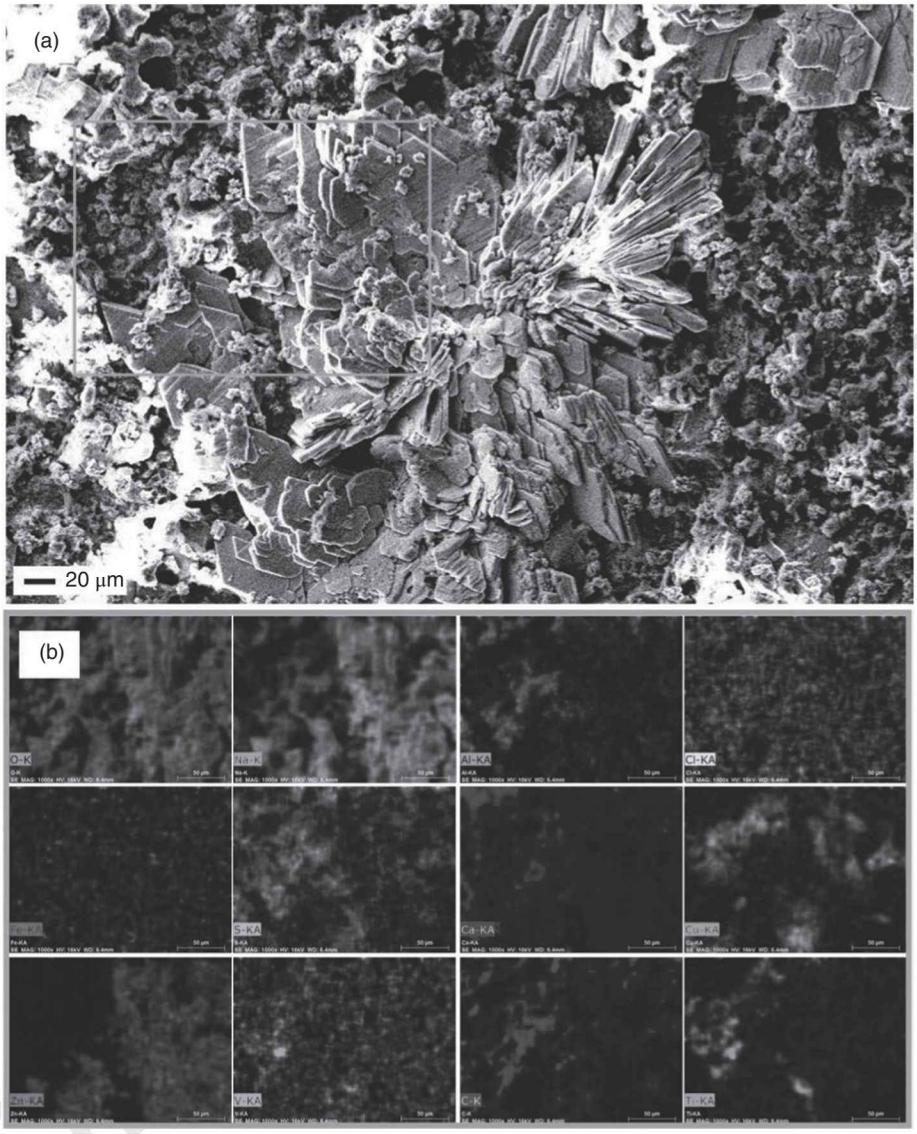

Figure 10.9 FE-SEM/EDX analysis. (a) Top view of the deposits overlying the NT layer in the black TiO_2 electrode at the end of the ED remediation treatment. The green inlet highlights the area analyzed through EDX. (b) Elemental mapping of the analyzed area.

Further evidence was derived by the target metal distribution in the analyzed fraction, which would suggests the progressive growth of a solid layer on the cathodic side of the CEM surface. This could mean increased maintenance costs and energy loss. In this scenario, the strategy to improve the process's sustainability for its scalability based on H_2 recovery could be ineffective. An experimental

UNCORRECTED PROOFS

Trim Size: 170mm x 244mm Single Column Loose Ribeiro670117 c10.tex V1 - 12/11/2020 11:54pm Page 244

campaign to further investigate strategies to prevent the formation of a solid layer and the related costs is required but is beyond the scope of the present work.

Coming back to H_2 recovery, the results achieved with black TiO_2 in this preliminary study pave the way to exploiting electrochemical production methods as a tool for tuning catalyst features to improve their activity: for instance, higher specific surfaces through increases in NTs density (decreasing cell voltage during potentiostatic anodization) and length (increasing anodization time), rather than through increases in the Ti^{3+} state's concentration through the electrochemical reduction step after anodization (increasing duration or current). At the same time, it must be taken into account that competitive electrodeposition phenomena occur during the current flow, highlighting the need for further studies about their effect on electrodes activity and durability.

Acknowledgments

This project has received funding from the European Union's Horizon 2020 research and innovation program under the Marie Skłodowska-Curie grant agreement No. 778045. FCT/MCTES is acknowledged through grant UIDB/04085/2020 (research unit CENSE, "Center for Environmental and Sustainability Research"); and Fundação para a Ciência e a Tecnologia for P. Guedes' fellowship (SFRH/BPD/114660/2016), and N. Couto's contract established under Individual Call to Scientific Employment Stimulus (CEECIND/04210/2017).

References

1 Hammons, T.J. (1992). Remote renewable energy resources. *IEEE Power Engineering Review* 12 (6): 3.

2 Momirlan, M. and Veziroglu, T.N. (2005). The properties of hydrogen as fuel tomorrow in sustainable energy system for a cleaner planet. *International Journal of Hydrogen Energy* 30 (7): 795–802.

3 Bureika, G., Matijošius, J., and Rimkus, A. (2020). *Alternative Carbonless Fuels for Internal Combustion Engines of Vehicles*, 1–49. Cham: Springer.

4 Yilanci, A., Dincer, I., and Ozturk, H.K. (2009). A review on solar-hydrogen/fuel cell hybrid energy systems for stationary applications. *Progress in Energy and Combustion Science* 35 (3): 231–244.

5 Coutanceau, C., Baranton, S., and Audichon, T. (2018). *Hydrogen Electrochemical Production*, 1–6.

AQ2

6 Edwards, P.P., Kuznetsov, V.L., David, W.I.F., and Brandon, N.P. (2008). Hydrogen and fuel cells: towards a sustainable energy future. *Energy Policy* 36 (12): 4356–4362.

7 Mazloomi, S.K. and Sulaiman, N. (2012). Influencing factors of water electrolysis electrical efficiency. *Renewable and Sustainable Energy Reviews* 16 (6): 4257–4263.

UNCORRECTED PROOFS

Trim Size: 170mm x 244mm Single Column Loose Ribeiro670117 c10.tex V1 - 12/11/2020 11:54pm Page 245

8 Hu, W., Chen, S., and Xia, Q. (2014). IrO_2/Nb-TiO_2 electrocatalyst for oxygen evolution reaction in acidic medium. *International Journal of Hydrogen Energy* 39 (13): 6967–6976.

9 Yan, Y., Xia, B.Y., Zhao, B., and Wang, X. (2016). A review on noble-metal-free bifunctional heterogeneous catalysts for overall electrochemical water splitting. *Journal of Materials Chemistry A* 4 (45): 17587–17603.

10 Yan, Y., Xia, B., Xu, Z., and Wang, X. (2014). Recent development of molybdenum sulfides as advanced electrocatalysts for hydrogen evolution reaction. *ACS Catalysis* 4 (6): 1693–1705.

11 Wang, J., Cui, W., Liu, Q. et al. (2016). Recent progress in cobalt-based heterogeneous catalysts for electrochemical water splitting. *Advanced Materials* 28 (2): 215–230.

12 Tahira, A., Ibupoto, Z.H., Mazzaro, R. et al. (2019). Advanced electrocatalysts for hydrogen evolution reaction based on core-shell MoS_2/TiO_2 nanostructures in acidic and alkaline media. *ACS Applied Energy Materials* 2 (3): 2053–2062.

13 Chen, L., Dong, X., Wang, Y., and Xia, Y. (2016). Separating hydrogen and oxygen evolution in alkaline water electrolysis using nickel hydroxide. *Nature Communications* 7 (May): 1–8.

14 Rong, F., Zhao, J., Yang, Q., and Li, C. (2016). Nanostructured hybrid NiFeOOH/CNT electrocatalysts for oxygen evolution reaction with low overpotential. *RSC Advances* 6 (78): 74536–74544.

15 Lu, J., Lei, Y., Lau, K.C. et al. (2013). A nanostructured cathode architecture for low charge overpotential in lithium-oxygen batteries. *Nature Communications* 4 (1): 2383.

16 Chik, H. and Xu, J.M. (2004). Nanometric superlattices: non-lithographic fabrication, materials, and prospects. *Materials Science & Engineering R: Reports* 43 (4): 103–138.

17 Magro, C., Almeida, J., Paz-Garcia, J.M. et al. (2019). Exploring hydrogen production for self-energy generation in electroremediation: a proof of concept. *Applied Energy* 255: 113839.

18 Ribeiro, A.B., Mateus, E.P., and Couto, N. (eds.) (2016). El[illegible]kinetics across disciplines and continents: new strategies for sustainable development. In: *Electrokinetics across Disciplines and Continents: New Strategies for Sustainable Development*, [illegible]427, https://doi.org/10.1007/978-3-319-20179-5, 20[illegible]–453. Springer International Publishing.

19 Reddy, K.R. and Cameselle, C. (eds.) (2009). *Electrochemical Remediation Technologies for Polluted Soils, Sediments and Groundwater*, 1–732. Hoboken, NJ, USA: Wiley.

20 Ottosen, L.M., Pedersen, A.J., Ribeiro, A.B., and Hansen, H.K. (2005). Case study on the strategy and application of enhancement solutions to improve remediation of soils contaminated with cu, Pb and Zn by means of electrodialysis. *Engineering Geology* 77 (3–4 SPEC. ISS): 317–329.

21 Guedes, P., Couto, N., Ottosen, L.M., and Ribeiro, A.B. (2014). Phosphorus recovery from sewage sludge ash through an electrodialytic process. *Waste Management* 34 (5): 886–892.

UNCORRECTED PROOFS

Trim Size: 170mm x 244mm Single Column Loose Ribeiro670117 c10.tex V1 - 12/11/2020 11:54pm Page 246

22 Guedes, P., Mateus, E.P., Almeida, J. et al. (2016). Electrodialytic treatment of sewage sludge: current intensity influence on phosphorus recovery and organic contaminants removal. *Chemical Engineering Journal* 306: 1058–1066.

23 Ottosen, L.M., Hansen, H.K., and Hansen, C.B. (2000). Water splitting at ion-exchange membranes and potential differences in soil during electrodialytic soil remediation. *Journal of Applied Electrochemistry* 30 (11): 1199–1207.

24 Ottosen, L.M., Hansen, H.K., Laursen, S., and Villumsen, A. (1997). Electrodialytic remediation of soil polluted with copper from wood preservation industry. *Environmental Science and Technology* 31 (6): 1711–1715.

25 Sun, T.R. and Ottosen, L.M. (2012). Effects of pulse current on energy consumption and removal of heavy metals during electrodialytic soil remediation. AQ3 *Electrochimica Acta*: 28–35.

26 Rojo, A. and Cubillos, L. (2009). Electrodialytic remediation of copper mine tailings using bipolar electrodes. *Journal of Hazardous Materials* 168 (2–3): 1177–1183.

27 Chou, S.Y., Krauss, P.R., Renstrom, P.J. et al. (2014). Nanoimprint lithography. *Journal of Vacuum Science & Technology B: Microelectronics and Nanometer Structures* 4129 (1996): 9–14.

28 Tartaj, P., Morales, M.P., González-Carreño, T. et al. (2005). Advances in magnetic nanoparticles for biotechnology applications. *Journal of Magnetism and Magnetic Materials* 290–291, Part 1:: 28–34.

29 Murray, B.J., Li, Q., Newberg, J.T. et al. (2005). Shape- and size-selective electrochemical synthesis of dispersed silver(l) oxide colloids. *Nano Letters* 5 (11): 2319–2324.

30 Zhao, Z., Chamele, N., Kozicki, M. et al. (2019). Photochemical synthesis of dendritic silver nano-particles for anti-counterfeiting. *Journal of Materials Chemistry C* 7 (20): 6099–6104.

31 MacWan, D.P., Dave, P.N., and Chaturvedi, S. (2011). A review on nano-TiO_2 sol-gel type syntheses and its applications. *Journal of Materials Science* 46: 3669–3686.

32 Jiang, S.P. (2006). A review of wet impregnation - an alternative method for the fabrication of high performance and nanostructured electrodes of solid oxide fuel cells. *Materials Science and Engineering A* 418 (1–2): 199–210.

33 Milchev, A. (2002). *Electrocrystallization*. Boston: Kluwer Academic Publishers.

34 Schiavi, P.G., Altimari, P., Zanoni, R., and Pagnanelli, F. (2016). Morphology-controlled synthesis of cobalt nanostructures by facile electrodeposition: transition from hexagonal nanoplatelets to nanoflakes. *Electrochimica Acta* 220: 405–416.

35 Altimari, P., Schiavi, P.G., Rubino, A., and Pagnanelli, F. (2019). Electrodeposition of cobalt nanoparticles: an analysis of the mechanisms behind the deviation from three-dimensional diffusion-control. *Journal of Electroanalytical Chemistry* 851: 113413.

36 Vignarooban, K., Lin, J., Arvay, A. et al. (2015). Nano-electrocatalyst materials for low temperature fuel cells: a review. *Cuihua Xuebao/Chinese Journal of Catalysis. Science Press* 36: 458–472.

UNCORRECTED PROOFS

Trim Size: 170mm x 244mm Single Column Loose Ribeiro670117 c10.tex V1 - 12/11/2020 11:54pm Page 247

37 Grimes, C.A. and Mor, G.K. (2009). *TiO2 Nanotube Arrays: Synthesis, Properties, and Applications*. Springer.

38 Paulose, M., Prakasam, H.E., Varghese, O.K. et al. (2007). TiO_2 nanotube arrays of 1000 μm length by anodization of titanium foil: phenol red diffusion. *Journal of Physical Chemistry C* 111 (41): 14992–14997.

39 Sánchez-Tovar, R., Paramasivam, I., Lee, K., and Schmuki, P. (2012). Influence of hydrodynamic conditions on growth and geometry of anodic TiO_2 nanotubes and their use towards optimized DSSCs. *Journal of Materials Chemistry* 22 (25): 12792–12795.

40 Mohapatra, S.K., Raja, K.S., Mahajan, V.K., and Misra, M. (2008). Efficient photoelectrolysis of water using TiO_2 nanotube arrays by minimizing recombination losses with organic additives. *Journal of Physical Chemistry C* 112 (29): 11007–11012.

41 Wang, J., Ji, G., Liu, Y. et al. (2014). Cu_2O/TiO_2 heterostructure nanotube arrays prepared by an electrodeposition method exhibiting enhanced photocatalytic activity for CO_2 reduction to methanol. *Catalysis Communications* 46: 17–21.

42 Auer, A. and Kunze-Liebhäuser, J. (2019). Recent progress in understanding ion storage in self-organized anodic TiO_2 nanotubes. *Small Methods* 3 (8): 1800385.

43 Zhou, H. and Zhang, Y. (2014). Electrochemically self-doped TiO_2 nanotube arrays for supercapacitors. *Journal of Physical Chemistry C* 118 (11): 5626–5636.

44 Feng, H., Xu, Z., Ren, L. et al. (2018). Activating Titania for efficient electrocatalysis by vacancy engineering. *ACS Catalysis* 8 (5): 4288–4293.

45 Tsui, L. and Zangari, G. (2014). Titania nanotubes by electrochemical Anodization for solar energy conversion. *Journal of the Electrochemical Society* 161 (7): D3066–D3077.

46 Mir, N., Lee, K., Paramasivam, I., and Schmuki, P. (2012). Optimizing TiO_2 nanotube top geometry for use in dye-sensitized solar cells. *Chemistry - A European Journal* 18 (38): 11862–11866.

47 Tsui, L.K., Homma, T., and Zangari, G. (2013). Photocurrent conversion in anodized TiO_2 nanotube arrays: effect of the water content in anodizing solutions. *Journal of Physical Chemistry C* 117 (14): 6979–6989.

48 Momeni, M.M. and Ghayeb, Y. (2015). Photoelectrochemical water splitting on chromium-doped titanium dioxide nanotube photoanodes prepared by single-step anodizing. *Journal of Alloys and Compounds* 637: 393–400.

49 Regonini, D., Bowen, C.R., Stevens, R. et al. (2007). Anodised TiO_2 nano-tubes: voltage ramp influence on the nanostructured oxide and investigation of phase changes promoted by thermal treatments. In: Phys. *Status Solidi A Applications and Materials Science* 204 (6): 1814–1819.

50 Rubino, A., Schiavi, P.G., Altimari, P., and Pagnanelli F. (2019). $Ti/TiO_2/Cu_2O$ electrodes for photocatalytic applications: Synthesis and characterization. AIP Conference Proceedings.

51 Rubino A., Agostini, M., Schiavi, P.G. et al. (2020). TiO_2 nanotubes in lithium-ion batteries. AIP Conference Proceedings.

UNCORRECTED PROOFS

Trim Size: 170mm x 244mm Single Column Loose Ribeiro670117 c10.tex V1 - 12/11/2020 11:54pm Page 248

52 Albu, S.P. and Schmuki, P. (2010). TiO_2 nanotubes grown in different organic electrolytes: two-size self-organization, single vs. double-walled tubes, and giant diameters. *Physica Status Solidi Rapid Research Letters* 4 (8–9): 215–217.

53 Macak, J.M., Tsuchiya, H., Ghicov, A. et al. (2007). TiO_2 nanotubes: self-organized electrochemical formation, properties and applications. *Current Opinion in Solid State & Materials Science* 11 (1–2): 3–18.

54 Ghicov, A., Tsuchiya, H., MacAk, J.M., and Schmuki, P. (2005). Titanium oxide nanotubes prepared in phosphate electrolytes. *Electrochemistry Communications* 7 (5): 505–509.

55 Roy, P., Berger, S., and Schmuki, P. (2011). TiO_2 nanotubes: synthesis and applications. *Angewandte Chemie, International Edition* 50 (13): 2904–2939.

56 Raja, K.S., Gandhi, T., and Misra, M. (2007). Effect of water content of ethylene glycol as electrolyte for synthesis of ordered titania nanotubes. *Electrochemistry Communications* 9 (5): 1069–1076.

57 Dumitriu, C., Pirvu, C., and Demetrescu, I. (2013). The electrochemical formation and shielding mechanism of TiO_2 nanotubes in organic electrolytes with different viscosity. *Journal of the Electrochemical Society* 160 (2): G55–G60.

58 Malgras, V., Ataee-Esfahani, H., Wang, H. et al. (2016). Nanoarchitectures for Mesoporous metals. *Advanced Materials* 28 (6): 993–1010.

59 Leng, Y.X., Huang, N., Yang, P. et al. (2002). Influence of oxygen pressure on the properties and biocompatibility of titanium oxide fabricated by metal plasma ion implantation and deposition. *Thin Solid Films* 420–421: 408–413.

60 Sankar, S. and Gopchandran, K.G. (2009). Effect of annealing on the structural, electrical and optical properties of nanostructured TiO_2 thin films. *Crystal Research and Technology* 44 (9): 989–994.

61 Yoriya, S., Mor, G.K., Sharma, S., and Grimes, C.A. (2008). Synthesis of ordered arrays of discrete, partially crystalline titania nanotubes by Ti anodization using diethylene glycol electrolytes. *Journal of Materials Chemistry* 18 (28): 3332–3336.

62 Giorgi, L., Dikonimos, T., Giorgi, R. et al. (2018). Electrochemical synthesis of self-organized TiO_2 crystalline nanotubes without annealing. *Nanotechnology* 29 (9): 1–14.

63 Jun, W. and Zhiqun, L. (2009). Anodic formation of ordered TiO 2 nanotube arrays: effects of electrolyte temperature and anodization potential. *Journal of Physical Chemistry* 113 (10): 4026–4030.

64 Tsui, L.K., Nguyen, N.T., Wang, L. et al. (2015). Hierarchical decoration of anodic TiO_2 nanorods for enhanced photocatalytic degradation properties. *Electrochimica Acta* 155: 244–250.

65 Nasirpouri, F., Peighambardoust, P.D., Samardak, A. et al. (2017). Structural defect-induced bandgap narrowing in dopant-free anodic TiO_2 nanotubes. *ChemElectroChem* 4 (5): 1227–1235.

66 Yang, B., Ng, C.K., Fung, M.K. et al. (2011). Annealing study of titanium oxide nanotube arrays. *Materials Chemistry and Physics* 130 (3): 1227–1231.

67 Xiao, P., Liu, D., Garcia, B.B. et al. (2008). Electrochemical and photoelectrical properties of titania nanotube arrays annealed in different gases. *Sensors and Actuators B: Chemical* 134 (2): 367–372.

UNCORRECTED PROOFS

Trim Size: 170mm x 244mm Single Column Loose Ribeiro670117 c10.tex V1 - 12/11/2020 11:54pm Page 249

68 Ansari, S.A., Khan, M.M., Ansari, M.O., and Cho, M.H. (2016). Nitrogen-doped titanium dioxide (N-doped TiO_2) for visible light photocatalysis. *New Journal of Chemistry*. Royal Society of Chemistry; 40: 3000–3009.

69 Mao, C., Zuo, F., Hou, Y. et al. (2014). In situ preparation of a Ti^{3+} self-doped TiO_2 film with enhanced activity as Photoanode by N_2H_4 reduction. *Angewandte Chemie, International Edition* 53 (39): 10485–10489.

70 Zhang, Z., Hedhili, M.N., Zhu, H., and Wang, P. (2013). Electrochemical reduction induced self-doping of Ti^{3+} for efficient water splitting performance on TiO_2 based photoelectrodes. *Physical Chemistry Chemical Physics* 15 (37): 15637–15644.

71 Astolfi, M.L., Protano, C., Marconi, E. et al. (2020). A new rapid treatment of human hair for elemental determination by inductively coupled mass spectrometry. *Analytical Methods* 12 (14): 1906–1918.

72 Carlson, K., Elliott, C., Walker, S. et al. (2016). An effective, point-of-use water disinfection device using immobilized black TiO_2 nanotubes as an electrocatalyst. *Journal of the Electrochemical Society* 163 (6): H395–H401.

73 Chen, X., Liu, L., Liu, Z. et al. (2013). Properties of disorder-engineered black titanium dioxide nanoparticles through hydrogenation. *Scientific Reports* 3: 1–7.

74 Liu, N., Schneider, C., Freitag, D. et al. (2014). Black TiO_2 nanotubes: cocatalyst-free open-circuit hydrogen generation. *Nano Letters* 14 (6): 3309–3313.

75 Teng, Y. and Teng, F. (2017). Investigation on surface metal vacancy electrochemistry. *Electrochimica Acta* 244: 1–7.

76 Wang, Y., Zhang, Y., Liu, Z. et al. (2017). Layered double hydroxide Nanosheets with multiple vacancies obtained by dry exfoliation as highly efficient oxygen evolution electrocatalysts. *Angewandte Chemie, International Edition* 56 (21): 5867–5871.

77 Kirkelund, G.M., Jensen, P.E., and Ottosen, L.M. (2013). Electrodialytic extraction of heavy metals from greenlandic MSWI fly ash as a function of remediation time and L/S ratio. In: *ISCORD 2013*, 87–96. Reston, VA: ASociety CE.

UNCORRECTED PROOFS

Trim Size: 170mm x 244mm Single Column Loose Ribeiro670117 c10.tex V1 - 12/11/2020 11:54pm Page 250

UNCORRECTED PROOFS

Trim Size: 170mm x 244mm Single Column Loose Ribeiro670117 c11.tex V1 - 12/11/2020 11:54pm Page 251

11

Hydrogen Recovery in Electrodialytic-Based Technologies Applied to Environmental Contaminated Matrices

Cátia Magro[1], Joana Almeida[1], Juan Manuel Paz-Garcia[2], Eduardo P. Mateus[1], and Alexandra B. Ribeiro[1]

[1]CENSE – Center for Environmental and Sustainability Research, Department of Environmental Sciences and Engineering, NOVA School of Science and Technology, NOVA University Lisbon, Caparica 2829-516, Portugal
[2]Department of Chemical Engineering, Faculty of Sciences, University of Malaga, Malaga 29010, Spain

11.1 Scope

It is widely known that "without a technological shift, the EU will fail on its 2050 ambitions" [1]. In this context, hydrogen-based energy has the potential to play a major role in decarbonizing the European energy landscape in the coming decades. Hydrogen provides a clean alternative energy carrier that can be easily produced from several kinds of primary energy sources, stored, and distributed. Its relevance is transverse to the entire energy sector, such as transportation, buildings, utilities, and industry. Through combination with fuel cells, power can be generated in the desired quantities and with no additional greenhouse gas emissions.

Hydrogen can be produced using an extensive range of fuels (e.g. natural gas and coal, biomass, non-food crops, nuclear energy) [2] and renewable energy (e.g. wind, solar, geothermal, and hydroelectric power) [3] through advanced technologies, in centralized or distributed production facilities. The diversity of supply sources is one of the primary reasons hydrogen is a promising energy carrier. Hydrogen can be obtained using electricity from renewable energy sources to produce water electrolysis, i.e. the decomposition of water into hydrogen and oxygen gases [4], leading to a carbon-neutral mechanism. Hydrogen can be generated from other industrial processes through electrochemical processes, such as the production of caustic soda [5]. Steam reforming (of natural gas and biogas), an endothermic process where methane is converted to hydrogen when pure water vapor is used as the oxidant, is nowadays the most common strategy to produce hydrogen [6].

Technologies such as electrokinetic and electrodialytic (ED) remediation can also be regarded as hydrogen producers. In these processes, applying a low current intensity between a pair of electrodes promotes the removal, degradation, or recovery of organic and inorganic compounds from polluted solid [7–11] and liquid matrices [12, 13]. The electrochemically induced transport phenomena consist of different transport contributors, such as electroosmosis, electrophoresis,

Electrokinetic Remediation for Environmental Security and Sustainability, First Edition.
Edited by Alexandra B. Ribeiro and M.N.V. Prasad.
© 2021 John Wiley & Sons Ltd. Published 2021 by John Wiley & Sons Ltd.

UNCORRECTED PROOFS

Trim Size: 170mm x 244mm Single Column Loose Ribeiro670117 c11.tex V1 - 12/11/2020 11:54pm Page 252

and electromigration. In particular, ionic species are primarily transported by electromigration toward the electrode of different charges, while non-ionic species are transported mainly by electroosmosis.

In electrokinetic or electrodialytic processes, hydrogen and oxygen gases are generated by the water electrolysis reactions. At the anode, water oxidation produces protons and oxygen gas, as shown in Eq. (11.1), while at the cathode, water is reduced to gaseous hydrogen and hydroxide ions according to Eq. (11.3). Depending on the process, matrix, and contaminants, different competitive redox reactions may occur at the electrode: For example, chlorine gas production at the anode (Eq. (11.2)) or metals deposition (Eq. (11.4)) at the cathode.

Anode reactions:

$$O_2(g) + 4H^+ + 4e^- = 2H_2O \quad E^0(O_2/H_2O) = 1.229\,V \tag{11.1}$$

$$Cl_2(g) + 2e^- = 2Cl^- \; E^0(Cl_2/2Cl^-) = 1.358\;\; V \tag{11.2}$$

Cathode reactions:

$$2H_2O + 2e^- = H_2(g) + 2OH^- \; E^0(H_2O/H_2) = -0.828\,V \tag{11.3}$$

$$Me^{2+} + 2e^- = Me^0 \tag{11.4}$$

Unlike at the anode, in electrokinetic and electrodialytic remediation processes, there are not many competitive electrochemical reactions that produce gases at the cathode electrode. The gas produced at the cathode has a high H_2 concentration (near 100% purity) and can therefore be collected, stored, and sold as a byproduct. Thus, the hydrogen inherently produced as a byproduct of electroremediation processes turns the technology into a symbiotic system, where the remediation treatment can take advantage of the energy generated. This will drive the technology's maturity toward market trends, enhancing the technology readiness level (TRL) and minimizing one of the downsides for scaling up.

Furthermore, the hydrogen formed in the cathode compartment may be used in situ as fuel in a proton-exchange membrane fuel cell (PEMFC) to produce electrical energy and reduce the energy requirements of the electroremediation process. The setup of an electrokinetic or electrodialytic reactor may be redesigned to incorporate gas collectors, avoiding hydrogen dissipation while remediating environmental matrices. The hydrogen produced can be collected for further reuse and purposes.

Fuel cells and hydrogen are key enablers for a competitive, inclusive, low-carbon society. Global hydrogen demand increased ~21% between 2013 and 2020 [14], corroborating the market search for new, innovative technologies and strategies to target hydrogen demand in the near future. Regarding the current paradigm in electroremediation strategies and global energy consumption, the development of hydrogen-smart technologies may be a key factor in the shift to a low-carbon economy [15].

Magro et al. [16] studied the potential to collect and reuse self-produced hydrogen from electrodialytic treatment. In line with Magro et al. [16], the following work is discussed in this chapter: (i) key components of the technology concept – electroremediation processes producing hydrogen while decontaminating environmental matrices; and (ii) market drivers for successful applications.

UNCORRECTED PROOFS

Trim Size: 170mm x 244mm Single Column Loose Ribeiro670117 c11.tex V1 - 12/11/2020 11:54pm Page 253

11.2 Technology Concept

11.2.1 Potential Secondary Resources

The reuse of potential secondary resources for different industrial purposes has been empowered by the European Commission [17]. These resources may be regarded as alternative supplies to replace primary sources, increasing the sustainability of industrial processes while closing materials loops. Hydrogen recovery was recently tested for briny water, wastewater, sewage sludge, and mine residue suspensions [16, 18]. An initial characterization of the tested secondary sources is shown in Table 11.1.

When secondary solid and liquid matrices were submitted to electrochemical treatment to extract target contaminants, cathodic hydrogen was produced with an average purity of ≈98% mol mol^{-1}. This corroborates the absence of gas-releasing competitive cathodic reactions [16]. However, Almeida et al. [18] tested sewage sludge treatment (collected from a wastewater treatment plant), where lower hydrogen purity was reported (≈33%). The generation of methane (CH_4), commonly produced by methanogenic organisms present in mixed cultures, may have affected the purity of the hydrogen collected. Hydrogenotrophic organisms may transform CO_2 and H_2 to produce CH_4 [19]. Bacteria could move together with the direct current applied through electroosmosis and electrophoresis phenomena [20]. Furthermore, some bacteria can adhere to organic/inorganic substrates or other microorganisms [21], also promoting their movement to the cathode compartment. Microorganisms form clusters due to their natural behavior and can interact with the media under the imposed experimental conditions [22].

As shown in Table 11.1, each tested matrix has different properties, meaning different targets for removal and separation of substances. Mine residue suspensions may represent significant concern due to the presence of harmful elements such as arsenic.

Nevertheless, the purity of hydrogen may be affected by the nature of the matrix at low-level current density due to the release of volatile organic compounds (VOCs) at the cathode end.

Table 11.1 Initial characterization of briny water, wastewater, and mine residue suspensions.

Matrix tested	pH	Conductivity (mS cm^{-1})	Major elements reported
Briny water	6.89 ± 0.08	1.81 ± 0.11	Ca, K, Mg, Na, P, S, Cu, Zn, Cl, S, N
Wastewater	7.67 ± 0.16	2.41 ± 2.12	
Sewage sludge	6.68 ± 0.02	0.81 ± 0.02	Ca, K, Mg, Na, P, S, Cu, Zn, Cl, S, Sn, W
Mine residues suspension	4.57 ± 1.74	0.84 ± 0.52	Ca, P, S, As, Cu, Sn, W

Source: Adapted from Magro et al. [16] and Almeida et al. [18].

UNCORRECTED PROOFS

Trim Size: 170mm x 244mm Single Column Loose Ribeiro670117 c11.tex V1 - 12/11/2020 11:54pm Page 254

Regarding the elements of concern and other chemical and physical properties of the matrices reported, recovering hydrogen may have the potential for secondary resources where electro-based technologies are applicable, once electrodialytic remediation has been reported as a feasible technology to remediate other secondary resources such as soil [23], wood [24], cork [25], sewage sludge [8], fly ash [26], and its water-washed [27] and other secondary mining resources [28].

11.2.2 Electrodialytic Reactor

The electrodialytic reactor for hydrogen recovery was preliminarily tested with a three-compartment sealed reactor, with an internal diameter of 8 cm and the central and electrolyte compartments 5 cm long. The reactor is composed of ion-exchange membranes and electrodes, where a direct electrical current density on the order of the 0.1–1 mA cm^{-2} is applied to promote the degradation of contaminants and species transport. When using suspensions, a stirrer system is needed in the sample compartment to ensure proper mixing. In both setups studied [16, 18], with 0.1 or 1 mA cm^{-2} of current applied, the final pH in the anode and cathode end reached ∼2 and ∼12, respectively. Also, despite the use of the ion-exchange membrane, in the sample compartment, the pH tends to decrease due to the moderately high perm-selectivity of the anion-exchange membrane (AEM) with respect to protons.

Hydrogen production occurs at the cathode end and may be influenced by the components involved in the reactor design: electrodes, membranes, and matrices [16]. Although gas production was verified during all electrodialytic tests performed in a three-compartment reactor with a current density of 1 mA cm^{-2}, two distinct scenarios were observed in terms of purity: (i) the composition of effluent, mine tailings, and brine water did not affect hydrogen purity [16]; and (ii) the composition of sewage sludge alone and coupled with mining residues affected hydrogen purity [18].

Additionally, overpotential on the cathode is directly related to the formation of hydrogen. Hydrogen generation is intrinsically determined by the bond between hydrogen and the electrode surface. Palladium has the lowest heat of adsorption of hydrogen (83.5 kJ mol^{-1}) as compared to 105 kJ mol^{-1} for Ni, for example [29].

11.2.2.1 Electrodes

The electrodes play an important role not only in energy consumption during the removal of elements but also in generating hydrogen flow [30]. The proof of concept for electrodialytic hydrogen recovery included titanium/mixed-metal-oxides (Ti/MMO) as working electrodes [16]. Ti/MMO electrode morphologies were analyzed by scanning electron microscopy (SEM) at 1.5 kV (Figure 11.1) due to its relevance for water electrolysis phenomena and consequent hydrogen generation at the cathode end.

Figure 11.1 shows Ti/MMO electrodes after all the experiments conducted in Magro et al. [16]. There is a homogeneous morphology with nonvisual damage, proving their reusability and long-term workability. MMOs have exhibited high

UNCORRECTED PROOFS

Trim Size: 170mm x 244mm Single Column Loose Ribeiro670117 c11.tex V1 - 12/11/2020 11:54pm Page 255

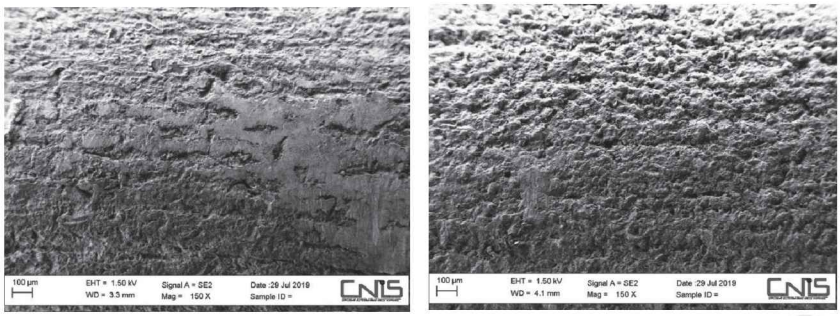

(b) (b)

Figure 11.1 SEM images from the anode and cathode. Source: Following Magro et al. [16] experiments.

technological performance and thus attracted wide attention due to high coating stability, high conductivity, low cost, electrode dimensional stability, and commercial applications [31]. Generally, MMO electrodes advantages and feature are as follows [32]:

- Significant reduction in anode overpotential and therefore cell voltage.
- Low bandgap energies and high specific surface areas as well as good thermal and chemical stability.
- Ti/MMO electrodes are semiconductors with a favorable electron transfer property due to their heterojunction structure [33].

Although the results for Ti/MMO composite electrodes corroborate a promising option for hydrogen production ($1.4\,mL\,min^{-1}$) with a current density of 100 mA ($1\,mA\,cm^{-2}$) in Magro et al. [16], other alternatives aiming for a gas flow upgrade can be considered. Adding metals with good workability functions may prevent electron-hole recombination, increasing electrode performance. For instance, synthesis methods and metal loadings (e.g. Au, Pt) positively affect hydrogen production [34]. Platinum is commonly used for water electrolysis, although the costs are high. Thus, other non-metals and transitions metal composites have been tested for hydrogen production. Copper can also be a feasible substitute, despite its high current density due to corrosive properties. However, when carbon is coated onto a copper substrate, the oxidation rate of the copper electrode decreases, causing stability in short-term hydrogen production. When 60 mA of current intensity was applied, the amount of hydrogen production reached ~120 µmol in 30 minutes and remained constant afterward [35]. Graphene also conducts electricity efficiently. Thus, including a single-layer graphene on a copper substrate may inhibit the corrosion of copper electrodes [35]. Kovendhan et al. [36] used stainless steel electrodes annealed at high temperature, with and without a hydrogen and argon environment, and tested the samples for hydrogen production in seawater conditions (3.5% NaCl). When 30, 60, and 90 mA current intensities were applied, in two minutes, the H_2 production was 0, 48, and 169 µmol, respectively [36]. On the other hand, Ganci et al. [37] studied a Ni nanostructured electrode as a

UNCORRECTED PROOFS

Trim Size: 170mm x 244mm Single Column Loose Ribeiro670117 c11.tex V1 - 12/11/2020 11:54pm Page 256

cathode and IrO_2 as an anode to assess the performance of nanostructured Ni for hydrogen production in alkaline solution. The authors found that after 60 hours of working at 0.5 A cm^{-2} constant current, the electrode potential decayed about 6.5%, which was an encouraging finding [37]. Summing up, the performance of the cathode electrode for hydrogen production should be tuned in terms of resistance to matrices in extreme conditions. According to the literature studied on hydrogen production, scientific research generally has documented simple matrices (e.g. deionized water or salty water) and highly controlled media conditions.

11.2.2.2 Ion-Exchange Membranes

Membranes are essential to guarantee the efficiency of the process of removing elements [38]. In particular, the ion-exchange membranes are ion-selective membranes comprised of cross-linked co-polymers of vinyl monomers and containing quaternary ammonium anion-exchange groups or sulfonic acid cation-exchange groups. The properties of these membranes are determined by the density of the polymer network, the hydrophobic or hydrophilic character of the matrix polymer, the type of concentration of the charges in the polymer, and the morphology of the membrane itself [39].

Ion-exchange membranes are integrated into the electrodialytic process as a key point since the membrane surface attracts dissolved ions, with the opposite charge (counter-ions) from the pore water of the membranes. The counter-ions are transported through the membrane due to the electrical current, and the co-ions (with the same charge as the surface of the membrane) are rejected. With these characteristics, it is possible to prevent/prohibit the passage of ions from electrode compartments, as well as the mixed gases produced. With the ion-exchange membranes, anion and cation, ion fluxes are regulated, and therefore a selection of ions reach the electrode compartments. A concentration gradient is thus essential for the flow of ions and water throughout the system [40].

The characteristics of the membranes are crucial for the phenomena involved in the removal and separation of substances in an electrodialytic reactor. Thus, the primary features of ion-exchange membranes are (adapted from [39–41]):

- Low electrical resistance
- High perm-selectivity
- Rugged construction and high burst strength
- Excellent long-term stability at up to 65 °C
- Long-term resistance to aqueous acid solutions
- High dimensional stability in solutions of different compositions
- High resistance to fouling by organic materials

Regarding different applications, the economic feasibility of processes with ion-exchange membranes is determined to a large extent by the chemical stability of the membranes under the process conditions. The structure and the mechanical properties of the membranes can be affected by degradation of the basic polymer or recrystallization and aging due to loss of water or plasticizing agents [39]. The deterioration of the electrical chemical properties can be caused by the loss of fixed

UNCORRECTED PROOFS

Trim Size: 170mm x 244mm Single Column Loose Ribeiro670117 c11.tex V1 - 12/11/2020 11:54pm Page 257

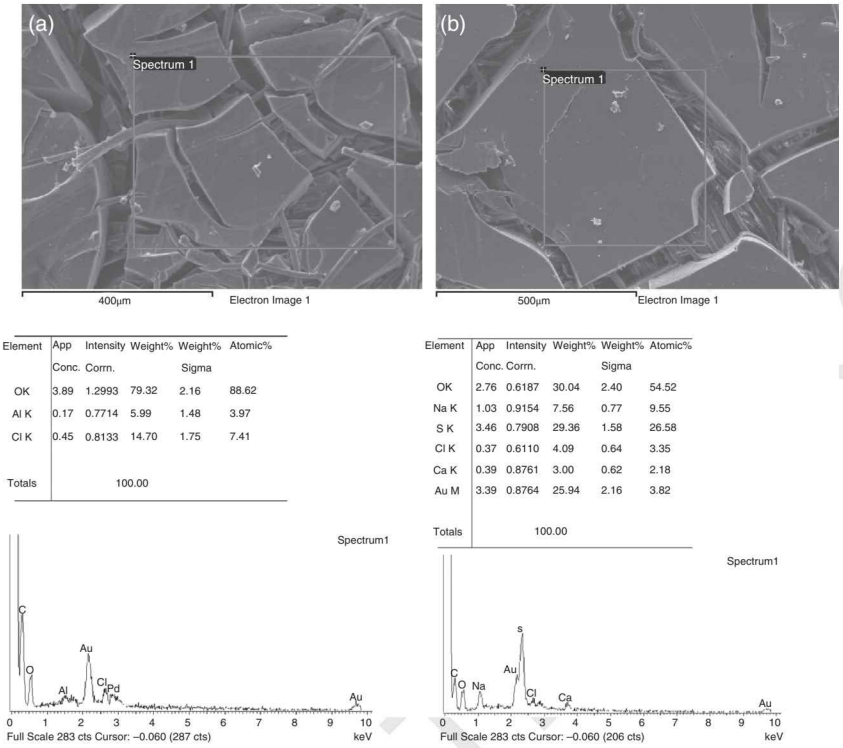

Figure 11.2 SEM/EDS analysis of ionic exchange membranes. (a) Anion-exchange membrane; (b) cation-exchange membrane.

charges due to the splitting-off of functional ion-exchange groups [41]. Generally, changes in membrane properties are related to time and are temperature-dependent. For that reason, it was important to understand the morphology of the membranes: if they were in good and stable condition after long-term use during electrodialytic treatments (temperature rise in the reactor). A characterization of the anion and cation-exchange membranes (CEMs) was performed after electrodialytic experiments with wastewater and mine residues, by a field emission SEM (Analytical FEG-SEM, JEOL 7001F with Oxford INCA light elements EDS detector) operating at 15 keV. A thin gold film was coated on the surface before SEM analysis to prevent buildup charging.

From the EDS experimental evidence (Figure 11.2), there are two layers in the membranes (commercially purchased): the elements founded in accordance with the typical composition of anion- and cation-exchange membranes [39, 42, 43]. Cl and O are predominant in the AEM, and S, O, and Na are prevalent in the CEM.

Regarding the purpose of hydrogen production by the electrodialytic process, there is no need for an efficient ion-exchange membrane. A diaphragm with high ion permeability can prevent the merge of the two gases and is sufficient to separate the solutions in the cathode and anode compartments. On the other hand, if a simultaneous system is proposed (as in Magro et al. [16]), the ion-exchange membranes are key

UNCORRECTED PROOFS

Trim Size: 170mm x 244mm Single Column Loose Ribeiro670117 c11.tex V1 - 12/11/2020 11:54pm Page 258

factors for (i) separating the contaminants from the media to the electrolytes, and (ii) hydrogen production at the cathode end, with the permeability of the gas through the membrane [39]. Also, the significant role of counter-ions in hydrogen generation and hydroxyl ions is proved. An exponential decrease in the flux of hydroxyl or hydrogen ions is established when the Gibbs energy of counter-ion hydration increases [24].

11.2.2.3 PEMFC System

Currently, society is moving from a highly centralized to a more decentralized energy system, relying on distributed energy generation and storage, and active involvement of consumers through demand response [44]. A fuel cell might be a feasible alternative technology with extensive applications, such as stationary power plants and portable power sources.

A *fuel cell* is a device that converts chemical potential energy (energy stored in molecular bonds) into electrical energy. A PEMFC uses hydrogen gas as fuel to react with oxygen (from air) and produce water, electricity, and heat without emitting other products that are different from the water formed in the reaction [45]:

$$H_2 + \frac{1}{2}O_2 \longrightarrow H_2O \tag{11.5}$$

A fuel cell, unlike a battery, produces electricity as long as fuel is supplied, never losing its charge. The pollution-free production of energy and high power density make fuel cell technology a viable approach for future energy industries [46]. Fuel cells show high energy conversion efficiency, up to 60%, greater than traditional internal combustion engines [47]. This efficiency can increase up to 80% with heat-recovery systems [48]. This is a huge improvement over internal combustion engines, coal-burning power plants, and nuclear power plants, all of which produce harmful byproducts [49]. Compared to the direct burning of hydrogen fuel, using fuel cells allows the in situ production of electricity with significantly lower heat losses. Since oxygen is readily available in the atmosphere, there is only the need to supply the fuel cell with hydrogen (which may come from the electrolysis process).

The primary advantages of this technology are as follows:

- By converting chemical potential energy directly into electrical energy, fuel cells avoid the "thermal bottleneck" (a consequence of the second law of thermodynamics). Thus, they are inherently more efficient than combustion engines, which convert chemical potential energy first into heat and then into mechanical work and/or electricity.
- Direct emissions from a fuel cell vehicle are reduced to water and vestigial heat. This is a step forward compared to the internal combustion engine's litany of greenhouse gases.
- Fuel cells have no moving components and are more reliable than traditional engines.

As a consequence of the primary advantages of the PEMFC, its development and optimization are now receiving increased attention [15]. To better recognize and assess the research status of fuel cell technologies, a bibliometric study was performed (February 2020), making use of the online version of SCOPUS. With the

UNCORRECTED PROOFS

Trim Size: 170mm x 244mm Single Column Loose Ribeiro670117 c11.tex V1 - 12/11/2020 11:54pm Page 259

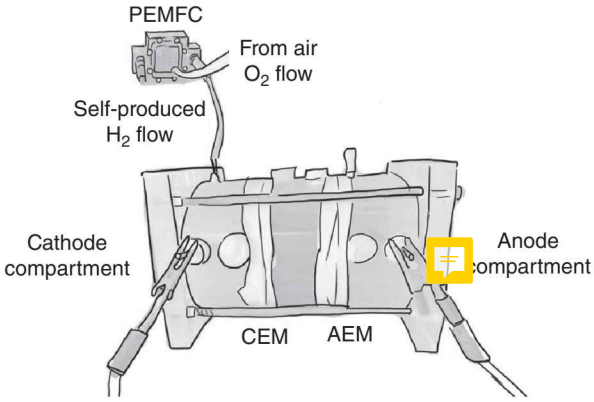

Figure 11.3 Electrodialytic reactor with three compartments (ø = 8 cm, central and electrolyte compartments with $L = 5$ cm; CEM, cation-exchange membrane; AEM, anion-exchange membrane) connected to a proton-exchange membrane fuel cell. Source: adapted from Almeida, Magro, and Ribeiro [18].

search term "fuel cell," a total of 108 841 scientific papers (articles and reviews) were obtained. The dominant research areas are engineering (19.8%), energy (18.3%), and chemistry (15.8%); and the US, China, and Japan are the top three countries, contributing 40.5% of the scientific articles. The search term "fuel cell" was refined with the sub-subject "proton-exchange membrane fuel cell," obtaining 27 537 papers from 1960 to 2020, meaning 25.3% of all fuel cell technologies.

PEMFC is reported as the most versatile fuel cell device available in the market. PEMFCs are easy to adapt to different energy production strategies since they are lightweight, have high power density, and have a cold-start capability so they can operate at low temperatures (<90 °C). Thus, to test a proof of concept of electrical energy generation from hydrogen production, a PEMFC was selected to be coupled with the electrodialytic reactor (Figure 11.3) [16].

The drawbacks found in the current literature are associated with the reactor design. Most electrodialytic setups are designed to allow the produced gases to flow freely into the atmosphere while aiming to reduce pressure-related transport mechanisms. Magro et al. [16] showed that there are new possibilities for saving energy and producing H_2 for different purposes in electrodialytic treatment, leading to an increase in the sustainability and applicability of the electro-remediation, decontamination, or of contaminant degradation processes. Thus, a gas-collection strategy during treatment is included in the system, preventing gas losses to the atmosphere; additionally, as an energy carrier, H_2 can be used to accumulate energy during electric power demand valleys and generate electric power during peaks. Therefore, a reservoir can be integrated into the ED system to recover and use the H_2 produced for various purposes.

Although studies have shown the feasibility of fuel cells to recover and reuse hydrogen for different purposes, research gaps and barriers still need to be addressed regarding scaling up the technology. Some examples are the infrastructures for

UNCORRECTED PROOFS

Trim Size: 170mm x 244mm Single Column Loose Ribeiro670117 c11.tex V1 - 12/11/2020 11:54pm Page 260

hydrogen production and storage, government initiatives to promote technical and social acceptance, and knowledge about the devices' end of life [15].

11.3 Economic Assessment of PEMFC Coupled with Electroremediation

11.3.1 Scenario Analysis

The scenario analysis aims to evaluate the impacts of possible future events on system performance. This analysis was carried out in a process forecasting perspective, considering a period of time and the occurrence of various situations. In addition, changes in system parameters in an uncertain environment were considered. Scenario analysis can be used to estimate the behavior of the system in response to an unexpected event. These studies may be helpful to explore changes in system performance, considering a theoretical best case (optimistic) or worst case (pessimistic) scenario. It may also provide guidelines for an investment strategy [50].

A PEMFC *core* is a membrane-electrode assembly consisting of a proton-exchange membrane and catalyst electrodes. The membrane-electrode is sandwiched by gas-diffusion layers, bipolar plates, current collectors, and compression plates to form a cell stack [4]. The bipolar plates and gas diffusion layers allow the diffusion of the reacting gases toward the electrodes. The catalyst is a special material that facilitates the reaction of oxygen and hydrogen by protonating the hydrogen gas; it is usually made of platinum nanoparticles thinly coated onto conductive carbon paper [51]. The catalyst coated over the side of the membrane facing the hydrogen gas inlet promotes the dissociation of the gas into protons and electrons according to

$$H_2\,(g) = 2H^+ + 2e^- \tag{11.6}$$

The protons migrate through the proton-exchange membrane toward the other electrode, while the electrons are conducted through an external circuit, as the membrane is electrically insulating. This means the catalytic membrane allows protons to pass through while blocking electrons and oxygen. Electrons are conducted toward the other side of the membrane through an electrical circuit (producing electricity) and are available for the reduction of oxygen gas. On the catalysts at the cathode end of the membrane, the oxygen molecules (from air) react with the circulating electrons and protons that diffuse through the membrane to form water [51]. The overall chemical reaction at the fuel cell is therefore

$$H_2\,(g) + {}^1\!/_2\,O_2\,(g) = H_2O \tag{11.7}$$

The electrical efficiency of PEMFCs depends on the material and working temperature; but currently, commercialized fuel cells can operate at an optimal temperature of around 85 °C and obtain efficiencies near 70% [47].

Let us assume an electrodialytic treatment submitted to a DC of I (A). The electrical energy necessary to maintain this current will depend on the cell voltage, ϕ_{cell}

UNCORRECTED PROOFS

Trim Size: 170mm x 244mm Single Column Loose Ribeiro670117 c11.tex V1 - 12/11/2020 11:54pm Page 261

(V), which can be considered the combination of different electric potential drops in series given by

$$\phi_{cell} = (\phi + \xi)_{anode} + \frac{I}{\sigma_{anol}} + \Delta\phi_{AEM} + \frac{I}{\sigma_{sample}} + \Delta\phi_{CEM} + \frac{1}{\sigma_{cathol}} + (\phi + \xi)_{cathode} \tag{11.8}$$

where $\phi + \xi$ (V) are the electrode potential and the overpotential in each electrode, σ (Ω) is the conductivity of the electrolyte (at the anolyte, the sample electrolyte, or the catholyte), and $\Delta\phi_{AEM}$ and $\Delta\phi_{CEM}$ (V) are the electric potential drops through the anion- and the cation-exchange membrane, respectively.

As the conductivity of the anolyte and the catholyte is normally very high, ensured by the pH changes produced by means of the electrode reactions, the electric potential related to ohmic losses in the electrolytes is negligible compared to the other terms. In the case of the sample compartments, this assumption is also valid for liquid solutions or suspensions that are properly stirred and have enough conductivity. The electrode potentials for standard conditions are given in Eqs. (11.1, 11.3), assuming water electrolysis. The potential will be on the order of approximately 2 V, depending on the pH changes on the media and the overpotentials. These overpotentials are expected, as the releasing gas forms attached bubbles over the surface of the electrodes that reduce the available reacting surface. As mentioned before, there are electrode materials that favor the release of these bubbles and impose lower overpotentials in the water electrolysis system. It is known that a minimum of 2.5 V is necessary to trigger the electrolysis of water and that the overpotentials increase with the applied current. With respect to the membrane potential, the rejection of charged species due to the internal membrane charge produces an electric potential drop through the membrane, which depends on the membrane's fixed charge, thickness, and material.

Summing up, the cell voltage in an electrodialytic reactor will have a minimum value of 2 V and will increase depending on the contribution of the different resistances. Taking into account the minimum value of $\phi_{cell}^{min} = 2$ V, assuming a faradic efficiency at the cathode of 100% with respect to the production of hydrogen gas, the higher heat value of H_2 of 286 kJ mol^{-1}, and fuel cell efficiency of 70%, it could be possible to recuperate up to 50% of the electrical energy applied to produce the electrolysis reactions. As discussed earlier, to achieve recuperations as close as possible to this theoretical maximum of 50%, proper design should take into account the adequate selection of electrode and membrane materials, as well as proper geometry and conductivity of the electrolyte compartments.

It has to be pointed out that the presented maximum recovery value has been calculated with respect to the energy used for the electrolysis reactions and that the electrodialytic reactor may have additional energy requirements, such as, for example, the energy necessary to pump and stir the electrolytes.

Furthermore, it is also worth mentioning that the theoretical maximum could increase if fuel cells are used for the gases produced at the anode compartment. For example, if high concentrations of chlorine gas are expected from the system, it could be possible to incorporate gas collectors at the anode and Cl_2 fuel cells to avoid the

UNCORRECTED PROOFS

Trim Size: 170mm x 244mm Single Column Loose Ribeiro670117 c11.tex V1 - 12/11/2020 11:54pm Page 262

release of the gas into the atmosphere during the treatment and increase the energy recovery potential.

11.3.2 Hydrogen Business Model Canvas

The continuous demand for hydrogen recovery processes is increasing awareness in the market. It is also expected that the fuel cell technologies market will reach USD $10.25 billion by 2025 (from ~USD $0.68 billion) [52]. Some of the primary tools in a preliminary market evaluation were used to understand the drivers and barriers for hydrogen self-produced by electrodialytic technology, to potentiate its further introduction into the market.

Thousands of publications (bibliometric evaluation through SCOPUS, with keywords "electrochemical process" and "electrokinetic process") have sought to develop new technologies or improve existing processes. Now, at the end of this long period, very few are being applied at their full scale, and most of them remain at the stage of "promising" technologies. Many strategies have recognizable benefits, but technological difficulties and handicaps can be identified. These disadvantages are related to missing components in the technology's value chain and the existence of only a few highly specialized stakeholders [53].

It is imperative to show what the needs are to begin with, aiming at a strategy and a clarified overview of a potential market approach.

Thus, a top-down approach was applied to build up the business model canvas (BMC). The BMC was designed for marketing the electrodialytic reactor coupled with the PEMFC, keeping in mind the possibility to decentralize the energy produced by this technology, as shown in Figure 11.4. This business model covered the primary drivers and propositions for a further introduction of this new concept on a larger scale.

This model was conducted considering a costumer segment example: industries facing economic and social issues related to energy, and looking for innovative technologies for sustainable production. Toward that end, the value proposition should include (i) a technology assessment that includes the components involved in the reactor concept; (ii) the benefits this technology will bring, which are a low CO_2 footprint and an add-in to conventional current processes; and (iii) opportunities that may accompany this new strategy, including the possibility to treat a broad range of substances from environmental matrices.

The channels to attract new customers are also crucial in market research. Today, the Web is a valid strategy to disseminate new ideas and reach people around the world. Thus, a clear, concise website outlining the advantages and details of the technology concept, acquisition, maintenance, and contacts, will help customers during the first step. Later, face-to-face meetings will be useful to explain doubts and concerns and improve trust in the company and, consequently, in the new products. Fairs, brochures, and direct sales will also potentiate contact and affirmation of the company in related events.

UNCORRECTED PROOFS

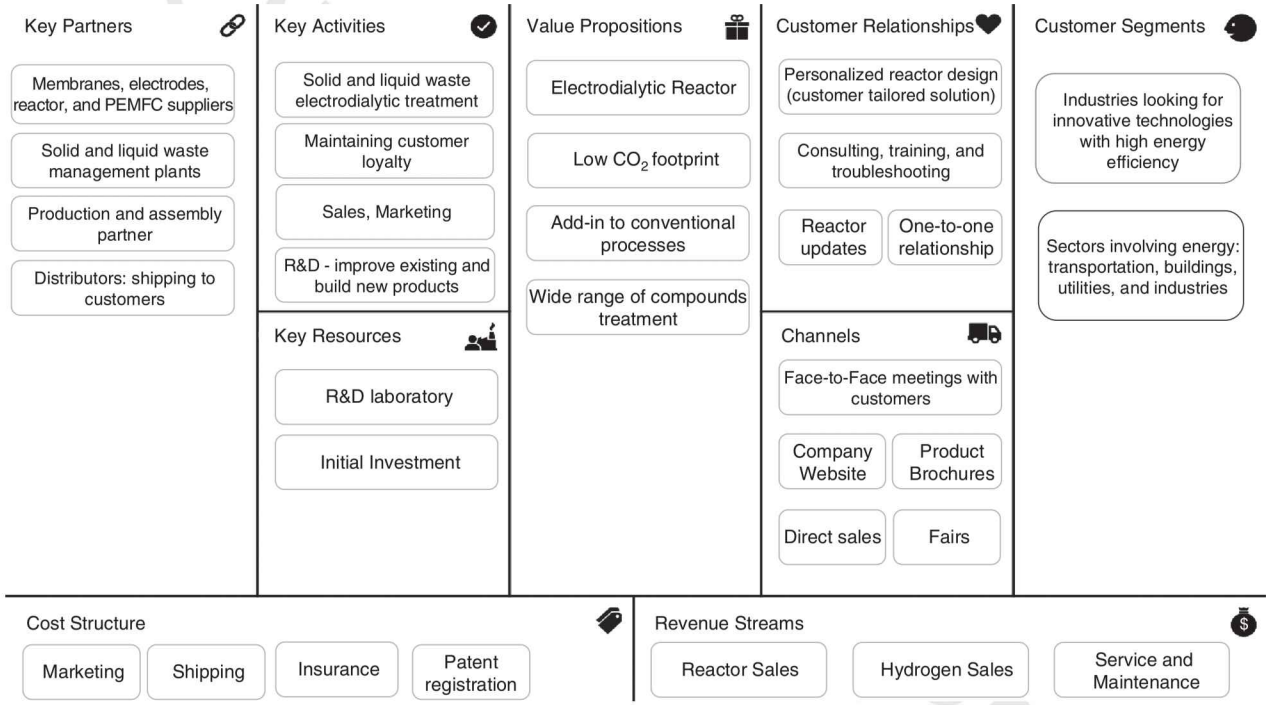

Figure 11.4 Business model canvas regarding the proton-exchange membrane fuel cell on hydrogen technology.

UNCORRECTED PROOFS

Trim Size: 170mm x 244mm Single Column Loose
Ribeiro670117 c11.tex V1 - 12/11/2020 11:54pm Page 263

Trim Size: 170mm x 244mm Single Column Loose Ribeiro670117 c11.tex V1 - 12/11/2020 11:54pm Page 264

Key resources are the primary inputs that companies use to create a value proposition, service their customer segment, and deliver the product to the customer. Considering a technology that is customizable according to the industrial sector target, it is imperative to include a research and development laboratory. Additionally, the market entry strategy should focus on scaling up with an industrial partner in a *win-win* solution to test full-scale product feasibility.

Key activities must be carried out to fulfill the business purpose. These activities should sustain customer relationships while providing long-term revenue streams. Considering the typology of the reactor, solid and liquid waste are the target sources of this strategy. Through some promising matrices, it will be possible to keep intensifying sales and marketing activities and research and development work to improve existing reactors and build new products, maintaining consumer loyalty [54].

Key partners are helpful in doing the work of the business model in areas that are not among the company's core activities. These partnerships might be with suppliers, manufacturers, or other business partners. Thus, it is crucial to find (i) suppliers of membranes, electrodes, reactors, and PEMFC; (ii) solid and liquid waste management plants interested in the technology; (iii) production and assembly partners; and (iv) distributors that will be responsible for shipping the reactor to customers.

The cost structure should be defined considering fixed and variable costs of the technology. Four elements that must be considered in the first stage are the marketing strategy, shipping of the electrodialytic reactors, insurance, and patent registration [54]. Revenue streams will guarantee the sustenance of the company, in this case through sales of the reactor and hydrogen and from the provision of services and maintenance.

11.3.3 SWOT Analysis

The overview of hydrogen recovery within the electrodialytic process called up several promising prospects for future research. Accordingly, a SWOT (strengths, weaknesses, opportunities, and threats) analysis of the potential market is presented (Table 11.2).

The SWOT analysis suggests the potential of the electrodialytic reactor for the hydrogen recovery market, primarily due to the purity of the hydrogen produced coupled with the generation of non-toxic byproducts. This represents an opportunity not only for strategy development but also to compete with primary energy sources. However, the high cost of investment should be overcome and supported by a structured conceptual strategy and market roadmap. Currently, existing legislation regarding hydrogen production and storage issues is underdeveloped, which may influence the standardization of new technologies.

11.4 Final Remarks

The global availability of clean and affordable energy by the use/reuse of renewable energy systems is at the top of the list. Hydrogen is gaining prominence as

UNCORRECTED PROOFS

Trim Size: 170mm x 244mm Single Column Loose Ribeiro670117 c11.tex V1 - 12/11/2020 11:54pm Page 265

Table 11.2 SWOT analysis of the electrodialytic reactor for the hydrogen recovery market.

	Helpful factors	**Harmful factors**
	Strengths	Weaknesses
Internal origin	• Product or process of manufacture can be patented • Performance advantage: high purity of hydrogen • High dynamic operation • Compact and multitasking system design • Product's long-run cash-flow potential • Non-toxic energy	• Development of the conceptual strategy and market roadmap • Partially established high cost of components
	Opportunities	Threats
External origin	• Market allies or partners • Market growth • Trialability • Increasing future expansion opportunities (increment of fossil fuel prices) • Increasing cooperation: collaboration between academic institutions, research institutes, online knowledge transfer to economic operators • Increasing energy efficiency through the efficient use of energy resources throughout the energy cycle – production, transport, storage, distribution, and final consumption • Current mindset toward energy decentralization	• Effectiveness of patent protection • Trade secret protection common and effective • Reactor involves comparatively high costs (of acquisition) • Storage • Immaturity of the legislative framework

an enabler of the transition to clean energy. Technologies for hydrogen production are taking advantage of the current market expansion, promoting their optimization and development to higher maturity levels. Electrodialytic technologies can be upgraded due to the natural electrolysis of water that occurs at the electrodes during the remediation process. H^+ is generated by water oxidation at the anode and OH^- by water reduction at the cathode end. This phenomenon is a powerful feature when remediation, degradation, removal, and recovery processes are involved since the generated byproduct can be used as fuel in PEMFCs. Self-produced hydrogen can be applied to electrical energy production to alleviate electroremediation energy costs and add value to the technology. Moreover, as an energy carrier, hydrogen can be stored during electric power demand valleys and can generate electric power during peak periods.

In this chapter, the crucial elements involved in electrodialytic remediation were analyzed. In particular, electrode composition and ion-exchange membranes

UNCORRECTED PROOFS

Trim Size: 170mm x 244mm Single Column Loose Ribeiro670117 c11.tex V1 - 12/11/2020 11:54pm Page 266

directly affect the quality of the hydrogen produced. The optimization of reactor components will promote an increase in the hydrogen-generation ratio and application to a broad range of matrices with different chemical and physical properties.

A business plan was built to summarize the economic study and the possibilities for marketing the technology, from a bottom-up approach to top-down next actions. The electrodialytic reactor, coupled with a PEMFC, was also subjected to a SWOT analysis. This study demonstrated not only the opportunity to develop electrodialytic-based technologies but also the feasibility of its introduction in the market to compete with primary energy sources.

Acknowledgments

This work has received funding from the European Union's Horizon 2020 research and innovation program under Grant Agreement No. 776811, under the Marie Skłodowska-Curie grant agreement No. 778045. The authors also acknowledge and appreciate the support given to CENSE by the Portuguese Foundation for Science and Technology (FCT) through the strategic project UIDB/04085/2020. C. Magro and J. Almeida acknowledge Fundação para a Ciência e a Tecnologia for their PhD fellowships: SFRH/BD/114674/2016 and PD\BD\135170\2017 (EcoCoRe Doctoral Program), respectively. The authors would also like to acknowledge Professor Susana Sério and Isabel Dias Nogueira for the SEM/EDS analysis for ion-exchange membranes. Also, we thank Professor Francesca Pagnanelli and Antonio Rubino for their help with the electrode SEM characterization, performed at Sapienza Università di Roma. This work is anchored by the RESOLUTION LAB, a laboratory at the NOVA School of Science and Technology.

References

1 European Commission. (2010). A strategy for competitive, sustainable and secure energy – energy 2020.
2 Gaudernack, B. (1998). Hydrogen production from fossil fuels. In: *Hydrogen Power: Theoretical and Engineering Solutions* (ed. T.O. Saetre), 75–89. Netherlands, Dordrecht: Springer.
3 Abdol Rahim, A.H., Tijani, A.S., Wan Mohamed, W.A.N. et al. (2014). An overview of hydrogen production from renewable energy source for remote area application. *Applied Mechanics and Materials* 699: 474–479.
4 Shiva Kumar, S. and Himabindu, V. (2019). Hydrogen production by PEM water electrolysis – a review. *Materials Science for Energy Technologies* 2 (3): 442–454.
5 Haneda, T. and Akisawa, A. (2017). Technological assessment of PEFC power generation system using by-product hydrogen produced from a caustic soda plant. *International Journal of Hydrogen Energy* 42 (5): 3240–3249.

UNCORRECTED PROOFS

Trim Size: 170mm x 244mm Single Column Loose Ribeiro670117 c11.tex V1 - 12/11/2020 11:54pm Page 267

6 Tuna, C.E., Silveira, J.L., da Silva, M.E. et al. (2018). Biogas steam reformer for hydrogen production: evaluation of the reformer prototype and catalysts. *International Journal of Hydrogen Energy* 43 (4): 2108–2120.

7 Magro, C.J.C. (2014). Electrodialytic remediation of two types of air pollution control residues and their applicability in construction materials. Master's thesis, NOVA School of Sciences and Technology, NOVA University Lisbon.

8 Guedes, P., Mateus, E., Almeida, J. et al. (2016). Electrodialytic treatment of sewage sludge: current intensity influence on phosphorus recovery and organic contaminants removal. *Chemical Engineering Journal* 306: 1058–1066.

9 Tunsu, C., Menard, Y., Eriksen, D.Ø. et al. (2019). Recovery of critical materials from mine tailings: a comparative study of the solvent extraction of rare earths using acidic, solvating and mixed extractant systems. *Journal of Cleaner Production* 218: 425–437.

10 Almeida, J., Craveiro, R., Faria, P. et al. (2020). Electrodialytic removal of tungsten and arsenic from secondary mine resources – deep eutectic solvents enhancement. *Science of the Total Environment* 710: 136364.

11 Ribeiro, A.B. and Rodríguez-Maroto, J.M. (2006). Electroremediation of heavy metal-contaminated soils -processes and applications. In: *Trace Elements in the Environment: Biogeochemistry, Biotechnology, and Bioremediation* (eds. M.N.V. Prasad, K.S. Sajwan and R. Naidu), 341–368. Florida, USA: CRC Press.

12 Magro, C., Mateus, E.P., Paz-Garcia, J.M., and Ribeiro, A.B. (2020). Emerging organic contaminants in wastewater: understanding electrochemical reactors for triclosan and its by-products degradation. *Chemosphere* 247: 125758.

13 Ferreira, A.R., Couto, N., Guedes, P. et al. (2018). Electrodialytic 2-compartment cells for emerging organic contaminants removal from effluent. *Journal of Hazardous Materials* 358: 467–474.

14 Wang, M., Wang, G., and Sun, Z. (2019). Review of renewable energy-based hydrogen production processes for sustainable energy innovation. *Global Energy Interconnection* 2: 43–44.

15 Valente, A., Iribarren, D., and Dufour, J. (2019). End of life of fuel cells and hydrogen products: from technologies to strategies. *International Journal of Hydrogen Energy* 44 (38): 20965–20977.

16 Magro, C., Almeida, J., Paz-Garcia, J.M. et al. (2019). Exploring hydrogen production for self-energy generation in electroremediation: a proof of concept. *Applied Energy* 255: 113839.

17 European Commission (2015) Closing the loop - An EU action plan for the Circular Economy.

18 Almeida, J., Magro, C., Mateus, E.P., and Ribeiro, A.B. (2020). Electrodialytic hydrogen production and critical raw materials recovery from secondary resources. *Water* 12 (5): 1262.

19 Rivera, I., Schröder, U., and Patil, S.A. (2019). Microbial electrolysis for biohydrogen production: technical aspects and scale-up experiences. In: *Microbial Electrochemical Technology* (eds. S.V. Mohan, S. Varjani and A. Pandey), 871–898. Elsevier.

UNCORRECTED PROOFS

Trim Size: 170mm x 244mm Single Column Loose Ribeiro670117 c11.tex V1 - 12/11/2020 11:54pm Page 268

20 Li, P.C.H. and Harrison, D.J. (1997). Transport, manipulation, and reaction of biological cells on-chip using electrokinetic effects. *Analytical Chemistry* 69 (8): 1564–1566.

21 Gill, R.T., Harbottle, M.J., Smith, J.W.N., and Thornton, S.F. (2014). Electrokinetic-enhanced bioremediation of organic contaminants: a review of processes and environmental applications. *Chemosphere* 107: 31–42.

22 Szumski, M., Kłodzińska, E., and Buszewski, B. (2005). Separation of microorganisms using electromigration techniques. *Journal of Chromatography. A* 1084 (1–2): 186–193.

23 Ferreira, A.R., Guedes, P., Mateus, E.P. et al. (2017). Influence of the cell design in the electroremoval of PPCPs from soil slurry. *Chemical Engineering Journal* 326: 162–168.

24 Ribeiro, A.B., Rodríguez-Maroto, J.M., Mateus, E.P. et al. (2007). Modeling of electrodialytic and dialytic removal of Cr, Cu and As from CCA-treated wood chips. *Chemosphere* 66 (9): 1716–1726.

25 Guedes, P., Mateus, E.P., Fernandes, J.P., and Ribeiro, A.B. (2019). Electro-technologies for the removal of 2,4,6-trichloroanisole from naturally contaminated cork discs: reactor design and proof of concept. *Chemical Engineering Journal* 361: 80–88.

26 Ferreira, C., Jensen, P., Ottosen, L., and Ribeiro, A. (2005). Removal of selected heavy metals from MSW fly ash by the electrodialytic process. *Engineering Geology* 77: 339–347.

27 Chen, W., Kirkelund, G.M., Jensen, P.E., and Ottosen, L.M. (2018). Electrodialytic extraction of Cr from water-washed MSWI fly ash by changing pH and redox conditions. *Waste Management* 71: 215–223.

28 Hansen, H.K., Lamas, V., Gutierrez, C. et al. (2013). Electro-remediation of copper mine tailings. Comparing copper removal efficiencies for two tailings of different age. *Minerals Engineering* 41: 1–8.

29 Stolten, D. and Emonts, B. (2016). *Hydrogen Science and Engineering: Materials, Processes, Systems and Technology*. INC.

30 Slama, R.B. (2013). Hydrogen production by water electrolysis effects of the electrodes materials nature on the solar water electrolysis performances. *Natural Resources* 4 (1): 1–7.

31 Pouladvand, I., Asl, S.K., Hoseini, M.G., and Rezvani, M. (2019). Characterization and electrochemical behavior of Ti/TiO2–RuO2–IrO2–SnO2 anodes prepared by sol–gel process. *Journal of Sol-Gel Science and Technology* 89 (2): 553–561.

32 Niksa, M.J. and Rudd, E.J. (2019). Precious metal containing mixed metal oxide (MMO) electrodes. Water Star Inc.

33 Jafari Foruzin, L., Rezvani, Z., Nejati, K. et al. (2019). High quantum efficiency of photocatalytic water oxidation over the TiO2/MMO nanocomposite under visible-light irradiation. *Journal of Molecular Liquids* 288: 111035.

34 Liao, C.H., Huang, C.W., and Wu, J.C.S. (2012). Hydrogen production from semiconductor-based photocatalysis via water splitting. *Catalysts* 2 (4): 490–516.

UNCORRECTED PROOFS

Trim Size: 170mm x 244mm Single Column Loose Ribeiro670117 c11.tex V1 - 12/11/2020 11:54pm Page 269

35 Youn, J.S., Jeong, S., Kang, H. et al. (2019). Effect of carbon coating on Cu electrodes for hydrogen production by water splitting. *International Journal of Hydrogen Energy* 44 (37): 20641–20648.

36 Kovendhan, M., Kang, H., Youn, J.S. et al. (2019). Alternative cost-effective electrodes for hydrogen production in saline water condition. *International Journal of Hydrogen Energy* 44 (11): 5090–5098.

37 Ganci, F., Lombardo, S., Sunseri, C., and Inguanta, R. (2018). Nanostructured electrodes for hydrogen production in alkaline electrolyzer. *Renewable Energy* 123: 117–124.

38 Yuzer, B., Selcuk, H., Chehade, G. et al. (2020). Evaluation of hydrogen production via electrolysis with ion exchange membranes. *Energy* 190: 116420.

39 Strathmann, H. (2004). Preparation and characterization of ion-exchange membranes. In: *Ion-Exchange Membrane Separation Processes* (ed. H. Strathmann), 89–146. Elsevier.

40 Hansen, H.K. (1995). Practical and theoretical aspects concerning the use of ion exchange membranes and resins in electrokinetic soil remediation. PhD thesis, Technical University of Denmark.

41 Strathmann, H. (2004). Overview of ion-exchange membrane processes. In: *Ion-Exchange Membrane Separation Processes* (ed. H. Strathmann), 1–22. Elsevier.

42 Pham, T.H., Olsson, J.S., and Jannasch, P. (2017). N -spirocyclic quaternary ammonium ionenes for anion-exchange membranes. *Journal of the American Chemical Society* 139 (8): 2888–2891.

43 Paidar, M., Fateev, V., and Bouzek, K. (2016). Membrane electrolysis – history, current status and perspective. *Electrochimica Acta* 209: 737–756.

44 Altmann, M., Brenninkmeijer, A., Lanoix, J-C. et al. (2010). Decentralised energy systems. European Parliament. EU Publications, No. IP/A/ITRE/ST/2009-16.

45 Kone, J.-P., Zhang, X., Yan, Y. et al. (2018). CFD modeling and simulation of PEM fuel cell using OpenFOAM. *Energy Procedia* 145: 64–69.

46 Pei, P., Jia, X., Xu, H. et al. (2018). The recovery mechanism of proton exchange membrane fuel cell in micro-current operation. *Applied Energy* 226: 1–9.

47 Staffell, I., Green, R., and Kendall, K. (2008). Cost targets for domestic fuel cell CHP. *Journal of Power Sources* 181 (2): 339–349.

48 Ahmadi, M.H., Mohammadi, A., Pourfayaz, F. et al. (2016). Thermodynamic analysis and optimization of a waste heat recovery system for proton exchange membrane fuel cell using transcritical carbon dioxide cycle and cold energy of liquefied natural gas. *Journal of Natural Gas Science and Engineering* 34: 428–438.

49 Lopes, V.V., Rangel, C.M., and Novais, A.Q. (2011). Fractional-order transfer functions applied to the modeling of hydrogen PEM fuel cells. In: *21 European Symposium on Computer Aided Process Engineering*, vol. 29 (eds. E.N. Pistikopoulos, M.C. Georgiadis and A.C. Kokossis). Computer Aided Chemical Engineering, 1748–1752. Elsevier.

50 Balaman, Ş.Y. (2019). Uncertainty issues in biomass-based production chains. In: *Decision-Making for Biomass-Based Production Chains* (eds. Ş. Balaman and T.B. Yılmaz), 113–142. Elsevier.

UNCORRECTED PROOFS

Trim Size: 170mm x 244mm Single Column Loose Ribeiro670117 c11.tex V1 - 12/11/2020 11:54pm Page 270

51 Ozden, A., Shahgaldi, S., Li, X., and Hamdullahpur, F. (2019). A review of gas diffusion layers for proton exchange membrane fuel cells – with a focus on characteristics, characterization techniques, materials and designs. *Progress in Energy and Combustion Science* 74: 50–102.

52 Market Research Future (2019). Fuel cell technology market research report - global forecast till 2025. MRFR/E&P/0302-CR.

53 Lacasa, E., Cotillas, S., Saez, C. et al. (2019). Environmental applications of electrochemical technology. What is needed to enable full-scale applications? *Current Opinion in Electrochemistry* 16: 149–156.

54 Schiltz, E.N. (2018). How can high-growth business opportunities for a cutting-edge technology be discovered? Master's thesis, NOVA School of Business and Economics, NOVA University, Lisbon.

UNCORRECTED PROOFS

Trim Size: 170mm x 244mm Single Column Loose Ribeiro670117 c12.tex V1 - 12/11/2020 11:55pm Page 271

12

Electrokinetic-Phytoremediation of Mixed Contaminated Soil for Environmental Remediation

Joana Dionísio[1], Nazaré Couto[1], Paula Guedes[1,2], Cristiana Gonçalves[1], and Alexandra B. Ribeiro[1]

[1]CENSE – Center for Environmental and Sustainability Research, Department of Environmental Sciences and Engineering, NOVA School of Science and Technology, NOVA University Lisbon, 2829-516 Caparica, Portugal
[2]Instituto de Tecnologia Química e Biológica António Xavier, NOVA University Lisbon, 2780-157 Oeiras, Portugal

12.1 Soil Contamination

Due to pollution related to anthropogenic factors, many toxic materials have been released and accumulated in soils that have consequently becoming profoundly polluted [1]. Contamination caused by diffuse or point sources may damage the valuable resources and services these ecosystems provide [2].

Soils are often polluted by a complex mixture of inorganic and organic contaminants. The most usual inorganic contaminants are the heavy metals, while the organic contaminants include polycyclic aromatic hydrocarbons (PAHs), pesticides, biocides, pharmaceuticals and personal care products (PPCPs), flame retardants, surfactants, polychlorinated biphenyls (PCBs), etc. [3, 4].

Organic contaminants (OCs) reach the soil through several routes. For example, primary sources in the environment of PAHs that are associated with petroleum and classified according to their aromatic benzene ring number are combustion, extraction, and use of fossil fuels, as well as industrial processes. PPCPs comprise a diverse group of chemicals present in several products, such as analgesics, antibiotics, cytostatic hormones, disinfectants, and antiseptics [5]. Post-use, they can be directly and indirectly released into soil: for instance, through wastewater effluent irrigation or landfill sites. Pesticides are regularly applied to soil, sometimes in an incautious manner. When these distinct OCs reach the environment, the extent of damage varies according to the physicochemical properties of both contaminants and soils. The overwhelming use of these chemicals has caused harmful effects on the environment. They are responsible for exerting pressure on soil communities, irreversibly affecting them, and compromising soil functions. Due to their lipophilic nature, OCs tend to accumulate in the adipose tissues of living organisms, and even though they are commonly present at low concentrations, chronic exposure is linked to harmful effects in the development of wildlife [2]. PAHs, for example, have been

Electrokinetic Remediation for Environmental Security and Sustainability, First Edition.
Edited by Alexandra B. Ribeiro and M.N.V. Prasad.
© 2021 John Wiley & Sons Ltd. Published 2021 by John Wiley & Sons Ltd.

UNCORRECTED PROOFS

Trim Size: 170mm x 244mm Single Column Loose Ribeiro670117 c12.tex V1 - 12/11/2020 11:55pm Page 272

linked to several cancers such as skin, lung, bladder, liver, and stomach by several studies concerning animal and human health [6], and soils contaminated with these chemicals often also contain high concentrations of metals originating from similar sources [7].

In soil contamination, the most commonly found metals are lead (Pb), chromium (Cr), arsenic (As), zinc (Zn), cadmium (Cd), copper (Cu), mercury (Hg), and nickel (Ni). These inorganic chemicals enter the environment through natural and anthropogenic sources [8]. The most relevant anthropogenic sources encompass mining, smelting, electroplating, fertilizers, pesticides, animal manures, sludge dumping, industrial discharge, atmospheric deposition, etc. [9]. Heavy metal pollution may result in adverse impacts on the overall living systems dependent on soil functions. Metals can damage the microbial community by altering their dimension, composition, and even activity. Uptake of heavy metals by plants can also harm their quality, even culminating in their death if the heavy metal concentration is too high [10]. Heavy metals in urban soils may reach the human body through skin absorption, inhalation of dust, or the consumption of contaminated produce or plants, with adverse impacts on human health as a consequence of bioaccumulation and biomagnification [11].

Soil remediation may not be easily accomplished because removal techniques are not always well-matched. Research has shown that heavy metal and organic contamination (depending on the type of contaminant) can pose synergistic or antagonistic effects, compromising soil's natural resilience. A majority of the methods available for their removal have the disadvantage of being expensive and occasionally require the translocation of contaminated substrates to specific treatment sites, adding risks of secondary contamination. Thus, in situ methods like phytoremediation, which are less environmentally disruptive [12], may be preferable.

12.2 Phytoremediation

Phytoremediation is an eco-friendly approach that relies on the natural processes of plants and microorganisms to remove pollutants or render them harmless. It can be used to decontaminate several matrices, as it successfully acts on soil, sediments, water, and air. Phytoremediation is primarily solar-powered and considered a low-cost, sustainable means to improve the economies of developing countries since it has the potential to be a viable solution for impoverished farmers [13–15].

Phytoremediation comprises five different processes: phytodegradation, phytostabilization, rhizoremediation, phytovolatilization, and phytoextraction [9]. Each mechanism contributes in a specific way according to the physicochemical properties of the contaminants that need to be removed or mitigated. Some of the variables that determine chemical uptake and distribution within plants encompass properties of compounds such as water solubility, vapor pressure, molecular weight, octanol-water partition coefficient (K_{ow}), environmental characteristics, and plant characteristics [16].

UNCORRECTED PROOFS

Trim Size: 170mm x 244mm Single Column Loose Ribeiro670117 c12.tex V1 - 12/11/2020 11:55pm Page 273

In *phytodegradation*, organic chemicals are absorbed and degraded inside the plant by metabolic processes that break down contaminants into simpler molecular forms, ultimately accumulating and incorporating them into their tissues [15, 17]. The water solubility, lipophilicity, and log K_{ow} between 0.5 and 3.5 that characterize the majority of organic contaminants enables their translocation to the plant tissues [18].

Phytostabilization acts on contaminants such as heavy metals by decreasing their movement in the polluted medium – that is, immobilizing them, which limits their diffusion in soil. Harmful compounds are altered into simpler forms, adhered to plant surfaces, and adsorbed into the root system [14, 19, 20].

In *rhizoremediation*, organic contaminants present in the rhizosphere are degraded by bacteria and fungi, stimulated by root exudates and enzymes. In this case, the plant does not directly degrade contaminants; instead, it creates the necessary conditions for the development of fungi and bacteria that degrade the contaminants [21].

Through *phytovolatization*, organic contaminants are converted into nontoxic forms, transferred from roots to leaves, and volatilized into the atmosphere at relatively low concentrations [17, 19, 22].

Phytoextraction is the process of extracting organic and inorganic substances, such as heavy metals, from solution media through transport; and concentrating compounds from the substrate into harvestable parts of plants such as above-ground shoots and (occasionally) parts of the rooting system. Through phytoextraction, these substances are removed from soil and relocated in harvestable parts of plants until they need to be replaced. Compared to soil, and depending on the heavy metals, the recycling, disposal, treatment, or oxidation of plants is a less costly investment [14, 15, 20, 22, 23].

Hyperaccumulator plants are fundamental to the phytoextraction success, as these plant species can accumulate high concentrations of metals and other pollutants in their shoots without demonstrating significant signs of toxicity [22–24]. Hyperaccumulation of metals relies on the bioavailability of the metals in soil, the expression of detoxification genes and metal transporters provided by the plant, and the plant-associated microbiota [9, 25]. The most used families of plants for this type of remediation include Asteraceae, Brassicaceae, Buxaceae, Celastraceae, Commelinaceae, Crassulaceae, Cunoniaceae, Euphorbiaceae, Fabaceae, Gleicheniaceae, Lamiaceae, Linderniaceae, Malvaceae, Myrtaceae Orobanchaceae, Pteridaceae, Polygonaceae, Phyllanthaceae, Proteaceae, Salicaceae, and Violaceae [26]. It has been reported that metal-hyperaccumulating plant species, in general, accumulate more than 100 μM of Cd, while normal plants accumulate only about 0.5–5 μM of Cd [27].

Despite its advantages, phytoremediation is not free of limitations. Plants can only act within a limited depth, as they are limited to their root length. After phytoextraction, landfilling, incineration, and composting may be options to dispose of or recycle the metals, although this depends upon the results of a toxicity characteristic leaching procedure (TCLP) and cost.

UNCORRECTED PROOFS

Trim Size: 170mm x 244mm Single Column Loose Ribeiro670117 c12.tex V1 - 12/11/2020 11:55pm Page 274

Although phytoremediation is a reliable technique for treating mixed contaminated soils, it is not exempt from constraints. This type of restoration requires a long treatment time since it is intensely conditioned by the plants' growth rate and biological cycles. In addition, its efficiency relies on the degree and location of contamination. Target substances must be at the surface or shallow depths and bioavailable, but their concentration cannot be excessive [4].

By coupling phytoremediation with electrokinetic (EK) remediation, most of the limitations can be overcome, and the processes can even profit from a synergistic effect [28]. However, it is critical to consider all the possible positive or negative effects of the electric field on the plant.

12.3 Electroremediation

EK as a remediation technique for contaminated soil was primarily studied and developed in the late 1980s to make it faster and easier to extract contaminants from soils with fine grains and low hydraulic conductivity (less than 10^{-4} cm s^{-1}). A decade later, various research had evaluated the role of electroosmosis and ion migration for the extraction of heavy metals and ions. Since then, numerous studies have highlighted the need for and made efforts to enhance this process to improve extraction from both solid and liquid matrices [29, 30].

EK remediation is based on applying a low-level direct current to the polluted porous matrix to be decontaminated [31, 32]. A pair of electrodes – the anode and cathode – are inserted, and a voltage drop is applied. The electric field causes the mobilization and transportation of target compounds or, if feasible, their degradation. Compounds that cannot be degraded may be transported through the substrate toward the electrodes, where they are collected, pumped out, and safely discarded after treatment [21].

This treatment technology can be applied in situ or ex situ. Although in situ technologies are favored because they usually result in lower costs (no excavation) and less disruption of the environment, an ex situ configuration provides a more controllable environment and greater operational control. The duration of treatment can vary from days to several months or years; therefore, it is necessary to apply a low current to avoid adverse heating effects caused by ohmic heating generated in the system [33, 34].

As mentioned earlier, EK remediation encompasses several complex mechanisms that promote the transport of contaminants (inorganic and organic species) through four primary mechanisms: electromigration, electroosmosis, electrophoresis, and diffusion. *Electromigration* describes the transport of ion complexes toward the opposite charge; cations are attracted to the anode and anions to the cathode [32, 35]. *Electrophoresis* refers to the movement of electrically charged particles or colloids that, again, cause them to move toward the opposite-charge electrode. *Electroosmosis* is caused by the movement of ions under an applied electrical potential: as they dislocate, they drag along the water by viscous force, resulting in the movement of soil moisture from anode to cathode. The electroosmotic flux

UNCORRECTED PROOFS

Trim Size: 170mm x 244mm Single Column Loose Ribeiro670117 c12.tex V1 - 12/11/2020 11:55pm Page 275

(EOF) is the primary mechanism for removing uncharged or weakly dissociated organic contaminants [36]. *Diffusion* refers to the mass transport caused by the difference in a concentration gradient. Previous processes like electromigration and electroosmosis generate this concentration gradient and, consequently, diffusive transport, which is slower than the previously mentioned mechanisms [1].

Individually or combined, these processes act to enhance the transport of contaminants. Each transport process's contribution depends on several variables intrinsic to the contaminants and the medium to be treated, such as soil mineralogy, pore fluid composition, conductivity, and electrochemical properties of the species present.

During EK treatment, the primary electrode reactions are electrolysis of water at the anode (Eq. (12.1)), which generates hydrogen ions (H^+) and oxygen gas, as well as an acid pH; and reduction of water at the cathode (Eq. (12.2)), producing hydroxyl ions (OH^-) and hydrogen gas, and creating an alkaline front [1, 21]:

$$H_2O \rightarrow 2H^+ + \frac{1}{2}O_2(g) + 2e^- \tag{12.1}$$

$$2H_2O + 2e^- \rightarrow 2OH^- + H_2(g) \tag{12.2}$$

Water electrolysis is considered the dominant electron transfer reaction and significantly affects the EK process. The generated H^+ and OH^- ions are moved through the soil in opposite directions by electroosmosis, advection, and diffusion. The counteracting EOF and H^+ greater ionic mobility, in comparison to OH^-, causes the acid front to dominate the chemistry of the soil, except for small sections near the cathode. The soil pH values will differ depending on the level of transport of H^+ and OH^- ions and characteristics of the soil [35]. The electrolysis reactions have substantial implications for the absorption/desorption of the contaminants, dissolution/precipitation reactions, chemical speciation, and the degradation of the contaminants, therefore impacting the EK treatment's efficiency [21].

This technology has been applied to different matrices to remediate organic and inorganic contaminants [37, 38]. However, it is not exempt from limitations, as this can be a long process, and removing contaminants located at deeper depth or the presence of large amounts of non-targeted contaminants can pose a challenge.

Phytoremediation and EK treatment are highly compatible technologies, and combining them allows efficient removal by overcoming their specific difficulties, such as the phytoremediation challenge of applying phytoextraction to deep subsurface contaminants [39].

12.3.1 EK Process Coupled with Phytoremediation

The EK-assisted phytoremediation technology consists of applying a low-intensity electric field to the contaminated soil in the vicinity of growing plants [40]. This process's primary goals are to facilitate phytoextraction by making contaminants more bioavailable and to use plants' capacities to rehabilitate soil properties that may be altered or damaged due to the effects of EK [37].

Applying a low-level current improves phytoremediation by mobilizing nutrients and contaminants, making them more available for plant uptake or more subject

UNCORRECTED PROOFS

Trim Size: 170mm x 244mm Single Column Loose Ribeiro670117 c12.tex V1 - 12/11/2020 11:55pm Page 276

to degradation through indigenous bacteria in the rhizosphere [41], simultaneously promoting plant and microflora growth [40].

A combination of phytoremediation and EK was tested to remediate Cd, Pb, and Cu from water using *Eichhornia crassipes* [42]. Three operating conditions were assessed: phytoremediation system only, electroremediation only, and a combination of phytoremediation and electroremediation. In EK setups, 4 V were applied for 2 hours per day for 25 days. The results showed that *E. crassipes* stimulated by an electric field grew better and assimilated more metal. The maximum amount of metal reduced by *E. crassipes* was achieved when applying an electric field: after 10 days for Cu, and after 15 days for Cd and Pb. Also, under electric stimulation, the maximum amount of Cd and Cu was accumulated in the aerial parts of the plant, while Pb was attained by roots. Improved growth and chlorophyll synthesis were identified in *E. crassipes,* and overall phytoremediation capacity was enhanced by using the current [42].

The type of electrodes used and their configuration can influence the effectiveness of the coupled EK-assisted phytoremediation technology. The spatial distribution of the electrodes has a decisive impact on the distribution of the electric field [32]. Thus, a proper configuration should be assessed based on specific variables of the treatment site: contamination type, location, and the depth of both roots and contamination must be considered [40]. Achieving a successful arrangement will prevent leaching of contaminants to groundwater and expand the remediation radius deeper than the depth of the roots. The most common material used for electrodes is graphite, due to its low cost and inertness. However, other materials have been successfully used, such as steel, stainless steel, Zn-coated iron, and others. Depending on the desired configuration and the previously described variables, different materials can be chosen for the anode and cathode [43–45].

Another crucial parameter is the intensity of the electric field; as the rhizosphere is the place where degradation primarily occurs, it is essential to adjust the intensity to a value that does not affect microorganisms [46]. Using AC or DC, the voltage level, and continuous or periodic voltage application are also factors to consider [37].

The primary electrode reactions induce changes in the soil's chemistry, the most common being acidification of the soil by the acid front produced at the anode. The resulting low pH values are harmful to microbiota, and if the soil becomes highly acidic, it can result in their elimination [21]. However, the low-intensity electric field stimulates biomass production, favoring the soil's natural processes that increase microbial activity [21]. An investigation regarding bioavailability and bioaccumulation of Pb, As, and Cs in paddy soil under an electrokinetic field was performed by Mao et al. [45]. This study concluded that the EK process effectively increased the dissolution of metalloids by lowering pH close to the anode (pH 1.5), meaning this acidification efficiently increased the metalloids' overall solubility and bioavailability without compromising the removal efficiency of Indian mustard, spinach, and cabbage [45]. As lowering soil pH near the anode increased water-soluble and exchangeable forms of Pb, As, and Cs, thus enhancing solubility and bioavailability, more metal(loid)s were accumulated in plant roots and shoots [45].

UNCORRECTED PROOFS

Trim Size: 170mm x 244mm Single Column Loose Ribeiro670117 c12.tex V1 - 12/11/2020 11:55pm Page 277

In addition to simultaneous application, these technologies can be executed in sequence, applying phytoremediation after EK to assist in removing possible residual contaminants. The efficiency and duration of treatment depend on the aspects previously mentioned but can be increased by adding enhancing agents to improve bioremediation, mobility, and bioavailability of the contaminants.

In bioremediation, bacteria degrade contaminants into nontoxic products. To enhance bioremediation, genetic engineering can be used to modify microorganisms' metabolic pathways so their capacity to degrade the target contaminant is improved, or even make microorganisms more tolerant to high contaminant concentration in soils [47]. Chelating agents can also be employed to increase heavy metal mobility and bioavailability: acetic acid, citric acid, pyridine-2,6-dicarboxylic acid (PDA), ethylenediaminetetraacetic acid (EDTA), and sodium metabisulfite ($Na_2S_2O_5$) are all agents that have been used to remove heavy metals from soils used in phytoremediation and EK.

12.3.2 EK-Assisted Bioremediation in the Treatment of Inorganic Contaminants

Metals, heavy metals, and metalloids do not suffer degradation as OCs, so their long-term deposition in soils can lead to accumulation. However, other plant species can be used to achieve favorable results; for example, potato has been successfully used to treat soil contaminated with a mixture of Zn, Pb, Cu, and Cd under the influence of EK [48]. Aboughalma et al. [48] concluded that biomass production of the plants was 72% higher under AC treatment, and there was a greater accumulation of Zn and Cu in the plant roots treated with electrical fields [48]. Regarding pH distribution, there was no significant metal redistribution and pH variation between anode and cathode in the AC soil profile, although soil pH varied from anode to cathode, reaching a minimum of pH 3 near the anode and a maximum of pH 8 near the cathode in the DC-treated soil profile.

Bi et al. [28] used rapeseed and tobacco to remediate soil contaminated with Cd, Zn, and Pb. The researched conditions were (i) no electrical field and (ii) electrical field application in alternating mode (AC, 1 V cm^{-1}) and direct mode (DC, 1 V cm^{-1}), switching polarity every 3 hours. The duration of treatment using tobacco plants was 90 days and for rapeseed was 30 days. In this study, no pH variation was created between electrodes by switching the polarity of the DC. In the applied conditions, metal uptake per rapeseed plant shoot was enhanced by applying an AC field; and while rapeseed biomass was enhanced due to the EK process, tobacco was not [28].

Occasionally, target inorganic contaminants can have poor conductivity or be present in a metallic form requiring preliminary dissolution. Choosing an electrolyte based on the type of chemical used (anolyte) and metal remediated may increase removal rates [22]. Another common practice in both EK and phytoremediation to enhance removal is using chelating agents to increase heavy metal mobility and bioavailability, with EDTA being one of the most commonly used [21]. A chelate forms a complex with the heavy metal, freeing the heavy metal from the soil cation exchange sites; thus, as a chelate-metal complex, the chelated metal species can

UNCORRECTED PROOFS

Trim Size: 170mm x 244mm Single Column Loose Ribeiro670117 c12.tex V1 - 12/11/2020 11:55pm Page 278

migrate more readily in soil. After the metal has been removed from the cation exchange sites, it can be taken up by plant roots in the immediate vicinity [49].

Gidarakos and Giannis [50] analyzed the viability of using chelating agents to enhance EK remediation of soils contaminated with heavy metals. The authors used chelating agents as washing solutions and as purging solutions at the electrode compartments. To prevent metal from precipitating as a hydroxide, acid was added in the cathode compartment. This allowed the dissolved heavy metals to move toward the anode or cathode according to their charges. Three different acids were tested for the EK extraction of Cd: acetic acid, citric acid, and PDA, as washing and purging solutions. EDTA as a washing solution and sodium metabisulfite ($Na_2S_2O_5$) as purging solution were tested for removing Zn. The results showed that 90% of Cd removal was achieved using acetic acid as a purging solution, and more than 95% for PDA. Removal of Zn greater than 96% was achieved when $Na_2S_2O_5$ was used as a washing solution, explained by the weakening of the Zn-soil bond. Additional conclusions were that using acetic acid as a washing solution did not accelerate the desorption of Cd from the soil surface, although citric acid seemed to be very effective at low pH values [50].

Tahmasbian and Sinegani [51] performed a study to investigate the effects of electrical fields and chelating agents on the phytoremediation efficiency of *Helianthus annuus* (sunflower). Three distinct chelating agents were tested: poultry manure extract (PME), cow manure extract (CME), and EDTA. Results indicated that the Pb metal uptake index increased in the 10 V EDTA treatment by 500% compared to a control; and under 30 V, soil-available Pb significantly increased. In conclusion, this EK remediation coupled with phytoextraction significantly increased phytoremediation efficiency with the application of EDTA [51]. EDTA was also used in a phytoremediation study with lemongrass (Cymbopogon). The investigators concluded that the growth of lemongrass was stimulated by adding chelators such as EDTA, diethylenetriaminepentaacetic acid (DTPA), and citric acid [52]. When applying this type of enhancement agents, it is necessary to acknowledge the potential leaching of metals into surrounding environments [53].

Efficient removal has been reported by Luo et al. [54], who concluded that a vertical electric field with moderate voltage (2 V) achieved the optimal effect on metal decontamination and leachate interception in the phytoremediation processes, even improving biomass yield, which increased from 2.71 kg in a control to 3.45 kg during treatments [54].

In addition to the improvement of removal rates, applying an electric field increases plant development. As studied by [55], applying 0.2 DC V cm^{-1} in clean soil near ryegrass seeds enhanced germination by 75%. In addition, tests performed for a month with AC current, 1 V cm^{-1} applied for 4 hours twice a day (4 hours on to 8 hours off), revealed the greatest biomass production [55].

12.3.3 EK-Assisted Bioremediation in the Treatment of Organic Contaminants

Organic contaminants (OCs) are a significant concern at many polluted sites. Coupling EK with phytoremediation has proven to be an effective process for the

UNCORRECTED PROOFS

Trim Size: 170mm x 244mm Single Column Loose Ribeiro670117 c12.tex V1 - 12/11/2020 11:55pm Page 279

degradation and removal of OCs from soil and can simultaneously enhance soil properties [46]. As previously mentioned, in the presence of a low-intensity electric field, plants are stimulated to grow, increasing their biomass production. While EK enhances plant growth, greater biomass production increases other physiological and enzymatic processes in the rhizosphere, thus resulting in greater degradation of OCs [56].

Sánchez et al. [39] performed a test using maize (*Zea mays L.*) to assess how a created electric field enhanced plant uptake and degradation of atrazine in spiked soils. By coupling EK with phytoremediation, the removal of atrazine increased 36.5% compared to the setting without applied electricity. Periodic polarity inversion prevented significant changes from occurring in soil pH [39].

OCs with high or moderate solubility in water can be removed, altering the physicochemical conditions to more suitable conditions, and thus enhancing desorption of the contaminant. For instance, co-solvents, cyclodextrins, and surfactants are the most widely used solubilizing agents in EK to improve PAH desorption [57].

According to Cameselle et al. [21], using EK-phytoremediation is limited, although their combined application can result in improved remediation of both organic- and inorganic-contaminated soil and led to overall homogenization of the removals during the studies.

12.4 Case Study of EK and Electrokinetic-Assisted Phytoremediation

A two-phased study to examine the removal efficiency of metalloids applying EK-assisted phytoremediation was performed [37, 58]. The target substances were As and Sb, both hazardous to human health and considered priority pollutants by the European Union (EU) and the US EPA.

The viability of the EK process alone for the remediation of a sandy clay mine soil contaminated with these metalloids was first analyzed. The soil contained 66 and 547 mg kg^{-1} of As and Sb, respectively, with $43 \pm 6\%$ of the As and $4.8 \pm 0.1\%$ of the Sb being present in a mobile form. To improve the remediation, pH control in the anolyte and phosphate amendment were applied. Both the initial soil and the soil after EK were submitted to a simple two-step extraction procedure, to simulate the mobile and mobilizable fractions of As and Sb. Only the mobilizable As fraction showed alteration compared to the initial soil, suggesting that As was still passing to lower energy bounded forms in the soil due to the applied low-level DC. Managing pH values proved to be advantageous for increasing contaminant solubilization and migration from the soil areas closer to the anode. Both anolyte conditioning and phosphate amendment achieved the best removal rates, about 17% and 2% for As and Sb, respectively, indicating that As was easier to remove than Sb. However, greater extraction occurred when no amendment was added (pH 13.5, 98% for As, and 28% for Sb). Figure 12.1 summarizes these results.

Due to the lower remediation efficiencies obtained, enhanced-EK remediation using phosphate amendment and pH control was not a feasible option in the

UNCORRECTED PROOFS

Trim Size: 170mm x 244mm Single Column Loose Ribeiro670117 c12.tex V1 - 12/11/2020 11:55pm Page 280

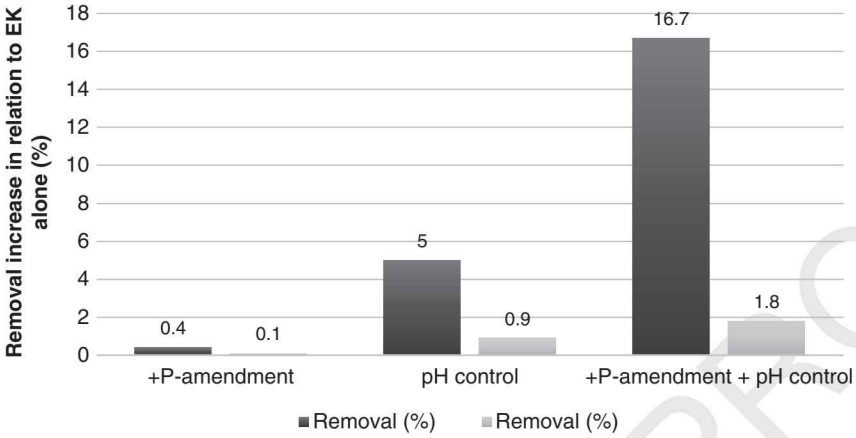

Figure 12.1 Removal of As and Sb using the different applied strategies (P-amendment, pH control, P-amendment + pH control) compared to EK alone.

analyzed case. The best approach was the simultaneously combination of these enhancements.

In phase two of the study [58], the primary goal was to understand the removal rates of EK-assisted phytoremediation of As and Sb from mine soil using two different plant species. Soil fertilized with a solution of 0.99 g of urea and 0.96 g of monopotassium phosphate was poured into rectangular plastic containers. Each container was divided into three compartments (cathode:central:anode) using a vertical nylon mesh in the cathode and anode regions and 900 g of soil; 1200 g were in the central compartment, for a total of 3000 g. Before the experiment, the soil was incubated with 70% of its water holding capacity for seven days, which was maintained for the duration of the test. Four graphite rods were vertically inserted into the treated matrix on opposite sides and used as working electrodes. Indian mustard (*Brassica juncea*) and ryegrass (*Lolium perenne*), as pregerminated seedlings, were transplanted to experimental boxes and grew for 10 days. In this trial, four different setups were tested: (i) plant alone (ryegrass or Indian mustard); (ii) lant and phosphate amendment; (iii) plant and EK process; and (iv) plant, phosphate amendment, and EK process. Every test with EK remediation was performed by applying 20 V DC current for 8 hours per day for 15 days, and phosphate amendment was applied in a concentration of 0.5 M of PO_4^{2-} (as KH_2PO_4).

The P-amendment as a fertilizer resulted in Indian mustard root being statistically greater than the control in the central compartment ($301 \pm 108\%$). Between plant species, there was an analogous pattern of nutrient distribution, suggesting that, in the present set conditions, DC application affected the distribution of nutrients more than plants. Potassium electromigrated toward the cathode compartment in the treatment with combined technologies, and nitrate was redistributed between soil compartments in the presence of EK, independent of using a phosphate amendment.

UNCORRECTED PROOFS

Trim Size: 170mm x 244mm Single Column Loose Ribeiro670117 c12.tex V1 - 12/11/2020 11:55pm Page 281

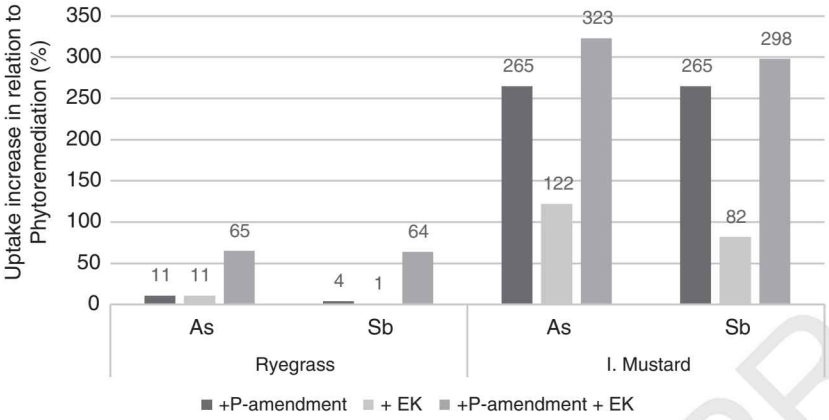

Figure 12.2 Uptake of As and Sb obtained for phytoremediation using ryegrass and Indian mustard according to the different applied strategies (P-amendment, EK, P-amendment + EK).

The enhanced concentration of elements in soil solution and their increased bioavailability, by applying an electric field, resulted in a positive effect on the growth of both species. For the Indian mustard, EK treatment enhanced below-ground biomass at the central compartment (approx. 124% more), but lower effects were observed in ryegrass. By combining P-amendment and EK, increased shoot and root biomass were detected in both plants (the central compartment), but more pronouncedly in Indian mustard than the plant alone (approx. 263% more). Indian mustard shoot and root tissues had a greater concentration of the studied metalloids than ryegrass did. Regarding the root system, Indian mustard accumulated 64% more As and 62% more Sb; with P-amendment, 89% and 81% more; with the EK process, 71% and 48% more; and with the coupled technology (P-amendment and EK process), 91% and 72% more, respectively (Figure 12.2).

12.5 Conclusions

The complex nature and heterogeneity of mixed soil contamination hinder its remediation. EK-assisted bioremediation is a remediation technology effective in the treatment of organic and inorganic contaminants present in soil.

Using an electric field in the vicinity of plants has a positive effect on the plants' germination and development. Mobilization and electromigration of essential nutrients caused by the imposed electric field are the primary mechanisms associated with this improvement. The biomass increase favors phytoremediation processes and stimulates microflora present in the rhizosphere, improving the efficacy and removal rates of contaminants. Further research is necessary to elucidate the intrinsic mechanisms associated with the interaction of the electric fields and the growing

UNCORRECTED PROOFS

Trim Size: 170mm x 244mm Single Column Loose Ribeiro670117 c12.tex V1 - 12/11/2020 11:55pm Page 282

plants. Further studies with longer duration and applied to real contamination soils should be carried out to deem EK-assisted bioremediation a practical remediation technology.

Acknowledgments

This work has received funding from the European Union's Horizon 2020 research and innovation program under the Marie Skłodowska-Curie grant agreement No. 778045; project CEMOWAS2 (SOE2/P5/F0505), co-financed by the European Regional Development Fund (FEDER); and Portuguese Foundation for Science and Technology (FCT) through grants UIDB/04085/2020 (strategic project for CENSE). FCT is also acknowledged for P. Guedes' fellowship (SFRH/BPD/114660/2016), and N. Couto's contract established under Individual Call to Scientific Employment Stimulus (CEECIND/04210/2017). This work is anchored by the RESOLUTION LAB, a laboratory at NOVA School of Science and Technology.

References

1 Sharma, H.D. (2004). *Geoenvironmental Engineering: Site Remediation, Waste Containment, and Emerging Waste Management Technologies*, vol. 35, 50–55. Hoboken, NJ Environ Int.: Wiley.

2 Valentín, L., Nousiainen, A., and Mikkonen, A. (2013). Introduction to organic contaminants in soil: concepts and risks. In: *Emerging Organic Contaminants in Sludges: Analysis, Fate and Biological Treatment* (eds. T. Vicent, G. Caminal, E. Eljarrat and D. Barceló), 1–29. Berlin, Heidelberg: Springer Berlin Heidelberg.

3 Duarte, R.M.B.O., Matos, J.T.V., and Senesi, N. (2017). Chapter 5, Organic pollutants in soils [Internet]. In: *Soil Pollution: From Monitoring to Remediation* (eds. A.C. Duarte, A. Cachada and T. Rocha-Santos), 103–126. Elsevier Inc.

4 Ramamurthy, A.S. and Memarian, R. (2012). Phytoremediation of mixed soil contaminants. *Water, Air, and Soil Pollution* 223 (2): 511–518.

5 Dey, S., Bano, F., and Malik, A. (2019). Chapter 1, Pharmaceuticals and personal care product (PPCP) contamination—a global discharge inventory [Internet]. In: *Pharmaceuticals and Personal Care Products: Waste Management and Treatment Technology* (eds. M.N.V. Prasad, M. Vithanage and A. Kapley), 1–26. Elsevier Inc.

6 Liao, X., Wu, Z., Li, Y. et al. (2019). Effect of various chemical oxidation reagents on soil indigenous microbial diversity in remediation of soil contaminated by PAHs. *Chemosphere* 226: 483–491.

7 Biswas, B., Sarkar, B., Mandal, A., and Naidu, R. (2015). Heavy metal-immobilizing organoclay facilitates polycyclic aromatic hydrocarbon biodegradation in mixed-contaminated soil. *Journal of Hazardous Materials* 298: 129–137.

UNCORRECTED PROOFS

Trim Size: 170mm x 244mm Single Column Loose Ribeiro670117 c12.tex V1 - 12/11/2020 11:55pm Page 283

8 Wuana, R.A. and Okieimen, F.E. (2011). Heavy metals in contaminated soils: a review of sources, chemistry, risks and best available strategies for remediation. *ISRN Ecology* 2011: 1–20.

9 Ali, H., Khan, E., and Sajad, M.A. (2013). Phytoremediation of heavy metals-concepts and applications. *Chemosphere* 91 (7): 869–881.

10 Singh, D.J. and Kalamdhad, A. (2011). Effects of heavy metals on soil, plants, human health and aquatic life. *International Journal of Research in Chemistry and Environment* 1: 15–21.

11 Su, C., Jiang, L., and Zhang, W. (2014). A review on heavy metal contamination in the soil worldwide: situation, impact and remediation techniques. *Environmental Skeptics and Critics* 3 (2): 24–38.

12 Reddy, K.R. and Chirakkara, R.A. (2019). Phytoremediation of field soil with mixed contamination. In: *Proceedings of the 8th International Congress on Environmental Geotechnics*, vol. 1 (eds. L. Zhan, Y. Chen and A. Bouazza), 624–629. Singapore: Springer Singapore.

13 Imadi, S.R., Shah, S.W., Kazi, A.G. et al. (2015). Phytoremediation of saline soils for sustainable agricultural productivity. *Plant Metal Interaction: Emerging Remediation Technology*: 455–468.

14 Upadhyay, A.K., Singh, D.P., Singh, N.K. et al. (2019). Chapter 11, Sustainable phytoremediation strategies for river water rejuvenation. In: *Phytomanagement of Polluted Sites* (eds. V.M. Pandey and K. Bauddh), 301–311. Elsevier Inc.

15 Garbisu, C. and Alkorta, I. (2001). Phytoextraction: a cost-effective plant-based technology for the removal of metals from the environment. *Bioresource Technology* 77 (3): 229–236.

16 Susarla, S., Medina, V., and Mccutcheon, S. (2002). Phytoremediation: an ecological solution to organic chemical contamination. *Ecological Engineering* 18: 647–658.

17 Dineshkumar, M., Seenuvasan, M., and Sarojini, G. (2019). Phytoremediation strategies on heavy metal removal. In: *Water and Wastewater Treatment Technologies. Energy, Environment, and Sustainability* (eds. X.T. Bui, C. Chiemchaisri, T. Fujioka and S. Varjani), 81–101. Singapore: Springer.

18 Syranidou, E., Christofilopoulos, S., Politi, M. et al. (2017). Bisphenol-a removal by the halophyte Juncus acutus in a phytoremediation pilot: characterization and potential role of the endophytic community. *Journal of Hazardous Materials* 323: 350–358.

19 Favas, P.J.C., Pratas, J., Paul, M.S., and Prasad, M.N.V. (2019). Chapter 10, Remediation of uranium-contaminated sites by phytoremediation and natural attenuation. In: *Phytomanagement of Polluted Sites* (eds. V.M. Pandey and K. Bauddh), 277–300. Elsevier https://doi.org/10.1016/B978-0-12-813912-7.00010-7. ISBN: 9780128139127.

20 Pandey, V.C. and Bajpai, O. (2019). Chapter 1, Phytoremediation: from theory toward practice. In: *Phytomanagement of Polluted Sites* (eds. V.M. Pandey and K. Bauddh), 1–49. Elsevier Inc. https://doi.org/10.1016/B978-0-12-813912-7.00001-6.

21 Cameselle, C., Chirakkara, R.A., and Reddy, K.R. (2013). Electrokinetic-enhanced phytoremediation of soils: status and opportunities. *Chemosphere* 93 (4): 626–636.

UNCORRECTED PROOFS

Trim Size: 170mm x 244mm Single Column Loose Ribeiro670117 c12.tex V1 - 12/11/2020 11:55pm Page 284

22 Khalid, S., Shahid, M., Niazi, N.K. et al. (2017). A comparison of technologies for remediation of heavy metal contaminated soils. *Journal of Geochemical Exploration* 182: 247–268.

23 Bolan, N.S., Park, J.H., Robinson, B. et al. (2011). Phytostabilization. A green approach to contaminant containment. *Advances in Agronomy* 112: 145–204.

24 Keeran, N.S., Balasundaram, U., Govindan, G., and Parida, A.K. (2018). Chapter 18, *Prosopis juliflora*: A potential plant for mining of genes for genetic engineering to enhance phytoremediation of metals. a potential plant for mining of genes for genetic engineering to enhance phytoremediation of metals. In: *Transgenic Plant Technology for Remediation of Toxic Metals and Metalloids* (eds. M. Narasimha and V. Prasad), 381–393. Elsevier Inc.

25 Thijs, S., Langill, T., and Vangronsveld, J. (2017). The bacterial and fungal microbiota of hyperaccumulator plants: small organisms, large influence. *Advances in Botanical Research* 83: 43–86.

26 Reeves, R.D., Baker, A.J.M., Jaffré, T. et al. (2018). A global database for plants that hyperaccumulate metal and metalloid trace elements. *The New Phytologist* 218 (2): 407–411.

27 Chaney, R.L., Malik, M., Li, Y.M. et al. (1997). Phytoremediation of soil metals. *Current Opinion in Biotechnology* 8 (3): 279–284.

28 Bi, R., Schlaak, M., Siefert, E. et al. (2011). Influence of electrical fields (AC and DC) on phytoremediation of metal polluted soils with rapeseed (*Brassica napus*) and tobacco (*Nicotiana tabacum*). *Chemosphere* 83 (3): 318–326.

29 Alshawabkeh, A.N. (2009). Electrokinetic soil remediation: challenges and opportunities. *Separation Science and Technology* 44 (10): 2171–2187.

30 Jorfi, S., Pourfadakari, S., and Ahmadi, M. (2017). Electrokinetic treatment of high saline petrochemical wastewater: evaluation and scale-up. *Journal of Environmental Management* 204: 221–229.

31 Acar, Y.B. and Alshawabkeh, A.N. (1993). Principles of electrokinetic remediation. *Environmental Science & Technology* 27 (13): 2638–2647.

32 Ribeiro, A.B. and Rodríguez-Maroto, J.M. (2006). Chapter 1, Electroremediation of heavy metal-contaminated soils. Processes and applications. In: *Trace Elements in the Environment: Biogeochemistry, Biotechnology and Bioremediation* (eds. M.N.V. Prasad, K.S. Sajwan and R. Naidu), 341–368. FL, USA: Taylor & Francis/CRC Press. ISBN: 1-56670-685-8.

33 Page, M.M. and Page, C.L. (2002). Electroremediation of contaminated soils. *Journal of Environmental Engineering* 128 (3): 208–219.

34 Ekwue, E.I. and Bartholomew, J. (2011). Electrical conductivity of some soils in Trinidad as affected by density, water and peat content. *Biosystems Engineering* 108 (2): 95–103.

35 Jamshidi-Zanjani, K.A. (2017). A review on enhancement techniques of electrokinetic soil remediation. *Pollution* 3 (1): 157–166.

36 Rittirong, A., Douglas, R.S., Shang, J.Q., and Lee, E.C. (2008). Electrokinetic improvement of soft clay using electrical vertical drains. *Geosynthetics International* 15 (5): 369–381.

UNCORRECTED PROOFS

Trim Size: 170mm x 244mm Single Column Loose Ribeiro670117 c12.tex V1 - 12/11/2020 11:55pm Page 285

37 Guedes, P. (2015). Electrokinetic treatment of environmental matrices. Contaminants removal and phosphorus recovery. PhD thesis, Universidade NOVA de Lisboa, Faculdade de Ciências e Tecnologia.

38 Ribeiro, A.B., Mateus, E.P., and Couto, N. (eds.) (2016). *Electrokinetics Across Disciplines and Continents - New Strategies for Sustainable Development*. Springer International Publishing 427 pp. doi: https://doi.org/10.1007/978-3-319-20179-5.

39 Sánchez, V., López-Bellido, F.J., Cañizares, P., and Rodríguez, L. (2018). Can electrochemistry enhance the removal of organic pollutants by phytoremediation? *Journal of Environmental Management* 225: 280–287.

40 Rada, E.C., Andreottola, G., Istrate, I.A. et al. (2019). Remediation of soil polluted by organic compounds through chemical oxidation and phytoremediation combined with DCT. *International Journal of Environmental Research and Public Health* 16 (17): 3179.

41 Rocha, I.M.V., Silva, K.N.O., Silva, D.R. et al. (2019). Coupling electrokinetic remediation with phytoremediation for depolluting soil with petroleum and the use of electrochemical technologies for treating the effluent generated. *Separation and Purification Technology* 208: 194–200.

42 Pillai, H.P.S. and Tharayil, M. (2017). Treatment of heavy metals from water by electro-phytoremediation technique. *Journal of Ecological Engineering* 18 (5): 17–26.

43 Cang, L., Zhou, D.M., Wang, Q.Y., and Fan, G.P. (2012). Impact of electrokinetic-assisted phytoremediation of heavy metal contaminated soil on its physicochemical properties, enzymatic and microbial activities. *Electrochimica Acta* 86: 41–48.

44 O'Connor, C.S., Lepp, N.W., Edwards, R., and Sunderland, G. (2003). The combined use of electrokinetic remediation and phytoremediation to decontaminate metal-polluted soils: a laboratory-scale feasibility study. *Environmental Monitoring and Assessment* 84 (1–2): 141–158.

45 Mao, X., Han, F.X., Shao, X. et al. (2016). Electrkinetic remediation coupled with phytoremediation to remove lead, arsenic and cesium from contaminated paddy soil. *Ecotoxicology and Environmental Safety* 125: 16–24.

46 Cameselle, C. and Gouveia, S. (2018). Electrokinetic remediation for the removal of organic contaminants in soils. *Current Opinion in Electrochemistry* 11: 41–47.

47 Hassan, I., Mohamedelhassan, E., Yanful, E., and Yuan, Z.-C. (2018). Chapter 10, Enhancement of bioremediation and phytoremediation using Electrokinetics. In: *Advances in Bioremediation and Phytoremediation* (ed. N. Shiomi), 169–189. IntechOpen https://doi.org/10.5772/intechopen.73202.

48 Aboughalma, H., Bi, R., and Schlaak, M. (2008). Electrokinetic enhancement on phytoremediation in Zn, Pb, Cu and Cd contaminated soil using potato plants. *Journal of Environmental Science and Health, Part A: Toxic/Hazardous Substances and Environmental Engineering* 43 (8): 926–933.

49 Dipu, S., Kumar, A., and Thanga, S.G. (2012). Effect of chelating agents in phytoremediation of heavy metals. *Remediation Journal* 22 (2): 133–146.

UNCORRECTED PROOFS

Trim Size: 170mm x 244mm Single Column Loose Ribeiro670117 c12.tex V1 - 12/11/2020 11:55pm Page 286

50 Gidarakos, E. and Giannis, A. (2006). Chelate agents enhanced electrokinetic remediation for removal cadmium and zinc by conditioning catholyte pH. *Water, Air, and Soil Pollution* 172 (1–4): 295–312.

51 Tahmasbian, I. and Safari Sinegani, A.A. (2016). Improving the efficiency of phytoremediation using electrically charged plant and chelating agents. *Environmental Science and Pollution Research* 23 (3): 2479–2486.

52 Patra, D.K., Pradhan, C., and Patra, H.K. (2018). Chelate based phytoremediation study for attenuation of chromium toxicity stress using lemongrass: *Cymbopogon flexuosus* (nees ex steud.) W. Watson. *International Journal of Phytoremediation* 20 (13): 1324–1329.

53 Lestan, D., Luo, C., and Li, X.-D. (2008). The use of chelating agents in the remediation of metal-contaminated soils: a review. *Environmental Pollution* 153: 3–13.

54 Luo, J., Ye, L., Qi, S. et al. (2018). Effect of electrode configurations on phytoremediation efficiency and environmental risk. *Plant and Soil* 424 (1–2): 607–617.

55 Acosta-Santoyo, G., Cameselle, C., and Bustos, E. (2017). Electrokinetic – enhanced ryegrass cultures in soils polluted with organic and inorganic compounds. *Environmental Research* 158 (June): 118–125.

56 Gill, R., Harbottle, M., Smith, J., and Thornton, S. (2014). Electrokinetic-enhanced bioremediation of organic contaminants: a review of processes and environmental applications. *Chemosphere* 107: 31–42.

57 Gitipour, S., Sorial, G.A., Ghasemi, S., and Bazyari, M. (2018). Treatment technologies for PAH-contaminated sites: a critical review. *Environmental Monitoring and Assessment* 190 (9): 546.

58 Couto, N., Guedes, P., Zhou, D.M., and Ribeiro, A.B. (2015). Integrated perspectives of a greenhouse study to upgrade an antimony and arsenic mine soil - potential of enhanced phytotechnologies. *Chemical Engineering Journal* 262: 563–570.

UNCORRECTED PROOFS

Trim Size: 170mm x 244mm Single Column Loose Ribeiro670117 c13.tex V1 - 12/11/2020 11:55pm Page 287

13

Enhanced Electrokinetic Techniques in Soil Remediation for Removal of Heavy Metals

Sadia Ilyas[1], Rajiv Ranjan Srivastava[2,3], Hyunjung Kim[1,4], and HummaAkram Cheema[5]

[1] *Department of Mineral Resources and Energy Engineering, Jeonbuk National University, Jeonju, Jeonbuk 54896, Republic of Korea*
[2] *Center for Advanced Chemistry, Institute of Research and Development, Duy Tan University, Da Nang 550000, Vietnam*
[3] *Faculty of Natural Sciences, Duy Tan University, Da Nang 550000, Vietnam*
[4] *Department of Environment and Energy, Jeonbuk National University, Jeonju, Jeonbuk 54896, Republic of Korea*
[5] *Mineral and Material Chemistry Lab, Department of Chemistry, University of Agriculture, Faisalabad 38040, Pakistan*

13.1 Introduction

Anthropogenic activities generate millions of tons of hazardous waste worldwide every year. In the waste volume, heavy metals and metalloids predominantly come from mining, mineral processing, smelting, industrial discharge, agricultural applications, and the landfill disposal of end-of-life devices as electronic waste. Improper handling of these waste heavy metals often exposes them in the environment due to leakage into soil and groundwater through slow leaching [1, 2]. The potential toxicity of heavy metals has an enormous impact on the quality of soil and groundwater and poses significant risks to human health and biota [3]. Notably, heavy metals and metalloids are non-biodegradable substances, in contrast to many organic pollutants [4], and therefore, active remediation is often required for proper handling of metal-contaminated soils and sediments. In this context, numerous innovative soil remediation techniques have been explored, including chemical oxidation, bioremediation, phytoremediation, soil washing, flotation, soil vapor extraction, thermal desorption, and ultrasonication [5–8]. The primary bottleneck in their application for in situ treatment is that they are limited to a particular type of contaminant or site conditions [9]. Developing other effective techniques to remediate heavy metal contamination of soil could lead to providing a more efficient method by applying an electric field to the ground for removal of contaminated soil, either a constant voltage or a direct current (DC) [10, 11]. This remediation technique is called electrokinetic remediation (ER).

Electrokinetic Remediation for Environmental Security and Sustainability, First Edition.
Edited by Alexandra B. Ribeiro and M.N.V. Prasad.
© 2021 John Wiley & Sons Ltd. Published 2021 by John Wiley & Sons Ltd.

UNCORRECTED PROOFS

Trim Size: 170mm x 244mm Single Column Loose Ribeiro670117 c13.tex V1 - 12/11/2020 11:55pm Page 288

13.2 Electrokinetic Mechanism and Phenomenon

The conceptual working mechanism of an electrokinetic system is shown in Figure 13.1. It involves applying a low DC or low-potential gradient to electrodes inserted into the ground and encompassing the contaminated zone. Due to the current, electrolysis reactions generate protons (H^+) and oxygen (O_2) at the anode, while hydroxyl ions (OH^-) and hydrogen (H_2) are generated at the cathode. The electron transfer reactions in an electrokinetic process can be written as the electrolysis of water at the anode

$$H_2O \rightarrow 2H^+ + \frac{1}{2}O_{2(g)} + 2e^- \tag{13.1}$$

and at the cathode:

$$2H_2O + 2e^- \rightarrow 2OH^- + H_{2(g)} \tag{13.2}$$

Further, protons migrate from the anode through the soil as a carrier toward the cathode, whereas OH^- ions in the cathode migrate toward the anode. Depending on the extent of proton and hydroxyl ion migration, the pH varies across the soil. Proton generation decreases the pH near the anode, while a simultaneous increase in the OH^- ion concentration increases the pH near the cathode. Such a change in soil pH significantly affects the occurrence of physico-chemical processes on the soil surface (facilitating the oxidation–reduction, adsorption–desorption, and precipitation–dissolution reactions) that dictate the partitioning and speciation of heavy metal contaminants in the soil [12]. It is imperative to note that because

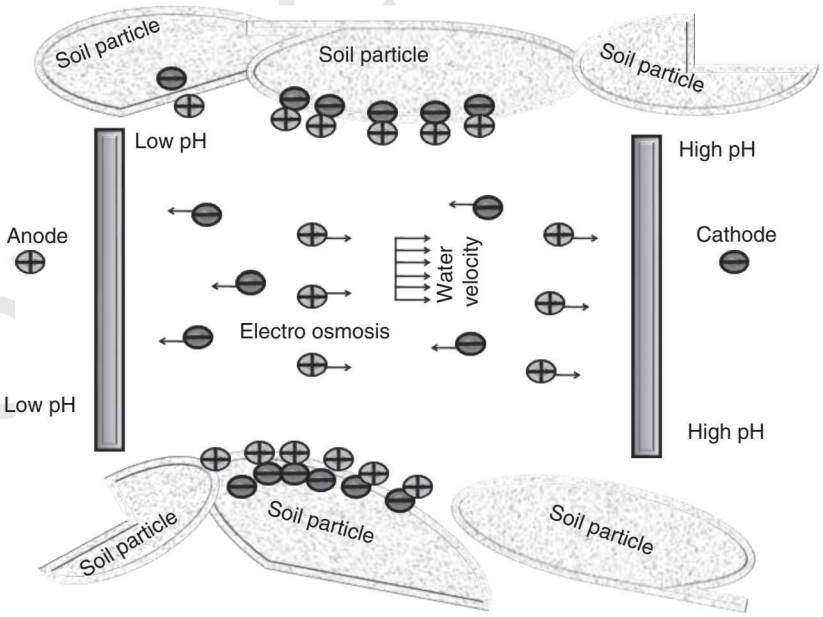

Figure 13.1 Conceptual schematic for the movement of charged ions in an electrokinetic system.

UNCORRECTED PROOFS

Trim Size: 170mm x 244mm Single Column Loose Ribeiro670117 c13.tex V1 - 12/11/2020 11:55pm Page 289

Table 13.1 The phenomena of different mechanisms occurring in electrokinetic remediation.

Electrokinetic mechanism	Phenomena
Electroosmosis	The movement of soil moisture or groundwater from anode to cathode in an electrolytic cell.
Electromigration	Transportation of ions and ion complexes toward the opposite charge, commonly occurring when ionic inorganic species like heavy metal cations exist.
Electrophoresis	Transportation of charged particles or colloids under the influence of an electric field. The contaminants bound to the particulate matter in mobility can be transported in this manner.

Sources: Based on Acar and Alshawabkeh [13]; Pamukcu and Wittle [14]; and Shapiro and Probstein [15].

ER is based on ion transport, the existence of contaminants in a soluble ionic form is preferable. Three different types of mechanisms are primarily responsible for the transportation of contaminants toward the electrodes: electroosmosis, electromigration, and electrophoresis (see Table 13.1) [13–15].

Among the three phenomena, the chances of contaminant transportation through electromigration are one to two orders greater than through other mechanisms; hence, it is considered to be the dominant mechanism in ER. However, due to the counteracting electroosmosis flow and greater ionic mobility of proton ions as compared to hydroxyl ions, the acid front dominates the soil chemistry, except for small sections near the cathode [16–18]. Therefore, the zeta potential (ζ) – the potential difference between the shearing surface and the bulk fluid – has been identified as a significant factor, depending on the pH [9, 19]. A lower value of ζ increases the electroosmosis flow rate and transportation of organic contaminants toward the cathode [20]; the more negative ζ, the greater the electroosmosis flow rate [21]. According to the Helmholtz and Smoluchovski theory, electroosmotic pore fluid flux (q_e) in the absence of hydraulic head is influenced by the soil ζ, pore water viscosity (η), and electric potential (E), as follows [13]:

$$q_e = \varepsilon \zeta n \nabla(-E)/(\eta\sigma) \tag{13.3}$$

where n is the soil porosity, ε is the permittivity of the medium, and σ is the effective bulk electric conductivity.

13.3 Limitations of the Electrokinetic Remediation Process

It should be noted that ζ is usually negative for water-saturated clays and silts [8]. Once ζ becomes positive, reverse electroosmosis seriously affects contaminant removal efficiency [22]. Hence, ER of heavy metals from clays requires maintaining

UNCORRECTED PROOFS

Trim Size: 170mm x 244mm Single Column Loose Ribeiro670117 c13.tex V1 - 12/11/2020 11:55pm Page 290

the soil pH low enough to keep the contaminant metals dissolved, in contrast to keeping the pH high enough to maintain a negative value of ζ [23].

For example, Yang et al. [4] used dry soil mixed with deionized water (EK1 and EK3) or pretreated with 0.1 M NaOH (EK2) or 0.1 M H_3PO_4 (EK4), giving 20% of the initial water content. In these systems, the final pH of EK1 and EK2 was ∼11.5 due to anolyte conditioning with NaOH, yielding highly negative ζ values with a point of zero charge value of 3.4. Acidifying the soil in EK3 and EK4 to pH ∼3.5 changed the ζ value from negative to about zero during the electrokinetic process. In addition, the transport of As, Cu, Pb, and Zn from soils during electrokinetics was investigated. The As concentration in the soil near the cathode in EK3 and EK4 was found to be lower than that near the anode, in contrast to Cu and Zn, whose concentrations in EK3 and EK4 were higher near the cathode than near the anode. The sequential extraction results indicated that significant changes occurred in the metal fractionation during electrokinetic treatment. It was observed that the ER efficiencies and changes in metal distribution (as shown in Figure 13.2) were affected by the physico-chemical reactions in the pore water and electrolyte solutions. It revealed that the removal time, chemical dosage, and energy consumption could be reduced by pretreating the soil and using adequate electrolytes. The simultaneous need to maintain the opposite condition is the primary obstacle for an ER process.

13.4 Need for Enhancement in the Electrokinetic Remediation Process

The poor solubility of heavy metals, weak desorption of adsorbed contaminants, and low removal efficiency of non-polar contaminants are the primary identified disadvantages of the ER process [10]. To overcome these bottlenecks, enhanced ER techniques or integrating the ER process with other useful technique is desirable, with a clear target in terms of the following:

- Solubilization of heavy metal contaminants
- Adjusting/controlling the soil pH in a suitable working range for ER
- Breaking down, transforming, or destroying the contaminants

The electrode surface attracts the gas generated during the ER process and increases resistance, significantly slowing the remediation process [24]. During the prolonged ER process, gas bubbles released from electrolytic dissociation slowly cover the entire surface of the cathode, causing increased resistance. Therefore, to further the ER process, the input voltage must be increased to supply the same current, resulting in an increased voltage gradient. Hydroxyl ions generated during electrolytic dissociation react with cations to form a sediment that plugs the spaces between soil particles, hindering the electrical current and decreasing the diffusive flow over time [24].

To address these issues, several enhancement techniques employing surface modification, chelating and complexing agents, pH control, bioremediation, ultrasonication, and permeable reactive barriers have been examined in combination

UNCORRECTED PROOFS

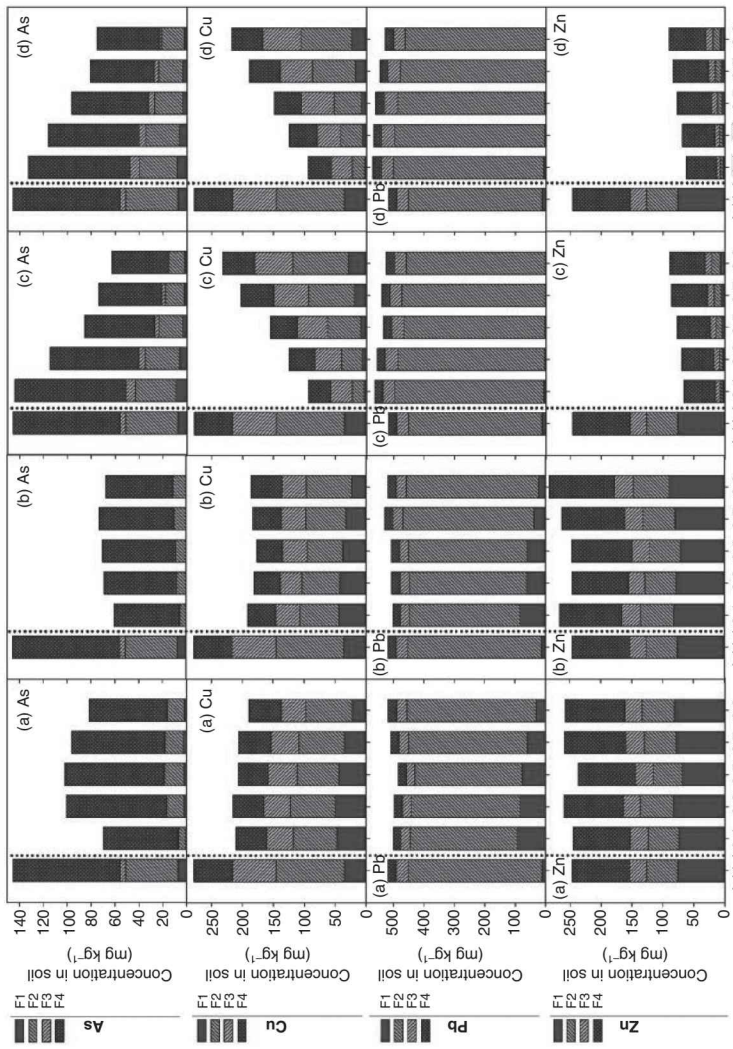

Figure 13.2 Distribution of metals in four different types of soil (EK1 and EK2, soil mixed with deionized water; EK3, pretreated with 0.1 M NaOH; EK4, pretreated with 0.1 M H_3PO_4). Source: Adapted from Yang et al. [4], © 2014 Elsevier.

UNCORRECTED PROOFS

Trim Size: 170mm x 244mm Single Column Loose Ribeiro670117 c13.tex V1 - 12/11/2020 11:55pm Page 292

with the ER technique to enhance the efficacy of soil remediation. In the following, enhancement techniques applied to soil remediation to remove heavy metals are discussed.

13.5 Enhancement Techniques

13.5.1 Surface Modification

To modify the surface of any liquid or solid by changing the surface tension, surfactants can act as wetting agents, adhesives, foaming agents, flocculating agents, detergents, penetrants, dispersants, and demulsifiers [11, 20]. Three primary types of surfactants are used for these purposes: (i) cationic surfactants (e.g. CTAC), (ii) anionic surfactants (e.g. sodium dodecyl sulfonate, SDS), and (iii) non-ionic surfactants (e.g. Tween 80). However, because cationic surfactants exhibit high toxicity and anionic surfactants lead to electromigration in the opposite direction compared to electroosmosis in the ER process; they are less frequently used in ER. In contrast, non-ionic and biological surfactants are often selected because they are less toxic and are environmentally benign. The schematic of electrokinetic enhancement using a surfactant is shown in Figure 13.3.

The negative impact of hard water, surfactants adsorbed onto solid surfaces, degradation, and difficulty recovering or regenerating surfactants are the primary limitations for enhancing the ER process (Harwell et al. 1992). Further, to overcome such limitations, adding co-solvents like alcohols, acetone, tetrahydrofuran, and butylamine can enhance the aqueous solubility of organic contaminants such as benzene ring and long-chain hydrocarbons and enable better transport with electroosmosis flow [25–28].

AQ1

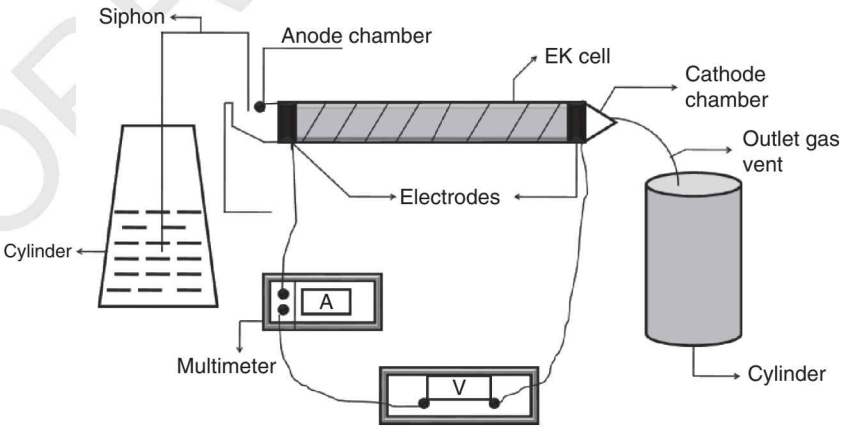

Figure 13.3 Schematic for a surfactant-enhanced electrokinetic remediation system. Source: Used by Yeung and Gu [20], © 2011 Elsevier.

UNCORRECTED PROOFS

Trim Size: 170mm x 244mm Single Column Loose Ribeiro670117 c13.tex V1 - 12/11/2020 11:55pm Page 293

13.6 Cation-Selective Membranes

High pH due to hydroxyl ion accumulation near the cathode causes the hydroxide precipitation of heavy metals adsorption onto the soil particles, which hinders the entire removal process. Several studies revealed the possibility of dealing with the pH impact [25, 29, 30]. They observed that the pH-buffer capacity and cation-exchange capacity (CEC) of the medium and solution-to-soil interactions might affect the speed of the advancement of the acidic and basic fronts and the location of the pH jump. To reduce the relative volume of water and conductive solution in the system, a cation-selective membrane is placed in front of the cathode [25, 29, 30], as shown in Figure 13.4.

As can be seen from Figure 13.4, the electrokinetic cell consists of the soil, conductive solution between the soil and the membrane, and the cathode compartment with electrolyte solution between the membrane and the cathode. Ions start to move to the electrodes when an electric current is applied. The cation-selective membrane is placed between the soil surface and the cathode, which selectively helps cations to pass through it, keeping the hydroxyl ions that are produced at the cathode in the same compartment as the cell membrane. Protons generated at the anode move through the soil by passing through the membrane, which drives the primary pH change near the membrane [25, 29, 30]. The process maintains a low soil pH during

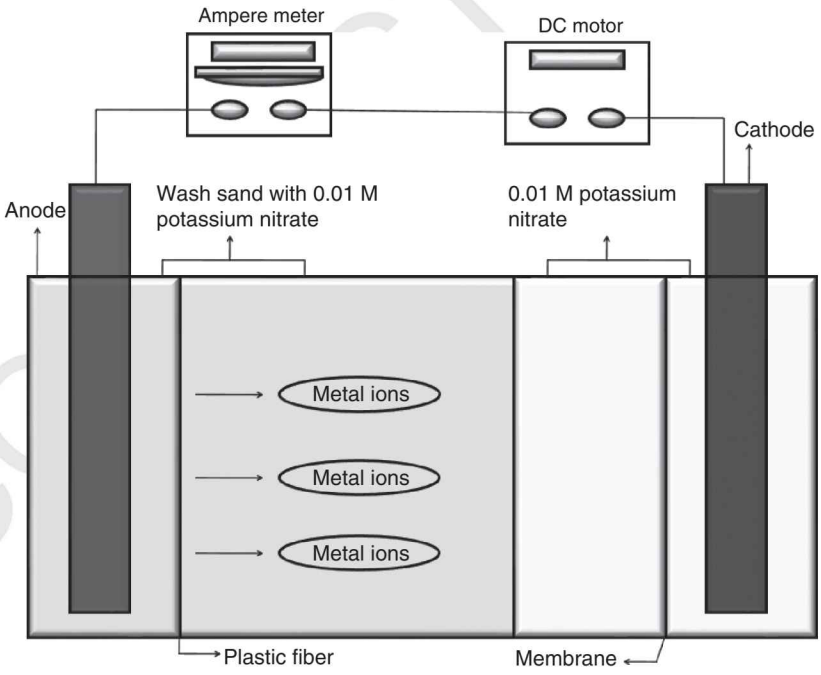

Figure 13.4 Schematic of the electrokinetic cell with a cation-selective membrane for a surfactant-enhanced ER process.

UNCORRECTED PROOFS

Trim Size: 170mm x 244mm Single Column Loose Ribeiro670117 c13.tex V1 - 12/11/2020 11:55pm Page 294

the ER process and significantly reduces the required amount of conductive solution. It has been found that a smaller volume of conductive solution gives a higher pH, and more anions leak through it [8]. A small number of anions passing through the membrane may not have any adverse effect, as the hydroxyl precipitation of heavy metals simultaneously reduces their concentration in the solution and reduces back-diffusion of contaminant metals because their concentration near the membrane does not exceed their solubility limit. Also, the precipitation of heavy metals causes a decrease in electrical energy consumption due to a potential drop between the electrodes, and remediation time is proportional to the distance between the electrodes [29].

13.7 Electro-Bioremediation

This technique employs the synergistic effects of both ER and microorganism-driven degradation processes to remove pollutants from soil [31]. Microorganisms take up carbon, phosphorus, nitrogen, and sulfur from the soil as their growth media and secrete biogenic acid; the heavy metals are further mobilized via their dissolution in the metabolic acid [32–34]. However, in cases like soils with low hydraulic conductivity, microorganism growth in the absence of required electron acceptors or nutrients is difficult [20]. This can be remedied by providing contaminants as nutrients to the microorganisms through electroosmotic flow to promote the microorganisms' metabolic growth [8]. A typical schematic of the electro-bioremediation technology is depicted in Figure 13.5.

Although microbial technology is a slow process compared to other physicochemical techniques, which often depend on the ability of the microorganisms used and the conditions of microbial growth [1], it is a low-cost process and also degrades organic contaminants into less toxic products and oxidizes them into CO_2 and H_2O [10]. The primary problem in carrying out remediation of clays using this combination method is maintaining optimal microbial degradation conditions. The primary advantage of an electrokinetic-enhanced bioremediation process is the increased remediation rate for biodegradable pollutants through the electrokinetic transport phenomenon [35, 36]. This phenomenon is also known as *electrophoresis* [37]. In areas with a cold climate, the heat produced by high ohmic drops due to the electrical field applied to the soil increases the rate of bioremediation to provide suitable growth temperatures for microbes based on their class (mesophilic, moderate heterotrophic, or heterotrophic) [38]. Mena et al. [39] have also suggested coupling electrokinetic soil flushing (EKSF) technology with a bioremediation system using microbial permeable reactive barriers. They observed efficient transportation of nutrients and sodium dodecyl sulfate in the combined process through the electromigration and electroosmotic processes. However, microorganisms have limited tolerance for heavy metals. Toxicity caused by a high concentration of heavy metals adversely affects their growth, and they may die sooner than usual. Moreover, aerobic conditions are more favorable than supplying nitrate or sulfate as alternative electron acceptors [40], albeit a few studies have shown the influence

UNCORRECTED PROOFS

Trim Size: 170mm x 244mm Single Column Loose Ribeiro670117 c13.tex V1 - 12/11/2020 11:55pm Page 295

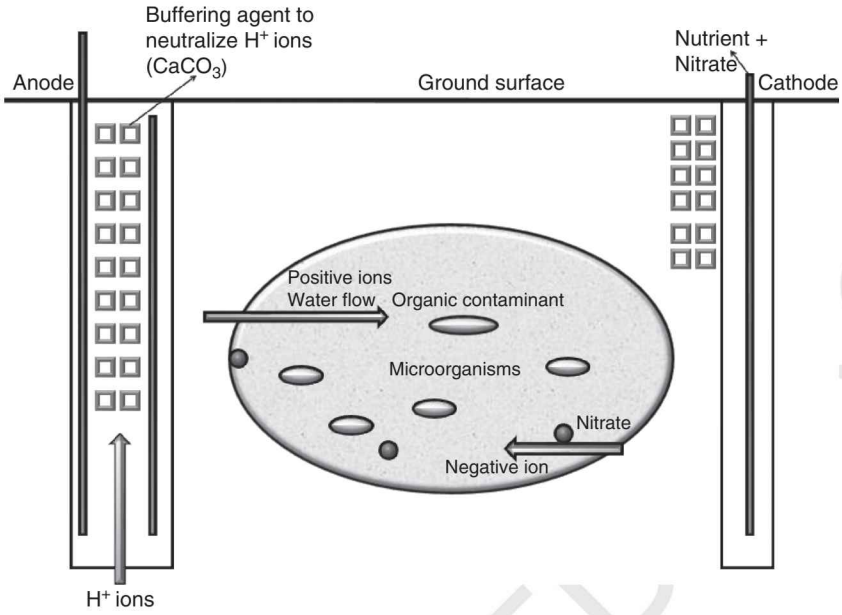

Figure 13.5 Schematic of the electro-bioremediation process.

of dissolved oxygen in an electro-bioremediation process [1]. It is also observed that applying a high electric current did not increase the concentration of dissolved oxygen in the soil, possibly indicating low permeability of clay soils. As a result, oxygen generated in the anode compartment could not be transported through the soil, and hence, in anaerobic treatment of low-permeability soils, the oxygen that evolves at the surface of the anode via Eq. (13.1) does not adequately meet the oxygen requirements.

13.8 Electro-Geochemical Oxidation

Geochemical technology coupled with electrokinetics plays an active role in initiating physical and/or chemical changes in soil and providing ER [41]. It also contributes to improved electrokinetic techniques for the transportation of heavy metal species and water molecules across fine-grained, low-permeability soils (like clays) contaminated with organic and inorganic compounds. Applying an electrical current to probes driven into the ground creates favorable conditions for redox reactions that lead to the immobilization of heavy metal contaminants in the soil/groundwater matrix between the electrode locations without requiring the introduction of external catalysts to drive the redox reactions. Using as the anode electrode for soil reinforcement along with needle-punched electro-geokinetic as the cathode, an improvement in the reinforcement bond and shear strength

UNCORRECTED PROOFS

Trim Size: 170mm x 244mm Single Column Loose Ribeiro670117 c13.tex V1 - 12/11/2020 11:55pm Page 296

of more than 200% was observed in comparison to using the geosynthetics technique without coupling it with electrokinetics [42]. Primarily, three fundamental applications work in this direction [43]:

- Electrophoretic action to rapidly settle out heavy metals
- Electroosmotic action to dewater the soil
- Strength enhancement by consolidation with electroosmotic action

However, the prolonged remediation time and lack of proven results are the disadvantages of this technique.

13.9 Lasagna™ Process

This technique was developed to remove heavy metals from heterogeneous and low-permeability soils in Kentucky [44, 45]. It involves creating several permeable treatment zones in close proximity throughout the soil matrix by adding catalytic reagents, sorbents, oxidizing agents, and buffering solutions, and applying an electrical current to transport heavy metals into the treatment zones. The primary identified advantage of this process is the possibility of recycling the cathode effluent back to the anode compartment to neutralize the pH and simplify water management and reverse fluid flow by switching the polarity. By switching polarity, multiple contaminants can pass through the treatment zones and diminish the possibility of non-uniform potential and pH jumps in the system. Two different configurations, the horizontal and vertical Lasagna™, respectively, are shown in Figure 13.6a,b.

Because the treatment zones are layered, this approach is named *Lasagna*. The formation of horizontal fractures on clay surfaces through horizontal electrodes and vertical pressure allows the removal of heavy metal contaminants deep in the soil [45]. For shallow contamination, the vertical treatment configuration is more appropriate [44]. However, there are some limitations, which include trapped gas that caused by electrolysis. A few attempts have also been made to introduce bioremediation into the treatment zones with the Lasagna process to significantly increase the overall removal of heavy metals from contaminated soils/clays [8].

13.10 Other Potential Processes

Electrosorb™ technology involves cylindrical electrodes coated with a specially designed polymer material impregnated with pH-regulating chemicals to prevent pH jumps [2]. During the ER process, ions move through the pore water to the electrode and are trapped in the polymer matrix. The electrochemical ion-exchange process is another promising technique in which a series of electrodes are placed in porous castings with circulating electrolytes. During the ER process, contaminant ions are captured into electrolytes and pumped to the surface, where they are passed through an electrochemical ion exchanger. Although it is expensive, removal

UNCORRECTED PROOFS

Trim Size: 170mm x 244mm Single Column Loose Ribeiro670117 c13.tex V1 - 12/11/2020 11:55pm Page 297

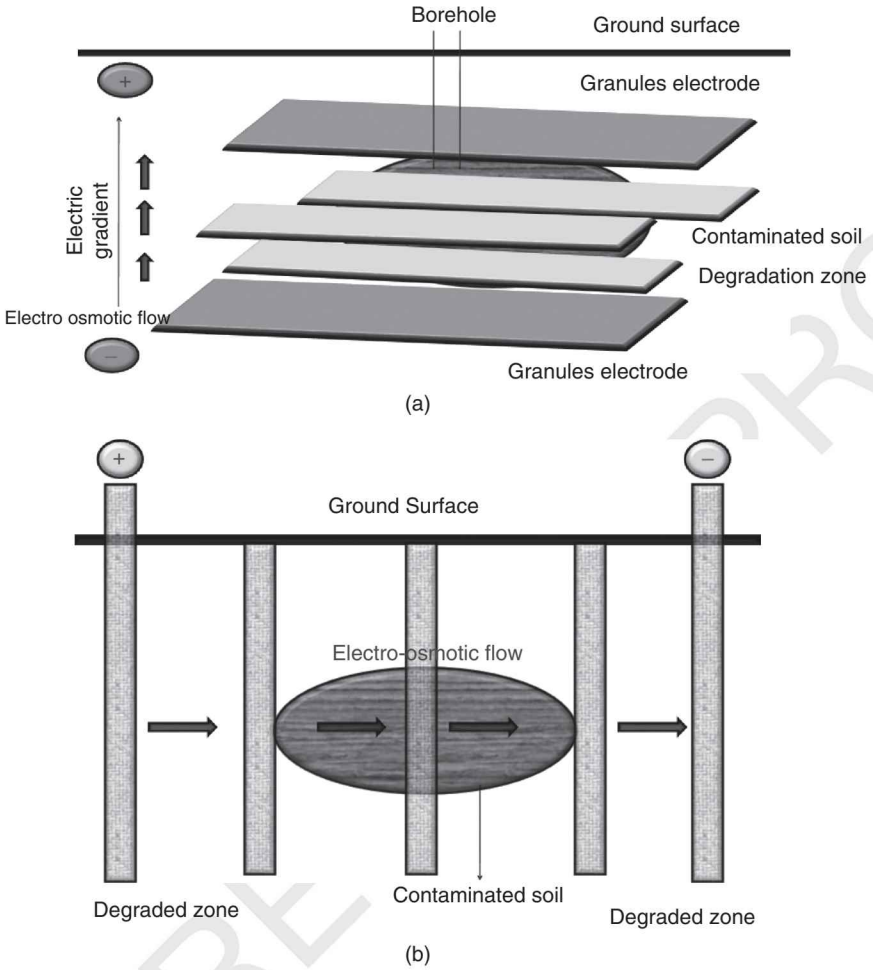

Figure 13.6 (a) Horizontal Lasagna configuration; (b) vertical Lasagna configuration. Source: Adapted from Ho et al. [44], © 1997 Elsevier.

efficiency for low concentrations of heavy metals is quite good. Electro-Klean™ is a new approach to remove heavy metals, radionuclides, and specific volatile organic contaminants from soils and sediments. In it, two DC electrodes are applied directly into the contaminated soil mass. To improve ER efficiency, acids are added to the soil as enhancement fluids. The high buffering capacity of the soil and various coexisting chemicals are the significant limitations of this process.

To decrease the focusing effect in the area where the acid and base fronts meet, an approaching anode technique is employed by some researchers [46]. The schematic of residual soil remediation from a chromite ore processing site using the approaching anode technique is shown in Figure 13.7. It involves sequentially approaching the anode near the fixed cathode after starting the electrokinetic process, to continuously decrease the pH near the anode and compress the precipitation zone.

UNCORRECTED PROOFS

Trim Size: 170mm x 244mm Single Column Loose Ribeiro670117 c13.tex V1 - 12/11/2020 11:55pm Page 298

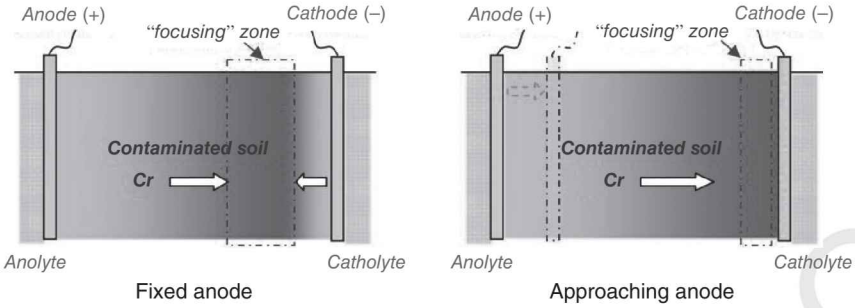

Figure 13.7 Schematic difference between the use of a fixed anode and an approaching anode ER process. Source: Adapted from Li et al. [46], © 2012 Elsevier.

Shen et al. [47] have reported that the ER process is accelerated, and this process could save energy (about 44%) and time (about 40%) by providing high proton and redox potentials that accelerate the migration of heavy metals to the cathode. Citric acid as the catholyte is found to be more suitable for reducing the focusing effect and improving the ER of heavy metals. Li et al. [46] have used four different ER systems to compare the effect of approaching and fixed anodes and observed that the approaching anode ER process can increase the current and simultaneously decrease the pH of the soil, yielding 92.5% removal efficiency for Cr(VI).

13.11 Summary

ER is a promising in situ remediation technology, specifically to efficiently remediate heavy metals from a fine-grained soil matrix. Despite the advantages of the ER process, it also has constraints, such as pH-dependent solubility limits on removing heavy metals, requiring an enhancing solution, decreased efficacy as a result of in situ temperature increases when high current is applied, and hindrances caused by the common presence of hematite and carbonate minerals in soils. Thus enhancement techniques are required to achieve the desired removal of heavy metals. The review of the primary enhancement techniques (including surface modification, cation-selective membranes, electro-bioremediation, electro-geochemical oxidation, and the Lasagna process) demonstrate the enhancements caused by improving the solubility of heavy metals in contaminated soil. Factors such as soil pH and zeta potential can be influential in controlling electroosmotic flow and removal efficiency. Combinational bioremediation improves the degradation of organic pollutants through bacterial activity using carbonaceous matter as an energy growth source. ER coupled with permeable reactive barriers has been shown to be an effective technique when contaminant metals are solubilized and transported through electroosmotic flow. Moreover, selecting the best combination technique to enhance the ER process depends on the heavy metals' speciation with changing solution pH and soil types. Therefore, to achieve efficient ER of contaminated soil, investigations of physico-chemical interactions with the soil (to be treated) and the

UNCORRECTED PROOFS

Trim Size: 170mm x 244mm Single Column Loose Ribeiro670117 c13.tex V1 - 12/11/2020 11:55pm Page 299

impact of enhancing agents on those interactions, the influence of organic matter in the soil, and the occurrence of reverse electroosmotic flow have been found to be very important.

Acknowledgments

This work was supported by the Brain Pool Program through the National Research Foundation of Korea (NRF) funded by the Ministry of Science and ICT (Grant No. 2019H1D3A2A02101993) and Basic Science Research Program through the National Research Foundation of Korea (NRF) funded by the Ministry of Education (Project no. 2020R1I1A1A01074249).

References

AQ2

1 Ramírez, E.M., Camacho, J.V., Rodrigo, M.R., and Cañizares, P.C. (2014). Feasibility of electrokinetic oxygen supply for soil bioremediation purposes. *Chemosphere* 117: 382–387.
2 Reddy, K.R. and Chinthamreddy, S. (1999). Electrokinetic remediation of heavy metal-contaminated soils under reducing environments. *Waste Management* 19: 269–282.
3 Ilyas, N., Ilyas, S., Yousaf, S. et al. (2018). Removal of copper from an electroplating industrial effluent using the native and modified spirogyra. *Water Science and Technology* 78: 147–155.
4 Yang, J.S., Kwon, M.J., Choi, J. et al. (2014). The transport behavior of as, Cu, Pb, and Zn during electrokinetic remediation of a contaminated soil using electrolyte conditioning. *Chemosphere* 117: 79–86.
5 Gomes, H.I., Dias-Ferreira, C., and Ribeiro, A.B. (2012). Electrokinetic remediation of organochlorines in soil: enhancement techniques and integration with other remediation technologies. *Chemosphere* 87: 1077–1090.
6 Habibul, N., Hu, Y., and Sheng, G.P. (2016). Microbial fuel cell driving electrokinetic remediation of toxic metal contaminated soils. *Journal of Hazardous Materials* 318: 9–14.
7 Pedersen, K.B., Lejon, T., Jensen, P.E., and Ottosen, L.M. (2016). Degradation of oil products in a soil from a Russian Barents hot-spot during electrodialytic remediation. *Springerplus* 5: 168.
8 Virkutyte, J., Sillanpää, M., and Latostenmaa, P. (2002). Electrokinetic soil remediation—critical overview. *Science of the Total Environment* 289: 97–121.
9 Moghadam, M.J., Moayedi, H., Sadeghi, M.M., and Hajiannia, A. (2016). A review of combinations of electrokinetic applications. *Environmental Geochemistry and Health* 38: 1217–1227.
10 Huang, D., Xu, Q., Cheng, J. et al. (2012). Electrokinetic remediation and its combined technologies for removal of organic pollutants from contaminated soils. *International Journal of Electrochemical Science* 7: 4528–4544.

UNCORRECTED PROOFS

Trim Size: 170mm x 244mm Single Column Loose Ribeiro670117 c13.tex V1 - 12/11/2020 11:55pm Page 300

11 Mulligan, C.N., Yong, R.N., and Gibbs, B.F. (2001). An evaluation of technologies for the heavy metal remediation of dredged sediments. *Journal of Hazardous Materials* 85: 145–163.

12 Reddy, K.R., Xu, C.Y., and Chinthamreddy, S. (2001). Assessment of electrokinetic removal of heavy metals from soils by sequential extraction analysis. *Journal of Hazardous Materials* 84: 279–296.

13 Acar, Y.B. and Alshawabkeh, A.N. (1993). Principles of electrokinetic remediation. *Environmental Science & Technology* 27: 2638–2647.

14 Pamukcu, S. and Kenneth Wittle, J. (1992). Electrokinetic removal of selected heavy metals from soil. *Environmental Progress* 11: 241–250.

15 Shapiro, A.P. and Probstein, R.F. (1993). Removal of contaminants from saturated clay by electroosmosis. *Environmental Science & Technology* 27: 283–291.

16 Acar, Y.B., Gale, R.J., Putnam, G.A. et al. (1990). Electrochemical processing of soils: theory of pH gradient development by diffusion, migration, and linear convection. *Journal of Environmental Science & Health Part A* 25: 687–714.

17 Alshawabkeh, A.N. and Acar, Y.B. (1992). Removal of contaminants from soils by electrokinetics: a theoretical treatise. *Journal of Environmental Science & Health Part A* 27: 1835–1861.

18 Probstein, R.F. and Hicks, R.E. (1993). Removal of contaminants from soils by electric fields. *Science* 260: 498–503.

19 Page, M.M. and Page, C.L. (2002). Electroremediation of contaminated soils. *Journal of Environmental Engineering* 128: 208–219.

20 Yeung, A.T. and Gu, Y.Y. (2011). A review on techniques to enhance electrochemical remediation of contaminated soils. *Journal of Hazardous Materials* 195: 11–29.

21 Kim, D.H., Ryu, B.G., Park, S.W. et al. (2009). Electrokinetic remediation of Zn and Ni-contaminated soil. *Journal of Hazardous Materials* 165: 501–505.

22 Saeidi, M., Jamshidi, A., Shariatmadri, N., and Falamaki, A. (2009). An investigation on the efficiency of electro kinetic coupled with carbon active barrier to remediate nickel contaminated clay. *International Journal of Environmental Research* 3 (4): 629–636.

23 Yeung, A.T., Hsu, C.N., and Menon, R.M. (1997). Physicochemical soil-contaminant interactions during electrokinetic extraction. *Journal of Hazardous Materials* 55: 221–237.

24 Sah, J.G. and Chen, J.Y. (1998). Study of the electrokinetic process on Cd and Pb spiked soils. *Journal of Hazardous Materials* 58: 301–315.

25 Li, A., Cheung, K.A., and Reddy, K.R. (2000). Cosolvent-enhanced electrokinetic remediation of soils contaminated with phenanthrene. *Journal of Environmental Engineering* 126: 527–533.

26 Maturi, K. and Reddy, K.R. (2008). Cosolvent enhanced desorption and transport of heavy metals and organic contaminants in soils during electrokinetic remediation. *Water, Air, and Soil Pollution* 189: 199–211.

27 Saichek, R.E. and Reddy, K.R. (2003). Effects of system variables on surfactant enhanced electrokinetic removal of polycyclic aromatic hydrocarbons from clayey soils. *Environmental Technology* 24: 503–515.

UNCORRECTED PROOFS

Trim Size: 170mm x 244mm Single Column Loose Ribeiro670117 c13.tex V1 - 12/11/2020 11:55pm Page 301

28 Wan, J., Yuan, S., Chen, J. et al. (2009). Solubility-enhanced electrokinetic movement of hexachlorobenzene in sediments: a comparison of cosolvent and cyclodextrin. *Journal of Hazardous Materials* 166: 221–226.

29 Li, Z., Yu, J.W., and Neretnieks, I. (1997). Removal of Pb (II), Cd (II) and Cr (III) from sand by electromigration. *Journal of Hazardous Materials* 55: 295–304.

30 Li, R.S. and Li, L.Y. (2000). Enhancement of electrokinetic extraction from lead-spiked soils. *Journal of Environmental Engineering* 126: 849–857.

31 Wick, L.Y., Shi, L., and Harms, H. (2007). Electro-bioremediation of hydrophobic organic soil-contaminants: a review of fundamental interactions. *Electrochimica Acta* 52: 3441–3448.

32 Ilyas, S., Anwar, M.A., Niazi, S.B., and Ghauri, M.A. (2007). Bioleaching of metals from electronic scrap by moderately thermophilic acidophilic bacteria. *Hydrometallurgy* 88 (1–4): 180–188.

33 Ilyas, S., Ruan, C., Bhatti, H. et al. (2010). Column bioleaching of metals from electronic scrap. *Hydrometallurgy* 101 (3–4): 135–140.

34 Niqui-Arroyo, J.L. and Ortega-Calvo, J.J. (2007). Integrating biodegradation and electroosmosis for the enhanced removal of polycyclic aromatic hydrocarbons from creosote-polluted soils. *Journal of Environmental Quality* 36: 1444–1451.

35 Lear, G., Harbottle, M.J., Sills, G. et al. (2007). Impact of electrokinetic remediation on microbial communities within PCP contaminated soil. *Environmental Pollution* 146: 139–146.

36 Mena, E., Rubio, P., Cañizares, P. et al. (2012). Electrokinetic transport of diesel-degrading microorganisms through soils of different textures using electric fields. *Journal of Environmental Science and Health, Part A* 47: 274–279.

37 Mena, E., Villaseñor, J., Cañizares, P., and Rodrigo, M.A. (2011). Influence of soil texture on the electrokinetic transport of diesel-degrading microorganisms. *Journal of Environmental Science and Health, Part A* 46: 914–919.

38 Suni, S., Malinen, E., Kosonen, J. et al. (2007). Electrokinetically enhanced bioremediation of creosote-contaminated soil: laboratory and field studies. *Journal of Environmental Science and Health, Part A* 42: 277–287.

39 Mena, E., Ruiz, C., Villaseñor, J. et al. (2015). Biological permeable reactive barriers coupled with electrokinetic soil flushing for the treatment of diesel-polluted clay soil. *Journal of Hazardous Materials* 283: 131–139.

40 Spence, M.J., Bottrell, S.H., Thornton, S.F. et al. (2005). Hydrochemical and isotopic effects associated with petroleum fuel biodegradation pathways in a chalk aquifer. *Journal of Contaminant Hydrology* 79: 67–88.

41 Glendinning, S., Jones, C.J., and Pugh, R.C. (2005). Reinforced soil using cohesive fill and electrokineticgeosynthetics. *International Journal of Geomechanics* 5: 138–146.

42 Hamir, R.B., Jones, C.J.F.P., and Clarke, B.G. (2001). Electrically conductive geosynthetics for consolidation and reinforced soil. *Geotextiles and Geomembranes* 19: 455–482.

43 Jones, C.J., Lamont-Black, J., and Glendinning, S. (2011). Electrokineticgeosynthetics in hydraulic applications. *Geotextiles and Geomembranes* 29: 381–390.

UNCORRECTED PROOFS

Trim Size: 170mm x 244mm Single Column Loose Ribeiro670117 c13.tex V1 - 12/11/2020 11:55pm Page 302

44 Ho, S.V., Athmer, C.J., Sheridan, P.W., and Shapiro, A.P. (1997). Scale-up aspects of the lasagna™ process for in situ soil decontamination. *Journal of Hazardous Materials* 55: 39–60.

45 Ho, S.V., Athmer, C., Sheridan, P.W. et al. (1999). The lasagna technology for in situ soil remediation. 1. Small field test. *Environmental Science & Technology* 33: 1086–1091.

46 Li, G., Guo, S., Li, S. et al. (2012). Comparison of approaching and fixed anodes for avoiding the 'focusing' effect during electrokinetic remediation of chromium-contaminated soil. *Chemical Engineering Journal* 203: 231–238.

47 Shen, Z., Chen, X., Jia, J. et al. (2007). Comparison of electrokinetic soil remediation methods using one fixed anode and approaching anodes. *Environmental Pollution* 150: 193–199.

48 Li, Z., Yu, J.W., and Neretnieks, I. (1998). Electroremediation: removal of heavy metals from soils by using cation selective membrane. *Environmental Science & Technology* 32: 394–397.

UNCORRECTED PROOFS

Trim Size: 170mm x 244mm Single Column Loose Ribeiro670117 c14.tex V1 - 12/11/2020 7:06pm Page 303

14

Assessment of Soil Fertility and Microbial Activity by Direct Impact of an Electrokinetic Process on Chromium-Contaminated Soil

Prem Prakash, Prasun Kumar Chakraborty, and Brijesh Kumar Mishra

Department of Environmental Science and Engineering, Indian Institute of Technology (ISM), Dhanbad, Jharkhand 826004, India

14.1 Introduction

Exposure of human beings to chromium comes from both natural and anthropogenic sources. Chromium is present naturally in the Earth's crust, varying from 100 to 300 ppm. Most chromium ores consist of the mineral chromite ($FeCr_2O_4$), which is widely present as a natural deposit. Chromium is usually contaminated with oxygen, magnesium, silica, aluminum, and chromite at concentrations varying between 42% and 56%. Anthropogenic releases of chromium into the environment include the use of chromium in the tanning, metallurgy, electroplating, power generation, and dyeing industries [1, 2]. South Africa is one of the leading producers of chromite ore. Other countries that have chromite ore include Turkey, Finland, Kazakhstan, India, and Brazil. It is estimated that in India alone, about 2000–3000 tons of Cr escape into the environment annually from tanning industries. Due to the complex geochemical properties of soil, removing chromium is a challenging task [3]. Chromium exists in two oxidation states in soil, [Cr (III)] and [Cr (VI)], which have different toxicity and transport characteristics. pH (acidic or alkaline conditions) and Eh (reducing or oxidizing conditions) are the dominating factors that result in the formation and interaction of chromium, particularly in groundwater. In general, Cr (VI) predominates under oxidizing conditions, and Cr (III) predominates under more reducing conditions [4].

Cr (VI) occurs as $HCrO_4^-$ (bichromate ion), CrO_4^{2-} (chromate ion), and $Cr_2O_7^{2-}$ (dichromate ion). Cr (III) mainly exists as $Cr(OH)_3$, which is amphoteric in nature: when dissolved in an acidic solution, it form $[Cr(H_2O)_6]^{3+}$; and in a basic solution, it forms $[Cr(OH)_6]^{3-}$ [1]. Cr (VI) has greater toxicity, carcinogenic properties, and mobility, and it is soluble in a wider pH range of soils than Cr (III).

The primary impact of chromium includes damage to the respiratory, immunological, and gastrointestinal systems; Cr (VI) possesses mutagenic and carcinogenic properties [5]. As per a report by the WHO, more than 8000 workers in tannery industries in Hazaribagh, Bangladesh suffer from dermatological, gastrointestinal,

Electrokinetic Remediation for Environmental Security and Sustainability, First Edition.
Edited by Alexandra B. Ribeiro and M.N.V. Prasad.
© 2021 John Wiley & Sons Ltd. Published 2021 by John Wiley & Sons Ltd.

UNCORRECTED PROOFS

Trim Size: 170mm x 244mm Single Column Loose Ribeiro670117 c14.tex V1 - 12/11/2020 7:06pm Page 304

and other diseases, and of those workers, 90% die before 50 years of age [6]. It has been estimated that more than 50000 Ha of agricultural land in Tamil Nadu have been contaminated due to the disposal of tannery waste [7]. Thus, remediation of Cr (VI) is of utmost importance for public health and preventing illnesses.

Several physical, chemical, and biological methods of remediating chromium are available, including membrane filtration, soil washing, adsorption, phytoremediation, bioremediation, thermal desorption, electrokinetic remediation, ion exchange, and sorption [8–11]. However, electrokinetic remediation is the most efficient method to remediate chromium from polluted soils, as the process is suitable for fine-grained soil with low permeability, and it achieves high removal efficiency in a short time [12].

Electrokinetic remediation is an in situ process that creates an electric field in soil/sludge by applying a low-voltage electric current between electrodes to remove contaminates. Applying direct current causes the movement of electrolytes; through the processes of electromigration, electroosmosis, electrophoresis, and electrolysis of water, heavy metals bound in the soil are mobilized and can be removed. *Electromigration* is the passage of material induced by the progressive transport of ions in a conductor due to mass transfer between conducting electrons and diffusing metal ions. *Electroosmosis* is the transfer of fluid induced by an applied electric potential across a material [13]. The direct application of current lead to electrolysis of water, which produces hydrogen ions and hydroxyl ions. The movement of H^+ ions generated at the anode is toward the cathode through the soil, whereas OH^- ions migrate toward the anode. Chemical characteristic changes in the soil such as the zeta potential, pH of the soil, concentration of electrolytes, etc. are associated with the application of direct current and have a substantial impact on the effectiveness of electrokinetic remediation [14].

During the electrokinetic process, an electric field is used to encourage the movement of contaminants toward the electrode; however, other compounds present in the ground can also be circulated. There was limited research measuring soil fertility after electrokinetic treatment. Thus, in this study, we performed electrokinetic treatment of chromium-contaminated soil and measured its impact on soil fertility. The performance of organic acid as an electrolyte is evaluated based on operational parameters during the electrokinetic (EK) process. The behavior of organic carbon, macronutrients, and microbial biomass carbon (MBC) content is also delineated.

14.2 Experimental Section

14.2.1 Soil Characteristics and Preparation of Contaminated Soil

The soil used in the study was collected from an agricultural area at Nirsa (23.78°N 86.72°E) in the Dhanbad district of India. The soil was collected from a field at a depth of 5–25 cm and was air-dried at room temperature. Stones, roots, and sticks were manually removed. The soil sample's grain size was kept less than 2 mm by sieving through a 2 mm Indian Standard sieve. The physico-chemical characteristics of the soil used in this study are summarized in Table 14.1.

UNCORRECTED PROOFS

Trim Size: 170mm x 244mm Single Column Loose Ribeiro670117 c14.tex V1 - 12/11/2020 7:06pm Page 305

Table 14.1 Physical and chemical characteristics of agriculture soil before contamination.

S no.	Characteristics	Measurement
1.	Particle size analysis	
a)	Sand	39%
b)	Silt	38%
c)	Clay	23%
2.	Liquid limit	32.23%
3.	Plastic limit	24.47%
4.	Porosity	42%
5.	Void ratio	0.66
6.	pH	4.68
7.	Conductivity	0.166 mS cm^{-1}
8.	Moisture content	20.70%
9.	Organic carbon	3.07%
10.	Organic matter	5.32%
11.	Water holding capacity	25.35%
12.	Calcium	17.6 mg kg^{-1}
13.	Potassium	33.6 mg kg^{-1}

The soil was then artificially spiked with Cr (VI): 2 kg of the soil sample were mixed with 1 l of 1000 mg l^{-1} $K_2Cr_2O_7$ to make a mixture concentration of 500 mg kg^{-1}. To age the chromium, the soil was stored in a plastic container in an aphotic room for two months. After that time, the speciation of total Cr in the contaminated soil was studied, and it was observed that chromium in the soil was found in the form of Cr (III) only due to the reduction of Cr (VI) to Cr (III).

14.2.2 Electrokinetic Tests, Experimental Setup, and Procedure

A schematic diagram of the EK setup is shown in Figure 14.1. The setup consists of two electrode chambers ($4 \times 4 \times 4\,cm^3$), one soil chamber ($4 \times 4 \times 20\,cm^3$), two electrolyte solution reservoirs (1 l), and a direct control electricity supply (0–300 V, 0–1 A). Two sets of plate-type graphite electrodes ($3.9 \times 3.9\,cm^2$) were employed in the experiments. To prevent soil from escaping from the cell to the electrode chamber, pierced Plexiglas plates with a paper filter were used. The soil cell was separated into four equal compartments numbered I to IV, each about 5 cm, with the first compartment closest to the anode. A constant voltage of 2 V cm^{-1} was applied throughout, and a flow rate of 2 ml min^{-1} was maintained using a peristaltic pump (Ravel Hiteks Pvt. Ltd., India).

UNCORRECTED PROOFS

Trim Size: 170mm x 244mm Single Column Loose Ribeiro670117 c14.tex V1 - 12/11/2020 7:06pm Page 306

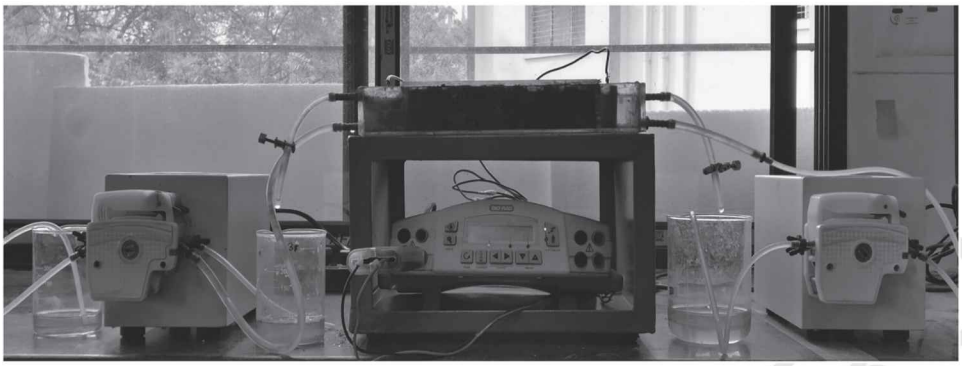

Figure 14.1 Design of the electrokinetic setup.

14.2.3 Testing Procedure

A set of experiments was carried out for 10 days. Citric acid (1 M) was employed as an electrolyte and was refreshed every two days during the EK process. Citric acid was used due to its high buffering capacity, to avoid pH jump and promote electroosmotic flow [15–17].

The soil sample from each section was collected after remediation and preserved at 4 °C. The pH and conductivity of the soil samples were analyzed (using a ratio of 1 : 2.5 of soil/distilled water) using a pH and conductivity meter (Hanna instrument, HI5521, USA). The soil's organic carbon and macronutrients were monitored at two-day intervals (as per the method described in the next section). The voltage and current intensity of the electrolytes in the electrode chambers were monitored periodically using a Power Pac (Bio-Rad, 164-5052) during the EK remediation.

14.2.4 Extraction and Analytical Methods

Cr (total) in the soil was digested using a microwave digester: 0.2 g of soil sample was mixed with 6 ml HNO_3 (65% purity), 2 ml HF, and 2 ml H_2O_2. Cr (total) in the soil was analyzed using an atomic absorbance spectrometer (AAS) (GBC Avanta PM, Dandenong, Victoria, Australia). Similarly, the metal ion concentrations of zinc, manganese, copper, and cadmium in the initial soil sample were calculated by the acid digestion method and were analyzed by AAS. The initial concentration of metal ions is summarized in Table 14.2.

14.2.5 Soil Nutrients

The available nitrogen in the soil was measured by the Kjeldahl method. The available phosphorus was determined by Oleson's method by extracting phosphorus from the soil with 0.5 M $NaHCO_3$ (pH 8.5) and further analyzed using a spectrophotometer (Lab Tech, UV9100A, China). Exchangeable potassium, sodium, and calcium in the soil were determined by centrifuging 5 g of the soil sample in 25 ml ammonium acetate solution, 1(N), and further analyzed by with a flame photometer at 767 nm

UNCORRECTED PROOFS

Trim Size: 170mm x 244mm Single Column Loose Ribeiro670117 c14.tex V1 - 12/11/2020 7:06pm Page 307

Table 14.2 Metal ion concentration in the initial soil sample.

Metal species	Metal ion concentration (mg kg^{-1})
Chromium	92.5
Zinc	148
Manganese	176.5
Copper	80.25
Cadmium	4.1

wavelength (ESICO, 1385, India). The standard curve was prepared from a stock solution of K, Na, and Ca.

14.2.6 Soil Microbial Biomass Carbon Analysis

The soil MBC was analyzed by the chloroform fumigation extraction method [18] using a correction factor of 0.33 [19]. Three 12.5 g soil samples were treated with chloroform ($CHCl_3$) exposed in a vacuum desiccator at 25 °C for 24 hours. Then the fumigated soil was kept in an oven at 105 °C for 24 hours. Extraction of the fumigated soil was accomplished by adding 25 ml 0.5 N K_2SO_4 and shaking for 30 min. The same protocol (except for chloroform treatment) was applied to estimate the non-fumigated biomass of the soil after each EK process. After that, 8 ml of the filtrate were taken, and 2 ml $K_2Cr_2O_7$, 10 ml H_2SO_4, 2.5 ml orthophosphoric acid, and 2 drops of diphenylamine indicator were added; the mixture was titrated with 0.4 N ferrous ammonium sulfate until a tea green color developed. The total MBC was formulated as follows:

$$\text{MBC} = (\text{OCF} - \text{OCNF}) \times 10^4 \div 0.33$$

where OCF is the organic carbon extracted from fumigated soil, and OCNF is the organic carbon extracted from non-fumigated soil.

The microbial biomass of the soil sample was analyzed at the beginning and end of the experiment to determine the impact of EK remediation.

14.2.7 Quality Control and Quality Assurance

To ensure proper quality control and quality assurance (QA/QC), correct effort and care were taken in the laboratory to guarantee purity of the sample and reliable data. Standard reference materials (SRM) – AccuStandard Inc., AccuTrace, USA; CRM uncertainity ± 5%, Matrix 2–5% nitric acid, verified against NIST SRM# 3112 for Cr; 3136 for Ni; 3108 for Cd; 3128 for Pb; 3113 for Co; 3132 for Mn; 3114 for Cu; 3168a for Zn – were used for calibration and preparation [20]. The recovery percentage of metals in the SRM samples for soil were 81%–103%. Calibration coefficients were maintained at ≥ 0.99. Repeated analysis of selected samples was performed to correlate inter-batch studies (less than 10% relative variation). Accuracy and precision

UNCORRECTED PROOFS

Trim Size: 170mm x 244mm Single Column Loose Ribeiro670117 c14.tex V1 - 12/11/2020 7:06pm Page 308

Table 14.3 QA/QC detection limit.

Metal	Detection limit (mg kg^{-1})	Characteristic concentration (mg kg^{-1})
Cr	0.003	0.05
Zn	0.0005	0.008
Ni	0.009	0.04
Co	0.004	0.05
Mn	0.0015	0.02
Pb	0.01	0.04
Cu	0.001	0.02
Cd	0.0004	0.0009

were checked using duplicate analysis of the sample (less than 10% relative variation). By running standard solutions after every 15 samples, the accuracy of the analytical procedure used for flame atomic absorption spectroscopy (FAAS) analysis was checked (Table 14.3).

14.3 Results and Discussion

14.3.1 Electrokinetic Remediation of Chromium-Contaminated Soil

14.3.1.1 Electrical Current Changes During the Electrokinetic Experiment

Electric current is an important parameter in EK remediation; it represents an ion electromigration [21]. Figure 14.2 shows the variation of electrical current over time. The current first increased significantly and reached a maximum value of 0.16 A within three days; it then gradually decreased and remained constant, stabilizing at a value of 0.09 A. The reason is that when a constant voltage of 2 V cm^{-1} was applied, an electric field was established, and current began to flow due to the movement of ions present in the soil. Current in the early days showed a slight increase because of the time required for the electrolyte to penetrate the soil and mobilize minerals that were in a bound or complex form. The later increase in electric current was caused by desorption of ions from soil particles to the soil solution, marked by a higher concentration of ions in pore water [22]. After three days, there was a constant decrease in current as the migration of ions from the anode to the cathode gradually declined; further, ions in mobile form in the soil were carried by the electrolyte, which were refreshed after two days, resulting in the loss of ions. Several researchers obtained a similar trend of current variation [23, 24]. The experiment was discontinued after 10 days as there was no substantial change in electric current, which indicated no movement of ions.

UNCORRECTED PROOFS

Trim Size: 170mm x 244mm Single Column Loose Ribeiro670117 c14.tex V1 - 12/11/2020 7:06pm Page 309

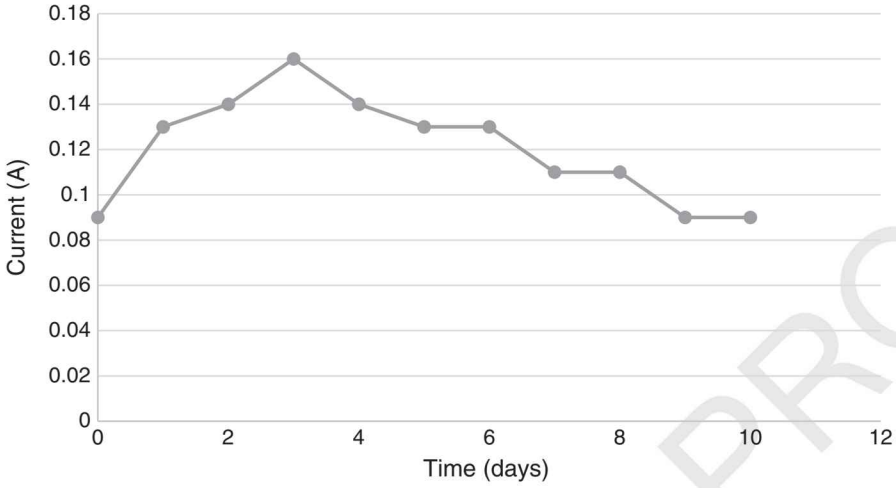

Figure 14.2 Variation of current with time during the electrokinetic experiment.

14.3.2 pH Distribution in Soil During and After the Electrokinetic Experiment

Soil pH has a significant impact on plant growth. It also has a powerful impact on nutrient transformation, solubility, and availability, and it affects the activity and type of microorganisms in the soil [25].

During the experiment, pH variation in the anode and cathode electrolyte reservoirs was monitored periodically every day. Figure 14.3 shows that the pH of the anode purging solution changed from 2.34 to 1.69, and pH at the cathode increased from 2.34 to 7.68. At the culmination of the experiment, the soil section was split into four components (equal in size), and their pH was recorded as shown in Figure 14.4. The pH ranged from 3.41 to 7.23, increasing with distance from the anode. The electrolysis of water in the anode compartment produced hydrogen ions, which were transported toward the cathode region, resulting in a decrease in pH in the anode compartment over time. Similarly, an increase in the pH of the soil in the cathode region was noted due to the generation of hydroxide ions from the electrolysis of water [26]. A similar trend of increase in pH near the cathode reservoir and decrease of pH near the anode reservoir was showed during remediation of hexachlorobenzene and manganese from the soil [27, 28]. The low pH near the anode promotes the desorption of most heavy metals and cations, which enhances the proportion of metallic contaminants removed [14, 29]; further, low pH in the soil augmented negative electroosmotic flow, resulting in removing metal contaminants [29]. As the electrolyte used in this experiment was 1 M citric acid of pH 2.17, the pH of the electrolyte never increased beyond 7.68. Thus, in a homogenous soil mixture, the pH varied between 2.34 and 7.68 on proceeding toward the cathode from the anode.

UNCORRECTED PROOFS

Trim Size: 170mm x 244mm Single Column Loose Ribeiro670117 c14.tex V1 - 12/11/2020 7:06pm Page 310

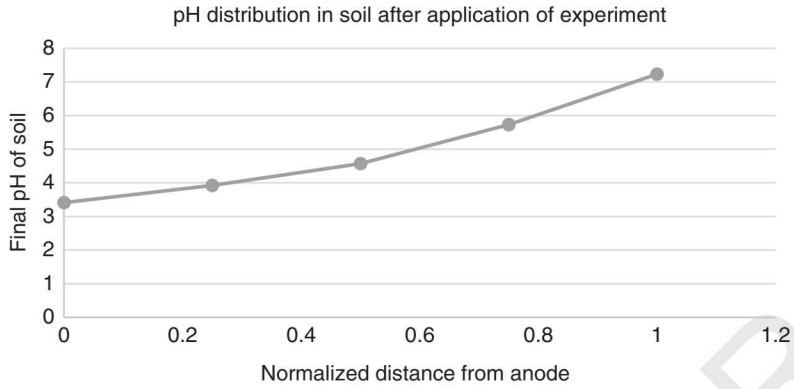

AQ2

Figure 14.3 Variation in electrolyte pH.

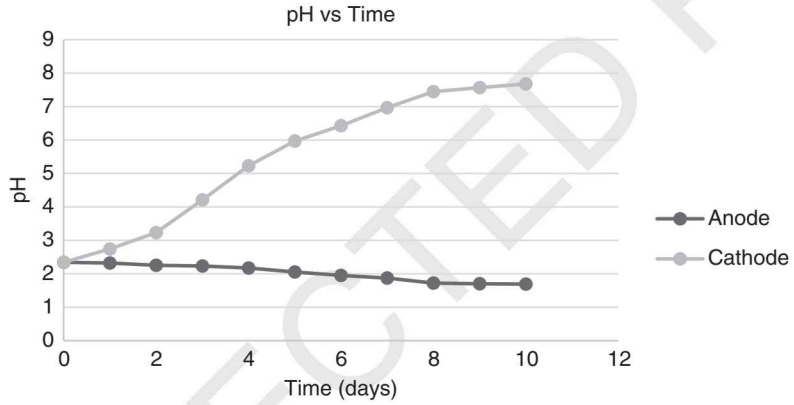

Figure 14.4 pH distribution in the soil after the experiment.

14.4 Removal of Cr

14.4.1 The Distribution of Total Cr and Its Electroosmotic Flow During the Electrokinetic Experiment

When an external electric field is applied to a material, it interferes with surplus charged ions, resulting in the movement of bulk liquid. This is known as *electroosmotic flow* [30]. A reduction in the cathode's pH makes it easier to extract pollutants, whichever species precipitates near the cathode. At an acidic pH, the surface charge of soil particles is positive, so electroosmotic flow moves rapidly toward the anode [31]. Figure 14.5 shows the electroosmotic flow with time; the experiment showed considerable electroosmotic flow in the first five days of treatment, when 60% of total accumulated electroosmosis flow (EOF) was observed; it increased with duration. The total volume collected at the cathode was 1910 ml; volume loss was primarily due to losses during measurement of the electrolyte pH during the experiment; in addition, some loss resulted from adsorption of Cr by the graphite electrode. With

UNCORRECTED PROOFS

Trim Size: 170mm x 244mm Single Column Loose Ribeiro670117 c14.tex V1 - 12/11/2020 7:06pm Page 311

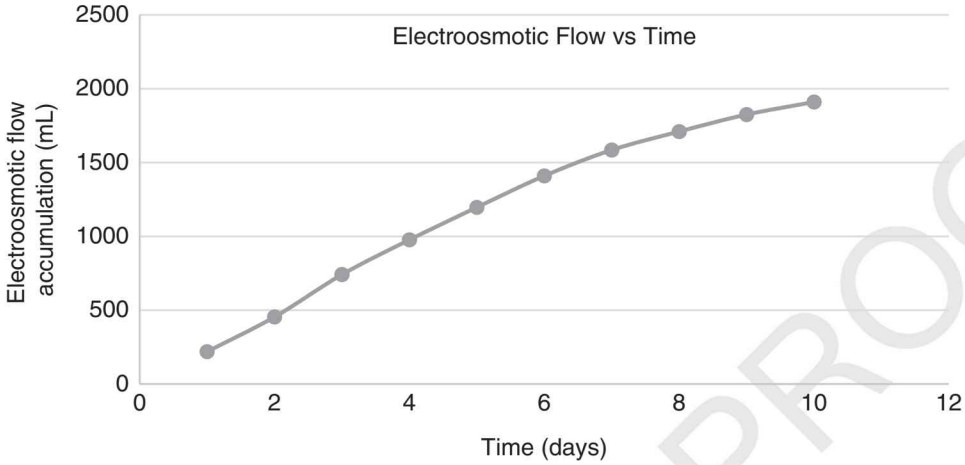

Figure 14.5 Electroosmotic flow during the electrokinetic experiment.

constant porosity and a coefficient of electroosmotic permeability, an increase in the electrical potential gradient resulted in an increase in electroosmotic flow. Electric current is directly proportional to the potential gradient; there was an increase in electroosmotic flow at the end of the experiment as there was a decrease in electrical current [32].

Figure 14.6 shows the normalized concentration of Cr (total) in the soil specimen at the conclusion of the trial. As shown in the figure, heavy metals are dissolved near the anode due to acidification of the soil, and the Cr (total) migrated toward the cathode. As the pH of the cathode was higher than the anode, some of the metal ions precipitated near the cathode. Over time, electromigration and electroosmotic flow decreased, so metal concentration increased with the increase in distance from the anode. The removal efficiency with time, as shown in Figure 14.7, was estimated by collecting soil near the anode and cathode, and the percentage of metal recovered was determined. The removal efficiency of Cr was 51.2% at the anode and 78.7% at

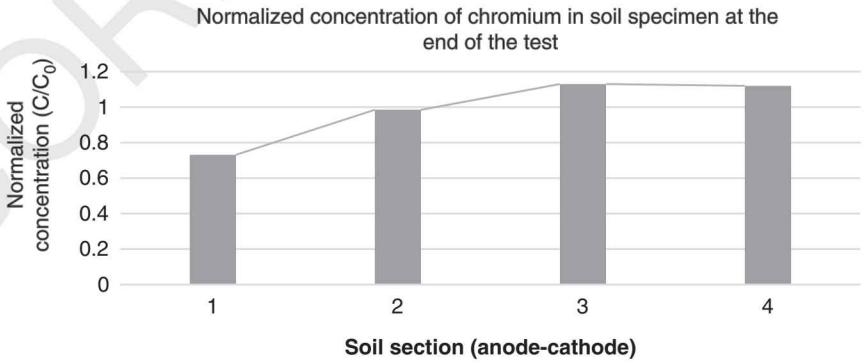

Figure 14.6 Normalized concentration of chromium in the soil specimen at the end of the test.

UNCORRECTED PROOFS

Trim Size: 170mm x 244mm Single Column Loose Ribeiro670117 c14.tex V1 - 12/11/2020 7:06pm Page 312

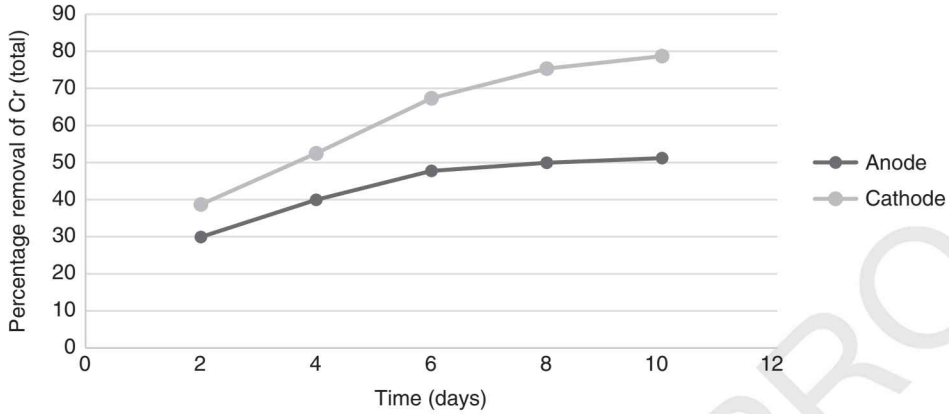

Figure 14.7 Percentage of chromium removed with time.

the cathode. At the end of the test, 303.488 mg kg^{-1} and 466.29 mg kg^{-1} of Cr were removed. Removal efficiency of Cr in sediments was 77.33%; using 1 M citric acid increased removal efficiency. This higher removal efficiency using 1 M citric acid may be attributed to citric acid acting as a complexing agent in the role of activation and compound assemblage in the soil, thus increasing contact time and mobilizing the ions, which accelerated the removal of chromium from the soil.

14.5 Effects of the Electrokinetic Process on Some Soil Properties

14.5.1 Soil Organic Carbon

Total organic carbon in soil is the measure of carbon stored in soil organic matter. Microorganisms require an energy source to break down food material. This energy source is provided by soil organic carbon. It releases nutrients for plant growth, improves the biological and physical health of the soil, and acts as a buffer against deleterious substances. An increase in soil organic carbon has two major benefits: it helps alleviate climate change and improves soil health and fertility [33].

Figure 14.8 shows the variation of organic carbon in chromium-contaminated soil over time. The graph exhibits a considerable increase in organic carbon from 2.97% to 17.12% within 10 days using 1 M citric acid as an electrolyte. Citric acid is a weak organic tricarboxylic acid with chemical formula $C_6H_8O_7$. The tricarboxylic acid cycle, also known as the citric acid cycle, is a prime source of energy for cells and an essential step in aerobic respiration. In the trichloroacetate (TCA) cycle, a six-carbon sugar is oxidized to produce CO_2 and H_2O, which are used by plants, fungi, and bacteria to convert organic compounds to energy. Hence, using citric acid as an electrolyte not only enhanced removal efficiency but was also effective in enriching the soil's organic carbon – an important parameter for the sustained

UNCORRECTED PROOFS

Trim Size: 170mm x 244mm Single Column Loose Ribeiro670117 c14.tex V1 - 12/11/2020 7:06pm Page 313

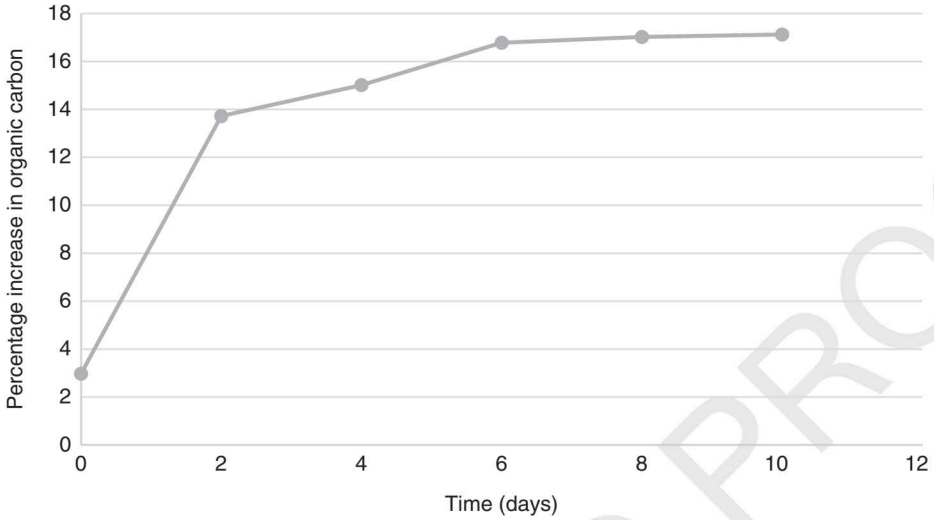

Figure 14.8 Percentage increase in organic carbon during the electrokinetic experiment.

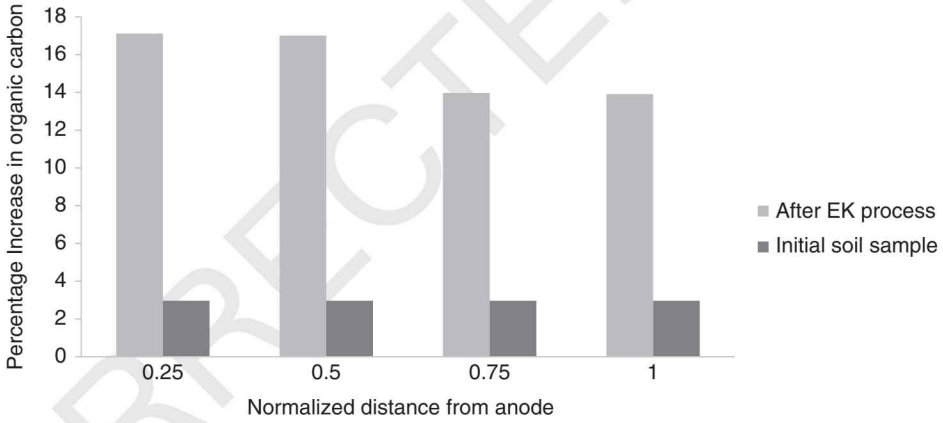

Figure 14.9 Organic carbon in soil after the electrokinetic process.

supply of nitrogen and maintaining appropriate soil quality, including permeability, water-holding capacity, aeration, and nutrient-preserving capacity [34].

The distribution of organic carbon in soil after the EK process is shown in Figure 14.9. Organic carbon increased near the anode and decreased with the distance from the anode. The reason was the accumulation of citric acid near the anode: as mentioned earlier, citric acid encourages high viscosity, so a clogging phenomenon was observed in the soil near the anode. Further, the mobility of ions decreased after 10 days, so citric acid near the anode could not flow toward the cathode due to high resistance and low electrical conductivity.

UNCORRECTED PROOFS

Trim Size: 170mm x 244mm Single Column Loose Ribeiro670117 c14.tex V1 - 12/11/2020 7:06pm Page 314

14.5.2 Soil-Available Nitrogen, Phosphorus, Potassium, and Calcium

Nutrients in the soil are essential for plant growth and metabolism; without them, plants are unable to complete a normal cycle life. Macronutrients obtained from soil include nitrogen, phosphorus, potassium, and calcium. The fundamental processes of nutrient uptake from soil by plants are simple diffusion, active transport, and facilitated diffusion. When an electric field was applied, the movement of chromium toward the electrode chamber was observed. However, other native compounds present in the soil, such as nitrogen, potassium, and calcium, were also mobilized [34]. Macronutrients in soil are present in complex chemical forms that can't be directly used by the plant; the plant consumes the available nutrients. The present study evaluated the impact of the EK test on the soil-available nutrients. For this reason, initial soil nutrients were measured, and after two days, the available nitrogen, phosphorus, potassium, calcium, and sodium were observed. After the experiment was complete, the soil section was divided into four equal parts, and their available nutrients were measured.

Figure 14.10 demonstrates the effects of the EK process on available soil nutrients over time. As shown in the figure, the average concentration of available nitrogen decreased from 84 to 75.7 mg kg^{-1}. The likely cause of the decline in nitrogen content was the application of the direct electric current, which caused the available nitrogen to be carried toward cathode by electroosmosis, along with the electrolyte; this mobile form of nitrogen was removed along with the electrolyte. Further, available nitrogen might have been transformed into organic nitrogen and inorganic nitrogen by hydrolysis of water. A similar trend of available nitrogen transformation was observed in fluorine-contaminated soil [35]. Figure 14.11 shows the distribution of available soil nitrogen with the normalized distance from the anode after EK treatment. It was found that maximum available nitrogen accumulated near the anode and decreased as the distance increased. The explanation was that the mobility of ions decreased after 10 days, so ions accumulated near the anode.

Available phosphorus was found in a trace amount in the soil sample and experienced a slight increase in value from 3.96 mg kg^{-1} to 5.072 mg kg^{-1}, as shown in Figure 14.10. An increase in the value of available phosphorus was observed. The change in available phosphorus with increased distance from the anode, as shown in Figure 14.12, remained almost constant. Soil nutrients consist of an available fraction, which is mobilized by the application of direct current, and an unavailable fraction, which remains in the soil [36–38]. The conversion of available phosphorus to a mobile form stimulated its removal from the soil, and the hydrolysis of unavailable phosphorus to available phosphorus increased its value by 28% (Figure 14.10).

The variation of soil-available potassium over time is shown in Figure 14.10. The available potassium in the soil increased from 17.6 to 24.8 mg kg^{-1} within six days of treatment. A decrease in value was observed after that, to 21 mg kg^{-1}. The sharp decrease in value was due to the transfer of potassium ions from the soil to the electrolyte by electroosmosis and electromigration; the ions were carried by the electrolyte over time. The variation of potassium at the end of the experiment is shown in

UNCORRECTED PROOFS

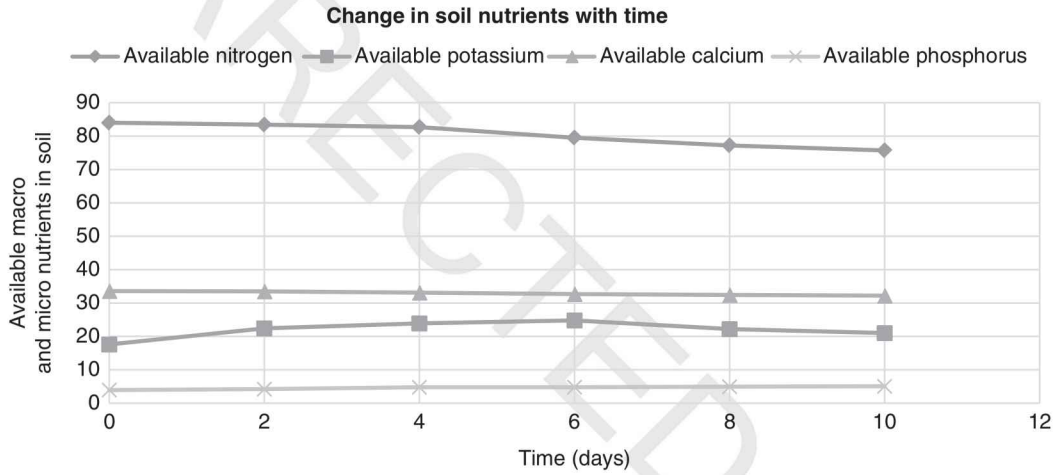

Figure 14.10 Change in soil nutrients with time.

UNCORRECTED PROOFS

Trim Size: 170mm x 244mm Single Column Loose

Ribeiro670117 c14.tex V1 - 12/11/2020 7:06pm Page 315

Trim Size: 170mm x 244mm Single Column Loose Ribeiro670117 c14.tex V1 - 12/11/2020 7:06pm Page 316

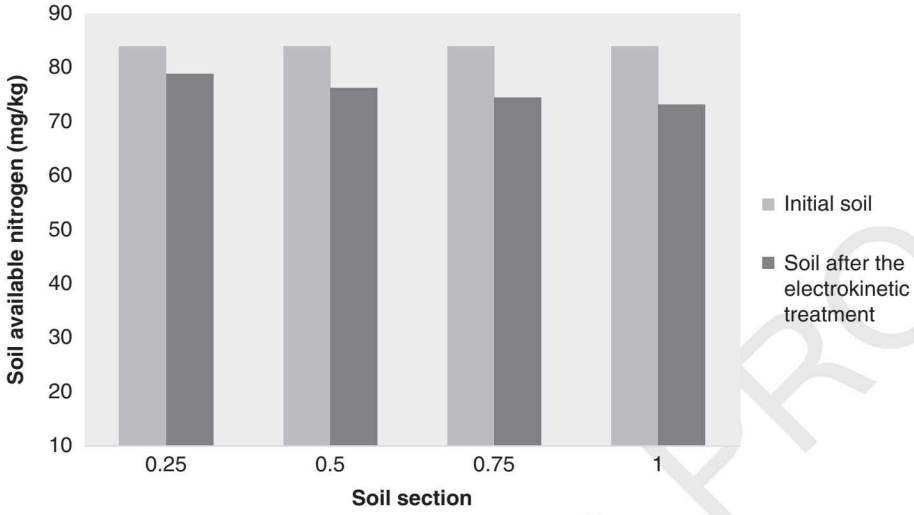

Figure 14.11 Distribution of soil-available nitrogen after the electrokinetic process.

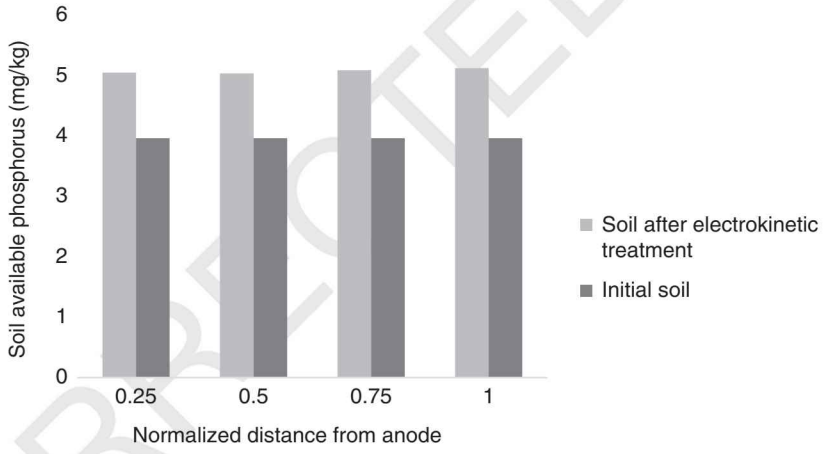

Figure 14.12 Distribution of soil-available phosphorus after the electrokinetic process.

Figure 14.13: the decreased from 21.7 to 18.48 mg kg^{-1}, resulting in the accumulation of bound potassium near the anode.

Figure 14.14 shows the variation of soil-available calcium after the end of the experiment with normalized distance from the anode. Available calcium did not show much variation and changed from 33.6 to 32.2 mg kg^{-1}. The magnitude of electron drift speed is the product of electron mobility and the electric field applied: with a constant electric field, it varies with variation in ionic mobility, which is given by $\mu = ze/6\pi\eta\alpha$; i.e. μ is inversely proportional to α, where α is the hydrodynamic radius. However, the hydrodynamic radius depends upon the solvent molecules around the ion. The effective size of solvation is related to how attractive metal ions appear on

UNCORRECTED PROOFS

Trim Size: 170mm x 244mm Single Column Loose Ribeiro670117 c14.tex V1 - 12/11/2020 7:06pm Page 317

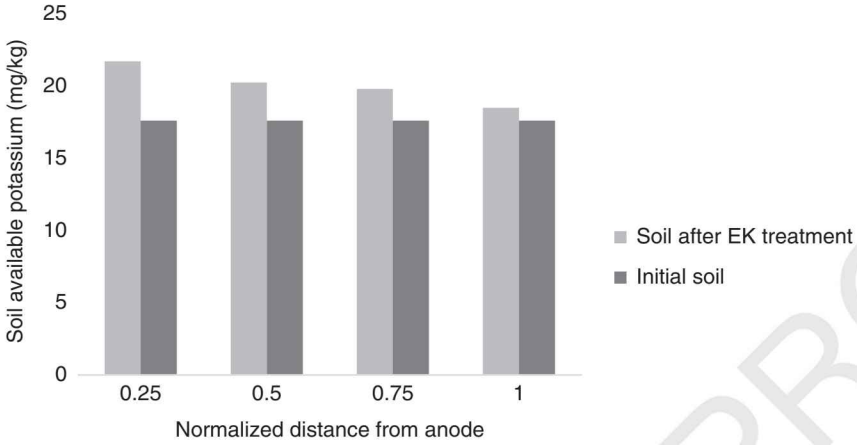

Figure 14.13 Distribution of soil-available potassium after the electrokinetic process.

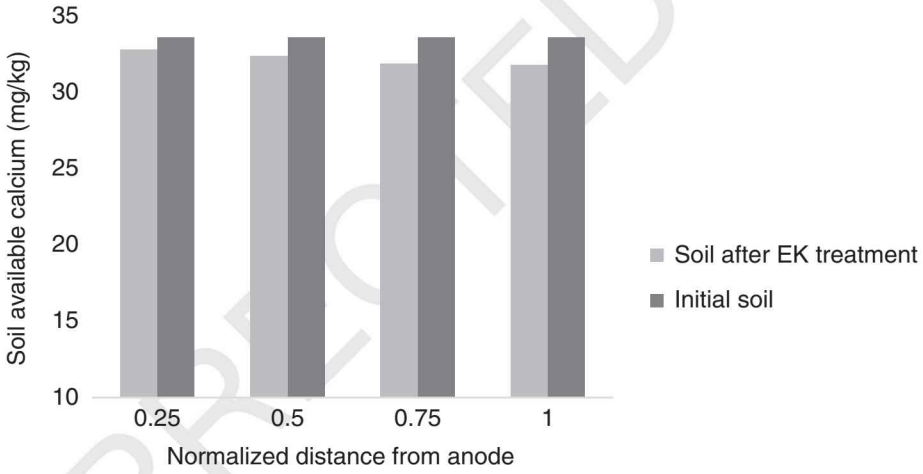

Figure 14.14 Distribution of soil-available calcium after the electrokinetic process.

the solvent molecule; for spherical ions, it is given by $E \propto ze/r^2$, where r is the atomic radius. Thus calcium ions are capable of attracting large solvent molecules, hindering movement; as a result, calcium ions accumulated in the soil sample, while a decrease in value was observed as the distance from the anode increased. Citric acid has an appreciably low affinity for alkaline earth and alkaline metals: i.e. calcium and potassium were responsible for less desorption of metal from the soil [39], so its convergence to a mobile form was not successful. As a result, its value decreased over time, as shown in Figure 14.10.

A minute amount of sodium was present in the soil and was not detected by the flame photometer.

UNCORRECTED PROOFS

Trim Size: 170mm x 244mm Single Column Loose Ribeiro670117 c14.tex V1 - 12/11/2020 7:06pm Page 318

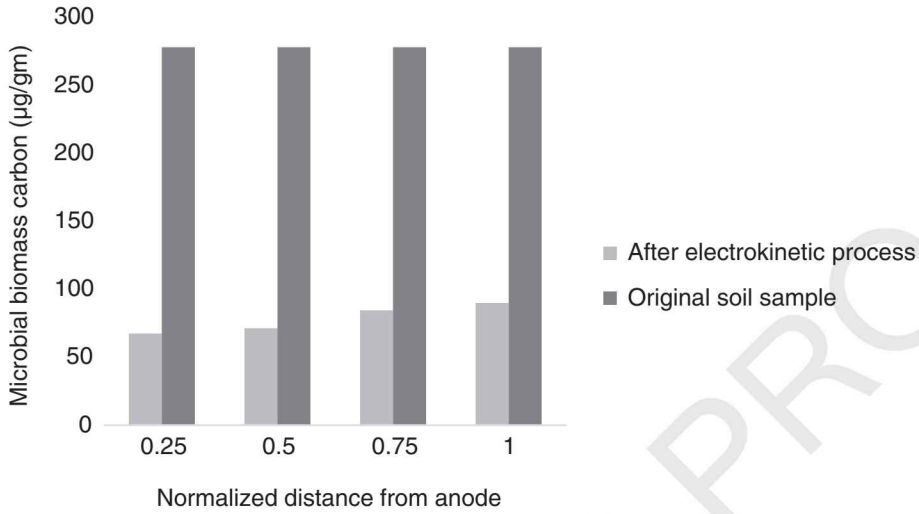

Figure 14.15 Distribution of soil microbial biomass carbon.

14.5.3 Soil Microbial Biomass Carbon

MBC showed a value of 287.87 µg g^{-1} at the start of the experiment; the value was reduced to 78.84 µg g^{-1} after EK treatment. The substantial reduction in MBC was primarily due to a change in the pH of the soil, which is an influential parameter for the survival of bacteria. Further, changes in moisture content, refreshing the electrolyte, electrical conductivity, and changes in soil properties are attributed to change in MBC. Previous studies also reported that the optimal pH range for most bacteria to survive lies between 6 and 7.5 [39]. An MBC value of 78.23 µg g^{-1} suggested that after an EK process using citric acid as an electrolyte, microbes can survive in the soil and can be revived later when exposed to a natural, open atmosphere. As depicted in Figure 14.15, the MBC count of soil in the cathode region was higher than in the anode region, as acidification of soil in the anode region meant fewer microbes survived. A negative correlation exists between pH and microbial biomass, which inhibited the increase in pH as observed in soil in the cathode region [40].

14.6 Conclusion

Application of 1 mol l^{-1} citric acid as an electrolyte can effectively remove chromium from soil and elicit a substantial impact on soil fertility. A further EK experiment has promising results regarding the distribution of soil macronutrients. Experimental results indicated that EK using a weak organic acid does not significantly impact soil-available nitrogen, phosphorus, and potassium. Available nitrogen, potassium, and calcium decreased from the anode to the cathode, while the available phosphorus concentration remained almost constant. MBC decreased significantly during the EK experiments, but the survival of some microbes indicated that they could be

UNCORRECTED PROOFS

Trim Size: 170mm x 244mm Single Column Loose Ribeiro670117 c14.tex V1 - 12/11/2020 7:06pm Page 319

regenerated when exposed to an open environment; thus, when this soil was exposed to the atmosphere, the pH would recover and MBC would increase. This experiment suggested that using organic acid as an electrolyte can return soil to its initial condition with an increase in soil fertility within a short time.

References

1 Reddy, K.R., Parupudi, U.S., Devulapalli, S.N., and Xu, C.Y. (1997). Effects of soil composition on the removal of chromium by electrokinetics. *Journal of Hazardous Materials* 55 (1–3): 135–158.

2 Capeáns, P.P., Alonso, M.C., Barrera, A.B., and Barrera, P.B. (2005). Chromium available fraction in aurosa sediments using a modified microve BCR protocol based on microwave assisted extraction. *Talanta* 65 (3): 678–685.

3 Li, G., Guo, S., Li, S. et al. (2012). Comparison of approaching and fixed anodes for avoiding the 'focusing' effect during electrokinetic remediation of chromium-contaminated soil. *Chemical Engineering Journal* 203: 231–238.

4 Stanin, F.T. and Pirnie, M. (2004). The transport and fate of Cr (VI) in the environment. In: *Chromium (VI) Handbook* (eds. C.P. Avakian, J. Guertin and J.A. Jacobs), 165–214. CRC Press.

5 Stearns, D.M., Wise, J.P. Sr.,, Patierno, S.R., and Wetterhahn, K.E. (1995). Chromium (III) picolinate produces chromosome damage in Chinese hamster ovary cells 1. *The FASEB Journal* 9 (15): 1643–1649.

6 Maurice, J. (2001). Tannery pollution threatens health of half-million Bangladesh residents. *Bulletin of the WHO* 79 (1): 78–79.

7 Rangasamy, S., Purushothaman, G., Alagirisamy, B., and Santiago, M. (2015). Chromium contamination in soil and groundwater due to tannery wastes disposals at Vellore district of Tamil Nadu. *International Journal of Environmental Sciences* 6 (1): 114–124.

8 Castilhos, D.D., Tedesco, M.J., and Vidor, C. (2002). Rendimentos de culturas e alterações químicas do solo tratado com resíduos de curtume e crômio hexavalente. *Revista Brasileira de Ciência do Solo* 26 (4): 1083–1092.

9 Fonseca, B., Pazos, M., Tavares, T., and Sanromán, M.A. (2012). Removal of hexavalent chromium of contaminated soil by coupling electrokinetic remediation and permeable reactive biobarriers. *Environmental Science and Pollution Research* 19 (5): 1800–1808.

10 Aboughalma, H., Bi, R., and Schlaak, M. (2008). Electrokinetic enhancement on phytoremediation in Zn, Pb, Cu and Cd contaminated soil using potato plants. *Journal of Environmental Science and Health Part A* 43 (8): 926–933.

11 Ryu, B.G., Park, G.Y., Yang, J.W., and Baek, K. (2011). Electrolyte conditioning for electrokinetic remediation of As, Cu, and Pb-contaminated soil. *Separation and Purification Technology* 79 (2): 170–176.

12 Alshawabkeh, A.N. (2009). Electrokinetic soil remediation: challenges and opportunities. *Separation Science and Technology* 44 (10): 2171–2187.

UNCORRECTED PROOFS

Trim Size: 170mm x 244mm Single Column Loose Ribeiro670117 c14.tex V1 - 12/11/2020 7:06pm Page 320

13 Buchireddy, P.R., Bricka, R.M., and Gent, D.B. (2009). Electrokinetic remediation of wood preservative contaminated soil containing copper, chromium, and arsenic. *Journal of Hazardous Materials* 162 (1): 490–497.

14 Lu, P., Feng, Q., Meng, Q., and Yuan, T. (2012). Electrokinetic remediation of chromium-and cadmium-contaminated soil from abandoned industrial site. *Separation and Purification Technology* 98: 216–220.

15 Pazos, M., Alcántara, M.T., Cameselle, C., and Sanromán, M.A. (2009). Evaluation of electrokinetic technique for industrial waste decontamination. *Separation Science and Technology* 44 (10): 2304–2321.

16 Eykholt, G.R. and Daniel, D.E. (1994). Impact of system chemistry on electroosmosis in contaminated soil. *Journal of Geotechnical Engineering* 120 (5): 797–815.

17 Yang, G.C. and Lin, S.L. (1998). Removal of lead from a silt loam soil by electrokinetic remediation. *Journal of Hazardous Materials* 58 (1–3): 285–299.

18 Vance, E.D., Brookes, P.C., and Jenkinson, D.S. (1987). An extraction method for measuring soil microbial biomass C. *Soil Biology and Biochemistry* 19 (6): 703–707.

19 Sparling, G.P. and West, A.W. (1988). A direct extraction method to estimate soil microbial C: calibration in situ using microbial respiration and 14C labelled cells. *Soil Biology and Biochemistry* 20 (3): 337–343.

20 Kumar, A. and Maiti, S.K. (2015). Assessment of potentially toxic heavy metal contamination in agricultural fields, sediment, and water from an abandoned chromite-asbestos mine waste of Roro hill, Chaibasa, India. *Environmental Earth Sciences* 74 (3): 2617–2633.

21 Shenbagavalli, S. and Mahimairaja, S. (2010). Electro kinetic remediation of contaminated habitats. *African Journal of Environmental Science and Technology* 4 (13): 930–935.

22 Kim, D.H., Jeon, C.S., Baek, K. et al. (2009). Electrokinetic remediation of fluorine-contaminated soil: conditioning of anolyte. *Journal of Hazardous Materials* 161 (1): 565–569.

23 Eykholt, G.R. (1992). Driving and complicating features of electrokinetic treatment of soils. PhD dissertation, University of Texas.

24 Grundl, T. and Michalski, P. (1996). Electroosmotically driven water flow in sediments. *Water Research* 30 (4): 811–818.

25 Zhou, M., Wang, H., Zhu, S. et al. (2015). Electrokinetic remediation of fluorine-contaminated soil and its impact on soil fertility. *Environmental Science and Pollution Research* 22 (21): 16907–16913.

26 Acar, Y.B. and Alshawabkeh, A.N. (1993). Principles of electrokinetic remediation. *Environmental Science & Technology* 27 (13): 2638–2647.

27 Reddy, K.R., Darko-Kagya, K., and Al-Hamdan, A.Z. (2011). Electrokinetic remediation of pentachlorophenol contaminated clay soil. *Water, Air, and Soil Pollution* 221 (1–4): 35–44.

28 Ricart, M.T., Hansen, H.K., Cameselle, C., and Lema, J.M. (2005). Electrochemical treatment of a polluted sludge: different methods and conditions for manganese removal. *Separation Science and Technology* 39 (15): 3679–3689.

UNCORRECTED PROOFS

Trim Size: 170mm x 244mm Single Column Loose Ribeiro670117 c14.tex V1 - 12/11/2020 7:06pm Page 321

29 Yeung, A.T., Hsu, C.N., and Menon, R.M. (1997). Physicochemical soil-contaminant interactions during electrokinetic extraction. *Journal of Hazardous Materials* 55 (1–3): 221–237.

30 Erickson, D. (2015). Electroosmotic flow over heterogeneous surfaces. In: *Encyclopedia of Microfluidics and Nanofluidics* (ed. D. Li). New York: Springer.

31 Kim, D.H., Ryu, B.G., Park, S.W. et al. (2009). Electrokinetic remediation of Zn and Ni-contaminated soil. *Journal of Hazardous Materials* 165 (1–3): 501–505.

32 Kim, D.H., Jo, S.U., Choi, J.H. et al. (2012). Hexagonal two dimensional electrokinetic systems for restoration of saline agricultural lands: a pilot study. *Chemical Engineering Journal* 198: 110–121.

33 Chan, Y. (2008). Increasing soil organic carbon of agricultural land. *Primefact* 735: 1–5.

34 Smith, P., Davies, C.A., Ogle, S. et al. (2012 Jul). Towards an integrated global framework to assess the impacts of land use and management change on soil carbon: current capability and future vision. *Global Change Biology* 18 (7): 2089–2101.

35 Gosling, P. and Shepherd, M. (2005 Jan 1). Long-term changes in soil fertility in organic arable farming systems in England, with particular reference to phosphorus and potassium. *Agriculture, Ecosystems and Environment* 105 (1–2): 425–432.

36 Bedmar, M.L., Perez-Sanz, A., Martinez-Inigo, M.J., and Benito, A.P. (2009). *Electrochemical Remediation Technology for Polluted Soils, Sediment and Ground Water*, 417–433. Hoboken, NJ: Wiley.

37 Gonzini, O., Plaza, A., Di Palma, L., and Lobo, M.C. (2010). Electrokinetic remediation of gasoil contaminated soil enhanced by rhamnolipid. *Journal of Applied Electrochemistry* 40 (6): 1239–1248.

38 Steger, H., Zorn, R., Gregolec, G. et al. (2005). Soil structure changing caused by electrokinetic processes. 5th Symposium on Electrokinetic Remediation, May, Ferrara, Italy.

39 Bassi, R., Prasher, S.O., and Simpson, B.K. (2000). Extraction of metals from a contaminated sandy soil using citric acid. *Environmental Progress* 19 (4): 275–282.

40 Card, S.M. and Quideau, S.A. (2010). Microbial community structure in restored riparian soils of the Canadian prairie pothole region. *Soil Biology and Biochemistry* 42 (9): 1463–1471.

UNCORRECTED PROOFS

UNCORRECTED PROOFS

Trim Size: 170mm x 244mm Single Column Loose Ribeiro670117 c15.tex V1 - 12/11/2020 12:32pm Page 323

15

Management of Clay Properties Based on Electrokinetic Nanotechnology

D.S. Nesterov and V.A. Korolev

Department of Engineering and Ecological Geology, Faculty of Geology, M.V. Lomonosov Moscow State University, Moscow 119991, Russia

15.1 Introduction

The ultrafine-dispersed fraction of clay soils (<0.1 μm) represented predominantly by clay minerals can be considered natural nanoparticles [1, 2]. Accordingly, the term *nanotechnology* applies to the methods that affect the parameters of clay nanoparticles to control the macroscopic properties of clay soils.

Texture, physico-chemical properties, and physico-mechanical properties of clay soils depend on the parameters of the electrical double layer (EDL) formed around their particles. In turn, the EDL parameters (including electrokinetic potential ζ) of soil are controlled by the sign and value of the net particle electrical charge σ_P. Thus, studies of electrical charge components in clay soils and the regularities of their formation attract considerable attention from various researchers [3–14].

The electrical charge of clay nanoparticles forms for three reasons: (i) isomorphic substitutions within the crystalline lattice of clay minerals, (ii) protonation/deprotonation of nanoparticle surfaces, and (iii) adsorption of ions (different from H^+ и OH^-) from the pore solution [4–7, 12–18]. Accordingly, total particle surface-charge density (σ_P) is the sum of structural (σ_0), proton (σ_H), and ion-sorbed (σ_S) surface-charge densities, respectively [7, 10, 13, 19]:

AQ1

$$\sigma_P = \sigma_0 + \sigma_H + \sigma_S \tag{15.1}$$

The sum of structural and proton surface-charge densities is called the *intrinsic surface-charge density*, σ_{in} [7]:

$$\sigma_{in} = \sigma_0 + \sigma_H \tag{15.2}$$

In turn, the net ion-adsorbed (or Stern layer) surface-charge density (σ_S) is composed of inner-sphere (σ_{IS}) and outer-sphere (σ_{OS}) complex surface-charge densities [3, 5–7]:

$$\sigma_S = \sigma_{IS} + \sigma_{OS} \tag{15.3}$$

Electrokinetic Remediation for Environmental Security and Sustainability, First Edition.
Edited by Alexandra B. Ribeiro and M.N.V. Prasad.
© 2021 John Wiley & Sons Ltd. Published 2021 by John Wiley & Sons Ltd.

UNCORRECTED PROOFS

Trim Size: 170mm x 244mm Single Column Loose Ribeiro670117 c15.tex V1 - 12/11/2020 12:32pm Page 324

Overall, the net total particle charge density (σ_P) is equalized by the diffuse layer surface-charge density (σ_d) [3, 5–7]:

$$\sigma_P = -\sigma_d \tag{15.4}$$

Accordingly, the charge balance equation for a clay nanoparticle can be written in this form [3, 5–7]:

$$\sigma_0 + \sigma_H + \sigma_{IS} + \sigma_{OS} = -\sigma_d \tag{15.5}$$

Further, the Stern layer (σ_S) and diffuse layer (σ_d) surface-charge densities compose the adsorbed ion charge density (Δq) [3, 5–7]:

$$\Delta q = \sigma_{IS} + \sigma_{OS} + \sigma_d \tag{15.6}$$

The surface-charge components play different roles for various clay minerals.

The structural surface-charge density (σ_0) is defined generally by the crystallochemical features of a clay mineral. It is strongly influenced by the type and location of isomorphic substitutions. Kaolinite represents a *T-O* clay mineral: isomorphism occurs in the tetrahedral layer. Its structural charge (σ_0) is relatively small since in general, isomorphic substitutions are rare for this mineral. So, the total surface-charge density (σ_P) of kaolinite forms primarily due to σ_H and σ_S.

Illite and smectite mineral groups are examples of *T-O-T* clay minerals: their structural charge (σ_0) is relatively significant. Illites possess isomorphic substitutions in the tetrahedral layer, whereas smectites' are in the octahedral layer. Illite crystallites are firmly bound due to the inner-sphere complexation of K^+ ions in the crystallite interlayers. On the other hand, smectite crystallites can swell since they are bonded primarily by outer-sphere complexing ions such as Na^+, Ca^{2+}, and Mg^{2+} [7]. In general, σ_0 is negative for all clay minerals.

The structural surface-charge density (σ_0) does not depend on physico-chemical factors of the medium except for extreme pH conditions, when a partial dissolution of clay crystals is possible. In contrast, the surface-charge components σ_H and σ_S strongly depend on physico-chemical factors of the pore solution, such as pH and electrolyte concentration.

The proton surface-charge density (σ_H) generally originates from the hydroxylation of the particle surface. It results from isomorphic substitutions, which cause OH-group formation at the basal planes and disruption of valency bonds (at the particle edges). This surface-charge parameter varies with pH: in the most common case, it is negative in neutral and alkaline media and positive in acidic media.

In turn, the Stern layer surface-charge density (σ_S) is formed by nonstructural (exchangeable) ions (usually cations) due to their equivalent exchange for H^+ in surface OH-groups. In contrast to σ_H, this surface-charge component is positive in the neutral and alkaline pH range (due to cation adsorption) and negative in the acidic range (due to anion bonding). So, σ_S compensates for the intrinsic charge σ_{in} partially at any pH value. Also, the influence of exchangeable cations on the surface charge of clay particles is different in solutions of supporting, or indifferent (no influence on σ_{in}), and non-indifferent (σ_{in} alteration) electrolytes due to the ability of these ions to complete the crystalline lattice of a particle) electrolytes [12].

UNCORRECTED PROOFS

Trim Size: 170mm x 244mm Single Column Loose Ribeiro670117 c15.tex V1 - 12/11/2020 12:32pm Page 325

So, generally, clay nanoparticles can change the sign of their charge (σ_P) with variation in external conditions (pH, E_h, and electrolyte concentration).

Accordingly, several characteristic pH parameters, which describe the sign alteration for various charge components, were introduced by Sposito and coauthors [3–7]. These parameters reflect the pH values at which significant EDL transformations occur for soil particles. The *point of zero charge* ($pH_{p.z.c.}$) is the pH value where $\sigma_P = 0$. In turn, adsorbed ion charge density (Δq) is zero at the *point of zero net charge* ($pH_{p.z.n.c.}$). At this pH value, the structural charge density (σ_0) is equalized only by the proton charge density (σ_H). The *point of zero net proton charge* ($pH_{p.z.n.p.c.}$) represents pH value where $\sigma_H = 0$. The structural charge density (σ_0) is equalized by adsorbed ion charge density (Δq) only at this pH. Furthermore, the *point of zero salt effect* ($pH_{p.z.s.e.}$) is the pH value where no effect of the solution ionic strength (I) on proton surface charge density σ_H is observed:

$$(\partial\sigma_H/\partial I)_{T,P} = 0 \tag{15.7}$$

In the case of clay minerals, $pH_{p.z.s.e.}$ usually coincides with $pH_{p.z.n.c.}$.

At the specific pH values, the electrokinetic potential ζ of soil particles is equal to zero. This pH value is called the *isoelectric point* ($pH_{i.e.p.}$). Since ζ is a linear function of the total particle surface-charge density (σ_P), the isoelectric point where σ_P changes its sign coincides with the point of zero charge ($pH_{p.z.c.}$).

Many researchers have thoroughly studied the mechanisms of surface-charge formation and alteration with the variation of external conditions for clay nanoparticles [3, 4, 7–10, 17, 18, 20–22]. In turn, the authors of the present chapter studied the variation of surface-charge and EDL characteristics among various clay soils for many years [12, 14, 23]. However, many features of electrical charge parameters in soils and the possibility of their purposeful regulation have still not been studied in full.

For instance, the influence of clay mineral composition (kaolinite, illite, smectite) on the soil-particle points of zero charge has not been studied entirely. Some relations of surface-charge parameters and medium factors such as solution concentration, pH, oxidation-reduction potential (E_h), moisture content, and temperature also have not been clarified. In addition, the influence of the value and sign of the particle surface charge on physico-chemical and physico-mechanical properties of clay soils is still an open problem.

Varying external physico-chemical factors results in the transformation of the sign and value of the nanoparticle surface charge due to σ_H and σ_S changing. In turn, they alter the clay nanoparticle EDL parameters and subsequently transform soil properties. Consequently, transforming the clay surface-charge characteristics can purposefully regulate their properties. The same variation in physico-chemical medium parameters will induce different transformations in properties for various clay soils.

The promising technology for regulating surface-charge characteristics and, consequently, macroscopic parameters of clay soils in situ is electrokinetics. The authors have also studied the influence of applying an electric field on the properties of various soil types for a long time [24].

UNCORRECTED PROOFS

Trim Size: 170mm x 244mm Single Column Loose Ribeiro670117 c15.tex V1 - 12/11/2020 12:32pm Page 326

Thus, this study aimed to elucidate the influence of mineral composition, external medium factors, and electric field application on the value and sign of the nanoparticle surface charge and, accordingly, the macroscopic parameters of clay to regulate its various properties.

15.2 Objects of the Study

The research was carried out using predominantly monomineralic clay samples, representing the primary mineral types of clays. The clays studied included three kaolinite soils, two illite soils, three smectite (montmorillonite) soils, and one polymineral soil. Glukhovtsy and Polozhsk kaolins (Glukhovtsy and Polozhky hamlets, Ukraine, respectively) were the kaolinitic soils. Illite clays used in the study were Cambrian (Leningrad Oblast, Russia) and Biyasalin (Prokhladnoe village, Crimea). Montmorillonite clays under study were Kil (Prokhladnoe village, Crimea) and Oglanly (Oglanly village, Turkmenistan) bentonites and monomineralic Askan-gel (or Makharadzian montmorillonite, from Askania village, Georgia). Moscow Quaternary mantle till loam was used as an example of a polymineralic clay.

Oglanly bentonite and Askan-gel were represented by their Na-forms, and Polozhsk kaolin and illite clays by their Ca-forms. The Cd-form of Kil clay was studied in this research. In the case of Glukhovtsy kaolin, two mono-ionic forms were used: Na and Ca. However, their physico-chemical properties did not differ significantly due to their low ion-exchange capacity.

The specific particle density (specific gravity) ρ_s of soils was determined using the kerosene pycnometer method in a way similar to that described in ASTM water and gas pycnometer methods [25, 26]. The liquid limit (LL) and plasticity index (PI) were calculated according to the ASTM method [27]. The cation-exchange capacity (CEC) was estimated by calculating the exchangeable cations sum and methylene blue adsorption methods [16, 28, 29]. The Brunauer-Emmett-Teller equation, Ovcharenko method, and SEM calculation were used to determine the specific surface area (SSA) [16, 30–32]. The soils were also classified by their granulometric composition (texture) following the GOST and ISO classifications [33, 34]. In the case of the kaolins, the Hinckley index (X-ray coefficient of kaolinite crystallinity degree) was estimated as well (Table 15.1). Characteristics of the clays studied are shown in Table 15.1.

The mineral composition of the clays studied, obtained by the X-ray diffraction method [32], is given in Table 15.2. Polozhsk kaolin and all bentonites were monomineralic clays. Glukhovtsy kaolin and Biyasalin illite clay contained > 70% of the primary clay mineral and a significant share of quartz or other minerals. Moscow loam and Cambrian illite clay were polymineral soils with the content of the primary mineral within the range of 50 to 60%.

In general, the physico-chemical activity of the clays and their corresponding parameters (LL, PI, CEC, and SSA) increased from mantle till loam to Askan-gel.

UNCORRECTED PROOFS

UNCORRECTED PROOFS

Trim Size: 170mm x 244mm Single Column Loose

Table 15.1 Characterization of the soils studied.

No	Clay	GI	Soil classification GOST/ISO	ρ_s, gcm^{-3}	LL, % dry weight	PI, %	CEC, meq (100 g dry soil)$^{-1}$	SSA, m^2g^{-1}	HI*, units
1	Moscow mantle till loam	prQ_{III}	Sandy loam/mSi	2.77	23	5	1.5	9.7 (BET)	–
2	Glukhovtsy kaolin (Na-form)	eN_1	Light silty clay/fsiCl	2.64	50	19	4	18 (BET)*	0.90
3	Glukhovtsy kaolin (Ca-form)						3.1	17.6 (BET)[1]	
4	Polozhsk kaolin	eN_1	Light silty clay/fsiCl	2.63	55	17	4*	23.5 (BET)*	0.58
5	Cambrian illite clay	$m\acute{E}_1$	Light silty clay/fsiCl	2.84	46	21	10.7	51.6 (BET)	–
6	Biyasalin illite clay	mK_1a	Heavy silty loam/fsiCl	2.75	48	15	13*	74.4 (BET)*	–
7	Kil bentonite	mK_2sn	Heavy clay/Cl	2.55	77**	32**	94*	790 (Ovcharenko)*	–
8	Oglanly bentonite	emP_2	Heavy clay/Cl	2.64	114	70	84*	620 (SEM)	–
9	Askan-gel	hdP_2	Heavy clay/Cl	2.50	102	45	68 (MB)*	910 (Ovcharenko)	–

GI, geological index of a clay stratum; ρ_s, specific particle density of a soil; PI, plasticity index; CEC, cation-exchange capacity; SSA, specific surface area; HI, Hinckley index; MB, methylene blue adsorption method; BET, Brunauer-Emmett-Teller method; Ovcharenko, Ovcharenko method; SEM, calculation by the SEM-image of dispersed suspension.
Sources: Data from Tarasevich and Ovcharenko* [16]; Korolev** [35].

Ribeiro670117 c15.tex V1 - 12/11/2020 12:32pm Page 327

Trim Size: 170mm x 244mm Single Column Loose Ribeiro670117 c15.tex V1 - 12/11/2020 12:32pm Page 328

Table 15.2 Mineral composition of the clays studied, % weight.

Number	Soil	K	I	S	Ch	Q	Pl	Kfs	Cl	C	D	G
1	Moscow mantle till loam	0	6	15	1	59	6	11	2	0	0	0
2–3	Glukhovtsy kaolin	75	5	0	0	18	0	0	0	0	0	2
4	Polozhsk kaolin	98	0	0	0	2	0	0	0	0	0	0
5	Cambrian illite clay	8	53	4	3	24	1	7	0	0	0	0
6	Biyasalin illite clay	10	70	5	10	4	0	0	0	0	1	0
7*	Kil bentonite	0	0	95	2	0	0	0	0	3	0	0
8	Oglanly bentonite	0	3	93	0	0	3	0	0	1	0	0
9	Askan-gel	0	0	100	0	0	0	0	0	0	0	0

K, kaolinite; I, minerals of illite group; S, smectite minerals; Ch, chlorite; Q, quartz; Pl, plagioclases; Kfs, potassium feldspar; Cl, clinoptilolite; C, calcite; D, dolomite; G, gypsum.
Source: Data from Korolev [35].

15.3 Methods of the Study

The present research consisted of two study cases: static and dynamic. The *static* case included estimating the effect of the physico-chemical medium parameters on the clay surface charge and EDL parameters. The *dynamic* case represented a study of the influence of applying a DC field and the processes induced by it (electroosmosis, electromigration, and electrolysis) on a soil mass and its various parameters. In this case, the parameters under study were soil composition (including EDL characteristics), texture and structure, consistency, and properties.

In the static case, the parameters used to characterize the alteration of the surface charge and EDL of clay particles were (i) electrokinetic potential ζ, (ii) point of zero charge $pH_{p.z.c.}$ ($\sigma_P = 0$), and (iii) point of zero net proton charge $pH_{p.z.n.p.c.}$ ($\sigma_H = 0$).

This part of the study was carried out using clayey suspensions prepared from the clay samples. Two series of suspensions were analyzed: (i) for the ζ measurement in the wide range of pH-E_h conditions using micro-electrophoresis and (ii) to determine $pH_{p.z.n.p.c.}$ of the clays at various ionic strength values using acid-base titration.

The first series included three groups of suspensions. In the case of clay numbers 2, 4, and 6–8, rows of three suspensions were prepared: in distilled water, 0.001 M HCl, and NaOH solutions. So, pH values of ~ 7, 3, and 11, respectively, were obtained for these suspensions. For clays number 3, 5, and 9, around 11 suspensions with a pH range of ~1–11 were prepared for each clay. For this purpose, clay specimens were suspended in distilled water, 0.009–0.00009 M $Ca(OH)_2$, and 0.001–0.1 M HCl. The third group included five suspensions of the loam (sample number 1) prepared at various pH values with a constant ionic strength of the solution. Solutions of various $CaCl_2$/HCl and $CaCl_2/Ca(OH)_2$ volume ratios were used to achieve different pH values. The solid/liquid ratio of the suspension was 1 : 20 for the first group and 1 : 40 for the second and third groups. Ionic strength was kept constant only in the case of the third group of suspensions.

UNCORRECTED PROOFS

Trim Size: 170mm x 244mm Single Column Loose Ribeiro670117 c15.tex V1 - 12/11/2020 12:32pm Page 329

The second series of suspensions included three groups as well. Clay samples number 2, 4, and 6–8 were suspended in 0.001, 0.01, and 0.1 M $NaNO_3$ solutions. The suspensions of clays number 2, 4, and 8 were prepared using $CaCl_2$ solutions of various ionic strength (I = 0.003, 0.03, and 0.3 M). Several $NaNO_3$ solutions (with I = 0.01, 0.05, and 0.1 M) were used for the sample 1 suspension. The solid/liquid ratio was 1 : 10 for the first and third groups of suspensions and 1 : 20 for the second group.

In the first suspension series, pH, E_h, total dissolved solids (TDS), and specific electrical conductivity ($æ_d$) were determined along with the ζ-potential of clay nanoparticles. pH-061 and ORP-169B instruments were used to measure pH and E_h values. TDS and $æ_d$ were estimated using a salt gauge HM Digital COM-80. In the case of suspensions prepared using concentrated HCl solutions, electric conductivity was measured with an MMZ4-04 conductometer [32]. TDS were expressed via equivalent KCl concentration. In addition, the same parameters were obtained for blank solutions of the same composition and concentration.

The electrokinetic potential ζ of the soil particles was measured by the micro-electrophoresis method using a Horiba SZ-100 nanoparticle laser analyzer [32]. For each suspension, four or five measurements were carried out. After this, the average ζ value was calculated. Then, $pH_{i.e.p.}$ ($\zeta = 0$) values were determined in $\zeta = f(pH)$ graph. The $pH_{p.z.c.}$ of clay soil was estimated as the $pH_{i.e.p.}$ value where the surface-charge sign changed.

Acid-base titration was applied to find the $pH_{p.z.n.p.c.}$ values of the studied soils [20]. In the case of clays number 2, 4, and 6–8, solutions of 0.01 M HCl and NaOH were used as titrants. Titration of clays number 3, 5, and 9 was carried out using 0.01 M HCl and 0.009 M $Ca(OH)_2$. The mantle till loam (sample 1) was titrated using 0.055 M HCl and 0.035 M KOH. Also, blank solutions of the buffer electrolytes with the same ionic strength values were titrated by the corresponding titrants.

The proton surface-charge density(σ_H, C m^{-2}) was calculated using the simplified formula (similar to Eq. (15.3) in [36]):

$$\sigma_H = [(V_s - V_b) * c * F]/[m * z * SSA] \tag{15.8}$$

where V_s and V_b are titrant volumes used to titrate a soil suspension and blank solution, respectively, in L; c is the titrant concentration in M; F is the Faraday number in C mol^{-1}; m is the mass of a soil specimen in g; z is the equivalency number of an ion in units; and SSA is in m^2 g^{-1}.

The point of zero net proton charge $pH_{p.z.n.p.c.}$ was determined in $\sigma_H = f(pH)$ graphs as the pH value where $\sigma_H = 0$.

The dynamic case study included electrokinetic treatment of the clay soil in a one-compartment cell by the isolated drainage mass scheme (with no additional water influx), with effluent able to escape in the cathodic zone. These test conditions were applied to achieve the most significant transformation of soil parameters under the DC electric field. The electric current was kept constant (10 mA) during treatment by the gradual increase of voltage [14]. The corresponding current density achieved was 34 A m^{-2}. The tests were ceased when the electric current declined drastically or voltage exceeded 200 V.

UNCORRECTED PROOFS

Trim Size: 170mm x 244mm Single Column Loose Ribeiro670117 c15.tex V1 - 12/11/2020 12:32pm Page 330

The soils used in this part of the research were Moscow loam, Glukhovtsy kaolin (Ca-form), Biyasalin illite clay, and Askan-gel. For these experiments, clayey pastes were prepared at the moisture content of LL since clay particle EDLs are the most developed and no electrophoresis occurs in these conditions. In this case, 0.01 M $CaCl_2$ was used as the pore solution.

After the treatment, a soil sample was divided into five parts. Moisture content (W), pH, moist density (ρ_m), and electrokinetic potential (ζ) were determined in each soil fragment [37]. Dry density (ρ_d), total porosity (n), and liquidity index (LI) were calculated for all the segments as well [37–39]. Also, samples were taken in the anodic and cathodic zones for SEM analysis. In the case of the loam, the micro-aggregate size (d_{50}) was measured using the Horiba SZ-100. The same parameters were determined for the initial clayey pastes.

All tests were conducted at a temperature of 21–23 °C and standard atmospheric pressure.

15.4 Results and Discussion

The following section describes altering the clay parameters under the influence of the DC electric field (dynamic study case). The experimental data on altering soil parameters are presented in the following logical order: (i) parameters of the pore solution, (ii) surface-charge characteristics, (iii) EDL parameters, (iv) soil texture and structure, (v) macroscopic soil properties." The results of the static case study are discussed in Sections 15.4.3 and 15.4.4.

15.4.1 Regulation of Soil pH

Pore-water electrolysis reactions occur during the application of a DC electric field to water-saturated clay soil. Water oxidation takes place at the anode, followed by the emission of H^+ ions into the solution and oxygen as a gas [40, 41]:

$$2H_2O - 4e^- \rightarrow O_2 \uparrow + 4H^+ \tag{15.9}$$

In turn, at the cathode, water reduces to gaseous H_2 with the simultaneous release of OH^- into the pore solution [40, 41]:

$$4H_2O + 4e^- \rightarrow 2H_2 \uparrow + 4OH^- \tag{15.10}$$

As a result, an acidic and oxidative medium usually forms near the anode, whereas an alkaline and reductive medium is generated near the cathode. Consequently, pH and E_h gradients are formed along the soil sample length between the electrodes [41]. The maximum pH gradient occurs in the soil system with no external water influx: $pH \leq 1$ near the anode and $pH \geq 13$ near the cathode.

The result of altering the pore-solution pH for the clays studied under the DC electric field is shown in Figure 15.1. The initial clayey paste reaction was neutral for the loam, kaolin, and illite clay, whereas it was alkaline for Askan-gel. An alkaline medium formed in the cathodic zone, and an acidic medium was generated near the

UNCORRECTED PROOFS

Trim Size: 170mm x 244mm Single Column Loose Ribeiro670117 c15.tex V1 - 12/11/2020 12:32pm Page 331

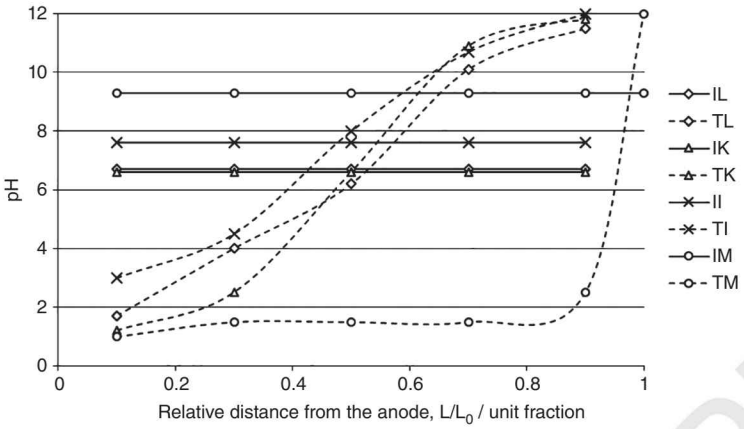

Figure 15.1 Distribution of the clay soil pore-solution pH along the soil sample length: initial and after electroosmosis. IL, initial loam; TL, treated loam; IK, initial kaolin, TK, treated kaolin; II, initial illite clay, TI, treated illite clay; IM, initial montmorillonite, TM, treated montmorillonite.

anode due to the electrolysis reactions (see Figure 15.1). Thus, a pH gradient formed along the sample length during electroosmosis [41]:

$$grad(\mathrm{pH}) = \partial(\mathrm{pH})/\partial L \neq 0 \tag{15.11}$$

where L is the distance from the anode.

The pH gradient formed was almost the same for the loam, kaolin, and illite clay [42]. The pH values of Biyasalin illite clay were slightly higher than those of the loam and kaolin at the same points between the electrodes. This phenomenon is likely to be caused by partial dissolution of dolomite in the acidic medium near the anode. In the case of Askan-gel, rapid acidification occurred in the entire space between the electrodes, except for the very cathodic zone. It probably resulted from the high electromigration velocity of H^+ ions in the smectite clay supported by the electroosmotic flow in the same direction [40].

Altering the pore-solution pH always induces various physico-chemical processes in clay soil. Desorption of cations (such as alkaline, alkaline-earth, and heavy metals) and anion adsorption (like $Cr_2O_7^{2-}$) onto the soil solids takes place in the acidic medium [41]. At the same time, these reactions occur in the opposite direction in the alkaline medium. In addition, transforming the pore-solution pH induces dissolution and precipitation reactions in the clay soil. Examples of these reactions are carbonate dissolution at low pH and hydroxide ($Al(OH)_3$, $Pb(OH)_2$, etc.) precipitation in the alkaline medium [40, 41].

Thus, applying a DC electric field to soil allows the regulation of its pore-solution pH in a wide range. In turn, it encourages the transformation of the soil properties, which directly depend on its pH.

UNCORRECTED PROOFS

Trim Size: 170mm x 244mm Single Column Loose Ribeiro670117 c15.tex V1 - 12/11/2020 12:32pm Page 332

15.4.2 Regulation of Oxidation-Reduction Potential

The oxidation-reduction potential (E_h) of the pore solution affects the EDL parameters of clay soils along with pH. The E_h gradient forms in soil between the electrodes along with the pH gradient under a DC electric field:

$$grad(E_h) = \partial(E_h)/\partial L \neq 0 \tag{15.12}$$

The E_h values in soils studied ranged from +80 to +120 mV.

The oxidation-reduction potential transformation under the DC electric field induces alterations of the pore-solution composition. For instance, oxidation of heavy metal cations (such as $Cr^{3+} \rightarrow Cr^{6+}$) and some anions (including organic complexes) can occur in the anodic zone. In turn, reduction reactions take place near the cathode [41].

Thus, regulating the pore-solution E_h in the near-electrode zones induces oxidation-reduction reactions. In turn, it promotes adsorption or desorption of metal ions, which is essential for environmental applications.

15.4.3 Regulation of Soil Particle Surface-Charge Density

The surface-charge density and EDL parameters influence various macroscopic properties of soil (such as CEC, density, and porosity). So, altering the surface charge of soil nanoparticles and their EDL characteristics allows the purposeful regulation of clay properties. This relation is a basis for electrokinetic nanotechnology to regulate the clay parameters, which is being actively developed worldwide.

Regulating the sign and value of the nanoparticle charge and its EDL parameters through electrokinetics transforms soil texture, structure, and physical properties in the desired direction. In particular, one can increase or decrease the soil's density and porosity, bearing capability, sorption characteristics, and permeability. In the same way, oil recovery can be increased, and migration of toxicants (heavy metals, radionuclides, and organic pollutants) can be promoted or mitigated through clays.

The surface-charge and EDL parameters primarily depend on the pore solution pH and its concentration. So, the mechanism of the influence on surface-charge density via electrokinetics is the following. An acidic medium ($pH < 2$) is generated near the anode, while an alkaline medium ($pH = 12$) forms near the cathode in clay soil under a DC electric field. That allows soil pH regulation within a broad range, and, thus, alteration of the surface-charge sign and value.

The ratio of different surface-charge components (σ_0, σ_H, and σ_S) varies among clay minerals, as mentioned before. In addition, it is essential to consider the inhomogeneity of the electric charge location in different parts of a clay-mineral nanoparticle. In turn, it creates the heterogeneity of the compensating ions' electric field and EDL around a soil particle. The inhomogeneity of the electric field around a particle plays an especially significant role in the case of pH variation.

Figure 15.2 demonstrates the decline of the surface electric potential (ϕ) within the particle EDL with the distance from the solid surface (x) [43]. Figure 15.2a–c show the influence of the pore-solution pH on this function, whereas Figure 15.2d

UNCORRECTED PROOFS

Trim Size: 170mm x 244mm Single Column Loose Ribeiro670117 c15.tex V1 - 12/11/2020 12:32pm Page 333

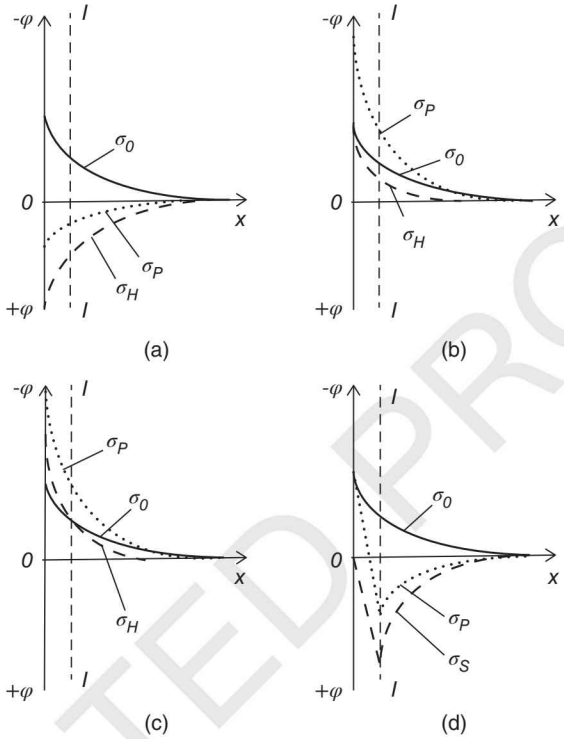

Figure 15.2 Scheme of the potential (ϕ) drop within the electrical double layer (EDL) during the clay-particle charge alterations, caused by the pH transformations of the supporting electrolyte pore solution at a distance x [43]: (a) acidic medium; (b) neutral medium; (c) alkaline medium; (d) resulted from ion sorption. Surface-charge density components: σ_0 – structural surface-charge density; σ_H – net proton (or hydroxylation) surface-charge density; σ_S – Stern-layer surface-charge density (created by the ions immobilized in surface complexes); σ_P – total particle surface-charge density. *I-I*– Stern-layer outer boundary.

reveals the impact of indifferent electrolyte ions. Overall, these diagrams exhibit the relationships $\phi = f(x)$ of the electric-potential decline near the particle surface due to the contribution of different surface-charge components ($\sigma_0, \sigma_H, \sigma_S$) and net particle charge (σ_P) in total with the pH variation. These schemes explain the impact of the pore-solution pH on the sign and value of the particle surface-charge characteristics.

As one can see in the diagrams (Figure 15.2), the structural surface-charge density σ_0 of clay nanoparticles generally does not depend on pH. So, the function $\sigma_0 = f(x)$ remains the same at any pH value (in acidic, neutral, and alkaline media). On the other hand, the proton surface-charge density σ_H is strongly governed by pH, so its value determines the behavior of the function $\sigma_P = f(x)$ in total.

Clay mineral nanoparticles are charged negatively ($\sigma_P < 0$) in a neutral medium (see Figure 15.2b). The pH increase causes the intensification of surface dissociation – more accurately, deprotonation (or hydroxylation). This process is accompanied by the release of H^+ ions, which cause the increase in the negative value of σ_P in the alkaline medium due to the increase in the magnitude of its component σ_H (see Figure 15.2c). The dissociation mechanism changes to the opposite (protonation) as the pH drops when the acidic medium forms. In this case, clay particles release OH^- ions into the solution (or attach protons). So, the sign of the total clay-particle surface-charge density can change to positive in the acidic medium ($\sigma_P > 0$) (see Figure 15.2a).

UNCORRECTED PROOFS

Trim Size: 170mm x 244mm Single Column Loose Ribeiro670117 c15.tex V1 - 12/11/2020 12:32pm Page 334

Some contributions to altering the nanoparticle charge may be made by adsorption of ions (see Figure 15.2d). This phenomenon causes the formation of the Stern-layer surface-charge density (σ_S), which has the opposite sign from the intrinsic charge (σ_{in}).

So, σ_P sign change takes place primarily due to the contribution of its component σ_H, which can be either negative (Figure 15.2b,c) or positive (Figure 15.2a).The σ_H sign changes with the pH variation due to deprotonation (which increases the total negative σ_P value) or protonation (which decreases the σ_H until its sigh changes to positive).

Thus, the surface-charge density of the clay nanoparticles can be regulated by altering the pore-solution pH through its impact on the sign and value of σ_H. In the present research, acid-base titration was applied to obtain the functions $\sigma_H = f(\mathrm{pH})$ for the clays studied and their $\mathrm{pH}_{\mathrm{p.z.n.p.c.}}$ values. The titration results are given in Figures 15.3 and 15.4 and Table 15.3 [43].

The diagrams show that the titration curves of Glukhovtsy kaolin (both Na- and Ca-forms) and Biyasalin illite clay at various ionic strength values of the solution intersected at one point (see Figure 15.3a,b,e). The pH value at the intersection of the curves represents the *point of zero salt effect* $\mathrm{pH}_{\mathrm{p.z.s.e.}}$ of the clay. At the same time, the increase in the solution ionic strength induced the increase in the σ_H magnitude in the entire pH range for these clays.

In contrast, the titration curves of Polozhsk kaolin, Cambrian illite clay, Oglanly bentonite, and Askan-gel did not intersect at one point. They pass conformally in the entire pH range; there was no intersection at any point in the case of montmorillonite clays (see Figure 15.3c,d,g,h). The surface-charge density became more positive at the same pH value for this type of curve as the ionic strength of the solution was increased. In turn, the titration curves of Kil bentonite (Cd-form) expressed intermediate behavior: each pair of curves intersected, but no intercrossing point for all three curves was observed (see Figure 15.3f). The specific influence of ionic strength on the Kil particle σ_H can be explained by the complicated effect of Cd^{2+} inner-sphere complexation with montmorillonite nanoparticles.

The relationship $\sigma_H = f(\mathrm{pH})$ for the polymineral mantle till loam (see Figure 15.4) was similar to those of inactive clays: the titration curves coincided at one point. The diagram demonstrates that the loam particles were negatively charged at $\mathrm{pH} > \mathrm{pH}_{\mathrm{p.z.n.p.c.}}$ (in an alkaline medium), while they possessed a positive charge at $\mathrm{pH} < \mathrm{pH}_{\mathrm{p.z.n.p.c.}}$, the same as monomineralic clays.

The clays whose titration curves intersected at one point (see Figures 15.3a,b,e and 15.4) had small structural surface-charge density values (σ_0) [7]. Only local electrostatic fields are formed around the basis planes and edges of their particles. In this case, the increase in the pore-solution ionic strength promoted the ion-exchange reactions: the substitution of H^+ or OH^- ions within the surface OH-groups by the corresponding ions of the buffer electrolyte. These ions did not participate in the neutralization reactions during acid-base titration within the significant pH range. So, this could be the probable reason for the σ_H magnitude to increase with the increase in the pore-solution ionic strength within the range studied.

UNCORRECTED PROOFS

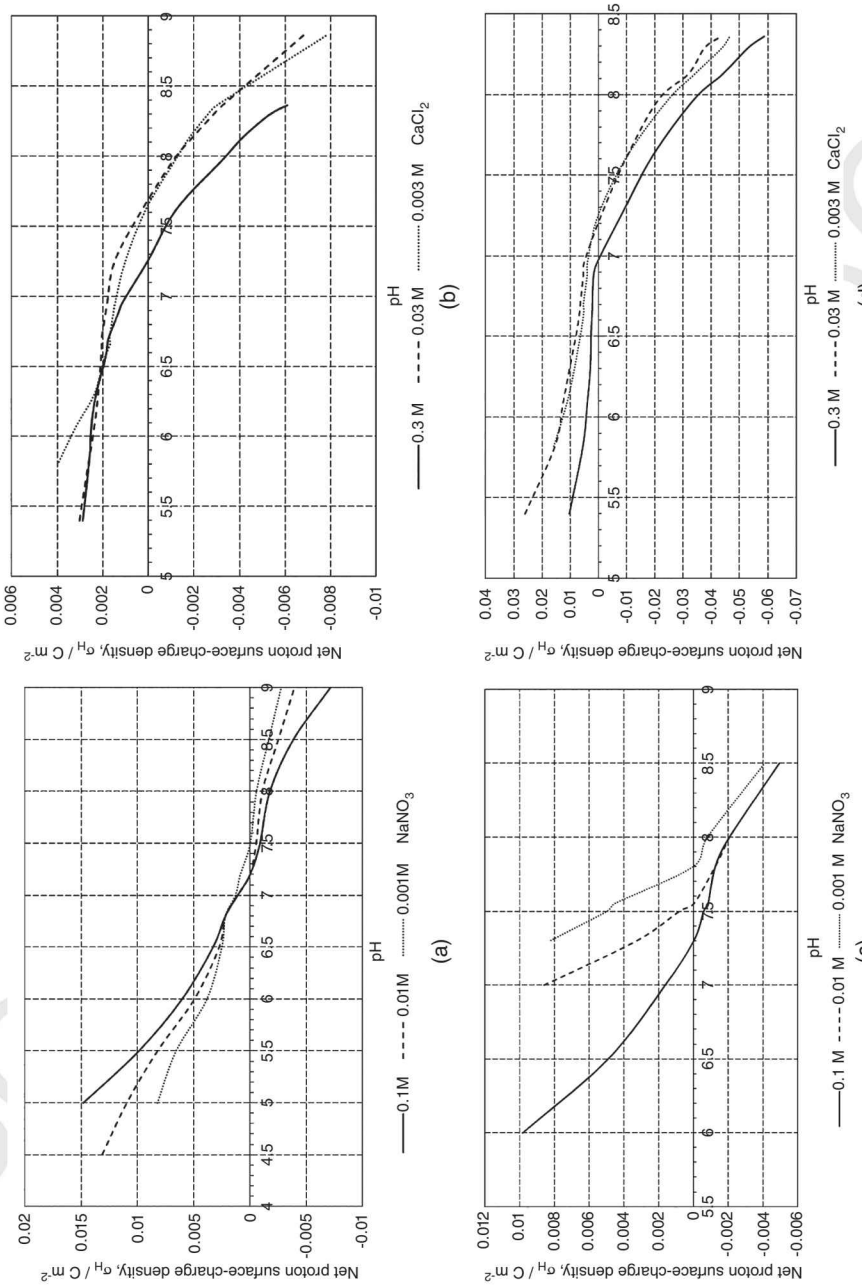

Figure 15.3 Relation between net proton surface-charge density (σ_H) of soil particles and soil pore-solution pH at various ionic strength values of bulk electrolyte solution [42]: (a) Glukhovtsy kaolin, Na-form; (b) Glukhovtsy kaolin, Ca-form; (c) Polozhsk kaolin (Ca-form); (d) Cambrian illite clay (Ca-form); (e) Biyasalin illite clay (Ca-form); (f) Kil bentonite (Cd-form); (g) Oglanly bentonite (Na-form); (h) Makharadzian montmorillonite or Askan-gel (Na-form).

UNCORRECTED PROOFS

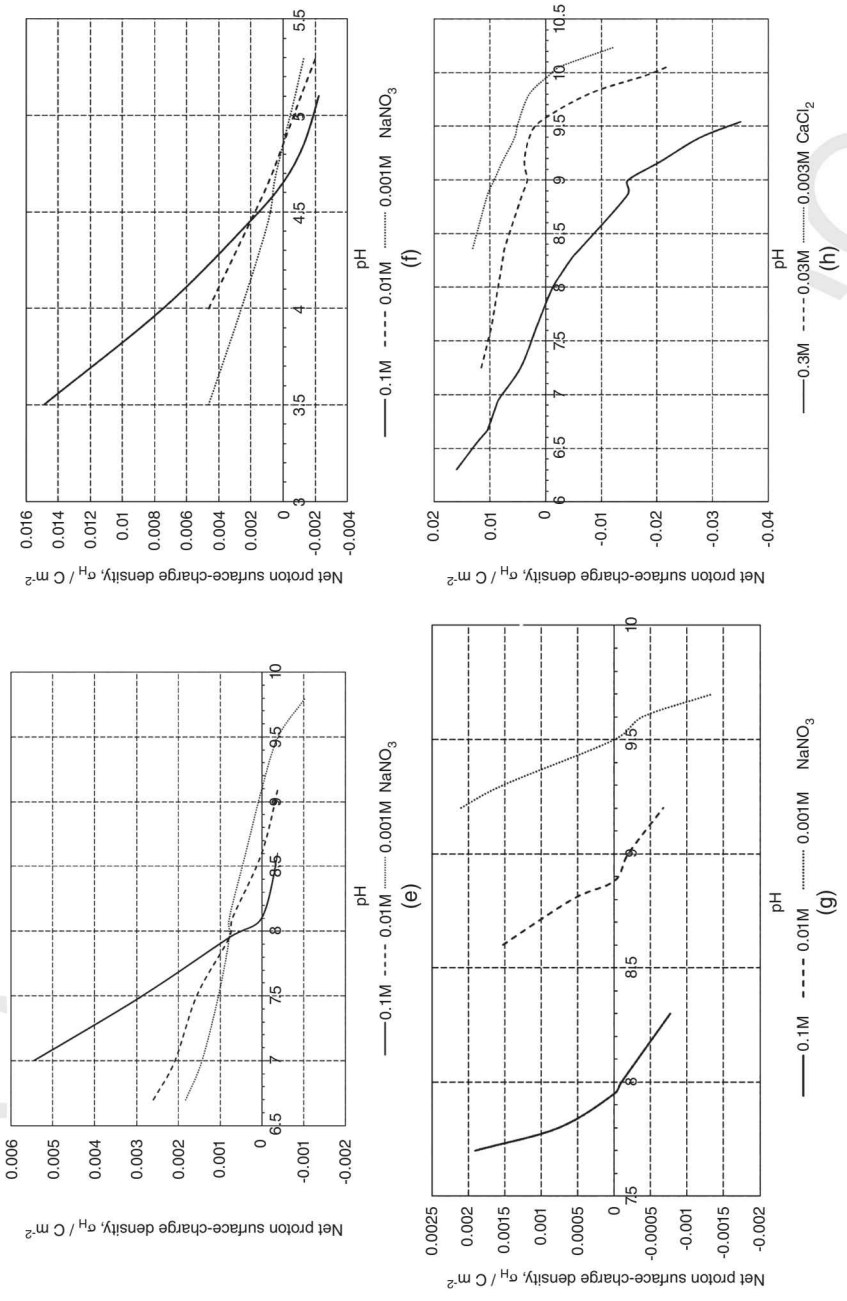

Figure 15.3 (*Continued*)

UNCORRECTED PROOFS

Trim Size: 170mm x 244mm Single Column Loose Ribeiro670117 c15.tex V1 - 12/11/2020 12:32pm Page 337

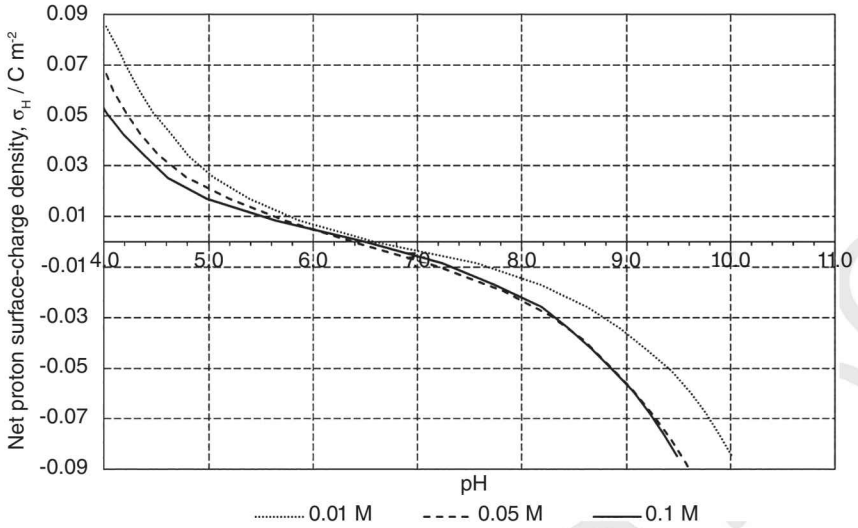

Figure 15.4 Relation between net proton surface-charge density (σ_H) of Quaternary mantle till loam at various ionic strength values of $NaNO_3$ bulk solutions. Source: The titration data for this plot was provided by I.V. Romanova.

In contrast, the clay nanoparticles whose titration curves had no intersection point (see Figure 15.3c,d,g,h) had significant structural charge density ($\sigma_0 < <0$) [7, 22]. Such particles formed a relatively strong single electrostatic field around all their planes. Accordingly, in this case, the increase in the pore-solution ionic strength caused the particles to aggregate so that part of the particle edges became sealed inside the aggregates. Hence, only the basis planes remained subjected to the influence of the pore solution. Therefore, the increase in the ionic strength of the pore solution caused the σ_H values to become more negative at the same pH for these clays.

In general, $pH_{p.z.n.p.c.}$ values decreased as the ionic strength of the clay pore solution increased. At the same time, they increased with the increase in physico-chemical activity of clays, within the row loam – kaolin – illite clay – bentonite and one mineral type. The same trend was observed for the $pH_{p.z.s.e.}$ values in the range Moscow loam – Ca-Glukhovtsy kaolin – Na-Glukhovtsy kaolin – Biyasalin illite clay.

The $pH_{p.z.n.p.c.}$ values determined in this study correspond to the data published for clays of a similar mineral composition. For example, the $pH_{p.z.n.p.c.}$ values of Glukhovtsy and Polozhsk kaolins at 0.1 M $NaNO_3$ are close to those obtained by Wieland and Stumm [44] for well-crystallized Cornish China kaolin in 0.1 M NaCl solution ($pH_{p.z.n.p.c.} \approx 7.5$). Moreover, the $pH_{p.z.n.p.c.}$ of Glukhovtsy kaolin in $NaNO_3$ solutions at I = 0.01–0.1 and I = 0.001 M coincide with those of purified Na-Tabarka ($pH_{p.z.n.p.c.} \approx 6.9–7.1$) and pure Kasserine ($pH_{p.z.n.p.c.} \approx 7.5$) kaolinites, respectively, in 0.001–0.1 M NaCl solutions, as reported by Kriaa et al. [45].

The $pH_{p.z.n.p.c.}$ values obtained for Biyasalin illite clay correspond to those of Kriaa et al. [21] for Tunisian chlorite-illite clay at the ionic strength of buffer NaCl solutions

UNCORRECTED PROOFS

Trim Size: 170mm x 244mm Single Column Loose Ribeiro670117 c15.tex V1 - 12/11/2020 12:32pm Page 338

Table 15.3 Point of zero net proton charge ($pH_{p.z.n.p.c.}$) values of the clays studied.

	$pH_{p.z.n.p.c.}$ at various ionic strength I of solution			$pH_{p.z.s.e.}$
	KNO_3			
Clay soil	**0.1 M**	**0.05 M**	**0.01 M**	
Moscow mantle till loam[a)]	6.6	6.4	6.52	6.0
		$NaNO_3$		
	0.1 M	0.01 M	0.001 M	
Glukhovtsy kaolin (Na-form)	7.2	7.2	7.5	6.8
Polozhsk kaolin (Ca-form)	7.3	7.55	7.8	n/o
Biyasalin illite clay (Ca-form)	8.1	8.6	9.1	7.95
Kil bentonite (Cd-form)	4.65	4.85	4.85	a (4.45–4.85)
Oglanly bentonite (Na-form)	7.95	8.9	9.5	n/o
		$CaCl_2$		
	0.3 M	0.03 M	0.003 M	
Glukhovtsy kaolin (Ca-form)	7.3	7.7	7.7	6.4
Cambrian illite clay (Ca-form)	7.0	7.2	7.3	n/o
Askan-gel (Na-form)	7.85	9.6	9.95	n/o

n/o, not observed in the entire pH range; a, ambiguous (no single exact value).
a) Data provided by I.V. Romanova.
Source: Based on Korolev and Nesterov [23, 43].

of 0.001–0.1 M ($pH_{p.z.n.p.c.} \approx 8.2–8.7$ for the It(Ha) sample). In addition, the $pH_{p.z.n.p.c.}$ results for Biyasalin illite clay and Oglanly bentonite in 0.001 M $NaNO_3$ are close to the data of Hao et al. [36] for illite IMt-2 ($pH_{p.z.n.p.c.} \approx 9.23$) and montmorillonite SWy-2 ($pH_{p.z.n.p.c.} \approx 9.77$), respectively.

Also, the data obtained for Oglanly bentonite in 0.1 M $NaNO_3$ coincide with that provided by Avena et al. for Argentinian montmorillonite from the Cerra Bandera site ($pH_{p.z.n.p.c.} \approx 7.9$) [46] and Kriaa et al. for Tunisian smectite ($pH_{p.z.n.p.c.} \approx 8.0$) [47] (both in 0.1 M NaCl). In addition, the results of $pH_{p.z.n.p.c.}$ determination for Oglanly bentonite in $NaNO_3$ solutions (I = 0.001–0.1 M) resemble those of Avena and De Pauli [20] for Na-Argentinian montmorillonite in 0.002–0.088 M NaCl ($pH_{p.z.n.p.c.} \approx 7.6–8.6$).

UNCORRECTED PROOFS

Trim Size: 170mm x 244mm Single Column Loose Ribeiro670117 c15.tex V1 - 12/11/2020 12:32pm Page 339

Thus, a zone with the proton surface-charge density of clay nanoparticles close to zero ($\sigma_H = 0$) should form in the middle of the inter-electrode space under a DC electric field. Therein, σ_H has the maximum negative values ($\sigma_H < 0$) at the cathode, while it possesses the maximum positive values ($\sigma_H > 0$) near the anode. Consequently, gradients of proton and total surface-charge densities form between the electrodes:

$$grad(\sigma_H) = \partial(\sigma_H)/\partial L \neq 0 \tag{15.13}$$

$$grad(\sigma_P) = \partial(\sigma_P)/\partial L \neq 0 \tag{15.14}$$

15.4.4 EDL Parameter Regulation

Since the electrokinetic potential ζ is a linear function of σ_P and depends strongly on σ_H, regulating them utilizing pH alteration or electrokinetics allows affecting ζ as well. The particle ζ values for the clays studied are shown in Table 15.4 and Figures 15.5 (static case), 15.6 (dynamic case), and 15.7 (static case).

According to the data in Table 15.4, the clays had negative ζ values in a neutral medium, up to −40 mV for kaolinites and illites and −67 mV for montmorillonites.

Electrokinetic potential (ζ) values depend on the *concentration* of the supporting electrolyte at a constant pH. Figure 15.5 demonstrates the relation of ζ values for various clays (including their monoionic forms) and the concentration of the contacting pore electrolyte C_0. In this case, the ζ values of the clays studied were calculated with a correction for surface conductivity. The maximum ζ-potential values for these soils were in the range from −20 to −70 mV.

Figure 15.5 demonstrates that the increase in electrolyte concentration generally caused the ζ potential to decrease for all the clays studied. This effect can be explained by the compression of the EDL diffuse part. The corresponding results

Table 15.4 Electrokinetic potential (ζ) value variation with pH for the clays studied.

Clay soil	Electrokinetic potential ζ (mV) at pH		
	3.0	7.0	11.0
Moscow mantle till loam	+24	No data	−33.8
Glukhovtsy kaolin (Na-form)	−30.8	−14	−55
Glukhovtsy kaolin(Ca-form)	−15	−40	−60
Polozhsk kaolin (Ca-form)	+14.9	−11.3	−103.4
Cambrian illite clay (Ca-form)	−10	−40	No data
Biyasalin illite clay (Ca-form)	−54.1	−13.2	−57
Kil bentonite (Cd-form)	−41.7	−47.4	−108.3
Oglanly bentonite (Na-form)	−12.5	−67	−115.7
Askan-gel (Na-form)	+25	−20	−75

Source: Based on Korolev and Nesterov [23, 43].

UNCORRECTED PROOFS

Trim Size: 170mm x 244mm Single Column Loose Ribeiro670117 c15.tex V1 - 12/11/2020 12:32pm Page 340

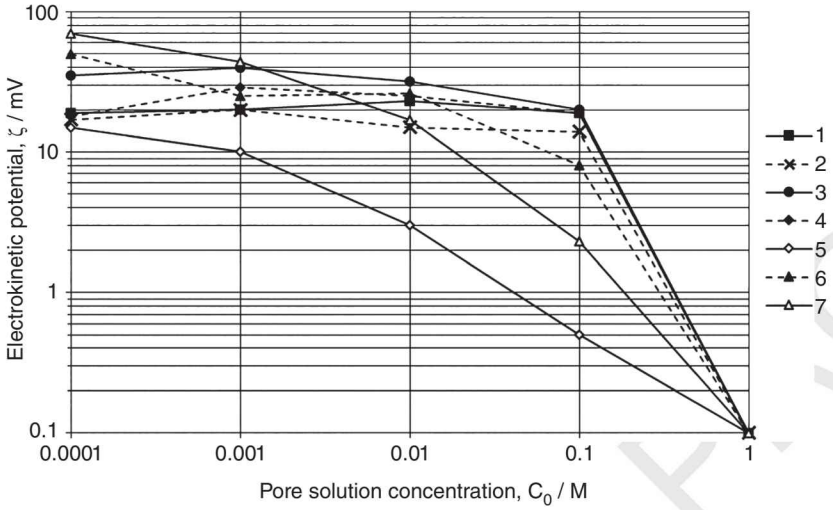

Figure 15.5 Relation between the electrokinetic potential (ζ) of clay-soil particles and soil pore-solution concentration (C_0, M): 1 – Polozhsk kaolin (natural form); 2 – Cambrian illite clay; 3 – Askan-gel (natural montmorillonite); 4 – Na-kaolin (Polozhsk); 5 – Ca-kaolin (Polozhsk); 6 – Na- montmorillonite; 7 – Ca- montmorillonite.

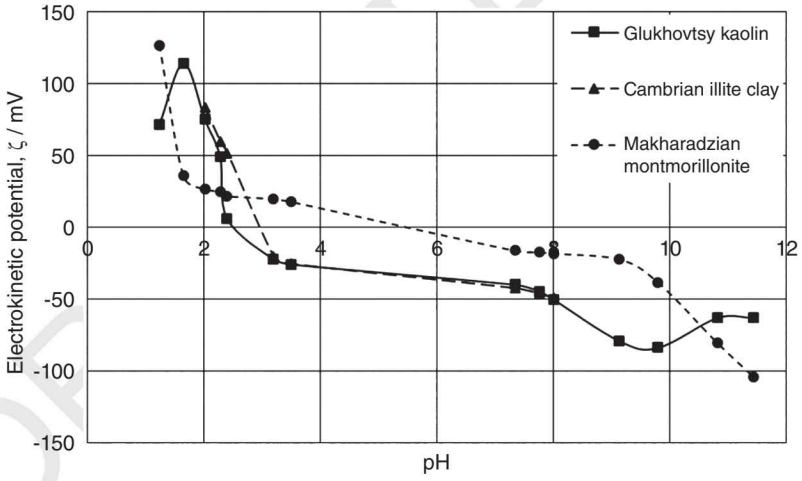

Figure 15.6 Relation between the electrokinetic potential of particles for various clays and their bulk-solution pH. Source: Data from Korolev and Nesterov [23, 43].

were observed by Delgado et al. [48] for the ζ values of Almeria montmorillonite (Spain). A similar impact of electrolyte concentration on EDL thickness was shown by Bharat and Das [49] in their theoretical calculations and experimental study with Kutch and Barmer bentonites (India).

Accordingly, the largest ζ values for the clays were observed in dilute electrolyte solutions (concentration < 0.001 M). The maximum electrokinetic potential of

UNCORRECTED PROOFS

Trim Size: 170mm x 244mm Single Column Loose Ribeiro670117 c15.tex V1 - 12/11/2020 12:32pm Page 341

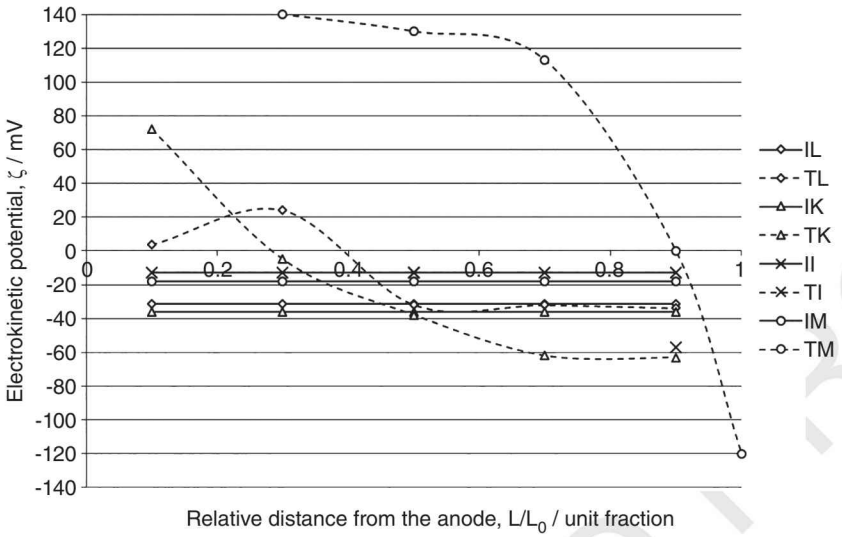

Figure 15.7 Distribution of the electrokinetic potential of clay-soil particles: initial and after electroosmosis (for the legend, see Figure 15.1).

Cambrian illite clay, Na-Polozhsk kaolin, and natural Askan-gel was observed in 0.001 M electrolyte solution. In contrast, that of natural Polozhsk kaolin occurred at a concentration of 0.01 M. This regulation is likely to originate from the different nature of surface dissociation of the EDL ions for these clays. The most drastic decline of ζ-potential with an increase in electrolyte concentration took place in∼0.1 M solution. Consequently, this concentration is a threshold for the clays studied, and exceeding it will cause intense aggregation of clay nanoparticles. This value is close to those observed by Santamarina et al. [50], where rapid "edge-to-face" flocculation occurred for kaolinite and "face-to-face" aggregation took place in the case of montmorillonite.

The influence of the pore-solution *pH* on ζ is significant as well (see Table 15.4). The increase in pH caused the negative ζ values of clay particles to grow due to the corresponding increase in negative σ_H values. Simultaneously, negative ζ potential decreased in magnitude in the acidic medium because of the growth in positive σ_H. For some clays (such as Polozhsk kaolin and Askam-gel), the pH decline caused the recharge of clay particles and the subsequent change of the ζ sign. In general, ζ potential increased in magnitude at the same pH value in the range kaolin – illite clay – bentonite.

The influence of pH on the particle ζ potential was studied in detail for three clays of various mineral types (see Figure 15.6). In the initial neutral medium, ζ was negative (from −15 to −40 mV). As the pH increased, ζ values increased in magnitude up to a range from −50 to −100 mV in the high-alkaline medium. In contrast, ζ decreased in magnitude for all the clays in the low-acidic medium. Electrokinetic potential changed its sign at the $pH_{p.z.c.}$ ($\zeta = 0$), and its positive value grew

UNCORRECTED PROOFS

Trim Size: 170mm x 244mm Single Column Loose Ribeiro670117 c15.tex V1 - 12/11/2020 12:32pm Page 342

with the further decline in pH. In the acidic medium, ζ potential reached its maximum positive values of +100–130 mV at $pH < 2$. In the case of kaolin, ζ magnitudes declined in the extreme pH conditions ($pH < 1.7$ and $pH > 9.8$) [23] due to the contraction of the kaolinite EDLs and subsequent particle "face-to-face" aggregation at the relatively low ionic strength [51]. Overall, as the physico-chemical activity of the clays increased in the row kaolin – illite clay – bentonite, the pH value of the clay-particle recharge was increased, i.e. the $pH_{p.z.c.}$ shifted to the alkaline pH zone (see Figure 15.6).

The number of surface OH-groups in the volume unit generally grows in the row kaolinite – illite – montmorillonite. Accordingly, this favors the more intense exchange of clay EDL cations for H^+ (as described in [48]) and the consequent generation of an alkaline medium. So, it could be a possible reason for the $pH_{p.z.c.}$ values to increase in this row (the σ_P sign change occurred at the higher pH).

The data obtained for Glukhovtsy kaolin are comparable to those reported in the literature: for example, by Yukselen-Aksoy and Kaya [52–54] for Georgian kaolinite (ζ ranged from −25 to −42 mV at pH = 3–11) and Sumbarda Ramos [55] for natural Sigma Aldrich kaolin (−39 mV in distilled water). Moayedi et al. detected the change of the ζ-potential sign at $pH_{p.z.c.} \approx 3.15$ [56]. Also, it should be noted that many researchers (for example, [20, 46, 53]) did not observe the recharge of montmorillonite particles in the entire pH range (pH = 2.5–10.5) during electrophoretic studies. This may relate to the different crystallochemical features of various smectite clays.

In the dynamic study, the electrokinetic potential of the initial clay soils was negative as well (Figure 15.7). As the electrokinetic treatment proceeded, the ζ magnitude increased generally both in the anodic and cathodic zones. However, the clay particles were charged oppositely in these zones. The electrokinetic potential became more negative in the alkaline medium near the cathode. At the same time, ζ changed its sign to positive near the anode. The ζ potential alteration along the sample length during electroosmosis was alike for the mantle till loam and Glukhovtsy kaolin. However, the positive ζ value decreased directly at the anode due to its EDL contraction in the high-acidic medium [24]. In the case of the kaolin, the ζ measurement results were comparable to those obtained by Liaki et al. (∼−5 mV near the anode and ∼ −50 mV at the cathode) for English China clay [57, 58]. However, no particle recharge was observed by these authors in the anodic zone since they used a flow-through electrokinetic setup in these studies and the lowest pH value obtained was ∼3.5.

For Askan-gel, rapid acidification occurred (see Figure 15.1), so its ζ-potential sign changed in almost the entire space between the electrodes, except for the cathodic zone. The ζ-sign change caused the formation of the inverse electroosmotic flow, which caused a rapid fading of electroosmosis in this soil system (1.5 hours of treatment for Askan-gel vs. 4–4.5 hours for the other soils).

Thus, the formation of the pH gradient in soil between the electrodes generated the gradient of electrokinetic potential for the soil particles (see Figure 15.7) [24]:

$$grad(\zeta) = \partial\zeta / \partial L \neq 0 \tag{15.15}$$

UNCORRECTED PROOFS

Trim Size: 170mm x 244mm Single Column Loose Ribeiro670117 c15.tex V1 - 12/11/2020 12:32pm Page 343

Table 15.5 $pH_{p.z.c.}$ and $E_{h\ p.z.c.}$ values for the clays studied.

Clay soil	$pH_{p.z.c.}$	$E_{h\ p.z.c.}$, mV
Glukhovtsy kaolin (Ca-formϕ орма)	2.5	+420
Cambrian illite clay	~2.9	+330
Askan-gel (Makharadzian montmorillonite)	~5.4	+180

Source: Based on Korolev and Nesterov [23, 43].

The recharge of clay particles ($\sigma_P = 0$) can probably occur with E_h variation the same way as in the case of pH. So, this E_h value is appropriate to name the point of zero charge $E_{h\ p.z.c.}$ by analogy with $pH_{p.z.c.}$ [43]. Both of these parameters for the clays studied are listed in Table 15.5.

An oxidative medium of the pore solution is generated by the presence of free protons, H^+ (and the corresponding lack of electrons e^-). Under these conditions, clay particles are positively charged ($\sigma_P > 0$). In turn, a reductive medium derives from the lack of protons (and subsequent excess of free electrons) and dominance of OH^- in the solution. Accordingly, the clay particles are negatively charged ($\sigma_P < 0$) in this case.

The relation of particle ζ and oxidation-reduction potential of the medium is depicted in Figure 15.8 (static case). Generally, the medium reaction became more reductive in the clayey suspensions at the same concentration of electrolyte solution in the row kaolin – illite clay – bentonite due to the corresponding pH variation in this range. The chart shows that the ζ values of the clay particles became more positive as the medium E_h grew. Accordingly, following the $pH_{p.z.c.}$ trend, the corresponding $E_{h\ p.z.c.}$ values declined in the row kaolin – illite clay – bentonite. So, the medium where the particle surface-charge density sign changed became more reductive in this range. Also, ζ values became more positive in this row at the same E_h.

Of note, in this study, the E_h alteration resulted from varying pH. So, a separate study should be conducted to examine the independent influence of E_h on the σ_P and ζ values of clay particles and prove the existence of the $E_{h\ p.z.c.}$ as an individual parameter.

Thus, the electrokinetic treatment can be applied to regulate ζ (as the primary EDL parameter) of clay soil between the electrodes in a wide range of values.

15.4.5 Regulation of Clay CEC

The interaction of clay minerals with acidic and alkaline solutions is pronounced in ion exchange on the basal planes of particles and neutralization reactions on the entire particle surface. As mentioned before, neutralization occurs as a surface dissociation of clay minerals with the release of H^+ ions in the alkaline medium and OH^- emission (or H^+ bonding) in the acidic medium. Ion exchange on a clay surface is accompanied by a partial uptake of H^+ or OH^- from the pore solution into

UNCORRECTED PROOFS

Trim Size: 170mm x 244mm Single Column Loose Ribeiro670117 c15.tex V1 - 12/11/2020 12:32pm Page 344

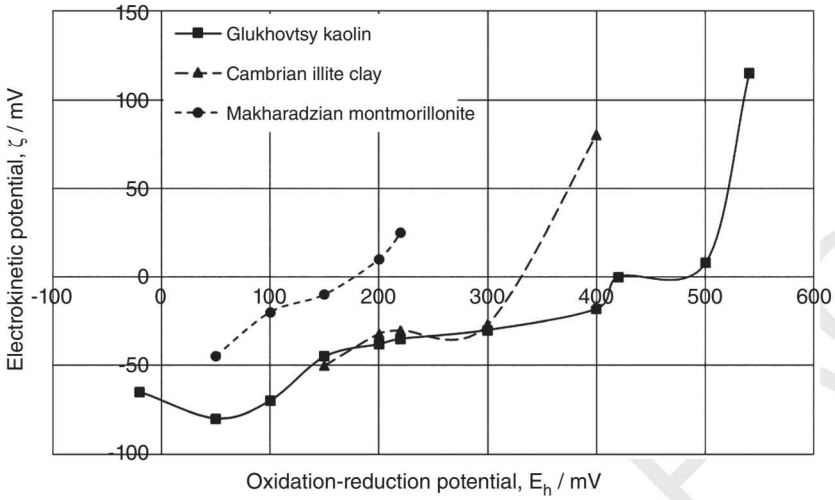

Figure 15.8 Relation between the electrokinetic potential of clay-soil particles and oxidation-reduction potential of a bulk solution. Source: Data from Korolev and Nesterov [43].

the clay's ion-exchangeable complex. Since the clay particles are negatively charged in most of the pH range, their surfaces absorb H^+ or compensating cations predominantly. CEC increases in the range kaolinite – illite – montmorillonite so that the pH of clay suspensions at the same pore-electrolyte concentration increases in this row as well.

The increase in CEC from kaolinites to montmorillonites results in an increase in the effective number of active exchangeable ions. Accordingly, it causes growth in salinity and specific electrical conductivity at the same pore-solution concentration for suspensions in this row of clay minerals [12, 43].

An increase in pH causes the negative ζ value of clay particles to increase. Accordingly, its growth increases the number of cations attracted to a clay particle. So, the clay CEC increases as the pore-solution pH grows [59–61]. At the $pH < pH_{p.z.c.}$, soil switches its CEC to anion-exchange capacity (AEC).

Applying a DC electric field to soil induces the pH alteration in a broad range, as was mentioned before (see Figure 15.1). Consequently, this effect can be used to regulate the CEC of clay soil as well. Accordingly, the clay CEC will decrease in the anodic zone (acidic medium) and increase in the cathodic zone (alkaline conditions). Notably, the CEC of clay near the cathode can be boosted many times over its value in the neutral medium (the central part of the soil sample between the electrodes).

This circumstance is essential to consider while applying electrokinetic technologies for the treatment of clay soils from various toxicants. For instance, generating acidic conditions and decreasing CEC near the anode will promote desorption of heavy metals and their easy removal from this zone.

UNCORRECTED PROOFS

Trim Size: 170mm x 244mm Single Column Loose Ribeiro670117 c15.tex V1 - 12/11/2020 12:32pm Page 345

15.4.6 Regulation of Physico-Chemical Parameters of Soils

Electrokinetic treatment can be applied to regulate various physico-chemical soil parameters. For example, electrokinetics is an effective method for regulating clay *plasticity*. This way, Liaki and coauthors demonstrated the considerable change in kaolin plasticity during the electrokinetic experiments by a flow-through scheme using inert electrodes [57]. The authors found that the decline in the pore-solution pH caused the LL to grow, while the increase in pH caused a drop in LL. Accordingly, LL values grew in the anodic zone (from initial 55.5 to 58.5%) and decreased near the cathode (from 55.5 to 54%). However, the kaolin LL grew in almost the entire inter-electrode space except for the very cathodic zone. Similarly, the soil PL increased along the entire sample length and in the direction from the cathode to the anode.

Such pH–LL and pH–PL trends resulted from the flocculation of kaolinite particles in the acidic medium (pH $\approx$ 3) and their disaggregation in the alkaline one (pH $\approx$ 9), as mentioned before. Plasticity and liquidity limits of clay represent the two critical moisture-content values, where a change in the predominant contact type between the soil particles occurs. In the case of PL, the transformation from transient (dry) contacts to near-coagulation ones takes place. In turn, far-coagulation contacts cease to exist, and no contacts exist between the particles at LL. Consequently, since the particle flocculation increases the number of contacts among the clay aggregates, greater water content must change the contact type to a weaker one. So, the flocculation of particles promotes an increase in soil LL. The opposite effect is observed in the case of particles' disaggregation.

The same authors also reported the effect of electrokinetic treatment using iron electrodes [58]. In this case, a more drastic increase in LL occurred in the anodic zone (from 55.5 to 61%), and a more significant LL decrease took place in the cathodic zone (from 55.5 to 53.5%). Such a trend near the anode resulted from the dissolution of iron electrodes and octahedral kaolinite sheets. It caused the release of Fe^{3+} and Al^{3+} ions into the pore solution, their subsequent sorption (first Fe^{3+}, then Al^{3+}) on the particle surfaces, and EDL contraction. Accordingly, particle flocculation (or aggregation) took place, and consequently, the kaolinite LL increased. In turn, the more significant decline in LL near the cathode seems to be caused by $Al(OH)_3$ precipitation on the soil particles there. This phenomenon could decrease the number of hydrophilic sites at the particle surfaces and cause the consequent drop in LL. The pH–PL trend was less pronounced in this study.

These effects are widely used for soil stabilization. For example, James et al. [62] reported the results of a high-plasticity clay stabilization using $CaCl_2$ and $Ca(OH)_2$ as stabilizing agents. In this research, the average LL of the clay decreased, while its PL increased during electrokinetic treatment. Overall, it resulted in a drop in the soil PI during the experiments. The more pronounced alterations were detected in the tests with $CaCl_2$ (for instance, PI decreased from 40 to 15%).

Electrokinetics can also be applied to reduce *swelling* of clay. Reduction of clay swelling is much in demand for industrial applications, especially in the oil industry, to prevent reservoir rocks from being damaged or clogged by tiny clay particles [63]. As an example, the authors of the just-mentioned study [62] reported a drop in the

UNCORRECTED PROOFS

Trim Size: 170mm x 244mm Single Column Loose Ribeiro670117 c15.tex V1 - 12/11/2020 12:32pm Page 346

free-swell index W_{sw} for the same clay after tests using both $CaCl_2$ and $Ca(OH)_2$ stabilizing solutions, from an initial 121% to 100 and 73%, respectively.

Shrestha et al. [64] demonstrated that the electrokinetic delivery of 0.01–0.1 M $CaCl_2$ could be applied to reduce the swelling (in terms of volume increase) of bentonite and bentonite-sand mixtures. The authors reported a significant decrease in clay swelling since the ζ-potential magnitudes of the $CaCl_2$-treated specimens were less than the initial value, even at higher final pH values.

15.4.7 Regulation of Soil Texture and Structure

Altering the clay ζ potential and particle EDLs generally results in a transformation of the soil microtexture that is pronounced in the change in the clay's microaggregate size. Also, the combined effect of the clay-mineral EDL transformation and electroosmotic flow causes the reorientation of clay nanoparticles, i.e. structural changes in soil.

In this chapter, soil texture and structure are given from the British-US standpoint. In this terminology, soil texture is represented as a description of the size, shape, and contact type of solid soil parts (particles, grains, microaggregates, etc.) [65]. Soil structure is defined as an arrangement of these solid parts and pores located between them [66]. In particular, soil structure is described by its anisotropy index. In contrast, *soil texture* and *soil structure* have the opposite meanings in the French-German-Russian classification system.

Microtextural transformations of clay due to electroosmosis occur the most clearly in the anodic and cathodic zones. The primary effects that cause textural alterations in soil due to the influence of a DC-field application are [14]:

1) Hardening of soil in the anodic zone due to electroosmotic drainage
2) Soil softening near the cathode due to its moisturization
3) Electrocoagulation at the anode and dipolophoresis of nanoparticles, particularly in the cathodic zone
4) pH change in both near-electrode zones
5) Concentration of some ions near the anode or cathode due to their electromigration
6) Electro-heating in the anodic zone

In the present study, transforming the microtexture under electroosmosis was studied in detail for the mantle till loam and Glukhovtsy kaolin (Figures 15.9–15.12). All the alterations were attributed to the change in EDL parameters of the soil nanoparticles and the influence of electroosmotic flow [24]. For example, analysis of the large-scale SEM images of the loam revealed that contacts of basis-edge type dominated between the clay-mineral particles in the initial sample. Overall, its microtexture was of the card-house type [63, 67].

During the treatment, the clay nanoparticles formed microaggregates merged by the basis planes in the alkaline medium near the cathode, thus forming basis-basis contacts. This effect was caused by the increase in the ionic strength (which exceeded the critical value for particle coagulation) and consequent particle

UNCORRECTED PROOFS

Trim Size: 170mm x 244mm Single Column Loose
Ribeiro670117 c15.tex V1 - 12/11/2020 12:32pm Page 347

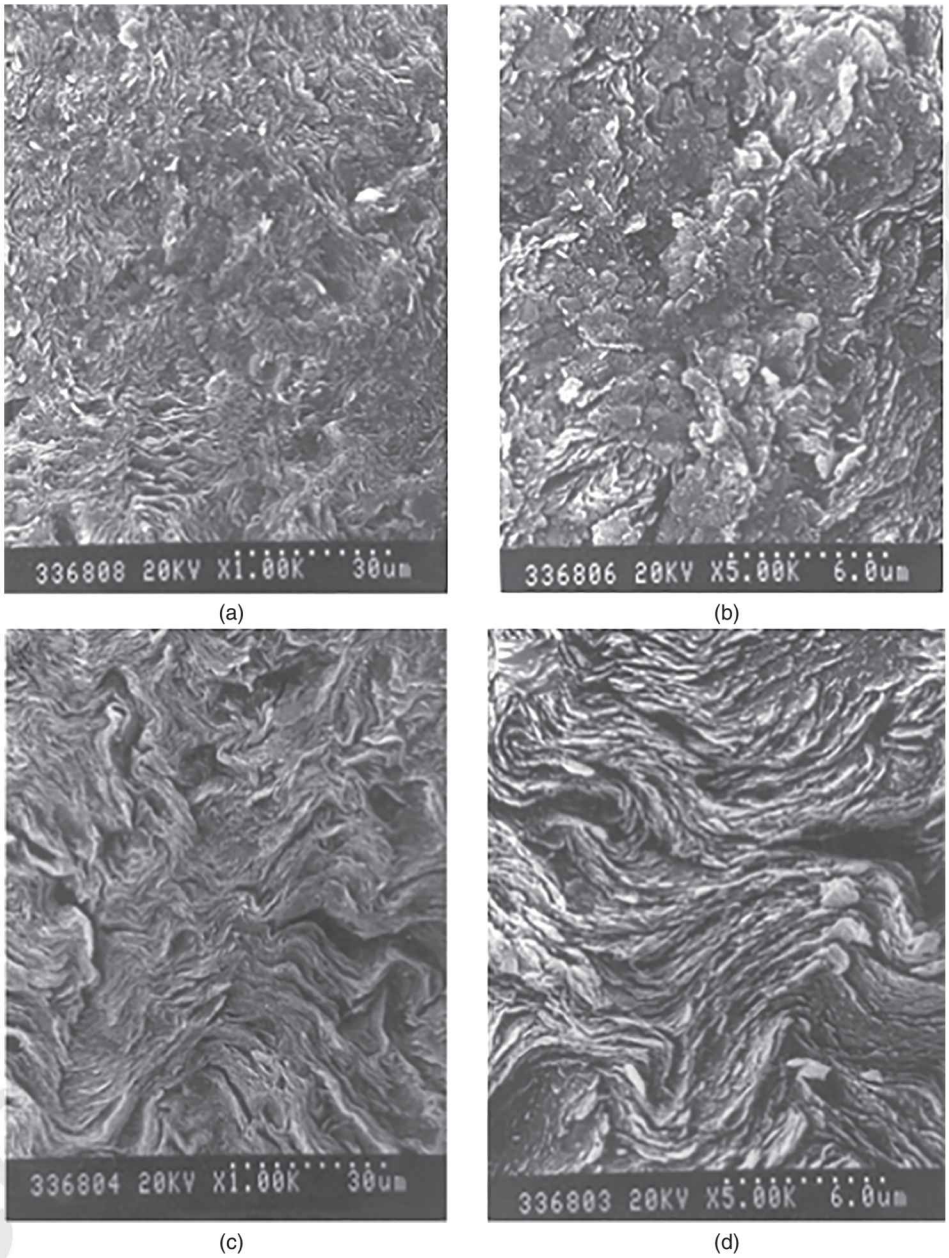

Figure 15.9 Microstructure of kaolinite clay (Glukhovtsy kaolin) in the anodic (a, b) and cathodic (c, d) zones as a result of electroosmosis.

UNCORRECTED PROOFS

Trim Size: 170mm x 244mm Single Column Loose Ribeiro670117 c15.tex V1 - 12/11/2020 12:32pm Page 348

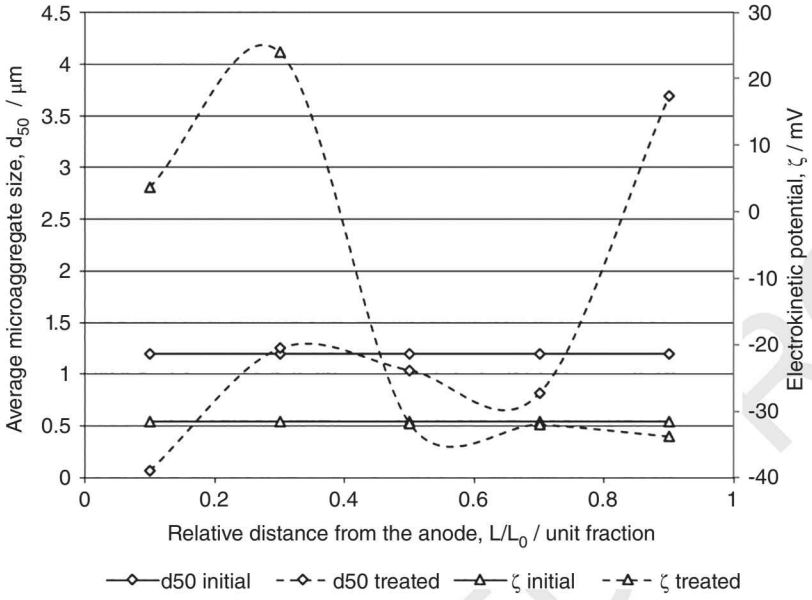

Figure 15.10 Distribution of loam's average microaggregate size d_{50} and the electrokinetic potential ζ of its particles: initial and after electroosmosis (treated).

aggregation around large non-clay grains. In the anodic zone, the clay particles became aggregated as well. However, some of them formed microaggregates with a basis-edge contact type since various particle surfaces were oppositely charged in the wide pH range [63]. In turn, analysis of the small-scale loam SEM images discovered that the share of large micropores (10–100 µm by Osipov and Sokolov classification [67]) increased near both the anode and cathode after electroosmosis [24].

The microtexture of Glukhovtsy kaolin was altered significantly during electroosmosis as well. For instance, kaolinite nanoparticle packages aggregated by the basis-basis type dominated in the initial sample texture. At the same time, these packages were oriented randomly so that the clay structure was isotropic. Part of the separate well-crystallized kaolinite particles and their ultra-microaggregates were merged with the packages via basis-edge contacts [24].

Figure 15.9 shows the SEM images of the kaolin microtexture in the anodic and cathodic zones after electroosmosis [14]. As can be seen in the large-scale images (see Figure 15.9a,c), the packages became oriented in the direction of the electroosmotic flow. However, this orientation was more pronounced in the cathodic zone. Also, the kaolinite particles formed microaggregates up to 20 µm in size near the cathode.

Comparing the kaolin microtexture in the anodic and cathodic zones in the small-scale images (see Figure 15.9b,d), one can see that it became denser near the anode (see Figure 15.9b) due to electroosmotic drainage. Large micropores (10–100 µm) filled with water almost disappeared here. Instead, the share of small

UNCORRECTED PROOFS

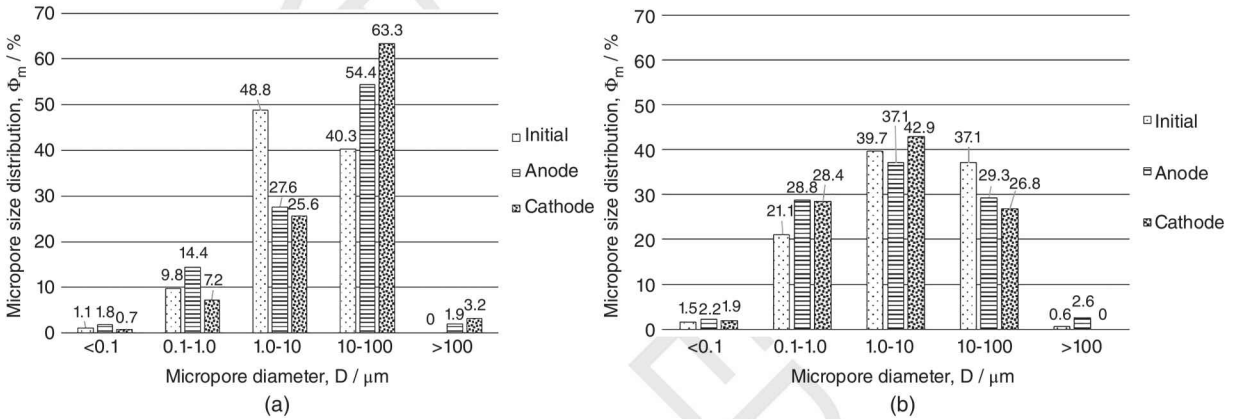

Figure 15.11 Micropore-diameter distribution in initial soil and near-electrode zones of the soil sample after electroosmosis: (a) mantle till loam; (b) Glukhovtsy kaolin. Source: Based on Korolev and Nesterov [24].

UNCORRECTED PROOFS

Trim Size: 170mm x 244mm Single Column Loose
Ribeiro670117 c15.tex V1 - 12/11/2020 12:32pm Page 349

Trim Size: 170mm x 244mm Single Column Loose Ribeiro670117 c15.tex V1 - 12/11/2020 12:32pm Page 350

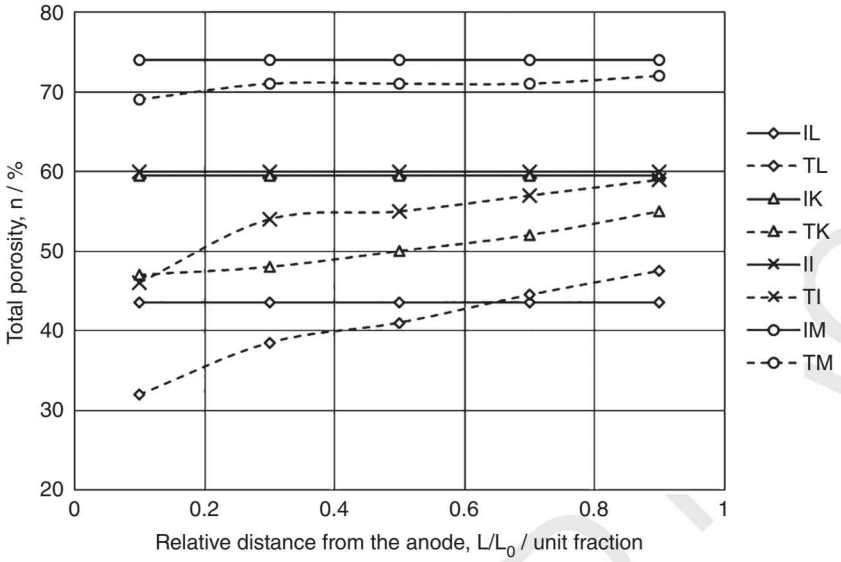

Figure 15.12 Distribution of total porosity of clay soils: initial and after electroosmosis (for the legend, see Figure 15.1).

(1–10 μm) and fine (0.1–1 μm) micropores, according to the soil pore-size classification by Osipov and Sokolov [67], increased. In contrast, comparatively more loose microtexture formed in the cathodic zone (see Figure 15.9c) due to electroosmosis. Large micropores filled with water can be seen distinctly. However, their total share decreased in both the anodic and cathodic zones compared to the initial kaolin. The kaolin microstructure became pseudo-turbulent near the cathode due to the intense water migration. Also, the pores within this clay became anisotropic in both zones. The same effect of electroosmosis on the kaolin microstructure during its treatment with the injection of Ca^{2+} ions was revealed in [68].

Microtextural transformations of the soils studied (such as microaggregate size and type of contacts) during electroosmosis were attributed to the change in pore-solution pH, particle EDL alterations, and modification in the soil moisture content (see Section 15.4.8). Altering the pore-solution pH (i.e. the formation of acidic and alkaline medium near the anode and cathode, respectively) resulted in a crucial change in the soil particle EDLs. The clay texture was transformed significantly due to the aggregation or disaggregation of the soil particles. At the same time, electrophoresis of the dispersed clay particles seems to be negligible since they were in constrained conditions.

In the case of mantle till loam, a considerable alteration of its microaggregate (or, more precisely, ultra-microaggregate) size due to the DC-field influence was observed (see Figure 15.10). Notably, the measured average microaggregate diameter d_{50} of the loam particles should be attributed only to smectite ultra-microaggregates. For example, the d_{50} value decreased in the cathodic zone ($L/L_0 = 0.7$) in comparison to the initial value. This seems to be caused by the increase in the share

UNCORRECTED PROOFS

Trim Size: 170mm x 244mm Single Column Loose Ribeiro670117 c15.tex V1 - 12/11/2020 12:32pm Page 351

of negatively charged particles and their consequent disaggregation due to the ion-electrostatic repulsion of the similarly charged EDLs [24]. In turn, d_{50} increased drastically directly near the cathode ($L/L_0 = 0.9$). The ionic strength of the pore solution doubled, so it could cause the loam particle EDLs to contract and the ultra-microaggregates to form. At the same time, the average particle electrokinetic potential ζ increased slightly in both zones compared to the initial value (see Figure 15.10). Such a relation between d_{50} and ζ can be explained by a small percent of clay minerals in the loam composition (see Table 15.2).

Ultra-microaggregates also formed in the acidic medium in the anodic zone ($L/L_0 = 0.3$). This effect was provoked by an increase in the relative share of positively charged particles, while some of them remained negatively charged [24]. So, the formation of dense ultra-microaggregates conjoint by electrostatic attraction forces took place. At the same time, ζ changed its sign and decreased in magnitude. However, the measured d_{50} declined in the high-acidic medium near the anode ($L/L_0 = 0.1$). This phenomenon could be caused probably by the partial dissolution of the octahedral layers of clay nanoparticles in the concentrated acid ($pH \approx 1.7$) and their partial disruption [69, 70]. So, the real microaggregate size should increase further in this zone due to significant EDL contraction. This assumption is proved correct in part by a drastic decrease in the ζ value, which should favor particle aggregation.

The data presented are in accord with the results of the SEM quantitative analysis (see Figure 15.11). Microporosity (n_μ) of the loam calculated by SEM-image analysis increased near the electrodes (22 and 24% at the cathode and anode, respectively) in comparison to that of the initial sample (20%). These results prove the aggregation of clay particles around large mineral grains and the consequent formation of large micropores (10–100 μm) in the near-electrode zones. This assumption is confirmed by the visible increase in the share of large micropores and consequent decrease in the percent of small (1–10 μm) micropores detected by the SEM analysis (see Figure 15.11a). In addition, the more significant increase in n_μ of the loam near the anode can be related to intense gas generation here due to water electrolysis. The gas emissions caused by electrolysis reactions at the electrodes resulted in the formation of mesopores (> 100 μm by [67]) during electroosmosis (see Figure 15.11a).

Microporosity of the kaolin decreased in both the anodic and cathodic zones (from initial 27% to 25 and 24%, respectively) during the treatment. The decline in the kaolin's n_μ values during the experiments can be attributed to kaolinite-particle reorientation and overall soil compaction under the electroosmotic flow. Accordingly, the percent of large micropores decreased while the share of fine micropores (0.1–1 μm) increased within the kaolin structure (see Figure 15.11b).

The anisotropy coefficient K_A of both soils studied also increased: from 10.6% to 16.6 and 25.9% (in the anodic and cathodic zones, respectively) for the loam and from 3.1% to 30.2 and 40.4% (near the anode and cathode, respectively) for the kaolin. So, in general, the microstructure of both the soils became oriented to a different extent. The maximum K_A values occurred in the cathodic zone since the electroosmotic flow impact was the most intense here.

UNCORRECTED PROOFS

Trim Size: 170mm x 244mm Single Column Loose Ribeiro670117 c15.tex V1 - 12/11/2020 12:32pm Page 352

Thus, the electroosmotic treatment resulted in the formation of aggregated microtexture and anisotropic microstructure both for the loam and kaolin. However, in the loam, the share of large micropores increased within its structure, while the percent of fine micropores increased for the kaolin [24, 71].

Figure 15.12 demonstrates the change in total soil porosity (n) during the experiments. In general, porosity decreased for all the soils studied. Thus, soil structure became denser in each case. Porosity slightly increased in the cathodic zone of the loam, possibly due to its intense moisturization and consequent softening. The highest decline in porosity occurred in the case of Glukhovtsy kaolin, and the least pronounced decrease in this parameter was observed for two soils: loam and bentonite. As for the mantle till loam, it occurred due to the low intensity of electroosmosis in this soil. In contrast, the rapid fading of electroosmosis caused an insignificant alteration of total porosity in Askan-gel. The primary trend observed was an increase in porosity from the anode to the cathode for each soil.

15.4.8 Regulation of Physical Clay Properties

Applying a DC field is known to cause *water content* (W) redistribution between the electrodes in water-saturated soils [12, 14, 40]. The moisture percent decreased during the treatment for each soil. On average, it declined from 25 to 20% for the loam, from 50 to 34% for Glukhovtsy kaolin, from 45 to 39% for Biyasalin illite clay, and from 99 to 94% for Askan-gel. Thus, the most pronounced drainage effect occurred in the kaolin. Also, the moisture content of clay soils decreased from the cathode to the anode. In total, electrokinetics caused the formation of a moisture-content gradient between the electrodes:

$$grad\,\mathrm{W} = \partial W/\partial L \neq 0 \tag{15.16}$$

Altering the water percent, as well as clay compaction under the hydraulic pressure of the electroosmotic flow, caused a change in soil *density* (ρ_m). Its average value increased after the treatment from 1.56 to 1.78 g cm^{-3} for the kaolin, from 1.59 to 1.74 g cm^{-3} for the illite clay, and from 1.29 to 1.42 g cm^{-3} for Askan-gel. In contrast, the average moist density (1.92 g cm^{-3}) of the loam did not change. As for the loam, this parameter declined in the cathodic zone due to the soil moisturization and loosening there. Generally, moist density decreased from the anode to the cathode. The greatest average increase in moist density occurred for the kaolin.

The influence of electroosmosis on clay soils and their subsequent drainage transforms their *consistency* as well. These changes were analyzed using the liquidity limit (LI) of soil (Figure 15.13).The initial pastes of kaolin, illite clay, and bentonite were free-flowing, while the loam had a very soft consistency. Generally, LI values decreased relative to the initial values for each soil after applying the DC field. The most significant change in soil consistency took place in the case of the kaolin. It obtained solid and semi-solid consistency throughout most of the inter-electrode space.

Since electrokinetic treatment can be used to affect soil porosity, it is also applicable to regulate soil *permeability*. Technologies based on electrokinetics are widely

UNCORRECTED PROOFS

Trim Size: 170mm x 244mm Single Column Loose Ribeiro670117 c15.tex V1 - 12/11/2020 12:32pm Page 353

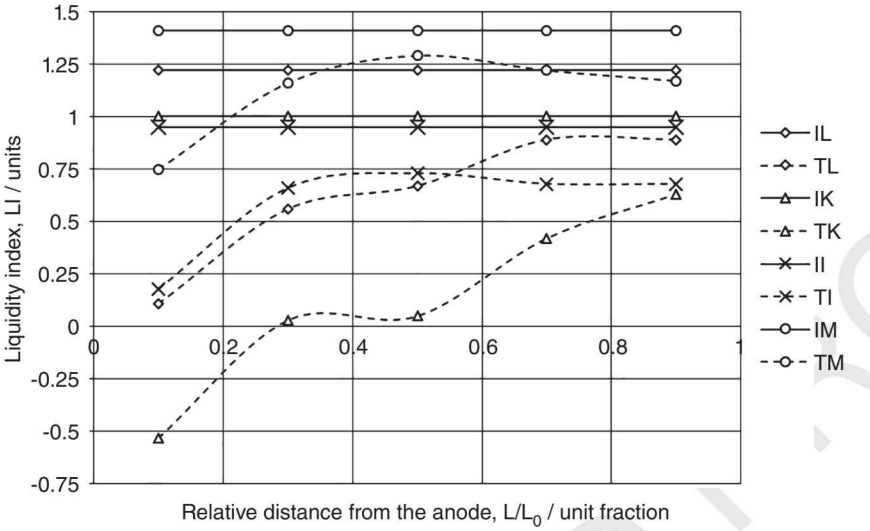

Figure 15.13 Distribution of soil liquidity index: initial and after electroosmosis (for the legend, see Figure 21.1).

applied in the oil industry to increase the permeability of collector sandstone cores. For example, Al-Shalabi et al. reported enhancing sandstone permeability by 40% after electrokinetic treatment with brine [72]. This effect seems to be caused by the disruption of pore-lining clay layers due to the aggregation of their particles in the concentrated solution and crack formation under electroosmotic flow pressure.

Thus, electrokinetics can be applied to purposefully transform the physical properties of clay soils to a great extent. The chemical-mineral composition of soil affects this transformation significantly.

15.4.9 Regulation of Soil Strength and Deformability

As demonstrated above, electrokinetic treatment of clay soil affects its texture, structure, and density greatly. So, it significantly alters soil strength as well. For example, the present data suggest that the strength characteristics of all the soils studied increased after the tests since their density increased.

Electroosmosis alone is widely applied in the construction industry to increase soil-strength parameters using the same regularities as described in this study. For example, Hansbo reported the results of a field implementation of electroosmosis to increase the bearing capacity of soil [73]. The *undrained shear strength* (c_u) increased in the entire soil space between the electrodes (except for the cathodic zone), on average by 40%. At the same time, it declined by 25% in 0.5 m proximity from the cathode. Also, Jayasekera demonstrated an increase in *compressive strength* (R_s) of two clay soils during electrokinetic lab tests by 175 and 200% under certain voltage gradients and test times [74]. The increase in soil strength during electroosmosis is attributed to particle EDL alterations and the hydraulic impact of water flow.

UNCORRECTED PROOFS

Trim Size: 170mm x 244mm Single Column Loose Ribeiro670117 c15.tex V1 - 12/11/2020 12:32pm Page 354

However, a more significant increase in soil strength can be achieved by electrochemical treatment of soil using sacrificial electrodes or stabilizing agents. For instance, Liaki et al. demonstrated that the undrained shear strength of kaolin generally decreased (by 15%) during electrokinetic treatment by a flow-through scheme using inert electrodes [57]. This effect resulted from an overall increase in the moisture content of the kaolin. The most significant decline in soil shear strength (25%) occurred at the cathode due to the greatest increase in water percent. It could be caused in part by the increase in the pore-solution pH and consequent soil disaggregation and loosening.

Notably, these authors reported distinct results in the same tests but with steel electrodes [58]. The undrained shear strength of the kaolin increased near the anode (by 20%), and it again declined at the cathode (by 15%). However, the undrained shear strength in the cathodic zone increased relatively against its values for the untreated kaolin at the same water content (maximum 250%). This data can be explained by the significant kaolinite EDL transformation at the anode and the formation of precipitates near the cathode (see Section 15.4.6).

Ayodele et al. showed that the treatment of kaolin with a (PO_4^{3-})-containing solution (injected through the anode) caused an increase in *constrained* (M_{max}) and *shear* (G_{max}) *moduli* of soil near the cathode by 15 and 20%, respectively [68]. G_{max} in the central soil section also increased by the same 20%. This phenomenon could be caused by phosphate precipitation in the kaolin pores and the formation of firmly bound floccules. However, tests run with a (Ca^{2+})-containing solution (injected through the cathode) resulted in a slight G_{max} decrease.

Thus, electrokinetic (or electrochemical) treatment can be applied successfully to regulate the strength and deformability parameters of soil.

15.5 Conclusions

Changing external physico-chemical parameters such as pH, E_h, composition, and ionic strength of the pore solution significantly alters the surface-charge characteristics of clay nanoparticles. Accordingly, changes in the sign and value of surface charge cause the significant transformation of the clay-particle EDLs.

In the present study, the following trends in the change of the clay-particle surface-charge characteristics with varying pore-solution parameters were found:

1) In general, clay nanoparticles were negatively charged in the neutral and alkaline media and positively charged in the acidic medium.
2) As the physico-chemical parameters of the clay soils (such as PI, CEC, and SSA) increased within the row kaolin – illite clay – bentonite, their $pH_{p.z.n.p.c.}$ and $pH_{p.z.c.}$ values shifted to the alkaline pH region.
3) $pH_{p.z.n.p.c.}$ of clays shifted to the acidic pH region of as the pore-solution ionic strength increased.
4) An increase in pore-solution E_h is hypothesized to result in the reduction in negative ζ-potential value until its sign changes at the $E_{h\ p.z.c.}$.

UNCORRECTED PROOFS

Trim Size: 170mm x 244mm Single Column Loose Ribeiro670117 c15.tex V1 - 12/11/2020 12:32pm Page 355

In turn, EDL characteristics influence macroscopic soil properties to a large extent. Thus, adjusting the pore-solution medium by electrokinetics allows regulating the soil properties via the impact on the soil's EDL parameters. Electrokinetic treatment alters the soil's texture and structure, its physical and physico-chemical properties. In general, applying a DC electric field results in the formation of various gradients (W, σ_P, ζ, etc.) in soil between the electrodes.

The data obtained can be used to justify the regulation of clay-soil properties. In particular, it can play a crucial role in the design of protective sorption barriers (PRBs) using clays on the migration path of toxicant solutions having various pH values. Since altering the EDL parameters directly affects the properties of clay soils, it allows the development of clay and clay-based sorbents with predetermined characteristics in a wide pH range.

Acknowledgments

The present study was conducted with the partial use of equipment (X-ray diffractometer ULTIMA-IV, SEM LEO 1450VP, and laser analyzer Horiba SZ-100) obtained as a part of the Lomonosov Moscow State University Development Program, and the authors acknowledge this support.

Also, the authors want to express their sincere gratitude to Dr. M.S. Chernov and Professors V.N. Sokolov and E.N. Samarin for their help with the analysis of SEM images and acid-base titration data. We would like to thank I.V. Romanova especially for the data provided.

Abbreviations

AEC	Anion-exchange capacity of soil, meq (100 g dry soil)$^{-1}$
c	Concentration of a titrant, M
c_u	Undrained shear strength, kPa
C_0	Initial concentration of pore solution, M
CEC	Cation-exchange capacity of soil, meq (100 g dry soil)$^{-1}$
d_{50}	Average microaggregate size, μm
D	Micropore diameter, μm
EDL	Electrical double layer
E_h	Oxidation-reduction potential, mV
$E_{h\ p.z.c.}$	Point of zero charge (oxidation–reduction potential), mV
F	Faraday number, C mol^{-1}
G_{max}	Shear modulus of soil, MPa
HI	Hinckley index, units
I	Ionic strength of solution, M
K_A	Anisotropy coefficient, %
L	Distance from the anode, cm
L_0	Sample length, cm

UNCORRECTED PROOFS

Trim Size: 170mm x 244mm Single Column Loose Ribeiro670117 c15.tex V1 - 12/11/2020 12:32pm Page 356

L_0/L	Relative distance from the anode, unit fraction
LI	Liquidity index, units
LL	Liquid limit, % dry weight
m	Mass of dry soil sample, g
M_{max}	Constrained modulus of soil, MPa
n	Total soil porosity, % volume
n_μ	Microporosity of soil (calculated by SEM image), % volume
$pH_{i.e.p.}$	Isoelectric point (pH), units of pH
$pH_{p.z.c.}$	Point of zero charge (pH), units of pH
$pH_{p.z.n.c.}$	Point of zero net charge (pH), units of pH
$pH_{p.z.n.p.c.}$	Point of zero net proton charge (pH), units of pH
$pH_{p.z.s.e.}$	Point of zero salt effect (pH), units of pH
P	Pressure, Pa
PI	Plasticity index, %
PL	Plasticity limit, % dry weight
PRB	Permeable reactive barrier
R_s	Compressive strength of soil, kPa
SEM	Scanning electron microscopy (or scanning electron microscope)
SSA	Specific surface area of soil, $m^2\ g^{-1}$
T	Temperature, °C
TDS	Total dissolved solids, ppm
V_b	Titrant volume used to titrate a blank solution, L
V_s	Titrant volume used to titrate a soil suspension, L
W	Moisture content of soil, % dry weight
W_{sw}	Free-swell index (moisture content), % dry weight
x	Distance from the particle surface, μm
z	Equivalency number of an ion, units
Δq	Adsorbed ion charge density, $C\ m^{-2}$
ζ	Electrokinetic potential, mV
ρ_d	Dry soil density, $g\ cm^{-3}$
ρ_m	Moist soil density, $g\ cm^{-3}$
ρ_s	Specific particle density of soil, $g\ cm^{-3}$
σ_0	Net structural surface-charge density, $C\ m^{-2}$
σ_d	Diffuse layer surface-charge density, $C\ m^{-2}$
σ_H	Net proton surface-charge density, $C\ m^{-2}$
σ_{in}	Intrinsic surface-charge density, $C\ m^{-2}$
σ_{IS}	Net inner-sphere complex surface-charge density, $C\ m^{-2}$
σ_{OS}	Net outer-sphere complex surface-charge density, $C\ m^{-2}$
σ_P	Net total particle surface-charge density, $C\ m^{-2}$
σ_S	Net Stern-layer surface-charge density, $C\ m^{-2}$
ϕ	Electric potential, V
Φ_m	Share of micropore category, %
æ$_d$	Specific electrical conductivity of a solution or suspension, $S\ m^{-1}$

UNCORRECTED PROOFS

Trim Size: 170mm x 244mm Single Column Loose Ribeiro670117 c15.tex V1 - 12/11/2020 12:32pm Page 357

References

1 Sokolov, V.N., Chernov, M.S., Shlykov, V.G. et al. (2008). Mineral nanoparticles in dispersed soils. *Journal of Surface Investigation: X-Ray, Synchrotron and Neutron Techniques* 2 (5): 759–763. https://doi.org/10.1134/S1027451008050169.

2 Sokolov, V.N. and Chernov, M.S. (2013). Mineral nanostructures of clay rocks. *Doklady Earth Sciences* 449 (1): 290–292. https://doi.org/10.1134/S1028334X13030161.

3 Chorover, J. and Sposito, G. (1995). Surface charge characteristics of kaolinitic tropical soils. *Geochimica et Cosmochimica Acta* 59 (5): 875–884. https://doi.org/10.1016/0016-7037(94)00357-2.

4 Schroth, B.K. and Sposito, G. (1997). Surface charge properties of kaolinite. *Clays and Clay Minerals* 45 (1): 85–91. https://doi.org/10.1346/CCMN.1997.0450110.

5 Sposito, G. (1998). On points of zero charge. *Environmental Science & Technology* 32 (19): 2815–2819. https://doi.org/10.1021/es9802347.

6 Chorover, J. (2005). Zero-charge points. In: *Encyclopedia of Soils in the Environment* (ed. D. Hillel), 367–373. New York: Elsevier Ltd https://doi.org/10.1016/B0-12-348530-4/00154-5.

7 Sposito, G. (2008). *The Chemistry of Soils*, *6*e. Oxford, UK: Oxford University Press.

8 Kriaa, A., Hamdi, N., Goncalves, M.A. et al. (2009). Acid-base properties of Tunisian glauconite in aqueous suspensions. *International Journal of Electrochemical Science* 4: 535–550.

9 Arfaoui, S., Hamdi, N., Frini-Srasra, N. et al. (2012). Determination of point of zero charge of PILCS with single and mixed oxide pillars prepared from Tunisian-smectite. *Geochemistry International* 50 (5): 447–454. https://doi.org/10.1134/S0016702912030020.

10 Hamdi, N. and Srasra, E. (2014). Acid-base properties of organosmectite in aqueous suspension. *Applied Clay Science* 99: 1–6. https://doi.org/10.1016/j.clay.2014.07.009.

11 Rengasamy, P., Tavakkoli, E., and Mcdonald, G.K. (2016). Exchangeable cations and clay dispersion: net dispersive charge, a new concept for dispersive soil: net dispersive charge in soil. *European Journal of Soil Science* 67 (5): 1–7. https://doi.org/10.1111/ejss.12369.

12 Zlochevskaya, R.I. and Korolev, V.A. (1988). *Electro-Surface Phenomena in Clay Soils*. Moscow, Russia: MSU Publishing House [in Russian].

13 Trofimov, V.T., Korolev, V.A., Voznesensky, E.A. et al. (eds.) (2005). *Ground Science*, *6*e. Moscow, Russia: MSU Publishing House [in Russian].

14 Korolev, V.A. (2015). *Theory of Electro-Surface Phenomena in Soils and their Application*. Moscow: Sam Polygraphist, Ltd [in Russian].

15 Tombácz, E., Szekeres, M., and Tóth, I.Y. (2018). Potentiometric characterization of protonation/deprotonation equilibria in aqueous colloids. In: *Titration: Theory, Types, Techniques and Uses* (ed. T.L. Joshi), 145–174. New York: Nova Science Publishers, Inc.

UNCORRECTED PROOFS

Trim Size: 170mm x 244mm Single Column Loose Ribeiro670117 c15.tex V1 - 12/11/2020 12:32pm Page 358

16 Tarasevich, Y.I. and Ovcharenko, F.D. (1975). *Adsorption on Clay Minerals*. Kyiv, USSR: Naukova Dumka [in Russian].

17 Mdivinishvili, O.M. (1983). *Crystallochemical Basis for the Regulation of the Properties of Natural Sorbents*. Tbilisi, USSR: Metsniereba [inRussian].

18 Paschenko, A.A. (ed.) (1986). *Physical Chemistry of Silicates*. Moscow, USSR: Higher School [in Russian].

19 Korolev, V.A., Nesterov, D.S., and Chernov, M.S. (2017). The regulation ofclay particle charge in relation to the technologies of protective barrier construction. In: *Proceedings of the 19th Sergeev Readings. 'Geoecological Safety of Mineral Deposits Exploitation',* Moscow, Russia (4-5 April 2017). Moscow, Russia: PFUR Publishing House [in Russian].

20 Avena, M.J. and De Pauli, C.P. (1998). Proton adsorption and electrokinetics of an Argentinean montmorillonite. *Journal of Colloid and Interface Science* 202 (1): 195–204. https://doi.org/10.1006/jcis.1998.5402.

21 Kriaa, A., Hamdi, N., and Srasra, E. (2009). Proton adsorption and acid-base properties of Tunisian illites in aqueous solution. *Journal of Structural Chemistry* 50 (2): 288–301. https://doi.org/10.1007/s10947-009-0039-6.

22 Stathi, P., Papadas, I.T., Tselepidou, A. et al. (2010). Heavy-metal uptake by a high cation-exchange-capacity montmorillonite: the role of permanent charge sites. *Global NEST Journal* 12 (3): 248–255.

23 Korolev, V.A. and Nesterov, D.S. (2018). Regulation of clay particles charge for design of protective electrokinetic barriers. *Journal of Hazardous Materials* 358: 165–170. https://doi.org/10.1016/j.jhazmat.2018.06.023.

24 Korolev, V.A. and Nesterov, D.S. (2019). Influence of electro-osmosis on physicochemical parameters and microstructure of clay soils. *Journal of Environmental Science and Health – Part A. Toxic/Hazardous Substances and Environmental Engineering* 54 (6): 570–581. https://doi.org/10.1080/10934529.2019.1571321.

25 D854-92, A.S.T.M. (1994). *Standard Test Method for Specific Gravity of Soil Solids by Water Pycnometer*. West Conshohocken, PA: ASTM.

26 ASTM D5550-06 (2014). *Standard Test Method for Specific Gravity of Soil Solids by Gas Pycnometer*. West Conshohocken, PA: ASTM.

27 ASTM D4318 (2010). *Standard Test Methods for Liquid Limit, Plastic Limit, and Plasticity Index of Soils*. West Conshohocken, PA: ASTM.

28 Cokca, E. and Birand, A. (1993). Determination of cation exchange capacity of clayey soils by the methylene blue test. *Geotechnical Testing Journal* 16 (4): 518–524. https://doi.org/10.1520/GTJ10291J.

29 Kahr, G. and Madsen, F.T. (1995). Determination of the cation exchange capacity and the surface area of bentonite, illite and kaolinite by methylene blue adsorption. *Applied Clay Science* 9 (5): 327–336. https://doi.org/10.1016/0169-1317(94)00028-O.

30 Brunauer, S., Emmett, P.H., and Teller, E. (1938). Adsorption of gases in multimolecular layers. *Journal of the American Chemical Society* 60 (2): 309–319. https://doi.org/10.1021/ja01269a023.

UNCORRECTED PROOFS

Trim Size: 170mm x 244mm Single Column Loose Ribeiro670117 c15.tex V1 - 12/11/2020 12:32pm Page 359

31 Mills, O.P. and Rose, W.I. (2010). Shape and surface area measurements using scanning electron microscope stereo-pair images of volcanic ash particles. *Geosphere* 6 (6): 805–811. https://doi.org/10.1130/GES00558.1.

32 Trofimov, V.T. and Korolev, V.A. (eds.) (2017). *Lab Works on Ground Science: Study Book*, *3*e. Moscow, Russia: University Book House [in Russian].

33 GOST 25100-2011 (2011). *Soils. Classification*. Moscow: Federal Agency on Technical Regulation and Metrology. [in Russian].

34 EN ISO 14688-1:2018 E (2018). *Geotechnical Investigation and Testing Identification and Classification of Soil - Part 1: Identification and Description (ISO 146881:2017)*. Dublin: CEN.

35 Korolev, V.A. (1986). Engineering-geological specifics of clay soils in the south western part of Crimean Mountains. *MSU Bulletin*. Series 4. Geology 3: 69–81. [in Russian].

36 Hao, W., Flynn, S.L., Alessi, D.S. et al. (2018). Change of the point of zero net proton charge (pH_{PZNPC}) of clay minerals with ionic strength. *Chemical Geology* 493: 458–463. https://doi.org/10.1016/j.chemgeo.2018.06.023.

37 ASTM D7263-09 (2018). *Standard Test Methods for Laboratory Determination of Density (Unit Weight) of Soil Specimens*. West Conshohocken, PA: ASTM.

38 Terzaghi, K. (1936). Stability of slopes of natural clay. In: *Proceedings of the 1st International Conference on Soil Mechanics, Volume 1*,Cambridge, MA(22-26 June 1936). Cambridge, MA: Harvard University Press.

39 Skempton, A.W. (1953). The colloidal "activity" of clays. In: *Proceedings of the 3rd International Conference on Soil Mechanics and Foundation Engineering,* Zurich, Switzerland (16-27 August 1953). Zurich, Switzerland: ICOSOMEF.

40 Pamukcu, S. (2009). Electrochemical transport and transformations. In: *Electrochemical Remediation Technologies for Polluted Soils, Sediments and Groundwater* (eds. K.R. Reddy and C. Cameselle), 29–64. Hoboken, NJ: Wiley.

41 Yeung, A.T. (2009). Geochemical processes affecting electrochemical remediation. In: *Electrochemical Remediation Technologies for Polluted Soils, Sediments and Groundwater* (eds. K.R. Reddy and C. Cameselle), 65–94. Hoboken, NJ: Wiley.

42 Nesterov, D.S. and Korolev, V.A. (2018). Alteration of the physico-chemical soil specifics during electroosmosis. In: *Proceedings of the International Scientific-Practical Conference 'Strategy for the Development of Geological Study on Subsurface Resources: Present and Future (to 100-Anniversary of the MGRI-RSGPU)', Volume 2,* Moscow, Russia (4-6 April 2018). Moscow, Russia: Research and Development enterprise 'Filtrotkani' [in Russian].

43 Korolev, V.A. and Nesterov, D.S. (2017). Physico-chemical regularities of changes of the clay soil particles electrical charge. *Engineering Geology (Russian)* 12 (4): 50–60. [in Russian]. https://doi.org/10.25296/1993-5056-2017-4-50-60.

44 Wieland, E. and Stumm, W. (1992). Dissolution kinetics of kaolinite in acidic solutions at 25°C. *Geochimica et Cosmochimica Acta* 56 (9): 3339–3355. https://doi.org/10.1016/0016-7037(92)90382-S.

45 Kriaa, A., Hamdi, N., and Srasra, E. (2008). Determination of point of zero charge of Tunisian kaolinites by potentiometric and mass titration methods.

UNCORRECTED PROOFS

Trim Size: 170mm x 244mm Single Column Loose Ribeiro670117 c15.tex V1 - 12/11/2020 12:32pm Page 360

Journal of the Chinese Chemical Society 55: 53–61. https://doi.org/10.1002/jccs.200800010.

46 Avena, M.J., Cabrol, R., and De Pauli, C.P. (1990). Study of some physicochemical properties of pillared montmorillonites: acid-base potentiometric titrations and electrophoretic measurements. *Clays and Clay Minerals* 38 (4): 356–362. https://doi.org/10.1346/CCMN.1990.0380404.

47 Kriaa, A., Hamdi, N., and Srasra, E. (2007). Acid–base chemistry of montmorillonitic and beidellitic-montmorillonitic smectite. *Russian Journal of Electrochemistry* 43 (2): 167–177. https://doi.org/10.1134/S102319350702005X.

48 Delgado, A., González-Caballero, F., and Bruque, M.J. (1986). On the zeta potential and surface charge density of montmorillonite in aqueous electrolyte solutions. *Journal of Colloid and Interface Science* 113 (1): 203–211. https://doi.org/10.1016/0021-9797(86)90220-1.

49 Bharat, T.V. and Das, D.S. (2017). Physicochemical approach for analyzing equilibrium volume of clay sediments in salt solutions. *Applied Clay Science* 136: 164–175. https://doi.org/10.1016/j.clay.2016.11.021.

50 Santamarina, J.C., Klein, K.A., Palomino, A.M. et al. (2002). Micro-scale aspects of chemical-mechanical coupling: Interparticle forces and fabric. In: *Chemo-Mechanical Coupling in Clays: From Nano-Scale to Engineering Applications. Proceedings of the Workshop, Maratea, 28–30 June 2001* (ed. C. DiMaio), 48–59. London, UK: Taylor & Francis Group https://doi.org/10.1201/9781315139289.

51 Palomino, A.M. and Santamarina, J.C. (2005). Fabric map for kaolinite: effects of pH and ionic concentration on behavior. *Clays and Clay Minerals* 53 (3): 209–222. https://doi.org/10.1346/CCMN.2005.0530302.

52 Yukselen, Y. and Kaya, A. (2003). Zeta potential of kaolinite in the presence of alkali, alkaline earth and hydrolysable metal ions. *Water, Air, and Soil Pollution* 145 (1): 155–168. https://doi.org/10.1023/A:1023684213383.

53 Kaya, A. and Yukselen, Y. (2005). Zeta potential of soils with surfactants and its relevance to electrokinetic remediation. *Journal of Hazardous Materials* B120 (1–3): 119–126. https://doi.org/10.1016/j.jhazmat.2004.12.023.

54 Yukselen-Aksoy, Y. and Kaya, A. (2011). A study of factors affecting on the zeta potential of kaolinite and quartz powder. *Environmental Earth Sciences* 62 (4): 697–705. https://doi.org/10.1007/s12665-010-0556-9.

55 Sumbarda-Ramos, E.G., Oropeza-Guzmán, M.T., Salgado-Rodríguez, R. et al. (2011). Potential measurements used to study the bentonite-pollutant and kaolin-pollutant interphase. *ECS Transactions* 36 (1): 341–347. https://doi.org/10.1149/1.3660628.

56 Moayedi, H., Huat, B.B.K., Kazemian, S. et al. (2011). Electrophoresis of suspended kaolinite in multivalent electrolyte solution. *International Journal of Electrochemical Science* 6: 6514–6524.

57 Liaki, C., Rogers, C.D.F., and Boardman, D.I. (2008). Physicochemical effects on uncontaminated kaolinite due to electrokinetic treatment using inert electrodes.

UNCORRECTED PROOFS

Trim Size: 170mm x 244mm Single Column Loose Ribeiro670117 c15.tex V1 - 12/11/2020 12:32pm Page 361

Journal of Environmental Science and Health – Part A. Toxic/Hazardous Substances and Environmental Engineering 43 (8): 810–822. https://doi.org/10.1080/10934520801973972.

58 Liaki, C., Rogers, C.D.F., and Boardman, D.I. (2010). Physicochemical effects on clay due to electromigration using stainless steel electrodes. *Journal of Applied Electrochemistry* 40 (6): 1225–1237. https://doi.org/10.1007/s10800-010-0096-8.

59 Sawhney, B.L., Frink, C.R., and Hill, D.E. (1970). Components of pH-dependent cation exchange capacity. *Soil Science* 109 (5): 272–278. https://doi.org/10.1097/00010694-197005000-00002.

60 Curtin, D. and Smillie, G.W. (1979). Origin of the pH-dependent cation exchange capacities of Irish soil clays. *Geoderma* 22 (3): 213–224. https://doi.org/10.1016/0016-7061(79)90020-X.

61 Meyer, W.L., Marsh, M., and Arp, P.A. (1994). Cation exchange capacities of upland soils in eastern Canada. *Canadian Journal of Soil Science* 74 (4): 393–408. https://doi.org/10.4141/cjss94-053.

62 James, J., James, A., Kumar, A. et al. (2019). Plasticity and swell-shrink behaviour of electrokinetically stabilized virgin expansive soil using calcium hydroxide and calcium chloride solutions as cationic fluids. *Civil and Environmental Engineering Reports* 29 (1): 128–146. https://doi.org/10.2478/ceer-2019-0010.

63 Wilson, M.J., Wilson, L., and Patey, I.T.M. (2014). The influence of individual clay minerals of formation damage of reservoir sandstones: a critical review with some new insights. *Clay Minerals* 49 (2): 147–164. https://doi.org/10.1180/claymin.2014.049.2.02.

64 Shrestha, R.A., Zhang, A.P., Mateus, E.P. et al. (2016). Electrokinetically enabled de-swelling of clay. In: *Electrokinetics across Disciplines and Continents. New Strategies for Sustainable Development* (eds. A.B. Ribeiro, E.P. Mateus and N. Couto), 43–56. Zurich, Switzerland: Springer International Publishing https://doi.org/10.1007/978-3-319-20179-5_3.

65 Ditzler, C., Scheffe, K., and Monger, H.C. (eds.) (2017). *Soil Survey Manual. USDA Handbook 18*. Washington, D.C.: Government Printing Office.

66 Dexter, A.R. (1988). Advances in characterization of soil structure. *Soil and Tillage Research* 11 (3–4): 199–238. https://doi.org/10.1016/0167-1987(88)90002-5.

67 Osipov, V.I. and Sokolov, V.N. (2013). *Clays and their Properties. Composition, Structure, and Properties Formation*. Moscow, Russia: GEOS [in Russian].

68 Ayodele, A.L., Pamukcu, S., Shrestha, R.A. et al. (2018). Electrochemical soil stabilization and verification. *Geotechnical and Geological Engineering* 36: 1283–1293. https://doi.org/10.1007/s10706-017-0392-8.

69 Ottosen, L.M., Christensen, I.V., Rörig-Dalgård, I. et al. (2008). Utilization of electromigration in civil and environmental engineering – processes, transport rates and matrix changes. *Journal of Environmental Science and Health – Part A. Toxic/Hazardous Substances and Environmental Engineering* 43 (8): 795–809. https://doi.org/10.1080/10934520801973949.

UNCORRECTED PROOFS

Trim Size: 170mm x 244mm Single Column Loose Ribeiro670117 c15.tex V1 - 12/11/2020 12:32pm Page 362

70 Skibsted, G., Ottosen, L.M., Elektorowicz, M. et al. (2017). Effect of long-term electrodialytic soil remediation on Pb removal and soil weathering. In: *Proceedings of the 15th Symposium on Electrokinetic Remediation (EREM 2017)*, Montreal, Canada (6-8 August 2017). Montreal, Canada: Concordia University.

71 Nesterov, D.S., Korolev, V.A., and Chernov, M.S. (2019). Transformations of the texture and properties of clay soil of various mineral types during their electro-osmotic treatment for the resolution of environmental problems in mining practice. In: *Proceedings of the 6th International Scientific-Practical Conference 'Resolution of Environmental and Technologicproblems in Mining Practice on the Territory of Russia, CIS and Non-CIS States'*, Moscow, Russia (21-23March 2019). Moscow, Russia: 'VNIPI Industrial Technologies', Ltd. [in Russian].

72 Al Shalabi, E.W., Ghosh, B., Haroun, M. et al. (2012). The application of direct current potential to enhancing waterflood recovery efficiency. *Petroleum Science and Technology* 30 (20): 2160–2168. https://doi.org/10.1080/10916466.2010.547902.

73 Hansbo, S. (2008). Soil improvement by means of electro-osmosis. 6th International Conference on Case Histories in Geotechnical Engineering.

74 Jayasekera, S. (2015). Electrokinetics to modify strength characteristics of soft clayey soils: a laboratory based investigation. *Electrochimica Acta* 181 (1): 39–47. https://doi.org/10.1016/j.electacta.2015.06.064.

UNCORRECTED PROOFS

Trim Size: 170mm x 244mm Single Column Loose Ribeiro670117 c16.tex V1 - 12/11/2020 10:16pm Page 363

16

Technologies to Create Electrokinetic Protective Barriers

D.S. Nesterov and V.A. Korolev

Faculty of Geology, Department of Engineering and Ecological Geology, Lomonosov Moscow State University, Moscow 119991, Russia

16.1 Introduction

Remediating a contaminated site usually requires materials, economic resources, and time. However, the soil treatment process can be a source of secondary environmental issues such as greenhouse gas emissions [1]. Consequently, when a pollutant spill occurs, the best strategy is to *prevent* contamination of soil and groundwater using a protective barrier.

In this context, applying electrokinetic methods to prevent the migration of toxicants is a promising option. Electrokinetic systems are easy to install in field conditions, even in densely built-up areas, and they are environmentally friendly in general. An *electrokinetic barrier* (EKB) can be applied as a specific technology to protect subsurface objects such as engineering structures, water-intake systems, storage facilities, and agricultural sites from contaminants [2] – most commonly, to prevent groundwater contamination [3, 4]. Studies of EKB applications show that they can prevent the migration of heavy metals, nitrates, organic pollutants (including hydrocarbons and organochlorine contaminants), and radionuclides [5–7].

Such a barrier is usually constructed by installing electrodes in dispersive soil and applying a direct current (DC) electric field. The primary principle of EKB performance is the development of a counterflow, which prevents toxicant migration (Figure 16.1). The predominant mechanisms to oppose the hydraulic flow are electroosmosis and electromigration. In brief, the EKB concept differs from the classic electrokinetic remediation of soil in the following ways [3]:

- The primary purpose of an EKB installation is to prevent contamination of clean land, not to remediate a polluted soil mass.
- A partial hydraulic barrier can form if soil pores are clogged by contaminant accumulation (adsorption, precipitation, or colmatation) near the electrodes.
- Electromigration of ions while the barrier is functioning promotes the formation of ion-depleted zones and a consequent increase in soil electrical resistance.

Electrokinetic Remediation for Environmental Security and Sustainability, First Edition.
Edited by Alexandra B. Ribeiro and M.N.V. Prasad.
© 2021 John Wiley & Sons Ltd. Published 2021 by John Wiley & Sons Ltd.

UNCORRECTED PROOFS

Trim Size: 170mm x 244mm Single Column Loose Ribeiro670117 c16.tex V1 - 12/11/2020 10:16pm Page 364

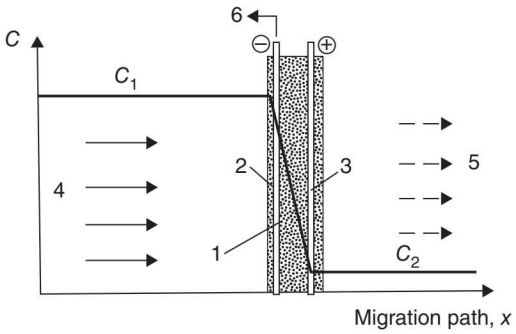

Figure 16.1 Concept of an electrokinetic barrier: plan view. Symbols: 1, area under protection; 2, anodes; 3, cathodes; 4, contaminated groundwater flow; 5, electroosmotic counterflow. Source: Based on Mitchell and Yeung [2].

Hence, the power consumption required for barrier maintenance declines significantly with time.

When an EKB is launched, the electrically induced counterflow restricts the direct contaminated flux. Hydraulic flow and diffusion are the primary driving forces for pollutant propagation within the soil mass. At the same time, when the barrier is applied, ion migration is mainly hindered by electroosmosis and electromigration. Thus, the common critical condition for proper EKB functioning is [3]

$$\nu_{EO} + \nu_{EM\,i} \geq \nu_h + \nu_{di} \tag{16.1}$$

where ν_{EO} is the contaminant migration velocity under electroosmosis, $\nu_{EM\,i}$ is the electromigration velocity of a charged species i, ν_h is its velocity in the hydraulic flow, and ν_{di} is the diffusion velocity of a solute i.

The following equation describes electroosmotic flux in soil [3, 4]:

$$\nu_{EO} = -\cdot K_{EO} \cdot \mathrm{grad}(\varphi) \tag{16.2}$$

where K_{EO} is electroosmotic conductivity ($m^2\ V^{-1}\ s^{-1}$) of the soil, φ – electric potential (V). In turn, K_{EO} depends on various parameters of the soil and pore solution [8]:

$$K_{EO} = -(\zeta \cdot \varepsilon \cdot \varepsilon_0 \cdot n \cdot \tau)/\eta \tag{16.3}$$

where ζ is the electrokinetic potential of soil solids (V), ε is the dielectric constant of the pore solution (units), ε_0 is the the vacuum permittivity ($\approx 8.85\,10^{-12}$ F m^{-1}), n is the soil porosity (% volume), τ is the tortuosity of the soil (units), and η is the viscosity of the pore solution (Pa s). The value of the electroosmotic conductivity K_{EO} varies slightly among different soil types, from 1×10^{-10} ($m\ V^{-1}\ s^{-1}$) for fine sands to 1×10^{-9} ($m\ V^{-1}\ s^{-1}$) for heavy clays [9].

Next, the electromigration velocity of an ion is defined by the following equation [10–12]:

$$\nu_{EM\,i} = -[(D_i \cdot n \cdot \tau \cdot z_i \cdot F)/(R \cdot T)] \cdot \mathrm{grad}(\varphi) \tag{16.4}$$

where D_i is the diffusion coefficient of a species i in free solution ($cm^2\ s^{-1}$), z_i is the charge of an ion i (units), F is the Faraday constant ($\approx 96\,485$ C mol^{-1}), R is the universal gas constant (8.314 $Jmol^{-1}\ K^{-1}$), and T is the absolute temperature (K).

UNCORRECTED PROOFS

Trim Size: 170mm x 244mm Single Column Loose Ribeiro670117 c16.tex V1 - 12/11/2020 10:16pm Page 365

Darcy's law governs the hydraulic velocity ν_h in soils [13]:

$$\nu_h = -K_h \cdot \mathrm{grad}(H) \tag{16.5}$$

where K_h is the soil hydraulic conductivity ($m\,s^{-1}$), H is the hydraulic head of groundwater flow (m). The K_h values vary in a wide range across various soils: between 1×10^{-3} m s^{-1} for coarse sand and 1×10^{-12} m s^{-1} for dense clay [4].

Finally, diffusion is described by Fick's law [14]:

$$\nu_{di} = -D_i \cdot n \cdot \tau \cdot V_{si} \cdot \mathrm{grad}(c_i) \tag{16.6}$$

where V_{si} is the volume fraction of a solute i ($l\,mol^{-1}$) [15, 16], and c_i is the solute concentration (M). In the majority of EKB applications, the ion diffusion rate ν_{di} can be neglected in comparison with the hydraulic velocity ν_h.

Diffusion must be taken into account during the design and validation of an EKB in heavy clay reservoirs for radioactive waste (RW) containment. The reliability of RW storage facilities is usually calculated for long terms (from decades to centuries), and the diffusion contribution is significant for such a duration. In this case, barrier validation should meet the following condition (see Eq. 16.1):

$$[(\zeta \cdot \varepsilon \cdot \varepsilon_0)/\eta + (D_i \cdot z_i \cdot F)/(R \cdot T)]n \cdot \tau \cdot \mathrm{grad}(\varphi) \geq K_h \cdot \mathrm{grad}(H) + D_i \cdot n \cdot \tau \cdot V_{si} \cdot \mathrm{grad}(c_i) \tag{16.7}$$

In contrast, the inequation for most EKB applications for soils varying from fine sands (fSa) to clays (Cl) [17] considers only ν_{EO}, $\nu_{EM\,i}$, and ν_h:

$$\nu_{EO} + \nu_{EM\,i} \geq \nu_h \tag{16.8}$$

$$[(\zeta \cdot \varepsilon \cdot \varepsilon_0)/\eta + (D_i \cdot z_i \cdot F)/(R \cdot T)]n \cdot \tau \cdot \mathrm{grad}(\varphi) \geq K_h \cdot \mathrm{grad}(H) \tag{16.9}$$

At the same time, the contribution of electroosmosis is negligible in coarse soils such as coarse or medium sands (cSa and mSa) [17], so barrier workability depends only on ion electromigration and hydraulic flow rates:

$$\nu_{EM\,i} \geq \nu_h \tag{16.10}$$

$$[(D_i \cdot z_i \cdot F)/(R \cdot T)]n \cdot \tau \cdot \mathrm{grad}(\varphi) \geq K_h \cdot \mathrm{grad}(H) \tag{16.11}$$

Finally, when a contaminant is represented by an uncharged species (e.g. organics), its movement in clay soil is ruled primarily by electroosmosis and hydraulic flow:

$$\nu_{EO} \geq \nu_h \tag{16.12}$$

$$[(\zeta \cdot \varepsilon \cdot \varepsilon_0 n \cdot \tau)/\eta] \cdot \mathrm{grad}(\varphi) \geq K_h \cdot \mathrm{grad}(H) \tag{16.13}$$

Notably, Eqs. (16.1, 16.8, 16.10, 16.12) represent simplified conditions with the assumption that no chemical reactions occur within the soil. However, more complicated models are often required for valid barrier utilization due to co-occurring electrochemical phenomena and soil-contaminant inter-reactions. The processes to be considered are water electrolysis (and consequent pH change) at the electrodes, soil-solution interactions, and reactions between solution components (e.g. adsorption/desorption, precipitation/dissolution, and oxidation/reduction) [16, 18].

UNCORRECTED PROOFS

Trim Size: 170mm x 244mm Single Column Loose Ribeiro670117 c16.tex V1 - 12/11/2020 10:16pm Page 366

16.2 Conventional Electrokinetic Barriers

Several researchers conducted lab tests on the applicability of the EKB concept to hinder the migration of different contaminants. These studies are crucial for understanding the essence of phenomena occurring in the soil as the result of barrier application. The data from such studies are widely used to design combined protective barriers.

16.2.1 Cationic Contaminants

EKBs are usually developed to halt the movement of cationic species such as heavy metals. Because the solid particles are charged negatively in a wide pH range for most soils [19–25], electroosmotic flux is usually directed toward the cathode. So, the arrangement of the electrodes to create a counterflow, in this scenario, should be the following: the cathode is up-gradient, and the anode is down-gradient relative to the contaminated flux.

The first papers on EKBs considered alkaline metals (Na, K) as model pollutants. The results of these studies are of interest for two reasons. First, EKB applications to hinder the movement of such ions represent the simplest cases. So, the results of these tests can be used to study the phenomena in detail and model more complicated cases when soil-contaminant interaction occurs or the pollutant can change its oxidation state. Second, these data are suitable to design field EKB systems to resist seawater intrusions in coastal areas or protect fresh groundwater aquifers from brine injection in arid regions.

For example, Mitchel and Yeung demonstrated the consistency of a periodically applied (1 h d^{-1}) voltage gradient of 1 V cm^{-1} to prevent the progression of Na ions under grad(H) = 50 in Altamont silty clay for 20 days [2]. The propagation of Na ions was five times less when the barrier was applied compared to the system without an EKB. However, the migration of Cl ions was accelerated around 2.5 times with the barrier functioning, compared to when no EKB was used. Narasimhan and Sri Ranjan developed a simulation model for NaCl solution component migration in the presence of an EKB [12] under the same conditions as in [2]. Their modeling results showed good agreement with the experimental data of Yeung and Mitchell.

Also, Narasimhan reported data on an EKB application to prevent the migration of K ions [26]. In this study, an electrical strength grad(φ) = 1 V cm^{-1} halted K^+ movement in 0.02 M KCl pore solution under grad(H) = 3.75. The voltage was applied for 32 days in a periodic mode with a cycle of 2 hours on and 22 hours off. K propagation was reduced by 20 times compared to that in the test with no electric field.

However, the majority of experimental studies deal with applying a barrier against heavy metal contamination. For instance, Lynch et al. showed that Cd movement in illitic-kaolinitic clay under grad(H) = 7 could be restricted successfully by an electric counter-gradient of 0.5 V cm^{-1} [27]. At the same time, applying grad(φ) = 0.85 V cm^{-1} resulted in a partial driving back of Cd up-gradient of the hydraulic flow. In the case of a 1 : 4 mixture of kaolinite clay and quartz sand, even

UNCORRECTED PROOFS

Trim Size: 170mm x 244mm Single Column Loose Ribeiro670117 c16.tex V1 - 12/11/2020 10:16pm Page 367

a relatively small voltage gradient (grad(φ) = 0.5 V cm^{-1}) was enough to prevent Cd from entering the clean soil.

Similar tests with the same soils were conducted by Rugery with Zn ions [28]. He found that a voltage gradient of only 1.25 V cm^{-1} was enough to hinder Zn migration almost entirely for both the soils. Under this electric strength, only 1–3% of the initial Zn concentration (2000 ppm) moved into clean soil fragments down-gradient of the contaminated flow.

The suitability of the EKB concept to prevent Cu propagation in silica silt was tested in [9]. The authors conducted flat tank experiments (the same as were in [29]) with 1000 ppm Cu solution under grad(H) = 1.3 and different voltage gradients. At grad(φ) = 0.96 V cm^{-1}, the intrusion of copper into clean soil was entirely prevented. Some infiltration of Cu (on an average level of 300 ppm) occurred when grad(φ) = 0.77 V cm^{-1} was applied, but the contaminant did not pass the anode.

16.2.2 Anionic Pollutants

EKB technology can be used to contain anionic species within the electrodes as well. In this case, the electrode positioning should be reversed. In particular, the potential for EKB use to prevent nitrate contamination was studied extensively.

For example, Eid et al. induced 6 mA current in a 0.3 m silica sand sample to confront NO_3^- movement under $\nu_h = 0.17$ m h^{-1} [30]. It was enough to hold the contaminant up-gradient at the anode during 12-hour experiments. Manokararajah and Sri Ranjan showed that applied grad(φ) = 1 V cm^{-1} was able to prevent the advance of 500 ppm KNO_3 solution in silty loam under grad(H) = 1.25 for at least 13 days [31]. In a parallel study, the same authors demonstrated that reversing the polarity of the electrodes caused the reduction of NO_3^- to gaseous N_2 at the cathode in the acidic medium [32]. Thus, by changing the electrode polarity at times, one can achieve complete cleaning of nitrates from soil.

Note that the electroosmotic flow was in the opposite direction (from the anode to the cathode), toward the electromigration of anionic species, in the mentioned papers [30–32]. So, electroosmosis should have hindered the counterflow and, consequently, facilitated the direct hydraulic flux. However, ν_{EO} seems to be negligible (in silica sand) or rather weak (in silty loam) compared to the electromigration rate.

On the other hand, the electroosmotic flow makes a significant contribution to total contaminant movement in active clays. Accordingly, it should be diminished or reversed. A promising approach is to affect the clay's ζ-potential, e.g. by soil acidification, since ζ is positive or close to zero at low pH [19, 25, 33].

In the same manner, moderate alkalization can be used to increase the absolute value of clay ζ and, consequently, enhance the electroosmotic flow in EKBs developed to use against heavy metals. Intense alkaline treatment can cause heavy metals to precipitate, thus clogging soil pores and reducing hydraulic flow.

16.2.3 Advanced EKB Implementations

Since the maintenance of an EKB requires much less electric power than conventional electrokinetic remediation, using solar panels as a promising source of energy

UNCORRECTED PROOFS

Trim Size: 170mm x 244mm Single Column Loose Ribeiro670117 c16.tex V1 - 12/11/2020 10:16pm Page 368

is an attractive idea. Nowicki et al. conducted tank tests of the applicability of an EKB supported with a chargeable solar panel to prevent Cu contamination [34]. The tests were carried out for three days in December when the light part of the day was shortest. A solar battery was charged for 2 hours; after this, the barrier functioned for 28 hours. Copper was largely prevented from advancing in the soil during these tests.

The further development of this technology requires eliminating the chargeable battery in the solar panel. So, the barrier should be able to work and hinder the movement of a pollutant properly during daylight hours only: i.e. function in a pulsed-voltage mode. Reeve and Lynch carried out a study of the ability of such an EKB to prevent the intrusion of 1000 ppm Cu solution [35]. The voltage application cycles were nine hours on and three hours off for the first two rounds, and then six hours on and six hours off. The barrier contained the contamination for at least 96 hours. After that period, the power was switched off, and Cu breakthrough through the EKB occurred immediately.

Mohamedelhassan reported the results of applying a solar-powered EKB to prevent Cd pollution [36]. In this study, EKBs powered by solar panels (with peak $\text{grad}(\varphi) = 1\,\text{V cm}^{-1}$ for a single panel and $\text{grad}(\varphi) = 2\,\text{V cm}^{-1}$ for two interconnected panels) were compared with the barriers supplied by a continuous DC field of the same voltage gradient. The electric field generated by solar panels functioned during daytime only (around 15 hours). The solar-powered EKBs proved to be as efficient as the continuously powered barriers to counteract grad(H) = 10 and even to move Cd up-gradient from the hydraulic flow.

It is worth mentioning that when an EKB is installed in the field, the soil can be treated before the EKB's deployment. For example, it can be acid-base treated to adjust its ζ-potential or densified to decrease its K_h value.

16.2.4 Using EKBs for Soil Remediation

An EKB in the field can be used in combination with other technologies to remediate soil. For instance, such a barrier can be applied to lower the groundwater-table level to facilitate the treatment of hydrocarbon-contaminated sites by the vapor-extraction method [4, 37]. Since this method is most efficient when the contaminated zone becomes unsaturated, using an EKB can provide significantly more remediation. The simulation conducted by Narasimhan and Sri Ranjan demonstrated that a voltage gradient of $0.25\,\text{V cm}^{-1}$ applied to 11 m embedded electrodes with a 2 m anode-cathode separation depressed the water table by 14 m [37]. Also, Simpanen et al. reported the successful application of vapor extraction (for five months) to reduce the concentration of petroleum-derived volatile organics from 10 000 ppm to ~200 ppm after the six-month electroosmotic dewatering of a contaminated site under $\text{grad}(\varphi) = 0.5\,\text{V cm}^{-1}$ [38].

A conventional EKB can also enhance the remediation of soluble species by the pump-and-treat method [4, 37]. In this application, the arrangement of the electrodes should be reversed so that electroosmotic flow can provide the required water and promote contaminant dissolution. Thus, the EKB is used to elevate the water

UNCORRECTED PROOFS

Trim Size: 170mm x 244mm Single Column Loose Ribeiro670117 c16.tex V1 - 12/11/2020 10:16pm Page 369

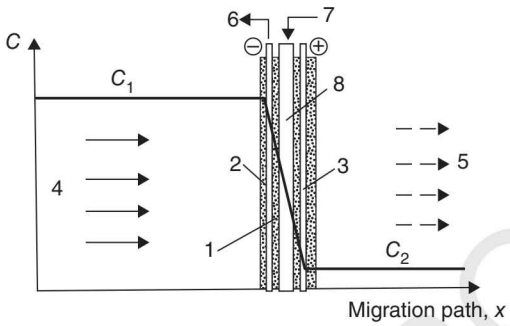

Figure 16.2 Conceptual scheme of a conventional electrokinetic barrier (EKB) applied with simultaneous pumping out (elevation view): 1, electrokinetic barrier zone; 2, cathode; 3, anode; 4, contaminated flow; 5, purified flow; 6, contaminated filtrate being piped out; *C*, contaminant concentration; C_1, initial contaminant concentration; C_2, contaminant concentration after treatment.

table at a contaminated site to facilitate migrating and pumping out a pollutant such as a heavy metal. Combining an EKB with the pump-and-treat method is the simplest and the most widely used variant. In this case, a contaminant is pumped out directly through one of the electrodes. The basic scheme of a conventional EKB against a cationic pollutant with simultaneous pumping-out is shown in Figure 16.2. Incorporating an EKB with other techniques is discussed in the following sections.

16.3 Electrokinetic Barrier with Ion-Selective Membranes (IS-EKB)

This type of protective EKB is shown in Figure 16.3. The chart depicts an EKB provided with ion-selective membranes (IS-EKB) along with the simultaneous application of the pump-and-treat technology. Just like a conventional EKB, it consists of the barrier working zone within the soil (1), and anode (2) and cathode rows. However, it also contains an ion-selective membrane (3), which passes the contaminant toward the corresponding electrode but stops all other ions. For such an EKB, the electrodes are installed in the inversed order. Thus, the electroosmotic flow coincides with the direction in which the contaminant is moving (4) and, consequently, facilitates its migration to the filtering electrodes.

The scheme shows the IS-EKB implementation for a cationic pollutant. In this arrangement, the ion-selective membranes (3) are adjacent to the filtering cathodes so that a cationic toxicant can be pumped out. These ion-exchange membranes can pass only cations of a specific size and hinder the others. Then a motor siphons off the electroosmotic filtrate (6), which contains only the toxic substances. Consequently, it allows the regulation of the groundwater-remediation process by pumping out only specific toxicants. Other, non-toxic solutes are left alone by the treatment.

Ion-exchange membranes can also be used to regulate soil pH to facilitate the functioning of an EKB. For instance, a cation-exchange membrane (CEM) installed near the cathode hinders the propagation of the alkaline front since it does not pass OH^- ions into the soil [39, 40]. When no other membrane is applied, a CEM promotes the acidification of soil during EKB exploitation. In turn, it can be used during EKB development against anionic toxicants (see Section 16.2.2) when the electroosmotic flow should be diminished or reversed.

UNCORRECTED PROOFS

Trim Size: 170mm x 244mm Single Column Loose Ribeiro670117 c16.tex V1 - 12/11/2020 10:16pm Page 370

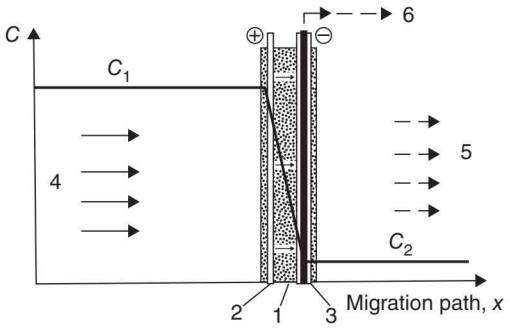

Figure 16.3 Conceptual scheme of an electrokinetic barrier with ion-selective membranes (IS-EKB): 1, electrokinetic barrier zone; 2, anode; 3, ion-selective membranes at the cathode; 4, contaminated flow; 5, purified flow; 6, contaminated filtrate being piped out; C, contaminant concentration; C_1, initial contaminant concentration; C_2, contaminant concentration after treatment.

In contrast, an anion-exchange membrane (AEM) can help stop the movement of the acidic front by preventing H^+ from entering the soil [41, 42]. So, it facilitates the movement of the alkaline front if no other membranes are set within the barrier system. In turn, soil alkalization enhances the direct electroosmotic flow (from the anode to the cathode). Also, heavy metals (such as Cu, Pb, Cd) will form hydroxides and precipitate in the high-alkaline medium near the cathode. That way, a partial hydraulic barrier can be formed in the way of the contaminated flow. Thus, an AEM is the most effective ~~barrier~~ in a barrier system developed against heavy metal pollution.

Furthermore, using both ion-exchange membrane types (CEM at the cathode and AEM at the anode) alongside the pump-and-treat technique allows the remediation of heavy metals from groundwater flow. In this case, the soil pH is maintained at the same level during the entire barrier application, so heavy-metal mobility does not change within the inter-electrode space (no additional mobilization near the anode or precipitation at the cathode). Thus, a toxicant can be hindered by the barrier and simultaneously siphoned off through the filtering cathode.

To sum up, using ion-exchange membranes in an EKB system affects the contaminant mobilization rate and soil electrokinetic parameters ~~via the impact of the pore-solution~~ via its impact on the pore-solution pH.

16.4 Electrokinetic Barrier Based on Geosynthetics (EKG-B)

The concept of electrokinetic geosynthetics (EKGs) was developed at Newcastle University (UK) and later presented at the Third International Symposium on Geosynthetics in Japan in 1996 [43]. This technology uses geosynthetic film materials, which can act as semi-permeable membranes and are conventionally used for soil drainage, containment, or reinforcement. In addition to standard geosynthetic design, EKGs are provided with electroconductive elements that develop electrokinetic phenomena in the soil adjacent to the EKG material.

Generally, an EKG can be designed as a single electroconductive fabric or a composite material containing electrically conductive elements. The EKG materials currently used in geotechnical practice include conductive needle-punched geotextiles,

UNCORRECTED PROOFS

Trim Size: 170mm x 244mm Single Column Loose Ribeiro670117 c16.tex V1 - 12/11/2020 10:16pm Page 371

carbon-fiber materials, and modified-polyester reinforcing tapes [44, 45]. The latter can carry electric current due to the presence of conductive stringers aligned parallel to polyester reinforcing elements [45].

Recent studies undertaken in different countries (UK, USA, Australia, China, etc.) demonstrated that EKGs could be used effectively in an array of field applications [45–49]. They include but are not limited to dewatering sediments, sludges, or waste slurries; consolidating soft clays; strengthening soil; and regulating oxidation-reduction processes (in areas such as soil conditioning or sewage composting) [44, 45, 47, 50–52]. Thus, it suggests that EKGs may be applicable for use in specific electrokinetic barriers (EKG-B).

Studies of the consolidation of fine-grained soils demonstrated that EKGs could function as effectively as copper electrodes. At the same time, EKG electrodes in all the trials showed better resistance to corrosion compared to the metal ones in both normal and reverse-polarity modes [43, 53–55]. These findings also suggest that using an EKG material can provide more durability and cost efficiency of EKBs.

Table 16.1 shows 14 different functions of EKG that are the essence of this technology, and their possible applicability to EKBs [44, 45, 52]. Notably, in addition to the electrokinetic functions of a conventional EKB (retention of water and solutes, electrically induced chemical reactions), an EKG-B can provide specific effects of geosynthetics that may be useful to halt contaminant movement. These effects include membrane action and sorption by geotextile material so that a contaminant can be retained by additional physical, physico-chemical, or chemical means. Considering the membrane action of geosynthetic material, one can conclude that an EKG-B will function as an IS-EKB (see Section 16.3). Also, soil reinforcement in the barrier zone is a valuable addition provided by geosynthetics.

Table 16.2 lists the primary processes that take place during EKG application and their possible use in EKG-Bs.

The heat produced by the passage of current can be a beneficial addition if EKG is used in a bio-electrokinetic fence since it increases microbial activity (see Section 16.5).

The form of an EKG used in EKB development depends primarily on the field in which it will be practically applied. The most suitable form for a conventional barrier based on EKG against a polluted flow is an electrokinetic filtration drainage curtain (eFDC). In the case of toxicant containment within a waste reservoir (landfill or tailings basin), the proper EKG configuration should be an electrokinetic mat (eMat) [44].

EKBs are often applied in combination with the pump-and-treat technique through filtering electrodes (usually, cathodes). In this scenario, the most suitable EKG forms are electrokinetic prefabricated vertical drains (ePVDs) or, in some cases, electrokinetic prefabricated (horizontal or subhorizontal) drains (ePDs) [44].

16.5 Bio-Electrokinetic Protective Barrier (Bio-EKB)

Numerous organic contaminants can be biologically destroyed by using microorganisms. A combination of bio-reclamation techniques and an EKB (bio-electrokinetic

UNCORRECTED PROOFS

Trim Size: 170mm x 244mm Single Column Loose Ribeiro670117 c16.tex V1 - 12/11/2020 10:16pm Page 372

Table 16.1 Functions of electrokinetic geosynthetics (EKG) with respect to their possible application in EKB development.

	Function	Effect
Electrokinetic (electrically induced) EK	*Electroosmosis*	*Water flow (counterflow against hydraulic flux)*
		Pore-water pressure change
		Volume change
	Electrophoresis	*Particle movement (retaining charged micellar contaminants)*
		Particle orientation
	Electromigration	*Solute movement (hindering ionic contaminants)*
	Electrolysis of water	*Oxygen emission (oxidizing contaminants/pathogens at the anode)*
		Hydrogen emission (reducing contaminants at the cathode)
		Change in pH of the soil pore solution (increase or decrease in the mobility of ions)
	Heating	Joule heating (electrode)
		Resistive heating (soil)
	Oxidation reactions	Soil cementation Reduction in soil plasticity
		Oxidation of a contaminant
	Reducing reactions	Electro-winning of metal ions
		Evolution of ammonia *Reduction of a contaminant*
Geosynthetic G	Drainage	Water flow Gas flow
	Reinforcement	Tensile strength
		In-plane stiffness
	Filtration	Barrier to solids entrained in the flow
	Separation	Strengthening and prevention of mixing
	Containment	Mechanical containment of solids
	Membrane action	*Barrier to liquid flow (containing dissolved pollutants)*
	Sorption	*Capturing liquids or solutes*

Note. The effects applicable to the electrokinetic barrier (EKB) implementation are shown in *italics*.
Source: Based on Jones, Lamont-Black, and Glendinning [44]; Jones, Lamont-Black, and Huntley [45]; Jones, Lamont-Black, and Glendinning [52].

UNCORRECTED PROOFS

Trim Size: 170mm x 244mm Single Column Loose Ribeiro670117 c16.tex V1 - 12/11/2020 10:16pm Page 373

Table 16.2 Primary contributing processes and their critical parameters, effects, and practical applications for EKGs with a focus on their possible use in EKB operations.

Contributing process	Parameter	Effect	Practical application
Electroosmosis	Water flow volumetric rate $q_{EO} = K_{EO} \cdot A \cdot \text{grad}(\varphi)$	Drainage or moisturization	Draining fine-grained materials (soft soils, tailings, or sludges)
			Electroosmotic counterflow to the direct hydraulic water flow
			Draining or moisturizing the contaminated zone for remediation purposes
	Porewater pressure $u = (K_{EO}/K_h) \cdot \text{grad}(\varphi)$	Consolidating or loosening soil	Consolidating compressible materials
Electrolysis	$\Delta pH = f(j)$	Acidifying or alkalizing soil	Controlling pH
			Transforming contaminant mobility
			Contaminant precipitation at an electrode; decreasing soil K_h
	$\Delta[O_2], [H_2] = f(j)$	Changing soil redox potential	Promoting root growth and soil microbial activity
			Oxidizing or reducing a contaminant
Electrokinetic strengthening	f(pH, CEC, electrode material)	Stiffening soil or waste	Stabilizing soft soils, instable slopes, or tailings
Joule heating	$Q = i^2 R_e$ and thermal conductivity of the material (λ)	Generating heat	Increasing chemical or microbial activity

Note. Issues useful for electrokinetic barrier development are given in *italics*; f, function.
Source: Based on Jones, Lamont-Black, and Glendinning [44]; Jones, Lamont-Black, and Huntley [45]; Jones, Lamont-Black, and Glendinning [52].

UNCORRECTED PROOFS

Trim Size: 170mm x 244mm Single Column Loose Ribeiro670117 c16.tex V1 - 12/11/2020 10:16pm Page 374

barrier or Bio-EKB) can be applied to prevent the spread of an organic contaminant plume. The primary idea of deploying a biofence is to provide a homogeneous spread of microorganisms in the path of or inside the pollutant plume and create sufficient conditions for them to function [56]. Accordingly, a Bio-EKB is usually an elongated structure compared to a conventional EKB. Since many microbes are charged species, their dispersion within the contaminated soil can be achieved by electrokinetics (electrophoresis).

Successful use of microorganisms to degrade toxic organic compounds requires the delivery of nutrients within the biofence area. Such nutrients include NH_4^+-, PO_4^{3-}-, K^+-compounds, oxygen donors, and micronutrients [57]. These components, once dissolved in water, can be injected through the electrodes and dispersed in soil electrokinetically along with microorganisms.

The majority of applied microorganisms need neutral pH conditions. Therefore, a biofence is usually constructed with an electrolyte-circulation system [56]. It mixes the anolyte and catholyte, prevents soil acidification/alkalinization, and maintains an electrolyte pH $\approx$ 7.

The heat generated at the electrodes provides an additional benefit for microorganism activity. The optimum temperature for bioreclamation in a city environment is around 40–50 °C [58].

An electrokinetic biofence was used to remediate a site at Waldervank (the Netherlands) contaminated with volatile organic compounds (VOCs) [56, 57]. The initial concentration of volatile chlorinated hydrocarbons in the soil was around 10 000 ppm. In this project, the biofence was installed perpendicularly to the groundwater flow to ensure the dispersion of charged nutrient species by electromigration. The solid nutrients were packed into infiltration wells up-gradient to the contaminated flow so that they could dissolve gradually during the remediation. After the Bio-EKB had run for about two years, most of the perchloroethylene (PCE) had degraded to vinyl chloride, and its concentration decreased by a factor of 4. Electric energy was provided by solar panels in this study or obtained from the grid at night and on cloudy days.

A similar technique was used to treat soil contaminated with chlorinated compounds at Zeist [58]. In this case, the reclamation project included two separate stages. First, the soil was heated electrically for two years to volatilize part of chlorinated solvents and pump them as vapor. The electrode setup functioned as a Bio-EKB for 2.5 years to biodegrade the heavy fractions of contamination. After 4.5 years of reclamation, the soil was almost entirely clean.

Another variant of Bio-EKB deployment is shown in Figure 16.4. This barrier consists of at least two rows of anodes (3) and cathodes (2) installed in the soil (1). In this configuration, electroosmotic flow hinders the propagation of contaminated flow. The soil between the electrodes can be optionally consolidated to decrease its hydraulic permeability.

An additional row of infiltration wells (8) is established between the electrodes. These wells are used to inject the microorganism-containing solution (7), which destroys or chemically transforms the contaminant (4). Part of the electroosmotic filtrate containing the contaminant (6) can be pumped out of the filtering cathodes

UNCORRECTED PROOFS

Trim Size: 170mm x 244mm Single Column Loose Ribeiro670117 c16.tex V1 - 12/11/2020 10:16pm Page 375

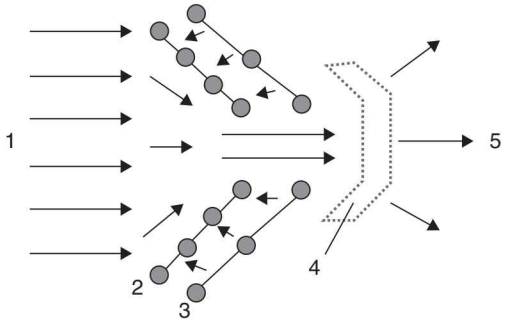

Figure 16.4 Cross-section of a bio-electrokinetic protective barrier (Bio-EKB): 1, semi-permeable barrier zone; 2, cathode; 3, anode; 4, contaminated flow; 5, purified flow; 6, contaminated filtrate being piped out; 7, microorganism-carrying solution being injected; 8, infiltration well; C, contaminant concentration; C_1, initial contaminant concentration; C_2, contaminant concentration after treatment.

(2) if necessary. As a result, the contaminated flow (4) can be treated successfully, and the contaminant level in the flow behind the fence (5) will meet the legal requirements.

The microorganism culture is chosen primarily based on the nature of the contaminant. Other issues to be taken into account are the strain's living conditions (T, nutrient concentration, etc.) and its ζ potential so that it migrates in the desired direction.

In addition, this configuration allows the regulation of temperature in the soil body of the fence (1), which is essential for microorganism activity. This barrier can also be supplied with sensors for temperature or strain concentration, which can be used to monitor the reclamation process.

Several lab-scale studies were carried out to prove the applicability of bio-electrokinetic reactive barriers (Bio-EKBs or Bio-PRBs) to remediate soil. This type of biofence is created by saturating the soil segment between the electrodes with a microbial strain and nutrients.

For instance, Mena Ramírez et al. developed an electrokinetic Bio-PRB in the form of a biofilm reactor against diesel contamination [59]. The voltage gradient applied was $1\,V\,cm^{-1}$. Sodium dodecyl sulfate was used in this study to emulsify hydrocarbons and increase their bio-availability. As a result, 39% of the biodegradable hydrocarbon fraction was removed, and the total diesel removal rate was 27% after the barrier had functioned for 336 hours.

Barba and co-authors conducted tests on the applicability of an electrokinetic Bio-PRB against 2,4-dichlorophenoxyacetic acid. The trials continued for 10 days with $\text{grad}(\varphi) = 1\,V\,cm^{-1}$ and electrode-polarity reversal two times per day [60]. The total removal efficiency achieved was 85%. The same researchers carried out similar lab tests on the bio-degradation of oxyfluorfen [61]. However, the maximum removal rate achieved in the two-week experiment was only 11% for this contaminant.

UNCORRECTED PROOFS

Trim Size: 170mm x 244mm Single Column Loose Ribeiro670117 c16.tex V1 - 12/11/2020 10:16pm Page 376

Finally, Bio-EKBs can remove some inorganic pollutants. Kaimbi and Chirwa applied a biofence with cultures of *Bacillus mycoides*, *Lysinibacillus fusiformis*, and *Micrococcus lylae* for the reduction of Cr(VI) to Cr(III) [62]. The transformation rate of Cr(VI) was 75% within 63 days of barrier use. After that, Cr(III) precipitates were removed by washing the soil with acid.

16.6 Electrokinetic Permeable Reactive Barriers (EK-PRB)

A permeable reactive barrier (PRB) represents a protective buffer wall made of a reactive material within the soil mass in the path of contaminated groundwater flow. A conventional PRB is semipermeable: it passes water but accumulates the targeted contaminant by various means. The development of such protective fences is more effective in many cases than the construction of absolutely impermeable barriers.

For instance, partial barrier permeability is essential for constructing accumulation reservoirs containing liquid, toxic wastes. The rapid filling of such reservoirs with impermeable beds lowers their effectiveness and requires new storage basins. However, when the floor of such a basin can infiltrate water but hinder pollutant migration, its effectiveness increases many times over.

In EK-PRB technology, semipermeable barriers are used together with electrokinetic fences [63]. The activity of these combined barriers can be achieved in many ways: chemical, physical, physico-chemical, and biological. Chemical activity is provided with toxicant chemosorption or chemical degradation. Physical approaches include mechanical colmatation or the impact of various physical fields (usually thermal or electromagnetic). In turn, the physico-chemical mechanism is represented by adsorption. Finally, using various microorganisms can provide a biological protection mechanism, as described in Section 16.5.

The basis for such barriers is a reactive segment embedded into dispersive soil. This reactive part is framed with compacted soil (from clays to silty sands in granulometric composition) so that the width of the entire barrier zone reaches at least 50–100 cm. The electrokinetic function of an EK-PRB is provided by installing anodic and cathodic rows.

The primary processes that occur within the barrier body are as follows:

a) Accumulation (adsorption, colmatation) or transformation (oxidation/reduction, decomposition) of the contaminant
b) Electromigration of solute species
c) Electroosmotic filtration of water

As a result of applying an EK-PRB, the contaminant concentration in the filtrating flux decreases to an acceptable value so that the clean flow releases the reactive barrier sector.

There are several possible designs for installing an EK-PRB in the field. For example, a popular approach is the “funnel-and-gate” technique [64, 65]. In this technology, an active barrier is installed in the path of contaminated groundwater

UNCORRECTED PROOFS

Trim Size: 170mm x 244mm Single Column Loose Ribeiro670117 c16.tex V1 - 12/11/2020 10:16pm Page 377

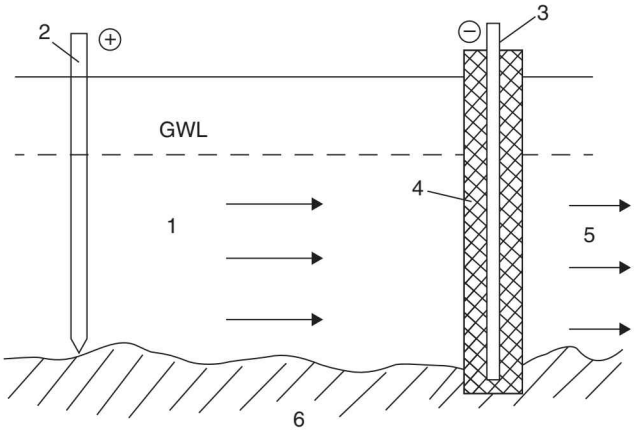

Figure 16.5 General draft (plan view) for the funnel-and-gate design of an electrokinetic permeable reactive barrier (EK-PRB) on the migration path of contaminated groundwater: 1, contaminated-water flow direction; 2, cathode row; 3, anode row; 4, reactive sorption-filtration gate; 5, purified groundwater flow.

flow (1), which is directed by an electrokinetic fence (Figure 16.5). The rows of cathodes (2) and anodes (3) are installed angle-wise to the contaminated flow (1). Electroosmotic flow counteracts the hydraulic flux and directs it toward the PRB (4). Physico-chemical interaction between the toxicant and reactive material occurs here, and clean water (5) passes behind the barrier.

The other configuration for an EK-PRB is shown in Figure 16.6. In this variant, the cathodes (3) are installed straight into the PRB body, while the anodes (2) are set up-gradient to the contaminated flow. Electroosmosis promotes the filtration of the contaminated groundwater (1) into the reactive barrier sector (4), toxicants are accumulated within it, and clean water (5) passes behind the PRB.

An EK-PRB can also be used with other techniques such as pump-and-treat. In this case, the cathodes may be used as filtering electrodes so that they can periodically pump out the accumulated toxicants. That can be achieved using desorbing agents within the barrier body when the power is off. Thus, the functional life of a PRB can be prolonged.

An overview of the applicability of various reactive materials in EK-PRBs is given next.

16.6.1 EK-PRBs Based on Activated Carbon

Activated carbon (AC) and carbon-containing products can be applied against both inorganic (heavy metals) and organic pollutants. The primary reactive mechanism of this material is adsorption for both types of contaminants.

For instance, an EK-PRB made with AC placed near the cathode was deployed by Zhao and co-authors against 2000 ppm Cu^{2+} contamination in kaolin [66]. The voltage gradient applied was 1 V cm^{-1}. The average removal efficiency achieved

UNCORRECTED PROOFS

Trim Size: 170mm x 244mm Single Column Loose Ribeiro670117 c16.tex V1 - 12/11/2020 10:16pm Page 378

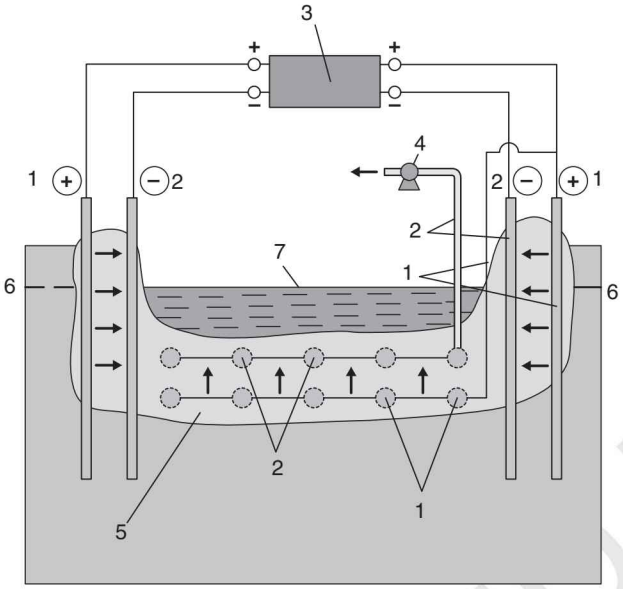

Figure 16.6 Cross-section of a combined electrokinetic permeable reactive barrier (EK-PRB): 1, contaminated groundwater flow; 2, anode; 3, cathode; 4, permeable reactive barrier; 5, purified groundwater flow; 6, underlying bed; GWL, groundwater level.

was around 97% for four days. In this lab-scale study, pH control (citric acid-sodium citrate buffer) was used to prevent the formation of Cu precipitates in the cathodic zone.

Ghobadi et al. studied the feasibility of using AC and biochar (BC) to remove Cu^{2+} from kaolinitic clay as well [67]. Trials under the constant grad(φ) = 1 V cm^{-1} demonstrated better Cu^{2+} uptake by BC (27%) than by AC (10%). Additional tests conducted with a constant current (i = 20 mA) showed almost total cleanup of Cu from the anodic and central zones but no general improvement in the total barrier adsorption rate. Leaching experiments showed around 99% Cu recovery for BC and 78% for AC, proving that the metal can be remediated successfully from the barrier body.

Vieira dos Santos et al. reported the results of a study applying granulated activated carbon (GAC) as a reactive medium combined with a reversible electrokinetic barrier (REKB) technique against herbicides [68]. The herbicides under study were atrazine and oxyfluorfen. Sodium dodecyl sulfate was used as a flushing solution. Using periodic polarity reversal prevented soil acidification and provided optimal conditions for the PRB to function. After 15 days, only 10% of the initial herbicide remained in the soil.

A study by Rodrigo's group revealed the successful application of a similar GAC-based PRB coupled with the REKB technique to remove clopyralid from clay soil [69]. Within 30 days, 57% removal was achieved.

UNCORRECTED PROOFS

Trim Size: 170mm x 244mm Single Column Loose Ribeiro670117 c16.tex V1 - 12/11/2020 10:16pm Page 379

16.6.2 EK-PRBs Based on Iron Compounds

This type of EK-PRB is the most widely used for remediating groundwater and soils. Iron-based barriers can be developed against heavy metals both as cations (Pb^{2+}, Cd^{2+}) and anions ($Cr_2O_7^{2-}$, AsO_4^{3-}) and chlorinated organic compounds. Such PRBs include two primary variants: zero-valent iron (ZVI) barriers and barriers based on ferric/ferrous compounds.

16.6.2.1 ZVI-Based EK-PRBs

ZVI is the most popular reactive material used for subsurface remediation. It was successfully used in conventional PRBs to remove such contaminants as dense non-aqueous-phase liquids (DNAPLs) and Cr(VI) [70–73]. The primary reason to use ZVI is that it can destroy recalcitrant pollutants, creating non-toxic products; it is also relatively inexpensive [63]. The main flaw of this material is that it corrodes quickly in the presence of oxygen. So, a ZVI-PRB can stop functioning before the desired remediation level is achieved for the targeted contaminant because of low hydraulic velocity in fine-grained soils. Combining electrokinetics with the PRB can overcome this limitation [63, 65].

Many researchers have studied the applicability of Fe^0 for use in an EK-PRB system. One of the most investigated fields is applying such a barrier against Cr(VI) contamination. The preliminary remediation mechanism, in this case, is the reduction of $Cr_2O_7^{2-}$, CrO_4^{2-}, or $HCrO_4^-$ to Cr^{3+} in the acidic medium [63]. This process can occur in a wide pH range (up to pH = 7). However, the reaction proceeds most rapidly in an acidic medium (pH < 3.5) so the Cr(VI)-contaminated water does not need to travel as far before total recovery. Also, partial dissolution of Fe^0 by acid takes place with the release of iron into solution as Fe^0 or Fe^{2+}. These species can react with Cr(VI) compounds as well, reducing them to Cr^{3+}.

An additional effect of Cr(VI) removal is its adsorption onto Fe^0 microparticles, which is also favored by acidic conditions. Thus, soil acidification may promote all three mechanisms of Cr(VI) removal, and thinner barriers will be needed for complete soil and groundwater remediation [63].

Weng et al. demonstrated the applicability of a ZVI-PRB coupled with electrokinetics to remediate 1150 ppm Cr(VI) pollution from clay soil and groundwater [74]. The barrier was composed of ZVI and silica sand at a 1 : 1 weight ratio (w/w) and functioned under $\text{grad}(\varphi) = 2\ \text{V cm}^{-1}$. The six-day run of the EK-PRB resulted in the complete reduction of Cr(VI) compounds (100%) and a total recovery rate of 60–70%. The optimal barrier position was near the cathode or in the middle of the soil section to achieve the highest electroosmotic permeability of the entire soil system.

A study by Weng's group investigated the ability of a similar barrier to recover hyper-Cr(VI)-contaminated clay (2497 ppm) under various electric gradients [75]. In this study, the barrier was placed in the middle section of the soil specimen. Reversed electroosmotic flow was observed during the tests, possibly due to high concentrations of CrO_4^{2-} and $HCrO_4^-$ and their dominance in soil EDLs. This effect hindered the movement of H^+ ions into the soil and promoted the propagation of the alkaline front. In turn, it increased Cr(VI) desorption but decreased the rate of its reduction to

UNCORRECTED PROOFS

Trim Size: 170mm x 244mm Single Column Loose Ribeiro670117 c16.tex V1 - 12/11/2020 10:16pm Page 380

Cr^{3+}. The maximum Cr(VI) reduction efficiencies achieved were 86 and 93% under voltage gradients of 1 and 2 V cm^{-1}, respectively.

The other promising direction for ZVI use in EK-PRB systems is recovering metalloid compounds (such as As and Se). The preliminary removal mechanisms, in this case, are adsorption and surface precipitation onto barrier compounds. Yuan and Chiang investigated the effectiveness of ZVI and goethite (FeOOH) as a PRB medium in silty loam against anionic As(V) contamination of 966 ppm [76]. The As(V) species were represented by AsO_4^{3-} and $HAsO_4^{2-}$ ions. The PRB was placed in the middle of the soil specimen, and the operating voltage gradient was 2 V cm^{-1}. The barrier medium was a mixture of a reactive material and silica sand in a 1 : 2 w/w ratio. The maximum removal efficiency achieved within five days for the ZVI barrier was 51%. Interestingly, the PRB made of FeOOH demonstrated better results, with an As(V) recovery rate of 60% during the same term. This was attributed to the larger surface area of goethite in comparison to ZVI. Generally, As(V) removal was enhanced 1.6–2.2 times compared to the system without a barrier.

Yao et al. reported data on remediating actual As-contaminated soil using an EK-PRB based on Fe^0 under grad(φ) = 1 V cm^{-1} for 96 hours [77]. Applying a ZVI-PRB resulted in the reduction of As(V) concentrations in the central and anodic parts of the soil specimen and a total recovery rate of 20%. In addition, the EK-PRB combined with an approaching cathode allowed As removal of 45%. This effect is likely due to the propagation of the alkaline front enhancing desorption of As(V) from the soil particles.

Huang et al. investigated the behavior of ZVI nanoparticles (nZVI) carried by AC as a reactive medium to recover Se(VI)-contamination with an EK-PRB [78]. A maximum Se(VI) removal efficiency of 94% with a corresponding reduction rate of 68% was achieved under optimal test conditions: grad(φ) = 2 V cm^{-1}, initial pH = 4, 20% w/w rate of nZVI-AC in the PRB composition, and treatment time of six days.

Fe^0 barriers can also be deployed to retain cationic contaminants. For instance, Robles et al. conducted a study of soil remediation from Hg^{2+} (656 ppm) using electrokinetic treatment and Fe^0-PRB sequentially [79]. The voltage gradient applied was 3.3 V cm^{-1}. Ethylenediaminetetraacetic acid (EDTA) was used as a complexing agent for Hg^{2+} to enhance its removal in the form of $[Hg\text{-}EDTA]^{2-}$. These complexes moved to the anode due to electromigration. The removal rate of Hg^{2+} from the soil by the EK treatment was 76% after 72 hours. Water enriched with $[Hg\text{-}EDTA]^{2-}$ was then pumped from the anodic compartment and filtered through the ZVI-PRB. The recovery efficiency of Hg^{2+} from the water was 85%. Mercury ions were retained by the barrier due to their co-complexation with iron microparticles.

Finally, a ZVI-PRB coupled with electrokinetic remediation can be a useful measure against organic pollutants. Chang and Cheng evaluated the feasibility of an EK-PRB based on Fe^0 fill to remediate sandy loam polluted with PCE [80]. The initial PCE concentration was 60 ppm. The optimal voltage gradient applied was 1 V cm^{-1}. Sodium carbonate (0.01 M) was used as a buffering solution to prevent soil acidification. The study showed that the best barrier placement was near the cathode. The recovery rates achieved in this configuration within 10 days were 99 and 85% for the porewater and soil, respectively. The performance of zero-valent zinc (ZVZ) as a

UNCORRECTED PROOFS

Trim Size: 170mm x 244mm Single Column Loose Ribeiro670117 c16.tex V1 - 12/11/2020 10:16pm Page 381

reactive material under the same conditions (optimal electric strength of 2 V cm^{-1}) was even better, showing 90% recovery efficiency for soil.

Similar research was carried out by Kebria et al. [81]. A Fe^0 barrier 1 cm thick was installed in the middle of the electrokinetic cell. Triton X-100 (TX-100) served as a surfactant in this study. The optimum conditions for the trials were grad(φ) = 2 V cm^{-1} and 0.005 M TX-100. A maximum average PCE removal rate of ~66% was achieved in the 10-day run (with 78% removal in the anodic zone).

Ren et al. conducted a study to estimate the effectiveness of ZVI/AC (Fe/C) mixture as a reactive medium in an EK-PRB to remediate phenanthrene (189 ppm) from soil [82]. The PRB was placed near the cathode. The optimal remediation conditions were Fe/C mass ratio of 4 : 1, grad(φ) = 2 V cm^{-1}, and applying Tween 80 as a surfactant and NaOH as a buffering agent. The best removal rate of phenanthrene from the soil, achieved under these conditions after five days of treatment, was 26%, including 23% by EK-PRB action alone.

Summing up, a ZVI-PRB, coupled with EK treatment, proved to be a feasible technology for removing numerous contaminants in a lab. However, its performance in field conditions can deteriorate due to the following effects [63]:

- Pores being clogged by the precipitation of Cr^{3+}, Fe^{3+}, Fe^{2+}, etc.
- Fe^0 corrosion caused by O_2 dissolved in water and generated at the anode
- Reaction of Fe^{2+} species with other anions occurring in groundwater such as sulfates, chlorides, carbonates, or phosphates

Using iron-reducing bacteria can recover the remedial properties of a Fe^0-PRB (by converting Fe^{3+} to Fe^{2+}) and promote its long-term performance [83].

16.6.2.2 EK-PRBs Based on Ferric/Ferrous Compounds

The other type of Fe-PRBs is based on Fe^{2+} or Fe^{3+} species. A promising reactive material of that kind is atomizing slag, usually containing around 25–40% Fe_2O_3. Chung and Lee tested the ability of slag to recover trichloroethylene (TCE) and Cd (both 300 ppm concentration) from natural clayey soil under a voltage gradient of 2 V cm^{-1} [84]. Two slag-based PRBs were placed in the electrode compartments. The average removal effectiveness after 200 hours of treatment was 90% for Cd and 85% for TCE.

Later, these authors conducted field trials of removing chlorine and arsenic compounds from the soil at a landfill area using an EK-PRB system based on atomizing slag [65]. The increase in Cl^- concentration observed during the tests marked the destruction of chlorine organic species due to their reaction with the slag. Significant retention of As by the PRB also took place during the treatment process. The arsenic removal rate was ~2.5 times higher than that in system with EK only.

Another promising remediation technology is the construction of Fe barriers (iron pans) within the soil using electrokinetics (in situ) [85–87]. Sacrificial iron electrodes are used as a source of iron ions in this technique. Applying a low-intensity DC electric field provokes the formation of a pH gradient between the electrodes: pH ≈ 2 near the anode and pH > 13 at the cathode. The acidic conditions cause the dissolution of the sacrificial anodes and release of Fe^0, Fe^{2+}, or Fe^{3+} species in the pore

UNCORRECTED PROOFS

Trim Size: 170mm x 244mm Single Column Loose Ribeiro670117 c16.tex V1 - 12/11/2020 10:16pm Page 382

solution. They move to the cathode by electromigration and electroosmosis and precipitate in the middle of the treated soil mass as the soil pH increases. Thus, a PRB made of native iron, ferric and ferrous oxides, and oxyhydroxides is formed, possessing a large surface area.

Such a barrier was developed by Cundy and Hopkins in batch-scale tests of remediating contaminated Cumbria sediment [85]. The voltage gradient of 0.09 V cm^{-1} was applied for 410 hours (17 days) to create a Fe-rich band within the sediment. The pH gradient developed within 15 days of the treatment was 2–13. Significant enrichment of the barrier body by contaminants, compared to their initial levels, was observed within the barrier body: 50% for radionuclide ^{60}Co and 100% of As. An additional benefit was an increase in the sediment's unconfined shear strength, which became comparable to that of moderately lithified sandstone.

Faulkner et al. demonstrated that the size of the created iron band strongly depends on the electric strength applied [86]. The Fe-rich barrier thickness was only 1 cm at grad(φ) = 0.13 V cm^{-1}, while it reached the entire 6 cm when grad(φ) = 0.53 V cm^{-1} was applied. This study also showed the ability of a Fe-PRB constructed in sand to self-heal under the same voltage gradient after a rupture.

Finally, Cundy et al. proved the feasibility of an iron pan to accumulate Zn^{2+} ions [87]. The enrichment of the barrier with this contaminant was up to 100% compared to its initial level in the soil.

16.6.3 EK-PRBs Based on Red Mud

Red mud is a residue of bauxite refinement in the aluminum production process. This by-product can be treated later to make it environmentally safe, thus forming transformed red mud (TRM). TRM is a mixture of Al- and Fe-containing minerals such as gibbsite, hematite, hydrotalcite, diaspor, and others. This material possesses a large surface area and can serve as a remedial media for PRB construction.

De Gioannis et al. applied an EK-PRB made from TRM (Bauxsol) to remediate 1000 ppm Cr(VI) contamination from kaolin [88]. The electric gradient induced was 1 V cm^{-1}, and the barrier was adjacent to the anode. When the PRB consisted of 15 g TRM (0.75% w/w of the entire soil mass) and the test was run for six days, Cr(VI) removal reached 54%, with 34% trapped by the barrier. Increasing the TRM mass to 30 g (1.5% w/w) and extending the trial duration to 12 days resulted in removing 93% of total Cr(VI), with 40% trapped by the PRB.

The primary remedial mechanism of TRM for Cr(VI) removal is suppressing the acidic front generated at the anode. It promotes Cr(VI) desorption under alkaline conditions and prevents its reduction to less mobile Cr^{3+}. In the mentioned study, the Cr(VI) transformation rate decreased in the EK-PRB tests as compared to the EK-only trials, from 72 to 42% and 93 to 60% for the 6- and 12-days runs, respectively. At the same time, the interaction of TRM with acid improves PRB adsorptive properties due to the increase in its surface area.

A subsequent study by Muntoni's research group assessed the ability of the TRM-based EK-PRB to treat illitic-kaolinitic soil with 1000 ppm Cr(VI) and 100 ppm As contamination under the same experimental conditions [89]. The

UNCORRECTED PROOFS

Trim Size: 170mm x 244mm Single Column Loose Ribeiro670117 c16.tex V1 - 12/11/2020 10:16pm Page 383

Cr(VI) recovery rate was 40% (with 21% trapped by the PRB) after six days and 87% (with 26% captured by the barrier) for the 12-day run. When the TRM content was increased to 8.3% w/w of the entire soil mass, 61% of total Cr(VI) was retained in the PRB after 12 days. However, EK-PRB treatment was not efficient for As removal in any test configurations.

16.6.4 EK-PRBs Based on Zeolites

Zeolites are an attractive material for remediating soils contaminated with heavy metals due to their high adsorption capacity. However, their applicability is hindered by the low leachability of some contaminants after uptake by a zeolite-based PRB [90]. So, zeolite barrier material cannot be treated in situ after it loses its effectiveness and requires an exchange. A promising solution is a surface modification of zeolites or their application in combination with other reactive materials.

Yu et al. conducted tests using zeolite-based EK-PRBs to recover Cr(VI)-contaminated soil [91]. A zeolite modified with cetyltrimethylammonium bromide (CTMAB-Z) and a mixture of CTMAB-Z and Fe^0 were used as reactive media for the barrier. Each PRB was placed at the anode. The highest removal efficiency (81%) was achieved during the application of mixed PRB at grad(φ) = 2.5 V cm^{-1} with 0.15 M DL-tartaric acid as the pore solution after eight days.

Zhou et al. evaluated the behavior of an EK-PRB based on a mixture of zeolite and ZVI at 1 : 1 w/w to remediate kaolin contaminated with 300 ppm Cd [92]. A new style of EK setup was used in this study: the cathode was installed inside the PRB, and several anodes surrounded the cathode. The highest remediation rate (93%) was achieved after five days under an electric gradient of 3 V cm^{-1} and with a soil moisture content of 40%.

16.6.5 EK-PRBs Based on Clays or Modified Soils

In some cases, soils themselves can serve as reactive materials against various contaminants. One option is active clays (ranging from poorly crystallized kaolins to bentonites), which can be used to adsorb toxicants such as heavy metals and function as a material for protective liners in landfills or contaminant-storage reservoirs [93, 94]. Coupling clay liners with electrokinetic barriers can be a promising technique to contain various toxicants.

The effectiveness of an EK-PRB made from clay depends greatly on the parameters of its electric double layer (EDL). Considering the dependence of the clay-particle ζ potential on the pore-solution pH (see Chapter 15 of this book), one can assume that it is possible to regulate the protective adsorption properties of clay by varying its pH [25].

High pH increases the magnitude of a negative ζ potential and decreases the permeability of clay. So, an alkaline medium generally improves the ability of clay to adsorb cationic pollutants such as heavy metals. Kaolins possess positive ζ values in acidic conditions (pH < 2) [19, 25]. However, most studies did not observe a change in the surface-charge sign of clay particles for illite clays and bentonites [21, 23].

UNCORRECTED PROOFS

Trim Size: 170mm x 244mm Single Column Loose Ribeiro670117 c16.tex V1 - 12/11/2020 10:16pm Page 384

Consequently, the ability of clay minerals to retain anionic pollutants (e.g. $HCrO_4^-$ or $HAsO_4^{2-}$) is limited to kaolins in strongly acidic conditions.

Furthermore, the range of maximum positive ζ potential values observed for Ca-Glukhovtsy kaolin was capped at 0.8 pH units versus 2.8 pH units of extreme negative ζ magnitudes observed in the alkaline region (see Figure 16.6, Chapter 15). So, the optimum parameters for anionic species retention appear under particular conditions. Thus, generally, the applicability of clays to constrain toxic anions is scant.

The other possible reactive material is sandy or silty soil modified to increase its sorption capacity or reactivity while saving its permeability. These approaches include injection of stabilizing agents based on oxalate-silicate or synthetic resin (e.g. phenol-formaldehyde) composition or soil modification using chemical additives (such as lime). As a result of stabilization, sandy-gel soil is generated, which can accumulate specific toxicants and pass water.

16.6.6 Other Materials for the Creation of EK-PRBs

Some other materials can also act as reactive media to remove contaminants. Kim and Han reported on applying food scrap ash (FSA) in an EK-PRB system to remediate kaolin contaminated with Cu (500 ppm) and phenanthrene (1000 ppm) [95]. The barrier was installed at a relative distance from the anode $L/L_0 = 0.75$, and the voltage gradient induced was 1 V cm^{-1}. The tests were run for 10 days with various media used as a pore solution: double distilled water (DDW), 0.05 M acetic acid, and 0.01 M Brij 30. The removal rate of Cu was in the range 84 to 90%, with the lowest result for DDW and the highest for acetic acid. In contrast, the removal of phenanthrene was low in all the trials and did not exceed 1–2%.

Zhou et al. studied the efficacy of activated Al_2O_3 as a reactive material for the electrokinetic treatment of F-contaminated soil [96]. The electric gradient was 2 V cm^{-1}, and the PRB was situated in the center of the soil sample. The removal rate of fluorine was 76% for a 240-hour run.

The performance of a layered double hydroxide, hydrocalumite (CaAl-LDH), in an EK-PRB against Cr(VI) was estimated by Xu and co-authors [97]. The barrier was installed at $L/L_0 = 0.14$. The removal efficiency of Cr(VI) achieved 96% after 120 hours for the test executed under grad(φ) = 2.5 V cm^{-1}, in contrast to 85.5% in an EK system without the PRB. The total removal rate of Cr in the EK-PRB trial was 69%.

Zero-valent metals other than ZVI can also be used as a fill for PRBs. The performance of Zn^0 against PCE was described earlier (see Section 16.6.2.1).

The reported data for EK-PRB trials using multiple materials are summarized in Table 16.3. An overview of the applicability of various reactive media is given in Table 16.4.

UNCORRECTED PROOFS

UNCORRECTED PROOFS

Trim Size: 170mm x 244mm Single Column Loose

Table 16.3 Comparison of experimental trials utilizing EK-PRBs with various reactive materials.

			EK treatment parameters						
Reactive material	**Contaminant**	**Soil**	**Electrodes**	**grad (φ), V cm^{-1}**	**Pore solution or anolyte/ catholyte**	**Duration**	**PRB position**	**Removal rate, %**	**Reference**
Activated carbon (AC)	Cu^{2+} 1000 ppm	Spiked kaolin	Graphite plates	1	0.1 M $NaNO_3$	4 d	Close to cathode	89	Zhao et al., 2016 [66]
	Cu^{2+} 1500 ppm							92	
	Cu^{2+} 2000 ppm							97	
	U_3O_8 1000 ppm	Local U-polluted soil	Graphite plates	2	0.1 M CA + 0.03 M $FeCl_3$	5 d	Close to anode	~70	Xiao et al., 2020 [98]
Granular activated carbon (GAC)	Cu^{2+} 1000 ppm	Spiked kaolin	Graphite rods	1	Distilled water (DW)	7 d	Close to cathode	10	Ghobadi et al., 2020 [67]
	Atrazine 100 ppm; oxyfluorfen 100 ppm	Spiked kaolin	Graphite plates	1	Sodium dodecyl sulfate 1000 ppm	15 d	Middle	90	Vieira dos Santos et al., 2017 [68]
	Clopyralid 30 ppm	Spiked silty loam	Graphite rods	1	Water	30 d	Middle	57 (with electrode reversal) 45 (no reversal)	Rodrigo et al., 2018 [69]

Ribeiro670117 c16.tex V1 - 12/11/2020 10:16pm Page 385

UNCORRECTED PROOFS

Trim Size: 170mm x 244mm Single Column Loose

Table 16.3 (Continued)

			EK treatment parameters						
Reactive material	**Contaminant**	**Soil**	**Electrodes**	**grad (φ), V cm^{-1}**	**Pore solution or anolyte/ catholyte**	**Duration**	**PRB position**	**Removal rate, %**	**Reference**
Biochar (BC)	Cu^{2+} 1000 ppm	Spiked kaolin	Graphite rods	1	Distilled water (DW)	7 d	Close to cathode	27	Ghobadi et al., 2020 [67]
ZVI/sand 1 : 1 w/w	Cr(VI) 1150 ppm	Spiked clay	Graphite rods	2	Groundwater (GW)	6 d	Close to anode	100 (67% for total Cr)	Weng et al., 2006 [74]
							Middle	100 (71% for total Cr)	
							Close to cathode	100 (60% for total Cr)	
	Cr(VI) 2497 ppm	Spiked clay	Graphite rods	1	GW	6 d	Middle	86	Weng et al., 2007 [75]
				2				93	
ZVI/sand 1 : 2 w/w	As(V) 966 ppm	Spiked silty loam	Graphite rods	2	GW	5 d	Middle	51	Yuan and Chiang, 2007 [76]
ZVI	PCE 60 ppm	Spiked sandy loam	Graphite rods	1	0.01 M Na_2CO_3	10 d	Close to anode	85	Chang and Cheng, 2006 [80]
	Hg^{2+} 656 ppm	Local Hg-polluted sandy loam	Ti plates	3.3	EDTA	72 hr	Outside the soil, after EK treatment	76 (85% for water)	Robles et al., 2015 [79]

Ribeiro670117 c16.tex V1 - 12/11/2020 10:16pm Page 386

UNCORRECTED PROOFS

Trim Size: 170mm x 244mm Single Column Loose

Table 16.3 (Continued)

Reactive material	Contaminant	Soil	EK treatment parameters				PRB position	Removal rate, %	Reference
			Electrodes	grad (φ), V cm^{-1}	Pore solution or anolyte/ catholyte	Duration			
	PCE 600 ppm	Spiked clay	Graphite plates	2	0.005 M Triton X-100	10 d	Middle	66	Kebria et al., 2016 [81]
	As(V) 185 ppm	Local As-polluted clay	Graphite plates	1	0.1 M Na_2HPO_4+ 0.1 M KH_2PO_4	96 hr	Close to anode	20 (45% with approaching cathode)	Yao et al., 2019 [77]
	U_3O_8 1000 ppm	Local U-polluted soil	Graphite plates	2	0.1 M CA + 0.03 M $FeCl_3$	5 d	Close to anode	49	Xiao et al., 2020 [98]
ZVI/AC 4 : 1 w/w	Phenanthrene (PHE) 189 ppm	Spiked sandy loam	Graphite rods	1	DW	5 d	Close to cathode	14	Ren et al., 2019 [82]
				1	Tween 80 (1.5 g l^{-1})			19	
				2	Tween 80 (1.5 g l^{-1})			27	
				2	Tween 80 (1.5 g l^{-1}) + NaOH			26	
ZVI/AC 5 : 1 w/w	U_3O_8 1000 ppm	Local U-polluted soil	Graphite plates	2	0.1 M CA + 0.03 M $FeCl_3$	5 d	1 close to anode	73	Xiao et al., 2020 [98]

Ribeiro670117 c16.tex V1 - 12/11/2020 10:16pm Page 387

Table 16.3 (Continued)

Reactive material	Contaminant	Soil	EK treatment parameters: Electrodes	grad (φ), V cm^{-1}	Pore solution or anolyte/ catholyte	Duration	PRB position	Removal rate, %	Reference
							1 close to anode and 1 at $L/L_0 = 0.6$	73	
							1 close to anode and 1 in the middle	81	
							4 at $L/L_0 =$ 0.25 from each other	75	
nZVI/AC	Se(VI) and Se(IV) 4500 ppm	Synthetic soil (kaolin 50%, gypsum 49%, Na_2SeO_3 1%)	Graphite (anode), stainless steel (cathode)	0.5	0.01 M H_3PO_4 + 0.01 M K_2HPO_4	3 d	1 at anode	84	Huang et al., 2019 [78] [a)]
				1		6 d	1 at anode	85	
				2			3 barriers: 1 close to the anode, then at $L/L_0 =$ 0.33 from each other	93	
				1		9 d	6 barriers: 1 close to the anode, then at $L/L_0 =$ 0.16 from each other	89	

UNCORRECTED PROOFS

Trim Size: 170mm x 244mm Single Column Loose

Ribeiro670117 c16.tex V1 - 12/11/2020 10:16pm Page 388

UNCORRECTED PROOFS

Trim Size: 170mm x 244mm Single Column Loose

Ribeiro670117 c16.tex V1 - 12/11/2020 10:16pm Page 389

Table 16.3 (Continued)

			EK treatment parameters						
Reactive material	**Contaminant**	**Soil**	**Electrodes**	**grad (φ), V cm^{-1}**	**Pore solution or anolyte/ catholyte**	**Duration**	**PRB position**	**Removal rate, %**	**Reference**
				2			2 barriers: 1 close to anode and 1 at $L/L_0 = 0.4$	88	
				1.5		12 d	2 barriers: 1 close to anode and 1 at $L/L_0 = 0.4$	92	
FeOOH/sand 1 : 2 w/w	As(V) 966 ppm	Spiked silty loam	Graphite rods	2	GW	5 d	Middle	60	Yuan and Chiang, 2007 [76]
Atomizing slag (~30% Fe_2O_3)	Cd^{2+} 300 ppm	Spiked Kimpo clay	Graphite plates	2	Deionized water (DIW)	200 hr	2 in the electrode compartments	90	Chung and Lee, 2007 [84]
	Trichloroethylene (TCE) 300 ppm							85	
	Chlorine compounds 16 ppm	*Local contaminated soil at a landfill site*	*Stainless steel*	*1*	*GW*	*50 hr*	*At cathode*	*~80*	*Chung and Lee, 2009* [65]
	As(V) 0.08 ppm							*~60*	
	Pb^{2+} 0.8 ppm							*~75*	

UNCORRECTED PROOFS

Trim Size: 170mm x 244mm Single Column Loose

Table 16.3 (Continued)

			EK treatment parameters						
Reactive material	**Contaminant**	**Soil**	**Electrodes**	**grad (φ), V cm^{-1}**	**Pore solution or anolyte/ catholyte**	**Duration**	**PRB position**	**Removal rate, %**	**Reference**
Iron pans (Fe^0, Fe^{2+}, and Fe^{3+} compounds)	^{60}Co 0.022 Bq g^{-1}	Local multi-contaminated sediment	Fe sacrificial rods	0.09	GW	17 d	The barrier is generated within the soil (middle)	~30	Cundy and Hopkins, 2005 [85]
	As(V) 11 ppm							~20	
	Zn^{2+} 600 ppm	Local Zn-contaminated soil	Fe sacrificial rods	0.09	GW	~400 hr	The barrier is generated within the soil (middle)	~50	Cundy et al., 2007 [87]
ZVZ	PCE 60 ppm	Spiked sandy loam	Graphite rods	1	0.01 M Na_2CO_3	10 d	Close to anode	90	Chang and Cheng, 2006 [80]
Transformed red mud (TRM or Bauxsol) 0.75% w/w	Cr(VI) 1000 ppm	Spiked kaolin	Pt-covered Ti electrodes	1	DIW	6 d	Close to anode	54 (34% by the PRB)	De Gioannis et al., 2008 [88]
TRM 1.5% w/w						12 d		93 (40% by the PRB)	
TRM 1% w/w	Cr(VI) 1000 ppm	Spiked illitic-kaolinitic soil	Pt-covered Ti electrodes	1	DIW	6 d	Close to anode	39 (21% by the PRB)	Cappai et al., 2012 [89]
TRM 2% w/w						12 d		86 (25% by the PRB)	

Ribeiro670117 c16.tex V1 - 12/11/2020 10:16pm Page 390

UNCORRECTED PROOFS

Trim Size: 170mm x 244mm Single Column Loose

Ribeiro670117 c16.tex V1 - 12/11/2020 10:16pm Page 391

Table 16.3 (Continued)

			EK treatment parameters						
Reactive material	**Contaminant**	**Soil**	**Electrodes**	**grad (φ), V cm^{-1}**	**Pore solution or anolyte/ catholyte**	**Duration**	**PRB position**	**Removal rate, %**	**Reference**
TRM 8.3% w/w								61 (by the PRB only)	
TRM 1.3% w/w	As(V) 100 ppm					6 d		2 (by the PRB only)	
TRM 2.7% w/w						12 d		9 (by the PRB only)	
Zeolite modified with cethyl-trimethyl-ammonium bromide (CTMAB-Z)	Cr(VI) 504 ppm	Local Cr-polluted soil	Graphite (anode), stainless steel (cathode)	2	0.1 M KCl	5 d	Close to anode	26	Yu et al., 2019 [91][a)]
CTMAB-Z/Fe^0					0.1 M KCl			28	
					0.1 M KCl/0.1 M DL-tartaric acid			66	
					0.1 M KCl/0.1% Tween 80			58	
					0.1 M KCl/0.1 M DL-tartaric acid + 0.1% Tween 80			56	
				1.5	0.1 M KCl/0.05 M DL-tartaric acid	4 d		50	

UNCORRECTED PROOFS

Trim Size: 170mm x 244mm Single Column Loose

Table 16.3 (Continued)

			EK treatment parameters						
Reactive material	**Contaminant**	**Soil**	**Electrodes**	**grad (φ), V cm^{-1}**	**Pore solution or anolyte/ catholyte**	**Duration**	**PRB position**	**Removal rate, %**	**Reference**
				2.5	0.1 M KCl/0.15 M DL-tartaric acid			57	
				2		6 d		73	
					0.1 M KCl/0.05 M DL-tartaric acid	8 d		71	
				2.5	0.1 M KCl/0.1 M DL-tartaric acid			78	
Zeolite/ZVI 1 : 1 w/w	Cd^{2+} 300 ppm	Spiked kaolin W = 25%	Graphite columns	1.5	0.1 M citric acid (CA)	5 d	Around cathode	85	Zhou et al., 2020 [92] [a)]
				2				89	
				2.5				90	
				3				91	
		Spiked kaolin W = 40%		1.5				87	
				2				92	
				2.5				93	
				3				93	

Ribeiro670117 c16.tex V1 - 12/11/2020 10:16pm Page 392

Table 16.3 (Continued)

Reactive material	Contaminant	Soil	EK treatment parameters: Electrodes	grad (φ), V cm^{-1}	Pore solution or anolyte/ catholyte	Duration	PRB position	Removal rate, %	Reference
Food scrap ash (FSA)	Cu^{2+} 500 ppm PHE 1000 ppm	Spiked kaolin	Graphite electrodes	1	Double distilled water (DDW)	10 d	At $L/L_0 = 0.75$ from the anode	73 ~0	Kim and Han, 2020 [95]
	Cu^{2+} 500 ppm (with PHE in 1 trial)				DDW			75	
					0.05 M acetic acid			84	
					0.01 M Brij 30			81	
	PHE 1000 ppm (with Cu^{2+} in 1 trial)				DDW			~0	
					0.05 M acetic acid				
					0.01 M Brij 30				
Activated Al_2O_3	F^- 1334 ppm	Local F-contaminated soil	Graphite sheet	2	0.1 M NaOH/DW	10 d	Middle	74	Zhou et al., 2016 [96]
Activated Al_2O_3/ unpolluted sandy loam 1 : 1 w/w								76	

UNCORRECTED PROOFS

Trim Size: 170mm x 244mm Single Column Loose

Ribeiro670117 c16.tex V1 - 12/11/2020 10:16pm Page 393

UNCORRECTED PROOFS

Trim Size: 170mm x 244mm Single Column Loose

Table 16.3 (Continued)

			EK treatment parameters						
Reactive material	**Contaminant**	**Soil**	**Electrodes**	**grad (φ), V cm^{-1}**	**Pore solution or anolyte/ catholyte**	**Duration**	**PRB position**	**Removal rate, %**	**Reference**
Hydrocalumite (CaAl-LDH)	Cr(VI) 956 ppm	Spiked clay	Graphite plates	1	GW	5 d	Close to anode ($L/L_0 = 0.14$)	96 for Cr(VI)	Xu et al., 2017 [97]
	Total Cr (tCr) 1017 ppm							69 for tCr	
				1.5				52 for tCr	
				2				50 for tCr	

Note. W, moisture content, %.
a) Selected trials are given; field (in situ) test are shown in *italics*.
Source: Based onWeng [63].

Ribeiro670117 c16.tex V1 - 12/11/2020 10:16pm Page 394

Trim Size: 170mm x 244mm Single Column Loose Ribeiro670117 c16.tex V1 - 12/11/2020 10:16pm Page 395

Table 16.4 Characterization of reactive materials for their use in an EK-PRB.

PRB material	Treatable contaminants	Removal mechanism	Advantages	Disadvantages
Activated carbon (AC)/biochar (BC)	Cu^{2+} U_3O_8 Atrazine $C_8H_{14}ClN_5$, oxyfluorfen $C_{15}H_{11}ClF_3NO_4$, clopyralid $C_6H_3Cl_2NO_2$	Adsorption	High adsorption capacity Inexpensive material Good performance against Cu^{2+}, U_3O_8, and herbicides	No single recovery strategy: leaching is expensive; thermal recovery produces CO_2 and deteriorates adsorption capacity; electrochemical regeneration is still being developed [99]
Food scrap ash (FSA)	Cu^{2+} Phenanthrene $C_{14}H_{10}$	Adsorption	Recyclable material Good performance against Cu^{2+}, easy leaching of adsorbed Cu^{2+}	No effect on the removal of polycyclic aromatic compounds (PAHs)
Fe^0	CrO_4^{2-}, $HCrO_4^-$, $Cr_2O_7^{2-}$ AsO_4^{3-}, $HAsO_4^{2-}$ SeO_3^{2-}, $HSeO_3^-$, SeO_4^{2-}, $HSeO_4^-$ Hg^{2+} U_3O_8 Perchloro-ethylene C_2Cl_4, phenanthrene $C_{14}H_{10}$	Chemical reduction Adsorption Precipitation	High reactivity Multiple removal mechanisms Good performance against Cr(VI), PCE, Se(VI), and Se(IV)	Pore clogging by Fe and Cr precipitates Corrodibility by dissolved O_2 Consumption of Fe^{2+} by anions in groundwater
FeOOH	AsO_4^{3-}, $HAsO_4^{2-}$	Adsorption	The most common natural Fe mineral Large surface area (greater than that of Fe^0) Better performance for As(V) removal than Fe^0	Behavior against various toxicants is not studied enough Poor performance at high pH

UNCORRECTED PROOFS

Trim Size: 170mm x 244mm Single Column Loose Ribeiro670117 c16.tex V1 - 12/11/2020 10:16pm Page 396

Table 16.4 (Continued)

PRB material	Treatable contaminants	Removal mechanism	Advantages	Disadvantages
Atomizing slag (~30% Fe_2O_3)	Cd^{2+}, Pb^{2+} AsO_4^{3-}, $HAsO_4^{2-}$ Trichloro-ethylene C_2HCl_3, other organic chlorine compounds	Adsorption Chemical reduction	Relatively inexpensive (compared to Fe^0 or zeolite) Good performance against Cd^{2+} and TCE Performance was proved in the field	The behavior against various toxicants is not studied enough
Iron pans (Fe^0, Fe^{2+}, and Fe^{3+} compounds)	Zn^{2+} ^{60}Co AsO_4^{3-}, $HAsO_4^{2-}$	Adsorption Precipitation Chemical reduction	Constructed in situ, no excavation of soil Low energy and material consumption during construction Self-regeneration under a DC field in case of rupture	No removal of cationic contaminants behind the barrier (near the cathode)
Activated Al_2O_3	F^- and F complexes (such as AlF^{2+})	Precipitation	Good performance against F-compounds	Common Al_2O_3 requires surface modification
TRM	CrO_4^{2-}, $HCrO_4^-$, $Cr_2O_7^{2-}$ AsO_4^{3-}, $HAsO_4^{2-}$	Suppression of the acidic front, propagation of the alkaline front Adsorption	Good performance against Cr(VI)	Some co-occurring fractions of metals can barely be remobilized after adsorption; they tend to form highly insoluble minerals [88]
Zn^0	Perchloro-ethylene C_2Cl_4	Chemical reduction Adsorption Precipitation	High reactivity Multiple removal mechanisms Good performance against PCE	Pore clogging by Zn precipitates Corrodibility by dissolved O_2

UNCORRECTED PROOFS

Trim Size: 170mm x 244mm Single Column Loose Ribeiro670117 c16.tex V1 - 12/11/2020 10:16pm Page 397

Table 16.4 (Continued)

PRB material	Treatable contaminants	Removal mechanism	Advantages	Disadvantages
Zeolites	Cd^{2+} CrO_4^{2-}, $HCrO_4^-$, $Cr_2O_7^{2-}$	Adsorption	Natural compounds	Low leachability of adsorbed contaminants; require modification or use in mixture
Clays	Pb^{2+}, Cd^{2+}, Cu^{2+}, Zn^{2+} HF	Adsorption	Natural compounds Clays are widespread, can be found at the site	Require special treatment (leaching) after use
Modified soils	Pb^{2+}, Cd^{2+}, Cu^{2+}, Zn^{2+}	Adsorption	Can be modified in situ, no excavation of soil The soil can be adjusted by chemicals to adsorb a specific contaminant	Require special treatment (leaching) after use
Hydrocalumite (CaAl-LDH) $Ca_4Al_2(OH)_{12}(Cl,CO_3,OH)_2 \cdot 4H_2O$	CrO_4^{2-}, $HCrO_4^-$, $Cr_2O_7^{2-}$, various Cr^{3+} species	Suppression of the acidic front, propagation of the alkaline front Adsorption	Promising behavior to treat Cr(VI)	Performance against various toxicants is not studied sufficiently enough

16.7 Electrokinetic Permeable Reactive Barriers to Prevent Radionuclide Contamination

Electrokinetic permeable reactive barriers (EK-PRBs) can also be applied to localize radionuclide-polluted spots or RW reservoirs. It is a relevant problem for some developing countries where RW is still stored as liquid residues in accumulation basins. The draft of an EK-PRB system for RW containment is shown in Figure 16.7.

Such a barrier can be created using fillings and loamy or other soil (5), modified by a stabilizing agent (see Section 16.6.5) in the lower part of the construction, under the accumulation basin (7). Rows of filtering anodes are installed horizontally within the barrier body, and rows of filtering cathodes are set above them. The same rows of filtering electrodes are also deployed on the reservoir perimeter to develop an electrokinetic fence against the migration of RW. The electrode system is plugged into a DC supply, and then the filtering cathodes are connected to a vacuum pump

UNCORRECTED PROOFS

Trim Size: 170mm x 244mm Single Column Loose Ribeiro670117 c16.tex V1 - 12/11/2020 10:16pm Page 398

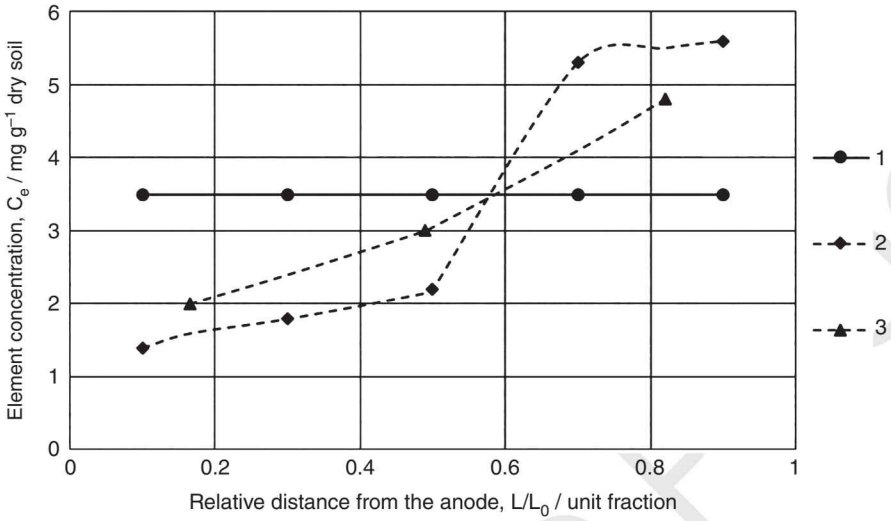

Figure 16.7 Elevation view of an electrokinetic permeable reactive barrier (EK-PRB) for a radioactive-waste (RW) containment reservoir: 1, anodes; 2, cathodes; 3, DC power supply; 4, water pump; 5, permeable reactive barrier; 6, groundwater level; 7, accumulation reservoir containing liquid RW. The arrows show the direction of electroosmotic migration.

with elastic hoses. Thus, the filtrate, enriched with radionuclides, can periodically be pumped out.

However, the protective properties of the PRB are depleted with time since it accumulates radionuclides. Electrochemical leaching can serve as an effective technique to recover the protective capacity of the barrier. This method remediates accumulated radionuclides from the PRB body without excavation of the polluted soil. During this process, a leaching anolyte is injected through the anode wells and siphoned off from the cathode wells, both under the action of a DC field. So, the entire EK-PRB system should work not only in electrokinetic protection mode but also in a containment regime accompanied by electrochemical leaching.

A project using such an electrokinetic fence was proposed by Lageman to contain the radioactive spill that occurred at the Fukushima nuclear power plant in 2011 [98]. Coupling an EK fence with a suitable PRB could make this system even more beneficial.

Another possible application of the described technology is the removal of radionuclides from already polluted soil. Xiao et al. investigated the recovery of soil contaminated with U(VI) in the form of U_3O_8 using a ZVI/AC barrier coupled with electrokinetics [100]. A set of experiments was conducted to evaluate the impact of various PRB locations: one thick barrier at the anode, one barrier at the anode and one in the center, or a series of barriers located $L/L_0 = 0.25$ from each other. The voltage gradient applied was 2 V cm^{-1}. A mixture of citric acid and $FeCl_3$ served as the pore solution. The removal efficacy achieved under the optimal conditions (two ZVI/AC barriers placed at the anode and in the center) was 81%.

UNCORRECTED PROOFS

Trim Size: 170mm x 244mm Single Column Loose Ribeiro670117 c16.tex V1 - 12/11/2020 10:16pm Page 399

The authors' research group also investigated the applicability of modified soils as a material for an EK-PRB in RW containment [101]. In particular, the study aimed to substantiate the electrokinetic method to recover the protective properties of a PRB made from sandy-gel soil. The gel:sand ratio was 1 : 2.5 w/w for the soil samples studied. This type of soil was able to adsorb the primary radioactive isotopes (such as Cs_{137}, Sr_{85}, or Ra_{226}) but passed water.

Solutions of $Sr(NO_3)_2$ and CsCl with a concentration of 10 g l^{-1} were used to model radionuclide contamination. The sandy-gel soil samples prepared using these solutions were then placed into a closed electrokinetic cell and held inside an exicator for one day to achieve physico-chemical equilibrium. After that, the cell was taken out and connected to a DC power supply. Electric current was the controlled parameter during the trials. It was held at a constant level of 20 mA by a slight increase in voltage from 20 to 30 V in the Sr experiment. In the Cs test, it was maintained at a constant value of 40 mA by a voltage increase from 18 to 27 V.

The experiments were finished after 6–6.5 hours; the samples were taken out of the cells and divided into several fragments. The final concentration of Sr or Cs in each fragment was determined by atomic-adsorption spectrometry. Then diagrams of the element distribution along the sample length were plotted according to the spectrometry data (Figure 16.8).

The chart shows that the final concentrations of Sr and Cs changed due to electromigration and electroosmotic advection. The initial concentration of both elements was 3.5 mg g^{-1}. It decreased almost twice to 1.5–2.0 mg g^{-1} in the anodic zone and increased to 4.8–5.6 mg g^{-1} in the cathodic zone. As the electroosmotic drainage of

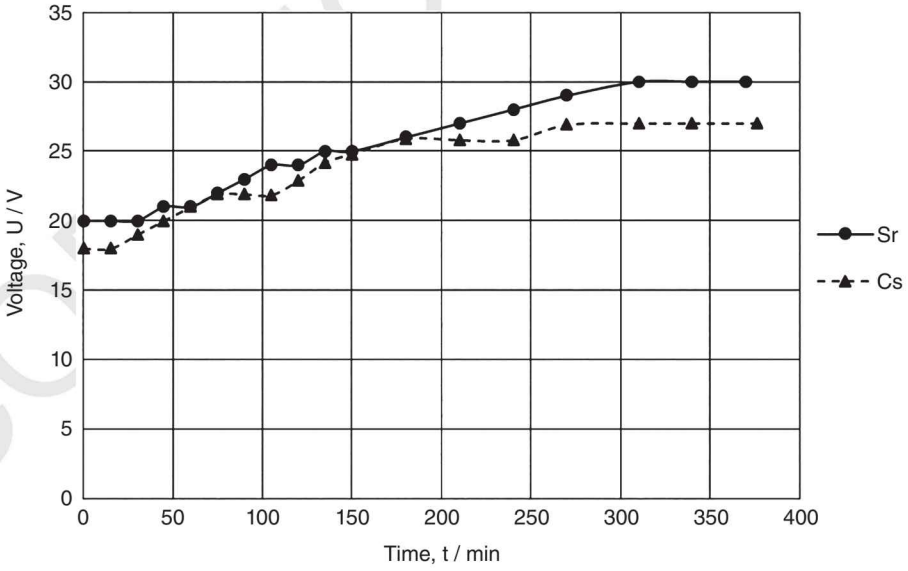

Figure 16.8 Distribution of the total Sr and Cs concentration along the length of a sandy-gel sample as a result of electrokinetic treatment: 1, initial concentration of each element; final concentration after the treatment: 2, Sr, 3, Cs.

UNCORRECTED PROOFS

Trim Size: 170mm x 244mm Single Column Loose Ribeiro670117 c16.tex V1 - 12/11/2020 10:16pm Page 400

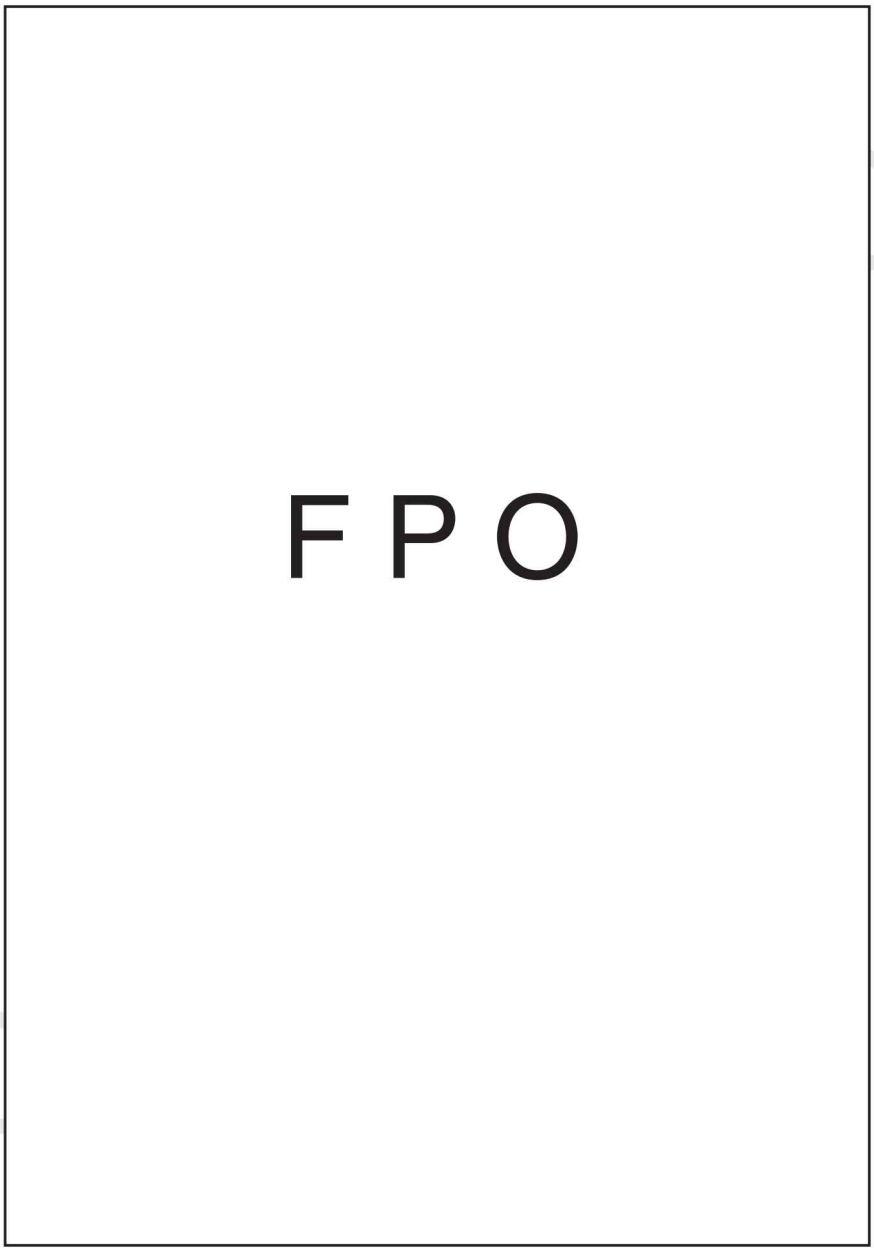

Figure 16.9 Voltage alteration in the sandy-gel samples during electrokinetic treatment for Sr and Cs at constant electric current (i = 20 mA).

UNCORRECTED PROOFS

Trim Size: 170mm x 244mm Single Column Loose Ribeiro670117 c16.tex V1 - 12/11/2020 10:16pm Page 401

the sandy-gel soil proceeded, the electric current decreased so that maintaining it at a constant level of 10 mA required a gradual increase in voltage. The voltage kinetics during the treatment are shown in Figure 16.9: the voltage increased slightly by the end of the tests (i.e. after 6–6.6 hours with the voltage on).

These trials demonstrate that sandy-gel, semipermeable walls can be used effectively to create EK-PRBs against radionuclides. Such barriers possess sufficient adsorption capacity for Sr and Cs and can be recovered from these elements electrochemically. Electrochemical regeneration of PRBs can elongate the duration of their use in industrial conditions, which sufficiently reduces economic expenditures for their maintenance.

16.8 Conclusion

Today, variants of EKBs – conventional EKB, Bio-EKB, and EK-PRB setups – have been proposed. Using them allows the efficient protection and remediation of soil and groundwater from multiple contaminants, including heavy metals, inorganic anions, organic compounds, and radionuclides.

Various barrier configurations and reactive materials were evaluated in this chapter based on their ability to remove specific contaminants. Also, possible emerging arrangements (IS-EKB and EKG-B) were suggested for practical use based on the successful application of conventional electrokinetic treatment using specific devices (ion-exchange membranes and EKG) to remediate contaminated soils.

Acknowledgments

The authors would like to thank V.V. Kucherov for his valuable contribution to the experimental data used in this chapter.

Abbreviations

A	Cross-sectional area, m^2
AC	Activated carbon
AEM	Anion-exchange membrane
BC	Biochar
Bio-EKB	Bio-electrokinetic barrier
Bio-PRB	Biological permeable reactive barrier
c_i	Solute concentration, M
C	Toxicant concentration, ppm
C_1	Initial toxicant concentration, ppm
C_2	Toxicant concentration after treatment (behind the barrier), ppm
CA	Citric acid
C_e	Element concentration, mg g^{-1} dry soil

UNCORRECTED PROOFS

Trim Size: 170mm x 244mm Single Column Loose Ribeiro670117 c16.tex V1 - 12/11/2020 10:16pm Page 402

CEM	Cation-exchange membrane
CEC	Cation-exchange capacity of the soil, meq (100 g dry soil)$^{-1}$
CTMAB-Z	Zeolite modified with cetyltrimethylammonium bromide
DC	Direct current
DDW	Double distilled water
D_i	Diffusion coefficient of a species i in dilute solution, cm^2 s^{-1}
DIW	De-ionized water
DNAPL	Dense non-aqueous-phase liquid
DW	Distilled water
eFDC	Electrokinetic filtration drainage curtain
eMat	Electrokinetic mat
ePD	Electrokinetic prefabricated drain
ePVD	Electrokinetic prefabricated vertical drain
EDL	Electric double layer
EK	Electrokinetic
EKB	Electrokinetic barrier
EDTA	Ethylenediaminetetraacetic acid
EKG	Electrokinetic geosynthetics
EKG-B	Electrokinetic barrier based on geosynthetics
EK-PRB	Electrokinetic permeable reactive barrier
F	Faraday constant, C mol^{-1}
FSA	Food scrap ash
GAC	Granulated activated carbon
GW	Groundwater
GWL	Groundwater level
H	Hydraulic head of groundwater flow, m
i	Electric current, mA
IS-EKB	Electrokinetic barrier with ion-selective membranes
j	Electric current density, A m^{-2}
K_{EO}	Electroosmotic conductivity, m^2 V^{-1} s^{-1}
K_h	Hydraulic conductivity, m s^{-1}
L	Distance from the anode, cm
L_0	Sample length, cm
L_0/L	Relative distance from the anode, unit fraction
LDH	Layered double hydroxide
n	Soil porosity, % volume
nZVI	Zero-valent iron nanoparticles
nZVI-AC	Nanoscale zero-valent iron carried by activated carbon
PAH	Polycyclic aromatic hydrocarbon
PCE	Perchloroethylene
PHE	Phenanthrene
PRB	Permeable reactive barrier
q_{EO}	Volumetric water flux of electroosmosis, m^3 s^{-1}
Q	Thermal flux, W
R	Universal gas constant, J mol^{-1} K^{-1}

UNCORRECTED PROOFS

Trim Size: 170mm x 244mm Single Column Loose Ribeiro670117 c16.tex V1 - 12/11/2020 10:16pm Page 403

R_e	Electrical resistance, Ω
REKB	Reversible electrokinetic barrier
RW	Radioactive waste
t	Time, min
T	Absolute temperature, K
TCE	Trichloroethylene
TRM	Transformed red mud
TX-100	Triton X-100 (surfactant)
u	Porewater pressure, Pa
U	Voltage, V
V_{si}	Volume fraction of a solute i (partial molar volume), l mol^{-1}
VOC	Volatile organic compound
w/w	Weight ratio
W	Moisture content of soil, % weight
x	Distance on the migration path of a toxicant, m
z_i	Ionic charge, units
ZVI	Zero-valent iron
ZVI-PRB	Permeable reactive barrier based on zero-valent iron
ZVZ	Zero-valent zinc
ε	Dielectric constant of the pore solution, units
ε_0	Permittivity of the vacuum, F m^{-1}
ζ	Electrokinetic potential of soil particles, V
η	Viscosity of the pore solution, Pa s
λ	Thermal conductivity of the material, W K^{-1}
ν_{di}	Diffusion velocity of a solute i, m s^{-1}
$\nu_{EM\,i}$	Electromigration velocity of a charged species i, m s^{-1}
ν_{EO}	Contaminant migration velocity under electroosmosis, m s^{-1}
ν_h	Solute velocity in hydraulic flow, m s^{-1}
τ	Soil tortuosity, units
φ	Electric potential, V
$[H_2]$	Concentration of aqueous and gaseous hydrogen, ppm
$[O_2]$	Concentration of aqueous and gaseous oxygen, ppm

References

1 Reddy, K.R., Cameselle, C., and Adams, J.A. (2019). *Sustainable Engineering: Drivers, Metrics, Tools, and Applications*. Hoboken, NJ: Wiley.

2 Mitchell, J.K. and Yeung, A.T. (1990). Electro-kinetic flow barriers in compacted clay. *Transportation Research Record* 1288: 1–9.

3 Lynch, R. (2009). Electrokinetic barriers for preventing groundwater pollution. In: *Electrochemical Remediation Technologies for Polluted Soils, Sediments and Groundwater* (eds. K.R. Reddy and C. Cameselle), 335–356. Hoboken, NJ: Wiley.

UNCORRECTED PROOFS

Trim Size: 170mm x 244mm Single Column Loose Ribeiro670117 c16.tex V1 - 12/11/2020 10:16pm Page 404

4 Sri Ranjan, R. (2009). Electrokinetic barriers: modeling and validation. In: *Electrochemical Remediation Technologies for Polluted Soils, Sediments and Groundwater* (eds. K.R. Reddy and C. Cameselle), 563–580. Hoboken, NJ: Wiley.

5 Chung, H.I. and Lee, M.H. (2009). Coupled electrokinetic PRB for remediation of metals in groundwater. In: *Electrochemical Remediation Technologies for Polluted Soils, Sediments and Groundwater* (eds. K.R. Reddy and C. Cameselle), 647–660. Hoboken, NJ: Wiley.

6 Korolev, V.A. (2009). Electrokinetic removal of radionuclides. In: *Electrochemical Remediation Technologies for Polluted Soils, Sediments and Groundwater* (eds. K.R. Reddy and C. Cameselle), 127–140. Hoboken, NJ: Wiley.

7 Korolev, V.A. (2015). *Theory of Electro-Surface Phenomena in Soils and their Application*. Moscow, Russia: Sam Polygraphist, Ltd. [in Russian].

8 Casagrande, L. (1949). Electroosmosis in soils. *Géotechnique* 1 (3): 159–177.

9 Mitchell, J.K. (1993). *Fundamentals of Soil Behaviour*, *2*e. New York: Wiley.

10 Koryta, J. (1982). *Ions, Electrodes, and Membranes*. New York: Wiley.

11 Acar, Y.B. and Alshawabkeh, A.N. (1993). Principles of electrokinetic remediation. *Environmental Science & Technology* 27 (13): 2638–2647. https://doi.org/10.1021/es00049a002.

12 Narasimhan, B. and Sri Ranjan, R. (2000). Electrokinetic barrier to prevent subsurface contaminant migration: theoretical model development and validation. *Journal of Contaminant Hydrology* 42 (1): 1–17. https://doi.org/10.1016/S0169-7722(99)00089-3.

13 Darcy, H. (1856). *Les Fontaines Publiques de la Ville de Dijon. Exposition et Application des Principes à Suivre et des Formules à Employer dans les Questions de Distribution d'Eau: Ouvrage Terminé par un Appendice Relatif aux Fournitures d'Eau de Plusieurs Villes au Filtrage des Eaux et à la Fabrication des Tuyaux de Fonte, de Plomb, de Tole et de Bitume*. Paris: Dalmont. [in French].

14 Fick, A. (1855). Ueber diffusion. *Annalen der Physik* 94 (1): 59–86. [in German]. https://doi.org/10.1002/andp.18551700105.

15 Yeung, A.T. and Mitchell, J.K. (1993). Coupled fluid, electrical, and chemical flows in soil. *Géotechnique* 43 (1): 121–134. https://doi.org/10.1680/geot.1993.43.1.121.

16 Olsen, H.W., Gui, S., and Lu, N. (2000). Critical review of coupled flow theories for clay barriers. *Transportation Research Record* 1714 (1): 57–64. https://doi.org/10.3141/1714-08.

17 EN ISO 14688-1:2018 E (2018). *Geotechnical Investigation and Testing Identification and Classification of Soil - Part 1: Identification and Description (ISO 146881:2017)*. Dublin: CEN.

18 Alshawabkeh, A. and Acar, Y.B. (1992). Removal of contaminants from soils by electrokinetics: a theoretical treatise. *Journal of Environmental Science and Health – Part A. Environmental Science and Engineering & Toxic and Hazardous Substance Control* 7 (A27): 1835–1865. https://doi.org/10.1080/10934529209375828.

UNCORRECTED PROOFS

Trim Size: 170mm x 244mm Single Column Loose Ribeiro670117 c16.tex V1 - 12/11/2020 10:16pm Page 405

19 Lorenz, P.B. (1969). Surface conductance and electrokinetic properties of kaolinite beds. *Clays and Clay Minerals* 17 (4): 223–231. https://doi.org/10.1346/CCMN.1969.0170405.

20 Yeung, A.T., Hsu, C., and Menon, R.M. (1997). Physicochemical soil-contaminant interactions during electrokinetic extraction. *Journal of Hazardous Materials* 55 (1): 221–237. https://doi.org/10.1016/S0304-3894(97)00017-4.

21 Avena, M.J. and De Pauli, C.P. (1998). Proton adsorption and electrokinetics of an Argentinean montmorillonite. *Journal of Colloid and Interface Science* 202 (1): 195–204. https://doi.org/10.1006/jcis.1998.5402.

22 Liaki, C., Rogers, C.D.F., and Boardman, D.I. (2008). Physicochemical effects on uncontaminated kaolinite due to electrokinetic treatment using inert electrodes. *Journal of Environmental Science and Health – Part A. Toxic/Hazardous Substances and Environmental Engineering* 43 (8): 810–822. https://doi.org/10.1080/10934520801973972.

23 Sumbarda-Ramos, E.G., Oropeza-Guzmán, M.T., Salgado-Rodríguez, R. et al. (2011). Potential measurements used to study the bentonite-pollutant and kaolin-pollutant interphase. *ECS Transactions* 36 (1): 341–347. https://doi.org/10.1149/1.3660628.

24 Yukselen-Aksoy, Y. and Kaya, A. (2011). A study of factors affecting on the zeta potential of kaolinite and quartz powder. *Environmental Earth Sciences* 62 (4): 697–705. https://doi.org/10.1007/s12665-010-0556-9.

25 Korolev, V.A. and Nesterov, D.S. (2018). Regulation of clay particles charge for design of protective electrokinetic barriers. *Journal of Hazardous Materials* 358: 165–170. https://doi.org/10.1016/j.jhazmat.2018.06.023.

26 Narasimhan, B. (1999). *Electrokinetic Barriers to Contaminant Transport: Numerical Modelling and Laboratory Scale Experimentation*. Master of Science thesis: University of Manitoba.

27 Lynch, R.J., Muntoni, A., Ruggeri, R. et al. (2007). Preliminary tests of an electrokinetic barrier to prevent heavy metal pollution of soils. *Electrochimica Acta* 52 (10): 3432–3440. https://doi.org/10.1016/j.electacta.2006.06.049.

28 Ruggeri, R. (2005). Applicazione dell'elettrocinesi. PhD thesis. DIGITA, University of Cagliari [in Italian].

29 Lynch, R.J., Muntoni, A., Ruggeri, R. et al. (2005). Optimization of energy consumption by using a pulsed electrokinetic barrier to prevent Zn and Cd spread over an uncontaminated site. Operation of the barrier in model tank tests. Fifth Symposium on Electrokinetic Remediation – EREM, Ferrara, Italy (22–25 May). Ferrara, Italy: University of Ferrara.

30 Eid, N., Elshorbagy, W., Larson, D. et al. (2000). Electro-migration of nitrate in sandy soil. *Journal of Hazardous Materials* B79 (1–2): 133–149. https://doi.org/10.1016/S0304-3894(00)00238-7.

31 Manokararajah, K.K. and Sri Ranjan, R. (2005). Creation of a barrier for nitrate ions using electrokinetic methods in a silty loam soil. *Canadian Biosystems Engineering/Le Genie des biosystems au Canada* 47: 1.15–1.21.

UNCORRECTED PROOFS

Trim Size: 170mm x 244mm Single Column Loose Ribeiro670117 c16.tex V1 - 12/11/2020 10:16pm Page 406

32 Manokararajah, K.K. and Sri Ranjan, R. (2005). Electrokinetic retention, migration, and remediation of nitrates in silty loam soil under hydraulic gradient. *Engineering Geology* 77 (3–4): 263–272. https://doi.org/10.1016/j.enggeo.2004.07.017.

33 Moayedi, H., Huat, B.B.K., Kazemian, S. et al. (2011). Electrophoresis of suspended kaolinite in multivalent electrolyte solution. *International Journal of Electrochemical Science* 6 (12): 6514–6524.

34 Nowicki, M.A., Lynch, R.J., and Amaratunga, G. (2005). Stand-alone solarpowered electrokinetic fence for preventing heavy metal pollution of groundwater. 20th EU Photovoltaic Solar Energy Conference, Barcelona, Spain (6–10 June).

35 Reeve, J. and Lynch, R.J. (2007). Use of a pulsed electric field for resisting groundwater pollution. 6th Symposium on Electrokinetic Remediation (EREM), Vigo, Spain (12–15 June).

36 Mohamedelhassan, E. (2011). Laboratory study on integrated solar electrokinetic barrier for preventing cadmium contamination. *Research Journal of Environmental and Earth Sciences* 3 (5): 521–533.

37 Narasimhan, B. and Sri Ranjan, R. (1999). Creation of a subsurface barrier to contaminant transport using electrical potential gradients. ASAE/CSAE – SCGR Annual International Meeting, St. Joseph, MI (18–21 July).

38 Simpanen, S., Yu, D., Makela, R. et al. (2018). Soil vapor extraction of wet gasoline-contaminated soil made possible by electroosmotic dewatering–lab simulations applied at a field site. *Journal of Soils and Sediments* 18: 3303–3309. https://doi.org/10.1007/s11368-017-1717-1.

39 Amrate, S., Akretche, D.E., Innocent, C. et al. (2006). Use of cation-exchange membranes for simultaneous recovery of lead and EDTA during electrokinetic extraction. *Desalination* 193 (1–3): 405–410. https://doi.org/10.1016/j.desal.2005.06.071.

40 Song, Y., Cang, L., Zuo, Y. et al. (2020). EDTA-enhanced electrokinetic remediation of aged electroplating contaminated soil assisted by combining dual cation-exchange membranes and circulation methods. *Chemosphere* 243: 1–12. https://doi.org/10.1016/j.chemosphere.2019.125439.

41 Ebbers, B., Ottosen, L.M., and Jensen, P.E. (2015). Comparison of two different electrodialytic cells for separation of phosphorus and heavy metals from sewage sludge ash. *Chemosphere* 125: 122–129. https://doi.org/10.1016/j.chemosphere.2014.12.013.

42 Pedersen, K.B., Ottosen, L.M., Jensen, P.E. et al. (2015). Comparison of 2-compartment, 3-compartment and stack designs for electrodialytic removal of heavy metals from harbour sediments. *Electrochimica Acta* 181: 48–57. https://doi.org/10.1016/j.electacta.2014.12.003.

43 Jones, C.J.F.P., Fakher, A., Hamir, R. et al. (1997). Geosynthetic materials with improved reinforcement capabilities. In: *Earth Reinforcement, Volume 2* (eds. H. Ochiai, N. Yasufuku and K. Omine), 865–887. Rotterdam, the Netherlands: Balkema.

UNCORRECTED PROOFS

Trim Size: 170mm x 244mm Single Column Loose Ribeiro670117 c16.tex V1 - 12/11/2020 10:16pm Page 407

44 Jones, C.J.F.P., Lamont-Black, J., Glendinning, S. et al. (2008). Recent research and applications in the use of electro-kinetic geosynthetics. Fourth European Geosynthetics Conference (EuroGeo 4), Edinburgh, UK (7–10 September).

45 Jones, C.J.F.P., Lamont-Black, J., Huntley, D. et al. (2017). Electrokinetic geosynthetics: from research to hype to practice. *Civil Engineering* 170 (CE3): 127–134. https://doi.org/10.1680/jcien.16.00039.

46 Lamont-Black, J., Jones, C.J.F.P., and White, C. (2015). Electrokinetic geosynthetic dewatering of nuclear contaminated waste. *Geotextiles and Geomembranes* 43 (4): 359–362. https://doi.org/10.1016/j.geotexmem.2015.04.005.

47 Jones, C.J.F.P. and Adler, D. (2018). Electrokinetic treatment of soils to: aid dewatering, accelerate consolidation, enhance soil strength, control pore water pressure. Theory and recent practice. Presentation at the BGA evening meeting in London, UK (7 March).

48 Transport Research Laboratory. (2018). Innovative geotechnical repair techniques: effectiveness of electrokinetic geosynthetics. TRL published project report PPR890.

49 Zhuang, Y., Liu, Z., Li, Z. et al. (2018). Upward gradient EKG and electroosmosis for deep soft ground consolidation. In: *Proceedings of the 11th International Conference on Geosynthetics*, Seoul, Republic of Korea (16–21 September 2018). Seoul, Republic of Korea: KGSS.

50 Hall, J., Glendinning, S., Lamont-Black, J. et al. (2008). Dewatering of waste slurries using electrokinetic geosynthetic (EKG) filter bags. In: *Proceedings of the Fourth European Geosynthetics Conference (EuroGeo 4)*, Edinburgh, UK, (7–10 September 2008). Edinburgh, UK: Heriot-Watt University.

51 White, C., Glendinning, S., Lamont-Black, J. et al. (2008). The application of electrokinetic geosynthetics in the advanced conditioning and composting processing of sewage sludge. In: *Proceedings of the Fourth European Geosynthetics Conference (EuroGeo 4)*, Edinburgh, UK, (7–10 September 2008). Edinburgh, UK: Heriot-Watt University.

52 Jones, C.J.F.P., Lamont-Black, J., and Glendinning, S. (2011). Electrokinetic geosynthetics in hydraulic applications. *Geotextiles and Geomembranes* 29 (4): 381–390. https://doi.org/10.1016/j.geotexmem.2010.11.011.

53 Jones, C.J.F.P. (2000). Developments and innovations in reinforced soil technology. In: *Landmarks in Earth Reinforcement, Volume 1* (eds. H. Ochiai, K. Omine, J. Otani and N. Yasufuku), 1047–1061. Lisse, the Netherlands: Balkema.

54 Hamir, R.B., Jones, C.J.F.P., and Clarke, B.G. (2001). Electrically conductive geosynthetics for consolidation and reinforced soil. *Geotextiles and Geomembranes* 19 (8): 455–482. https://doi.org/10.1016/S0266-1144(01)00021-8.

55 Jones, C.J.F.P., Glendinning, S., and Shim, G.S.C. (2002). Soil consolidation using electrically conductive geosynthetics. In: *Geosynthetics: State of the Art, Recent Developments, Volume 3* (eds. P. Delmas and J.P. Gourc), 1039–1042. Lisse, the Netherlands: Balkema.

56 Lageman, R. and Pool, W. (2009). Electrokinetic biofences. In: *Electrochemical Remediation Technologies for Polluted Soils, Sediments and Groundwater* (eds. K.R. Reddy and C. Cameselle), 357–366. Hoboken, NJ: Wiley.

UNCORRECTED PROOFS

Trim Size: 170mm x 244mm Single Column Loose Ribeiro670117 c16.tex V1 - 12/11/2020 10:16pm Page 408

57 Godschalk, M.S. and Lageman, R. (2005). Electrokinetic biofence, remediation of VOCs with solar energy and bacteria. *Engineering Geology* 77 (3–4): 225–231. https://doi.org/10.1016/j.enggeo.2004.07.013.

58 Lageman, R. and Godschalk, M.S. (2007). Electro-bioreclamation: a combination of in situ remediation techniques proves successful at a site in Zeist, the Netherlands. *Electrochimica Acta* 52 (10): 3449–3453. https://doi.org/10.1016/j.electacta.2006.01.089.

59 Mena Ramírez, E., Sáez Jiménez, C., Villaseñor Camacho, J. et al. (2015). Feasibility of coupling permeable bio-barriers and electrokinetics for the treatment of diesel hydrocarbons polluted soils. *Electrochimica Acta* 181: 192–199. https://doi.org/10.1016/j.electacta.2015.02.201.

60 Barba, S., Carvela, M., Villaseñor Camacho, J. et al. (2019). Fixed-bed biological barrier coupled with electrokinetics for the in situ electrobioremediation of 2,4-dichlorophenoxyacetic acid polluted soil. *Journal of Chemical Technology & Biotechnology* 94 (8): 2684–2692. https://doi.org/10.1002/jctb.6079.

61 Barba, S., Ocaña, H., Villaseñor Camacho, J. et al. (2019). Electrobioremediation of oxyfluorfen-polluted soil by means of a fixed-bed permeable biological barrier. *Water, Air, and Soil Pollution* 230 (6) https://doi.org/10.1007/s11270-019-4183-0.

62 Kaimbi, L.A. and Chirwa, E.M.N. (2018). Efficiency of remobilisation of chromium precipitates in an aquifer permeable reactive barrier. *Chemical Engineering Transactions* 70: 1795–1800. https://doi.org/10.3303/CET1870300.

63 Weng, C.-H. (2009). Coupled electrokinetic-permeable reactive barriers. In: *Electrochemical Remediation Technologies for Polluted Soils, Sediments and Groundwater* (eds. K.R. Reddy and C. Cameselle), 483–503. Hoboken, NJ: Wiley.

64 US EPA. (1998). Permeable reactive barrier technologies for contaminant remediation. Research report EPA/600/R-98/125.

65 Chung, H.I. and Lee, M.H. (2009). Coupled electrokinetic PRB for remediation of metals in groundwater. In: *Electrochemical Remediation Technologies for Polluted Soils, Sediments and Groundwater* (eds. K.R. Reddy and C. Cameselle), 357–366. Hoboken, NJ: Wiley.

66 Zhao, S., Fan, L., Zhou, M. et al. (2016). Remediation of copper contaminated kaolin by electrokinetics coupled with permeable reactive barrier. *Procedia Environmental Sciences* 31: 274–279. https://doi.org/10.1016/j.proenv.2016.02.036.

67 Ghobadi, R., Altaee, A., Zhou, J.L. et al. (2020). Copper removal from contaminated soil through electrokinetic process with reactive filter media. *Chemosphere* 252: 126607. https://doi.org/10.1016/j.chemosphere.2020.126607.

68 Vieira dos Santos, E., Sáez, C., Cañizares, P. et al. (2017). Reversible electrokinetic adsorption barriers for the removal of atrazine and oxyfluorfen from spiked soils. *Journal of Hazardous Materials* 322 (Pt B): 413–420. https://doi.org/10.1016/j.jhazmat.2016.10.032.

69 Rodrigo, S., Saez, C., Cañizares, P. et al. (2018). Reversible electrokinetic adsorption barriers for the removal of organochlorine herbicide from spiked

UNCORRECTED PROOFS

Trim Size: 170mm x 244mm Single Column Loose Ribeiro670117 c16.tex V1 - 12/11/2020 10:16pm Page 409

soils. *Science of the Total Environment* 640–641: 629–636. https://doi.org/10.1016/j.scitotenv.2018.05.364.

70 Blowes, D.W., Ptacek, C.J., Benner, S.G. et al. (2000). Treatment of inorganic contaminants using permeable reactive barriers. *Journal of Contaminant Hydrology* 45 (1–2): 123–137. https://doi.org/10.1016/S0169-7722(00)00122-4.

71 Simon, F.G., Meggyes, T.T., Czurda, K. et al. (2001). Long-term behaviour of permeable reactive barriers used for the remediation of contaminated groundwater. In: *Proceedings of the 8th International Conference on Radioactive Waste Management and Environmental Remediation, Volume 1*, Bruges, Belgium, (30 September - 4 October 2001). Bruges, Belgium: ICEM, ASME.

72 Wilkin, R.T., Su, C., Ford, R.G. et al. (2005). Chromium removal processes during groundwater remediation by a zero valent iron permeable reactive barrier. *Environmental Science and Technology* 39 (12): 4599–4605. https://doi.org/10.1021/es050157x.

73 Ebert, M., Kober, R., Parbs, A. et al. (2006). Assessing degradation rates of chlorinated ethylenes in column experiments with commercial iron materials used in permeable reactive barriers. *Environmental Science and Technology* 40 (6): 2004–2010. https://doi.org/10.1021/es051720e.

74 Weng, C.H., Lin, T.Y., Chu, S.H. et al. (2006). Laboratory-scale evaluation of Cr(VI) removal from clay by electrokinetics incorporated with Fe(0) barrier. *Practice Periodical of Hazardous, Toxic, Waste Management* 10 (3): 171–178. https://doi.org/10.1061/(ASCE)1090-025X(2006)10:3(171).

75 Weng, C.H., Lin, Y.T., Lin, T.Y. et al. (2007). Enhancement of electrokinetic remediation of hyper-Cr(VI) contaminated clay by zero-valent iron. *Journal of Hazardous Materials* 149 (2): 292–302. https://doi.org/10.1016/j.jhazmat.2007.03.076.

76 Yuan, C. and Chiang, T.S. (2007). The mechanisms of arsenic removal from soil by electrokinetic process coupled with iron permeable reaction barrier. *Chemosphere* 67 (8): 1533–1542. https://doi.org/10.1016/j.chemosphere.2006.12.008.

77 Yao, W., Cai, Z., Sun, S. et al. (2019). Electrokinetic-enhanced remediation of actual arsenic-contaminated soils with approaching cathode and Fe0 permeable reactive barrier. *Journal of Soils and Sediments* 20 (3): 1526–1533. https://doi.org/10.1007/s11368-019-02459-4.

78 Huang, T., Liu, L., Zhang, S. et al. (2019). Evaluation of electrokinetics coupled with a reactive barrier of activated carbon loaded with a nanoscale zero-valent iron for selenite removal from contaminated soils. *Journal of Hazardous Materials* 368: 104–114. https://doi.org/10.1016/j.jhazmat.2019.01.036.

79 Robles, I., Lozano, M.J., Solís-Valdez, S. et al. (2015). Electrokinetic treatment of mercury-polluted soil facilitated by ethylenediaminetetraacetic acid coupled with a reactor with a permeable reactive barrier of iron to recover mercury (II) from water. *Electrochimica Acta* 181: 68–72. https://doi.org/10.1016/j.electacta.2015.04.099.

UNCORRECTED PROOFS

Trim Size: 170mm x 244mm Single Column Loose Ribeiro670117 c16.tex V1 - 12/11/2020 10:16pm Page 410

80 Chang, J.H. and Cheng, S.F. (2006). The remediation performance of a specific electrokinetics integrated with zero-valent metals for perchloroethylene contaminated soils. *Journal of Hazardous Materials* 131 (1–3): 153–162. https://doi.org/10.1016/j.jhazmat.2005.09.026.

81 Kebria, D.Y., Taghizadeh, M., Villaseñor Camacho, J. et al. (2016). Remediation of PCE contaminated clay soil by coupling electrokinetics with zero-valent iron permeable reactive barrier. *Environmental Earth Sciences* 75 (8): 699. https://doi.org/10.1007/s12665-016-5466-z.

82 Ren, D., Li, S., Wu, J. et al. (2019). Remediation of phenanthrene-contaminated soil by electrokinetics coupled with iron/carbon permeable reactive barrier. *Environmental Engineering Science* 36 (9): 1224–1235. https://doi.org/10.1089/ees.2019.0066.

83 Shin, H.Y., Singhal, N., and Park, J.W. (2007). Regeneration of iron for trichloroethylene reduction by Shewanella alga BrY. *Chemosphere* 68 (6): 1129–1134. https://doi.org/10.1016/j.chemosphere.2007.01.059.

84 Chung, H.I. and Lee, M.H. (2007). A new method for remedial treatment of contaminated clayey soils by electrokinetics coupled with permeable reactive barriers. *Electrochimica Acta* 52 (10): 3427–3431. https://doi.org/10.1016/j.electacta.2006.08.074.

85 Cundy, A.B. and Hopkinson, L. (2005). Electrokinetic iron pan generation in unconsolidated sediments: implications for contaminated land remediation and soil engineering. *Applied Geochemistry* 20 (5): 841–848. https://doi.org/10.1016/j.apgeochem.2004.11.014.

86 Faulkner, D., Hopkinson, L., and Cundy, A.B. (2005). Electrokinetic generation of reactive iron-rich barriers in wet sediments: implications for contaminated land management. *Mineralogical Magazine* 69 (5): 749–757. https://doi.org/10.1180/0026461056950285.

87 Cundy, A.B., Hopkinson, L., and Whitby, R.L.D. (2008). Use of iron-based technologies in contaminated land and groundwater remediation: a review. *Science of the Total Environment* 400 (1–3): 42–51. https://doi.org/10.1016/j.scitotenv.2008.07.002.

88 De Gioannis, G., Muntoni, A., Ruggeri, R. et al. (2008). Chromate adsorption in a transformed red mud permeable reactive barrier using electrokinesis. *Journal of Environmental Science and Health Part A. Toxic/Hazardous Substances and Environmental Engineering* 43 (8): 969–974. https://doi.org/10.1080/10934520801974582.

89 Cappai, G., De Gioannis, G., Muntoni, A. et al. (2011). Combined use of a transformed red mud reactive barrier and electrokinetics for remediation of Cr/As contaminated soil. *Chemosphere* 86 (4): 400–408. https://doi.org/10.1016/j.chemosphere.2011.10.053.

90 Carvalho Rocha, L.C. and Zuquette, L.V. (2020). Evaluation of zeolite as a potential reactive medium in a permeable reactive barrier (PRB): batch and column studies. *Geosciences (Switzerland)* 10 (2): 59. https://doi.org/10.3390/geosciences10020059.

UNCORRECTED PROOFS

Trim Size: 170mm x 244mm Single Column Loose Ribeiro670117 c16.tex V1 - 12/11/2020 10:16pm Page 411

91 Yu, X., Muhammad, F., Yan, Y. et al. (2019). Effect of chemical additives on electrokinetic remediation of Cr-contaminated soil coupled with a permeable reactive barrier. *Royal Society Open Science* 6 (5) https://doi.org/10.1098/rsos.182138.

92 Zhou, H., Xu, J., Lv, S. et al. (2020). Removal of cadmium in contaminated kaolin by new-style electrokinetic remediation using array electrodes coupled with permeable reactive barrier. *Separation and Purification Technology* 239: 116544. https://doi.org/10.1016/j.seppur.2020.116544.

93 Hamdi, N. and Srasra, E. (2008). Interaction of aqueous acidic-fluoride waste with natural Tunisian soil. *Clays and Clay Minerals* 56 (2): 259–271. https://doi.org/10.1346/CCMN.2008.0560209.

94 Cuevas, J., Ruiz, A.I., De Soto García, I.S. et al. (2012). The performance of natural clay as a barrier to the diffusion of municipal solid waste landfill leachates. *Journal of Environmental Management* 95 (Supplement): S175–S181. https://doi.org/10.1016/j.jenvman.2011.02.014.

95 Kim, D. and Han, J. (2020). Remediation of multiply contaminated ground via permeable reactive barrier and electrokinetic using recyclable food scrap ash (FSA). *Applied Sciences* 10 (4): 1194. https://doi.org/10.3390/app10041194.

96 Zhou, M., Zhu, S., Yi, Y. et al. (2016). An electrokinetic/activated alumina permeable reactive barrier-system for the treatment of fluorine-contaminated soil. *Clean Technologies and Environmental Policy* 18: 2691–2699. https://doi.org/10.1007/s10098-016-1156-5.

97 Xu, Y., Xia, W., Hou, H. et al. (2017). Remediation of chromium-contaminated soil by electrokinetics and electrokinetics coupled with CaAl-LDH permeable reaction barrier. *Environmental Science and Pollution Research* 24 (12): 20479–20486. https://doi.org/10.1007/s11356-017-9705-y.

98 Lageman, R. (2015). Preliminary assessment of applying an electrokinetic ring fence for the removal of radionuclides from groundwater at Fukushima Daiichi Nuclear Power Plant. Lambda Consulting. 10.13140/RG.2.1.1398.4084

99 Cameselle, C. and Gouveia, S. (2019). Electrochemical regeneration of activated carbon. The problem of the end-waste effluent. In: *Proceedings of the 17th International Symposium on Electrochemical Remediation EREM-2019, Book of Abstracts - Keynotes*, San Miguel de Allende, Mexico, (22–27 September 2019). Querétaro, Mexico: CIDETEQ.

100 Xiao, J., Pang, Z., Zhou, S. et al. (2020). The mechanism of acid-washed zero-valent iron/activated carbon as permeable reactive barrier enhanced electrokinetic remediation of uranium-contaminated soil. *Separation and Purification Technology* 244 https://doi.org/10.1016/j.seppur.2020.116667.

101 Kucherov, V.V. and Korolev, V.A. (2005). Electrokinetic treatment of artificial soils in the foundations of storage reservoirs for liquid radioactive wastes. In: *Proceedings of the 7th Sergeev Readings. Materials of the Annual Session of the RAS Scientific Council. Engineering-Geological and Geo-Ecological Issues of Utilization and Dumping of Wastes. Volume 7*, Moscow, Russia, (23 March 2005). Moscow, Russia: GEOS [in Russian].

UNCORRECTED PROOFS

UNCORRECTED PROOFS

Trim Size: 170mm x 244mm Single Column Loose Ribeiro670117 c17.tex V1 - 12/11/2020 5:48pm Page 413

17

Emerging Contaminants in Wastewater: Sensor Potential for Monitoring Electroremediation Systems

Cátia Magro[1], Eduardo P. Mateus[1], Maria de Fátima Raposo[2], and Alexandra B. Ribeiro[1]

[1]CENSE – Center for Environmental and Sustainability Research, Department of Environmental Sciences and Engineering, NOVA School of Science and Technology, NOVA University Lisbon, 2829-516 Caparica, Portugal
[2]CEFITEC, Department of Physics, NOVA School of Science and Technology, NOVA University Lisbon, 2829-516 Caparica, Portugal

17.1 Scope

Today, more than 700 emerging contaminants and their metabolites and transformation products are listed as being present in European bodies of water [1]. Emerging contaminants are defined as "synthetic or naturally occurring chemicals that are not commonly monitored in the environment, but which have the potential to enter the environment and cause known or suspected adverse ecological and (or) human health effects." In some cases, release of emerging contaminants into the environment has likely occurred for a long time but may not have been recognized until new detection methods were developed [2]. Emerging contaminants are currently not included in (inter)national routine monitoring programs, and their fate, behavior, and eco-toxicological effects are often not well understood. They can be released from point pollution sources, e.g. wastewater treatment plants from urban or industrial areas, or from diffuse sources through atmospheric deposition, or from crop and animal production. Emerging contaminants are categorized into more than 20 classes related to their origin: pharmaceuticals, pesticides, disinfection by-products, wood preservation, and industrial chemicals [1].

Another relevant issue is regulatory frameworks affecting emerging contaminants. For example, the REACH regulation registers, evaluates, authorizes, and restricts the use of nearly all chemical substances manufactured or imported into the EU [3]. In terms of point source pollution, several directives and regulations are relevant: The Industrial Emissions Directive [4], the European Pollutant Release and Transfer Register [5], and the Urban Wastewater Treatment Directive [6]. Finally, regulating the presence of emerging contaminants in the environment, the Water Framework Directive [7] provides a safety net, including identification, monitoring,

Electrokinetic Remediation for Environmental Security and Sustainability, First Edition.
Edited by Alexandra B. Ribeiro and M.N.V. Prasad.
© 2021 John Wiley & Sons Ltd. Published 2021 by John Wiley & Sons Ltd.

UNCORRECTED PROOFS

Trim Size: 170mm x 244mm Single Column Loose Ribeiro670117 c17.tex V1 - 12/11/2020 5:48pm Page 414

and a list of priority substances for which concentration limits are defined in the Environmental Quality Standards Directive [8]. These regulations are the legislative basis for efficient resource management. The combination of regulations, using data from monitoring tools, and its application for risk assessment enables the elaboration of sustainable water resource management that takes into consideration economically possible solutions.

Detection, identification, quantification, and removal of emerging contaminants and their transformation products in the various environmental compartments is essential for learning about their occurrence, fate, and remediation. Current state-of-the-art techniques for sampling, analysis, and removal vary among laboratories and research teams. They are typically dedicated to specific emerging contaminant classes and do not cover the full range of analytes of potential concern. Although significant advances have been made in detecting and analyzing trace contaminants in recent decades, due to the continued development and refinement of specific analytical techniques and methodologies, the choice of the best tools to monitor these contaminants in the various environmental matrices is not a closed issue [9]. In addition, the search for efficient methodologies that promote the removal of these contaminants is another important subject. In recent years, several electro-based cleanup technologies were developed and studied to improve the quality and safety of water. Sensors have come to be considered future monitoring tools, since compared to traditional sampling and analysis, they have the potential to provide fast responses to output data in a timely, continuous, safe, and cost-effective fashion.

Among sensors, the electronic tongue (e-tongue) has proved to be an interesting approach for liquid environmental matrices contaminated with emerging organic contaminants (EOCs) [10]. A feature in the development of electronic languages for the purpose of multi-analyte determination is the use of sensor arrays composed of highly miniaturized signal transducer elements, which allow parallel monitoring, in real time, of several species in a single sample analysis [11, 12]. Using nanomaterials to perform the analysis as sensor layers will improve the device's sensitivity and performance due to their unique physical and chemical properties [13], such as more conductivity and/or resistivity to changes in the target analyte, high relative surface area, and size versatility. The type of thin-film or sensorial layer chosen is a critical step for building a reliable qualitative and quantitative device.

Therefore, sensors used in association with electro-based removal technologies could play a role in the control, monitoring, and trending of contamination (Figure 17.1).

This chapter describes electro-based removal technologies, as well as current advances in the e-tongue, potential thin-film coatings, nanomaterials used, assembly techniques, and the highest potential electrical transducer: impedance spectroscopy. The last section is dedicated to an overview of e-tongues coupled to electroremediation treatment reactors.

UNCORRECTED PROOFS

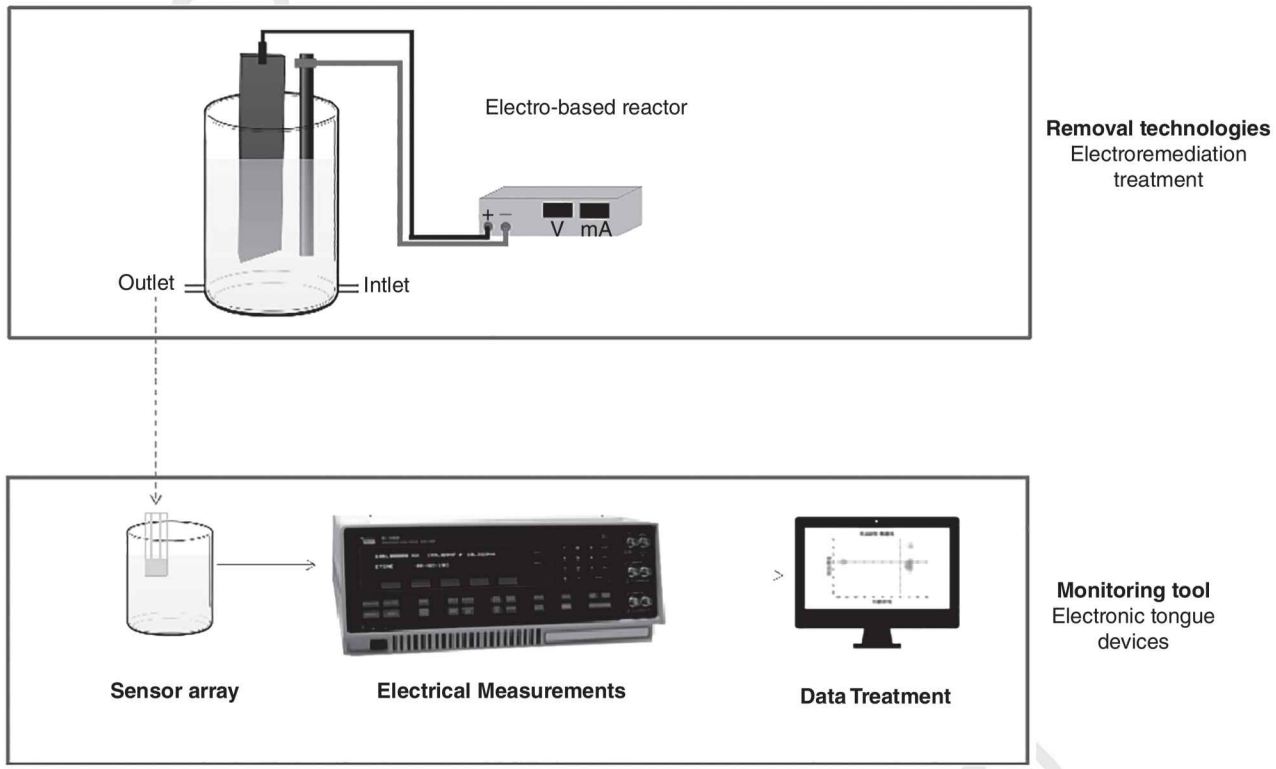

Figure 17.1 Electro-based removal technologies combined in a cutting-edge monitoring tool. Source: Adapted from Magro et al. [14].

UNCORRECTED PROOFS

Trim Size: 170mm x 244mm Single Column Loose
Ribeiro670117 c17.tex V1 - 12/11/2020 5:48pm Page 415

Trim Size: 170mm x 244mm Single Column Loose Ribeiro670117 c17.tex V1 - 12/11/2020 5:48pm Page 416

17.2 Removal Technologies: Electroremediation Treatment

Over the years, the electrokinetic (EK) process, or electroremediation treatment, has proved to be an effective and versatile technology to separate, remove, or degrade different type of contaminants. The EK process is based on the application of a low-level current (direct or alternate) density, on the order of a few mA/cm, and a low potential gradient, on the order of V/cm [15] between a pair (or multiple pairs) of electrodes. The electric field generated between suitably located electrodes induces physico-chemical changes in the applied media. These changes lead to species transport by coupled mechanisms, which acts as a "cleaning agent" by which the contaminants are moved out of the matrix toward one of the electrode compartments, where they can be concentrated and may be removed. The transport processes include:

- *Electromigration*: The physical transport mechanism that is primarily responsible for moving ions through water or a moist matrix by an applied electrical field. The electrical current tends to go where the electrical resistance is lower. When an electric current is applied to a moist porous material, the ions flow naturally to the opposite charged electrode. Electromigration flux is dependent on the ionic mobility, tortuosity factor, porosity of the material, and charge of ions [15].
- *Electroosmosis*: The movement of the pore water under the influence of an electric field. For removing uncharged species or weakly dissociated organic contaminants like phenols, electroosmotic flux is predominant and normally goes from the anode to cathode as the species in the diffusive double layer are often cations [16].
- *Electrophoresis*: The opposite of electromigration. The movement of larger units, such as protein molecules or colloidal particles, under a potential gradient.
- *Diffusion*: The movement of species under a chemical concentration gradient. In general, this is significant movement in volumes of the matrix where gradients are especially high (such as areas where acid and basic fronts or metal cations and hydroxyl ions meet).

Electrokinetic treatment relies on several interacting mechanisms. Depending on the process, matrix, and contaminants, different competitive redox reactions may occur at the electrode, such as chlorine gas production at the anode (Eq. (17.2)) or metals deposition (Eq. (17.4)) at the cathode.

Anode reactions:

$$O_2(g) + 4H^+ + 4e^- = 2H_2O \quad E^0(O_2/H_2O) = 1.229\,V \tag{17.1}$$

$$Cl_2(g) + 2e^- = 2Cl^- \quad E^0(Cl_2/2Cl^-) = 1.358\ V \tag{17.2}$$

Cathode reactions:

$$2H_2O + 2e^- = H_2(g) + 2OH^- \quad E^0(H_2O/H_2) = -0.828\,V \tag{17.3}$$

$$Me^{2+} + 2e^- = Me^0 \tag{17.4}$$

UNCORRECTED PROOFS

Trim Size: 170mm x 244mm Single Column Loose Ribeiro670117 c17.tex V1 - 12/11/2020 5:48pm Page 417

The electrodialytic (ED) process is based on the combination of the EK movement of ions and electrodialysis. In the electrodialytic process, ion-exchange membranes are used instead of passive membranes as in the EK process. Two types of membranes are key to the ED process: the cation-exchange membrane (CEM) and the anion-exchange membrane (AEM). These membranes have high permselectivity, low electric resistance, good mechanical/form stability, and high chemical and thermal stability [17]. The CEM allows only the passage of cations, unlike the AEM, which allows the passage of anions and H^+ ions to the matrix compartment. The surface attracts dissolved ions with an opposite charge (counter-ions) from the pore water of the membranes.

Using AEMs and CEMs has several advantages [17]:

- Allows the passage of ions from polluted media to the electrode compartments
- Prevents/prohibits the passage of ions from electrode compartments back to the contaminated media
- Maintains the ions removed from the matrix compartment in the electrolytes
- Prevents the produced acid and base at the anode and the cathode, respectively, from entering the matrix and being transported through the media, thus saving energy

The membranes allow the regulation of the ion fluxes, thus selecting the ions that reach the electrode compartments. A concentration gradient is therefore essential for the flow of ions and water throughout the system. It is expected that the application of a low-level current onto a pair of electrodes in the moist contaminated matrix will result in both electroosmotic and electromigration flows. For this reason, using the ED process allows selective accumulation of organic contaminants and heavy metals in the anode or at the cathode end.

In addition, removing contaminants from the contaminated matrix by electric potential, when the reactor scheme is designed to place the electrodes in contact with the matrix, generates $^{\cdot}OH$ and therefore enhances the oxidation of EOCs [18]. Thus, the degradation is attributed to direct anodic oxidation, or indirect oxidation in the liquid bulk. Direct anodic oxidation occurs as the contaminants come in contact with the anode surface and are destroyed by the electron transfer reaction. Indirect oxidation in the liquid bulk is mediated by the oxidants that are formed electrochemically, such as chlorine, hypochlorite, hydroxyl radicals, ozone, and hydrogen peroxide [19].

17.3 Monitoring Tool: Electronic Tongues Devices

Conceptually, using sensors as monitoring tools for emerging contaminants is a cutting-edge idea that, with the right approval, support from governmental agencies, and increased quality of produced analytical data, may become a routine procedure in modern environmental monitoring laboratories [20]. On top of that, environmental monitoring in real-time mode and operating in the long term can allow the collection of data that may be vital to understand the full range of potential

UNCORRECTED PROOFS

Trim Size: 170mm x 244mm Single Column Loose Ribeiro670117 c17.tex V1 - 12/11/2020 5:48pm Page 418

contamination in all its phases and all environmental segments. To be reliable for environmental monitoring of emerging contaminants in wastewater matrices, the first line of contamination, the sensing units must be selective for target compounds and sensitive enough to detect them at trace levels. One of the challenges related to the development of a sensor at both the technological and scientific levels is analyte selectivity (adaptation to each type of target molecule) and sensitivity. Analytes must be detected at trace levels in environmentally complex matrices containing countless spurious molecules, potential interfering compounds, and microscopic life [21] that can jeopardize the analysis of a target molecule due to matrix effects. Due to differences in samples, an ideal real-time measurement technology should (i) be robust (able to be used in adverse environment, e.g. high humidity, high or low temperature, high airborne dust levels); (ii) have a low weight; (iii) be sensitive, generating data similar to the equipment in a laboratory; (iv) be versatile, allowing rapid analysis and the ability to operate with simple infrastructure; and (v) use a portable energy source [20, 22].

The electronic tongue has emerged as a powerful tool for the rapid assessment of information from complex liquid systems [23]. Its applicability in environmental contaminated matrices is potentially relevant due to advantages such as the ability to deal with multicomponent data, making possible the interpretation of complex media composition; multi-selectivity, allowing the analysis of different analytes in the same sample; clarification of the target species and their interferents; and even making the distinction between false and true positives signals (one of the biggest challenges for sensing systems) [24]. Since the first prototype in 1990 by Hayashi et al. [25], the e-tongue is seen as one of the most promising tools to develop a fast, cheap, objective method to evaluate different matrices. The e-tongue is "a multisensory system, formed by an array of low-selective sensors, combined with advanced mathematical procedures for output signal processing based on pattern recognition and/or multivariate data analysis" [26]. If configured and properly "trained," the e-tongue can be used to characterize complex aqueous matrices and recognize the qualitative and quantitative composition of multi-species solutions [27].

17.3.1 Sensor Design

The working electrodes in the e-tongue array can be covered with films (coatings), improving the sensitivity of the electrical measurements (Figure 17.2). The ability to tune the composition of nanostructured thin films allows for an improvement in the sensor's intrinsic (chemical or physical) properties for sensing applications [28]. Riul et al. and Olivati et al. [29, 30] reported using impedance spectroscopy for e-tongues, which is advantageous since the materials composing the sensing units do not need to be electroactive and a reference electrode is not required, in contrast to the conventional electrochemical methods. In this technique, the impedance of the entire system is measured for varying frequencies of the signal applied on interdigitated electrodes covered with thin films of different materials. This system is accounting with the highest potential for the combination with EK processes, since it can be described by an equivalent electrical circuit in which the double layer formed at the

UNCORRECTED PROOFS

Trim Size: 170mm x 244mm Single Column Loose Ribeiro670117 c17.tex V1 - 12/11/2020 5:48pm Page 419



Array of sensors: The e-tongue



Interdigitated
Electrodes: The sensor

+

Coating

Film coating deposition techniques:
- Layer-by-layer
- Sputtering

Figure 17.2 Electronic tongue, sensor, and coating concepts.

electrode/electrolyte interface controls the response at low frequencies, the solution conductance and ultrathin films coating the electrodes rule the total impedance at intermediate frequencies, and the geometric capacitance is most relevant at higher frequencies [31].

17.3.1.1 Thin-Film Nanomaterials

Sensors can be made from various materials depending on the purposes they serve. High sensitivity, fast response, and good selectivity are the general requirements for a good sensor [32]. For large-scale applications, low material cost and easy fabrication are also required. In recent decades, significant advances have been made in the synthesis and application of nanomaterials with highly controllable size, shape, surface charge, and physicochemical characteristics [33]. Briefly, the ability to precisely engineer nanomaterials and tailor their properties has culminated in highly robust and sensitive active layers. Because of the inherent properties of nanomaterials, such as super-small size and large surface/volume ratio, they can dramatically improve the sensitivity of the sensors as compared to traditional materials. By judiciously coating the nanoparticle surface composition, unique target binding characters can be achieved to allow great selectivity for emergent pollutants in various environmental matrices.

Nanomaterials can be organized into four material-based categories [34]:

- *Carbon-based*: Nanomaterials that contain carbon, found in morphologies such as hollow tubes, ellipsoids, or spheres. Fullerenes, carbon nanotubes, carbon nanofibers, carbon black, graphene, and carbon onions are included in this category. Laser ablation, arc discharge, and chemical vapor deposition are the important production methods for these carbon-based materials' fabrication [35].
- *Inorganic-based*: Metal and metal oxide nanomaterials, which can be synthesized into metals such as Au or Ag nanoparticles, metal oxides such as TiO_2 and ZnO,

UNCORRECTED PROOFS

Trim Size: 170mm x 244mm Single Column Loose Ribeiro670117 c17.tex V1 - 12/11/2020 5:48pm Page 420

and semiconductors such as silicon and ceramics. Physical vapor deposition is an important production method for these materials' fabrication.

- *Organic-based*: Nanomaterials made mostly from organic matter, excluding carbon-based or inorganic-based. Using noncovalent interactions for the self-assembly and design of molecules helps to transform organic nanomaterials such as polyelectrolytes (e.g. poly(allylamine hydrochloride), poly(ethyleneimine), and poly(sodium 4-styrene sulfonate)), dendrimers, micelles, and liposomes [36], into desired structures. The layer-by-layer (LbL) technique is an important production method for these materials' fabrication [37]. Other layers using micro-imprinting polymers (MIPs) can be also detect selectively low concentrations of spurious molecules [38].
- *Composite-based*: Multiphase nanoparticles and nanostructured materials with one phase on the nanoscale dimension that can either combine nanoparticles with other nanoparticles or combine nanoparticles with larger or with bulk-type materials (e.g. hybrid nanofibers) or more complicated structures, such as a metal-organic framework. The composites may be any combinations of carbon-based, metal-based, or organic-based nanomaterials with any form of metal, ceramic, or polymer bulk materials.

17.3.1.2 Promising Thin-Film Deposition Techniques

17.3.1.2.1 Layer-by-Layer Technique

Thin film formation is the primary successfully and most-used approach to produce organized nanostructures at the molecular level, where sensitive layers can be achieved by different techniques and used as a sensing platform. In this context, the most commonly employed technique for nanostructured films as sensor platforms is LbL [23]. This technique allows the formation of highly organized and morphologically controlled films, providing suitable tools for sensors.

The LbL technique [39] consists of the alternate adsorption from solution of positive and negative polyelectrolyte molecules. The electrostatic interaction is the primary driving force for LbL assembly, which in this case requires that the building blocks be water-soluble, multi-charged species such as polyelectrolytes. The LbL nano-assembly technique is flexible, easily scaled, reproducible, and versatile, allowing precise control over the film thickness and architecture. It is consistent with dedicated patterning techniques, including microcontact printing, conventional photolithography, photochemistry, and chemical selectivity [40], thus allowing molecules to be adsorbed onto a determined spatial region or pattern. These concepts can be used for the development of lab-on-a-chip sensors, which is a relevant issue for development of in situ sensors.

When organic films are used in the LbL technique, the film stability is related to electrostatic interactions in the range of 100 kJ/mol between the opposite ionized groups of cationic and polyelectrolyte molecules [41, 42]. Therefore, electrostatic interactions play a vital role in the adsorption of these molecular bilayers; but they are also strongly pH-dependent since the degree of ionization of each polyelectrolyte is a function of pH [41, 42]. Thus, if the goal is developing a sensor dedicated to detecting a specific molecule in complex media that can present different pH values,

UNCORRECTED PROOFS

Trim Size: 170mm x 244mm Single Column Loose Ribeiro670117 c17.tex V1 - 12/11/2020 5:48pm Page 421

the electrostatic interactions must be studied. Moreover, salts and/or other elements present in the environmental matrices may change the degree of ionization of LbL films and molecules involved [43] and therefore affect the sensor's electrical properties. It is crucial that studies of thin-film desorption or adsorption be performed to ascertain which sensor has the best features for detecting each emerging pollutant.

Desorption occurs with losses in electrostatic interactions between the opposite charge thin films. This could be explained by (i) more surface-located layers not being properly adsorbed during the film preparation, so that when immersed, they suffer a washing process that results in a loss of previous adsorbed matter; (ii) the presence of ions such as Mg^{2+}, Na^{+}, and SO_4^{2-}, which interact strongly with the polyelectrolyte outer layer, facilitating a change of charge within the polyelectrolyte layer from negatively charged to predominantly neutral and thus weakening the strong electrostatic interactions between the polyelectrolyte outer layer and the remaining layers and leading to polyelectrolyte molecules detachment [44]; or (iii) the effect of matrix pH on the degree of ionization of the polyelectrolyte, leading to film molecules losing much of their charge. The adsorption phenomenon in these cases has additional relevance aside from the detection factor, as it can be used to remove emerging pollutant from matrices. Moreover, and highly dependent on the chemical structure (e.g. target contaminants' pKa) of the molecule and the polyelectrolyte used, the adsorption observed could be a result of either the formation of hydrogen bonds or the interactions of π-π stacking [45]. The best LbL combination is one where the molecules under study are repelled by the films and not adsorbed on the surface, and desorption is not observed.

17.3.1.2.2 Sputtering Technique

Sputter deposition is a widely used technique to deposit thin films on substrates. This technique is based on ion bombardment of a source material: the target. Ion bombardment results in a vapor due to a purely physical process, i.e. the sputtering of the target material. This technique is part of the class of physical vapor deposition techniques, which includes thermal evaporation and pulsed laser deposition.

The most common approach for growing thin films by sputter deposition uses a magnetron source in which positive ions present in the plasma of a magnetically enhanced glow discharge bombard the target [46]. The target can be powered in different ways, ranging from direct current for conductive targets to radio frequency for nonconductive targets to various other ways of applying current and/or voltage pulses. Since sputtering is a purely physical process, adding chemistry to, for example, deposit a compound layer must be done ad hoc by adding a reactive gas to the plasma, i.e. reactive sputtering. The undesirable reaction of the reactive gas with the target material results in a nonlinear behavior of the deposition parameters as a function of the reactive gas flow. To model this behavior, the fluxes of the various species toward the target must be determined. Equally important are the fluxes of species incident at the substrate, because they not only influence the reactive sputter deposition process but also control the growth of the desired film [46].

Magro et al. [14] used this technique to build up some of the thin-film layers presented in an e-tongue array, to detect triclosan and its byproducts in a wastewater

UNCORRECTED PROOFS

Trim Size: 170mm x 244mm Single Column Loose Ribeiro670117 c17.tex V1 - 12/11/2020 5:48pm Page 422

matrix. These authors concluded that thickness and hydrophobic or hydrophilic final character are crucial for detection and semi-quantification of target compounds. Thus, a thin film with a more hydrophobic character, such as TiO2/ZnO and ZnO, is better suited for analytes with higher Log k_{ow}. However, for analytes with lower molecular dimension and less lipophilic potential, the hydrophobic character related to higher thickness will permit molecule semi-permeability through the thin-film net, giving the molecules a fluid character; this may mask their detection if the molecules' movement through the hole structures is too fast, not allowing for complete analysis.

17.3.1.3 Electrical Measurements: Impedance Spectroscopy

Impedance – the frequency-dependent ratio between the two fundamental electrical parameters, voltage and current – is a ubiquitous quantity, widely used to realize sensors at different size scales. Briefly, Ohm's law, $V = IR$, describes the relationship of voltage (V) to a direct current (I) passing through a resistor (R). Impedance extends the concept of resistance to an alternating current circuit and is generally represented as Z. It should be clear that the impedance measurement, therefore, can be made by applying an oscillating voltage, $V(t) = |V|sin(\omega t)$, and measuring the (oscillating) current response, $I(t) = |I|sin(\omega t + \theta)$, where $|V|$ is the amplitude of the voltage signal and $\omega = 2\pi f$ is the angular frequency. The response will be a current with an amplitude $|I|$, which is also shifted in phase from the applied signal $V(t)$. The current is shifted in phase because of reactance (e.g. catytpacitance or inductance) in addition to resistance which changes the amplitude of signal. The impedance can therefore be expressed by $Z = V(t)/I(t)$.

To simplify, one can consider Euler's formula, and the previous equation can be rewritten using complex numbers, $Z^* = Z' + jZ''$. Note that j is the imaginary unit, which we use instead of i to avoid confusion with the symbol for electrical current. Thus, dividing the complex impedance into the real and imaginary parts Z' and Z'' are the resistive and reactive parts of the impedance, respectively. Z^* can be represented on an Argand diagram, the basis for the Nyquist plot, which is the plot of the real and imaginary parts of the impedance (the most often used). An impedance measurement for a single frequency is a single point on a Nyquist plot. Moreover, the ratio of an oscillating voltage to an oscillating current is the impedance, which has a magnitude $|Z|$ and a phase angle θ.

These measurements are the basis of impedance spectroscopy, in which the Cartesian complex plane is used for representation. An impedance spectrum is therefore a series of points, where each point is a different frequency; whereas, characteristic shapes can appear in Nyquist plots. The shapes can represent characteristics of specific elements or combinations of elements, so they are (often, but not always) visually useful for quickly understanding something about the system to be measured. Also note that impedance spectroscopy is a popular analytical tool in materials research and development because it involves a relatively simple electrical measurement that can readily be automated and whose results may often be correlated with many complex materials variables from mass transport, rates of chemical reactions, corrosion, and dielectric properties to defects, microstructure,

UNCORRECTED PROOFS

Trim Size: 170mm x 244mm Single Column Loose Ribeiro670117 c17.tex V1 - 12/11/2020 5:48pm Page 423

and compositional influences on the conductance of solids. Impedance spectroscopy is useful as an empirical quality control procedure, yet it can also contribute to the interpretation of fundamental electrochemical and electronic processes [47].

A physical quantity becomes detectable by means of impedance (i.e. converted into a measurable electrical signal) when a variation of such a quantity reflects into a variation of the impedance of the sensor [48]. Typically, impedance sensors are passive: energy is not directly transferred from the physical domain to the electrical domain, as in the case of optical and radiation sensors, where photons are converted into electrons, or of electrochemical sensors, where charge is transferred from ions to metal electrodes during a redox reaction. Here, external events change the sensor impedance, and a stimulation source is required to inject some energy into the sensor (either a voltage or a current) to detect such a variation. The former attribute is granted by the adjustable penetration of the electric field in the matter, while the latter is due to charge induction–capacitive coupling [48]. The interface between the physical domain (i.e. the sensing material/device) and the electrical domain is the electrodes. Although the design of the electrodes is often overlooked, the code sign of the electrodes and the readout electronics is a key point to achieve optimal performance [48].

Sensors based on impedance transduction have been well consolidated in the industry for decades. Today, downscaling the size of sensing elements to micrometric and sub-micrometric dimensions is enabled by the diffusion of lithographic processes and fostered by the convergence of complementary disciplines such as microelectronics, photonics, biology, electrochemistry, and material science, all focusing on energy and information manipulation at the micro- and nanoscale. Although such a miniaturization trend is pivotal in supporting the pervasiveness of sensors (in the context of mass deployment paradigms such as smart city, home, and body monitoring networks and the Internet of Things), it also presents new challenges for detection [48].

The rapidly growing demands on sensing, detection, and determination of a vast variety of compounds in wide ranges of test systems under very different conditions emphasize the need for intense methodological research. To meet these requirements, all imaginable measuring principles are being tested and, where possible, developed and applied. A good example is the measurement of the electrical impedance of test systems, for several reasons:

- Technical developments have made measurements simple, flexible, and cheap.
- The technique is portable and user friendly.
- It does not require sample preparation.
- It is a non-destructive technique.
- Using substantially lower frequencies of the applied signal has led to better definition of the output, which is more easily interpreted.
- The universal detection character and the separation of the sensing elements from the test medium make the technique attractive for analyses of complex mixtures of similar analytes.

UNCORRECTED PROOFS

Trim Size: 170mm x 244mm Single Column Loose Ribeiro670117 c17.tex V1 - 12/11/2020 5:48pm Page 424

17.3.2 Data Treatment

An essential step when using artificial electronic sensors is data analysis. Since the number of samples may be very large, and many measurements are needed to distinguish the samples, the volume of data generated is tremendous [49]. Therefore, using chemometrics or pattern-recognition techniques is inevitable.

These tools consist of the following sequential stages: signal preprocessing, dimensionality reduction, and prediction/validation [50]. Signal preprocessing prepares the feature vector for future processing. It includes compensation for sensor drift, scaling of the data, and extracting representative parameters [51]. The intrinsic complexity, richness, and cross-selectivity of the signals generated by sensor arrays provide certain advantages, as the resulting dataset contains meaningful information about the sample. The choice of method depends on the type of available input data acquired from the sensors and the type of information that is sought.

The digital output generated by e-tongue sensors needs to be analyzed and interpreted in order to provide useful information to the operator [52]. Essential methods used to process data obtained from sensor arrays are principal component analysis (PCA), multivariate linear regression, linear discriminant analysis, principal component regression, partial least squares, cluster analysis, artificial neural networks, and fuzzy logic [53]. Of these, PCA is the most used methodology in the literature for e-tongues; it is based on an unsupervised method for determining similarity of the input data by comparing the relative location of the associated so-called principal components in a PCA plot. The corresponding score plots correlate the observations or experiments, grouping samples that can be used for further classification [23].

17.4 Critical View on Coupling EK and Electronic Tongues

The quantitative analysis of all components in a complex sample is a utopia, unless dedicated sensors can be obtained for each molecule to be detected. Global biological measurements provide information about the effects produced by a cocktail of contaminants; however, the total composition is unknown [54, 55]. As analytical methodologies, e-tongues, chromatography, and mass spectrometric techniques are under constant improvement. If classical chromatographic/mass spectrometric techniques are currently considered the gold standard for detection, e-tongues are seen as the new generation of detection devices for liquid samples (Table 17.1). With e-tongues, a reduction in sample manipulation is possible and will avoid sample preparation steps. Nevertheless, traditional techniques are superior in terms of simultaneous multi-analyte identification. Indeed, the e-tongue is highly sensitive to small changes in the system (even low limit of detection [LOD] and limit of quantification [LOQ] are achieved, compared to high-performance liquid chromatography with a diode-array detector [HPLC-DAD]), but not as selective as a mass spectrometry instrument, i.e. liquid chromatography–mass spectrometry (LC/MS), which can provide, at the same time, selectivity and excellent reliability of results.

UNCORRECTED PROOFS

Trim Size: 170mm x 244mm Single Column Loose Ribeiro670117 c17.tex V1 - 12/11/2020 5:48pm Page 425

Table 17.1 Comparative features of traditional methods vs. e-tongue for environmental analysis.

Chromatography techniques	E-tongue
■ Analysis of an aliquot of the extract ■ High sample volumes of water are necessary ■ Fewer matrix effects ■ Disposable cartridges ■ Sequential extraction and possibility of using different combinations of cartridges connected in series ■ Manipulation of the sample; possibility of contamination ■ Risk of degradation of compounds (longer overall analysis time) ■ Consumption of organic solvents for elution and eluents ■ Possible loss of analytes during elution step ■ Several measurements can be performed with the same extract ■ Longer analysis time ■ Expensive equipment	■ Small sample volumes ■ Matrix effects: depending on electrical principle and transduction element ■ Direct analysis of the sample; minimal sample preparation ■ Limited multi-analyte determination: good response in detection, range of contamination concentration achieved, but not specific analyte identification ■ Possible automatization of the system ■ Minimal degradation ■ Avoids consumption of organic solvents ■ Minimal, non-contaminating waste ■ Faster analysis ■ Real-time detection and high throughput ■ Portable systems ■ Applicability to early-warning and on-site monitoring ■ Non-qualified personnel required: user friendly ■ Cost-effective equipment

Source: Adapted from Magro et al. [10]; Farré et al. [54]; Rodriguez-Mozaz, Lopez de Alda, and Barceló [55]; Bourgeois et al. [56].

Magro et al. [14] coupled an electroremediation reactor to a hybrid e-tongue array and proved that the array of sensors is capable of checking the degradation pathway, making it possible to understand the plume of contamination (kinetics of degradation). Electroremediation technologies have been used since the early nineteenth century for different type of contaminants, to remove, separate, and promote degradation, targeting soil remediation [15]. Promising results have been observed for removing EOCs from soil [57, 58], sludge [59], and effluent [60]. Today, electro-based technologies are at a turning point, since at the end of a long experimental proof-of-concept period, these treatments are now in the position to improve the maturity of their technology and play a role in practical solutions.

To do that, critical technological difficulties and cost handicaps must be overcome. Compared to the traditional sampling and analysis currently used to monitor electroremediation treatment, sensors like e-tongues can provide a faster response to the output data in a continuous, cost-effective way, thus improving market competitiveness and increasing removal performance and technology payback. A SWOT (Strengths, Weaknesses, Opportunities, Threats) analysis of the strengths, weaknesses, opportunities, and threats regarding electro-based technology's real-time monitoring by e-tongues is presented in Figure 17.3.

The SWOT analysis suggests promising prospects for future research on real-time sensing applied to remediation techniques. The concept will take advantage of

UNCORRECTED PROOFS

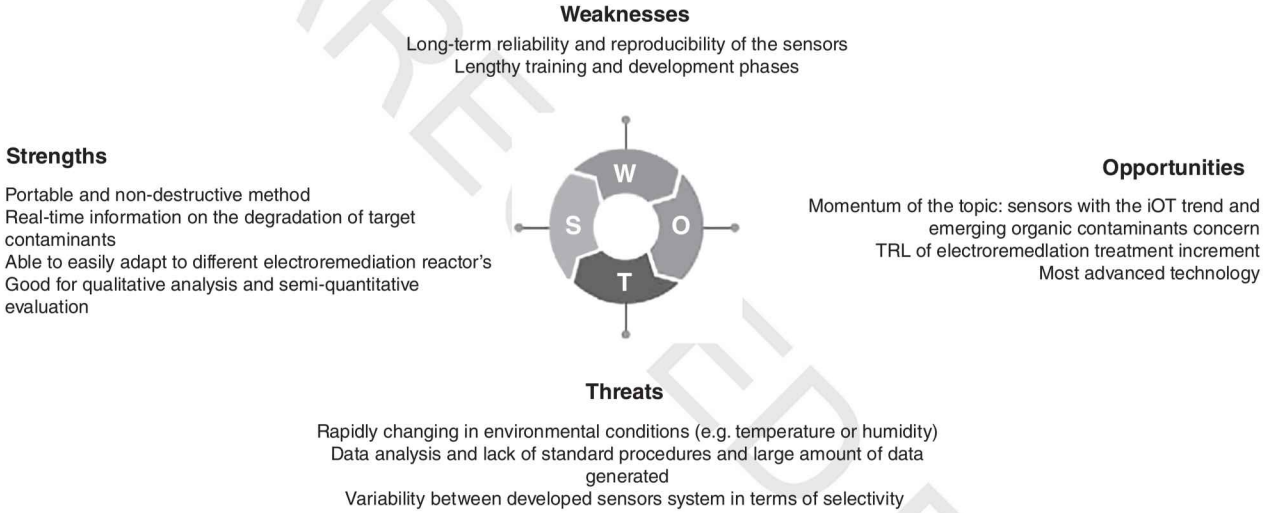

Figure 17.3 SWOT analysis of the electro-based technologies coupled to sensors in a market prospective. Source: Data from Magro et al. [10]; Bourgeois et al. [56].

UNCORRECTED PROOFS

Trim Size: 170mm x 244mm Single Column Loose

Ribeiro670117 c17.tex V1 - 12/11/2020 5:48pm Page 426

Trim Size: 170mm x 244mm Single Column Loose Ribeiro670117 c17.tex V1 - 12/11/2020 5:48pm Page 427

sensors, momentum regarding emerging contaminants, and, above all, the design flexibility of electroremediation technologies, which can easily be adapted based on the target contaminants and application. Additionally, real-time information will decrease the cost of electro-technologies by reducing the duration of monitoring, as they can follow the contaminants' concentration decay and are a non-destructive method for analyzing matrices.

The major drawback of using the e-tongue as a monitoring, semi-quantitative, and qualitative tool for emerging contaminants in a dynamic process such as electroremediation would be to have a system with the ability to systematically reduce the dimensionality of the incoming electrical data while preserving all relevant information. So far, there has been no systematic approach to the problem of data preprocessing and analysis. It seems that the choice of suitable output (e.g. desorption signal, baseline, transient/maximum response) and analysis protocol (e.g. PCA, partial least squares, artificial neural networks) is often the result of trial and error, primarily based on personal intuition or experience [56]. This has shown serious consequences for the classification of results and also underlined the difficulty of modeling this effect with a calibration mixture. The primary challenge for e-tongues is the low reproducibility of sensor manufacturing, which implies a learning phase for the array. Also, pH changes can occur in electrochemical remediation, leading to losses in the thin-film structures. Thus, the design of the reactor may be built to allow pH stability, and/or the thin films should be mechanically stable under pH fluctuations.

Although not many sensor systems can compete with conventional analytical methods in terms of accuracy and reproducibility, they can be used in a dynamic removal process and applied to industry, since they can provide enough information for routine testing and screening environmental aqueous matrices in terms of concentration range. E-tongues are not intended to replace traditional methods, but they can be useful and complementary tools when speed and a lower-cost response are required.

17.5 Final Remarks

This chapter has presented the state-of-art as well as drawbacks, challenges, and advantages, demonstrating that sensors based on the electronic tongue concept can be coupled with EK processes to detect EOCs in wastewater. If the concept is applied to EK technologies, the potential for in situ monitoring is amplified for the supervision of these type of contaminants.

The key to developing sensor devices with sub-picomolar detection capabilities is based on

- The choice of a sensor array system
- The measuring technique
- The preparation of data libraries to support data analysis, particularly concerning sample classification using supervised and unsupervised pattern recognition techniques

UNCORRECTED PROOFS

Trim Size: 170mm x 244mm Single Column Loose Ribeiro670117 c17.tex V1 - 12/11/2020 5:48pm Page 428

Acknowledgments

This work has received funding from the European Union's Horizon 2020 research and innovation program under Grant Agreement No. 776811, under the Marie Skłodowska-Curie grant agreement No. 778045. The authors also acknowledge and apprciate the support given to CENSE by the Portuguese Foundation for Science and Technology (FCT) through the strategic project UIDB/04085/2020. UID/FIS/00068/2020 and supported by the project "Development of Nanostructures for Detection of Triclosan Traces on Aquatic Environments" (PTDC/FIS-NAN/0909/2014). C. Magro acknowledges Fundação para a Ciência e a Tecnologia for her PhD fellowship SFRH/BD/114674/2016. This work is anchored by the RESOLUTION LAB, a laboratory at NOVA School of Science and Technology.

References

1 Brack, W., Dulio, V., and Slobodnik, J. (2012). The NORMAN network and its activities on emerging environmental substances with a focus on effect-directed analysis of complex environmental contamination. *Environmental Sciences Europe* 24 (1): 29.

2 Geissen, V., Mol, H., Klumpp, E. et al. (2015). Emerging pollutants in the environment: a challenge for water resource management. *International Soil and Water Conservation Research* 3 (1): 57–65.

3 EU (2006). Regulation No 1907/2006 of the European Parliament and of the Council of 18 December 2006 concerning the registration, evaluation, authorisation and restriction of chemicals (REACH), establishing a European Chemicals Agency, amending Directive 1999/45/ EC and repealing Council Regulation (EEC) No 793/93. *Official Journal of the European Union* L 39611.

4 EU (2010). Directive 2010/75/EU of the European Parliament and of the Council of 24 November 2010 on industrial emissions (integrated pollution prevention and control). *Official Journal of the European Union* L 334 (17.12.2010): 17–119.

5 European Commission (2006). Regulation No 166/2006 of the European Parliament and of the Council of 18 January 2006 concerning the establishment of a European pollutant release and transfer register and amending council directives 91/689/EEC and 96/61/EC. *Official Journal of the European Union* L 33 (4.2.2006): 1–17.

6 EEC Council (1991). Council Directive 91/271/EEC of 21 May 1991 concerning urban wastewater treatment. *Official Journal of the European Union* L 135 (30.5.1991): 40–52.

7 European Commission (2000). Directive 2000/60/EC of the European Parliament and of the Council of 23 October 2000 establishing a framework for community action in the field of water policy. *Official Journal of the European Union* L 327 (22.12.2000): 1–73.

8 European Parliament (2008). Directive 2008/105/EC of the European Parliament and of the Council of 16 December 2008 on environmental quality

UNCORRECTED PROOFS

Trim Size: 170mm x 244mm Single Column Loose Ribeiro670117 c17.tex V1 - 12/11/2020 5:48pm Page 429

standards in the field of water policy. *Official Journal of the European Union* L 348 (24.12.2008): 84–97.

9 Gavrilescu, M., Demnerová, K., Aamand, J. et al. (2015). Emerging pollutants in the environment: present and future challenges in biomonitoring, ecological risks and bioremediation. *New Biotechnology* 32 (1): 147–156.

10 Magro, C., Mateus, E.P., Raposo, M., and Ribeiro, A.B. (2019). Overview of electronic tongue sensing in environmental aqueous matrices: potential for monitoring emerging organic contaminants. *Environmental Reviews* 27 (2): 202–214.

11 Liu, X., Feng, H., Liu, X., and Wong, D.K.Y. (2011). Electrocatalytic detection of phenolic estrogenic compounds at NiTPPS|carbon nanotube composite electrodes. *Analytica Chimica Acta* 689 (2): 212–218.

12 Facure, M.H.M., Mercante, L.A., Mattoso, L.H.C., and Correa, D.S. (2017). Detection of trace levels of organophosphate pesticides using an electronic tongue based on graphene hybrid nanocomposites. *Talanta* 167: 59–66.

13 Jianrong, C., Yuqing, M., Nongyue, H. et al. (2004). Nanotechnology and biosensors. *Biotechnology Advances* 22 (7): 505–518.

14 Magro, C., Mateus, E.P., Paz-Garcia, J.M. et al. (2019). Electronic tongue coupled to an electrochemical flow reactor for emerging organic contaminants real time monitoring. *Sensors* 19 (24): 5349.

15 Acar, Y.B. and Alshawabkeh, A.N. (1993). Principles of electrokinetic remediation. *Environmental Science & Technology* 27 (13): 2638–2647.

16 Acar, Y.B., Rabbi, M.F., Gale, R.J. et al. (1996). Enhance soil bioremediation with electric fields. *ChemTech* 26 (4): 40–43.

17 Strathmann, H. (2004). Overview of ion-exchange membrane processes. In: *Ion-Exchange Membrane Separation Processes* (ed. H. Strathmann), 1–22. Elsevier.

18 Magro, C., Mateus, E.P., Paz-Garcia, J.M., and Ribeiro, A.B. (2020). Emerging organic contaminants in wastewater: understanding electrochemical reactors for triclosan and its by-products degradation. *Chemosphere* 247: 125758.

19 Klavarioti, M., Mantzavinos, D., and Kassinos, D. (2009). Removal of residual pharmaceuticals from aqueous systems by advanced oxidation processes. *Environment International* 35 (2): 402–417.

20 Gałuszka, A., Migaszewski, Z.M., and Namieśnik, J. (2015). Moving your laboratories to the field – advantages and limitations of the use of field portable instruments in environmental sample analysis. *Environmental Research* 140: 593–603.

21 Albareda-Sirvent, M., Merkoçi, A., and Alegret, S. (2001). Pesticide determination in tap water and juice samples using disposable amperometric biosensors made using thick-film technology. *Analytica Chimica Acta* 442 (1): 35–44.

22 De Marco, R., Clarke, G., and Pejcic, B. (2007). Ion-selective electrode potentiometry in environmental analysis. *Electroanalysis* 19 (19–20): 1987–2001.

23 Correa, D.S., Pavinatto, A., Mercante, L.A. et al. (2017). Chemical sensors based on hybrid nanomaterials for food analysis. In: *Nanobiosensors* (ed. A.M. Grumezescu), 205–244. Elsevier.

24 del Valle, M. (2010). Electronic tongues employing electrochemical sensors. *Electroanalysis* 22 (14): 1539–1555.

UNCORRECTED PROOFS

Trim Size: 170mm x 244mm Single Column Loose Ribeiro670117 c17.tex V1 - 12/11/2020 5:48pm Page 430

25 Hayashi, K., Yamanaka, M., Toko, K., and Yamafuji, K. (1990). Multichannel taste sensor using lipid membranes. *Sensors and Actuators B: Chemical* 2 (3): 205–213.

26 Vlasov, Y., Legin, A., Rudnitskaya, A. et al. (2005). Nonspecific sensor arrays ("electronic tongue") for chemical analysis of liquids (IUPAC technical report). *Pure and Applied Chemistry* 77 (11): 1965–1983.

27 Escuder-gilabert, L. and Peris, M. (2010). Highlights in recent applications of electronic tongues in food analysis. *Analytica Chimica Acta* 665 (1): 15–25.

28 Magro, C. (2019). Advances in applied electrokinetics: Treatment, by-products reuse and sensors' system. PhD thesis, NOVA School of Sciences and Technology, NOVA University, Lisbon.

29 Riul, A., Dos Santos, D.S., Wohnrath, K. et al. (2002). Artificial taste sensor: efficient combination of sensors made from Langmuir-Blodgett films of conducting polymers and a ruthenium complex and self-assembled films of an azobenzene-containing polymer. *Langmuir* 18 (1): 239–245.

30 Olivati, C.A., Riul, A., Balogh, D.T. et al. (2009). Detection of phenolic compounds using impedance spectroscopy measurements. *Bioprocess and Biosystems Engineering* 32 (1): 41–46.

31 Taylor, D.M. and Macdonald, A.G. (1987). AC admittance of the metal/insulator/electrolyte interface. *Journal of Physics D: Applied Physics* 20 (10): 1277.

32 Bai, J. and Zhou, B. (2014). Titanium dioxide nanomaterials for sensor applications. *Chemical Reviews* 114 (19): 10131–10176.

33 Chen, A. and Chatterjee, S. (2013). Nanomaterials based electrochemical sensors for biomedical applications. *Chemical Society Reviews* 42 (12): 5425.

34 Jeevanandam, J., Barhoum, A., Chan, Y.S. et al. (2018). Review on nanoparticles and nanostructured materials: history, sources, toxicity and regulations. *Beilstein Journal of Nanotechnology* 9: 1050–1074.

35 Chandran, G.T., Li, X., Ogata, A., and Penner, R.M. (2016). Carbon-based nanomaterials. In: *Essentials in Nanoscience and Nanotechnology* (eds. N. Kumar and S. Kumbhat), 189–236. Wiley.

36 Duarte, A.A., Botelho do Rego, A.M., Salerno, M. et al. (2015). DPPG liposomes adsorbed on polymer cushions: effect of roughness on amount, surface composition and topography. *The Journal of Physical Chemistry. B* 119 (27): 8544–8552.

37 Zhao, S., Caruso, F., Dähne, L. et al. (2019). The future of layer-by-layer assembly: atribute to ACS nano associate editor Helmuth Möhwald. *ACS Nano* 13 (6): 6151–6169.

38 Motia, S., Tudor, I.A., Ribeiro, P.A. et al. (2019). Electrochemical sensor based on molecularly imprinted polymer for sensitive triclosan detection in wastewater and mineral water. *Science of the Total Environment* 664: 647–658.

39 Decher, G., Hong, J.D., and Schmitt, J. (1992). Buildup of ultrathin multilayer films by a self-assembly process: III. Consecutively alternating adsorption of anionic and cationic polyelectrolytes on charged surfaces. *Thin Solid Films* 210–211: 831–835.

UNCORRECTED PROOFS

Trim Size: 170mm x 244mm Single Column Loose Ribeiro670117 c17.tex V1 - 12/11/2020 5:48pm Page 431

40 Veiseh, M., Zareie, M.H., and Zhang, M. (2002). Highly selective protein patterning on gold-silicon substrates for biosensor applications. *Langmuir* 18 (17): 6671–6678.

41 Ferreira, Q., Gomes, P.J., Ribeiro, P.A. et al. (2013). Determination of degree of ionization of poly(allylamine hydrochloride) (PAH) and poly[1-[4-(3-carboxy-4 hydroxyphenylazo)benzene sulfonamido]-1,2- ethanediyl, sodium salt] (PAZO) in layer-by-layer films using vacuum photoabsorption spectroscopy. *Langmuir* 29 (1): 448–455.

42 Raposo, M. and Oliveira, O.N. (2000). Energies of adsorption of poly(o-methoxyaniline) layer-by-layer films. *Langmuir* 16 (6): 2839–2844.

43 Raposo, M., Lourenço, J.M.C., Botelho do Rego, A.M. et al. (2012). Counterions – a new approach to control the degree of ionization of polyelectrolytes in layer-by-layer films. *Colloids and Surfaces A Physicochemical and Engineering Aspects* 412: 1–10.

44 Chang, C.-W., Kumar, S.R., Wong, C.-B. et al. (2018). Graphene oxide-cation interaction: inter-layer spacing and zeta potential changes in response to various salt solutions. *Journal of Membrane Science* 554: 253–263.

45 Raposo, M. and Oliveira, O.N. Jr. (1998). Adsorption mechanisms in layer-by-layer films. *Brazilian Journal of Physics* 28 (4): 1–14.

46 Depla, D., Mahieu, S., and Greene, J.E. (2010). Sputter deposition processes. In: *Handbook of Deposition Technologies for Films and Coatings* (ed. P.M. Martin), 253–296. Elsevier.

47 Barsoukov, E. and Macdonald, J.R. (2005). *Impedance Spectroscopy*. Wiley.

48 Carminati, M. (2017). Advances in high-resolution microscale impedance sensors. *Journal of Sensors* 2017: 1–15.

49 Wilson, A.D. (2012). Review of electronic-nose technologies and algorithms to detect hazardous chemicals in the environment. *Procedia Technology* 1: 453–463.

50 Rodríguez Méndez, M.L. (2016). Preface. In: *Electronic Noses and Tongues in Food Science* (ed. M.L.R. Méndez), xv. San Diego: Elsevier.

51 Raposo, M., Ribeiro, P.A., El Bari, N., and Bouchikhi, B. (2016). Sensing of component traces in complex systems. In: *Electrokinetics across Disciplines and Continents* (eds. B.A. Ribeiro, P.E. Mateus and N. Couto), 401–426. Cham: Springer International Publishing.

52 Wilson, A.D. and Baietto, M. (2009). Applications and advances in electronic-nose technologies. *Sensors* 9 (1): 5099–5148.

53 Riul, A. Jr., Dantas, C.A.R., Miyazaki, C.M., and Oliveira, O.N. Jr. (2010). Recent advances in electronic tongues. *Analyst* 135 (10): 2481.

54 Farré, M., Kantiani, L., Pérez, S. et al. (2009). Sensors and biosensors in support of EU directives. *TrAC Trends in Analytical Chemistry* 28 (2): 170–185.

55 Rodriguez-Mozaz, S., Lopez de Alda, M.J., and Barceló, D. (2007). Advantages and limitations of on-line solid phase extraction coupled to liquid chromatography-mass spectrometry technologies versus biosensors for monitoring of emerging contaminants in water. *Journal of Chromatography. A* 1152 (1–2): 97–115.

UNCORRECTED PROOFS

Trim Size: 170mm x 244mm Single Column Loose Ribeiro670117 c17.tex V1 - 12/11/2020 5:48pm Page 432

56 Bourgeois, W., Romain, A.-C., Nicolas, J., and Stuetz, R.M. (2003). The use of sensor arrays for environmental monitoring: interests and limitations. *Journal of Environmental Monitoring* 5: 852–860.

57 Gomes, H.I., Dias-Ferreira, C., and Ribeiro, A.B. (2013). Overview of in situ and ex situ remediation technologies for PCB-contaminated soils and sediments and obstacles for full-scale application. *Science of the Total Environment* 445–446: 237–260.

58 Guedes, P., Mateus, E.P., Couto, N. et al. (2014). Electrokinetic remediation of six emerging organic contaminants from soil. *Chemosphere* 117 (1): 124–131.

59 Guedes, P., Magro, C., Couto, N. et al. (2015). Potential of the electrodialytic process for emerging organic contaminants remediation and phosphorus separation from sewage sludge. *Electrochimica Acta* 181: 109–117.

60 Ferreira, A.R., Couto, N., Guedes, P. et al. (2018). Electrodialytic 2-compartment cells for emerging organic contaminants removal from effluent. *Journal of Hazardous Materials* 358: 467–474.

UNCORRECTED PROOFS

Trim Size: 170mm x 244mm Single Column Loose Ribeiro670117 c18.tex V1 - 12/11/2020 5:49pm Page 433

18

Perspectives on Electrokinetic Remediation of Contaminants of Emerging Concern in Soil

Paula Guedes[1,2], Nazaré Couto[1], Eduardo Mateus[1], Cristina Silva Pereira[2], and Alexandra B. Ribeiro[1]

[1]CENSE – Center for Environmental and Sustainability Research, Department of Environmental Sciences and Engineering, NOVA School of Science and Technology, NOVA University Lisbon, 2829-516 Caparica, Portugal
[2]Instituto de Tecnologia Química e Biológica António Xavier, NOVA University Lisbon, 2780-157 Oeiras, Portugal

18.1 Introduction

18.1.1 Soil Pollution

Soil, a complex and dynamic system, should be regarded as a non-renewable resource on a human scale. Soil contributes to the maintenance of all forms of life that occur on the terrestrial surface. It also has several other functions such as providing biomass and raw materials; storing, filtering, and transforming substances; and acting as a carbon and biodiversity pool, as a platform for human activities and the landscape, and as a heritage archive [1]. There are many threats to soil – erosion, sealing, compaction, landslides, loss of organic matter, salinization, and contamination – all of which potentially promote loss of biodiversity [1]. These threats have proven difficult to tackle and continue to be a challenge, particularly in line with expected future developments in urbanization, intensive agriculture, and industrialization.

The Intergovernmental Technical Panel of Soil (ITPS) identified soil contamination as the third threat to soil functions in Europe [2]. Soil pollution can be defined as "the occurrence of pollutants in soil above a certain level causing a deterioration or loss of one or more soil functions and that has adverse effects on any non-targeted organism" [1, 3]. There are more than 22.8 million potentially contaminated sites in the 28 EU Member States [1], representing lost economic opportunities and threatening human health and the ecosystem.

Soils play an essential role in health and environmental preservation. Thus, soil protection was included in one of the most important legal frameworks for development in the upcoming decades: the proposal of Sustainable Development Goals (SDGs) approved by the United Nations General Assembly in September 2015. The SDGs mention soil contamination twice: SDG 3.9 proposes to reduce the

Electrokinetic Remediation for Environmental Security and Sustainability, First Edition.
Edited by Alexandra B. Ribeiro and M.N.V. Prasad.
© 2021 John Wiley & Sons Ltd. Published 2021 by John Wiley & Sons Ltd.

UNCORRECTED PROOFS

Trim Size: 170mm x 244mm Single Column Loose Ribeiro670117 c18.tex V1 - 12/11/2020 5:49pm Page 434

effect of hazardous substances present in air, water, and soils; and SDG 12.4 aims to promote better management of chemicals and waste, reducing their release into air, water, and soils to minimize their adverse impacts on human health and the environment [1].

Anthropogenic sources of soil pollution are usually caused by chemicals used in or produced as byproducts of industrial and domestic, activities, livestock, municipal wastes (including wastewater), agrochemicals, and petroleum-derived products [1, 3]. Today, concerns are being raised about emerging pollutants such as pharmaceuticals, endocrine disruptors, hormones, toxins, and biological pollutants, such as micropollutants in soils, including bacteria and viruses [3].

18.1.2 Contaminants of Emerging Concern

Contaminants of emerging concern (CECs) are chemical compounds that have been detected in drinking water, wastewater, and the aquatic environment. Pharmaceuticals and personal care products (PPCPs) and endocrine-disrupting chemicals (EDCs) are included in the CECs. These compounds usually have biological activity on different organisms, and their physicochemical properties determine their persistence in the environment and facilitate their bioaccumulation. There are many potential sources of CECs release into the environment (Figure 18.1). CECs are released worldwide from either point or non-point sources, including effluent, biosolids, landfill leachate, aquaculture, and livestock [2, 4–8]. Wastewater treatment plants are considered one of the primary sources of CECs environmental spread [9].

When treated wastewater – reclaimed wastewater (RWW) – is used for agricultural irrigation or treated sewage sludge (biosolids) is used as fertilizer, CECs present in these matrices are transferred into the soil. Once in the soil, the CECs' behavior will vary according to their characteristics and soil type [10–12]. The environmental abundance of many potentially toxic emerging pollutants strengthens the need to better understand the occurrence, fate, and ecological impact of CECs [9].

A study conducted in 2018 [13] showed that pharmaceuticals were detected in effluent (3–41 $\mu g\, l^{-1}$) and surface soil (2 and 15 $ng\, g^{-1}$) samples. Some of the detected compounds reached a depth of 150 cm, indicating that they can undergo leaching associated with heavy rain episodes. The soil presented a predominance of analgesics and anti-inflammatories (maximum of 10.05 $ng\, g^{-1}$), followed by antibiotics and psychiatric drugs (maximum of 5.45 and 3.78 $ng\, g^{-1}$, respectively). Once in the soil, these contaminants can transfer to crops through root uptake and translocation; the potential risk is greater for products consumed raw (e.g. fresh fruits and vegetables) [14]. It has been documented that certain antibiotics, including tetracyclines, amoxicillin, and fluoroquinolones, can be taken up by crop plants [15], while other CECs, such as miconazole (fungicide) and fluoxetine (antidepressants), are not present in crops despite their persistence in the soil [16].

A significant problem today, associated with the presence of CECs in the environment, is that some of these contaminants can promote bacterial resistance in the environment [17–19]. The United Nations General Assembly has recognized

UNCORRECTED PROOFS

Trim Size: 170mm x 244mm Single Column Loose Ribeiro670117 c18.tex V1 - 12/11/2020 5:49pm Page 435

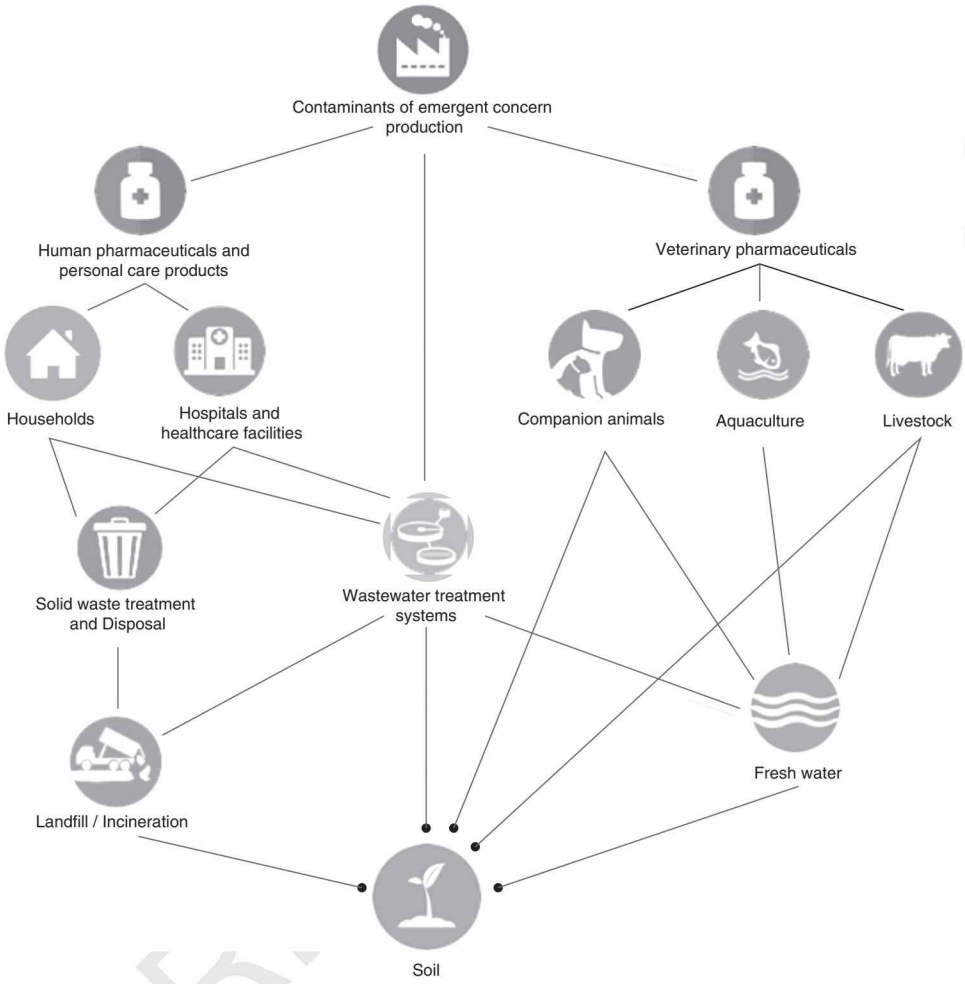

Figure 18.1 Simplified pathway for soil exposure to contaminants of emerging concern.

the need to address antimicrobial resistance and reduce antimicrobial residues in soils [3, 20].

The presence of these contaminants in soil is receiving increased attention worldwide, with the objective of protecting fresh water due to the scarcity of water and promoting the reuse of wastewater. These important topics are acknowledged and embedded within European and national strategies. The UN SDG on Water (SDG 6) specifically targets a substantial increase in recycling and safe reuse globally by 2030. Water reuse is a top priority area in the Strategic Implementation Plan of the European Innovation Partnership on Water [21], and the maximization of water reuse is a specific objective in the Communication "Blueprint to safeguard Europe's water resources" [22]. Using RWW for irrigation purposes can be a source of diverse nutrients for plants once its quality and usage requirements are complied with. The levels

UNCORRECTED PROOFS

Trim Size: 170mm x 244mm Single Column Loose Ribeiro670117 c18.tex V1 - 12/11/2020 5:49pm Page 436

of salts, heavy metals, and pathogens in RWW are critical parameters [23, 24] since they directly impact the quality of the soil and could potentially have adverse effects on both humans and plants. The presence of CECs is not included in the usage requirements of RWW. However, the dissemination of CECs in agricultural soils irrigated with RWW has been made apparent, as shown above, with potential health implications [14]. Although several technologies that are currently being developed for wastewater treatment address the removal of CECs, there is a need to address legacy pollution in soils. Thus, the worldwide occurrence of CECs in soil requires effective and economical treatments to eliminate them.

18.2 Electrokinetic Process

The electrokinetic (EK) process relies on applying a low-level current density between at least two electrodes. When applied to soil, this process may help overcome some of the problems associated with soil remediation technologies. The EK process presents some advantages in comparison with conventional remediation methods: (i) simplicity and safety; (ii) effectiveness for remediation of a wide range of contaminants (e.g. metals, organic compounds, radionuclides) alone or mixed; (iii) can be combined with other technologies; (iv) applicability both in situ and ex situ; and (v) cost-effectiveness [25–27].

When the EK process is applied, it generates a potential gradient that initiates electrochemical reactions (water electrolysis, redox, adsorption-desorption, and dissolution-precipitation reactions) and the movement of the contaminants through electromigration (movement of ions), electroosmosis (movement of the fluid), and electrophoresis (mechanical movement of colloidal particles or microorganisms present in the soil) [28, 29]. Upon their migration to the electrodes, contaminants may be removed or, in the case of organic contaminants, degraded by direct or indirect oxidation reactions (and/or through bioremediation in synergistic systems).

Still, the EK process is not without constraints. For example, the potential application of EK in situ is advantageous, as it avoids excavation of soil, thus minimizing changes in the soil's geotechnical and biological properties [25, 30]. However, the electrolysis of water generates pH changes near the electrodes that, if not appropriately controlled, may negatively influence soil properties and affect biodiversity [31, 32].

EK technologies have been extensively applied to soil contaminated with heavy metals and other inorganic pollutants [25–27, 33]. To remove organic pollution, most works are dedicated to remediating petroleum-derived contamination: polycyclic aromatic hydrocarbons (PAHs) [30, 34, 35]. Applying the EK technique to remediate soils contaminated with CECs is still in the early stages, with few studies fulfilling this aim [36–42].

The overall EK efficiency of CECs remediation is based on two primary mechanisms: (i) extracting contaminants from soil by electroosmosis and electromigration and (ii) destroying CECs by induced electrochemical reactions. In the specific case of in situ soil remediation, in mild conditions, biodegradation plays an important role.

UNCORRECTED PROOFS

Trim Size: 170mm x 244mm Single Column Loose Ribeiro670117 c18.tex V1 - 12/11/2020 5:49pm Page 437

Thus, the following sections focus on these three basic mechanisms and potential applications to soils contaminated with CECs.

18.2.1 Removal Mechanisms

In most studies, the anode and cathode are in a chamber filled with a solution that enhances the removal of contaminants. This chamber is then inserted into the soil (Figure 18.2). EK remediation of non-polar organic contaminants relies on electroosmosis as the primary removal mechanism. Thus, the effectiveness of the EK process is highly dependent on compounds being soluble in the pore fluid or being converted into a soluble form.

The strategy to increase contaminant desorption and solubilization has been to employ surfactants, co-solvents, and chelating and complexing agents [43]. Since they may react differently with different contaminants, compatibility of flushing solutions and contaminants needs to be considered for process optimization [43]. It has been demonstrated for the removal of bisphenol A that using NaCl enhanced system efficiency compared to other tested electrolytes (deionized water, Na_2SO_4, citric acid, and NaOH) [41]. It was concluded that both the type of electrode (binary metallic, discussed below) and the processing fluid played key roles in enhancing the electrochemical degradation of bisphenol A. In addition, the compound pKa is an essential player in removal mechanisms. The pKa of bisphenol A is 9.6; thus, at higher pH, it could migrate either toward the anode reservoir by electromigration or toward the cathode reservoir by electroosmotic flow. In this case, electromigration toward the anode reservoir was predominant; once at the anode chamber, it suffered anodic oxidation [41]. On the other hand, in a similar system, nonylphenol solubility in the processing fluid significantly influenced its removal toward the cathode chamber by electroosmosis, with four types of processing fluid (deionized water, citric acid, NaCl, and methanol) being tested [44]. In this case, by increasing nonylphenol solubility in the processing fluid, the removal toward the reservoirs also increased. Methanol was the processing fluid that allowed the greatest nonylphenol removal [44].

When the EK process is used to remove compounds that have a low polarity or are non-polar, the control of electroosmosis (the primary removal mechanism for these compounds) is of the utmost importance [43]. It has been noted that maintaining pH at 7 in the anode chamber and increasing the electric charge accelerates the electroosmotic flow through soil, leading to increased mobilization and removal of low-polarity contaminants like PAHs [34]. The same is true for the removal of CECs. In a study conducted with two soils (loamy sand and silty loam), applying the EK process using $NaNO_3$ (0.01 M) as both anolyte and catholyte was efficient in the removal of six CECs (bisphenol A, 17α-ethinylestradiol, 17β-oestradiol, *p*-nonylphenol, *p*-octylphenol, and triclosan) in four days [36]. The results showed that by increasing the anolyte pH to 13, increased electroosmotic flow was achieved, consequently increasing CECs removal from the soil. The extent of mobilization toward the cathode end was primarily dependent on compound solubility and the octanol-water partition coefficient. Accordingly, bisphenol A presented the

UNCORRECTED PROOFS

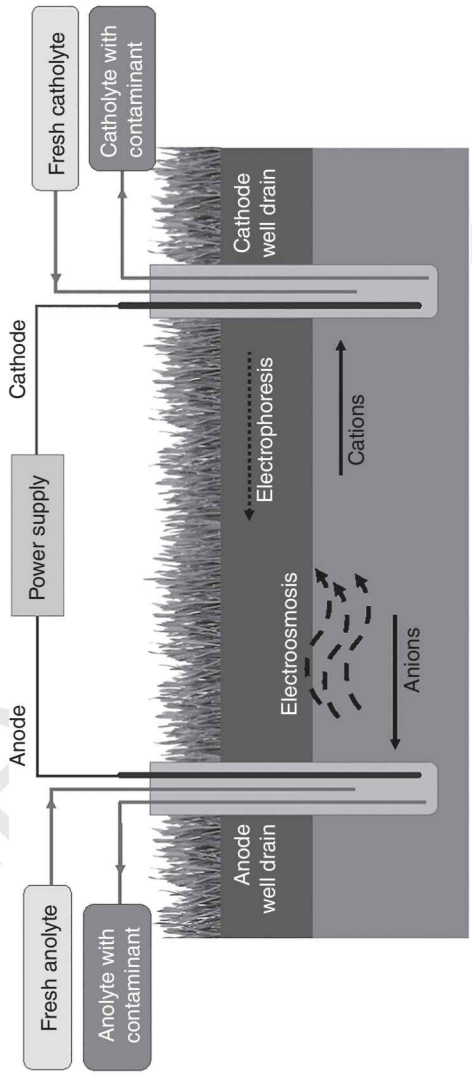

Figure 18.2 Schematic representation of the electrokinetic process.

UNCORRECTED PROOFS

Trim Size: 170mm x 244mm Single Column Loose Ribeiro670117 c18.tex V1 - 12/11/2020 5:49pm Page 439

highest mobilization rate, and *p*-nonylphenol was not detected in the catholyte. Again, for less soluble compounds, controlling the pH of the system based on the compound pKa is of interest. For example, triclosan has a pKa of 7.9; hence, at a pH greater than its pKa, triclosan will be predominantly ionized. This results in greater solubility and faster mobilization through electroosmosis toward the cathode [36]. The type of electrodes also influences electroosmotic flow: for example, higher values of electroosmosis are achieved with RuO_2/Ti and Pd/Ti comparing to Ti electrodes [41]. Thus, the type of electrodes cannot be disregarded in the control of electroosmotic flow.

When a mixture of CECs is under study for removal, it may not always be possible to adjust the system pH according to a specific compound pKa to increase its mobilization. CECs physicochemical properties vary among compounds, and their behavior is often controlled by interactions with specific functional groups or complex pH-dependent speciation; hence their removal behavior may be difficult to predict in the design of an EK process. Still, the solution might pass through spatial and temporal changes of pH and/or processing fluid that lead to dynamic changes in geochemistry and chemical compound speciation, which in turn improves removal kinetics for different compounds during treatment.

Most EK approaches used for soil require a processing fluid that might influence soil properties [36, 39, 41, 44]. Although the moderate use of a processing fluid might not disturb soil properties, if the flushing is too strong, it will remove other elements from the soil. The same is true for direct insertion of the electrodes into the soil without using a processing fluid; if the current is not properly controlled, other ions (including nutrients) and microorganisms will be mobilized, promoting a heterogeneous distribution within the soil column. In both cases, the soil pH may change dramatically if the water electrolysis is not appropriately controlled, which may help CECs mobilization and/or degradation but may also negatively affect the soil's microbiological community.

18.2.2 Electro-Degradation Mechanisms

Once contaminants are concentrated in the electrolyte solution (either cathode or anode), one option is to promote their degradation by electrochemical reactions. If CECs are in the anode compartment, the contaminants will suffer both direct and indirect degradation, whereas in the cathode, they will only undergo indirect degradation [45]. In this case, several types of electrodes can be employed: noble metals; metal alloys; mixed metal oxide (MMO), commercially known as dimensionally stable anodes (DSA®); carbon and graphite, boron-doped diamond (BDD), and others [46]. However, some of these materials present drawbacks such as passivation, polarization, and corrosion. Passivation is usually caused by polymeric and oligomeric compounds formed during electrode reactions [46]. Polarization is caused by poor mass transfer and accumulation of gases at the electrodes, which leads to the depletion of species in the boundary level of the electrode [46, 47]. These processes influence electrode stability, life expectancy, and reaction mechanisms, which consequently influence EK efficiency. Still, these problems

UNCORRECTED PROOFS

Trim Size: 170mm x 244mm Single Column Loose Ribeiro670117 c18.tex V1 - 12/11/2020 5:49pm Page 440

can be overcome by choosing the correct electrode materials and/or developing new electrode materials (preventing corrosion) and by powerful agitation of the electrolyte (preventing polarization and passivation) [46].

Electrodes can be divided into two classes: active and non-active [48], referring to activity related to the interaction between the anodes and formed hydroxyl radicals ($^{\cdot}OH$). Several authors have studied these interactions and the underlying oxidation mechanism extensively [40, 46, 48, 49]. In aqueous electrochemical reactions, the direct oxidation of organic contaminants usually occurs via the oxidation of water molecules on the electrode surface (MO_x), which leads to the formation of $^{\cdot}OH$ (Eq. (18.1)). Then, the $^{\cdot}OH$ may oxidize the underlying oxide lattice to a higher state, forming a *higher oxide* (Eq. (18.2)), which participates in the selective oxidation of the organic pollutant without complete mineralization (Eq. (18.3)).

$$H_2O + MO_x \rightarrow MO_x(^{\cdot}OH) + H^+ + e^- \quad (18.1)$$

$$MO_x(^{\cdot}OH) \rightarrow MO_x(O) + H^+ + e^- \quad (18.2)$$

$$MO_x(O) + R \rightarrow RO + MO \quad (18.3)$$

This behavior is typical for active electrodes (lower oxygen evolution reaction [OER] overpotential). For non-active electrodes (greater OER overpotential), the generated $^{\cdot}OH$ may directly oxidize the organic compound to CO_2 and H_2O via reaction with MO_x and $MO_x(^{\cdot}OH)$ (Eq. (18.4)), where m and n are the stoichiometric coefficients.

$$MO_x(^{\cdot}OH) + R \rightarrow M + mCO_2 + MO_x + nH + ne^- \quad (18.4)$$

A recent study employed graphite electrodes, which are cheap and commercially available, to remove CECs from clay soil [37]. The tested electrodes, directly inserted in the soil, were unstable in currents above 10 mA (3.5 mA cm^{-2}). For example, when 50 or 100 mA was used (approximately 17 and 35 mA cm^{-2}), the electrodes showed significant signs of corrosion [37]. At 10 mA, the electrodes endured the EK conditions for seven days without signs of deterioration while promoting CECs degradation (either by electrochemical reactions or by enhancing bioremediation) between 13% and 85% (depending on the current strategy employed).

The most common electrodes used for CECs removal (from aqueous matrices) are BDD and MMO electrodes such as Ti/Ta_2O_5–IrO_2, Ti/SnO_2–IrO_2, Ti/RuO_2–IrO_2, Ti/Sb–SnO_2, Ti/SnO_2–Sb_2O_5–RuO_2, and Ti/TiO_2–IrO_2, among others [46].

Platinized titanium electrodes have been tested to remediate soil polluted with CECs, inserted in the electrolyte compartments [36] and/or in direct contact with a soil slurry [38]. Using an EK soil-flushing system, a degradation efficiency of 52–66% for remediating six CECs (17β-estradiol, 17α-ethinylestradiol, bisphenol A, nonylphenol, octylphenol, and triclosan) was reported in the $NaNO_3$ solution applying 10–20 mA after a four-day treatment. Their degradation was primarily attributed to photo- and electrochemical (indirect) reactions [36]. The platinized titanium bars were also effective in removing CECs in three different cell designs, including electrodialytic systems [38]. The authors tested a three-compartment cell (soil in the middle separated from the electrodes by ion-exchange membranes), a two-compartment cell (soil in the cathode compartment separated from the anode

UNCORRECTED PROOFS

Trim Size: 170mm x 244mm Single Column Loose Ribeiro670117 c18.tex V1 - 12/11/2020 5:49pm Page 441

by an anion-exchange membrane), and a one-compartment cell (no separation) [38]. In this case, removal was between 44 and 100% (through mobilization and/or degradation) after 72 hours for the three studied CECs (bisphenol A, oxybenzone, and 17α-ethinylestradiol). The cell design influenced CECs removal, which allowed an understanding of the contaminants' behavior and the removal mechanisms involved. Using cells with divided compartments (three or two), bisphenol A and oxybenzone were primarily mobilized toward the anode compartment through electromigration, whereas 17α-ethinylestradiol suffered degradation [38]. In the two-compartment cell, when the soil was placed in the cathode compartment, greater degradation was obtained for oxybenzone. In this case, the soil slurry's pH influenced oxybenzone behavior (pH > pKa), making it more mobile, so it reached the anode side more quickly. The higher residence time in the anode compartment gave more time for oxybenzone to suffer anodic oxidation [38]. If the objective is to achieve greater and more homogeneous degradation rates, the best option is to place both electrodes (cathode and anode) in direct contact with the soil slurry [38].

In soil, RuO_2/Ti, Pd/Ti (binary metallic), and Ti have been employed for bisphenol A removal [41]. More bisphenol A was removed from soil with RuO_2/Ti than when Pd/Ti electrodes were used (1.4–1.8 times greater; deionized water as the processing fluid; 2 V cm^{-1} for five days) [41]. When NaCl was used as an electrolyte, 67.3% and 64.4% of bisphenol A was degraded with RuO_2/Ti and Pd/Ti electrodes, respectively.

EK technology coupled with RuO_2/Ni foam has also been tested for the removal of ibuprofen [40]. Results indicate that the EK effect is more evident in the ibuprofen degradation than on its removal by electromigration (depending on soil pH): remediation efficiency is highly dependent on the potential gradient applied. In this case, it was also concluded that increasing the electrode area would not significantly enhance ibuprofen remediation efficiency [40].

One option to improve contaminant degradation in the electrolyte well is to promote the electro-Fenton reaction. Basically, the electro-Fenton process has two different configurations: (i) Fenton reagents are added to the reactor from outside, and inert electrodes with high catalytic activity are used as anode material; or (ii) only hydrogen peroxide is added to the system, and Fe^{2+} is provided from sacrificial cast iron anodes [50]. The removal and degradation of ibuprofen from soil have been successfully achieved using Al/Fe oxidation electrodes as an anode and stainless steel as a cathode [39]. The Al plays the role of electron donor, so the Fenton–like reaction can continuously produce $^{\cdot}OH$. Using this system, the authors increased the remediation efficiency of ibuprofen to 70.1–94.6%. Two of the key factors were determined to be the H_2O_2 addition and the electrode area [39]. Still, the Fenton process is only effective at low pH (3–5), which may require pH adjustment during the remediation process [51].

It is relevant to mention that, in addition to direct and indirect electrochemical reactions, electro-degradation mechanisms may also be promoted further from the electrodes. In this case, soil particles may act as micro-electrodes (due to the double layer), inducing redox reactions [52] that may degrade CECs. Clay particles can be thought of as micro-electrodes possessing a compact Stern layer and a diffuse layer that mediates faradic reactions [52]. As donated/accepted electrons pass across the

UNCORRECTED PROOFS

Trim Size: 170mm x 244mm Single Column Loose Ribeiro670117 c18.tex V1 - 12/11/2020 5:49pm Page 442

electrical double layer into the bulk of the fluid, the available species are converted into others through redox reactions [52]. Thus, CECs further from the electrodes can also undergo redox reactions due to a wider electrochemical degradation range [37]. This is especially important if CECs with lower mobilization velocities, or even immobile compounds, are being treated. Still, very few studies focus on this degradation mechanism, and further research is needed.

18.2.3 Enhanced Bio-Degradation

In soil, CECs may suffer bioremediation, but its efficiency is site-specific and often limited by (i) mass transfer of electron acceptors/nutrients to microorganisms responsible for biodegradation; (ii) limited bio-accessibility of contaminants; and (iii) adaptation of indigenous microorganisms for biodegradation [27]. These limitations can be overcome by coupling bioremediation with the EK process. When applied in mild conditions, EK technology has the potential to increase biodegradation efficiency, primarily by mobilizing pollutants and bacteria and stimulating bacterial activity.

When using the EK process to enhance bioremediation, the primary objective is to make compounds, nutrients, and electron acceptors bioavailable [27, 32, 46, 53]. Electrophoresis will carry bacteria and charged colloids to the positive electrode (anode); nutrients, charged CECs, and other substances will electromigrate to the electrode with the opposite charge; and electroosmosis will carry bacteria, contaminants, nutrients, and electron acceptors toward the negative electrode (cathode) (Figure 18.3). The mobility of indigenous bacteria under an EK field is mostly influenced by electroosmosis ($> 90\%$) and electrophoresis ($< 20\%$) in clay soils [54], depending on the applied electric field. It has been determined in capillaries [55] that at electric fields above $0.3\,\mathrm{V\,cm^{-1}}$, *Escherichia coli* moves

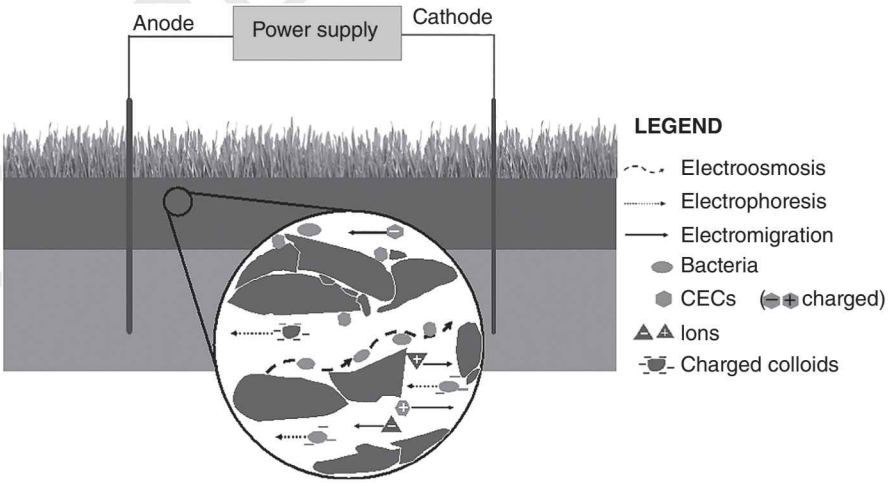

Figure 18.3 Schematic representation of electrokinetic-enhanced bioremediation. Source: Adapted from Gill et al. [27].

UNCORRECTED PROOFS

Trim Size: 170mm x 244mm Single Column Loose Ribeiro670117 c18.tex V1 - 12/11/2020 5:49pm Page 443

exclusively by electroosmosis. But at values below $0.2\,V\,cm^{-1}$, *E. coli* moves at different average speeds toward both anode and cathode due to the superimposed effects of electroosmotic flow, electrophoresis, galvanotaxis, and random motility.

Contaminant bioavailability, as well as its homogeneous distribution, significantly influences bioremediation efficiency [56]. The application of an electric field helps to overcome contaminant bioavailability constraints through contaminant desorption and redistribution on both a micro and a macro scale [33, 53]. The positive effects of the EK process also include the generation of oxidizing and reducing zones that are favorable for biodegradation of contaminants close to the electrodes [27]. However, when the current is applied, the soil pH can change dramatically if the water electrolysis is not appropriately controlled. Although these pH changes may help with CECs mobilization and/or degradation, they can also negatively affect the soil's microbial community [27, 51]. Thus, pH is one of the key parameters when EK is used in combination with bioremediation.

The pH along the soil column is modified by the generation of H^+ and OH^- (anode and cathode, respectively). The acid front generated at the anode migrates toward the cathode, and the alkaline front migrates in the opposite direction. H^+ presents greater mobility in relation to OH^-; and as it moves alongside electroosmosis, water will be generated at two-thirds of the distance from the anode where the acid and alkaline fronts meet [57]. However, this behavior depends on soil characteristics such as buffering capacity, which may hinder H^+ mobility [33]. On the other hand, the alkaline front may cause the precipitation of metals (e.g. as hydroxide and carbonate salts), which may block the pores of the soil and influence pollutant mobilization [33]. Microorganisms will be influenced by these soil pH variations, especially near the electrodes, where extreme pH changes may occur [32, 58–63]. By controlling the soil pH and moisture content, the EK process enhances microbial dehydrogenase activity, thus promoting a positive effect on biodegradation (in this case, of pentachlorophenol) [64]. But if extreme pH variations occur ($3 >$ soil $pH > 9$), they may interfere with microbial metabolism, gas solubility, and nutrient (bio)availability in the pore fluid and inhibit microbial growth [31, 47, 63–65], thus negatively affecting biodegradation.

The usual strategies to control soil pH are using conditioning agents/circulation methods and current strategies (polarity reversal, ON/OFF periods) [37, 66, 67].

The choice of a circulating agent can be a challenge as the reagent needs to be environmentally friendly and compatible with the soil microbiota and, at the same time, provide effective pH regulation at the anode and cathode sides. Also, using the electrolyte and circulation system will increase the treatment cost. Thus, alternatives that provide significant removal efficiency and do not require additional chemicals are good options.

Various current strategies have been applied to control pH [37, 40, 41, 53, 61, 64, 68]. The advantage of using current strategies is the possibility of also controlling the mobilization of nutrients, microorganisms, and pore fluid. Some strategies have been successfully applied to remediate soils contaminated with hydrocarbons and pentachlorophenol [53, 63, 69]. The most common strategy is periodic polarity reversal, in which electrode polarity is reversed at fixed time intervals; as a result,

UNCORRECTED PROOFS

Trim Size: 170mm x 244mm Single Column Loose Ribeiro670117 c18.tex V1 - 12/11/2020 5:49pm Page 444

the electrochemical reactions are interchanged between the electrodes, reversing the EK mechanisms. This strategy allows controlling the pH [37, 63, 64] while simultaneously reversing the direction of electroosmotic flow, electromigration, and electrophoresis, promoting a more homogenous distribution of water, nutrients, and bacteria [27]. This strategy may result in slightly greater current densities when the direction of the electric field is reversed [70]. This effect has been attributed to a change in the charge of the double layer that increases consumption of the capacitive part of the current due to the double layer discharging or recharging [70]. Another option to control pH changes with the current is to use ON/OFF periods, depending on total treatment time [37]. If the current is kept ON for 12 hours and then switched OFF for 12 hours, pH changes after seven days of treatment are not significant compared to initial soil pH. In contrast, a 24-hour ON/OFF period increases pH variation [37].

A study carried out in a microcosm using a clay soil (graphite electrodes inserted in the soil; no electrolyte; spiking only at the central soil section; seven days of treatment) allowed hypothesizing about some of the mechanism involved in CECs removal [37]. It has been hypothesized that caffeine (virtually immobile) suffers mostly electrochemically induced degradation when 12-hour OFF periods are followed by 12 hours of electric current application. This is probably related to the time needed for caffeine to suffer desorption from soil particles (the desorption coefficient logarithm is 2.87 and 3.89 for silt and sandy loam soils, respectively). Sulphamethoxazole and triclosan degradation increase with water mobility (and possibly also with that of soil microbes), with sulphamethoxazole biodegradation being favored away from the electrodes [37]. Thus, in both cases, if ON/OFF periods or polarity reversal is used, degradation decreases. It should also be noted that under constant application of a unidirectional current, the high mobility of CECs toward the electrodes will contribute to their degradation (electro and bio) [37]. However, near the electrodes, soil pH suffers more pronounced changes, which may negatively affect biodegradation around the electrodes [32, 60], where CECs will mostly undergo electrochemical degradation [37].

The removal of three antibiotics (tetracyclines) in soil using EK-Bio achieved average removal rates between 35 and 40% after seven days [42]. The degradation was primarily attributed to direct or indirect electrochemical reactions as well as indigenous biological processes. The innovation in this study was that the fate of antibiotic-resistant bacteria and antibiotic resistance genes were also evaluated. The study concluded that using EK technology reduced the tetracycline resistance genes in a ratio between 12.4 and 61.2%, with the abundance of total bacteria and antibiotic-resistant bacteria also decreasing [42]. These findings suggest that EK treatment is a promising technology to reduce the environmental and human risks associated with the spread of antibiotic resistance vectors. Still, studies are needed to understand how the EK process influenced the reduction of antibiotic resistance genes in the soil compared to the control. It has been suggested that direct and indirect action of the electric field inactivated antibiotic-resistant bacteria in the soil, especially on both sides near the electrode compartments [42]. Another hypothesis is that by applying the EK process, the amount of tetracycline that suffered

UNCORRECTED PROOFS

Trim Size: 170mm x 244mm Single Column Loose Ribeiro670117 c18.tex V1 - 12/11/2020 5:49pm Page 445

bioremediation decreased, as it mostly underwent electrochemical-induced degradation.

Little is known about the degradation pathways and removal mechanisms involved in EK-enhanced bioremediation of different CECs and its influence on contaminants and microbiota distribution along the soil column. This should be included as a focus of upcoming studies and may help to more effectively develop synergies between EK and the soil microbiological community.

18.3 Conclusion

The EK process is a promising technology for remediating CECs in soil. It has the potential not only to promote electro-degradation and removal of these contaminants but also to effectively enhance bioremediation processes. This is of special interest given the EK technology's capacity to perform remediation in physically heterogeneous or low-permeability matrices, where alternative technologies are usually ineffective. Still, although the basics and principles of EK remediation of soils seem simple, numerous physico-chemical processes are involved that rely on both soil composition and the properties of target compounds. This combination results in a highly complex system that needs to be understood to allow operational optimization and control.

Most EK studies focus on remediating heavy metals and petroleum-derived contamination. Little is known about applying the EK process to soil contaminated with CECs; however, most published studies present promising results that deserve further attention – especially those that present in situ approaches. Soils are complex systems made of water, gases, and mineral matter containing a diverse range of organisms and materials of biological origin. Soil microorganisms play critical roles, for example, in nutrient cycling and carbon sequestration. Thus, one of the priorities when developing in situ remediation approaches for contaminated soils should be balancing their effectiveness with preventing negative effects on soil microbial communities. If not appropriately applied, the EK technology may cause detrimental effects on the soil microbial community and soil health. If microorganisms are negatively impacted, their bioremediation capacity and tolerance to CECs may also be impaired. This means that, after EK treatment, any byproducts formed may remain in the soil longer, as the community would need time to recover. EK technology should be used whenever appropriate to potentiate both electro- and bio-degradation mechanisms.

In this chapter, the primary CECs removal mechanism was reviewed and the following conclusions were drawn:

- Electrode configurations and treatment optimization are needed to study electrode behavior due to soil heterogeneity and complexity and understand how it affects microbial communities.
- Many degradation mechanisms are involved in remediating different CECs, and further studies are needed to disclose both the electro-degradation and biodegradation pathways.

UNCORRECTED PROOFS

Trim Size: 170mm x 244mm Single Column Loose Ribeiro670117 c18.tex V1 - 12/11/2020 5:49pm Page 446

- Myriad byproducts are formed during the EK(-Bio) remediation process, indicating a need to analyze the response (and contribution) of the soil microbiota to their removal after the EK process is shut down.
- Most studies focus on the microcosm setup, and studies at a larger scale are needed to better understand the limitations involved in the process and thus design more suitable approaches.

The efficiency of every remediation technique is site-specific as it depends on soil properties and the combination of pollutants. Hopefully, more studies on EK remediation of soils polluted with CECs will be published in the near future, promoting essential advances in the field.

Acknowledgments

This work has received funding from the European Union's Horizon 2020 research and innovation program under Marie Skłodowska-Curie grant agreement No. 778045; project CEMOWAS2 (SOE2/P5/F0505), co-financed by the European Regional Development Fund (FEDER). The authors acknowledge and appreciate the support given by the Portuguese Foundation for Science and Technology (FCT) to CENSE through the strategic project UIDB/04085/2020 and the Project MOSTMICRO-ITQB with refs UIDB/04612/2020 and UIDP/04612/2020. FCT is also acknowledged for P. Guedes' (SFRH/BPD/114660/2016) fellowship, and N. Couto's contract established under Individual Call to Scientific Employment Stimulus (CEECIND/04210/2017). This work is anchored by the RESOLUTION LAB, a laboratory at the NOVA School of Science and Technology.

References

1 Pérez, A.P. and Eugenio, N.R. (2018). Status of local soil contamination in Europe: Revision of the indicator "progress in the management of contaminated sites in Europe." EUR 29124 EN. Luxembourg: Publications Office of the European Union.
2 FAO and ITPS. (2015). Status of the world's soil resources (SWSR) – main report. Rome, Italy.
3 Rodríguez-Eugenio, N., McLaughlin, M., and Pennock, D. (2018). *Soil Pollution: A Hidden Reality*. Rome: FAO.
4 Ratola, N., Cincinelli, A., Alves, A., and Katsoyiannis, A. (2012). Occurrence of organic microcontaminants in the wastewater treatment process. A mini review. *Journal of Hazardous Materials* 239–240: 1–18.
5 Paíga, P., Correia, M., Fernandes, M.J. et al. (2019). Assessment of 83 pharmaceuticals in WWTP influent and effluent samples by UHPLC-MS/MS: hourly variation. *Science of the Total Environment* 648: 582–600.

UNCORRECTED PROOFS

Trim Size: 170mm x 244mm Single Column Loose Ribeiro670117 c18.tex V1 - 12/11/2020 5:49pm Page 447

6 Boxall, A.B.A., Rudd, M.A., Brooks, B.W. et al. (2012). Pharmaceuticals and personal care products in the environment: what are the big questions? *Environmental Health Perspectives* 120 (9): 1221–1229.

7 Beretta, M., Britto, V., Tavares, T.M. et al. (2014). Occurrence of pharmaceutical and personal care products (PPCPs) in marine sediments in the Todos os Santos Bay and the north coast of Salvador, Bahia, Brazil. *Journal of Soils and Sediments* 14 (7): 1278–1286.

8 Ghirardini, A., Grillini, V., and Verlicchi, P. (2020). A review of the occurrence of selected micropollutants and microorganisms in different raw and treated manure – environmental risk due to antibiotics after application to soil. *Science of the Total Environment* 707: 136118.

9 Petrie, B., Barden, R., and Kasprzyk-Hordern, B. (2015). A review on emerging contaminants in wastewaters and the environment: current knowledge, understudied areas and recommendations for future monitoring. *Water Research* 72: 3–27.

10 Li, W.C. (2014). Occurrence, sources, and fate of pharmaceuticals in aquatic environment and soil. *Environmental Pollution* 187: 193–201.

11 Wojsławski, J., Białk-Bielińska, A., Stepnowski, P., and Dołżonek, J. (2019). Leaching behavior of pharmaceuticals and their metabolites in the soil environment. *Chemosphere* 231: 269–275.

12 Kodešová, R., Grabic, R., Kočárek, M. et al. (2015). Pharmaceuticals' sorptions relative to properties of thirteen different soils. *Science of the Total Environment* 511: 435–443.

13 Biel-Maeso, M., Corada-Fernández, C., and Lara-Martín, P.A. (2018). Monitoring the occurrence of pharmaceuticals in soils irrigated with reclaimed wastewater. *Environmental Pollution* 235: 312–321.

14 Pan, M. and Chu, L.M. (2017). Fate of antibiotics in soil and their uptake by edible crops. *Science of the Total Environment* 599–600: 500–512.

15 Azanu, D., Mortey, C., Darko, G. et al. (2016). Uptake of antibiotics from irrigation water by plants. *Chemosphere* 157: 107–114.

16 Gottschall, N., Topp, E., Metcalfe, C. et al. (2012). Pharmaceutical and personal care products in groundwater, subsurface drainage, soil, and wheat grain, following a high single application of municipal biosolids to a field. *Chemosphere* 87 (2): 194–203.

17 Wang, Y., Lu, J., Mao, L. et al. (2019). Antiepileptic drug carbamazepine promotes horizontal transfer of plasmid-borne multi-antibiotic resistance genes within and across bacterial genera. *The ISME Journal* 13 (2): 509–522.

18 Lu, J., Jin, M., Nguyen, S.H. et al. (2018). Non-antibiotic antimicrobial triclosan induces multiple antibiotic resistance through genetic mutation. *Environment International* 118: 257–265.

19 Shen, Y., Stedtfeld, R.D., Guo, X. et al. (2019). Pharmaceutical exposure changed antibiotic resistance genes and bacterial communities in soil-surface- and overhead-irrigated greenhouse lettuce. *Environment International* 131: 105031.

UNCORRECTED PROOFS

Trim Size: 170mm x 244mm Single Column Loose Ribeiro670117 c18.tex V1 - 12/11/2020 5:49pm Page 448

20 UN. (2019). Follow-up to the political declaration of high-level meeting of the General Assembly on antimicrobial resistance. A/73/869.

21 European Innovation Partnership. (2012). Strategic Implementation Plan on Water. 1–22.

22 European Commission. (2012). The blueprint to safeguard Europe's water resources. COM(2012)673.

23 European Commission. (2018) Proposal for a regulation of the European Parliament and of the Council on Minimum Requirements for water reuse. COM(2018)337.

24 Presidency of the Council of Ministers. (2019). Decreto-Lei no. 119/2019, Diário da República n.º 159/2019, Série I de 2019-08-21. Portugal.

25 Virkutyte, J., Sillanpää, M., and Latostenmaa, P. (2002). Electrokinetic soil remediation – critical overview. *Science of the Total Environment* 289 (1): 97–121.

26 Lima, A.T., Hofmann, A., Reynolds, D. et al. (2017). Environmental electrokinetics for a sustainable subsurface. *Chemosphere* 181: 122–133.

27 Gill, R.T., Harbottle, M.J., Smith, J.W.N., and Thornton, S.F. (2014). Electrokinetic-enhanced bioremediation of organic contaminants: a review of processes and environmental applications. *Chemosphere* 107: 31–42.

28 Mulligan, C.N., Yong, R.N., and Gibbs, B.F. (2001). An evaluation of technologies for the heavy metal remediation of dredged sediments. *Journal of Hazardous Materials* 85 (1–2): 145–163.

29 Acar, Y.B. and Alshawabkeh, A.N. (1993). Principles of electrokinetic remediation. *Environmental Science & Technology* 27 (13): 2638–2647.

30 Saichek, R.E. and Reddy, K.R. (2005). Electrokinetically enhanced remediation of hydrophobic organic compounds in soils: a review. *Critical Reviews in Environmental Science and Technology* 35 (2): 115–192.

31 Kim, S.H., Han, H.Y., Lee, Y.J. et al. (2010). Effect of electrokinetic remediation on indigenous microbial activity and community within diesel contaminated soil. *Science of the Total Environment* 408 (16): 3162–3168.

32 Lear, G., Harbottle, M.J., Van Der Gast, C.J. et al. (2004). The effect of electrokinetics on soil microbial communities. *Soil Biology and Biochemistry* 36 (11): 1751–1760.

33 Reddy, K.R. and Cameselle, C. (2009). Overview of electrochemical remediation technologies. In: *Electrochemical Remediation Technologies for Polluted Soils, Sediments and Groundwater* (eds. K.R. Reddy and C. Cameselle), 1–28. Wiley.

34 Alcántara, M.T., Gómez, J., Pazos, M., and Sanromán, M.A. (2010). Electrokinetic remediation of PAH mixtures from kaolin. *Journal of Hazardous Materials* 179 (1–3): 1156–1160.

35 Alcántara, M.T., Gómez, J., Pazos, M., and Sanromán, M.A. (2012). Electrokinetic remediation of lead and phenanthrene polluted soils. *Geoderma* 173–174: 128–133.

36 Guedes, P., Mateus, E.P., Couto, N. et al. (2014). Electrokinetic remediation of six emerging organic contaminants from soil. *Chemosphere* 117: 124–131.

UNCORRECTED PROOFS

Trim Size: 170mm x 244mm Single Column Loose Ribeiro670117 c18.tex V1 - 12/11/2020 5:49pm Page 449

37 Guedes, P., Lopes, V., Couto, N. et al. (2019). Electrokinetic remediation of contaminants of emergent concern in clay soil: effect of operating parameters. *Environmental Pollution* 253: 625–635.

38 Ferreira, A.R., Guedes, P., Mateus, E.P. et al. (2017). Influence of the cell design in the electroremoval of PPCPs from soil slurry. *Chemical Engineering Journal* 326: 162–168.

39 Hung, C.H., Yuan, C., Wu, M.H., and Chang, Y.C. (2018). Electrochemical degradation of ibuprofen-contaminated soils over Fe/Al oxidation electrodes. *Science of the Total Environment* 640–641: 1205–1213.

40 Yuan, C., Hung, C.H., and Huang, T.Y. (2018). Application of RuO2/Ni foam electrodes for remediation of ibuprofen in soil matrix – the effect of electrokinetic parameters. *Environmental Science and Pollution Research* 25 (6): 5181–5190.

41 Yuan, C., Chen, C.Y., and Hung, C.H. (2013). Electrochemical remediation of BPA in a soil matrix by Pd/Ti and RuO 2/Ti electrodes. *Journal of Applied Electrochemistry* 43 (12): 1163–1174.

42 Li, H., Li, B., Ma, J. et al. (2018). Fate of antibiotic-resistant bacteria and antibiotic resistance genes in the electrokinetic treatment of antibiotic-polluted soil. *Chemical Engineering Journal* 337: 584–594.

43 Pham, T.D. and Sillanpää, M. (2015). Electrokinetic remediation of organic contamination. *Environmental Technology Reviews* 4 (1): 103–117.

44 Hung, C.H., Yuan, C., and Chen, K.C. (2010). Effect of processing fluid and initial concentration on electrokinetic removal of environmental hormone-nonylphenol (NP) from soil matrix. *Journal of Applied Electrochemistry* 40 (6): 1123–1130.

45 Ferreira, A.R., Couto, N., Guedes, P. et al. (2018). Electrodialytic 2-compartment cells for emerging organic contaminants removal from effluent. *Journal of Hazardous Materials* 358: 467–474.

46 Shestakova, M. and Sillanpää, M. (2017). Electrode materials used for electrochemical oxidation of organic compounds in wastewater. *Reviews in Environmental Science and Biotechnology* 16 (2): 223–238.

47 Lee, B.S., Park, H.Y., Choi, I. et al. (2016). Polarization characteristics of a low catalyst loading PEM water electrolyzer operating at elevated temperature. *Journal of Power Sources* 309: 127–134.

48 Comninellis, C. (1994). Electrocatalysis in the electrochemical conversion/combustion of organic pollutants for waste water treatment. *Electrochimica Acta* 39 (1): 1857–1862.

49 Awad, H.S. and Galwa, N.A. (2005). Electrochemical degradation of acid blue and basic brown dyes on Pb/PbO2 electrode in the presence of different conductive electrolyte and effect of various operating factors. *Chemosphere* 61 (9): 1327–1335.

50 Nidheesh, P.V. and Gandhimathi, R. (2012). Trends in electro-Fenton process for water and wastewater treatment: an overview. *Desalination* 299: 1–15.

UNCORRECTED PROOFS

Trim Size: 170mm x 244mm Single Column Loose Ribeiro670117 c18.tex V1 - 12/11/2020 5:49pm Page 450

51 Yeung, A.T. and Gu, Y.Y. (2011). A review on techniques to enhance electrochemical remediation of contaminated soils. *Journal of Hazardous Materials* 195: 11–29.

52 Pamukcu, S. (2009). Electrochemical transport and transformations. In: *In: Electrochemical Remediation Technologies for Polluted Soils, Sediments and Groundwater* (eds. K.R. Reddy and C. Cameselle), 29–64. Wiley.

53 Harbottle, M.J., Lear, G., Sills, G.C., and Thompson, I.P. (2009). Enhanced biodegradation of pentachlorophenol in unsaturated soil using reversed field electrokinetics. *Journal of Environmental Management* 90 (5): 1893–1900.

54 Wick, L.Y., Mattle, P.A., Wattiau, P., and Harm, H. (2004). Electrokinetic transport of PAH-degrading bacteria in model aquifers and soil. *Environmental Science & Technology* 38: 4596–4602.

55 Liu, Z., Chen, W., and Papadopoulos, K.D. (1999). Electrokinetic movement of *Escherichia coli* in capillaries. *Environmental Microbiology* 1 (1): 99–102.

56 Reid, B.J., Jones, K.C., and Semple, K.T. (2000). Bioavailability of persistent organic pollutants in soils and sediments – a perspective on mechanisms, consequences and assessment. *Environmental Pollution* 108 (1): 103–112.

57 Acar, Y.B., Gale, R.J., Alshawabkeh, A.N. et al. (1995). Electrokinetic remediation: basics and technology status. *Journal of Hazardous Materials* 40 (2): 117–137.

58 Jackman, S.A., Maini, G., Sharman, A.K. et al. (2001). Electrokinetic movement and biodegradation of 2,4-dichlorophenoxyacetic acid in silt soil. *Biotechnology and Bioengineering* 74 (1): 40–48.

59 Page, M.M. and Page, C.L. (2002). Electroremediation of contaminated soils. *Journal of Environmental Engineering* 128 (3): 208–219.

60 Lear, G., Harbottle, M.J., Sills, G. et al. (2007). Impact of electrokinetic remediation on microbial communities within PCP contaminated soil. *Environmental Pollution* 146 (1): 139–146.

61 Luo, Q., Wang, H., Zhang, X. et al. (2006). In situ bioelectrokinetic remediation of phenol-contaminated soil by use of an electrode matrix and a rotational operation mode. *Chemosphere* 64 (3): 415–422.

62 Wick, L.Y., Buchholz, F., Fetzer, I. et al. (2010). Responses of soil microbial communities to weak electric fields. *Science of the Total Environment* 408 (20): 4886–4893.

63 Mena, E., Villaseñor, J., Cañizares, P., and Rodrigo, M.A. (2016). Effect of electric field on the performance of soil electro-bioremediation with a periodic polarity reversal strategy. *Chemosphere* 146: 300–307.

64 Huang, D., Guo, S., Li, T., and Wu, B. (2013). Coupling interactions between electrokinetics and bioremediation for pyrene removal from soil under polarity reversal conditions. *Clean - Soil, Air, Water* 41 (4): 383–389.

65 Juwarkar, A.A., Singh, S.K., and Mudhoo, A. (2010). A comprehensive overview of elements in bioremediation. *Reviews in Environmental Science and Biotechnology* 9 (3): 215–288.

UNCORRECTED PROOFS

Trim Size: 170mm x 244mm Single Column Loose Ribeiro670117 c18.tex V1 - 12/11/2020 5:49pm Page 451

66 Lee, H.H. and Yang, J.W. (2000). A new method to control electrolytes pH by circulation system in electrokinetic soil remediation. *Journal of Hazardous Materials* 77 (1–3): 227–240.

67 Moliterni, E., Jiménez-Tusset, R.G., Villar Rayo, M. et al. (2012). Kinetics of biodegradation of diesel fuel by enriched microbial consortia from polluted soils. *International journal of Environmental Science and Technology* 9 (4): 749–758.

68 Liu, B., Tu, C., Hu, S. et al. (2007). Effect of organic, sustainable, and conventional management strategies in grower fields on soil physical, chemical, and biological factors and the incidence of southern blight. *Applied Soil Ecology* 37 (3): 202–214.

69 Luo, Q., Zhang, X., Wang, H., and Qian, Y. (2005). The use of non-uniform electrokinetics to enhance in situ bioremediation of phenol-contaminated soil. *Journal of Hazardous Materials* 121 (1–3): 187–194.

70 Röhrs, J., Ludwig, G., and Rahner, D. (2002). Electrochemically induced reactions in soils – a new approach to the in-situ remediation of contaminated soils? Part 1: the microconductor principle. *Electrochimica Acta* 47 (9): 1395–1403.

UNCORRECTED PROOFS

UNCORRECTED PROOFS

Trim Size: 170mm x 244mm Single Column Loose Ribeiro670117 c19.tex V1 - 12/11/2020 5:50pm Page 453

19

Electrokinetic Remediation for the Removal of Organic Waste in Soil and Sediments

S.M.P.A Koliyabandara[1], Chamika Siriwardhana[1], Sakuni M. De Silva[2], Janitha Walpita[2], and Asitha T. Cooray[1,2]

[1] *Department of Chemistry, Faculty of Applied Sciences, University of Sri Jayewardenepura, Nugegoda 10250, Sri Lanka*
[2] *Instrument Centre, Office of the Dean, Faculty of Applied Sciences, University of Sri Jayewardenepura, Nugegoda 10250, Sri Lanka*

19.1 Introduction

Soil is a complex mixture of minerals, organic material, dead and living micro- and macro-organisms, air, and water. It forms at the earth's surface under the influence of climate, topography, organisms, parent material, and time. Soil formation is a slow process that takes up to thousands of years to create an inch of topsoil. Soil is a limited natural resource, and it is the primary provider and storage place of nutrients and water for all the ecosystems on earth. It is considered a renewable resource; however, as mentioned, soil formation – particularly in dry and cold environments – occurs very slowly. Sediment, on the other hand, is a naturally occurring material that is transported by the action of wind (aeolian processes), water (fluvial processes), or ice (glacial deposits). For example, sand dunes in deserts and beaches are a result of aeolian and fluvial processes, respectively.

Soil contamination has been referred to as "invisible contamination" because it is not as easily observable as water and atmospheric pollution [1]. Most soil pollutants are toxic to humans, animals, and plants; persistent in the environment; and bioaccumulative. Volatile and semi-volatile organic pollutants undergo air-soil exchange at high air temperatures, enabling long-term atmospheric transport. Heavy metal and nutrient pollution are usually observed close to their sources; however, organic pollutants have been observed in high concentrations far from their sources – even in remote areas, such as polar regions, due to atmospheric transport [2]. As a result, the remediation of organically polluted soil is a priority worldwide.

19.2 Organic Soil Pollution

A wide array of organic pollutants can readily be found in the environment due to anthropogenic and natural activities. Such organic pollutants include

Electrokinetic Remediation for Environmental Security and Sustainability, First Edition.
Edited by Alexandra B. Ribeiro and M.N.V. Prasad.
© 2021 John Wiley & Sons Ltd. Published 2021 by John Wiley & Sons Ltd.

UNCORRECTED PROOFS

Trim Size: 170mm x 244mm Single Column Loose Ribeiro670117 c19.tex V1 - 12/11/2020 5:50pm Page 454

pesticides, biocides, pharmaceuticals, surfactants, flame retardants, polycyclic aromatic hydrocarbons (PAHs), polychlorinated biphenyls (PCBs), polychlorinated dibenzo-p-dioxins (PCDDs), and polychlorinated dibenzofurans (PCDFs) [3–5].

Hydrophobic organic contaminants (HOCs) are derived from various persistent toxic contaminants that are mostly resistant to chemical attack and have low aqueous solubility [6]. Their chemical properties have made them one of the most widespread environmental contaminants [7]. Solubility is an important factor during contaminant treatment, as the primary aim is to solubilize the pollutants via an extracting solution, which is responsible for cleaning HOCs from the soil matrix [8]. HOCs are persistent in most hazardous organic contaminants in soil, sludge, and sediment. Commonly, the literature targets the treatment of soluble organics in soil. However, many sites worldwide are contaminated with HOCs, and no sustainable technology is available to remediate these sites. Organic pollutants, especially HOCs, are difficult to treat due to their higher retention time, lower solubility ($<30\,mg\,l^{-1}$), high lipophilicity, semi-volatility, and low degradability. Therefore, HOCs, including PAHs, are concentrated in the soil for a long time [5]. HOCs like chlorophenols, trichloroacetate (TCA), chlorobenzene, pentachloroethylene (PCE), and PAHs have been of concern for decades. Among them, persistent organic pollutants (POPs) have been identified and are sometimes referred to as "forever chemicals."

Most PAHs that are considered POPs are used in activities such as agriculture and industrial applications. They are primarily organochlorine compounds (OCs). Some POPs, including dioxins, furans, and PAHs, are combustion products, which complicates the control of their emissions into the environment. The United Nations Environment Program (UNEP) POP list adopted at the Stockholm Convention identifies POPs including aldrin, hexachlorobenzene, toxaphene, mirex, dioxins, PCBs, furans, dichlorodiphenyltrichloroethane (DDT), heptachlor, chlordane, dieldrin, chlordecone, endrin, hexabromobiphenyl, PAHs, etc. [2].

In terms of structure, PAHs include two or more fused benzene rings. They are known for their cytotoxic, mutagenic, and carcinogenic effects [9, 10]. PAHs are distinguished by their strong hydrophobic nature. They exhibit low vapor pressure and low aqueous solubility. Their properties are linked to the molecular weight and structures of the compounds. Incomplete combustion of organic matter and fossil fuel generates PAHs. Oil spill accidents and wastewater discharge are recognized as sources of PAHs [10, 11]. The US Environmental Protection Agency and European Union have stated that 16 PAH compounds are considered priority pollutants (Table 19.1) [12].

The other common organic contaminant group is PCBs: organochlorides used by industries. Industrial production of PCBs was banned in the 1970s due to their high persistence and toxicity; however, they still pose a threat to the environment [13]. Wastewater plant effluents have been identified as a source of organo-halogenated compounds that pollute soils and sediments. The accumulation of these pollutants results from sources such as agricultural runoff and rainfall. The properties of both PCBs and organochlorides have shown similar physical and chemical characteristics in sediments [14, 15].

UNCORRECTED PROOFS

Trim Size: 170mm x 244mm Single Column Loose Ribeiro670117 c19.tex V1 - 12/11/2020 5:50pm Page 455

Table 19.1 Polycyclic aromatic hydrocarbons listed by priority.

Name	Chemical formula	Human carcinogenicity
Naphthalene	$C_{10}H_8$	No information
Acenaphthene	$C_{12}H_{10}$	No information
Acenaphthylene	$C_{12}H_{10}$	No information
Anthracene	$C_{14}H_{10}$	No information
Fluorene	$C_{13}H_{10}$	No information
Phenanthrene	$C_{14}H_{10}$	No information
Fluoranthene	$C_{16}H_{10}$	No information
Pyrene	$C_{16}H_{10}$	No information
Chrysene	$C_{18}H_{12}$	Probable human carcinogen
Benz(a)anthracene	$C_{18}H_{12}$	Probable human carcinogen
Benzo(b)fluoranthene	$C_{20}H_{12}$	Probable human carcinogen
Benzo(k)fluoranthene	$C_{20}H_{12}$	Probable human carcinogen
Benzo(a)pyrene	$C_{20}H_{12}$	Probable human carcinogen
Dibenz(a,h)anthracene	$C_{22}H_{14}$	Probable human carcinogen
Indeno(1,2,3-cd)pyrene	$C_{22}H_{12}$	Probable human carcinogen
Benzo(g,h,i)perylene	$C_{22}H_{12}$	No information

Source: Adapted from Ravindra et al. [12].

19.2.1 The Fate of Organic Soil Pollutants

In natural conditions, soil acts as a sink for many pollutants. They enter the soil from natural or anthropogenic sources. Once organic pollutants are in the soil, their fate depends on environmental factors such as precipitation and temperature; soil properties such as moisture, pH, organic matter availability; and properties of organic pollutant such as vapor pressure, hydrophobicity, and stability [16]. Many mechanisms can transport these pollutants through soil [17]. The most prominent are leaching and erosion, volatilization, and suspension of soil particles, all of which transfer contaminants through soil, water, and air and then into the food chain.

19.2.2 Biomagnification and Bioaccumulation of Soil Pollutants

POPs including PCBs, PBDEs, PCDDs, and furans can be retained in food chains and food webs for years due to their lipophilicity, low biodegradability, and refractory nature. This results in bioaccumulation of these organics in high concentrations; and eventually, organisms may accumulate relatively higher concentrations of hazardous pollutants than in the environment. The adverse concentrations of these contaminants lead to negative reproductive effects and endocrine disruption or immune dysfunction [18]. Due to the "cold trapping" effect, in cold environments, POP concentration levels are relatively high. In addition, the dietary pattern, growth

UNCORRECTED PROOFS

Trim Size: 170mm x 244mm Single Column Loose Ribeiro670117 c19.tex V1 - 12/11/2020 5:50pm Page 456

rate, age, and lipid content of organisms (mostly fish) can affect bioaccumulation in aquatic food chains in remote areas [19].

Biomagnification is the accumulation of xenobiotic substances in an organism, which are transferred from food and result in higher concentration within the organism compared to the food source [19, 20]. According to Gary and coworkers [21], PAHs may not show biomagnification, while PCBs and DDT have shown comparatively high biomagnification. Two models have been proposed to explain the biomagnification process. The first model explains that passive diffusion is the predominant activity to pass intestinally absorbed hydrophobic organic substances from the gastrointestinal tract to the organism's tissue. According to the second model, biomagnification occurs in organism tissues but not in the gastrointestinal tract [22]. It has been shown that in *Mytilus galloprovincialis* (Mediterranean mussel) and *Dicentrarchus labrax* (European seabass), uptake of PAHs is greater in mussels than fish. Thus, in this case, mussels are effective bio-concentrators and pose a high risk for humans [23].

19.3 Soil Remediation Methods

Soil is a significant constituent of the ecosystem, and it is essential to conduct efficient remediation methods to maintain the ecological environment, safe food production, and sustainable agriculture. Many countries have passed laws and acts to regulate and raise concerns about this global issue, and therefore commercial industries are paying attention and investing in cost-effective remediation methods [24]. The remediation techniques employed on polluted soil and sediments depend on the concentration and physical status of pollutants and the type of soil [25]. Remediation techniques work in different ways; ex situ treatment methods involve excavation of contaminated soils and subsequent treatment at the surface or at a different site. In situ treatment methods treat the contaminated soil without removing it. In recent decades, different soil and sediment remediation methods, including physical, chemical, and biological techniques, have been invented and applied to remove or reduce the hazardous chemical activities of organic pollutants.

19.3.1 Physical Methods

Physical remediation techniques are applied to prevent soil damage due to organic pollutants, and these techniques include capping and thermal treatments. Thermal techniques like thermal desorption [26, 27] and soil vapor extraction (SVE) [28] remove OPs from contaminated soil using a gas or liquid solvent [1, 29].

19.3.1.1 Capping

In situ, capping is not truly a soil "remediation" method but only covers the contaminated soil with waterproof material (Figure 19.1) and minimizes its exposure to the environment. Some capping materials are clay, concrete, asphalt, and high-density polyethylene (HDPL); these materials act as a stable, inactive protective coat over

UNCORRECTED PROOFS

Trim Size: 170mm x 244mm Single Column Loose Ribeiro670117 c19.tex V1 - 12/11/2020 5:50pm Page 457

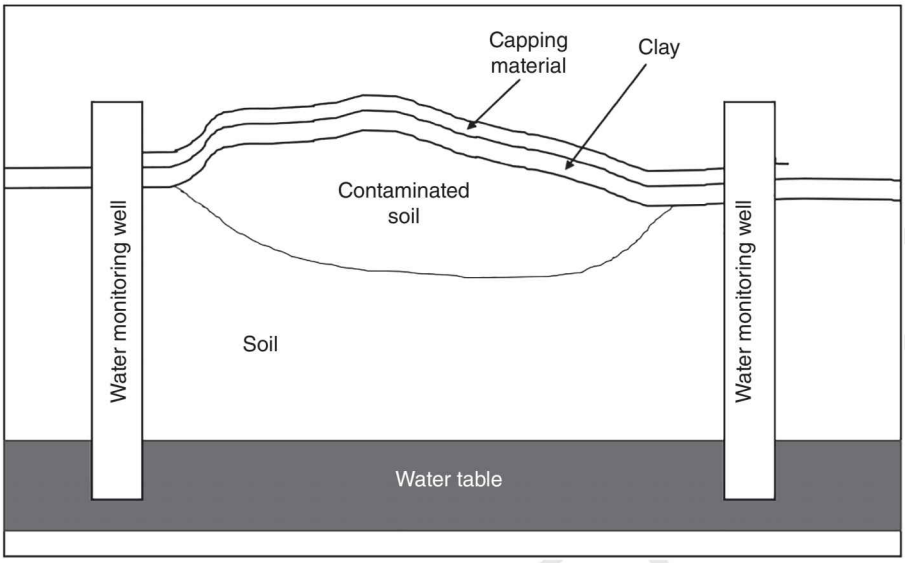

Figure 19.1 Schematic diagram for soil capping as a physical treatment method for contaminated soils/sediments.

contaminated soil. The purpose of these methods is the stabilization of contaminated sites, physical isolation, and reduction of contaminant transportation [1, 30]. During capping design, few factors to consider include site orientation, type of contaminant, concentration of the contaminant, rainfall, and future use of the land. The design can be single-layered or multi-layered depending on contamination severity. For example, asphalt is commonly used to cover soil with low levels of contamination for future use as a parking lot. If soil is contaminated with a highly hazardous contaminant, it may require multiple layers during the capping process, including a vegetative layer, drainage layer, geomembrane, and clay layer [31]. The primary limitations of soil capping as a final remediation technique are long-term maintenance of the cover and soil monitoring to ensure that the cover remains intact and effective.

19.3.1.2 Thermal Desorption

During the thermal desorption remediation method, a heat source (electrical resistive heating, conductive heating, steam-based, or radio-frequency heating) is used to improve the evaporation of POPs and volatile organic contaminants (VOCs). Microwave heating is attractive in thermal desorption because it prevents the overheating of the soil surface [1]. Zhao et al. have shown that thermal desorption is effective for semi-volatile POPs such as PCBs [27]. Gao et al. found that organochlorine pesticides (OCPs) in agricultural sites can be removed using combined remediation methods like thermal desorption and solvent washing [26].

Although thermal desorption has some attractive features, the contaminated material must be excavated and stored. This can increase the cost of the process and require a large land footprint. Therefore, this method shows limited usage due to

UNCORRECTED PROOFS

Trim Size: 170mm x 244mm Single Column Loose Ribeiro670117 c19.tex V1 - 12/11/2020 5:50pm Page 458

its high capital and operational costs [1]. Furthermore, the possibility of generating toxic particulate matter upon heating makes it a questionable approach for certain polluted soils and sediments.

19.3.1.3 Soil Vapor Extraction (SVE)

This method is efficient for semi-volatile and volatile OCs. Vacuum blowers are used to apply a vacuum to the soil, and this air flow extracts VOCs to extraction wells based on mass transfer. This method has overcome the drawbacks of thermal desorption because pollutants are not exposed to the environment. Extracted pollutants are treated in above-ground systems. Studies have demonstrated that SVE is effective for benzene removal, and the removal efficiency for sandy soils and humus soils is 92% and 78%, respectively [28]. The primary disadvantage of this technique is that it is more efficient for soils with high permeability. But when permeability decreases, the approach is less cost-effective because it requires more energy to extract VOCs through contaminated soil. To obtain an efficient result using SVE, the subsurface should have a gas phase to pass the contaminants. When permeability decreases, contaminants travel more slowly [32].

19.3.1.4 Incineration

Soils polluted with organic compounds can be treated with incineration. This is a widely used method. Incineration removes organic contaminants from soil and permanently destroys them. These systems include complex steps including preparation, feeding, combustion, and emission control. However, this method is not cost-effective, and it can sometimes cause problems with air pollution [33].

19.3.1.5 Air Sparging

This is an in situ remediation technique that forces air to bubble through groundwater or *sparge* through contaminated soils to volatilize VOCs. Sparging air eliminates VOCs, in particular, compared to nonvolatile organics embedded in soil particles and dissolved in groundwater. Hence, this method is used to remove VOCs from both soil particles and the groundwater phase.

SVE can be used to collect vaporized VOCs, and air sparging can improve the efficiency of both SVE and biodegradation. Since air sparging facilitates the growth of aerobic microorganisms to degrade organic contaminants, it is also combined with bioremediation techniques [34]. The major limitation of efficient air sparging is the presence of low-permeable zones over the contaminated zone [35].

19.3.2 Chemical Methods

In chemical remediation methods, chemicals, chemical reactions, and chemical principles are used to extract undesired organic pollutants. These methods include soil washing/flushing, electrochemical remediation, chemical oxidation remediation, etc. Chemical methods are highly effective at field scale because they enhance the in situ degradation of organic pollutants by reducing or removing their hazardous nature. Compared to physical treatment methods, chemical remediation techniques are more effective, less time consuming, and cost-effective.

UNCORRECTED PROOFS

Trim Size: 170mm x 244mm Single Column Loose Ribeiro670117 c19.tex V1 - 12/11/2020 5:50pm Page 459

19.3.2.1 Soil Washing/Flushing

In situ flushing is carried out by passing a suitable extraction fluid through the soil, after which the fluid is recovered and the contaminants are extracted. Commonly used extracting agents are surfactants, cosolvents, cyclodextrin (CD), chelates, and weak acids. Flushing is an effective method for sites contaminated with HOCs. Previous studies have shown that CDs are effective against PAHs. Chelating agents like ethylenediaminetetraacetic acid (EDTA) and diethylenetriaminepentaacetic acid (DTPA) along with cosolvents and CDs, have been used in soils contaminated with metals and PAHs, benzene, and phenols [29, 36, 37].

Soil washing or solvent extraction is mostly a water-based ex situ technique that dissolves or suspends PAHs in the soil using aqueous-based or organic solvent solutions. This method requires high shear energy to separate pollutants from the solid phase to the liquid phase. Nonpolar organic solvents such as 1-pentanol, n-hexane, toluene, dichloromethane, and benzene have lipophilic characteristics and are commonly used to extract hydrophobic contaminants such as PAHs [9].

19.3.2.2 Chemical Oxidation Remediation

19.3.2.2.1 Fenton Oxidation and Fenton-Like Oxidation

Traditional Fenton's reagent is a solution of $Fe^{2+/}H_2O_2$, and it can effectively degrade numerous OPs such as phenol, benzoic acid, aniline, etc. The primary Fenton oxidation reaction is

$$H_2O_2 + Fe^{2+} \rightarrow Fe^{3+} + OH^{\cdot} + OH^{-}$$

Hydroxyl free radicals are responsible for the oxidization of organic contaminants. This primary reaction, followed by a series of reactions, produces free radicals that facilitate the degradation of hydrocarbons [38, 39]:

$$Fe^{2+} + H_2O_2 \rightarrow Fe^{3+} + OH^{\cdot} + OH^{-}$$
$$Fe^{3+} + H_2O_2 \rightarrow Fe^{2+} + HO_2^{\cdot} + H^{+}$$

The overall reaction is as follows:

$$2H_2O_2 \rightarrow OH^{\cdot} + HO_2^{\cdot} + H_2O$$
$$OH^{\cdot} + \text{organics} \rightarrow CO_2 + H_2O + \text{other products}$$

The optimal pH for the reaction is 3, which is the major drawback of this oxidation process. Since Fenton and Fenton-like oxidation methods require large amounts of chemicals, they become cost-inefficient. Further, this technique cannot be used for soils with low permeability [1].

19.3.2.2.2 Photocatalytic Remediation

Semiconductor-mediated photocatalysis is a well-studied research area in the field of environmental science. Photosensitizers like TiO_2 and Fe_2O_3 are used to accelerate the photoreaction; by absorbing light, these photosensitizers produce hydroxyl and superoxide free radicals from water, which can oxidize target organic contaminants [1]. Activated semiconductor surface-generated electron-hole pairs oxidize water and form superoxide, and then the superoxide produces its protonated form:

UNCORRECTED PROOFS

Trim Size: 170mm x 244mm Single Column Loose Ribeiro670117 c19.tex V1 - 12/11/2020 5:50pm Page 460

the hydroperoxyl radical ($HO_2^{\bullet}$) and ultimately H_2O_2. Organic contaminants are degraded by the mechanism of titania-assisted photocatalysis to generate CO_2, H_2O, and the relevant acid, given O_2, TiO_2, and energy. the target contaminant's absorptivity is related to the photodegradation rate.

Photocatalytic remediation process and Fenton-like oxidation are referred to as advanced oxidation processes (AOP). Both methods form highly reactive free radicals that can be used to degrade organic compounds [40]. A previous study has shown that photoirradiation in the presence of TiO_2 significantly reduced P-nitrophenol [5]. The major drawback of photocatalytic remediation is that it is limited by soil thickness: it requires photons (UV or visible light) to penetrate the soil.

19.3.3 Bioremediation

Bioremediation uses aerobic and anaerobic microorganisms, especially bacteria and fungi, to digest soil contaminants – sometimes even persistent organic contaminants like PAHs. Microbial and phytoremediation are the two primary bioremediation techniques and depend on bacteria, fungi, and plants to degrade organic contaminants from soil.

19.3.3.1 Microbial Remediation

Microbial remediation primarily uses bacteria and fungi to degrade organic contaminants. These organisms use organic substances as their food source and degrade them into CO_2 and H_2O. This process takes considerable time and therefore is not suitable for quick remediation. Studies have proved that *Pseudomonas* sp. and fungi are effective for degrading PAHs [41]. Temperature, moisture content, pH, and soil humidity affect the growth and activity of microorganisms [42]. However, this process is relatively cost-effective and environmentally friendly. One of the most prominent examples is microbial remediation of petroleum hydrocarbon contaminants [43].

19.3.3.2 Phytoremediation

Phytoremediation uses natural fauna and their associated microbes to treat contaminants through biological, chemical, and physical activities and processes, as shown in Figure 19.2. Toxic compounds are converted into non-toxic compounds by root-colonizing microbes or by the plant itself [44]. Phytoremediation is widely used to clean up metals, pesticides, petroleum products, explosives, PAHs, and other organic compounds. Alfalfa, flat pea, and switchgrass are effective against PCBs [41]. Even though this remediation process is cost-beneficial, it also takes more time to degrade organic contaminants, as in microbial remediation.

UNCORRECTED PROOFS

Trim Size: 170mm x 244mm Single Column Loose Ribeiro670117 c19.tex V1 - 12/11/2020 5:50pm Page 461

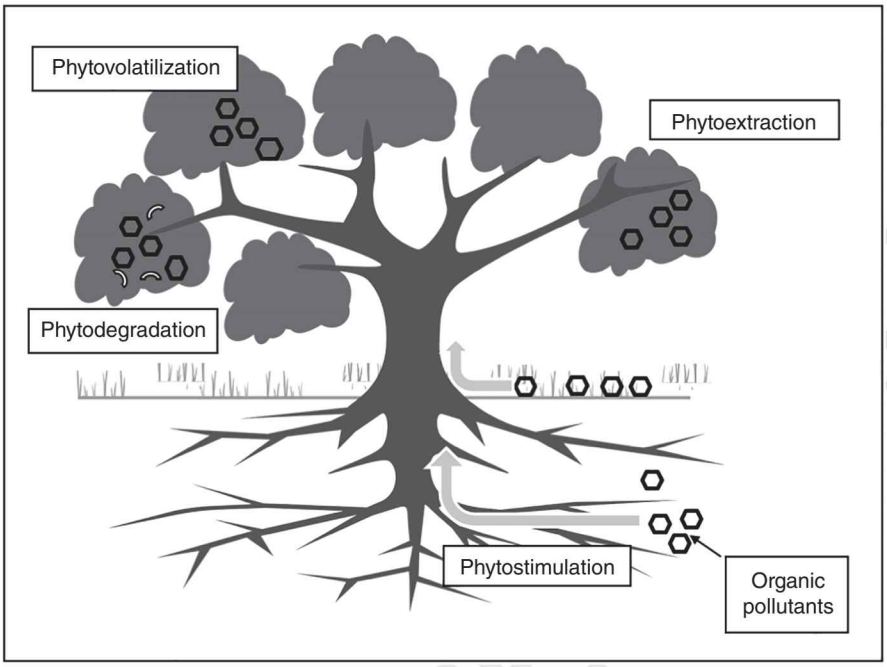

Figure 19.2 Processes in the phytoremediation technique.

19.4 Electrokinetic Remediation (EKR)

Today, significant attention is being paid to the electrokinetic remediation (EKR) of OPs due to this approach's distinctive advantages: it can be used in low-permeability solids and for in situ remediation, it requires a short remediation time, and it is low cost. Most importantly, EKR has been proven effective in reducing metals, radionuclides, and OPs, including semi-volatile organic compounds such as PAHs and PCBs; VOCs like trichloroethane, trichloroethylene, benzene, toluene, ethylbenzene, and xylene; and total petroleum hydrocarbons in both soil and groundwater [45]. In addition, EKR can be readily combined with other remediation methods to enhance the efficiency of EKR and overcome the drawbacks of other remediation methods.

19.4.1 Basic Principles of EKR

Electrokinetic (EK) soil remediation has emerged as a novel technology in the last two decades to remove heavy metals and organic contaminants from low-permeability soil under a low-level direct current (DC) [46]. In 1808, Reuss

UNCORRECTED PROOFS

Trim Size: 170mm x 244mm Single Column Loose Ribeiro670117 c19.tex V1 - 12/11/2020 5:50pm Page 462

first identified the electrokinetic phenomenon by applying DC to a clay-water mixture. The Helmholtz-Smoluchowski theory (H-S theory) is the theory of the electroosmotic velocity of a fluid, and it is commonly used as the basis of EKR [47].

In EKR, low-level DC or potential gradient is applied to electrodes inserted into contaminated soil. Several important mechanisms are observed under this potential gradient at the electrodes, including electrolysis, electroosmosis, electromigration, and electrophoresis. These mechanisms are responsible for the mobilization and transportation of charged species in contaminants formed by the electric field. Electrolysis of water is the basic and primary electron transfer reaction after low-level DC is applied to electrodes [48]. The basic EKR approach is shown in Figure 19.3.

19.4.1.1 Electrolysis of Pore Water

Electrolysis of water creates oppositely charged electrodes and produces acid and base fronts [50].

Oxidization at the anode is as follows:

$$2\,H_2O \rightarrow 4H^+ + O_2\,(g) + 4e^- E = -1.229\,V$$

And reduction occurs at the cathode:

$$2H_2O + 2e^- \rightarrow 2OH^- + H_2\,(g)\,E = -0.828\,V$$

Accumulation of hydrogen ions at the anode lowers the pH at the anode and makes an acid front. But at the cathode, a base front is created due to the formation of hydroxyl ions, and the pH at the cathode increases. Formation of cations (hydrogen ions) is greater than anions (hydroxyl ions), making the anode more acidic, and the migration of the acid front to the cathode also increases due to the higher mobility of H^+ ions. Through mechanisms like electrical migration, diffusion, and advection, the acid front migrates to the cathode. Advection occurs by electroosmotic flow and an externally applied hydraulic gradient.

19.4.1.2 Electromigration

The term *electromigration* is used to explain how the electric current is moved by ions in moist, porous material. The movement of ions is triggered by the direct electric current (DC) field. Anions are expected to move to the anode, and cations to the cathode. Electromigration of ions occurs along field lines, which are controlled by the electron placement [51]. The method can be used in both fine- and coarse-grained soils as electromigration does not affect the pore size [48]. Even though the ion migration rate is comparatively higher in sandy soils than clayey soil, compared to the ion transfer according to the hydraulic gradient, it has shown to have less difference for both soils [52].

Electromigration depends on factors such as electrolyte concentration, strength of the electric field, and ionic mobility. This process is relatively faster than the other migrating routes, electroosmosis, and electrophoresis. Hence, it acts as the dominant mechanism for metal ions, polar organic compounds, and ionic micelles during remediation.

UNCORRECTED PROOFS

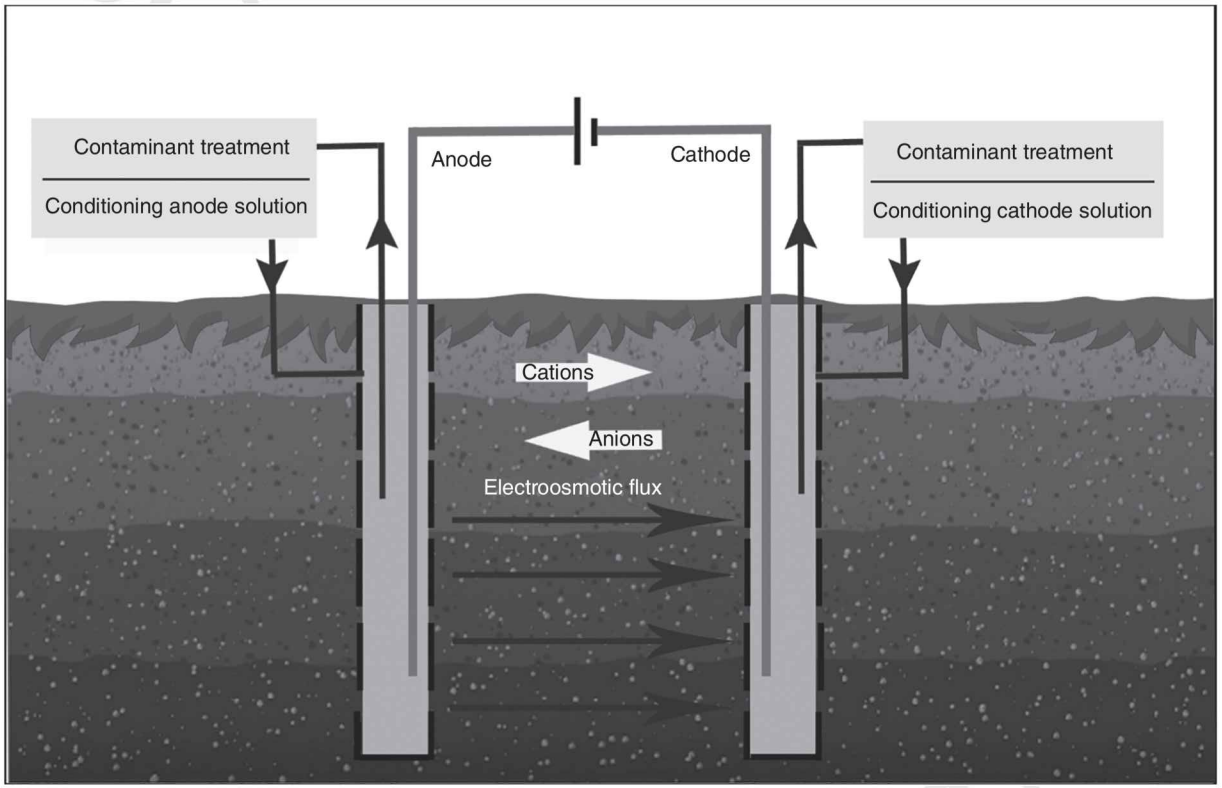

Figure 19.3 Electroosmotic flux and conditioning of anodic solution and conditioning of cathodic solution. Source: Adapted from Cameselle et al. [49].

UNCORRECTED PROOFS

Trim Size: 170mm x 244mm Single Column Loose
Ribeiro670117 c19.tex V1 - 12/11/2020 5:50pm Page 463

Trim Size: 170mm x 244mm Single Column Loose Ribeiro670117 c19.tex V1 - 12/11/2020 5:50pm Page 464

19.4.1.3 Electroosmosis

The electric potential difference incurred at the electrodes results in the electroosmosis-generated flushing of differently charged species in a porous media [48]. *Electroosmosis* is the migration of soil moisture and groundwater from anode to cathode using the capillary influence of the supplied low-level DC. A diffuse double layer is formed since soil particles are negatively charged and water and cations around the soil particles are oppositely charged [45]. Electroosmosis depends on the thickness of the diffuse double layer: the greater the thickness, the greater the electroosmosis. A wider diffuse double layer determines the magnitude of the charge density on the soil surface, ion concentration of the pore fluid, valence of the cations, and dielectric properties of the pore fluid [53]. Electroosmosis does not depend on the pore size distribution or the presence of macropores [45]. It has been proved that an electric potential gradient is more effective than a hydraulic gradient for the migration of fluid through less permeable soil or fine-grained soil. Unlike metal ions, organic contaminants, especially HOCs, are mobilized through electroosmosis in a solubilized form [54].

19.4.1.4 Electrophoresis

Electrophoresis is the migration of colloids, clay particles, and organic particles, usually micelles. The electric field influences the process. Mass transport by electrophoresis in low-permeability soils is insignificant relative to electroosmosis and electromigration. Contaminants bound to mobile particulate matter can be transferred using this method. Electrophoresis is efficient in remediating slurries; when it is applied to EKR, surfactants should be added to the processing fluid to enhance the formation of micelles [47].

19.5 EKR for the Treatment of Soils and Sediments

Processes like electromigration, electrophoresis, and electroosmosis can remove contaminants under an electric voltage in a soil column [55]. This method has even been used to remove PCBs and PAHs [56]. Initially, EKR studies were focused on removing heavy metals from soil. Later, the possibility of eliminating soluble organic pollutants was tested, with positive results. EKR has been suggested as a successful technique for treating organically and inorganically contaminated low-permeability material [51]. EKR is considered unsuitable for HOCs, which have a significant likelihood of being adsorbed into soil and are not soluble in water. Methods that can improve the solubility of HOCs have been recommended to be coupled with EKR [47, 48]. Processes like biodegradation and chemical oxidation can help remove PAHs from soil when combined with EKR [57, 58].

Electrokinetic soil flushing has been tested on removing PAHs [59]. To increase its efficiency, the interaction between soil-solution contaminant and the mobilization of solubilized contaminants has been identified. The electroosmosis phenomenon in EKR creates possible pathways to increase the soil-solution-contaminant interaction in low-permeability regions, thus reducing costs, tailings, and remediation

UNCORRECTED PROOFS

Trim Size: 170mm x 244mm Single Column Loose Ribeiro670117 c19.tex V1 - 12/11/2020 5:50pm Page 465

time [5]. Researchers have concluded that maintaining an optimum osmotic flow was one of the significant considerations for achieving high removal efficiency. An alkaline solution has been used to buffer the anode to maintain electroosmotic flow [51].

In situ and ex situ treatments for removing organic pollutants from soil and sludge and EKR have shown promising results [60–62]. Methods that use one or more electrodes to remove contaminants from saturated and unsaturated soils have received patents [63, 64].

The productiveness of EKR depends primarily on properties such as organic matter content, buffer capacity, and mineralogy. Mechanisms such as ion exchange, surface complexation, and sorption primarily prevent the mobilization of metals from negatively charged particles. The addition of chemical agents such as EDTA has been identified to trigger contaminant solubilization and movement. If a chemical agent is not used, a suitable pretreatment, such as an ultra-sonic treatment, is recommended [62, 65]. EKR offers promising advantages, such as the possibility of using it in situ so it can be adopted where pollutants need to be removed. The ability to remove pollutants from low-permeability materials and manage costs by using a low-voltage application are also advantages. EKR represents a single-stage option to remove both organic and inorganic material and also dewater and consolidate soils and sediments.

Theoretically, the EKR method can be altered by precipitation reactions, competition between species, side reactions, parasite current generation, etc. [51]. Among the recorded EKR remediation processes, most data is available to apply EKR for dewatering and triggering sediment consolidation [66, 67]. Confined disposal facilities (CDFs) are used for sediment disposal and sediment management. Fast consolidation can be useful in this regard. The process may not be fast due to low-speed consolidation caused by high water content and low hydraulic conductivity of sediments [67].

EKR has been used in land reclamation programs combining preloading and prefabricated drains to maximize the mechanical strength of marine sediments. A non-insulated electrode was used for the process, and an intermittent current was applied [68]. The outcome from the application showed that the mechanical properties of sediments were improved in the vicinity of the electrodes after 22–34 days. The applied voltage gradient ranged between 9.5 and 28.2 $V\,m^{-1}$. A test run for marine sediments using a cell test has also shown that combining EKR and preloading improves dewatering and sediment mechanical properties [69].

EKR has shown promising results compared to chemical coagulation and has been tested to improve the free settling velocity and solids concentration of river sediments. Conditioning with $FeCl_3$ in combination with EKR has given the best results in this case [70]. Unenhanced EKR has been tested on high acid buffering spiked glacial till soils. The observations showed that very low removal of cationic contaminants occurred under high pH levels [71, 72]. Experiments were carried out by Reddy and Ala [4] to remove organic pollutants from lake sediments. The sediment was characterized by 19% organic content, a pH of 7, a wide range of PAHs, upper concentrations of heavy metals, and high buffering capacity.

UNCORRECTED PROOFS

Trim Size: 170mm x 244mm Single Column Loose Ribeiro670117 c19.tex V1 - 12/11/2020 5:50pm Page 466

19.5.1 Enhancement Techniques Coupled with EKR

Enhancement techniques are useful for efficiently managing EKR. The EKR process tends to depend on low pH as it is linked with metal release into the solution. When soil buffering capacity is high, it hinders the acidic nature required for EKR [47]. In addition, acidification of soils may not be environmentally friendly. Therefore, different techniques are coupled with EKR to enhance and synergize the remediation of soil up to an acceptable level. Like many other remediation methods, EKR also requires solubilized contaminants in pore fluids and colloidal species suspended in pore fluid for proper extraction. When soil pH alters due to the acid and base fronts produced during the electrolysis mechanism, the solubility of contaminants is reduced, and the effectiveness of EKR also drops [52]. The primary objectives of enhancing techniques for EKR include solubilizing contaminants; maintaining a soil pH favorable for effective EKR; and destroying, breaking down, and transforming contaminants to make them mobile [73].

19.5.1.1 Techniques Used to Enhance the Solubility of Contaminants

The solubility of contaminant species can be obtained by lowering the soil pH and introducing enhancement agents in the soil [51]. Some contaminants are immobile due to persistence in soil precipitation and sorb into soil particles. Soil pH can be controlled by adding acids. If the acid/base buffer capacity is lower in soils, it is enough to use weak acids such as citric acid and acetic acid to reduce the soil pH. However, when the acid/base buffer capacity is higher, strong acids should be applied. It is essential to maintain soil pH above the point of zero charge. Otherwise, the direction of electroosmosis, which is from anode to cathode, is reversed.

In addition, contaminant species can be made soluble by using enhancement agents such as chelates (carboxylates, organophosphates, and polyamines), complexing agents (I^-, OH^-, Cl^-, NH_3^-, acetic acid, cyclodextrins, ammonium acetate), surfactants [74] and cosolvents (sodium dedocylbenzenesulfonate, alkylpolyglucoside, sodium dodecyl sulfate), oxidizing/reducing agents (ozone, chlorine, H_2O_2, $KMnO_4$, $NaMnO_4$), and cation solutions [75]. A mixture of a chelating agent (EDTA) and cosolvent (n-propanol), coupled with EKR, has been shown to be effective against HOCs in diesel-contaminated soil [76].

19.5.1.2 Techniques to Control Soil pH

Soil pH varies during electrolysis because H^+ ions generate an acidic medium, and OH^- ions generate a basic medium; therefore, the soil pH changes during the remediation process, and eventually the process's effectiveness is reduced. Hence, a constant pH must be maintained during EKR to effectively remediate contaminated species. Soil pH can be maintained by electrode conditioning and the use of an ion-exchange membrane [51].

In electrode conditioning, weak acids and buffer solutions such as acetic acid/acetate and $H_2CO_3/NaHCO_3$ are used to control the pH of electrode reservoir electrolytes and thereby control the electroosmotic flow direction and rate. Previous studies have shown that external circulation of the electrolyte solution from cathode to anode controls the soil pH [77].

UNCORRECTED PROOFS

Trim Size: 170mm x 244mm Single Column Loose Ribeiro670117 c19.tex V1 - 12/11/2020 5:50pm Page 467

An ion-exchange membrane can be either a cation ion-exchange membrane or an anion ion-exchange membrane. A cation ion-exchange membrane allows only cations to pass through; keeping the membrane near the cathode prevents OH^- accumulation at the cathode and controls pH. However, it results in the fouling of the membrane due to OH^- deposition on the surface [73].

19.5.1.3 Coupling with Other Remediation Techniques

Since different soil remediation techniques have advantages and disadvantages as introduced earlier, by coupling these methods, the drawbacks can be reduced and the advantages can be synergized. EKR can be combined with permeable reactive barriers (PRBs), oxidation/reduction, bioremediation, phytoremediation, and ultrasonication techniques. The Fenton process is the most commonly used oxidation/reduction technique for soil remediation, especially for organic contaminants in soil.

Hydroxyl radicals ($OH^{\cdot}$) only react with freely available mobile organic contaminants, not with contaminants bound to soil particles. But hydroperoxyl radicals (HO_2), superoxide anions (O_2^-), and hydroperoxide anions (HO_2^-) are highly reactive species, and they can degrade organic contaminants even in a bound form. Soil contaminated with aqueous phenol solution with 90–115 mg kg^{-1} concentration was remediated with EKR coupled with the Fenton process along with 0.3% H_2O_2 for 10 days. The results showed that the destruction efficiency for phenol was 99.7% [78].

EKR combined bioremediation is used for low-permeability soils and when contaminants are embedded in soil particles. EKR can mobilize contaminants and nutrients and make them freely available for microorganisms in low-permeability soil [51]. A combination of electrokinetic soil flushing and bioremediation and daily polarity reversal of the electric field for 14 days removed 20% of diesel from contaminated soil [79].

PRBs are made of reactive treatment media and placed across the flowing pathway of contaminated groundwater and ultimately degrade contaminants on the surface of the barrier. By combining them with EKR, contaminants may flow across the barriers not only by advection but also through electroosmosis, electromigration, and electrophoresis, thereby enhancing the contamination rate on the barriers. Since EKR efficiency is pH-dependent, several steps and processes can be applied to maintain the pH, including the Lasagna process, zero-valent iron PRBs, and PRBs with different reactive media [73]. EKR coupled with phytoremediation allows plants to absorb contaminants, especially metal ions, more easily due to the activity of the DC electric field. The electric field enhances the bioavailability of contaminants, and microbial communities close to plant roots can easily absorb these minerals and other nutrients [50].

Ultrasonication is an environmentally friendly method used to increase the kinetic energy of soil pore fluid, decrease the velocity of soil pore fluid, increase the molecular motion of contaminant species, and make soil permeable by cavitation in soil pore fluid. This approach facilitates the mass transfer of the reaction solution, activates the electrode surface, and enhances electrolytic current mode [80]. All these characteristics enhance the fluid flow rate and also increase the porosity of the soil.

UNCORRECTED PROOFS

Trim Size: 170mm x 244mm Single Column Loose Ribeiro670117 c19.tex V1 - 12/11/2020 5:50pm Page 468

In addition, organic contaminants can be degraded by pyrolysis, and oxidation processes occur during ultrasonication. A study has concluded that soil containing three POPs (hexachlorobenzene, phenanthrene, and fluoranthene) showed higher electroosmotic flow, higher current, and better performance when EKR was coupled with ultrasonication [54].

19.5.2 Facilitating Agents for PAH Removal

Using facilitating agents for solubilization/desorption of organic contaminants is productive in soil remediation processes. Four groups of facilitating agents have been used in this regard: cyclodextrins [81], surfactants [75, 82, 83], cosolvents [3], and biosurfactants [84]. These facilitating agents have been widely used to enhance EKR, and some examples are discussed here.

19.5.2.1 Cyclodextrin-Enhanced EK

Using an altered cyclodextrin called hydroxypropyl β-cyclodextrin (HPCD) as a facilitator offers biodegradability, minimal soil adsorption, non-toxicity, and appreciable PAH solubility. EKR experiments have been conducted using HPCD concentrations in the range of 1.37 to 6.85 mM. The elimination of phenanthrene in model clay was primarily influenced by the concentration of HPCD; other factors, like cumulative volume of electroosmotic flow and longer operation time, were less effective. Once the HPCD concentration was increased to 6.85 mM, 56% phenanthrene removal was observed for six days (due to lower electroosmotic flow) compared to using HPCD for 14 days at 1.37 mM. The highest overall removal (about 75%) was achieved using the highest concentration of HPCD with a buffer solution to improve the electroosmotic washing time [81].

Experiments carried out in the soil-flushing column using CDs such as β – CD and HPCD increased the extraction of PAHs from soils contaminated by industrial effluents. The eradication of PAHs was improved by increasing the cyclodextrin concentration [59]. Researchers state that the desorption of PAH might be inhibited by competitive hydrophobic interactions of pollutants with CD molecules and organic matter, and their co-sorption [85].

19.5.2.2 Surfactant-Enhanced EK

Nonpolar organic transportation has used nonionic surfactant materials with osmotic flow. The materials used are APG (alkyl polyglycolides) [86], Tween 80 (polyoxyethylene (20) sorbitan monooleate) [83], Brij 30 (polyoxyethylene-4-lauryl ether) [87], etc. According to Helmholtz-Smoluchowski (H-S) theory, electroosmotic flow is directly proportional to the dielectric constant of the fluid [47]. The dielectric constant of water is greater than both surfactant and cosolvent solutions. The viscosity of the cosolvent can be greater than water. The reduction in electroosmotic flow by facilitating agents occurs for this reason [51].

Increased transport of pollutants, desorption, and solubilization have been observed near the anode when 3% Tween 80 was applied to an EKR system to

UNCORRECTED PROOFS

Trim Size: 170mm x 244mm Single Column Loose Ribeiro670117 c19.tex V1 - 12/11/2020 5:50pm Page 469

eradicate phenanthrene from kaolin and glacial till. Phenanthrene concentration was higher in the cathodic and central region due to insufficient electroosmotic flow and because surfactant adsorption changing the soil chemistry [83].

Using surfactants has further shown that 3% Tween 80 is not effective in removing PAHs from soils containing a large amount of organic matter. PAH removal has been observed closer to the anodic region, and 3% Tween 80 is not enough to solubilize phenanthrene [4, 75]. It is essential to use higher Tween 80 concentrations or regulate pH to achieve full electrokinetic treatment of soil polluted with PAH. Researchers have shown promising results for the nonionic surfactant Igepal CA-720 among different surfactant/cosolvent mixtures for removing PAHs [51]. Phenanthrene removal was comparatively higher when the surfactant was applied [83]. Using Igepal CA-720 as the coordinating agent eliminated more than 90% of PAHs by periodic application of high-voltage gradient [72]. Removing ethylbenzene with anionic–nonionic mixed surfactants also had positive results. A combined system of 0.5% SDS (sodium dodecyl sulfate) and 2.0% PANNOX 110 (nonylphenol polyethylene glycol ether) led to ethylbenzene removal (98%) [88].

19.5.3 Cosolvent-Enhanced EKR

It has been shown that n-butylamine as a cosolvent can influence electroosmotic flow and the mobility of phenanthrene. About 20% greater removal of phenanthrene was observed than in the cosolvent (10%) due to increased solubilization. The cosolvent must be optimized while permitting sustained electroosmotic flow. However, with an increase in cosolvent concentration, the removal of phenanthrene is reduced [3].

EKR studies have shown the use of ethanol as a solubility-enhancing agent. Phenanthrene solubilization, desorption, and migration near the anode in a soil solution have been observed with 40% ethanol but not with a 3% Tween 80 surfactant solution [89].

19.5.4 Biosurfactant–Enhanced EKR

Biosurfactants can trigger HOC availability by improving their solubility. Rhamnolipids produced by *Pseudomonas aeruginosa* have been tested by researchers to improve the EKR process to remove phenanthrene from soil. Biosurfactants therefore enhance biodegradation, solubilization, and desorption of PAHs in electrokinetic processes [84]. Two biosurfactants, Mannosylerythritol lipid (MEL) and BS–UC (a kind of biosurfactant produced by *Candida antarctica* while growing on n-undecane), produced by *Candida Antarctica*, have been tested to remediate phenanthrene in kaolinite soils [90]. The efficacy of biosurfactant usage was tested in conjunction with synthetic surfactants, where removal efficiencies were recorded as MEL 16.2%, BS–UC 17.4%, and APG, Brij 30, and SDS in the range of 6.3 to 11.1%. Higher removal was observed with biosurfactants. Low-toxicity biosurfactants and good biodegradability are expected to lead to successful electrokinetic flushing.

UNCORRECTED PROOFS

Trim Size: 170mm x 244mm Single Column Loose Ribeiro670117 c19.tex V1 - 12/11/2020 5:50pm Page 470

19.6 Factors Affecting the Efficiency of Electrokinetic Remediation

Soil characteristics, voltage gradient, pH, ionic strength, zeta potential, etc. are generally considered factors that influence EKR remediation efficiency. The process of electroosmosis is equally essential for remediating nonpolar organic compounds like PAHs. In the same manner, solutions to enhance solubility are also needed [51].

19.6.1 Effect of pH

EKR prefers a neutral or basic pH for the process of maintaining a negative zeta potential. With such a negative zeta potential, high electroosmotic flow is critical in removing nonpolar organics [51]. Electroosmotic flow is not constant in the EK system, resulting in a low hydraulic conductivity zone in the reactor's center. The soil pH must be uniformly regulated to sustain a consistent high electroosmotic flow. pH regulation is usually achieved using bases or pH buffering solutions in analytes; however, these materials can alter the interaction of solubility-improving solutions with PAHs and soil [51]. In systems where surfactants or cyclodextrin are used to improve electroosmotic flow, acetate buffer and carbonate buffer solutions have shown promising results [81, 87].

19.6.2 Effect of Electrolytes

An electrolyte moves the current in the pore fluid, while the electric potential and consumption of power are linked with its concentration. Less surfactant adsorption and increased micellization can be expected when critical micelle concentrations (CMCs) of a surfactant are reduced due to the solution depolarization effect that occurs in the presence of an electrolyte. The electrolyte reduces the CMC of the surfactant [89]. A study showed that increases in ion intensity triggered a decrease in soil surface zeta potential and a decrease in electroosmotic flow, which resulted in almost no removal of phenanthrene [51]. To strengthen micellization and increase electroosmotic flow, it is necessary to maintain an optimum electrolyte concentration [51].

19.6.3 Effect of Soil Characteristics

Kaolin has been used as the medium in many laboratory EKR experiments. It consists primarily of kaolinite, which is characterized by low cation exchange capacity, low organic content, consistent mineralogy, and nonreactivity compared to clay types like illite and montmorillonite [83, 91]. Nevertheless, it is not an acceptable replica for very heterogeneous soils with high concentrations of organic matter and diverse mineralogy. In electrokinetic phenanthrene removal studies, Reddy and Saichek [83] have compared two clay soils, kaolin, and glacial till. Compared to kaolin, glacial till has more diverse mineralogy, and carbonates are also high. These ions heighten conductivity, increasing the osmotic flow in all samples including soil, surfactant, and cosolvent. Contaminants like PAHs are harder to remove from

UNCORRECTED PROOFS

Trim Size: 170mm x 244mm Single Column Loose Ribeiro670117 c19.tex V1 - 12/11/2020 5:50pm Page 471

glacial till due to interactions with organic matter. In tests of dredged sediment and soil from gas plants, substantial electroosmotic flow was generated due to high acid buffering ability. However, phenanthrene removal efficiency was very poor because PAHs were strongly adsorbed to organic matter; the proportion of organic matter in sediment and soils from manufactured gas plants (MGPs) was 19% and 4%, respectively [4].

Several experiments have examined the impact of soils with more heterogeneous compositions on surfactant-enhanced EKR [5]. A set of bench-scale experiments were performed using two soils (sand and kaolin) with different heterogeneities, such as sprayed, lens, and mixed soil configurations. Sample soils treated with nonionic surfactant Igepal CA-720 showed the highest phenanthrene extraction, while lower remediation levels were observed in soils with elevated concentrations of kaolin [74].

19.6.4 Effect of the Voltage Gradient

An increased voltage generates higher osmotic pressure due to the correlation between velocity and electroosmotic flow and potential gradient. The periodic use of electrical potential has been proposed to enhance the efficiency of pollutant removal while triggering the solubilization of micelles [92]. Discontinuous application of voltage has shown greater pollutant removal in contrast to periodic voltage [93].

19.7 Conclusions and Future Perspective

EKR is effective for removing organic waste from soil and sediments. However, it should be emphasized that this remediation method is highly site-specific. Therefore, results obtained from one study or site cannot be applied directly to another site. In addition, chemicals used to enhance treatment efficiency can complicate the behavior of contaminants at each site, making the process. For this reason, it is common to use other remediation techniques in combination with EKR to improve the remediation results. EKR has been considered unsuitable for HOCs, which are likely to be adsorbed onto soil and lack solubility in water. Hence, methods that can improve the solubility of HOCs are recommended to be coupled with EKR. For specific complex contamination scenarios, electrokinetics can be used in combination with other techniques. Such combinations result in efficient, cost-effective remediation methods for contaminated sites.

Acknowledgments

The authors would like to thank the Department of Chemistry, Faculty of Applied Sciences, University of Sri Jayewardenepura; Instrument Centre, Faculty of Applied Sciences, University of Sri Jayewardenepura; and Ecosphere Resilience Research Center, Faculty of Applied Sciences, University of Sri Jayewardenepura, Sri Lanka, for their support.

UNCORRECTED PROOFS

Trim Size: 170mm x 244mm Single Column Loose Ribeiro670117 c19.tex V1 - 12/11/2020 5:50pm Page 472

References

1 Zhang, H., Ma, D., Qiu, R. et al. (2017). Non-thermal plasma technology for organic contaminated soil remediation: a review. *Chemical Engineering Journal* 313: 157–170.

2 Fernández, P. and Grimalt, J.O. (2003). On the global distribution of persistent organic pollutants. *Chimia International Journal for Chemistry* 57: 514–521.

3 Maturi, K. and Reddy, K.R. (2008a). Cosolvent-enhanced desorption and transport of heavy metals and organic contaminants in soils during electrokinetic remediation. *Water, Air, and Soil Pollution* 189: 199–211.

4 Reddy, K.R. and Ala, P.R. (2006). Electrokinetic remediation of contaminated dredged sediment. *Journal of ASTM International* 3: 254–267.

5 Saichek, R.E. and Reddy, K.R. (2005a). Electrokinetically enhanced remediation of hydrophobic organic compounds in soils: a review. *Critical Reviews in Environmental Science and Technology* 35: 115–192.

6 Gillette, J.S., Luthy, R.G., Clemett, S.J., and Zare, R.N. (1999). Direct observation of polycyclic aromatic hydrocarbons on geosorbents at the subparticle scale. *Environmental Science & Technology* 33: 1185–1192.

7 Connell, D. (2005). Soaps and detergents. In: *Basic Concepts of Environmental Chemistry*, 209–222. Florida, USA: CRS Press.

8 Valsaraj, K.T. and Melvin, E.M. (2000). *Elements of Environmental Engineering: Thermodynamics and Kinetics*. CRC Press.

9 Von Lau, E., Gan, S., Ng, H.K., and Poh, P.E. (2014). Extraction agents for the removal of polycyclic aromatic hydrocarbons (PAHs) from soil in soil washing technologies. *Environmental Pollution* 184: 640–649.

10 Wilcke, W. (2000). Synopsis polycyclic aromatic hydrocarbons (PAHs) in soil – a review. *Journal of Plant Nutrition and Soil Science* 163: 229–248.

11 Rivas, F.J. (2006). Polycyclic aromatic hydrocarbons sorbed on soils: a short review of chemical oxidation based treatments. *Journal of Hazardous Materials* 138: 234–251.

12 Ravindra, K., Sokhi, R., and Van Grieken, R. (2008). Atmospheric polycyclic aromatic hydrocarbons: source attribution, emission factors and regulation. *Atmospheric Environment* 42: 2895–2921.

13 Fan, G., Cang, L., Fang, G., and Zhou, D. (2014). Surfactant and oxidant enhanced electrokinetic remediation of a PCBs polluted soil. *Separation and Purification Technology* 123: 106–113.

14 Falandysz, J., Brudnowska, B., Kawano, M., and Wakimoto, T. (2001). Polychlorinated biphenyls and organochlorine pesticides in soils from the southern part of Poland. *Archives of Environmental Contamination and Toxicology* 40: 173–178.

15 Guzzella, L. (1997). PCBs and organochlorine pesticides in Lake Orta (Northern Italy) sediments. *Water, Air, and Soil Pollution* 99: 245–254.

16 Peijnenburg, W. (2004). Fate of contaminants in soil. In: *Developments in Soil Science* (eds. P. Doelman and H.J.P. Eijacskers), 245–280. Elsevier.

UNCORRECTED PROOFS

Trim Size: 170mm x 244mm Single Column Loose Ribeiro670117 c19.tex V1 - 12/11/2020 5:50pm Page 473

17 Biswas, B., Qi, F., Biswas, J.K. et al. (2018). The fate of chemical pollutants with soil properties and processes in the climate change paradigm – a review. *Soil Systems* 2: 51.

18 Romero-Romero, S., Herrero, L., Fernández, M. et al. (2017). Biomagnification of persistent organic pollutants in a deep-sea, temperate food web. *Science of the Total Environment* 605: 589–597.

19 Ren, J., Wang, X., Wang, C. et al. (2017). Biomagnification of persistent organic pollutants along a high-altitude aquatic food chain in the Tibetan Plateau: processes and mechanisms. *Environmental Pollution* 220: 636–643.

20 Gray, J.S. (2002). Biomagnification in marine systems: the perspective of an ecologist. *Marine Pollution Bulletin* 45: 46–52.

21 Gary, J. (2002). Biomagnifications of methyl mercury in marine systems the perspective of and ecologist. *Marine Pollution Bulletin* 45: 46–52.

22 Gobas, F.A., Mccorquodale, J.R., and Haffner, G. (1993). Intestinal absorption and biomagnification of organochlorines. *Environmental Toxicology and Chemistry: An International Journal* 12: 567–576.

23 D'adamo, R., Pelosi, S., Trotta, P., and Sansone, G. (1997). Bioaccumulation and biomagnification of polycyclic aromatic hydrocarbons in aquatic organisms. *Marine Chemistry* 56: 45–49.

24 Sharma, S., Tiwari, S., Hasan, A. et al. (2018). Recent advances in conventional and contemporary methods for remediation of heavy metal-contaminated soils. *3Biotech* 8: 216.

25 Rulkens, W., Tichy, R., and Grotenhuis, J. (1998). Remediation of polluted soil and sediment: perspectives and failures. *Water Science and Technology* 37: 27–35.

26 Gao, Y.F., Yang, H., Zhan, X.H., and Zhou, L.X. (2013). Scavenging of BHCs and DDTs from soil by thermal desorption and solvent washing. *Environmental Science and Pollution Research* 20: 1482–1492.

27 Zhao, Z., Ni, M., Li, X., and Buekens, A. (2016). Thermal desorption for remediating PCB-contaminated soil. *International Journal of Environment and Pollution* 60: 171–189.

28 Soares, A.A., Albergaria, J.T., Domingues, V.F. et al. (2010). Remediation of soils combining soil vapor extraction and bioremediation: benzene. *Chemosphere* 80: 823–828.

29 Wolff, M.S., Teitelbaum, S.L., Mcgovern, K. et al. (2015). Environmental phenols and pubertal development in girls. *Environment International* 84: 174–180.

30 Liu, L., Li, W., Song, W., and Guo, M. (2018). Remediation techniques for heavy metal-contaminated soils: principles and applicability. *Science of the Total Environment* 633: 206–219.

31 Palermo, M.R. (1998). Design considerations for in-situ capping of contaminated sediments. *Water Science and Technology* 37: 315.

32 Brusseau, M.L. and Maier, R.M. (2004). Soil and groundwater remediation. In: *Environmental Monitoring and Characterization* (eds. J. Artiola, I. Pepper and M. Brusseau), 335–356. Elsevier Inc.

UNCORRECTED PROOFS

Trim Size: 170mm x 244mm Single Column Loose Ribeiro670117 c19.tex V1 - 12/11/2020 5:50pm Page 474

33 Flores, R., García, M., Peralta-Hernández, J. et al. (2012). Electro-remediation in the presence of ferrous sulfate as an ex-situ alternative treatment for hydrocarbon polluted soil. *International Journal of Electrochemical Science* 7: 2230–2239.

34 Fox, R.D. (1996). Physical/chemical treatment of organically contaminated soils and sediments. *Journal of the Air & Waste Management Association* 46: 391–413.

35 Brusseau, M.L. (2019). Soil and groundwater remediation. In: *Environmental and Pollution Science* (eds. M.L. Brusseau, I.L. Pepper and C.P. Gerba), 329–354. Academic Press.

36 Maturi, K. and Reddy, K.R. (2008b). Extractants for the removal of mixed contaminants from soils. *Soil & Sediment Contamination* 17: 586–608.

37 Mousset, E., Oturan, M.A., Van Hullebusch, E.D. et al. (2014). Soil washing/flushing treatments of organic pollutants enhanced by cyclodextrins and integrated treatments: state of the art. *Critical Reviews in Environmental Science and Technology* 44: 705–795.

38 Talvenmäki, H., Lallukka, N., Survo, S., and Romantschuk, M. (2019). Fenton's reaction-based chemical oxidation in suboptimal conditions can lead to mobilization of oil hydrocarbons but also contribute to the total removal of volatile compounds. *Environmental Science and Pollution Research* 26: 34670–34684.

39 Tisa, F., Raman, A.A.A., and Daud, W.M.A.W. (2014). Applicability of fluidized bed reactor in recalcitrant compound degradation through advanced oxidation processes: a review. *Journal of Environmental Management* 146: 260–275.

40 Gaya, U.I. and Abdullah, A.H. (2008). Heterogeneous photocatalytic degradation of organic contaminants over titanium dioxide: a review of fundamentals, progress and problems. *Journal of Photochemistry and Photobiology C: Photochemistry Reviews* 9: 1–12.

41 Kang, J.W. (2014). Removing environmental organic pollutants with bioremediation and phytoremediation. *Biotechnology Letters* 36: 1129–1139.

42 Marttinen, S.K., Kettunen, R.H., and Rintala, J.A. (2003). Occurrence and removal of organic pollutants in sewages and landfill leachates. *Science of the Total Environment* 301: 1–12.

43 Das, N. and Chandran, P. (2011). Microbial degradation of petroleum hydrocarbon contaminants: an overview. *Biotechnology Research International* 2011: 941810.

44 Suresh, B. and Ravishankar, G. (2004). Phytoremediation – a novel and promising approach for environmental clean-up. *Critical Reviews in Biotechnology* 24: 97–124.

45 Niroumand, H., Nazir, R., and Kassim, K.A. (2012). The performance of electrochemical remediation technologies in soil mechanics. *International Journal of Electrochemical Science* 7: 5708–5715.

46 Alcantara, T., Pazos, M., Gouveia, S. et al. (2008). Remediation of phenanthrene from contaminated kaolinite by electroremediation-Fenton technology. *Journal of Environmental Science and Health. Part A, Toxic/Hazardous Substances & Environmental Engineering* 43: 901–906.

47 Virkutyte, J., Sillanpää, M., and Latostenmaa, P. (2002). Electrokinetic soil remediation – critical overview. *Science of the Total Environment* 289: 97–121.

UNCORRECTED PROOFS

Trim Size: 170mm x 244mm Single Column Loose Ribeiro670117 c19.tex V1 - 12/11/2020 5:50pm Page 475

48 Acar, Y.B., Gale, R.J., Alshawabkeh, A.N. et al. (1995). Electrokinetic remediation: basics and technology status. *Journal of Hazardous Materials* 40: 117–137.

49 Cameselle, C., Gouveia, S., Akretche, D.E., and Belhadj, B. (2013). Advances in electrokinetic remediation for the removal of organic contaminants in soils. In: *Organic Pollutants-Monitoring, Risk and Treatment* (ed. M.N. Rashid), 210–229. London: IntechOpen.

50 Gill, R., Harbottle, M.J., Smith, J., and Thornton, S. (2014). Electrokinetic-enhanced bioremediation of organic contaminants: a review of processes and environmental applications. *Chemosphere* 107: 31–42.

51 Reddy, K.R. and Cameselle, C. (2009). *Electrochemical Remediation Technologies for Polluted Soils, Sediments and Groundwater*. Wiley.

52 Alshawabkeh, A.N. (2009). Electrokinetic soil remediation: challenges and opportunities. *Separation Science and Technology* 44: 2171–2187.

53 Mosavat, N., Oh, E., and Chai, G. (2012). A review of electrokinetic treatment technique for improving the engineering characteristics of low permeable problematic soils. *International Journal of GEOMATE* 2: 266–272.

54 Pham, T.D., Shrestha, R.A., Virkutyte, J., and Sillanpää, M. (2009). Combined ultrasonication and electrokinetic remediation for persistent organic removal from contaminated kaolin. *Electrochimica Acta* 54: 1403–1407.

55 Acar, Y.B. and Alshawabkeh, A.N. (1993). Principles of electrokinetic remediation. *Environmental Science & Technology* 27: 2638–2647.

56 Garbisu, C. and Alkorta, I. (1997). Bioremediation: principles and future. *Journal of Clean Technology, Environmental Toxicology and Occupational Medicine* 6: 351–366.

57 Kim, W.S., Kim, S.O., and Kim, K.W. (2005). Enhanced electrokinetic extraction of heavy metals from soils assisted by ion exchange membranes. *Journal of Hazardous Materials* 118: 93–102.

58 Niqui-Arroyo, J.L. and Ortega-Calvo, J.J. (2007). Integrating biodegradation and electroosmosis for the enhanced removal of polycyclic aromatic hydrocarbons from creosote-polluted soils. *Journal of Environmental Quality* 36: 1444–1451.

59 Viglianti, C., Hanna, K., De Brauer, C., and Germain, P. (2006). Removal of polycyclic aromatic hydrocarbons from aged-contaminated soil using cyclodextrins: experimental study. *Environmental Pollution* 140: 427–435.

60 Lageman, R., Pool, W., and Seffinga, G. (1989). Electro-reclamation: theory and practice. *Chemistry and Industry* 9: 585–590.

61 Probstein, R.F., Renaud, P.C., and Shapiro, A.P. (1991). Electroosmosis techniques for removing materials from soil. United States, 12/24/1991

62 Yeung, A.T. and Hsu, C.N. (2005). Electrokinetic remediation of cadmium-contaminated clay. *Journal of Environmental Engineering* 131: 298–304.

63 Probstein, R.F. and Hicks, R.E. (1993). Removal of contaminants from soils by electric fields. *Science* 260: 498–503.

64 Wittle, J.K. and Pamukcu, S. (1997). Electrochemical system and method for the removal of charged species from contaminated liquid and solid wastes. United States, 03/25/1997.

UNCORRECTED PROOFS

Trim Size: 170mm x 244mm Single Column Loose Ribeiro670117 c19.tex V1 - 12/11/2020 5:50pm Page 476

65 Chung, H.I. and Kamon, M. (2005). The coupled effect of electrokinetic and ultrasonic remediation for the treatment of contaminated sediments. Fifteenth International Offshore and Polar Engineering Conference, 19–24 June, Seoul, Korea. International Society of Offshore and Polar Engineers.

66 Mohamedelhassan, E. and Shang, J. (2001). Analysis of electrokinetic sedimentation of dredged Welland River sediment. *Journal of Hazardous Materials* 85: 91–109.

67 Reddy, K.R., Urbanek, A., and Khodadoust, A.P. (2006). Electroosmotic dewatering of dredged sediments: bench-scale investigation. *Journal of Environmental Management* 78: 200–208.

68 Lo, K., Micic, S., Shang, J. et al. (2000). Electrokinetic strengthening of a soft marine sediment. *International Journal of Offshore and Polar Engineering* 10: 1–8.

69 Micic, S., Shang, J., Lo, K. et al. (2001). Electrokinetic strengthening of a marine sediment using intermittent current. *Canadian Geotechnical Journal* 38: 287–302.

70 Buckland, D.G., Shang, J., and Mohamedelhassan, E. (2000). Electrokinetic sedimentation of contaminated Welland River sediment. *Canadian Geotechnical Journal* 37: 735–747.

71 De Gioannis, G., Muntoni, A., Polettini, A., and Pomi, R. (2008). Enhanced electrokinetic treatment of different marine sediments contaminated by heavy metals. *Journal of Environmental Science and Health, Part A* 43: 852–865.

72 Reddy, K.R. and Chinthamreddy, S. (2004). Enhanced electrokinetic remediation of heavy metals in glacial till soils using different electrolyte solutions. *Journal of Environmental Engineering* 130: 442–455.

73 Yeung, A.T. and Gu, Y.Y. (2011). A review on techniques to enhance electrochemical remediation of contaminated soils. *Journal of Hazardous Materials* 195: 11–29.

74 Saichek, R.E. and Reddy, K.R. (2005b). Surfactant-enhanced electrokinetic remediation of polycyclic aromatic hydrocarbons in heterogeneous subsurface environments. *Journal of Environmental Engineering and Science* 4: 327–339.

75 Saichek, R., Reddy, E., and Krishna, R. (2004). Evaluation of surfactants/cosolvents for desorption/solubilization of phenanthrene in clayey soils. *International Journal of Environmental Studies* 61: 587–604.

76 Han, H., Lee, Y.J., Kim, S.H., and Yang, J.W. (2009). Electrokinetic remediation of soil contaminated with diesel oil using EDTA–cosolvent solutions. *Separation Science and Technology* 44: 2437–2454.

77 Li, R.S. and Li, L.Y. (2000). Enhancement of electrokinetic extraction from lead-spiked soils. *Journal of Environmental Engineering* 126: 849–857.

78 Yang, G.C. and Long, Y.-W. (1999). Removal and degradation of phenol in a saturated flow by in-situ electrokinetic remediation and Fenton-like process. *Journal of Hazardous Materials* 69: 259–271.

79 Ramírez, E.M.,.C.J.V.,.R.M.A.&.C.P. (2015). Combination of bioremediation and electrokinetics for the in-situ treatment of diesel polluted soil: a comparison of strategies. *Science of the Total Environment* 533: 307–316.

UNCORRECTED PROOFS

Trim Size: 170mm x 244mm Single Column Loose Ribeiro670117 c19.tex V1 - 12/11/2020 5:50pm Page 477

80 Pham, T.D. and Sillanpää, M. (2020). Ultrasonic and electrokinetic remediation of low permeability soil contaminated with persistent organic pollutants. In: *Advanced Water Treatment* (ed. M. Sillanpää), 227–310. Elsevier.

81 Ko, S.O., Schlautman, M.A., and Carraway, E.R. (2000). Cyclodextrin-enhanced electrokinetic removal of phenanthrene from a model clay soil. *Environmental Science & Technology* 34: 1535–1541.

82 Gezer, A. and Karagunduz, A. (2010). Use of surfactants in soil and groundwater remediation. In: *Survival and Sustainability. Environmental Earth Sciences* (eds. H. Gökçekus, U. Türker and J. LaMoreaux), 995–1004. Berlin, Heidelberg: Springer.

83 Reddy, K.R. and Saichek, R.E. (2003). Effect of soil type on electrokinetic removal of phenanthrene using surfactants and cosolvents. *Journal of Environmental Engineering* 129: 336–346.

84 Ju, L. and Elektorowicz, M. (2000). *In - situ* phenanthrene removal provoked by electrokinetic transport of on - site produced biosurfactants. Annual conference, Canadian Society for Civil Engineering, May, London.

85 Badr, T., Hanna, K., and De Brauer, C. (2004). Enhanced solubilization and removal of naphthalene and phenanthrene by cyclodextrins from two contaminated soils. *Journal of Hazardous Materials* 112: 215–223.

86 Yang, J.W., Lee, Y.J., Park, J.-Y. et al. (2005). Application of APG and Calfax 16L-35 on surfactant-enhanced electrokinetic removal of phenanthrene from kaolinite. *Engineering Geology* 77: 243–251.

87 Park, J.Y., Lee, H.H., Kim, S.-J. et al. (2007). Surfactant-enhanced electrokinetic removal of phenanthrene from kaolinite. *Journal of Hazardous Materials* 140: 230–236.

88 Yuan, C. and Weng, C.H. (2004). Remediating ethylbenzene-contaminated clayey soil by a surfactant-aided electrokinetic (SAEK) process. *Chemosphere* 57: 225–232.

89 Saichek, R.E. and Reddy, K.R. (2003). Effect of pH control at the anode for the electrokinetic removal of phenanthrene from kaolin soil. *Chemosphere* 51: 273–287.

90 Park, J.Y., Chen, Y., Chen, J., and Yang, J.-W. (2002). Removal of phenanthrene from soil by additive-enhanced electrokinetics. *Geosciences Journal* 6: 1.

91 Pierzynski, G.M., Vance, G.F., and Sims, J.T. (2005). *Soils and Environmental Quality*. CRC Press.

92 Yeom, I.T., Ghosh, M.M., and Cox, C.D. (1996). Kinetic aspects of surfactant solubilization of soil-bound polycyclic aromatic hydrocarbons. *Environmental Science & Technology* 30: 1589–1595.

93 Reddy, K.R. and Saichek, R.E. (2004). Enhanced electrokinetic removal of phenanthrene from clay soil by periodic electric potential application. *Journal of Environmental Science and Health, Part A* 39: 1189–1212.

UNCORRECTED PROOFS

UNCORRECTED PROOFS

Trim Size: 170mm x 244mm Single Column Loose Ribeiro670117 c20.tex V1 - 12/11/2020 5:51pm Page 479

20

The Integration of Electrokinetics and In Situ Chemical Oxidation Processes for the Remediation of Organically Polluted Soils

Long Cang[1], Qiao Huang[1,2], Hongting Xu[1], and Mingzhu Zhou[1]

[1] *Key Laboratory of Soil Environment and Pollution Remediation, Institute of Soil Science, Chinese Academy of Sciences, Nanjing 210008, China*
[2] *College of Resources and Environment, University of the Chinese Academy of Sciences, Beijing 100049, China*

20.1 Introduction

The rapid development of industry has meant that soil contamination by organic pollutants is now a serious environmental problem. A large variety of technologies have been developed to remediate contaminated soils, including physical (e.g. thermal desorption [1] and soil washing [2, 3]), chemical (e.g. chemical oxidation [4, 5] and chemical reduction [6]), and biological processes (e.g. microbial remediation [7, 8]). Among these technologies, chemical treatment is a widely used approach for soil and groundwater remediation because of its wide applicability, relatively fast treatment times, simplicity of operation, and cost-effectiveness [9, 10]. According to the Superfund Remedy Report [11], chemical treatment was one of the most frequently selected in situ methods (27 ~ 42%), and more than half of the chosen chemical treatments involved chemical oxidation.

The primary principle of in situ chemical oxidation (ISCO) is the introduction of a chemical oxidant into the soil/groundwater subsurface to transform organic contaminants into less harmful chemical species. Many oxidants, such as persulfate, permanganate, and hydrogen peroxide, have been widely used in ISCO processes to treat organically contaminated soil and groundwater. However, applying ISCO to low-permeability soils is limited because of the difficulty in delivering oxidants to such soils ([12], [13]. In recent years, researchers have combined electrokinetic remediation with ISCO when attempting to remediate organically contaminated soil.

Electrokinetic remediation (EKR), also known as electrokinetic soil remediation (ESR)), is a soil and groundwater remediation technology introduced in the 1980s. The technology applies a direct current (DC) electric field to the soil to generate a voltage gradient that drives soluble pollutants out of the soil by electromigration, electroosmosis flow (EOF), and/or electrophoresis [14–16]. The electrolysis of water leads to an oxidation and reduction environment near the anode and cathode,

Electrokinetic Remediation for Environmental Security and Sustainability, First Edition.
Edited by Alexandra B. Ribeiro and M.N.V. Prasad.
© 2021 John Wiley & Sons Ltd. Published 2021 by John Wiley & Sons Ltd.

UNCORRECTED PROOFS

Trim Size: 170mm x 244mm Single Column Loose Ribeiro670117 c20.tex V1 - 12/11/2020 5:51pm Page 480

respectively. In addition, some soluble additive substances, such as chelates and oxidants, can migrate into the soil by electromigration and electroosmotic flow under a DC electric field. The electromigration and electroosmosis equations show that hydraulic permeability is more affected by soil texture than the electromigration and electroosmosis velocities [14]. Therefore, EK-enhanced ISCO technology is an alternative approach that can be used to remediate organically contaminated soils, especially low-permeability soils.

The objective of this chapter is to examine the state of knowledge on electrokinetic in situ chemical oxidation technology (EK-ISCO) and discuss the mechanisms underlying the EK-ISCO remediation process. In this chapter, various oxidants (persulfate, hydrogen peroxide, permanganate, etc.) and enhanced methods for removing organic pollutants are investigated. A number of possible enhancement mechanisms are also discussed. In addition, this chapter focuses on the fundamental principles and governing factors underlying EK-ISCO technology and the relevant remediation equipment. It also discusses the results of pilot/field-scale experiments. Finally, the concluding remarks and perspectives will inform future studies on the EK-ISCO remediation of soils contaminated with organic pollutants.

20.2 Principles Underlying EK-ISCO Remediation Technology

EK-ISCO remediation methods use a DC electric field to remove pollutants and oxidants. They also degrade organic pollutants using oxidants and anode reactions. The basic principle is to strengthen the desorption and migration of pollutants and the migration of oxidants using electromigration and electroosmotic flow. This means the pollutants can be efficiently desorbed from the soil and migrate and degrade under the action of an electric field and oxidants. The primary processes used by EK-ISCO technologies include desorption and migration of organic pollutants; migration of oxidants; removal and degradation of organic pollutants by oxidants; and degradation of organic pollutants by electrode reactions in the anode and cathode. A schematic diagram of EK-ISCO remediation is shown in Figure 20.1.

20.2.1 Desorption and Migration of Organic Pollutants

Many organically contaminated soils can be treated using EK-ISCO technology. According to the published literature, these organic pollutants include phenol [17, 18], trichloroethylene (TCE) [19, 20], tetrachloroethylene (PCE) [21], chlorobenzenes (such as hexachlorobenzene [HCB]) [22], polycyclic aromatic hydrocarbons (PAHs) [23, 24], polychlorinated biphenyls (PCBs) [13, 25, 26], phthalates (PAEs) [27], organochlorine pesticides (OCs) [28], and petroleum hydrocarbons [29, 30]. These pollutants, with the exception of phenol, which has a high aqueous solubility (6.67 g/100 ml, 25 °C), have a very low solubility or are insoluble in water. Phenol (C_6H_5OH) can be hydrolyzed into H^+ and $C_6H_5O^-$, and the latter is an anion that can migrate to the anode under a DC electric field.

UNCORRECTED PROOFS

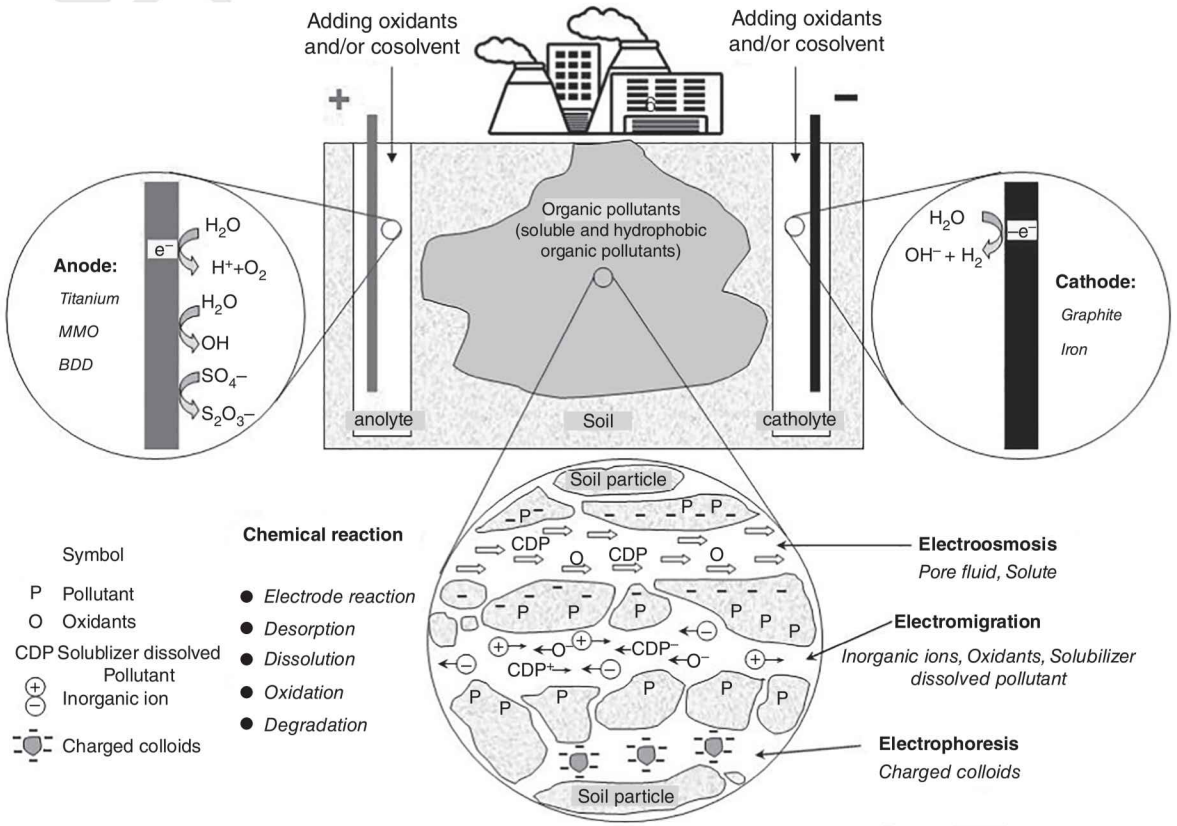

Figure 20.1 Schematic diagram showing EK-ISCO remediation of organically polluted soil. Expanded bubbles detail EK migration and chemical reactions. MMO, mixed metal oxides electrode; BDD, boron-doped diamond electrode).

UNCORRECTED PROOFS

Trim Size: 170mm x 244mm Single Column Loose
Ribeiro670117 c20.tex V1 - 12/11/2020 5:51pm Page 481

Trim Size: 170mm x 244mm Single Column Loose Ribeiro670117 c20.tex V1 - 12/11/2020 5:51pm Page 482

However, it is difficult to desorb insoluble organic pollutants from the surface of soil particles so that they can migrate in a DC electric field. This is because they are strongly adsorbed onto the soil organic matter (SOM). Therefore, it is generally necessary to add cosolvents to increase the solubility of organic pollutants and accelerate their migration under a DC electric field.

Many solubilizers (surfactants, cosolvents, and other reagents) are used in the EKR process. The surfactant category includes cationic surfactants, such as hexadecyl trimethyl ammonium bromide (CATB) [31]; anionic surfactants, such as sodium dodecyl sulfate (SDS), rhamnolipid, and dodecyl sulfate [32]; and nonionic surfactants, such as polyethylene lauryl ether (Brij 35), Igepal CA-720, and Tween 80 [28, 33, 34]. There are also other types of solubilizers, such as n-butylamine, alkyl polyglucoside (APG), and hydroxypropyl-alkyl-cyclodextrin (HPCD) [32, 33]. These solubilizers can desorb organic pollutants from the soil and increase the solubility of organic pollutants by forming micelles. Cationic and anionic surfactants form micelles with positive or negative charges that can carry organic pollutants and migrate to the cathode or anode under a DC electric field via electromigration. The nonionic surfactant has a neutral charge, which means the pollutant can be removed from the soil by electroosmotic flow under a DC electric field. The cyclodextrin cosolvents can combine the organic pollutant molecules in the cyclodextrin cavity and carry the pollutant out of the soil under a DC electric field. Furthermore, HPCD can significantly increase the desorption of bromodiphenyl ether (BDE) from the soil because of its relatively hydrophobic interior "hole" and high aqueous solubility [35].

Reddy and Ala [33] used 5% Igepal CA-720 to restore a phenanthrene-contaminated soil. Over 90% of phenanthrene was removed from the soil after applying an intermittent current for 148 days. Park et al. [32] used surfactants (alkyl polyglucoside, Brij 35, and SDS) to enhance EK removal of phenanthrene from kaolin, and found that Brij 35 was the best surfactant. Karagunduz et al. [36] used surfactants (7.5 g/l sodium dodecylbenzene sulfonate [SDBS] or Tween 80) to enhance EK removal of DDT from a soil, and Wan et al. [37] used 20–50% ethanol and 20–50 g/l methyl-β-cyclodextrin (MCD) to enhance the EK removal of HCB-contaminated sediments. The relevant studies are shown in Table 20.1.

20.2.2 Oxidant Migration

Oxidants that are commonly used in EK-ISCO remediation processes include hydrogen peroxide (H_2O_2, HP), persulfate (PS), potassium permanganate ($KMnO_4$, PM), sodium hypochlorite (NaClO), and permonosulfate (PMS). Oxidant migration under a DC electric field is primarily related to the oxidant charge. Hydrogen peroxide has no charge and primarily migrates in soil by electroosmotic flow under a DC electric field. However, the PS, $KMnO_4$, and NaClO oxidation groups are all negatively charged, meaning they move to the anode under a DC electric field. During the EK process, the electroosmotic flow generally moves toward the cathode because of the negative charge on the soil particle surface, which is opposite the general migration

UNCORRECTED PROOFS

Trim Size: 170mm x 244mm Single Column Loose Ribeiro670117 c20.tex V1 - 12/11/2020 5:51pm Page 483

Table 20.1 Solubilizer-enhanced EK remediation of organically contaminated soil.

References	Pollutants	Solubilizers	Voltage/current	Time	Important results
[33]	PAHs: 677 mg/kg	5% Igepal CA-720, 20% n-butylamine, 3% Tween 80, 10% HPCD	2 V/cm	148 d, pulse current	Igepal CA-720 and n-butylamine were valid.
[34]	HCB: 55 mg/kg	1% Tween 80, 1% β-CD	1 V/cm	7–11 d	β-CD was better than Tween 80.
[32]	Phenanthrene: 600–700 mg/kg	5 g/L alkyl polyglucoside, 5 g/L Brij 35, 5 g/L SDS	10 mA (0.8 mA/cm^2)	14–28 d	Brij 35 was the best solubilizer.
[36]	DDT: 1.92 mg/kg	7.5 g/L SDBS, 7.5 g/L Tween 80	1.3–2 V/cm	10–20 d	SDBS was better than Tween 80.
[37]	HCB: 14.3 mg/kg	20–50% ethanol, 20–50 g/L MCD	2 V/cm	14–21 d	MCD was better than ethanol.
[28]	OCs: 100 mg/kg	10% Tween 80, 6.4% GLDA	2 V/cm	7, 15 d	Tween 80 was better than GLDA.

OCs, organochlorine pesticides; MCD, methyl-β-cyclodextrin; GLDA, N,N-dicarboxymethyl glutamic acid tetrasodium salt; SDS, sodium dodecyl sulfate; SDBS, sodium dodecylbenzene sulfonate; APG, alkyl polyglucoside; HPCD, hydroxypropyl-alkyl-cyclodextrin.

direction of the oxidation groups. Therefore, the migration rates and direction of the different oxidation groups need to be carefully evaluated.

Potassium permanganate is a common oxidant that migrates as ions in soil. Thepsithar and Roberts [18] studied the removal of phenol from contaminated kaolin using EK-ISCO after adding PM to the catholyte. Over 90% of the phenol in the 15 cm-long container was removed after five days of treatment. Chowdhury [38] successfully transported PM into the silt layer using a DC electric field, whereas PM could only reach the edge of the silt layer without the electric field. The most commonly used oxidant in practical engineering is PS, which has a high redox potential (E = 2.40 mV) and high aqueous solubility and stability, and is inexpensive. There is a strong reduction condition near the cathode during the EK process. When a DC electric field is applied, any anion oxidant that has been added to the cathode pool will migrate to the anode. During this process, the oxidant will undergo a reduction reaction near the cathode, which leads to oxidant losses. For example, PS is consumed by reductive H_2 and redundant electrons, resulting in depolarizing of the cathode and mass loss of PS near the cathode [20, 39]. To avoid the loss of oxidant

UNCORRECTED PROOFS

Trim Size: 170mm x 244mm Single Column Loose Ribeiro670117 c20.tex V1 - 12/11/2020 5:51pm Page 484

Table 20.2 Migration of oxidants during the EK process.

References	Pollutants	Oxidant	Injection spot	Voltage/ current	Time	Important results
Thepsithar and Roberts, 2006 [17]	Phenol: 1 g/kg	9 g/l PM	Cathode	1 V/cm	5 d	PM ions could be detected throughout the soil after 72 h.
[13, 26]	PCBs: 46.2 mg/kg	20% PS	Anode, cathode, both electrodes	1 V/cm	15 d	Anode was the best injection spot.
Chowdhury et al. 2017a,b [36, 41]	TCE: 771 mg/l	30 g/l PM	Cathode	5.1 A/m^2	40 d	EK increased 3–4 times of PM migration rates.
[42]	OPs: 18 510 mg/kg	10% H_2O_2	Anode	3 V/cm	15 d	EK enhanced the migration of H_2O_2.
[40]		20% PS	Anode, anode with CEM	1 V/cm	10 d	The latter treatment increased the migration of PS and reduced the loss of PS.

PM, permanganate; PS, persulfate; OCs, organochlorine pesticides; CEM, cation-exchange membrane.

near the cathode, extra oxidant can be added to the anode pool and moved into the soil by electroosmotic flow [13]. In addition, the oxidant can be isolated from the reduction conditions near the cathode by placing a cation-exchange membrane in the cathode pool, which will prevent oxidant losses and improve oxidant migration through the soil [40]. The relevant studies are shown in Table 20.2.

20.3 Factors that Influence EK-ISCO Technology

20.3.1 Soil Properties

A detailed study of the soil properties needs to be undertaken if EK-ISCO remediation technology is to remove pollutants efficiently. Some factors, such as soil pH, OM, conductivity, metal content, buffering capacity, soil texture, and porosity, may significantly affect the EK-ISCO remediation process [43, 44]. Some researchers have pointed out that low acid buffering capacities, iron concentrations, and OM levels generally improve treatment efficiency [45].

The soil OM has a great influence on the remediation process because high levels increase the sorption of organic pollutants into soil, which may decrease migration, reduce contact between the organic pollutants and the oxidant, and limit the extent of the oxidation reaction. Furthermore, soil OM competes with the oxidation

UNCORRECTED PROOFS

Trim Size: 170mm x 244mm Single Column Loose Ribeiro670117 c20.tex V1 - 12/11/2020 5:51pm Page 485

reaction for oxidants, and a proportion of the oxidants may be consumed by OM [46–48] reported that the degradation of phenanthrene and fluorene by oxidation treatment was inhibited by fulvic acid, possibly because the PAHs (e.g. phenanthrene [PHE] and fluorine) that are bound to the fulvic acid are considered to be unreactive.

The acid buffering capacity of soil has an important influence on remediation efficiency. Kim et al. [49] chose two different soils to investigate the effects of soil acid buffering capacity and Fe oxide contents. A higher acid buffering capacity led to a larger EOF, which accelerated the migration of PHE in the soil. In addition, clay particles are more reactive than any other size fractions in soils because of their high surface charge, surface area, and adsorption capacity. Furthermore, soils with high clay contents usually have low permeability, which is not conducive to the desorption and migration of organic pollutants [50].

20.3.2 Dosage and Methods Used to Add Oxidants to Soil

The dosage and methods used to add oxidants are important factors that affect remediation efficiency, and they particularly affect engineering applications. The oxidant concentrations are dependent on the pollution characteristics and vary considerably among different studies [51]. Generally, the concentrations of the H_2O_2 solution ranged from 0.3 to 30%, but they were primarily between 5 and 10%; the PS concentrations were 1–200 g/l [13, 20, 25]), and the PM concentrations were 2–10 g/l (Thepsithar and Robert, 2006 [17]; [52]). Reddy et al. (2008) [50] investigated the EK remediation of PHE contamination using 5, 10, 20, and 30% H_2O_2 solution concentrations. Oxidation of PHE increased as the H_2O_2 concentration rose, and the maximum oxidation level (56%) was observed at 30% H_2O_2. Similar results were reported by Reddy et al. [23], where 49.8–82.3% of PAHs were oxidized as the H_2O_2 concentration increased from 5 to 10%. However, excess oxidants may scavenge the radicals (OH·and SO_4) and facilitate the decomposition of oxidants [50, 53]. Therefore, the oxidant dosage needs to be carefully determined.

The methods used to add oxidants affect the migration and stability of the oxidants, which influences pollutant removal efficiency. Alcantara et al. [51] compared the effect of the H_2O_2 (10%) anode-addition method with the anode-and-cathode-addition method on PHE removal and found that the removal efficiency of the latter method (99%) was significantly higher than the former (68%). Fan et al. [13] reported similar results for PCBs removal efficiency when the both-electrodes-addition (41%) method and anode-addition (35%) method were compared. Oonnittan et al. [22] studied the effect of different addition orders and times for two oxidants (H_2O_2 and $FeSO_4$) on the EK-Fenton remediation of HCB-contaminated kaolin. The results showed that adding H_2O_2 and $FeSO_4$ at intervals of five days led to the highest HCB removal efficiency.

Wu et al. [21] developed a new numerical EOF and reactive transport model and suggested that the placement of the injection well was very important because coverage generally increased as the number of injection wells rose. This result will help engineers to more accurately predict the number of injection wells needed and determine their placement in future remediation projects.

UNCORRECTED PROOFS

Trim Size: 170mm x 244mm Single Column Loose Ribeiro670117 c20.tex V1 - 12/11/2020 5:51pm Page 486

20.3.3 Concentration and Aging of Organic Pollutants

Generally, soils that are highly polluted with organics are treated by thermal desorption, whereas biological treatment is more appropriate and cheaper when contamination levels are lower. However, biological degradation is limited by the low availability of most organic pollutants [54, 55]. It has been suggested that the EK-ISCO method can be used as an alternative remediation process for moderately polluted soil. Previous studies have shown that the general concentration range is 90–1000 mg/kg for phenol, 130–200 mg/kg for TCE, 200–500 mg/kg for PHE, 400–500 mg/kg for PAHs, 100 mg/kg for HCB, 300–10 000 mg/kg for diesel, 50–107 mg/kg for PCBs, and 5 mg/kg for PAEs.

The aging of organic pollutants can also directly affect pollutant removal efficiency. Lemaire et al. [56] compared the PAH oxidation efficiency in two aged soils to a spiked soil. The results showed that the highest PAH degradation rate was 30% for the aged soils and 55% for the spiked soil. PAH availability (extraction with a cyclodextrin) was an important parameter that affected these results, but other parameters (soil pH, OM, calcite content, etc.) were also important. Lemaire et al. [56] also showed that aged soil samples were difficult to treat with Fenton's reagent (maximum degradation ratio: 45%). This was primarily due to the very poor PAH availability. Therefore, improved methods need to be developed for aged soil.

20.4 Enhanced EK-ISCO Remediation Methods

20.4.1 Electro-Fenton Process

Organic compounds in soil can be treated in situ using the electro-Fenton method, which combines the EK and Fenton processes. The combined process has the migration advantages of the EK process and the degradation advantages of the Fenton process.

Yang and Long [17] were the first to report a laboratory study that combined the EK process with a Fenton-like process to remediate a phenol-spiked sandy loam soil. They carried out experiments to study the effects of a scrap iron powder (SIP) bed (1.05–32.69 g, located 5 cm from the anode reservoir) and treatment time on electroosmosis permeability and phenol removal efficiency. The aim was to determine the feasibility of EK-Fenton enhanced remediation with 0.3% H_2O_2. They found that the maximum overall phenol removal rate and destruction efficiency reached 99.7% when a 1.05 g SIP bed was added, and a longer treatment time improved the chemical destruction of phenols. However, the reaction mechanisms underlying the EK-Fenton process and the possible pathways driving phenol degradation were not investigated.

Many factors can impact the remediation performance of an in situ EK-Fenton process. Therefore, Yang and Liu [19] evaluated the effect of electrode material, soil type, catalyst type, and catalyst dosage on trichloroethylene (TCE) treatment efficiency. They compared loamy sand and a sandy loam that contained 1.56 and 3.53% OM, respectively. They found that the sandy loam had a lower removal efficiency

UNCORRECTED PROOFS

Trim Size: 170mm x 244mm Single Column Loose Ribeiro670117 c20.tex V1 - 12/11/2020 5:51pm Page 487

than the loamy sand because it had higher organic matter content, which meant it consumed more hydrogen peroxide. This resulted in reducing the breakdown of organic contaminants. Graphite electrodes produced greater TCE treatment efficiencies than stainless steel electrodes because the EOF levels and electroosmosis permeability were higher. The SIP process had greater treatment efficiency than $FeSO_4$ when different catalysts were added. This indicated that the destruction mechanism dominated when SIP was used in the EK-Fenton process, whereas the removal mechanism was most important when $FeSO_4$ was used. In a study similar to those undertaken by Yang and Long and Yang and Liu [17, 19], Ni et al. [42] installed a $FeSO_4$ barrier at a distance of 6 cm from the anode chamber and established an EK-Fenton remediation system to remediate soils contaminated with OCs. After 15 days of remediation, the removal efficiencies in the EK-Fenton treatment were 40.0–60.9%, higher than the EK removal efficiencies (25.9–30.5%).

In contrast to the previous studies, Kim et al. [57] injected 3.5–7% H_2O_2 into the anode reservoir without adding iron to the soil column and studied the effect of the EK-Fenton process on the remediation of phenanthrene-contaminated kaolinite. The results showed that the EK-only treatment had no significant effect on PHE removal, but H_2O_2 addition enhanced the EK treatment and decreased the PHE concentration in the kaolinite. They also found that adding dilute acid significantly improved H_2O_2 stability and increased PHE removal efficiency (74%). However, the PHE removal efficiency in the soil section near the cathode was sub-optimal, which was attributed to the low H_2O_2 concentration and high soil pH. Based on this study, Alcantara et al. [51] improved the experimental treatment and added H_2O_2 to both the anode and cathode pools. This treatment increased the PHE removal efficiency to 99%.

20.4.2 pH Control

In a standard EK-ISCO remediation process, the high pH of the soil and soil solution near the cathode can cause metals to precipitate and clog soil pores, which decreases EOF and pollutant migration and removal efficiency [45]. This suggests that maintaining a low pH in the cathode reservoir might improve efficiency. Kim et al. [57] studied a mineral catalyst enhanced EK-Fenton process that was intended to remediate phenanthrene-contaminated kaolinite soil. The aim was to explore the correlation between phenanthrene treatment and H_2O_2 behavior. They found that the H_2O_2 decomposition rate decreased when the acid front extended to the regions that were adjacent to the cathode, which showed that acid addition increased H_2O_2 stability and improved phenanthrene treatment efficiency. Xu et al. [40] found that controlling the catholyte pH at pH = 4 produced the highest PAH removal efficiency (93.1%), which suggested that a lower pH improved the oxidation of $S_2O_8^{2-}$. Many other studies have produced similar results [24, 58]. Therefore, maintaining a lower pH seems to be important when remediating organically polluted soils using EK-ISCO technology. However, a pH that is too low is also detrimental to pollutant removal efficiency. Alcantara et al. [51] reported that the PHE removal efficiency was only 15% when the kaolinite pH was lower than 2.5. Although many studies

UNCORRECTED PROOFS

Trim Size: 170mm x 244mm Single Column Loose Ribeiro670117 c20.tex V1 - 12/11/2020 5:51pm Page 488

have reported that an acid pH favored PHE removal, extremely low pHs eliminated the EOF, and PHE removal decreased dramatically. Similar results were obtained by Bocos et al. [45].

In contrast, a high pH may increase oxidation efficiency during the alkaline activation of PS. Fan et al. [25] investigated various activation methods. Zero-valent iron, citric acid chelated Fe^{2+}, iron electrodes, alkaline pHs, and peroxide were evaluated to see if they enhanced the activity of PS delivered by EK when it was used to treat PCB-contaminated soil. The results showed that the PCB removal efficiency was highest when alkaline activation was used. Furthermore, the activation effect was highly dependent on the ratio of activator to persulfate.

In general, pH control needs to add acid or alkali to the remediation system. However, this introduces large numbers of ions and increases the electric current and power cost. In addition, high or low pH controls have been shown to significantly change soil properties, which can have negative effects [25, 40].

20.4.3 Ion-Exchange Membranes

There is a strong reduction environment near the cathode during the EK-ISCO process. When the anion oxidant (PS, PM) is added to the cathode pool and then moved to the anode by electromigration, the oxidant undergoes a reduction reaction near the cathode, which leads to oxidant loss [20, 39]. When the oxidant is added to the anode pool and moved to the cathode by EOF, the oxidants that migrate near the cathode also undergo a reduction reaction. For example, PS can be consumed by reductive H_2 and redundant electrons, which results in the cathode becoming depolarized and causes the mass loss of PS near the cathode [12, 13].

Ion-exchange membranes (IEMs) are often applied to the EK remediation of soils contaminated with heavy metals [57, 59–61]. Xu et al. [40] were the first to report that IEMs enhanced EK-ISCO when attempting to remediate soils polluted with PAHs. They carried out quartz sand column experiments and soil matrix experiments to investigate the effects of IEMs on $S_2O_8^{2-}$ migration and PAH removal efficiency. The results showed that IEMs could control oxidation-reduction potential changes and prevent $S_2O_8^{2-}$ from contacting the cathode, which significantly improved the $S_2O_8^{2-}$ concentration in the soil solution. An 87.1% PAH removal efficiency was achieved by the IEM treatment, which was higher than for the treatment without an IEM (33.1%).

IEMs have some disadvantages, such as the high cost of IEM materials and limited service life. These limitations need to be considered when undertaking a remediation project because using IEMs may increase the material costs despite reducing power losses and oxidant costs.

20.4.4 Adding Solubilizers

A major challenge in the EK-ISCO treatment of organically contaminated soil, particularly aged soils, is limited mass transfer due to the strong sorption and low aqueous solubility of most organic pollutants [50]. However, enhanced methods, such as

UNCORRECTED PROOFS

Trim Size: 170mm x 244mm Single Column Loose Ribeiro670117 c20.tex V1 - 12/11/2020 5:51pm Page 489

adding solubilizers, can be used to improve the solubility and migration of organic pollutants in soils subjected to EK-ISCO.

Fan et al. [26] investigated using Igepal CA-720 surfactant and PS oxidant to remediate PCB-polluted soil. They found that 2% Igepal CA-720 solubilized some PCBs in the soil and led to the PCBs migrating toward the cathode under an EOF electrical field. The results also showed that using Igepal CA-720 and PS produced the greatest PAH removal efficiencies (38.0%), whereas the removal efficiency was only 14.9% in the EK-only treatment and 21.0% in the EK + Igepal CA-720 treatment. Abtahi et al. [62] improved PS-assisted EK remediation of pyrene-contaminated soil by adding 20 mL Tween 80 per kilogram soil. The pyrene removal efficiency was 76% when Tween 80 was added but only 64% without Tween 80, which indicated that Tween 80 increased the pyrene removal efficiency by enhancing the aqueous solubility of pyrene. Tween 80 was also used by Suanon et al. [28] to remediate OC-contaminated soil. The results indicated that incorporating Tween 80 with PS significantly promoted oxidation and removed 60–82% of the OCs within 10 days. Adding Tween 80 improved EK by 20–30% compared to the control treatment (without Tween 80).

Cyclodextrins are also commonly used when remediating organically contaminated soil by EK-ISCO. Ni et al. [42] investigated whether adding 1% β-cyclodextrin could increase the removal efficiency of the EK-Fenton remediation process. The results showed that β-cyclodextrin facilitated the solubility of OCs and increased the EK-Fenton oxidation efficiency.

However, cosolvents are organic compounds that can be oxidized by oxidants during the EK-ISCO process. Therefore, attention must be paid to the dosage and residual compounds produced by the cosolvents, particularly during in situ remediation.

20.4.5 Electrode Activation/Electrode Thermal Activation

The electrode reaction is an important process during EK remediation. It is the process whereby electrons are lost from the anode and gained at the cathode. Some researchers have investigated using iron electrode corrosion–enhanced EK-ISCO to remediate contaminated soil. Tsai et al. [29] found that EK enhanced oxidation with H_2O_2 combined with iron electrode corrosion (Fe_3O_4) resulted in a higher diesel removal efficiency (97%) compared to EK (55%) or Fenton oxidation (27%) alone. However, Fan et al. [25] reported that the iron anode corrosion treatment used in their study produced the lowest PCB removal efficiency (similar to the control treatment). They suggested that the low EOF inhibited the transportation of PS in soil. Therefore, the remediation effect of iron anode corrosion treatments needs to be carefully evaluated.

Electrode thermal activation is another potential PS activation method. Chowdhury et al. [38, 63] adopted a novel approach when they combined EK-ISCO with low electrical resistivity heating (ERH) to activate PS. The EK first delivered unactivated PS throughout the silt, and then the ERH generated and sustained the target temperature needed to activate the PS. The results showed that the method reduced the TCE concentration to below the detection limit in the silt within a few weeks.

During the EK-ISCO process, oxidants are continuously consumed due to contaminant degradation reactions and reduction of the cathode, which means

UNCORRECTED PROOFS

Trim Size: 170mm x 244mm Single Column Loose Ribeiro670117 c20.tex V1 - 12/11/2020 5:51pm Page 490

the oxidant dosage and cost of remediation increase. One way to potentially solve this problem is to maintain the generation of oxidants during EK-ISCO instead of adding oxidants. Farhat et al. [64] first proposed and verified the generation of sulfate radicals in sodium sulfate solution using a boro-doped diamond (BDD) electrode. However, the BDD electrode was very expensive and difficult to apply at a large scale. Therefore, Song et al. [30] introduced a new approach to remediate diesel-contaminated sand. They used an EK delivery anodic in situ generated active chlorine system with a normal Ti/RuO_2 anode. The results showed that the maximum diesel removal was 67.1% when a 20 g/l NaCl solution was added, and the DC potential was 2 V/cm. Furthermore, the remediation cost significantly decreased compared to the oxidant-addition treatment.

20.4.6 Nanomaterial-Enhanced Methods

Nanomaterials have been widely used in soil and groundwater remediation. At present, the most widely used nanomaterials are nano zero-valent iron (nZVI) and nano Fe_3O_4, both of which have large specific surface areas and high catalytic activities. They can be used to effectively catalyze the reduction of various organic halides, such as OCs, halogenated alkanes, and halogenated aromatic hydrocarbons. In addition, nZVI and nano Fe_3O_4 are good PS activating agents. The activating capacity of nano Fe_3O_4 is lower than that of nZVI, but it is more stable and easier to use [65].

Yang and Yeh [20] evaluated the effect of nano Fe_3O_4 on PS activation during the EK-ISCO remediation of TCE-contaminated clay soil. The results showed that nano Fe_3O_4 played a significant role in activating PS oxidation, and the coupled process could effectively destroy TCE in the soil and electrode compartments. Then Yang et al. [27] studied the mechanism underlying nano Fe_3O_4 enhancement and found that the injected nano Fe_3O_4 slurry in the anode reservoir was transported into the soil by EOF. This suggested that the Fe^{2+} and Fe^{3+} derived from nano Fe_3O_4 dissociation formed precipitates in the soil pores, which decreased the EOF rate. In a study by Suanon et al. [28], an nZVI reactive barrier was set up 5 cm from the anode to enhance the EK remediation of OC contaminated soil when PS and HP were used as oxidants. However, adding the nZVI reactive barrier did not significantly improve the OC remediation efficiency after seven days.

In general, applying nanomaterials to EK-ISCO remediation depends on the dispersion and migration of the nanomaterials. It seems that the easy aggregation and sedimentation of nanoparticles, due to their strong van der Waals forces and magnetic attraction, limited their delivery in soil and their oxidation activities.

20.5 Pilot/Field-Scale Studies of EK-ISCO Remediation Technologies

20.5.1 Experimental Design

20.5.1.1 Electrode Materials

The electrode materials used in EK remediation generally include graphite, iron, platinum, titanium, and alloys [41]. During the EK process, an electron

UNCORRECTED PROOFS

Trim Size: 170mm x 244mm Single Column Loose Ribeiro670117 c20.tex V1 - 12/11/2020 5:51pm Page 491

loss reaction occurs at the anode. Furthermore, the anode is always in an acidic environment because of the hydrolysis reaction. Therefore, the anode material must be corrosion-resistant or inexpensive to replace. In contrast, the cathode only needs to have good conductivity relative to the anode. Generally, the materials used to make electrodes should meet the following criteria: good conductivity, corrosion resistant, inexpensive, and easy to obtain. Contaminated site remediation is a large-scale operation. Therefore, the cost of the electrode materials needs to be seriously considered. In the EK-ISCO remediation process, the electrode should be processed into a porous, hollow structure because the electrolyte usually needs to be recycled. This means easy processing and installation of the electrode are also very important.

Graphite, iron, and titanium are usually selected as the electrode materials and have been used in many studies. Yang and Liu [19] reported the effects of electrode materials on the EK-Fenton remediation of TCE-contaminated soil and found that graphite electrodes were superior to stainless steel electrodes. After this report, many researchers began to use graphite for electrodes [20, 28, 42]. Titanium is also used for electrodes during the EK-ICO process because of its hardness, corrosion resistance, and electron conductivity [13, 25, 26, 66, 67].

Recently, a BDD electrode was used with EK oxidation to treat contaminated soil because it can produce sulfate radicals in Na_2SO_4 solution, which can effectively degrade organic pollutants [64]. However, the BDD electrode is expensive and difficult to use in large-scale practical applications. The binary metallic oxidation electrode, a type of reactive electrode, is another type of electrode that has been used in EK-chemical oxidation processes. Finally, Yuan et al. [68] reported a new electrode material, RuO_2/Ni foam, which was successfully used in the EK-oxidation remediation of ibuprofen (IBP)-contaminated soil.

20.5.1.2 Configuring Electrode Settings

In laboratory studies of EK remediation, a one-dimensional (1D) electrode configuration (equal number of anodes and cathodes) is often used to set a uniform electric field. This type of electric field is easy to set up, but the uniformity of the electric field depends on the spacing between the anodes or cathodes. When the spacing is large, there is a certain inactive (dead) electric field between electrodes with the same polarity [41], which affects the migration of pollutants and oxidants and thus EK-ISCO remediation efficiency. In addition, the anodes may be expensive because they are more resistant to corrosion.

In pilot and field experiments, the appropriate electrode configuration is directly related to remediation cost and pollutant removal efficiency. This is because contaminated sites are large and have diverse soil properties. Therefore, a two-dimensional (2D) electrode configuration (unequal number of anodes and cathodes) is often used in pilot and field experiments. In the 2D electrode configuration, a cathode or anode is placed in the center. It is then surrounded by an array of anodes or cathodes, and the positive/negative pollutants migrate from the surrounding pool to the center pool under the DC electric field. The electrode configuration can be divided into triangles, squares, hexagons, etc. (Figure 20.2). This electrode arrangement can effectively expand the DC electric field, but the electric field

UNCORRECTED PROOFS

Trim Size: 170mm x 244mm Single Column Loose Ribeiro670117 c20.tex V1 - 12/11/2020 5:51pm Page 492

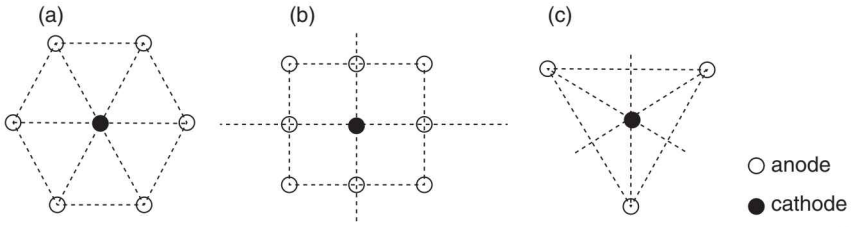

Figure 20.2 Examples of two-dimensional electrode configurations (a) Hexagonal; (b) square; (c) triangular. Source: Alshawabkeh, Yeung, and Bricka [41].

is non-uniform [41, 69]. Previous mathematical simulation research has shown that the hexagon configuration was the optimal electrode setup because it can maintain the stability of the system and the uniformity of pollutant removal [70]. Furthermore, the hexagon configuration can also be used to migrate heavy metals and saline compounds from the soil [71–73]. However, the effects of electrode configuration on EK-ISCO are unclear and need further research.

In these electrode configurations, the cathode and anode are usually fixed, which means part of the restored soil could still be subject to EK treatment; therefore, more time and power are required to remove pollutants from the soil. Shen et al. [74] used the approaching-anodes method (gradually reducing the distance between the anode and cathode) to increase the intensity of the electric field and improved the migration of pollutants to the cathode. In addition, the regular exchange of the anode and cathode or intermittent current is considered to improve remediation efficiencies [75].

20.5.1.3 Power Supply Modes

In general, constant voltage or constant current power modes are used during EK remediation. Under the constant voltage mode, the electric current changes along with the change in soil electrical conductivity. During EK remediation, the conductivity of the soil and the current will gradually decline because the soil conductive particles move to the anode and cathode [76]. Therefore, the available current does not exceed the maximum current of the DC power supply. Under the constant current mode, the voltage will increase with the gradual decline in soil conductivity during the EK remediation process [77]. Sometimes the voltage will exceed the maximum voltage of the DC power supply, which means a higher-voltage DC power supply is required. In general, the voltage gradient in EK remediation is 50–150 V/m, and the current density is 1–10 A/m^2 [41, 78]. The steady voltage mode is used in most studies on EK remediation, including laboratory, pilot, and field-scale experiments. However, the specific power supply mode and applied electric field intensity depend on the actual on-site situation.

In recent years, there have also been some reports [79–82] of new power supply methods, such as galvanic cells, solar energy, and wind energy. These methods make full use of natural energy and reduce power consumption, but their effects on the efficiency and stability of EK remediation require further study.

UNCORRECTED PROOFS

Trim Size: 170mm x 244mm Single Column Loose Ribeiro670117 c20.tex V1 - 12/11/2020 5:51pm Page 493

Table 20.3 Pilot and field-scale studies of EK-ISCO remediation of organically contaminated soil.

References	Soil	Volume (L × W × H) (m × m × m)	Pollutants	Voltage ($V\,m^{-1}$)	Current ($A\,m^{-2}$)	Duration	Removal (%)
[39, 85]	Sediment	0.98 × 0.98 × 0.5	HCB: 14.4–36.3 mg/kg	20–40	5–7	100 d	12%
[86]	Soil	0.7 × 0.5 × 0.5	Phenanthrene: 500 mg/kg	100	1.3–5.5	2800 h	25%
Ochoa et al. 2016 [87]	Soil	3.3 m^3	Gasoline: 1126 mg/kg	20	9	20 d (4.5 h/d)	80%
[88]	Soil	0.175 m^3, 16 m^3	2,4-D: 20 mg/kg	100	–	–	–

20.5.2 Pilot Cases

There have been some pilot and field studies of EK remediation of soil contaminated with heavy metals [72, 73, 78, 83, 84]). However, few studies have focused on EK-ISCO remediation of organically contaminated soil at the pilot and field scale (Table 20.3), and there have been no specific reports of field trials. Li et al. [85] were the first to conduct an EK-oxidation remediation test of actual HCB-contaminated sediment (14.4–36.3 mg/kg). The experiment consisted of a $0.98 \times 0.98 \times 0.54\,m^3$ experimental box with graphite and iron rods as the anode and cathode, respectively. After adding HPCD as a cosolvent, they found that the HPCD migrated from the anode to the cathode by electroosmotic flow, which caused the HCB to migrate out of the soil. Based on the mass balance calculations, approximately 12% of the HCB was degraded after EK remediation, which was probably due to the reduction in HCB dechlorination near the cathode.

Lopez-Vizcaino et al. [86] carried out a pilot EK remediation study that lasted 2800 hours. They used PHE-contaminated soil (500 mg/kg) with two rows of six electrodes. The size of the system was $0.7 \times 0.5 \times 0.5\,m^3$, and adding anionic surfactant dodecyl sulfate (10 g/l) increased the solubility and mobility of PHE. The results showed that the thermal effect of the electric field had a significant influence on phenanthrene removal and that phenanthrene migration from the soil was primarily due to electroosmotic flow. However, the phenanthrene removal rate was only 25%, whereas energy consumption reached 540 kWh/m^3.

Ochoa et al. [89] investigated the EK treatment of gasoline-polluted soil coupled to an advanced oxidation process that treated the associated wastewater. In this study, a pilot-level EK (3.3 m^3) test cell was used. It contained a circular arrangement of electrodes with a Ti cathode in the middle of the cell surrounded by six anodes. Hydrocarbons were directed toward the cathode by electroosmosis, and 80% of the hydrocarbons were removed. The wastewater was collected in a central compartment and subsequently treated with a Fenton-type advanced oxidation process.

UNCORRECTED PROOFS

Trim Size: 170mm x 244mm Single Column Loose Ribeiro670117 c20.tex V1 - 12/11/2020 5:51pm Page 494

The pilot studies mentioned showed that the pollutant removal efficiencies in most studies were lower than in bench studies. In the pilot studies, the enhanced methods tested in the bench studies were not applied, which may be one of the reasons for the low removal rates. In addition, the larger processing scale may have reduced removal efficiency [88].

20.6 Conclusions

The EK-ISCO method is a promising technology that could be applied to the in situ remediation of soils contaminated with organics. It has the potential to effectively enhance chemical oxidation remediation in low-permeability soils where alternative technologies may be ineffective or expensive. This review focused on the state of knowledge about EK-ISCO and discussed enhanced mechanisms that could be used in the EK-ISCO remediation process. It reviewed the following areas and made some important conclusions:

- The mechanisms underlying the EK-ISCO remediation process were discussed, including physical mechanisms (electromigration, electroosmosis, etc.) and chemical mechanisms (electrode reaction, desorption, dissolution, oxidation, degradation).
- The factors that influence EK-ISCO remediation (soil properties, oxidant dosage, and contamination status) were analyzed.
- Various enhanced methods that can be used to improve EK-ISCO remediation were discussed, and the most effective methods were identified. However, the methods chosen must be based on the specific soil and pollutant conditions.
- Some important practical aspects and design criteria (such as electrode materials, configuration, and power supply) for EK-ISCO were investigated.

The review outcomes suggested that future research on EK-ISCO technology should focus on the following areas:

- The reactions at the electrodes need to be investigated if organic pollutant degradation is to improve.
- It is important to investigate the effects of combined technology and enhanced methods on EK-ISCO remediation.
- More pilot/field-scale studies are needed.
- Good practice guidelines for EK-ISCO implementation could be developed to support future applications at the pilot/field scale.

Acknowledgments

This research was financially supported by the National Key R&D Program of China (Grant Nos. 2018YFC1802005) and the Natural Science Foundation of China (41471261).

UNCORRECTED PROOFS

Trim Size: 170mm x 244mm Single Column Loose Ribeiro670117 c20.tex V1 - 12/11/2020 5:51pm Page 495

References

AQ3

1 Zhao, C., Dong, Y., Feng, Y.P. et al. (2019). Thermal desorption for remediation of contaminated soil: a review. *Chemosphere* 221: 841–855.

2 Yang, K., Zhu, L., and Xing, B. (2006). Enhanced soil washing of phenanthrene by mixed solutions of TX100 and SDBS. *Environmental Science & Technology* 40: 4274–4280.

3 Dermont, G., Bergeron, M., Mercier, G., and Richer-Lafleche, M. (2008). Soil washing for metal removal: a review of physical/chemical technologies and field applications. *Journal of Hazardous Materials* 152: 1–31.

4 Ferrarese, E., Andreottola, G., and Oprer, I.A. (2008). Remediation of PAH-contaminated sediments by chemical oxidation. *Journal of Hazardous Materials* 152: 128–139.

5 Gryzenia, J., Cassidy, D., and Hampton, D. (2009). Production and accumulation of surfactants during the chemical oxidation of PAH in soil. *Chemosphere* 77: 540–545.

6 Gu, Y.W., Wang, B.B., He, F. et al. (2017). Mechanochemically Sulfidated microscale zero Valent iron: pathways, kinetics, mechanism, and efficiency of richloroethylene Dechlorination. *Environmental Science & Technology* 51: 12653–12662.

7 Juhasz, A.L. and Naidu, R. (2000). Bioremediation of high molecular weight polycyclic aromatic hydrocarbons: a review of the microbial degradation of benzo[a]pyrene. *International Biodeterioration and Biodegradation* 45: 57–88.

8 Bento, F.M., Camargo, F.A.O., Okeke, B.C., and Frankenberger, W.T. (2005). Comparative bioremediation of soils contaminated with diesel oil by natural attenuation, biostimulation and bioaugmentation. *Bioresource Technology* 96: 1049–1055.

9 Rastogi, A., Al-Abed, S.R., and Dionysiou, D.D. (2009). Sulfate radical-based ferrous–peroxymonosulfate oxidative system for PCBs degradation in aqueous and sediment systems. *Applied Catalysis B: Environmental* 85: 171–179.

10 Tsitonaki, A., Petri, B., Crimi, M. et al. (2010). In situ chemical oxidation of contaminated soil and groundwater using Persulfate: a review. *Critical Reviews in Environmental Science and Technology* 10: 55–91.

11 United States Environmental Protection Agency. (2017). Superfund Remedy Report, 15th ed. EPA-542-R-17-001. www.epa.gov/remedytech/superfund-remedy-report.

12 Yukselen-Aksoy, Y. and Reddy, K.R. (2012). Effect of soil composition on electrokinetically enhanced persulfate oxidation of polychlorobiphenyls. *Electrochimica Acta* 86: 164–169.

13 Fan, G.P., Cang, L., Fang, G.D., and Zhou, D.M. (2014a). Electrokinetic delivery of persulfate to remediate PCBs polluted soils: effect of injection spot. *Chemosphere* 117: 410–418.

14 Acar, Y.B. and Alshawabkeh, A.N. (1993). Principles of electrokinetic remediation. *Environmental Science & Technology* 27: 2638–2647.

UNCORRECTED PROOFS

Trim Size: 170mm x 244mm Single Column Loose Ribeiro670117 c20.tex V1 - 12/11/2020 5:51pm Page 496

15 Probstein, R.F. and Hicks, R.E. (1993). Removal of contaminants from soils by electric-fields. *Science* 260 (5107): 498–503.

16 Reddy, K.R., Park, W., Sin, B.C. et al. (2009). Synthesis of electrically conductive and superparamagnetic monodispersed iron oxide-conjugated polymer composite nanoparticles by in situ chemical oxidative polymerization. *Journal of Colloid and Interface Science* 335 (1): 34–39.

17 Yang, G.C.C. and Long, Y.W. (1999). Removal and degradation of phenol in a saturated flow by in-suit electrokinetic remediation and Fenton-like process. *Journal of Hazardous Materials* B69: 259–271.

18 Thepsithar, P. and Roberts, E.P.L. (2006). Removal of phenol from contaminated kaolin using Electrokinetically enhanced in situ chemical oxidation. *Environmental Science & Technology* 40: 6098–6103.

19 Yang, G.C.C. and Liu, C.Y. (2001). Remediation of TCE contaminated soils by in situ EK-Fenton process. *Journal of Hazardous Materials* B85: 317–331.

20 Yang, G.C.C. and Yeh, C.F. (2011). Enhanced nano-$Fe_3O_4/S_2O_8^{2-}$ oxidation of trichloroethylene in a clayed soil by electrokinetics. *Separation and Purification Technology* 79: 264–271.

21 Wu, M.Z., Reynolds, D.A., Fourie, A., and Thomas, D.G. (2013). Optimal field approaches for electrokinetic in situ oxidation remediation. *Ground Water Monitoring & Remediation* 33 (1): 62–74.

22 Oonnittan, A., Isosaari, P., and Sillanpaa, M. (2010). Oxidant availability in soil and its effect on HCB removal during electrokinetic Fenton process. *Separation and Purification Technology* 76: 146–150.

23 Reddy, K.R. and Chandhuri, K.S. (2009). Fenton-like oxidation of polycyclic aromatic hydrocarbons in soils using Electrokinetics. *Journal of Geotechnical and Geoenviromental Engineering* 135: 1429–1439.

24 Cang, L., Fan, G.P., Zhou, D.M., and Wang, Q.Y. (2013). Enhanced-electrokinetic remediation of copper-pyrene co-contaminated soil with different oxidants and pH control. *Chemosphere* 90: 2326–2331.

25 Fan, G.P., Cang, L., Gomes, H.I. et al. (2016). Electrokinetic delivery of persulfate to remediate PCBs polluted soils: effect of different activation methods. *Chemosphere* 144: 138–147.

26 Fan, G.P., Cang, L., Fang, G.D. et al. (2014b). Surfactant and oxidant enhanced electrokinetic remediation of a PCBs polluted soil. *Separation and Purification Technology* 123: 106–111.

27 Yang, G.C.C., Chiu, Y.H., and Wang, C.L. (2015). Integration of electrokinetic process and nano-$Fe_3O_4/S_2O_8^{2-}$ oxidation process for remediation of phthalate esters in river sediment. *Electrochimica Acta* 181: 217–227.

28 Suanon, F., Tang, L., Sheng, H. et al. (2020). TW80 and GLDA-enhanced oxidation under electrokinetic remediation for aged contaminated-soil: Does it worth? *Chemical Engineering Journal* 385: 123934.

29 Tsai, T.T., Sah, J., and Kao, C. (2010). Application of iron electrode corrosion enhanced electrokinetic-Fenton oxidation to remediation diesel contaminated soils: a laboratory feasibility study. *Journal of Hydrology* 380: 4–13.

UNCORRECTED PROOFS

Trim Size: 170mm x 244mm Single Column Loose Ribeiro670117 c20.tex V1 - 12/11/2020 5:51pm Page 497

30 Song, Y., Cang, L., Fang, G.D. et al. (2018). Electrokinetic delivery of anodic in situ generated active chlorine to remediate diesel-contaminated sand. *Chemical Engineering Journal* 337: 499–505.

31 Ranjan, R.S., Qian, Y., and Krishnapillai, M. (2006). Effects of electrokinetics and cationic surfactant cetltrimethylammonium bromide[CTAB] on the hydrocarbon removal and retention from contaminated soils. *Environmental Technology* 27: 767–776.

32 Park, J.Y., Lee, H.H., Kim, S.J. et al. (2007). Surfactant-enhanced electrokinetic removal of phenanthrene from kaolinite. *Journal of Hazardous Materials* 140: 230–236.

33 Reddy, K.R. and Ala, P.R. (2006). Electrokinetic remediation of contaminated dredged sediment. *Journal of ASTM International* 3 (6): 13344.

34 Yuan, S.H., Tian, M., and Lu, X.H. (2006). Electrokinetic movement of hexachlorobenzene in clayed soils enhanced by tween 80 and β-cyclodextrin. *Journal of Hazardous Materials* 137 (2): 1218–1225.

35 Wang, X.J. and Brusseau, M.L. (1993). Solubilization of some low-polarity organic-compounds by hydroxypropyl-beta-cyclodextrin. *Environmental Science & Technology* 27 (13): 2821–2825.

36 Karagunduz, A., Gezer, A., and Karasuloglu, G. (2007). Surfactant enhanced electrokinetic remediation of DDT from soils. *Science of the Total Environment* 385: 1–11.

37 Wan, J., Yuan, S.H., Chen, J. et al. (2009). Solubility-enhanced electrokinetic movement of hexachlorobenzene in sediments: a comparison of cosolvent and cyclodextrin. *Journal of Hazardous Materials* 166: 221–226.

38 Chowdhury, A.I.A., Gerhard, J.I., Reynolds, D. et al. (2017a). Electrokinetic-enhanced permanganate delivery and remediation of contaminated low permeability porous media. *Water Research* 113: 215–222.

39 Li, J., Fu, Q., Liao, Q. et al. (2009). Persulfate: a self-activated cathodic electron acceptor for microbial fuel cell. *Journal of Power Sources* 194: 269–274.

40 Xu, H.T., Song, Y., Cang, L. et al. (2020). Ion exchange membranes enhance the electrokinetic in situ chemical oxidation of PAH-contaminated soil. *Journal of Hazardous Materials* 382: 121042.

41 Alshawabkeh, A.N., Yeung, A.T., and Bricka, M.R. (1999a). Practical aspects of in-suit electrokinetic extraction. *Journal of Environmental Engineering* 125 (1): 27–35.

42 Ni, M., Tian, S., Huang, Q. et al. (2018). Electrokinetic-Fenton remediation of organochlorine pesticides from historically polluted soil. *Environmental Science and Pollution Research* 25: 12159–12168.

43 Bogan, B.W. and Trbovic, V. (2003). Effects of sequestration on PAH degradability with Fenton's reagent: roles of total organic carbon, humin, and soil porostity. *Journal of Hazardous Materials* 100 (1): 285–300.

44 Venny, Gan, S., and Ng, H.K. (2012). Current status and prospects of Fenton oxidation for the decontamination of persistent organic pollutants (POPs) in soils. *Chemical Engineering Journal* 213: 295–317.

UNCORRECTED PROOFS

Trim Size: 170mm x 244mm Single Column Loose Ribeiro670117 c20.tex V1 - 12/11/2020 5:51pm Page 498

45 Bocos, E., Fernandez-Costas, C., Pazos, M. et al. (2015). Removal of PAHs and pesticides from polluted soils by enhanced electrokinetic-Fenton treatment. *Chemosphere* 125: 168–174.

46 Sirguey, C., de Souza, S., Paula, T. et al. (2008). Impact of chemical oxidation on soil quality. *Chemosphere* 72 (2): 282–289.

47 Jonsson, S., Persson, Y., Frankki, S. et al. (2006). Comparison of Fenton reagent and ozone oxidation of polycyclic aromatic hydrocarbon in aged contaminated soils. *Journal of Soils and Sediments* 6 (4): 208–214.

48 Lindsey, M.E. and Tarr, M.A. (2000). Inhibited hydroxyl radical degradation of aromatic hydrocarbons in the presence of dissolved fulvic acid. *Waster Research* 34 (8): 2385–2389.

49 Kim, J.H., Han, S.J., Kim, S.S. et al. (2006). Effect of soil chemical properties on the remediation of phenanthrene-contaminated soil by electrokinetic-Fenton process. *Chemosphere* 63: 1667–1676.

50 Yap, C.L., Gan, S.G., and Ng, H.K. (2011). Fenton based remediation of polycyclic aromatic hydrocarbons-contaminated soils. *Chemosphere* 83: 1414–1430.

51 Alcantara, T., Pazos, M., Gouveia, S. et al. (2008). Remediation of phenanthrene from contaminated kaolinite by electroremediation-Fenton technology. *Journal of Environmental Science and Health Part A* 43: 901–906.

52 Wu, M.Z., Reynolds, D.A., Fourie, A. et al. (2012). Electrokinetic in situ oxidation remediation: assessment of parameter sensitivities and the influence of aquifer heterogeneity on remediation efficiency. *Journal of Contaminant Hydrology* 136-137: 72–85.

53 Kulick, N., Goi, A., Trapido, M. et al. (2006). Degradation of polycyclic aromatic hydrocarbons by combined chemical pre-oxidation and bioremediation in creosote contaminated soil. *Journal of Environmental Management* 78: 382–391.

54 Chung, N.H. and Alexander, M. (1998). Differences in sequestration and bioavailability of organic compounds aged in dissimilar soils. *Environmental Science & Technology* 32 (7): 855–860.

55 Haapea, P. and Tuhkanen, T. (2016). Integrated treatment of PAH contaminated soil by soil washing, ozonation and biological treatment. *Journal of Hazardous Materials* 136 (2): 244–250.

56 Lemaire, J., Laurent, F., Leyval, C. et al. (2013). PAH oxidation in aged and spiked soils investigated by column experiments. *Chemosphere* 91 (3): 406–414.

57 Kim, S.S., Kim, J.H., and Han, S.J. (2005a). Application of the electrokinetic-Fenton process for the remediation of kaolinite contaminated with phenanthrene. *Journal of Hazardous Materials* 118: 121–131.

58 Pazos, M., Teresa, A.M., Rosales, E. et al. (2011). Hybrid technologies for the remediation of diesel fuel polluted soil. *Chemical Engineering & Technology* 34 (12): 2077–2082.

59 Li, Z., Yu, J.W., and Neretnieks, I. (1998). Electroremediation: removal of heavy metals from soils by using Cation selective membrane. *Environmental Science & Technology* 32: 394–397.

UNCORRECTED PROOFS

Trim Size: 170mm x 244mm Single Column Loose Ribeiro670117 c20.tex V1 - 12/11/2020 5:51pm Page 499

60 Ottosen, L.M., Hansen, H.K., and Hansen, C.B. (2000). Water splitting at ion-exchange membranes and potential differences in soil during electrodialytic soil remediation. *Journal of Applied Electrochemistry* 30: 1199–1207.

61 Kim, W.S., Kim, S.O., and Kim, K.W. (2005b). Enhanced electrokinetic extraction of heavy metals from soils assisted by ion exchange membranes. *Journal of Hazardous Materials* 118: 93–102.

62 Abtahi, M., Jorfi, S., Mehrabi, N. et al. (2018). A novel combination of surfactant addition and Persulfate-assisted Electrokinetic oxidation for remediation of Pyrene-contaminated soil. *Chemical and Biochemical Engineering Quarterly* 32 (1): 55–70.

63 Chowdhury, A.I.A., Gerhard, J.I., Reynolds, D. et al. (2017b). Low permeability zone remediation via oxidant delivered by electrokinetics and activated by electrical resistance heating: proof of concept. *Environmental Science & Technology* 51 (22): 13295–13303.

64 Farhat, A., Keller, J., Tait, S. et al. (2015). Removal of persistent organic contaminants by electrochemically activated sulfate. *Environmental Science & Technology* 49 (24): 14326–14333.

65 Wang, J. and Wang, S. (2018). Activation of persulfate (PS) and peroxymonosulfate (PMS) and application for the degradation of emerging contaminants. *Chemical Engineering Journal* 334: 1502–1517.

66 Gomes, H.I., Fan, G.P., Mateus, E.P. et al. (2014). Assessment of combined electro–nanoremediation of molinate contaminated soil. *Science of the Total Environment* 493: 178–184.

67 Mendez, E., Perez, M., Romero, O. et al. (2012). Effects of electrode material on the efficiency of hydrocarbon removal by an electrokinetic remediation process. *Electrochimica Acta* 86: 148–156.

68 Yuan, C., Hung, C.H., and Huang, T.Y. (2018). Application of RuO2/Ni foam electrodes for remediation of ibuprofen in soil matrix—the effect of electrokinetic parameters. *Environmental Science and Pollution Research* 25: 5181–5190.

69 Virkutyte, J., Sillanpaa, M., and Latostenmaa, P. (2002). Electrokinetic soil remediation-critical overview. *The Science of the Total Environment* 289: 97–121.

70 Alshawabkeh, A.N., Gale, R.J., Ozsu-Acar, E. et al. (1999b). Optimization of 2-D electrode configuration for electrokinetic remediation. *Journal of Soil Contamination* 8 (6): 617–635.

71 Fan, X.Y., Wang, H., Luo, Q.S. et al. (2007). The use of 2D non-uniform electric field to enhance in situ bioremediation of 2,4-dichlorophenol-contaminated soil. *Journal of Hazardous Materials* 148: 29–37.

72 Kim, D.H., Jo, S.U., Choi, J.H. et al. (2012a). Hexagonal two dimensional electrokinetic systems for restoration of saline agricultural lands: a pilot study. *Chemical Engineering Journal* 198–199: 110–121.

73 Kim, Y.H., Kim, D.H., Jung, H.B. et al. (2012). Pilot scale ex-situ electrokinetic remediation of arsenic-contaminated soil. *Separation Science and Technology* 47: 2230–2234.

UNCORRECTED PROOFS

Trim Size: 170mm x 244mm Single Column Loose Ribeiro670117 c20.tex V1 - 12/11/2020 5:51pm Page 500

74 Shen, Z.M., Chen, X.J., Jia, J.P. et al. (2007). Comparison of electrokinetic soil remediation methods using one fixed anode and approaching anodes. *Environmental Pollution* 150 (2): 193–199.

75 Lopez-Vizcaino, R., Yustres, A., Saez, C. et al. (2017). Effect of polarity reversal on the enhanced electrokinetic remediation of 2,4-D-polluted soils: a numerical study. *Electrochimica Acta* 258: 414–422.

76 Zhou, D.M., Deng, C.F., and Cang, L. (2004). Electrokinetic remediation of a cu contaminated red soil by conditioning catholyte pH with different enhancing chemical reagents. *Chemosphere* 56: 265–273.

77 Yuan, H.S., Liu, Y.G., Li, X. et al. (2007). Analyzing flexibility of electroremediation techniques to Pb contaminated red soils. *Journal of University of South China (Science and Technology)* 21 (1): 82–85.

78 Zhou, D.M., Cang, L., Alshawabkeh, A.N. et al. (2006). Pilot-scale electrokinetic treatment of a Cu contaminated red soil. *Chemosphere* 63 (6): 964–971.

79 Yuan, S.H., Zheng, Z.H., Chen, J. et al. (2009a). Use of solar cell in electrokinetic remediation of cadmium-contaminated soil. *Journal of Hazardous Materials* 162: 1583–1587.

80 Yuan, S.H., Wu, C., Wan, J.Z. et al. (2009b). In situ removal of copper from sediments by a galvanic cell. *Journal of Environmental Management* 90: 421–427.

81 Souza, F.L., Saez, C., Llanos, J. et al. (2016a). Solar-powered electrokinetic remediation for the treatment of soil polluted with the herbicide 2,4-D. *Electrochimica Acta* 190: 371–377.

82 Souza, F.L., Llanos, J., Saez, C. et al. (2016b). Performance of wind-powered soil electroremediation process for the removal of 2,4-D from soil. *Journal of Environmental Management* 171: 128–132.

83 Acar, Y.B. and Alshawabkeh, A.N. (1996). Electrokinetic remediation I. pilot-scale tests with lead-spiked kaolinite. *Journal of Geotechnical Engineering* 122: 173–185.

84 Kim, S.O., Moon, S.H., Kim, K.W. et al. (2002). Pilot scale study on the ex situ electrokinetic removal of heavy metals from municipal wastewater sludges. *Water Research* 36: 4765–4774.

85 Li, T.P., Yuan, S.H., and Wan, J.Z. (2009). Pilot-scale electrokinetic movement of HCB and Zn in real contaminated sediments enhanced with hydroxypropyl-beta-cyclodextrin. *Chemosphere* 76: 1226–1232.

86 Lopez-Vizcaino, R., Alonso, J., and Canizares, P. (2014). Electroremediation of a natural soil polluted with phenanthrene in a pilot plant. *Journal of Hazardous Materials* 265: 142–150.

87 Ranc, B., Faure, P., Croze, V. et al. (2016). Selection of oxidant doses for in situ chemical oxidation of soils contaminated by polycyclic aromatic hydrocarbons (PAHs): a review. *Journal of Hazardous Materials* 312: 280–297.

88 Lopez-Vizcaino, R., Navarro, V., Leon, M.J. et al. (2016). Scale-up on electrokinetic remediation: engineering and technological parameters. *Journal of Hazadous Materials* 315: 135–143.

UNCORRECTED PROOFS

Trim Size: 170mm x 244mm Single Column Loose Ribeiro670117 c20.tex V1 - 12/11/2020 5:51pm Page 501

89 Ochoa, B., Ramos, L., Garibay, A. et al. (2016). Electrokinetic treatment of polluted soil at pilot level coupled to an advanced oxidation process of its wastewater. *Physics and Chemistry of the Earth* 91: 68–76.

90 Reddy, K.R. and Madhusudhana, R.K. (2008). Effect of oxidant dosage on integrated electrochemical remediation of contaminant mixtures in soils. *Journal of Environmental Science and Health Part A* 43: 881–893.

91 Julien, L., Michel, B., Tanina, K. et al. (2013). Oxidant selection to treat an aged PAH contaminated soil by in situ chemical oxidation. *Journal of Environmental Chemical Engineering* 1: 1261–1268.

UNCORRECTED PROOFS

UNCORRECTED PROOFS

Trim Size: 170mm x 244mm Single Column Loose Ribeiro670117 c21.tex V1 - 12/11/2020 8:30pm Page 503

21

Electrokinetic and Electrochemical Removal of Chlorinated Ethenes: Application in Low- and High-Permeability Saturated Soils

Bente H. Hyldegaard and Lisbeth M. Ottosen

Department of Civil Engineering, Technical University of Denmark, 2800 Lyngby, Denmark

21.1 Introduction

To engineer remediation efforts, e.g. the use of electric currents for environmental security and sustainability, it is essential to sufficiently understand the contaminant of concern and the environmental settings. Only then robust remedies can be designed, which can cope with the complexity and diversity of contaminated sites.

In this chapter, the focus is on in situ remediation using electric currents to remove hazardous chlorinated ethenes, which are detected in soils of both low and high permeability. Soils with low and high permeability differ in characteristics, challenges, and thereby requirements for remediation. Using electric currents may overcome some of the challenges currently faced during the removal of chlorinated ethenes in both low- and high-permeability soils. However, even when applying electric currents, the relevant processes differ in these zones with different permeabilities. In low-permeability soils, electrokinetics offer advantages due to improved transport and thereby deliver amendments for subsequent degradation of chlorinated ethenes. In high-permeability soils, electrochemically generated reactants can transform chlorinated ethenes directly. The concepts of applied electrokinetics and electrochemistry for remediating chlorinated ethenes in low- and high-permeability soils are presented along with the related degradation pathways, the current state of development, and suggestions to focus areas of future work.

21.1.1 Chlorinated Ethenes

Chlorinated ethenes, commonly known as chlorinated solvents, are organic compounds with two carbon atoms and one or more chloride ions bound to the carbon atom(s). Most common are tetrachloroethylene (PCE) and trichloroethylene (TCE), which are used in e.g. dry-cleaning and for metal degreasing [1]. These chemicals were consumed in large quantities in the US and Europe in the 1960s and 1970s, but their use decreased in the 1980s due to awareness of their hazardous side effects [1, 2]. Nevertheless, the global market for chlorinated ethenes is increasing primarily due to a growing market in Asia [2].

Electrokinetic Remediation for Environmental Security and Sustainability, First Edition.
Edited by Alexandra B. Ribeiro and M.N.V. Prasad.
© 2021 John Wiley & Sons Ltd. Published 2021 by John Wiley & Sons Ltd.

UNCORRECTED PROOFS

Trim Size: 170mm x 244mm Single Column Loose Ribeiro670117 c21.tex V1 - 12/11/2020 8:30pm Page 504

Due to leakage in infrastructure or improper handling, chlorinated ethenes have been introduced into the environment. Because chlorinated ethenes are denser than water and have low sorption, high relative solubility, and high volatilization [1], they can distribute into low-permeability soils, high-permeability soils, soil vapor, and indoor air (Figure 21.1). Due to this complex spreading pattern, the source zone(s)

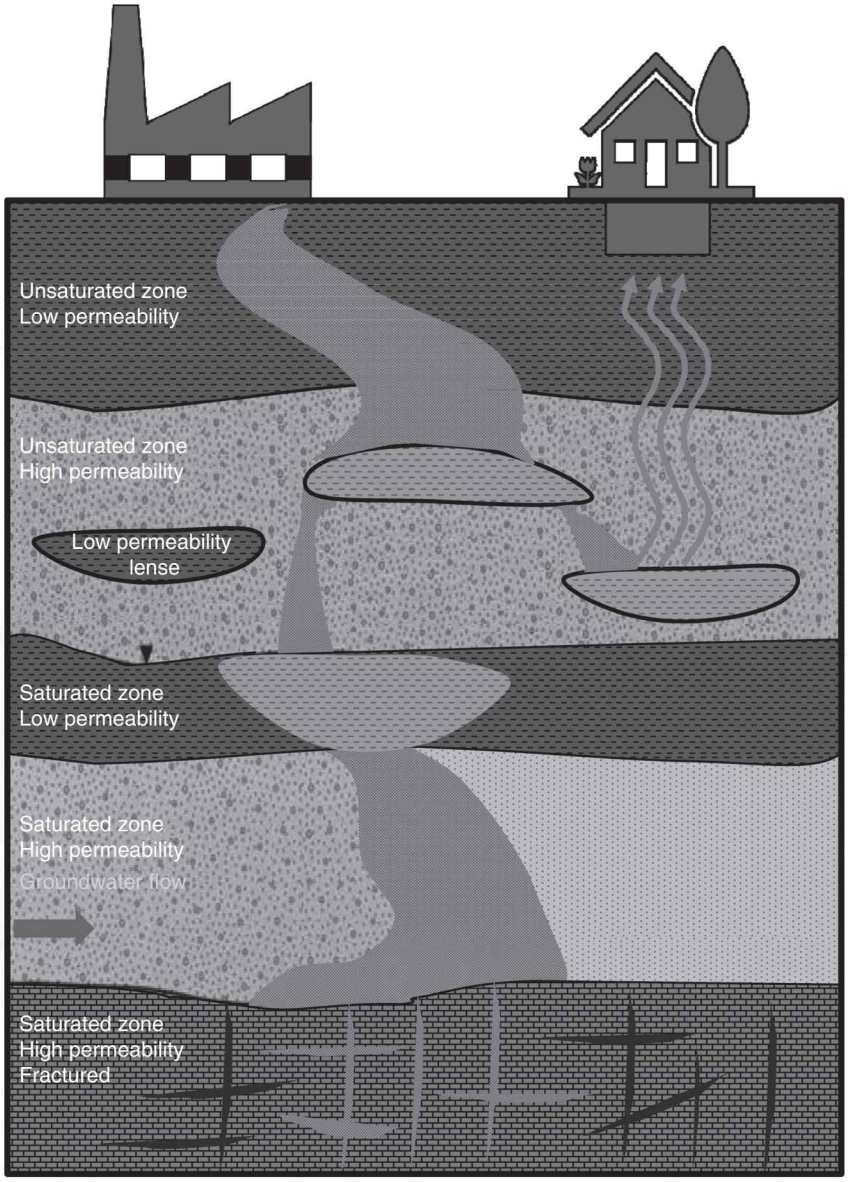

Figure 21.1 Conceptual illustration of the fate of harmful chlorinated ethenes once they enter the environment. Contamination of indoor air, low- and high-permeability soils, and groundwater may occur.

UNCORRECTED PROOFS

Trim Size: 170mm x 244mm Single Column Loose Ribeiro670117 c21.tex V1 - 12/11/2020 8:30pm Page 505

can be difficult to identify and hence constitute a long-term source of continuous release of chlorinated ethenes into e.g. indoor air and groundwater [3, 4]. Therefore, means to remediate low- and high-permeability soils are necessary to protect residential areas, drinking water, and the environment.

Several degradation pathways exist for chlorinated ethenes, including abiotic reduction, abiotic oxidation, and biotic reduction (Figure 21.2). Abiotically,

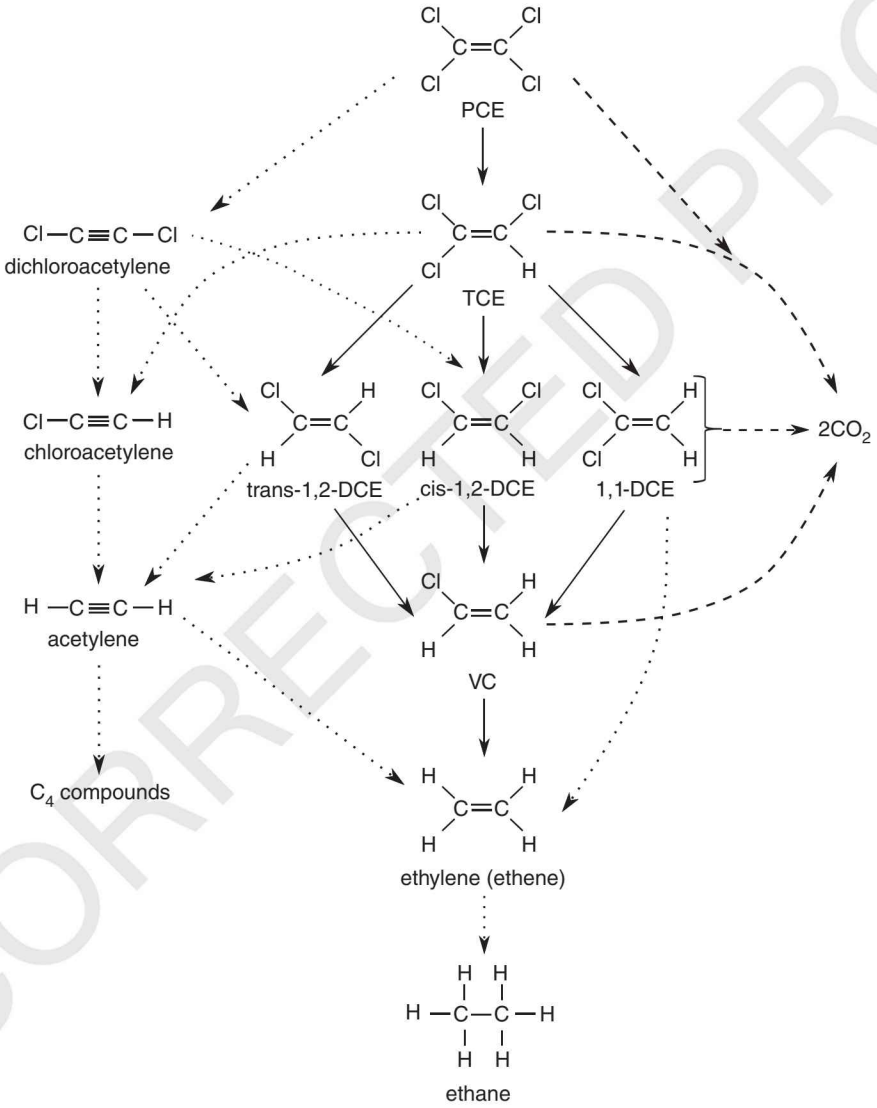

Figure 21.2 Common degradation pathways for tetrachloroethylene (PCE), trichloroethylene (TCE), dichloroethylenes (DCEs), and vinyl chloride (VC): abiotic reduction (dotted arrows), biotic reduction (solid arrows), and abiotic oxidation (dashed arrows). Source: Ottosen et al. [5].

UNCORRECTED PROOFS

Trim Size: 170mm x 244mm Single Column Loose Ribeiro670117 c21.tex V1 - 12/11/2020 8:30pm Page 506

chlorinated ethenes can be reduced to ethene and ethane (Figure 21.2, dotted arrows) [6]. The abiotic oxidation can completely mineralize chlorinated ethenes to water and carbon dioxide (Figure 21.2, dashed arrows) [7, 8]. And biologically, under specific conditions, PCE and TCE can be sequentially degraded to cis-1,2-dichloroethylene (cis-DCE), trans-1,2-dichloroethylene (trans-DCE), 1,1-dichloroethylene (1,1-DCE), vinyl chloride (VC), and ultimately ethylene and ethane (Figure 21.2, solid arrows). This sequential biodegradation requires strict anaerobic conditions, the presence of an electron donor, and specific microbial cultures containing the *vcrA* gene, e.g. *Dehalococcoides* [9–12]. However, one or more of these requirements are often lacking, resulting in the accumulation of cis-DCE and/or VC in the environment [13–15]. Both the parent components (PCE and TCE) and the degradation intermediates (DCEs and VC) are hazardous contaminants, and the degradation intermediates pose the greatest health risks [16]. The harmful health effects include carcinogenicity, reproductive toxicity, and organ toxicity [16–18]. Consequently, the regulatory maximum contaminant levels (MCL) for chlorinated ethenes are low. For example, in the US, the MCLs in drinking water for PCE and TCE are $5\,\mu g\,l^{-1}$, $7\,\mu g\,l^{-1}$ for 1,1-DCE, $70\,\mu g\,l^{-1}$ for cis-DCE, $100\,\mu g\,l^{-1}$ for trans-DCE, and $2\,\mu g\,l^{-1}$ for VC [19]; and in Denmark, the MCLs for PCE, TCE, and DCEs are $1\,\mu g\,l^{-1}$, and $0.2\,\mu g\,l^{-1}$ for VC [20].

Contamination with chlorinated ethenes is a widespread environmental problem. Mapping of the extent of contamination is lacking on a global scale [21]. In the US, chlorinated ethenes are among the most frequently detected contaminants and have been detected in 17% of >5000 sampled groundwater wells throughout the country and at 50% of the >3200 contaminated sites under the Department of Defense [21–23]. In residential areas and in regions using groundwater as drinking water, chlorinated ethene contaminations are of the greatest concern when considering human health. Groundwater accounts for approximately 99% of liquid freshwater on Earth. On a global basis, approximately 70% of extracted groundwater is used for irrigation, approximately 21% for domestic water supplies, and approximately 9% in industry, and the extracted volume is increasing [21, 24]. The groundwater resource is currently used to supply drinking water to approximately 50% of the world's population [24]. Several cities and countries rely entirely on groundwater for the supply of drinking water [21]. Thus, remediating sites contaminated with chlorinated ethenes is inescapable, and it is a comprehensive task. Different strategies are used to target chlorinated ethenes in soil and groundwater, depending on e.g. the permeability of the soil. General characteristics of low- and high-permeability soils and the related challenges are outlined in Sections 21.1.2 and 21.1.3, respectively.

21.1.2 Low-Permeability Saturated Soils

Soils with low permeability can be relatively homogenous layers of various sizes and thicknesses or heterogeneous soils with e.g. tight clay lenses (Figure 21.1). Low-permeability geologies include clay and peat with porosities of 0.3–0.9 [25]. The composition of low-permeability soils is beyond the scope of this chapter, but specifically for clay minerals, it is essential to point out that the surfaces are

UNCORRECTED PROOFS

Trim Size: 170mm x 244mm Single Column Loose Ribeiro670117 c21.tex V1 - 12/11/2020 8:30pm Page 507

often negatively charged [26], which enables an additional transport mechanism in applied electric fields as discussed in Section 21.2. These soils are usually well sorted with small grain sizes [27]. Consequently, low hydraulic conductivities of $<10^{-7}$ m s^{-1} are common [27]. Thus, contaminants will slowly diffuse into and, in particular, out of these soils, so low-permeability soils can constitute a source of long-term contamination [28, 29].

Today, common strategies for remediating low-permeability soils include enhanced reductive dechlorination (ERD), in situ chemical oxidation (ISCO), and in situ chemical reduction (ISCR), including permeable reactive barriers (PRBs). Common among these remedies is that their performance depends on contact between amendments and contaminants. Hence, sufficient distribution of amendments, whether microbial cultures, electron donors, or chemical reactants, is essential. However, in low-permeability and/or tight geologies, sufficient delivery is the key challenge [8, 30]. Therefore, several optimized delivery strategies have been tested, e.g. hydraulic and pneumatic fracturing, for better fracture connectivity in the geological matrix. Despite using a dense network of boreholes to install fracturing tools, such techniques introduce preferential pathways for amendments rather than a uniform distribution through the geological matrix. Instead, applying electrokinetics is suggested for enhanced delivery of the amendments in low-permeability saturated soils and thereby forms the basis of improved remedial performance, as described in Section 21.2.

21.1.3 High-Permeability Saturated Soils

Soils with high permeability may consist of homogeneous and heterogeneous layers, as illustrated in Figure 21.1. Typical geologies with high permeabilities are gravel, sand, and limestone, and the porosities are in the range of 0.15–0.35 [25, 31, 32]. The composition of high-permeability soils is not discussed here, but two characteristics are important in the context of applying electric currents (Section 21.3): (i) the surfaces of soil particles in high-permeability geologies are usually not charged [5, 32, 33], and (ii) the content of carbonate-containing minerals can be high, and they can buffer acidic fronts established near anodes [32, 34, 35]. These soils are often poorly sorted and have larger grain sizes than low-permeability soils [27]. High-permeability bedrock may also be fractured [31]. Therefore, the hydraulic conductivities are high, $>10^{-4}$ m s^{-1} [25, 27]. Consequently, chlorinated ethenes can be extensively distributed in these soils.

To manage plumes of chlorinated ethenes in high-permeability soils, commonly applied remediation methods include pump-and-treat (P&T) [36, 37], ERD [1, 37], ISCO [7, 8], and ISCR including PRB [6, 38]. In high-permeability soils, the performance of ERD, ISCO, and PRB also relies on sufficient delivery of amendments, which can be challenging [8, 39]. In addition, short reactant lifetimes and/or consumption of reactants by naturally present substances are observed [8, 40, 41]. For P&T, chlorinated ethenes adsorb onto e.g. activated carbon, which has a limited efficiency toward chlorinated degradation intermediates [42, 43]. Also, sorption is a nondestructive method that generates a secondary waste stream, which needs

UNCORRECTED PROOFS

Trim Size: 170mm x 244mm Single Column Loose Ribeiro670117 c21.tex V1 - 12/11/2020 8:30pm Page 508

to be handled offsite [42]. Therefore, optimizing current remediation strategies or developing alternatives is required. It is suggested that the challenges sometimes faced by current remediation strategies in high-permeability saturated soils may be overcome by applying electrochemistry, as described in Section 21.3.

21.2 Electrokinetically Enhanced Remediation in Low-Permeability Saturated Soils

Electrokinetics is the most studied and mature aspect of applying an electric field to manage chlorinated ethenes and other contaminants. Hence, the principles have been described thoroughly [44–48]. Whether the strategy is to remove contaminants or deliver amendments, the concept is to move charged species through porous matrices of low permeability via conduction toward the electrode(s) of opposite polarity or neutral species by advection in mobilized porewater. The transport processes for species in the electric field in low-permeability saturated matrices include electromigration (EM) of charged species, electrophoresis (EP) of charged particles, and electroosmotic flow (EOF) of porewater due to the charged surface of e.g. clay minerals (Section 21.1.2), and thereby advection of the species toward the cathode. The electric transport gradients may prompt velocities that are up to 1000 times faster than by natural hydraulic gradients [45].

The primary advantage of electrokinetic methods, from the perspective of chlorinated ethene contamination, is related to enhanced delivery of amendments and not actual contaminant degradation induced by electrokinetics. With the often challenging delivery of amendments in present remediation efforts, as discussed in Section 21.1.2, electrokinetics complement the other remediation techniques. Consequently, electrokinetics can be combined with established methods for electrokinetic enhancement of e.g. bioremediation (EK-BIO, Section 21.2.1), ISCO (EK-ISCO, Section 21.2.2), and PRBs (EK-PRB, Section 21.2.3). The resulting transport rates with EM, EP, and advection in the EOF are calculated and presented in the following sections based on published studies. However, there is no standardized way of reporting the relevant experimental data, so orders of magnitudes rather than specific figures should be considered.

21.2.1 Electrokinetically Enhanced Bioremediation (EK-BIO)

The concept of EK-BIO covers both EK-bioaugmentation and EK-biostimulation [46]. In EK-bioaugmentation, an electric field is used for the optimized delivery of specific microbial cultures into a contaminated zone. In EK-biostimulation, electrokinetics is used for enhanced delivery of electron donors, e.g. lactate, to feed the naturally present microbial community. Bioaugmentation and biostimulation are often combined to reduce both the risk of accumulating degradation intermediates (Figure 21.2, solid arrows) and the remediation time frame. One concern related to the applied current density during EK-BIO is that it may inhibit microbial cultures [49]. However, no studies have reported such inhibition of chlorinated ethene degrading microorganisms in the current intensity range applied for remediation.

UNCORRECTED PROOFS

Trim Size: 170mm x 244mm Single Column Loose Ribeiro670117 c21.tex V1 - 12/11/2020 8:30pm Page 509

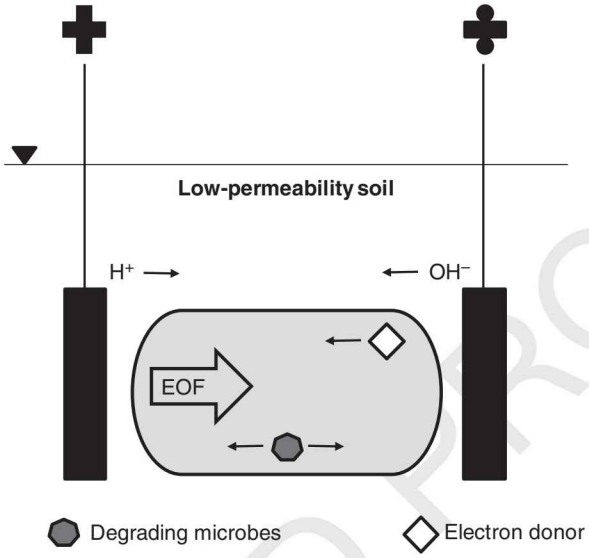

Figure 21.3 Simplified illustration of the EK-BIO concept for enhanced delivery of degrading microbial cultures and an electron donor into the contaminated zone (light gray oval) by electromigration, electrophoresis, or advection in the electroosmotic flow (EOF). The established transport velocities of these EK mechanisms are site- and system-specific.

Also, resulting changes in soil pH and redox conditions may influence microbial cultures, but this can be overcome by managing such side effects [50, 51]. For EK-BIO, microbial cultures can be delivered by electrokinetics via EP and advection in the EOF, while delivering electron donors is primarily by EM, as described in the following. A simplified illustration of the EK-BIO concept is presented in Figure 21.3.

21.2.1.1 EK-Induced Delivery of Microbial Cultures and Electron Donors

Delivering microbial cultures by EP is governed by the cell surface characteristics of the microbes, properties of the porous matrix, and pH of the porewater [52–54]. The cell surface charge of microbes is often weak negative at neutral pH with a specific strength of each culture [55]. Hence, EP transport velocities vary but are usually directed toward the anode. The influence of porous matrices is related to the sizes of the pore spaces versus the size of the microbes and possible adsorption of microbes onto the soil particles. Sizes of relevant microbial cultures in the range of 0.62 to 2 μm have been reported [55–58], while the pore spaces in soils differ greatly. For example, in bryozoan limestone, a pore size of 0.06–1.56 μm for 95% of the pores has been reported [32]. In clay, pore sizes of 0.5–30 μm are measured [59, 60]. In a sandy loam, pore sizes >500 μm are documented [61]. Thus, in some soils, the sizes of the pore spaces and microbes are in the same range, so electrokinetic delivery of the microbes into the smallest pores may be restricted. This can be overcome by the abilities of the microbial cultures since microbes have been shown to grow and divide into pore spaces smaller than the size of the microbial cells [62]. Last, acidic porewater pH may hinder EP, as observed in a study by DeFlaun and Condee [54]. The effect of pH on the EP of microbes may be due to changes in the strength of their surface charge; at low pH, a net neutralization or even positive polarization of the cell surfaces is possible [54]. Despite these influential factors on EP transport,

UNCORRECTED PROOFS

Trim Size: 170mm x 244mm Single Column Loose Ribeiro670117 c21.tex V1 - 12/11/2020 8:30pm Page 510

delivery of microbial cultures by EP has been demonstrated in sandy sediment [54], sandy/silty loam [54], clay [52, 63], and limestone [32]. The greatest EP velocities have been reported for sand (7.2–14.4 $cm^2\ V^{-1}d^{-1}$), while they are in the range of 2.4 to 3.6 $cm^2\ V^{-1}d^{-1}$ in silty loam [54] and 5.8 $cm^2\ V^{-1}d^{-1}$ in clay [52]. EP rates that are lower in silty and clayey soils than in sand could indicate EOF in the opposite direction.

Transport of microbial cultures via advection in the EOF is directed toward the cathode, i.e. in the opposite direction than EP. Thus, EOF can counteract the magnitude of EP transport. The magnitude of advection in the EOF is influenced by the soil properties and porewater chemistry. Important soil properties include pore spaces and zeta potential. The higher the relative surface charge of the soil, i.e. the smaller the pore spaces, the more significant the advective transport in the EOF [64]. Thus, at contaminated sites, EOF transport is most significant in clayey soils, while it may be non-existent in limestone and sandy soils [32, 64]. The charge of the soil particles is also influenced by the pH of the porewater [65]. In addition, the EOF is more pronounced when the ionic strength of the bulk porewater is low [5]. In terms of practical considerations, this implies that at sites with a high contaminant concentration, the EOF may be insignificant [66]. Since the ionic strength of the soil porewater changes over time during the application of electrokinetics, as the pH fronts and/or supplied amendment fronts are migrating into the soil, the EOF is subject to nonlinear and transient changes [5]. Nevertheless, transport of microbial cultures by advection in the EOF has been observed. In clayey soils, transport rates in the EOF for *Sphingomonas* of 0–3.8 $cm^2\ V^{-1}d^{-1}$ [52], *M. frederiksbergense* of 3.4–6.7 $cm^2\ V^{-1}d^{-1}$ [52], and specific chlorinated ethene–degrading microbes *Dehalococcoides* of 0.4 $cm^2\ V^{-1}d^{-1}$ [5, 63] have been observed. However, the transport rates of advection in the EOF and EP are system-specific, so the dominating transport mechanism varies from site to site [5]. Therefore, depending on the resulting transport rates in the EOF and by EP, which are in opposite directions, the net electrokinetically induced delivery of microbes can be directed toward both the anode and the cathode. Since the transport directions influence the design of the EK-BIO, these are important aspects to consider and investigate.

Lactate has proven to be an efficient electron donor for stimulating biodegradation and hence is often supplied together with microbial cultures. Lactate is negatively charged, so it can be transported by EM toward the anode [32, 63, 67]. Transport by EM is influenced by the properties of the ion and the soil system. For example, adsorption and high natural oxygen demand impact the mobility and availability of the electron donor, respectively [67]. EM of lactate in various soil types has been reported. In three clayey soils, transport rates of lactate by EM of 3.2–4 $cm^2\ V^{-1}d^{-1}$ have been observed [5, 63, 67, 68]. In sandy sediment, a rate of 8.9 $cm^2\ V^{-1}d^{-1}$ is seen [5, 67]. The lower EM rate in the clayey soils compared to sandy soil could be due to counteracting EOF in clayey soils.

21.2.1.2 Current State of Development from an Applied Perspective

The EK-BIO strategy has primarily been studied under controlled and simplified conditions in the lab, where it has demonstrated promising results. However, field

UNCORRECTED PROOFS

Trim Size: 170mm x 244mm Single Column Loose
Ribeiro670117 c21.tex V1 - 12/11/2020 8:30pm Page 511

implementations appear to be limited. To date, based on conference contributions, company web pages, and literature, pilot demonstration of EK-BIO have been carried out at sites in the Netherlands, US, Canada, and Denmark, and the first full-scale remediation has been completed at a site in Denmark. Of these field applications, only two of the pilot demonstrations have been published.

The pilot demonstration in the Netherlands aimed at enhancing the distribution of nutrients for bioremediation of a source zone containing PCE, TCE, cis-DCE, and VC in a fine-grained soil with a seepage velocity of 3 m yr^{-1} [69]. Three cathodes and two anodes were installed in a row, spaced 5 m apart, perpendicular to the groundwater flow direction. A total of 24 infiltration wells were installed 2 m upgradient from the electrodes to supply the nutrients nitrogen and phosphorus along with an electron donor. An increase in the concentration of these amendments was observed. This resulted in a decrease in the concentration of PCE and TCE and an increase in cis-DCE and VC. Over time, the concentration of degradation intermediates also decreased. This pilot demonstration was operated for three years, and the energy input was coupled with solar panels [69].

The pilot demonstration in the US was installed in a clayey soil in the source zone of a PCE contamination [70]. The treatment area was approximately 12×12 m at a depth of 5–7 m. A total of nine electrode wells and eight injection wells were used to distribute lactate and the microbial culture KB-1®. To manage pH developments, potassium carbonate was added. The pilot demonstration was operated for five months following a six-month incubation periods before a second stage of five months was applied. With this strategy, >60% degradation of PCE was achieved in both the soil and groundwater. An accumulation of VC and non-chlorinated end products was observed in sampled groundwater but not in soil. Growth of the distributed *Dehalococcoides* by >10% was measured [70]. Furthermore, a modeling study of EK-BIO has been performed to assist in understanding mobilization, degradation, and design [71].

To improve understanding of the resulting transport and degradation mechanisms and rates, and thereby the applicability of EK-BIO, the focus needs to be on performance in realistic environmental settings [33, 72], and subsequent publication of findings is important to collectively be able to mature and model the technology. Relevant site characteristics to address, and their influence on EK-BIO, include geological heterogeneities, water content, and groundwater flow gradients. Also, the extent of the oxidizing zone generated around the anode must be assessed, in that strict anaerobic conditions are a prerequisite for biodegradation by *Dehalococcoides* [5].

21.2.2 Electrokinetically Enhanced In Situ Chemical Oxidation (EK-ISCO)

The purpose of EK-ISCO is to enhance delivery of chemical oxidants by EK transport mechanisms into a contaminated zone. For complete oxidation of chlorinated ethenes (Figure 21.2, dashed arrows), permanganate (MnO_4^-) and persulfate (SO_2^{5-}, $S_2O_8^{2-}$) are commonly used ISCO reactants [73]. If these reactants are successfully delivered, ISCO is a promising technology. Delivering these chemical

UNCORRECTED PROOFS

Trim Size: 170mm x 244mm Single Column Loose Ribeiro670117 c21.tex V1 - 12/11/2020 8:30pm Page 512

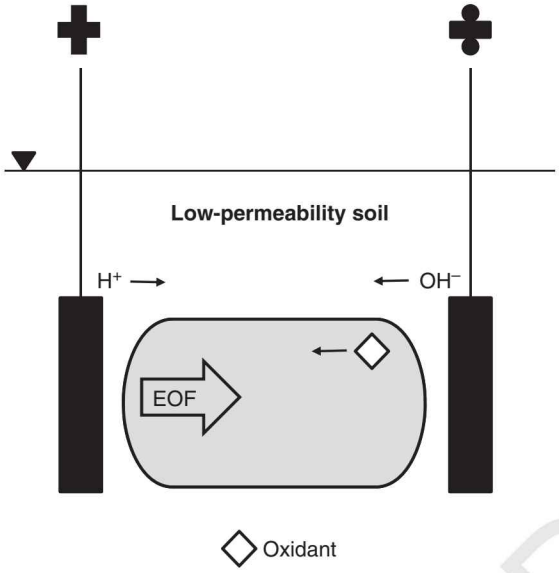

Figure 21.4 Simplified illustration of the EK-ISCO concept for enhanced delivery of oxidants into the contaminated zone (light gray oval) by electromigration or advection in the electroosmotic flow (EOF). The established transport velocities of these EK mechanisms are site- and system-specific.

oxidants can be by EM toward the anode, which may be counteracted by advection in an EOF toward the cathode. Specifically, for EK-ISCO, it is important to manage the reducing zone of the cathode. Otherwise, the amount of oxidant spent on competing reactions instead of contaminant degradation will increase, requiring a continuous additional supply of the oxidant, or remediation efficiency will decrease [5]. A simplified illustration of the EK-ISCO concept is presented in Figure 21.4.

21.2.2.1 EK-Induced Delivery of Oxidants

The advantages offered by permanganate are related to its high oxidation potential, stability, reactivity at a pH of 3.5–12, and lack of a need for subsequent activation [74]. When combined with EK, pH in the vicinity of the anode may become <3.5. If so, permanganate is no longer an active oxidant because it is reduced to Mn^{2+} [75]. Thus, managing pH fronts generated at the electrodes is essential during EK-ISCO. Otherwise, EM from the cathode toward the anode has shown to be limited [75]. In kaolinite, an EM transport rate of 2.3 $cm^2\ V^{-1}d^{-1}$ has been observed, but the distribution was uneven [76].

The EM transport of permanganate into low-permeability lenses has been studied visually, which is possible due to the pink color of permanganate. Such studies demonstrate enhanced distribution of permanganate into low-permeability lenses when electric fields are applied [74, 77]. This observed EK-enhanced delivery of oxidants into low-permeability lenses is promising for overcoming the challenges related to slow back-diffusion from tight matrices [74], which otherwise constitute a long-term source of groundwater and indoor air contaminations.

The advantages of using persulfate to oxidize contaminants are related to its high aqueous solubility, stability, and reduced cost [78]. However, persulfate needs to be activated. Depending on site characteristics, e.g. hydrogeology [79], persulfate can

UNCORRECTED PROOFS

Trim Size: 170mm x 244mm Single Column Loose Ribeiro670117 c21.tex V1 - 12/11/2020 8:30pm Page 513

be activated by high pH, heat, UV, or mineral-containing activators [78]. Thus, in contrast to using permanganate, persulfate must be distributed and subsequently activated to initiate the remediation. Due to persulfate's negative charge, it can EM toward the anode. In non-contaminated sand, an EM transport rate of 12 $cm^2\ V^{-1}d^{-1}$ is reported, which was found to be linearly correlated to voltages of 1–4 $V\ cm^{-1}$ [64]. In non-contaminated silt, an increased EM transport rate of 19.8 $cm^2\ V^{-1}d^{-1}$ is seen, explained by higher electrical conductivities in silt than sand [64]. In contaminated silt, with the addition of phosphate buffer at the electrodes, EM transport rates of $3.1 \pm 1.1\ cm^2\ V^{-1}d^{-1}$ are observed, with resulting persulfate concentrations near the anode of $9\ g\,l^{-1}$ and complete degradation of PCE [80]. Without managing pH, transport of persulfate by advection in the EOF in a field-sampled soil has exceeded the EM transport, but breakthrough into the catholyte was lacking [81]. The advective transport of persulfate in the EOF was sensitive to the activation strategy, with the highest transport rates observed during high pH activation, while the lowest transport rates were seen when using an iron electrode to activate the persulfate [81].

With these reported transports of persulfate by both EM and EOF, a strategy could be the supply of persulfate at both electrodes. This has been studied and resulted in a non-uniform distribution of the persulfate in the soil [81]. Since persulfate needs to be activated, and the activation strategy influences the EK-enhanced delivery of the persulfate, the use of persulfate as an oxidant in EK-ISCO adds complexity to the method. In addition, the essential pH buffering at the electrodes is challenging when using persulfate because the relevant oxidative radicals formed tend to react with anions of the buffering system instead of with the contaminants and thereby impact remediation efficiency [82].

21.2.2.2 Current State of Development from an Applied Perspective

EK-ISCO has shown encouraging results in terms of improved remediation of chlorinated ethenes in low-permeability soils in laboratory setups. However, there are few studies; and based on the literature, no field implementations have been carried out. One pilot study of EK-ISCO using persulfate and thermal activation (EK-TAP) has been carried out in Denmark but has not been published. Another study of EK-TAP is currently ongoing in the US (ESTCP project ER-201626). As more data become available on this technology, modeling of the system may provide relevant information at a lower cost and in a shorter time frame than field-testing. One modeling study of EK-ISCO targeting chlorinated ethenes has been performed to assess the influence of various design options [83].

Future work should focus on EM transport velocities of the oxidants and achieve an even distribution of these to improve the conditions for subsequent contaminant degradation [76]. To design a robust remediation technology, the influence of soil type and other relevant field parameters on the EM must also be investigated [5]. Specific for EK-ISCO using persulfate, identification of a pH buffer having a low consumption of formed oxidative radicals, and thereby a low impact on contaminant degradation, is important.

UNCORRECTED PROOFS

Trim Size: 170mm x 244mm Single Column Loose Ribeiro670117 c21.tex V1 - 12/11/2020 8:30pm Page 514

21.2.3 Electrokinetically Enhanced Permeable Reactive Barriers (EK-PRB)

The traditional PRB concept is to distribute reactive media across the flow of the contaminant plume to degrade contaminants as they passively flow through the barrier [84]. In combination with EK, the strategy can be twofold: enhanced transport of chlorinated ethenes toward the PRB by advection in the EOF and EM [85], or preventing passivation of the filling material [86, 87]. For this type of remediation of chlorinated ethenes, the dominant degradation pathway is abiotic reduction (Figure 21.2, dotted arrows). A third strategy is to distribute the reactant by EK transport mechanisms to the contaminated area [88–90], but this has not been studied for remediating chlorinated ethenes. By combining EK and PRB, enhanced remediation of chlorinated ethenes has been reported. For degrading TCE in laboratory testing, EK-PRB enhances remediation compared to conventional PRB by up to eight times [86, 91, 92]. If EK is applied to transport chlorinated ethenes toward the PRB, then neutralization of pH changes is essential since pH influences the EOF [5]. A simplified illustration of the EK-PRB concept of mobilizing contaminants is presented in Figure 21.5.

21.2.3.1 EK-Induced Mobilization of Chlorinated Ethenes

In an electric field, chlorinated ethenes have been shown to be transported by advection in the EOF [93] and by EM due to the formation of positively charged ion pairs with protons [63], i.e. in both cases toward the cathode. By advection in the EOF in a field-sampled sandy clay, the transport of PCE appears to be slower than TCE, which could be due to PCE's lower solubility [94]. In fine-grained soil, a TCE transport rate in the EOF of 2.4 $cm^2\ V^{-1}d^{-1}$ has been observed [95]. In a kaolin clay, an EOF-induced transport rate of TCE is found to be 2 $cm^2\ V^{-1}d^{-1}$ [93]; however, in field-sampled clays, lower TCE transport rates in the EOF of 0.6–0.8 $cm^2\ V^{-1}d^{-1}$ are

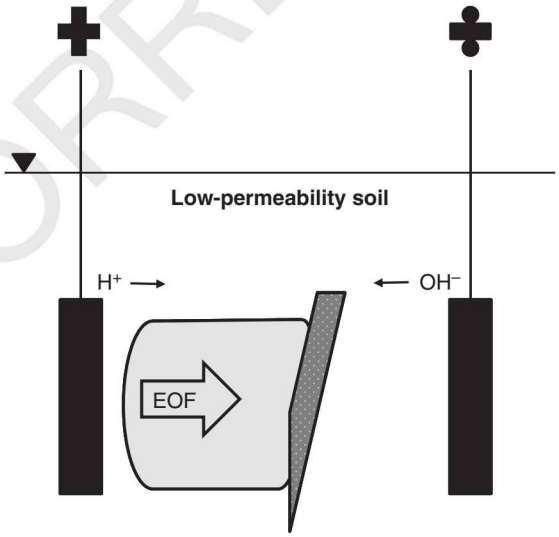

Figure 21.5 Simplified illustration of one EK-PRB concept: enhanced mobilization of the contaminants (light gray oval) toward the reactive filling material (dark gray transverse barrier) by advection in the electroosmotic flow (EOF). The established transport velocity is site- and system-specific.

UNCORRECTED PROOFS

Trim Size: 170mm x 244mm Single Column Loose Ribeiro670117 c21.tex V1 - 12/11/2020 8:30pm Page 515

reported [94, 96, 97], and for PCE of 0.5 $cm^2\ V^{-1}d^{-1}$ [97]. In sandy soil, the transport of PCE is limited [98]. These studies report EK-PRB performance in removing chlorinated ethenes of 85%–99% for PCE [97, 98] and 70%–100% for TCE [92, 94–97].

21.2.3.2 EK-Controlled Reactivity of the Filling Material

Zero-valent iron (ZVI) is often used as a filling material in EK-PRB for degrading chlorinated ethenes [85, 86, 91, 98]. However, zero-valent zinc may perform better than ZVI for degrading PCE [98]. When these filling materials oxidize, i.e. corrode, chlorinated ethenes can be reduced. The formation of oxides on the surface of the filling material passivates the PRB over time and may reduce the barrier's permeability. The longevity of the filling material depends on the rate of oxide formation and, thus, corrosion. It can be prolonged if the filling material is cathodically protected, i.e. by placing the cathode within the PRB and the anode downstream [86]. In this design, the reducing zone of the cathode can assist in increased abiotic reduction of chlorinated ethenes [86, 91]. On the other hand, corrosion can be accelerated to increase the reduction of chlorinated ethenes if anodically protected, i.e. when the anode is placed within the PRB and the cathode downstream of the PRB [86]. When the anode is placed within the PRB, the acid produced during electrolysis prevents iron oxides from forming on the surface of the filling material, thereby maintaining its reactivity [92]. The most effective design for EK-PRB in terms of chlorinated ethene degradation appears to be dependent on more parameters than just the electrode arrangement, e.g. the soil, in that different studies report both design options to be superior [86, 91, 92, 98].

21.2.3.3 Current State of Development from an Applied Perspective

In the field, several full-scale EK-PRB applications have been carried out in the US for remediating chlorinated ethenes in low-permeability soils. Common to these studies is that they investigated Lasagna™ processes, which use electric current to transport contaminants into a layered treatment zone of e.g. ZVI. The sites were contaminated with TCE. The first field application was installed horizontally [99].

Ahead of this full-scale application, a smaller pilot-scale test was carried out [100]. The pilot test (L: 4.6 m, W: 3 m, D: 4.6 m) aimed at demonstrating transport of TCE by advection in the EOF toward the treatment zone. Therefore, the filling material was granular activated carbon for sorption of TCE instead of degradation, to document the enhanced mobility. The pilot test was operated for four months at a constant current of 40 A with an electrode spacing of 3 m. Mobilization of TCE was observed, and approximately three pore volumes were transported. The resulting transport rate of TCE was 1.04 $cm^2\ V^{-1}d^{-1}$, similar to that observed at lab scale, with 92%–99.8% removal of TCE from the clay [100].

The subsequent horizontal full-scale application (L: 6.4 m, W: 9.2 m, D: 13.7 m) demonstrated the effective degradation of TCE. An iron filling material was chosen. The full-scale application was operated for a year at an initial constant voltage of 150 V (110 A), which after two months was adjusted to 200 V (200 A) and after five months to 120 V (120 A). The electrode spacing was 6.3 m. Again, TCE was mobilized, corresponding to approximately 2.8 pore volumes. Within the PRB, 96%–99%

UNCORRECTED PROOFS

Trim Size: 170mm x 244mm Single Column Loose Ribeiro670117 c21.tex V1 - 12/11/2020 8:30pm Page 516

of TCE was removed from the soil, while 70% was removed between the cathode and the PRB, and 43% was removed between the anode and the PRB [99].

Despite the good results of these horizontal EK-PRB field applications, vertical installations appeared more practical [101]. One such field application has been carried out to remediate a partially degraded TCE contamination in clay underneath buildings [102]. Three areas were remediated (L: 33 m, W: 21 m, D: 6 m; L: 20 m, W: 15 m, D: 6 m; L: 15 m, W: 15 m, D: 6 m) using iron fillings. Again, the contamination was mobilized, and degradation of TCE by 76%–83% was observed [102].

EK-PRBs have demonstrated a significant potential to efficiently remediate TCE-contaminated sites. Since little is known about the influence of the soil and groundwater composition, this should be the focus of future work. Also, means to lower the cost of EK-PRB or reduce its carbon footprint may strengthen the method's position in the market. Furthermore, only the EK-PRB strategy focusing on enhanced contaminant transport has been tested in the field. The strategy of preventing passivation of the filling material is less matured, and since it may improve the performance of traditional PRB, this strategy should be assessed.

21.3 Electrochemical Remediation in High-Permeability Saturated Soils

The electrochemical remediation strategy, as opposed to electrokinetics, induces actual degradation of contamination. It also differs by targeting high-permeability soils (Figure 21.1). Degradation is stimulated through the establishment of suitable redox zones and electrogenerated reactants. It relies on electrode processes, i.e. electrolysis, which establishes a reducing zone around the cathode and an oxidizing zone around the anode [44, 45]. Thus, the fundamentals of in situ electrochemical and electrokinetic remediation are similar, but the utilized processes and mechanisms are different. Since the foundation for electrochemical remediation is the electrode process, no buffering solutions should be used, as is the case during electrokinetically enhanced remediation. Instead, several design parameters influence the performance, e.g. electrode material, electrode configuration, and electrode shape. This is reviewed and studied in a project by Hyldegaard [103].

The primary advantages of the electrochemical method, from the perspective of chlorinated ethene degradation, are related to (i) the resulting reduction and oxidation processes, which facilitate concurrent degradation of the parent compounds and degradation intermediates, and possibly mixtures of contaminants; (ii) the flexible design, where the sequence of redox zones can be engineered, and the number of electrodes depends on the dimensions of the contaminant plume; (iii) the lack of a need for amendments, e.g. buffer solutions; (iv) the option of remote control; and (v) the option of coupling with renewable energy sources, which makes the method a sustainable alternative [45, 47, 104, 105].

Electrochemical degradation of chlorinated ethenes was initially studied and developed for wastewater treatment [106]. Later, the method was adapted to remediate contaminated sites. Overall, two concepts of in situ electrochemical remediation

UNCORRECTED PROOFS

Trim Size: 170mm x 244mm Single Column Loose Ribeiro670117 c21.tex V1 - 12/11/2020 8:30pm Page 517

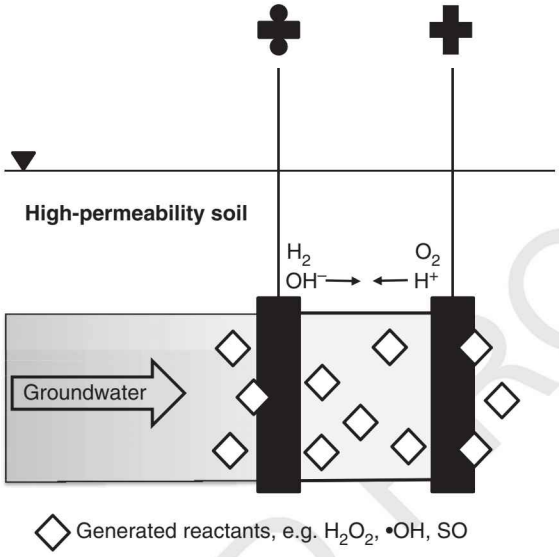

Figure 21.6 Simplified illustration of one electrochemical remediation concept: in-between well treatment of the contaminants (light gray square) by in situ generated reactants and redox conditions as the contamination flows with the groundwater through the electrochemical zone. The specific reactants and concentrations formed are site- and system-specific.

of chlorinated ethenes are studied. One is designed for in-well treatment, so the electrodes are installed in the same well and hence in a fully water-filled setting [107]. The other is aimed at in-between well treatment, where the electrodes are installed in separate wells to form a chemical barrier within a porous matrix in which a chlorinated ethene plume is treated as it flows through the electrochemical zone [108]. Since the electric field in the latter concept is installed across a soil, many factors affect the generated electrochemistry and subsequent contaminant degradation. A simplified illustration of the electrochemical remediation concept of in-between well treatment of contaminants is presented in Figure 21.6.

21.3.1 Electrochemistry in Complex Environmental Settings

Within the electrochemical zone of mixed redox conditions, chlorinated ethenes are subject to the overall indirect degradation pathways illustrated in Figure 21.2. However, electrochemical degradation processes are more complex. Chlorinated ethenes may also be reduced and oxidized directly on the electrode surfaces. Thus, concurrent degradation processes include direct abiotic reduction, indirect abiotic reduction, direct abiotic oxidation, indirect abiotic oxidation, and possible stimulation of biodegradation by naturally present specific microbial cultures [105, 109]. Direct abiotic reduction requires adsorption of chlorinated ethenes onto the surface of the cathode, which allows a direct transfer of electrons to the chlorinated ethenes [110–112]. However, during indirect abiotic reduction, electrons are transferred via electrolytically formed hydrogen [110, 111]. Similarly, during direct abiotic oxidation, electrons are transferred directly to the anode via the adsorbed chlorinated ethenes [105, 113] but via electrogenerated reactants during indirect abiotic oxidation [114, 115]. The electrogenerated reactants and radicals that can form within the electrochemical zone when established in soil

UNCORRECTED PROOFS

Trim Size: 170mm x 244mm Single Column Loose Ribeiro670117 c21.tex V1 - 12/11/2020 8:30pm Page 518

and groundwater systems include, but are not limited to, H_2O_2, ·OH, $SO_4^{\cdot-}$, Cl_2, HClO, and ClO^- [105, 115, 116]. Finally, electrochemical zones have been shown to stimulate biotic reduction [109, 117, 118] and biotic oxidation [119, 120]. The governing degradation pathways in an electrochemical zone depend on e.g. the electrode material and current intensity applied [105, 121].

For realistic current intensities, a potential for the reducing zone around the cathode of –600 mV vs. the standard hydrogen electrode (SHE) is feasible and capable of reducing chlorinated ethenes [107, 109]. Generally, chlorinated ethenes can be reduced in zones of lower potentials than those of the chlorinated ethene transformation reactions while oxidized in zones of higher potentials. Reported transformation potentials of chlorinated ethenes are listed in Table 21.1. Since the reaction potentials express the energy yield of a specific reaction and thereby the reaction readiness [125, 126], Table 21.1 reveals several patterns for degrading chlorinated ethenes in electrochemical zones. For example, chlorinated ethenes are more prone to abiotic reduction than biotic reduction, given optimal conditions. For the abiotic reduction of chlorinated ethenes, the specific pathway of elimination – where two Cl^- atoms are released – is more likely than hydrogenolysis, where one Cl^- atom is replaced by hydrogen. This is ideal since no unwanted chlorinated intermediates are formed with this pathway. Last, PCE and TCE are easier to reduce than the DCEs and VC, which have a higher affinity for oxidation. Thus, by designing the electrochemical zone such that the reducing zone is followed by an oxidizing zone, the

Table 21.1 Reported reduction and oxidation potentials of chlorinated ethenes following abiotic and biotic degradation pathways.

	Abiotic reduction		Abiotic	Biotic reduction	Biotic
Chlorinated ethene	**Hydrogenolysis[a] [mV vs. SHE]**	**Elimination[b] [mV vs. SHE]**	**Oxidation[c] [mV vs. SHE]**	**Hydrogenolysis[a] [mV vs. SHE]**	**Oxidation[c] [mV vs. SHE]**
PCE	592 [122]	631 [122] 795 [112]		430 [123]	
TCE	509–530 [122]	599 [122] 757 [112]	540 [113]	420 [123]	
cis-DCE	407 [122]	568 [122] 718 [112]		310 [123]	700 [123]
trans-DCE	428 [122]	589 [122] 718 [112]			700 [123]
1,1-DCE	423 [122] 655 [112]	Not applicable [122]			700 [123]
VC	481 [122]	Not applicable [122]		380 [123]	500 [123]

a) Figure 21.2 solid arrows and dotted arrows between chlorinated acetylenes [124].
b) Figure 21.2 dotted arrows between chlorinated ethenes and (chlorinated) acetylenes [124].
c) Figure 21.2 dashed arrows.
Source: Modified from Hyldegaard [103].

UNCORRECTED PROOFS

Trim Size: 170mm x 244mm Single Column Loose Ribeiro670117 c21.tex V1 - 12/11/2020 8:30pm Page 519

parent components will be degraded first, and any present intermediates may then be captured in the oxidizing zone.

At contaminated sites, hydrogeochemistry contains a variety of chemical species. These species may compete with chlorinated ethenes for oxidation and reduction within the electrochemical zone and thereby potentially reduce the degradation performance. A list of reaction potentials for chemical species often found in the environment is presented in Table 21.2.

The specific potentials established in an electrochemical zone depend on the current or voltage input. However, oxygen evolution at the anode occurs at a potential of −1229 mV, while hydrogen evolution at the cathode occurs at a potential of −828 mV (Table 21.2). By comparing these potentials of electrolysis to the specific potentials of soil and groundwater species listed in Table 21.2, potentially competing redox reactions can be identified. Those include reduction of CO_2, Fe^{2+}, Fe^{3+}, O_2 to H_2O_2, S, and Zn^{2+}, and oxidation of Cl^-, HClO, $HClO_2$, ClO_3^-, Fe^{2+}, Mn^{2+}, and O_2. Few studies have assessed the isolated influence of environmental chemical species on the electrochemical degradation of chlorinated ethenes in simplified systems of synthetic groundwater. One study found that the presence of Fe^{2+} and S^{2-} in the solution enhanced the electrochemical degradation of chlorinated ethenes [116]. However, the presence of humic substances [130, 131], HCO_3^- [132], chromate, selenate, and NO_3^- [131, 133, 134] have been shown to negatively influence the electrochemical remediation performance. This highlights the need to assess the influence of mixtures of a wide range of common environmental species, i.e. testing under more realistic environmental conditions.

21.3.2 Electrochemical Remediation in Complex Environmental Settings

Assessing the performance of electrochemical remediation in systems representing contaminated sites combines mechanisms such as electromigration, advection, dispersion, precipitation, dissolution, and other chemical transformations. Therefore, distinguishing what design or field-realistic parameters are most influential on electrochemical performance in such systems is challenging. The influence of electrochemical design parameters, e.g. electrode material, electrode spacing, electrode configuration, current intensity, polarity reversal, etc. has been studied in flow-through reactors of simple solutions and inert porous matrices [133–140].

One strategy to improve understanding of the influence of field-realistic parameters is to model the system. A simple one-dimensional equilibrium model in the software PRHEEQC [141], where pH was forced to decrease and increase to represent the anode and cathode, respectively, has been shown to capture changes in groundwater composition as observed in laboratory tests [34]. Another strategy is to gradually make the experimental system more complex by adding relevant environmental parameters step by step to an experimental baseline of synthetic groundwater and an inert porous matrix. This approach has been employed in a study of the influence of a field-realistic flow rate, field-extracted groundwater containing a partially degraded PCE contamination, sandy sediment, groundwater

UNCORRECTED PROOFS

Trim Size: 170mm x 244mm Single Column Loose Ribeiro670117 c21.tex V1 - 12/11/2020 8:30pm Page 520

Table 21.2 Listed standard potentials (E°) of chemical elements possibly encountered in soil and groundwater systems.

Species	Half reaction	E° [mV]	Ref.
Al	$Al^{3+} + 3e^- \Leftrightarrow Al_{(s)}$	−1680	[127]
	$Al(OH)_4^- + 3e^- \Leftrightarrow Al_{(s)} + 4OH^-$	−2310	[127, 128]
Ca	$Ca^{2+} + 2e^- \Leftrightarrow Ca_{(s)}$	−2840	[127]
Cl	$Cl_{2(g)} + 2e^- \Leftrightarrow 2Cl^-$	1360	[127, 128]
	$HClO + H^+ + 2e^- \Leftrightarrow Cl^- + H_2O$	1490	[127]
	$HClO_2 + 2H^+ + 2e^- \Leftrightarrow HClO + H_2O$	1700	[127]
	$ClO_3^- + 3H^+ + 2e^- \Leftrightarrow HClO_2 + H_2O$	1180	[127]
	$ClO_4^- + 2H^+ + 2e^- \Leftrightarrow ClO_3^- + H_2O$	1200	[127]
CO_2	$CO_{2(g)} + 8H^+ + 8e^- \Leftrightarrow CH_{4(g)} + 2H_2O$	170	[128]
Fe	$Fe^{2+} + 2e^- \Leftrightarrow Fe_{(s)}$	−447	[127–129]
	$Fe^{3+} + 3e^- \Leftrightarrow Fe_{(s)}$	−37	[127]
	$Fe^{3+} + e^- \Leftrightarrow Fe^{2+}$	771	[127–129]
	$FeO_4^{2-} + 8H^+ + 3e^- \Leftrightarrow Fe^{3+} + 4H_2O$	2200	[127]
	$Fe(OH)_3 + 3H^+ + e^- \Leftrightarrow Fe^{2+} + 3H_2O$	−980	[129]
H	$2H^+ + 2e^- \Leftrightarrow H_{2(g)}$	0	[127, 128]
	$2H_2O + 2e^- \Leftrightarrow H_{2(g)} + 2OH^-$	−828	[127]
	$H_2O_2 + 2H^+ + 2e^- \Leftrightarrow 2H_2O$	1760	[127, 128]
K	$K^+ + e^- \Leftrightarrow K_{(s)}$	−2920	[127]
Mg	$Mg^{2+} + 2e^- \Leftrightarrow Mg_{(s)}$	−2360	[127, 128]
Mn	$Mn^{2+} + 2e^- \Leftrightarrow Mn_{(s)}$	−1190	[127]
	$MnO_2 + 4H^+ + 2e^- \Leftrightarrow Mn^{2+} + 2H_2O$	1220	[127, 129]
	$MnO_4^- + 8H^+ + 5e^- \Leftrightarrow Mn^{2+} + 4H_2O$	1510	[127]
Na	$Na^+ + e^- \Leftrightarrow Na_{(s)}$	−2710	[127]
NO_3	$NO_3^- + 10H^+ + 8e^- \Leftrightarrow NH_4 + 3H_2O$	880	[128]
	$NO_3^- + 2H^+ + 2e^- \Leftrightarrow NO_2^- + H_2O$	830	[128]
O	$O_{2(g)} + 4H^+ + 4e^- \Leftrightarrow 2H_2O$	1229	[127–129]
	$O_2 + 2H^+ + 2e^- \Leftrightarrow H_2O_2$	695	[127]
	$O_2 + 2H_2O + 2e^- \Leftrightarrow H_2O_2 + 2OH^-$	−146	[127]
	$O_3 + H_2O + 2e^- \Leftrightarrow O_2 + 2OH^-$	1250	[127, 128]
S	$S_{(s)} + 2H^+ + 2e^- \Leftrightarrow H_2S$	142	[127, 128]
	$SO_4^{2-} + 10H^+ + 8e^- \Leftrightarrow H_2S + 4H_2O$	340	[128]
Zn	$Zn^{2+} + 2e^- \Leftrightarrow Zn_{(s)}$	−762	[127, 128]

Note that the reactions are written in the state of reduction, regardless of some species being spontaneously oxidized.
Source: Modified from Hyldegaard [103].

UNCORRECTED PROOFS

Trim Size: 170mm x 244mm Single Column Loose Ribeiro670117 c21.tex V1 - 12/11/2020 8:30pm Page 521

temperatures of 8–10 °C and 22 °C, and extended test duration [35]. The purpose of the study was to evaluate the influence of the field-realistic parameters on the electrochemical degradation performance and the effect of the introduced electrochemistry on natural hydrogeochemistry, i.e. not to demonstrate complete remediation, so the electrochemical reactor was not fully optimized. A constant current of 120 mA was supplied to a palladium-coated Fe foam cathode and a downgradient mixed metal oxide mesh anode for a total of 30 hours. Introducing the electrochemistry to the reactor containing an inert porous matrix and synthetic groundwater flowing through at a realistic seepage velocity of 150 m y^{-1} resulted in a 50% ± 8.6% degradation of PCE to a concentration of approximately 17 µg l^{-1} [35]. When the synthetic groundwater was replaced with field-extracted groundwater containing a partially degraded PCE contamination, the degradation of PCE increased to 70% ± 9% to a concentration of 13 ± 4 µg l^{-1}, while TCE and cis-DCE were degraded completely [35]. Despite possible competition from a wide range of groundwater species with the degradation of chlorinated ethenes, this study suggests that the influence of natural hydrochemistry is a net enhancement. Combining the system of field-realistic flow rate and field-extracted groundwater with sandy sediment resulted in 81% ± 7% degradation of PCE, reaching a concentration of 7.8 ± 2.3 µg l^{-1}, and complete degradation of TCE and cis-DCE. This is not statistically significant compared to testing with field-extracted groundwater, but the tendency is enhanced performance in sandy sediment [35]. Then the electrochemical performance was studied in the complex field-realistic system at a temperature of 8–10 °C, which is the common temperature of groundwater in e.g. North America and northern Europe, because chemical reaction rates are temperature dependent [142, 143]. The resulting degradation of PCE was 74% ± 7.5% to a concentration of 19.3 ± 6.3 µg l^{-1}. The influence of lower temperatures was not statistically significant from the performance in field-extracted groundwater but indicated some adverse influence of reduced temperature [35]. Lastly, the test duration was extended to 50 hours for testing with field-extracted groundwater and sandy sediment at 22 °C. The electrochemical remediation then demonstrated degradation of PCE, TCE, and cis-DCE to below the detection limits, i.e. to concentrations of <0.25 µg l^{-1}. Thereby, the electrochemical remediation was shown to be able to obey e.g. the Danish and American MCLs of chlorinated ethenes in groundwater and drinking water. The contribution of volatilization to these degradation percentages accounted for <0.15% [35, 103].

Another study assessed electrochemical degradation performance for PCE in a synthetic solution flowing through a sandy sediment with the application of a constant voltage [104]. At 10 V, 50% of PCE was degraded, while an enhancement was observed at 30 V to 85% degradation, reaching a concentration of 500 µg l^{-1} [104].

A third study assessed the electrochemical degradation of TCE in field-extracted groundwater flowing through a sandy sediment under constant potentials of 2.5, 5, 10, and 20 V [108]. The greatest TCE degradation of 82% was observed for an applied voltage of 20 V, reaching a concentration of 70 µg l^{-1} [108].

In the study of stepwise addition of field-realistic parameters, changes in dominating degradation pathways for chlorinated ethenes were observed, which were

UNCORRECTED PROOFS

Trim Size: 170mm x 244mm Single Column Loose Ribeiro670117 c21.tex V1 - 12/11/2020 8:30pm Page 522

primarily influenced by the porous matrix [103]. In tests incorporating both the inert porous matrix and sandy sediment, the strong oxidant H_2O_2 was formed near the anode in concentrations of up to 4000 $\mu g\,l^{-1}$ [35]. However, the distribution of formed H_2O_2 varied between these porous matrices. In the tests with an inert porous matrix, H_2O_2 was distributed over time throughout the electrochemical reactor. Thus, the extent of the reducing zone of the cathode was not sustained, and the predominant degradation pathway for chlorinated ethenes in an inert porous matrix consequently was indirect abiotic oxidation. However, in sandy sediment, the distribution of electrogenerated H_2O_2 was restricted to the vicinity of the anode, and the reducing zone of the cathode was maintained. Since PCE was primarily degraded near the cathode for testing in the sandy sediment, a shift in the degradation pathway to abiotic reduction was observed [103]. In the study, foam and mesh electrodes were used, and the specific contribution of direct and indirect pathways to the observed degradation of PCE in sandy sediment was unclear.

Comparing to an observed degradation of chlorinated ethenes in a similar study using electrode rods, where only a small amount of the contamination was in contact with the electrodes, the governing reduction pathway for PCE appears to be indirect reduction [34, 103]. Based on the reported tendency of greater degradation of PCE during testing in sandy sediment, in which the distribution of H_2O_2 was limited, the reduction of PCE could be superior to oxidation. This agrees with the reaction potentials of reduction and oxidation listed in Table 21.2, where reduction is favorable from a perspective of gain in energy. No chlorinated intermediates accumulated in the porewater as a result of the electrochemical reduction of PCE [35]. This could be due to subsequent fast reduction of the intermediates, but it could also indicate reduction via the elimination pathway, which proceeds via the formation of chlorinated acetylenes (Figure 21.2). TCE and cis-DCE were subject to both reduction and oxidation [103].

21.3.2.1 Electrochemically Induced Changes in Hydrogeochemistry

The electrochemical remediation method changes the pH and redox conditions of the system to which it is applied. In addition, strong oxidants are electrogenerated, so changes to the natural hydrogeochemistry are inevitable. Electrochemical application to a system of field-extracted groundwater and sandy sediment showed that an electrode configuration of a cathode followed by an anode was least intrusive to the hydrogeochemistry [103]. Despite pH and conductivity changing near the electrodes, initial levels were maintained both up- and downgradient of the electrochemical zone [34, 35]. In addition, the strength of the acidic front of the anode was weak due to the buffering of calcium carbonate present in the sandy sediment [34, 35]. Thus, when electrochemistry is applied to a complex field-realistic system, the induced changes in pH and conductivity are less than otherwise observed in simplified systems.

Within the electrochemical zone, EM and the changes in pH and redox conditions influence hydrogeochemical species. Therefore, the fate of hydrogeochemical species due to introduced electrochemistry depends on the established sequence of redox conditions, i.e. on the applied electrode configuration [144]. In the system of

UNCORRECTED PROOFS

Trim Size: 170mm x 244mm Single Column Loose Ribeiro670117 c21.tex V1 - 12/11/2020 8:30pm Page 523

field-extracted groundwater and sandy sediment, changes were primarily observed for Ca, Mg, K, Na, Si, SO_4^{2-}, Cl^-, and NO_3^- [35, 103]. For an electrode configuration of a cathode followed by an anode, the following changes in hydrogeochemistry have been observed based on porewater samples:

- pH increased near the cathode and decreased near the anode. Downgradient from the electrochemical zone, a near-neutral pH was maintained [34, 35].
- Ca appeared to form colloids in the reducing zone, transported by advection and dissolved in the downgradient oxidizing zone. Overall, the concentration of Ca decreased downgradient from the electrochemical zone, indicating net precipitation of Ca [34, 35].
- Mg co-precipitated with Ca in the reducing zone and dissolved in the oxidizing zone. Overall, the concentration of Mg decreased downgradient from the electrochemical zone, indicating net precipitation of Mg [34].
- K was subject to cation exchange onto formed colloids in the reducing zone. This was reversed in the reducing zone but resulted in an overall decrease in the concentration of K downgradient from the electrochemical zone, indicating that the cation exchange was only partly reversible [34, 103].
- Na accumulated near the cathode, indicating EM of Na [103, 145]. Overall, Na decreased in concentration downgradient from the electrochemical zone [34].
- Si increased in concentration, possibly due to dissolution of silicate minerals, i.e. weathering of the sandy sediment [35, 146].
- SO_4^{2-} decreased in concentration in the reducing zone and increased in the oxidizing zone, indicating EM toward the anode, reduction near the cathode, and subsequent oxidation near the anode [103]. Overall, the concentration increased downgradient from the electrochemical zone, possible due to dissolution of pyrite in the sandy sediment [34].
- Cl^- decreased in concentration in the reducing zone and increased in the oxidizing zone, indicative of EM toward the anode [34, 35]. Overall, deviating trends in the concentration of Cl^- downgradient from the electrochemical zone have been observed [34, 35]. An increase in concentration could be due to the release of Cl^- as chlorinated ethenes are degraded, while a decrease may be due to the formation of reactive species, e.g. HClO, ClO_3^-, and Cl_2 [103].
- NO_3^- decreased and increased in concentration in the reducing and oxidizing zone, respectively, explained by EM and redox reactions [103]. No clear trend was observed in the concentration downgradient from the electrochemical zone [34, 35].

For an electrode configuration of an anode followed by a cathode, the following changes in hydrogeochemistry in a system of field-extracted groundwater and sandy sediment have been reported and are based on porewater samples:

- pH decreased near the anode and increased near the cathode. Downgradient from the electrochemical zone, the pH was alkaline [144].
- Ca formed precipitates in the reducing zone, which remained bound downgradient from the electrochemical zone, causing a more pronounced decrease

UNCORRECTED PROOFS

Trim Size: 170mm x 244mm Single Column Loose Ribeiro670117 c21.tex V1 - 12/11/2020 8:30pm Page 524

in concentration than the opposite electrode configuration [144]. Continuous precipitation may lead to clogging of the pore spaces.

- Mg complexes formed in the reducing zone and remained bound downgradient from the electrochemical zone, resulting in a significant decrease in concentration [144].
- Na decreased in the oxidizing zone and increased in the reducing zone, possibly controlled by the pH conditions and the related dominant form of the carbonate system species (HCO_3^-/CO_3^{2-}), and EM. Overall, the concentration of Na downgradient from the electrochemical zone recovered to pre-treatment levels [144].
- SO_4^{2-} increased in concentration within the oxidizing zone and decreased in the subsequent reducing zone, indicating EM toward the anode and redox reactions. Consequently, SO_4^{2-} was removed from the porewater downgradient from the electrochemical zone [144].
- Cl^- increased in concentration in the oxidizing zone and decreased in the following reducing zone, possibly due to EM toward the anode. Overall, Cl^- was removed from the porewater downgradient from the electrochemical zone [144].

The reported changes in hydrogeochemistry within electrochemical zones of opposite electrode configurations are summarized schematically in Figure 21.7.

In the study of stepwise addition of field-realistic parameters to the electrochemical reactor, a correlation between the presence of sandy sediment and formation of

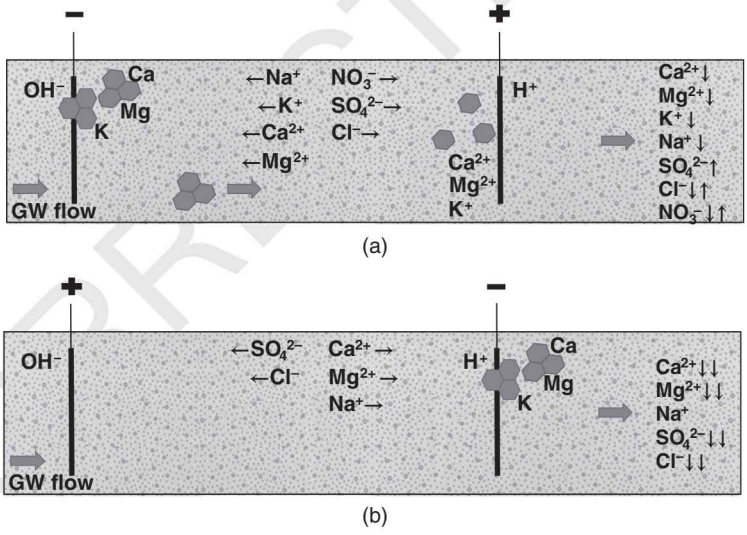

Figure 21.7 Summary of the reported fates of common hydrogeochemical species within the electrochemical zone of (a) reduction followed by oxidation and (b) oxidation followed by reduction when applied in realistic systems of field-extracted groundwater flowing through a sandy sediment. The hydrogeochemical species were subject to electromigration (horizontal arrows), advection, reduction, oxidation, colloid formation/precipitation (hexagons), and/or cation exchange. Induced overall change in concentration downgradient from the electrochemical zone of these species is indicated (vertical arrows). Source: Modified from Hyldegaard [103].

UNCORRECTED PROOFS

Trim Size: 170mm x 244mm Single Column Loose Ribeiro670117 c21.tex V1 - 12/11/2020 8:30pm Page 525

trichloromethane (TCM), commonly known as chloroform, was observed [35]. TCM was formed in the vicinity of the anode. The formation of TCM is undesirable due to its inherent toxic and health hazardous effects [18]. The concentrations of TCM measured were significant and could not be explained stoichiometrically by degradation of chlorinated ethenes. Instead, it was explained by oxidation of organic matter embedded in the sandy sediment in the presence of free Cl^-, which was supplied in sufficient levels with the field-extracted groundwater [35, 147–150]. Oxidation of the naturally present organic matter could be induced by the electrogenerated H_2O_2 at the anode, and the H_2O_2 consumption by organic matter could also explain the observed restricted distribution of H_2O_2 to the vicinity of the anode when installed in sandy sediment. The concentration of TCM decreased over time [35, 103], which could indicate exhaustion of the fraction of organic matter within the sandy sediment, thereby changing the geochemical composition. A subsequent electrochemically induced degradation of TCM is also conceivable [151–155].

21.3.2.2 Current State of Development from an Applied Perspective

Most experience with electrochemical remediation of chlorinated ethenes has been gained through bench-scale testing in simplified conditions, with few studies incorporating natural groundwater and geology. Field implementations appear to be limited. Based on published work, including patents and conference contributions, one pilot test [156, 157] and two full-scale implementations [158] have been carried out in the field. The pilot test and full-scale implementations differ in strategy and thereby applied electrochemical design.

In the pilot test, a connected electrode barrier was installed across the contaminant plume to treat the contaminated groundwater as it naturally flowed through the electrode barrier [156, 157]. In the full-scale implementations, the electrodes were installed in wells in which the reactants were continuously generated and distributed [159, 160]. With these differences in test design, the resulting dominant degradation pathways of the field implementations may vary. In the pilot test, with flow through the electrodes, the governing degradation pathway could be direct oxidation and reduction. In the full-scale implementations, with electrodes installed in wells, indirect pathways are most significant (Section 21.3.1).

The pilot test was conducted in the US to remediate a TCE plume containing 300 µg l^{-1} [156]. A trench was excavated across the contaminant plume into which constructed electrode panels (total L: 9.2 m, H: 1.9 m) were installed. The electrode panels consisted of three mixed metal oxide mesh electrodes, each with an internal spacing of 2 cm in a configuration in the groundwater flow direction of anode – cathode – bipolar electrode. The electrode barrier was installed in sandy soil with a seepage velocity of approximately 0.1 m d^{-1} [156]. The electrochemical remediation was operated continuously for 36 months [156, 157]. A constant voltage of 3.1 V was applied for the first 120 days followed by 6.5 V through day 290, 4.9 V through day 399, 3.1 V through day 500 [156], and primarily 4 V through the conclusion of the test at day 1070 [157]. The greatest degradation of dissolved TCE of 95% was observed for application of 6.5 V to a concentration below the MCL immediately downgradient from the electrode barrier [156, 157]. The degradation

UNCORRECTED PROOFS

Trim Size: 170mm x 244mm Single Column Loose Ribeiro670117 c21.tex V1 - 12/11/2020 8:30pm Page 526

intermediate cis-DCE was detected within the electrode barrier during the first 18 months of operation but did not distribute downgradient from the barrier [156]. In addition, TCM was quantified downgradient from the electrode barrier, but during application of 6.5 V only, and it could not be quantified 4 m downgradient from the electrode barrier [156, 157]. Therefore, the operation of the electrode barrier was continued at lower voltages [157]. An overall decrease in dissolved TCE concentration of 75% was observed during the concluding 18 months with the application of 4 V, and no degradation intermediates or TCM accumulated downgradient from the electrode barrier [157]. A large snowstorm set in on day 600, and the subsequent thawing resulted in increased infiltration and dilution of the TCE plume, which led to an order of magnitude drop in concentration. Over time, the concentration of TCE rebounded, but the event obscured the performance of the electrode barrier [157]. TCM formation at 6.5 V was investigated and explained by oxidation of organic matter in the construction material [156]. Oxidizing conditions were established both upgradient and downgradient of the electrode barrier, but a reducing zone near the cathode was maintained, and an increase in pH was observed [156]. Consequently, calcium deposited due to the electrochemical application; but with weekly polarity reversals of 12 hours to remove scale on the cathode, no impact on remediation performance was observed [156]. pH was maintained neutral at distances of 0.5 m to the electrode barrier but decreased in the proximity of the electrode panels [156]. An increase in biomass was observed in the soil downgradient from the electrode barrier [157]. Generally, the components of the electrode barrier remained functional for the 36 months of operation [157]. During the first 18 months of application, 2240 kWh was consumed to treat approximately 238 m^3 of contaminated water, i.e. the average energy consumption was 9.4 kWh m^{-3} treated [156]. Based on the design strategy of installing an electrode mesh barrier across the contaminant plume, the feasibility and applicability of the electrochemical strategy investigated were evaluated to decrease with depth to the dissolved contamination [156].

Two full-scale implementations applying the remediation technology known as Provect-"EBR®" have been carried out in Israel, but with a few details being provided on only one of these applications [158]. At this site, a plume of a partially degraded PCE contamination was identified. High concentrations were measured: PCE 257 µg l^{-1}, TCE 25146 µg l^{-1}, and DCE 47 µg l^{-1}. One electrode well was installed with three electrodes mounted [158]. The three electrodes served individual purposes and were activated in a sequence. First, one catalytic cathode of diamond-doped titanium was activated for in situ formation of H_2O_2. Second, an iron anode was activated to release Fe^{2+}. Third, a one-dimensionally stable anode (mixed metal oxide) was activated to produce oxygen via electrolysis. The shift in activation of each electrode was remotely controlled based on real-time monitoring of temperature, pH, oxygen concentration, oxidation–reduction potential, current density, and conductivity within the electrode well [159]. With this sequential electrode activation, strong oxidants like H_2O_2, $^{\cdot}HO_2$, $^{\cdot}O_2$, and $^{\cdot}OH$ were formed in situ [159, 160]. Sufficient distribution of the electrogenerated reactants was observed with a radius of influence of 2–4 m, depending on site characteristics,

UNCORRECTED PROOFS

Trim Size: 170mm x 244mm Single Column Loose Ribeiro670117 c21.tex V1 - 12/11/2020 8:30pm Page 527

leading to an applied electrode spacing of 4–7 m [160]. The electrochemical strategy was applied for 60 days. The resulting degradation of chlorinated ethenes was >99% within 30 days of application [158], with no formation of degradation intermediates [160]. During the following 30 days of application (days 30–60), some rebound or loss of efficiency was observed, with concentrations increasing for PCE from <2 to 5 $\mu g\,l^{-1}$, TCE from <2 to 15 $\mu g\,l^{-1}$, and DCE from <1 to 8 $\mu g\,l^{-1}$ [158]. For this specific application, the radius of influence observed downgradient from the electrode well was 20 m [158]. The number of electrode wells required depend on the site characteristics and dimensions of the contaminant plume [158]. The longevity of this electrochemical remediation technology is five to more than seven years [160]. The Provect-"EBR®" method has also been applied for remediating sites contaminated with MTBE and BTEX in both groundwater and soil [158, 159].

One modeling study of electrochemical application has been performed, which focused on physico-chemical changes within the electrochemical reactor [161]. The model was validated against observed physico-chemical changes in experimental work on electrochemical degradation of chlorinated ethenes [161] but omitted the fate of the contaminants. An electrochemical model that includes the contaminant fate and is validated against performed field applications could provide relevant insight into a complex system at a cost-effective rate.

With the observed degradation performances of the outlined pilot and full-scale field implementations, the electrochemical method has demonstrated promising potential for in situ remediation of chlorinated ethenes. Since the number of field applications and the available details are still sparse, future work should focus on field applications, the influence of site characteristics on design and performance, long-term performance, operation and maintenance requirements, and cost-competitiveness. Also, implementation of the electrochemical method near underground infrastructure, e.g. piping, and means to protect the existing infrastructure are relevant for the applicability of the method.

21.4 Summary

Hazardous chlorinated ethenes are found in low- and high-permeability soils worldwide and have resulted in contamination of e.g. groundwater and indoor air in residential areas. These contaminants are challenging to remediate, and uses of electric fields for in situ enhancement of current remediation technologies or as new alternatives are being investigated. Electrokinetics have been used to enhance the contact between reactants and contaminants in low-permeability soils through improved delivery of reactants or mobilization of contaminants. The electrokinetic concept utilizes transport mechanisms and is therefore combined with other remediation technologies for subsequent contaminant degradation, e.g. EK-BIO, EK-ISCO, and EK-PRB. On the other hand, electrochemistry is investigated for in situ electrogeneration of reactants and redox zones in high-permeability soils and can degrade chlorinated ethenes through intelligent engineering of electrode processes.

UNCORRECTED PROOFS

Trim Size: 170mm x 244mm Single Column Loose Ribeiro670117 c21.tex V1 - 12/11/2020 8:30pm Page 528

In this chapter, the current state of development of EK-BIO, EK-ISCO, EK-PRB, and electrochemical remediation was outlined, with a focus on in situ application. Electrokinetic and electrochemical strategies have demonstrated promising results in the field. However, these remediation methods are still novel and suffer from a lack of published findings. More field implementations and sharing of findings are needed for a joint maturing of these methods toward becoming commercially robust and competitive remediation technologies.

References

1 Pankow, J.F., Feenstra, S., Cherry, J.A., and Ryan, C.M. (1996). DENSE CHLORINATED SOLVENTS and other DNAPLs in Groundwater: history, behavior, and remediation. In: *DENSE CHLORINATED SOLVENTS and Other DNAPLs in Groundwater: history, behavior, and remediation* (ed. J. Pankow), 1–522. Portland, OR: Waterloo Press.

2 Wolf, K. and Chesnutt, T.W. (1987). Chlorinated solvents: market interactions and regulation. *Journal of Hazardous Materials* 15 (1–2): 137–161.

3 Parker, B.L., Cherry, J.A., Chapman, S.W., and Guilbeault, M.A. (2003). Review and analysis of chlorinated solvent dense nonaqueous phase liquid distributions in five Sandy aquifers. *Vadose Zone Journal* 2 (2): 116–137.

4 Kueper BH, Wealthall GP, Smith JWN et al. (2003). An illustrated handbook of DNAPL transport and fate in the subsurface. Environment Agency R&D Publication 133. www.environment-agency.gov.uk.

5 Ottosen, L.M., Larsen, T.H., Jensen, P.E. et al. (2019). Electrokinetics applied in remediation of subsurface soil contaminated with chlorinated ethenes – a review. *Chemosphere* 235: 113–125. https://linkinghub.elsevier.com/retrieve/pii/S0045653519313207.

6 He, Y.T., Wilson, J.T., Su, C., and Wilkin, R.T. (2015). Review of abiotic degradation of chlorinated solvents by reactive iron minerals in aquifers. *Groundwater Monitoring and Remediation* 35 (3): 57–75.

7 Kueper, B.H., Stroo, H.F., Vogel, C.M., and Ward, C.H. (2014). *Chlorinated Solvent Source Zone Remediation. Chlorinated Solvent Source Zone Remediation*, 1–759. New York, USA: Springer.

8 Siegrist, R.L., Crimi, M., Broholm, M.M. et al. (2012). Advances in groundwater remediation: achieving effective in situ delivery of chemical oxidants and amendments. In: *Clean Soil and Safe Water* (eds. F.F. Quercia and D. Vidojevic), 197–212. Dordrecht, The Netherlands: Springer.

9 Maymó-gatell, X., Chien, Y., Gossett, J.M., and Zinder, S.H. (1997). Isolation of a bacterium that reductively dechlorinates tetrachloroethene to ethene. *Science* 276: 1568–1571.

10 Van Der Zaan, B., Hannes, F., Hoekstra, N. et al. (2010). Correlation of Dehalococcoides 16S rRNA and chloroethene-reductive dehalogenase genes with geochemical conditions in chloroethene-contaminated groundwater. *Applied and Environmental Microbiology* 76 (3): 843–850.

UNCORRECTED PROOFS

Trim Size: 170mm x 244mm Single Column Loose Ribeiro670117 c21.tex V1 - 12/11/2020 8:30pm Page 529

11 Scheutz, C., Durant, N.D., Dennis, P. et al. (2008). Concurrent ethene generation and growth of Dehalococcoides containing vinyl chloride reductive dehalogenase genes during an enhanced reductive dechlorination field demonstration. *Environmental Science & Technology* 42 (24): 9302–9309.

12 Fennell, D.E., Gossett, J.M., and Zinder, S.H. (1997). Comparison of butyric acid, ethanol, lactic acid, and propionic acid as hydrogen donors for the reductive dechlorination of tetrachloroethene. *Environmental Science & Technology* 31 (3): 918–926.

13 Lee, P.K.H., Cheng, D., West, K.A. et al. (2013). Isolation of two new Dehalococcoides mccartyi strains with dissimilar dechlorination functions and their characterization by comparative genomics via microarray analysis. *Environmental Microbiology* 15 (8): 2293–2305.

14 Maymó-Gatell, X., Anguish, T., and Zinder, S.H. (1999). Reductive dechlorination of chlorinated ethenes and 1,2-dichloroethane by "dehalococcoides ethenogenes" 195. *Applied and Environmental Microbiology* 65 (7): 3108–3113.

15 Heimann, A.C., Friis, A.K., Scheutz, C., and Jakobsen, R. (2007). Dynamics of reductive TCE dechlorination in two distinct H_2 supply scenarios and at various temperatures. *Biodegradation* 18 (2): 167–179.

16 World Health Organization. (2020). International Programme on Chemical Safety - environmental health criteria. https://www.who.int/ipcs/publications/ehc/en.

17 Rudén, C. (2006). Science and policy in risk assessments of chlorinated ethenes. *Annals of the New York Academy of Sciences* 1076: 191–206.

18 Ruder, A.M. (2006). Potential health effects of occupational chlorinated solvent exposure. *Annals of the New York Academy of Sciences* 1076: 207–227.

19 US Environmental Protection Agency. (2018). Drinking water standards and health advisories. EPA 822-F-18-001.

20 Miljøstyrelsen (Danish EPA). (2018). Liste over kvalitetskriterier i relation til forurenet jord og kvalitetskriterier for drikkevand.

21 Margat, J. and van der Gun, J. (2013). *Groundwater around the World. A Geographic Synopsis*, 1–372. Boca Raton, USA: CRC Press/Taylor & Francis Group.

22 Moran, M.J., Zogorski, J.S., and Squillace, P.J. (2007). Chlorinated solvents in groundwater of the United States. *Environmental Science & Technology* 41 (1): 74–81.

23 Parsons Engineering Science Inc (2000). *Remediation of Chlorinated Solvent Contamination on Industrial and Airfield Sites*. Denver, USA: United States Air Force Environmental Restoration Program.

24 Groundwater Governance - A Global Framework for Action (2016). *Global Diagnostic on Groundwater Governance* (ed. J. Burke). Food and Agriculture Organization of the United Nations (FAO) http://www.fao.org/3/a-i5706e.pdf.

25 Appelo, C.A.J. and Postma, D. (2010). Flow and transport. In: *Geochemistry, Groundwater and Pollution*, 2e (eds. C.A.J. Appelo and D. Postma), 63–118. Leiden, The Netherlands: CRC Press LLC.

UNCORRECTED PROOFS

Trim Size: 170mm x 244mm Single Column Loose Ribeiro670117 c21.tex V1 - 12/11/2020 8:30pm Page 530

26 Appelo, C.A.J. and Postma, D. (2010). Ion exchange. In: *Geochemistry, Groundwater and Pollution*, 2e (eds. C.A.J. Appelo and D. Postma), 241–310. Leiden, The Netherlands: CRC Press LLC.

27 Nazaroff, W.W. and Alvarez-Cohen, L. (2000). Transport phenomena. In: *Environmental Engineering Science*, 1e (eds. W.W. Nazaroff and L. Alvarez-Cohen), 159–206. New York, USA: Wiley.

28 Chapman, S.W. and Parker, B.L. (2005). Plume persistence due to aquitard back diffusion following dense nonaqueous phase liquid source removal or isolation. *Water Resources Research* 41 (12): 1–16. http://doi.wiley.com/10.1029/2005WR004224.

29 Parker, B.L., Chapman, S.W., and Guilbeault, M.A. (2008). Plume persistence caused by back diffusion from thin clay layers in a sand aquifer following TCE source-zone hydraulic isolation. *Journal of Contaminant Hydrology* 102 (1–2): 86–104. http://dx.doi.org/10.1016/j.jconhyd.2008.07.003.

30 Scheutz, C., Broholm, M.M., Durant, N.D. et al. (2010). Field evaluation of biological enhanced reductive dechlorination of chloroethenes in clayey till. *Environmental Science & Technology* 44 (13): 5134–5141.

31 Appelo, C.A.J. and Postma, D. (2010). Carbonates and carbon dioxide. In: *Geochemistry, Groundwater and Pollution*, 2e (eds. C.A.J. Appelo and D. Postma), 175–240. Leiden, The Netherlands: CRC Press LLC.

32 Hansen, B.H., Nedergaard, L.W., Ottosen, L.M. et al. (2015). Experimental design for assessment of electrokinetically enhanced delivery of lactate and bacteria in 1,2-cis-dichloroethylene contaminated limestone. *Environmental Technology and Innovation* 4: 73–81. http://dx.doi.org/10.1016/j.eti.2015.04.006.

33 Gill, R.T., Harbottle, M.J., Smith, J.W.N., and Thornton, S.F. (2014). Electrokinetic-enhanced bioremediation of organic contaminants: a review of processes and environmental applications. *Chemosphere* 107: 31–42. http://linkinghub.elsevier.com/retrieve/pii/S0045653514003683.

34 Hyldegaard, B.H., Jakobsen, R., Weeth, E.B. et al. (2019). Challenges in electrochemical remediation of chlorinated solvents in natural groundwater aquifer settings. *Journal of Hazardous Materials* 368: 680–688. https://doi.org/10.1016/j.jhazmat.2018.12.064.

35 Hyldegaard, B.H., Jakobsen, R., and Ottosen, L.M. (2020). Electrochemical transformation of an aged tetrachloroethylene contamination in realistic aquifer settings. *Chemosphere* 243: 125340. https://linkinghub.elsevier.com/retrieve/pii/S0045653519325809.

36 Mackay, D.M. and Cherry, J.A. (1989). Groundwater contamination: pump-and-treat remediation. *Environmental Science & Technology* 23 (6): 630–636.

37 Interstate Technology & Regulatory Council (2011). *Integrated DNAPL Site Strategy*, 1–209. www.itrcweb.org.

38 Interstate Technology & Regulatory Council (2005). *Permeable Reactive Barriers: Lessons Learned/New Directions. PRB-4*, 1–202. Washington, DC, USA: Interstate Technology & Regulatory Council, Permeable reactive Barrier Team.

UNCORRECTED PROOFS

Trim Size: 170mm x 244mm Single Column Loose Ribeiro670117 c21.tex V1 - 12/11/2020 8:30pm Page 531

39 Stroo, H.F., Leeson, A., Marqusee, J.A. et al. (2012). Chlorinated Ethene source remediation: lessons learned. *Environmental Science & Technology* 46 (12): 6438–6447. http://pubs.acs.org/doi/10.1021/es204714w.

40 Aulenta, F., Pera, A., Rossetti, S. et al. (2007). Relevance of side reactions in anaerobic reductive dechlorination microcosms amended with different electron donors. *Water Research* 41 (1): 27–38.

41 O'Connor, D., Hou, D., Ok, Y.S. et al. (2018). Sustainable in situ remediation of recalcitrant organic pollutants in groundwater with controlled release materials: a review. *Journal of Controlled Release* 283 (May): 200–213. https://doi.org/10.1016/j.jconrel.2018.06.007.

42 Stenzel, M.H. and Gupta, U.S. (1985). Treatment of contaminated groundwaters with granular activated carbon and air stripping. *Journal of the Air Pollution Control Association* 35 (12): 1304–1309.

43 Urano, K., Yamamoto, E., Tonegawa, M., and Fujie, K. (1991). Adsorption of chlorinated organic compounds on activated carbon from water. *Water Research* 25 (12): 1459–1464.

44 Acar, Y.B. and Alshawabkeh, A.N. (1993). Principles of electrokinetic remediation. *Environmental Science & Technology* 27 (13): 2638–2647.

45 Alshawabkeh, A.N. (2009). Electrokinetic soil remediation: challenges and opportunities. *Separation Science and Technology* 44 (10): 2171–2187.

46 Lima, A.T., Hofmann, A., Reynolds, D. et al. (2017). Environmental electrokinetics for a sustainable subsurface. *Chemosphere* 181: 122–133. http://dx.doi.org/10.1016/j.chemosphere.2017.03.143.

47 Reddy, K.R. and Cameselle, C. (2009). *Electrochemical Remediation Technologies for Polluted Soils, Sediments and Groundwater* (eds. K.R. Reddy and C. Cameselle), 1–732. Hobroken, NJ: Wiley.

48 Ribeiro, A.B., Mateus, E.P., and Couto, N. (2016). *Electrokinetics across Disciplines and Continents, New Strategies for Sustainable Development* (eds. A.B. Ribeiro, E.P. Mateus and N. Couto), 1–469. London: Springer International Publishing.

49 Beretta, G., Mastorgio, A.F., Pedrali, L. et al. (2019). The effects of electric, magnetic and electromagnetic fields on microorganisms in the perspective of bioremediation. *Reviews in Environmental Science and Biotechnology* 18 (1): 29–75. https://doi.org/10.1007/s11157-018-09491-9.

50 Lear, G., Harbottle, M.J., Van Der Gast, C.J. et al. (2004). The effect of electrokinetics on soil microbial communities. *Soil Biology and Biochemistry* 36 (11): 1751–1760.

51 Shi, L., Müller, S., Harms, H., and Wick, L.Y. (2008). Effect of electrokinetic transport on the vulnerability of PAH-degrading bacteria in a model aquifer. *Environmental Geochemistry and Health* 30 (2): 177–182.

52 Wick, L.Y., Mattle, P.A., Wattiau, P., and Harms, H. (2004). Electrokinetic transport of PAH-degrading bacteria in model aquifers and soil. *Environmental Science & Technology* 38 (17): 4596–4602.

UNCORRECTED PROOFS

Trim Size: 170mm x 244mm Single Column Loose Ribeiro670117 c21.tex V1 - 12/11/2020 8:30pm Page 532

53 Shi, L., Müller, S., Harms, H., and Wick, L.Y. (2008). Factors influencing the electrokinetic dispersion of PAH-degrading bacteria in a laboratory model aquifer. *Applied Microbiology and Biotechnology* 80 (3): 507–515.

54 Deflaun, M.F. and Condee, C.W. (1997). Electrokinetic transport of bacteria. *Journal of Hazardous Materials* 55 (1–3): 263–277.

55 Zhang, H., Ulrich, A.C., and Liu, Y. (2015). Retention and transport of an anaerobic trichloroethene dechlorinating microbial culture in anaerobic porous media. *Colloids and Surfaces. B, Biointerfaces* 130: 110–118. http://dx.doi.org/10.1016/j.colsurfb.2015.04.020.

56 Adrian, L., Szewzyk, U., Wecke, J., and Görisch, H. (2000). Bacterial dehalorespiration with chlorinated benzenes. *Nature* 408 (6812): 580–583. http://proquest.umi.com/pqdweb?did=65143990&Fmt=7&clientId=20870&RQT=309&VName=PQD%5Cn.

57 He, J., Ritalahti, K.M., Yang, K.-L. et al. (2003). Detoxification of vinyl chloride to ethene coupled to growth of an anaerobic bacterium. *Nature* 424 (6944): 62–65. http://www.nature.com/articles/nature01717.

58 Cheng, D. and He, J. (2009). Isolation and characterization of "Dehalococcoides" sp. strain MB, which dechlorinates tetrachloroethene to trans-1,2-dichloroethene. *Applied and Environmental Microbiology* 75 (18): 5910–5918.

59 Lu, C., Broholm, M.M., Fabricius, I.L., and Bjerg, P.L. (2014). Determination of matrix pore size distribution in fractured clayey till and assessment of matrix migration of dechlorinating bacteria. *Bioremediation Journal* 18 (4): 295–308.

60 Ninjgarav, E., Chung, S.-G., Jang, W.-Y., and Ryu, C.-K. (2007). Pore size distribution of pusan clay measured by mercury intrusion porosimetry. *KSCE Journal of Civil Engineering* 11 (3): 133–139. http://link.springer.com/10.1007/BF02823892.

61 Pires, L.F., Borges, F.S., Passoni, S., and Pereira, A.B. (2013). Soil pore characterization using free software and a portable optical microscope. *Pedosphere* 23 (4): 503–510. http://dx.doi.org/10.1016/S1002-0160(13)60043-0.

62 Männik, J., Driessen, R., Galajda, P. et al. (2009). Bacterial growth and motility in sub-micron constrictions. *Proceedings of the National Academy of Sciences of the United States of America* 106 (35): 14861–14866. http://www.pnas.org/cgi/doi/10.1073/pnas.0907542106.

63 Mao, X., Wang, J., Ciblak, A. et al. (2012). Electrokinetic-enhanced bioaugmentation for remediation of chlorinated solvents contaminated clay. *Journal of Hazardous Materials* 213–214: 311–317. https://linkinghub.elsevier.com/retrieve/pii/S0304389412001379.

64 Mikkola, H., Schmale, J.Y., Wesner, W., and Petkovska, S. (2008). Laboratory pre-assays for soil remediation by electro synthesis of oxidants and their electrokinetic distribution. *Journal of Environmental Science and Health Part A* 43 (8): 907–912. http://www.tandfonline.com/doi/abs/10.1080/10934520801974426.

65 Cherepy, N.J. and Wildenschild, D. (2003). Electrolyte Management for Effective Long-Term Electro-Osmotic Transport in Low-Permeability Soils.

UNCORRECTED PROOFS

Trim Size: 170mm x 244mm Single Column Loose Ribeiro670117 c21.tex V1 - 12/11/2020 8:30pm Page 533

Environmental Science & Technology 37 (13): 3024–3030. https://pubs.acs.org/doi/10.1021/es026095h.

66 West, L.J., Stewart, D.I., Binley, A.M., and Shaw, B. (1999). Resistivity imaging of soil during electrokinetic transport. *Engineering Geology* 53 (2): 205–215. https://linkinghub.elsevier.com/retrieve/pii/S0013795299000344.

67 Wu, X., Alshawabkeh, A.N., Gent, D.B. et al. (2007). Lactate Transport in Soil by DC Fields. *Journal of Geotechnical and Geoenviromental Engineering* 133 (12): 1587–1596. http://ascelibrary.org/doi/10.1061/%28ASCE%291090-0241%282007%29133%3A12%281587%29.

68 Wu, X., Gent, D.B., Davis, J.L., and Alshawabkeh, A.N. (2012). Lactate injection by electric currents for bioremediation of tetrachloroethylene in clay. *Electrochimica Acta* 86: 157–163. https://linkinghub.elsevier.com/retrieve/pii/S0013468612010213.

69 Lageman, R. and Pool, W. (2009). Electrokinetic biofences. In: *Electrochemical Remediation Technologies for Polluted Soils, Sediments and Groundwater* (eds. K.R. Reddy and C. Cameselle), 357–366. Hobroken, USA: Wiley.

70 Cox, E., Wang, J., Reynolds, D.et al. (2018). Electrokinetic-enhanced (EK-Enhanced) amendment delivery for remediation of low permeability and heterogene materials. https://clu-in.org/download/techfocus/electrokinetics/EK-ER-201325-FR.pdf.

71 Sprocati, R. and Rolle, M. (2019). Charge interactions, reaction kinetics and dimensionality effects on electrokinetic remediation: a model-based analysis. *Journal of Contaminant Hydrology* (October): 103567. https://linkinghub.elsevier.com/retrieve/pii/S0169772219302736.

72 Gomes, H.I., Dias-Ferreira, C., and Ribeiro, A.B. (2012). Electrokinetic remediation of organochlorines in soil: enhancement techniques and integration with other remediation technologies. *Chemosphere* 87 (10): 1077–1090. http://dx.doi.org/10.1016/j.chemosphere.2012.02.037.

73 Siegrist, R.L., Crimi, M., Thomson, N.R. et al. (2014). In situ chemical oxidation. In: *Chlorinated Solvent Source Zone Remediation*, vol. 7 (eds. B.H. Kueper, H.F. Stroo, C.M. Vogel and C.H. Ward), 253–305. SERDP/ESTC Environmental Remediation Technology.

74 AIA, C., Gerhard, J.I., Reynolds, D. et al. (2017). Electrokinetic-enhanced permanganate delivery and remediation of contaminated low permeability porous media. *Water Research* 113: 215–222. https://linkinghub.elsevier.com/retrieve/pii/S0043135417300805.

75 Roach, N. and Reddy, K.R. (2006). Electrokinetic delivery of permanganate into low-permeability soils. *International Journal of Environment and Waste Management* 1 (1): 4–19. http://www.inderscience.com/link.php?id=11122.

76 Hodges, D., Fourie, A., Thomas, D., and Reynolds, D. (2013). Overcoming permanganate stalling during electromigration. *Journal of Environmental Engineering* 139 (5): 677–684. http://ascelibrary.org/doi/10.1061/%28ASCE%29EE.1943-7870.0000660.

UNCORRECTED PROOFS

Trim Size: 170mm x 244mm Single Column Loose Ribeiro670117 c21.tex V1 - 12/11/2020 8:30pm Page 534

77 Reynolds, D.A., Jones, E.H., Gillen, M. et al. (2008). Electrokinetic migration of permanganate through low-permeability media. *Ground Water* 46 (4): 629–637. http://doi.wiley.com/10.1111/j.1745-6584.2008.00415.x.

78 Matzek, L.W. and Carter, K.E. (2016). Activated persulfate for organic chemical degradation: a review. *Chemosphere* 151: 178–188. https://linkinghub.elsevier.com/retrieve/pii/S0045653516302077.

79 Yukselen-Aksoy, Y. and Reddy, K.R. (2012). Effect of soil composition on electrokinetically enhanced persulfate oxidation of polychlorobiphenyls. *Electrochimica Acta* 86: 164–169.

80 Chowdhury, A.I.A., Gerhard, J.I., Reynolds, D., and O'Carroll, D.M. (2017). Low permeability zone remediation via oxidant delivered by electrokinetics and activated by electrical resistance heating: proof of concept. *Environmental Science & Technology* 51 (22): 13295–13303. https://pubs.acs.org/doi/10.1021/acs.est.7b02231.

81 Fan, G., Cang, L., Fang, G. et al. (2014). Electrokinetic delivery of persulfate to remediate PCBs polluted soils: effect of injection spot. *Chemosphere* 117 (1): 410–418. http://dx.doi.org/10.1016/j.chemosphere.2014.08.006.

82 Zhao, Y., Zhao, Y., Li, Q. et al. (2016). Effect of common inorganic ions on aniline degradation in groundwater by activated persulfate with ferrous iron. *Water Science and Technology: Water Supply* 16 (3): 667–674. https://iwaponline.com/ws/article/16/3/667/27747/Effect-of-common-inorganic-ions-on-aniline.

83 Wu, M.Z., Reynolds, D.A., Fourie, A., and Thomas, D.G. (2013). Optimal field approaches for electrokinetic in situ oxidation remediation. *Ground Water Monitoring & Remediation* 31 (1): 62–74. http://onlinelibrary.wiley.com/doi/10.1111/j.1745-6592.2011.01346.x/abstract.

84 Obiri-Nyarko, F., Grajales-Mesa, S.J., and Malina, G. (2014). An overview of permeable reactive barriers for in situ sustainable groundwater remediation. *Chemosphere* 111: 243–259. http://dx.doi.org/10.1016/j.chemosphere.2014.03.112.

85 Weng, C.H. (2009). Coupled electrokinetic-permeable reactive barriers. In: *Electrochemical Remediation Technologies for Polluted Soils, Sediments and Groundwater* (eds. K.R. Reddy and C. Cameselle), 483–504. Hobroken, NJ: Wiley.

86 Roh, Y., Lee, S.Y., Elless, M.P., and Cho, K.-S. (2000). Electro-enhanced remediation of radionuclide-contaminated groundwater using zero-valent iron. *Journal of Environmental Science and Health Part A* 35 (7): 1043–1059. http://www.tandfonline.com/doi/abs/10.1080/10934520009377019.

87 Zhang, M., Wang, H., Jin, S. et al. (2016). Electrochemically enhanced reduction of trichloroethene by passivated zero-valent iron. *Journal of Environmental Chemical Engineering* 4 (1): 599–604. http://dx.doi.org/10.1016/j.jece.2015.12.013.

88 Pamukcu, S., Hannum, L., and Wittle, J.K. (2008). Delivery and activation of nano-iron by DC electric field. *Journal of Environmental Science and Health Part A* 43 (8): 934–944. http://www.tandfonline.com/doi/abs/10.1080/10934520801974483.

UNCORRECTED PROOFS

Trim Size: 170mm x 244mm Single Column Loose Ribeiro670117 c21.tex V1 - 12/11/2020 8:30pm Page 535

89 Jones, E.H., Reynolds, D.A., Wood, A.L., and Thomas, D.G. (2011). Use of electrophoresis for transporting nano-iron in porous media. *Ground Water* 49 (2): 172–183.

90 Gomes, H.I., Dias-Ferreira, C., Ribeiro, A.B., and Pamukcu, S. (2012). Electrokinetic enhanced transport of zero valent iron nanoparticles for chromium(VI) reduction in soils. *Chemical Engineering Transactions* 28 (Iii): 139–144.

91 Moon, J.-W., Moon, H.-S., Kim, H., and Roh, Y. (2005). Remediation of TCE-contaminated groundwater using zero valent iron and direct current: experimental results and electron competition model. *Environmental Geology* 48 (6): 805–817.

92 Liu, C.-C., Liau, S.-F., and Tseng, D.-H. (2006). Effects of the electrode arrangements on reductive Dechlorination of trichloroethylene in an electro-enhanced Iron wall. *Environmental Technology* 27 (6): 683–693. http://www.tandfonline.com/doi/abs/10.1080/09593332708618681.

93 Bruell, C.J., Segall, B.A., and Walsh, M.T. (1992). Electroosmotic removal of gasoline hydrocarbons and TCE from clay. *Journal of Environmental Engineering* 118: 68–83.

94 Yang, G.C.C. and Yeh, C.-F. (2011). Enhanced nano-Fe3O4/S2O82− oxidation of trichloroethylene in a clayey soil by electrokinetics. *Separation and Purification Technology* 79 (2): 264–271. https://linkinghub.elsevier.com/retrieve/pii/S1383586611001493.

95 Weng, C.-H., Yuan, C., and Tu, H.-H. (2003). Removal of trichloroethylene from clay soil by series-electrokinetic process. *Practice Periodical of Hazardous, Toxic, and Radioactive Waste Management* 7 (1): 25–30. http://ascelibrary.org/doi/10.1061/%28ASCE%291090-025X%282003%297%3A1%2825%29.

96 Chung, H.I. and Lee, M. (2007). A new method for remedial treatment of contaminated clayey soils by electrokinetics coupled with permeable reactive barriers. *Electrochimica Acta* 52 (10): 3427–3431. https://linkinghub.elsevier.com/retrieve/pii/S0013468606010103.

97 Chang, J.H., Qiang, Z., and Huang, C.P. (2006). Remediation and stimulation of selected chlorinated organic solvents in unsaturated soil by a specific enhanced electrokinetics. *Colloids and Surfaces A: Physicochemical and Engineering Aspects* 287 (1–3): 86–93.

98 Chang, J. and Cheng, S. (2006). The remediation performance of a specific electrokinetics integrated with zero-valent metals for perchloroethylene contaminated soils. *Journal of Hazardous Materials* 131 (1–3): 153–162. https://linkinghub.elsevier.com/retrieve/pii/S0304389405005601.

99 Ho, S.V., Athmer, C., Sheridan, P.W. et al. (1999). The Lasagna Technology for In Situ Soil Remediation. 2. Large Field Test. *Environmental Science & Technology* 33 (7): 1092–1099.

100 Ho, S.V., Athmer, C., Sheridan, P.W. et al. (1999). The Lasagna Technology for In situ soil remediation. 1. Small Field Test. *Environmental Science & Technology* 33 (7): 1086–1091.

UNCORRECTED PROOFS

Trim Size: 170mm x 244mm Single Column Loose Ribeiro670117 c21.tex V1 - 12/11/2020 8:30pm Page 536

101 Athmer, C. and Ho, S.V. (2009). Field studies: organic - contaminated soil remediation with lasagna technology. In: *Electrochemical Remediation Technologies for Polluted Soils, Sediments and Groundwater* (eds. K.R. Reddy and C. Cameselle), 625–646. Hobroken, NJ: Wiley.

102 Athmer, C.J. (2014). Use of large-scale electrokinetic and ZVI treatment for chlorinated solvent remediation at an active industrial facility. *Remediation Journal* 24 (4): 41–51. http://doi.wiley.com/10.1002/rem.21403.

103 Hyldegaard, B.H. (2020). *Electrochemical Zone for Degradation of Chlorinated Ethenes in Aquifers*. Technical University of Denmark.

104 Gilbert, D., Sale, T., and Petersen, M.A. (2010). In Situ Remediation of Chlorinated Solvent Plumes. In: *In Situ Remediation of Chlorinated Solvent Plumes* (eds. H.F. Stroo and C.H. Ward), 573–590. New York, NY: Springer New York http://link.springer.com/10.1007/978-1-4419-1401-9.

105 Martínez-Huitle, C.A., Rodrigo, M.A., Sirés, I., and Scialdone, O. (2015). Single and coupled electrochemical processes and reactors for the abatement of organic water pollutants: a critical review. *Chemical Reviews* 115 (24): 13362–13407.

106 Tezuka, M. and Yajima, T. (1991). Electroreductive dechlorination of chloroethylenes. *Denki Kagaku oyobi Kogyo Butsuri Kagaku* 59 (6): 517–518. https://www.jstage.jst.go.jp/article/kogyobutsurikagaku/59/6/59_517/_article.

107 Mao, X., Ciblak, A., Amiri, M., and Alshawabkeh, A.N. (2011). Redox control for electrochemical Dechlorination of trichloroethylene in bicarbonate aqueous media. *Environmental Science & Technology* 45 (15): 6517–6523.

108 Petersen, M.A., Sale, T.C., and Reardon, K.F. (2007). Electrolytic trichloroethene degradation using mixed metal oxide coated titanium mesh electrodes. *Chemosphere* 67 (8): 1573–1581.

109 Aulenta, F., Tocca, L., Verdini, R. et al. (2011). Dechlorination of trichloroethene in a continuous-flow bioelectrochemical reactor: effect of cathode potential on rate, selectivity, and electron transfer mechanisms. *Environmental Science & Technology* 45 (19): 8444–8451.

110 Farrell, J., Melitas, N., Kason, M., and Li, T. (2000). Electrochemical and column investigation of iron-mediated reductive dechlorination of trichloroethylene and perchloroethylene. *Environmental Science & Technology* 34 (12): 2549–2556.

111 Wang, J. and Farrell, J. (2003). Investigating the role of atomic hydrogen on chloroethene reactions with iron using Tafel analysis and electrochemical impedance spectroscopy. *Environmental Science & Technology* 37 (17): 3891–3896.

112 Huang, B., Long, J., Chen, W. et al. (2016). Linear free energy relationships of electrochemical and thermodynamic parameters for the electrochemical reductive dechlorination of chlorinated volatile organic compounds (Cl-VOCs). *Electrochimica Acta* 208: 195–201. http://linkinghub.elsevier.com/retrieve/pii/S0013468616310702.

113 Lakshmipathiraj, P., Bhaskar Raju, G., Sakai, Y. et al. (2012). Studies on electrochemical detoxification of trichloroethene (TCE) on Ti/IrO_2-Ta_2O_5 electrode

UNCORRECTED PROOFS

Trim Size: 170mm x 244mm Single Column Loose Ribeiro670117 c21.tex V1 - 12/11/2020 8:30pm Page 537

from aqueous solution. *Chemical Engineering Journal* 198–199: 211–218. http://dx.doi.org/10.1016/j.cej.2012.05.092.

114 Cheng, M., Zeng, G., Huang, D. et al. (2016). Hydroxyl radicals based advanced oxidation processes (AOPs) for remediation of soils contaminated with organic compounds: A review. *Chemical Engineering Journal* 284: 582–598. http://dx.doi.org/10.1016/j.cej.2015.09.001.

115 Yuan, S., Mao, X., and Alshawabkeh, A.N. (2012). Efficient degradation of TCE in groundwater using Pd and electro-generated H_2 and O_2: a shift in pathway from Hydrodechlorination to oxidation in the presence of ferrous ions. *Environmental Science & Technology* 46 (6): 3398–3405.

116 Yuan, S., Chen, M., Mao, X., and Alshawabkeh, A.N. (2013). A three-electrode column for Pd-catalytic oxidation of TCE in groundwater with automatic pH-regulation and resistance to reduced sulfur compound foiling. *Water Research* 47 (1): 269–278. http://dx.doi.org/10.1016/j.watres.2012.10.009.

117 Verdini, R., Aulenta, F., de Tora, F. et al. (2015). Relative contribution of set cathode potential and external mass transport on TCE dechlorination in a continuous-flow bioelectrochemical reactor. *Chemosphere* 136: 72–78. http://linkinghub.elsevier.com/retrieve/pii/S0045653515003422.

118 Lohner, S.T., Becker, D., Mangold, K.M., and Tiehm, A. (2011). Sequential reductive and oxidative biodegradation of chloroethenes stimulated in a coupled bioelectro-process. *Environmental Science & Technology* 45 (15): 6491–6497.

119 Aulenta, F., Verdini, R., Zeppilli, M. et al. (2013). Electrochemical stimulation of microbial cis-dichloroethene (cis-DCE) oxidation by an ethene-assimilating culture. *New Biotechnology* 30 (6): 749–755. http://dx.doi.org/10.1016/j.nbt.2013.04.003.

120 Tiehm, A., Lohner, S.T., and Augenstein, T. (2009). Effects of direct electric current and electrode reactions on vinyl chloride degrading microorganisms. *Electrochimica Acta* 54 (12): 3453–3459.

121 Brewster, J.H. (1954). Mechanisms of Reductions at Metal Surfaces. I. A General Working Hypothesis. *Journal of the American Chemical Society* 76 (24): 6361–6363. http://pubs.acs.org/doi/abs/10.1021/ja01653a034.

122 Roberts, A.L., Totten, L.A., Arnold, W.A. et al. (1996). Reductive elimination of chlorinated ethylenes by zero-valent metals. *Environmental Science & Technology* 30 (8): 2654–2659.

123 Wiedemeier, T.H., Rifai, H.S., Newell, C.J., and Wilson, J.T. (1999). Overview of intrinsic bioremediation. In: *Natural Attenuation of Fuels and Chlorinated Solvents in the Subsurface* (eds. T.H. Wiedemeier, H.S. Rifai, C.J. Newell and J.T. Wilson), 162–188. Wiley https://linkinghub.elsevier.com/retrieve/pii/S0169772299000996.

124 Arnold, W.A. and Roberts, A.L. (2000). Pathways and kinetics of chlorinated ethylene and chlorinated acetylene reaction with Fe(O) particles. *Environmental Science & Technology* 34: 1794–1805.

125 Zumdahl, S.S. (2009). Electrochemistry. In: *Chemical Principles*, 6e (eds. R.B. Schwartz, C.L. Brooks and A. Galvin), 472–520. Boston, MA: Houghton Mifflin Company.

UNCORRECTED PROOFS

Trim Size: 170mm x 244mm Single Column Loose Ribeiro670117 c21.tex V1 - 12/11/2020 8:30pm Page 538

126 Fallgren, P.H., Eisenbeis, J.J., and Jin, S. (2018). In situ electrochemical manipulation of oxidation-reduction potential in saturated subsurface matrices. *Journal of Environmental Science and Health Part A* 53 (6): 517–523. https://doi.org/10.1080/10934529.2017.1422951.

127 Strandgaard Andersen, E., Jespersgaard, P., and Østergaard, O. (1993). Datbog fysik kemi. In: , 8e (eds. E. Strandgaard Andersen, P. Jespersgaard and O. Østergaard), 1–272. Copenhagen, DK: F & K Forlaget.

128 Nazaroff, W.W. and Alvarez-Cohen, L. (eds.) (2010). A Further Look at Transformation Processes. In: *Environmental Engineering Science*, 641–650. New York, USA: Wiley.

129 Appelo, C.A.J. and Postma, D. (2010). Redox Processes. In: *Geochemistry, Groundwater and Pollution*, 2e (eds. C.A.J. Appelo and D. Postma), 415–487. Leiden, The Netherlands: CRC Press LLC.

130 Rajic, L., Fallahpour, N., Nazari, R., and Alshawabkeh, A.N. (2015). Influence of humic substances on electrochemical degradation of trichloroethylene in limestone aquifers. *Electrochimica Acta* 181: 123–129. http://dx.doi.org/10.1016/j.electacta.2015.03.121.

131 Fallahpour, N., Mao, X., Rajic, L. et al. (2017). Electrochemical dechlorination of trichloroethylene in the presence of natural organic matter, metal ions and nitrates in a simulated karst media. *Journal of Environmental Chemical Engineering* 5 (1): 240–245. http://dx.doi.org/10.1016/j.jece.2016.11.046.

132 Xie, W., Yuan, S., Mao, X. et al. (2013). Electrocatalytic activity of Pd-loaded Ti/TiO2 nanotubes cathode for TCE reduction in groundwater. *Water Research* 47 (11): 3573–3582. http://dx.doi.org/10.1016/j.watres.2013.04.004.

133 Mao, X., Yuan, S., Fallahpour, N. et al. (2012). Electrochemically induced dual reactive barriers for transformation of TCE and mixture of contaminants in groundwater. *Environmental Science & Technology* 46 (21): 12003–12011. https://doi.org/10.0.3.253/es301711a.

134 Rajic, L., Fallahpour, N., Podlaha, E., and Alshawabkeh, A.N. (2016). The influence of cathode material on electrochemical degradation of trichloroethylene in aqueous solution. *Chemosphere* 147: 98–104. http://linkinghub.elsevier.com/retrieve/pii/S0045653515305506.

135 Hyldegaard, B.H., Ottosen, L.M., and Alshawabkeh, A.N. (2020). Transformation of tetrachloroethylene in a flow-through electrochemical reactor. *Science of the Total Environment* 707: 135566. https://doi.org/10.1016/j.scitotenv.2019.135566.

136 Rajic, L., Fallahpour, N., and Alshawabkeh, A.N. (2015). Impact of electrode sequence on electrochemical removal of trichloroethylene from aqueous solution. *Applied Catalysis B: Environmental* 174–175: 427–434. http://dx.doi.org/10.1016/j.apcatb.2015.03.018.

137 Rajic, L., Fallahpour, N., Yuan, S., and Alshawabkeh, A.N. (2014). Electrochemical transformation of trichloroethylene in aqueous solution by electrode polarity reversal. *Water Research* 67: 267–275. http://dx.doi.org/10.1016/j.watres.2014.09.017.

UNCORRECTED PROOFS

Trim Size: 170mm x 244mm Single Column Loose Ribeiro670117 c21.tex V1 - 12/11/2020 8:30pm Page 539

138 Rajic, L., Fallahpour, N., Oguzie, E., and Alshawabkeh, A.N. (2015). Electrochemical transformation of thichloroethylene in groundwater by Ni-containing cathodes. *Electrochimica Acta* 181: 118–122.

139 Rajic, L., Nazari, R., Fallahpour, N., and Alshawabkeh, A.N. (2016). Electrochemical degradation of trichloroethylene in aqueous solution by bipolar graphite electrodes. *Journal of Environmental Chemical Engineering* 4 (1): 197–202. http://www.ncbi.nlm.nih.gov/pubmed/26955517.

140 Carter, K.E. and Farrell, J. (2009). Electrochemical oxidation of trichloroethylene using boron-doped diamond film electrodes. *Environmental Science & Technology* 43 (21): 8350–8354.

141 Parkhurst, D.L. and Appelo, C.A.J. (2013). Description of input and examples for PHREEQC version 3 - A computer program for speciation, batch-reaction, one-dimensional transport, and inverse geochemical calculations. U.S. Geological Survey Techniques and Methods, book 6, chapter A43, p. 497. http://pubs.usgs.gov/tm/06/a43.

142 Leenson, I.A. (2009). Old rule of thumb and the Arrhenius equation. *Journal of Chemical Education* 76 (10): 1459–1460.

143 Sundstrom, D.W., Klei, H.E., Nalette, T.A. et al. (1986). Destruction of halogenated Aliphatics by ultraviolet catalyzed oxidation with hydrogen peroxide. *Hazardous Waste & Hazardous Materials* 3 (1): 101–110. http://www.liebertpub.com/doi/10.1089/hwm.1986.3.101.

144 Hyldegaard, B.H. and Ottosen, L.M. (2020). Selecting electrode materials and sequence for electrochemical removal of chlorinated ethenes in groundwater. *Water, Air, and Soil Pollution* 231 (6) https://doi.org/10.1007/s11270-020-04641-8.

145 Pamukcu, S., Ghazanfari, E., and Wittle, K. (2014). Reduction of Contaminants in Soil and Water By Direct Electric Current. In: *Electrokinetics for Petroleum and Environmental Engineers* (eds. G.V. Chilingar and M. Haroun), 33–101. Wiley.

146 Skibsted, G., Ottosen, L.M., Elektorowicz, M., and Jensen, P.E. (2018). Effect of long-term electrodialytic soil remediation on Pb removal and soil weathering. *Journal of Hazardous Materials* 358 (October 2017): 459–466. https://doi.org/10.1016/j.jhazmat.2018.05.033.

147 Bagastyo, A.Y., Radjenovic, J., Mu, Y. et al. (2011). Electrochemical oxidation of reverse osmosis concentrate on mixed metal oxide (MMO) titanium coated electrodes. *Water Research* 45 (16): 4951–4959.

148 Zhao, Y., Yang, H., Liu, S. et al. (2016). Effects of metal ions on disinfection byproduct formation during chlorination of natural organic matter and surrogates. *Chemosphere* 144: 1074–1082. http://dx.doi.org/10.1016/j.chemosphere.2015.09.095.

149 Rebelo, A., Ferra, I., Marques, A., and Silva, M.M. (2016). Wastewater reuse: modeling chloroform formation. *Environmental Science and Pollution Research* 23 (24): 24560–24566. http://dx.doi.org/10.1007/s11356-016-7749-z.

UNCORRECTED PROOFS

Trim Size: 170mm x 244mm Single Column Loose Ribeiro670117 c21.tex V1 - 12/11/2020 8:30pm Page 540

150 Chaidou, C.I., Georgakilas, V.I., Stalikas, C. et al. (1999). Formation of chloroform by aqueous chlorination of organic compounds. *Chemosphere* 39 (4): 587–594.

151 Sonoyama, N. and Sakata, T. (1999). Electrochemical continuous decomposition of chloroform and other volatile chlorinated hydrocarbons in water using a column type metal impregnated carbon fiber electrode. *Environmental Science & Technology* 33 (19): 3438–3442. https://pubs.acs.org/doi/10.1021/es980903g.

152 Chen, G., Betterton, E.A., Arnold, R.G., and Ela, W.P. (2003). Electrolytic reduction of trichloroethylene and chloroform at a Pt- or Pd-coated ceramic cathode. *Journal of Applied Electrochemistry* 33 (2): 161–169.

153 Velázquez, J.C., Leekumjorn, S., Hopkins, G.D. et al. (2016). High activity and regenerability of a palladium–gold catalyst for chloroform degradation. *Journal of Chemical Technology and Biotechnology* 91 (10): 2590–2596.

154 McNab, W.W. and Ruiz, R. (1998). Palladium-catalyzed reductive dehalogenation of dissolved chlorinated aliphatics using electrolytically-generated hydrogen. *Chemosphere* 37 (5): 925–936.

155 Molina, V.M., González-Arjona, D., Roldán, E., and Dominguez, M. (2002). Electrochemical reduction of tetrachloromethane. Electrolytic conversion to chloroform. *Collection of Czechoslovak Chemical Communications* 67 (3): 279–292.

156 Sale, T., Petersen, M.A., and Gilbert, D. (2005). Electrically induced redox barriers for treatment of groundwater. https://clu-in.org/download/contaminantfocus/dnapl/Treatment_Technologies/CU-0112-fr-01.pdf.

157 Sale, T., Petersen, M.A., and Gilbert, D. (2008). Electrically induced redox barriers for treatment of groundwater. Technical report.

158 Mandelbaum, R., Mandelbaum, G., Elgressy, E., et al. (2019). Integrated biogeochemical / electrochemical method for remediation of contaminated groundwater. 5th International Symposium on Bioremediation & Sustainable Technologies (Battelle), Baltimore, USA. Provectus Environmental Products. https://www.provectusenvironmental.com/ebr/Mueller_EBR_Final.pdf.

159 Elgressy, E. (2015). Breakdown of fuel components and solvents in groundwater and contaminated soil. US patent 9975156B2, filed 3 December 2015, issued 22 May 2018. www.provectusenvironmental.com/p-ebr/US9975156B2.pdf.

160 Provectus Environmental Products. (2019). Provect-EBR® ISCO Generator technical data sheet. https://www.provectusenvironmental.com/p-ebr/Provect-EBR_TDS_FINAL.pdf.

161 Hojabri, S., Rajic, L., and Alshawabkeh, A.N. (2018). Transient reactive transport model for physico-chemical transformation by electrochemical reactive barriers. *Journal of Hazardous Materials* 358 (June): 171–177. https://doi.org/10.1016/j.jhazmat.2018.06.051.

UNCORRECTED PROOFS

Trim Size: 170mm x 244mm Single Column Loose Ribeiro670117 c22.tex V1 - 12/12/2020 12:31am Page 541

22

Chlorophenolic Compounds and Their Transformation Products by the Heterogeneous Fenton Process: A Review

Cetin Kantar and Ozlem Oral

Department of Environmental Engineering, Canakkale Onsekiz Mart University, Canakkale 17020, Turkey

22.1 Introduction

Chlorophenols (CPs) are prevalent refractory organic contaminants that enter natural systems through industrial activities involving the production of paper, pharmaceuticals, pesticides, fungicides, herbicides, antiseptics, dye, and plastics [1–3]. CPs have also been used as wood preservatives in many countries [4]. In addition, they are produced as reaction by-products during chlorine disinfection of drinking water, biodegradation of chlorinated organic compounds, and incomplete incineration of organic hazardous waste [2, 5, 6]. Worldwide CP production exceeding 200 000 tons per year has been reported in the literature [6]. Due to their low biodegradability, high toxicity, and mutagenic, teratogenic, and carcinogenic characteristics [7–9], several CPs are classified as priority toxic compounds by the US EPA under the Clean Water Act [10] and by the European Parliament under Decision No. 2455/2001/CE.

Chlorophenols are phenolic compounds with one [e.g. 2-CP, 3-CP, 4-CP, etc.] or more chlorine atoms [e.g. 2,3-DCP, 2,3,4-TCP, 2,3,5-TCP, 2,4,5-TCP, 2,3,4,6-TeCP, PCP] attached to the benzene ring. A list of chlorophenolic compounds with selected physical and chemical properties is given in Table 22.1. The toxicity of chlorophenols varies depending on the position and number of Cl atoms associated with the benzene structure [11]. For instance, CPs with a Cl atom attached to position 2 (*ortho*) in the benzene ring relative to the phenolic group (OH^-) have been shown to exhibit the least toxic properties, as opposed to CPs with Cl atoms located on the *meta* or *para* position [11]. Also, the toxicity of CPs is observed to increase when the number of Cl atoms in the benzene ring decreases [11, 12].

The mobility of CPs in natural systems depends greatly on the degree of their water solubility, their partition coefficient (pK_a), and their hydrophobic characteristics ($\log K_{ow}$). As shown in Table 22.1, the solubility of CPs decreases when the number of Cl atoms increases, suggesting that monochlorophenols are more mobile in the environment relative to multichlorophenols. Due to their relatively high solubility in water, CPs can migrate rapidly through different layers of environmental

Electrokinetic Remediation for Environmental Security and Sustainability, First Edition.
Edited by Alexandra B. Ribeiro and M.N.V. Prasad.
© 2021 John Wiley & Sons Ltd. Published 2021 by John Wiley & Sons Ltd.

UNCORRECTED PROOFS

Trim Size: 170mm x 244mm Single Column Loose Ribeiro670117 c22.tex V1 - 12/12/2020 12:31am Page 542

Table 22.1 Selected physical and chemicals properties of chlorophenols.

Compound	Chemical formula	Solubility (mg/L) (20 °C)	pK_a	Log K_{ow}	Henry's Law constant (atm-cu m/mol at 25 °C)
2-chlorophenol (2-CP)	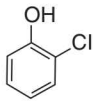	11 300	8.56	2.15	1.12×10^{-5}
3-chlorophenol (3-CP)	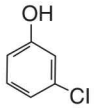	26 000	9.12	2.5	3.45×10^{-7}
4-chlorophenol (4-CP)	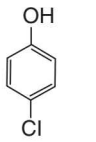	24 000	9.41	2.39	6.27×10^{-7}
2,3-dichlorophenol (2,3-DCP)	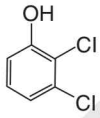	3 600	7.7	2.84	3.08×10^{-7}
2,4-dichlorophenol (2,4-DCP)	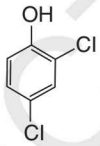	6 000	7.9	3.06	4.29×10^{-6}
2,6-dichlorophenol (2,6-DCP)	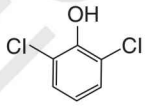	1900	6.79	2.75	2.67×10^{-6}
3,5-dichlorophenol (3,5-DCP)	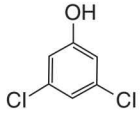	5380	8.18	3.62	2.44×10^{-7}
2,4,5-trichlorophenol (2,4,5-TCP)	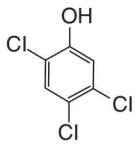	1200	7.43	3.72	2.21×10^{-6}
2,4,6-trichlorophenol (2,4,6-TCP)	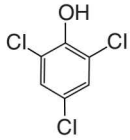	500	6.23	3.69	4.2×10^{-6}

(*continued*)

UNCORRECTED PROOFS

Trim Size: 170mm x 244mm Single Column Loose Ribeiro670117 c22.tex V1 - 12/12/2020 12:31am Page 543

Table 22.1 (Continued)

Compound	Chemical formula	Solubility (mg/L) (20 °C)	pK_a	Log K_{ow}	Henry's Law constant (atm-cu m/mol at 25 °C)
3,4,5-trichlorophenol (3,4,5-TCP)	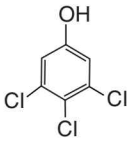	<1000	7.84	4.01	2.3×10^{-7}
2,3,4,6-tetrachlorophenol (2,3,4,6-TeCP)	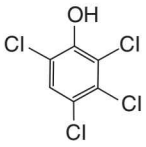	1000	5.22	4.45	1.3×10^{-6}
2,3,5,6-tetrachlorophenol (2,3,5,6-TeCP)	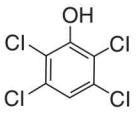	<1000	5.14	3.88	3.5×10^{-7}
Pentachlorophenol (PCP)	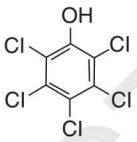	14	4.70	5.12	2.45×10^{-8}

Source: Chemical data from [147, 148].

systems and easily enter the food chain, thus creating a significant health concern for humans and other living organisms. For instance, although CP concentrations reported for natural systems are usually in the ng/l to μg/l range [11, 13–16], CP concentrations up to 190 mg l^{-1} in have been reported in polluted surface and groundwater [17, 18]. Due to their relatively high log K_{ow} values, they can also interact with hydrophobic cell membranes via hydrophobic bonding and thus bio-accumulate in living organisms and organic matter fractions of soils, thereby causing acute and chronic toxicity in aquatic organisms [6, 19, 20]. As shown in Table 22.1, the pK_a values, which show the degree and extent of ionization, decrease with an increasing number of Cl atoms associated with the aromatic ring. This suggests that chlorophenols with high pK_a values (e.g. multichlorophenols) interact more strongly with oxide surfaces via chemical bonding (e.g. ≡FeO—CP) than monochlorophenols do, leading to their accumulation in soils and sediments [20] because CPs with high pK_a values dissociate at high pH values.

A number of chemical and biological treatment methods have been proposed for treating wastewater containing CPs. Degrading CPs by biological methods can be achieved under both aerobic and anaerobic conditions using bacteria and fungi [20–26]. Despite the low cost of biodegradation, biological treatment methods suffer from some significant drawbacks, usually associated with the toxic nature of chlorophenolic compounds, which leads to a significant inhibition in biomass growth and process sustainability [23, 27, 28]. The incomplete biodegradation

UNCORRECTED PROOFS

Trim Size: 170mm x 244mm Single Column Loose Ribeiro670117 c22.tex V1 - 12/12/2020 12:31am Page 544

of CPs is usually explained through difficulties in the breakage of C—Cl bonds associated with the aromatic structure as well as the generation of more toxic and less biodegradable reaction intermediate species [27, 28].

Alternatives to biological treatment methods are chemical processes, including adsorption, air stripping, solvent extraction, and chemical oxidation using strong oxidants [12, 26, 29, 30]. Of all these treatment methods, advanced oxidation processes (AOPs) have received significant attention from researchers due to their high removal efficiency, high reaction rates, low waste (e.g. sludge) generation, and applicability to a wide variety of wastewaters containing recalcitrant compounds [31–35]. The Fenton process is a widely used AOP for treating biologically low-degradable organic compounds due to its simplicity, ease of operation, short reaction times, high level of performance, and low capital cost [32, 35–39]. The Fenton process relies on generating peroxy (HO_2^*) and reactive hydroxyl radicals (HO^*) via a reaction involving H_2O_2 as the oxidant and Fe^{2+} as the catalyst [40, 41]:

$$Fe^{2+} + H_2O_2 = Fe^{3+} + HO^* + OH^* \quad (22.1)$$

$$Fe^{3+} + H_2O_2 = Fe^{2+} + HO_2^* + H^+ \quad (22.2)$$

Of all the radicals, HO^* has been reported to be the most significant and dominant radical responsible for degrading chlorophenolic compounds with the Fenton process [5, 42–46]. In the conventional homogenous Fenton process, Fe^{2+} is supplied to the reactor in the form of soluble $FeSO_4$, and thus, radical generation (Reactions (22.1) and (22.2)) and the degradation of organic contaminants takes place in solution under acidic conditions (pH < 4). Despite the fact that the conventional homogenous Fenton process has been widely used in treating chlorophenolic compounds [5, 7, 42–52], it has some significant drawbacks, including high chemical cost, excess sludge production in the form of $Fe(OH)_{3[S]}$, limited pH application range (pH 2–4), and problems associated with catalyst recycling and sludge handling [32]. In addition, the conventional Fenton reaction requires very high catalyst dosages of more than 80 mg l^{-1} to achieve desired contaminant removal efficiencies [32]. While the initial reaction rate is fast due to the fast generation and high oxidation capacity ($E^0 = 2.80$ V) of HO^* radicals, the degradation reaction rate decreases with time due to the depletion of Fe^{2+} and subsequent generation of Fe^{3+} in the bulk solution (Reaction 22.1); this in turn reacts with H_2O_2 to form HO_2* radicals with a much lower potential ($E^0 = 1.65$ V) [53]. Also, the rapid precipitation of Fe^{3+} to $Fe(OH)_{3[S]}$ sludge in the system at pH > 4 may lead to an inhibition of further Fenton reactions [54, 55]. The efficiency of the Fenton process is highly dependent on systems conditions. For instance, the presence of excess concentrations of catalyst and H_2O_2 can adversely affect process efficiency due to their scavenging effect on HO^* radicals [54]:

$$Fe^{2+} + HO^* = Fe^{3+} + OH^- \quad (22.3)$$

$$HO^* + H_2O_2 = HO_2^* + H_2O \quad (22.4)$$

UNCORRECTED PROOFS

Trim Size: 170mm x 244mm Single Column Loose Ribeiro670117 c22.tex V1 - 12/12/2020 12:31am Page 545

An alternative to the conventional Fenton process is the heterogeneous Fenton process, which uses a solid-based catalyst material instead of $FeSO_4$. Unlike the homogenous Fenton process, heterogeneous Fenton processes allow the generation of HO^* radicals on the catalyst surface and extend the application pH range higher than pH 4 without requiring effluent neutralization after the Fenton process [35]. The catalysts used are environmentally friendly and non-corrosive and can be found in large quantities in the environment [35]. Removing organic contaminants via heterogeneous Fenton reactions may be explained through several different mechanisms, including (i) the sorption of contaminants onto the catalyst surface followed by oxidative degradation with in situ generated surface HO^* radicals; and (ii) homogenous oxidative degradation of organic contaminants in the bulk phase caused by surface-dissolved iron [56, 57]. Although a number of excellent review papers have been published on CP treatment by the conventional Fenton process (e.g. [5]), there is no paper summarizing data on the performance of heterogeneous Fenton processes for degrading CPs. This chapter focuses on new developments regarding the application of heterogeneous Fenton processes to treat chlorophenolic compounds with physical/chemical factors affecting CP degradation. Reaction mechanisms, the type and toxicity of reaction intermediates, and possible reactor configurations are also discussed.

22.2 Heterogeneous Fenton Processes

Heterogeneous Fenton processes have many advantages over the homogenous Fenton process, including a much wider optimum pH range, higher removal efficiency, low chemical cost, less iron leaching, reduced sludge production, and long-term use (stability) of catalyst materials. The catalyst surfaces remain active during successive treatments by continuously generating in situ HO^* radicals from H_2O_2, and thus minimizing Fe precipitation on the surface [58]. Due to the low generation of sludge, the extra cost associated with sludge handling after the treatment is minimized [59–64]. Heterogeneous catalyst materials can also allow the in situ generation of H_2O_2 on the catalyst surface, thus minimizing the external use of excess H_2O_2 and making it possible to directly oxidize the organic contaminant on the catalyst surface [65–69]. In the heterogeneous Fenton process, reaction efficiency is greatly influenced by physical and chemical catalyst properties including catalyst size, surface area, surface morphology, porosity, and type and number of surface groups associated with the catalyst [35, 59]. Catalytic activity can also be enhanced through surface amendments and modifications [57, 70, 71]. On the other hand, mass-transfer limitations may have a major influence on reaction rates because oxidation reactions take place directly on the catalyst surface [72]. The heterogeneous Fenton process may also suffer from the oxidation and accumulation of Fe [III] as $Fe(OH)_{3(S)}$ on the catalyst surface, thus leading to surface passivation and inhibition of further Fenton reactions [56, 57].

UNCORRECTED PROOFS

Trim Size: 170mm x 244mm Single Column Loose Ribeiro670117 c22.tex V1 - 12/12/2020 12:31am Page 546

22.2.1 Effect of Catalyst Type and Possible Reaction Mechanisms

Both natural and synthetic materials have been widely used as Fe sources (catalysts) in heterogeneous Fenton treatment of chlorophenolic compounds. The most common solid catalyst materials used include Fe (hydr)oxide and sulfides (e.g. pyrite (FeS_2) ([56, 57, 73]), magnetite (Fe_3O_4) ([3, 61, 63, 74, 75], hematite (Fe_2O_3) [3], ferrihydrite [76], goethite (α-FeOOH) [35, 59, 69, 76, 77]), zero-valent iron (ZVI) (Fe^0) [3, 62, 64, 65, 78–80], multimetallic iron particles [9, 25, 62, 75, 81–87], supported iron-based materials [87–100], and horseradish peroxidase (HRP)-based materials [101].

Of the natural catalyst materials, pyrite and magnetite are most commonly used to treat chlorinated organic compounds since they are easily accessible and cheap due to their natural formation in the Earth's crust [102, 103]. In heterogeneous Fenton systems involving natural catalysts such as pyrite, removing chlorophenolic compounds is primarily controlled by combining organic compound degradation with heterogeneous surface-bound HO^* radicals and homogeneous solution-bound HO^* radicals regulated by iron leaching from the catalyst surface [56, 57]. However, the aggregation of nano- or micro-sized pyrite or magnetite particles due to intraparticle interactions and Fe precipitation associated with Fe leaching from the catalyst surface hurt process efficiency and sustainability [35, 102].

In addition to natural catalyst materials, iron-based synthesized catalysts including ZVI, multimetallic, and supported iron-based materials have also been used in treating chlorophenols [3, 61–64]. They offer solutions to overcome difficulties associated with the homogenous or heterogeneous Fenton process with natural catalysts, including limited operating pH range, iron leaching from the catalyst surface, aggregation of catalyst particles, sludge processing after pH adjustment, decreasing catalytic activity caused by catalyst consumption, and slow reaction kinetics. These synthesized catalysts can easily be separated from the effluent after reaction and are generally reusable for a number of treatment cycles [61, 75, 79, 84, 89, 90, 97]. These materials are usually synthesized in the nano scale to increase their surface area and surface reactivity. They are also specifically modified so that iron becomes trapped within the solid matrix or within the interlayer space of the porous structure to prevent iron leaching and subsequent Fe precipitation [58]. Therefore, the catalyst surface can preserve its ability to produce HO^* radicals from the decomposition of H_2O_2.

In supported iron-based catalysts, the support materials used include carbon-based materials (e.g. activated carbon, graphite, graphene oxide [GO], and carbon nanotubes [CNTs]), aerogels, ion-exchange resins, organic polymers (e.g. alginate), and silicate-based materials (e.g. zeolite, quartz, sepiolite, and pillared interlayered clays [PILCs]) [35, 102, 104, 105]. Incorporating iron oxides/particles as a catalyst into highly porous structures such as activated carbon and clays as the support materials reduces the risk of particle aggregation and thus improves the stability and reactivity of iron oxides/particles [25, 35]. Although the role of adsorption for pollutant removal is not clearly established, several authors report that, due to their highly porous structure and high surface area, these

UNCORRECTED PROOFS

Trim Size: 170mm x 244mm Single Column Loose Ribeiro670117 c22.tex V1 - 12/12/2020 12:31am Page 547

support materials contain a large number of reactive binding sites. The presence of such reactive sites creates a synergistic effect for the adsorption and subsequent oxidation of pollutants on the catalyst surface [35]. But other authors argue that the pollutants adsorbed onto support materials such as activated carbon become non-reactive and thus are not available for oxidation with HO^* radicals [106]. Unlike homogenous systems or heterogeneous systems with natural catalysts, in systems involving synthesized catalysts, organic compounds are oxidized by surface-bound HO^* radicals generated from surface reactions. The reaction mechanism is rather complex and involves a series of surface reactions occurring consecutively (i.e. pollutant sorption onto the catalyst surface, followed by surface-bound Fenton oxidation with interfacial HO^* radicals) [56, 57, 72]. Although several studies report on the role of support materials to decompose H_2O_2, the decomposition of H_2O_2 to HO^* radicals is still believed to be primarily driven by iron materials [72, 107].

A number of authors have recently focused on incorporating other metals into iron-based materials to enhance in situ catalytic transformation of O_2 into H_2O_2 by Fe or Fe-containing materials and thus improving the generation of HO^* radicals from the decomposition of H_2O_2 [69, 81, 85, 86]. The most common metals used are C(IV), Cu(II), Ni (II), Co(III), and Mn (III or V). In this multimetallic systems, while the second metal improves reactivity by enhancing the Fe redox cycle and activating H_2O_2 decomposition, the decomposition of H_2O_2 to HO^* radicals is primarily driven by Fe [25, 69, 72, 82, 83, 108].

22.2.1.1 Iron Oxides

Iron oxide minerals are ubiquitous in natural systems and can act as a catalyst in the heterogeneous Fenton degradation of chlorophenolic compounds [61, 76, 77, 109]. A list of studies using Fe-oxides as the catalyst in the Fenton degradation of CPs is shown in Table 22.2. In addition to being abundant in nature, Fe oxides such as magnetite (Fe_3O_4) have very high Fe^{2+} and Fe^{3+} content and exhibit magnetic properties, making it possible for these materials to be easily separated from the effluent and used in the next treatment cycle.

The most common oxide minerals used as a catalyst in the Fenton process include goethite, ferrihydrite, hematite, and magnetite [61, 63, 76, 110]. The efficacy of oxide minerals to generate HO^* radicals from H_2O_2 is greatly influenced by several factors including H_2O_2 concentration, type of oxide mineral, particle size, solution pH, and contaminant properties [58, 59, 61, 77, 109]. For instance, a study by Huang et al. [76] showed that although the catalytic activity of oxide minerals for H_2O_2 decomposition decreased in the order ferrihydrite > goethite > hematite, the highest 2-CP removal was achieved in systems with hematite as the catalyst. Lu [59] showed that 2-CP removal with a goethite-Fenton system was significantly related to the goethite particle size, with 2-CP oxidation increasing with a decrease in particle size. Although a number of different reaction mechanisms involving adsorption and oxidation have been proposed, CP degradation by Fe-oxide Fenton systems is shown to be primarily regulated by the degree of Fe^{2+} leaching from the catalyst surface, followed by homogenous generation of HO^* radicals in the bulk solution (Reaction (22.1)) [59, 77, 110]. For instance, Xu and Wang [61] showed that while

UNCORRECTED PROOFS

UNCORRECTED PROOFS

Trim Size: 170mm x 244mm Single Column Loose

Table 22.2 Monometallic catalysts including Fe-oxides, pyrite, and zero-valent iron for CP degradation in Fenton reactions.

Compound	CP concentration	Catalyst	Experimental conditions	Treatment efficiency	Rate constant (min^{-1})	By-products	Ref
2-CP	50 mg l^{-1}	Zero valent iron	pH = 3 Catalyst = 0–44 mg l^{-1}	80%	—	Chlorobenzoquinone Chlorohydroquinone	[78]
2-CP	52.2 mg l^{-1}	Goethite	pH = 3 Catalyst = 0.5–2 g l^{-1}	99%	—	Chlorobenzoquinone Chlorohydroquinone	[77]
2-CP	0.31 mM	Goethite	pH = 3 Catalyst = 0.2–0.8 g l^{-1} Ligand = 0.1–1 mM H_2O_2 = 0-3.92 mM	100%	—	—	[110]
2-CP	15 mg l^{-1}	Iron oxides	pH = 5.8-8.4 Catalyst = 9.8–17.8 mM H_2O_2 = 0.98-9.8 mM	4% (granular ferrihydrite) 9% (goethite) 15% (hematite)	—	—	[76]
2-CP	50 mg l^{-1}	Goethite	pH = 3 Catalyst = 0.1–0.8 g l^{-1} catalyst diameter = 0.21–0.044 mm H_2O_2 = 75 m g l^{-1}	100%	—	—	[59]
4-CP	0.2 mM	Zero valent iron	pH = 7 Catalyst = 1 g l^{-1} Ligand = 2 mM	56.2%	—	—	[71]
4-CP	128.6 mg l^{-1}	Pyrite	pH = 5–11 H_2O_2 = 0–50 mM	99% (FeS_2@GO) 97% (FeS_2)	—	Oxalic acid Acetic acid Chloroacetic acid	[73]

Ribeiro67017 c22.tex V1 - 12/12/2020 12:31am Page 548

4-CP	100 mg l^{-1}	Zero valent iron	pH = 3–4 Catalyst = 0.1–1 g l^{-1} H_2O_2 = 94.9–39.16 mM	100%	—	—	[111]
4-CP	50–200 mg l^{-1}	Zero valent iron	pH = 3–5 Catalyst = 0.1–10 g l^{-1} H_2O_2 = 2–20%	100%	0.567	4-chlorocatechol Catechol and maleic acid hydroquinone	[112]
4-CP	0.42–1.67 mM	Zero valent iron	pH = 3 Catalyst = 2 mg l^{-1} H_2O_2 = 10 mM	100%	—	4-chlorocatechol Perchlorylbenzene 2-(2,4-Dichlorophenoxy) phenol 5-Chloro-2-(2-chloro-4-hydroxyphenoxy)phenol	[113]
4-CP	1 g l^{-1}	Zero valent iron Graphite Activated carbon	pH = 3 catalyst = 1 g l^{-1} H_2O_2 = 15 ml l^{-1}	60% (zero-valent iron) 35% (graphite) 25% (activated carbon)	—	—	[114]
2,4-DCP	30– 100 mg l^{-1}	Fe-NPs	pH = 3–7 H_2O_2 = 2.5–15 mM Catalyst = 1 g l^{-1} T = 293–313 K	67.5%	—	2-chlorohydroquinone Acetic acid acetaldehyde	[64]

(*continued*)

UNCORRECTED PROOFS

Trim Size: 170mm x 244mm Single Column Loose

Ribeiro67017 c22.tex V1 - 12/12/2020 12:31am Page 549

UNCORRECTED PROOFS

Trim Size: 170mm x 244mm Single Column Loose

Table 22.2 (Continued)

Compound	CP concentration	Catalyst	Experimental conditions	Treatment efficiency	Rate constant (min^{-1})	By-products	Ref
2,4-DCP	50 g l^{-1}	Fe-NPs	pH = 6.8 H_2O_2 = 10 mM Catalyst = 1 g l^{-1}	64%	—	Acetone Acetic acid	[3]
2,4-DCP	50–250 mg l^{-1}	Fe-NPs	pH = 1–5 H_2O_2 = 1–15 mM Catalyst = 0.5–2 g l^{-1} T = 10–40 °C	57.87% (nZVI)	7.4*10^{-3} (nZVI)	3,5-dichloro-2-hydroxy-1, 4-benzoquinone Maleic acid	[62]
2,4-DCP	30–100 mg l^{-1}	Fe-NPs (Fe^{2+}, nFe_3O_4, nZVI)	pH = 3–7 Persultafe = 6.4–24 mg l^{-1} Catalyst = 1–2 g l^{-1}	98%	7.1*10^{-2}	3,5-dichloro-2-hydroxy-1, 4-benzoquinone Maleic acid	[63]
2,4-DCP	20– 100 mg l^{-1}	Fe_3O_4	pH = 2, 3, 3.9, 4.6, 5 H_2O_2 = 0.6–30 mM Catalyst = 0.2–2 g l^{-1}	100%	0.064	2-Chlorohydroquinone 4,6-Dichlororesorcinol Acetic acid Formic acid	[61]
CPs (2-CP, 4-CP, 2,3-DCP, 2,4-DCP, 2,4,6-TCP, 2,3,4,6-TeCP)	100–500 mg l^{-1}	Pyrite	pH = 3–5 H_2O_2 = 0.3 M Catalyst = 0.25–1 g l^{-1}	100% (2-CP) 100% (4-CP) 100% (2,3-DCP) 100% (2,4-DCP) 100% (2,4,6-TCP) 100% (2,3,4,6-TeCP)	−0.1637 (2-CP) −0.2411 (4-CP) −0.2269 (2,3-DCP) −0.1045 (2,4-DCP) −0.0721 (2,4,6-TCP) −0.3389 (2,3,4,6-TeCP)	4-chloro-1,3-benzenendiol 2,4,5-trichlorophenol Chloroacetic acid Phenol, 2,4-bis (1,1-dimethylethyl) 4-chlorophenol Acetic acid Formic acid Maleic acid	[56]

Ribeiro670117 c22.tex V1 - 12/12/2020 12:31am Page 550

CPs (2-CP, 4-CP, 2,3-DCP, 2,4-DCP, 2,4,6-TCP, 2,3,4,6-TeCP)	100 mg l^{-1}	Pyrite	Batch reactor experiments pH = 3 H_2O_2 = 0.3 M Catalyst = 1 g l^{-1} Ligand = 0–10^{-3} M Column experiments pH = 4 H_2O_2 = 0.02 M Ligand = 0–10^{-3} M	100%	−0.1637 (2-CP) −0.2411 (4-CP) −0.2269 (2,3-DCP) −0.1045 (2,4-DCP) −0.0721 (2,4,6-TCP) −0.3389 (2,3,4,6-TeCP)	4-chloro-1,3-benzenendiol 2,4,5-trichlorophenol Chloroacetic acid Phenol, 2,4-bis (1,1-dimethylethyl) 4-chlorophenol Acetic acid Formic acid Maleic acid	[57]
PCP	1 mg l^{-1}	Zero-valent iron	pH = 3–7 Catalyst = 5 mg l^{-1} H_2O_2 = 2.5 mg l^{-1}	90%	—	—	[80]
PCP	50 mg l^{-1}	Nano zero-valent iron	pH = 5 H_2O_2 = 1–10% Catalyst = 15 mg of particles per test	57%	—	—	[79]
PCP	50 mg l^{-1}	Magnetite	pH = 7 Catalyst = 2 g l^{-1} H_2O_2/Fe = 100 Ligand = 1 mM T = 20 °C	100%	—	—	[74]
PCP	0.0375 mM	Goethite Hematite	pH = 3.5 Catalyst = 0.4 g l^{-1} Ligand = 0–2 mM	68% (goethite) 83% (hematite)	—	Tetrachlorocatechol 2,3,5,6-tetrachloro-1, 4-hydroquinone o-chloranil p-chloranil	[109]

UNCORRECTED PROOFS

Trim Size: 170mm x 244mm Single Column Loose
Ribeiro67017 c22.tex V1 - 12/12/2020 12:31am Page 551

Trim Size: 170mm x 244mm Single Column Loose Ribeiro670117 c22.tex V1 - 12/12/2020 12:31am Page 552

surface HO^* radicals played an important role in 2,4-DCP removal by magnetite, the 2,4-DCP degradation was primarily driven by the HO^* radicals generated in the bulk solution. Similarly, several researchers (e.g. [59, 110]) showed a direct correlation between Fe^{2+} leaching from goethite and 2-CP degradation in the presence of H_2O_2:

$$\alpha - FeOOH_{(s)} + 2H^+ + 0.5H_2O_2 = Fe^{2+} + 0.5O_2 + 2H_2O \quad (22.5)$$

Some authors have also studied the role of adsorption on CP removal by Fe oxides. Bandara et al. [115], for instance, reported that CP adsorption onto Fe oxides (e.g. hematite, goethite) was very low and decreased in the order 2-CP > 2,4-DCP > 2,3-DCP > 2,4,6-TCP. Fe oxides exhibit hydrophilic properties and thus are not suitable sorbents for hydrophobic compounds such as CPs. Kuntail et al. [116] found that pentachlorophenol (PCP) adsorption onto magnetite occurred through Fe-Cl interaction.

22.2.1.2 Pyrite

Pyrite is an abundant iron sulfide mineral (FeS_2) in the environment that has often been used as a catalyst material in the Fenton degradation of chlorophenols due to its very low cost and high Fe^{2+} content [56, 57, 117]. A list of studies using pyrite as the catalyst in the Fenton degradation of CPs is shown in Table 22.2. In addition to its catalytic properties, the oxidation of pyrite by O_2 and H_2O_2 leads to the release of Fe^{2+} and H_2SO_4 into the bulk solution, thus bringing the system to the acidic conditions (pH 3–4) required for optimum Fenton operations [55–57, 118, 119]:

$$2FeS_2 + 7O_2 + 2H_2O = 2Fe^{2+} + 4SO_4^{2-} + 4H^+ \quad (22.6)$$

$$2FeS_2 + 15H_2O_2 = 2Fe^{3+} + 4SO_4^{2-} + 2H^+ + 14H_2O \quad (22.7)$$

Fe^{2+} ions released from pyrite can interact with H_2O_2 to form HO^* radicals in the bulk solution (Reaction (22.1)). The Fe redox cycle (i.e. Fe(II)/Fe(III) redox couple) plays an important role in Fe^{2+} leaching from pyrite and process sustainability [56, 120, 121]. Under acidic conditions, Fe^{3+} ions released from pyrite (Reaction (22.7)) can react with the disulfide functional group on the pyrite surface, thus releasing Fe^{2+} ions into the bulk solution, followed by homogenous HO^* radical generation in the bulk solution [56, 57]:

$$FeS_2 + 14Fe^{3+} + 8H_2O = 15Fe^{2+} + 2SO_4^{2-} + 16H^+ \quad (22.8)$$

The direct adsorption and heterogeneous catalytic decomposition of H_2O_2 into HO^* and $HO_2{}^*$ radicals on the pyrite surface have also been reported in the literature [56]:

$$Fe^{II}S_2 + H_2O_2 = Fe^{III}S_2 + \equiv OH^*_{ads} + OH^- \quad (22.9)$$

$$Fe^{III}S_2 + H_2O_2 = Fe^{II}S_2 + \equiv HO^*_{2(ads)} + OH^- \quad (22.10)$$

A number of different mechanisms have been postulated for the Fenton oxidation of organic pollutants in systems involving pyrite as the catalyst [54–57]. According

UNCORRECTED PROOFS

Trim Size: 170mm x 244mm Single Column Loose Ribeiro670117 c22.tex V1 - 12/12/2020 12:31am Page 553

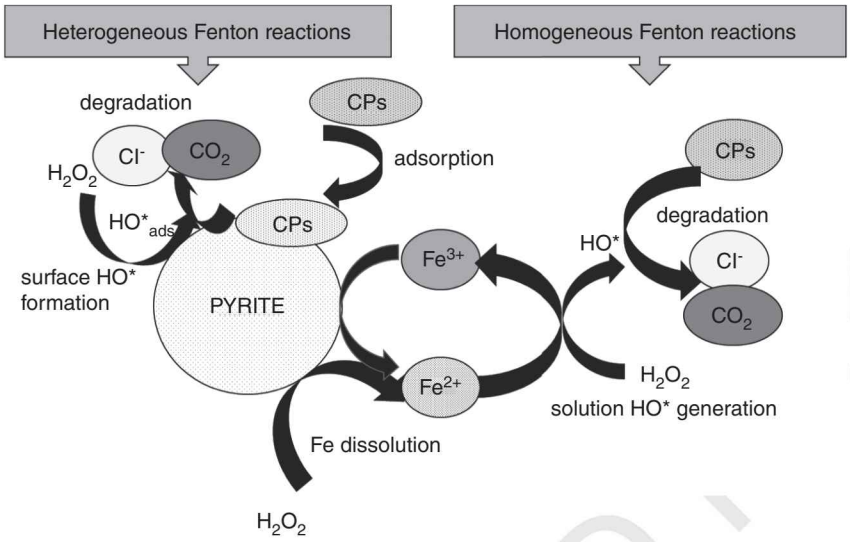

Figure 22.1 Schematic description of CP degradation with the pyrite-Fenton system.

to Kantar et al. [56], for instance, the CP degradation by pyrite is regulated by several concurrently and consecutively occurring reactions, including (i) CP adsorption onto the pyrite surface via hydrophobic bonding, followed by oxidative degradation with heterogeneous HO^* radicals; and (ii) oxidative degradation with homogenous HO^* radicals generated by Fe leaching from pyrite (Reactions (22.6) and (22.8)). The schematic description of CP degradation with a pyrite-Fenton reaction is summarized in Figure 22.1. Pyrite exhibits both hydrophilic and hydrophobic properties depending on the system conditions (e.g. pH) and serves as a good sorbent for hydrophobic compounds such as CPs [65, 122]. As shown in Figure 22.2, CP adsorption by pyrite is greatly dependent on the type of CP, and the extent of CP sorption increases with increasing CP hydrophobicity, suggesting that, in addition to oxidative degradation, CP adsorption onto pyrite via hydrophobic bonding also plays a critical role in removing multichlorophenolic compounds. According to Weerasooriya et al. [122], CP adsorption onto pyrite is primarily driven by Fe-Cl interactions. Similarly, data by Weerasooriya et al. [65] show that the presence of oxidized species on pyrite (i.e. ≡FeOOH) not only favors the adsorption of 4-CP but also enhances H_2O_2 and HO^* radical generation on the pyrite surface, implying that the oxidized pyrite surface acts as a Fe-oxide.

22.2.1.3 Zero-Valent Iron (ZVI)

An alternative catalyst used in the Fenton process is ZVI (Fe^0), which exhibits excellent catalytic activity for degrading chlorinated organic compounds such as chlorophenols [3, 62, 80, 111, 112, 114, 123]. A list of studies using ZVI as the catalyst in the Fenton degradation of CPs is shown in Table 22.2. ZVI is generated in the lab in different sizes ranging from nano- to micro-sized [3, 31]. Despite the aggregation problem associated with nano-scale ZVI, it exhibits very high reactivity

UNCORRECTED PROOFS

Trim Size: 170mm x 244mm Single Column Loose Ribeiro670117 c22.tex V1 - 12/12/2020 12:31am Page 554

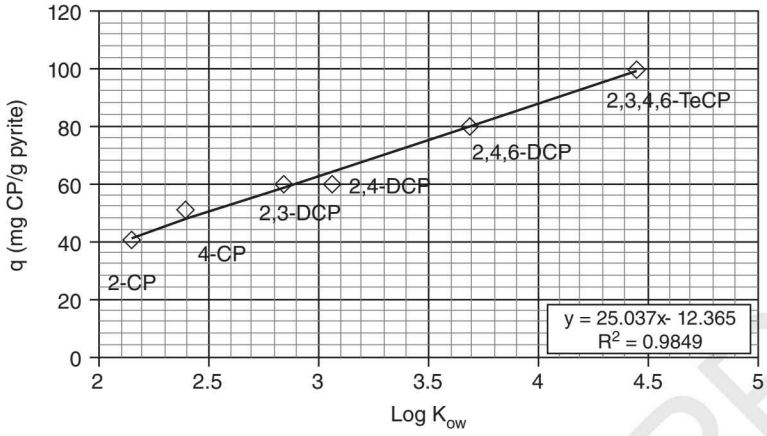

Figure 22.2 The role of CP type on CP sorption onto pyrite at pH 3, 100 mg l^{-1} CP, and 1 g l^{-1} pyrite. The data were plotted in terms of the amount of CP adsorbed (mg/g) as a function of log K_{ow} of CPs. Source: Data adapted with permission from Kantar et al. [56]. Copyright Elsevier (2020).

toward chlorinated compounds under acidic conditions [62, 63, 79, 112]. A number of different mechanisms for degrading organic compounds with the ZVI-Fenton system have been proposed, involving surface catalysis and homogenous Fenton reaction [64]. A schematic diagram showing the possible reaction mechanisms for CP degradation with the ZVI-Fenton system is shown in Figure 22.3. The corrosion of ZVI with O_2 and H_2O_2 leads to in situ generation of Fe^{2+} followed by homogenous radical generation in the bulk phase according to Reaction (22.1) [78, 112, 113, 124]:

$$Fe^0 + O_2 + 2H^+ = Fe^{2+} + H_2O_2 \quad (22.11)$$

$$Fe^0 + H_2O_2 + 2H^+ = Fe^{2+} + 2H_2O \quad (22.12)$$

According to several authors [62, 78, 80, 111, 114], CP degradation with the ZVI-Fenton process under acidic conditions occurs through a homogenous Fenton reaction, which is accelerated by Fe^{2+} leaching from ZVI according to Reactions (22.11) and (22.12). Zhou et al. [112] reported that 4-CP degradation with the ZVI-Fenton system followed a two-stage process, with the first slow stage – primarily initiated by kinetically controlled heterogeneous Fenton reactions – followed by a rapid second stage controlled by bulk-phase homogenous Fenton reactions initiated by Fe^{2+} leaching from ZVI. On the other hand, Gan et al. [64] emphasized the role of adsorption and subsequent surface-catalyzed oxidation of 2,4-DCP with Fenton-like reactions using Fe nanoparticles. Regardless of where the reaction takes place, like the pyrite-Fenton system, the Fe redox cycle plays a key role in process efficiency and sustainability for the ZVI-Fenton system by continuously generating Fe^{2+} ions through ZVI oxidation with Fe^{3+} ions [112]:

$$2Fe^{3+} + Fe^0 = 3Fe^{2+} \quad (22.13)$$

UNCORRECTED PROOFS

Trim Size: 170mm x 244mm Single Column Loose Ribeiro670117 c22.tex V1 - 12/12/2020 12:31am Page 555

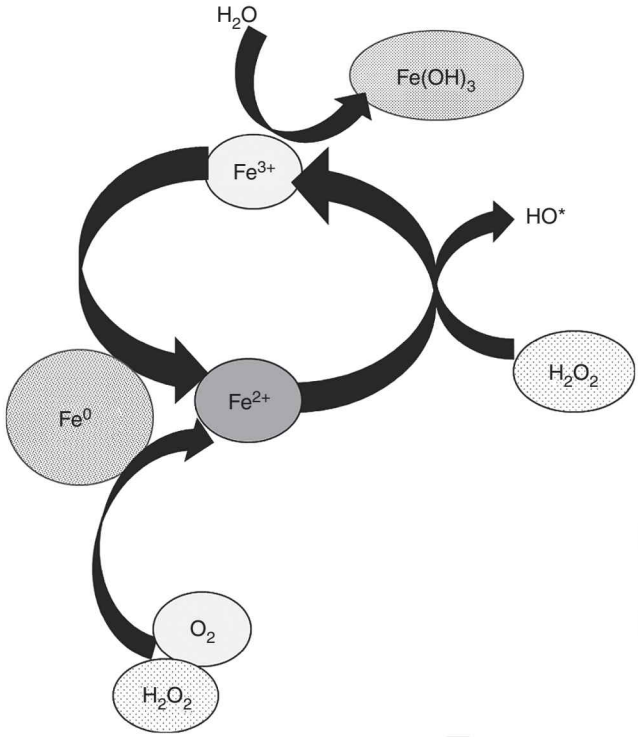

Figure 22.3 Schematic description of CP degradation with the ZVI/H_2O_2 system.

22.2.1.4 Multimetallic Iron-Based Catalysts

Many multimetallic composite materials have been synthesized to accelerate H_2O_2 decomposition with Fe and enhance the subsequent generation of interfacial HO^* radicals for CP degradation (e.g. [81]). A second metal incorporated into an iron oxide/particle can also accelerate the Fe redox cycle (i.e. corrosion), thus improving catalyst stability and sustainability under a wide pH range [61, 75, 82, 83, 93, 125, 126]. These multimetallic catalysts are usually synthesized at the nano scale to increase their reactivity and may contain magnetic materials such as Fe_3O_4 for easy separation and recovery [75, 82, 83]. For instance, Liu et al. [83] found that the Au-Fe_3O_4 catalyst effectively oxidized 4-CP up to pH 5 while keeping its stability and reusability even after a number of treatment cycles. An extensive list of studies using multimetallic materials as the catalyst in Fenton degradation of CPs is shown in Table 22.3. The multimetallic catalysts used for CP degradation include Ni/Fe [62, 126, 136], Pd/Fe [62, 133–135], Fe/CeO_2 [132], Cu/Fe [128], Fe_3O_4/MnO_2 [93], Al-Fe/O_2 [130], Cu/Fe_3O_4 [125], $Ni_xZn_{1-x}Fe_2O_4$ [81], Ni/Fe/Fe_3O_4 [82], Au/Fe_3O_4 [83], Mg/Fe-O_2 [69], and Fe_3O_4/CeO_2 [75].

While CP oxidation primarily occurs on the catalyst surface via heterogeneous Fenton reaction catalyzed by the second metal (e.g. CeO_2) [69, 81, 130, 133–136], CP removal by a homogenous Fenton process initiated by Fe^{2+} leaching from the catalyst has also been reported in a number of articles [63, 72, 83, 128]. For

UNCORRECTED PROOFS

UNCORRECTED PROOFS

Trim Size: 170mm x 244mm Single Column Loose

Table 22.3 Multimetallic catalyst materials used in the Fenton degradation of chlorophenols.

Compound	CP concentration	Catalyst	Experimental conditions	Treatment efficiency	Rate constant (min^{-1})	By-products	Ref
p-CP	0.625 mM	Ni/Fe	pH = 3-6.5 Catalyst = 0.16–0.48 $g\,l^{-1}$	100%	—	—	[127]
4-CP	25–75 $mg\,l^{-1}$	Mg/Fe-O_2	pH = 2–5 Catalyst = 1–4 $g\,l^{-1}$	100%	—	—	[69]
4-CP	0.1 mM	Cu^0/Fe_3O_4	pH = 3–10 Catalyst = 1 $g\,l^{-1}$	100%	—	—	[125]
4-CP	1.1 mmol	Fe/Ni	pH = 6	89%	—	Phenol p-benzoquinone Hydroquinone	[126]
4-CP	50 $mg\,l^{-1}$	Cu/Fe	pH = 1-5 Catalyst = 100 $g\,l^{-1}$	70% (Cu)	—	Phenol	[128]
4-CP	25 $mg\,l^{-1}$	Au-Fe_3O_4 magnetic nanocomposites	pH = 3-11 Catalyst = 0.050.1 $g\,l^{-1}$ H_2O_2 = 0.25–1.5 $g\,l^{-1}$ T = 293–313 K	97.6%		Hydroquinone Formic acid Fumaric acid Acetic acid Malonic acid	[83]
4-CP	25–100 $mg\,l^{-1}$	Fe_3O_4-MnO_2 core Shell nanocomposite	pH = 4.5–9.5 Catalyst = 0.1–1 $g\,l^{-1}$	100%	—	—	[93]
4-CP	0.75–2 $g\,l^{-1}$	Ni/Zn – Fe_2O_4	pH = 6.67–6.86 H_2O_2 = 39.16 mM Catalyst = NixZn1 – xFe2O4 (x = 0.0, 0.25, 0.5, 0.75, 1.0) T = 25–70 °C	100%	—	Triacetone peroxide Acetone 4-hydroxy 4-methyl 2-pentanone 2,5-hexane dione Xylenes Benzoquinone	[81]

Ribeiro670117 c22.tex V1 - 12/12/2020 12:31am Page 556

4-CP	1.1 mM	$Fe@Fe_2O_3$	pH = 2.7 Catalyst = 0.1 g $^{-1}$ Ligand = 2 mM	100%	—	4-chlorocatechol 4-chlororesorcinol	[129]
4-CP	5–200 mg l^{-1}	Al-Fe/O_2	pH = 2.5-9 Catalyst = 1.01–20.02 g l^{-1} Ligand = 20.46–188.71 mg l^{-1}	100%	—	4-chlorocatechol p-benzoquinone Maleic acid	[130]
4-CP	0.78 mM	Fe_3O_4/CeO_2	pH = 2.2–5.3 Catalyst = 1–2.5 g l^{-1} H_2O_2 = 6–50 mM	100%	—	Hydroquinone Fumaric acid Malonic acid Acetic acid Formic acid	[131]
2,4-DCP	20 mg l^{-1}	Ni/Fe-Fe_3O_4	pH = 3–10 Catalyst = 3 g l^{-1}	91.5%	—	—	[82]
2,4-DCP	50–250 mg l^{-1}	Iron-based nanoparticles	pH = 1–5 H_2O_2 = 1–15 mM Catalyst = 0.5–2 g l^{-1} T = 10–40 °C	27.94% (n-Pd/Fe) 34.23% (n-Ni/Fe) 19.61% (Fe^{2+})	$9.7*10^{-3}$ (n-Pd/Fe) $3.4*10^{-3}$ (n-Ni/Fe) $8.2*10^{-3}$ (Fe^{2+})	3,5-dichloro-2-hydroxy-1, 4-benzoquinone Maleic acid	[62]

(*continued*)

UNCORRECTED PROOFS

Trim Size: 170mm x 244mm Single Column Loose

Ribeiro670117 c22.tex V1 - 12/12/2020 12:31am Page 557

UNCORRECTED PROOFS

Trim Size: 170mm x 244mm Single Column Loose

Table 22.3 (Continued)

Compound	CP concentration	Catalyst	Experimental conditions	Treatment efficiency	Rate constant (min^{-1})	By-products	Ref
2,4,6-TCP	20-100 mg l^{-1}	Fe_3O_4/CeO_2	pH = 2–4 H_2O_2 = 6–30 mM Catalyst = 0.5–2.5 g l^{-1}	99%	$4.6*10^{-2}$	2,6-dichloro-1, 4-benzoquinone 3,5-dichloro-1, 2-benzoquinone 2-chloro-1, 4-benzoquinone 2-hydroxycyclohexa-2, 5-diene-1,4-dione Succialdehyde (E)but-2-enoic acid Oxoacetic acid Acetic acid Formic acid	[75]
CPs (4-CP, 2,4-DCP, 2,4,6-TCP, PCP)	50 mg l^{-1}	Fe^0/CeO_2	pH = 2.8-6.2 Catalyst = 1 g l^{-1}	100% (PCP) 60% (2,4-DCP) 40% (2,4,6-TCP) 10% (4-CP)	—	—	[132]
CPs (4-CP,2,4-DCP,2,4,6-TCP)	20 mg l^{-1}	Pd/Fe	pH = 5.5 Catalyst = 5 g l^{-1}	94% (2,4,6-TCP)	—	—	[133]
CPs (p-CP,o-CP,m-CP)	20 mg l^{-1}	Pd/Fe	T = 28 °C	100%	0.0215(o-CP) 0.0155(m-CP) 0.0112(p-CP)	—	[134]

Ribeiro67017 c22.tex V1 - 12/12/2020 12:31am Page 558

PCP	10 mg l^{-1}	Zerovalent Pd/Fe	Catalyst = 3.13, 6.25, 12.5 g l^{-1} T = 5–45 °C	98%	—	Phenol 2-CP 4-CP 3-CP 2,3-DCP 2,6-DCP 3,4-DCP 2,3,5-TCP 2,4,6-TCP 2,4,5-TCP 2,3,4-TCP 2,3,6-TCP 3,4,5-TCP 2,3,4,5-TeCP 2,3,4,6-TeCP 2,3,5,6-TeCP	[135]

UNCORRECTED PROOFS

Trim Size: 170mm x 244mm Single Column Loose

Ribeiro670117 c22.tex V1 - 12/12/2020 12:31am Page 559

Trim Size: 170mm x 244mm Single Column Loose Ribeiro670117 c22.tex V1 - 12/12/2020 12:31am Page 560

instance, studies by Xu and Wang [131, 132] showed that the presence of CeO_2 promoted the dissolution of Fe^0 and magnetite, thus releasing Fe^{2+} into the bulk solution and subsequently leading to enhanced CP degradation under the combined effect of homogenous and heterogeneous Fenton reactions. On the other hand, a study by Shih et al. [135] emphasized the role of PCP adsorption and subsequent dechlorination with Pd/Fe nanoparticles. Similarly, the Al-Fe/O_2 system exhibited excellent reactivity due to in situ H_2O_2 generation induced by electron transfer from Al to oxygen [130]. Incorporating Zn into the nickel ferrite system extended the optimum pH range to neutral pH conditions with very little Fe leaching and significantly improved 4-CP removal depending on the Zn/Ni ratio [81]. This enhanced 4-CP degradation with Zn substitution was attributed to a reduction in particle size and change in the $NiFe_2O_4$ structure from inverse spinel to a mixed spinel structure, thus creating a stable Fe^{2+}/Fe^{3+} redox couple.

22.2.1.5 Supported Iron-Based Catalyst Materials

A wide range of support materials, including carbon-based materials such as activated carbon, graphite, GO, CNTs, aerogels, ion exchange resins, and polymers (e.g. alginate) [73, 84, 85, 89–91, 96–98, 104, 137, 138], silicate-based materials such as zeolite, quartz, rectorite, PILCs [25, 87, 88, 92, 99, 100, 139–141], alumina [108, 142], and TiO_2 [9], have been incorporated into iron oxides/particles to overcome problems associated with homogenous or nano-scale heterogeneous catalysts such as particle aggregation due to intraparticle forces and Fe leaching from the catalyst. Heterogeneous catalysts embedded into support materials may also facilitate Fenton-like reactions up to slightly alkaline pH conditions due to limited iron leaching from the catalyst since Fe^{3+} becomes immobilized within the solid matrix and porous interlayer of the clay structure [58]. Multiple different reaction mechanisms have been proposed for the oxidative degradation of chlorophenols with heterogeneous catalysts using support materials, including pollutant adsorption followed by catalytic oxidation on the catalyst surface [84].

Due to their low cost and high surface area, clay minerals such as bentonite, sepiolite, and zeolite are an effective choice as catalyst support for the oxidative degradation of CPs with mono- or multimetallic catalyst materials [25, 87, 88, 92, 99, 100, 139, 141]. An extensive list of studies involving supported iron catalysts in the Fenton degradation of CPs is shown in Table 22.4. A study by Zhou et al. [25], for instance, found that bentonite-supported bimetallic Fe/Pd nanoparticles exhibited excellent catalytic activity for 4-CP degradation up to pH 7. Nano-ZVI particles supported with hydrophobic organic surfactant–coated bentonite enhanced CP adsorption via hydrophobic bonding and minimized the aggregation of ZVI particles [94, 140].

Recently, organic support materials such as CNTs, organic polymers, and GO significantly improved the catalytic activity of bimetallic catalyst materials [73, 84, 85, 89–91, 95–98, 104, 137, 138, 140]. For instance, Yang et al. [84] successfully synthesized a catalyst material by incorporating Zn-Fe_3O_4 bimetallic materials into CNTs for the effective degradation of 4-CP. Similarly, Zn/Fe bimetallic composite supported with CNTs led to the in situ generation of H_2O_2 via Zn-C galvanic cells, thus activating O_2 to facilitate interfacial HO^* generation for 4-CP oxidation [85]. While

UNCORRECTED PROOFS

UNCORRECTED PROOFS

Trim Size: 170mm x 244mm Single Column Loose

Ribeiro67017 c22.tex V1 - 12/12/2020 12:31am Page 561

Table 22.4 Supported-iron catalysts for heterogeneous Fenton degradation of chlorophenols.

Compound	CP concentration	Catalyst	Experimental conditions	Treatment efficiency	Rate constant (min^{-1})	By-products	Ref
p-chlorophenol	100 mg l^{-1}	Ag_3PO_4/Fe_3O_4/GO	pH = 3 Catalyst = 0.4 g l^{-1}	96.1%	—	—	[95]
p-chlorophenol	60–110 mg l^{-1}	nZVI/Rectorite	pH = 5–9 H_2O_2 = 0.1–1 ml Catalyst = 0.003–0.1 g	100%	—	—	[87]
p-chlorophenol	60–110 mg l^{-1}	Fe_3O_4/Rectorite nano-Fe_3O_4	pH = 2–9 H_2O_2 = 0.05–1 ml Catalyst = 0.005–0.04 g	100%	—	—	[92]
p-chlorophenol	50 mg l^{-1}	B/Pd/Fe	pH = 6.7 Catalyst = 2–5 g l^{-1}	100%	—	—	[25]
p-chlorophenol	1 g l^{-1}	AlFePILCs	pH = 3.5 H_2O_2:4-CP = 2.7 : 1 Catalyst = 1 g l^{-1} T = 50 °C	100%	—	4-chlorophenol 2,4-dichlorophenol Hydroquinone Chlorocatechol Chlorohydroquinone Dichlorocatechol 5-chloro-1,2,4-benzenetriol	[88]
2-CP	50 mg l^{-1}	Fe-PILCs	pH = 3-7 Catalyst = 0.2–1 g l^{-1} H_2O_2 = 265 mg l^{-1}	100%	—	—	[99]

(*continued*)

UNCORRECTED PROOFS

Trim Size: 170mm x 244mm Single Column Loose

Ribeiro67017 c22.tex V1 - 12/12/2020 12:31am Page 562

Table 22.4 (Continued)

Compound	CP concentration	Catalyst	Experimental conditions	Treatment efficiency	Rate constant (min^{-1})	By-products	Ref
2-CP	100 mg l^{-1}	Ak/rGO	pH = 4–9 Catalyst = 1 g l^{-1} H_2O_2 = 100 mM	100%	—	—	[137]
4-CP	0.78 mM	Fe/Cu/γ-Al_2O_3	pH = 7 Catalyst = 0-2.5 g l^{-1} H_2O_2 = 0-40 mM	99.7%	—		[108]
4-CP	50–150 mg l^{-1}	Zn-Fe-CNTs	pH = 2–5 Catalyst = 0.4–1.2 g l^{-1}	90.8%	—	Hydroquinone benzoquinone formic acid acetic acid oxalic acid	[85]
4-CP	25–250 mg l^{-1}	Zn0-CNTs-Fe_3O_4	pH = 1–4 Catalyst = 0.5–4 g l^{-1}	99%	—	4-chlorocatechol Formic acid Acetic acid Oxalic acid	[84]
4-CP	100 mg l^{-1}	Pd-Ni/MWCNTs/GF	pH = 2.5–11.5	100%	—	—	[138]
4-CP	25–100 mg l^{-1}	NZVI-Ag immobilized in alginate	pH = 3–5 Catalyst = 5 g l^{-1} H_2O_2 = 90–180 mg l^{-1}	100%	–	Chlorocatechol	[104]
4-CP	100 mg l^{-1}	Fe_3O_4@β-CD	pH = 2–8 Catalyst = 0.5–2 g l^{-1} H_2O_2 = 10–50 mM	100%	—	Hydroquinone Formic acid Fumaric acid Acetic acid Malonic acid	[96]

UNCORRECTED PROOFS

Trim Size: 170mm x 244mm Single Column Loose

4-CP	128.6 mg l^{-1}	FeS_2@GO	pH = 5–11 H_2O_2 = 0–50 mM	99% (FeS_2@GO) 97% (FeS_2)	—	Oxalic acid Acetic acid Chloroacetic acid	[73]
4-CP	100 mg l^{-1}	Iron-glutamate-silicotungstate ternary complex (Fe^{III}GluSiW)	pH = 3–8 H_2O_2 = 10–20 mM Catalyst = 0.2–2 g l^{-1}	100%	—	—	[97]
4-CP	100 mg l^{-1}	Iron-containing silicotungstate (Fe^{III}AspSiW)	pH = 3–9 H_2O_2 = 10–30 mM Catalyst = 0.1–1 g l^{-1}	100%	—	—	[91]
4-CP	0.48 mM	FeO_x/TiO $CuFe_2O_4$	pH = 7.4 H_2O_2 = 16 mM	100%	—	—	[9]
4-CP	3.1	Fe(OMC)	pH = 2-5 H_2O_2 = 3.1–6.6 mM T = 30–60 °C	96.1%			[90]
4-CP	100 mg l^{-1}	Fe^{III}containing polyoxometalate (POM)	pH = 3.2–10.1 H_2O_2 = 10–20 mM Catalyst = 0.2–1 g l^{-1} T = 25 ± 2 °C	100% (TOC)	—	—	[89]
4-CP	2.76 mM	Al-Fe/Cu-PILC	Catalyst = 1 g l^{-1} H_2O_2 = 36.27 mM T = 40 °C	100%	—	—	[141]
4-CP	155.6 µmol l^{-1}	Al-Fe-PILC	pH = 3.5–5 Catalyst = 0.5 g l^{-1} H_2O_2 = 2625.3 µmol l^{-1}	100%	—	4-chlorocatechol	[139]

(*continued*)

Ribeiro67017 c22.tex V1 - 12/12/2020 12:31am Page 563

UNCORRECTED PROOFS

Trim Size: 170mm x 244mm Single Column Loose

Table 22.4 (Continued)

Compound	CP concentration	Catalyst	Experimental conditions	Treatment efficiency	Rate constant (min^{-1})	By-products	Ref
2,4-DCP	0.5 mM	Sep-Fe/Ni	pH = 1-11 Catalyst = 0.025–0.75 g	100%	—	Phenol	[100]
2,4-DCP	50 mg l^{-1}	nZVI/B	Catalyst = 0.075 g	73.5 (nZVI/DK1) 46.1 (nZVI/DK3) 27.1 (nZVI/DK5) 25.7 (nZVI/B)	—	—	[94]
CPs (2-CP, 4-CP, 2,4-DCP, 2,4,6-TCP)	50 mg l^{-1}	Pd@Fe_3O_4@MOF	pH = 3–4 H_2O_2 = 1–10 mM Catalyst = 0.5 g l^{-1}	Phenol 100% 2-CP 100% 4-CP 100% 2,4-DCP 100% 2,4,6-TCP 75%	0.036 (2-CP) 0.586 (4-CP) 0.48 (DCP) 0.007 (TCP)	—	[98]
CPs (2-CP, 4-CP, 2,4-DCP, 2,4,6-TCP, PCP)	0.5 mM	NZVI/CTMA-Bent	pH = 5.5 iron dose = 0.6 g l^{-1}	87.1% (2-CP) 88.9% (2,4-DCP) 93.1% (2,4,6-TCP) 93.4% (PCP)	—	—	[140]
CPs (4-CP, 2,4-DCP, 2,4,6-TCP)	200 mg l^{-1} (4-CP, 2,4-DCP 100 mg l^{-1} (2,4,6-TCP)	Pd-Fe/γ-Al_2O_3	Catalyst = 2 g l^{-1} H_2O_2 = 250 mg l^{-1}	100%	—	Maleic acid Malonic acid Oxalic acid Acetic acid Formic acid	[142]

Ribeiro670117 c22.tex V1 - 12/12/2020 12:31am Page 564

Trim Size: 170mm x 244mm Single Column Loose Ribeiro670117 c22.tex V1 - 12/12/2020 12:31am Page 565

using GO as a support material with Fe oxides (e.g. Fe_3O_4, FeOOH) was shown to enhance Fenton-like oxidation of CPs via strong Fe-O-C interaction [95, 137], Fe leaching from pyrite supported with GO played a key role in homogenous 4-CP degradation [73]. Despite Fe leaching, FeS_2@GO was still effective in 4-CP degradation even at neutral pH conditions. Studies performed with other organic-based support materials such as alginate and metal-organic frameworks (MOF) exhibit similar improvements in catalyst stability and reusability under a wide range of pH values (pH < 7) [89–91, 96–98, 104].

Even though most studies have reported on using support materials that can accumulate the pollutants near highly reactive surface sites (e.g. Fe-sites) for enhanced surface catalytic activity toward CP degradation [94, 108], some researchers have also proposed a homogenous reaction for CP degradation with bimetallic particles, Fe-oxides, or Fe sulfides supported on TiO_2, GO, or clays [9, 73, 139]. For instance, according to Catrinescu et al. [139], incorporating Al/Fe into the clay structure (Al/Fe PILC) enhanced 4-CP oxidation via a combined effect of surface catalysis and homogenous Fenton reaction catalyzed from Fe leaching.

22.3 Factors Affecting CP Removal Efficiency in Heterogeneous Fenton Processes

22.3.1 Effect of Catalyst Size

One of the key factors affecting CP removal efficiency with Fe-containing heterogeneous Fenton systems is the catalyst size, which relates to surface reactivity [59]. The degradation rates of CPs with heterogeneous Fenton processes were observed to be parallel to the surface area (i.e. decrease in size) [31]. For instance, Lu [59] reported a direct relationship between 2-CP removal and goethite surface area, with 2-CP removal increasing with an increase in particle surface area. Despite the enhanced CP removal with nano-sized particles (e.g. [62, 78]), particle aggregation due to intraparticle forces, including van der Waals forces, leads to a significant decrease in catalyst stability [73]. To overcome this problem, researchers have lately focused on the synthesis of multimetallic or Fe catalysts with support materials [25, 100]. The studies performed with these materials seem to show some promising results in terms of particle stability and reusability [87–89, 91, 92, 100, 139, 141].

22.3.2 Effect of Catalyst Dosage

The catalyst dose in heterogeneous Fenton-like processes is one of the critical parameters affecting CP removal efficiency by both (i) increasing the number of surface sites on the catalyst surface for enhanced adsorption and (ii) increasing Fe leaching from the catalyst for homogenous Fenton oxidation [56, 73, 83, 111, 112]. For instance, Kantar et al. [56] found that increasing pyrite dose significantly improved CP removal by pyrite-Fenton due to enhanced CP adsorption and Fe^{2+} leaching from pyrite, contributing to homogenous CP degradation in the bulk solution. Similarly, Zhou et al. [112] reported enhanced CP removal with ZVI loading, resulting

UNCORRECTED PROOFS

Trim Size: 170mm x 244mm Single Column Loose Ribeiro670117 c22.tex V1 - 12/12/2020 12:31am Page 566

in enhanced Fe^{2+} leaching and subsequent homogenous CP oxidation. In another study, Li et al. [63] showed that increasing the ZVI dose from 1 to 2 g l^{-1} improved CP removal efficiency by more than 100%. This enhanced CP removal was attributed to Fe^{2+} release from ZVI, which can then catalyze H_2O_2 to generate HO^* radicals. Zhou et al. [133] demonstrated that the dechlorination rate constants for 2,4,6-TCP increased with increasing the initial catalyst dose of bimetallic Pd/Fe nanoparticles due to an increase in catalyst surface area. Similarly, increasing the dose of bimetallic Ni/Fe particles led to an increase in surface catalytic dechlorination of 4-CP from 15 to 91% within less than 20 minutes of reaction time [136]. Yang et al. [69] explained the enhanced CP removal with increasing the concentration of bimetallic Mg/Fe particles through an increase in the number of reactive sites for O_2 reduction and subsequent generation of more oxidizing agents such as H_2O_2 and HO^* radicals.

A catalyst overdose, on the other hand, can have an adverse effect on CP degradation with heterogeneous catalyst materials due to the scavenging effect of enhanced Fe^{2+} leaching on HO^* radicals (Reaction (22.3)) [56, 143]. Excess Fe^{2+} ions in solution competes with CPs for HO^* radicals, and thus inhibits CP degradation. Liu et al. [130] showed that while increasing the dose of bimetallic Al/Fe particles from 1.01 to 5.05 g l^{-1} improved 4-CP degradation with surface-catalyzed Fenton reactions, a catalyst dose over 5.05 g l^{-1} led to a decrease in 4-CP degradation due to excessive consumption of HO^* radicals (Reaction (22.3)). Similarly, Liu et al. [83] reported that although increasing the catalyst dose from 0.05 to 0.1 g l^{-1} for a Au/Fe_3O_4 bimetallic system increased 4-CP degradation from 62 to 95%, a catalyst dose greater than 0.1 g l^{-1} had little or no effect on 4-CP degradation. According to the authors, this was caused by the agglomeration of catalyst particles and the scavenging effect induced by excess Fe ions.

22.3.3 Effect of pH

Solution pH significantly impacts homogenous/heterogeneous Fenton degradation of chlorophenolic compounds by changing the catalyst surface properties and the ionization of chlorophenolic compounds [112]. In general, CP removal with Fe-bearing materials used as the catalyst in heterogeneous Fenton reactions decreases with increasing solution pH [25, 56, 64, 73, 80, 112]. The decrease in CP degradation may be attributed to a number of factors, including (i) change in surface properties of Fe catalysts and (ii) decrease in Fe^{2+}/Fe^{3+} solubility with increasing pH [56, 61, 64, 73, 80, 111, 112]. The Fenton reactions are more effectively carried out at acidic pH conditions (pH < 4) due to the low solubility of Fe species under slightly acidic to alkaline pH conditions [56, 57]. It is known that the solubility of Fe^{3+}/Fe^{2+} ions decreases with increasing pH. As a result, Fe ions precipitate as $Fe(OH)_{3[S]}/Fe(OH)_{2[S]}$ sludge on the catalyst surface, leading to the inactivation and thus inhibition of further HO^* generation on the catalyst surface [56]. The decrease in Fe^{2+} solubility from the catalyst with increasing pH can also adversely affect homogenous Fenton oxidation of CPs due to limited Fe^{2+} leaching from the catalyst surface [56, 62, 73, 114].

UNCORRECTED PROOFS

Trim Size: 170mm x 244mm Single Column Loose Ribeiro670117 c22.tex V1 - 12/12/2020 12:31am Page 567

In addition to Fe solubility, the catalyst surface properties also show variations depending on solution pH. While the surface of Fe oxides/sulfides is usually positively charged under acidic conditions, the surface charge changes from positive to negative with increasing solution pH, especially at pH values > pH_{pzc} of the Fe materials [93]. Note that while the pH_{pzc} of pyrite is 2, that for Fe-oxides lies in the range from 7 to 9 [56, 120]. On the other hand, as shown in Table 22.1, the dissociation constants (pK_a) for CPs range from 4.7 for PCP to 9.41 for 4-CP, suggesting that the ionization of multichlorophenols (e.g. PCP) starts at much lower pH values; thus the electrostatic repulsive forces between negatively charged CPs and negatively charged catalyst surfaces become dominant, leading to a decrease in CP adsorption onto Fe-oxides under alkaline pH conditions. A study by Bandara et al. [115] shows that CP adsorption onto Fe-oxides decreased with increasing pH and exhibited dependence on CP type, with monochlorophenolic compounds exhibiting a much higher sorptive affinity relative to multichlorophenolic compounds. According to Xu and Wang [61], enhanced CP removal in Fe_3O_4/H_2O_2 system under acidic conditions was caused by several factors including the higher oxidation power of HO^* radicals, more Fe leaching, much greater stability of H_2O_2 in an acidic environment, and enhanced adsorption of CPs onto the catalyst surface through the formation of an inner-sphere Fe-oxide-CP surface complex [≡FeO-Cl-C], which may, in turn, contribute to surface catalytic CP degradation through heterogeneous Fenton reactions. A similar effect of solution pH on CP degradation was also reported for sulfide minerals such as pyrite [56]. Low CP removal with increasing pH was found to parallel a decrease in Fe solubility and change in pyrite surface properties [56]. As stated previously, adding H_2O_2 leads to Fe^{3+} leaching from pyrite (Reaction (22.7)), which, in turn, oxidizes the pyrite surface (Reaction (22.8)) to produce Fe^{2+} for subsequent homogenous Fenton reactions in an acidic environment (Reaction (22.1)). However, under alkaline pH conditions, Fe-oxides accumulate on the pyrite surface and change the pH_{pzc} value to higher pH values. This, then, leads to electrostatic repulsion between the negatively charged surface and negatively charged CP molecules. Similarly, in systems containing ZVI, adding H_2O_2 oxidized the ZVI surface, thereby leading to the deposition of iron oxides on the ZVI surface (e.g. magnetite and lepidocrocite) and subsequent loss of its catalytic activity in an alkaline environment [112].

Although the introduction of bimetallic particles or Fe catalysts with support materials extended the optimum pH range to neutral pH conditions by accelerating the Fe redox cycle and CP adsorption as well as minimizing Fe leaching from the catalyst surface, pH is still an important parameter for controlling CP degradation with heterogeneous Fenton reactions in an alkaline environment [25, 32, 82, 83, 100, 104, 111, 130, 140].

22.3.4 Effect of Hydrogen Peroxide Dose

The in situ generation or external addition of H_2O_2 is a necessity to produce homogenous or heterogeneous HO^* radicals on the catalyst surface or in the bulk solution (Reaction 22.1). Studies performed with heterogeneous catalysts show that while CP

UNCORRECTED PROOFS

Trim Size: 170mm x 244mm Single Column Loose Ribeiro670117 c22.tex V1 - 12/12/2020 12:31am Page 568

degradation increases with increasing H_2O_2 dose due to enhanced HO^* radical generation, using an excess H_2O_2 dose can adversely affect process efficiency due to the scavenging effect of excess H_2O_2 on HO^* radicals [32, 64, 90, 112]:

$$HO^* + H_2O_2 = HO_2^* + H_2O \tag{22.14}$$

Gan et al. [64] reported a close relationship between H_2O_2 dose and 2,4-DCP removal by ZVI due to the enhanced generation of HO radicals in accordance with Reaction (22.1). However, the authors also found that adding H_2O_2 at > 15 mM resulted in a significant reduction in 2,4-DCP degradation, in parallel with the scavenging effect of H_2O_2 on HO^* radicals (Reaction 22.14). In a study with a ZVI-Fenton system, similarly, Zhou et al. [112] observed that while increasing the H_2O_2 concentration significantly improved 4-CP degradation, H_2O_2 applied at higher doses reduced 4-CP degradation. Unlike the system with ZVI, on the other hand, studies performed with Fe-oxides show no direct relationship between H_2O_2 dose and CP degradation [61, 110].

The scavenging effect induced by H_2O_2 was reported to decline in multimetallic Fe catalysts and Fe catalysts with support materials [73, 87, 92]. In systems with pyrite supported with GO, for instance, Liu et al. [73] observed that 4-CP removal increased with increasing H_2O_2 concentration even though the extent of the rate increase became smaller at higher H_2O_2 concentrations. The authors attributed the increase in 4-CP degradation to Fe^{2+} dissolution from pyrite in accordance with Reactions (22.7) and (22.8). Similarly, using rectorite-supported nano-Fe_3O_4 composite material as the catalyst, Bao et al. [92] reported an increase in 4-CP degradation with increasing H_2O_2 concentration due to enhanced Fe^{2+} leaching, which catalyzed homogenous Fenton degradation. The authors also showed that an excess H_2O_2 dose did not have any further effect on 4-CP degradation.

Recently, Fe catalysts with support materials have been modified to allow in situ generation of H_2O_2 on the catalyst surface for Fenton-like CP degradation (e.g. [[84, 85]). For instance, Yang et al. [84] synthesized a Zn-Fe_3O_4 composite supported with CNTs that could interact with O_2 to form H_2O_2 and HO^* radicals on the catalyst surface. Liu et al. [85] report H_2O_2 generation up to 40 mg l^{-1} at pH 2 in a system with bimetallic composite Zn-Fe supported with CNTs. The in situ generation of H_2O_2 and HO^* radicals on the pyrite surface has also been reported by Weerasooriya et al. [65].

22.3.5 Effect of Organic Ligands

The corrosion and accumulation of surface precipitates containing Fe-oxides on the catalyst surface have been shown to have an adverse effect on CP Fenton degradation with heterogeneous Fe catalysts under slightly acidic to alkaline pH conditions [56, 71, 74]. Organic chelating agents such as ethylenediaminetetraacetic acid (EDTA), citrate, and oxalate can improve Fenton reactions by (i) strongly complexing with Fe^{2+}/Fe^{3+} and accelerating the Fe redox cycle, and (ii) removing surface precipitates through the formation of highly soluble Fe-ligand complexes [57, 71, 130]. Liu et al. [130], for instance, report that adding EDTA to a system

UNCORRECTED PROOFS

Trim Size: 170mm x 244mm Single Column Loose Ribeiro670117 c22.tex V1 - 12/12/2020 12:31am Page 569

containing bimetallic Al/Fe catalyst improved 4-CP removal by accelerating H_2O_2 production through (i) strong complexation of EDTA with Fe^{2+}/Fe^{3+}, which leads to enhanced H_2O_2 generation; and (ii) electron transfer from Al to O_2. Similarly, Huang et al. [129] observed that EDTA accelerated 4-CP degradation with the $Fe@Fe_2O_3$ system by enhancing HO^* radical generation. Xu et al. [71] reported that citrate, an organic ligand, increased 4-CP degradation with ZVI by (i) enhancing Fe^{2+} leaching from ZVI, and subsequently leading to generating more radicals for Fenton degradation; and (ii) the adsorption of $FeCit^-$ complex onto Fe^0 surface, which expedited electron transfer from ZVI to O_2 to promote interfacial HO radical generation. According to Xue et al. [74], the stimulatory effect of chelating agents on PCP degradation with an Fe_3O_4/H_2O_2 system is not directly related to magnetite dissolution but rather explained by the adsorption of ligands onto the Fe_3O_4 surface, which, in turn, accelerates the Fe^{3+}/Fe^{2+} redox cycle and catalyzes more radical production by Fenton reactions.

On the other hand, Lu et al. [110] found that although the chelating agent oxalate enhanced Fe^{2+}/Fe^{3+} leaching from goethite, it had an adverse effect on 2-CP degradation with a goethite-Fenton system. According to Kantar et al. [57], adding chelating agents can improve Fenton degradation of CPs in heterogeneous catalyst systems such as pyrite as long as the catalyst dose is high enough to overcome the competitive effect induced by the chelating agents to consume HO^* radicals.

22.4 Reaction By-Products

Degrading CPs with a heterogeneous Fenton process is complex and may involve consecutively and concurrently occurring multiple different reaction pathways [56, 61, 62, 75, 112, 130, 141, 142]. A rough representative diagram showing the reaction pathways for degrading CPs with a heterogeneous Fenton process is shown in Figure 22.4. CP degradation with heterogeneous Fenton reactions is usually represented by a short initial period of rapid degradation, followed by a much slower degradation period. The initial stage occurs within seconds to minutes and involves the rapid oxidation of the mother chlorophenolic compound to short-chain organic acids such as acetic acid, formic acid, maleic, oxalic acid, etc. via the attack of HO radicals at the ortho and para positions in the aromatic benzene ring. This results in the conversion and polymerization of the mother compound to aromatic and chlorinated aromatic intermediate by-products containing phenols, quinones, hydroquinones, chlorohydroquinones, benzoquinones, highly chlorinated compounds, and chlorocatechols [25, 32, 56, 57, 62, 75, 83–85, 88, 112, 142]. A sizable list of intermediate compounds formed depending on the type of catalyst system used and the type of CP degraded is shown in Tables 22.2–22.4. The slower second stage is caused by the oxidation of short-chain organic acids to CO_2 [56, 57, 61, 62, 73]. The type and concentration of intermediate by-products formed depend on a number of factors, including the type of CP degraded, catalyst type and dose, H_2O_2 dose, solution pH, and reaction time [3, 56, 57, 62, 64, 73, 85, 88, 96, 128, 129]. According to Catrinescu et al. [88], for instance, degrading 4-CP with a bimetallic

UNCORRECTED PROOFS

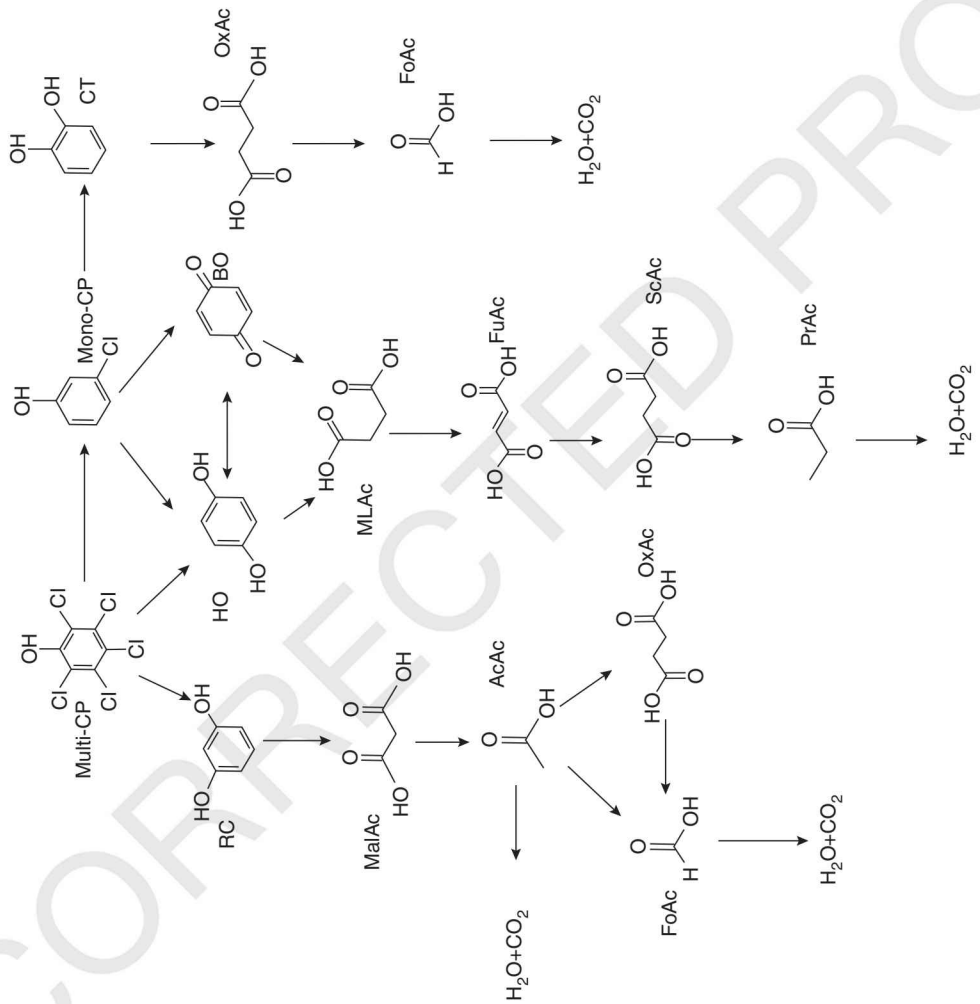

Figure 22.4 Representative CP degradation pathways for CP degradation with heterogeneous Fenton reactions. AcAc, acetic acid; BQ, benzoquinone; CT, catechol; FoAc, formic acid; FuAc, fumaric acid; HQ, hydroquinone; MLAc, maleic acid; MalAc, malonic acid; PrAc, propanoic acid; RC, resorcinol; ScAc, succinic acid.

UNCORRECTED PROOFS

Trim Size: 170mm x 244mm Single Column Loose Ribeiro670117 c22.tex V1 - 12/12/2020 12:31am Page 571

Al/Fe catalyst supported with PILCs resulted in the formation of intermediate compounds containing hydroquinone, 4-chlorocatechol, chlorohydroquinone, 2,4-dichlorophenol, dichlorocatechol, and 5 chloro-1,2,4 benzenetriol. Similarly, in pyrite supported with a GO system [73], the intermediate compounds detected for 4-CP degradation included oxalic acid, acetic acid, and chloroacetic acid, and their concentrations changed as a function of reaction time. Wang et al. [96] demonstrated that 4-CP degradation by Fe_3O_4 supported with a β-cylcodextrin nanocomposite follows a reaction pathway involving the attack of HO^* radicals to hydroxyl groups located at the para position to produce hydroquinone, followed by the dehydrogenation of hydroquinone to benzoquinone. Subsequently, the oxidation cycle continued to ultimately generate short-chain organic acids such as fumaric, formic, acetic, and malonic acids. In a study involving 4-CP degradation with a CNT-supported Zn/Fe_3O_4 composite material, Yang et al. [84] reported that the oxidation reaction was initiated by HO^* attack at the hydroxyl group located in the ortho position to generate 4-chlorocatachol. Li et al. [62] show that while the initial degradation of 2,4-DCP with a nano-scaled ZVI/H_2O_2 system occurred very fast, within less than 50 minutes of reaction time, the complete mineralization of intermediates species containing phenol, 2-CP, 3,5-dichlorocatechol, hydroquinone, maleic acid, etc. took much longer to complete. Using the pyrite-Fenton system for degrading 2,4-DCP, while several different intermediate compounds including chloroacetic acid, acetic acid, maleic acid, formic acid 4-chloro-1,3-benzenediol, and 2,4,5-trichlorophenol were detected in a batch system with very low pyrite loading [56], the only intermediate compounds observed in the effluent of column studies with very high pyrite loading were short-chain organic acids such as formic and oxalic acids [57]. Similarly, acetic acid and formic acid were reported as the final degradation products of 2,4-DCP degradation with Fe_3O_4 as the catalyst used in the Fenton reaction [61].

22.5 Mode of Implementation, Reactor Configuration, and Biodegradability

Due to the toxicity and low biodegradability of chlorophenolic compounds, AOPs such as the Fenton process can be applied as (i) the only treatment process [104], (ii) a pretreatment step before biodegradation [52], or (iii) a post-treatment step [20] following biodegradation, depending on the quality of CP-containing wastewater (Figure 22.5). A complete CP and total organic carbon (TOC) removal can only be achieved in large reactors using high dosages of chemicals, when the heterogeneous Fenton process is used as the sole treatment method [52, 144]. For instance, Barreto-Rodrigues et al. [104] determined that although CP degradation with Fe/Ag composite material immobilized in alginate was achieved within 30 minutes of reaction time, it required more than 90 minutes to completely mineralize all intermediate reaction compounds. Using nano-ZVI as the catalyst, Li et al. [62] found that while 2,4-DCP removal reached 93% at $t = 180$ minutes, the TOC removal efficiency was only 30% at the same reaction time, suggesting the formation of chemically less-degradable compounds that require much longer reaction times to mineralize.

UNCORRECTED PROOFS

Trim Size: 170mm x 244mm Single Column Loose Ribeiro670117 c22.tex V1 - 12/12/2020 12:31am Page 572

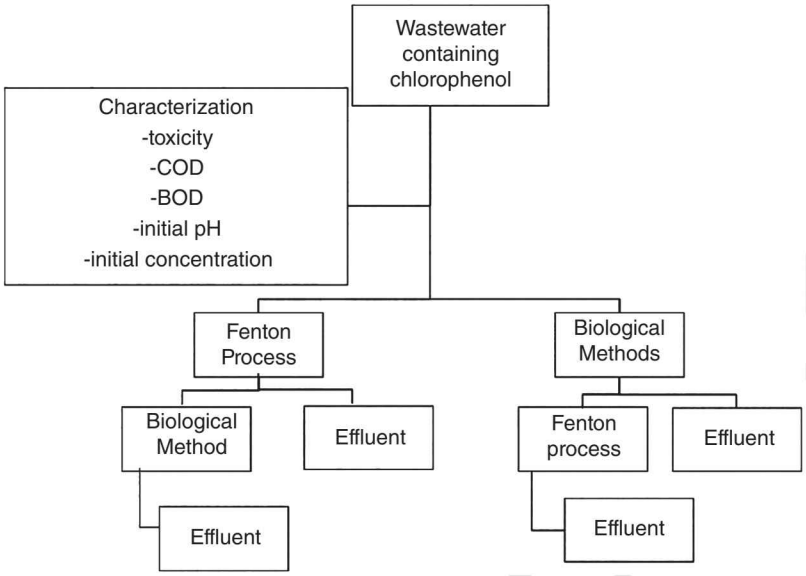

Figure 22.5 Incorporating the Fenton process into biological degradation for CP treatment.

The toxicity of reaction by-products of heterogeneous Fenton oxidation of chlorophenols depends on the type of species formed [42, 145]. Except for a limited number of studies reporting that pretreatment with Fenton oxidationdid not change the toxicity, or produced more toxic compounds than the mother compound [42], in general, Fenton oxidation of CPs has been shown to produce intermediate species with much lower toxicity [46, 75, 142, 146]. For instance, Munoz et al. [142] found that while the Fenton treatment of chlorophenols with a heterogeneous Pd/Fe catalyst supported with alumina resulted in limited TOC removal, the reaction by-products following Fenton oxidation were much less toxic than their mother compounds. Pretreating 4-CP with bentonite-supported bimetallic Fe/Pd nanoparticles significantly improved the biodegradability of 4-CP with a bacterial strain, *Bacillus-fusiformis,* without any observed adverse effects on cell growth. Similarly, a batch study by Xu and Wang [75] suggested that while 2,4-6-TCP treatment with nanoscaled-Fe_3O_4/CeO_2 composite material significantly reduced the toxicity of 2,4,6-TCP, the TOC removal remained at 65%, implying that Fenton oxidation can be used as a pretreatment stage to decrease the toxicity and enhance the biodegradability of 2,4,6-TCP prior to biodegradation. A typical reactor configuration combining heterogeneous Fenton reactions with biological processes for CP degradation is shown in Figure 22.6.

22.6 Conclusions

Chlorophenolic compounds are persistent contaminants commonly observed in contaminated soil and groundwater due to their high toxicity and low biodegradability. While the classical homogenous Fenton process suffers from

UNCORRECTED PROOFS

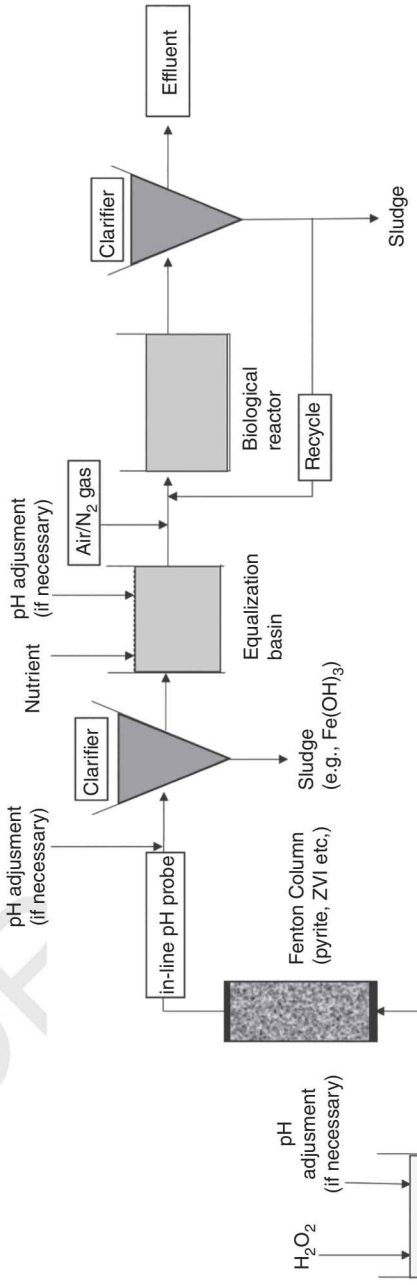

Figure 22.6 Reactor configuration for sequential heterogeneous Fenton-biological CP treatment.

UNCORRECTED PROOFS

Trim Size: 170mm x 244mm Single Column Loose Ribeiro670117 c22.tex V1 - 12/12/2020 12:31am Page 574

high operating costs and excessive sludge formation, heterogeneous Fenton processes are a viable, cost-effective solution to the oxidative dehalogenation of chlorophenolic compounds by using solid-based catalyst materials (e.g. ZVI and pyrite) with much lower chemical costs and reduced sludge production. The heterogeneous processes use different catalyst materials, including monometallic Fe materials (e.g. Fe oxides/sulfides), multimetallic Fe composites, and Fe catalysts with support materials. Monometallic Fe catalysts such as pyrite, ZVI, and Fe_3O_4 exhibit very high catalytic efficiency toward heterogeneous Fenton degradation of chlorophenols with much less sludge production than homogenous Fenton processes, and the reaction mechanism for the Fenton degradation of CPs with monometallic catalysts is usually attributed to homogenous Fenton degradation regulated by the extent of Fe^{2+} leaching from the catalyst. The reaction mechanism involved in multimetallic Fe catalyst systems can be explained through a combined effect of surface catalysis through interfacial HO^* generation and homogenous Fenton oxidation induced by Fe^{2+} leaching from the catalyst surface. However, multimetallic catalysts may suffer from the aggregation of nanoparticles, which, in turn, may create problems in terms of process efficiency and sustainability. Fe catalysts with support materials, on the other hand, minimize the risk of particle aggregation and reduce Fe^{2+} leaching from the catalyst, and thus the degradation of CPs is usually dominated by surface catalysis driven by interfacial HO^* radicals.

The Fenton degradation of CPs with heterogeneous catalysts usually produces intermediate reaction by-products containing aromatic (e.g. phenols, quinones, hydroquinones, chlorohydroquinones, benzoquinones, highly chlorinated compounds, and chlorocatechols) and aliphatic (e.g. short-chain organic acids) organic compounds, depending on the catalyst type, size, and dose, and type; concentration of CP treated; reaction time; H_2O_2 concentration; etc. The reaction by-products are usually less toxic than the mother compound and thus can be treated in a biological reactor to meet the discharge criteria set for wastewaters containing CPs.

References

1 Tai, C. and Jiang, G. (2005). Dechlorination and destruction of 2, 4, 6-trichlorophenol and pentachlorophenol using hydrogen peroxide as the oxidant catalyzed by molybdate ions under basic condition. *Chemosphere* 59 (3): 321–326.

2 Vlastos, D., Antonopoulou, M., and Konstantinou, I. (2016). Evaluation of toxicity and genotoxicity of 2-chlorophenol on bacteria, fish and human cells. *Science of the Total Environment* 551: 649–655.

3 Guo, M., Weng, X., Wang, T., and Chen, Z. (2017). Biosynthesized iron-based nanoparticles used as a heterogeneous catalyst for the removal of 2,4-dichlorophenol. *Separation and Purification Technology* 175: 222–228.

4 Yu, C., Wang, C., Lu, Z. et al. (2019). The endocrine-disrupting potential of four chlorophenols by in vitro and in silico assay. *Chemosphere* 218: 941–947.

UNCORRECTED PROOFS

Trim Size: 170mm x 244mm Single Column Loose Ribeiro670117 c22.tex V1 - 12/12/2020 12:31am Page 575

5 Pera-Titus, M., Garcia-Molina, V., Banos, M.A. et al. (2004). Degradation of chlorophenols by means of advanced oxidation processes: a general review. *Applied Catalysis B: Environmental* 47: 219–256.

6 Ge, T., Han, J., Qi, Y. et al. (2017). The toxic effects of chlorophenols and associated mechansims in fish. *Aquatic Toxicology* 184: 78–93.

7 Du, Y., Zhou, M., and Lei, L. (2006). Role of the intermediates in the degradation of phenolic compounds by Fenton-like process. *Journal of Hazardous Materials* 136 (3): 859–865.

8 Sharma, S., Mukhopadhyay, M., and Murthy, Z.V.P. (2013). Treatment of chlorophenols from wastewaters by advanced oxidation processes. *Separation and Purification Reviews* 42 (4): 263–295.

9 Kuan, C.C., Chang, S.Y., and Schroeder, S.L. (2015). Fenton-like oxidation of 4-chlorophenol: homogeneous or heterogeneous? *Industrial & Engineering Chemistry Research* 54 (33): 8122–8129.

10 ATSDR, Agency for Toxic Substances and Disease Registry. (2007). Comprehensive Environmental Response, Compensation and Liability Act (CERCLA) Priority List of Hazardous Substances. https://www.atsdr.cdc.gov/spl/previous/07list.html.

11 Czaplicka, M. (2004). Sources and transformations of chlorophenols in the natural environment. *Science of the Total Environment* 322 (1-3): 21–39.

12 Garba, Z.N., Zhou, W., Lawan, I. et al. (2019). An overview of chlorophenols as contaminants and their removal from wastewater by adsorption: a review. *Journal of Environmental Management* 241: 59–75.

13 Gao, J., Liu, L., Liu, X. et al. (2008). Levels and spatial distribution of chlorophenols −2,4-dichlorophenol, 2,4,6-trichlorophenol, and pentachlorophenol in surface water of China. *Chemosphere* 71: 1181–1187.

14 Sim, W.-J., Lee, S.-H., Lee, I.-S. et al. (2009). Distribution and formation of chlorophenols and bromophenols in marine and river environments. *Chemosphere* 77: 552–558.

15 Igbinosa, E.O., Odjadjare, E.E., Chigor, V.N. et al. (2013). Toxicological profile of chlorophenols and their derivatives in the environment: the public health perspective. *Scientific World Journal* 2013, Article ID: 460215: 1–11.

16 Antonopoulou, M., Vlastos, D., and Konstantinou, I.K. (2015). Photocatalytic degradation of pentachlorophenol by Ni-F-TiO_2: identification of intermediates, mechanism involved, genotoxicity and ecotoxicity evaluation. *Photochemical & Photobiological Sciences* 14: 520–527.

17 Zilouei, H., Guieysse, B., and Mattiasson, B. (2006). Biological degradation of chlorophenols in packed-bed reactors using mixed bacterial consortia. *Process Biochemistry* 41: 1083–1089.

18 Olaniran, A.O. and Igbinosa, E.O. (2011). Chlorophenols and other related derivatives of environmental concern: properties, distribution and microbial degradation processes. *Chemosphere* 83 (10): 1297–1306.

19 Pedroza, A.M., Mosqueda, R., Alonso-Vante, N., and Rodriguez-Vazquez, R. (2007). Sequential treatment via *Tamtes versicolor* and UV/TiO_2/Ru_xSe_y to

UNCORRECTED PROOFS

Trim Size: 170mm x 244mm Single Column Loose Ribeiro670117 c22.tex V1 - 12/12/2020 12:31am Page 576

reduce contaminants in wastewater resulting from the bioleaching process during paper production. *Chemosphere* 67: 793–801.

20 González, L.F., Sarria, V., and Sánchez, O.F. (2010). Degradation of chlorophenols by sequential biological-advanced oxidative process using Trametes pubescens and TiO_2/UV. *Bioresource Technology* 101 (10): 3493–3499.

21 Chang, C.-C., Tseng, S.-K., Chang, C.-C., and Ho, C.-M. (2004). Degradation of 2-chlorophenol via a hydrogenotrophic biofilm under different reductive conditions. *Chemosphere* 56: 989–997.

22 Bajaj, M., Gallert, C., and Winter, J. (2008). Anaerobic biodegradation of high strength 2-chlorophenol-containing synthetic wastewater in a fixed bed reactor. *Chemosphere* 73: 705–710.

23 Liu, X.-P. (2009). Kinetics of cometabolic degradation of 2-chlorophenol and phenol by *Pseudomonas putida*. *Water Science and Engineering* 2 (3): 110–120.

24 Khan, M.Z., Mondal, P.K., and Sabir, S. (2011). Bioremediation of 2-chlorophenol containing wastewater by aerobic granules-kinetics and toxicity. *Journal of Hazardous Materials* 190: 222–228.

25 Zhou, Y., Kuang, Y., Li, W. et al. (2013). A combination of bentonite-supported bimetallic Fe/Pd nanoparticles and biodegradation for the remediation of p-chlorophenol in wastewater. *Chemical Engineering Journal* 223: 68–75.

26 Moussavi, G., Ghodrati, S., and Mohseni-Bandpei, A. (2014). The biodegradation and COD removal of 2-chlorophenol in a granular anoxic baffled reactor. *Journal of Biotechnology* 184: 111–117.

27 Farrell, A. and Quilty, B. (1999). Degradation of mono-chlorophenols by a mixed community via a meta-cleavage pathway. *Biodegradation* 10: 353–362.

28 Farrell, A. and Quilty, B. (2002). The enhancement of 2-chlorophenol degradation by a mixed microbial community when augmented with *Pseudomonas putida* CP1. *Water Research* 36: 2443–2450.

29 Monsalvo, V.M., Mohendano, A.F., Casa, J.A., and Rodrigues, J.J. (2009). Cometabolic biodegradation of 4-chlorophenol by sequencing batch reactors at different temperatures. *Bioresource Technology* 100: 4572–4578.

30 Zahouane-Boudiaf, H. and Boutahala, M. (2011). Kinetic analysis of 2,4,5-trichlorophenol adsorption onto acid-activated montmorillonite from aqueous solution. *International Journal of Mineral Processing* 100: 72–78.

31 Ambika, S., Devasena, M., and Nambi, I.M. (2016). Synthesis, characterization and performance of high energy ball milled meso-scale zero valent iron in Fenton reaction. *Journal of Environmental Management* 181: 847–855.

32 Wang, N., Zheng, T., Zhang, G., and Wang, P. (2016). A review on Fenton-like processes for organic wastewater treatment. *Journal of Environmental Chemical Engineering* 4 (1): 762–787.

33 Boczkaj, C. and Fernandes, A. (2017). Wastewater treatment by means of advanced oxidation processes at basic pH conditions: a review. *Chemical Engineering Journal* 320: 608–633.

34 Huang, D., Hu, C., Zeng, G. et al. (2017). Combination of Fenton processes and biotreatment for wastewater treatment and soil remediation. *Science of the Total Environment* 574: 1599–1610.

UNCORRECTED PROOFS

Trim Size: 170mm x 244mm Single Column Loose Ribeiro670117 c22.tex V1 - 12/12/2020 12:31am Page 577

35 Mirzaei, A., Chen, Z., Haghighat, F., and Yerushalmi, L. (2017). Removal of pharmaceuticals from water by homo/heterogonous Fenton-type processes- a review. *Chemosphere* 174: 665–688.

36 Tekin, H., Bilkay, O., Ataberk, S.S. et al. (2006). Use of Fenton oxidation to improve the biodegradability of a pharmaceutical wastewater. *Journal of Hazardous Materials* 136 (2): 258–265.

37 Perez-Estrada, L.A., Maldonado, M.I., Gernjak, W. et al. (2005). Decomposition of diclofenac by solar driven photocatalysis at pilot plant scale. *Catalysis Today* 101: 219–226.

38 Kajitvichyanukul, P. and Suntronvipart, N. (2006). Evaluation of biodegradability and oxidation degree of hospital wastewater using photo-Fenton process as the pretreatment method. *Journal of Hazardous Materials* 138: 384–391.

39 Velasquez, M., Santander, I.P., Contreras, D.R. et al. (2014). Oxidative degradation of sulfathiazole by Fenton and photo-Fenton reactions. *Journal of Environmental Science and Health, Part A Environmental Science* 49: 661–670.

40 Hartmann, M., Kullmann, S., and Keller, H. (2010). Wastewater treatment with heterogeneous Fenton-type catalysts based on porous materials. *Journal of Materials Chemistry* 20: 9002–9017.

41 Maezono, T., Tokumura, M., Sekine, M., and Kawase, Y. (2011). Hydroxyl radical concentration profile in photo-Fenton oxidation process: generation and consumption of hydroxyl radicals during the discoloration of azo-dye Orange II. *Chemosphere* 82: 1422–1430.

42 Perez-Moya, M., Graells, M., del Valle, L.J. et al. (2007). Fenton and photo-Fenton degradation of 2-chlorophenol: multivariate analysis and toxicity monitoring. *Catalysis Today* 124 (3–4): 163–171.

43 Poerschmann, J., Trommler, U., Gorecki, T., and Kopinke, F.-D. (2009). Formation of chlorinated biphenyls, diphenyl ethers and benzofurans as a result of Fenton-driven oxidation of 2-chlorophenol. *Chemosphere* 75: 772–780.

44 Zimbron, J.A. and Reardon, K.F. (2009). Fenton's oxidation of pentachlorophenol. *Water Research* 43 (7): 1831–1840.

45 Munoz, M., de Pedro, Z.M., Casas, J.A., and Rodriguez, J.J. (2011). Assessment of the generation of chlorinated byproducts upon Fenton-like oxidation of chlorophenols at different conditions. *Journal of Hazardous Materials* 190: 993–1000.

46 Karci, A., Arslan-Alaton, I., Olmez-Hanci, T., and Bekbölet, M. (2012). Transformation of 2,4-dichlorophenol by H2O2/UV-C, Fenton and photo-Fenton processes: oxidation products and toxicity evolution. *Journal of Photochemistry and Photobiology A: Chemistry* 230: 65–73.

47 Detomaso, A., Lopez, A., Lovecchio, G. et al. (2003). Practical applications of the Fenton reaction to the removal of chlorinated aromatic pollutants. *Environmental Science and Pollution Research* 10 (6): 379.

48 Kong, S.-H., Watts, R.J., and Choi, J.H. (1998). Treatment of petroleum-contaminated soils using iron mineral catalyzed hydrogen peroxide. *Chemosphere* 37 (8): 1473–1482.

UNCORRECTED PROOFS

Trim Size: 170mm x 244mm Single Column Loose Ribeiro670117 c22.tex V1 - 12/12/2020 12:31am Page 578

49 Du, Y., Zhou, M., and Lei, L. (2007). The role of oxygen in the degradation of p-chlorophenol by Fenton system. *Journal of Hazardous Materials* 139 (1): 108–115.

50 Hong, S.-H., Kwon, B.-H., Lee, J.-K., and Kim, H.-K. (2008). Degradation of 2-chlorophenol by Fenton and photo-Fenton processes. *Korean Journal of Chemical Engineering* 25 (1): 46–52.

51 Poerschmann, J. and Trommler, U. (2009). Pathways of advanced oxidation of phenol by Fenton's reagent – identification of oxidative coupling intermediates by extractive acetylation. *Journal of Chromatography, A* 1216: 5570–5579.

52 Zimbron, J.A. and Reardon, K.F. (2011). Continuous combined Fenton's oxidation and biodegradation for the treatment of pentachlorophenol-contaminated water. *Water Research* 45 (17): 5705–5714.

53 de Luna, M.D.G., Briones, R.M., Su, C.-C., and Lu, M.-C. (2013). Kinetics of acetaminophen degradation by Fenton oxidation in a fluidized-bed reactor. *Chemosphere* 90: 1444–1448.

54 Che, H. and Lee, W. (2011). Selective redox degradation of chlorinated aliphatic compounds by Fenton reaction in pyrite suspension. *Chemosphere* 82 (8): 1103–1108.

55 Bae, S., Kim, D., and Lee, W. (2013). Degradation of diclofenac by pyrite catalyzed Fenton oxidation. *Applied Catalysis B: Environmental* 134–135: 93–102.

56 Kantar, C., Oral, O., Urken, O. et al. (2019). Oxidative degradation of chlorophenolic compounds with pyrite-Fenton process. *Environmental Pollution* 247: 349–361.

57 Kantar, C., Oral, O., Urken, O., and Oz, N.A. (2019). Role of complexing agents on oxidative degradation of chlorophenolic compounds by pyrite-Fenton process: batch and column experiments. *Journal of Hazardous Materials* 373: 160–167.

58 Garrido-Ramírez, E.G., Theng, B.K.G., and Mora, M.L. (2010). Clays and oxide minerals as catalysts and nanocatalysts in Fenton-like reactions—a review. *Applied Clay Science* 47 (3–4): 182–192.

59 Lu, M.-C. (2000). Oxidation of chlorophenols with hydrogen peroxide in the presence of goethite. *Chemosphere* 40: 125–130.

60 Lee, S., Oh, J., and Park, Y. (2006). Degradation of phenol with Fenton-like treatment by using heterogeneous catalyst [modified iron oxide] and hydrogen peroxide. *Bulletin of the Korean Chemical Society* 27: 4489–4494.

61 Xu, L. and Wang, J. (2012). Fenton-like degradation of 2,4-dichlorophenol using Fe_3O_4 magnetic nanoparticles. *Applied Catalysis B: Environmental* 123–124: 117–126.

62 Li, R., Gao, Y., Jin, X. et al. (2015). Fenton-like oxidation of 2,4-DCP in aqueous solution using iron-based nanoparticles as the heterogeneous catalyst. *Journal of Colloid and Interface Science* 438: 87–93.

63 Li, R., Jin, X., Megharaj, M. et al. (2015). Heterogeneous Fenton oxidation of 2,4-dichlorophenol using iron-based nanoparticles and persulfate system. *Chemical Engineering Journal* 264: 587–594.

UNCORRECTED PROOFS

Trim Size: 170mm x 244mm Single Column Loose Ribeiro670117 c22.tex V1 - 12/12/2020 12:31am Page 579

64 Gan, L., Li, B., Guo, M. et al. (2018). Mechanism for removing 2,4-dichlorophenol via adsorption and Fenton-like oxidation using iron-based nanoparticles. *Chemosphere* 206: 168–174.

65 Weerasooriya, R., Makehelwala, M., and Bandara, A. (2010). Probing reactivity sites on pyrite-oxidative interactions with 4-chlorophenol. *Colloids and Surfaces A: Physicochemical and Engineering Aspects* 367 (1-3): 65–69.

66 Zhou, T., Lim, T.-K., Lu, X. et al. (2009). Simultaneous degradation of 4-CP and EDTA in a heterogeneous ultrasound/Fenton like system at ambient circumstance. *Separation and Purification Technology* 68: 367–374.

67 Wang, W., Qu, Y., Yang, B. et al. (2012). Lactate oxidation in pyrite suspension: a Fenton-like process in situ generating H_2O_2. *Chemosphere* 86: 376–382.

68 Wang, Y.R. and Chu, W. (2013). Photo-assisted degradation of 2,4,5-trichlorophenol by electro-Fe(II)/Oxone process using a sacrificial iron anode: performance optimization and reaction mechanism. *Chemical Engineering Journal* 215–216: 643–650.

69 Yang, Z., Zhang, X., Pu, S. et al. (2019). Novel Fenton-like system [mg/Fe-O_2] for degradation of 4-chlorophenol. *Environmental Pollution* 250: 906–913.

70 Zhang, Y. and Zhou, M. (2019). A critical review of the application of chelating agents to enable Fenton and Fenton-like reactions at high pH values. *Journal of Hazardous Materials* 362: 436–450.

71 Xu, Y., Zeng, L., Li, L. et al. (2019). Enhanced oxidative activity of zero-valent iron by citric acid complexation. *Chemical Engineering Journal* 373: 891–901.

72 He, J., Yang, X., Men, B., and Wang, D. (2016). Interfacial mechanisms of heterogeneous Fenton reactions catalyzed by iron-based materials: a review. *Journal of Environmental Sciences* 39: 97–109.

73 Liu, W., Xu, L., Li, X. et al. (2015). High-dispersive FeS2 on graphene oxide for effective degradation of 4-chlorophenol. *RSC Advances* 5 (4): 2449–2456.

74 Xue, X., Hanna, K., Despas, C. et al. (2009). Effect of chelating agent on the oxidation rate of PCP in the magnetite/H_2O_2 system at neutral pH. *Journal of Molecular Catalysis A: Chemical* 311 (1–2): 29–35.

75 Xu, L. and Wang, J. (2015). Degradation of 2,4,6-trichlorophenol using magnetic nanoscaled Fe3O4/CeO2 composite as a heterogeneous Fenton-like catalyst. *Separation and Purification Technology* 149: 255–264.

76 Huang, H.-H., Lu, M.-C., and Chen, J.-N. (2001). Catalytic decomposition of hydrogen peroxide and 2-Chlorophenol with iron oxides. *Water Research* 35 (9): 2291–2299.

77 de la Plata, G.B.O., Alfano, O.M., and Cassano, A.E. (2010). Decomposition of 2-chlorophenol employing goethite as Fenton catalyst. I. Proposal of a feasible, combined reaction scheme of heterogeneous and homogeneous reactions. *Applied Catalysis B: Environmental* 95 (1–2): 1–13.

78 de la Plata, G.B.O., Alfano, O.M., and Cassano, A.E. (2012). 2-Chlorophenol degradation via photo Fenton reaction employing zero valent iron nanoparticles. *Journal of Photochemistry and Photobiology A: Chemistry* 233: 53–59.

UNCORRECTED PROOFS

Trim Size: 170mm x 244mm Single Column Loose Ribeiro670117 c22.tex V1 - 12/12/2020 12:31am Page 580

79 Cheng, R., Cheng, C., Liu, G.H. et al. (2015). Removing pentachlorophenol from water using a nanoscale zero-valent iron/H_2O_2 system. *Chemosphere* 141: 138–143.

80 Santos-Juanes, L., García-Ballesteros, S., Vercher, R.F. et al. (2019). Commercial steel wool used for zero Valent iron and as a source of dissolved iron in a combined red-ox process for pentachlorophenol degradation in tap water. *Catalysis Today* 328: 252–258.

81 Kurian, M. and Nair, D.S. (2015). Heterogeneous Fenton behavior of nano nickel zinc ferrite catalysts in the degradation of 4-chlorophenol from water under neutral conditions. *Journal of Water Process Engineering* 8: e37–e49.

82 Xu, C., Liu, R., Chen, L., and Tang, J. (2016). Enhanced dechlorination of 2, 4-dichlorophenol by recoverable Ni/Fe–Fe_3O_4 nanocomposites. *Journal of Environmental Sciences* 48: 92–101.

83 Liu, J., Zhao, Z., Ding, Z. et al. (2016). Degradation of 4-chlorophenol in a Fenton-like system using au–Fe_3O_4 magnetic nanocomposites as the heterogeneous catalyst at near neutral conditions. *RSC Advances* 6 (58): 53080–53088.

84 Yang, Z., Gong, X., Peng, L. et al. (2018). Zn^0-CNTs-Fe_3O_4 catalytic in situ generation of H2O2 for heterogeneous Fenton degradation of 4-chlorophenol. *Chemosphere* 208: 665–673.

85 Liu, Y., Fan, Q., Liu, Y., and Wang, J. (2018). Fenton-like oxidation of 4-chlorophenol using H_2O_2 in situ generated by Zn-Fe-CNTs composite. *Journal of Environmental Management* 214: 252–260.

86 Choi, K.-H., Min, J., Park, S.-Y. et al. (2019). Enhanced photocatalytic degradation of tri-clorophenol by Fe_3O_4@TiO_2@Au photocatalyst under visible-light. *Ceramics Internatonal* 45: 9477–9482.

87 Bao, T., Damtie, M.M., Wu, K. et al. (2019). Rectorite-supported nano-Fe3O4 composite materials as catalyst for P-chlorophenol degradation: preparation, characterization, and mechanism. *Applied Clay Science* 176: 66–77.

88 Catrinescu, C., Arsene, D., and Teodosiu, C. (2011). Catalytic wet hydrogen peroxide oxidation of para-chlorophenol over Al/Fe pillared clays [AlFePILCs] prepared from different host clays. *Applied Catalysis B: Environmental* 101 (3–4): 451–460.

89 Zhang, L., Zeng, H., Zeng, Y. et al. (2014). Heterogeneous Fenton-like degradation of 4-chlorophenol using a novel Fe^{III}-containing polyoxometalate as the catalyst. *Journal of Molecular Catalysis A: Chemical* 392: 202–207.

90 Duan, F., Yang, Y., Li, Y. et al. (2014). Heterogeneous Fenton-like degradation of 4-chlorophenol using iron/ordered mesoporous carbon catalyst. *Journal of Environmental Sciences* 26: 1171–1179.

91 Chen, H., Zhang, L., Zeng, H. et al. (2015). Highly active iron-containing silicotungstate catalyst for heterogeneous Fenton oxidation of 4-chlorophenol. *Journal of Molecular Catalysis A: Chemical* 406: 72–77.

92 Bao, T., Damtie, M.M., Wu, K. et al. (2019). Rectorite-supported nano-Fe3O4 composite materials as catalyst for P-chlorophenol degradation: preparation, characterization, and mechanism. *Applied Clay Science* 176: 66–77.

UNCORRECTED PROOFS

Trim Size: 170mm x 244mm Single Column Loose Ribeiro670117 c22.tex V1 - 12/12/2020 12:31am Page 581

93 Liu, J., Zhao, Z., Shao, P., and Cui, F. (2015). Activation of peroxymonosulfate with magnetic Fe_3O_4–MnO_2 core–shell nanocomposites for 4-chlorophenol degradation. *Chemical Engineering Journal* 262: 854–861.

94 Li, G., Xu, Q., Jin, X. et al. (2018). Enhanced adsorption and Fenton oxidation of 2, 4-dichlorophenol in aqueous solution using organobentonite supported nZVI. *Separation and Purification Technology* 197: 401–406.

95 Jin, H. and Dong, J. (2019). Enhanced performance of Ag_3PO_4/Fe_3O_4/GO bifunctional catalysts on p-chlorophenol degradation in advanced catalytic oxidation systems. *Colloids and Surfaces, A: Physicochemical and Engineering Aspects* 581: 123803.

96 Wang, M., Fang, G., Liu, P. et al. (2016). Fe3O4@β-CD nanocomposite as heterogeneous Fenton-like catalyst for enhanced degradation of 4-chlorophenol [4-CP]. *Applied Catalysis B: Environmental* 188: 113–122.

97 Yin, D., Zhang, L., Zhao, X. et al. (2015). Iron-glutamate-silicotungstate ternary complex as highly active heterogeneous Fenton-like catalyst for 4-chlorophenol degradation. *Chinese Journal of Catalysis* 36: 2203–2210.

98 Niu, H., Zheng, Y., Wang, S. et al. (2018). Continuous generation of hydroxyl radicals for highly efficient elimination of chlorophenols and phenols catalyzed by heterogeneousFenton-like catalysts yolk/shell Pd@Fe_3O_4@metal organic frameworks. *Journal of Hazardous Materials* 346: 174–183.

99 Leon, M.A.D., Segio, M., bussi, J. et al. (2019). Heterogeneous photo-Fenton process using iron-modified regional clays as catalysts: photonic and quantum efficiencies. *Environmental Science and Pollution Research* 26: 12720–12730.

100 Ezzatahmadi, N., Marshall, D.L., Hou, K. et al. (2019). Simultaneous adsorption and degradation of 2, 4-dichlorophenol on sepiolite-supported bimetallic Fe/Ni nanoparticles. *Journal of Environmental Chemical Engineering* 7 (2): 102955.

101 Sarno, M. and Iuliano, M. (2020). New nano-biocatalyst for 4-chlorophenols removal from wastewater. *Materials Today: Proceedings* 20: 74–81.

102 Pouran, S.R., Raman, A.A.A., and Daud, W.M.A.W. (2014). Review on the application of modified iron oxides as heterogeneous catalysts in Fenton reactions. *Journal of Cleaner Production* 64: 24–35.

103 Munoz, M., de Pedro, Z.M., Casas, A., and Rodriguez, J.J. (2015). Preparation of magnetite-based catalysts and their application in heterogeneous Fenton oxidation – a review. *Applied Catalysis B: Environmental* 176–177: 249–265.

104 Barreto-Rodrigues, M., Silveira, J., García-Muñoz, P., and Rodriguez, J.J. (2017). Dechlorination and oxidative degradation of 4-chlorophenol with nanostructured iron-silver alginate beads. *Journal of Environmental Chemical Engineering* 5 (1): 838–842.

105 Poza-Nogueiras, V., Rosales, E., Pazos, M., and Sanroman, M.A. (2018). Current advances and treands in electro-Fenton process using heterogeneous catalysts-a review. *Chemosphere* 201: 399–416.

106 Giorgi, A. and Kopinke, F.-D. (2005). Interaction of adsorption and catalytic reactions in water decontamination processes: part I. oxidation of organic contaminants with hydrogen peroxide catalyzed by activated carbon. *Applied Catalysis B: Environmental* 58: 9–18.

UNCORRECTED PROOFS

Trim Size: 170mm x 244mm Single Column Loose Ribeiro670117 c22.tex V1 - 12/12/2020 12:31am Page 582

107 Hu, X., Liu, B., Deng, Y. et al. (2011). Adsorption and heterogeneous Fenton degradation of 17 alpha-methylestosterone on nano Fe_3O_4/MWCNTs in aqueous solution. *Applied Catalysis B: Environmental* 107: 274–283.

108 Huang, Z., Chen, Z., Chen, Y., and Hu, Y. (2018). Synergistic effects in iron-copper bimetal doped mesoporous γ-Al_2O_3 for Fenton-like oxidation of 4-chlorophenol: structure, composition, electrochemical behaviors and catalytic performance. *Chemosphere* 203: 442–449.

109 Lan, Q., Li, F.B., Sun, C.X. et al. (2010). Heterogeneous photodegradation of pentachlorophenol and iron cycling with goethite, hematite and oxalate under UVA illumination. *Journal of Hazardous Materials* 174 (1–3): 64–70.

110 Lu, M.C., Chen, J.N., and Huang, H.H. (2002). Role of goethite dissolution in the oxidation of 2-chlorophenol with hydrogen peroxide. *Chemosphere* 46 (1): 131–136.

111 Yin, X., Liu, W., and Ni, J. (2014). Removal of coexisting Cr [VI] and 4-chlorophenol through reduction and Fenton reaction in a single system. *Chemical Engineering Journal* 248: 89–97.

112 Zhou, T., Li, Y., Ji, J. et al. (2008). Oxidation of 4-chlorophenol in a heterogeneous zero valent iron/H_2O_2 Fenton-like system: kinetic, pathway and effect factors. *Separation and Purification Technology* 62: 551–558.

AQ2

113 Raja, P., Bozzi, A., Jardim, W.F. et al. (2005). Reductive/oxidative treatment with superior performance relative to oxidative treatment during the degradation of 4-chlorophenol. *Applied Catalysis B: Environmental* 59 (3–4): 249–257.

114 Lücking, F., Köser, H., Jank, M., and Ritter, A. (1998). Iron powder, graphite and activated carbon as catalysts for the oxidation of 4-chlorophenol with hydrogen peroxide in aqueous solution. *Water Research* 32 (9): 2607–2614.

115 Bandara, J., Mielczarski, J.A., and Kiwi, J. (2001). I. Adsorption mechanism of chlorophenols on iron oxides, titanium oxide and aluminum oxide as detected by infrared spectroscopy. *Applied Catalysis B: Environmental* 34 (4): 307–320.

116 Kuntail, J., Jain, Y.M., Shukla, M., and Sinha, I. (2019). Adsorption mechanism of phenol, p-chlorophenol, and p-nitrophenol on magnetite surface: a molecular dynamics study. *Journal of Molecular Liquids* 288: 111053.

117 Khabbaz, M. and Entezari, M.H. (2017). Degradation of Diclofenac by sonosynthesis of pyrite nanoparticles. *Journal of Environmental Management* 187: 416–423.

118 Ganiyu, S.O., Zhou, M., and Martinez-Huitle, C.A. (2018). Heterogeneous electro-Fenton and photoelectron-Fenton processes: a critical review of fundamental principles and application for water/wastewater treatment. *Applied Catalysis B: Environmental* 235: 103–129.

119 Oral, O. and Kantar, C. (2019). Diclofenac removal by pyrite-Fenton process: performance in batch and fixed-bed continuous flow systems. *Science of the Total Environment* 664: 817–823.

AQ3

120 Kantar, C., Ari, C., and Keskin, S. (2015). Comparison of different chelating agents to enhance reductive Cr [VI] removal by pyrite treatment procedure. *Water Research* 76: 66–75.

UNCORRECTED PROOFS

Trim Size: 170mm x 244mm Single Column Loose Ribeiro670117 c22.tex V1 - 12/12/2020 12:31am Page 583

121 Kantar, C., Ari, C., Keskin, S. et al. (2015). Cr (VI) removal from aqueous systems using pyrite as the reducing agent: batch, spectroscopic and column experiments. *Journal of Contaminant Hydrology* 174: 28–38.

122 Weerasooriya, R., Makehelwala, M., Miedaner, M.M., and Tobschall, H.J. (2006). Thermodynamics of monochlorophenol isomers and pyrite interfacial interactions in the activation state. *Journal of Colloid and Interface Science* 297 (1): 31–37.

123 Segura, Y., Martinez, F., and Melero, J.A. (2013). Effective pharmaceutical wastewater degradation by Fenton oxidation with zero-valent iron. *Applied Catalysis B: Environmental* 136–137: 64–69.

124 Keenan, C.R. and Sedlak, D.L. (2008). Factor affecting the yield of oxidants from the reaction of nanoparticulate zero-valent iron and oxygen. *Environmental Science & Technology* 42: 1262–1267.

125 Ding, Y., Ruan, Y., Zhu, L., and Tang, H. (2017). Efficient oxidative degradation of chlorophenols by using magnetic surface carboxylated Cu0/Fe3O4 nanocomposites in a wide pH range. *Journal of Environmental Chemical Engineering* 5 (3): 2681–2690.

126 Shen, W., Mu, Y., Wang, B. et al. (2017). Enhanced aerobic degradation of 4-chlorophenol with iron-nickel nanoparticles. *Applied Surface Science* 393: 316–324.

127 Zhang, W.H., Xie, Q.U.A.N., and Zhang, Z.Y. (2007). Catalytic reductive dechlorination of p-chlorophenol in water using Ni/Fe nanoscale particles. *Journal of Environmental Sciences* 19 (3): 362–366.

128 Duan, J., Zhu, H., Xu, F., and Zhao, J. (2016). A new approach to 4-chlorophenol dechlorination on monometallic copper compared to its cu/Fe bimetallic system. *Chemical Engineering Journal* 304: 282–288.

129 Huang, Q., Cao, M., Ai, Z., and Zhang, L. (2015). Reactive oxygen species dependent degradation pathway of 4-chlorophenol with Fe@Fe_2O_3 core–shell nanowires. *Applied Catalysis B: Environmental* 162: 319–326.

130 Liu, X., Fan, J.H., and Ma, L.M. (2014). Elimination of 4-chlorophenol in aqueous solution by the bimetallic Al–Fe/O_2 at normal temperature and pressure. *Chemical Engineering Journal* 236: 274–284.

131 Xu, L. and Wang, J. (2012). Magnetic nanoscaled Fe_3O_4/CeO_2 composite as an efficient Fenton-like heterogeneous catalyst for degradation of 4-chlorophenol. *Environmental Science & Technology* 46 (318): 10145–10153.

132 Xu, L.J. and Wang, J.L. (2013). Degradation of chlorophenols using a novel Fe0/CeO2 composite. *Applied Catalysis B: Environmental* 142: 396–405.

133 Zhou, T., Li, Y., and Lim, T.T. (2010). Catalytic hydrodechlorination of chlorophenols by Pd/Fe nanoparticles: comparisons with other bimetallic systems, kinetics and mechanism. *Separation and Purification Technology* 76 (2): 206–214.

134 Liu, Y., Yang, F., Yue, P.L., and Chen, G. (2001). Catalytic dechlorination of chlorophenols in water by palladium/iron. *Water Research* 35 (8): 1887–1890.

UNCORRECTED PROOFS

Trim Size: 170mm x 244mm Single Column Loose Ribeiro670117 c22.tex V1 - 12/12/2020 12:31am Page 584

135 Shih, Y.H., Chen, M.Y., Su, Y.F., and Tso, C.P. (2016). Concurrent oxidation and reduction of pentachlorophenol by bimetallic zerovalent Pd/Fe nanoparticles in an oxic water. *Journal of Hazardous Materials* 301: 416–423.

136 Wei-hua, Z., Xie, Q., and Zhuo-yong, Z. (2007). Catalytic reductive dechlorination of p-chlorophenol in water using Ni/Fe nanoscale particles. *Journal of Environmental Sciences* 19: 362–366.

137 Xiao, F., Li, W., Fang, L., and Wang, D. (2016). Synthesis of akageneite [beta-FeOOH]/reduced graphene oxide nanocomposites for oxidative decomposition of 2-chlorophenol by Fenton-like reaction. *Journal of Hazardous Materials* 308: 11–20.

138 Wu, Y., Gan, L., Zhang, S. et al. (2018). Carbon-nanotube-doped Pd-Ni bimetallic three-dimensional electrode for electrocatalytic hydrodechlorination of 4-chlorophenol: enhanced activity and stability. *Journal of Hazardous Materials* 356: 17–25.

139 Catrinescu, C., Arsene, D., Apopei, P., and Teodosiu, C. (2012). Degradation of 4-chlorophenol from wastewater through heterogeneous Fenton and photo-Fenton process, catalyzed by Al–Fe PILC. *Applied Clay Science* 58: 96–101.

140 Li, Y., Zhang, Y., Li, J. et al. (2013). Enhanced reduction of chlorophenols by nanoscale zerovalent iron supported on organobentonite. *Chemosphere* 92 (4): 368–374.

141 Zhou, S., Zhang, C., Hu, X. et al. (2014). Catalytic wet peroxide oxidation of 4-chlorophenol over Al-Fe-, Al-cu-, and Al-Fe-cu-pillared clays: sensitivity, kinetics and mechanism. *Applied Clay Science* 95: 275–283.

142 Munoz, M., de Pedro, Z.M., Casas, J.A., and Rodriguez, J.J. (2013). Chlorophenols breakdown by a sequential hydrodechlorination-oxidation treatment with a magnetic Pd–Fe/γ-Al_2O_3 catalyst. *Water Research* 47 (9): 3070–3080.

143 Liao, Q., Sun, J., and Gao, L. (2009). Degradation of phenol by heterogeneous Fenton reaction using multi-walled carbon nanotube supported Fe_2O_3 catalysts. *Colloids and Surfaces A: Physicochemical and Engineering Aspects* 345: 95–100.

144 Gomez-Herrero, E., Tobajas, M., Polo, A. et al. (2019). Removal of imidazolium-based ionic liquid by coupling Fenton and biological oxidation. *Journal of Hazardous Materials* 365: 289–296.

145 Stowell, J.P., Jensen, J.N., and Weber, A.S. (1992). Sequential chemical/biological oxidation of 2-chlorophenol. *Water Science and Technology* 26 (9–11): 2085–2087.

146 Kastanek, F., Maleterova, Y., and Kastanek, P. (2007). Combination of advanced oxidation and/or reductive dehalogenation and biodegradation for the decontamination of waters contaminated with chlorinated organic compounds. *Separation Science and Technology* 42 (7): 1613–1625.

147 Sangster, J. (1997). *Octanol-Water Partition Coefficients: Fundamentals and Physical Chemistry*. Wiley.

UNCORRECTED PROOFS

Trim Size: 170mm x 244mm Single Column Loose Ribeiro670117 c22.tex V1 - 12/12/2020 12:31am Page 585

148 National Center for Biotechnology Information. (2018). PubChem compound database. US National Library of Medicine. https://www.ncbi.nlm.nih.gov/pccompound.

149 Kantar, C., Oral, O., and Oz, N.A. (2019). Ligand enhanced pharmaceutical wastewater treatment with Fenton process using pyrite as the catalyst: column experiments. *Chemosphere* 237: 124440.

UNCORRECTED PROOFS

UNCORRECTED PROOFS

Trim Size: 170mm x 244mm Single Column Loose Ribeiro670117 c23.tex V1 - 12/11/2020 6:01pm Page 587

23

Clays and Clay Polymer Composites for Electrokinetic Remediation of Soil

Jayasankar Janeni[1] *and Nadeesh M. Adassooriya*[2]

[1] *Postgraduate Institute of Science, University of Peradeniya, Peradeniya 20400, Sri Lanka*
[2] *Department of Food Science & Technology, Wayamba University of Sri Lanka, Makandura 60170, Sri Lanka*

23.1 Introduction

Human activities and industrialization have resulted in a surge in pollution in soil and groundwater due to improper management and frequent spills of harmful chemicals. Toxic chemical structures such as total petroleum hydrocarbons, metals and related metal ions (Cd, Zn, Cr, Pb, Hg, As, Cs), pesticides, and radionuclides pose a potential danger to human health and the environment. In particular, soil includes clay and humic substances that can accumulate significant amounts of toxic metals, resulting in their gradual release into porewater and leading to pollution of surface and groundwater. Thus, there is a need for innovative, cost-effective technologies for environmental remediation to improve public health and environmental safety [1]. In this context, electrokinetic remediation (EKR) can play a significant role in decontaminating soil by extracting toxic metals and other chemical substances like persistent organic pollutants (POPs) via in situ configurations (ex situ technology is also available) [2]. Hence, the in-situ methods usually provide overall cost effectiveness and convenience due to the limited matrix displacement.

EKR is a fine approach that is sustainable and accessible for both on-site and off-site interventions [3]. The method applies an electric field through the soil matrix using an electrochemical system [4]. Interstitial fluid in the soil is induced by the electric field, and electroosmotic flow is generated toward the cathode [5]. An electrical gradient is induced by the direct current (DC) electric field in addition to the hydraulic fluid gradient. This technique is primarily applicable for low-permeability and heterogeneous soils (e.g. glacial tills, lacustrine clays and silts, alluvial deposits, and saprolitic formations) [5].

Clay soils have fine grains and thus low hydraulic conductivity and large specific area [6]. This chapter focuses on the decontamination of clay soils using the EKR technique and discusses the modification of clay soils using different polymers (cationic, anionic, and nonionic) to improve and increase the removal efficiency of the decontamination process. The chapter first explains the fundamental aspects

Electrokinetic Remediation for Environmental Security and Sustainability, First Edition.
Edited by Alexandra B. Ribeiro and M.N.V. Prasad.
© 2021 John Wiley & Sons Ltd. Published 2021 by John Wiley & Sons Ltd.

UNCORRECTED PROOFS

Trim Size: 170mm x 244mm Single Column Loose Ribeiro670117 c23.tex V1 - 12/11/2020 6:01pm Page 588

of clay minerals, including their structure, properties, and modifications. Factors affecting EKR and the efficiency of contaminant removal are discussed. Several studies have been conducted to determine the influence of the properties and chemical nature of clay soil on the applicability and effectiveness of the EKR method.

23.2 Electrokinetic Remediation Technique: An Overview

EKR is based on applying a low-level direct current (DC) on the order of mA cm^{-2} across the soil zone between two electrodes to remove contaminants. The electrodes are usually immersed in wells containing electrolytic solutions. Most commonly, these wells are permeable to liquids and ionic species, where they facilitate hydraulic communication with the soil [3].

Physicochemical and hydrological changes occur in the soil mass due to the low DC, resulting in species being transported through various mechanisms [7]. These mechanisms consist of three primary transportation paths: *electroosmosis* is the primary mechanism, whereby water passes through the porous media of fine grains toward the two electrochemical reaction, which means migration of ions – cations migrate to the cathode, and the anions move toward the anode [8]; *electrophoresis* is the transportation of large colloidal particles and charged particles through the soil; and *electromigration* is the movement of ionic species in the pore fluid toward the oppositely charged electrode, followed by electrodeposition [4, 9]. The EKR technique is used to extract pollutants such as heavy metal ions [10], organic pollutants [5, 11], and inorganic contaminants, as widely reported in the literature.

23.3 Clay Soil and Minerals

Clay minerals possess a wide range of applications in wastewater treatment, oil spill control, drilling, and remediation techniques [12–14]. They are phyllosilicates (layered silicates) consisting primarily of the fine-grained fraction of soils and sediments. The word *clay* indicates a fine-grained texture in naturally occurring materials that becomes plastic when wet and hardens when dried [15, 16]. The most common clay minerals in environmental applications are montmorillonite (MMT) (a mineral in the smectite group and type of bentonite clay), kaolinite, palygorskite, and halloysite.

Before continuing with the main topic of this chapter, it is important to be familiar with the overall classifications, structure, and properties of clay minerals. Clay soil is most commonly a composition of several minerals, either clay with sand and slits or clay-rich soil. Clay soils are usually found in sites such as agricultural, irrigation, and coastal areas [15, 16]. Clay minerals have a wide range of applications in diverse sectors including environmental remediation [17], cosmetics, construction, and agriculture.

UNCORRECTED PROOFS

Trim Size: 170mm x 244mm Single Column Loose Ribeiro670117 c23.tex V1 - 12/11/2020 6:01pm Page 589

23.4 Clay Mineral Classifications and Structure

Clay materials belong to a class of layered materials classified into two groups: cationic clay and anionic clay. Cationic clays are made up of layered silicates. They consist of negatively charged aluminosilicate or magnesiosilicate layers and interlayer charge-balancing cations. The building blocks of the layered lattice are formed by the fusion of $(SiO_4)^{4-}$ tetrahedra units with $Al_2(OH)_6$ or Mg $(OH)_2$ octahedra. The silicate tetrahedra and $Al_2(OH)_6$ or $Mg(OH)_2$ octahedra are covalently linked via apical tetrahedral oxygen. Due to the symmetry and dimensional similarities of the tetrahedral and octahedral sheets, they can be combined in different structural arrangements, resulting in a variety of cationic clay mineral subgroups [12, 16].

Condensation of one tetrahedral (T) sheet with one octahedral (O) sheet results in a structure referred to as a *1: 1 group*, as in kaolinite. In a 1: 1-layer structure, the unit cell includes six octahedral sites and four tetrahedral sites. The combination of another tetrahedral sheet on the opposite side of the octahedral sheet in a 1: 1-layer results in a 2: 1 group (e.g. pyrophyllite, smectite group). In addition, six octahedral sites and eight tetrahedral sites are included in the unit cell of a 2: 1 layered structure. Structures with all six octahedral sites occupied are known as trioctahedral; and if only four of the six octahedra are occupied, the structures are referred to as dioctahedral [12].

In anionic clay, the structure is layered double hydroxide (LDH); for example, consider the structure of brucite, $Mg(OH)_2$, in which the Mg^{2+} ions are octahedrally coordinated to hydroxyl groups. The octahedral units share edges to form infinite neutral, stacked layers, leading to a layered network held together by hydrogen bonding. In an LDH, some of the divalent ions undergo isomorphous substitution by higher-valent ions of comparable size, generating a positive charge on the layers. This positive charge on the layers requires interlayer charge-balancing anions to maintain total charge neutrality. Another group of LDHs could be explained by considering the structure of gibbsite. In gibbsite, one-third of the octahedral sites are initially vacant but may be filled by appropriately sized cations, leading to a net positive charge on the layers.

LDHs may be represented by the general formula $[M^{2+}_{(1-x)}\ M^{3+}_{x}(OH)_2A^{n-}_{x/n}]_m.\ H_2O$, where M^{3+} and M^{2+} are divalent and trivalent cations, respectively. X is $(M^{3+}/(M^{3+}+M^{2+}))$, and A is the interlayer charge-balancing anion of valence n. A strong H-bonding network within the layers also facilitates inserting other neutral molecules with electronegative functional groups. LDHs are available as both naturally occurring (hydrotalcite, brucite) and synthetic minerals [12, 18].

The literature also highlights a common classification of clay minerals in four primary groups: kaolinite, illite, smectite, and vermiculite. The kaolinite group comprises kaolinite, dickite, nacrite, and halloysite; they are formed by the decomposition of orthoclase feldspar (e.g. in granite). The illite group includes hydrous micas, phengite, brammalite, celadonite, and glauconite (a green clay sand) formed by the decomposition of some micas and feldspars; they are predominant in marine clays and shales. The smectite group includes MMT, bentonite, hectorite, nontronite, saponite, and sauconite [14, 18]. This chapter primarily discusses EKR

UNCORRECTED PROOFS

Trim Size: 170mm x 244mm Single Column Loose Ribeiro670117 c23.tex V1 - 12/11/2020 6:01pm Page 590

of soils that are rich in clay minerals, especially the most common clay types such as kaolinite, bentonite, MMT, illite, etc.

23.5 Layer Charge

Layers in cationic clays are negatively charged due to isomorphous substitution when tetrahedral sites, which are primarily occupied by Si^{4+}, are subjected to partial isomorphous substitution by lower-valance cations like Al^{3+}. Also, Mg^{2+} present in octahedral sites undergo partial isomorphous substitution with Li^{+} or Al^{3+}. In all these cases, cations are intercalated between the layers to maintain the charge balance. Substitution in the octahedral sheets creates a delocalized charge deficiency over 10 basal oxygen atoms, and substitution in the tetrahedral sites forms a more localized charge over only three oxygen atoms present in the basal layer.

Ismadji et al. [14] explain the charge in clay minerals and the effect of charge on their properties. Most commonly, tetrahedral and octahedral clay mineral sheets have a charge. Two forms of clay charge exist: structural and surface charge. Structural charge is formed within the interior of the layers and caused by ion substitutions: it is a permanent charge, and the value of pH is a factor. Surface charge originates on the basal surface of tetrahedral sheets in 2: 1-layer clay minerals; it comes from both tetrahedral and octahedral sheets in 1 : 1-layer clay. The boundaries of the sheets in both 1: 1 and 2 : 1 clay contribute to the surface charge [14].

23.6 Active Bond Sites in Clay Minerals

Bergaya et al.[12] highlighted the active sites present in clay minerals. Several active sites are available on clay materials, such as the following [12]:

- *Neutral siloxane surface* – Caused by the presence of siloxane groups. The surface is hydrophobic due to a strong bond between Si and O atoms.
- *Isomorphic substitution sites* – Due to the partial replacement of tetrahedral Si^{4+} ions and octahedral Al^{3+} by lower-valance ions.
- *Exchangeable cations* – Charge-balancing cations in the interlayer region.
- *Polarized water molecules surrounded by exchangeable cations* – These molecules and uncoordinated surface atoms can donate protons (surface Brønsted acidity) more readily than bulk water to promote various chemical reactions.
- *Broken edge sites or pH-dependent active sites* – Uncoordinated metal ions present at broken edges and surface of the clay react with water to form surface hydroxyl groups to complete the coordination sphere. These sites contribute more than 20% of the ion-exchange capacity, and they strongly depend on the size and the shape of the clay particles.

UNCORRECTED PROOFS

Trim Size: 170mm x 244mm Single Column Loose Ribeiro670117 c23.tex V1 - 12/11/2020 6:01pm Page 591

23.7 Properties of Clay Minerals

The presence of charge in clay minerals is the fundamental reason for cation exchange and the swelling properties of these minerals. An essential property of clay mineral is the cation exchange capacity (CEC): a measure of the capacity of clay minerals to exchange cations from solution and, at the same time, a measure of the concentration of unfixed cations in the interlayers and surface layers that relies on the magnitude of the total layer charge. CEC is measured at pH 7; hence the surface layer charge is a function of pH. Ca^{2+}, Mg^{2+}, Na^{+}, and K^{+} are common metallic cations found in exchange positions in clay minerals [14]. In addition, clay minerals have properties such as adsorption [19], colloidal behavior, and swelling capacity [20].

23.8 Clay Minerals and Their Modifications

Clay minerals can be chemically modified in different ways to impart specific properties that suit the final application, thanks to their low permeability and leachate. In recent years, organic substances such as polymers, biopolymers, and surfactants have been used in a broad range of soil-improvement applications, and several works have demonstrated their ability to improve the shear strength, soil remediation, and erosion resistance of geomaterials [1]. In this context, polymer- and surfactant-modified clay (organoclay), acid-leached clay, and acid- and base-impregnated clay are widely studied by researchers [13, 21, 22]. Using surfactants and polymers to modify clays and enhance their engineering properties is an interesting solution to improve their applicability for geotechnical applications, including decontamination [23]. Surfactants (surface-active agents) can change various fluid-interface properties. Several studies have been conducted that deal with surfactants (anionic, cationic, and nonionic), modified clays (Surfactant modified clays or surfactant–clay complexes). Akbulut et al. [24] studied the effect of surfactants on smectite-rich clay's contact angles and consistency limits [24].

23.9 Organoclays and Their Properties

Clay interacts with a polymer, resulting in the polymer's functional groups make bonding with clay faces (basal planes and edges), exchangeable cations and water molecules. This polymer interaction changes the surface properties and water interaction of the modified clay [25, 26]. The intercalation of surfactant ions onto the clay mineral structure converts the initially hydrophilic clay mineral particles into hydrophobic organoclays [27]. Several studies have been carried out to investigate enhancing the electrokinetic properties of clay minerals by treating them with surfactants or polymers.

UNCORRECTED PROOFS

Trim Size: 170mm x 244mm Single Column Loose
Ribeiro670117 c23.tex V1 - 12/11/2020 6:01pm Page 592

Zhao et al. [28] explain the properties of organic compound modified clays, including geochemical properties like electrokinetic potential, absorptivity, attenuation of nonpolar compounds, hydrophobicity, and electrical conductivity; and physical properties such as hydraulic conductivity, strength, and dynamic properties [28]. Organic compounds such as surfactants – quaternary ammonium cations (QACs), e.g. tetramethylammonium chloride (TMA $(CH_3)_4NCl$), tetraethylammonium bromide (TEA $(CH_2CH_3)_4NBr$), tetrabutylammonium bromide (TBA $((CH_2)_3(CH_3))_4NBr$), and decyl trimethylammonium bromide (DTMA $(CH_3)_3 NC_{10}H_{21}Br$]) [23] – and many other compounds like polymeric quaternary alkylammonium salts and copolymers, biopolymers [1], alcohols, and aldehydes have been widely discussed [28].

Behavioral changes in organoclays after the intercalation of polymeric surfactants have been widely studied by several researchers. Zhao and Burns [29] studied the sorption behaviors of QAC $((CH_3)_3NR^+)$-intercalated clay with the use of benzene molecules in a simulation of molecular dynamics. In their observations, the simulation results confirmed that the sorption mechanism of organoclays is controlled by the arrangement of the surfactants. Benzene molecules were observed to interact with the clay surface in the presence of TMA cations and tend to interact with the aliphatic chain of the hexadecyltrimethylammonium (HDTMA) cation in clay interlayers [29]. Zhu et al. [30] studied the intercalation mechanism of zwitterionic surfactant-modified MMT. They stated that MMT can form amphoteric surfaces as it has surface negative charge and metal cations in the interlayers; this is called a zwitterion or inner salt.

It is well known that ion-exchange reactions can be used to synthesize conventional organoclays. Reactions happen under mild conditions between organic cationic surfactants and the smectite family of clay minerals, where exchangeable metal cations are easily replaced by the organic cations of surfactant molecules. During the reaction of MMT with a zwitterionic surfactant (SB16), the negative clay layer surface is connected with the positive ends of SB16 (quaternary ammonium), and the negative ends of SB16 are linked to interlayer metal cations. This process is driven by an ion-dipole interaction between the SB16 head-groups and the MMT surface, with cations rather than an exchange reaction [30].

Huang et al. [31] reviewed techniques combined with EKR, including adding surfactants. Surfactants or co-solvents penetrate and permeate deep into the soil, where they interact and bind with organic pollutants. This process forms migratory compounds through the physio-chemical actions of desorption, dissolution or complexation, and chelation. [31]. Most commonly, surfactants and complexing agents are used to increase the desorption and solubility rates of organic and metal pollutants during EKR [32].

Sarkar et al. [33] explains that the presence of hydrated cations in the interlayer of natural clay minerals makes the clay hydrophilic. Hydrated cations are replaced with hydrophobic organic cations during the interaction of quaternary ammonium compounds with clay minerals, that makes the resultant organoclays become hydrophobic. Therefore, the interaction of the organoclay deviates from the normal clay interaction with the environment. Usually, this transformation into

UNCORRECTED PROOFS

Trim Size: 170mm x 244mm Single Column Loose Ribeiro670117 c23.tex V1 - 12/11/2020 6:01pm Page 593

a hydrophobic material greatly enhances the organoclay's affinity to hydrophobic organic compounds (e.g. PAHs). In contrast, the affinity to hydrophilic impurities (e.g. toxic metal cations) may decrease significantly [33].

Bate and Burns [34] determined the complex dielectric permittivity of different organoclays and investigated the impact of organic carbon on those organoclays [34]. Not only the intercalation of organic surfactants converts the hydrophilic environment of clays to hydrophobic but also it increases the interlayer spacing as well [35]. Since this chapter emphasizes how changes in clay soil can affect the EKR process, discussing such property modifications is significant. Properties of the surface and microstructure of the interlayers of clayey material are related to its physical and chemical properties [17].

23.10 Factors Affecting the Mechanism of Transporting Contaminants in Clay Soils

23.10.1 Structural Parameters

Ion distribution (charge distribution) near the surface is explained by numerous models in negatively charged clay minerals in an aqueous environment, as follows. Next to the clay mineral's surface is the Stern layer or Helmholtz plane: a thin layer of ions and surface-bound water molecules with less mobility [36]. Most ions have a positive charge. The electrical diffuse layer (EDL) is outside the Stern layer; in the bulk fluid, charge-balancing ions accumulate a charge cloud consisting of mostly cations and fewer anions [28, 36, 37]. This charge cloud can be calculated using Guoy-Chapman theory. This entire system of the Stern layer and EDL forms the electrical double layer illustrated in Figure 23.1. Interactions between clay particles occur primarily through the electrical double layer. The thickness of the diffuse layer (ϑ) is determined by classical Derjaguin-Landau-Verwey-Overbeek (DLVO) theory [28, 36]:

$$\vartheta = \sqrt{\frac{\varepsilon_0 k}{2e_0^2 N_{av}}} \cdot \sqrt{\frac{\kappa T}{cz^2}} \tag{23.1}$$

where $\varepsilon_0 = 8.85 \times 10^{-12}$ F/m is the permittivity of free space, k (Boltzmann's constant) $= 1.38 \times 10^{-23}$ J/K, e_0 (electron charge) $= 1.602 \times 10^{-19}$ C, Avogadro's number is $N_{av} = 6.022 \times 10^{23}$ mol^{-1}, κ is the real relative permittivity of the fluid, T is the absolute temperature (K), c is the bulk fluid concentration (mol/l), and z is the ionic valence. Considering Eq. (23.1), both higher concentration and higher valence reduce the thickness of the diffuse layer, thus bringing MMT particles closer to each other.

23.10.2 Mass Transport

Mass transport driven by EK phenomena in a porous medium is of special interest to soil scientists and environmental and geotechnical engineers due to

UNCORRECTED PROOFS

Trim Size: 170mm x 244mm Single Column Loose Ribeiro670117 c23.tex V1 - 12/11/2020 6:01pm Page 594

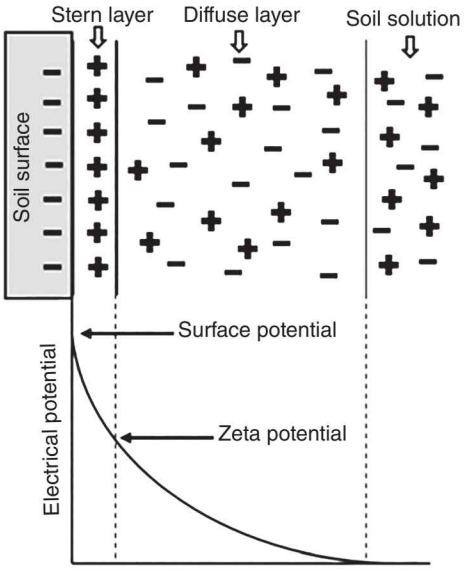

Figure 23.1 Electric double layer of a negatively charged soil particle.

its ability to help remove or extract contaminants from less porous geological materials such as clay soil. Numerous theories explaining electroosmosis, including Helmholtz-Smoluchowski theory, Schmid theory, the Spiegler friction model, Buckingham π theory, and ion hydration theory, have been widely reported [8, 38].

Electroosmotic flow is induced by ionic fluxes leading from the fluid surrounding the soil particles. The flow of water molecules in the bulk phase can also occur, with the fluid carrying soil particles in the same flow direction. Drag action is the primary cause of the electro-osmotic flow which means the interaction between the first region (flow in the fluid surrounding the soil particles) and the second region (flow in the bulk phase) enables the movement of water in the bulk phase. Therefore, the total observed electro-osmotic flow is considered as the movement of these two water layers [8].

A positive surface charge has a divergent effect, which means electroosmotic flow occurs from cathode to anode [5, 8]. Electroosmosis decreases drastically during pH and zeta (ζ) potential drops in the later stages of a sustained EK process under a constant electric field. Electrophoresis may become significant during the formation of micelles (charged aggregate of molecules or particles) with other species in the processing fluid or when dealing with slurries. Pham and Sillanpaa [39] emphasize that the type of soil, soil pH value, and degree of saturation significantly affect EKR efficiency. pH changes can affect the chemical state of contaminants. In addition, they affect the transport of contaminants in soil pore fluid due to changes in the magnitude and direction of electroosmotic flow. The direction of electroosmotic flow is reversed from the cathode toward the anode when the soil pH is lower than the point of zero charge (pzc: zero zeta-potential of the soil particle surface). Both electroosmosis and ionic migration are affected by the degree of saturation. Soils with high water content and low ionic strength offer satisfactory conditions for transporting pollutants by electroosmotic and ionic migration [39].

UNCORRECTED PROOFS

Trim Size: 170mm x 244mm Single Column Loose Ribeiro670117 c23.tex V1 - 12/11/2020 6:01pm Page 595

Electromigration of a specific ion relies on the soil's conductivity, porosity, pH gradient, applied electric potential, initial concentration of the ion, and other competitive ions. Heavy metals are removed primarily by electromigration, and organic pollutants are removed by electroosmosis. The presence of heavy metals affects the electroosmotic flow and sorption of contaminants because it causes the zeta potential of the soil to become less negative or even have a positive value [5, 40].

Helmholtz first studied electroosmotic phenomena analytically in 1879 and found a mathematical model. Later, Smoluchowski (1914) modified this model to also apply to electrophoretic velocity; this is known as the Helmholtz–Smoluchowski (H-S) theory [5]. The equation of the H-S model is as follows

$$v_{eo} = \frac{\varepsilon_s \xi}{\eta} . \frac{\partial \phi}{\partial x} = k_{eo} E \tag{23.2}$$

where v_{eo} is the electroosmotic (electrophoretic) velocity, ε_s is the permittivity of the pore fluid, η is the viscosity of the solvent or pore fluid, k_{eo} is the coefficient of electroosmotic conductivity, and $\vartheta\phi/\vartheta x = E =$ electric field.

The ζ (zeta) potential in Eq. (23.2) is not constant during electroosmotic transport in a clay medium because it varies with the pore fluid's pH and ionic concentration and the electric field. This phenomenon makes it difficult to assess velocity when making temporal and spatial distribution predictions for electroosmotic transport. Experiments exhibited that v_{eo}/E increased with E, hence making the other parameters in Eq. (23.2) functions of the electrical field.

23.10.3 Electrokinetic Potential (Zeta Potential)

The ζ (zeta) potential is the electrical potential at the junction between the fixed and mobile parts of the electrical double layer (see Figure 23.1). The type and concentration of electrolytes added to the particle suspension affect the ζ potential. The magnitude and sign of the ζ potential are greatly dependent on the pore fluid chemistry [5].

ζ potential variations in fine-grained soils are due to positive ions balancing negative charges that occur during isomorphous substitution and broken bonds in soil particles [41]. The ζ potential value is usually negative for clay soils due to the net negative charge on the clay particle surfaces. At low enough pH, the ζ potential may become positive. As potential-determining ions, the H^+ and OH^- concentrations vary. Hence a lower pH will reduce the ζ potential (magnitude) for most clay-rich soils [5, 40].

Researchers have found that the ζ potential of fine-grained soils plays an essential role in the efficiency of EKR. The reason is that the direction and rate of electroosmotic flow are ζ potential–dependent, as in

$$k_{eo} = \frac{\varepsilon_s n_e \zeta}{\eta \tau} \tag{23.3}$$

where k_{eo} is electroosmotic permeability (ranges between 10^{-9} and 10^{-8} m^2V^{-1} s^{-1}), n_e is the effective porosity, and τ is the tortuosity [40, 42].

Numerous simultaneous reactions such as electrolysis, acidification, adsorption, and precipitation of the soil surface, fluid, and contaminants may occur

UNCORRECTED PROOFS

Trim Size: 170mm x 244mm Single Column Loose Ribeiro670117 c23.tex V1 - 12/11/2020 6:01pm Page 596

[4, 43]. During EK treatment, fine-grained soils like clay, which are electrically active and have a large specific surface area, can further complicate these reactions. Thus, understanding the reactions and interactions happening at the soil–liquid–contamination interface is necessary to improve removal efficiency. Pollutants that are adsorbed on the soil or present as a precipitate or immiscible liquid form cannot be effectively removed by an EK remediation technique unless these species have been absorbed into the aqueous phase. In this scenario, the solubility of heavy metals may be substantially reduced at usual pH values [41].

23.10.4 Polymeric Agent Enhanced Electrokinetic Decontamination of Clay Soils

Several studies were reported to enhance EK remediation efficiency by introducing surfactants into the soils because surfactants affect electrical double layer interactions and Van-der-Waals interactions. A number of studies indicate the significance of the soil's ζ potential on EKR efficiency, and research has been conducted based on the effect of polymeric surfactants on the ζ potential. Kayaa and Yukselen [41] investigated the effect of surfactants (cationic, anionic, and nonionic) on the ζ potentials of different clay samples of kaolinite, MMT, and quartz powder with metal ions (Li^{+}, Ca^{+2}, Cu^{+2}, Pb^{+2}, and Al^{+3}). The results indicated that an anionic surfactant produces negative ζ potential values. The other soil ζ potential values varied with the surfactants, yielding positive and negative values [41, 44].

Zhuang et al. state that Clay particles with a ζ potential value greater than +30 mV or lower than −30 mV are considered stable suspensions. Therefore, they can form more stable connections with the phase and create connections in a uniform and non-aggregated way in both the polar and nonpolar phases. This is advantageous for uniform osmotic flow when considering the practical applicability of EKR. Monteiro et al. [45] modified calcium bentonite clay by using different polymeric surfactants to investigate several parameters, including contact angle and ζ potential. They found that bentonite modified with a mixture of cetyltrimethylammonium bromide (CTAB), sodium dodecyl sulfate (SDS), and lauryl alcohol ethoxylated (ALEO) (OBent-III with CTAB + SDS + ALEO) could establish a more stable connection in the phase and hence had a ζ potential value of >30 mV according to the clarifications done by Zhuang et al. [45].

The scenario of using charged polymers or surfactants for the desorption of metal ions is reported. The desorption of metal ions from clay minerals (already absorbed metals ions, due to CEC: e.g. MMTs partially form strong inner-sphere complexes with Cs ions) could be facilitated by introducing suitable cationic polyelectrolytes and polymers that are bound or intercalated with the clay soil and tend to be an advantage during the EKR. A highly charged cationic polyelectrolyte, polyethyleneimine (PEI), intercalated into the negatively charged MMT interlayers substantially replaced Cs ions adsorbed on the interlayers of MMT. Further, Cs ion desorption is enhanced by additional $NH4^{+}$ treatment. This synergetic treatment desorbed 95% of Cs ion from MMT interlayers [46]. Stojiljkovic et al. [47] studied the

UNCORRECTED PROOFS

Trim Size: 170mm x 244mm Single Column Loose Ribeiro670117 c23.tex V1 - 12/11/2020 6:01pm Page 597

electrokinetic properties of bentonite modified by polyvinyl pyrolidone, soy isolates, and Carbopol at different temperatures. They showed that adding polymers has a significant effect on pH and electrical conductivity. The values varied according to the concentration and temperature [47]. Careful control of pH is also necessary to improve the efficiency of the decontamination process, especially given the solubility of heavy metals, which is strongly correlated with the pH of the system. Metals may remain as precipitates in the soil matrix at relatively higher pH values. Therefore, metals must be free to move in solution to be eradicated by the drag of the electric field. For this reason, it is frequently necessary to add substances that maintain or enhance the solubility of the metal, even in unfavorable pH conditions [32].

Zou et al. [48] studied the efficiency of EK removal in clay soil artificially polluted with the hydrophobic organic pollutant pyrene. They carefully controlled the pH· and added a biosurfactant (rhamnolipid) to enhance the EK removal process. An increase in rhamnolipid concentration (ranging from 0.5 to 2 g l^{-1}) increased the pyrene removal efficiency from 14.74 to 24.81%, reaching 93.60% in the area closest to the anode [48]. In another study, kaolin clay and sandy soil containing lead (Pb) and phenanthrene (PHE) was decontaminated using the EK technique. The authors used a processing fluid combination of 1% Tween 80 and 0.1 M EDTA for solubility enhancement. The system showed nearly 90% removal efficiency of Pb and PHE in clay soil [32]. Gu et al. performed desorption that showed 75% of sorbed cadmium could be dissolved into solution when using 0.1 mol l^{-1} organophosphonates or EDTA in a wide pH range [1–11]. They observed migration of cadmium, which spiked in the specimen due to enhancement with nitrilotrimethylene triphosphonate (NTMP) and (ethylenedinitrilo)-tetramethylenephosphonate (EDTMP), and EDTA under a constant voltage gradient of approximately 1.0 V cm^{-1}. The results showed average removal efficiencies of cadmium from the soil moderated by NTMP (22.8%) and EDTMP (22.4%) after five days of EK removal; these were greater than the removal efficiency for EDTA (15.1%). EDTA is a widely used chelating agent for EKR.

23.10.5 Future Perspectives

EKR technology is a popular technique, but it has drawbacks in terms of applicability and efficiency control. Careful control of processing parameters should be studied and focused on during the implementation of EKR systems at relevant sites.

Environmental pollution is becoming a significant issue worldwide, including an increase in contaminants such as toxic metals, PAHs, and POPs in the soil and groundwater with the potential to harm human health and the environment. This chapter has primarily focused on clay soils, which are a viable matrix for EKR for decontamination. However, controlling process parameters such as pH, conductivity, and the nature of the soil is challenging.

Presently, there are various modification techniques, including coupling EKR with other popular decontamination technologies. For example, removal of

UNCORRECTED PROOFS

Trim Size: 170mm x 244mm Single Column Loose Ribeiro670117 c23.tex V1 - 12/11/2020 6:01pm Page 598

polychlorinated biphenyls (PCBs) solely by EKR is less effective due to the strong absorption of PCBs into soils; therefore, enhanced technologies are widely discussed [49]. EK can also be coupled with nanotechnology, bioremediation, and chemical oxidation [49]. For nanotechnological applications, the problem of limited transport in low-permeability soils is enhanced by incorporating polymer-modified, zero-valent iron (nZVI) nanoparticles in groundwater remediation [50]. Vocciante et al. [51] reported the Global Warming Potential impact of an electrokinetic method. This had been assessed in terms of kilograms of equivalent CO_2 m^{-2} of a multi-metal-contaminated soil [51]. Considering the environmental impacts of the decontamination process is essential for a sustainable future.

23.11 Summary

EKR is a successful technique for remediating soils, sediments, and sludges polluted with inorganic and organic contaminants. The principle of EKR depends on imparting a low-intensity direct current through contaminated soil between two electrodes (cathode and anode). The EKR technique is more suitable for fine-grained soils like clay because of adverse factors that can affect decontamination, such as the low permeability of clay soils. DC electric fields tend to facilitate the flow of decontaminants along with the flow fluid. The chapter initially emphasized the fundamental theory related to clay minerals and their structures. Enhancing clay soils by using chemical reagents like organic compounds (polymers) is useful to improve efficiency. The chapter's final focus was on factors that influence the EKR process with enhancements applied to clay soils. Finally, significant challenges faced by the environmental and industrial sectors to decontaminate clay soils using the EKR technique were described.

References

AQ1

1 Cao, S.C., Bate, B., Hu, J.W., and Jung, J. (2016). Engineering behavior and characteristics of water-soluble polymers: implication on soil remediation and enhanced oil recovery. *Sustainability* 8 (3).

2 Acar, Y.B. and Alshawabkeh, A.N. (1993). Principles of electrokinetic remediation. *Environmental Science & Technology* 27 (13): 2638–2647.

3 Rosestolato, D., Bagatin, R., and Ferro, S. (2015). Electrokinetic remediation of soils polluted by heavy metals (mercury in particular). *Chemical Engineering Journal* [Internet]. Elsevier B.V. 264: 16–23. Available from: http://dx.doi.org/10.1016/j.cej.2014.11.074.

4 Virkutyte, J., Sillanpaa, M., and Latostenmaa, P. (2002). Electrokinetic soil remediation - critical overview. *Science of the Total Environment*: 97–121.

5 Reddy, K.R. (2009). *Electrochemical Remediation Technologies for Poluted Soils, Sediments and Ground Water* (eds. K.R. Reddy and C. Cameselle). Hoboken, NJ: Wiley. 719 p.

UNCORRECTED PROOFS

Trim Size: 170mm x 244mm Single Column Loose Ribeiro670117 c23.tex V1 - 12/11/2020 6:01pm Page 599

6 Mascia, M., Vacca, A., and Palmas, S. (2014). Effect of surface equilibria on the electrokinetic behaviour of Pb and Cd ions in kaolinite. *Society of Chemical Industry*: 1290–1298.

7 Gonzini, O., Plaza, A., Di Palma, L., and Lobo, M.C. (2010). Electrokinetic remediation of gasoil contaminated soil enhanced by rhamnolipid. *Journal of Applied Electrochemistry* 40 (6): 1239–1248.

8 Asadi, A., Huat, B.B.K., Nahazanan, H., and Keykhah, H.A. (2013). Theory of electroosmosis in soil. *International Journal of Electrochemical Science* 8 (1): 1016–1025.

9 Estabragh, A.R., Lahoori, M., Javadi, A.A., and Abdollahi, J. (2019). Effect of a surfactant on enhancing efficiency of the electrokinetic method in removing anthracene from a clay soil. *Journal of Environmental Chemical Engineering* [Internet]. Elsevier 7 (5): 103298. Available from: https://doi.org/10.1016/j.jece.2019.103298.

10 Liu, L., Li, W., Song, W., and Guo, M. (2018). Remediation techniques for heavy metal-contaminated soils: principles and applicability. *Science of the Total Environment* [Internet]. Elsevier B.V. 633: 206–219. Available from: https://doi.org/10.1016/j.scitotenv.2018.03.161.

11 Ma, Y., Li, X., Mao, H. et al. (2018). Remediation of hydrocarbon – heavy metal co-contaminated soil by electrokinetics combined with biostimulation. *Chemical Engineering Journal* 353 (April): 410–418.

12 Bergaya, F., Theng, B.K.G., and Lagaly, G. (2006). *Handbook of Clay Science*, 1e, vol. 53, 1689–1699. Elsevier.

13 Leporatti, S. (2019). Polymer clay nano-composites. *Polymers (Basel)* 11 (9): 1445.

14 Ismadji, S., Soetaredjo, F.E., and Ayucitra, A. (2015). *Clay Materials for Environmental Remediation* (ed. S.K. Sharma). Cham Heidelberg/New York/Dordrecht London: Springer Briefs in Molecular Science. 124 p.

15 Buehrer, T.F. (1952). Role of chemical properties of clays in soil science. *Clays and Clay Minerals* 1 (1): 177–187.

16 Theng, B.K.G. (2012). *Developments in Clay Science*, 2e. Elsevier Science 526 p.

17 Lee, J., Park, S., Jeon, E., and Baek, K. (2017). Applied geochemistry selective and irreversible adsorption mechanism of cesium on illite. *Applied Geochemistry* [Internet]. Elsevier Ltd: 1–6. Available from: http://dx.doi.org/10.1016/j.apgeochem.2017.05.019.

18 Bergaya, F., Lagaly, G., and Vayer, M. (eds.) (2013). *Handbook of Clay Science* [Internet], Developments in Clay Science, 2e, vol. 5, 333–359. Elsevier Available from: http://www.sciencedirect.com/science/article/pii/B9780080982595000135.

19 Javadi, S., Ghavami, M., Zhao, Q., and Bate, B. (2017). Advection and retardation of nonpolar contaminants in compacted clay barrier material with organoclay amendment. *Applied Clay Science* [Internet]. Elsevier B.V. 142 (November): 30–39. Available from: http://dx.doi.org/10.1016/j.clay.2016.10.041.

20 Yuan, G.D., Theng, B.K.G., Churchman, G.J., and Gates, W.P. (2013). Clays and clay minerals for pollution control. In: *Handbook of Clay Science* [Internet], 2e (eds. F. Bergaya and G. Lagaly), 587–644. Elsevier Ltd Available from: http://dx.doi.org/10.1016/B978-0-08-098259-5.00021-4.

UNCORRECTED PROOFS

Trim Size: 170mm x 244mm Single Column Loose Ribeiro670117 c23.tex V1 - 12/11/2020 6:01pm Page 600

21 Ismadji, S., Soetaredjo, F.E., and Ayucitra, A. (2015). Modification of clay minerals for adsorption purpose. In: *Clay Materials for Environmental Remediation* (eds. M. Mercurio, B. Sarkar and A. Langella), 5–37. SpringerBriefs in Molecular Science Available from: http://link.springer.com/10.1007/978-3-319-16712-1.

22 Yu, C., Ke, Y., Hu, X. et al. (2019). Effect of bifunctional montmorillonite on the thermal and tribological properties of polystyrene/montmorillonite nanocomposites. *Polymers (Basel)* 11: 834.

23 Bate, B., Choo, H., and Burns, S.E. (2013). Dynamic properties of fine-grained soils engineered with a controlled organic phase. *Soil Dynamics and Earthquake Engineering* [Internet]. Elsevier 53: 176–186. Available from: http://dx.doi.org/10.1016/j.soildyn.2013.07.005.

24 Akbulut, S., Kurt, Z.N., and Arasan, S. (2012). Surfactant modified clays consistency limits and contact angles. *Earth Science Research Journal* 16 (2): 95–101.

25 Lieske, W., Verst, R., and Baille, W. (2019). Polymer modification of bentonite: impact of molar mass. XVII Eur Conf Soil Mech Geotech Eng (ECSMGE).

26 Chenu, C., Le Bissonnais, Y., and Arrouays, D. (2000). Organic matter influence on clay wettability and soil aggregate stability. *Soil Science Society of America Journal* 64 (4): 1479–1486.

27 Shang, H. and Sun, Z. (2019). PAHs (naphthalene) removal from stormwater runoff by organoclay amended pervious concrete. *Construction and Building Materials* [Internet]. Elsevier Ltd 200 (December): 170–180. Available from:: https://doi.org/10.1016/j.conbuildmat.2018.12.096.

28 Zhao, Q., Choo, H., Bhatt, A. et al. (2016). Review of the fundamental geochemical and physical behaviors of organoclays in barrier applications. *Applied Clay Science* [Internet]. Elsevier B.V. 142(October 2017): 2–20. Available from: http://dx.doi.org/10.1016/j.clay.2016.11.024.

29 Zhao, Q. and Burns, S.E. (2012). Molecular dynamics simulation of secondary sorption behavior of montmorillonite modified by single chain quaternary ammonium cations. *Environmental Science & Technology* 46 (7): 3999–4007.

30 Zhu, J., Zhang, P., Qing, Y. et al. (2017). Novel intercalation mechanism of zwitterionic surfactant modified montmorillonites. *Applied Clay Science* [Internet]. Elsevier B.V. 141: 265–271. Available from: http://dx.doi.org/10.1016/j.clay.2017.03.002.

31 Huang, D., Xu, Q., Cheng, J. et al. (2012). Electrokinetic remediation and its combined technologies for removal of organic pollutants from contaminated soils. *International Journal of Electrochemical Science* 7: 4528–4544.

32 Alcántara, M.T., Gómez, J., Pazos, M., and Sanromán, M.A. (2012). Electrokinetic remediation of lead and phenanthrene polluted soils. *Geoderma* [Internet]. Elsevier B.V. 173–174: 128–133. Available from: http://dx.doi.org/10.1016/j.geoderma.2011.12.009.

33 Sarkar, B., Rusmin, R., Ugochukwu, U.C. et al. (2019). Modified clay minerals for environmental applications. In: *Modified Clay and Zeolite Nanocomposite Materials* [Internet] (eds. M. Mercurio, B. Sarkar and A. Langella), 113–127. Elsevier Inc. Available from: http://dx.doi.org/10.1016/B978-0-12-814617-0.00003-7.

UNCORRECTED PROOFS

Trim Size: 170mm x 244mm Single Column Loose Ribeiro670117 c23.tex V1 - 12/11/2020 6:01pm Page 601

34 Bate, B. and Burns, S.E. (2014). Complex dielectric permittivity of organically modified bentonite suspensions (0.2-1.3 GHz). *Canadian Geotechnical Journal* 51 (7): 782–794.

35 Ghavami, M. (2017). *Cationic Surfactant Modification and its Impact on the Engineering Behaviors of Montmorillonite*. University of Louisville.

36 Ohshima, H. (2014). Interaction of colloidal particles. In: *Colloid and Interface Science in Pharmaceutical Research and Development* [Internet], 1–28. Elsevier B.V Available from: http://dx.doi.org/10.1016/B978-0-444-62614-1.00001-6.

37 Israelachvili, J.N. (2011). *Intermolecular and Surface Forces*, 3e. Elsevier.

38 Gray, D.H. (1970). Electrochemical hardening of clay soils. *Geotechnique* 20 (1): 81–93.

39 Pham, T.D. and Sillanpää, M. (2015). Electrokinetic remediation of organic contamination. *Environmental Technology Review* 4 (1): 103–117.

40 Shang, J.Q. (1997). Zeta potential and electroosmotic permeability of clay soils. *Canadian Geotechnical Journal* 34 (4): 627–631.

41 Kaya, A. and Yukselen, Y. (2005). Zeta potential of soils with surfactants and its relevance to electrokinetic remediation. *Journal of Hazardous Materials B* 120: 119–126.

42 Cameselle, C. (2015). Enhancement of electroosmotic flow during the electrokinetic treatment of a contaminated soil. *Electrochimica Acta*. Elsevier Ltd: 4–11.

43 Song, Y., Ammami, M.T., Benamar, A. et al. (2016). Effect of EDTA, EDDS, NTA and citric acid on electrokinetic remediation of As, Cd, Cr, Cu, Ni, Pb and Zn contaminated dredged marine sediment. *Environmental Science and Pollution Research* 23 (11): 10577–10586. Available from: http://dx.doi.org/10.1007/s11356-015-5966-5.

44 Al-Faze, R. and Kooli, F. (2014). Eosin removal properties of organo-local clay from aqueous solution. *Oriental Journal of Chemistry* 30 (2): 675–680.

45 Monteiro, M.K.S., de Oliveira, V.R.L., dos Santos, F.K.G. et al. (2018). Influence of the ionic and nonionic surfactants mixture in the structure and properties of the modified bentonite clay. *Journal of Molecular Liquids* [Internet]. Elsevier B.V 272: 990–998. Available from: https://doi.org/10.1016/j.molliq.2018.10.113.

46 Chan, A., Park, W., Hyun, B. et al. (2016). Enhanced desorption of Cs from clays by a polymeric cation-exchange agent. *Journal of Hazardous Materials* [Internet]. Elsevier B.V. Available from: http://dx.doi.org/10.1016/j.jhazmat.2016.12.037.

47 Stojiljkovic, S., Miljkovic, V., Nikolic, G. et al. (2014). The influence of the addition of polymers on the physico-chemical properties of bentonite suspensions. *Science of Sintering* 46 (1): 65–73.

48 Zou, H., Du, W., Ji, M., and Zhu, R. (2016). Enhanced electrokinetic remediation of pyrene-contaminated soil through pH control and rhamnolipid addition. *Environmental Engineering Science* 33 (7): 507–513.

49 Fan, G., Wang, Y., Fang, G. et al. (2016). Review of chemical and electrokinetic remediation of PCBs contaminated soils and sediments. *Environmental Science. Processes & Impacts* [Internet]. Royal Society of Chemistry 18 (9): 1140–1156. Available from: http://dx.doi.org/10.1039/C6EM00320F.

UNCORRECTED PROOFS

Trim Size: 170mm x 244mm Single Column Loose Ribeiro670117 c23.tex V1 - 12/11/2020 6:01pm Page 602

50 Gomes, H.I., Dias-Ferreira, C., Ribeiro, A.B., and Pamukcu, S. (2013). Enhanced transport and transformation of zerovalent nanoiron in clay using direct electric current. *Water, Air, and Soil Pollution* 224 (12): 1–12.

51 Vocciante, M., Caretta, A., Bua, L. et al. (2016). Enhancements in Electrokinetic remediation technology : environmental assessment in comparison with other configurations and consolidated solutions. *Chemical Engineering Journal* [Internet]. Elsevier B.V. 289: 123–134. Available from: http://dx.doi.org/10.1016/j.cej.2015.12.065.

UNCORRECTED PROOFS

Trim Size: 170mm x 244mm Single Column Loose Ribeiro670117 c24.tex V1 - 12/11/2020 11:32pm Page 603

24

Enhanced Remediation and Recovery of Metal-Contaminated Soil Using Electrokinetic Soil Flushing

Yudha Gusti Wibowo[1] *and Bimastyaji Surya Ramadan*[2]

[1] *Department of Environmental Science, School of Postgraduate Studies, Universitas Jambi, Jambi 36122, Indonesia*
[2] *Department of Environmental Engineering, Faculty of Engineering, Universitas Diponegoro, Semarang 50277, Indonesia*

24.1 Introduction

Mining is an industrial activity that causes a significant impact on the environment. Open mining activities lead to significant changes in the landscape [1]. Some countries with the largest coal reserves, such as China, Indonesia, and the US, are at the greatest risk of damage to the quality and quantity of soil and groundwater caused by mining activities. This risk has received increasing worldwide attention over the past few decades and has led to a booming global market for remediation activities [2]. Compared to other remediation strategies, electrokinetic (EK) treatment is very effective in reducing soil pollution, but its effectiveness is limited to specific parameters such as metals and other ionic pollutants. The EK method's effectiveness for treating some parameters of soil pollutants is still unknown [3].

Soil remediation using EK methods has been implemented and reduced the content of Cu in the soil [4]. Cr(IV) in contaminated soil was also successfully reduced by 87% after the EK method was applied for five days [5]. The longer the EK process was carried out, the greater the decrease in metals in the soil. It was noted that the decrease in lead (Pb) and cadmium (Cd), respectively, reached 49.8 and 67.6% after four days of EK treatment [6]. The EK method also succeeded in reducing total petroleum hydrocarbons and Ni to 77.4 and 58.5%, respectively, after treatment for 30 days [7]. However, successful application of EK techniques on real contaminated soil is still limited [4]. Electrokinetic soil flushing (EKSF) is an EK development method that utilizes a specific flushing fluid to increase metal solubility in soil pores [8]. EKSF can increase the soil's electrical conductivity (for a particular ionic flushing fluid) so the rate of electroosmosis in the soil increases. This phenomenon increases the amount of metals removed. It is also claimed to be a sustainable method that can be applied in a long-term remediation strategy [9].

Although remediation of soils using the EKSF method has been extensively investigated, the study of EK applications in metal-contaminated soils is limited to batch

Electrokinetic Remediation for Environmental Security and Sustainability, First Edition.
Edited by Alexandra B. Ribeiro and M.N.V. Prasad.
© 2021 John Wiley & Sons Ltd. Published 2021 by John Wiley & Sons Ltd.

UNCORRECTED PROOFS

Trim Size: 170mm x 244mm Single Column Loose Ribeiro670117 c24.tex V1 - 12/11/2020 11:32pm Page 604

experiments in the laboratory [4]. This chapter aims to provide insight into using flushing solutions and possible strategies to improve the effectiveness of EK remediation of metal-contaminated soil. In addition, it is hoped that this chapter can be a reference for the development of EKSF technology, especially for removing metal contaminants in mining areas.

24.2 Metal Contamination in Mining Areas

Environmental damage caused by industrial activities since 1750 has affected all aspects of life and significantly impacted environmental quality, especially soil conditions. Soil damage caused by industrial activities has decreased the soil's acidity and increased its metal content. Metals can affect human health, plants, and agricultural products and can lead to the loss of microorganisms in the soil [10]. Soil is an environmental component, and industrial mining activity primarily contaminates it through dry and wet emission deposits from smelters and the accumulation of waste runoff.

In contaminated areas such as mining sites, the relevant aspect of soil geochemistry is the partition of metal elements in the soil fraction, called *fractionation*, controlled by the chemical properties of the soil and its composition such as pH, ion exchange capacity, mineral content, and soil organic matter. Oxidation occurs when the soil is contaminated with wastewater, and contaminated water turns into acid mine drainage. Conversely, acid mine drainage contributes to an increase in metal content in the soil. In mining areas, saturated soil turns into sludge, which is difficult to control. The sludge distributes pollution in a broader area [1].

Soil and groundwater pollution in former mining regions continues to increase as fossil energy use expands. More than 5 million mining areas have contaminated soil and groundwater. For example, the former Abbadia San Salvator mine in Italy has experienced pollution characterized by high Hg, As, and Sb content. Geochemical processes have caused sulfide minerals in coal and the topsoil to burst, contaminating the surrounding area. This area is called "mercury belt" because of the very high mercury content [11]. Mining exploitation in the Biga Peninsula (Turkey) also poses environmental risks due to the release of arsenic metals into soil and bodies of water [12]. Oil and gas mining areas have also polluted the surrounding environment with metals and hydrocarbons [7].

Around 20 million hectares in the area have been contaminated by metals [13]. In China, 1.01 million square kilometers exceeded local environmental quality standards for soil. The Advanced Industrial Research Institute predicts that China needs funds reaching 682.1 billion yuan to repair contaminated sites [14]. Europe identified 80 000 contaminated sites in 2007 and 2.5 million potentially contaminated sites in 2013 [15]. In the United States, 294 000 mercury contaminated sites were found. Recent studies reported that those contaminated sites need 31 years to remediate. This treatment is estimated to require 209 billion USD, and the cost will increase by about 650 billion USD in the next 30–35 years. Australia has confirmed 160 000 potential contaminated sites from more than 50 000 contaminated sites.

UNCORRECTED PROOFS

Trim Size: 170mm x 244mm Single Column Loose Ribeiro670117 c24.tex V1 - 12/11/2020 11:32pm Page 605

Annual maintenance costs are estimated to exceed USD 3 billion. And Japan has more than 500 000 PCS, and their annual maintenance costs are around USD 3 billion in 2010 [2]. Effective and efficient environmental remediation is required to reduce environmental losses and benefit companies and local governments.

24.3 Treatment of Metal-Contaminated Soil Using EKSF

24.3.1 Soil Flushing

Soil flushing is a method of contaminated soil remediation that uses pressure to inject a flushing solution into soil pores. This method is known to effectively reduce organic pollutants and metals in the soil [16]. Soil flushing is also known as *soil washing* in terms of ex situ treatment. Pressure and EK methods are used to flush the solution when working with in situ remediation. [17–19].

The soil-flushing process can be divided into three phenomena: physical separation, chemical extraction, and the combination of both [20, 21]. Physical separation in soil flushing is influenced by several factors, such as the type and concentration of metals in the soil and the soil's characteristics (density, size, magnetism, and hydrophobic surface properties) [22, 23]. Physical separation can be implemented if contaminants (metals) are in the form of particulates. Furthermore, chemical extraction is used as a soil-washing method to detach metals from soil particle surface by using chemical reagents such as acids or chelating agents [24, 25]. In this case, chemical extraction involves metal desorption or dissolution. Chemical separation is suitable for ionic forms adsorbed on soil or non-detrital metals [26, 27].

Physical and chemical separation techniques have been widely evaluated in recent literature. Unfortunately, the use of this technology is still limited to a few metals that are often measured, such as Cr, Cu, Pb, and Zn [28–30]. The separation of other metals using the soil-flushing method is rarely discussed.

A physical separation process cannot be used on metal-contaminated soil since adsorption is the primary phenomenon that can explain the desorption process [31, 32]. Also, the process of separating metals using physical methods in soil flushing is still limited by the mineralogical aspects of the contaminants (shape and mineralogical and morphological associations) [33] and physical properties of the soil (particle size, particle shape, clay content, humic content, water content, heterogeneity of the soil matrix, hydrophobic properties of the soil particle surface, differences in density between soil matrices, and magnetic properties and types of contaminants) [34, 35]. A physical separation method cannot be used in metal-contaminated soils that are highly bound to soil particles due to the significant variability in metal chemistry, high humic content, and high viscosity of organic compounds [36–41].

To overcome that problem, chemical extraction or separation is highly recommended to remediate polluted anthropogenic soils in urban or industrial areas. Chemical extraction is part of soil-flushing remediation. Commonly used chemicals are acids, bases, surfactants, chelating agents, salts, and redox agents that function as reagents to transfer metals from the soil to the flushing solution [42–44]. In soil

UNCORRECTED PROOFS

Trim Size: 170mm x 244mm Single Column Loose Ribeiro670117 c24.tex V1 - 12/11/2020 11:32pm Page 606

remediation, a concentrated solution affects the solubility of metals. This interesting condition can be achieved by converting metal compounds into more soluble forms (for example, converting metals into metal salts with changes in valence) [45–48].

Although chemical extraction technology methods are better for reducing pollutants in polluted soils, some limitations must be overcome. Using chemical compounds increases the cost of remediation. The processed soil may not be suitable for revegetation due to changes in physical and microbiological properties. The presence of certain chemical compounds can make it difficult to recycle and treat water. Processing metal-contaminated sludge is also challenging. In addition, the possibility of soil contamination from the chemical compounds is a consideration [49–53]. The uses of flushing fluid in the remediation of contaminated soil are listed in Table 24.1.

24.3.2 Fundamental Equation for EK Remediation

The EK soil remediation method uses a low electrical gradient to induce the migration of contaminants. In 1879, Helmholtz first introduced the theory of electroosmosis. The theory was modified by Smoluchowski in 1914. Although the theory is more appropriate when used in soils with high permeability values, it can be applied to various soil types. The Helmholtz-Smoluchowski (HS) theory can be written with Eq. (24.1):

$$v_{eo} = -\frac{D\varsigma Ez}{\eta} \tag{24.1}$$

where the electroosmotic flow velocity (v_{eo}) is proportional to the specific voltage (Ez), zeta potential (ζ), and dielectric constant of the fluid (D) and inversely proportional to the viscosity of the aqueous solution used as a flushing solution (η). The HS equation is considered valid when the thickness of the double layer (λ) is smaller than that of the capillary radius (a) so that the surface of the particle can be considered flat. The HS equation is limited to $\kappa a > 100$, where κ is $1/\lambda$ and a is the radius of capillary curvature. The HS equations can also be written

$$q_{eo} = -\frac{D\varsigma Ez}{\eta} n.A \tag{24.2}$$

where n is porosity and A is the specimen cross-sectional area. Furthermore, it should be noted that using effective porosity (ne) or porosity (n) divided by quadratic tortuosity (n/τ^2) may be more accurate than using porosity (n) that can be described in Eq. (24.3):

$$k_{eo} = -\frac{D\varsigma n}{\eta} \tag{24.3}$$

Moreover, the volumetric flow rate equation becomes

$$q_{eo} = k_{eo}.Ez.A \tag{24.4}$$

Now, electroosmotic flow can be compared to hydraulic flow using the famous hydraulic equation given by Darcy's law:

$$q = kiA \tag{24.5}$$

UNCORRECTED PROOFS

UNCORRECTED PROOFS

Trim Size: 170mm x 244mm Single Column Loose

Ribeiro670117 c24.tex V1 - 12/11/2020 11:32pm Page 607

Table 24.1 Soil-flushing remediation around the world and its application.

Location	Type of remediation	Type	Metal(s)	Flushing fluid	Removal efficiency (%)	Short description of the remediation treatment	References
Canada	In situ and ex situ	PS	Hg	EDTA	50	Gravity concentration, screening, froth flotation, hydro-cyclone	[20]
USA	In situ	CE	Zn Pb	sodium metabisulfite ($Na_2S_2O_5$) and EDTA	28.27 75.14	Flushing with sodium metabisulfite ($Na_2S_2O_5$) and EDTA	[54]
Nigeria	Ex situ	CE	Ni Cu Zn Cd Pb	EDTA	63 72 60 60 58	Flushing with EDTA	[55]
Korea	Ex situ	PS/CE	Us Ni Zn	sodium borohydride, sodium hydroxide, HCl	75 60 45	Chemically enhanced scrubbing by acid leaching and fine separation	[56]
Canada	Ex situ	PS/CE	Cu Ni Pb Zn	EDTA and HCl	86 82 87 93	PS: hydro-cyclone, screening, attrition scrubbing, separation of density CE: acid leaching followed by ion-exchange chelating resin	[57]
No information	In situ	PS	Pb	–	20.2	Attrition scrubbing and gravity concentration	[58]

(Continued)

UNCORRECTED PROOFS

Trim Size: 170mm x 244mm Single Column Loose

Table 24.1 (Continued)

Location	Type of remediation	Type	Metal(s)	Flushing fluid	Removal efficiency (%)	Short description of the remediation treatment	References
China	In situ	CE	Cu Ni Zn	EDTA-organic acids	84 86 80	Flushing with EDTA-organic acids	[59]
China	In situ	CE	Zn Pb Cd	EDTMP and PAA	20 58 72	Flushing with EDTMP and PAA	[60]
China	Ex situ	CE	PAH	Tween 80	90	Flushing with Tween 80	[61]
China	Ex situ	CE	V Cr	FVAs	57.09 94.72	Flushing with FVAs derived from food waste as washing agents	[62]
Canada	In situ	PS/CE	Pb	EDTA	20	PS: Size separation CE: precipitation and leaching	[63]
China	Ex situ	CE	Cd Pb	EDTA	88.07 37.78	Combination of freeze trawling and soil flushing with EDTA	[64]

Note: PS, physical separation; CE, chemical extraction; PS/CE, combination of both.

Ribeiro670117 c24.tex V1 - 12/11/2020 11:32pm Page 608

Trim Size: 170mm x 244mm Single Column Loose Ribeiro670117 c24.tex V1 - 12/11/2020 11:32pm Page 609

where q is the rate of hydraulic flow through the cross-sectional area A, k is the hydraulic conductivity, and i is the hydraulic gradient or head loss per unit length. If two volumetric flow rates, electroosmotic and hydraulic, are considered the same, the electrical gradient is set to a typical value of $1\,V\,cm^{-1}$, and the electroosmotic permeability (k_{eo}) and hydraulic conductivity (k) are known. The hydraulic gradient (i) needed to induce electroosmotic flow can be calculated through Eq. (24.6):

$$i = -\frac{k_{eo}}{k}(Ez) \tag{24.6}$$

where $k_{eo} = 4.1 \times 10^{-5}\ (cm\,s^{-1})/(V\,cm^{-1})$ for fine sand and soil with sand type estimated $k = 10^{-4}\,cm\,s^{-1}$. However, in soils with lower permeability, such as kaolin, $k_{eo} = 5.7 \times 10^{-5}\ (cm\,s^{-1})/(V\,cm^{-1})$ and estimated $k = 10^{-7}\,cm\,s^{-1}$.

On EK cell electrodes, hydrolysis occurs. The electrolysis reaction produces oxygen gas and hydrogen (H^+) ions, or protons, at the anode and hydrogen gas and hydroxyl ions (OH^-) at the cathode. This reaction can be written as in Eqs. (24.7 and 24.8):

$$H_2O \rightarrow {}^1\!/_2O_{2(g)} + 2H^+_{(aq)} + 2e^- \quad \text{The reactants are oxidized at the anode.} \tag{24.7}$$

$$2H_2O + 2e^- \Rightarrow H_{2\,(g)} + 2OH^-_{(aq)} \quad \text{The reactants are reduced at the cathode.} \tag{24.8}$$

The EK method is often combined with flushing fluid (EKSF) to enhance remediation efficiency. Because enhancing agents must be used during EK experiments, it is important to assess the solution's effects. The ability of an electrolyte solution to support the flow of electricity depends on the mobility of dissolved ions in the electric field (E). The ions are targeted for the frictional force (K_r) given by the Stokes formula

$$K_r = 6\pi\eta r v \tag{24.9}$$

where η is the viscosity of the solution, r is the radius of the ion, and v is the speed of the ion. The frictional force K_r is also equal to the ion charge (Z_{eo}) multiplied by the electric force of the field (E) and the speed of the ion terminal. The explanation above is then written with Eq. (24.10) [65]:

$$V_{max} = \frac{Zeo\,E}{6\prod \eta\, r} \tag{24.10}$$

24.3.3 Electrokinetic Soil Flushing (EKSF)

Many researchers have investigated combining the EK method with various flushing fluids as the oxidant. EKSF has been proven effective for reducing pollution in soil and shows a significant reduction of various hydrocarbons and metals (diesel fuel and mineral oil) in soils that have historically been contaminated. EKSF is stable and is better than the EK method without a flushing fluid [66]. EKSF aims to increase

UNCORRECTED PROOFS

Trim Size: 170mm x 244mm Single Column Loose Ribeiro670117 c24.tex V1 - 12/11/2020 11:32pm Page 610

the soil's permeability so metals can be desorbed and recovered. The remediation scheme of the EKSF method can be seen in Figure 24.1.

$$Me + L \leftrightarrow MeL \tag{24.11}$$

where K = [MeL]/[Me][L]

where Me is the metal cation, L is the anion's ligand, and K is the formation constant. EK flushing with a pump increases the pressure of the solution used to wash the soil, and this combination follows Eq. (24.12):

$$j = \left[\left(k_o + k_m\right)\nabla\varphi + k_h\nabla p\right]\ C - \frac{D}{\sigma^2}\nabla C \tag{24.12}$$

where j is the molar flux of the species per unit of pore area, k_o is the electroosmotic permeability, k_m is the electromigration coefficient, k_h is the hydraulic permeability, p is the pressure, C is the molar concentration, D is the diffusion coefficient, and σ is nondimensional tortuosity. Some EKSF successes at treating metal-contaminated soil are listed in Table 24.1.

24.3.4 Flushing Fluid Enhanced EKSF Performance

Table 24.2 shows the various EKSF methods for reducing metals in polluted soils. The most frequently used flushing fluids is EDTA (ethylenediaminetetraacetic acid) because it is proven to remove metal cations better than other flushing fluids. In addition, EDTA's physical and chemical impacts on the soil matrix are classified as very small [84–86]. EDTA is a tetrapotic acid (H_4Y), where Y is the ethylene diamine tetraacetate ion (EDTA) [87]. EDTA is a polyprotic acid with an electron pair in two amine groups and four in its carboxylic group. It does not dissolve easily in water and has a parent acid deionization constant to produce H_3Y^-, H_2Y^{2-}, HY^{3-}, and Y^{4-}, respectively, with values 10^{-2}, 2.16×10^{-3} 6.92×10^{-7}, and 5.50×10^{-1} [87]. Each EDTA ion can bind metal ions at six different sites: four for each acetate ion and two nitrogen atoms. It has three pairs of valence electrons that can be used to form coordinate bonds [88]. This compound is a hexadentate ligand (six pairs of free electrons), and these usually form a stable chelate complex. In chelating formation, the six electron donor atoms follow the nucleus ions by forming a chelate circle [89]. EDTA is an essential chelating agent in the industry, forming a very stable complex with divalent and trivalent metal ions [90]. Metals in the soil can be removed with the addition of EDTA because EDTA compounds can bind and pull the metal ions out of the soil. The reaction between the metal-binding agent (EDTA) and metal ions causes the metal ions to lose their ionic properties and causes the metal to lose most of its toxicity, making it easier for metals in the soil to migrate to the anode. For these reasons, EDTA is the most frequent and most effective flushing agent for reducing pollutant parameters in contaminated soil.

In contrast, humic acid has the least ability to reduce soil pollutants. This compound is often used for soil phytoremediation [91]. However, humic acid compounds are not very suitable for use as flushing fluids in EKSF treatment of metal contamination. Deionized water is also often used in the remediation of contaminated soils using the EK method. It is not as effective as EDTA, but using deionized water

UNCORRECTED PROOFS

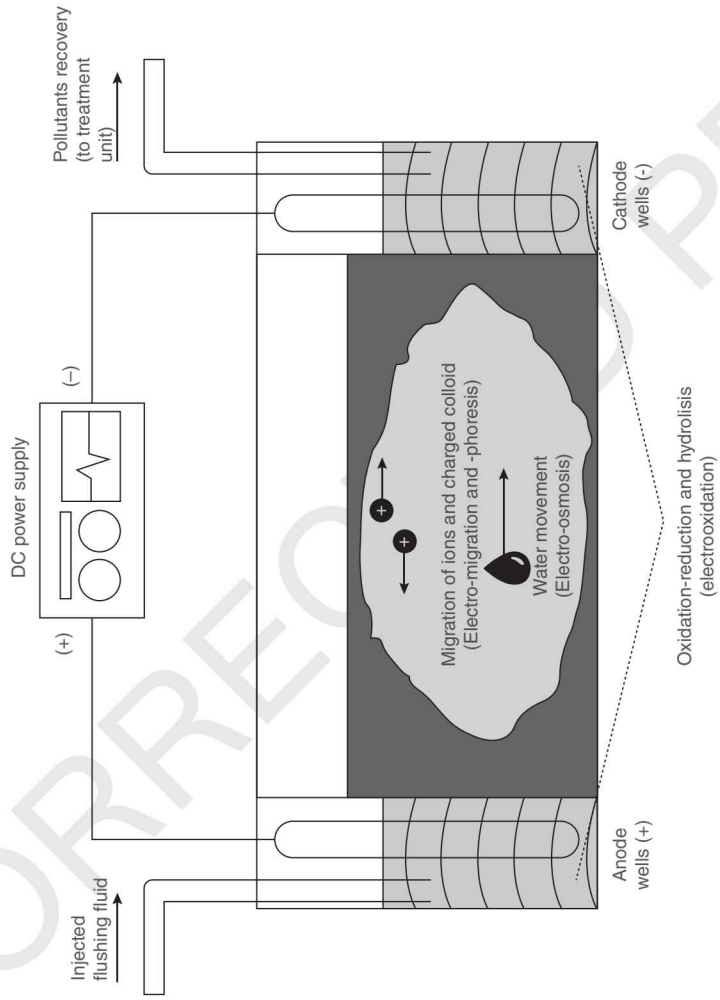

Figure 24.1 EKSF remediation scheme.

UNCORRECTED PROOFS

UNCORRECTED PROOFS

Trim Size: 170mm x 244mm Single Column Loose

Ribeiro670117 c24.tex V1 - 12/11/2020 11:32pm Page 612

Table 24.2 EKSF for treating metal-contaminated soil.

Contaminant	Location	Soil characteristics	Electrodes	Flushing fluid	Greatest removal efficiency	Operational time	References
Co^{2+} and Cs^{+}	Contaminated soil in a nuclear facility	SiO_2 64%, Al_2O_3 16.7%, K_2O 9.5%, etc.	Titanium	EDTA (cathode)	92.1% Co and 83.1 Cs	15 d	[67]
Cr	Contaminated soil from an industrial area	pH 4.10, moisture 23.1%, electrical conductivity (EC) 1620 µs cm^{-1}	Stainless steel	Deionized water (both)	94.27 ± 0.51	7 d	[66]
As	Contaminated soil around a smelter	pH 5.5, EC 88.6, sand 41%, silt 32%, clay 27%	Iridium-coated titanium oxide	Deionized water (both)	25%	22 d	[68]
Cr(IV)	Contaminated soil from chromite ore processing	pH 8.15, organic content (OM) 4.6%, specific gravity (Sg) 16%, 90% of particle size is 283.1 µm	Iron	Natural rainfall (anode)	59.5%	150 min	[69]
Pb	Artificial sandy soil	pH 3.97, Sg 2.5, EC 5.1, OM 5.1 meq/100 g	Cylindrical graphite	Deionized water (both)	96.98%	25 hr	[70]
^{60}Co and ^{137}Cs	Contaminated soil from a Korean power plant	Saturation degree (SD) 26.3%, pH 6.3, porosity 0.40, bulk density 1.57 g cm^{-3}, hydraulic conductivity (HC) 1.8×10^{-3} cm s^{-1}	Electrode plate (no information)	EDTA (cathode)	99.9%	50 d	[71]

UNCORRECTED PROOFS

Trim Size: 170mm x 244mm Single Column Loose

Cu	Kaolinite soil from laboratory		Granular graphite	Deionized water (both)	75%	180 hr	[9]
Co and Cs	Real soil from TRIGA research reactor	SD 38.8, pH 6.9, SiO_2 65.2%, Al_2O_3 16.7%, K_2O 8.3%, etc.	Filter paper and titanium	Oxalic acid (anode)	90.5%	10 d	[72]
Cd	Real soil from China	SG 2.73, liquid limit 36%, plastic limit 19%, plastic index 19%, pH 8.29, OC 0.18%, total carbon content 8.52 g kg^{-1}, EC 0.339	Stainless steel	Organophosphates (cathode)	75%	5 d	[73]
Pb	Contaminated soil	Sand 19.3%, silt 62.4%, clay 18.3%	Graphite	Deionized water (both)	87.7%	192 hr	[74]
Pb	Lead-polluted soil	pH 7.9, EC 6.1–6.8%, cation exchange capacity (CEC) 69 mol kg^{-1}	Stainless steel	EDTA (cathode)	79%	10 d	[75]
Cr(VI)	Loam and kaolin	No information	Graphite	EDTA (cathode)	80%	30 hr	[76]
Cd	Real soil	pH 7.42, gravel 1%, sand 19%, silt 70%, OC 2.15%	Graphite	EDTA (cathode)	95%	25 d	[77]
Cr, Cu, Ni	Real soil from the electroplating industry	Clay 34%, silt 58%, sand 7.53%, pH 4.8%, CEC 18.4 cmol kg^{-1}, EC 130 μS cm^{-1}	Stainless steel	EDTA (cathode)	Cr 54.6 Cu 34% Ni 3.5%	10 d	[78]

(Continued)

Ribeiro670117 c24.tex V1 - 12/11/2020 11:32pm Page 613

UNCORRECTED PROOFS

Trim Size: 170mm x 244mm Single Column Loose

Ribeiro670117 c24.tex V1 - 12/11/2020 11:32pm Page 614

Table 24.2 (Continued)

Contaminant	Location	Soil characteristics	Electrodes	Flushing fluid	Greatest removal efficiency	Operational time	References
As	Artificial As-contaminated soil	pH 8.59, EC 167.05, organic 28.9%, carbon 2.85%	Graphite	Humic acid (anode)	31.8%	25 d	[79]
As, Al, Fe, and Mn	Mining site soil	pH 3.35, EC 2427, Sg 2.45 g cm^{-3}, permeability 6.45×10^{-6}	Graphite	Deionized water (both)	As 6% Al 45% Fe 13% Mn 99%	No information	[12]
Cd	Agriculture contaminated soil	Quartz 9.5%, illite 46.5%, kaolinite 42%, albite 2%, OC 1.53%	Graphite	sodium dodecyl sulfate-SDS (cathode)	90%	18 d	[80]
Cr(VI), Ni(II), and Cd(II)	Kaolinite soil	pH 3.79, SG 2.5, CEC 5.1 meq, organic matter 1.4%	Stainless steel	Deionized water (both)	Cr(VI) 42%; Ni(II) 30%; Cd(II) 28%	10 d	[81]
Cu and Zn	Real contaminated soil	Kaolinite 100%. pH 4.9, CEC 1.0–1.6	Graphite	EDTA (cathode)	Cu 63% Zn 65%	554 hr	[82]
Pb	Real contaminated soil	Kaolinite 100%	Graphite	EDTA (cathode)	20.45%	25 hr	[83]

Trim Size: 170mm x 244mm Single Column Loose Ribeiro670117 c24.tex V1 - 12/11/2020 11:32pm Page 615

as a flushing fluid is far more economical than EDTA. In addition, the nature of electricity to flow in water increases the electroosmosis of soil pollutants.

Another flushing fluid is SDS, a compound that is often used as an anionic surfactant. It can increase the density and turtousity of the electrolyte, thus reducing electroosmotic flow. This molecule has a hydrophobic part containing 12 carbon atoms and binds to sulfate groups that make it an amphiphilic compound [92]. Although it can significantly reduce metal levels, the use of SDS is still infrequent and limited to detergents, soaps, and various other cleaning products.

The type of flushing fluid is the most critical factor in reducing metals using EKSF [77]. In general, EDTA is ubiquitous and is often used in EKSF to remove metals from contaminated soil [73, 75, 78]. EDTA is the most effective chelating agent for removing metals from soil [93]. The combination of EK and EDTA as flushing fluid is known to reduce Pb levels significantly. This statement is reinforced by the increased electroosmosis and electromigration caused by the use of EDTA. The concentration of EDTA used is the critical parameter to increase its ability to reduce metals in soil. The study reported that 0.1 M EDTA could reduce Pb by 79% in six days (with contamination $\pm 4000\,\mathrm{mg\,kg^{-1}}$) from contaminated agricultural soil [76].

Further research on optimizing operating conditions and recycling chelating agents will improve the cost-effectiveness of this new approach [78]. Removal of Cr(VI) after 150 minutes was achieved by Li et al. (2018) using EKSF. Interestingly, the flushing fluid used was rainwater because it was considered to enlarge the soil's pores and neutralize the soil pH. The longer the kinetic desorption process is implemented, the greater the percent removal of Cr, until no Cr is released back into the environment [69]. Although using rainwater looks promising, an efficiency of 59.5% is not considered high enough compared to using EDTA and citric acid. Although EDTA to remove significant amounts of metals, Gu et al. (2018) stated that EDTA was expensive. Flushing solution substitution was a concern for other researchers [73].

In addition to EDTA, a weak organic acid salt compound (such as citric and acetic acid) is an environmentally friendly material that can be used to remediate soils contaminated by metals. These compounds can increase soil aggregation and dissolve only small amounts of macronutrients from the soil [77]. Kim et al. (2009) confirmed that using acetic acid, oxalic acid, and citric acid was better than using EDTA, where the reduction efficiency of Co with each flushing fluid was EDTA 83.5%, oxalic acid 90.5%, citric acid 86.9%, and acetic acid 92.1%. EK remediation using acetic acid has the highest value of cobalt remediation efficiency compared to the other two types of fluid [71]. Ryu et al. [68] stated that citrate was better than EDTA and oxalate for reducing As from contaminated soil. Kantar and Honeyman (2006) also mentioned the possible reactions with citric acid, as shown in Eqs. (24.13 and 24.14) [19]:

$$2H_2O + 4e^- \rightarrow O_2 + 4H^+ + NaOH \tag{24.13}$$

$$Fe\ (II) + C_6H_8O_7 + O_2 \rightarrow Fe\ (III) + C_6H_8O_7 + H_2O_2/O^{2-} \tag{24.14}$$

UNCORRECTED PROOFS

Trim Size: 170mm x 244mm Single Column Loose Ribeiro670117 c24.tex V1 - 12/11/2020 11:32pm Page 616

The formation of H_2O_2 and Fe(III) is considered to trigger a Fenton reaction so As can be properly mediated. This phenomenon occurs because Fenton affects H_2O_2 in the anode, enhancing the EK method's effectiveness; but it needs to be stressed that the injection must be at the required concentration – using a dose greater than required reduces the electroosmosis flow rate. However, iron oxidation has the potential to cause blockages in soil pores. Kim et al. got the same result [67], where EDTA was the least effective flushing fluid for removing Co^{2+} and Cs^{+} from contaminated soil. Comparing EDTA, oxalic acid, and citric acid, acetic acid produced the largest percentage of removal for Co^{2+} and Cs^{+}, at 92.1 and 83.1%, respectively. In that study, the flushing fluid succeeded in increasing the permeability of cobalt-contaminated soil and had a higher efficiency value [67].

Nitric acid has an excellent ability to reduce Co and Cs compared to EK methods using constant current of 10 mA/cm^{-2} working for 20 days without flushing or using acetic acid reagents. Using a vertical EK method with nitric acid as an electrolyte is also very efficient for reducing Cd metal content, followed by Zn and Pb. The decrease in Pb is very small because Pb has a stronger adsorption value than other metals. Some studies also show that Pb is the most difficult metal to remove from contaminated soil. Increasing the EK contact duration causes metals to migrate upward (to the cathode). The metal moves out of the soil in the cathode effluent or is deposited on the surface of the cathode [77].

Chen et al. (2011) also tried ammonium (0.01 M) as an anolyte. According to the reaction between copper and ammonium [15], high pH close to the cathode supports the copper-ammonium complex reaction, thereby increasing the level of solubility and removal of copper during the remediation process. The reaction between copper and ammonium can be seen in the Eq. (24.15) [9]:

$$\begin{aligned}
&NH_4{}^{+} \leftrightarrow NH_3 + H^{+} && pKa = 9.25\\
&Cu^{2+} + NH_3 \leftrightarrow Cu\left(NH_3\right)^{2+} && pK1 = -4.31\\
&Cu^{2+} + 2NH^{3} \leftrightarrow Cu\left(NH_3\right)^{2+} && pK2 = -7.98\\
&Cu^{2+} + 3NH^{3} \leftrightarrow Cu\left(NH_3\right)^{2+} && pK3 = -11.02\\
&Cu^{2+} + 4NH^{3} \leftrightarrow Cu\left(NH_3\right)^{2+} && pK4 = -13.32\\
&Cu\,(OH)_{2(s)} \leftrightarrow Cu^{2+} + 2OH^{-} && pKsp = 19.66
\end{aligned} \tag{24.15}$$

According to Gu et al. (2018), organophosphonates such as nitrilotrimethylene triphosphonate (NTMP) and (ethylenedinitrilo)-tetramethylenephosphonate (EDTMP) have proven to be efficient supplementary agents for EK remediation of metal-contaminated soils. The absorption of 75% of cadmium in a 0.1 mol l^{-1} organophosphonate solution proves this explanation. Humic acid (HA) and fulvic acid (FA) can also be used as an alternative booster and increase the efficiency of EK remediation. EK combined with FA has greater effectiveness than HA. This result is due to FA containing more bound oxygen than HA. The greater ability of HA to remove metals is caused by HA consisting of micro molecules with long carbon chains, whereas FA consists of small molecules with short carbon chains. The combination of HA and FA may increase EK ability. In addition, competitive adsorption, reductive dissolution, and complexation processes occur [79].

UNCORRECTED PROOFS

Trim Size: 170mm x 244mm Single Column Loose Ribeiro670117 c24.tex V1 - 12/11/2020 11:32pm Page 617

24.3.5 Preventing pH from Acidification

Maintaining pH is an essential part of increasing the efficiency of metal removal using EK. Efforts are made to maintain the value in acidic soil such as adding a chemical solution (acid or base), changing the position of the anode and cathode, or using a circulation method. Maturi and Reddy [82] used hydroxypropyl b-cyclodextrin (HPCD) to remove nickel and phenanthrene. Cyclodextrins have no direct effect on the migration of Ni^{2+} ions. However, the rate of electroosmosis increases ion removal. At the cathode, most of the Ni^{2+} ions are deposited as $Ni(OH)_2$ due to high-pH conditions. Cyclodextrin at high concentrations (10%) can maintain low soil pH near the cathode, and this condition affects the efficiency of metal removal [82]. The addition of persulfate is also considered to increase the mobilization of metals in the soil due to the oxidation process of organic materials/metal complex sulfides to persulfate compounds [94]. The persulfate solution added to the EK method can produce many ions such as Na^+ and $SO_4{}^{2-}$. The reactions that occur with the addition of persulfate are

$$FeO + 2S_2O_8{}^{2-} \rightarrow Fe^{2+} + 2SO_4{}^{2-} + 2SO_4 \tag{24.16}$$

Soil conditions that are very acidic cause no precipitation, so the efficiency of pollutant reduction is higher. In line with this statement, Reddy et al. (2010) argue that deionized water at neutral pH does not contribute to the removal of metals with or without the application of voltage gradients. This argument shows that the metal has been absorbed into the soil matrix. It is also possible that the concentration of contaminants decreases due to natural processes such as rain or washing caused by groundwater [95]. However, conditions that are too acidic cause a decrease in the rate of electroosmosis and electromigration. Maintaining the pH at neutral conditions is very important in EKSF. Therefore, pH-control strategies need to be implemented to maintain a neutral pH to enhance the ability to decrease pollutants [96, 97]. In addition to using acidic or basic solutions, pH control can be achieved with synthetic lime (CaO) or shellfish waste that is high in calcium carbonate ($CaCO_3$) content. This compound can be synthesized using a simple reactor to produce CaO at temperatures above 400 °C. The process releases O_2 into the environment and forms CaO. The process that occurs in the calcination of $CaCO_3$ to CaO is shown in Eq. (24.17):

$$CaCO_3 \rightarrow CaO + O_2 \tag{24.17}$$

Periodic application of FeO to the catholyte produces $SO_4{}^{2-}$ continuously, which is transferred to the soil chamber by electromigration. This phenomenon can increase the ability of an EK method to reduce pollutant parameters in contaminated soil [94]. The correct pH buffer must be determined to improve the efficiency of remediation using chelating agents [75]. Circulation methods can increase the effectiveness of chelating agents: this method increases Ni and Cu removal, eliminates the effects of metal accumulation, and reduces highly acidic areas from 80 to 20%. Compared to the acidification effect, EDTA has no significant chelating effect on Ni and Cu compared to other chelating agents.

UNCORRECTED PROOFS

Trim Size: 170mm x 244mm Single Column Loose Ribeiro670117 c24.tex V1 - 12/11/2020 11:32pm Page 618

As explained previously, acidic soil conditions increases the mobilization of metals and pollutants. Polarity reversal can overcome this problem and extract more metals from soil than conventional EK methods. Cai et al. (2015) said that this is consistent with the initial assumption that variations in changes in polarity can extract more metals from soil, thereby increasing the efficiency of reducing Pb in polluted soils. The conventional EK method can reduce Pb by 61.8% in contaminated soil during 192 hours of treatment, while the polarity exchange technique on soils with pH conditions 5–9 has succeeded in reducing Pb by 77.1 and 87% in 96 and 48 hours, respectively. The efficiency of metal degradation is enhanced due to the exchange of polarity to prevent Pb precipitation in alkaline soils. This method is also useful for preventing Pb from returning to the environment [74]. And it does not require chemicals like flushing, so it is more economical and sustainable.

24.3.6 Other Factors that Enhance EKSF Performance

Normalizing the distance from the anode identifies differences in the percentage of removal for each contaminant. EK methods that are not equipped with specific flushing solutions have a decreased capability at increasingly longer anode distances. The more flushing solution is added to the soil, the better the value of the metal reduction efficiency [98–100]. The effect of this distance has also been evaluated by Zulfiqar et al. (2017), where the anode distance affects the percentage decrease in Fe and Pb. The results of their research showed that the greater the distance from the anode, the lower the Fe and Pb content. Soil type and contact time are other factors that influence the rate of metal migration to the cathode. A recent study analyzed the electromigration effect of Cr(VI) metal in two types of soil (kaolin and glacial soil). Unlike kaolin, glacial soil does not affect nickel and cadmium migration due to its high buffering capacity. In both kaolin and glacial soil, the rate of Cr(VI) migration to the anode increases with greater contact time. However, Cr(VI) migration is greater in glacial soil than kaolin due to the high pH in glacial soil. Some Cr(VI) is also reduced to Cr(III), and the rate of reduction of Cr(VI) to Cr(III) and Cr(III) migration is affected by the time of treatment. Overall, this study shows that electroosmotic flow and direction of migration depend on polarity, soil type, and length of treatment [101]. Also, the decrease in metal content in natural soils is much greater than in kaolin in more saturated conditions. High water content and better permeability of natural soil are known to increase the EK effect in natural soils [102, 103]. Stress variations do not have a significant effect on pH, soil, temperature, and humidity, but voltage gradients have a significant effect on electroosmotic fluxes. The higher the applied voltage, the greater the transfer rate [8, 104]

24.3.7 Energy Requirements and Future Perspectives

Issues that are important and need to be addressed in EK applications in the field are energy requirements and the drastic increase in soil temperature caused by

UNCORRECTED PROOFS

Trim Size: 170mm x 244mm Single Column Loose Ribeiro670117 c24.tex V1 - 12/11/2020 11:32pm Page 619

the application of electrical energy. Although high temperatures can enhance the process of removing metals from soil particles, an increase in temperature potentially accelerates soil drying and ultimately reduces remediation efficiency [66, 105]. The difference in temperature increase may be influenced by the soil's ionic strength. Fu et al. (2017) tried to solve this problem by applying EKSF to remediate Cr and Cr^{6+}, using citric acid (CA) and polyaspartic acid (PASP) as electrolytes. These electrolytes increase the efficiency of Cr^{6+} removal because CA and PASP reduce the valence of Cr from 6+ to 3+. When using CA and PASP as electrolytes, the -OH and -COOH groups play an important role in remediating chromium. Relatively lower transfer efficiency of total Cr was found when using PASP as an electrolyte. PASP supports the transformation of Cr into carbon-bound Cr, which has a lower migration rate. However, using electrolyte solutions increases energy consumption. This phenomenon, of course, is accompanied by an increase in soil temperature that is faster than when using deionized water. The energy used in this experiment can be calculated using Eq. (24.18) [66]:

$$W = \int_0^t UIdt \tag{24.18}$$

Moreover, the total Cr lost can be calculated by Eq. (24.19):

$$\eta = \frac{Co - Ct}{Ct} \times 100\% \tag{24.19}$$

where U is the voltage between the electrodes (V), I is the electric current (A), and t is the duration of treatment (h), where Ct is the Cr concentration at t (mg g^{-1}) and Co is the initial concentration of Cr (mg g^{-1}). The energy needed is also different for each electrolyte used. Deionized water is the electrolyte that consumes the least energy, followed by PASP and CA [106, 107]. Ng et al. (2015) state that the lowest energy consumption of 45.04 kWh kg^{-1} Pb occurs in reactors that apply a voltage of 30 V, with flushing concentrations of 0.05 M and Pb concentrations of 1000 mg kg^{-1}. The average Pb loss uses a current of 16.01 mA [70].

The addition of a permeable reactive barrier (PRB) is promoted as a new technology for increasing the ability of EK methods [76, 108]. EK-PRB was found to reduce levels of Cu in the soil [4]. The results of this study show that Cu in contaminated soil can be reduced to 96.40% after four days with an initial concentration of Cu of 2000 mg kg^{-1} [4]. EK combination technology using a reactive barrier of red mud is also more effective than conventional EK methods. This method can reduce 19.4% of the total weight of Cr(IV) detected in the soil, and 20.6% of Cr is trapped on the reactive barrier of red mud after testing for six days [109]. However, these studies have not evaluated using EK-PRB with an electrolyte such as EDTA, citric acid, or acetic acid. The field-scale study of EK-PRB should be conducted to evaluate the possibility of commercializing this technology. Also, EKSF technology eliminates more than 80% of polar and non-polar pollutants due to EK flux and evaporation for some volatile pollutants. Most researchers only show that side effects from this process can be minimized by using adsorption or biological oxidation. Other side effects have not been studied much, so this is a direction for further research related to EKSF.

UNCORRECTED PROOFS

Trim Size: 170mm x 244mm Single Column Loose Ribeiro670117 c24.tex V1 - 12/11/2020 11:32pm Page 620

24.4 Conclusion

Remediation of contaminated soil using EKSF is still rarely found in the field. Some obstacles are the high cost of environmental management and technical issues such as high temperatures and evaporation rates, soil conditions, electrode corrosion, pH control, and the availability of electricity in isolated areas. Flushing fluids include EDTA, citric acid, Tween 80, humic acid, fulvic acid, acetic acid, and sodium dodecyl sulfate, but the most frequently used and highest-efficiency flushing fluid is EDTA. In addition, various types of anode and cathode materials have been used, such as stainless steel, graphite, iron, and titanium. Other factors that affect the ability to decrease soil pollutants are pH, electrodes, and the type of flushing fluid. The capacity-building strategy has been described. Therefore, the success rate for remediation of contaminated soils using EK and soil-flushing methods could be enhanced by combining them with other successful treatment methods.

References

1 Saini, A., Bekele, D.N., Chadalavada, S. et al. (2019). A review of electrokinetically enhanced bioremediation technologies for PHs. *Journal of Environmental Sciences* 88: 31–45.

AQ1

2 Naidu, R. and Birke, V. (2015). *Permeable Reactive Barrier*, 1e, 1–308. Boca Raton, FL: CRC Press/Taylor and Francis Group.

3 Nieto Castillo, A., García-Delgado, R.A., and Cala Rivero, V. (2012). Electrokinetic treatment of soils contaminated by tannery waste. *Electrochimica Acta* 86: 110–114.

4 Zhao, S., Fan, L., Zhou, M. et al. (2016). Remediation of copper contaminated kaolin by electrokinetics coupled with permeable reactive barrier. *Procedia Environmental Sciences* 31: 274–279.

5 Yan, Y., Li, H., Yu, X. et al. (2019). Efficient removal of chromium from the soil in a modified electrokinetic system using iron-treated activated carbon as a third electrode. *Journal of the Taiwan Institute of Chemical Engineers* 101: 15–23.

6 Kim, S., Moon, S., and Kim, K. (2001). Removal of heavy metals from soils using enhanced electrokinetic soil processing. *Water, Air, and Soil Pollution* 125: 259–272.

7 Li, X., Mao, H., Wang, B. et al. (2018). Remediation of hydrocarbons - heavy metal co-contaminated soils by electrokinetics combined with biostimulation. *Chemical Engineer* J353: 410–418.

8 Mena, E., Villaseñor, J., Rodrigo, M.A., and Cañizares, P. (2016). Electrokinetic remediation of soil polluted with insoluble organics using biological permeable reactive barriers: effect of periodic polarity reversal and voltage gradient. *Chemical Engineer* J299: 30–36.

9 Chen, J.L., Yang, S.F., Wu, C.C., and Ton, S. (2011). Effect of ammonia as a complexing agent on electrokinetic remediation of copper-contaminated soil. *Separation and Purification Technology* 79 (2): 157–163.

UNCORRECTED PROOFS

Trim Size: 170mm x 244mm Single Column Loose Ribeiro670117 c24.tex V1 - 12/11/2020 11:32pm Page 621

10 Surya, B., Lova, G., Tina, R., and Jatnika, A. (2018). An overview of electrokinetic soil flushing and its effect on bioremediation of hydrocarbon contaminated soil. *Journal of Environmental Management* 218: 309–321.

11 Protano, G. and Nannoni, F. (2018). Influence of ore processing activity on Hg, As and Sb contamination and fractionation in soils in a former mining site of Monte Amiata ore district (Italy). *Chemosphere* 199: 320–330.

12 Karaca, O., Cameselle, C., and Bozcu, M. (2019). Opportunities of electrokinetics for the remediation of mining sites in Biga peninsula, Turkey. *Chemosphere* 227: 606–613.

13 Wuana, R.A. and Okieimen, F.E. (2011). Heavy metals in contaminated soils: a review of sources, chemistry, risks, and best available strategies for remediation. *International Scholarly Research Network* 2011: 1–20.

14 Chinese Academy for Environmental Planning. (2018). Financing models for soil remediation in China. The International Institute for Sustainable Development and the CAEP. https://www.iisd.org/system/files/publications/financing-models-soil-remediation-china.pdf.

15 Panagos, P., Hiederer, R., Van Liedekerke, M., and Bampa, F. (2013). Estimating organic soil carbon in Europe based on data collected through an European network. *Ecological Indicators* 24: 439–450.

16 Abumaizar, R.J. and Smith, E.H. (1999). Heavy metal contaminants removal by soil washing. *Journal of Hazardous Materials* 70 (1–2): 71–86.

17 Reed, B.B.E., Member, A., Carriere, P.C., and Moore, R. (1996). Pb (II) contaminated soil using HC. *Journal of Environmental Engineering* 122 (ii): 48–50.

18 Khodadoust, A.P., Wagner, J.A., Suidan, M.T., and Safferman, S.I. (1994). Solvent washing of PCP contaminated soils with anaerobic treatment of wash fluids. *Water Environment Research* 66 (5): 692–697.

19 Kantar, C. and Honeyman, B.D. (2006). Citric acid enhanced remediation of soils contaminated withuranium by soil flushing and soil washing. *Journal of Environmental Engineering* 132 (2): 247–255.

20 Dermont, G., Bergeron, M., Mercier, G., and Richer-Laflèche, M. (2008). Soil washing for metal removal: a review of physical/chemical technologies and field applications. *Journal of Hazardous Materials* 152 (1): 1–31.

21 Blockley, S.P.E., Pyne-O'Donnell, S.D.F., Lowe, J.J. et al. (2005). A new and less destructive laboratory procedure for the physical separation of distal glass tephra shards from sediments. *Quaternary Science Reviews* 24 (16–17): 1952–1960.

22 Verma, A. and Stellacci, F. (2010). Effects of surface properties on nanoparticle-cell interactions. *Small* 6 (1): 12–21.

23 Brown, P., Bushmelev, A., Butts, C.P. et al. (2012). Magnetic control over liquid surface properties with responsive surfactants. *Angewandte Chemie, International Edition* 51 (10): 2414–2416.

24 Neale, C.N., Bricka, R.M., and Chao, A.C. (1997). Evaluating acids and chelating agents for removing heavy metals from contaminated soils. *Environmental Progress* 16 (4): 274–280.

UNCORRECTED PROOFS

Trim Size: 170mm x 244mm Single Column Loose Ribeiro670117 c24.tex V1 - 12/11/2020 11:32pm Page 622

25 Lim, T.T., Tay, J.H., and Wang, J.Y. (2004). Chelating-agent-enhanced heavy metal extraction from a contaminated acidic soil. *Journal of Environmental Engineering* 130 (1): 59–66.

26 Peters, R.W. (1999). Chelant extraction of heavy metals from contaminated soils. *Journal of Hazardous Materials* 66 (1–2): 151–210.

27 Bhandari, A., Surampalli, R.Y., Champagne, P. et al. (2007). *Remediation Technologies for Soils and Groundwater*.60, 1–449.

28 Wasay, S.A., Barrington, S., and Tokunaga, S. (1999). Efficiency of GAC for treatment of leachate from soil washing process. *Water, Air, and Soil Pollution* 116 (3–4): 449–460.

29 Kuo, S., Lai, M.S., and Lin, C.W. (2006). Influence of solution acidity and $CaCl_2$ concentration on the removal of heavy metals from metal-contaminated rice soils. *Environmental Pollution* 144 (3): 918–925.

30 Hansen, H.K., Ottosen, L.M., Kliem, B.K., and Villumsen, A. (1997). Electrodialytic remediation of polluted soils with Cu, Cr, Hg, Pb and Zn. *Journal of Chemical Technology and Biotechnology* 70 (1): 67–73.

31 Strawn, D.G. and Sparks, D.L. (2000). Effects of organic matter soil on the kinetics and mechanisms of Pb(II) sorption and desorption in soil. *Soil Science Society of America Journal* (J64, 1): 144–156.

32 Pigna, M., Krishnamurti, G.S.R., and Violante, A. (2006). Kinetics of arsenate sorption-desorption from metal oxides. *Soil Science Society of America Journal* J70 (6): 2017–2027.

33 Laperche, V., Traina, S.J., Gaddam, P., and Logan, T.J. (1996). Chemical and mineralogical characterizations of Pb in a contaminated sail: reactions with synthetic apatite. *Environmental Science & Technology* 30 (11): 3321–3326.

34 Ochoa-Loza, F.J., Noordman, W.H., Jannsen, D.B. et al. (2007). Effect of clays, metal oxides, and organic matter on rhamnolipid biosurfactant sorption by soil. *Chemosphere* 66 (9): 1634–1642.

35 Griffiths, R.A. (1995). Soil-washing technology and practice. *Journal of Hazardous Materials* 40 (2): 175–189.

36 Shim, H.Y., Lee, K.S., Lee, D.S. et al. (2014). Application of electrocoagulation and electrolysis on the precipitation of heavy metals and particulate solids in washwater from the soil washing. *Journal of Agricultural Chemistry and Environment* 03 (04): 130–138.

37 Gusiatin, Z.M. and Klimiuk, E. (2012). Metal (Cu, Cd and Zn) removal and stabilization during multiple soil washing by saponins. *Chemosphere* 86 (4): 383–391.

38 Mulligan, C.N., Yong, R.N., and Gibbs, B.F. (2001). An evaluation of technologies for the heavy metal remediation of dredged sediments. *Journal of Hazardous Materials* 85 (1–2): 145–163.

39 Zhang, M.K., He, Z.L., Calvert, D.V. et al. (2003). Phosphorus and heavy metal attachments and release in sandy soil aggregate fractions. *Soil Science Society of America Journal* 67 (4): 1158–1167.

UNCORRECTED PROOFS

Trim Size: 170mm x 244mm Single Column Loose Ribeiro670117 c24.tex V1 - 12/11/2020 11:32pm Page 623

40 Mclaughlin, M.J., Zarcinas, B.A., Stevens, D.P., and Cook, N. (2000). Soil testing for heavy metals. *Communications in Soil Science and Plant Analysis* 31 (11–14): 1661–1700.

41 Srivatsan, T.S., Ibrahim, I.A., Mohamed, F.A., and Lavernia, E.J. (1991). Processing techniques for particulate-reinforced metal aluminium matrix composites. *Journal of Materials Science* 26 (22): 5965–5978.

42 Van Benschoten, J.E., Reed, B.E., Matsumoto, M.R., and McGarvey, P.J. (1994). Metal removal by washing soil for an iron oxide coated sandy soil. *Water Environment Research* 66 (2): 168–174.

43 Mann, M.J. (1999). Full-scale and pilot-scale soil washing. *Journal of Hazardous Materials* 66 (1–2): 119–136.

44 Makino, T., Sugahara, K., Sakurai, Y. et al. (2006). Remediation of cadmium contamination in paddy soils by washing with chemicals: selection of washing chemicals. *Environmental Pollution* 144 (1): 2–10.

45 Rieuwerts, J.S., Thornton, I., Farago, M.E., and Ashmore, M.R. (1998). Factors influencing metal bioavailability in soils: preliminary investigations for the development of a critical loads approach for metals. *Chemical Speciation & Bioavailability* 10 (2): 61–75.

46 Hartley, F.R. (1973). Thermodynamic data for olefin and acetylene complexes of transition metals. *Chemical Reviews* 73 (2): 163–189.

47 Cataldo, D.A. and Wildung, R.E. (1978). Soil and plant factors influencing the accumulation of heavymetals by plants. *Environmental Health Perspectives* 27: 149–159.

48 Silveira, M.L.A., Alleoni, L.R.F., and Guilherme, L.R.G. (2003). Biosolids and heavy metals in soils. *Science in Agriculture* 60 (4): 793–806.

49 Zhang, W. (2015). Batch washing of saturated hydrocarbons and polycyclic aromatic hydrocarbons from crude oil contaminated soils using bio-surfactants. *Journal of Central South University* 22 (3): 895–903.

50 Kos, B. and Leštan, D. (2003). Induced phytoextraction/soil washing of leads using biodegradable chelates and permeable barriers. *Environmental Science & Technology* 37 (3): 624–629.

51 Almazán-Sánchez, P.T., Cotillas, S., Sáez, C. et al. (2017). Removal of pendimethalin from soil washing effluents using electrolytic and electro-irradiated technologies based on diamond anodes. *Applied Catalysis B: Environmental* 213: 190–197.

52 Shi, Z. and Chen, J. (2013). The influence of defoamer on removal of PAHs in soil washing. *Journal of the Air & Waste Management Association* 63 (1): 80–86.

53 Satyro, S., Race, M., Marotta, R. et al. (2017). Photocatalytic processes assisted by artificial solar light for soil washing effluent treatment. *Environmental Science and Pollution Research* 24 (7): 6353–6360.

54 Khan, L.I. and Abumaizar, R. (1996). Laboratory investigation of heavy metal removal by soil washing. *Journal of the Air & Waste Management Association* 46 (8): 765–768.

UNCORRECTED PROOFS

Trim Size: 170mm x 244mm Single Column Loose Ribeiro670117 c24.tex V1 - 12/11/2020 11:32pm Page 624

55 Wuana, R.A., Okieimen, F.E., and Imborvungu, J.A. (2010). Removal of heavy metals from a contaminated soil using organic chelating acids. *International Journal of Environmental Science and Technology* 7 (3): 485–496.

56 Ko, I., Lee, C., Lee, K. et al. (2006). Remediation of soil contaminated with arsenic, zinc, and nickel by pilot-scale. *Soil Washing* 25 (1): 39–48.

57 Applications, F., Dermont, G., Bergeron, M., and Mercier, G. (2008). Soil washing for metal removal: a review of physical/chemical technologies soil washing for metal removal: a review of physical/chemical technologies and field applications. *Journal of Hazardous Materials* 152: 1–31.

58 Marino, M.A., Box, O., Brica, R.M., and Neale, C.N. (1997). Heavy metal soil remediation: the effects of attrition scrubbing on a wet gravity concentration process. *Environmental Progress & Sustainable Energy* 16 (3): 208–214.

59 Cheng, S., Lin, Q., Wang, Y. et al. (2020). The removal of Cu, Ni, and Zn in industrial soils by washing with EDTA-organic acids. *Arabian Journal of Chemistry* 13 (4): 5160–5170.

60 Feng, W., Zhang, S., Zhong, Q. et al. (2020). Soil washing remediation of heavy metal from contaminated soil with EDTMP and PAA: properties, optimization, and risk assessment. *Journal of Hazardous Materials* 381: 120997.

61 Bai, X., Wang, Y., Zheng, X. et al. (2019). Remediation of phenanthrene contaminated soil by coupling soil washing with Tween 80, oxidation using the UV/$S_2O_8^{2-}$ process and recycling of the surfactant. *Chemical Engineering Journal* 369: 1014–1023.

62 Zou, Q., Xiang, H., Jiang, J. et al. (2019). Vanadium and chromium-contaminated soil remediation using VFAs derived from food waste as soil washing agents: a case study. *Journal of Environmental Management* 232: 895–901.

63 Mercier, G., Blais, J., and Chartier, M. (2007). Décontamination à l 'échelle pilote de sols pollués en métaux toxiques par des procédés miniers et lixiviation chimique. *Journal of Environmental Engineering and Science* 6 (1): 53–64.

64 Rui, D., Wu, Z., Ji, M. et al. (2019). Remediation of Cd and Pb-contaminated clay soils through combined freeze-thaw and soil washing. *Journal of Hazardous Materials* 369: 87–95.

65 Saichek, R.E. and Reddy, K.R. (2005). Electrokinetically enhanced remediation of hydrophobic organic compounds in soils: a review. *Critical Reviews in Environmental Science and Technology* 35 (2): 115–192.

66 Fu, R., Wen, D., Xia, X. et al. (2017). Electrokinetic remediation of chromium (Cr)-contaminated soil with citric acid (CA) and polyaspartic acid (PASP) as electrolytes. *Chemical Engineering Journal* 316: 601–608.

67 Kim, G.N., Jung, Y.H., Lee, J.J. et al. (2008). Development of electrokinetic-flushing technology for the remediation of contaminated soil around nuclear facilities. *Journal of Industrial and Engineering Chemistry* 14 (6): 732–738.

68 Ryu, S.R., Jeon, E.K., and Baek, K. (2017). A combination of reducing and chelating agents for electrolyte conditioning in electrokinetic remediation of

UNCORRECTED PROOFS

Trim Size: 170mm x 244mm Single Column Loose Ribeiro670117 c24.tex V1 - 12/11/2020 11:32pm Page 625

As-contaminated soil. *Journal of the Taiwan Institute of Chemical Engineers* 70: 252–259.

69 Li, D., Ji, G., Hu, J. et al. (2018). Remediation strategy and electrochemistry flushing & reduction technology for real Cr(VI)-contaminated soils. *Chemical Engineering Journal* 334: 1281–1288.

70 Ng, Y.S., Sen Gupta, B., and Hashim, M.A. (2015). Effects of operating parameters on the performance of washing-electrokinetic two stage process as soil remediation method for lead removal. *Separation and Purification Technology* 156: 403–413.

71 Kim, G.N., Yang, B.I.L., Choi, W.K., and Lee, K.W. (2009). Development of vertical electrokinetic-flushing decontamination technology to remove ^{60}Co and ^{137}Cs from a Korean nuclear facility site. *Separation and Purification Technology* 68 (2): 222–226.

72 Kim, G.N., Jung, Y.H., Lee, J.J. et al. (2008). An analysis of a flushing effect on the electrokinetic-flushing removal of cobalt and cesium from a soil around the decommissioning site. *Separation and Purification Technology* 63 (1): 116–121.

73 Gu, Y., Yeung, A.T., and Li, H. (2018). Enhanced electrokinetic remediation of cadmium-contaminated natural clay using organophosphonates in comparison with EDTA. *Chinese Journal of Chemical Engineering* 26 (5): 1152–1159.

74 Cai, Z.P., Van Doren, J., Fang, Z.Q., and Li, W.S. (2015). Improvement in electrokinetic remediation of Pb-contaminated soil near lead acid battery factory. *Transactions of the Nonferrous Metals Society of China* 25 (9): 3088–3095.

75 Chang, J.H., Dong, C.D., Huang, S.H., and Shen, S.Y. (2020). The study on lead desorption from the real-field contaminated soil by circulation-enhanced electrokinetics (CEEK) with EDTA. *Journal of Hazardous Materials* 383: 121194.

76 Zhang, J., Xu, Y., Li, W. et al. (2012). Enhanced remediation of Cr (VI) -contaminated soil by incorporating a calcined-hydrotal-based permeable reactive barrier with electrokinetics. *Journal of Hazardous Materials* 239-240: 128–134.

77 Giannis, A. and Gidarakos, E. (2005). Washing enhanced electrokinetic remediation for cadmium removal from real contaminated soil. *Journal of Hazardous Materials* 123 (1–3): 165–175.

78 Song, Y., Cang, L., Zuo, Y. et al. (2020). EDTA-enhanced electrokinetic remediation of aged electroplating contaminated soil assisted by combining dual cation-exchange membranes and circulation methods. *Chemosphere* 243: 125439.

79 Li, J., Ding, Y., Wang, K. et al. (2020). Comparison of humic and fulvic acid on remediation of arsenic contaminated soil by electrokinetic technology. *Chemosphere* 241: 125038.

80 Giannis, A., Gidarakos, E., and Skouta, A. (2007). Application of sodium dodecyl sulfate and humic acid as surfactants on electrokinetic remediation of cadmium-contaminated soil. *Desalination* 211 (1–3): 249–260.

81 Ng, Y.S., Sen Gupta, B., and Hashim, M.A. (2014). Performance evaluation of two-stage electrokinetic washing as soil remediation method for lead removal using different wash solutions. *Acta Electrochimica* 147: 9–18.

UNCORRECTED PROOFS

Trim Size: 170mm x 244mm Single Column Loose Ribeiro670117 c24.tex V1 - 12/11/2020 11:32pm Page 626

82 Maturi, K. and Reddy, K.R. (2006). Simultaneous removal of organic compounds and heavy metals from soils by electrokinetic remediation with a modified cyclodextrin. *Chemosphere* 63 (6): 1022–1031.

83 Al-Hamdan, A.Z. and Reddy, K.R. (2008). Transient behavior of heavy metals in soils during electrokinetic remediation. *Chemosphere* 71 (5): 860–8671.

84 Xia, W., Gao, H., Wang, X. et al. (2009). Application of EDTA decontamination on soils affected by mining activities and impacts of treatment on the geochemical partition of metal contaminants. *Journal of Hazardous Materials* 164 (2–3): 936–940.

85 Udovic, M. and Lestan, D. (2012). EDTA and HCl leaching of calcareous and acidic soils polluted with potentially toxic metals: remediation efficiency and soil impact. *Chemosphere* 88 (6): 718–724.

86 Kim, C., Lee, Y., and Ong, S.K. (2003). Factors affecting EDTA extraction of lead from lead-contaminated soils. *Chemosphere* 51 (9): 845–853.

87 Ait Ahmed, O., Derriche, Z., Kameche, M. et al. (2016). Electro-remediation of lead contaminated kaolinite: an electrokinetic treatment. *Chemical Engineering and Processing - Process Intensification* 100: 37–48.

88 Cockrell, G.M., Zhang, G., VanDerveer, D.G. et al. (2008). Enhanced metal ion selectivity of 2,9-di- (pyrid-2-yl) -1,10-phenanthroline and its use as a fluorescent sensor for cadmium (II). *Journal of the American Chemical Society* 130 (4): 1420–1430.

89 Matović, Z.D., Jeremić, M.S., Jelić, R.M. et al. (2013). Configurational, LFDFT and NBO analysis of chromium (III) complexes of edta-type ligands. *Polyhedron* 55: 131–143.

90 Edta, R.C.W., James, D.B., and Spedding, F.H. (1961). Cation-exchange elution sequences - I. *Journal of Inorganic and Nuclear Chemistry* 19 (1): 133–1341.

91 Vargas, C., Pérez-Esteban, J., Escolástico, C. et al. (2016). Phytoremediation of Cu and Zn by vetiver grass in mine soils amended with humic acids. *Environmental Science and Pollution Research* 23 (13): 13521–13530.

92 Duan, W.H., Wang, Q., and Collins, F. (2011). Dispersion of carbon nanotubes with SDS surfactants: a study from a binding energy perspective. *Chemical Science* 2 (7): 1407–1413.

93 Karim, M.A. and Khan, L.I. (2012). Enhancement of electrokinetic decontamination with EDTA. *Environmental Technology* (United Kingdom) 33 (20): 2291–2298.

94 Chen, F., Li, X., Ma, J. et al. (2019). Remediation of soil co-contaminated with decabromodiphenyl ether (BDE-209) and copper by enhanced electrokinetics-persulfate process. *Journal of Hazardous Materials* 369: 448–455.

95 Reddy, K.R., Cameselle, C., and Ala, P. (2010). Integrated electrokinetic-soil flushing to remove mixed organic and metal contaminants. *Journal of Applied Electrochemistry* 40 (6): 1269–1279.

96 Zhou, D.M., Deng, C.F., Cang, L., and Alshawabkeh, A.N. (2005). Electrokinetic remediation of a Cu-Zn contaminated red soil by controlling the voltage and conditioning catholyte pH. *Chemosphere* 61 (4): 519–527.

UNCORRECTED PROOFS

Trim Size: 170mm x 244mm Single Column Loose Ribeiro670117 c24.tex V1 - 12/11/2020 11:32pm Page 627

97 Lee, H.H. and Yang, J.W. (2000). A new method for control of electrolytes pH by circulation system in electrokinetic soil remediation. *Journal of Hazardous Materials* 77 (1–3): 227–240.

98 Sung, M., Teng, C.H., and Yang, T.H. (2017). Dissolution enhancement and mathematical modeling of removal of residual trichlorethene in sands by ozonation during flushing with micro-nano-bubble solution. *Journal of Contaminant Hydrology* 202: 1–10.

99 Palma, L., Ferrantelli, P., and Medici, F. (2005). Heavy metals extraction from contaminated soil: recovery of the flushing solution. *Journal of Environmental Management* 77 (3): 205–211.

100 Palma, L., Ferrantelli, P., Merli, C., and Biancifiori, F. (2003). Recovery of EDTA and metal precipitation from soil flushing solutions. *Journal of Hazardous Materials* 103 (1–2): 153–168.

101 Al-Hamdan, A.Z. and Reddy, K.R. (2008). Geochemical assessment of metal transport in glacial till during electrokinetic remediation. *Environmental Monitoring and Assessment* 139 (1–3): 137–149.

102 Choo, H., Song, J., Lee, W., and Lee, C. (2016). Effects of clay fraction and pore water conductivity on the electrical conductivity of sand-kaolinite mixed soils. *Journal of Petroleum Science and Engineering* 147: 735–745.

103 Yuan, S., Tian, M., and Lu, X. (2006). Electrokinetic movement of hexachlorobenzene in clayed soils enhanced by tween 80 and β-cyclodextrin. *Journal of Hazardous Materials* 137 (2): 1218–1225.

104 Ammami, M.T., Portet-Koltalo, F., Benamar, A. et al. (2015). Application of biosurfactants and periodic voltage gradients for enhanced electrokinetic remediation of metals and PAHs in dredged marine sediments. *Chemosphere* 125: 1–8.

105 Kim, W.S., Park, G.Y., Kim, D.H. et al. (2012). In situ field scale electrokinetic remediation of multi-metals contaminated paddy soil: influence of electrode configuration. *Electrochimica Acta* 86: 89–95.

106 Xiao, J., Zhou, S., Chu, L. et al. (2020). Electrokinetic remediation of uranium (VI)-contaminated red soil using composite electrolyte of citric acid and ferric chloride. *Environmental Science and Pollution Research* 27 (4): 4478–4488.

107 Sinn, C.G., Dimova, R., and Antonietti, M. (2004). Isothermal titration calorimetry of the polyelectrolyte/water interaction and binding of Ca^{2+}: effects determining the quality of polymeric scale inhibitors. *Macromolecules* 37 (9): 3444–3450.

108 Chung, H.I. and Lee, M.H. (2007). A new method for remedial treatment of contaminated clayey soils by electrokinetics coupled with permeable reactive barriers. *Acta Electrochimica* 52: 3427–3431.

109 Cappai, G., De Gioannis, G., Muntoni, A. et al. (2012). Combined use of a transformed red mud reactive barrier and electrokinetics for remediation of Cr/As contaminated soil. *Chemosphere* 86 (4): 400–408.

UNCORRECTED PROOFS

Trim Size: 170mm x 244mm Single Column Loose Ribeiro670117 c24.tex V1 - 12/11/2020 11:32pm Page 628

UNCORRECTED PROOFS

Trim Size: 170mm x 244mm Single Column Loose Ribeiro670117 c25.tex V1 - 12/11/2020 7:25pm Page 629

25

Recent Progress on Pressure-Driven Electro-Dewatering (PED) of Contaminated Sludge

Bimastyaji Surya Ramadan, Amelinda Dhiya Farhah, Mochtar Hadiwidodo, and Mochamad Arief Budihardjo

Department of Environmental Engineering, Faculty of Engineering, Universitas Diponegoro, Semarang, 50275, Indonesia

25.1 Introduction

In a sludge treatment process, sludge drying is a crucial stage that needs correct practical consideration [1]. This stage is the critical point of sludge treatment since the dried sludge will be burned for further processing or sent to hazardous treatment facilities. Therefore, effective drying is a must for efficient operational costs and energy consumption [2]. Conventionally, sludge drying can be done using freeze-thaw, centrifugal force, filter-press, or direct drying under the sun [3]. This process is not easy to handle because sludge has fine, colloidal-like, and gel-like particles [1, 4]. To overcome the limitations in the conventional sludge drying process, technologies such as water mineralization in sludge and peroxidation make it possible to reduce the excess water content [5]. Thus, sludge-dewatering processes, such as mechanical pressure systems [1, 6–8] and filtration [9–11], are commonly used in practical applications. However, when the sludge is saturated after pressure, its colloidal and compressive nature inhibits and slows the drying process [12].

An electro-dewatering (EDW) system is a cost-effective method compared to other conventional sludge treatments [3]. EDW is a technology that utilizes an electric field between the anode and cathode to increase the mobilization of charged ions (electro-migration) or particles (electrophoresis), as well as to mobilize water from the anode to the cathode by electroosmosis [10]. Given the difference in surface charge between particles, applying an electrochemical system can decontaminate and oxidize metal ions and organic matter [13]. EDW can keep the metals ion in the cathode side and increase the dewatering rate [14]. EDW systems have been widely used, especially for handling contaminated fine solid particles [15]. Examples include using EDW with mine tailings [16, 17], food waste [18], sewage sludge [19], river sediment, and other industries [20] where conventional methods are less successful [1]. The EDW system can be used as a post-treatment after conventional pressure-filtration [21], in a combined treatment, or as a single treatment system [22]. Before EDW, using

Electrokinetic Remediation for Environmental Security and Sustainability, First Edition.
Edited by Alexandra B. Ribeiro and M.N.V. Prasad.
© 2021 John Wiley & Sons Ltd. Published 2021 by John Wiley & Sons Ltd.

UNCORRECTED PROOFS

Trim Size: 170mm x 244mm Single Column Loose Ribeiro670117 c25.tex V1 - 12/11/2020 7:25pm Page 630

mechanical pressure systems can increase water reduction and save energy in dewatering systems [5].

Therefore, in this chapter, we provide a systematic review of recent progress on pressure-driven electro-dewatering (PED) systems. This technology is expected to increase the final solid dried concentration and speed up the drying process with lower energy consumption [23]. Sludge drying is done by applying low electric fields through a sludge cake (EDW) that was previously treated mechanically (filter-press), to increase the removal of pollutants in sludge and wastewater. We provide a solid dry concentration in various industrial sludge treatments using EDW and mechanical treatment systems. A potential alternative plan (pressure-driven EDW/PED) is discussed to improve sludge dewatering at the commercial/industrial scale.

25.2 Electro-Dewatering for Sludge Treatment

25.2.1 Conventional Sludge Treatment Systems

Sludge is a significant byproduct of wastewater treatment, and treating it is a complex environmental problem [24]. Sludge production is increasing due to firmer regulations for industry effluent discharge during wastewater treatment. Sludge waste typically contains metals, organic compounds, macronutrients, micronutrients, organic micropollutants, microorganisms, and parasitic organisms [20]. Thus, sludge from municipal wastewater treatment creates many environmental problems [25]. In recent years, increasingly stringent standards and guidelines have been put in place to better protect public health, leading to greater attention being paid to the sludge treatment process [26]. Most sludge produced from wastewater by physical and biological and secondary or primary treatment processes must be treated and disposed of properly – the more wastewater is treated, the more sludge is produced [27]. A well-designed, efficiently operated sludge treatment and disposal system is crucial for the overall success of the wastewater treatment effort [28].

Sludge management is a term used to describe planning, designing, and operating facilities to reuse or dispose of wastewater treatment residues. Sludge contains large amounts of water, biomass, and extracellular polymeric substances, which have weak water resistance. The sludge needs to be managed for storage and disposal to prevent polluting the environment. However, high handling costs for treatment require around 50% of the operating budget for wastewater treatment plants [24]. Other considerations include minimizing environmental impacts and meeting disposal requirements set by local regulations [29]. The choice of approach depends on an economic evaluation as well as local conditions. In cases where biological stabilization is not used, the dried solid undergoes thermal decomposition in either a furnace or incinerator [30].

25.2.2 Overview of Electro-Dewatering Systems

EDW is an alternative method for reducing water content in sludge by applying an electric field [6] between the anode and cathode to drive mobilization of charged

UNCORRECTED PROOFS

Trim Size: 170mm x 244mm Single Column Loose Ribeiro670117 c25.tex V1 - 12/11/2020 7:25pm Page 631

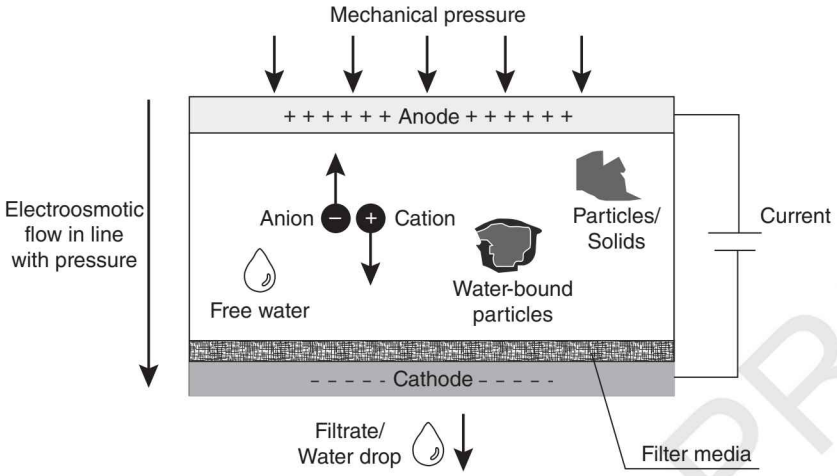

Figure 25.1 Schematic representation of the mechanism in a pressure driven electro-dewatering (PED) system. Source: Mahmoud et al. [21].

ions (electromigration) or particles (electrophoresis) and to move water molecules in porous media through the space between solid particles (pore) from the anode to the cathode side [31]. In the electrokinetic process, water movement is also known as the *electroosmotic process*; this process pushes water out of the system [32]. Commonly, sludge dewatering is done with various treatments including centrifugation [33], compression [34], filtration [21], and combustion [28], which require advanced equipment with relatively high maintenance costs, low treatment efficiency, and limited capacity [35]. The EDW method can increase the effectiveness of those treatments since the final solid concentration of the sludge is increased significantly to more than 35 wt% dry solid produced from conventional dewatering treatments [21]. EDW has advantages in terms of high efficiency, low energy consumption, low operational cost, and avoiding clogged filters caused by pressurized treatment [5, 10, 26]. A schematic representation of the EDW system is shown in Figure 25.1.

Applying an electric field produces electrochemical reactions that affect the performance of the EDW process. Possible reactions at the cathode and anode can be seen in Eqs. (25.1 and 25.2) [12].

On the cathode:

$$2H_2O + 2e^- \rightarrow H_{2\uparrow} + 2OH^- \tag{25.1}$$

$[H^+]$ reduced; pH increased

On the anode:

$$2H_2O \rightarrow 4H^+ + O_{2\uparrow} + 4e^- \tag{25.2}$$

$[H^+]$ increased; pH reduced

According to Werther and Ogada [24], the combined system of electro and mechanical dewatering (MDW) includes several stages. First, the MDW process

UNCORRECTED PROOFS

Trim Size: 170mm x 244mm Single Column Loose Ribeiro670117 c25.tex V1 - 12/11/2020 7:25pm Page 632

reduces the volume of pores and squeezes water out of the sludge. Then, charged particles move freely in fluid suspension and migrate to electrodes carrying opposite charges. When the sludge cake has formed, the particles are locked in position and cannot move. Ion-containing water is transported through viscous and molecular interactions and as a hydration casing. Electrochemical reactions on the electrodes form a charge balance that allows EDW to occur beyond the transient stage. Finally, water is no longer a continuous phase in the sludge cakes, and electrical resistance increases, causing ohmic heating [36]. The resulting reduction in liquid viscosity makes it easy to remove the remaining water [24].

After direct electric current is applied in the system, electrolysis of water in the anode and cathode sections induces the mobilization of charged ions (electromigration) or colloidal-charged particles (electrophoresis), and mobilization of water molecules (electroosmosis) [37]. *Electromigration* is a process of migrating metal ions, which produces more current in the conductor in the open circuit and can be overcome by obeying the current density limit [35]. Electromigration can be used to determine the phenomenon of ion migration through the diffusion coefficient in a specimen. Based on Lv et al. (2020), electromigration is the transfer of a charged ion in a solution [14]. *Electroosmosis* is a method for controlling water availability by utilizing a direct electric current (DC). Two electrodes are mounted on the sludge, and electricity flows; the water in the sludge moves from the positive electrode to the negative electrode [38]. The higher the voltage used, the more water is carried along with the flow of electricity [21]. According to Harris et al. (2018), electroosmosis consists of a mobile solution containing mobile ions relative to a stationary charged surface [39]. According to Shi et al. (2008), *electrophoresis* is a method of separating compounds that have a charge in the form of cations or anions by utilizing an electric field generated from electrodes with an electric source derived from DC or alternating electric current (AC). The movement rate of a molecule depends on the ratio of mass to charge and the molecular shape [40]. According to Yeung and Gu (2011), electrophoresis is the opposite of electroosmosis, where charged particles move relative to stationary fluids [41].

25.2.3 Fundamental Equations of EDW Systems

The effectiveness of EDW systems in laboratory and field-scale applications can be predicted using the Helmholtz-Smoluchowski (H-S) theory [42]. The rate of electroosmosis of water molecules in fine material can be described through Eq. (25.3)

$$Q_e = k_e i_e A \tag{25.3}$$

where Q_e represents the rate of electroosmosis ($m^3\ s^{-1}$), k_e is the coefficient of permeability of electroosmosis ($m^2\ Vs^{-1}$) whose magnitude is influenced by pore size, i_e is the potential gradient ($V\ m^{-1}$, the difference between the voltage V and the distance L, $\frac{\Delta V}{\Delta L}$), and A is the cross-sectional area (m^2). Equation (25.3) is similar to Darcy's equation, where the k_h notation replaces k_e. Electroosmotic permeability is inversely proportional to processing time [43]. In addition, over time, the rate of electroosmosis decreases due to the electrochemical reaction occurring at the anode, increasing

UNCORRECTED PROOFS

Trim Size: 170mm x 244mm Single Column Loose Ribeiro670117 c25.tex V1 - 12/11/2020 7:25pm Page 633

the sludge resistance [44]. This condition shows that electroosmotic permeability cannot be considered constant throughout processing.

In developing the EDW system model, several things are assumed [11, 45]: (i) sludge is considered homogeneous and saturated, (ii) there is no movement of charged colloids/particles due to electrophoresis, (iii) water molecules move in a one-dimensional direction, (iv) no other electrochemical reactions occur during the electroosmosis process, (v) electroosmosis permeability is considered constant over time [46], and (vi) Darcy and ohmic law are used in the dewatering cycle. Through these assumptions, two calculations can be produced by assuming EDW under constant voltage and current conditions. At a constant voltage (current varies, $V = \frac{I}{R}$ and $V = \frac{Q}{C}$, where R is the resistance, Q is the electric charge, and C is the electric capacity), the model formed from these assumptions can be seen in Eq. (25.4):

$$Vol(t) = \frac{k_e A V_0}{L}\left(1 - e^{\frac{-t}{R_D C}}\right) \tag{25.4}$$

where the permeability coefficient (k_e) is considered constant, $Vol(t)$ is the accumulated volume of water ($m^3\ s^{-1}$) that migrates at a particular operational time (t), $V_0$is the constant voltage (V) given, L is the distance between the electrodes (m), and R_D is a constant resistance (ohm/Ω). Under these conditions, H-S theory cannot explain the rate of electroosmosis. Under constant current, the model that describes the electroosmosis rate is shown in Eqs. (25.5 and 25.3).

$$Vol(t) = \frac{k_e A I R_0 t}{L} \tag{25.5}$$

During the application of constant current, the internal voltage gradient generated by the power supply is considered to be proportional to the voltage acting on the system. Equation (25.5) also shows that the electric field strength is always constant during dewatering using a constant current so that the rate of electroosmosis can be constant as the voltage increases.

Wu et al. (2020) also constructed models for the design and operation of EDW, where several parameters including volatile solids (VS,%), pH, electrical conductivity (EC, $mS\,cm^{-1}$), and zeta potential (ζ, mV) significantly affect the amount of dry solid produced (DS_f) and the electrical power requirements of the EDW process (P_E):

$$DS_f = 0.879 - 0.71VS - 0.011pH - 0.028EC + 0.002\zeta \tag{25.6}$$

$$P_E = -0.01 - 0.08VS - 0.004pH - 0.039EC + 0.003\zeta \tag{25.7}$$

However, this model cannot accurately predict electricity demand and dry solid concentration due to differences in reactor construction, dewatering time, and type of sludge used. The model might be suitable for predicting the final solid concentration and power required for the same vital parameters [47].

Several other factors, such as thickness, required current, voltage, pressure, and type of electrodes, must be determined in the EDW design. The thickness of the sludge significantly influence the drying process. After EDW is applied to the sludge, the dry solids concentration can be calculated using Eq. (25.8) (assuming a constant

UNCORRECTED PROOFS

Trim Size: 170mm x 244mm Single Column Loose Ribeiro670117 c25.tex V1 - 12/11/2020 7:25pm Page 634

current), and the processing time is calculated using Eq. (25.9)

$$DS_2 = \frac{DS_1}{1 - \frac{k_e I R_o t}{\rho_s L^2}} \tag{25.8}$$

$$t = \left(\frac{(DS_2 - DS_1)}{DS_2}\right) \frac{\rho_s L^2}{k_e R_o I} \tag{25.9}$$

where DS_2 is the final solid concentration after EDW is applied, DS_1 is the initial solid concentration, and ρ_s is the sludge mass density. From Eq. (25.8), it can be understood that the final solid concentration is a function of the sludge's thickness and a constant current. However, when the current is not constant, Eq. (25.8) is no longer valid. The rate of electroosmosis at a constant current can be understood through Eqs. (25.10 and 25.11).

$$R_o = \rho \frac{L}{A} \tag{25.10}$$

$$Q_e = k_e i_e \rho = k_e i_e A R_o \tag{25.11}$$

where ρ is the resistivity (Ωm) of the sludge through this equation, and changes in reactor dimensions, including height (h) and cross-sectional area (A) at the same volume, only affect the initial resistance (ρ). The equation models [10, 11] also show that when designing EDW under constant current, the reactor's dimensions do not affect the electroosmotic rate. Under constant voltage, the electroosmotic flow may change depending on the reactor dimension even at the same volume, as seen in Eq. (25.3) [11, 45].

Current has a significant effect on reducing the water content in sludge. The higher the current, the greater the charge given to the system. This condition speeds up the charge's movement. The movement of the charge attracts water and other charges. The pattern of relationships between currents and final solid concentration after a series of EDW treatments can be derived from Eq. (25.8). At a constant voltage of $1\,\mathrm{V\,cm^{-1}}$, the current must not be less than $\mathrm{R_0} \times 1\,\mathrm{V\,cm^{-1}}$:

$$I = \left(\frac{(DS_2 - DS_1)}{DS_2}\right) \frac{k_e R_o t}{\rho_s L^2} \tag{25.12}$$

Under a constant current, the rate of electroosmosis forms a linear curve illustrating when the sludge resistance becomes very large. Sludge resistance causes the current to slow, and the rate of electroosmosis decreases to form a sloping curve. Figure 25.2 illustrates the relationship of critical time (t_b) and its relation to the rate of electroosmosis under constant voltage and current. Equation (25.8) applies only as long as the relationship between the rate of electroosmosis and time forms a linear curve. Therefore, the processing time, as shown in Eq. (25.5), must be less than the critical processing time using EDW. Several things must be determined to enhance EDW related to Eqs. (25.8–25.12):

a) Optimal power supply voltage output [1]
b) Pressure as a pretreatment/combined treatment with EDW [2, 4]
c) Type of electrodes that have a low conductivity/electrochemical reaction rate [48]

UNCORRECTED PROOFS

UNCORRECTED PROOFS

Trim Size: 170mm x 244mm Single Column Loose

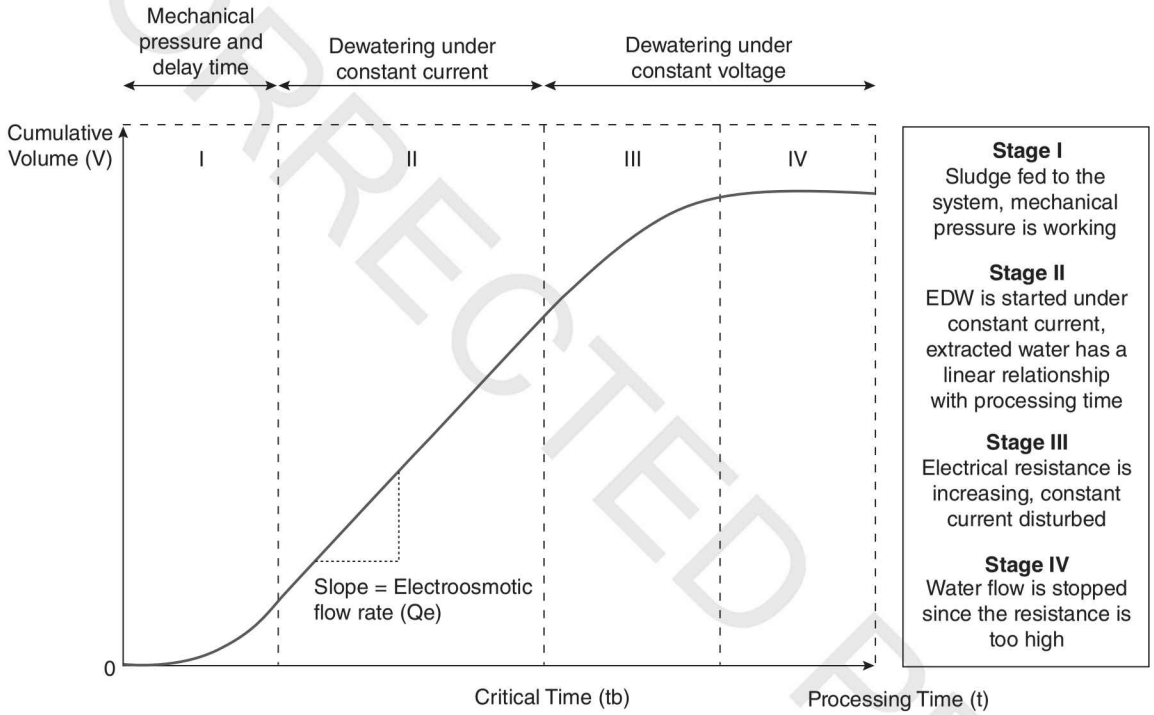

Figure 25.2 Typical relationship between cumulative volume and processing time under the applied electric field. Source: Glendinning et al. [11].

Ribeiro670117 c25.tex V1 - 12/11/2020 7:25pm Page 635

Trim Size: 170mm x 244mm Single Column Loose Ribeiro670117 c25.tex V1 - 12/11/2020 7:25pm Page 636

Figure 25.1 shows the presence of water-bound particles and free water in the PED system. The number of water-bound particles can be calculated using the following standard differential scanning calorimetry (DSC) approach

$$W_B = W_T - \frac{\Delta H}{\Delta H_0} \tag{25.13}$$

where W_B is the water-bound particle fraction (kg kg^{-1}), W_T is the total water content fraction in the mud sample (kg kg^{-1}), ΔH is the amount of energy absorbed in the sampled, and ΔH_0 is the standard energy (334.7 J g^{-1}) for ice to melt [49].

Mahmoud et al. (2016) proposed a tool to evaluate the economic feasibility (K_{si}) of EDW under specific power inputs (P, kWh), final dry solids mass (m_{DS}, kg), and processing time (t, hours), in the form of Eq. (25.14). This is a simple quantitative criterion used to determine optimal technology choices based on economic feasibility. If the K_{si} value of an EDW alternative is less than the value for others approaches, then the alternative is more acceptable and deserves to be applied.

$$Ksi_{EDW} = f(P, t, m_{DS}) = \left(\frac{P}{m_{DS}}\right).\left(\frac{t}{m_{DS}}\right) = E_{DW}.\theta \tag{25.14}$$

where E_{DW} is the electricity requirement per unit of kg dry solids (kWh kg$^{-1}{}_{\mathrm{DS}}$), and θ is the unit of processing time per kg of dry solids successfully treated (hours/kg$_{DS}$) [21].

Dizon and Orazem (2019) also developed an alternative model that can estimate economic feasibility (capital and operational costs) for scaling up a continuous EDW–belt press system under constant voltage for dewatering phosphatic clay. The model uses the relationship between energy consumption(P_E), voltage used (v), dry solid concentration (DS), length of the gap between the feed (d_1) and collection sides (d_2), wet-sludge production rate (m), and sludge density (ρ). The energy consumption is calculated using Eq. (25.15). Then, the operational cost can be generated from the electrical cost (c_{el}) times the energy consumption (Eq. (25.16)). The capital cost (c_{cap}) is dependent on the annualized capital cost (c_{annual}), the electrode width (W) and length (L), and the dry solid concentration generated from the EDW system times the wet-sludge production rate. Equation (25.17) explains the relationship of those parameters (with modification of symbols) [50]:

$$P_E = \frac{200{V_{max}}^2}{\rho w_c m(d_1 + d_2)} \tag{25.15}$$

$$c_{op} = c_{el} P_E \tag{25.16}$$

$$c_{cap} = c_{annual} \frac{100LW}{w_c m} \tag{25.17}$$

25.3 Design Considerations for PED Systems

Mechanical pressure as a pretreatment plays a significant role in improving EDW performance [6, 51]. Increasing the pressure (limited to 12 bar) can increase the percentage of water removed and the electrical contact between the electrode and the

UNCORRECTED PROOFS

Trim Size: 170mm x 244mm Single Column Loose Ribeiro670117 c25.tex V1 - 12/11/2020 7:25pm Page 637

solid fraction of sludge. Pressure above 12 bar is considered insignificant for removing water and consumes too much energy [21]. Mechanical pressure applied before EDW removes more free water, so this approach is recommended to optimize the process.

Mechanical pressure (0.1–2 bar) removes water quickly for the first 5 minutes, and as much as 30.3% of water content can be removed for 20 minutes. Therefore, the high pressure will eventually form a water clog. EDW can overcome this problem and eliminate 69% of water content in just seven to eight minutes. Different results may be produced at high pressures: at a pressure of 1 bar, 40% concentration of dry solids can be achieved in just five minutes. The concentration of dry solids from the initial sludge, which contains more water, may be slightly reduced after treatment by pressure or electrokinetics alone [34].

PED offers several advantages [48]:

- Pressure causes the sludge cakes to come into contact with the anode.
- Pressure causes water to flow faster to the filter media.
- The layer of gas on the surface of the sludge particles can be compressed maximally, reducing the sludge's resistance.

Therefore, when applying pressure together with EDW, some considerations have to be noted. When the pressure is greater than 5 bar, water removal becomes increasingly insignificant. At constant current, no applied pressure (0.5–12 bar) affects the water removal percentage. This may be the case because sludge resistance is strongly influenced by applied current, and at a constant voltage, the applied current varies depending on how much voltage is applied. At low pressure (below 0.5 bar), filter cloths and electrodes are quickly damaged. An increase in temperature on the anode side means the system needs to be stopped as soon as possible. These conditions indicate the importance of determining the minimum pressure limit to avoid loss of electrical contact between the electrode and treated sludge. The optimum range of pressure under constant voltage and current is relatively the same, around 4–6 bar. When mechanical pressure and EDW are applied simultaneously, a low electric field (20–30 V) at 2–6 bar pressure will impact the kinetics of sludge dewatering. However, with a high electric field (above 50 V), regardless of the pressure value, the final concentration of the dry solid produced does not change significantly [4, 21].

Before designing a PED system, the relationship between factors influencing the rate of electroosmosis must be known (see Figure 25.3) [45, 52]. Higher sludge conductivity, for instance, will increase the rate of electrons/protons passing through the sludge pores. Water removal efficiency will continue to increase, along with sludge conductivity [28]. Unfortunately, the greater the mineral content, the greater the chance of protons being trapped in the surface of the sludge particles, reducing the electroosmosis rate [16]. Similar to pore fluid conductivity, water removal efficiency increases with the increase in pore fluid conductivity because pore fluid can carry charged ions and particles outward. Energy consumption during EDW is less than during thermal drying. Energy consumption can also increase sharply due to greater resistance and the increase in voltage and current during treatment [53]. In line with Eqs. (25.3–23.5), electroosmosis is directly proportional to the voltage or

UNCORRECTED PROOFS

Trim Size: 170mm x 244mm Single Column Loose Ribeiro670117 c25.tex V1 - 12/11/2020 7:25pm Page 638

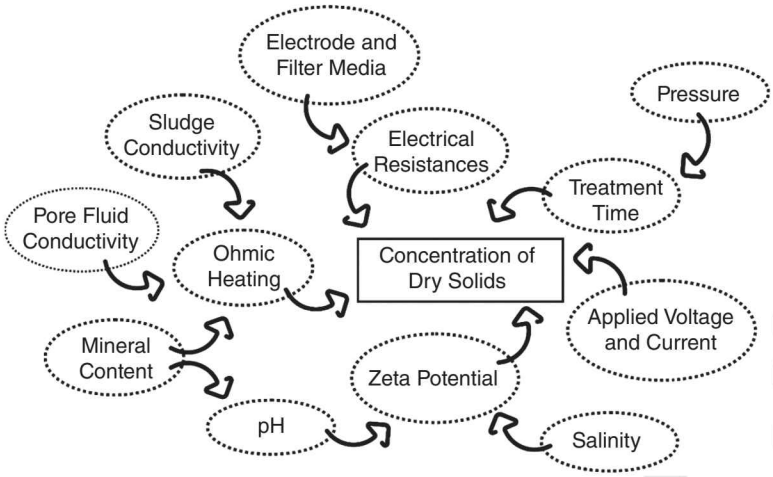

Figure 25.3 Relationship between factors affecting dry solids concentration.

current applied to the sludge. The following section discusses some enhancements to overcome the critical factors influencing PED.

25.3.1 Reducing Electrical Resistance in PED Systems

Electrical resistance is an essential factor when considering the maximum voltage that must be applied to the PED under constant voltage [54]. As the peak of the linear electroosmosis curve is reached, the current increases and is accompanied by an increase in voltage so that more energy is consumed, and eventually the PED system can no longer operate sufficiently [55]. In addition, applying pressure as a pretreatment before using the PED system is very important. Although pressure does not directly affect Eq. (25.3 or 25.4), applying pressure can reduce the concentration of air voids in the sludge sample. As a result, sludge resistance is reduced, and the efficiency of energy use increases in the PED system.

The relationship between electrical resistance and dry solid concentration in both types of PED has the same pattern. In the first stage, electrical resistance decreases with increasing dry solid concentration. This condition occurs below 9 wt% dry solid. Then, in the range of 22–44 wt% dry solid, electrical resistance increases slightly along with an increase in dry solid concentration due to an increase in the layer of unsaturated sludge. These conditions reduce the rate of electroosmosis, thereby reducing the concentration of dry solids formed. The electrical resistance becomes so large that electroosmosis does not occur at a dry solid concentration of more than 44%, and the PED process stops [54]. Electrical resistance increases significantly when the concentration of solids exceeds 44–45 wt% dry solid.

Placing electrodes against filter cloth is also important because the electrodes being in direct contact with the filter can increase energy consumption [56]. Using nonconductive materials in the filter cloth reduces electrical resistance and thus reduces the energy consumption of the entire process. The ease of cleaning

UNCORRECTED PROOFS

Trim Size: 170mm x 244mm Single Column Loose Ribeiro670117 c25.tex V1 - 12/11/2020 7:25pm Page 639

dewatered sludge from the filter cloth is also a significant consideration when choosing a good filter cloth.

Electrical resistance at the top of the sludge cake is greater than at the bottom. This condition happens because gas bubbles generated by the electrolysis reaction reduce the contact between the anode and the sludge cake, which increases electrical resistance [52]. Electromigration also has a tremendous impact because cations on the sludge's surface migrate to the cathode. H^+ ions generated at the anode move to the pore liquid, interact with anionic compounds on the surface of the solids, and form a nonionic chemical system classified as a bad electrical conductor [57]. The dryness that occurs in the top layer of sludge cake can increase electrical resistance sludge. When the solids concentration is below 20%, sludge resistance is affected by solids loading. Above 20%, resistance is affected by the dryness of the sludge cake. In a constant-voltage system, resistance does not change even if the voltage is increased from 30 to 50 V. However, the higher the current applied (from 200 to 400 mA), the smaller the resistance in the constant-current system. But when the dry solid content exceeds 44–45%, the increase in resistance is due not only to current but also to the type of filter used. The thickness of the sludge layer affects electrical resistance, where the thicker the sludge cakes, the higher the electric resistance [57]. Adding copper ions to the electrolyte was able to reduce electroosmosis. Conversely, adding sodium ions can increase the volume of removed water. This occurs because copper ions precipitate at the cathode, increasing electrical resistance in the area near the cathode [58].

Ohmic heating also needs to be considered in the PED system because it changes the viscosity and moisture content in the sludge cake. Ohmic heating heats the sludge and pushes moisture out of the sludge capillary, reducing the sludge resistance. Ohmic heating can also damage supporting equipment such as filter media, electrodes, and other equipment while disrupting the PED process. When the temperature increases sharply (more than 60 °C), the PED operator must stop the system immediately. Ohmic heating can be controlled by choosing the right washing solution and system and applying appropriate processing times, delay times, and electric fields (constant current or voltage) [12, 57, 59].

25.3.2 Maintaining Optimum pH and Salinity

The electric current applied to the sludge produces protons (H^+) at the anode and hydroxyl ion (OH^-) at the cathode. The proton velocity, which is faster than that of hydroxyl ions, causes the sludge to become acidic, affecting the zeta potential, which gradually becomes positive and reduces the rate of electroosmosis. A drastic decrease in pH also increases the ionic strength in the pore fluid, reducing the rate of electroosmosis [54]. A low pH value at the anode causes dryness, while the cathode (with a high pH value) is flooded by the electroosmotic effect. The rate of electroosmosis (v_e) in porous media is strongly dependent on the electrical potential (V), zeta potential (ξ), dielectric constant (D), viscosity (η), porosity (n), and length of the particle flow in the porous media (x). Therefore, the model that describes this relationship is shown in Eq. (25.18) as a derivative equation from Darcy's law [60]. Equation (25.18)

UNCORRECTED PROOFS

Trim Size: 170mm x 244mm Single Column Loose Ribeiro670117 c25.tex V1 - 12/11/2020 7:25pm Page 640

shows that the pH affects the zeta potential, affecting the electroosmotic flow. The higher the initial pH of solid media, the greater the electroosmotic rate. A higher initial soil pH will change the electric potential across solid media. When working with an initial lower pH, electrical resistance is higher, and conductivity is lower. This condition results in a higher voltage gradient at the end of treatment [58].

$$v_e = -\frac{\xi D}{\eta} n \frac{\partial V}{\partial x} \tag{25.18}$$

Salt increases the pH gradient and volume of ion transfer from the anode to the cathode. Adding a salt such as Na_2SO_4 or NaCl to the PED system under constant current may reduce the zeta potential of the sludge since salt compresses and changes the electrical double layer of sludge particles. That phenomenon leads to greater electroosmotic flow and shortens processing time. Thus, energy consumption is reduced. The efficiency of water reduction in the PED process reached 42.5% with a total dose of Na_2SO_4 given at 12.5 g kg^{-1} dry solids at a constant pressure of 0.01 bar and voltage of 20 V. Adding salt causes a considerable pH gradient due to the electrolysis reaction near the anode or cathode. The higher the electric current, the more significant the difference in pH between the upper (anode) and lower (cathode) layers. The anode produces hydroxide ions, while the cathode produces protons, so the middle part becomes neutral. The zeta potential is directly proportional to the pH gradient because it correlates with ionic strength. Zeta potential is also affected by the salinity of the sludge [61]. Under alkaline conditions that form around the cathode chamber, a thin layer of precipitate covers the cathode and the filter media's surface. Therefore, hardness and high temperature accelerate the formation of precipitates in the space around the cathode [2].

The PED process is more effective in low-salinity sludge because the particles in the sludge reach isoelectric conditions so that energy consumption increases. Water transfer in the PED with the addition of salt causes an increase in water evaporation. Premature drying conditions limit the PED process. The part closest to the anode dries quickly and decreases in zeta potential due to the accumulation of H^+ ions in the anode. Adding CaO during the EDW process can increase pH from 6 to 12.2 and conductivity from 368 ± 16 μS cm^{-1} to 6285 ± 21 μS cm^{-1} as the level of CaO increases. Zeta potential decreases when the CaO dose is added from -15.3 ± 0.6 mV to -8.8 ± 0.4 mV. Adding Ca^{2+} ions of more than 5% increases the inhibitory effect on the electrokinetic system [54].

Adding salt also causes ohmic heating. The temperature of the process due to ohmic heating is almost 100 °C. The water content of the sludge can be removed better at a lower salinity gradient. This may be because the Na^+ ions move faster than K^+ ions, following the nature of electronegativity, thus enhancing the displacement of the upper and lower layers during the rapid dewatering stage (see Figure 25.2, stage II). PED can remove more than 80% of Na^+ ions, which is very useful in subsequent sludge treatment processes. The dissolved sodium ions in sludge decrease dramatically but increase slowly during the rapid dewatering process. The efficiency of removing Na^+ during dewatering reaches 85 wt% dry solid. Na^+ concentration decreased in the upper layer from 34.3 to 9.0 g kg^{-1} for the middle layer from 37.9

UNCORRECTED PROOFS

Trim Size: 170mm x 244mm Single Column Loose
Ribeiro670117 c25.tex V1 - 12/11/2020 7:25pm Page 641

to 13.5 g kg^{-1}. The filtrate that came out also contained only 15.2 g kg^{-1} Na^+ ions. Adding salt during the dewatering process can increase organic matter in the upper and middle layers by as much as 55%. This result shows that organic matter moves from the cathode to the anode through the electrophoresis phenomenon induced by the addition of salt [14].

25.3.3 Determining Sludge Characteristics and Properties

The type of sludge also plays a role in the maximum value of electrical resistance since each sludge has solid-water bonds with different strengths. Sludge, which has a higher concentration of dry solids, has less water-bonding activity and greater resistivity, thereby inhibiting water removal. Industrial sludge tends to contain abundant organic compounds and stronger water bonds than river sediment. Meanwhile, river sediment has more significant water content and fewer organic compounds [47]. Zhang et al. stated that when working on different sludge properties, several operating parameters, such as the temperature gradient and pH, are important because they can cause an increase in cathode fouling at a constant PED voltage. In belt-press modified PED with a rotating system, the cathode must be cleaned continuously to maintain its effectiveness [2].

The specific contaminant properties are also essential factors. Based on research conducted by Tuan and Sillanpää [62] regarding the effect of stress on macro-fractionation and trace metals using the EDW method, lead metal fractions tend to be stable (immobile, challenging to move) but very easily oxidized and can migrate given longer processing times. This more stable metal fraction is more likely to remain intact in the sludge only by filtering and pressuring treatment. Lead migration can also be affected by extending the processing time so that lead can migrate from the sludge. This phenomenon occurs because a large proportion of the positively charged ions tend to migrate to the negatively charged cathode. Thus, migration and a decrease in high inorganic ion concentrations must occur in the area near the positively charged anode [62]. According to Hwang and Min [63], the effect of loading and filtering by gravity on reducing metals is not significant. The reduction in concentrations of metals such as Zn, Mn, Pb, Cd, and Ni in sludge was observed after MDW and PED. Adding PED solved the existing sludge management problem because it achieved low metal concentrations, resulting in lower leachate amounts and reducing unwanted contamination [63]. Iron (Fe) concentration is lower in sludge in the upper (anode) layer and lower (cathode) layer of sludge. This phenomenon occurs because there is a large proportion of the migration of positively charged ions to the negatively charged cathode [62]. According to Hwang and Min (2003), the effect of loading and filtering by gravity on reducing metals is not significant [63].

25.3.4 Operating PED Under Constant Voltage or Current

Lv et al. (2020) explained that a higher electric current shortens the processing time at the slow dewatering stage (see Figure 25.2, stage I): starting current of 5, 10, and

UNCORRECTED PROOFS

Trim Size: 170mm x 244mm Single Column Loose Ribeiro670117 c25.tex V1 - 12/11/2020 7:25pm Page 642

15 V yields a processing time of 450, 300, and 120 seconds, respectively. An increase in electric current in the dewatering process increases Na^+ and K^+ ion displacement. The amount of Na^+ and K^+ ions varies in each sludge, but the results of the PED process show that Na^+ ions are successfully separated from sludge up to 84.65%, and K^+ ions reach only 44.82% with 15 V contact treatment. Solid layers begin to form after the first stage of dewatering. Difficulty in the next dewatering stage, solids increase more – an increase in electric current causes more dry solids concentration to form [14]. Although constant current can increase dewatering performance, this method can also cause high voltage, so it is hazardous when working on a larger scale [15]. When constant voltage is applied, cathode fouling becomes a significant problem in PED performance. This cathode fouling can be overcome by maintaining the cleanliness of the filter media [15]. Cathode fouling can occur due to the presence of calcium carbonate and magnesium hydroxide compounds, where calcium (Ca^{2+}) and magnesium (Mg^{2+}) ions precipitate on the surface of the cathode [2].

Voltage settings at the start of operation are also essential. When the pressure is determined in advance (e.g. 1 bar), the rate of electroosmosis and resulting change in water content are greater than the operating pressure in each stage (e.g. 0.1–1 bar). However, gradually increasing the voltage changes the pH and lowers the temperature. These conditions decrease the cathode chamber's alkalinity, thus reducing the potential for cathode fouling. The increase in temperature due to ohmic heating can also be reduced to achieve the efficient use of electricity during the PED process. However, in thin sludge cakes (±1 cm) and smaller processing units, those phenomena may not be significant, so energy consumption is also not greater than in other treatments [48, 59].

Using high voltage can cause excessive energy consumption. The most energy is used during the initial dewatering stage (see Figure 25.2, stage I). Using low voltage to concentrate dissolved ions in the first stage and using a higher voltage in the next two stages in the dewatering process is more efficient. At the beginning of the dewatering process, a 5 V voltage was used to move ions. Then PED was carried out at 15 V for 2700 seconds, and energy consumption decreased from 350.08 to 295.88 kWh, with total solids reaching 41.35 wt% dry solid. This result is far better than heat drying, which consumes 600 kWh per ton of sludge with a result of 80 wt% dry solids [14, 30].

25.3.5 Determining Appropriate Electrodes (Anodes and Cathodes)

Electrodes are conductors used to allow electrons to flow from an external wire to a nonmetallic part or medium of a circuit (e.g. semiconductor, electrolyte, or vacuum). Electrodes in electrochemical cells can be referred to as *anodes* or *cathodes*. The type of electrode also indirectly influences the PED system's efficiency because the electrochemical reaction is highly dependent on the type of electrode. Electrodes with a higher electrochemical reaction rate accelerate the critical time (see Figure 25.2, t_b) more than those with low electrochemical reaction rates [64].

Carbon electrodes are far more economical than copper because carbon has a lower reactivity value, increasing overall process efficiency [65]. Also, copper

UNCORRECTED PROOFS

Trim Size: 170mm x 244mm Single Column Loose Ribeiro670117 c25.tex V1 - 12/11/2020 7:25pm Page 643

undergoes corrosion during the process, so it is not recommended for commercial use. In addition, electrodes containing two or more metals have two or more active sites that act as electrochemical catalysts [64]. Very efficient stainless-steel electrodes are used to degrade sludge contaminants through economic and environmentally friendly electrochemical processes [66]. However, ceramic-coating electrode pretreatment may be necessary to prevent stainless-steel electrodes from faster corrosion [67]. Dimensionally stable anodes (DSA) are mixed metal oxide layers protected by a titanium matrix in flat plates or grid-like structures. This material is excellent as a filter medium because it can reduce electrical resistance and energy consumption [48]. Determining the correct electrode type and configuration is a must to increase the PED system's efficiency.

25.3.6 Reducing Energy Consumption

On a commercial scale, PED is always competing against other technologies in terms of energy consumption, processing time, and efficiency of production results [68]. Therefore, the factors that support these three things need to be known. The PED process consumed 92.3% of the total energy when combined with a belt-press filter. The second biggest energy consumer is the high-pressure system for filter cleaning since some of the filtrates are reused and mixed with water from other sources. Only half of the filtrate is permitted to be used again in filter cleaning because of the high alkalinity of the filtrate and the possibility that it still contains pollutants that may clog filters. Although energy consumption increased, the results of the study show that the energy consumption of PED operated under constant voltage can also decrease due to several factors including failure at the anode to reduce electrical conductivity, fouling at the cathode, and blockage (clogging) in the filter media. This reduction in energy consumption can reduce dewatering performance, thereby increasing sludge processing time [2].

PED was proven to shorten the drying time in lab-scale, pilot-scale, and full-scale applications. Energy consumed in the field-scale application (electrically enhanced belt-press filter dewatering) is 0.06 kWh kg^{-1} dry solids with a maximum system capacity of 4 m^3 h^{-1} or an increase of 1.5–2 m^3 h^{-1} compared to conventional systems [23]. Significant improvement of PED was also obtained by Zhang et al. (2017), where the energy needed by PED for drying biosolids at industrial scale was 0.123 kWh kg^{-1} dry solids with a maximum capacity of 10 t h^{-1} sludges (total area of 3.84 m^2, height of cake layer 0.55 m). Energy consumption during the dewatering process using a filter belt press/centrifuge is 0.009–0.073 kWh m^{-3}, thermal treatment is 3534 kWh $kg_{DS}{}^{-1}$ in dry conditions and 0.617–1.2 kWh $kg_{water}{}^{-1}$ in wet conditions, and EDW is 0.027–0.315 kWh $kg_{water}{}^{-1}$ for industrial sludge and river sediment [47].

The provision of delay time in applying the electric field in the dewatering system reduced energy consumption between 10 and 12% when working under constant voltage (50 V, 5 bar) and 30–46% under constant current (300 mA, 5 bar). Energy consumption to reach 40 wt% dry solid under constant voltage is 1.38 kWh kg^{-1} dry sludge and decreases to 0.017 kWh kg^{-1} dry sludge given a delay time of (5 bar of

UNCORRECTED PROOFS

Trim Size: 170mm x 244mm Single Column Loose Ribeiro670117 c25.tex V1 - 12/11/2020 7:25pm Page 644

pressure) 120 minutes. Under constant current conditions, this decrease may reach up to 0.53 kWh kg^{-1} dry sludge. Providing delay time may be a useful finding when implementing PED on an industrial scale. However, this delay time adds to the total sludge processing time required to reach the same dry solid concentration. Thus, determining the right time for PED applications is one of the critical points in PED operations because it can save energy and increase process efficiency [21]. A delay time of approximately 24 hours before applying EDW also shows success in handling non-stabilized biological sludge. Delay time or *aging*, in this study, demonstrates a significant increase in dewatering when the delay time is 24 hours. A decrease in organic compound concentration and increase in sludge conductivity resulted during the delay [25].

25.4 Future Perspectives

A summary of practical considerations for enhancing PED performance can be seen in Table 25.1. However, other alternatives to increase PED efficiency were found by another researcher using various innovative approaches. Using ultrasonic energy, for example, may increase the effectiveness of electroosmotic dewatering. Ultrasonic energy can help electroosmosis by increasing the contact between water and electrodes, helping moisture pass through the filter, removing water from the filter, and helping to compact the cake and provide electrical continuity through a continuous humidity path to the optimal humidity removal point [59]. The electric field allows for increased electroosmosis and electrophoresis, while acoustic force helps maintain electrical continuity through the material by clumping and condensing the cake and keeping the filter material from sticking together [8]. In addition, magnetic microparticles (MMP) can also be used as a conditioner sludge to increase dewaterability. At a voltage of 44.67 V and 4 bar of pressure, a dry solid concentration of 53.52% was obtained. MMP reduces the compressibility of the sludge through the skeleton-building effect where the size, strength, and density of the sludge flocks increase so that the sludge is more easily dewatered [49].

PED is rarely used because the technology is very vulnerable to ohmic heating. In addition, the high energy consumption and potential for electrode corrosion make this technology less desirable. Also, the formation of extreme pH gradients between the filtrate and filter cake due to the electrolysis process can quickly stop the system. Zhang et al. [2] stated that problems at the commercial level include equipment service life and how to improve processing effectiveness. Depreciation of PED equipment is substantial, especially for anodes and filter media, which are very susceptible to saturation during the process. Filter media have experienced a price depreciation of 327.7% per year and anode plates of 138.4%. The most significant ratio in equipment operating costs is in the primary and supporting facilities of the belt press filter–PED system and anode plate replacement.

Thin filter media reduce obstacles in the filter medium, thereby reducing service life, and can only be used for a maximum of three months. The filter material accounts for 1.1% of the total operational costs of the equipment, and although this

UNCORRECTED PROOFS

UNCORRECTED PROOFS

Trim Size: 170mm x 244mm Single Column Loose

Table 25.1 Summary of PED system enhancement.

Sludge type	System enhancement	Type	Voltage or current	Pressure (bar)	Max power consumption (kWh kg^{-1})	Max dry sludge concentration (wt%)	References
Industrial sludge	Addition of Na^+ and K^+ ions	Lab scale	5–15 V 1.12–1.61 A	–	0.29	41.35	[14]
Industrial sludge	Addition of CaO 3–5% to the sludge mass	Lab scale	30 V	0.25	0.233–0.271	46.2	[54]
Municipal WWT sludge	Addition of Na_2SO_4 as much as 12.5 g kg^{-1} dry sludge	Lab scale	0–50 V 0–10 A	0.01	–	16.8	[61]
Activated and digested sludge	Filter cloth positioning	Lab scale	20–80 A	5	0.61	34.5	[69]
Municipal WWT sludge and river sediment	Voltage and sludge characteristic	Lab scale	10–20 V	0.3	0.953	42.9	[29]
Municipal WWT sludge	Polymer and stabilization of bio-sludge	Lab scale	10–20 V	0.3	0.083	39.3	[22]
Industrial sludge	Sediment sludge characteristic	Lab scale	20 V 4 A	0.5	0.032–0.315	11.4	[47]
Industrial sludge	Adding polyelectrolyte, salt, pH	Lab scale	80 A	5	0.25	40	[4]
Municipal WWT sludge	Application of different applied pressure and time delay	Lab scale	10–50 V	2–6	1.38	36	[21]

Ribeiro670117 c25.tex V1 - 12/11/2020 7:25pm Page 645

UNCORRECTED PROOFS

Trim Size: 170mm x 244mm Single Column Loose

Table 25.1 (Continued)

Sludge type	System enhancement	Type	Voltage or current	Pressure (bar)	Max power consumption (kWh kg^{-1})	Max dry sludge concentration (wt%)	References
Municipal WWT sludge	Pulsed electric	Lab scale	10–30 V	10–30	0.077–0.135	40	[59]
Sediment river	Electrical field	Lab scale	10–50 V	–	0.07–0.275	51	[20]
Mix industrial and municipal WWT sludge	• Modification of equipment, anode–cathode, filter, and pressure • Applying pilot and industrial scale	Lab-, pilot-, industrial scale	20–50 V	0.1–1	0.12 (lab scale) 1.23 (pilot scale) 0.12 (industrial scale)	40	[2]
Municipal WWT sludge	Filter cloth	Lab scale	8–12 V	0.07	0.043–0.075	40	[30]
Municipal WWT sludge	Electrode pretreatment (surface-coating)	Lab scale	5–15 V	3	0.287–0.495	45	[67]

Note: WWT, wastewater treatment.

Ribeiro670117 c25.tex V1 - 12/11/2020 7:25pm Page 646

Trim Size: 170mm x 244mm Single Column Loose Ribeiro670117 c25.tex V1 - 12/11/2020 7:25pm Page 647

value is quite small compared to the overall operational costs of the equipment per year, the filter media must be replaced every time its service life runs out. Anodes must be replaced regularly because nonconductive TiO_2 layers are formed during the process. Also, the active oxide coating dissolves, which increases stress due to increased sludge resistance. As a result, the performance of the dewatering process will decrease significantly. All components that directly or indirectly come into contact with sludge must be protected/coated to avoid corrosion.

Auxiliary systems to support the PED process are also essential. The on-time distribution of sludge must be ensured during operation. Reusing recycling water for filter cleaning and dehumidifying filter media is also critical to consider during the process. Monitoring equipment must always be maintained to remove water vapor, which can hamper recording system efficiency during dewatering [2, 22].

25.5 Conclusion

Electrokinetic systems typically work together with pressure in the dewatering process. However, applying pressure as a pretreatment improves process efficiency while reducing energy consumption. Pressure-driven EDW works at both constant current and constant voltage. At constant current, changes in reactor dimensions do not significantly affect the sludge treatment process. However, a significant increase in voltage can occur when electrical resistance reaches a critical value. Voltage control becomes necessary when working under such a system. Under constant voltage, electrical resistance does not change significantly, which is advantageous and does not harm the electrical system.

The successful implementation of a PED system is supported by several factors including electrical resistance, pH, salinity, sludge characteristics, electric fields, and electrodes. The enhancement method focused on a system that produces more dry solid concentration with low energy consumption. There are still gaps in its application on a commercial scale due to the high risk of ohmic heating, energy consumption, and operational costs.

Using other technologies as co-dewatering systems has also been introduced, such as using pulsed electricity, MMP conditioning, and nonconductive electrodes. Sustaining the performance of PED is still being studied by many researchers, especially in overcoming the formation of extreme pH gradients and increasing the equipment service life.

References

1 Mahmoud, A., Olivier, J., Vaxelaire, J., and Hoadley, A.F.A. (2010). Electrical field: a historical review of its application and contributions in wastewater sludge dewatering. *Water Research* 44 (8): 2381–2407.

2 Zhang, S., Yang, Z., Lv, X. et al. (2017). Novel electro-dewatering system for activated sludge biosolids in bench-scale, pilot-scale and industrial-scale applications. *Chemical Engineering Research and Design* 121: 44–56.

UNCORRECTED PROOFS

Trim Size: 170mm x 244mm Single Column Loose Ribeiro670117 c25.tex V1 - 12/11/2020 7:25pm Page 648

3 Yuan, C. and Weng, C.H. (2003). Sludge dewatering by electrokinetic technique: effect of processing time and potential gradient. *Advances in Environmental Research* 7 (3): 727–732.

4 Citeau, M., Larue, O., and Vorobiev, E. (2011). Influence of salt, pH and polyelectrolyte on the pressure electro-dewatering of sewage sludge. *Water Research* 45 (6): 2167–2180.

5 Mahmoud, A., Olivier, J., Vaxelaire, J., and Hoadley, A.F.A. (2013). Advances in mechanical dewatering of wastewater sludge treatment. In: *Wastewater Reuse and Management*, 253–303. Springer.

6 Tuan, P., Jurate, V., and Mika, S. (2008). Electro-dewatering of sludge under pressure and non-pressure conditions. *Environmental Technology* 29 (10): 1075–1084.

7 Vaxelaire, J., Bongiovanni, J.M., and Puiggali, J.R. (1999). Mechanical dewatering and thermal drying of residual sludge. *Environmental Technology* 20 (1): 29–36.

8 Jakobsson, J. (2017). Electro-assisted dewatering of cellulosic materials: A comparison between fibrillated materials. Master's thesis, Chalmera University of Technology.

9 Silva, F.L., Lanza, M.R.V., Saez, C., and Rodrigo, M.A. (2019). Electrochemical dewatering for the removal of hazardous species from sludge. *Journal of Environmental Management* 233: 768–773.

10 Mahmoud, A., Olivier, J., Vaxelaire, J., and Hoadley, A.F.A. (2011). Electro-dewatering of wastewater sludge: influence of the operating conditions and their interactions effects. *Water Research* 45 (9): 2795–2810.

11 Glendinning, S., Mok, C.K., Kalumba, D. et al. (2010). Design framework for electrokinetically enhanced dewatering of sludge. *Journal of Environmental Engineering* 136 (4): 417–426.

12 Loginov, M., Citeau, M., Lebovka, N., and Vorobiev, E. (2013). Electro-dewatering of drilling sludge with liming and electrode heating. *Separation and Purification Technology* 104: 89–99.

13 Citeau, M., Larue, O., and Vorobiev, E. (2015). Electric (electro/Dielectro-Phoretic)-force field assisted separators. In: *Progress in Filtration and Separation* (ed. E. Steven Tarleton), 325–397. Elsevier Ltd.

14 Lv, H., Xing, S., Liu, D. et al. (2020). Soluble metal ions migration and distribution in sludge electro-dewatering. *Environmental Research* 180.

15 Tuan, P.-A., Mika, S., and Pirjo, I. (2012). Sewage sludge electro-dewatering treatment—a review. *Drying Technology* 30 (7): 691–706.

16 Fourie, A.B. and Jones, C.J.F.P. (2010). Improved estimates of power consumption during dewatering of mine tailings using electrokinetic geosynthetics (EKGs). *Geotextiles and Geomembranes* 28 (2): 181–190.

17 Bourgès-Gastaud, S., Dolez, P., Blond, E., and Touze-Foltz, N. (2017). Dewatering of oil sands tailings with an electrokineticgeocomposite. *Minerals Engineering* 100: 177–186.

18 Menon, A., Mashyamombe, T.R., Kaygen, E. et al. (2019). Electro-osmosis dewatering as an energy efficient technique for drying food materials. *Energy Procedia* 161 (0): 123–132.

UNCORRECTED PROOFS

Trim Size: 170mm x 244mm Single Column Loose Ribeiro670117 c25.tex V1 - 12/11/2020 7:25pm Page 649

19 Wang, K., Wu, Y., Wang, Z. et al. (2018). Insight into effects of electro-dewatering pretreatment on nitrous oxide emission involved in related functional genes in sewage sludge composting. *Bioresource Technology* 265: 25–32.

20 Wu, P., Shi, Y., Wang, Z. et al. (2019). Effect of electric field strength on electro-dewatering efficiency for river sediments by horizontal electric field. *Science of the Total Environment* 647: 1333–1343.

21 Mahmoud, A., Hoadley, A.F.A., Conrardy, J.B. et al. (2016). Influence of process operating parameters on dryness level and energy saving during wastewater sludge electro-dewatering. *Water Research* 103: 109–123.

22 Visigalli, S., Turolla, A., Zhang, H. et al. (2017). Assessment of pressure-driven electro-dewatering as a single-stage treatment for stabilized sewage sludge. *Journal of Environmental Chemical Engineering* 5 (6): 6122–6131.

23 Raats, M.H.M., Van Diemen, A.J.G., Lavèn, J., and Stein, H.N. (2002). Full scale electrokinetic dewatering of waste sludge. *Colloids Surfaces A Physicochemical and Engineering Aspects* 210 (2–3): 231–241.

24 Werther, J. and Ogada, T. (1999). Sewage sludge combustion. *Progress in Energy and Combustion Science* 25 (1): 55–116.

25 Lv, H., Liu, D., Xing, S. et al. (2019). The effects of aging for improving wastewater sludge electro-dewatering performances. *Journal of Industrial and Engineering Chemistry* 80: 647–655.

26 Liu, S., Song, F., Zhu, N. et al. (2010). Chemical and microbial changes during autothermal thermophilic aerobic digestion (ATAD) of sewage sludge. *Bioresource Technology* 101 (24): 9438–9444.

27 Olivier, J., Mahmoud, A., Vaxelaire, J. et al. (2014). Electro-dewatering of anaerobically digested and activated sludges: an energy aspect analysis. *Drying Technology* 32 (9): 1091–1103.

28 Cao, B., Wang, R., Zhang, W. et al. (2019). Carbon-based materials reinforced waste activated sludge electro-dewatering for synchronous fuel treatment. *Water Research* 149: 533–542.

29 Visigalli, S., Turolla, A., Gronchi, P., and Canziani, R. (2017). Performance of electroosmotic dewatering on different types of sewage sludge. *Environmental Research* 157: 30–36.

30 Yu, X., Zhang, S., Xu, H. et al. (2010). Influence of filter cloth on the cathode on the electroosmotic dewatering of activated sludge. *Chinese Journal of Chemical Engineering* 18 (4): 562–568.

31 Reddy, K.R., Urbanek, A., and Khodadoust, A.P. (2006). Electroosmotic dewatering of dredged sediments: bench-scale investigation. *Journal of Environmental Management* 78 (2): 200–208.

32 Mena, E., Villaseñor, J., Rodrigo, M.A., and Cañizares, P. (2016). Electrokinetic remediation of soil polluted with insoluble organics using biological permeable reactive barriers: effect of periodic polarity reversal and voltage gradient. *Chemical Engineering Journal* 299: 30–36.

UNCORRECTED PROOFS

Trim Size: 170mm x 244mm Single Column Loose Ribeiro670117 c25.tex V1 - 12/11/2020 7:25pm Page 650

33 Hu, S., Hu, J., Liu, B. et al. (2018). In situ generation of zero valent iron for enhanced hydroxyl radical oxidation in an electrooxidation system for sewage sludge dewatering. *Water Research* 145: 162–171.

34 Feng, J., Wang, Y.L., and Ji, X.Y. (2014). Dynamic changes in the characteristics and components of activated sludge and filtrate during the pressurized electroosmotic dewatering process. *Separation and Purification Technology* 134: 1–11.

35 Iwata, M., Tanaka, T., and Jami, M.S. (2013). Application of electroosmosis for sludge dewatering—a review. *Drying Technology* 31 (2): 170–184.

36 Ammami, M.T., Song, Y., Benamar, A., and Wang, H. (2020). Electro-dewatering of dredged sediments by combined effects of mechanical and electrical processes: influence of operating conditions. *Electrochimica Acta* 353: 136462.

37 Xian-shu, D., Xiao-jie, H., Su-ling, Y. et al. (2009). Vacuum filter and direct current electroosmosis dewatering of fine coal slurry. *Procedia Earth and Planetary Science*. Elsevier B.V.: 685–693.

38 Curvers, D., Maes, K.C., Saveyn, H. et al. (2007). Modelling the electro-osmotically enhanced pressure dewatering of activated sludge. *Chemical Engineering Science* 62 (8): 2267–2276.

39 Harris, A., Nosrati, A., and Addai-mensah, J. (2018). The influence of pulp and interfacial chemistry and mode of electrical power input on electroosmotic dewatering of Na-exchanged smectite dispersions. *Applied Clay Science* 162: 214–222.

40 Shi, L., Müller, S., Harms, H., and Wick, L.Y. (2008). Factors influencing the electrokinetic dispersion of PAH-degrading bacteria in a laboratory model aquifer. *Applied Microbiology and Biotechnology* 80 (3): 507–515.

41 Yeung, A.T. and Gu, Y.Y. (2011). A review on techniques to enhance electrochemical remediation of contaminated soils. *Journal of Hazardous Materials* 195: 11–29.

42 Maturi, K., Reddy, K.R., and Cameselle, C. (2009). Surfactant-enhanced Electrokinetic remediation of mixed contamination in low permeability soil. *Separation Science and Technology* 44 (10): 2385–2409.

43 Sun, Z., Wu, B., Guo, P. et al. (2019). Enhanced electrokinetic remediation and simulation of cadmium-contaminated soil by superimposed electric field. *Chemosphere* 233: 17–24.

44 Gill, R.T., Harbottle, M.J., Smith, J.W.N., and Thornton, S.F. (2014). Electrokinetic-enhanced bioremediation of organic contaminants: a review of processes and environmental applications. *Chemosphere* 107: 31–42.

45 Mok, C.K. (2006). Design and modelling of electroosmotic dewatering. Thesis, Newcastle University.

46 Mena, E., Rubio, P., Cañizares, P. et al. (2012). Electrokinetic transport of diesel-degrading microorganisms through soils of different textures using electric fields. *Journal of Environmental Science and Health, Part A: Toxic/Hazardous Substances and Environmental Engineering* 47 (2): 274–279.

UNCORRECTED PROOFS

Trim Size: 170mm x 244mm Single Column Loose Ribeiro670117 c25.tex V1 - 12/11/2020 7:25pm Page 651

47 Wu, P., Pi, K., Shi, Y. et al. (2020). Dewaterability and energy consumption model construction by comparison of electro-dewatering for industry sludges and river sediments. *Environmental Research* 184: 109335.

48 Yang, Z., Lu, X., Zhang, S. et al. (2018). Pressurized electro-dewatering of activated sludge: analysis of electrode configurations (anode). *Waste Management* 81: 157–167.

49 Guo, X., Qian, X., Wang, Y., and Zheng, H. (2018). Magnetic micro-particle conditioning–pressurized vertical electroosmotic dewatering (MPEOD) of activated sludge: role and behavior of moisture and organics. *Journal of Environmental Sciences* 74: 147–158.

50 Dizon, A.R. and Orazem, M.E. (2019). Mathematical model and optimization of continuous electroosmotic dewatering. *Electrochimica Acta* 304: 42–53.

51 Zhang, Y., Lian, G., Dong, C. et al. (2020). Optimizing and understanding the pressurized vertical electroosmotic dewatering of activated sludge. *Process Safety and Environmental Protection* 140: 392–402.

52 Martin, L., Alizadeh, V., and Meegoda, J. (2019). Electro-osmosis treatment techniques and their effect on dewatering of soils, sediments, and sludge: a review. *Soils and Foundations* 59 (2): 407–418.

53 Harris, A., Nosrati, A., and Addai-Mensah, J. (2015). The effect of clay type and dispersion conditions on electroosmotic consolidation behaviour of model kaolinite and Na-exchanged smectite pulps. *Chemical Engineering Research and Design* 101: 56–64.

54 Wei, Y., Zhou, X., Zhou, L. et al. Electro-dewatering of sewage sludge: effect of near-anode sludge modification with different dosages of calcium oxide. *Environmental Research* 186: 109487.

55 Luo, Q., Zhang, X., Wang, H., and Qian, Y. (2005). The use of non-uniform electrokinetics to enhance in situ bioremediation of phenol-contaminated soil. *Journal of Hazardous Materials* 121 (1–3): 187–194.

56 Hassan, I., Mohamedelhassan, E., and Yanful, E.K. (2015). Solar powered electrokinetic remediation of Cu polluted soil using a novel anode configuration. *Electrochimica Acta* 181: 58–67.

57 Conrardy, J.B., Vaxelaire, J., and Olivier, J. (2016). Electro-dewatering of activated sludge: electrical resistance analysis. *Water Research* 100: 194–200.

58 Hu, L., Zhang, L., and Wu, H. (2019). Experimental study of the effects of soil pH and ionic species on the electroosmotic consolidation of kaolin. *Journal of Hazardous Materials* 368: 885–893.

59 Deng, W., Lai, Z., Hu, M. et al. (2020). Effects of frequency and duty cycle of pulsating direct current on the electro-dewatering performance of sewage sludge. *Chemosphere* 243: 125372.

60 Casagrande, L. (1949). Electro-osmosis in soils. *Geotechnique* 1 (3): 159–177.

61 Xiao, J., Wu, X., Yu, W. et al. (2017). Migration and distribution of sodium ions and organic matters during electro-dewatering of waste activated sludge at different dosages of sodium sulfate. *Chemosphere* 189: 67–75.

UNCORRECTED PROOFS

Trim Size: 170mm x 244mm Single Column Loose Ribeiro670117 c25.tex V1 - 12/11/2020 7:25pm Page 652

62 Tuan, P.A. and Sillanpää, M. (2010). Migration of ions and organic matter during electro-dewatering of anaerobic sludge. *Journal of Hazardous Materials* 173 (1–3): 54–61.

63 Hwang, S. and Min, K.S. (2003). Improved sludge dewatering by addition of electroosmosis to belt filter press. *Journal of Environmental Engineering and Science* 2 (2): 149–153.

64 Lee, Y.J., Choi, J.H., Lee, H.G. et al. (2012). Effect of electrode materials on electrokinetic reduction of soil salinity. *Separation Science and Technology* 47 (1): 22–29.

65 Peng, G. and Tian, G. (2010). Using electrode electrolytes to enhance electrokinetic removal of heavy metals from electroplating sludge. *Chemical Engineering Journal* 165 (2): 388–394.

66 Roulier, M., Kemper, M., Al-Abed, S. et al. (2000). Feasibility of electrokinetic soil remediation in horizontal lasagna (TM) cells. *Journal of Hazardous Materials* 77 (1–3): 161–176.

67 Gronchi, P., Canziani, R., Brenna, A. et al. (2017). Electrode surface treatments in sludge electroosmosis dewatering. *Materials and Manufacturing Processes* 32 (11): 1265–1273.

68 Olivier, J., Conrardy, J.B., Mahmoud, A., and Vaxelaire, J. (2015). Electro-dewatering of wastewater sludge: an investigation of the relationship between filtrate flow rate and electric current. *Water Research* 82: 66–77.

69 Mahmoud, A., Hoadley, A.F.A., Citeau, M. et al. (2018). A comparative study of electro-dewatering process performance for activated and digested wastewater sludge. *Water Research* 129: 66–82.

UNCORRECTED PROOFS

Trim Size: 170mm x 244mm Single Column Loose Ribeiro670117 c26.tex V1 - 12/11/2020 10:26pm Page 653

26

Removing Ionic and Nonionic Pollutants from Soil, Sludge, and Sediment Using Ultrasound-Assisted Electrokinetic Treatment

Bimastyaji Surya Ramadan[1], Marita Wulandari[2], Yudha Gusti Wibowo[3], Nurani Ikhlas[4], and Dimastyaji Yusron Nurseta[5]

[1]*Department of Environmental Engineering, Faculty of Engineering, Universitas Diponegoro, Semarang 50277, Indonesia*
[2]*Environmental Engineering Department, Institut Teknologi Kalimantan, Balikpapan 76127, Indonesia*
[3]*Department of Environmental Science, School of Postgraduate Studies, Universitas Jambi, Jambi 36122, Indonesia*
[4]*Department of Environmental Engineering, Faculty of Engineering, Institut Teknologi Pembangunan Surabaya, 60188, Indonesia*
[5]*Bioprocess Engineering, Department of Agricultural Engineering, Faculty of Agricultural Technology, Universitas Brawijaya, 65145, Indonesia*

26.1 Introduction

Remediating contaminated soil, sludge, and sediment (SSS) requires advanced technology and has high environmental costs, which leads to high annual operating costs [1]. Electrokinetic treatment can improve the quality of the environment. This technology is commonly known as electro-reclamation [2], electrochemical remediation [3], or electro-decontamination [4]. It is an emerging fine SSS treatment and recovery approach that utilizes direct current in improving the quality of SSS contaminated with ionic and nonionic materials [5]. Remediating SSS using electrokinetic treatment is rarely found in the field since this technology has many limitations, especially the treatment cost, high rate of evaporation, and need for a source of electricity in remote areas [4]. The treatment applies a direct electrical current to transfer contaminants from the solid surface to the electrolyte chamber [6]. In treating organic pollutants, surfactants are generally used to increase desorption and dissolution through the production of the micelle and decrease the surface tension of the contaminants [7]. Other technologies such as bioremediation [8], oxidation/reduction [9], permeable reactive barriers (PRBs) [7], nano-zero valent iron [10], lasagna [11], phytoremediation [12], and ultrasonication [13] can be integrated into a series of treatments to enhance the effectiveness of electrokinetic treatment [2].

Ultrasonication has been applied in several fields (such as soil remediation, organic synthesis, and industrial activities) [14, 15]. In the last two decades, the utilization of ultrasonic treatment in environmental cleanup has been widely studied. High-power ultrasonic energy is applied at a pilot scale rather than a lab scale,

Electrokinetic Remediation for Environmental Security and Sustainability, First Edition.
Edited by Alexandra B. Ribeiro and M.N.V. Prasad.
© 2021 John Wiley & Sons Ltd. Published 2021 by John Wiley & Sons Ltd.

UNCORRECTED PROOFS

Trim Size: 170mm x 244mm Single Column Loose Ribeiro670117 c26.tex V1 - 12/11/2020 10:26pm Page 654

with the primary focus of research on soil and sediment contamination by organic pollutants [16]. Ultrasonication is a process that utilizes sound with a frequency greater than 20 kHz [14]. When ultrasonication is applied to liquid or a slurry, it breaks down chemical bonds through sonolysis and produces free radicals [17]. Ultrasonication can also be used as a pretreatment in sludge treatment [18]: it is reported to reduce water in suspensions such as sludge and sediment. Ultrasonic pressure can also produce a kind of sponge effect to facilitate water migration, acoustic streaming, local heating, surface layer instability, agitation, cavitation, and solid/liquid separation [19]. Low-frequency ultrasonic energy can make sludge particles coalesce. In addition, low-frequency ultrasonic energy can enhance anaerobic processes, which requires a lengthy processing time and is low-efficiency [20]. Ultrasonic energy is better for use in sludge pretreatment since it can quickly reduce water and increase remediation efficiency [21]. Ultrasonic technology is not easy to apply in industrial processes because high-energy ultrasonic equipment is challenging to use. But the many studies that have been done indicate that ultrasonic technology can be a robust, sustainable, clean technology for treating SSS [22, 23].

The possibilities included in the description of ultrasonic-assisted electrokinetics (US-EK) indicate a positive correlation in integrating the two technologies, so they might feasibly be applied on a commercial scale. This chapter explains using electrokinetics to remove ionic and nonionic materials from polluted SSS. The chapter briefly discusses the mechanism of desorption and degradation of pollutants by ultrasonic and electrokinetic means. Then, an integrative processes using ultrasonication and electrokinetics are compared. The potential and limitations of using US-EK treatment for environmental remediation are also reviewed. This chapter also discusses the research that has been carried out so far.

26.2 Overview of Technologies

26.2.1 Ultrasonication

The discovery that ultrasound enhances SSS remediation has not been explicitly published based on evidence. In the 1950s, several companies began to develop ultrasonic treatment systems. Then, in 1995, research began into remediating contaminated soils using ultrasonic energy [24]. Ultrasonic energy can degrade contaminants, increase the porosity and percolation rate of the soil, and accelerate the desorption process from SSS minerals. Many studies have proven the success of ultrasonic technology in removing various contaminants such as metals and organic compounds from SSS. However, research into ultrasonic remediation on a field scale is limited [20]. Since the late 1990s, ultrasonic technology to remediate contaminated soils has continued to develop. Ultrasonication [16] is suitable for remediating persistent contaminants (phenolic compounds, chlorofluorocarbons [CFCs], chlorinated aliphatic hydrocarbons [CAHs], aromatic compounds, polychlorinated biphenyls [PCBs], polycyclic aromatic hydrocarbons [PAHs], pesticides, and other organochlorines) that are adsorbed into soil particles [13, 21–23].

UNCORRECTED PROOFS

Trim Size: 170mm x 244mm Single Column Loose Ribeiro670117 c26.tex V1 - 12/11/2020 10:26pm Page 655

Ultrasonication refers to sound waves that are above the limits humans can hear, commonly at frequencies between 20 kHz and 500 MHz [25]. The sound waves can be transmitted through elastic media including water, saturated water gas, and slurry and are usually applied to surface cleaning, mining processes, food technology, non-destructive testing, health technology, the welding industry, material science and nanotechnology, and environmental applications [26, 27]. Although ultrasonic applications for SSS remediation are currently limited and in development at the lab scale, it offers several benefits: it is environmentally friendly (no production of toxic chemicals), has low energy requirements, and is easy to place in remediation sites [21]. Various types of ultrasonic treatments have been developed to deal effectively with different situations. Some examples used in the lab are baths, probes, and a cup-horn system. The bath and probe types are usually operated at a fixed frequency depending on the transducer [26]. The type of ultrasonic technology is divided into two groups: static and continuous processing systems [28]. In a lab experiment, a probe and bath system is often used. The probe system can provide a better sonication effect than the bath system, but the probe system is limited to small volumes [25, 26, 28].

Park and Son reported an effective reactor design for treating metal-contaminated soil with a frequency of 28 kHz at the bottom of the reactor (bath). The reactor is also equipped with a 200 rpm stirrer and 250 W of power [23]. Meanwhile, Thangavadivel et al. found that using high-frequency ultrasonication using a probe-type reactor could degrade non-polar pollutants such as dichloro-diphenyl-trichloroethane (DDT) contaminating soil [29]. The sonication frequency of 20 kHz and 375 W of power can degrade 75% DDT in 20 minutes. However, when the frequency was increased to 1.6 MHz, it was only able to remove 10% of DDT in 90 minutes. Although the ultrasonic horn type (probe) is most widely used at lab scale, this type of technology has a disadvantage: it is not adequate in the field because the capacity to transition acoustic energy into large tanks tends to be weak. Therefore, an ultrasonic bath is usually used for a larger scale [23]. In a bath system, an ultrasonic transducer is placed under the bath to indirectly result in sonication. The bath system itself can be used as a reaction container for receiving ultrasonic waves. In general, ultrasonic baths use specific power and intensity, so they do not change during the reaction. Therefore, determining the uniformity of energy distribution is tricky [28]. In general, using more than one transducer is mandatory for large-scale ultrasonic processing applications [13, 30]. Figure 26.1 shows bath and probe ultrasonic systems.

Ultrasonication has been studied and applied in many sectors in environmental protection and remediation [15]. Ultrasonication usually is not referred to as technology itself but is integrated with several other techniques to develop conventional methods. For example, ultrasonication can be applied with soil washing or electrokinetic remediation [31, 32]. Like a static treatment system, the effects of cavitation from ultrasonic energy can result from two forces: surface cleaning and contaminant leaching [16]. In addition, applying ultrasonication to soil washing can improve the ability to reduce pollutants by increasing contaminant transport in solution [23].

UNCORRECTED PROOFS

Trim Size: 170mm x 244mm Single Column Loose Ribeiro670117 c26.tex V1 - 12/11/2020 10:26pm Page 656

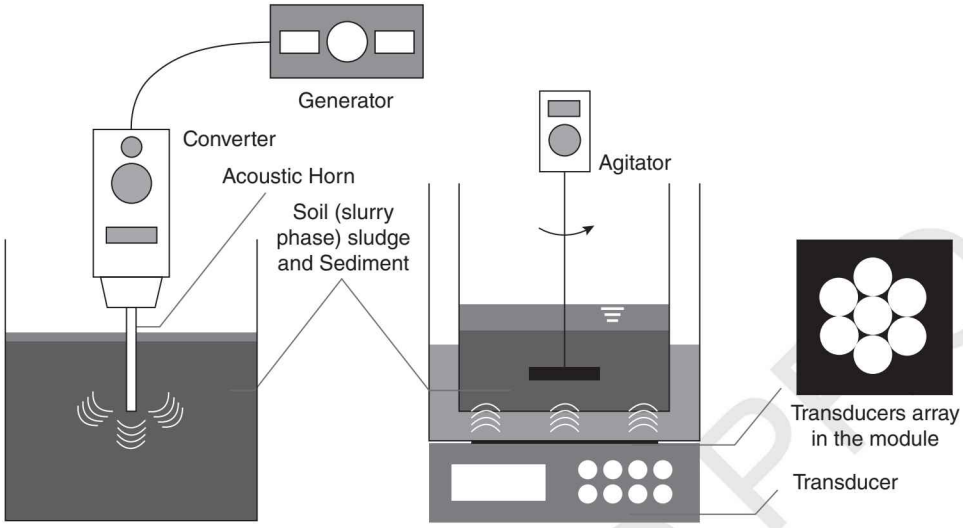

Figure 26.1 Ultrasonic probe (left) and bath system (right). Source: Adapted from Park and Son [23]; Abramov et al. [28]; Asgharzadehahmadi et al. [30].

Many studies discuss the effects of ultrasonic energy, especially in removing organic compounds from contaminated sites. Thangavadivel et al. used ultrasonic energy to enhance DDT desorption from clay-silt soils containing high organic content, with 80% desorption efficiency for 30 seconds at 20 kHz frequency [29]. Park and Son examined the effect of the solid-liquid ratio in ultrasonic remediation. The lower the soil/liquid rate (the greater the volume of solvent), the greater the removal efficiency [23]. Ultrasonication offers several advantages, including the following [15]:

- Faster rate of remediation than other existing technologies
- No sludge production
- Can be applied at room temperature
- Does not require massive areas of land
- Easy to implement
- Minimal maintenance costs

In general, ultrasonication produces two primary effects in SSS remediation. Desorption (physical force) occurs due to local turbulence reactions, and degradation (chemical effect) of contaminants results from free radical oxidation reactions. Soil type, soil/water ratio, temperature, frequency, and energy used are some factors that can influence the success rate of the ultrasonic method [1, 31].

26.2.2 Electrokinetic Remediation

Electrokinetic remediation is a technology that uses constant voltage and direct electrical current to generate the oxidation process: water, colloids, and ions migrate through SSS pores into the electrode chamber [33]. Electrokinetic remediation was

UNCORRECTED PROOFS

Trim Size: 170mm x 244mm Single Column Loose Ribeiro670117 c26.tex V1 - 12/11/2020 10:26pm Page 657

first discovered around the 1980s when organic metals were found in water, given a series of electric currents [2]. This technology was initially used as a water extractor (dewatering) in SSS [9]. This electrokinetic remediation method helps remove metals in situ and ex situ, especially in low-permeability soil [34]. This technology can also be used to recover metals contained in sludge and sediments. It is expected that inorganic and organic compounds can be moved and extracted from SSS in the electrode chamber [35]. Using electrokinetics in the remediation process is very beneficial, especially when dealing with contaminated soils with excessive clay content. The technology is still being explored, with research focusing on using various types of eluents, models, and configurations of electrodes, as well as integrative techniques to make it more effective and efficient [33, 36].

Electrokinetic remediation has also been analyzed economically as feasible in remediating polluted soils and water. This possibility increased researchers' interesting in determining the economic feasibility of the electrokinetic method. A feasibility study was carried out using the quantitative assessment of life cycle sustainability (QUALICS) framework by combining the Integrated Value Model for Sustainable Assessment and Analytical Hierarchy Process (AHP) methods. This method combines economic, environmental, and technological aspects in the feasibility analysis of using electrokinetic methods as an alternative technology in soil remediation. The electrokinetic process is one alternative to sustainable remediation technology [37].

In general, electrokinetic phenomena in a remediation system consist of electrolysis, electroosmosis, electromigration, electrophoresis, and electrooxidation. Electrolysis causes the formation of excessive H^+ ions and O_2 around the anode and OH^- ions around the cathode. As a result, the anode chamber becomes acidic, with a pH of 2–3, and the cathode chamber becomes very alkaline, with a pH of 10–12. This phenomenon causes the release of charged ions, colloids, and organic and inorganic compounds from the mineral surface to the fluid in the SSS pores [38]. SSS typically contains negative ions around the surface molecules so that the H^+ ions produced at the anode migrate toward the cathode and are trapped in the surface of clay minerals (electromigration). Due to the movement of excessive H^+ ions, the fluid in the pores of soil minerals are carried toward the cathode in a process called *electroosmosis* [39]. It causes non-polar compounds to move to the eluent in the electrode chamber [7]. Another mechanism that occurs is *electrophoresis*, in which charged colloidal particles migrate toward the poles with a charge the opposite of theirs [40]. Compounds can also be converted into new derivatives due to *electrooxidation* [9]. In addition to the phenomena mentioned earlier, diffusion or movement of ions and molecules from high to low concentrations also occurs [41]. Figure 26.2 shows the electrokinetic system that is implemented in SSS remediation.

Various developments in reducing pollutant parameters in contaminated soils have been developed, and multiple variations are being studied to find the most reasonable method. The integration of electrokinetic and bioremediation has been reported to remove organic contaminants effectively [43]. This technology effectively reduces various pollutants in saturated soils. The bioremediation itself consists of three types of biological processes: bio-attenuation,

UNCORRECTED PROOFS

Trim Size: 170mm x 244mm Single Column Loose Ribeiro670117 c26.tex V1 - 12/11/2020 10:26pm Page 658

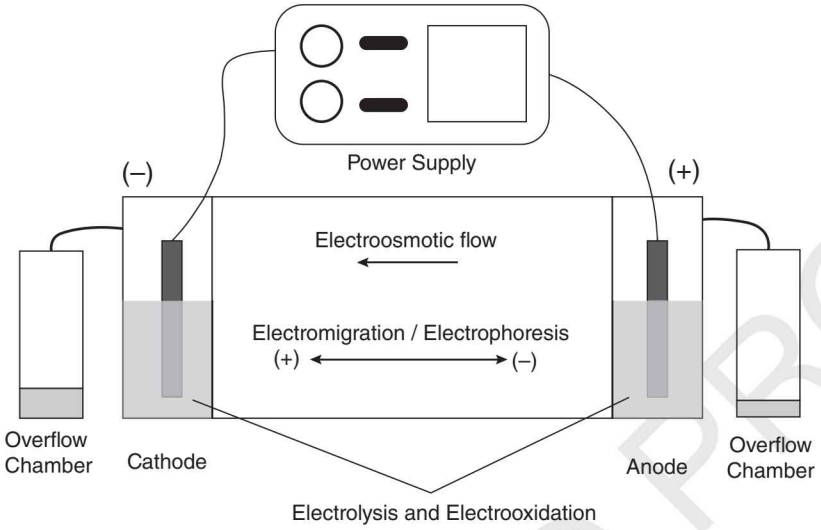

Figure 26.2 Electrokinetic system. Source: Ramadan, Effendi, and Helmy [42].

bio-stimulation, and bio-augmentation [4]. Other studies have suggested using a low-cost electrokinetic-Fenton (EK-Fenton) process by utilizing the trichloroethylene (TCE) oxidation process. Initial cost analysis shows that the EK-Fenton process used in that work is very cost-effective due to the destruction of TCE. In addition, other studies demonstrate that EK-Fenton integration has succeeded in reducing organic parameters [44]. Zhao et al. reported that the combination of electrokinetics and permeable reactive barriers (EK-PRB) reduce copper levels in soil up to 96.40% after four days of processing with an initial Cu concentration of 2000 mg kg^{-1} [45]. Combining electrokinetic methods with a reactive barrier using red mud has also been developed. Red mud in that study was produced from bauxite byproducts in alumina. The red mud used as a reactive barrier is placed close to the anode. This study demonstrates that the combination of EK technology and a reactive barrier made from red mud has greater effectiveness than conventional EK methods. This method can reduce 19.4% of the total weight of chromium (IV) detected in the soil, and 20.6% of chromium is trapped in the reactive barrier of red mud after testing for six days [46]. Electrokinetic and persulfate treatment also remediates soil contaminated with decabromodiphenyl ether and copper. The farther the distance from the anode, the lower the iron content is. At the opposite lead, the closer the anode is, the greater the decrease in lead content in the soil [39]. A combination of electrokinetics and ultrasonic (EK-US) remediation is the most effective treatment for removing organic and metal contaminants from contaminated SSS. Electrokinetic treatment is the most effective technique to remove metals and inorganic material but is less effective for removing organic compounds. However, ultrasonication is the most effective for removing organic compounds from contaminated soil [14, 21, 47].

UNCORRECTED PROOFS

Trim Size: 170mm x 244mm Single Column Loose Ribeiro670117 c26.tex V1 - 12/11/2020 10:26pm Page 659

26.3 Desorption and Degradation Mechanism

26.3.1 Removing Contaminants by Ultrasonication

Ultrasonication can remove contaminants by desorption (sound turbulence) and degradation (oxidation-reduction). SSS that has finer/smaller particles, more surface area, and greater capillary force increases the efficiency of contaminant reduction [48]. The effectiveness of decreasing contaminants increases along with power intensity, but only to a certain extent [49]. In general, the effects involved in the desorption of pollutants due to ultrasonication are as follows:

- Bubble decay (which is close to the surface of solids) is caused by the high-speed microjet process, which can increase the rate of transport and the surface area.
- Particle fragmentation due to collisions between particles can increase the area and encourage penetration of the leachate into the matrix.
- Acoustic streaming can disturb the diffusion layer on the surface.

The efficiency of contaminant release through diffusion to the outermost layer can be increased by applying ultrasonic energy that accelerates the kinetics of leaching contaminants in soil and sediment. Many studies state that contaminant leaching using ultrasonication yields greater removal efficiency with a shorter treatment time than mechanical stirring [50]. Contaminant leaching, in general, depends on the interaction between the solvent and soil particles. It is thought that ultrasonication produces microjet streams, dispersion, and turbulence, which increase solvent interaction and leaching efficiency [16]. Ultrasonic energy is transmitted through the medium by inducing sound waves into the medium so the molecules vibrate. As a result of the vibrations, the structure of the particles is stretched and compressed. The distance between molecules also changes due to molecular vibrations in the initial position. If the intensity of the ultrasonic waves in the water continues to increase, then a maximum condition is reached where the intramolecular force can no longer maintain the structure as it was initially. As a result, the molecule breaks down and forms a hole (cavity). This cavity is called a *cavitation bubble* [51, 52].

Oxidation reactions that usually occur at interphase or in the liquid phase play an essential role in the chemical degradation of organic pollutants due to ultrasonic remediation. Degradation resulting from ultrasonic cavitation occurs through two pathways [53, 54]:

- Sonolysis by free radicals
- Pyrolysis under specific pressure and temperature conditions

Oxidants (hydrogen, hydroxyl, hydroperoxyl) react with organic pollutants and cause changes in their chemical structure. Long carbon chains or aromatic hydrocarbons with complex structures and high molecular weight compounds can be broken down into simpler hydrocarbons [48, 54]. For instance, perchloroethylene (PCE) and TCE can be degraded into chloride ions, water, and carbon oxides [53, 55].

UNCORRECTED PROOFS

Trim Size: 170mm x 244mm Single Column Loose Ribeiro670117 c26.tex V1 - 12/11/2020 10:26pm Page 660

26.3.2 Ultrasonic Wave Effect

When ultrasonic energy is applied to the liquid or slurry phase of SSS, there are several physical and chemical effects, including cavitation and chemical, thermal, and biological impacts. Those effects are further discussed in the next section.

26.3.2.1 Cavitation

Cavitation is the formation, growth, and damage of microbubbles as a result of the effects of ultrasonic irradiation, which is also known to release a certain amount of energy at a certain point [30]. Research showed that high-frequency waves (>20 kHz) cause considerable mechanical distortion and "hot spots" at high temperatures and pressures in a liquid. Ultrasonic energy can be transmitted through elastic media and causes particle oscillations. When particle oscillations occur in a medium, a split occurs. The instability of the bubbles can cause cavitation due to interference from other bubbles that form and resonate around them. As a result, some bubbles undergo a sudden expansion so that they burst, as in Figure 26.3. Cavitation events with the bursting of the bubble cause a sonochemical reaction (radical formation) [23].

Figure 26.4 shows the ultrasonic effect on soil particles due to the jet stream phenomenon. In general, ultrasonic cavitation consists of three primary stages: nucleation or bubble formation, bubble growth, and bubble burst (implosive collapse). In the second stage, microbubbles grow and enlarge due to the high intensity of the ultrasonic waves. With ultrasonication at high intensity, microbubbles quickly increase, whereas at low intensity, the rate of growth of bubbles is slower. The bubbles go through several acoustic cycles before they finally enlarge. The third stage of cavitation occurs when the intensity of the ultrasonic waves exceeds the threshold of ultrasonic cavitation (20 kHz for liquids in general). At this stage, microbubbles continue to grow until they can no longer absorb the energy [56]. Eventually they burst (see Figure 26.4).

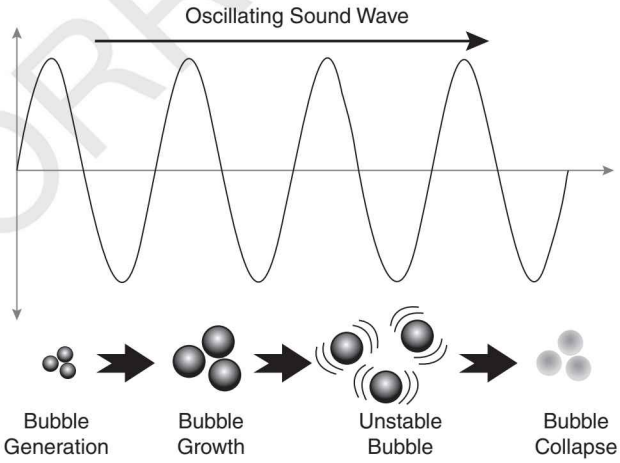

Figure 26.3 Cavitation mechanism caused by ultrasonic waves. Source: Seidi and Yamini [26].

UNCORRECTED PROOFS

Trim Size: 170mm x 244mm Single Column Loose Ribeiro670117 c26.tex V1 - 12/11/2020 10:26pm Page 661

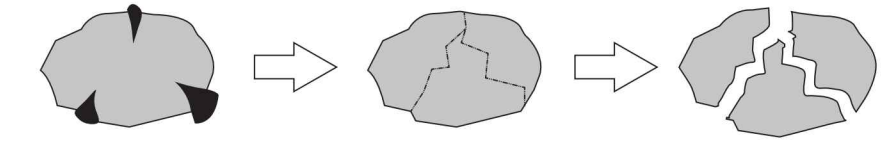

Figure 26.4 Overview of the effects of ultrasonic waves on the impact of jet streams on soil particles. Source: Bendicho et al. [56].

26.3.2.2 Thermal Effect

Two primary effects are related to changes in temperature in the medium irradiated by ultrasonic waves: high localized temperature and an increase in overall medium heat. The increase in temperature is caused by the cavitation process and the presence of dissolved gas in the medium. That cavitation, in addition to increased local temperatures, also sharply increases local pressure. A local temperature of 420 °K with local force can reach 975 bar [24]. This high localized temperature occurs during the cavitation process: when bubbles burst, temperatures rise in the area around the bursting bubbles. This temperature increase happens because the medium absorbs energy from ultrasonic waves during the radiation process; the lost energy is converted to heat, which then increases the temperature of the medium [57].

26.3.2.3 Chemical Effect

Ultrasonic irradiation in water causes growth and destruction of microbubbles and thus produces high temperatures and pressures, which trigger the formation of free radicals (OH radicals) through thermal dissociation between water and oxygen. These free radicals enter the water and oxidize contaminants in the water, combining with hydrogen atoms to produce hydrogen peroxide (H_2O_2) compounds. Volatile components are better able to diffuse to form cavitation bubbles and degrade faster through the pyrolysis reaction. During the destruction of microbubbles in the water, gas molecules from the water trapped in the bubbles undergo pyrolysis reactions that produce highly reactive radicals such as hydroxyl radicals. The hydroxyl radicals generated from this cavitation event can react in the gas phase, combined in colder regions such as the surface of the gas-liquid interface and the solution phases to produce hydrogen peroxide or water.

The reactions are as follows:

$$H_2O \leftrightarrow HO^{\cdot} + H^{\cdot} \tag{26.1}$$

$$H^{\cdot} + H^{\cdot} \leftrightarrow H_2 \tag{26.2}$$

$$^{\cdot}OH + {}^{\cdot}OH \leftrightarrow H_2O_2 \tag{26.3}$$

$$H^{\cdot} + O_2 \leftrightarrow HO_2^{\cdot} \tag{26.4}$$

$$H^{\cdot} + HO_2 \leftrightarrow H_2O_2 \tag{26.5}$$

$$HO_2^{\cdot} + HO_2^{\cdot} \leftrightarrow H_2O_2 + O_2 \tag{26.6}$$

$$H_2O^{\cdot} + {}^{\cdot}OH \leftrightarrow H_2O_2 + H^{\cdot} \tag{26.7}$$

UNCORRECTED PROOFS

Trim Size: 170mm x 244mm Single Column Loose Ribeiro670117 c26.tex V1 - 12/11/2020 10:26pm Page 662

If water is saturated with oxygen and peroxyl, more hydroxyl radicals are formed in the gas phase due to the decomposition of oxygen molecules. Hydroxyl radicals formed beforehand in the liquid-gas interface and the solution phase experience recombination with each other, thus creating hydrogen peroxide. Hydroxyl radicals formed in the bubble core are concentrated in the bubble surface with a concentration that can reach 4×10^{-3} M. Hydroxyl radicals and H_2O_2 degrade organic substances in the solution into smaller molecules until complete oxidation occurs [24, 51, 58].

26.3.2.4 Biological Effect

Several studies have found that sonication has a positive effect on biological processes [27]. Environmental factors such as ionic strength, pressure, temperature, and acid/base concentration affect sonication activity. Changes in cell membrane permeability and increased microscopic and macroscopic mixing are responsible for increased bacterial activity. Ultrasonic irradiation in a medium can have a sterilizing effect that kills microorganisms related to the cavitation process, which can increase local pressure at a sizeable micro scale that causes the cell to break. The types of microorganisms that have been identified as being affected are protozoa, *Escherichia coli*, arbacia eggs, and others. Vyas and Tin [27] also mentioned that ultrasound has a chemical effect (formation of OH radicals) that activates the bacteria *E. coli* and *Streptococcu* ssp. mutants. Furthermore, research showed that sonication plays an essential role in the release of enzymes during hydrolysis. Some proteins have also been shown to be susceptible to change due to free radicals produced with the ultrasonic method [59].

26.3.3 Electrokinetic Remediation Process

The electrokinetic method uses an electric current between the anode and cathode placed in contaminated SSS. This method was first carried out by F.F. Reuss in 1809 and continues to be utilized for sludge dewatering, fine soil stabilization, metal extraction, salinity control of agricultural soil, and reducing metal contamination [60]. Electrokinetic treatment is classified as an environmentally friendly technology because it uses electric current and does not produce waste. Anodes and cathodes that are planted during the electrokinetic process cause ions and colloids to move to electrodes with opposing charge. Electrokinetic phenomena consist of electrooxidation, electroosmosis, electrophoresis, and electromigration [9, 35, 61] (see Figure 26.5).

26.3.3.1 Electrolysis

Electrolysis is the oxidation reaction of water at the positive charge (anode) and water reduction at the negative charge electrode (cathode). When the electrode poles are planted in the SSS and electrified, an electrolysis process occurs in the area surrounding the electrodes, with the following equations:

$$\text{Anode (oxidation)} : 2H_2O_{(l)} \rightarrow 4e^- + O_{2(g)} + 4H^+{}_{(aq)} \tag{26.8}$$

$$\text{Cathode (reduction)} : 2H_2O_{(l)} + 2e^- \rightarrow H_{2(g)} + 2OH^-{}_{(aq)} \tag{26.9}$$

UNCORRECTED PROOFS

Trim Size: 170mm x 244mm Single Column Loose Ribeiro670117 c26.tex V1 - 12/11/2020 10:26pm Page 663

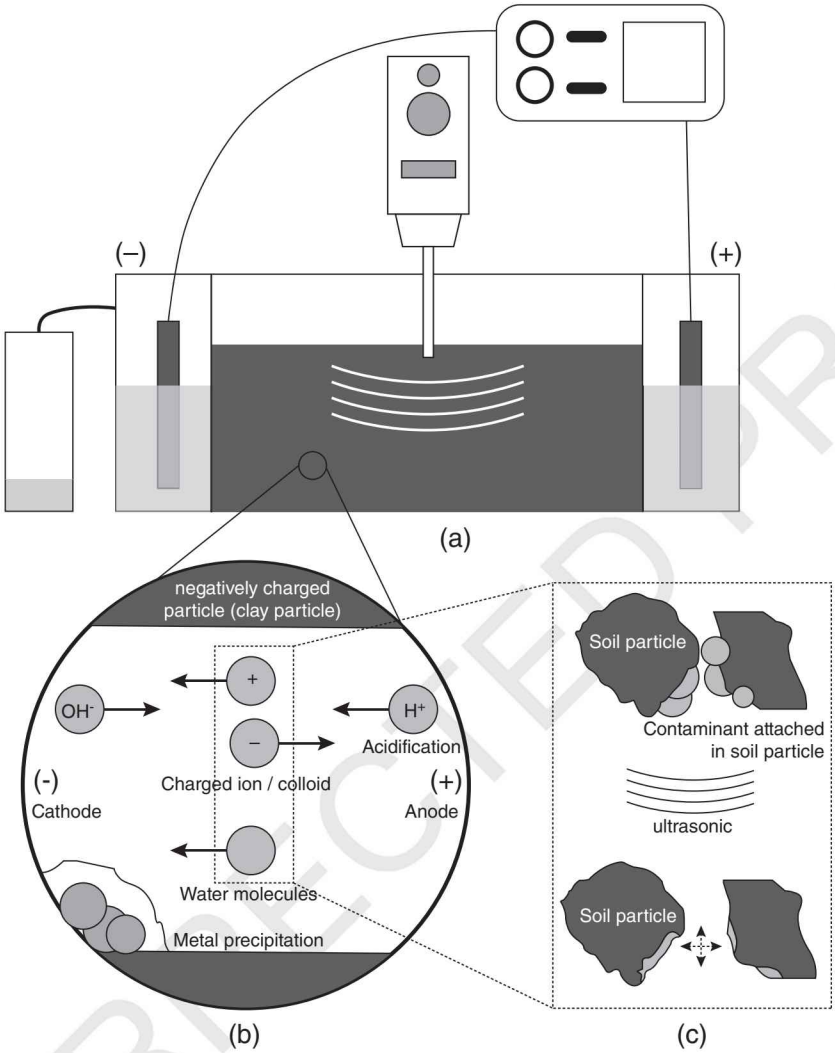

Figure 26.5 Conceptual picture of ultrasonication-assisted electrokinetic treatment: (a) system configuration; (b) electrokinetic process; (c) ultrasound illustration, where ultrasound increases pore stress, molecular movement, and cavitation. Source: Chung, Chun, and Lee [47].

The release of hydroxyl ions is followed by water formation at the anode and hydrogen formation at the cathode. The reactions can be seen in the following formulas:

$$\text{Anode}: 4OH^-_{(aq)} \rightarrow 2H_2O_{(l)} + O_{2(g)+} 4e^- \quad (26.10)$$

$$\text{Cathode}: 2e^- + 2H^+_{(aq)} \rightarrow H_{2(g)} \quad (26.11)$$

Although it appears that the anode can achieve equilibrium with the formation of water, in reality, the eluent at the anode decreases and at the cathode increases

UNCORRECTED PROOFS

Trim Size: 170mm x 244mm Single Column Loose Ribeiro670117 c26.tex V1 - 12/11/2020 10:26pm Page 664

dramatically due to electroosmosis, which is the residual effect of the above reaction [43, 62].

Hydrolysis of water molecules at the cathode and anode causes a high pH gradient. This phenomenon induces electromigration, electrophoresis, and electroosmosis. Uncontrolled pH gradients are often the cause of decreased contaminant removal efficiency. For example, when working with metals, a low pH increases the solubility of the metal in the fluids found in the SSS pores. At high pH, these metals precipitate and form a blockage that can hold the flow of water around the cathode chamber so that the system stops. Transport of H^+ ions is estimated to be two times faster than OH^- ions, so the soil tends to become acidic. Therefore, it is necessary to maintain a neutral soil pH to make the remediation system run optimally. Neutralization of pH can be done in various ways, including providing a buffer solution to the anode chamber, applying periodic polarity reversal, manipulating electrode placement (either cathode or anode), or using on-off systems by relying on the SSS buffering capacity [7, 9].

26.3.3.2 Electromigration and Electrophoresis

Electromigration is the movement of cations and anions due to the influence of a low-voltage electric field. Cations or (+)ions move toward the cathode with a negative charge, and anions or (−)ions move in the opposite direction. The ions approach the electrode through the fluid intermediary in the SSS pores and react in the electrode chamber. Electromigration plays a major role in the direct transport of pollutants for metal ions and charged colloids. Electromigration is also influenced by the conductivity and porosity of the soil, pH gradient, initial concentration of specific ions, and presence of other competitive ions. The electromigration rate (v_{em}) of an ion is proportional to the factors mentioned above, shown in the following equations

$$u_i = \frac{D_i z_i F}{RT} \tag{26.12}$$

$$v_{em} = u_i z_i n \tau F E \tag{26.13}$$

where u_i is the specific ion mobility ($m^2\ Vs^{-1}$), z_i is the valence of ions, n is porosity, τ is tortuosity, F is Faraday's constant (96.487 C mol^{-1}), D_i is the coefficient of molecular diffusion, R is the gas constant (8314 J $kmol^{-1}$), and E is the electrical energy potential (V m^{-1}). Electrophoresis is the movement of charged colloidal particles due to the presence of a low-voltage electric field applied to the SSS. It is more focused on the transport of charged colloids/particles. The electrophoresis phenomenon is often used to flush charged surfactants such as sodium dodecyl sulfate (SDS) and linear alkylbenzene sulfonates (LAS), which are placed in the anode chamber so the surfactant flows through the pores of the soil. It stimulates the formation of micelles after meeting with organic compounds such as hydrocarbons [36, 63].

26.3.3.3 Electroosmosis

Electroosmosis is water movement in SSS pores due to the application of a direct current electrical field. Factors affecting electroosmosis are soil type, moisture content, ion species, and ion concentration. In studies with higher voltage gradients, the electroosmotic rate is much faster. This phenomenon follows the

UNCORRECTED PROOFS

Trim Size: 170mm x 244mm Single Column Loose Ribeiro670117 c26.tex V1 - 12/11/2020 10:26pm Page 665

Helmholtz-Smoluchowski theory (H-S theory), where the increase in voltage is proportional to the rise in the flow rate of electroosmosis, zeta potential, and dielectric constant but inversely proportional to the viscosity of the liquid. Equation (26.13) illustrates this phenomenon of the electroosmosis rate

$$u_i = \frac{D\zeta E_z}{\eta} = nA\frac{D\zeta E_z}{\eta} \tag{26.14}$$

where D is the dielectric constant, ζ is the zeta potential, E_z is the applied voltage gradient, and η is the viscosity of the liquid. When liquid velocity is calculated on a volumetric scale, it is also necessary to know the area of the cross-section (A) and porosity of the soil (n). The rate of electroosmosis dramatically affects the rate of removal of pollutants, especially organic pollutants, which are not charged. Electroosmosis causes SSS to drain quickly and sends water to the cathode, so the volume of water at the cathode increases. Electroosmosis is then used for flushing enhancing agents and unloaded surfactants to remove organic contaminants that are tightly attached to the surface of the SSS [63].

26.3.3.4 Electrooxidation/Reduction

Organic contaminants are quite difficult to remediate using electrokinetics because of their low water solubility and hydrophobic nature. The mass transfer and transport process of organic contaminants using electrokinetics is also minimal. But phenols are exceptions because these compounds can dissolve in water and are protonated in an acidic atmosphere. Uncharged organic contaminants can be oxidized directly or indirectly in the electrokinetic process. Direct oxidation occurs when OH radicals appear at the cathode accompanied by oxygen reduction to form the following reactions:

$$\text{Water electrolysis} : H_2O \rightarrow H^+ + OH^* \tag{26.15}$$

$$\text{Oxygen reduction} : O_2 + 2H^+ + 2e^- \rightarrow 2H_2O_2 \tag{26.16}$$

$$\text{Perhydroxyl radical} : H_2O_2 + OH^* \rightarrow H_2O + HO_2{}^* \tag{26.17}$$

$$\text{Organic substrate conversion by } OH^* : RH + OH \ast\rightarrow R^* + H_2O + HO_2{}^* \tag{26.18}$$

$$\text{(Fenton reaction)} : R^* + Fe^{3+} \rightarrow Fe^{2+} + \text{products} \tag{26.19}$$

These hydroxyl radicals then indirectly bind to hydrogen peroxide due to atmospheric oxygen reduction and electrolysis of water. Hydroxyl radicals and hydrogen peroxide can occur due to the presence of ferrous ions in an acidic atmosphere. Charged soil particles act as micro-conductors and are polarized into monopolar and bipolar microelectrodes. This microelectrode causes indirect oxidation of organic compounds on the surface of the SSS. The output of this process is mineralized organic compounds, so no further processing is needed for the eluent produced [22, 44]. The initiation of the Fenton reaction on the microelectrode surface requires several Fe conditions, including:

- Fe binds to carbonates.
- Fe binds to iron or manganese oxides.
- Fe binds to organic material and sulfide.

UNCORRECTED PROOFS

Trim Size: 170mm x 244mm Single Column Loose Ribeiro670117 c26.tex V1 - 12/11/2020 10:26pm Page 666

26.4 Ultrasonication-Assisted Electrokinetic Remediation

26.4.1 Recent Progress in Ultrasonication-Assisted Electrokinetic Remediation (US-EK)

Ultrasonic technology is usually used with other conventional remediation techniques such as soil washing, electrokinetics, and Fenton oxidation. Chung and Kamon evaluated remediation of lead- and phenanthrene-contaminated soil using ultrasonication-assisted electrokinetics. The results showed that the removal rates for lead and phenanthrene were 91% and 90%, respectively [32]. Zhang et al. tried to combine ultrasonication and Fenton's reaction to treat oily sludge. The result showed that this integrated treatment could provide greater total petroleum hydrocarbon removal efficiency than ultrasonication alone [22]. Chung et al. also revealed that ultrasonication could increase remediation efficiency for oil-contaminated soil.

On the other hand, electrokinetic treatment effectively improves the removal of cadmium from contaminated soils [64]. Cadmium was removed due to electromigration phenomena caused by applying an electrical field. Therefore, US-EK is better at removing persistent organic pollutant (POP) contaminants than electrokinetics. US-EK also has greater electroosmotic flow than experiments with only electrokinetic treatment. In that case, the addition of ultrasonic energy can increase the organic pollutant removal rate by 10% since ultrasonication increases soil porosity and permeability [21]. Thus, ultrasonication enhances the desorption process of organic contaminants such as POPs, PAHs, and organochlorine compounds from soil. Regarding the cases mentioned before, electrokinetic and ultrasonic methods can be effective for removing ionic and nonionic pollutants [32].

Table 26.1 summarizes all of the research that evaluates the performance of ultrasound-assisted electrokinetic treatment. Figure 26.5 shows a typical system configuration for ultrasound-assisted electrokinetics in lab-scale experiments.

26.4.2 Factors Affecting Performance

Electrokinetics and ultrasonication produce an accumulated flow volume 1.8 times greater than conventional soil flushing. The effect of sonolysis may explain this phenomenon. The soil's pores are opened so that the flow rate of water in the pores increases, and electroosmotic flow carries most of the water from the soil to the electrode chamber. The intended sonolysis effect also causes soil permeability to increase, as shown in Figure 26.5. Integrative treatment is more robust for removing contaminants than electrokinetics, ultrasonication, or soil flushing alone. Pollutants migrate to the area near the cathode. Electrokinetic effects dominate the removal of metals, while hydrocarbons are dominated by the impact of soil flushing and ultrasonication [69].

26.4.2.1 System Parameters

Electrode materials also have a significant impact on the removal of organic pollutants. Occasionally, graphite and titanium are used as electrode materials for

UNCORRECTED PROOFS

Trim Size: 170mm x 244mm Single Column Loose Ribeiro670117 c26.tex V1 - 12/11/2020 10:26pm Page 667

Table 26.1 Research on ultrasound-assisted electrokinetic treatment.

Contaminant	Media	Electrokinetic characteristic	Ultrasonication characteristic	Highest removal efficiency	Operational time	References
Zinc (Zn); lead (Pb); copper (Cu); cadmium (Cd)	Municipal solid waste incineration fly ashes	Graphite and stainless steel electrodes; 2.0 V cm^{-1}	Bath system; 30 min acoustic time; 40 kHz; 60–180 W	69.84%; 64.24%; 67.74%; 59.93%	7 d	[65]
Arsenic, cadmium, lead	500 g sandy soil	Stainless steel electrodes; 1.5 V cm^{-1}	Probe system in batch-scale test; 200 kHz; 30 min d^{-1}	25.50%; 8.01%; 34.90%	25 d	[66]
100 mg kg^{-1} chrysene	Kaolin soil	Graphite electrodes; 1.5 V cm^{-1}	Acoustic horn (probe system); 30 kHz; 100 W; 5 h on the first day and 1 h the following days	>50%	10 d	[67]
Hexachloro-benzene, phenanthrene	Kaolin soil	The addition of surfactant; titanium electrodes	Probe system; 30 kHz; 100 W; 5 h on the first day and 1 h the following days	61% and 97%	14 d	[68]
100 mg kg^{-1} Hexachloro-benzene, phenanthrene, fluoranthene	500 g low permeability kaolin	Titanium electrodes; 0.5 V cm^{-1}	Probe system; 24 kHz; 100 W; 1 h d^{-1}	47–67%; 16–26%; 20–34%	15 d	[13]
100 mg kg^{-1} Chrysene (PAH)	500 g of clayey soil	Stainless steel electrodes; 1.5 V cm^{-1}	Probe system; 30 kHz; 100 W; 10 mm horn diameter; 5 h in the 1st day and 1 h in the following days	54%	10 d	[58]
100–500 mg kg^{-1} hexachloroben-zene, phenanthrene, fluoranthene	650 and 1000 g low permeability kaolin	Titanium electrodes; 1.5 V cm^{-1}	Probe system; 24 kHz; 100 and 200 W; 5 h in the 1st day and 1 h	36%; 50%; 60%	15 d	[14]
Diesel fuel and cadmium	Contaminated groundwater in a sandy layer	Graphite electrodes; 1.0 V cm^{-1}	Acoustic horn (probe system); 30 kHz; 200 W	87% and 83%	100 min	[69]
500 mg kg^{-1} lead (Pb) and 500 mg kg^{-1} ethylene glycol	Contaminated sand soil	Graphite electrodes; 1.0 V cm^{-1}	Acoustic horn (probe system); 30 kHz; 200 W	80% and 90%	170 min	[47]
500 mg kg^{-1} lead (Pb) and 500 mg kg^{-1} phenanthrene	Natural clay	Graphite electrodes; constant current 50 mA	Acoustic horn (probe system); 20 kHz; 200 W	91% and 90%	15 d	[32]

UNCORRECTED PROOFS

Trim Size: 170mm x 244mm Single Column Loose Ribeiro670117 c26.tex V1 - 12/11/2020 10:26pm Page 668

EK-US treatment. However, when iron electrodes are used, the removal percentage increases by 1% more than those electrodes. This could be the result of iron ions being broken down by electric current and increasing the electroconductivity of the flushing fluid. Using iron as an electrode increases the removal percentage by 5% around the electrode chamber. The presence of dissolved Fe ions due to electrolysis at the anode can increase hydraulic conductivity. Furthermore, the pH of the soil can be maintained so that electroosmosis continues. Interestingly, when electrodes are used to remove hydrocarbon compounds that have lower molecular mass, the removal efficiency increases by 10% compared to compounds with greater molecular mass. This result shows the relationship between remediation effectiveness and percentage of hydrocarbons removed. In electrokinetic reactors, contaminant removal is found to be most significant around the anode. This may occur due to electroosmosis of water in the pores. Moreover, there is a possibility of the compound being oxidized by oxygen radicals produced during the electrokinetic process. Conversely, in the US-EK reactor, the most significant removal was found at the cathode because of the high water content due to electroosmosis, which causes increased production of OH radicals [67].

When ultrasonication is integrated with soil flushing, the greater flushing rate is directly proportional to the increase in pollutant transport. However, when the rate of the flushing fluid is slow, the interaction between flushing fluid and organic composition is even more pronounced. In that case, the chances of pollutants being completely broken down are even greater. This phenomenon explains the enormous flushing rate; the efficiency of pollutant reduction is not sufficient because there is not enough time for the pollutants and flushing fluid to react [49]. In the case of metal removal, the activation system may increase the efficiency of remediation using EK-US treatment. The ultrasonic acidification pretreatment stage was proven to be more effective for improving the solubility and migration of metals than experiments using only nitric acid or with ultrasonication alone. Acidification may be a vital factor in removing metal pollutants because the crystalline phase of metalloid minerals can be destroyed, thus keeping the minerals dissolved. However, determining the concentration and type of acid solution is very important in suppressing the crystalline phase of metal minerals. The adoption of ultrasonication-acidification-assisted electrokinetic remediation in metal removal is considered better than using ultrasonication-assisted electrokinetics and electrokinetics alone. This hypothesis is indicated by the high level of solubility and metal migration in solid media [32].

At a constant voltage gradient, the value of currents in ultrasonication-assisted electrokinetic treatment tends to decrease because free ions present in the SSS are mobilized or neutralized in the electrode chamber. More pollutants are eliminated at the cathode because they are carried by electroosmosis currents flowing into the chamber. In this case, nonionic pollutants can be removed due to dilution from the production of water and electroosmosis compounds [58]. The residue of nonionic compounds is in the middle of the 2D horizontal reactor soon after applying US-EK. This condition can occur because pollutants in the anode are migrated to the cathode and oxidized by oxygen produced at the anode. Before reaching the cathode,

UNCORRECTED PROOFS

Trim Size: 170mm x 244mm Single Column Loose Ribeiro670117 c26.tex V1 - 12/11/2020 10:26pm Page 669

it is estimated that nonionic compounds are also decomposed due to the sonolysis process. Then, the concentration is drastically reduced in the cathode region [13]. However, different behaviors are shown in Pham et al.: the electrical current tends to increase first and then gradually becomes constant. At the beginning of the study, soil pores were open and permeable due to ultrasonication [14].

A new condition is demonstrated using EK-US at constant voltage: the current value of EK-US is slightly more significant than the EK test. This occurs because the conductivity of the pore solution can be maintained when using ultrasonication. Current values tend to decrease because the availability of mobile ions in the SSS is gradually reduced due to electromigration. In addition, excess ions around the electrode chamber undergo neutralization because they react with SSS particles, different species in solution, or the electrode. Electric current tends to decrease with time as moisture decreases due to evaporation. In the US-EK process, ultrasonication does not significantly affect pH reduction but is solely due to migration from excessive H^+. Ultrasonication can maintain pH slightly better than without ultrasonication due to an increase in water flow as a result of ultrasonic energy. The concentration of organic contaminant residues in US-EK is more homogeneously distributed than in electrokinetic soil flushing. US-EK can release organic contaminant bonds with soil particles and degrade them by oxidizing free radicals produced during cavitation [68]. The small voltage gradient also affects the hydrolysis rate, reducing all electrokinetic phenomena and extending the remediation time. However, too much voltage can also increase the rate of oxidation, accelerate the formation of complex compounds due to migration, and increase energy consumption. Therefore, an optimal voltage gradient is critical for optimal efficiency with low energy usage. Ultrasonication with a frequency of 40 kHz has a role in the extraction of metals and accelerates the mass transfer of ionic contaminants from the solid phase to the liquid phase. The removal of four metals (Zn, Pb, Cu, and Cd) increased gradually along with an increase in the voltage gradient of 0.5–2 V cm^{-1} [65].

Ultrasonic power affects the shear stresses of particle surfaces and cavitation so that the desorption rate of organic pollutants is higher. The time of sonication exposure is a significant factor in influencing integrative treatment. The longer the time, the more organic pollutants are removed (1–5 minutes). Interestingly, too much acoustic time is not significant for decreasing organic pollutants (>10 minutes). The release of organic contaminants after the optimal time is challenging because of the strong binding force between contaminants and soil particles. Power, frequency, temperature, acoustic time, and liquid level induce electrokinetic phenomena and accumulation of metal ions in the electrokinetic remediation system. With the same system parameters, acoustic time, reactor temperature, and power have different effects on metal removal. In general, the significant factors for three metal ions (Zn, Pb, Cd) sorted from greatest to least are acoustic time, reactor temperature, and power of ultrasonication [30, 65].

26.4.2.2 Contaminant and Environmental Parameters

The primary factor influencing the effectiveness of EK-US remediation technology is the chemical characteristics of organic compounds, especially water dissolution

UNCORRECTED PROOFS

Trim Size: 170mm x 244mm Single Column Loose Ribeiro670117 c26.tex V1 - 12/11/2020 10:26pm Page 670

and absorption into soil particles. However, with constant humidity, frequency, and ultrasonic power, the effectiveness of this combined remediation method also decreases with greater pollutant concentration. When the concentration of organic pollutants is lower, the contaminants are tightly attached to soil particles as monolayers, and only high desorption energy can release the bonds. When the pollutants are at a higher concentration, the molecules on the SSS surface particles attach as multilayers that have weak bonds. That causes ultrasound cavitation, quickly releasing the chemical bonds. Ultrasonication can encourage the formation of thermal decomposition, radical hydroxyl oxidation, high solid-liquid shear stresses, and sonolysis of organic compounds in SSS. The initial concentration of contaminants is an essential parameter for determining the effectiveness of removing nonionic pollutants in EK-US [14]. Given the same moisture content and processing system, the concentration of nonionic pollutants is inversely proportional to the efficiency of ultrasonication. The greater the initial level of pollutants, the lower the efficiency. Shrestha et al. reported that at a concentration of 100 mg kg^{-1} chrysene, the resulting efficiency was 45%; whereas at a level of 25 mg kg^{-1}, the average removal efficiency was 70%. Ultrasonication is useful for extracting metals and accelerating mass transfer from solid-liquid systems. The recommended ultrasonication time is more than 20 minutes based on the obtained removal efficiency [67].

Electrokinetic phenomena are influenced by various interactions, including hydraulic conductivity, chemical–physical components, and the interaction of SSS particles with electricity [3]. Sorption-desorption, precipitation-dissolution, and oxidation-reduction of compounds significantly affect removal efficiency. Sorption behavior is very dependent on the type of contaminants, the kind of SSS particles, and the character of the fluid present in the SSS pores. Changes in SSS pH when applying electrokinetics affect the sorption and desorption processes of contaminants [70]. Therefore, pH stabilization is a critical factor in the electrokinetic process. Excessive hydrogen ion migration is suppressed by using a buffer solution to prevent a drastic decrease in pH. EK and EK-US have no significant differences in pH values [14]. The pH continues to decrease over time and then becomes constant. Ultrasonication is unable to maintain a neutral soil pH. The pH is also lower at the anode side and tends to be higher on the cathode side [67]. However, controlling pH so it is consistently neutral is essential because electroosmosis occurs at neutral pH. Furthermore, the pH of the soil rapidly decreases, except in the area around the cathode.

As previously described, electrokinetic remediation is very useful when applied to SSS with low permeability and for removal of charged metals/colloidal pollutants. On the other hand, ultrasonication is specifically used to enhance extraction, desorption, destruction, and mobilization of organic pollutants. Combining the two may be beneficial in low-permeability SSS contaminated with organic compounds. Ultrasonication helps the electrokinetic process by stimulating shear stress, forming a means of thermal decomposition and radical hydroxyl oxidation that can initiate the sonolysis process of organic compounds in pore fluid. The decrease in pH also indicates continuous hydrolysis, which increases the number of protons

UNCORRECTED PROOFS

Trim Size: 170mm x 244mm Single Column Loose Ribeiro670117 c26.tex V1 - 12/11/2020 10:26pm Page 671

and is useful in the extraction and exchange of ions with metals attached to the soil particle [57, 65].

Maintaining an optimal water content is also a critical parameter during the US-EK process. H^+ ions at the anode are transferred to the cathode, and the migration speed of H^+ ions is 1.76 faster than OH^-. The phenomenon of electroosmotic flow in combining the two technologies is also explained by Chung and Kamon. Outflow in integrative treatment is greater than for electrokinetics alone. Lead hydroxide formed in soil pores causes a decrease in ionic strength throughout the process so that electroosmotic flow decreases [32]. However, when ultrasonication is applied, the soil's porosity and permeability increase so that the rate of electroosmosis is not reduced. In fluids, ultrasonication causes water to produce bubbles, which can turn into microjets or jet streams, as shown in Figure 26.5. Ultrasonication can increase permeability because of the influence of particle agitation and dislodging on soil pore [47]. Ultrasonication in the middle of the reactor does not affect the electrolyte pH. The anode chamber is filled with H^+, which is transported to the cathode.

26.4.3 Future Directions

Ultrasonication is useful for increasing the quantity of outflow and ensuring that electroosmosis can take place optimally. Meanwhile, electrokinetics are not significant in increasing liquid outflow because of the small current. This result may be different when US-EK is applied at a field scale with higher electricity demand, where electrokinetics may play an essential role in increasing outflow volume [69]. However, the removal of contaminants did not occur due to the amount of calcium in the soil. The complexity of geochemical factors, especially the interaction between natural electrolytes and differences in the composition of lab-test soils and field-test soils, are suspected to be factors causing this technology to fail on a field scale [15, 27, 71]. Pham et al. said that the right use of surfactants might increase the effectiveness of organic contaminant removal using EK-US. After the contaminants leach because of the ultrasound effect, electroosmosis plays a critical role in transporting contaminants from the soil pores into the electrode chamber. Since organic pollutants have larger molecular sizes, surfactants can convert these molecules into micelle oil, preventing soil pores from clogging [68]. However, there is a lack of research evaluating the potential of remediation systems using EK-US and surfactants. Other research related to using sustainable green energy that can provide green electricity may be explored and quantified [72]. Therefore, further research is also needed that can support applying this technology in the field.

26.5 Conclusions

Ultrasonication is very appropriate for pretreating and assisting electrokinetic remediation in removing ionic and nonionic pollutants from soil. However, some parameters must be highlighted to achieve optimal conditions. Acoustic time,

UNCORRECTED PROOFS

Trim Size: 170mm x 244mm Single Column Loose Ribeiro670117 c26.tex V1 - 12/11/2020 10:26pm Page 672

power, frequency, ambient temperature, concentration and type of contaminant, and soil/liquid ratio affect the efficiency of ultrasonication. Moreover, several critical electrokinetic parameters also influence the effectiveness of electrokinetic treatment, including soil type, ionic concentration, voltage gradient, electrode type, humidity, and pH control. Although this combination technology can provide high efficiency in the removal of hydrocarbon, organic, and metal pollutants, it is limited by the high investment costs and the high electricity load that must be provided to support the process. In addition, there is no empirical data that mentions the success of combining these two technologies at the field scale. Using various renewable technologies may reduce the environmental and investment costs of remediating the original contaminated soil.

References

1 Feng, D. and Aldrich, C. (2000). Sonochemical treatment of simulated soil contaminated with diesel. *Advances in Environmental Research* 4 (2): 103–112.
2 Gomes, H.I., Dias-Ferreira, C., and Ribeiro, A.B. (2012). Electrokinetic remediation of organochlorines in soil: enhancement techniques and integration with other remediation technologies. *Chemosphere* 87 (10): 1077–1090.
3 Yeung, A.T. and Gu, Y.Y. (2011). A review on techniques to enhance electrochemical remediation of contaminated soils. *Journal of Hazardous Materials* 195: 11–29.
4 Ramadan, B.S., Sari, G.L., Rosmalina, R.T. et al. (2018). An overview of electrokinetic soil flushing and its effect on bioremediation of hydrocarbon contaminated soil. *Journal of Environmental Management* 218: 309–321.
5 Benamar, A., Tian, Y., Portet-Koltalo, F. et al. (2019). Enhanced electrokinetic remediation of multi-contaminated dredged sediments and induced effect on their toxicity. *Chemosphere* 228: 744–755.
6 Risco, C., López-Vizcaíno, R., Sáez, C. et al. (2015). Remediation of soils polluted with 2,4-D by electrokinetic soil flushing with facing rows of electrodes: a case study in a pilot plant. *Chemical Engineering Journal* 285: 128–136.
7 Mena, E., Villaseñor, J., Rodrigo, M.A., and Cañizares, P. (2016). Electrokinetic remediation of soil polluted with insoluble organics using biological permeable reactive barriers: effect of periodic polarity reversal and voltage gradient. *Chemical Engineering Journal* 299: 30–36.
8 Li, W.W. and Yu, H.Q. (2015). Electro-assisted groundwater bioremediation: fundamentals, challenges and future perspectives. *Bioresource Technology* 196: 677–684.
9 Ferrarese, E. and Andreottola, G. (2007). Application of electrochemical techniques for the remediation of soils contaminated with organic pollutants. Assoc Environ Heal Sci - 23rd Annu Int Conf Soils, Sediments Water.
10 Xiao, J., Pang, Z., Zhou, S. et al. (2020). The mechanism of acid-washed zero-valent iron/activated carbon as permeable reactive barrier enhanced

UNCORRECTED PROOFS

Trim Size: 170mm x 244mm Single Column Loose Ribeiro670117 c26.tex V1 - 12/11/2020 10:26pm Page 673

electrokinetic remediation of uranium-contaminated soil. *Separation and Purification Technology* 244: 116667.

11 Roulier, M., Kemper, M., Al-Abed, S. et al. (2000). Feasibility of electrokinetic soil remediation in horizontal lasagna(TM) cells. *Journal of Hazardous Materials* 77 (1–3): 161–176.

12 Cameselle, C. and Gouveia, S. (2018). Electrokinetic remediation for the removal of organic contaminants in soils. *Current Opinion in Electrochemistry* 11: 41–47.

13 Pham, T.D., Shrestha, R.A., and Sillanpää, M. (2009). Electrokinetic and ultrasonic treatment of kaolin contaminated by POPs. *Separation Science and Technology* 44 (10): 2410–2420.

14 Pham, T.D., Shrestha, R.A., Virkutyte, J., and Sillanpää, M. (2009). Combined ultrasonication and electrokinetic remediation for persistent organic removal from contaminated kaolin. *Electrochimica Acta* 54 (5): 1403–1407.

15 Adewuyi, Y.G. (2001). Sonochemistry: environmental science and engineering applications. *Industrial & Engineering Chemistry Research* 40: 4681–4715.

16 Mason, T.J., Collings, A., and Sumel, A. (2004). Sonic and ultrasonic removal of chemical contaminants from soil in the laboratory and on a large scale. *Ultrasonics Sonochemistry* 11 (3–4): 205–210.

17 Wood, R.J., Lee, J., and Bussemaker, M.J. (2017). A parametric review of sonochemistry: control and augmentation of sonochemical activity in aqueous solutions. *Ultrasonics Sonochemistry* 38: 351–370.

18 Jiang, J., Zhao, Q., Zhang, J. et al. (2009). Electricity generation from bio-treatment of sewage sludge with microbial fuel cell. *Bioresource Technology* 100 (23): 5808–5812.

19 Mason, T.J. (2007). Developments in ultrasound – non-medical. *Progress in Biophysics and Molecular Biology* 93: 166–175.

20 Yin, X., Han, P., Lu, X., and Wang, Y. (2004). A review on the dewaterability of bio-sludge and ultrasound pretreatment. *Ultrasonics Sonochemistry* 11 (6): 337–348.

21 Shrestha, R.A., Pham, T.D., and Sillanpää, M. (2009). Effect of ultrasound on removal of persistent organic pollutants (POPs) from different types of soils. *Journal of Hazardous Materials* 170 (2–3): 871–875.

22 Zhang, J., Li, J., Thring, R., and Liu, L. (2013). Application of ultrasound and Fenton's reaction process for the treatment of oily sludge. *Procedia Environmental Sciences* 18: 686–693.

23 Park, B. and Son, Y. (2017). Ultrasonic and mechanical soil washing processes for the removal of heavy metals from soils. *Ultrasonics Sonochemistry* 35: 640–645.

24 Hoffmann, M.R., Hua, I., and Höchemer, R. (1996). Application of ultrasonic irradiation for the degradation of chemical contaminants in water. *Ultrasonics Sonochemistry* 3 (3): S163–S172.

25 Little, C., Hepher, M.J., and El-Sharif, M. (2002). The sono-degradation of phenanthrene in an aqueous environment. *Ultrasonics* 40 (1–8): 667–674.

UNCORRECTED PROOFS

Trim Size: 170mm x 244mm Single Column Loose Ribeiro670117 c26.tex V1 - 12/11/2020 10:26pm Page 674

26 Seidi, S. and Yamini, Y. (2012). Analytical sonochemistry; developments, applications, and hyphenations of ultrasound in sample preparation and analytical techniques. *Central European Journal of Chemistry* 10 (4): 938–976.

27 Vyas, S. and Ting, Y.P. (2018). A review of the application of ultrasound in bioleaching and insights from sonication in (bio)chemical processes. *Resources* 7 (1) https://www.mdpi.com/2079-9276/7/1/3.

28 Abramov, O.V., Abramov, V.O., Myasnikov, S.K., and Mullakaev, M.S. (2009). Extraction of bitumen, crude oil and its products from tar sand and contaminated sandy soil under effect of ultrasound. *Ultrasonics Sonochemistry* 16 (3): 408–416.

29 Thangavadivel, K., Megharaj, M., Smart, R.S.C. et al. (2011). Ultrasonic enhanced desorption of DDT from contaminated soils. *Water, Air, and Soil Pollution* 217 (1–4): 115–125.

30 Asgharzadehahmadi, S., Abdul, R.A.A., Parthasarathy, R., and Sajjadi, B. (2016). Sonochemical reactors: review on features, advantages and limitations. *Renewable and Sustainable Energy Reviews* 63: 302–314.

31 Kim, S.S. and Han, S.J. (2003). Application of an enhanced electrokinetic ion injection system to bioremediation. *Water, Air, and Soil Pollution* 146 (1–4): 365–377.

32 Chung, H.I. and Kamon, M. (2005). Ultrasonically enhanced electrokinetic remediation for removal of Pb and phenanthrene in contaminated soils. *Engineering Geology* 77 (3–4 Spec. Iss): 233–242.

33 Moghadam, M.J., Moayedi, H., Sadeghi, M.M., and Hajiannia, A. (2016). A review of combinations of electrokinetic applications. *Environmental Geochemistry and Health* 38 (6): 1217–1227.

34 Wick, L.Y., Shi, L., and Harms, H. (2007). Electro-bioremediation of hydrophobic organic soil-contaminants: a review of fundamental interactions. *Electrochimica Acta* 52 (10 Spec. Iss): 3441–3448.

35 Tahmasbian, I. (2012). Soil electerokinetic remediation and its effects on soil microbial activity- a review. *African Journal of Microbiology Research* 6 (10): 2233–2238.

36 Shi, L., Müller, S., Harms, H., and Wick, L.Y. (2008). Factors influencing the electrokinetic dispersion of PAH-degrading bacteria in a laboratory model aquifer. *Applied Microbiology and Biotechnology* 80 (3): 507–515.

37 Trentin, A.W.S., Reddy, K.R., Kumar, G. et al. (2019). Quantitative assessment of life cycle sustainability (QUALICS): framework and its application to assess electrokinetic remediation. *Chemosphere* 230: 92–106.

38 Harbottle, M.J., Lear, G., Sills, G.C., and Thompson, I.P. (2009). Enhanced biodegradation of pentachlorophenol in unsaturated soil using reversed field electrokinetics. *Journal of Environmental Management* 90 (5): 1893–1900.

39 Chen, F., Li, X., Ma, J. et al. (2019). Remediation of soil co-contaminated with decabromodiphenyl ether (BDE-209) and copper by enhanced electrokinetics-persulfate process. *Journal of Hazardous Materials* 369: 448–455.

UNCORRECTED PROOFS

Trim Size: 170mm x 244mm Single Column Loose Ribeiro670117 c26.tex V1 - 12/11/2020 10:26pm Page 675

40 Taccari, M., Milanovic, V., Comitini, F. et al. (2012). Effects of biostimulation and bioaugmentation on diesel removal and bacterial community. *International Biodeterioration and Biodegradation* 66 (1): 39–46.

41 Cuevas, J., Ruiz, A.I., de Soto, I.S. et al. (2012). The performance of natural clay as a barrier to the diffusion of municipal solid waste landfill leachates. *Journal of Environmental Management* 95: S175–S181.

42 Ramadan, B.S., Effendi, A.J., and Helmy, Q. (2018). Integrating electrokinetic and bioremediation process for treating oil contaminated low permeability soil. E3S Web of Conferences.

43 Rodrigo, M.A., Mena, E., Ruiz, C. et al. (2014). Combined electrokinetic soil flushing and bioremediation for the treatment of spiked soils polluted with organics. *Chemical Engineering Transactions* 41: 109–114.

44 Yang, G.C.C. (2018). Integrated electrokinetic processes for the remediation of phthalate esters in river sediments: a mini-review. *Science of the Total Environment* 659: 963–972.

45 Zhao, S., Fan, L., Zhou, M. et al. (2016). Remediation of copper contaminated kaolin by Electrokinetics coupled with permeable reactive barrier. *Procedia Environmental Sciences* 31: 274–279.

46 Cappai, G., De Gioannis, G., Muntoni, A. et al. (2012). Combined use of a transformed red mud reactive barrier and electrokinetics for remediation of Cr/As contaminated soil. *Chemosphere* 86 (4): 400–408.

47 Chung, H.I., Chun, B.S., and Lee, Y.J. (2006). The combined electrokinetic and ultrasonic remediation of sand contaminated with heavy metal and organic substance. *KSCE Journal of Civil Engineering* 10 (5): 325–331.

48 Lim, M.H., Kim, S.H., Kim, Y.U., and Khim, J. (2007). Sonolysis of chlorinated compounds in aqueous solution. *Ultrasonics Sonochemistry* 14 (2): 93–98.

49 Li, J., Song, X., Hu, G., and Thring, R.W. (2013). Ultrasonic desorption of petroleum hydrocarbons from crude oil contaminated soils. *Journal of Environmental Science and Health, Part A: Toxic/Hazardous Substances and Environmental Engineering* 48 (11): 1378–1389.

50 Son, Y., Nam, S., Ashokkumar, M., and Khim, J. (2012). Comparison of energy consumptions between ultrasonic, mechanical, and combined soil washing processes. *Ultrasonics Sonochemistry* 19 (3): 395–398.

51 Effendi, A.J., Wulandari, M., and Setiadi, T. (2019). Ultrasonic application in contaminated soil remediation. *Current Opinion in Environmental Science & Health* 12: 66–71.

52 Parveen, K., Rafique, U., Akhtar, M.J., and Ashokumar, M. (2018). Ultrasound-assisted synthesis of gallium hybrids for environmental remediation application. *Ultrasonics Sonochemistry* 49: 222–232.

53 Sáez, V., Esclapez, M.D., Bonete, P. et al. (2011). Sonochemical degradation of perchloroethylene: the influence of ultrasonic variables, and the identification of products. *Ultrasonics Sonochemistry* 18 (1): 104–113.

54 Dewulf, J., Van Langenhove, H., De Visscher, A., and Sabbe, S. (2001). Ultrasonic degradation of trichloroethylene and chlorobenzene at micromolar concentrations: kinetics and modelling. *Ultrasonics Sonochemistry* 8 (2): 143–150.

UNCORRECTED PROOFS

Trim Size: 170mm x 244mm Single Column Loose Ribeiro670117 c26.tex V1 - 12/11/2020 10:26pm Page 676

55 Lim, J.L. and Okada, M. (2005). Regeneration of granular activated carbon using ultrasound. *Ultrasonics Sonochemistry* 12 (4): 277–282.

56 Bendicho, C., De La Calle, I., Pena, F. et al. (2012). Ultrasound-assisted pretreatment of solid samples in the context of green analytical chemistry. *TrAC, Trends in Analytical Chemistry* 31: 50–60.

57 Mohammadian, E., Junin, R., Rahmani, O., and Idris, A.K. (2013). Effects of sonication radiation on oil recovery by ultrasonic waves stimulated water-flooding. *Ultrasonics* 53 (2): 607–614.

58 Shrestha, R.A., Pham, T.D., and Sillanpää, M. (2009). Remediation of chrysene from contaminated soil by enhanced electrokinetics. *International Journal of Electrochemical Science* 4 (10): 1387–1394.

59 Martín-Díaz, J., Lucena, F., Blanch, A.R., and Jofre, J. (2020). Review: indicator bacteriophages in sludge, biosolids, sediments and soils. *Environmental Research* 182: 109–133.

60 Zulfiqar, W., Iqbal, M.A., and Butt, M.K. (2017). Pb^{2+} ions mobility perturbation by iron particles during electrokinetic remediation of contaminated soil. *Chemosphere* 169: 257–261.

61 Maturi, K., Reddy, K.R., and Cameselle, C. (2009). Surfactant-enhanced electrokinetic remediation of mixed contamination in low permeability soil. *Separation Science and Technology* 44 (10): 2385–2409.

62 Streche, C., Badea, A., Istrate, I.A. et al. (2014). Experimental research regarding the application of electro-flushing method on diesel contaminated soils. *Present Environment and Sustainable Development* 8 (1): 37–44.

63 Reddy, K.R. and Chinthamreddy, S. (2004). Enhanced electrokinetic remediation of heavy metals in glacial till soils using different electrolyte solutions. *Journal of Environmental Engineering* 130 (4): 442–455.

64 Chung, H.I., Oh, I.K., and Kamon, M. (2002). The coupled effect of electrokinetic and ultrasonic remediation of contaminated soil. Brownfield Sites. 55:495–505. https://www.witpress.com/elibrary/wit-transactions-on-ecology-and-the-environment/55/1027.

65 Huang, T., Zhou, L., Liu, L., and Xia, M. (2018). Ultrasound-enhanced electrokinetic remediation for removal of Zn, Pb, Cu and Cd in municipal solid waste incineration fly ashes. *Waste Management* 75: 226–235.

66 Oh, S., Oh, M., and Lee, J.-Y. (2013). Removal of As, cadmium and lead in sandy soil with sonification-electrokinetic remediation. *Journal of Soil and Groundwater Environment* 18 (7): 1–11.

67 Shrestha, R.A., Pham, T.D., and Sillanpää, M. (2010). Electro ultrasonic remediation of polycyclic aromatic hydrocarbons from contaminated soil. *Journal of Applied Electrochemistry* 40 (7): 1407–1413.

68 Pham, T.D., Shrestha, R.A., and Sillanpää, M. (2010). Removal of hexachlorobenzene and phenanthrene from clayey soil by surfactant- and ultrasound-assisted electrokinetics. *Journal of Environmental Engineering* 136 (7): 739–742.

69 Chung, H.I. (2007). Treatment of contaminated groundwater in sandy layer under river bank by electrokinetic and ultrasonic technology. *Water Science and Technology* 55 (1–2): 329–338.

UNCORRECTED PROOFS

Trim Size: 170mm x 244mm Single Column Loose Ribeiro670117 c26.tex V1 - 12/11/2020 10:26pm Page 677

70 Niqui-Arroyo, J.L., Bueno-Montes, M., Posada-Baquero, R., and Ortega-Calvo, J.J. (2006). Electrokinetic enhancement of phenanthrene biodegradation in creosote-polluted clay soil. *Environmental Pollution* 142 (2): 326–332.

71 Gong, Y., Zhao, D., and Wang, Q. (2018). An overview of field-scale studies on remediation of soil contaminated with heavy metals and metalloids: technical progress over the last decade. *Water Research* 147: 440–460.

72 Hassan, I., Mohamedelhassan, E., and Yanful, E.K. (2015). Solar powered electrokinetic remediation of Cu polluted soil using a novel anode configuration. *Electrochimica Acta* 181: 58–67.

UNCORRECTED PROOFS

UNCORRECTED PROOFS